Robust and Imperceptible Region Based Watermarking on Medical Images

K. Swaraja, K. Meenakshi, Padmavathi Kora, and G. Karuna

Abstract Telemedicine is the remote delivery of health care services to evaluate, diagnose and treat patients using common technology, such as video conferencing and smart phones, without the need for an in-person visit. There is likelihood in altering the medical images purposely or unintentionally while transmitting over covert channel. The Physician confirms the diagnosis region obtained from the medical image as region of interest (ROI), prior to interpreting any report on evaluation. Watermarking scheme for medical images exploring DCT domain is conferred in this proposal. Fuzzy c algorithm is utilized in segmenting the assessment region (ROI) and non-interest region (RONI), further the watermark is inserted through modulation scheme termed as M-ary. The scheme efficacy is determined for MRI medical images through simulation by computation of quality metrics such as PSNR and NCC.

Keywords Medical image watermarking · Region of interest · Fuzzy c-means · M-ary modulation

1 Introduction

Internet is the most innovative improvement in the existing technology. In our existence, health care is the most significant application of internet to health concern providers as Electronic Patient Record (EPR) is transferred to dissimilar organizations. The watermarking schemes in the telemedicine area [1–3] entail extreme caution while inserting extra data inside the medical images as the added data need not distress the quality of the image. Therefore, to overcome the difficulty of memory exploitation as well as to defend the medical details against illicit handling, watermarking for medical images is employed. Thus in this work, a watermarking system exploiting the M-ary modulation scheme is proposed. The image with medical details

K. Swaraja (✉) · K. Meenakshi · P. Kora
Electronics and Communications Engineering, GRIET, Hyderabad, India

G. Karuna
Computer Science and Engineering, GRIET, Hyderabad, India

A. Kumar et al. (eds.), *ICDSMLA 2020*, Lecture Notes in Electrical Engineering 783,
https://doi.org/10.1007/978-981-16-3690-5_78

A Robust Watermarking Using RDWT and Slant Transform Using Hybrid Firefly and Differential Evolution Optimization Algorithm

K. Meenakshi, K. Swaraja, Padmavathi Kora, and G. Karuna

Abstract In this work, an optimized watermarking framework is proposed with the hybrid combination of two metaheuristic algorithms-firefly optimization and differential evolution, namely HFADE. The cover image is partitioned into 4×4 sub-blocks, and the watermark is concealed in the slant domain using Quantized Index Modulation (QIM). The optimized thresholds obtained with HFADE used in quantization to improve imperceptibility and robustness. Peak Signal to noise ratio(PSNR) and Normalized Cross Correlation (NCC) are used for evaluation of the proposed watermarking scheme. The fitness function for HFADE is taken as the reciprocal of mean square error between the watermarked and cover image. Simulation outcomes convey that the proposed scheme maintains improved imperceptibility, and the watermark extracted from a seriously distorted image.

Keywords Differential evolution · Firefly · Slant transform · Quantization index modulation

1 Introduction

The improvement of Internet and computer input-output devices has made the broadcast and alteration of digital content without difficulty. With the advanced editing technologies, an edited copy appears similar to the original. So, the security of ownership of digital content has become the utmost concern. Digital watermarking [1–16] is evolved to protect the interests of owners from the copyright infringement. The three trade-off parameters of watermarking scheme are transparency, robustness and capacity. Further, it must not suffer from the false positive problems. Optimization algorithms such as Fuzzy logic [17, 18], Genetic Algorithm [19], Differential Evolution (DE) [1] are used to optimize the mutually conflicting parameters of transparency and robustness.

K. Meenakshi (✉) · K. Swaraja · P. Kora · G. Karuna
Department of ECE, GRIET, Hyderabad, India
e-mail: mkollati@gmail.com

A. Kumar et al. (eds.), *ICDSMLA 2020*, Lecture Notes in Electrical Engineering 783,
https://doi.org/10.1007/978-981-16-3690-5_79

Artificial Intelligence Based Learning Approach for Leaf Disease Identification and Detection

G. Karuna, K. Sahithi, B. Rupa, R. Amani, K. Swaraja, and K. Meenakshi

Abstract Plants and Crops get diseased due to many reasons. It might be because of diseases of stems, leaves, roots etc. This Paper mainly congregates on leaves. Leaf Disease identification and Detection has many applications for cultivators and farmers to know whether the plant is diseased or not. So that they can retort in dwarf time and decreasing the loss and then can obtain immense profits. This paper mainly focused at learning the disease of plant through leaves. Here, we scrutinize the leaf through Image Processing and extract features of particular leaf and then utilizing those features as a dataset and done preprocessing and then administering them in Artificial Intelligence based learning algorithms like Convolutional Neural Networks to find disease.

Keywords Leaf disease · Neural networks · Features

1 Introduction

In the Earth, India is the second powerful Country in terms of population and also Food is one of the essential one to a person in order to survive. We are acquiring food from plants and so we have to safeguard our plants from diseases. Diseases of plants are normally due to insects, pests, pathogens and reduce the fertility to an extreme extent if not managed with in time.

Now-A-Days technology plays important role in most of the fields yet till this day we are applying some past approaches in farming. Knowing the plant's condition plays a vital role for productive farming [1]. Detection is happened normally by the scientists but due to the so many changes in the environment, the detection is becoming tough. So we can practice processing of image techniques for recognition of disease of a plant. Normally we can get to know the symptoms of diseases on stems, leafs, flowers etc. so here we mainly utilize leaves for recognition of diseased plants.

G. Karuna (✉) · K. Sahithi · B. Rupa · R. Amani
Computer Science and Engineering, GRIET, Hyderabad, India

K. Swaraja · K. Meenakshi
Electronics and Communications Engineering, GRIET, Hyderabad, India

A. Kumar et al. (eds.), *ICDSMLA 2020*, Lecture Notes in Electrical Engineering 783,
https://doi.org/10.1007/978-981-16-3690-5_77

Performance Analysis of Machine Learning Algorithms for Text Classification

Manda Thejaswee(✉), V. Srilakshmi, K. Anuradha, and G. Karuna

Computer Science and Engineering GRIET, Hyderabad, India

Abstract. In the current century, the number of complex documents and messages requiring a top-to-bottom understanding of ML strategies that precisely identify texts in different applications is increasing. In natural language processing, several ML techniques have produced impressive results. The achievement of these learning calculations relies on their ability to comprehend complex models and non-linear data relationships. In any case, identifying right text classification structures and procedures is still a test for researchers. A brief overview of text classification algorithms is presented in this paper. This review includes numerous methods of selecting text elements, current algorithms and techniques and methods of evaluation. In this analysis different TF-IDF Vectorizer features are compared to find the set that works best under different classification models. The objective of phishing website URLs is to purloin the personal information like user name, passwords and online banking transactions. Phishers use the websites which are visually and semantically similar to those real websites. As technology continues to grow, phishing techniques started to progress rapidly and this needs to be prevented by using anti-phishing mechanisms to detect phishing. Machine learning is a powerful tool used to strive against phishing attacks. This paper surveys the features used for detection and detection techniques using machine learning.

Keywords: Text mining · Text classification · Text categorization · Document classification

1 Introduction

In the last few decades, text classification issues have been discussed in many real-world applications [1, 2]. Classification Many researchers are interested in developing applications that relate to text classification methods, particularly with the latest developments in natural language processing (NLP) with text mining. Artificial Neural Networks were new emerging technologies that help solve problems with the classification of machine learning [20, 22]. Most text categorization systems can be divided into the following phases: pre-processing of text, selection of functions, selection of classifiers and evaluation.

A. K. Luhach et al. (Eds.): ICAICR 2020, CCIS 1393, pp. 414–424, 2021.
https://doi.org/10.1007/978-981-16-3660-8_39

International Conference on Information Processing

ICInPro 2021: **Data Science and Computational Intelligence** pp 353–365

ERDNS: Ensemble of Random Forest, Decision Tree, and Naive Bayes Kernel Through Stacking for Efficient Cross Site Scripting Attack Classification

A. Niranjan, K. M. Akshobhya, Arun Singh Chouhan & Praveen Tumuluru

Conference paper | First Online: 01 January 2022

Part of the Communications in Computer and Information Science book series (CCIS,volume 1483)

Abstract

Cross-Site Scripting (XSS) is a form of client-side code injection attack in which an attacker attempts to execute malicious scripts in the victim's web browser by embedding dangerous code in a legitimate web page or application. During such an attack, the attacker impersonates a victim user and performs any behavior that the user is capable of, as well as accessing any of his data. If the victim user has privileged access to the application, the attacker can take complete control of the app's features and data. XSS attacks are most common

Proceedings of the Third International Conference on Inventive Research in Computing Applications (ICIRCA-2021)
IEEE Xplore Part Number: CFP21N67-ART; ISBN: 978-0-7381-4627-0

An efficient smartphone based Parasite Malaria Detection with Deep Neural Networks

1st Rahul Das.P
Computer Science and Engineering,
GRIET
Hyderabad, Telangana, India
rahuldaspathlavath@gmail.com

2nd Karuna.G
Computer Science and Engineering,
GRIET
Hyderabad, Telangana, India
karunavenkatg@gmail.com

3rd Srilakshmi.V
Computer Science and Engineering,
GRIET
Hyderabad, Telangana, India
potlurisrilakshmi@gmail.com

4th Rupa.B
Computer Science and Engineering,
GRIET
Hyderabad, Telangana, India
rupa.bogolu@gmail.com

2021 Third International Conference on Inventive Research in Computing Applications (ICIRCA) | 978-1-6654-3877-3/21/$31.00 ©2021 IEEE | DOI: 10.1109/ICIRCA51532.2021.9544951

***Abstract* — Malaria is a serious infection caused by a blood parasite called Plasmodium spp. Every year, the**

World Health Organization [WHO] estimates 300-500 million malaria cases and over one deaths worldwide. Manually counting and arranging epithetical contaminated erythrocytes is a time-consuming and exhausting operation. Computerized parasite detection using mobile phones is a potential alternative to manual parasite meaning intestinal illness assessment, especially in remote areas without expert parasitologists. As a result, the relevance of developing novel devices to facilitate quick and simple detection of epithetical malaria in areas with limited access to social insurance administrations cannot be overstated. The preceding study investigates the possibility of epithetical mechanised intestinal illness parasite recognition trig thick blood distributes around cell phones. We have developed a primary deep learning approach that can recognize malaria parasites, generate dense blood smear images, and can run forth cell phones. Along with the aforementioned research, we created a dataset of 1819 thick smear images from 150 patients that is publicly accessible via examination network. *Keywords* — Deep learning, Convolutional neural networks, Malaria.

I. INTRODUCTION

Malaria is a main source epithetical bleakness & mortality in tropical & sub-tropical nations, amidst an expected epithetical 1-2 million passing each year. The visual discovery and acknowledgement of blood test Epithetical Plasmodium spp is possible and fruitful in addition to a material method known as Giemsa recoloring. The recoloring technique somewhat colorsizes erythrocytes, but it also contains Plasmodium sppparasites, white platelets (WBC), and old rarities. According to a few field experts, manual microscopy is not a reliable screening technique when conducted by non-specialists and is also time-consuming. It is also important to estimate the existence of parasites per tainted erythrocyte when evaluating hypothetical antimalarial therapies. In a current report, WHO [1,2] considers a specific current financing conveyance epithetical intestinal sickness control products that aren't tending via critical shortcomings in wellbeing frameworks for developing nations, proposing a specific imaginative ways that may endure required via rapidly extend access via malaria mediations. It merits underlining a certain cell phone is right now Africa's most significant advanced innovation, & similarly as African media communications generally skirted landline framework & went directly via cell phones, a few specialists state African medication canister skirt concentrated labs [4]. In addition, mix epithetical cell phones.

Concrete which repairs itself by biologically producing limestone to heal cracks that appear on the surface of concrete structures. It is also called bio-concrete. Whenever the concrete is damaged and water starts entering the cracks that appear in the concrete, the spores of the bacteria fertilize after coming in contact with water and nutrients will get activated. The bacteria start to feed the calcium lactate. As the bacteria consume oxygen, the soluble calcium lactate is converted to insoluble limestone. The limestone solidifies on the cracked surface, thereby sealing it up. The overall aim of this research was to quantitatively understand and assess the role of microbiologically induced calcium carbonate precipitation in enhancing the mechanical and durability characteristics of concrete incorporated with Sporosarcina pasteurii and evaluate its crack healing efficiency. Bacteriogenic calcite mineral precipitation using Sporosarcina pasteurii mechanism can be used effectively in improving the strength and durability properties can be attributed to the activity of Sporosarcina pasteurii in development of dense and refined microstructure of bacteria incorporated concrete.

Dr. V Srinivasa Reddy is a professor of civil engineering at Gokaraju Rangaraju Insitute of Engineering and Technology, Hyderabad, Telangana, India. Dr. M V Seshagir Rao is a professor of civil engineering at CVR college of Engineering, Hyderabad, Telangana, India. Dr K Satya Sai Trimurty Naidu is a Retired Executive Engineer at R&DM, Govt.of AP.

9 786203 201116

Fly Ash Based Bacterial Concrete

Vempada, Meduri, Kolla

Srinivasa Reddy Vempada
Seshagiri Rao Meduri
Satya Sai Trimurty Naidu Kolla

Fly Ash Based Bacterial Concrete

Performance and Crack Healing Efficiency Evaluation

LAP LAMBERT Academic Publishing

Srinivasa Reddy Vempada
Seshagiri Rao Meduri
Satya Sai Trimurty Naidu Kolla

Fly Ash Based Bacterial Concrete

Srinivasa Reddy Vempada
Seshagiri Rao Meduri
Satya Sai Trimurty Naidu Kolla

Fly Ash Based Bacterial Concrete

Performance and Crack Healing Efficiency Evaluation

LAP LAMBERT Academic Publishing

Imprint

Cover image: www.ingimage.com

Publisher:
LAP LAMBERT Academic Publishing
is a trademark of
International Book Market Service Ltd., member of OmniScriptum Publishing Group
17 Meldrum Street, Beau Bassin 71504, Mauritius
Printed at: see last page
ISBN: 978-620-3-20111-6

Contents

Chapter-1

INTRODUCTION

1.1 General

Concrete will continue to be the most important building material for infrastructure but most concrete structures are prone to cracking. Tiny cracks on the surface of the concrete make the whole structure vulnerable because water seeps in to degrade the concrete and corrode the steel reinforcement, greatly reducing the lifespan of a structure [1]. Concrete can withstand compressive forces very well but not tensile forces. When it is subjected to tension it starts to crack, which is why it is reinforced with steel; to withstand the tensile forces. Structures built in a high water environment, such as underground basements and marine structures, are particularly vulnerable to corrosion of steel reinforcement. Motorway bridges are also vulnerable because salts used to de-ice the roads penetrate into the cracks in the structures and can accelerate the corrosion of steel reinforcement [2][3]. In many civil engineering structures tensile forces can lead to cracks and these can occur relatively soon after the structure is built [4]. Repair of conventional concrete structures usually involves applying a concrete mortar which is bonded to the damaged surface. Sometimes, the mortar needs to be keyed into the existing structure with metal pins to ensure that it does not fall away. Repairs can be particularly time consuming and expensive because it is

often very difficult to gain access to the structure to make repairs, especially if they are underground or at a great height [7].

As we all know that, concrete is still one of the main materials used for any construction project, ranging from the foundation of buildings to the structure of bridges and underground parking lots. Concrete construction is widely preferred all over the globe due to the convenience in working and promising durability. But like the old idiom that states – 'Every coin has its two sides'; the concrete construction also has its share of problems. Some issues arising in concrete constructions are listed here under:

1. The formation of cracks in the concrete structure which ultimately affects its durability.
2. As the size of cracks become more, it damages the structural integrity.
3. The smaller millimeter-sized cracks might also result in durability problems.
4. Similarly, few connected cracks increase matrix permeability.
5. Ingress water and chemicals can cause premature concrete degradation and corrosion of steel reinforcement.

Self-healing concrete could solve the problem of concrete structures deteriorating well before the end of their service life. Concrete is still one of the main materials used in the construction industry, from the foundation of buildings to the structure of bridges and underground parking lots [8]. Traditional concrete has a flaw, it tends to crack when

subjected to tension. A healing agent that works when bacteria embedded in the concrete convert nutrients into limestone has been under development at the Civil Engineering and Geosciences Faculty in Delft since 2006 [14]. The project is part of a wider Mineral-producing bacteria have been found that could help mend micro-cracking in concrete. Dr Henk Jonkers, a microbiologist who specializes in the behaviour of bacteria in the environment, has developed self-healing concrete in the laboratory and full-scale outdoor testing was done in 2011 [15]. The first self-healing concrete products (successful research results permitting) are expected to hit the market in two years' time and are expected to increase the lifespan of many civil engineering structures [20].

1.2 Autonomous Healing

Concrete constructions are currently designed according to set norms that allow cracks to form up to 0.2 mm wide. Such micro cracks are generally considered acceptable, as these do not directly impair the safety and strength of a construction. Moreover, micro cracks sometimes heal themselves as many types of concrete feature a certain crack-healing capacity. Research has shown that this so called 'autonomous' healing capacity is largely related to the number of non-reacted cement particles present in the concrete matrix. On crack formation, ingress water reacts with these particles, resulting in closure of micro cracks. However, because of the variability of autonomous crack healing of concrete constructions, water leakage as a result of micro crack formation in tunnel

and underground structures can occur [22]. The Delft group quantified autonomous self-healing of control samples and compared that to the self-healing capacity of concrete with an inbuilt bacteria-based self-healing agent. While self-healing of 0.2 mm wide cracks occurred in 30% of the control samples, complete closure of all cracks was obtained in all bacteria-based samples. Moreover, the crack sealing capacity of the latter group was found to be extended to 0.5 mm cracks [25].

1.3 Self-healing concrete

Concrete which repairs itself by biologically producing limestone to heal cracks that appear on the surface of concrete structures. It is also called bio-concrete. There are selected types of the bacteria called Genus Bacillus, along with a calcium-based nutrient known as calcium lactate nitrogen and phosphorus, are added to the ingredients of the concrete when it is being mixed. These self-healing agents or self-healing concrete bacteria can remain alive in concrete up to 200 years [28]. Whenever the concrete is damaged and water starts entering the cracks that appear in the concrete, the spores of the bacteria fertilize after coming in contact with water and nutrients will get activated. The bacteria start to feed the calcium lactate. As the bacteria consume oxygen, the soluble calcium lactate is converted to insoluble limestone. The limestone solidifies on the cracked surface, thereby sealing it up [29].

Self-healing concrete technology has proved to be better than many conventional technologies because of its eco- friendly nature, self-healing

abilities and increase in durability of structure. Various researchers have successfully improved our understanding of the possibilities and limitations of biotechnological applications on building materials. Enhancement of compressive strength, reduction in permeability, water absorption, and reduced reinforcement corrosion have been seen in various cementations and stone materials [30. Self-healing concrete used in construction can reduce the problem of concrete structures deteriorating well before the end of their durable service life. Self-healing concrete is also known as a bio-concrete, self-fixing concrete, bacterial concrete, self-repairing concrete, bacterial self-healing concrete and bacteria healing concrete.

1.4 The Need of Self-Healing Bacterial Concrete / Bio-concrete

Concrete is the most important building material for the construction industry, but, the most concrete structures are affected by various types of cracking problems during its life span. Small cracks developing on the surface of the concrete make the whole structure appear vulnerable because water seeps into the ordinary concrete and starts degrading the same and corrode the steel reinforcement, greatly reducing the lifespan or durability of any structure. It is a well-known fact that concrete can withstand compressive forces very well but not tensile forces. When it is subjected to tensile force it starts to crack, this is why steel reinforcement is used to withstand the tensile forces and support concrete structures.

Structures built in high-water environment, such as underground basements and marine structures are particularly vulnerable to corrosion of steel reinforcement. Bridges are also affected by corrosion problems because salts used to de-ice the roads penetrates into the cracks in the structures and can accelerate the corrosion of steel reinforcement. In the majority of civil engineering structures, tensile forces can lead to cracks and these can occur relatively soon after the structure is constructed. Repair of conventional concrete construction is done by applying a concrete mortar which is bonded to the damaged surface. Sometimes, the mortar needs to be inserted into the existing structure's cracks with metal pins to ensure that it does not fall away [35]. Repairs are time-consuming and expensive because these are often very difficult to execute. Additional effort is required sometimes to gain access to the structure to make repairs, especially if these are underground or at a greater height.

As repair work and regular manual maintenance of concrete constructions are costly and, in some cases, not at all possible, hence it becomes necessary to find a recovery option for it, and the self-healing concrete is one such promising option. The adoption of an autonomous self-healing repair mechanism would be highly advantageous as it could both reduce maintenance and increase material durability [36].

1.5 History of Self – Healing Concrete

Self-healing concrete was invented by 'Hendrik Jonkers', microbiologist of the Delft University of Technology in the Netherlands. He was highly inspired by natural body processes in which bones heal through mineralization, and Jonkers implemented the idea whether this could be used in concrete at all [5].

Looking towards the unique properties and conditions of concrete, it was a challenging experiment that took Jonkers almost three years and saw him named as a finalist for the European Inventor Award 2015. We all know that concrete is an extremely alkaline material in the nature and finding some bacteria that could survive its dry, stone-like properties and remain dormant before being activated by water was not easy [15].

1.6 Self – Healing Concrete Mechanism

Self-healing concrete repairs itself by biologically producing limestone to heal cracks that appear on the surface of concrete structures. There are selected types of the bacteria called Genus Bacillus, along with a calcium-based nutrient known as calcium lactate nitrogen and phosphorus, are added to the ingredients of the concrete when it is being mixed [39].

These self-healing agents or self-healing concrete bacteria can remain alive in concrete up to 200 years. Whenever the concrete is damaged and water starts entering the cracks that appear in the concrete, the spores of the bacteria fertilize after coming in contact with water and nutrients will get activated. The bacteria start to feed the calcium lactate. As the bacteria

consume oxygen, the soluble calcium lactate is converted to insoluble limestone. The limestone solidifies on the cracked surface, thereby sealing it up [44].

It copies the process by which bone fractures in the human body are naturally healed by osteoblast cells that mineralize to re-form the bone. The consumption of oxygen, during bacterial conversion of calcium lactate to limestone has an additional advantage. As we know that, the oxygen is a major element in the process of corrosion of steel, here in this process, the bacterial activity has consumed it all increasing the durability of steel reinforced concrete constructions.

There are two self – repairing agents:

- The bacterial spores
- The calcium lactate-based nutrients

There are added to the concrete with separate expanded clay pellets 2-4 mm wide. This ensures that the self-healing bacteria will not be activated during the cement mixing process. When cracks in a concrete open up the pellets and infiltrating water brings the calcium lactate into contact with the bacteria activating this self-healing process [48].

Testing data expressed that when water enters into the concrete, the bacteria fertilize and multiply quickly. The bacteria transform the nutrients into limestone within seven days in the laboratory.

1.7 Incorporation of bacteria in concrete

The beginning of the research was to find bacteria capable of surviving in an extreme alkaline environment. Cement used in concrete may have pH value of up to 13 when mixed. Usually, in an adverse environment, most organisms die in an environment with a pH value of 10 or above. Therefore, the research is focused on microbes that can remain alive in alkaline environments which can be found in natural environments, such as alkali lakes in Russia, soda lakes in Egypt and carbonate-rich soils in the deserts of Spain [50].

At 'Delft University' the similar bacteria were grown in a flask of water that would then be used as the part of the water mix for the self-healing concrete. Various types of bacteria were added into a small block of concrete. Each block of concrete would be left for two months to become hard. Then the block would be crushed into small particle and the remains tested to see whether the bacteria had survived during a specified time period. From test results, it was found that only some of the bacteria that were able to survive were the ones that produced spores comparable to plant seeds. Such bacteria spores have extremely thick cell walls that enable them to remain intact for up to 200 years while waiting for a better environment to activate [15].

These bacteria would get activated when the concrete starts to crack, food becomes available, and water seeps into the structure. This germination process lowers the pH of the highly alkaline concrete to values in the range

(pH 10 to 11.5) where the bacterial spores become activated. For Finding a suitable food source for the bacteria that could survive in the self-repairing concrete took a long time and many different nutrients were tried until it was observed that calcium lactate was a carbon source that provides biomass. If it gets dissolved during the mixing process, calcium lactate does not interfere with the setting time of the concrete [53].

The Bacteria are identified as:

- Bacillus megaterium
- Bacillus pasteurii
- Bacillus sp. CT-5
- Bacillus subtilis
- Bacillus Aerius
- Sporosarcina pasteurii
- AKKR5
- Shewanella Species
- Bacillus flexus

It is found, that Bacillus megaterium can precipitate the maximum amount of calcite when compared to other positive bacteria, which results in increase in compressive strength and higher efficiency of crack-healing. The idea of bacteria healing concrete was first introduced by US academician in the late 1990s by the research group of 'Professor Sookie Bang' [27]. Testing and application of the theory were not investigated further because there was a lack of interest from the commercial branch

of engineering sector for such a product. But after recent research and development in bioconcrete, several big industries have created partnerships with Delft University to develop applications of self-fixing concrete. Investment funding from construction industry is now forthcoming. Delft University researchers are now therefore developing self-healing concrete products for specific civil engineering markets that will not be in competition with one another. They are developing the product for sectors such as tunnel-lining, structural basement walls, highway bridges, concrete floors, and marine structures [29].

For testing self-healing properties of concrete, the small concrete structure or part of a structure will be built with the self-healing material and observed over two to four years. The concrete structures will be attached to some panels of bacterial concrete and others with normal concrete so that the behavior of the two can be examined and compared. Cracks in concrete will be made much larger than the ones that have healed up in the laboratory to determine how well and fast they heal over the time. Commercial industrial partners have asked whether the process could be used to repair existing structures. To answer this question Delft University has just been given funding of €420,000 from the Dutch government [15]. Two post-doctorate scientists will spend two years for developing a self-healing system to be applied to existing structures.

For finding out the solution to this problem, researchers are testing two systems. The first technique is to see that the structure gets bacteria and

nutrients, as a self-healing mortar, so that they can be used to repair large-scale damage. The second technique will be to observe that the bacteria and food nutrients get dissolved into a liquid that is sprayed onto the surface of the concrete from where it can seep into the cracks after 200 years.

1.8 Advantages of Self – Healing Concrete

1. Overall maintenance cost of this concrete becomes low. The use of bio-concrete significantly enhances the strength of the concrete.
2. It has lower permeability when compared to conventional concrete.
3. It has also lower water absorption when compared to conventional concrete.
4. It offers great resistance against freeze and thaw attacks.
5. The chances of corrosion or reinforcement are reduced to negligible.
6. Redressing of cracks can be done efficiently.
7. It basically increases durability of the structure to a large extent.

1.9 Disadvantages of Self – Healing Concrete

1. Cost of this concrete is comparatively higher than conventional concrete; it's about 10-30% more than conventional concrete.
2. The germination of bacteria is not suitable in every possible environment.
3. The investigations to observe calcite precipitation are costly.
4. Bacteria that are used in concrete are not good for human health; hence its usage has to be limited to the structure.

5. No design guideline for bacterial concrete are yet available in Codes of Design.

1.10 Crack Repair in Concrete Using Biological Methods

Since the combined polymers used today to repair and restore concrete are harmful to the environment, the use of biological methods can be very effective. Bacillus bacteria consume nutrients, having calcium lactate, and absorb nitrogen and phosphorus from environment, and thus produce calcium carbonate. Calcium lactate is soluble and calcium carbonate is insoluble. Thus, calcium carbonate precipitates, then hardens and becomes resistant. In addition to this, environment oxygen consumption by bacteria and reduction of oxygen in small cracks causes the reduction of corrosion and decay potential of metal components in concrete. But the presence of bacterial spores and nutrients having calcium lactate are not enough to activate the process of calcium carbonate mineralization [61]. The process begins when hardening concrete removes microscopic cracks and leaking water enters the micro-cracks and reaches bacteria. Under such conditions, the mineralization of calcium carbonate and the self-healing of concrete begins and within a few days to a few weeks micro-cracks will be closed with a calcium carbonate gel precipitation, and a few months later the carbonate gel will harden and concrete will regain its lost resistance. In addition, since the calcium carbonate gel precipitation in the micro-cracks, leaking water cannot penetrate concrete anymore and metal

components in concrete become more resistant, and Bio concrete becomes more lasting.

Bacterial stimulated calcium carbonate precipitation is a recommended alternative to other cracks repair methods, because it is environment friendly.Types of bacteria,such as Baciluss Sphaericus, Bacillus Cohnii, Bacillus Pasteurii, Bacillus Lentus, Bacillus Sphaericus and Ureolytic, are capable to produce calcium carbonate precipitation [63].

Gollapudi et al. (1995) are the first scientists who introduced the biological method of cracks repair and its compatibility with the environment. Bacterial precipitation CaCO3 is governed by several factors: concentration dissolved inorganic carbon pH, calcium ions concentration and availability of nucleation sites [36]. The three mentioned factors are created through bacterial metabolism when the cellular membranes of the bacterium operate as a nucleation site [44].The only problem is that the bacterial cells cannot be added directly to the cement samples and, on the other hand, they decrease in the pH above 12 in concrete. Jonkers et al. showed that bacteria do not survive due to the decrease of cement diameter during hydration [15]. In this method bacteria produce urea, that catalyzes urea hydrolysis to ammonium and carbonate (CO_3^{-2}), and the reactions are as follows: First, one mole of urea is hydrolyzed into an intracellular mole of carbonate and one ammonium mole. Simultaneously, carbonate is hydrolyzed to create another mole of ammonium and carbonic acid. Then creates one mole of bicarbonate and 2 moles of ammonium

along with hydroxide ions. The final reaction happens to increase the pH, which provides the balance of the bicarbonate, and at the end produces carbonate ions [64].

1.11 Microbiologically induced calcium carbonate precipitation (MICP)

Microbiologically induced calcium carbonate precipitation (MICP) is a novel technique which to some extent has contributed to the decrease in porosity of concrete structures, as well as has offered higher strength, improved durability, good resistance to corrosion and has reduced water permeability. MICP is a bio-geochemical process that induces calcium carbonate precipitation within the concrete matrix. It comes under a broader category of science called bio mineralization. Bio mineralization is defined as a biologically induced precipitation in which an organism creates a local microenvironment, with conditions that allow optimal extracellular chemical precipitation of mineral [55]. Use of this bio mineralogy concept leads to the potential invention of new material "bacterial concrete" an inherent and self repairing biomaterial that can remediate the cracks and fissures in concrete. Microbiologically-induced $CaCO_3$ precipitation results from a series of complex biochemical reactions described below [39]. The microbial urease enzyme catalyzes the hydrolysis of urea into ammonium and carbonate (1), Due to presence of ammonia the pH of the surrounding increases.

$$CO(NH_2)_2 + H_2O \text{ ---> } NH_2COOH + NH_3 \qquad (1)$$

The compound formed then spontaneously hydrolyses into ammonia and carbonic acid that leads to the formation of bicarbonate and hydroxyl ions (2)(3)(4).

$NH_2COOH + H_2O \dashrightarrow NH_3 + H_2CO_3$ (2)

$2NH_3 + 2H_2O \dashrightarrow 2NH^+_4 + 2OH^-$ (3)

$H_2CO_3 \dashrightarrow HCO_3 + H^+$ (4)

The production of hydroxide ions results in the increase of pH, which in turn can shift the bicarbonate equilibrium, resulting in the formation of carbonate ions (5)

$HCO_3 + H^+ + 2NH^+_4 + 2OH^- \dashrightarrow CO_3^{-2} + 2NH^+_4 + 2H_2O$ (5)

The produced carbonate ions precipitate in the presence of calcium ions as calcium carbonate crystals (6).

$Ca^{+2} + CO_3^{-2} \dashrightarrow CaCO_3 \downarrow$ (6)

The formation of a monolayer of calcite further increases the affinity of the bacteria, resulting in the production of multiple layers of calcite.

1.12 Thesis Layout

The thesis is divided into ten chapters that are composed of Chapter 1 (Introduction), Chapter 2 (Literature Review), Chapter 3 (Research Objectives), Chapter 4 (Materials and Mix Proportions), Chapter 5 (Characterizations of Bacteria), Chapter 6 (Mechanical Properties), Chapter 7 (Performance Evaluation), Chapter 8 (Crack healing Efficiency), Chapter 9 (Cost Analysis) and finally Summary of Conclusions.

The descriptions for each chapter are as follows:

Chapter 1 demonstrates the general background of the study and thesis layout are also reported in this chapter.

Chapter 2 expresses a concise review of literature on bacterial concrete, bacterial effect on concrete strength and durability, and eventually micro-structural investigation on bacterial concrete.

Chapter 3 mentions the problem statements, research aim and objectives, scope of the study, and significance of research.

Chapter 4 presents all the materials used and mix proportions of M20 and M40 grades fly ash based bacterial concretes.

Chapter 5 characterizes the calcium carbonate precipitate in concrete.

Chapter 6 presents the mechanical properties of M20 and M40 grade fly ash aggregate based bacterial concretes and flexural behavior of fly ash aggregate based bacterial concrete beams.

Chapter 7 presents performance of M20 and M40 grade fly ash aggregate based bacterial concretes in terms of pore structure analysis using BET Nitrogen (N2) Adsorption method, permeation properties, and corrosion resistance capacities.

Chapter 8 presents the efficacy of microbiologically motivated crack healing in terms of strength recovery and enhancement of surface impermeability.

Chapter 9 estimates the costs involved in developing the M20 and M40 grade fly ash aggregate based bacterial concretes

Chapter 10 presents the conclusions drawn from the experimental investigations.

1.13 Summary

To sum up, self-healing concrete technology has proved to be better than many conventional technologies because of its eco- friendly nature, self-healing abilities and increase in durability of structure. Various researchers have successfully improved our understanding of the possibilities and limitations of biotechnological applications on building materials. Enhancement of compressive strength, reduction in permeability, water absorption, and reduced reinforcement corrosion have been seen in various cementations and stone materials. Formation of cementation by this method is very easy and convenient for usage. This will provide the basis for high-quality concrete structures that will be cost-effective and environmentally safe. However, more research work is required to be done to improve the feasibility of this technology from both economical as well as scalable practical view point.

Chapter-2

LITERATURE REVIEW

2.1 General

Bio-influenced self-healing concrete is expected to be a viable solution to the environmental concerns of carbon dioxide production by cement industries as well as durability of concrete structures. Due to these advantages it has been the focus of several research works and studies during the past few years. This chapter contains notable studies carried out on bio-influenced self-healing concrete. These research works have taken into account different variables contributing towards self-healing of concrete. Some of these variables are type of bacteria, pre-cursor compound and techniques used for incorporation of bacteria.

2.2 Bio-mineralization

The bio-mineralization process consists of the biological synthesis of minerals by microorganisms. In nature, bio-mineralization processes are widespread in different environments and they involve microorganisms of different taxonomies and with diverse metabolic pathways. Carbonates, phosphates, silicates, sulfates, sulfides, oxides, or hydroxides along with a variety of cations such as Ca^{2+}, Fe, Mg^{2+}, and MnO_2 form bio-minerals through microbial activity [1]. The process also involves organic macromolecules such as proteins, polysaccharides, glycoproteins, and proteoglycans, which function as skeletal support [6]. Bio-mineralization

is divided into three mechanisms: Biologically Controlled Mineralization (BCM), Biologically Induced Mineralization (BIM), and Biologically Mediated Mineralization (BMM) [8]. In BCM, the metabolic activity of the microorganism controls nucleation, composition, localization, and the morphology of bio-minerals. This mechanism could be an extracellular (BCMe), intracellular (BCMin) and an intercellular (BCMint) process with the participation of organic macromolecules exopolysaccharides (EPS) or vesicles. The importance of the regulation of genes on structure, composition, and intrinsic specific morphology of bio-minerals has also been mentioned previously [22].

In Biologically Induced Mineralization (BIM), minerals are precipitated indirectly due to the interactions between metabolic byproducts of microorganisms and ions present in the environment. However, the participation of microbial cells in composition, localization, and nucleation of minerals is limited. The minerals generated by BIM are characterized by their wide range in size of particulates, poor crystallinity, and morphology (Weiner and Dove, 2003) [9].

In Biologically Mediated Mineralization (BMM), mineral formation is the result of an interaction between an organic matrix and organic and/or inorganic compounds without the necessity of extracellular or intracellular biological activity. Dupraz et al. [25] excluded BIM and BMM from the bio-mineralization process and introduced a term organo-mineralization process for these mechanisms. The most abundant bio-minerals and

organo-minerals contain calcium as the principal ion due to its participation in several fundamental processes in the cellular metabolism of organisms. Calcium-bearing minerals comprise 50% of the total of biominerals and organominerals formed and calcium carbonate is one of the most abundant minerals on earth, comprising 4% in weight of the earth's crusts. The precipitation of $CaCO_3$ is a common phenomenon in marine waters, sediments, freshwater, soils and other environments, and this mechanism is known as the microbial precipitation of calcium carbonate (MCP) [29]. MCP can occur either actively or passively. BIM (active) known as Microbially Induced $CaCO_3$ Precipitation (MICP) and or passively BMM (passive) occurs through the interaction of the organic matrix (EPS) and calcium ions without the necessity of direct biological activity. In BMM, functional groups such as carboxylic acids (R-COOH), hydroxyl groups (R–OH), amino groups (R–NH2), sulfate- (R–O–SO_3H), and sulfhydryl groups (–SH), deprotonate due to an increase in pH, which results in an overall negative charge of extrapolysaccharides produced by the cell which facilitates its binding to metal ions [31].

2.3 Microbially Induced Calcium Carbonate Precipitation (MICP)

In MICP, calcium carbonate mineral formation is the result of the interaction among different metabolic byproducts, *viz.*, (HCO_3^-) and calcium ions present in the microenvironment [8] [48]. Though, it has been reported that MICP occurs only through extracellular means, several studies showed intracellular precipitation of calcium carbonates in

cyanobacteria [66][67][68]. Head et al. (2000) [67] reported that oxaliferum precipitates calcite crystals through intracellular means. They observed that more than 70% of the total volume of cells size is occupied by intracellular inclusions of calcium carbonate crystals, surrounded by membranes without vesicles formation. More recently, Xu et al. (2019) reported the calcite and aragonite precipitation through virus induced lysis of cyanobacteria cells and suggested that this new mechanism is expanding the calcium carbonate bio-mineralization process [115].

MICP has been reported as part of numerous biotechnological applications such as remediation of soil and water contaminated by heavy metals, metalloids and cations (Ca^{2+}) [80][91], in soil bio-consolidation [84], in CO_2 bio-sequestration [116], and in self-healing concrete (bioconcrete) [78][90][91][117].

2.4 Bio-concrète

Adolphe et al. (1990) are the pioneers of the incorporation of MICP for the restauration of surfaces of ornamental stone [64]. They obtained the patent for the MICP technique known as “bio-concept of calcite or bio-deposition,” and this patent was expired in 2010. Nowadays, this biomaterial is known as bio-concrete. Bio-concrete can be defined as the concrete prepared through the addition of bacteria with the capacity for precipitation of calcium carbonate (MICP), and aids in sealing the cracks that appear in it, which is characterized as a self-healing property (Jonkers, 2011)[72]. Thus, bio-concrete is considered as one of the most environmentally-

friendly and economic technologies since CO_2 emissions and the cost of maintenance and repair could be minimized. Bio-concrete has three constituents: microorganisms capable of MICP, nutrients and calcium ions which form cementitious materials [71]. Bio-concrete is gaining attention due to its self-healing feature and improvement of mechanical and durability properties of concrete structures. Several studies reported self-healing of cracks of (<0.5 mm) by Bacillus cohnii, B. pseudofirmus, B. subtilis, B. alkalinitrilicus, Pseudomonas aeruginosa, and Diaphorobacter nitroreducens [72][117]. Several studies have also been conducted in the restauration of historic monuments such as Thouars church tower [31.

In last two decades, there are various studies on the different implementation strategies, to enhance the performance of bioconcrete through the protection of cells such as the addition of nutrient sources and different materials e.g., polyurethane, sol-gel ceramics, calcium sulphoaluminate cement, and magnetic iron oxide nanoparticle (IONS). These methods can benefit the bacteria to survive under harsh concrete matrix conditions such as a high pH (~13.5), limitation of nutrient and water ingress. Bang et al. (2001) [29] incorporated Sporosarcina pasteurii immobilized on polyurethane, which increased compressive strength by 12%. It has also been reported that the addition of lactate in the concrete matrix increases compressive strength in a range of 10–17% over control. Chen et al. [80] showed an increment of compressive strength of 56–72% by immobilization of Bacillus mucilaginous L3 and Brewer's yeast JCS 05

C4 on ceramsite with sucrose and yeast extract as the nutrient sources. Wang et al. [54][117] employed microcapsules of spores enriched with urea, yeast extract, and calcium nitrate, and observed a 40% decrease in water permeability; however, compressive strength was reduced by 34%. However, Xu and Yang [115] reported that when encapsulating bacteria in low alkali and fast hardening cementitious material, calcium sulphoaluminate cement increased the regain ratio of the compressive strength and water tightness by 84 and 50%, respectively, but the ureolytic activity was found to be lower in encapsulated spores than in the free spores. It can be concluded that the success of a microencapsulation strategy depends on the compatibility of the material used for the capsule as well its size and distribution through the concrete matrix. Despite the fact that microencapsulation could affect mechanical properties like compressive strength, in some cases it is found to improve water tightness and aids in the activity of bacteria for a long period (120–150 days). Later, Seifan et al. [108] evaluated the potential of magnetic iron oxide nanoparticles' (IONs) addition in concrete mixtures, on growth and activity of bacterial cells. They observed that while 150 µg/ml of IONs significantly increased the growth of bacteria, 300 µg/ml of IONs achieved the maximum $CaCO_3$ precipitation of 34.54 g/l. More recently, Ruan et al. [106] reported higher curing of cracks by formation of hydrated magnesium carbonate (>150 µM) in comparison with MICP without addition of IONs. However, the use of these recent strategies involve a high

cost, for example €180 for 1 kg of nutrients to generate 13 L of bacterial culture and an equivalent production of 5.4×10^6 units of urease [91]. Earlier, to reduce the costs of nutrients added, Achal et al. [91] used industrial waste, such as Lactose Mother Liquor (LML) and Corn Steep Liquor (CSL) and obtained a 17% and 35% increase of compressive strength, respectively. Charpe et al. (2017) [83] observed a 23% increase of compressive strength through the use of lentil seeds as a protein source and sugar as a carbon source and demonstrated a reduction of the cost in comparison with use of peptone as a nutrient source. Later, Fang et al. (2019) [91] obtained 27.8% in compressive strength through the use of Tofu wastewater as a nutrient source. Zhang et al. (2017) [119] demonstrated the potential implementation of activated sludge microbial communities as an alternative source of bacteria and as well as an economic one for self-healing in concrete. They evaluated three microbial consortia under three conditions (aerobic, anaerobic, and facultative anaerobic) and observed that microbial consortia under aerobic conditions showed a more positive effect on inorganic carbon conversion (75.3 ± 3.8%), which was 1.2 ~ 1.8 times more than that of the conditions tested. Adzami et al. (2018) [77] evaluated the large-scale bio-production of calcium carbonate. They reported that agitation speed of 50 rpm and aeration rate of 2.0 vvm recorded the highest specific growth rate (0.141 h−1) of Bacillus sphaericus, which formed $CaCO_3$ crystals with 100% purity.

In the UK, the Resilient Materials for Life project led by Cardiff University in partnership with the universities of Cambridge, Bath and Bradford, have developed four self-healing techniques; the use of microcapsules containing mineral healing agents, bacterial healing, the use of a shape memory polymer based system for crack closure and the delivery of a mineral healing agent through a vascular flow network. They observed that all four techniques showed significant results of accelerated crack healing in the range of 14–28% and the Whole-Life Costing (WLC) analysis indicated a ~12% reduction in the cost of repairs and maintenance [85]. However, the microencapsulation technique did not show a significant effect on the compressive strength.

Adolphe et al. (1990) [64] were the pioneers in the incorporation of MICP for restoration of surfaces of ornamental stone. They obtained the patent for the MICP technique known as "bio-concept of calcite or bio-deposition," and this patent expired in 2010. Nowadays, this biomaterial is known as bio-concrete. Bio-concrete can be defined as the concrete prepared by addition of bacteria with the capacity for precipitation of calcium carbonate (MICP), which aids in sealing the cracks that form in it, which is characterized as a self-healing property (Jonkers, 2011)[72]. Bioconcrete has three constituents: microorganisms capable of MICP, nutrients and calcium ion to form cementitious materials. Several studies reported autogeneous healing in cracks of (<0.5 mm) by B. cohnii, Bacillus pseudofirmus, Bacillus subtilis, Bacillus alkalinitrilicus, Pseudomonas

aeruginosa, and Diaphorobacter nitroreducens [71][74][89]. In recent years, MICP has gained attention due to its self-healing properties, which is found to benefit the mechanical and durability properties of concrete. Further, it helps in reducing the negative impact on the environment in terms of CO_2 emissions by the construction sector and also lowers the cost of repairs of concrete structures in comparison to conventional methods. Moreover, the potential of a protein known as "Bio-remediase," which promotes bio-silicification has been reported. Bio-remediase is a silica leaching enzyme, and is 78% similar to bovine carbonic anhydrase II, but does not show carbonic anhydrase activity [92] [79]. Biswas et al. (2010) isolated Bioremediase protein from a novel bacterium BKH1 and reported an increase in compressive (>25%) and tensile (>20%) strengths by adding the enzyme powder to the concrete mixture [79]. However, self-healing of bioconcrete is not feasible with the addition of enzyme powder in comparison to the addition of cells which may extend the use and lifetime of bioconcrete by up to 200 years [72]. Bacteria have the ability to resist alkaline conditions by spore formation and reactivate their metabolic activity when water, CO_2, SO_4, and NO^{-}_3 and others substances ingress, due to the formation of cracks in the structure of concrete [109]. Majumdar et al. [79] showed 39.4% increment in compressive strength at 28-days cured samples and 42.4% at 120-days with a concentration of 10^5 cells of Bacterium BKH1. Interestingly, Alshalif et al. [78] genetically modified a spore forming Bacillus subtilis strain by incorporating the bioremediase

like protein gene. They observed that transformed bacterial cells survived for a long time within the cementitious environment and showed a ~16.6% increase in compressive strength and self-healed the cracks by formation of a novel Gehlenite (~85 nm diameter) along with calcite precipitation inside the mortar matrices. Later, Sarkar et al. (2019) showed an increase of >50% of compressive strength by addition of 10^4 cells.ml^{-1} of BKH4, an alkaliphilic bacterium isolated from Bakreshwar hot springs and tolerant to a pH of 12.

On the other hand, Ercole et al. [88] studied the metabolism of ureolytic Bacillus megaterium, B. pasteurii, and a non-ureolytic Bacillus cohnii in the absence of a substrate, nutrients and their effect on mechanical properties of concrete. They observed that in the absence of nutrient sources, bacteria used an alternate pathway and further, bacteria served as a heterogenous nucleation site, and induced the formation of calcite, and hydrated aluminosilicate phases like beidillite, gismondine. Formation of these crystals increased various mechanical properties of concrete, such as reduction in water absorption (~22%), volume of voids (~24%) and sulfate ion concentration (~26%) at 180 days [94].

Apart from the advantages discussed above, bioconcrete has also been reported to lower the contribution of carcinogens (one-thirtieth), ecotoxicity (one-tenth), and fossil fuels (six-sevenths) compared to traditional concrete (Gonsalves, 2011)[93]. However, the main

disadvantages are the generation of ammonia and the possibility of pathogens associated with urea hydrolysis that may harm the health of animals and humans [80]. It is predicted that real-scale production of bioconcrete based on urea hydrolisis could pollute more than 4.5×10^6 m^3 of drinking water and 100 km^3 of air. To combat this, Ivanov et al. (2019) [96] propose that MICP technology has to be combined with the proper ventilation of the biogrouting space, proper treatment of MICP effluent, and facilitation for the transformation of the ammonia containing gas to fertilizer. However, this would result in an increase in the cost of bioconcrete. However, alternate metabolic pathways, such as denitrification and sulfate reduction (Alshalif et al., 2016) [78], photosynthesis and methane oxidation (Okwadha and Li, 2011 [101]; Ersan et al., 2015 [89]; Zhu and Dittrich, 2016 [120]) also yielded promising results on MICP, but their environmental effects need to be researched further.

2.5 Microbial Metabolic Processes Involved in MICP

The major microbial metabolic processes involved in MICP are urea hydrolysis, ammonification of amino acids, denitrification, dissimilatory sulfate reduction and photosynthesis (Castanier et al., 1999 [82]; Dupraz et al., 2009 [87]). Among these metabolic pathways, urea hydrolysis is less complex (Achal et al. [8]) and urea hydrolytic strains showed more higher calcite precipitation (~20–80%) in comparison with other metabolic pathways and is therefore the most studied MICP process [91]

2.5.1 Urea Hydrolysis

A series of complex reactions in urea hydrolysis are driven by urease (EC 3.5.1.5) and carbonic anhydrase (EC 4.2.1.1) enzymes. One mole of urea is hydrolyzed by urease (UE) to one mole of ammonia and carbamate (Equation 1), and the carbamate is spontaneously hydrolyzed to produce one mole of ammonia and carbonic acid (Equation 2). Carbonic acid is converted to bicarbonate (Equation 3) by carbonic anhydrase (CA) and two moles of ammonium and hydroxide are formed due to ammonia hydrolysis (Equation 4). Consequently, pH is increased around the cell and induces precipitation of calcium carbonate in presence of soluble Ca^{2+} (Equations 5–7). Under unfavorable conditions, the cell survives by allowing the entry and accumulation of calcium ions, resulting in an excessive expulsion of protons. Subsequently, the cells actively export calcium and compensate the loss of protons. A low concentration of protons and a high concentration of Ca^{2+} in the microenvironment is required for secretion of carbonate ions while the supersaturation of carbonate induces precipitation of calcium carbonate on the surface of the cell. Exopolymers, biofilms and even inactive spores can provide nucleation sites for the above-mentioned reactions [115]. Earlier, Park and Hausinger (1995) [103] observed that activities of UE and CA are in synergy due to the incorporation of nickel in the active center of UE, which depends on the regulation of CO_2/HCO_3, a reaction catalyzed by CA.

$CO(NH_2)_2 + H_2 \rightarrow NH_2COOH + NH_3$ (1)

$NH_2\ COOH + H_2O \rightarrow NH_3 + H_2CO_3$ (2)

$H_2CO_3 \leftrightarrow HCO^-_3 + H^+$ (3)

$NH_3 + 2H_2O \rightarrow 2NH^+_4 + 2OH$ (4)

$HCO^-_3 + H^+ + 2NH^+_4 + 2OH \rightarrow CO^{2-}_3 + 2NH^+_4 + 2H_2O$ (5)

$Ca^{2+} + Cell \rightarrow Cell{-}Ca^{2+}$ (6)

$Cell{-}Ca^{2+} + CO_2{}^{-3} \rightarrow Cell{-}CaCO_3$ (7)

With respect to kinetics parameters (K_m and V_{max}) of UE and CA, a wide range have been reported. Stocks-Fischer et al. (1999) observed that pH influenced UE affinity to the substrate as well as the enzyme activity of Sporosarcina pasteurii. UE activity was found to be decreased at pH 7.0 and with K_m and V_{max} values of 41.6 mM and 3.55 mM min^{-1} mg^{-1} of protein, respectively. However, the affinity improved with pH increase, with a K_m of 26.2 mM and V_{max} of 1.72 mM min^{-1} mg^{-1} at pH of 8.3–9.0. Bachmeier et al. (2002) compared the urease activity of free and immobilized, recombinant Escherichia coli (HB101). Free suspended bacteria recorded a K_m and V_{max} of 17.3 mM and of 1.57mM min^{-1} mg^{-1}, respectively. On the other hand, polyurethane immobilized UE showed a K_m of 22.9 mM and V_{max} of 0.73 mM min−1 mg−1, which indicated that immobilized UE requires higher substrate concentrations than free cells.

This suggests that bacteria in bioconcrete conditions will be under stress because of a fault in adequate substrate concentrations for their activity. Similarly, Yadav et al. (2011) [118] reported that CA activity was five times lower in immobilized Single Enzyme Nanoparticles (SENs) than free CA activity. They observed that SENs showed a limitation of substrate transfer due to the presence of a hybrid layer between each carbonic anhydrase molecule and biopolymeric silica network. Achal et al. [91] characterized UE and CA from Bacillus megaterium, and confirmed the role of CA on UE activity and the importance of factors such as; the concentration of calcium ions, concentration of dissolved inorganic carbon, pH and availability of nucleation sites. Dhami et al. (2014) [86] highlighted the importance of the synergistic role of UE and CA in MICP formation. Apart from the precipitation of calcium carbonate, morphology of the formed crystals also play a significant role in their durability. Calcite, aragonite, and vaterite are some of the most representative biomineral polymorphs with different types of crystallization such as rhombohedral, orthorhombic, and hexagonal (Sarayu et al., 2014) [109]. Earlier, Achal et al. (2011) {8] reported that extracellular polymeric substances, biofilms, and amino acid residues have an impact on polymorphic nature of calcium carbonate biominerals. Sondi and Sondi (2005) demonstrated that interaction between Asp residues and UE molecules induce the formation of vaterite rather than calcite. Ercole et al. (2007) [16] showed that proteins present in organic matter regulate aragonite and vaterite precipitation in

Bacillus firmus and Bacillus sphaericus. In the case of Myxococcus sp., vaterite and calcite polyforms are more common precipitations [46].

2.5.2 Ammonification of Amino Acids

Another microbial mechanism is ammonification of amino acids, and in this process, microbial activity produces CO_2 and ammonia during metabolism of amino acids (Equation 8). Hydrolysis of ammonia produces ammonium and hydroxide ions around the cell (Equation 9), leading to their supersaturation, which consequently favors the precipitation of calcium carbonate (Equations 10, 11) (Zhu and Dittrich, 2016) [120].

$$\text{Amino acids} + O_2 \rightarrow NH_3 + CO_2 + H_2O \quad (8)$$

$$NH_3 + H_2O \rightarrow NH_4 + OH^- \quad (9)$$

$$CO_2 + OH \rightarrow HCO^{-3} \quad (10)$$

$$Ca^{2+} + HCO^{-3} \rightarrow CaCO_3 + H+ \quad (11)$$

Myxococcus xanthus is reported to use this mechanism during its growth in liquid and solid mediums and resulting in different polyforms [53]. Furthermore, it has been reported that Myxococcus xanthus precipitates uranium as meta-autunite (Turick and Berry, 2016) [114], which can protect concrete structures exposed to radioactive wastes.

2.5.3 Denitrification

In denitrification, MICP results from the oxidation of organic matter using NO_3^- as a final electron acceptor. The process produces NO_2, CO_2, and

OH−, (Equation 12) and the bacteria creates an alkaline microenvironment by the consumption of H+ in the presence of soluble calcium ions (Zhu and Dittrich, 2016) [120].

$$(CH_3COOH)_2Ca+NO^{3-}\rightarrow CaCO_3+N_2+3CO_2+3H_2O+OH \quad (12)$$

Ersan et al. (2015) [89] incorporated denitrifying and expanded clay particles immobilized Pseudomonas aeruginosa and Diaphorobacter nitroreducens and found that the addition closed micro cracks in the range of 200–250 µm size and the permeability was decreased by 42 and 47%, respectively. Ersan et al. (2018) [90] implemented special granules called "activated compact denitrifying core" (ACDC) and observed healing of cracks (>70%) larger than 400 µm. However, the denitrification process is inhibited by the accumulation of toxic byproducts generated such as nitrite and nitrous oxide. As mentioned previously, ureolysis showed more efficiency of calcium carbonate precipitation (<0.5 mm) than denitrification.

2.5.4 Dissimilatory Sulfate Reduction

In organic matter rich anaerobic environments, the presence of calcium induces the indirect formation of calcium carbonate minerals by sulfate-reducing bacteria (SRB) due to dissimilatory sulfate reduction process (Equation 13). It has been demonstrated that Desulfovibrio sp. has the ability to precipitate calcium carbonate through removal of sulfates from gypsum ($CaSO_4.H_2O$) by a combination of three mechanisms: dissolution, diffusion and calcium carbonate precipitation. Calcium ions released by

gypsum dissolution react with carbon dioxide (CO_2) under an alkaline pH microenvironment due to sulfide removal, which leads to calcium carbonate precipitation (Perito and Mastromei, [104]).

$$6CaSO_4+4H_2O+6CO_2 \rightarrow CaCO_3+4H_2S+2S+11O_2 \quad (13)$$

Recently Alshalif et al. (2016) [78] reported that the addition of sulfate-reducing bacteria in a concrete matrix increased the compressive strength of concrete by 13% and decreased water permeability by 8.5%. More recently, Tambunan et al. (2019) [113] reported an increase in compressive strength (60.87%) and flexural strength (52.30%) by adding SRB isolated from domestic acidic water. However, generation of H_2S can cause corrosion of the concrete structure, since H_2S reacts with oxygen to form elemental sulfur or a partially oxidized sulfur species, which are considered to be corrosion products of concrete surfaces (O'Connell et al., 2010) [100]. Few studies have showed improvement in calcium carbonate precipitation by association of SRB and cyanobacteria. Extracellular polymeric substances produced by cyanobacteria as heterogeneous nucleation sites, influence the diffusion barrier and calcium ions mobility, and improves the kinetics of precipitation by SRB [25]. Thus, microbial consortia of SRB and cyanobacteria appears to be potential candidates for application in bioconcrete technology, but requires more research on combining oxygen producing cyanobacteria with anaerobic SRB.

2.5.5 Photosynthesis

Apart from the above heterotrophic bacterial metabolic processes, the feasibility of MICP by autotrophic processes, such as photosynthesis and methane oxidation, have also been reported. Cyanobacteria and microalgae are the main photosynthetic microorganisms responsible for MICP in the aquatic environment. Calcium carbonate precipitation by photosynthetic microorganisms occurs due to HCO^{-}_{3} and CO_2^{-3} exchange (Equations 14, 15); HCO^{-}_{3} is diffused through the membrane and dissociates in cytosol of the cell into CO_2 and OH^- and this reaction is catalyzed by carbonic anhydrase (CA), leading to an increase of pH due to OH−generation, which along with calcium ions present in the microenvironment induces MICP (Equation 16) (Dhami et al., 2014) [86].

$$Ca^{2+}+2HCO^{-}_{3}\rightarrow CaCO_3+ CO_2+H_2O \quad (14)$$

$$Ca^{2+}+HCO^{-2}+OH-\rightarrow CaCO3+2H2O \quad (15)$$

$$2HCO^{-}_{2}\leftrightarrow CO_2+CO_2^{-3}+ H_2O \quad (16)$$

It should be mentioned however, that the application of photosynthetic microorganisms as agents of bioconcrete can be achieved only when structures are exposed to CO_2 and sunlight, which are principal components for photosynthesis process (Seifan et al., 2018) [110].

2.5.6 Methane Oxidation

In marine and freshwater sediments, the concentration of carbon dioxide is largely driven by methane oxidizing bacteria under both aerobic and

anoxic conditions. In aerobic conditions, this process is initiated with conversion of methane to methanol by methane mono-oxygenase activity in the presence of oxygen (Equation 17). In the periplasm of a cell, methanol (carbon source) is converted to formate through several enzymatic processes. Subsequently, when formate is in equilibrium with formic acid, methane mono-oxygenase oxidizes formic acid to C_{O2} by formate dehydrogenase activity (Equations 18–21). Carbon dioxide produced turns into CO_2^{-3}, and calcium carbonate is precipitated in presence of calcium ions (Equation 22) around the cells (Ersan, 2018)[90].

$$CH_4+O_2 \leftrightarrow CH_3OH+ H_2O \quad (17)$$

$$CH_3OH \rightarrow CHOH \quad (18)$$

$$CHOH+ H_2O \rightarrow HCOO^-+H+ \quad (19)$$

$$HCOO^-+ H_2O \leftrightarrow HCOOH+ OH^- \quad (20)$$

$$HCOOH \rightarrow CO_2 \quad (21)$$

$$Ca^{2+}+CO_2+ 2OH- \leftrightarrow CaCO_3+H_2O \quad (22)$$

Anaerobic methanotrophic bacteria too produces bicarbonate as a result of methane anaerobic oxidation, with sulfate as the final electron acceptor and in presence of calcium ions (Equations 23, 24) [110] [120].

$$CH_2^{-3} + H_2O \leftrightarrow HCO^{-3} \quad (23)$$

$$CH_4 + SO_2^{-4} \rightarrow HCO^{-3} + HS^- + H_2O \quad (24)$$

Recently, Caesar et al. (2019) [81] showed the potential of MICP in mitigation of methane release into the atmosphere due to anaerobic methane oxidation. However, there are no studies on the use of this mechanism in bioconcrete yet.

2.6 MICP in Concrete

Besides external application of bacteria in the case of remediation of cracks, microorganisms have also been applied in the concrete mixture. Until now, research has mainly focused on the consequences of this addition on the material properties of concrete, i.e. strength and durability. Both properties depend on the microstructure of the concrete.

Ramakrishnan et al. (2001) [27] [28] [29] studied the role of micro-organisms in remediation of cracks and their effect on compressive strength in mortar samples. Micro-organisms used in this research were Bacillus Pasteurii. For this purpose Portland cement mortar beams and beams of dimensions 25 x 25 x 150 mm and 50 x 50 x 50 mm respectively were made and 3.175 mm wide cracks with varying depths were produced. Cracks were filled with sand mixed with bacterial specimen of 3 x 10^8 cells/cm^3. Samples were placed in solutions of urea and $CaCl_2$ for 28 days. Compressive tests were performed to find out the compressive strength of samples. In addition to compressive tests, SEM and XRD tests were also

conducted to find out the crack healing efficiency of bacteria. Results showed that at lower concentrations B. Pasteurii increased the compressive strength of mortar sample. Microbiological remediation is more effective in shallow cracks as compared to deep cracks.

Ghosh et al. (2005) [40] studied the effect of anaerobic bacteria of Shewanella species and Escherichia Coli on the compressive strength of cement mortar. For this purpose mortar cubes specimens of 70.6 mm were studied. Different cell concentrations of both bacteria were used in these samples ranging from zero to 10^7 per ml. It was observed through results that Shewanella bacteria had a positive effect on compressive strength at a cell concentration of 10^5 per ml and increased compressive strength by 25%. However, by increasing its concentration further caused a decrease in compressive strength. On the other hand, addition of E.Coli bacteria had no significant effect on the compressive strength of mortar samples. In addition to compressive strength, SEM and MIP tests were also conducted on the samples. Results of these tests showed an improvement in pore size distribution at Shewanella cell concentration of 105 per ml. increase in compressive size was attributed to this improved pore size distribution in samples.

Jonkers et al. (2010) [55] studied the direct incorporation of bacteria along with nutrient compound in the concrete. Two different species of bacillus family were added (Bacillus Cohnii and Bacillus Pseudofirmus) in the concrete together with four different nutrient compounds including

calcium acetate, yeast, peptone and calcium lactate. Compression tests were conducted and results exhibited that calcium acetate and yeast lowered the strength of concrete to half to that of control specimen. Peptone addition resulted in complete detrimental effect on concrete. Only the incorporation of calcium lactate increased compressive strength of concrete in 28 days cured samples. Crack surfaces of both control and bacterial concrete samples was inspected and a difference was noted among them in 7 day cured samples but surfaces of both samples were not substantially different in 28 days cured samples. Copious amount of particles with size 20-80μm was found on crack surface of 7 days cured bacterial sample which was absent in 28 days cured samples. This along with results from most probable number (MPN) techniques proved that viability of bacterial spores decreases significantly over time.

De Belie and De Muynck (2008) [75] studied the effect of crack healing using bio deposition. Bacillus Sphaericus culture was used in this study. In order to study it standardized cracks of 0.3 mm were created by incorporating thin copper plates in concrete and pulling them out one day after casting or by performing split tensile tests on samples wrapped in fiber reinforced polymer. Cracked samples were cured in nutrient solution containing $CaCl_2$ or $Ca(NO_3)_2$. Bacteria were immobilized in silica gel and introduced in the concrete samples for protection. Visual inspection, ultrasound testing and water permeability tests were conducted. Visual inspection and ultrasound tests confirmed crack healing up to 0.3 mm in

width and 10 mm in depth. Water permeability tests showed that 0.6 mm wide cracks were healed through the process of bio deposition. In addition to that water permeability test also depicts that epoxy, BS+sol-gel+$CaCl_2$ and BS+sol-gel+$Ca(NO_3)_2$ were most efficient in reducing water permeability.

Van Tittelboom et al. (2010) [115] investigated the efficiency of bacteria to repair cracks in concrete in comparison with traditional crack repairing methods. During this study water permeability tests, ultrasound transmission measurements and visual examinations were conducted to determine the crack healing efficiency of various crack repairing techniques. Cracks were created by means of split tensile methods and by creating grooves using copper wire. Crack treatment with B.Sphaericus immobilized in silica gel showed increased ultrasonic pulse velocity. As it can be seen, bacterial solution incorporated in silica gel and treated with $CaCl_2$ had the least value of water permeability coefficient (K) and shows great reduction in water permeability as compared to untreated samples. In the same way, results for ultrasonic pulse velocity tests at the crack width of 10 mm show that maximum reduction in transmission time is observed in samples containing bacterial solution incorporated in silica gel and treated with $CaCl_2$. Through this increase in ultrasonic pulse velocity together with visual examination and water permeability tests, it was concluded that enhanced crack repair can be obtained by treating crack

with biological mix containing B.Sphaericus culture incorporated in silica gel along with calcium source.

Wang et al. (2012) [54] studied the possibility of using silica gel (SG) and polyurethane (PU) as a carrier for bacteria into the concrete mix. Bacteria used for this purpose was B.Sphaericus along with urea as the nutrient precursor compound. In order to identify the efficiency of bacteria, two different suspensions were prepared and incorporated with SG and PU. The bacterial suspensions containing bacteria in alive form were represented by "BS" and those containing dead bacteria were named "BSA". Bacteria together with nutrient and other compounds were encapsulated in glass tubes. When cracking occurred, glass tubes broke with it causing the encapsulate solution to release and heal the cracks.

It can be seen that specimen having bacteria incorporated in silica gel showed better conductivity as compared to those incorporated in polyurethane. Results showed calcium carbonate precipitation of 25% by mass in silica gel as compared to 10% by mass in polyurethane. Strength regain in case of silica gel was relatively low i.e. 5% as compared to 60% strength regain in polyurethane. Based on these conclusions polyurethane was nominated a better option as bacterial carrier.

Wiktor and Jonkers (2011) [72] carried out tests on cement mortar samples. During their research study bacteria were made inactive by heating them at 80°C for 30 minutes. Bacteria along with nutrient precursor were protected by infusing them in light weight aggregates

(LWA). Reinforced mortar specimen were made by using ordinary Portland cement, fine aggregate and LWA either soaked with bacteria and calcium lactate in case of bacterial specimen or non-impregnated in case of control specimen. After 56 days of curing, cracks were created and were re-cured. In the light of observations made by them, they concluded that width of completely healed cracks was more than double in bacterial specimen (46 mm) as compared to that in control specimen (18 mm).

Sierra-Beltran and Jonkers (2012) [71] discussed the effect and use of bio-based mortar for concrete repair. Initially, in this research four different types of ECC minerals were studied and depending upon their drying shrinkage and mechanical properties two of them were selected for further testing as bio based mortar. In these selected two material fillers, either sand or limestone was replaced with LWA having bacteria on them. Calcium lactate was used as nutrient precursor compound. The incorporation of healing agent had a negative impact on flexural strength and deflection but caused increase in compressive strength. However, all the test results exhibited that mortars having self-healing agent lied in the acceptable limit described in European standard EN 1504-3.

Wang et al. (2017) [119] conducted research study on self-healing efficiency of microencapsulated bacteria. During this study B.Sphaericus was used as a healing agent. Six different series of samples were prepared containing control specimen, specimens containing nutrients, with microcapsules, having both microcapsules and nutrients, containing

nutrients and 3% microencapsulated bacterial spores (NCS3%) and containing nutrients and 5% microencapsulated bacterial spores (NCS5%). Cracks were produced in these specimens and after that five different incubation techniques were used to check role of water in self-healing process. These incubation techniques included placing specimen in air conditioned room, immersion in water, immersion in deposition medium, wet-dry cycles with water and wet-dry cycles with deposition medium.

Observation were made 56 days after cracking, it was concluded that specimen in series NCS3% showed maximum crack healing while those of NCS5% gave lowest water permeability results because of the reason that greater amount of inert microencapsulation caused water-proofing effect and didn't allow contact of bacteria with water, hence decreasing self-healing ration and permeability. While observing effect of incubation techniques it was evident that wet dry cycle with water was the most effective technique as during wet cycle specimen absorbed water and during dry cycle it got more oxygen from atmosphere.

In addition to type of bacteria, selection of carrier is also a matter of great significance. When it comes to strength of concrete and viability of bacteria, carrier material is an important factor in the manufacturing of self-healing concrete Therefore, studies related to the carrier materials are also presented.

Gadea et al. (2010) [70] studied the use of polyurethane foam wastes (PFW) in making lightweight cement based mortar. During his research he grounded the PFW to the size less them 4 mm and gradually replaced fine aggregate with grounded PFW. Two types of cement were used in this study i.e. Cem I 42.5 R and Cem IV 42.5 N. mechanical properties including workability, permeability and strength were checked for each replacement level. It was found that inclusion of PFW increases the workability of mix and at the replacement level of 100% it increases the workability of mix by 120 min. on the other hand, effect of PFW on the flexural and compressive strength of mix at various checking days was devastating.

Sixuan (2012) [69] studied the possibility of using graphite nano platelets (GNP) in cement based construction materials. During his study, GNP particles were added in the cement mix and both mechanical and electrical properties of cement mix were studied. To study the compressive and flexural strength of cement mix two different kind of samples were made. 50 x 50 x 50 mm cubes were made to study the compressive strength of mortar and 40 x 40 x 160 mm prisms were made to study the flexural properties. During this experimental work it was found that increasing the amount of GNP in mortar has a better effect on the compressive and flexural properties of mortar. Three different percentages of 0.5, 1 and 1.5% were used. It was seen that mix with 1.5 % GNP had maximum compressive strength where mix with 1% GNP had maximum flexural

strength and flexural strength started to decrease when percentage was increased to 1.5%.

2.7 Summary

A review of previous studies on self-healing techniques has been presented. It is seen that quite limited type of bacteria and carrier compounds have been used in the previous studies. The purpose of this research is to collect sufficient data on the efficiency of Bacillus Subtilis and use of graphite nano platelets to check the possibility of an alternate bacteria and carrier compound for self-healing studies that can lead to most conducive and favourable outcome in self-healing of concrete.

Chapter-3

RESEARCH OBJECTIVES

3.1 General

The notion of self-healing concrete that can repair itself without human intervention seems to be the substance of science fiction till now but research conducted at JNTU Hyderabad on bacteria incorporated concrete apprehends the potential of this new field of bio-inspired self-repair innovation. The cracks and fissures in all concrete structures not only affect its aesthetics but also its strength and durability performance. Research has indicated that a concrete which is low in permeation properties lasts longer without exhibiting any signs of distress and deterioration. The deterioration of concrete structures usually involves the transport of aggressive substances from the surrounding environment followed by physical and chemical actions in its internal structure. The seepage of aggressive gases and liquids into concrete depends on its permeation characteristics. Therefore, permeation of concrete is one of the most significant parameters which governs the concrete durability in aggressive environments. Available literature has not reported any suitable self-healing system which has features such as long-term compatibility, eco-friendliness, good bonding with surrounding cement matrix, less human intervention, inexpensive and organic in nature.

3.2 Problem Statement

In recent times, it is discovered that bacterial calcite precipitation from biological activities of bacteria can enhance the overall behaviour of concrete. The urease enzyme existent in bacteria, breaks down urea by water to produce carbonate and in attendance of a calcium origin, calcite is voluntarily precipitated under these situations. Recent research has shown that specific species of bacteria can actually be useful to fill the concrete pores automatically by calcite precipitation as a result of microbial activities.

This new technique significantly reduce the bacterial concrete maintenance costs due to its service life span growth and subsequently will reduce the CO2 emission to atmosphere to help global warming partially by reduction of cement demand. Hence, in order to obtain more ability to realize the effects of bacteria in concrete, investigation on its characteristics is necessary.

It was an eminent fact that concrete structures are extremely susceptible to microcracking which allows water, gases and other potential harmful liquids enter and degrade the concrete, reducing the performance of the structure in terms of strength and durability aspects. To defeat this disadvantage it requires expensive continuous maintenance in the form of micro crack repairs. When these microcracks propagate further deep, not only the concrete itself will be damaged, but also leads to corrosion in the

steel reinforced concrete structures. Microcracks are therefore the major cause in reducing the durability of concrete structures. There are many crack repair techniques available to surmount this problem but each technique has its own advantages and disadvantages. Methods currently used for crack remediation often use synthetic polymers which are expensive, incompatible, doubtful long-term performance, needs skilled human assistance and aesthetically unpleasant (especially in repairing historic monuments) most importantly these methods are not environment friendly and are very expensive. The idea of self–crack healing mechanism in concrete is developed to circumvent the above stated disadvantages. One such alternative crack-repair mechanism is application of biominerilization of bacteria to seal and heal cracks in concrete. Synthetic polymers such as epoxy treatment etc, at present being used for repair of concrete, are harmful to the environment; therefore the use of a biological repair technique in concrete was focused upon. The principle of self crack healing mechanism is that certain kinds of healing agents will be released from the concrete when cracks occur. Every repair method follows the procedure of detection, monitoring and repair of cracks but in the self crack healing method the procedure of detection, monitoring and repair is autogeneous throughout the structure's life-cycle thus reducing the repair maintenance significantly. Repairs can be particularly time consuming and expensive because it is often very difficult to gain access to the structure to make repairs, especially if they are underground or at a great

height. Currently available concrete repair systems are largely based on environmental unfriendly material systems. So research is focused on the biotechnology based crack remediation in concrete to study the crack healing process of concrete with less or no human intervention and also examine the effect of biogenic calcite precipitation on the mechanical and durability aspects of concrete structures.

3.3 Research Significance

In reaction to the replacing of concrete progress, the prosperity of this study will be useful for the construction industry by using bacterial concrete towards green construction materials. This research describes a novel technique using living microorganism which investigates the process of ureolytic bacteria isolation to introduce in concrete to improve its characteristics by calcite precipitation. Moreover, this research provides a novel alternative material such as use of fly ash based artificial aggregate in concrete. In this research effect of biotic and abiotic factors are studied on the bacterial activity and their impact on the mechanical and durability properties of bacterial concrete made with fly ash based artificial coarse aggregate. Crack healing efficiency is evaluated.

In the recent past, investigations attempted to study about the application of biomineralization in civil engineering. As a part of those studies, researchers around the world started working on the use of specific bacteria in cementitious materials to self-heal and seal cracks without

human intervention. Available literature has not reported any such suitable self-healing system which has features such as long-term compatibility, eco-friendliness, good bonding with surrounding cement matrix, less human intervention, inexpensive and organic in nature. Though it is reported that the use of specific alkaliphilic mineral forming bacteria enhances the properties of cement mortar but there exists little understanding of the effect of bacteria on the mechanical and durability properties of concrete. In the present research work, studies related to characterization of mineral precipitation, permeation properties, resistance to aggressive environment, resistance to corrosion, behaviour at elevated temperature etc of bacteria incorporated concrete has been reported.

3.4 Gaps in the Literature

Not much work has been reported on the use of microorganism *Sporosarcina pasteurii*, and its calcite mineral precipitation efficiency using the nitrogen cycle as its microbial pathway in enhancing the mechanical and durability characteristics of different grades of concrete made with fly ash based artificial aggregate for Indian conditions. An exhaustive comparative study of mechanical and durability characteristics of ordinary grade (M20), standard grade (M40) concrete with and without addition of bacteria *Sporosarcina pasteurii* are made to understand the microstructure of bacteria incorporated concrete made with fly ash based

artificial aggregate at micro and macro level. Hence to address the gaps available in the research, investigations are planned to study the effect of calcite mineral producing bacteria *Sporosarcina pasteurii* on the microstructure of various grades of concrete and its impact on its mechanical and durability properties and its crack healing efficiency is evaluated. Once the gaps available in the literature are identified, the main research objectives of the present research work are outlined for obtaining detailed experimental data to address these gaps, which will help to understand the crack healing efficiency of bacteria incorporated concrete and its characteristics in terms of strength and durability aspects under Indian conditions.

3.5 Research Objectives

The overall aim of this research was to quantitatively understand and assess the role of microbiologically induced calcium carbonate precipitation in enhancing the mechanical and durability characteristics of concrete incorporated with *Sporosarcina pasteurii* and evaluate its crack healing efficiency. To achieve this aim the following objectives are framed:

1. To prepare fly ash based artificial coarse aggregates using cold bond technique and develop bacterial concrete made with treated fly ash based artificial coarse aggregates
2. To identify the appropriate bacteria with calcite precipitation capacity to introduce in structural concrete to enhance its properties

and to characterize the calcite precipitates in bacteria incorporated concrete using micro-scan observations

3. To establish the effect of appropriate concentration of bacteria on mechanical and durability aspects of concrete made with treated fly ash based artificial coarse aggregates
4. To investigate the crack healing efficiency of bacterially treated concrete specimens

The above objectives are outlined into detailed phases as shown:

Phase 1- Materials and Mix proportions

1. Physical and chemical properties of materials used
2. Preparation of fly ash based artificial coarse aggregates using cold bond technique.
3. Selection of suitable bacteria –its growth and culture
4. Determination of mix proportions for M20 and M40 grade concrete

Phase 2 - Optimization and Characterization of Bacteria

1. Optimum bacterial cell concentration for $CaCO_3$ Precipitation
2. Effect of biotic and abiotic factors on bacterial activity
3. Characterization of $CaCO_3$ precipitation using Scanning Electron Microscope (SEM), X-ray diffraction (XRD) , Thermo-gravimetric (TG) analyses and check for bacteria viability

Phase -3 Mechanical Properties

1. Determination of compressive, split-tensile and modulus of rupture of M20 and M40 grade bacterial concrete made with treated fly ash based artificial coarse aggregates
2. Quality Assessment of bacterial concrete by Non-Destructive methods
3. Evaluate the Stress-Strain Behavior of M20 and M40 grade bacterial concrete made with treated fly ash based artificial coarse aggregates
4. Modelling of Stress-Strain Behavior of M20 and M40 grade bacterial concrete made with treated fly ash based artificial coarse aggregates
5. Evaluation of Modulus of Elasticity and Toughness of M20 and M40 grade bacterial concrete made with treated fly ash based artificial coarse aggregates
6. Studies on Flexural Behavior of fly ash aggregate bacterial concrete reinforced beams and the parameters observed are first crack load, pre-cracking and post-cracking behavior, deflection pattern, crack development pattern and ultimate load carrying capacity of bacterial concrete beams.
7. Modelling of Flexural Behavior of fly ash aggregate bacterial concrete reinforced beams

Phase-4 Performance Evaluation

1. Pore Structure Analysis using BET Nitrogen (N2) Adsorption method concrete in terms of specific surface area, pore size distribution, and pore volume,
2. Determination of water permeability of M20 and M40 grades of bacteria incorporated concretes bacterial concrete made with treated fly ash based artificial coarse aggregates as per IS 3085 and DIN 1048.
3. Determination of water absorption capacity and porosity of M20 and M40 grades of bacteria incorporated concretes bacterial concrete made with treated fly ash based artificial coarse aggregates
4. Determination of Chloride Resistance of M20 and M40 grades of bacteria incorporated concretes bacterial concrete made with treated fly ash based artificial coarse aggregates using Rapid chloride penetration test expressed as the total electrical charge passed through the specimen, in coulombs.
5. Evaluation of Chloride ion diffusivity of M20 and M40 grades of bacteria incorporated concretes bacterial concrete made with treated fly ash based artificial coarse aggregates
6. Measurement of Resistivity and corrosion potentials of M20 and M40 grades of bacteria incorporated concretes bacterial concrete made with treated fly ash based artificial coarse aggregates

7. Determination of carbonation depth of M20 and M40 grades of bacteria incorporated concretes bacterial concrete made with treated fly ash based artificial coarse aggregates

Phase-5 Crack Healing Efficiency

1. To evaluate the efficiency of crack remediation technique using Sporosarcina pasteurii bacterial strain and determine the degree of strength regain in cracked concrete specimens.
2. Demonstrate the surface permeability of bacteria treated cement mortar specimen (immersed in Sporosarcina pasteurii bacterial strain suspension) and untreated cement mortar specimen (immersed in distilled water).
3. To assess the crack healing efficiency of fly ash aggregate concretes (FAAC) incorporated with Sporosarcina pasteurii bacterial strain using Ultrasonic pulse velocity measurements.
4. To evaluate the self-crack healing efficiency by assessing the water permeability of the microbially healed specimen
8. To evaluate the cost involved in the development of M20 and M40 grades of bacteria incorporated concretes bacterial concrete made with treated fly ash based artificial coarse aggregates

Chapter - 4

MATERIALS AND MIX PROPORTIONS

4.1 General

This chapter presents materials used and their properties and methodology for preparation of fly ash based artificial coarse aggregates and process of growing and culturing bacteria to be used in bacterial concrete along with the basic mix quantities required to prepare fly ash based bacterial concrete of grades M20 and M40.

4.2 Cement

Ordinary Portland cement of 53 Grade, conforming to IS: 12269-1987 was used in this investigation. The physical and chemical properties of Ordinary Portland cement (OPC) of 53 grade [IS: 12269-1987, Specifications for 53 Grade Ordinary Portland cement] tested in accordance with the IS: 12269 – 1987 and IS: 4031-1988 are tabulated in table 4.1

4.3 Indian standard sand (Ennore Sand)

Indian standard sand as per IS: 650-1991 is used to prepare cement mortar cubes. Now it is available at Ennore, Madras. Standard sand shall be of quartz material, free from silt and angular but a small percentage of flaky or rounded particle. All the particles of standard sand fall within the size range of 2 mm to 90 micron (Provided by Tamil Nadu minerals Limited) as shown in table 4.2 and 4.3

Table 4.1 - Physical and Chemical properties of Ordinary Portland Cement

Particulars	Requirement as per IS 12269-1987	Test Results Obtained
(A) Physical Properties		
1) Blaine's Fineness (Specific Surface)(m^2/kg)	225 (minimum)	330
2)Specific Gravity		3.13
3) Setting Time (in minutes) Initial Final	 30 (minimum) 600 (maximum)	 85 minutes 250 minutes
4)Soundness	10 mm (maximum)	2 mm
5) Compressive Strength 7 Days 28 Days	 37 MPa (minimum) 53 MPa (minimum)	 41.82 MPa 53.48 MPa
6) Average particle size		12µm
(B) Chemical Composition		
1) LSF CaO-$0.7SO_3/2.8SiO_2+1.2Al_2O_3+0.65Fe_2O_3$	0.8 to 1.02 (maximum)	0.90
2) Al_2O_3 / Fe_2O_3 (%)	0.66 (minimum)	1.20
3) Insoluble Residue (% by mass)	2.0	0.40 %
4) Magnesia (% by mass)	6 % (maximum)	1.40 %
5) Sulphuric Anhydrate (% by mass)	3 % (maximum)	2.20 %
6) Total Loss on Ignition (%)	4 % (maximum)	1.36 %
7) Total Chlorides (%)	0.05 (maximum)	0.012 %

Table 4.2 - Particle Size Distribution Of Standard Sand

Particle Size	Percentage
2 mm to 1 mm	33.33%
1 mm to 500 micron	33.33%
500 micron to 90 micron	33.33%

Table 4.3 - Physical and Chemical properties of Indian Standard sand

Physical properties	
Colour	Grayish White
Specific gravity	2.64
Absorption in 24 hours	0.80%
Shape of grains	Sub-angular
Chemical Properties	
Chemical analysis	
SiO2	99.30%
Al2O3	--
Fe2 O3	0.10%
CaO	--
Loss on extraction with hot HCI	0.11%
Loss on Ignition	-
Pertrographic analysis	
Quartz	97.40%
Feldspar	2.50%

4.4 Fine Aggregate

Locally available clean, well-graded, natural river sand having fineness modulus of 2.89 conforming to Zone II of IS 383-1970 was used as fine aggregate. In the present research work, locally available river sand conforming to Zone –II is adopted. Properties of river sand conforming to IS: 383 – 1970 and results of various tests conducted in accordance with IS: 2386 – 1963 are tabulated in table 4.4.

Table 4.4 - Physical properties of River Sand

S. No	Property	Fine Aggregate	Range as per IS: 383 -1970
1.	Specific gravity	2.55	2.30-2.90
2.	Bulk Density a) Loose b) Compacted	 1600 kg/m^3 1720 kg/m^3	1280-1920
3.	Bulking	6%	-
4.	Fineness Modulus	3.07	2.10-3.20
5.	Water absorption %	0.40 5	0-8
6.	Fines through 75µ, %	0.6	-

From Sieve analysis report, it is confirmed that River Sand used conform to Zone-II as suggested IS code of practice and is having a fine modulus of 2.88.

4.5 Mixing Water

Water used for mixing and curing is fresh potable water, conforming to IS: 3025 – 1986 and IS: 456 – 2000. Water used for mixing and curing is fresh potable water, conforming to IS: 3025 – 1986 and IS: 456 – 2000 and its properties are tabulated as table 4.5.

Table 4.5 - Properties of Water Sample

Parameter	Results	Limits as per IS 456 – 2000
pH	6.6	6.5 – 8.5
Chlorides (mg/l)	49	2000 (PCC) 500 (RCC)
Alkalinity (ml)	8	< 25
Sulphates (mg/l)	116	400
Fluorides (mg/l)	0.089	1.5
Organic Solids (mg/l)	53	200
Inorganic Solids (mg/l)	129	3000
Suspended matter (mg/l)	40	2000

4.6 Superplasticizer

Super plasticizer of Sulphonated Naphthalene Formaldehyde (SNF) based Conplast SP-430 was used as a water-reducing admixture. SP used is 0.6 % by weight of cement.

4.7 Natural Coarse Aggregate

Crushed granite angular aggregate of size 20 mm and 10 mm size from local source with specific gravity of 2.75 was used as coarse aggregate. Properties of coarse aggregate conforming to IS: 383 – 1970 and results of various tests conducted in accordance with IS: 2386 – 1963 are shown in table 4.6

Table 4.6 - Physical properties of Coarse aggregate

S. No	Property	Method	Coarse Aggregate
1.	Specific gravity	Pycnometer IS:2386 Part 3-1986	2.60
2.	Bulk Density (Loose) (Dense)	IS:2386 Part 3-1986	1390 kg/m^3 1560 kg/m^3
4.	Flakiness Index	(IS:2386 Part 2-1963)	2.41%
5.	Elongation Index	(IS:2386 Part 2-1963)	12.80%
6.	Fineness Modulus	Sieve Analysis (IS:2386 Part 2-1963)	7.19

Table 4.7 shows the sieve analysis of coarse aggregate, from which fineness modulus of coarse aggregate is found as 6.74. Size of the coarse aggregate used is 10mm

Table 4.7 - Sieve Analysis of Coarse Aggregate

The dry weight of aggregate = 5000 gm

Sieve size	Weight of material retained (gms)	% weight retained	Cumulative %weight retained	%weight passing
20mm	0	0	0	0
10mm	3700	74	74	26
4.75mm	1300	26	100	0
2.36mm	0	0	100	0
1.18mm	0	0	100	0
600µ	0	0	100	0
300µ	0	0	100	0
150µ	0	0	100	0

4.8 Artificial coarse aggregate – fly ash based

Fly ash, used in this investigation to make artificial coarse aggregate, was procured from Vijayawada Thermal Power Station, Andhra Pradesh, India. It conforms to grade I of IS: 3812 – 1981 [Specifications for fly ash for use as pozzolana and admixture]. It was tested in accordance with IS: 1727 – 1967 [Methods of test for pozzolana materials].The physical characteristics and chemical composition of fly ash used in the present investigation were given in table 4.8.

Table 4.8 – Physical and Chemical Composition of fly ash

(Source: Vijayawada Thermal Power Station, AP, India)

Characteristics	Result (%)	Requirements of IS:3812
Physical Properties		
Surface area m^2/kg	236	320
Specific Gravity	2.15	
Compressive strength at 28 days as percentage of strength of corresponding plain mortar cubes	86%	Not less than 80%
Chemical Properties		
Silica, SiO_2	60.9	35
Alumina Al_2O_3	31.01	-
Iron oxide Fe_2O_3	3.99	-
Lime CaO	0.70	-
Magnesia Mg O	1.50	5
Sulphar Trioxide SO_3	0.85	2.75
Na_2O	0.25	1.5
K_2O	0.91	-
TiO_2	1.95	
Loss on Ignition	0.20	12

The physical characteristics of fly ash based artificial coarse aggregate are tested in accordance with IS: 2386 – 1963 Parts I to VIII

4.8.1 Cold Bond technique

In the present study, Class 'F' fly ash is used along with alkaline activator solutions NaOH (optimum molarity) and Na_2SiO_3 for casting of mortar cubes of 70.6 mm x 70.6 mm x 70.6 mm size and tested for 28 days compressive strength. The optimum molar NaOH and Na_2SiO_3 proportion that yields the maximum strength when cured in oven for 24 hrs at 60°C after rest period of 24 hrs (Geo-polymerization), is utilized to make the fly

ash aggregate based bacterial concrete. Alkaline activators are mixed before 30 minutes of concrete making. Geo-polymerization process involves reaction between alumina-silicate oxides under alkaline conditions yielding polymetric Si-O-Al-O bonds. The normal consistency is found to be 35% for samples prepared with fly ash and cement in the ratio of 90:10, with various molarities of 8M, 10M, 12M, 14M and 16M NaOH and Na_2SiO_3 with SiO_2/Na_2O ratio= 2. The Na_2SiO_3/NaOH ratio is taken as 2.5 based on previous literature. Various mortar cubes are prepared with the above ingredients. It was found that 14M NaOH is the optimum molar at which maximum strength is achieved so this is used for further investigations.

To prepare fly ash aggregate, its dry mix quantities are calculates as shown below-

For 1 m^3 volume of paste mix, required quantities for the proportion of fly ash to cement as 90:10 with Na_2SiO_3 +NaOH to binder ratio as 0.35.

Specific gravity of fly ash and cement are 2.13 and 3.15. Density of water is 1 g/cm^3

1. Weight of fly ash = 0.90 x 2.13 g/cm^3 x 10^3= 1917 kg/m^3
2. Weight of cement= 0.10 x 3.15 g/cm^3x 10^3= 315 kg/m^3

Total Binder= 1917+315=2232 kg/m^3

Alkaline activator solution= 0.35 x 2232 = 781.2 kg/m^3

Na_2SiO_3/ NaOH= 2.5 i.e. Na_2SiO_3/ NaOH= 5/2

Na_2SiO_3 solution = 781.2 x 5/7 = 558 kg/m^3

NaOH solution = 781.2 x 2/7 = 223.2 kg/m^3

Calculation of NaOH flakes and water required for m^3 -

Molecular weight of NaOH=40 gm/mol. So for optimum 14M NaOH, flakes required are 14x40=560 gm for 1000ml of water (Solubility in water is 1110 gm/1000ml at 20°C). So to prepare 1000ml of NaOH solution dissolve 560 gm of NaOH flakes in 1000ml of water.

NaOH flakes/ Water= 560/1000=0.56

Sodium hydroxide solution = 0.56 x water + water = 1.56 x Weight of Water.

223.2 = 1.56 x Weight of Water

Therefore, weight of water required is 143 kg/m^3 to dissolve NaOH flakes of 80.2 kg/m^3

So quantity of NaOH= 80.2 kg/m^3

Quantity of Na_2SiO_3 = 80.2 x2.5= 200.5 kg/m^3

For 1 m^3 volume of dry mix, required quantities for the proportion of fly ash to cement is 90:10 are presented in table 4.9.

Table 4.9 - Quantities for 1 m^3 dry mix of paste

Material	Quantity (kg/m^3)	Proportions
Fly ash	1917	6.08
Cement	315	1
NaOH flakes	80.2	0.25
Na_2SiO_3	200.5	0.64

For the dry mix of fly ash and cement in the ratio of 90:10 as per weight and add alkaline activator solution and make paste. Now that paste is transferred to tray and compacted to required thickness of aggregate. Cut the compacted paste into required square size pellets and place in oven for 24 hrs at 60°C. After 24 hrs the hardened aggregates are kept in the mixer and rotate for 3-5 minutes then we obtained cubically angular shaped aggregates. Due to its high water absorption capacity of fly ash aggregates, these aggregates are treated (soaked) with bacterial solution before using in the concrete. In the present method of preparation of fly ash aggregates, cubical with angular shaped aggregates were obtained using cold bond technique but if pelletizing process is adopted, rounded aggregates will be obtained. These fly ash aggregates are tested for its suitability by conducting tests as per appropriate IS: 2386.

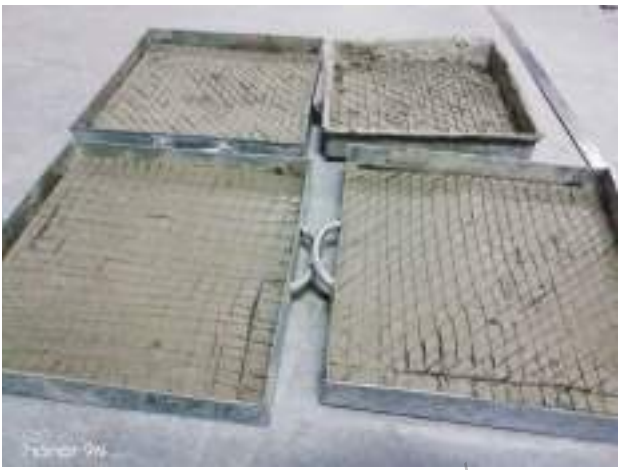

Figure 4.1 - Preparation of fly ash aggregates using cold bond technique

Figure 4.2 - Artificial coarse aggregate made with fly ash

Table 4.10 below presents the properties of the artificial coarse aggregate made with fly ash.

Table 4.10 - Properties of fly ash coarse aggregates

Test Conducted	Fly ash aggregates	Natural aggregates	Permissible limits		Property Of Aggregate
			For road pavements	For other structures	
Shape	Angular	Angular			
Bulk density (kg/ m3)	996	1675			
Size	12.5 to 20mm	12.5 to 20mm			
Fineness Modulus	7.5	7.1			
Specific gravity	1.84	2.55	2.5 to 2.9	2.5 to 2.9	Specific gravity
Aggregate crushing value	35.23%	27.51%	≤30%	≤45%	Crushing strength
Aggregate impact value	37.14%	27.94%	≤30%	≤45%	Toughness
Aggregate abrasion value	30%	26%	≤30%	≤50%	Wear and Tear
Water absorption (IS 2386- Part 3)	17.84% (Before Treatment) 0.4% (After Treatment)	0.6%	0.5 to 1%	1.0 to 2.0%	Porosity

4.9 Microorganism used - Sporosarcina pasteurii

Bacteria used is "*Sporosarcina pasteurii"* formerly known as *"Bacillus pasteurii"* which has an ability to precipitate calcite given a calcium source and urea through the process of MICP (microbiologically induced calcite precipitate). Bacillus pasteurizing is a gram-positive bacterium, with rod shaped cells that form chains-Medium-sized, smooth colonies with an entire margin. and also, Rod-shaped cells. Gram-variable, large, spore-forming rods with a diameter < 0.9µm. Catalase -positive. Lecithinase-negative. Does not attack sugars. Grow thing range of Temperature: 37˚C Optimum Temperature- 35-37˚C.

Pure culture of bacteria was obtained from NCIM-Pune, National Chemical Laboratory, in a slant cultured test tube, with nutrient agar.

Figure 4.3 - Slant culture of Sporosarcina pasteurii

Table 4.11 - Scientific classification of Bacillus pasteurii

Scientific classification	
Domain	Bacteria
Division	Firmicutes
Class	Bacilli
Order	Bacillales
Family	Planococcaceae
Genus	Sporosarcina
Species	Sporosarcina pasteurii

4.10 Nutrients

Nutrient broth: Added as food for bacteria while culturing.

It consists of

i. beef extract

ii. yeast extract

iii. peptone

iv. sodium chloride (NaCl)

Figure 4.4 - Nutrient broth in fine powdered form

4.10.1 Calcium carbonate ($CaCO_3$)

It acts as short-term calcium supplement for bacterial growth and crack healing. Calcium carbonate is a chemical compound with the formula $CaCO_3$. It is a common substance found in rocks as the minerals calcite and aragonite and is the main component of pearls and the shells of marine organisms, snails, and eggs.

Figure 4.5 - Calcium carbonate in fine white powder

4.10.2 Calcium lactate ($C_6H_{10}CaO_6$)

It is a white crystalline salt which forms several hydrates, most common being the pentahydrate. Calcium lactate can be prepared by the reaction of lactic acid with calcium carbonate or calcium hydroxide. Since the 19th century, the salt has been obtained industrially by fermentation of carbohydrates in the presence of calcium mineral sources such as calcium carbonate or calcium hydroxide.

Figure 4.6 -Calcium lactate in white or off-white powder form

Table 4.12 - Properties of calcium lactate

Chemical formula	$C_6H_{10}CaO_6$
Molar mass	218.22 g/mole
Appearance	white or off-white powder, slightly efflorescent
Density	1.494 g/cm^3
Melting point	240° (anhydrous) 120° (pentahydrate)
Acidity	6.0 – 8.5

Calcium lactate is added by 5% weight of cement to mortar to provide long term calcium supplement for bacterial activity.

4.11 Growth and Culture of Bacteria

Bacteria used in this study are "Sporosarcina pasteurii" which was previously known as Bacillus pasteurii that has a capability to precipitate calcite given a calcium supply through the process known as MICP (microbiologically induced calcite precipitate). Bacteria to culture is obtained from NCIM Pune National Chemical Laboratory, in a slant cultured test tube and maintained constantly on nutrient agar slants in the laboratory. To grow bacteria, a particular colony of the culture is inoculated or introduced into nutrient broth of 25 ml in a 100 ml conical flask and the growth environment are maintained at 37 ˚C temperature and placed in 125 rpm orbital shaker. Then obtained bacterial water is used in concrete at mixing phase to study its effect. Thirteen grams of nutrient broth is added to one litre of distilled water and stirred until a uniform mix is obtained. This solution (in properly plugged flasks) is kept in BOD incubator for 48 hours at a temperature of 37˚C. In aseptic medium, bacteria from the pure culture is scraped with sterilized loop (of diameter 5mm) is inoculated into the broth solution and mixed properly.

Two types of solutions were made in this study:

i. Bacterial solution without calcium supplement

ii. Bacterial solution with calcium supplement (where 5 grams of $CaCO_3$ is added along with nutrient broth).

Micro-organism must have a constant nutrient supply if they are to survive. Media may be liquid (broth) or solid(agar). Any desired nutrients

may be in corporate in to the broth (or) agar to grow bacteria. Organism grown in broth cultures causes' turbidity, (or) cloudiness, in the broth. On agar, masses of cells known as colonies, appear after a period of incubation certain separated on agar so that as the cell divines and produces a visible mass. The colony isolated from other colonies, isolated colonies are assumed to be pure culture. After introducing bacteria into media it is incubated in BOD incubator for 48 hours at 37 degrees temperature to gain required concentration of bacteria Cell concentration. Confirmation for bacterial growth is done if after incubation period the solution becomes turbid as shown below in figure 4.7 and 4.8

Figure 4.7 -Solution without $CaCO_3$

Figure 4.8 -Solution with $CaCO_3$

4.11.1 Cell Count

i. A cleaned Neubauer chamber and cover slip is taken and placed on flat surface. With pipette, 0.5 micro litre of uniformly mixed bacterial solution is drawn.

ii. The pipette tip is placed against the edge of the cover glass and liquid is slowly expelled into the chamber. Capillary action makes sure that the chamber is full.

iii. Neubauer chamber is placed under microscope and using 40X objective number of total cells are counted in entire 25 squares.

iv. A concentration of 500 cells was observed in 0.5 micro litre of bacterial solution. Which ultimately, provides a total concentration of 10^6 cells per 1 ml solution.

Figure 4.9 - Neubauer chamber

Figure 4.10 - Light microscope

4.11.2 Plating and CFU counting

In microbiology, a colony-forming unit (CFU) is a unit used to estimate the number of viable bacteria or fungal cells in a sample. Viable is defined as the ability to multiply via binary fission under the controlled conditions. Counting with colony-forming units requires culturing the microbes and counts only viable cells, in contrast with microscopic examination which

counts all cells, living or dead. The visual appearance of a colony in a cell culture requires significant growth, and when counting colonies, it is uncertain if the colony arose from one cell or a group of cells. Expressing results as colony-forming units reflects this uncertainty. It also helps in identifying if the prepared bacterial solution is contaminated or not, as the presence of any other organism or artefacts in solution would produce variant colony which is visible to naked eye.

4.11.3 Preparation of nutrient agar

50 ml of distilled water is taken in conical flask and 6.5g of nutrient broth, 1g of agar-agar is added and stirred well. Two petri plates with lids are taken. Plug the conical flasks with cotton to prevent contamination. Cover the cotton plugged conical flask and plates with newspaper separately to autoclave at 121° for 40 min approximately (autoclave machine takes 30 min to reach the desired temperature).

Figure 4.11 - Autoclave machine

After letting out steam, add the solution to petri plates equally and stay for few minutes to let it solidify. Place a drop of 0.005ml of bacterial solution with micro pipette and spread it into 3 lines and place the covered petal plates in incubator for 24 hrs. The growth of colonies for few bacterial cells cannot be counted on nutrient agar as it is pale in colour. So, blood agar medium is also used to clearly predict the presence of contamination, procedure being same. After 24 hours of incubation the samples are taken out and observed if growth is uneven or if different cell formation has happened.

Figure 4.12 - Colony growth in nutrient and blood agar petri plates

4.12 Mix Quantities and Proportions

Mix design can be defined as the process of selecting suitable ingredients of concrete such as cement, aggregates, water and determining their relative proportions in a range with the object of producing concrete of required minimum strength, workability and durability as economically as possible.

The grades of concrete used in the present study are M20 and M40 grades of concrete. The mix proportions of M20 and M40 grade concrete are designed using IS: 10262-2009. The mix proportions and materials required for one cubic meter of concrete for M20 and M40 grades of concrete are given below.

Ordinary Grade Concrete M20 Mix proportion 1: 2.27: 3.45: 0.54

Cement	Fine aggregate	Coarse aggregate	Water
320.4 kg	727.3 kg	1105.4 kg	173 L

Standard Grade Concrete (M40) Mix proportion 1: 1.47: 1.53: 0.35

Cement	Fine aggregate	Coarse aggregate	Water	Super plasticizer
390.7 kg	676 kg	1119.7 kg	164.1 L	2.5 kg

Two types of concrete mix of M20 and M40 grades i.e. one without bacteria and natural aggregate as coarse aggregate (reference sample) and one with bacteria and bio-treated fly ash aggregate as coarse aggregate (bacterial sample) were prepared for experimental investigations in the present research work. The mixes have similar proportions of sand, coarse aggregates, cement and water. However, the main difference was in the water component as bacterial and normal water will be used:

(1) Tap water is used for preparing reference concrete specimens made with natural aggregate as coarse aggregate and is without bacteria (for M20 and M40 grades)

(2) While *Sporosarcina pasteurii* bacterial suspension is used for preparing concrete specimens made with bio-treated fly ash aggregate as coarse aggregate (for M20 and M40 grades). For preparation of bacteria-nutrient suspension, optimum cell concentration of *Sporosarcina pasteurii* bacterial strain is grown in nutrient based distilled water in sterile conditions at biotechnology laboratory. The bacterial culture in suspension is added to fly ash aggregate concrete during concrete mixing process. Concrete shall be mixed in a mechanical mixer.

4.13 Workability

The slump values of ordinary (M20) and standard (M40) of conventional and bacteria incorporated concrete made with natural aggregate (NAC) and Fly ash aggregate (untreated and treated) are tabulated in table 4.13 below.

Table 4.13 – Slump values of M20 and M40 grades of concrete made with natural aggregate (NAC) and Fly ash aggregate bacterial concrete (FAABC)

Age of concrete	Slump (mm)
M20 Reference Concrete made with natural coarse aggregate (NAC)	128
M20 Bacterial Concrete made with untreated fly ash coarse aggregate	142
M20 Bacterial Concrete made with treated fly ash coarse aggregate (FAABC)	123
M40 Reference Concrete made with natural coarse aggregate (NAC)	100
M40 Bacterial Concrete made with untreated fly ash coarse aggregate	131
M40 Bacterial Concrete made with treated fly ash coarse aggregate (FAABC)	92

4.14 Summary

This section presents all the materials and their properties along with the mix quantities used to prepare bacterial concrete of M20 and M40 grades.

Page left blank intentionally

Chapter - 5

CHARACTERIZATION OF BACTERIA

5.1 General

This chapter characterizes the calcium carbonate precipitate in concrete. Characterization of bacteria includes determination of optimal cell concentration for enhanced performance of concrete along with identifying the calcite crystals are precipitated due to microbial activity alone not from other mechanisms in concrete.

5.2 Optimum bacterial cell concentration

This investigation was carried out primarily to understand the effect of bacterial cell concentration on the quantity of calcium carbonate precipitation. More bacteria with enough nutrients will precipitate more calcite in the laboratory conditions but in the cement-sand environment, bacteria mineral precipitating ability depends on its compatibility with cement-sand matrix. Bacteria incorporated into cement-sand medium should not affect the physio-chemical properties of cement-sand. Hence cell concentration of bacteria plays a key role in optimizing the performance of cementitious materials. The appropriate bacterial cell concentration for maximum calcium carbonate precipitation can be established by determining the 28 day compressive strengths of various cement-mortar specimens induced with different bacterial cell concentrations. The sample whose 28 day compressive strength was

highest determines the optimum cell concentration for high amount of crystalline calcite precipitation. Different cell concentrations were derived from the bacterial growth culture by serial dilution method.

Standard Cement-mortar cubes (70.6mm x 70.6mm x 70.6mm) incorporated with soil bacteria *Sporosarcina pasteurii* of different cell concentrations were cast, cured for 28 days and tested to study the compressive strength under axial compression as per IS 4031(Part 6)-2000. Various bacterial cell concentrations used are 10^3 cells/ml of mixing water, 10^4 cells/ml of mixing water, 10^5 cells/ml of mixing water, 10^6 cells/ml of mixing water and 10^7 cells/ml of mixing water. Reference control specimens (Cement-mortar cubes without bacteria) are also casted and tested for 28 day compressive strength.

Table 5.1 presents Compressive Strengths (MPa) of cement mortar specimens induced with various *Sporosarcina pasteurii* cell concentrations

Table 5.1- Compressive Strengths (MPa) of cement mortar specimens induced with various *Sporosarcina pasteurii* cell concentrations

Cell concentration/ml of mixing water	Average Compressive Strength (MPa) ± S.D	
	28 days	% Increase relative to control
Nil (Without Bacteria)	55.81±0.10	-
10^3	57.23±0.11	2.54
10^4	59.52±0.72	6.65
10^5	65.79±0.68	17.88
10^6	62.21±0.49	11.47
10^7	54.66±0.89	-2.06

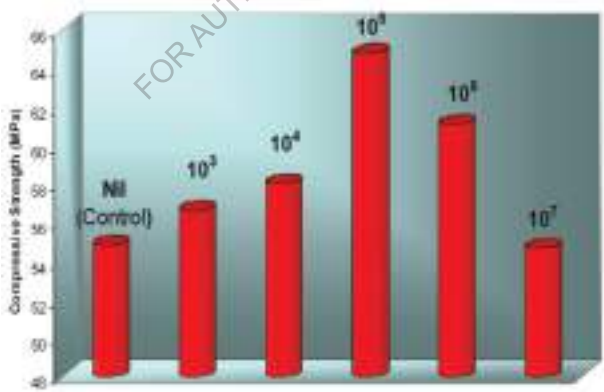

Figure 5.1- Effect of bacteria cell concentration on compressive strength

For cell concentration of 10^5 cells per ml of mixing water the 28 day compressive strength of bacteria incorporated cement mortar specimens is highest. This improvement in compressive strength was mainly due to metabolic deposition of $CaCO_3$ in the voids /or pores within cement–sand matrix modifying the pore structure of bacteria induced cement mortar specimens. During bacterial growth, the calcium precipitation process occurs continuously, clogging the internal pores with calcium precipitate. Fig above depicts the highest increase in compressive strength of cement mortar specimens incorporated with *Sporosarcina pasteurii* cell concentration of 10^5 cells per ml. The maximum percentage increase is found to be 17.88 % for 10^5 bacterial cells induced specimens. It is observed that for cement mortar specimens incorporated with *Bacillus subtilis* JC3 cell concentration of 10^7 cells per ml the compressive strength is reduced drastically. The gradual reduction of compressive strength of cement mortar cube specimens induced with bacterial cell concentrations more than 10^5 cells per ml of mixing water is attributed to the disruption of cement-mortar matrix integrity by the presence of organic matter (biomass) above the permissible limits as specified by IS 456. Maximum strength is observed for 10^5 cells/ml of mixing water so this is taken as optimum cell concentration to be used for further study to investigate the effect of bacteria on properties of concrete. Therefore, *Sporosarcina pasteurii* cell concentration of 10^5 cells/ml of mixing water generates the greatest reduction in porosity by precipitating calcite crystals optimally.

Reduction in pores due to such material precipitation (calcium carbonate) will eventually increase the concrete strength. Microbial calcite was precipitated on the surface of cells and eventually within the pores leading to their plugging which further lead to stoppage of flow of oxygen and nutrients to the cells. The cells either die or transformed into endospores that act as organic solid fibers.

5.3 Effect of biotic and abiotic factors on bacterial activity

This study enables us to understand the factors responsible for enhancement of strength and permeation properties in bacteria incorporated mortar specimens. The main significance of this study is to determine the strength enhancement in cement mortar specimens due to induction of bacteria. Bacteria precipitates minerals in the cement mortar during its metabolic activity by consuming nutrients and calcium supplements. Nutrients are used to culture bacteria into colonies or cells and calcium supplement is used to grow. During growth of bacteria calcium sources are consumed and calcite crystals are precipitated as a by-product of bio-mineralization. In the present study authors want to investigate the effect of nutrients and calcium sources on the biological process of precipitating calcite crystals and on subsequent increase in strength. It is also important to determine the microstructure of cement mortar specimens in terms of permeation properties to comprehend the durability of bacteria induced mortar specimens.

Various combinations of study are as follows:

1. Sample 1: Cement mortar specimen made with water
2. Sample 2: Cement mortar specimen made with (bacteria+ broth) solution
3. Sample 3: Cement mortar specimen made with (bacteria + broth) solution and calcium lactate
4. Sample 4: Cement mortar specimen made with (bacteria + broth + Ca supplement) solution
5. Sample 5: Cement mortar specimen made with (bacteria + broth + Ca supplement) solution and calcium lactate
6. Sample 6: Cement mortar specimen made with broth solution alone
7. Sample 7: Cement mortar specimen made with calcium lactate alone

Compressive strengths of above designated samples of cement mortar specimens are assessed to determine the role of bacteria and nutrients action in the strength improvement of cementitious materials and are presented below in Table 5.2 below

Table 5.2 - Compressive strengths of Samples considered

Sample compositions	Compressive strengths (MPa)			
	3 days	7 days	28 days	% increase
Sample A: Cement + Water	27.2	38.2	54.3	-
Sample B: Cement + (Bacteria + Nutrient broth) solution	30.1	40.8	56.2	3.5
Sample C: Cement + (Nutrient broth solution)	27.6	38.9	55.1	1.5
Sample D: Cement + (Bacteria + Nutrient broth + $CaCO_3$ supplement) solution	34.3	44.8	65.3	20.3
Sample E: Cement + (Bacteria + Broth) solution + Calcium lactate	**35.1**	**44.5**	**68.3**	**25.8**
Sample F: Cement + (Bacteria + Nutrient broth + $CaCO_3$ supplement) solution + Calcium lactate	35.9	45.8	68.4	25.9
Sample G: Cement + Calcium lactate	32.4	44.2	60.3	11.1

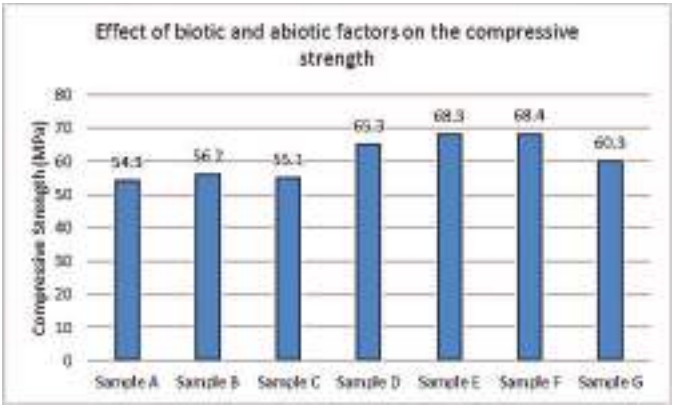

Figure 5.2 - Effect of biotic and abiotic factors on the compressive strength

Mortar samples made with bacteria, nutrients and calcium lactate yields maximum strength than any other samples. Calcium supplement in the nutrients is good enough for growth of bacteria and mineral precipitation for 28 days so calcium lactate is added by 5% weight of cement to mortar to provide long term calcium supplement for bacterial activity.

5.4 Water absorption and porosity

The total quantity of water absorbed is related to the total open porosity, while the kinetics of the process depends principally on the distribution of the pore sizes. This test also measures the capillary rise of water, the most common form of liquid water migration into cement mortar which is inversely proportional to the diameter of the pores. The smaller the diameter of the pores, the greater will be the capillary absorption.

Absorption is the capacity of a sample to hold water while capillary is the rate at which the water fills the sample.

Cement mortar cube samples of size 70.6 x 70.6 x 70.6 mm are casted and cured for 28 days for testing. Wash the samples in the de-ionized water before beginning this test in order to eliminate powdered material from the surface. Dry the samples in the oven for 24 hours at 60°C and record their weights. Repeat the drying process until the mass of each sample is constant, that is, until the difference between 2 successive measurements, at an interval of 24 hours, is no more than 0.1% of the mass of the sample. Once the samples have been completely dried and the constant mass is recorded (m_o), place them in a container or beaker, on a base of glass rods and slowly cover with de-ionized water until they are totally immersed with about 2 cm of water above them. At programmed intervals of time, take each sample out of the container, blot it quickly with a damp cloth to remove surface water, and then record the mass of the wet samples (m_i) and the time of measurement on the data sheet. Re-immerse the samples in water and continue measuring until the difference in weight between 2 successive measurements at 24-hour intervals is less than 1% of the amount of water absorbed. At this point, take the samples out of the water and dry them again in an oven at 60°C until they have reached constant mass (as above). Record this value (m_d) on the data sheet. At each interval, the quantity of water absorbed with respect to the mass of the dry sample is expressed as:

$$M_i\% = 100 \times (m_i - m_o)/m_o$$

Where m_i = weight (kg) of the wet sample at time t_i; m_o = weight (kg) of the dry sample.

Figure 5.3 - Samples placed in oven

Record these values on a data sheet and on a graph as a function of time. The length of the intervals during the first 24 hours depends on the absorption characteristics of the materials. Cement mortar samples should be weighed a few minutes after immersion, and then at increasing intervals (15 min, 30 min, 1 hour, etc.) for the first 3 hours. All samples should then be weighed 8 hours after the beginning of the test and then at 24- hour intervals until the quantity of water absorbed in two successive measurements is not more than 1% of the total mass. In the next step, the samples were put into a water bath with boiling water for 5 hours. Then

the samples were removed from the boiling water and left to cool for 12 hours. Then weights of the samples were measured (M_c). On the same day, the apparent weight of each sample (M_d) was measured by immersing the samples in the water using a hanging balance. Using the measured weights (M_a to M_d) and the equations from the ASTM C642 standard test, the following parameters are obtained.

Figure 5.4 - Samples placed in boiling water

Water Absorption Capacity (WAC) = $[(M_b-M_a)/ M_a] \times 100$

Bulk density = $g_1 = [(M_a)/ M_c- M_d]x \rho$

Apparant density $=g_2 = [(M_a)/ M_a- M_d]x \rho$

Volume of permeable voids (VPV) = $[(g_2 - g_1)/ g_2] \times 100$

Where: M_a = mass of oven-dried sample in air, kg; M_b = mass of surface-dry sample in air after immersion, kg; M_c = mass of surface-dry sample in

air after immersion and boiling, kg and M_d = apparent mass of sample suspended in water, kg.

g_1 = dry bulk density (kg/m^3) and g_2 = apparent density (kg/m^3)

ρ= density of water (1000 kg/m^3)

Finally, total porosity 'P' or percentage of interconnected pore space was calculated using the formula given below

Total porosity = $(V_v/V) = (W_{sat} - W_{dry}) / \rho_w V$

Where, V_v = volume of voids in cc= $W_{sat} - W_{dry}$ in grams;

V = total volume of specimen in cc = 7.06 x 7.06 x7.06 cm^3

Where ρ_w the unit mass of water =(1 g/cc)

W_{dry} and W_{sat} denote the weight of the dried and fully saturated samples, respectively.

The following equation was used to find the apparent porosity.

Apparent porosity (%) = $[(M_w - M_d)/ (M_w - M_s)]$ x100

Where M_w = weight of saturated specimen (after immersion in water for 48 hours, it is removed and surface dried), M_d = Weight of oven dried specimen and M_s = weight of specimen while suspended in water.

Figure 5.5 - Suspended weighing of cubes

Porosity of cement mortar is usually determined by dividing the volume of voids of the sample by its bulk volume. Bulk volume of each sample is determined using the measured lengths and diameters of the samples. Volume of voids for each sample is determined by subtracting its grain volume (the volume of the solid portion of cement mortar excluding the volume of pores) from its bulk volume. Total porosity therefore considers both permeable and impermeable voids whereas apparent porosity considers only impermeable voids.

Water Absorption Capacity and Porosity of various samples of cement mortar specimens are assessed to determine the role of bacteria and nutrients action in the strength improvement of cementitious materials and are presented in table 5.3 below.

Table 5.3 - Water Absorption Capacity and Porosity

Specimens	Water Absorption capacity (%)	Porosity (%)
Sample 1: cement + water	2.77	5.32
Sample 2:cement + (bacteria + nutrient broth) solution	2.78	4.18
Sample 3:cement + (nutrient broth solution)	2.11	5.32
Sample 4:cement + (bacteria + nutrient broth + $CaCO_3$ supplement) solution	1.19	2.28
Sample 5:cement + (bacteria +nutrient broth) solution + calcium lactate	**0.38**	**0.76**
Sample 6:cement + (bacteria + nutrient broth + $CaCO_3$ supplement) solution + calcium lactate	0.38	0.76
Sample 7:cement + calcium lactate	1.99	4.94

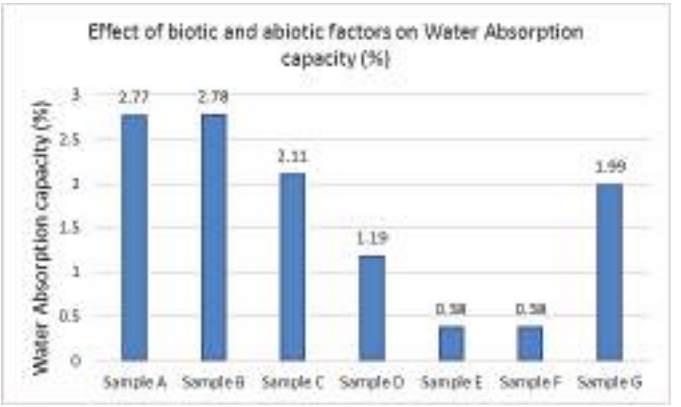

Figure 5.6 - Effect of biotic and abiotic factors on the Water absorption capacity

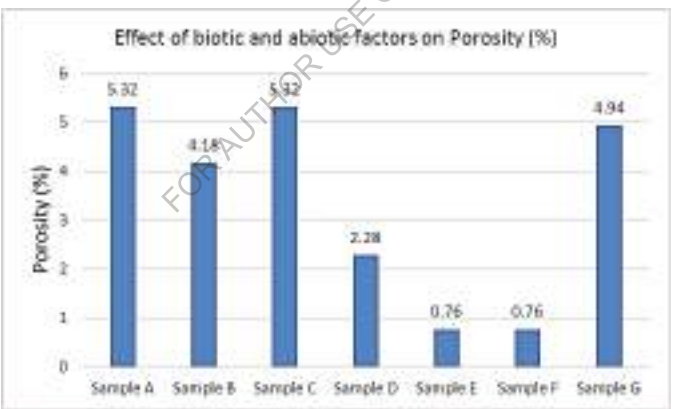

Figure 5.7 - Effect of biotic and abiotic factors on porosity

It was observed that nutrients and calcium lactate alone cannot have any effect on strength and durability of the cement mortar specimens. Incorporation of bacteria into cement mortar along with nutrients with calcium supplement and 5% calcium lactate gives best possible results in

terms of compressive strength and durability due to enhanced microstructure of the specimens due to refinement of concrete pore structure by plugging the voids /or the pores within cement–sand matrix, as part of metabolic activity, with deposition of $CaCO_3$ precipitate formed by *Sporosarcina pasteurii.* This dense growth of calcite precipitate refines the pore structure of cement mortar specimens resulting in the strength improvement and enhancement of permeation properties.

5.5 Characterization of $CaCO_3$ precipitate

Bacteria promote calcium carbonate precipitation in the form of calcite crystals due to its metabolic reactions. The formation of calcite ($CaCO_3$) by process of bio-mineralization can be analyzed using various characterization techniques/methods. The micro-structural observations could improve the understanding of the mechanism of self-healing phenomenon by calcifying bacteria. This chapter is focused on characterizing the mineral precipitation in concrete by *Sporosarcina pasteurii* bacterial strain as calcite using relevant nanocharacterization techniques such as Scanning Electron Microscope (SEM), X-ray diffraction (XRD) , Thermo-gravimetric (TG) analyses and to validate that cracks/ or pores in bacteria incorporated concrete were sealed up by the precipitation of calcium carbonate crystals grown due to complex metabolic mechanism through nitrogen cycle by *Sporosarcina pasteurii* bacterial strain. The above characterization studies establish the fact that the $CaCO_3$ is precipitated in the concrete by *Sporosarcina pasteurii* bacterial strain.

Microbial calcite precipitation was visualized by SEM, quantified by X-Ray Powder Diffraction (XRD) analysis and confirmed by TG/DTG, FT-IR and Raman spectrograph Analysis. The samples for the tests were collected, from the bacteria treated cement mortar samples and from control specimens i.e., samples without bacteria, in the form of powders and/or broken pieces.

5.5.1 Scanning Electron Microscope (SEM) Analysis

The purpose of this study was (1) to determine the reason for the increase in strength of the bacterially modified or bacterially induced mortar and (2) to characterize the microstructures of such mortar by identifying the new product formed by the bacteria within.

The test is to confirm the presence of bacteria precipitated calcite by generating high resolution images of bacteria induced concrete samples

Scanning Electron Microscope (SEM) analysis is made on the samples of 28 day old bacterial cement mortar specimens and control mortar specimens (without bacteria). Broken pieces of 28 day old cement mortar cubes from the compression test were examined under a SEM Hitachi-S520 using accelerating voltages ranging from 1to 30 KV in the research centre at CSIR- Indian Institute of Chemical Technology.

The test is to confirm the presence of bacteria precipitated calcite by generating high resolution images of bacteria induced concrete samples and shows spatial variations in chemical compositions. Fig 5.9 (a) and (b)

shows SEM scanning images of control cement mortar sample and bacteria induced cement mortar sample. Improvement in pore structure of cement-sand mortar samples treated with *Sporosarcina pasteurii* bacterial strain of 10^5 cell concentration per ml can be observed in a magnified view (2500x) of SEM micrograph as shown in Fig 5.9 (b).

Nil Cell Concentration

10^3 Cell Concentration

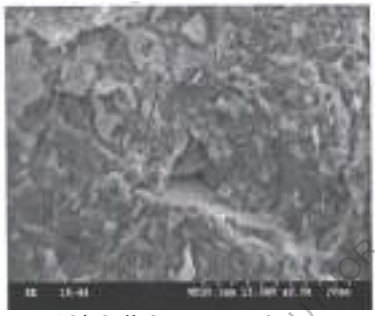

10^4 Cell Concentration

10^5 Cell Concentration

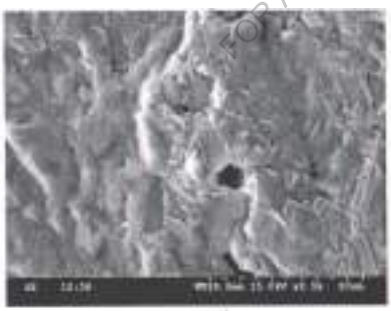

10^6 Cell Concentration

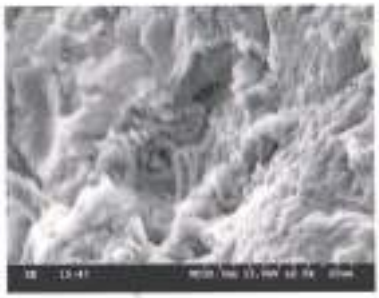

10^7 Cell Concentration

Figure 5.8 - SEM images of mortar specimens made with different bacterial cell counts

(a) Cell Concentration –Nil (Reference Specimen)

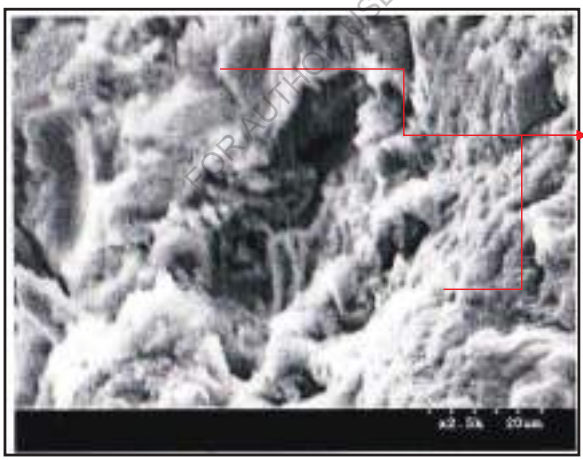

(b) Cell Concentration – 10^5/ml (Optimum)

Figure 5.9 - Magnified SEM Micrographs (2500x magnification): Hydrated Structure of Cement-sand Mortar without Bacteria and with optimum Bacteria incorporated

The difference between these two scanning electron micrographs shows that the in case of sample from bacteria induced cement mortar, formation of dense $CaCO_3$ precipitation spreading over the pores present inside, with rod-shaped impressions housed by *Sporosarcina pasteurii* bacterial strain can be observed. The morphology of the newly formed crystals of rhombohedra shape suggests that the mineral may be $CaCO_3$ and its formation could be the result of the metabolic conversion of the nutrients by *Sporosarcina pasteurii* bacterial strain. SEM examination shows that in a mortar made with a 10^5/ml cell concentration, the pores are almost completely filled with narrow strands of filler (calcite) and modification of pore size distribution is noticed. In case of control sample no filler material was observed.

From the above SEM investigations, the following conclusions are drawn:

1. Microbial calcium carbonate precipitation was visualized by SEM analysis.
2. The SEM analysis revealed the dense growth of calcite crystals embedded with bacterial cells in bacteria incorporated specimen.
3. Packing density of high calcium amounts in it confirmed that calcite was present in the form of calcium carbonate deposited by bacteria.
4. It can be concluded that the microbial activity of *Sporosarcina pasteurii* bacterial strain has precipitated dense $CaCO_3$ which may have caused the increase in 28 day compressive strength due to pore refinement in the concrete.

5.5.2 X-ray Diffraction (XRD) Analysis

X-Ray Powder Diffraction (XRD) analysis is powerful method by which X-rays of a known wavelength are passed through a sample to identify different phases of that sample. This test characterizes the crystalline materials present in the given sample. It provides information on crystalline phase, average size, atomic arrangement and imperfections. X-Ray Powder Diffraction is a physico-chemical analysis method commonly used to determine the reticular plane distance and for the identification of crystalline compounds by their diffraction pattern. To identify the presence of $CaCO_3$ precipitation in bacteria induced samples, X-ray diffraction (XRD) analysis was conducted.

The sample material should be grounded sufficiently fine so that it will pass through a 40 μm sieve. The quantity required is less than 10 gm which should be placed in the sample holder. The XRD Pattern was obtained by scanning from 2 to 80° 2θ using a vertical x-ray diffractometer. Powder diffraction patterns are typically plotted as the intensity of the diffracted X-rays vs. the angle 2θ. By measuring the 2θ values for each diffraction peak, we can calculate the d-spacing (the distance between the diffracting planes) for each diffraction peak. The data analysis software has a program for automatically calculating the d-spacings (reticular plane distance) for all of the peaks in the diffraction pattern. The constituents of the sample were identified by comparing d values of each diffraction peak

against the mineral XRD database (standard JCPDS files) established by the Joint Committee on Powder Diffraction Standards (JCPDS)-International Centre for Diffraction Data (ICDD). Mineralogical compositions of the bacteria deposited $CaCO_3$ crystals were investigated with X-ray powder diffraction analysis. Higher the peak suggests the more amount of presence of mineral. The areas under the peak are related to the amount of each mineral present in the sample. The widths of the peaks in a particular pattern provide an indication of the average crystallite size. Crystal identification is accomplished by comparing the data (peaks and relative intensities) from samples with "standard" data provided by the International Center for Diffraction Data (ICDD).

To identify the presence of $CaCO_3$ precipitation in bacteria induced samples, X-ray diffraction (XRD) analysis was conducted. This test characterizes the crystalline materials present in the given sample. Figures 5.10 and 5.11 depicts the profiles of XRD spectra of control and bacteria incorporated cement mortar samples. From the XRD spectrums for control mortar sample and the bacterial incorporated mortar sample, the principal calcite peaks can be observed at 26.82°. In the intensity mapping of the characteristic peaks of calcite, it is found that the higher calcite intensity peaks with reference to International Crystal Diffraction Database (ICDD) were formed for the bacterial incorporated specimen. This is an indication of presence of high percentage of calcite mineral in the bacteria incorporated specimen, which could be attributed to an formation of

$CaCO_3$ due to microbial activities of bacteria *Sporosarcina pasteurii* bacterial strain. This high amount of calcite precipitation, thus results in significant higher compressive strength than the control mortar samples. In the XRD pattern Fig 5.10 , of control cement mortar sample, the characteristic diffraction peak (100% intensity) occurred, at 2θ= 18.25º with reticular plane distance (d) value 3.342 (for quartz) which indicates presence of the relatively high amount of quartz mineral when compared to other minerals present in the sample. It can also be noted that the presence of calcite in control mortar sample is due to formation of hydrated C-S-H gel. In case of bacteria incorporated sample XRD spectra Fig 5.11, the characteristic diffraction peak (100% intensity) occurred at 2θ= 26.82º with d value 3.035 (for Calcite) which confirms the presence of relatively high amount of calcite crystals when compared to other minerals present in the sample. This can be attributed to the copious deposition of $CaCO_3$ in bacteria induced samples by *Sporosarcina pasteurii* bacterial strain during its microbial activity. So the presence of $CaCO_3$ was substantiated using X-Ray Diffraction (XRD) analysis. More number of calcite peaks suggests maximum calcite precipitation which would thereby reduce the pores in concrete.

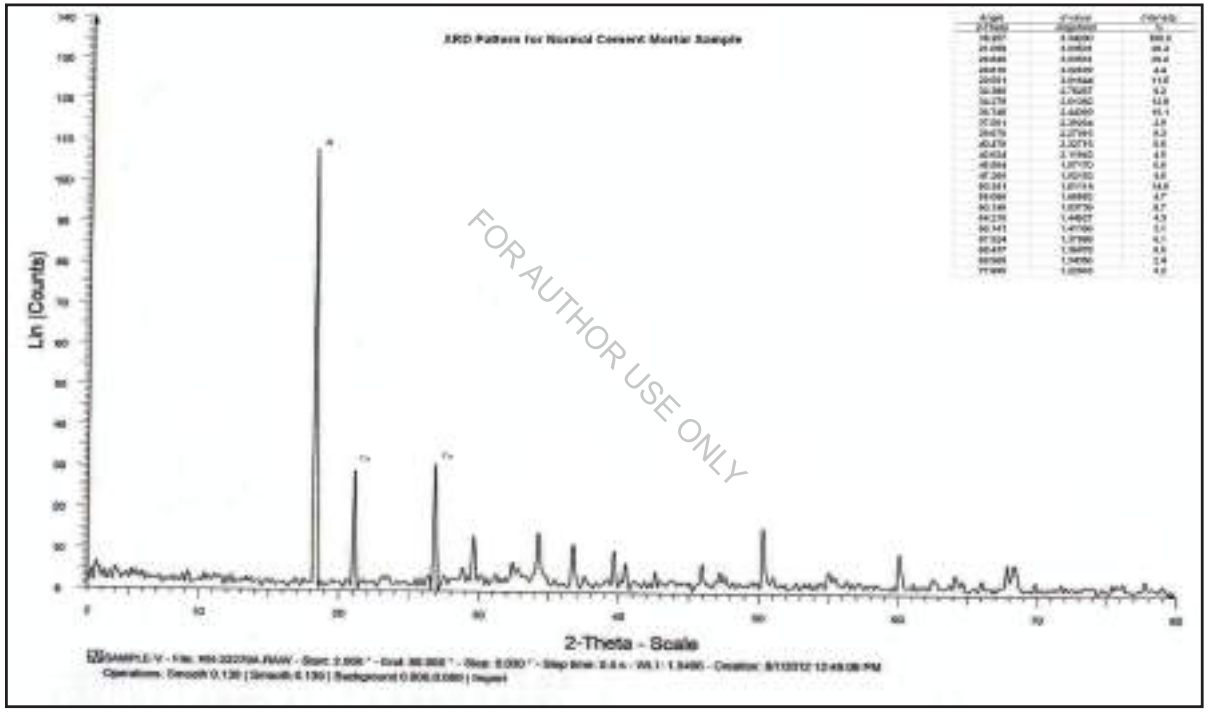

Figure 5. 10 - Diffractogram of normal cement mortar specimens

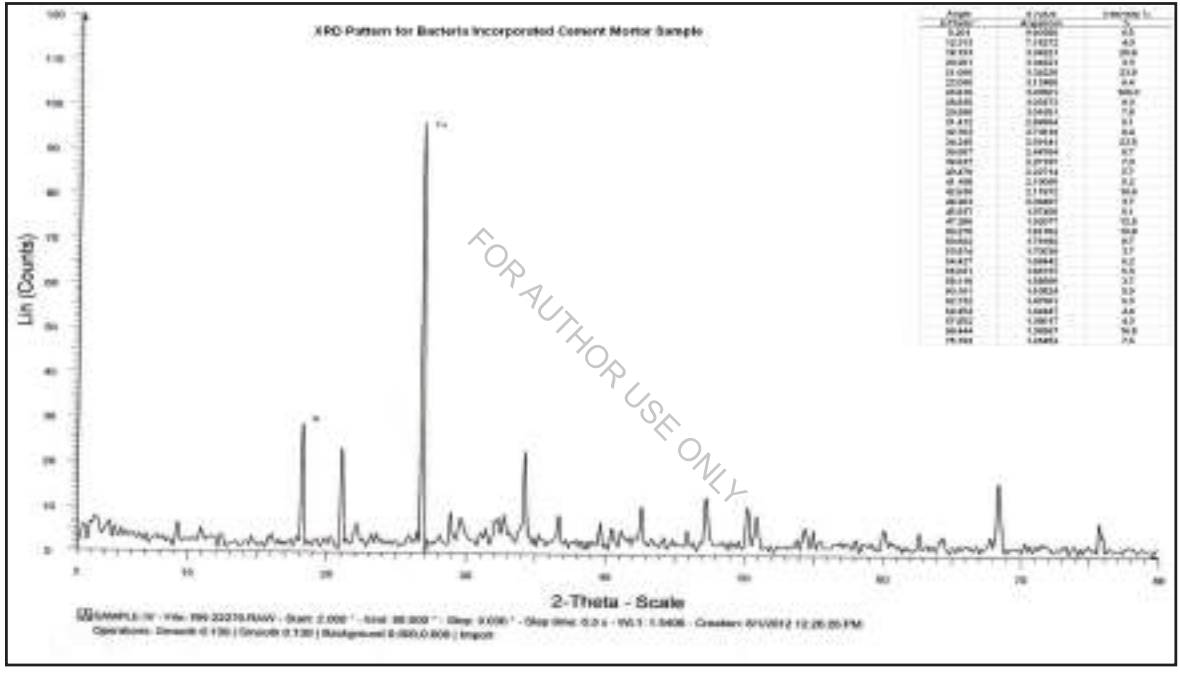

Figure 5.11 - Diffractogram of bacteria incorporated mortar specimen's shows the abundant presence of Ca and precipitation was inferred to as calcite ($CaCO_3$) crystals

From the XRD analysis, the following conclusions are drawn:

1. Microbial calcium carbonate precipitation was quantified by XRD analysis.
2. The XRD scanning image of powdered bacteria incorporated cement mortar sample confirms the presence of high amount of calcite mineral.
3. This can be attributed to the copious deposition of calcite ($CaCO_3$) in bacteria induced samples by *Sporosarcina pasteurii* bacterial strain during its microbial activity. This deposition of $CaCO_3$ in the pores will maximize the packing density of cement mortar consequently has great impact on the strength produced.

5.5.3 Thermo-gravimetric (TG) Analysis

Thermo-gravimetric Analysis (TGA) is a technique to characterize materials by measuring the sample's weight as it is heated or cooled in a furnace. TGA is commonly used to determine selected characteristics of materials that exhibit either mass loss or gain due to decomposition, oxidation, or loss of volatiles (such as moisture). This analysis is conducted to confirm the presence of calcite ($CaCO_3$) in bacteria induced samples by studying the properties of sample as they change with temperature.

A TGA analysis is performed by gradually raising the temperature of a sample in a furnace as its weight is measured on an analytical balance that remains outside of the furnace. So this test measures changes in weight in relation to changes in temperature. The measured weight loss

curve gives information on changes in sample composition and thermal stability**.** A derivative weight loss curve can be used to tell the point at which weight loss is most apparent. TGA thermal curve is drawn between temperature on x-axis and weight (mg) or weight percent (%) on y-axis. Derivative thermogravimetric (DTG) Curves are drawn between the rate of mass change (%/ ^{o}C) against temperature on the *x* axis, when substance is heated at uniform rate. For thermal analysis study, the sample size considered is 50mg. During the Thermogravimetric analysis, the precipitated calcite material in cement mortar specimen was exposed to temperatures ranging from 50 °C to 900 °C at a rate of 10 °C/min in an inert nitrogen atmosphere with a purge rate of 20 mL/minute. Through performance of the TGA analysis, the presence of $CaCO_3$ in the repair material is determined.

This analysis is conducted to confirm the presence of calcite ($CaCO_3$) in bacteria induced samples by studying the properties of sample as they change with temperature.

The descending TGA thermal curve indicates a weight loss occurred. When $CaCO_3$ crystals are present in the repair material, they will decompose into CaO and CO_2 upon heating ($CaCO_3 \rightarrow CaO + CO_2$). When TGA analysis is performed on powdered bacteria incorporated cement mortar sample, extreme loss of weight is observed at temperature range of 500–700°C. This is ascribed to $CaCO_3$ decomposition around that temperature interval. For the normal mortar specimens the weight loss is rather small

(2%) while for specimens with bacteria a significant decrease in weight is observed (20%) as shown in Fig 5.12**.** In first graph the percentage of weight loss is plotted against the temperature while in second graph the derivative of the weight loss (rate of mass change) is plotted against the temperature. As it can be observed from the first graph of Fig. 5.12, at about 100 - 200 °C the water in the samples evaporates, leading to a decrease in weight. Between 500 and 700 °C another decrease in weight is detected. This is due to the decomposition of $CaCO_3$. An apparent difference in weight loss can be observed between the samples treated with and without bacteria. These results provide evidence that particularly in the case of bacteria incorporated specimens; amount of $CaCO_3$ crystals present is high due to bio-mineralization by *Sporosarcina pasteurii* bacterial strain. In second graph, the derivative in weight loss is shown versus the temperature to indicate the points at which the weight loss is most evident. For specimens without bacteria only a small amount of $CaCO_3$ is decomposed at the temperature of 591°C. This decrease in weight may possibly be attributed to chemical precipitation of $CaCO_3$ during formation of hydrated C-S-H gel. For concrete specimens with bacteria, the observed peaks are more distinct.

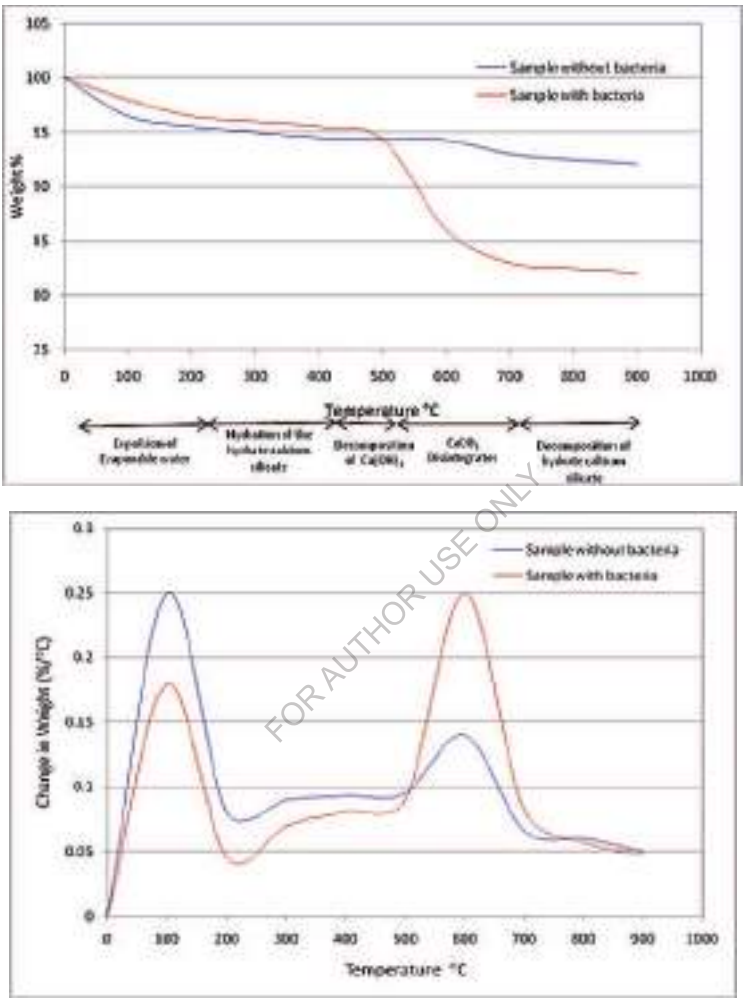

Figure 5.12 - TGA Results for cement mortar specimens with and without bacteria showing weight loss and Change in weight loss per ^{o}C

So it can be inferred that the behavior of both control specimens and bacteria incorporated specimens are identical when subjected to elevated temperatures. So these results provide evidence that the effect of bacteria on the properties of cementitious materials is neutralized at temperatures higher than 500°C. From the Thermogravimetric Analysis, the following conclusions are drawn:

1. TGA analysis performed on powdered bacteria incorporated cement mortar sample showed an extreme loss of weight at temperature range of 500–700°C confirming the presence of high amount of $CaCO_3$.
2. Thermogravimetric Analysis (TGA) confirms the presence of $CaCO_3$ in bacteria incorporated concrete specimens.
3. This presence of large amount of $CaCO_3$ can be credited to the precipitation of calcite ($CaCO_3$) in bacteria induced samples by *Sporosarcina pasteurii* bacterial strain during its microbial activity.
4. The behavior of control mortar specimens and bacteria incorporated mortar specimens are identical when subjected to elevated temperatures. This invalidates the use of calcite precipitating bacteria at higher temperatures.

5.6 Bacteria Viability

In this experiment it was tested how long the bacteria *Sporosarcina pasteurii* bacterial strain can remain viable and sustain high alkaline conditions of concrete environment. *Sporosarcina pasteurii* bacterial strain

being alkaliphilic and endospore-former is expected to tolerate harsh alkaline environment by remaining dormant, non-metabolically active and non-reproductive. When endospores of *Sporosarcina pasteurii* bacterial strain are exposed to a suitable environment then the spore can able to transform into a vegetative cell, capable of normal metabolic function. Since the microorganisms will be embedded within concrete, key challenges are determine whether bacteria *Sporosarcina pasteurii* bacterial strain can (1) tolerate the highly alkaline conditions (pH 12-13), (2) survive the mixing process used to prepare the concrete, and (3) survive with limited access to nutrients.

A piece of bacterial concrete of 365 days age was inoculated in nutrients broth and kept in orbital shaker for 24 hrs. After 24h incubation, a loop full of culture is taken from the broth and streaked on agar plate. Once colonies are formed their morphological characteristics and microscopic observations match with *Sporosarcina pasteurii* bacterial strain. This confirms the presence of *Sporosarcina pasteurii* bacterial strain even after 365 days in concrete. Photo contrast pictures shows that bacteria are still viable in concrete. Fig 5.13 shows Phase contrast microscopic pictures reveal that *Sporosarcina pasteurii* bacterial strain spores were produced within vegetative cells (endospores). and white calcium carbonate precipitation (calcite crystals) is formed around its cell. Vegetative *Sporosarcina pasteurii* bacterial strain cells were detected viable even after 365 days in mortar samples. These viable cells were detected as vegetative

cells (metabolically active) because when they are inoculated in nutrients broth, bacterial colonies are formed. It should be noted that as per the available literature on viability of microorganisms so far this is the longest survival period recorded for microorganisms in cement-based materials without any encapsulation. It has been found that spores of *Sporosarcina pasteurii* bacterial strain can tolerate high pH, and remained viable up to a year. Photo contrast pictures show the deposited calcite crystals by endospored *Sporosarcina pasteurii* bacterial strain in the concrete. This validates that the bacteria *Sporosarcina pasteurii* bacterial strain is alkaliphilic and endospore forming soil microorganism.

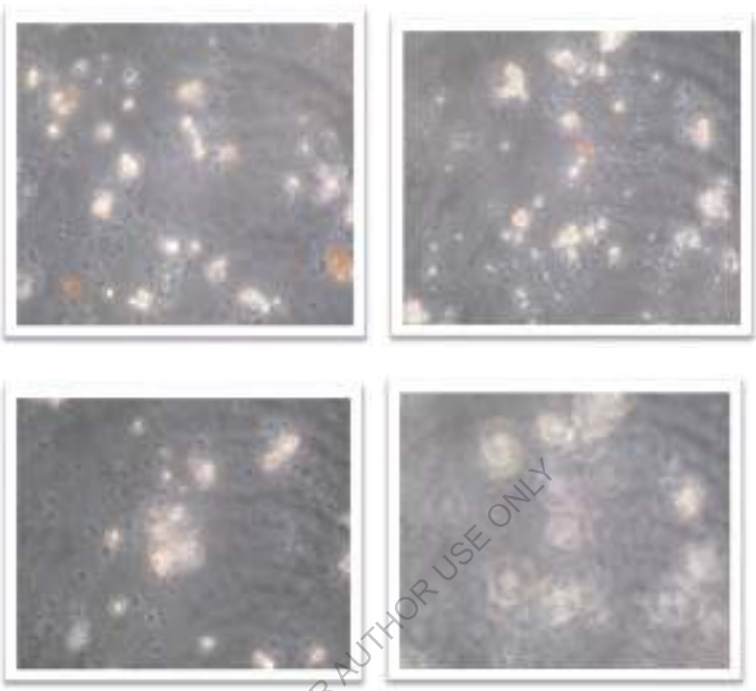

Figure 5.13 - Phase contrast microscopic images shows white calcium carbonate crystals formation

5.7 Summary

This section presents materials used and their properties (provided by the supplier) and methodology for preparation of fly ash based artificial coarse aggregates, process of growing and culturing bacteria, Optimum bacterial cell concentration for $CaCO_3$ Precipitation, effect of biotic and abiotic factors of bacterial activity on strength and durability of cementitious materials, Characterization of $CaCO_3$ precipitation, mix proportions of

M20 and M40 grade concretes, mechanical properties of M20 and M40 grade fly ash aggregate based bacterial concretes , Flexural Behavior of fly ash aggregate based bacterial concrete beams, Pore Structure Analysis, permeation properties, corrosion resistance of M20 and M40 grade fly ash aggregate based bacterial concretes using BET Nitrogen (N2) Adsorption method. Finally crack healing efficiency evaluation methods are discussed.

Page left blank intentionally

Chapter - 6

MECHANICAL PROPERTIES

6.1 General

This section presents the mechanical properties of M20 and M40 grade fly ash aggregate based bacterial concretes and flexural behavior of fly ash aggregate based bacterial concrete beams.

6.2 Compressive Strength

This investigation is carried out to study the compressive strength of ordinary (M20) and standard (M40) grades of conventional and bacterial concrete at 28, 60 and 90 days. Concrete cubes of 100 mm x 100 mm x 100 mm are cast with optimized cell concentration of *Sporosarcina pasteurii* (10^5 cells/ml of mixing water) and tested to study the compressive strength under axial compression on completion of 28, 60 and 90 days as per IS: 516-1999. The main objective of the present experimental investigations is to obtain specific experimental data, which helps to understand the mechanical characteristics of bacteria incorporated concrete.

The results of the compressive strength at 28, 60 and 90 days for ordinary (M20) and standard (M40) of conventional and bacteria incorporated concrete are tabulated in table 6.1 below.

Table 6.1 - Compressive Strength of M20 and M40 grades of concrete made with natural aggregate (NAC) and Fly ash aggregate bacterial concrete (FAABC)

Age of concrete	28 days	60 days	90 days
M20 Reference Concrete made with natural coarse aggregate (NAC)	28.18	32.44	33.27
M20 Bacterial Concrete made with untreated fly ash coarse aggregate	22.17	27.56	28.79
M20 Bacterial Concrete made with treated fly ash coarse aggregate (FAABC)	32.74	37.97	39.40
M40 Reference Concrete made with natural coarse aggregate (NAC)	52.01	56.47	57.96
M40 Bacterial Concrete made with untreated fly ash coarse aggregate	44.30	47.89	49.11
M40 Bacterial Concrete made with treated fly ash coarse aggregate (FAABC)	61.06	66.52	66.83

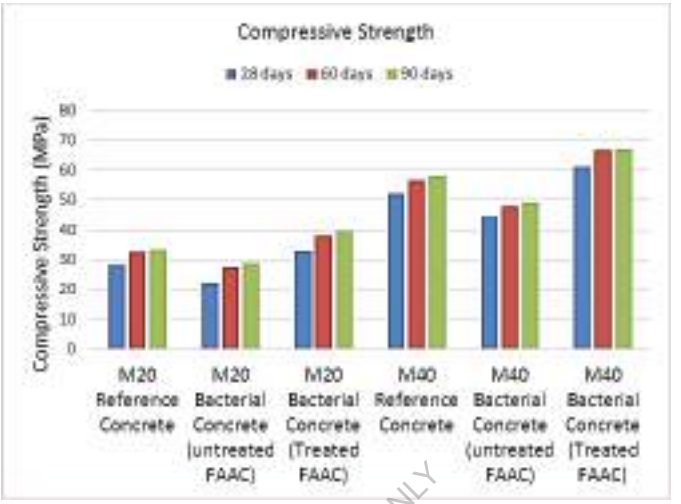

Figure 6.1- Compressive Strength of M20 and M40 grades of concrete made with natural aggregate (NAC) and Fly ash aggregate bacterial concrete (FAABC)

It is observed that in M20 grade concrete, with the addition of bacteria the compressive strength of concrete showed significant increase by 16.18% in cube specimens at 28 days. There is further percentage increase of compressive strength due to persistent calcium carbonate mineral precipitation by Bacillus pasteurii, which fills up the pores in the concrete making the concrete microstructure denser. In M40 grade concrete, it is observed that with the addition of bacteria the compressive strength of concrete showed significant increase by 17.54 %at 28 days.

The percentage of compressive strength has increased with the age of concrete due to incessant calcium carbonate mineral precipitation by

Bacillus Pasteurii. So the percentage increase of compressive strength will be more in high strength grades of bacteria incorporated concrete which is attributed to not only the presence of calcite crystals induced by Bacillus pasteurii in the concrete pores in the form of an extra cellular organic substance. Use of silica fume in high strength grades also acts as a micro-filler in making the concrete dense.

Based on the above studies, the following conclusions are drawn:

1. The addition of Sporosarcina pasteurii bacterial strain to concrete increases the compressive strength by 16-18% in M20 and M40.
2. The increase in compressive strength attributes to the bacteriogenic calcite mineral plugging in the concrete pores in the form of extra-cellular organic substance in the cement sand matrix modifying the microstructure of concrete.
3. The percentage of compressive strength has improved more with age due to continuous calcium carbonate mineral precipitation by Bacillus pasteurii.

6.3 Split tensile Strength

This investigation is carried out to study the split tensile strength of ordinary (M20) and standard (M40) grades of conventional and bacterial concrete at 28, 60 and 90 days. Cylinders of size 150 x 300 mm are cast and tested to study the split tensile strength as per IS: 5816 – 1999 and are tabulated in table 6.2 below.

Table 6.2- Split tensile strength of M20 and M40 grades of concrete made with natural aggregate (NAC) and Fly ash aggregate bacterial concrete (FAABC)

Age of concrete	28 days	60 days	90 days
M20 Reference Concrete made with natural coarse aggregate (NAC)	3.26	3.34	3.49
M20 Bacterial Concrete made with untreated fly ash coarse aggregate	3.11	3.17	3.22
M20 Bacterial Concrete made with treated fly ash coarse aggregate (FAABC)	3.73	3.89	4.04
M40 Reference Concrete made with natural coarse aggregate (NAC)	4.51	4.63	4.89
M40 Bacterial Concrete made with untreated fly ash coarse aggregate	4.34	4.45	4.51
M40 Bacterial Concrete made with treated fly ash coarse aggregate (FAABC)	5.13	5.41	5.65

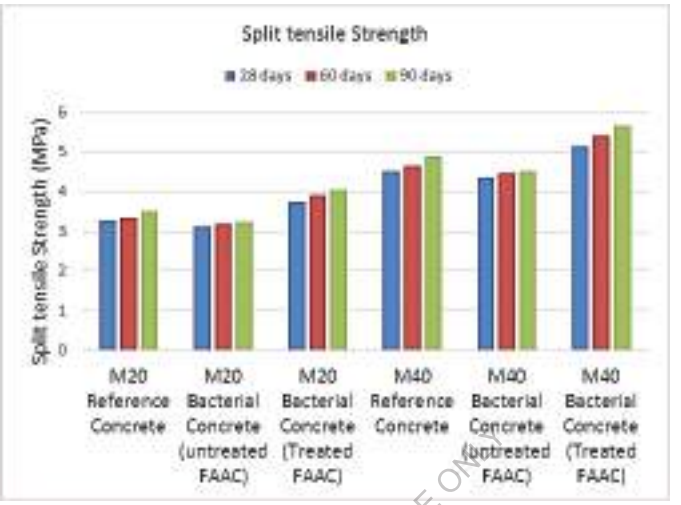

Figure 6.2 - Split tensile strength of M20 and M40 grades of concrete made with natural aggregate (NAC) and Fly ash aggregate bacterial concrete (FAABC)

In M20 grade concrete, it was observed that with the addition of bacteria there is a significant increase in the 28 day split tensile strength by 14.42%. In M40 grade of bacteria incorporated concrete the increase is by 13.75 % at 28 days. The percentage of split tensile strength increases with the increase in the age of concrete due to incessant calcite precipitation of Bacillus pasteurii. From the above experimental investigations, it is observed that the increase of split tensile strength in all grades of bacteria incorporated concrete is mainly due to filling up of voids/or pores in concrete with bacteriogenic calcite precipitates of Bacillus pasteurii.

6.4 Modulus of rupture or Flexural Strength

This investigation is carried out to study the flexural strength of ordinary (M20) and standard (M40) grades of conventional and bacterial concrete at 28, 60 and 90 days. Prisms of size 100 x100 x 500 mm are cast and tested to study the flexural strength of conventional and bacteria incorporated concretes of various grades as per IS:9399 – 1979 and are tabulated in table 6.3 below.

Table 6.3- Flexural strength of M20 and M40 grades of concrete made with natural aggregate (NAC) and Fly ash aggregate bacterial concrete (FAABC)

Age of concrete	28 days	60 days	90 days
M20 Reference Concrete made with natural coarse aggregate (NAC)	4.68	4.93	5.12
M20 Bacterial Concrete made with untreated fly ash coarse aggregate	4.42	4.56	4.67
M20 Bacterial Concrete made with treated fly ash coarse aggregate (FAABC)	6.11	6.32	6.51
M40 Reference Concrete made with natural coarse aggregate (NAC)	5.68	5.98	6.25
M40 Bacterial Concrete made with untreated fly ash coarse aggregate	4.79	4.88	4.98
M40 Bacterial Concrete made with treated fly ash coarse aggregate (FAABC)	7.25	7.47	7.65

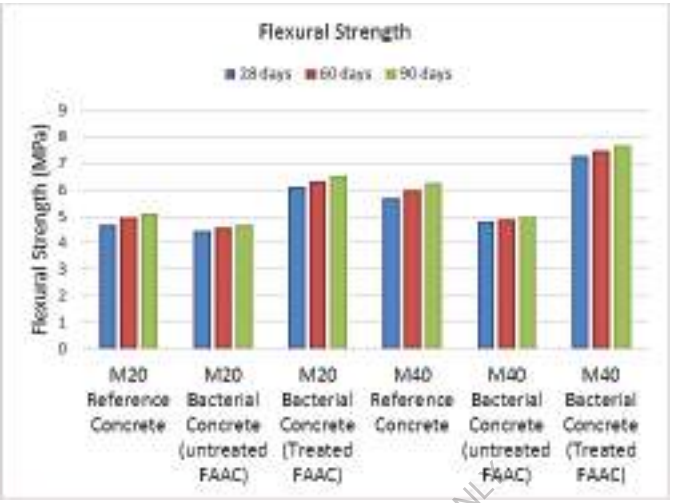

Figure 6.3 - Flexural strength of M20 and M40 grades of concrete made with natural aggregate (NAC) and Fly ash aggregate bacterial concrete (FAABC)

In M20 grade concrete, it is observed that with the addition of bacteria there is a significant increase in the 28 day flexural strength by 30.5%. In M40 grade bacteria incorporated concrete, the 28 day flexural strength increases by 27.6% at 28 days.

From the above discussion it can be concluded that the 28 day flexural strength increase in all grades of bacteria incorporated concrete. This increase of flexural strength in bacteria incorporated concrete is ascribed to filling up of voids/or pores in concrete with bacteriogenic calcite precipitates of Bacillus pasteurii. This growth of dense calcite as filler material improves pore structure giving better bonding at transition zone.

So the increase in flexural strength can be explained by the fact that the calcite precipitation increases the bond strength at the interfacial zone.

The following discussions are made from strength studies

1) The addition of *Sporosarcina pasteurii* bacterial strain improves the compressive strength of cement mortar.

2) The cement mortar cube specimens which contained cell concentration of 10^5 bacterial cells/ml of mixing water were found to attain higher compressive strength as compared to the control specimen. Microbial calcite was precipitated on the surface of cells and eventually within the pores leading to their plugging which further lead to stoppage of flow of oxygen and nutrients to the cells that able to precipitate calcite continuously. The mineral precipitation in cement mortar reduces the interconnectivity of the pore structure by decreasing the pore size (pores refinement), which is directly related to durability.

3) In M20 grade concrete the compressive strength is increased by 16.18% at 28 days, 17.04% at 60 days and 18.42% at 90 days by addition of Sporosarcina pasteurii bacterial strain when compared to conventional concrete. Similarly in M40 grade the percentage increase was found to be 17.54% at 28 days, 17.79% at 60 days and 16.32% at 90 days.

4) In M20 grade concrete the split tensile strength is increased by 14.42% at 28 days, 16.47% at 60 days and 15.76% at 90 days by addition of Sporosarcina pasteurii bacterial strain when compared to conventional

concrete. Similarly in M40 grade the percentage increase was found to be 13.75% at 28 days, 16.85% at 60 days and 15.54% at 90 days.

5) In M20 grade concrete the flexural strength is increased by 30.50% at 28 days, 28.20% at 60 days and 27.15% at 90 days by addition of Sporosarcina pasteurii bacterial strain when compared to conventional concrete. Similarly in M40 grade the percentage increase was found to be 27.60% at 28 days, 24.92% at 60 days and 22.40% at 90 days.

6) The percentage of compressive strength, split tensile strength and flexural strength has improved with age due to continuous calcium carbonate mineral precipitation by *Sporosarcina pasteurii* bacterial strain.

6.5 Quality Assessment by Non-Destructive methods

The main objective of the present experimental investigations is to assess the quality, structural integrity and compressive strength of M20 and M40 grade fly ash aggregate concretes (FAAC) incorporated with *Sporosarcina pasteurii* bacterial strain using Rebound hammer test and Ultrasonic pulse velocity measurements.

The Rebound Hammer Test is conducted as per IS: 13311 (Part 2) – 1992 on of M20 and M40 grade bacteria incorporated (Treated FAAC) and reference concretes (NAC) cubes of size 150x150x150mm. This test mainly evaluates the quality of surface hardness based on the rebound numbers obtained.

Table 6.4 - Quality of concrete based on Average Rebound Hammer as per IS: 13311 (Part 2) – 1992

Average rebound number	Quality of concrete
> 40	Very good hard layer
30 to 40	Good layer
20 to 30	Fair
< 20	Poor

Ultrasonic Pulse Velocity Test is conducted as per IS: 13311 (Part 1) – 1992 on M20 and M40 grade bacteria incorporated (Treated FAAC) and reference concretes (NAC) of size 150x150x150mm. This test qualitatively assesses the homogeneity and integrity of concrete. This test also determined the density and elastic properties of the concrete.

Table 6.5 -Concrete Quality based on USPV as per IS: 13311 (Part 1) – 1992

Pulse velocity	Concrete quality
>4.5 km/s	Excellent
3.5 – 4.5 km/s	Good
3.0 – 3.5 km/s	Medium
<3.0 km/s	Doubtful

To make a more realistic assessment of the quality and integrity of concrete, a prudent approach of combined use of Non–destructive tests viz ultrasonic pulse velocity and rebound hammer tests were used.

Mean rebound values and mean ultrasonic pulse velocities (USPV) are measured to understand the quality, integrity and strength of bacteria

incorporated concrete and compare with conventional concrete's corresponding properties. The table 6.6 lists the mean rebound values, mean pulse velocity values of M20 and M40 grade bacteria incorporated (Treated FAAC) and reference concretes (NAC) specimens at different ages, along with their estimated compressive strengths.

It is observed the ultrasonic pulse velocity and rebound number values increased due to refined pore structure and microstructure of hardened bacteria incorporated concrete making the concrete highly dense. Similar observation is noted in both the grades of bacteria treated concrete specimens. Since the rebound index is indicative of hardness of concrete up to a limited depth from the surface hence the internal cracks, flaws etc. or heterogeneity across the cross section will not be indicated by rebound numbers. So the ultrasonic pulse velocity measurements are obtained so that concrete density and modulus of elasticity can be understood. In order to assess particle continuity inside the concrete specimen, USPV test is performed on both grades of bacteria incorporated (Treated FAAC) and reference concretes (NAC) specimens at different ages. Therefore combined Rebound hammer and Ultrasonic Pulse Velocity measurement were used to assess the quality and strength of the concrete.

Table 6.6 - Combined Rebound hammer and Ultrasonic pulse velocity values of bacteria incorporated (Treated FAAC) and reference concretes (NAC)

Combined Rebound hammer and Ultrasonic Pulse Velocity values								
	M20 Reference Concrete (NAC)				M20 Bacterial Concrete (Treated FAAC)			
Age in days	Mean Rebound Number	Mean Pulse Velocity km/sec	Compressive Strength (f_{ck}) N/mm^2	Quality of Concrete	Mean Rebound Number	Mean Pulse Velocity km/sec	Compressive Strength (f_{ck}) N/mm^2	Quality of Concrete
28	25	4.26	28.18	Good	33	4.77	32.74	Excellent
60	28	4.36	32.44	Good	35	4.83	37.97	Excellent
90	29	4.41	33.27	Good	36	4.91	40.41	Excellent
	M40 Reference Concrete (NAC)				M40 Bacterial Concrete (Treated FAAC)			
Age in days	Mean Rebound Number	Mean Pulse Velocity km/sec	Compressive Strength (f_{ck}) N/mm^2	Quality of Concrete	Mean Rebound Number	Mean Pulse Velocity km/sec	Compressive Strength (f_{ck}) N/mm^2	Quality of Concrete
28	36	4.49	51.19	Good	41	4.93	60.17	Excellent
60	37	4.53	55.39	Excellent	43	4.99	63.35	Excellent
90	39	4.61	56.97	Excellent	45	5.02	66.27	Excellent

It can be concluded that for both grades of bacteria incorporated concrete (Treated FAAC), rebound numbers obtained indicate the superior surface hardness than reference concrete (NAC) and also the USPV measurements were greater than 4.5km/sec which denotes that both grades of bacteria induced concrete (Treated FAAC) are classified as excellent concretes in terms of strength and durability point of view due to improved pore structure of concrete through calcite precipitation by *Sporosarcina pasteurii* bacterial strain whereas referenced concretes (NAC) are classified from good to excellent.

6.6 Stress-Strain Behavior

The aim of this study is to determine the experimental stress-strain behavior of M20 and M40 grade fly ash aggregate concretes incorporated with *Sporosarcina pasteurii* bacterial strain and to validate proposed stress-strain mathematical model against the experimental stress-strain values.

6.6.1 Experimental Stress-strain curves

Cylinders of standard size 150 x 300 mm are cast with and without bacteria, cured for 28 days and tested in uni-axial compression under strain control as per IS: 516-1999 to understand the stress-strain behavior of *Sporosarcina pasteurii* bacterial strain incorporated concrete of M20 and M40 grades considered.

From the experimental values of stresses and strains (table 6.7 to 6.10), average stress-strain curve for each grade of bacteria incorporated

(Treated FAAC) and reference concretes (NAAC) are plotted (figure 6.5), taking the average values of the results of the three cylinders.

Figure 6.4 - Test setup for stress-strain measurements

Table 6.7- Experimental Stress –Strain values of M20 grade Reference concrete (NAC)

Experimental Values	
σ	E
0.00	0
3.20	0.00023
5.66	0.00035
8.49	0.0005
11.32	0.00068
14.15	0.00082
16.99	0.00103
19.82	0.00122
22.65	0.0015
24.25	0.002
22.65	0.00227
18.70	0.00257
14.90	0.00288

Table 6.8 - Experimental Stress –Strain values of M20 grade bacteria incorporated concrete (Treated FAAC)

Experimental Values	
σ	E
0.00	0
2.83	0.00006
5.66	0.00015
8.49	0.00025
11.32	0.00037
14.15	0.00047
16.99	0.00062
19.82	0.00082
22.65	0.00099
25.48	0.00132
28.31	0.0021
25.10	0.00266
18.00	0.00312

Table 6.9- Experimental Stress –Strain values of M40 grade reference concrete (NAC)

Experimental Values	
σ	E
0.00	0
2.83	0.00011
5.66	0.00021
8.49	0.00031
11.32	0.0004
14.15	0.00051
16.99	0.00059
19.82	0.00069
22.65	0.00077
25.48	0.00087
28.31	0.00103
31.14	0.00115
33.97	0.00131
36.80	0.00141
39.63	0.00162
42.46	0.00211
41.30	0.00238
36.80	0.00274
30.30	0.00308

Table 6.10 - Experimental Stress –Strain values of M40 grade bacteria incorporated concrete (Treated FAAC)

Experimental Values	
σ	E
0.00	0
2.83	0.00007
5.66	0.00013
8.49	0.0002
11.32	0.00027
14.15	0.00033
16.99	0.00038
19.82	0.00043
23.20	0.00052
25.70	0.0006
28.60	0.00071
31.14	0.0008
33.97	0.00095
36.80	0.00114
39.63	0.00126
42.46	0.00145
45.29	0.00169
48.12	0.0021
45.29	0.00258
42.46	0.00275
36.70	0.00306

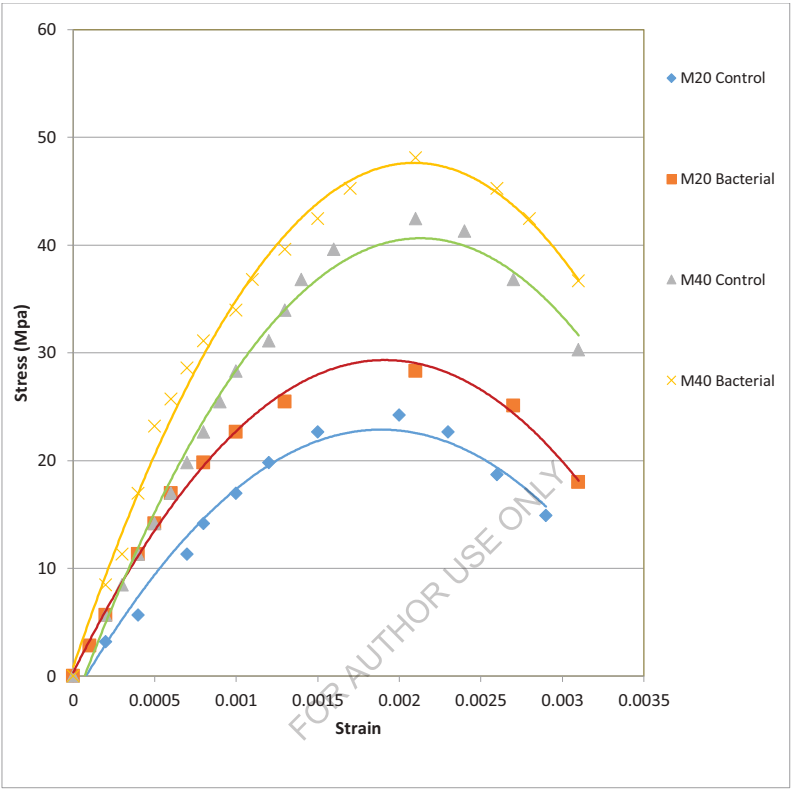

Figure 6.5- Experimental stress-strain curves

Table 6.11- Peak stress values and their corresponding strains

Grade of Concrete	Reference Concrete (NAC)		Bacteria incorporated concrete (Treated FAAC)	
	Peak Stress f_o	Corresponding strain at peak stress ϵ_o	Peak Stress f_o	Corresponding strain at peak stress ϵ_o
M20	24.25	0.0020	28.31	0.0021
M40	42.46	0.0021	48.12	0.0021

6.6.2 Analytical stress- strain curves

6.6.2.1 Proposed Mathematical Model

In order to study the stress-strain behavior of bacteria incorporated concrete, one of the most important steps is to establish appropriate analytic stress-strain models that capture the real (observable) behavior. The better the stress-strain model, the more reliable is the estimate of strength and deformation behavior of concrete structural members. Appropriate analytic stress-strain mathematical model is developed that can capture the real (observable) stress-strain behavior of bacteria induced concrete. This can be done by utilizing the best attributes of earlier models and proposing a stress-strain model that can well represent the overall stress-strain behavior of bacteria incorporated concrete. After obtaining

the stress-strain behavior of reference and bacteria incorporated concrete experimentally, empirical equations are developed to represent uni-axial stress-strain behavior of M20 and M40, grades of reference and bacteria incorporated concretes (Treated FAAC). From these empirical equations, theoretical stresses for reference and bacteria incorporated concrete are calculated and compared with experimental values.

Many models were developed for the stress-strain behavior prediction of concrete by many researchers. Some relevant models are considered below:

1) Desayi's and Krishnan's model (1964)

2) Modified Saenz Model (1964)

3) Hognestad Model (1955)

4) Wang *et al*, Model (1978)

5) Carriera and Chu Model (1985)

Of all the above stress-strain models, simplified and the modified single variable polynomial equations based on modified Saenz's model that fits with the developed normalized stress-strain curves seems to be valid for both ascending and descending portions of the curve. The developed equations for ascending and descending portions of analytical stress-strain curve are in the form of

$$y = \frac{Ax}{1 + Bx + Cx^2} \quad \text{and} \quad y = \frac{Dx}{1 + Ex + Fx^2}$$

where y is the stress at any level ; x is the corresponding strain at that level; A, B, C are the constants for ascending portion and D, E, F are the constants for descending portion of analytical stress-strain curve. Similarly, the equations for ascending and descending portions of non-dimensional stress-strain curve (normalized) are in the form of

$$f / f_o = A^1(\in / \in_o) \ / (1+ B^1(\in / \in_o) + C^1 (\in / \in_o)^2)$$

and

$$f / f_o = D^1 (\in / \in_o) + / (1+ E^1 (\in / \in_o) + F^1(\in / \in_o)^2)$$

A^1, B^1, C^1 are the constants for ascending portion and D^1, E^1, F^1 are the constants for descending portion of non-dimensional stress-strain curve. f / f_o is normalized stress(stress ratio) and $\in / \in_o$ is the normalized strain (strain ratio).

Constants are evaluated based on the boundary conditions of normalized stress-strain curves for both reference and bacteria incorporated concrete.

Boundary conditions for ascending and descending portions of stress-strain curves are,

(1) At the origin the ratio of stresses and strains are zero

i.*e.* at $(\in / \in_o) = 0, (f / f_o) = 0$

(2) The strain ratio $(\in / \in_o)$ and stress ratio at the peak of the non-dimensional stress-strain curve is unity.

i.*e* at $(\in / \in_0) = 1$, $(f / f_o) = 1$

(3) The slope of non-dimensional stress-strain curve at the peak is zero

i.*e* at $(\in / \in_0) = 1.0$, $d(f / f_o) / d(\in / \in_0) = 0$

(4) At 85% stress ratio, the corresponding values of strain ratio is recorded

i.*e* at $(f / f_o) = 0.85$, $(\in / \in_0)$=strain ratio corresponding to 0.85 stress ratio

where f_o - peak stress and $\in_0$ - strain at peak stress ; f and $\in$ corresponds to stress and strain values at any other point.

Boundary conditions (1), (2) and (3) are for determining the constants A^1, B^1, C^1 in the ascending portion of the normalized stress-strain curve and (2), (3) and (4) are for determining the constants D^1, E^1, F^1 in the descending portion of the curve. Corresponding A, B, C constants for ascending portion and D, E, F constants for descending portion of analytical stress-strain curve are then evaluated using equations

$$A = A^1 (f_o / \in_0),\ B = B^1 (1/ \in_0) \text{ and } C = C^1 (1/ \in_0)^2$$

and

$$D = D^1 (f_o / \in_0),\ E = E^1 (1/ \in_0) \text{ and } F = F^1 (1/ \in_0)^2$$

Constants and empirical analytical equations giving the complete stress-strain behavior are developed for reference and bacteria incorporated concretes (Treated FAAC) and are tabulated in tables 6.12 - 6.14below.

Table 6.12 -Constants for ascending and descending portions of non-dimensional stress-strain curve

Grade of Concrete	Reference Concrete						Bacteria incorporated concrete					
	Ascending portion Constants			Descending portion constants			Ascending portion Constants			Descending portion constants		
	A^1	B^1	C^1	D^1	E^1	F^1	A^1	B^1	C^1	D^1	E^1	F^1
M20	1.10	-0.90	1	1.40	-0.60	1	3.68	1.68	1	1.75	-0.25	1
M40	1.40	-0.60	1	2.56	0.56	1	1.78	-0.22	1	1.87	-0.13	1

Table 6.13 -Analytical equations for non-dimensional stress-strain curve

Grade of Concrete	Reference Concrete		Bacteria incorporated concrete	
	Ascending portion	Descending portion	Ascending portion	Descending portion
M20	$y = \frac{1.1x}{1-0.9x+x^2}$	$y = \frac{1.4x}{1-0.6x+x^2}$	$y = \frac{3.68x}{1+1.68x+x^2}$	$y = \frac{1.75x}{1-0.25x+x^2}$
M40	$y = \frac{1.4x}{1-0.6x+x^2}$	$y = \frac{2.56x}{1+0.56x+x^2}$	$y = \frac{1.78x}{1-0.22x+x^2}$	$y = \frac{1.87x}{1-0.13x+x^2}$

Table 6.14-Constants for ascending and descending portions of dimensional analytical stress-strain curve

Grade of Concrete	Reference Concrete					
	Ascending portion Constants			Descending portion constants		
	A	B	C	D	E	F
M20	13338	-450	250000	16975	-300	250000
M40	28092	-286	226757	51807	129	226757
	Bacteria incorporated concrete					
M20	49685	755	250000	23639	-165	250000
M40	40830	14	226757	42616	-62	226757

6.6.2.2 Calculation of Theoretical Stresses

Theoretical stresses have been calculated using proposed empirical equations for reference and bacteria incorporated concrete which are derived from modified Saenz's model in the form of

$$y = \frac{Ax}{1 + Bx + Cx^2}$$ For ascending portion

$$y = \frac{Dx}{1 + Ex + Fx^2}$$ For descending portion

Where y is the stress at any level ; x is the corresponding strain at that level.

After developing empirical equations for stress-strain curves of reference and bacteria incorporated concrete, theoretical values of stresses are calculated at different values of strains in concrete based on the developed empirical equations.

From the stress-strain values of reference and bacteria incorporated concrete grades the corresponding normalized stress-strain values are calculated by dividing each stress value by the peak stress and dividing each strain value by strain at peak stress. After an appropriate model for predicting stress- strain behaviour is selected, empirical equations are developed in the form of $y= Ax/(1+Bx+Cx^2)$ for ascending and descending portions of reference and bacteria incorporated concrete mixes for various grades of concrete in terms of unknown constants. Constants are computed based on the boundary conditions. Theoretical values of stresses are calculated at different values of strains in reference and bacteria incorporated concrete based on the developed empirical equations. These theoretical stress-strain curves are compared with experimental stress-strain curves and found that theoretical stress-strain curves have shown good correlation with experimental stress-strain curves for all grades of reference and bacteria incorporated concretes validating the proposed model adopted to study the stress-strain behavior of M20 and M40, grades of reference and bacteria incorporated concretes (Treated FAAC).

Table 6.15- Experimental and Theoretical Stress –Strain values of M20 grade Reference concrete (NAC)

Experimental Values		Theoretical Values	
σ	E	σ	ε
0.00	0	0.00	0
3.20	0.00023	3.33	0.00023
5.66	0.00035	5.89	0.00035
8.49	0.0005	8.83	0.0005
11.32	0.00068	11.78	0.00068
14.15	0.00082	14.72	0.00082
16.99	0.00103	17.66	0.00103
19.82	0.00122	20.61	0.00122
22.65	0.0015	23.55	0.0015
24.25	0.002	25.22	0.002
22.65	0.00227	23.55	0.00227
18.70	0.00257	19.45	0.00257
14.90	0.00288	15.50	0.00288

Table 6.16 - Experimental and Theoretical Stress –Strain values of M20 grade bacteria incorporated concrete (Treated FAAC)

Experimental Values		Theoretical Values	
σ	E	σ	ε
0.00	0	0.00	0
2.83	0.00006	2.94	0.00006
5.66	0.00015	5.89	0.00015
8.49	0.00025	8.83	0.00025
11.32	0.00037	11.78	0.00037
14.15	0.00047	14.72	0.00047
16.99	0.00062	17.66	0.00062
19.82	0.00082	20.61	0.00082
22.65	0.00099	23.55	0.00099
25.48	0.00132	26.50	0.00132
28.31	0.0021	29.44	0.0021
25.10	0.00266	26.10	0.00266
18.00	0.00312	18.72	0.00312

Table 6.17 - Experimental and Theoretical Stress –Strain values of M40 grade reference concrete (NAC)

Experimental Values		Theoretical Values	
σ	E	σ	ε
0.00	0	0.00	0
2.83	0.00011	2.94	0.00011
5.66	0.00021	5.89	0.00021
8.49	0.00031	8.83	0.00031
11.32	0.0004	11.78	0.0004
14.15	0.00051	14.72	0.00051
16.99	0.00059	17.66	0.00059
19.82	0.00069	20.61	0.00069
22.65	0.00077	23.55	0.00077
25.48	0.00087	26.50	0.00087
28.31	0.00103	29.44	0.00103
31.14	0.00115	32.38	0.00115
33.97	0.00131	35.33	0.00131
36.80	0.00141	38.27	0.00141
39.63	0.00162	41.22	0.00162
42.46	0.00211	44.16	0.00211
41.30	0.00238	42.95	0.00238
36.80	0.00274	38.27	0.00274
30.30	0.00308	31.51	0.00308

Table 6.18 - Experimental and Theoretical Stress –Strain values of M40 grade bacteria incorporated concrete (Treated FAAC)

Experimental Values		Theoretical Values	
σ	E	σ	ε
0.00	0	0.00	0
2.83	0.00007	2.94	0.00007
5.66	0.00013	5.89	0.00013
8.49	0.0002	8.83	0.0002
11.32	0.00027	11.78	0.00027
14.15	0.00033	14.72	0.00033
16.99	0.00038	17.66	0.00038
19.82	0.00043	20.61	0.00043
23.20	0.00052	24.13	0.00052
25.70	0.0006	26.73	0.0006
28.60	0.00071	29.74	0.00071
31.14	0.0008	32.38	0.0008
33.97	0.00095	35.33	0.00095
36.80	0.00114	38.27	0.00114
39.63	0.00126	41.22	0.00126
42.46	0.00145	44.16	0.00145
45.29	0.00169	47.11	0.00169
48.12	0.0021	50.05	0.0021
45.29	0.00258	47.11	0.00258
42.46	0.00275	44.16	0.00275
36.70	0.00306	38.17	0.00306

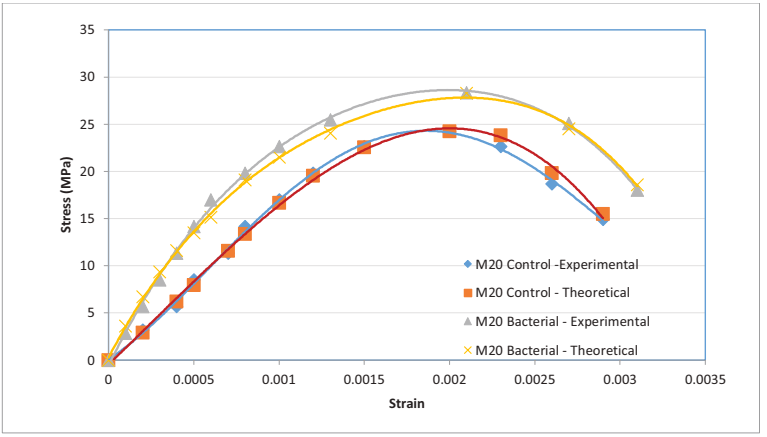

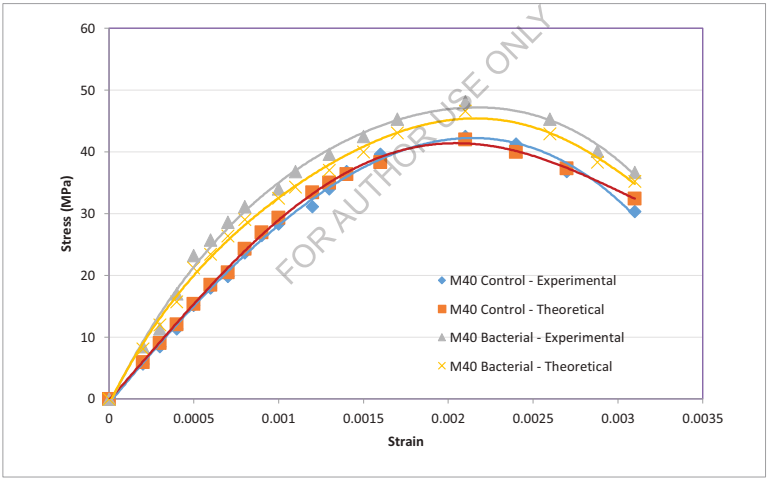

Figure 6.6- Graph showing Experimental and Theoretical stress strain values of reference and bacteria incorporated concrete in M20 and M40 grade concretes

From the observations made from stress-strain curves, the following conclusions are drawn:

Bacteria incorporated concrete has shown improved stress values for the same strain levels compared to that of reference concrete. The strain at peak stress is slightly higher, and the slope of the descending part is steeper due to the decrease in the extent of internal micro cracking in bacteria induced concrete.

The analytical equations for the stress-strain response of reference and bacteria incorporated concrete mixes have been proposed in the form of y = Ax / (1+Bx+Cx2), both for ascending and descending portions of the curves with different set of values for constants.

The results show that the above proposed model was validated against the experimental data and gave good predictions for both ascending and descending branches; it also demonstrates satisfactorily the effect of bacteria on the stress–strain curve.

The results show that the proposed model provides a good simulation to the experimental stress–strain curves. The stress-strain curves obtained in the experiment for different grades of reference and bacteria incorporated concrete exhibit a similar trend as that of stress-strain curves developed from the empirical equations of modified Saenz model. So Saenz mathematical model of second degree polynomial was successfully evaluated and validated for bacteria incorporated concrete to be better fit

to predict the stress-strain behavior of M20 and M40 grades of reference and bacteria incorporated concretes (Treated FAAC).

6.7 Modulus of Elasticity and Toughness

The relationship between stress and strain is important in understanding the basic elastic behavior of concrete in hardened state. From the plotted Stress-Strain curves, modulus of elasticity and modulus of toughness for M20 and M40 grades of reference and bacteria incorporated concretes (Treated FAAC) can be calculated. Modulus of elasticity will indicate the elastic behaviour of the material whereas toughness gives the ability of a material to counteract crack propagation by dissipating deformation energy. Modulus of elasticity can be evaluated from the slope of the stress-strain curve whereas toughness (amount of energy absorbed by the specimen under loading) can be determined by measuring the area (i.e., by taking the integral) underneath the stress-strain curve. Modulus of toughness is the energy needed to completely fracture the material (the total area up to fracture).

Modulus of Toughness and Modulus of Elasticity values of M20 and M40 grades of reference and bacteria incorporated concretes (Treated FAAC) are shown in table 6.19. The average value of area under stress-strain diagram for different grades of concrete for reference and bacteria incorporated concrete mixes are computed to evaluate energy absorption capacity. Toughness or energy absorption capacity of different grades of bacteria incorporated concrete mixes has shown an increase of 14-26% when

compared to same grades of reference concrete mixes. Materials showing good impact resistance are generally those with high moduli of toughness. It was observed that Modulus of Elasticity (E) is relatively more for all grades of bacteria incorporated concrete than the reference concrete by about 14-21%.

Table 6.19 - Modulus of Toughness and Elasticity values for different grades of reference and bacteria incorporated concretes

Grade of Concrete	Modulus of Toughness (MPa)		Secant Modulus Of Elasticity (GPa)	
	Reference Concrete	Bacteria incorporated concrete	Reference Concrete	Bacteria incorporated concrete
M20	0.035	0.044	22.4	27.2
M40	0.066	0.075	32.2	36.7

It can be concluded that toughness or energy absorption capacity of bacteria incorporated concrete of various grades are more when compared to same grades of reference concrete due to its enhanced ability to counteract crack propagation by dissipating deformation energy. High moduli of toughness in bacteria incorporated concrete signify its improved shock resistance. It is observed that modulus of elasticity (E) is relatively more for both grades of concrete in which bacteria is induced than the

reference concrete indicating its enhanced performance due to dense microstructure of bacteria incorporated concrete.

6.8 Flexural Behavior of fly ash aggregate bacterial concrete reinforced beams

To study the flexural behaviour of M20 and M40 grades of reference (NAC) (NAC) and bacteria incorporated concretes (Treated FAAC) under reinforced beams of size 1200 x 100 x 150 mm were cast and tested under third point loading and their behaviour in flexure was investigated to understand fly ash aggregate based *Sporosarcina pasteurii* bacterial strain incorporated concrete beams deflection characteristics and cracking behavior. Based on limit state method, the reinforcement required for balanced section was calculated first and then the amount of reinforcement for under-reinforced section was determined. The beams are tested under symmetrical two-point flexural loading as per IS: 9399 – 1979. From the above investigations, the parameters observed are first crack load, pre-cracking and post-cracking behavior, deflection pattern, crack development pattern and ultimate load carrying capacity of bacterial concrete beams. The beam sizes and length were chosen to ensure that the beams would fail in flexure. The beam dimensions were also sufficiently large to simulate a real structural element. The beam details are shown in Table 6.20 below and Fig 6.7 below shows reinforcement arrangement.

The beam specimen is 100 x 150 mm in cross-section and 1200 mm in length and simply supported over an effective span of 1000 mm. The clear cover of the beam was 20 mm. The geometry of the beam specimens is shown in Figure 6.7 below.

Table 6.20- Flexure Test beam details

Grade of Concrete	Grade of Steel	Tensile Reinforcement	Nominal Compression Reinforcement	Shear Reinforcement	Beam dimensions
M20	Fe 415	2 No - 10mmφ Tor steel bars	2 No - 6mm φ MS bars	2 legged - 6mm φ @75mm c/c	100 mm x 150 mm x 1200 mm
M40	Fe 415	2 No - 12mmφ Tor steel bars	2 No - 6mm φ MS bars	2 legged - 6mm φ @75mm c/c	100 mm x 150 mm x 1200 mm

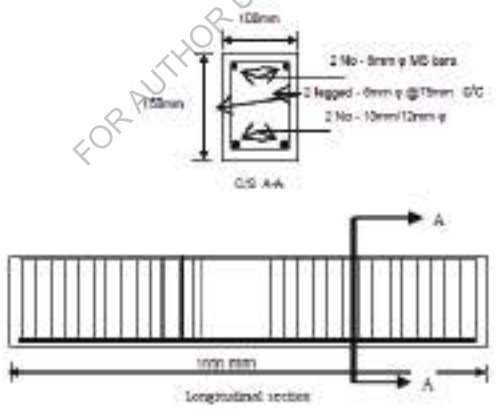

Figure 6.7 - The beam reinforcement details

In the pure bending zone (middle third), no stirrups were provided so as not to influence crack development in the constant moment zone. Two 6

mm steel bars were used as top reinforcement to hold stirrups in place in the shear span zone.

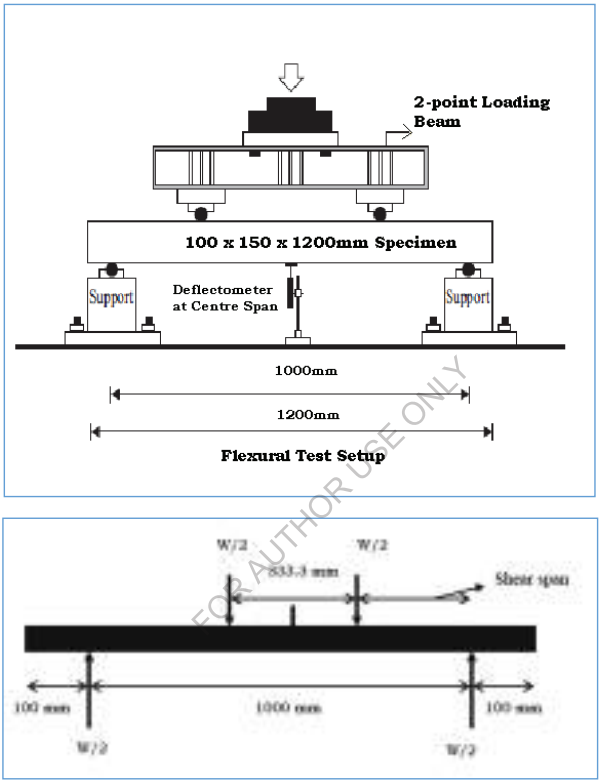

Figure 6.8 - Flexural Test Set up – Schematic Diagram

The test setup for the flexural test is shown in Figure 6.8. The test specimen was mounted in a UTM of 1000 kN capacity. The supports of the beam rested on an adjustable steel rollers. Dial gauges of 0.01 mm least count were used for measuring the deflections under the load points and

at mid span for measuring the deflection. The dial gauge readings were recorded at different loads.

One day before the testing, the cured beams are white washed and the locations of supports; load points and the central deflection gauge are marked with a pencil. Beams are subjected to symmetrical two-point flexural loading under strain rate control. Dial gauges of 0.001 mm least count were used for measuring the deflections at mid span for measuring the deflection. The dial gauge readings were recorded at different loads until failure. The load was applied at intervals of 2.5kN/sec until the first crack was observed. Subsequently, the load was applied in increments of 5kN/sec. The behavior of the beam was observed carefully and the first crack was identified using a hand held microscope. The failure mode of the beams was also recorded. Deflections at the central point and the ultimate load carrying capacity (Peak load) are measured for M20 and M40 grades of reference (NAC) (NAC) and bacteria incorporated concretes (Treated FAAC) under reinforced beams. The test is continued until the load drops to 15-20% of peak load recorded, in the descending portion of load deflection curves. At that stage the testing is stopped by gradually unloading.

The load was applied at intervals of 3kN/min. The behaviour of the beam was observed carefully and the first crack was identified with magnifying glass. The deflections and strain values were recorded for respective load increments until failure. The failure mode of the beams was also recorded.

The flexural test results for under-reinforced M20 and M40 grades of reference (NA) and bacteria incorporated (Treated FAAC) reinforced concrete beams are shown in Tables 6.21 – 6.24 below.

Table 6.21 – Flexural test results of M20 Under-reinforced Reference (NAC) concrete beam made with natural aggregate

M20-NA				
Load kN	Deflection Mm		1/R	Moment kN.m
	Centre	Under Load		
0	0	0	0	0
4	0.08	0.05	0	0.667
8	0.13	0.09	7.84E-07	1.333
12	0.24	0.21	7.84E-07	2.000
16	0.26	0.24	1.57E-06	2.667
20	0.32	0.26	1.57E-06	3.333
24	0.42	0.33	2.35E-06	4.000
28	0.55	0.39	2.35E-06	4.667
32	0.67	0.52	2.74E-06	5.333
36	0.82	0.61	3.14E-06	6.000
40	0.97	0.81	3.53E-06	6.667
44	1.11	0.93	3.92E-06	7.333
48	1.27	1.05	4.71E-06	8.000
52	1.53	1.2	4.71E-06	8.667
56	1.69	1.44	5.1E-06	9.333
60	1.76	1.61	5.88E-06	10.000
64	1.96	1.68	5.88E-06	10.667
68	2.16	1.88	6.67E-06	11.333
72	2.37	2.06	7.06E-06	12.000
76	2.56	2.23	7.06E-06	12.667
80	2.73	2.41	7.84E-06	13.333
83	2.84	2.59	8.23E-06	13.833

Table 6.22 – Flexural test results of M40 – Under-reinforced Reference (NAC) concrete beam made with natural aggregate

M40-NA				
Load kN	Deflection mm		1/R	Moment kN.m
	Centre	Under load		
0	0	0	0	0.000
5	0.11	0.06	1.21E-06	0.833
10	0.23	0.14	1.62E-06	1.667
15	0.35	0.23	2.43E-06	2.500
20	0.47	0.32	2.83E-06	3.333
25	0.59	0.41	3.64E-06	4.167
30	0.71	0.51	3.64E-06	5.000
35	0.83	0.61	4.45E-06	5.833
40	0.95	0.72	5.66E-06	6.667
45	1.08	0.83	6.47E-06	7.500
50	1.21	0.94	7.68E-06	8.333
55	1.34	1.05	8.49E-06	9.167
60	1.47	1.16	9.3E-06	10.000
65	1.62	1.28	1.09E-05	10.833
70	1.77	1.4	1.21E-05	11.667
75	1.92	1.53	1.29E-05	12.500
80	2.07	1.66	1.37E-05	13.333
85	2.22	1.79	1.45E-05	14.167
90	2.37	1.93	1.54E-05	15.000
95	2.53	2.06	1.62E-05	15.833
100	2.69	2.2	1.74E-05	16.667
105	2.85	2.34	1.82E-05	17.500
110	3.02	2.48	1.9E-05	18.333
115	3.19	2.63	2.02E-05	19.167
120	3.37	2.78	2.14E-05	20.000
125	3.55	2.93	2.26E-05	20.833
130	3.77	3.08	2.38E-05	21.667
135	4.03	3.28	2.63E-05	22.500
140	4.29	3.54	2.79E-05	23.333
145	4.55	3.8	2.95E-05	24.167
150	4.81	4.06	3.23E-05	25.000
155	5.07	4.32	3.52E-05	25.833
160	5.51	4.76	3.8E-05	26.667
165	6.05	5.3	4.2E-05	27.500
170	7.34	6.59	9.18E-05	29.833

Table 6.23 – Flexural test results of M20 – Under-reinforced bacteria incorporated concrete made with treated fly ash aggregates (FAAC)

M20 –RA-10%GGBS				
Load kN	Deflection mm		1/R	Moment kN-m
	Centre	Under load		
0	0	0	0	0
4	0.09	0.06	0	0.667
8	0.19	0.09	7.83E-07	1.333
12	0.28	0.11	7.83E-07	2.000
16	0.38	0.16	1.57E-06	2.667
20	0.53	0.19	1.57E-06	3.333
24	0.65	0.21	2.35E-06	4.000
28	0.77	0.39	2.74E-06	4.667
32	0.89	0.43	3.52E-06	5.333
36	0.99	0.55	3.92E-06	6.000
40	1.17	0.68	4.7E-06	6.667
44	1.35	0.81	5.48E-06	7.333
48	1.59	0.91	6.27E-06	8.000
52	1.67	1.06	7.05E-06	8.667
56	1.89	1.21	7.83E-06	9.333
60	2.09	1.38	8.62E-06	10.000
64	2.25	1.56	9.4E-06	10.667
68	2.45	1.74	1.02E-05	11.333
72	2.63	1.91	1.14E-05	12.000
76	2.85	2.08	1.25E-05	12.667
80	3.11	2.33	1.45E-05	13.333
84	3.43	2.65	1.68E-05	14.000
87	4.11	3.19	2.08E-05	14.500

Table 6.24 – Flexural test results of M40 – Under-reinforced bacteria incorporated concrete made with treated fly ash aggregates (FAAC)

M40 –RA-10%GGBS				
Load kN	Deflection mm		1/R	Moment kN.m
	Centre	Under load		
0	0	0	0	0.000
5	0.1	0.07	7.83E-07	0.833
10	0.21	0.15	1.57E-06	1.667
15	0.33	0.23	2.35E-06	2.500
20	0.45	0.32	3.13E-06	3.333
25	0.57	0.4	3.91E-06	4.167
30	0.69	0.51	4.31E-06	5.000
35	0.81	0.61	5.09E-06	5.833
40	0.93	0.72	6.26E-06	6.667
45	1.05	0.83	7.04E-06	7.500
50	1.18	0.94	7.83E-06	8.333
55	1.31	1.05	9E-06	9.167
60	1.44	1.16	9.78E-06	10.000
65	1.57	1.27	1.06E-05	10.833
70	1.71	1.41	1.17E-05	11.667
75	1.85	1.54	1.29E-05	12.500
80	1.99	1.66	1.33E-05	13.333
85	2.13	1.79	1.41E-05	14.167
90	2.27	1.93	1.49E-05	15.000
95	2.41	2.06	1.57E-05	15.833
100	2.56	2.2	1.64E-05	16.667
105	2.71	2.33	1.72E-05	17.500
110	2.86	2.47	1.8E-05	18.333
115	3.01	2.62	1.88E-05	19.167
120	3.16	2.76	2E-05	20.000
125	3.32	2.92	2.11E-05	20.833
130	3.48	3.07	2.23E-05	21.667

135	3.64	3.26	2.31E-05	22.500
140	3.8	3.42	2.43E-05	23.333
145	3.98	3.6	2.62E-05	24.167
150	4.24	3.86	2.86E-05	25.000
155	4.55	4.17	3.13E-05	25.833
160	4.93	4.55	3.44E-05	26.667
165	5.5	5.12	3.84E-05	27.500
170	6.34	5.96	4.46E-05	28.333
175	7.81	7.43	8.3E-05	29.167

Flexural behaviour characteristics of Under-reinforced Concrete beams made with natural aggregate (NA) and treated fly ash aggregate (FAA) are presented in Tables 6.25 and 6.26 below.

Table 6.25 – Flexural behaviour characteristics of Under-reinforced Concrete beams made with natural aggregate (NAC)

Grade of the Concrete Beam	Service load kN	Load at first crack (kN)	Ultimate Flexural Strength (kN)	Deflection at service load mm	Central Deflection at Failure (mm)	Deflection Under load at failure (mm)	Maximum Crack width at failure (mm)
M20	29	32	83	2.38	2.84	2.59	0.96
M40	49	65	170	3.72	7.34	6.59	1.14

Table 6.26 – Flexural behaviour characteristics of Under-reinforced bacteria incorporated concretes (Treated FAAC) beams

Grade of the Concrete Beam	Service load kN	Load at first crack (kN)	Ultimate Flexural Strength (kN)	Deflection at service load mm	Central Deflection at Failure (mm)	Deflection Under load at failure (mm)	Maximum Crack width at failure (mm)
M20	29	40	87	2.13	4.11	3.19	0.91
M40	49	70	175	3.69	7.81	7.43	1.09

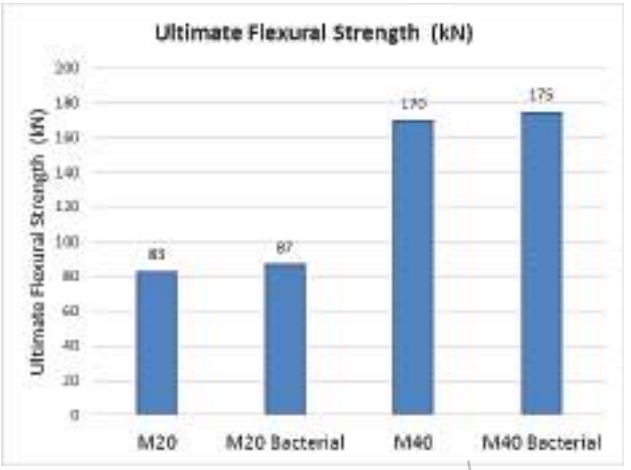

Figure 6.9 - Ultimate Flexural Strength of M20 and M40 grades of reference (NAC) and bacteria incorporated concretes (Treated FAAC) beams

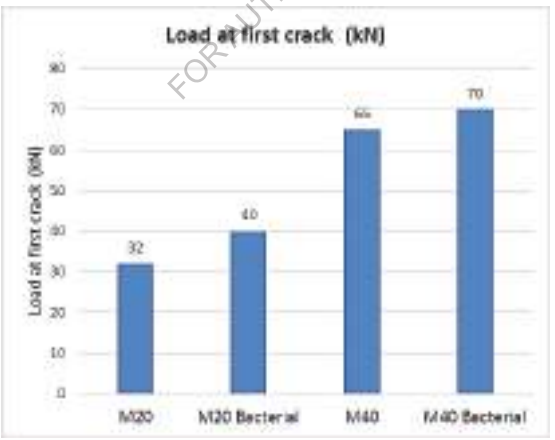

Figure 6.10 -Load at first crack of M20 and M40 grades of reference (NAC) and bacteria incorporated concretes (Treated FAAC) beams

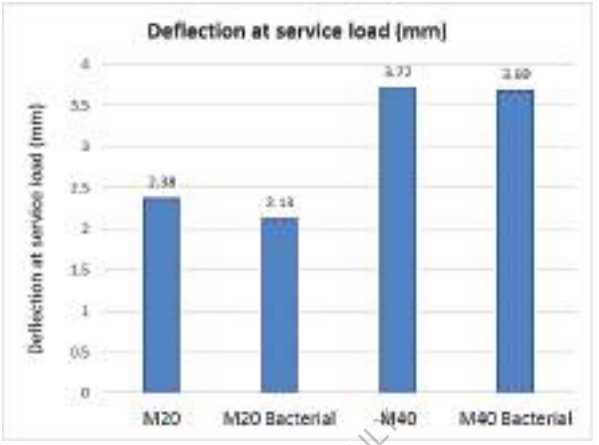

Figure 6.11- Deflection at service load of M20 and M40 grades of reference (NAC) and bacteria incorporated concretes (Treated FAAC) beams

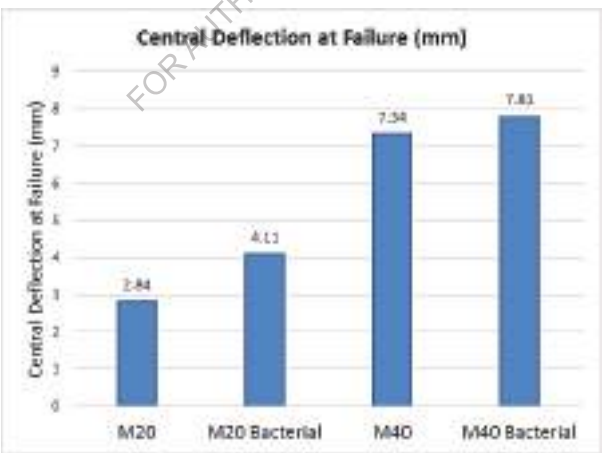

Figure 6.12- Central deflection at failure M20 and M40 grades of reference (NAC) and bacteria incorporated concretes (Treated FAAC) beams

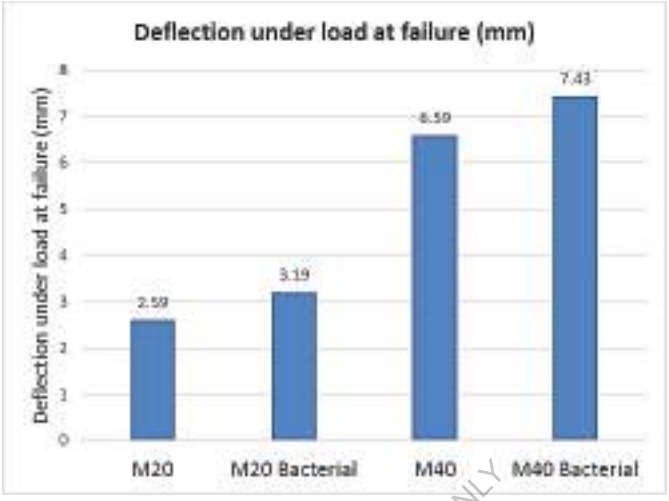

Figure 6.13 - Deflection under load at failure of M20 and M40 grades of reference (NAC) and bacteria incorporated concretes (Treated FAAC) beams

6.8.1 Theoretical Computation of Moments and Curvatures

Beams of under-reinforced are tested under two point loading and its load-deflection, moment curvature behaviour were investigated. The experimental results of moments have been analyzed by developing procedures for obtaining the complete theoretical moment-curvature diagrams. The models proposed for stress-strain behaviour of concrete mixes are used as the basis for prediction of the analytical behaviour of moment-curvature and in deriving the expressions of the resisting moments and curvatures. For obtaining the complete moment curvature relationship for any cross-section, discrete values of concrete strains (Є)

were selected such that even distribution of points on the plot, both before and after maximum was obtained.

The procedure used in the computation is given below.

1. For a selected values of Єc , the extreme fibre concrete strain, a neutral axis depth 'nd' is assumed initially.
2. For the assumed value of 'nd' the compressive force C_c and the value of moment M_c of this resultant compressive force about assumed neutral axis is calculated.
3. The strain in tension steel Єs is calculated on the basis of strain compatibility. Єc /nd= Єs /(d-nd)
4. The tensile force Ts, in the tension steel is arrived at by taking the corresponding stress from stress-strain diagram of steel and multiplying with the area of steel. The corresponding moments Ms about the assumed neutral axis is Ms= Ts (d-nd).
5. The values of C_c and T_s are compared. If C_c and T_s are same, then the assumed position of neutral axis is correct. Then moment M_c and curvature $Ø_c$ are calculated for a particular fibre strain.
6. If C_c is not equal to T_s a new value of neutral axis depth is assumed based on judgment whether C_c is greater or smaller than T_s .The above procedure is repeated until the equilibrium condition $C_c = T_s$ is satisfied.
7. The assumption made is variation of strain across the section is linear up to failure.

8. Displacement control is used to obtain complete profile of moment-curvature behavior, especially in the post ultimate region. Moment-curvature diagram is generated for all the beams based on the characteristic stress – strain diagram. The experimental values of moments and curvatures are plotted as discrete points on the moment-curvature diagrams. The experimental ultimate moments and theoretical moments computed based on the characteristic stress-strain curve of reinforced concrete are represented on a correlation diagram.

6.8.1.1 Calculation of neutral axis depth

The value of "nd" is calculated by equating force in tension and force in compression

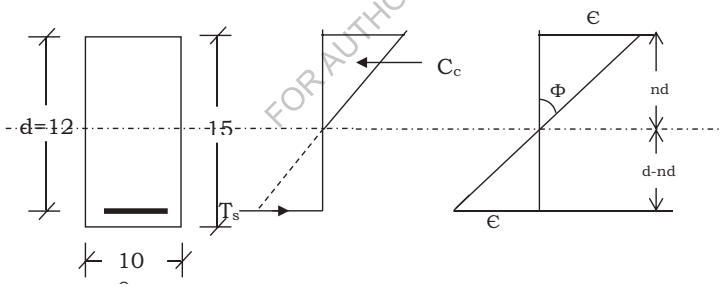

Distribution of stresses and strains over a cross- section

(1) Force in compression (C_c) can be obtained by

$$C_c = \frac{b.n.d}{Є} \int_0^{Є} \sigma \, d\varepsilon$$

Where $\sigma = \frac{A^1 \, Є}{1+B^1Є^2}$ where $A1 = (A.\sigma_0) / Є_0$ and $B^1 = B/Є_0^2$

$$\int \sigma \, d\varepsilon = \frac{A^1}{2\,B^1} \log (1 + B^1 \epsilon^2)$$

The constants A^1 and B^1 (constants for dimensional stress –strain curve) As two separate equations are proposed for ascending and descending portions of the stress-strain curve

$$C_c = \frac{b\,(nd)}{\epsilon} \left\{ \int_0^{\epsilon_0} \sigma_1 \, d\varepsilon + \int_{\epsilon_0}^{\epsilon_{0.85}} \sigma_2 \, d\varepsilon \right\}$$

σ_1 - Corresponds to ascending portion of stress-Strain curve

σ_2 - Corresponds to descending portion of stress-strain curve

(2) Force in tension (T_s) can be obtained by $T_s = A_{st} \times \sigma_{st}$

Where σ_{st} - is stress in steel and A_{st} - area of tensile reinforcement

The strains in tension steel are calculated based on the strain-compatibility and σ_{st} is arrived by taking the corresponding stresses from the stress-strain diagram of steel. Knowing the values of A^1 and B^1 for ascending and descending portions of stress-strain curves of all grades of concrete mixes made with recycled aggregate, for known values of strain in extreme fibre of concrete ϵ (say 0.0002, 0.0004 ---), the values of C_c and T_s can be determined.

Initially assuming n = 0.5d and ϵ = 0.0002, C_c and T_s can be determined. For equilibrium, $C_c = T_s$ should be satisfied. Hence for a given value of ϵ, by changing the values of 'n' till $C_c = T_s$ is satisfied, the neutral axis depth

coefficient 'n' for that given value of Є can be determined. By repeating the process, values of n for different values of Є can be determined. This is continued till Є = $Є_{0.85}$ or $1.9Є_{0.}$

Using the above procedure, for Є = 0.0002 the value of 'n' which satisfies $C_c=T_s$ is calculated. By changing the values of Є with increments of 0.0002 corresponding values of 'n' are calculated.

6.8.1.2 Moment of Resistance of concrete and steel

From the basics stress- strain compatibility of steel and concrete the theoretical moment – curvatures have been developed.

The moment of resistance offered by the concrete (M_c) can be determined by

$$M_c = b\,(n.d/Є)^2 \int_0^{Є} \sigma\, Є\, d\varepsilon$$

Where $\sigma = \dfrac{A^1\, Є}{1+B^1Є^2}$ and

$$\int \sigma\, Є d\varepsilon = \left[\frac{A^1}{B^1}.\, Є\right] - \left[\frac{A^1}{B^1\sqrt{B^1}}.\, \mathrm{Tan}^{-1}\,(\sqrt{B^1}.\, Є)\right]$$

As two separate equations are proposed for ascending and descending portions of the stress-strain curve

$$M_c = b\,(nd/Є)^2 \left\{ \int_0^{Є_0} \sigma_1\, Є\, d\varepsilon + \int_{Є_0}^{Є_{0.85}} \sigma_2\, Є\, d\varepsilon \right\}$$

$$= bd^2\,(n/Є)^2 \left\{ \int_0^{Є_0} \sigma_1\, Є\, d\varepsilon + \int_{Є_0}^{Є_{0.85}} \sigma_2\, Є\, d\varepsilon \right\}$$

For the given values of b, d and Є, the value of M_c for different values of 'n' can be determined using above relationship.

The moment of resistance offered by steel (M_s) can be determined by

$M_s = T_s (d-nd)$

$= \sigma_{st} \times Ast (d-nd)$

As the values of b, d, A_{st}, A^1, B^1, neutral axis depth and Ts for different values of Є are already known, just by substituting these values in the expressions of M_c and M_s, the moment of resistance offered by concrete and steel can be determined.

The moment of resistance 'M' of the section can be determined by moment of resistance offered by concrete and steel.

Knowing the values of Є and n, theoretical curvature (Φ) can be determined from strain distribution diagram. The curvature is given by the relationship $\Phi = (Є / n.d)$. The values of M are the theoretical moment values, knowing the values of Є and n, theoretical curvatures are calculated using the relation $\Phi = (Є / n.d)$ and the results are tabulated. Thus theoretical moment curvature values are calculated for M20 and M40 grades of reference (NAC) (NAC) and bacteria incorporated concretes (Treated FAAC) under reinforced beams.

The theoretical moment curvature values has been validated by conducting an experimental moment curvature values of M20 and M40 grades of reference (NAC) and bacteria incorporated concretes (Treated

FAAC) beams. The correlation between experimental and analytical values of moments and curvatures are arrived at.

6.8.1.3 Sample calculations

Deflection in mm= dial gauge reading X L.C (0.01)

- *Ec = (201.46- top strain gauge reading)/ 201.46*
- *Et = (bottom strain gauge reading -200.3)/ 200.3*
- *1/ R = (Ec + Et)/ d*
- *Support reaction = load/ 2*
- *Distance of support from application of load L/ 3 where L is 1m.*

So Maximum Moment in kN-m = (load/ 2)(L/ 3)*

= (load x L)/ 6 = load x 1.2 m/ 6

6.8.2 Load-Deflection and Moment –Curvature Relations

Deflections were measured at the central point and under the load using the deflection meters. The values of moments and curvatures are obtained. Load-deflection behavior of M20 and M40 grades of reference (NAC) and bacteria incorporated concretes (Treated FAAC) beams were studied using load –deflection plots.

Moment curvature relationships are very important to assess out ductility of the structure and the amount of possible redistribution of stresses. Ductility is the deformation capacity of a member or structure after the first yield. It gives a measure of energy dissipation capacity of a member or structure. Work done on a structure after yield cannot be stored in the material so it is converted into heat energy and is dissipated to the environment. Energy dissipation is desirable for structures because the heavy energy imparted by the ground motions, etc., are to be released.

The deformations measured are divided by the gauge length (200mm) to obtain the strains at the particular level. From the top and bottom strains, the average curvatures were calculated. Moment- curvature behavior of M20 and M40 grades of reference (NAC) and bacteria incorporated concretes (Treated FAAC) beams are also studied. From these results, M-Φ diagrams are plotted for under -reinforced M20 and M40 grades of reference (NAC) and bacteria incorporated concretes (Treated FAAC) beams are plotted.

The experimental results of moments have been analyzed by developing procedures for obtaining the complete theoretical moment-curvature diagrams. The models proposed for stress-strain behaviour of concrete mixes are used as the basis for prediction of the analytical behaviour of moment-curvature and in deriving the expressions of the resisting moments and curvatures. The models proposed for stress-strain behaviour of M20 and M40 grades of reference (NAC) and bacteria incorporated concretes (Treated FAAC) beams are used as the basis for prediction of the analytical behaviour of moment-curvature. The moment of resistance offered by the concrete (M_c) can be determined by $M_c = b (nd/\epsilon)^2 \int \sigma \epsilon \, d\varepsilon$

Where $\sigma = \frac{A^1 \epsilon}{(1+B^1\epsilon^2)}$ and

$$\int \sigma \epsilon d\varepsilon = \frac{A^1}{B^1}\epsilon - \frac{A^1}{B^1\sqrt{B^1}} \mathrm{Tan}^{-1} \sqrt{B^1}\ \epsilon$$

As two separate equations are proposed for ascending and descending portions of the stress-strain curve

$$M_c = b\,(nd/\epsilon)^2 \left\{ \int_0^{\epsilon_0} \sigma_1\, \epsilon\, d\varepsilon + \int_{\epsilon_0}^{\epsilon_{0.85}} \sigma_2\, \epsilon\, d\varepsilon \right\}$$

The moment of resistance offered by steel (Ms) can be determined by

$M_s = Ts\,(d-nd) = \sigma st \times Ast\,(d-nd)$

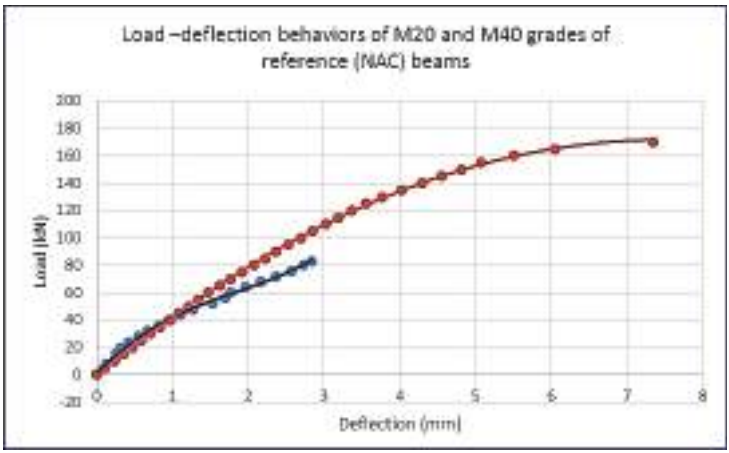

Figure 6.14 - Load –deflection behaviors of M20 and M40 grades of reference (NAC) beams

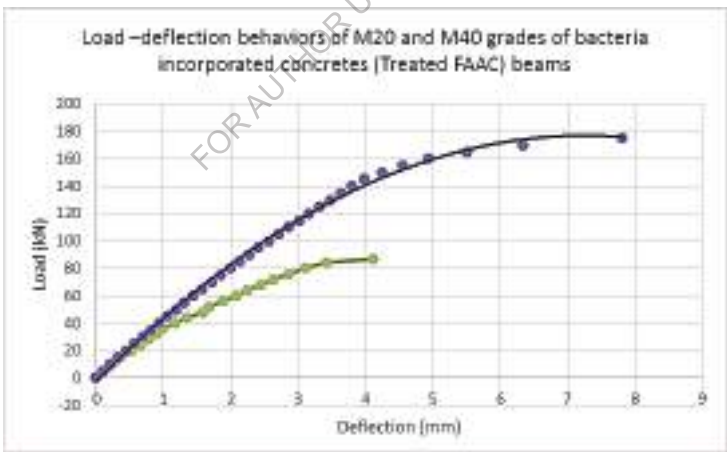

Figure 6.15 - Load –deflection behaviors of M20 and M40 grades of bacteria incorporated concretes (Treated FAAC) beams

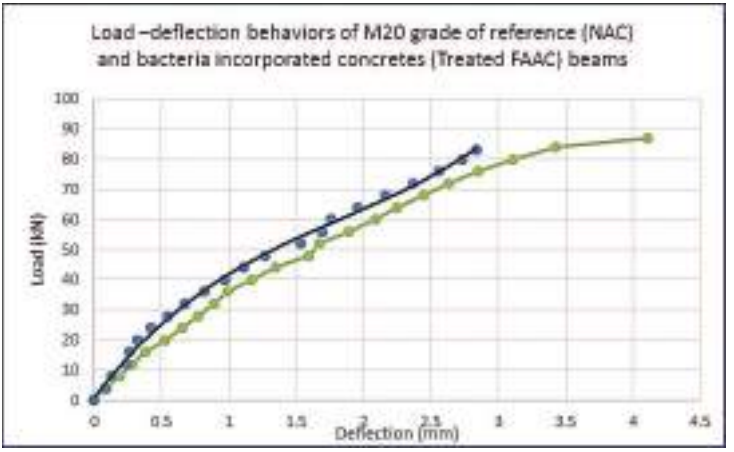

Figure 6.16 - Load –deflection behaviors of M20 grade of reference (NAC) and bacteria incorporated concretes (Treated FAAC) beams

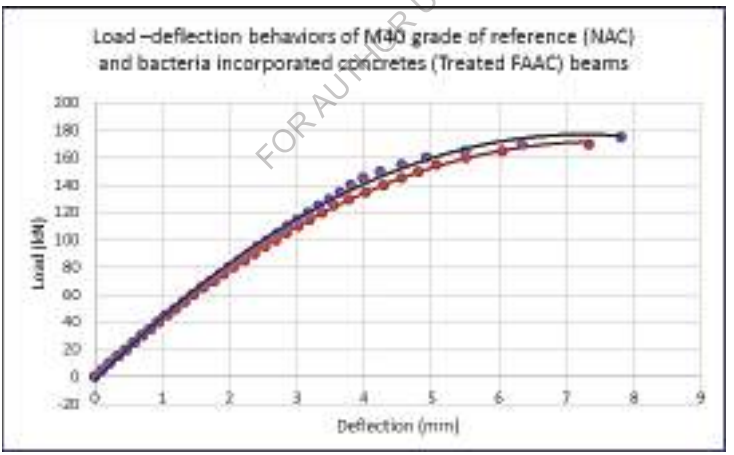

Figure 6.17 - Load –deflection behaviors of M40 grades of reference (NAC) and bacteria incorporated concretes (Treated FAAC) beams

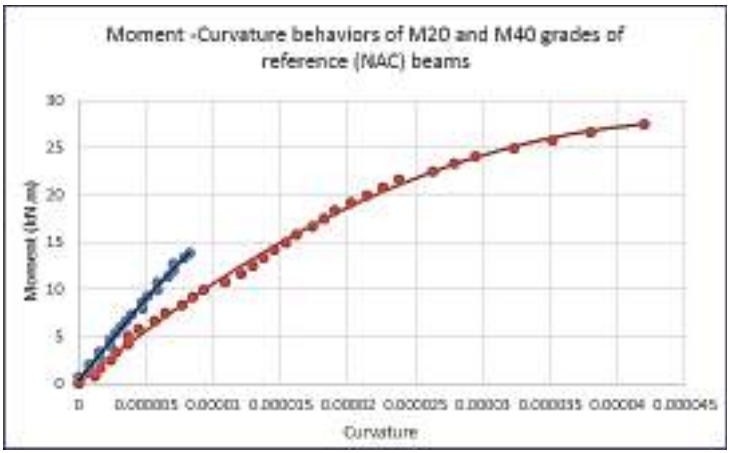

Figure 6.18 - Moment -Curvature behaviors of M20 and M40 grades of reference (NAC) beams

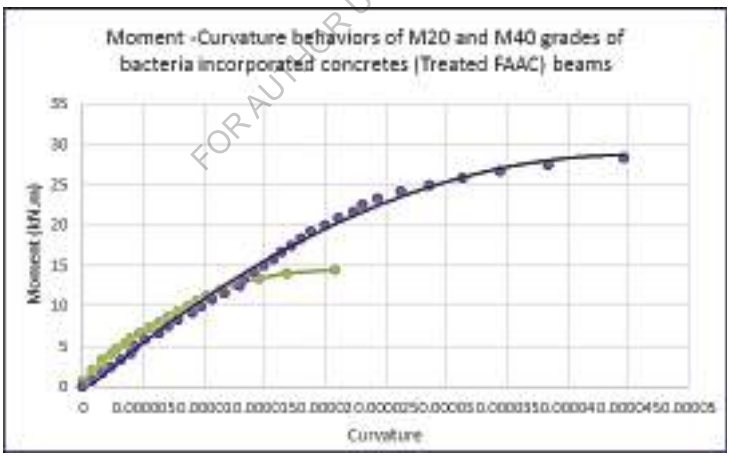

Figure 6.19 - Moment -Curvature behaviors of M20 and M40 grades of bacteria incorporated concretes (Treated FAAC) beams

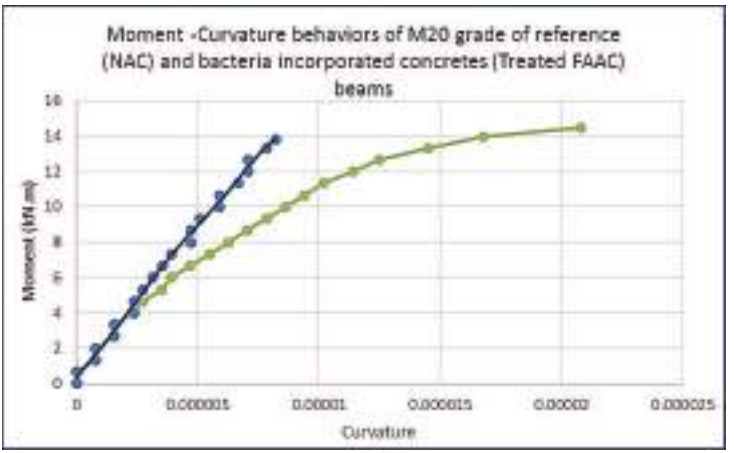

Figure 6.20 - Moment -Curvature behaviors of M20 grade of reference (NAC) and bacteria incorporated concretes (Treated FAAC) beams

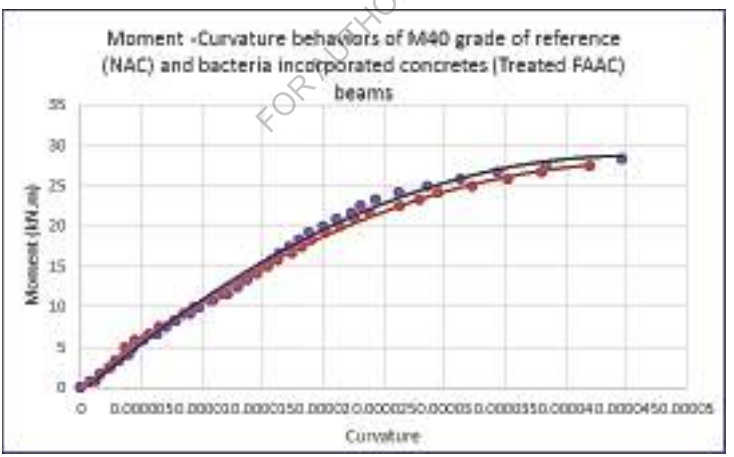

Figure 6.21 - Moment -Curvature behaviors of M40 grades of reference (NAC) and bacteria incorporated concretes (Treated FAAC) beams

No horizontal cracks were noticed at the level of the reinforcement indicating that there was no occurrence of bond failure. Vertical flexural cracks were observed in the middle third region (constant moment) and ultimate failure occurred due to crushing of the compression concrete with significant amount of deflection. The flexure cracks were the first to initiate in the Constant Bending moment Zone (middle third) as expected. Loads at first crack in bacteria incorporated concretes (Treated FAAC) beams are higher than the concrete made with natural aggregate concrete beams in all grades by 1.2 times confirming that microbiologically treated fly ash aggregate bacterial concrete beams offer greater resistance to cracking. First crack formation was delayed in microbiologically treated fly ash aggregate bacterial concrete beams due to its dense micro structure with low pore fraction and reduced pore size due to which fatigue strength is increased which in turn increases the time taken for first crack occurrence and thereby increasing the load carrying capacity. The deflection at the mid span increased in reinforced bacterial concrete beams which indicates the improved flexural stiffness of the elements thereby reducing the structural member's deformability. Mid-span deflections at peak load reduced as the grade of the concrete increases. The ultimate deflection in case of bacterial concrete beams is about 10-20 % more than that of conventional aggregate reinforced beams.

From the above investigations, it can be concluded that, the ultimate flexural strength of bacterial concrete beams have improved significantly when compared with natural aggregate reinforced beams due to better bond strength at the interfacial zones. The recovery of deflection after removal of the load was more in case of bacterial concrete beams indicating more elastic behaviour. Thus bacterial concrete beams are more suitable to take fatigue loads than natural aggregate reinforced beams. From the above investigations it is evident that the load at first crack, cracking behavior, deflection pattern, crack development pattern and ultimate load carrying capacity of bacterial concrete beams have improved enormously. Hence bacterial concrete beams will have dense micro structure with low pore fraction and reduced pore size due to which fatigue strength is increased which in turn increases the first crack load and the ultimate load carrying capacity in case of flexural loading.

For under reinforced beams with the increase in load the multiple cracks increased. After the multiple cracking stages, it is found that there is yield in steel so the P-δ curve become more or less flat till the ultimate load is reached. On further increase in load a drop in the load is observed with propagation of cracks. All the beams failed by compression of concrete and the load deformation curves are plotted up to failure stage. The same behavior was noticed in all the under-reinforced bacterial concrete beams. The differences noticed in the load deflection behavior of recycled aggregate beams and natural aggregate beams are the increase in the horizontal

plateau of the load-deflection curve and the increase in load at first crack and ultimate load in bacterial concrete beams than that in natural aggregate beams.

These moment curvature plots for under reinforced bacterial concrete beams observed to follow the similar pattern as that of load deflection plots of natural aggregate beams.

All the beams exhibited a tension failure which is a ductile failure. The cracks are accompanied by pronounced bulging. When the load is further increased, cracks propagated towards the top of the beam. As the beams are forced to deform further, the cracks became more pronounced and the concrete crushed at one or both the ends. With further increase in beam deflection, the load decreased, accompanied by concrete spalling. This crack pattern is observed to be same for all the natural aggregate and bacterial concrete beams.

Figure 6.22- Crack pattern of M20 and M40 grades of reference (NAC) and bacteria incorporated concretes (Treated FAAC) beams

In under-reinforced M20 and M40 grades of reference (NAC) and bacteria incorporated concretes (Treated FAAC) beams, the deflections at service loads are less than the maximum permissible deflection of 4.8 mm *i.e* Span/250 specified by IS 456-2000. Thus the reinforced fly ash aggregate bacterial concrete beams does not violate the serviceability norms of the codes of practice.

The load deflection and moment –distribution behaviour of M20 and M40 grades of reference (NAC) and bacteria incorporated concretes (Treated FAAC) beams is observed to be similar except the increased values of loads at ultimate and at first crack bacteria incorporated concrete.

In under reinforced beams with the increase in moment, curvature increased gradually up to the multiple cracking stages and beyond, and later curvature increased drastically at constant moment or with small variation in the moment. The M-Φ curve is more or less flat till the ultimate moment is reached. As all the beams failed by compression of concrete the moment curvature plots are drawn up to failure stage. The behaviour is similar in all grades of the under-reinforced bacterial concrete beams.

Load at first crack occurred during the experiment and also first crack load is determined from load-deflection plot corresponding to the point on the curve at which the curve deviated from linearity is observed. Load at first crack increased in bacteria incorporated beams which is due to the bond between the concrete and steel in beams due to formation of bacterial calcite precipitates. In bacterial concrete beams, the bondage is more

which arrests the micro cracks developed in the matrix which results in requirement of more energy. This lead to an improvement in load at first crack.

In under-reinforced beams after the multiple cracking stages, the yielding of steel was found to be more, and ultimate load corresponds to the yielding of steel and crushing of concrete. When micro cracks develop in the bacteria incorporated cement matrix, the microbially produced calcite precipitates will fill such micro cracks and prevent further propagation. Hence there is increase the ultimate load, as the cracks that appear inside the matrix will take meandering path, resulting in the demand for more energy for future propagation. The bacterial reinforced beams have shown improved ultimate load values compared to that of natural aggregate reinforced cement concrete beams.

The deflection at service load is determined from load deflection plot corresponding to a load of Pu/1.5. Deflections observed from the load-deflection curves for all the specimens at service loads (P_u/1.5) are less than the maximum permissible deflection of 4.8mm i.e span/250 specified by IS 456-2000.

From the crack pattern observed in under-reinforced reference (NAC) beams (NAC), the visible flexural cracks developed at 60% to 70% of the ultimate load of each beam and in bacteria incorporated beams (FAAC) they developed at 75% to 85% of the ultimate load of each beam. The crack started to widen considerably indicating higher strains in steel than the yield strain in steel. All the beams exhibited a tension failure which is a ductile failure. The cracks are accompanied by pronounced bulging. When the load is further increased, cracks propagated towards the top of the beam. As the beams are forced to deform further, the cracks became more pronounced and the concrete crushed at one or both the ends. With further increase in beam deflection, the load decreased, accompanied by concrete spalling. This crack pattern is observed to be same for all grades of under-reinforced bacteria incorporated concrete beams, except the spacing of the cracks.

The higher values of maximum deflection for under-reinforced beams are due to yielding of reinforcement at ultimate loads. Due to yielding of reinforcement at ultimate loads the under-reinforced beams has shown higher values of maximum curvature.

6.8.3 Experimental and Theoretical M & Φ values

Experimental and Theoretical M & Φ values of under-reinforced M20 and M40 grades of reference (NA) and bacteria incorporated (Treated FAAC) reinforced concrete beams are shown in Tables 6.27 to 6.30 below.

Table 6.27- Experimental and Theoretical M & Φ values of M20 grade natural aggregate concrete

Experimental Values		Theoretical Values	
Φ	M kN-m	Φ	M kN-m
0	0	0	0
7.84E-07	0.667	8.23E-07	1.39965
7.84E-07	1.333	8.23E-07	2.1
7.84E-07	2.000	1.65E-06	2.80035
1.57E-06	2.667	1.65E-06	3.49965
1.57E-06	3.333	2.47E-06	4.2
2.35E-06	4.000	2.47E-06	4.90035
2.35E-06	4.667	2.88E-06	5.59965
2.74E-06	5.333	3.3E-06	6.3
3.14E-06	6.000	3.71E-06	7.00035
3.53E-06	6.667	4.12E-06	7.69965
3.92E-06	7.333	4.95E-06	8.4
4.71E-06	8.000	4.95E-06	9.10035
4.71E-06	8.667	5.36E-06	9.79965
5.1E-06	9.333	6.17E-06	10.5
5.88E-06	10.000	6.17E-06	11.20035
5.88E-06	10.667	7E-06	11.89965
6.67E-06	11.333	7.41E-06	12.6
7.06E-06	12.000	7.41E-06	13.30035
7.06E-06	12.667	8.23E-06	13.99965
7.84E-06	13.333	8.64E-06	14.52465
8.23E-06	13.833		

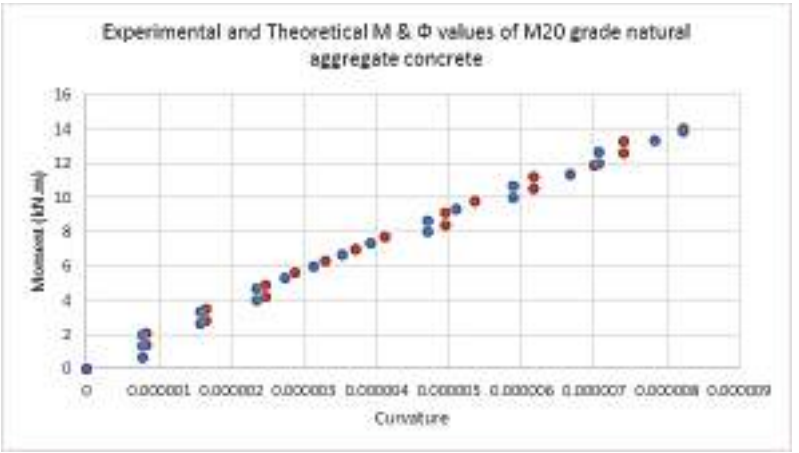

Figure 6.23 - Experimental and Theoretical M & Φ values of M20 grade natural aggregate concrete

Table 6.28 - Experimental and Theoretical M & Φ values of M20 grade bacteria incorporated concretes (Treated FAAC) beams

Experimental Values		Theoretical Values	
Φ	M kN-m	Φ	M kN-m
0	0	0	0
0	0.667	8.22E-07	1.39965
7.83E-07	1.333	8.22E-07	2.1
7.83E-07	2.000	1.65E-06	2.80035
1.57E-06	2.667	1.65E-06	3.49965
1.57E-06	3.333	2.47E-06	4.2
2.35E-06	4.000	2.88E-06	4.90035
2.74E-06	4.667	3.7E-06	5.59965
3.52E-06	5.333	4.12E-06	6.3
3.92E-06	6.000	4.94E-06	7.00035
4.7E-06	6.667	5.75E-06	7.69965
5.48E-06	7.333	6.58E-06	8.4
6.27E-06	8.000	7.4E-06	9.10035
7.05E-06	8.667	8.22E-06	9.79965
7.83E-06	9.333	9.05E-06	10.5
8.62E-06	10.000	9.87E-06	11.20035
9.4E-06	10.667	1.07E-05	11.89965
1.02E-05	11.333	1.2E-05	12.6
1.14E-05	12.000	1.31E-05	13.30035
1.25E-05	12.667	1.52E-05	13.99965
1.45E-05	13.333	1.76E-05	14.7
1.68E-05	14.000		

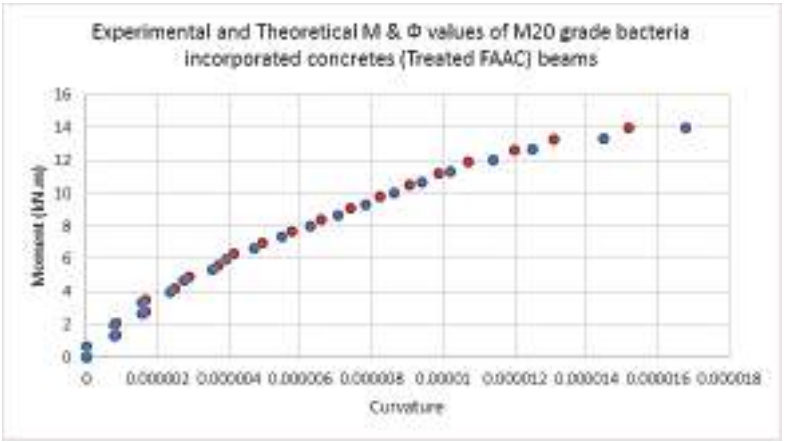

Figure 6.24- Experimental and Theoretical M & Φ values of M20 grade bacteria incorporated concretes (Treated FAAC) beams

Table 6.29 - Experimental and Theoretical M & Φ values of M40 grade natural aggregate concrete

Experimental Values		Theoretical Values	
Φ	M kN-m	Φ	M kN-m
0	0.000	0	0
1.21E-06	0.833	1.27E-06	0.87465
1.62E-06	1.667	1.7E-06	1.75035
2.43E-06	2.500	2.55E-06	2.625
2.83E-06	3.333	2.97E-06	3.49965
3.64E-06	4.167	3.82E-06	4.37535
3.64E-06	5.000	3.82E-06	5.25
4.45E-06	5.833	4.67E-06	6.12465
5.66E-06	6.667	5.94E-06	7.00035
6.47E-06	7.500	6.79E-06	7.875
7.68E-06	8.333	8.06E-06	8.74965
8.49E-06	9.167	8.91E-06	9.62535
9.3E-06	10.000	9.77E-06	10.5
1.09E-05	10.833	1.14E-05	11.37465
1.21E-05	11.667	1.27E-05	12.25035
1.29E-05	12.500	1.35E-05	13.125
1.37E-05	13.333	1.44E-05	13.99965
1.45E-05	14.167	1.52E-05	14.87535
1.54E-05	15.000	1.62E-05	15.75
1.62E-05	15.833	1.7E-05	16.62465
1.74E-05	16.667	1.83E-05	17.50035
1.82E-05	17.500	1.91E-05	18.375
1.9E-05	18.333	2E-05	19.24965
2.02E-05	19.167	2.12E-05	20.12535
2.14E-05	20.000	2.25E-05	21
2.26E-05	20.833	2.37E-05	21.87465

2.38E-05	21.667	2.5E-05	22.75035
2.63E-05	22.500	2.76E-05	23.625
2.79E-05	23.333	2.93E-05	24.49965
2.95E-05	24.167	3.1E-05	25.37535
3.23E-05	25.000	3.39E-05	26.25
3.52E-05	25.833	3.7E-05	27.12465
3.8E-05	26.667	3.99E-05	28.00035
4.2E-05	27.500	4.41E-05	28.875
9.18E-05	29.833	9.64E-05	31.32465

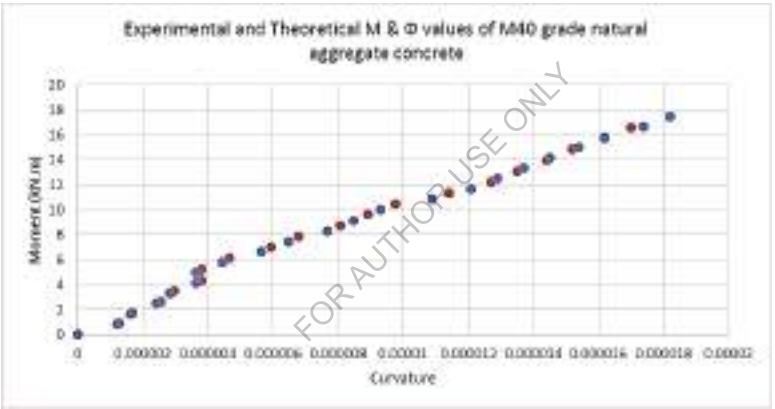

Figure 6.25- Experimental and Theoretical M & Φ values of M40 grade natural aggregate concrete

Table 6.30 - Experimental and Theoretical M & Φ values of M40 grade bacteria incorporated concretes (Treated FAAC) beams

Experimental Values		Theoretical Values	
Φ	M kN-m	Φ	M kN-m
0	0.000	0	0
7.83E-07	0.833	8.22E-07	0.87465
1.57E-06	1.667	1.65E-06	1.75035
2.35E-06	2.500	2.47E-06	2.625
3.13E-06	3.333	3.29E-06	3.49965
3.91E-06	4.167	4.11E-06	4.37535
4.31E-06	5.000	4.53E-06	5.25
5.09E-06	5.833	5.34E-06	6.12465
6.26E-06	6.667	6.57E-06	7.00035
7.04E-06	7.500	7.39E-06	7.875
7.83E-06	8.333	8.22E-06	8.74965
9E-06	9.167	9.45E-06	9.62535
9.78E-06	10.000	1.03E-05	10.5
1.06E-05	10.833	1.11E-05	11.37465
1.17E-05	11.667	1.23E-05	12.25035
1.29E-05	12.500	1.35E-05	13.125
1.33E-05	13.333	1.4E-05	13.99965
1.41E-05	14.167	1.48E-05	14.87535
1.49E-05	15.000	1.56E-05	15.75

1.57E-05	15.833	1.65E-05	16.62465
1.64E-05	16.667	1.72E-05	17.50035
1.72E-05	17.500	1.81E-05	18.375
1.8E-05	18.333	1.89E-05	19.24965
1.88E-05	19.167	1.97E-05	20.12535
2E-05	20.000	0.000021	21
2.11E-05	20.833	2.22E-05	21.87465
2.23E-05	21.667	2.34E-05	22.75035
2.31E-05	22.500	2.43E-05	23.625
2.43E-05	23.333	2.55E-05	24.49965
2.62E-05	24.167	2.75E-05	25.37535
2.86E-05	25.000	3E-05	26.25
3.13E-05	25.833	3.29E-05	27.12465
3.44E-05	26.667	3.61E-05	28.00035
3.84E-05	27.500	4.03E-05	28.875
4.46E-05	28.333	4.68E-05	29.74965
8.3E-05	29.167	8.72E-05	30.62535

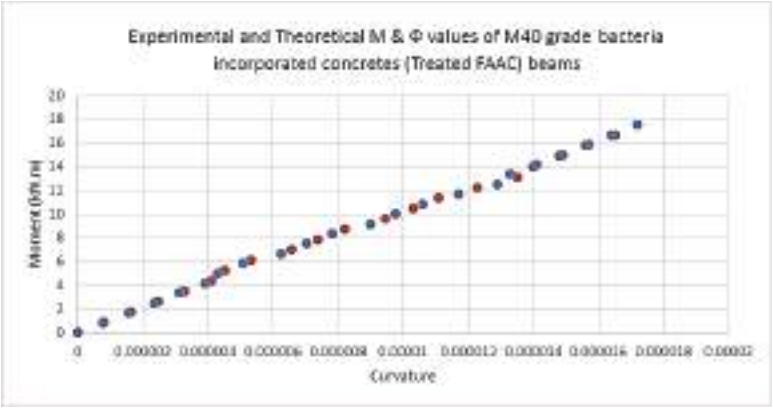

Figure 6.26- Experimental and Theoretical M & Φ values of M40 grade bacteria incorporated concretes (Treated FAAC) beams

Deflections for under reinforced bacteria incorporated concretes (Treated FAAC) beams at service loads are less than the maximum permissible deflection of 4 mm *i.e.* Span/250 specified by IS 456-2000. Thus, the use of bacteria incorporated concrete beams did not violate the serviceability norms of the codes of practice.

Load deflection behaviour for all grades of bacteria incorporated concrete is observed to have the increased values of loads at ultimate and at first crack.

Moment curvature plots for under reinforced bacteria incorporated concrete are observed to follow similar pattern as that of load deflection plots of natural aggregate concrete beams.

Theoretical moment-curvature relationships for bacteria incorporated concrete followed similar pattern as that of experimental values. This shows a good correlation between them.

6.9 Summary

This section presents materials used and their properties (provided by the supplier) and methodology for preparation of fly ash based artificial coarse aggregates, process of growing and culturing bacteria, Optimum bacterial cell concentration for $CaCO_3$ Precipitation, effect of biotic and abiotic factors of bacterial activity on strength and durability of cementitious materials, Characterization of $CaCO_3$ precipitation, mix proportions of M20 and M40 grade concretes, mechanical properties of M20 and M40 grade fly ash aggregate based bacterial concretes , Flexural Behavior of fly ash aggregate based bacterial concrete beams, Pore Structure Analysis, permeation properties, corrosion resistance of M20 and M40 grade fly ash aggregate based bacterial concretes using BET Nitrogen (N2) Adsorption method. Finally crack healing efficiency evaluation methods are discussed.

Chapter - 7

PERFORMANCE EVALUATION

7.1 General

This section presents performance of M20 and M40 grade fly ash aggregate based bacterial concretes in terms of pore structure analysis using BET Nitrogen (N2) Adsorption method, permeation properties, and corrosion resistance capacities.

7.2 Pore Structure Analysis using BET Nitrogen (N_2) Adsorption method

Two independent methods, proposed for pore structure analysis, for estimating pore volume and pore diameter, are the gas adsorption method (also known as the Brenauer- Emmett-Teller method) (BET) and the mercury porosimeter method (MIP). These two methods, with various modifications, are used by industry and in research. Results of the nitrogen adsorption technique cover both gel and capillary pores of the concrete mixtures, while entrapped air and capillary pores of diameter larger than 300nm are not accounted. The aim of this test is to study the pore structure characterization of bacteria incorporated concrete using Brenauer-Emmett-Teller's (BET) Nitrogen (N2) nitrogen adsorption method. This test confirms the modification in pore size distribution due to the addition of microorganisms. Porosity of concrete in terms of specific surface area, pore size distribution, and pore volume, was examined using the Brenauer-Emmett-Teller BET nitrogen adsorption method based on DIN 66131.

The BET nitrogen adsorption technique is appropriate to characterize the sizes and distribution of pores in the region of capillary pores (50 to 10 nm) and gel pores (< 10 nm). Small samples (2 g) were taken from concrete specimens that were moist cured for 28 days. Porosity characteristics of concrete including total volume of pores in concrete matrix, volume of micropores, pore size distribution and specific surface area were determined using the BET nitrogen adsorption method. The gas adsorption method is based on the phenomenon of gas condensation in narrow pores at pressures lower than saturated vapour pressure of the examined material. Classically, volumes of gas progressively adsorpted by the material, and those of gas progressively desorpted, are represented by the isotherms. Adsorption isotherms are used to calculate the specific surface area of materials, mean pore size or mean size of deposited particles, as well as pore size or particle size distribution. The method of Barrett-Joyner-Halenda (BJH) is used for calculating pore size distribution in a porous material using adsorption or desorption isotherms.

Pore diameter, Total pore surface area, Total pore volume and porosity of M20 and M40 grades of reference and bacteria incorporated concretes (Treated FAAC) obtained from the Adsorption isotherms and BJH isotherms are tabulated in Table 7.1 below and corresponding graphs 7.1 to 7.4 are plotted.

Table 7.1 - Pore diameter, Total pore surface area, Total pore volume and porosity of M20 and M40 grades of reference and bacteria incorporated concretes (Treated FAAC)

	M20 Reference Concrete (NAC)	M20 Bacteria incorporated concrete (FAAC)	M40 Reference Concrete (NAC)	M40 Bacteria incorporated concrete (FAAC)
Average Pore Diameter (nm)	19.121	3.386	5.084	3.097
Total Pore Surface Area (m^2/g)	1.747	5.047	3.346	5.088
Total pore volume (cc/g)	0.0161	0.0071	0.0137	0.0057
Porosity (%)	1.6	0.7	1.37	0.57

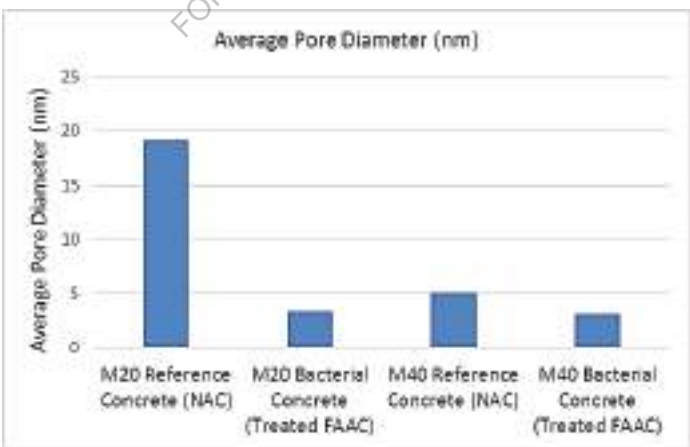

Figure 7.1 - Pore diameters of controlled and bacteria incorporated concretes of different grades

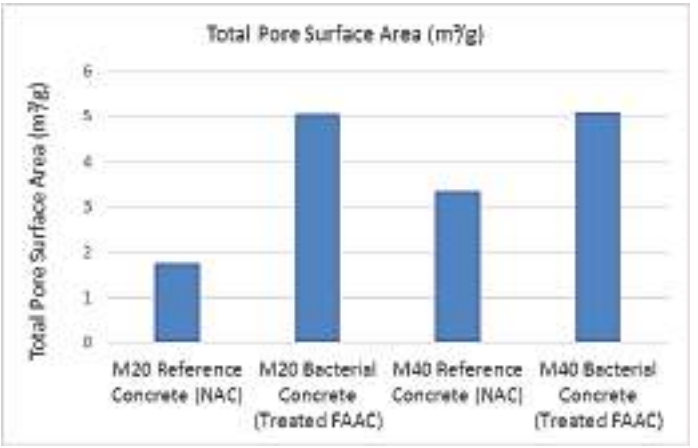

Figure 7.2 - Total pore surface area of controlled and bacteria incorporated concretes of different grades

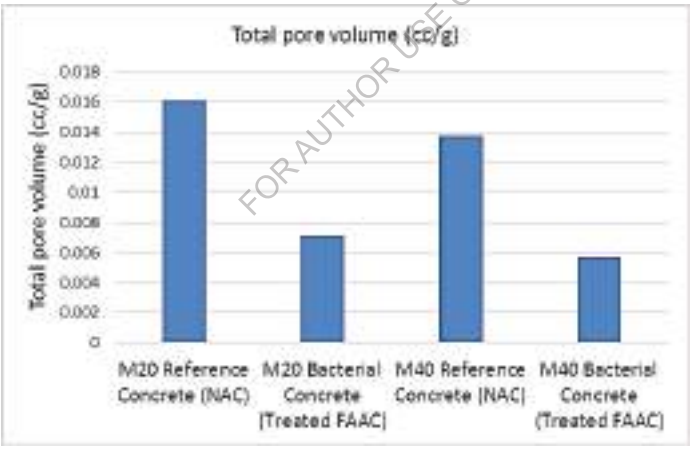

Figure 7.3 - Total pore volume of controlled and bacteria incorporated concretes of different grades

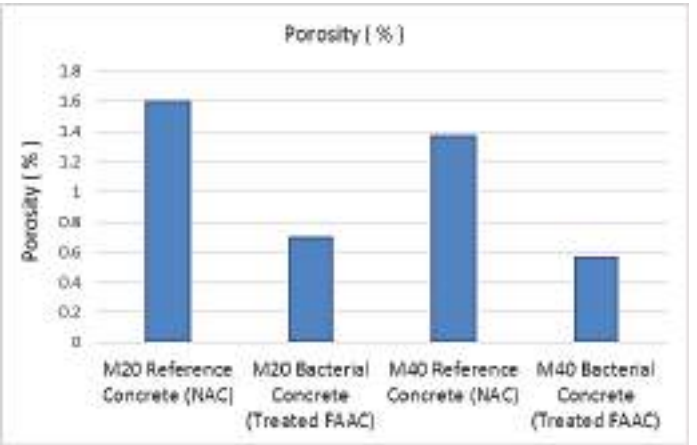

Figure 7.4 - Porosity of controlled and bacteria incorporated concretes of different grades using BET method

The analysis of the BET isotherms and hysteresis produced by the adsorption and desorption branches gives the following observations:

The shape of the isotherms in both the grades of controlled concrete specimens is of Type-1 isotherm representing micro porous solids of microstructure of continuously graded pores where as shape of the isotherm in both the grades of bacteria incorporated concrete specimens is of Type-2 and Type-3 isotherms indicating the characteristic of non-porous solids.

Average pore diameter, observed using BJH method, decreases from lower to higher grades of concrete and this observation is significant in bacteria incorporated concrete in which average pore diameter decreases drastically due to calcite mineral precipitation in the pores because of microbial metabolic activity of *Sporosarcina pasteurii* bacterial strain.

Total Pore Surface Area (from Multi-point BET data) increases with the grade of concrete. Surface area of bacteria incorporated concrete specimens of both grades is found to be more than surface area of referenced concrete specimens.

As average pore diameter decreases from lower to higher grades of concrete, total pore volume also decreased as grade increases. The decrease is more in case of bacteria incorporated concrete samples. Total porosity decreases as grade increases. This decrease is significant in bacterial specimens. As the pore diameter increases, the pore volume also increases leading to high porosity, possibility of water absorption and a decrease in density of concrete. Porosity in bacteria incorporated concretes is reduced by 20 to 60% for low to high grades. Total Pore volume in bacteria incorporated concretes is reduced by 20 to 60% for low to high grades.

A significant decrease in porosity and average pore diameter was observed in bacteria incorporated concrete by the addition of bacteria as compared to the reference concrete.

From the above observation, the following conclusions are drawn:

The porosity decreases significantly in all the grades of bacteria incorporated concrete in comparison with the porosities shown by the corresponding grades of reference concrete because pore diameter and total pore volume are very low in all grades of bacteria induced concrete due to calcite mineral precipitation in the pores by *Sporosarcina pasteurii* bacterial strain metabolic activity. Total pore surface area

increases in bacteria incorporated concrete specimens of different grades due to formation of dense microstructure.

7.3 Water permeability

Permeability is the most crucial internal factor in concrete durability. The permeability dictates the rate at which aggressive agents can penetrate to attack the concrete and the steel reinforcement. Water penetrability is defined as the degree to which a material permits the transport gases, liquids or ionic species through it. Water can be harmful for concrete, because of its ability to leach calcium hydroxide from the cement paste, to carry harmful dissolved species such as chlorides or acids into the concrete, to form ice in large pores in the paste, and to cause leaching of compounds from the concrete. Water absorption, sorptivity and water permeability measurement are some methods to determine the water penetrability of concrete. A triaxial cell permeability apparatus method used for determining water permeability of concrete utilizes Darcy's Law for steady flow so as to relate water permeability to the rate of water flow under a pressure head. The major drawbacks commonly encountered in triaxial cell permeability apparatus are addressed by evaluating the water permeability as per as per German standard DIN 1048(Part 5):1991 specifications and MORT&H (Ministry of Road Transport & Highways) 4th Revision specifications. Permeability measurement techniques and durability modeling are based on the Darcy equation for permeability based on measurement of flow rate, and the Valetta equation for permeability based on measurement of penetration depth and time. The

objective of this study is to determine water permeability of M20 and M40 grades of reference and bacteria incorporated concretes (Treated FAAC) as per IS 3085 and DIN 1048.

7.3.1 Water Permeability of Concrete as per IS 3085

Concrete water permeability test is conducted as per IS 3085:1965. The permeability tester used was a 1-cell tester, a pressure chamber and air compressor supplying water to the test samples under required pressure. Bacteria incorporated concrete cylindrical specimens and controlled cylindrical concrete specimens of diameter 150mm and height 150mm are casted and cured for 28 and 90 days. Then they are loaded in the specially designed cells and a constant air pressure of 15 kg/cm^2 is maintained by using air compressor throughout the experiment for a given interval of time. The standard test pressure head to be applied to the water should be 10 kg/cm^2. The quantity of percolated water collected is measured at periodic intervals. In the beginning, the rate of water intake is larger than the rate of outflow. As the steady state of flow is approached, the two rates tend to become equal and the outflow reaches maximum and stabilizes. With further passage of time both inflow and outflow generally register a gradual drop. Permeability test shall be continued for about 100 hours after the steady state of flow has been reached and the outflow shall be considered as average of all the outflows measured during the period of 100 hours. Then the coefficient of permeability (k, in m/sec) based on Darcy's law for a falling water head, which is applicable at steady state

flow conditions, can be computed on 28 and 60 days aged specimens, using the following formula

$$K = \frac{Q}{A \times T \times (H/L)}$$

Where K= Coefficient of permeability in m/sec

Q = Quantity of water collected in milliliters over the entire period of test

T = Time in seconds over which Q is measured = 100x60x60 sec = 360000sec

A = Area of the specimen face in m^2 = 0.01767 m^2

Water pressure=10 kg/cm^2 = 10^6 Pa

1Pa of water pressure = 0.0001m of pressure head (water at room temperature)

Pressure Head = 100 m (kept constant throughout the test)

H/L = ratio of pressure head to thickness of the specimen both expressed in metre = 100/0.15 = 666.67

Figure 7.5 - Concrete Water Permeability setup

Table 7.2- Coefficient of water permeability ranges as per IS: 3085-1965

Water Permeability	Very Low	Low	Medium	High
Coefficient of permeability (x 10^{-9} m/sec)	< 0.5	0.5-1.0	1.0-2.0	>2.0

7.3.2 Water Permeability of Concrete as per DIN 1048

The Darcy's Law can be applied only for steady state flows. It has been observed by many investigators that steady state flow conditions could not be achieved in concrete mixes having low permeability even after subjecting the test samples to pressures as high as 3.5 MPa for a test period extending up to several weeks. In such cases, some investigators have used the 'depth of penetration' to determine the water permeability of concrete of age 28 and 60 days. In our present study, for M20 and M40 grades of bacteria incorporated concretes (Treated FAAC) steady state conditions could not be achieved before 72 hours, so water permeability test, M20 and M40 grades of reference and bacteria incorporated concretes (Treated FAAC), as per German standard DIN 1048(Part 5):1991 specifications and MORT&H (Ministry of Road transport & Highways) 4th Revision Cl.1716.5 is carried out on 150mm cylindrical specimens. This test gives a measure of the resistance of concrete against the penetration of water exerting pressure. For this test, reference and bacteria treated specimens are casted and placed inside the permeability cell , the water is introduced on the top of the

cell and the pressure of 0.5 N/mm^2 is applied in way to force the water to penetrate through the sample. The determination of the permeability is carried out by measuring the water penetration depth after 96 hrs by a splitting the cylinder specimens. Water with a color indicator is used, which helps to determine the border of penetration depth. If water penetrates through to the underside of the specimen, the test may be terminated and considered as failed. The mean of the maximum depth of penetration from three specimens thus tested shall be taken as the test result. To measure the water coefficient by penetration at 28 and 90 days age, Valenta's law can be applied if the material is less permeable.

$$k = \frac{D^2 V}{2 H T}$$

Where, k= Water permeability coefficient (m/s)

D= depth of penetration (m)

V= Volume of voids filled by water in the penetrated zone

H= Applied pressure is 5 bar (1 bar = 10m)

T= Time to penetrate to depth D (s)

Table 7.3 - Permeability ranges according to standard DIN 1048 (Part 5):1991

Permeability as per to DIN 1048	Low	Medium	High
Penetration depth after 96 hrs	Less than 30 mm	30-60 mm	Greater than 60 mm

The tables 7.4 and 7.5 below presents the coefficients of permeability values determined as per IS 3085 for M20 and M40 grades of reference and bacteria incorporated concrete (Treated FAAC) specimens of age 28 and 60 days.

Table 7.4 - Coefficients of Permeability for M20 and M40 grades of reference and bacteria incorporated concrete (Treated FAAC) of age 28 days

Grade of Concrete	Type of specimen	Pressure head H (m)	Quantity of water collected (ml)	Coefficient of permeability x 10^{-9} m/sec	% Reduction
M 20	Reference Concrete (NAC)	100	9822	2.31	-
	Bacterial Concrete (FAAC)	100	1157	0.27	88
M 40	Reference Concrete (NAC)	100	7800	1.84	-
	Bacterial Concrete (FAAC)	100	1039	0.25	86

Table 7.5 - Coefficients of Permeability for M20 and M40 grades of reference and bacteria incorporated concrete (Treated FAAC) of age 60 days

Grade of Concrete	Type of specimen	Pressure head H (m)	Quantity of water collected (ml)	Coefficient of permeability x 10^{-9} m/sec	% Reduction
M 20	Reference Concrete (NAC)	100	9114	2.15	-
	Bacterial Concrete (FAAC)	100	1108	0.26	88
M 40	Reference Concrete (NAC)	100	7088	1.67	-
	Bacterial Concrete (FAAC)	100	1017	0.24	86

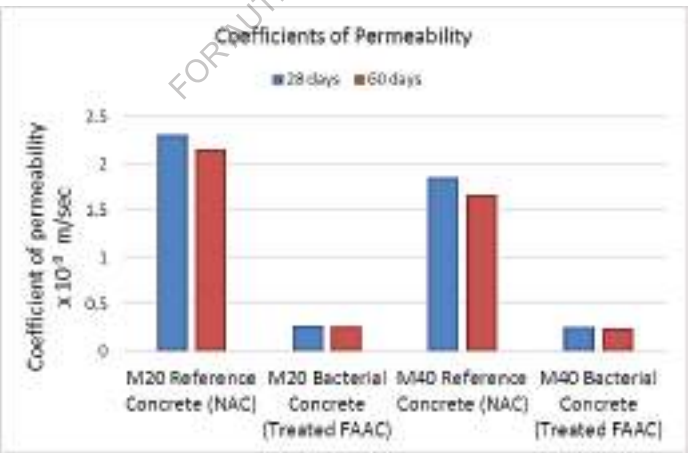

Figure 7.6 - Coefficients of Permeability for M20 and M40 grades of reference and bacteria incorporated concrete (Treated FAAC) of age 28 and 60 days

The Table 7.7 and 7.8 and Figure 7.7 presents the coefficients of permeability values for M20 and M40 grades of reference and bacteria incorporated concrete (Treated FAAC) of age 28 and 60 days determined as per DIN 1048.

Table 7.7 - Depth of Penetration for M20 and M40 grades of reference and bacteria incorporated concrete (Treated FAAC) of age 28 days

Grade of Concrete	Type of specimen	Depth of Water Penetration (mm)	Requirement as per MORT&H 4th Revision Clause 1716.5
M 20	Reference Concrete (NAC)	23	25mm (Maximum permissible limit for RCC strucutres)
	Bacterial Concrete (FAAC)	5	
M 40	Reference Concrete (NAC)	17	
	Bacterial Concrete (FAAC)	4	

Table 7.8 - Depth of Penetration for M20 and M40 grades of reference and bacteria incorporated concrete (Treated FAAC) of age 60 days

Grade of Concrete	Type of specimen	Depth of Water Penetration (mm)	Requirement as per MORT&H 4th Revision Clause 1716.5
M 20	Reference Concrete (NAC)	20	25mm (Maximum permissible limit)
	Bacterial Concrete (FAAC)	4	
M 40	Reference Concrete (NAC)	14	
	Bacterial Concrete (FAAC)	3	

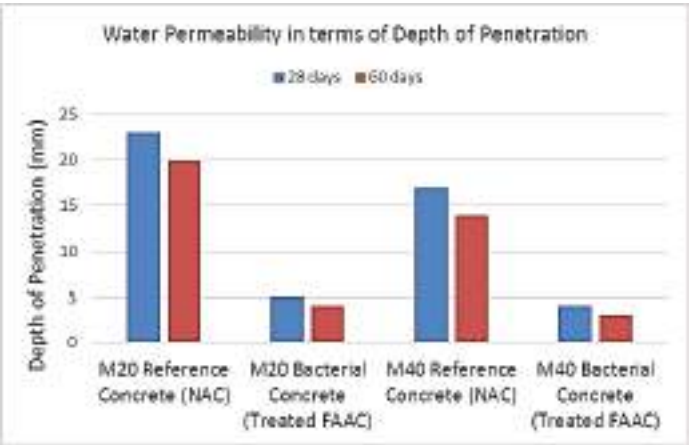

Figure 7.7 - Depth of Penetration for M20 and M40 grades of reference and bacteria incorporated concrete (Treated FAAC) of age 28 and 60 days

From the presented test results, it was observed that significantly lower water permeability is observed in bacteria induced specimens than controlled specimens under 100m water head. Results show that the presence of bacteria resulted in lower coefficient of permeability of range 0.24 – 0.27 x 10^{-9} m/sec in comparison to controlled concrete which has coefficient of permeability of 1.67 – 2.31 x 10^{-9} m/sec for various grades of concretes. Reduction in water permeability of specimens treated with bacteria is nearly 88%, 86% for M20 and M40 grades respectively, of age 28 and 60 days. It shows that bacteria incorporated concretes are less permeable than the reference concretes the reason attributed is that the bacteria incorporated concretes has improved pore structure due to precipitation of calcite crystals subsequently reduction in the porosity of the concrete which substantially reduces

the permeability of the concrete. The main idea of this test as per DIN 1048 is that water penetrates the concrete specimens under a set pressure for a set period of time. So depths of penetration are measured to evaluate the water impermeability of M20 and M40 grades of reference and bacteria incorporated concrete (Treated FAAC). The depth of water penetration measured in bacteria induced specimens when tested in DIN 1048 water permeability tests corresponds to the "very low permeability". Depth of penetration is reduced in bacteria built-in specimens by nearly 76% in all the grades of concrete.

In the case of Bacteria incorporated concrete, blocking of the pores due to calcite mineral precipitates reduces the water permeability so the depth of penetration is very low when compared with water penetration depths in controlled concrete.

The above investigations shows that bacteria incorporated concretes were less permeable than the control concretes the reason is that the bacteria incorporated concrete has improved pore structure due to precipitation of calcite crystals subsequently reduction in the porosity of the concrete which substantially reduces the permeability of the concrete. Water permeability reduces in bacteria incorporated concrete by nearly 80 % in comparison to controlled concrete confirming the bacteria incorporated concrete as impermeable.

7.4 Water Absorption Capacity and Porosity

The aim of this study is to determine the total water absorption capacity and measure the volume of voids present in M20 and M40 grades of reference and bacteria incorporated concrete (Treated FAAC) as per ASTM C642-13. The total quantity of water absorbed is related to the total open porosity, while the kinetics of the process depends principally on the distribution of the pore sizes. This test also measures the capillary rise of water, the most common form of liquid water migration into concrete which is inversely proportional to the diameter of the pores. The smaller the diameter of the pores, the greater will be the capillary absorption. Absorption is the capacity of a sample to hold water while capillary is the rate at which the water fills the sample.

Concrete cube samples of size 100 x 100 x 100 mm are casted and cured for 28 days for testing. Wash the samples in the de-ionized water before beginning this test in order to eliminate powdered material from the surface. Dry the samples in the oven for 24 hours at 60°C and record their weights. Repeat the drying process until the mass of the each sample is constant, that is, until the difference between 2 successive measurements, at an interval of 24 hours, is no more than 0.1% of the mass of the sample. Once the samples have been completely dried and the constant mass is recorded (m_o), place them in a container or beaker, on a base of glass rods and slowly cover with de-ionized water until they are totally immersed with about 2 cm of water above them. At programmed intervals of time, take each sample out of the container, blot it quickly with a damp cloth to remove surface water, and then

record the mass of the wet samples (m_i) and the time of measurement on the data sheet. Re-immerse the samples in water and continue measuring until the difference in weight between 2 successive measurements at 24-hour intervals is less than 1% of the amount of water absorbed. At this point, take the samples out of the water and dry them again in an oven at 60°C until they have reached constant mass (as above). Record this value (m_d) on the data sheet. At each interval, the quantity of water absorbed with respect to the mass of the dry sample is expressed as:

$$M_i\% = 100 \times (m_i - m_o)/m_o$$

Where m_i = weight (kg) of the wet sample at time t_i; m_o = weight (kg) of the dry sample.

Record these values on a data sheet and on a graph as a function of time. The length of the intervals during the first 24 hours depends on the absorption characteristics of the materials. Concrete samples should be weighed a few minutes after immersion, and then at increasing intervals (15 min, 30 min, 1 hour, etc.) for the first 3 hours. All samples should then be weighed 8 hours after the beginning of the test and then at 24- hour intervals until the quantity of water absorbed in two successive measurements is not more than 1% of the total mass.

For measuring the water absorption capacity and volume of permeable voids, a balance, water bath, and container suitable for immersing the specimen are needed for performing the test. After the 100x100x100 mm cube samples were cured for 28 days, three samples were put into an oven at 60° C for 24 hours. The dried samples were

taken from the oven and allowed to cool for about 30 minutes. The samples were then weighed (M_a) using a balance with an accuracy within 0.01 grams. The samples were submerged in the water tank for 24 hours. After 24 hours, the samples were removed from the water tank and their surface was dried with a paper towel to obtain a saturated surface dry (SSD) condition. The weight (M_b) of the SSD samples was measured. In the next step, the samples were put into a water bath with boiling water for 5 hours. Then the samples were removed from the boiling water and left to cool for 12 hours. Then weights of the samples were measured (M_c). On the same day, the apparent weight of each sample (M_d) was measured by immersing the samples in the water using a hanging balance. Using the measured weights (M_a to M_d) and the equations from the ASTM C642 standard test, the following parameters are obtained.

Water Absorption Capacity (WAC) = $[(M_b-M_a)/ M_a] \times 100$

Bulk density = $g_1 = [(M_a)/ M_c- M_d]x \rho$

Apparant density $=g_2 = [(M_a)/ M_a- M_d]x \rho$

Volume of permeable voids (VPV) = $[(g_2 - g_1)/ g_2] \times 100$

where: M_a = mass of oven-dried sample in air, kg; M_b = mass of surface-dry sample in air after immersion, kg ; M_c = mass of surface-dry sample in air after immersion and boiling, kg and M_d = apparent mass of sample suspended in water, kg.

g_1 = dry bulk density (kg/m^3) and g_2 = apparent density (kg/m^3)

ρ= density of water (1000 kg/m^3)

Finally total porosity 'P' or percentage of interconnected pore space was calculated using the formula given below

$$\text{Total porosity} = (V_v/V) = (W_{sat} - W_{dry}) / \rho_w V$$

Where, V_v = volume of voids in cc= W_{sat}- W_{dry} in grams;

V = total volume of specimen in cc = 100 x 100 x100 mm^3

Where ρ_w the unit mass of water (1 g/cc)

W_{dry} and W_{sat} denote the weight of the dried and fully saturated samples, respectively.

The following equation was used to find the apparent porosity.

$$\text{Apparent porosity (\%)} = [(M_w - M_d)/ (M_w - M_s)] \text{ x100}$$

Where M_w = weight of saturated specimen (after immersion in water for 48 hours, it is removed and surface dried), M_d = Weight of oven dried specimen and M_s = weight of specimen while suspended in water.

Porosity of concrete is usually determined by dividing the volume of voids of the sample by its bulk volume. Bulk volume of each sample is determined using the measured lengths and diameters of the samples. Volume of voids for each sample is determined by subtracting its grain volume (the volume of the solid portion of concrete excluding the volume of pores) from its bulk volume. Total porosity therefore considers both permeable and impermeable voids whereas apparent porosity considers only impermeable voids.

Table 7.9 - Durability Classification as per ASTM C 642

Classification	Volume of Permeable Voids (VPV) (% by volume)	Water Absorption Capacity (% by weight)
Excellent	<14	<5
Good	14-16	5-6
Normal	16-17	6-7
Marginal	17-19	7-8
Bad	>19	>8

The tables 7.10 to 7.14 below give the water absorption capacity (WAC), volume of permeable voids and apparent porosity of M20 and M40 grades of reference and bacteria incorporated concrete (Treated FAAC) specimens.

Table 7.10 - Water Absorption at different time intervals of M20 and M40 grades of reference (made with NA)

Measurement Intervals ti (min)	Reference Concrete (NAC)			
	M20		M40	
	mo= 2.49 kg		mo= 2.51 kg	
	mi(kg)	Mi(%)	mi(kg)	Mi(%)
0	2.49	0.00	2.51	0.00
15	2.51	0.80	2.55	1.59
30	2.59	4.02	2.56	1.99
60	2.60	4.42	2.58	2.79
90	2.61	4.82	2.58	2.79
180	2.62	5.22	2.58	2.79
480	2.62	5.22	2.58	2.79
1440	2.63	5.62	2.58	2.79
2880	2.63	5.62	2.58	2.79

Table 7.11 - Water Absorption at different time intervals of M20 and M40 grades of bacteria incorporated concrete (made with treated FAAC)

Measurement Intervals ti (min)	Bacteria incorporated concrete (FAAC)			
	M20		M40	
	mo= 2.51 kg		mo= 2.53 kg	
	mi(kg)	Mi(%)	mi(kg)	Mi(%)
0	2.51	0.00	2.53	0.00
15	2.52	0.40	2.54	0.40
30	2.54	1.20	2.55	0.79
60	2.56	1.99	2.55	0.79
90	2.58	2.79	2.56	1.19
180	2.58	2.79	2.56	1.19
480	2.58	2.79	2.56	1.19
1440	2.58	2.79	2.56	1.19
2880	2.58	2.79	2.56	1.19

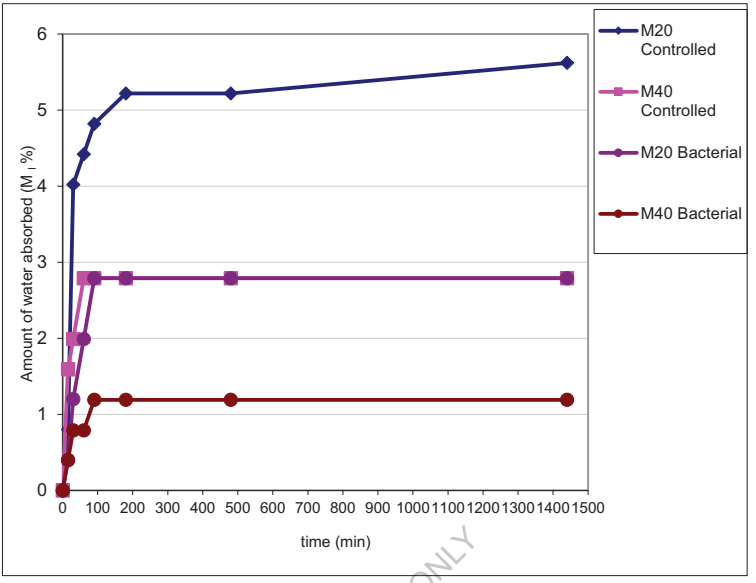

Figure 7.8 - Plot showing amount of water absorption with time for M20 and M40 grades of reference and bacteria incorporated concrete (Treated FAAC)

Table 7.12 - Water Absorption Capacity (WAC), Volume of Permeable Voids and Apparent porosity of M20 and M40 grades of reference and bacteria incorporated concrete (Treated FAAC)

	Controlled Concrete		Bacteria incorporated concrete	
	M20	M40	M20	M40
M_a	2.49	2.51	2.51	2.53
M_b	2.63	2.58	2.58	2.56
M_c	2.64	2.59	2.59	2.57
M_d	1.49	1.45	1.46	1.46
bulk density (g_1) (kg/m^3)	2184	2221	2241	2300
apparent density (g_2) (kg/m^3)	2490	2367	2390	2364
Water Absorption Capacity (WAC) (%)	5.62	2.79	2.79	1.19
Volume of permeable voids (VPV) (%)	12	6	6	3
Apparent porosity (%)	11.4	5.5	5.7	2.1

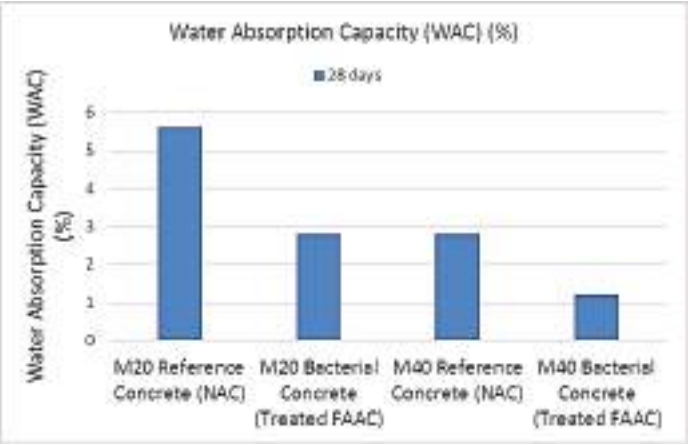

Figure 7.9 - Water Absorption Capacity (WAC of M20 and M40 grades of reference (made with NA) and bacteria incorporated concrete (made with treated FAAC)

Table 7.13 - Porosity of M20 and M40 grades of reference and bacteria incorporated concrete (Treated FAAC) at 28 days

	Controlled Concrete		Bacteria incorporated concrete	
	M20	M40	M20	M40
M_{sat} (kg)	2.63	2.58	2.55	2.56
M_{dry} (kg)	2.49	2.51	2.51	2.53
Porosity, P at 28 days	0.14	0.07	0.04	0.03
Decrease in Porosity	-	-	72%	57%

Table 7.14 - Porosity of M20 and M40 grades of reference and bacteria incorporated concrete (Treated FAAC) at 60 days

	Controlled Concrete		Bacteria incorporated concrete	
	M20	M40	M20	M40
M_{sat} (kg)	2.63	2.58	2.55	2.56
M_{dry} (kg)	2.52	2.53	2.52	2.54
Porosity, P at 60 days	0.11	0.05	0.03	0.02
Decrease in Porosity	-	-	73%	60%

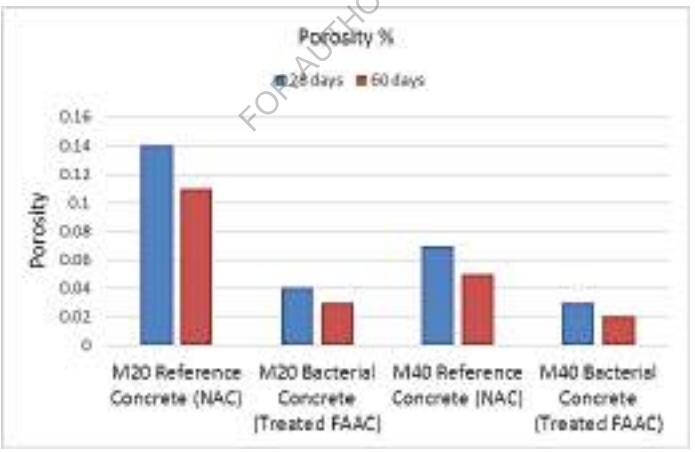

Figure 7.10 - Porosity of M20 and M40 grades of reference and bacteria incorporated concrete (Treated FAAC) at 28 and 60 days age of curing

Concrete specimens incorporated with bacteria showed significantly less water absorption capacity compared to reference specimens. This decrease in water absorption capacity of all grades of bacteria incorporated concretes is attributed to the reduction of pores in the concrete. Water Absorption Capacity (WAC) of bacteria incorporated concrete specimens is reduced by nearly 50 % as compared with WAC of reference concrete specimens due to pore plugging with bacteria produced calcite minerals thereby modifying the pore structure of the cement –sand matrix. The absorption characteristics indirectly represent the volume of pores and their connectivity. Porosity of concrete specimens is reduced by nearly 57 - 73% with induction of bacteria into concrete. The possible reason for this is calcite mineral precipitation in the pores reduced the average pore radius of concrete. This means that the time taken for the water to rise by capillary action in bacteria incorporated concrete is longer and thus proved that these bacteria induced concretes are less porous compared to the reference concrete. The rate of water absorbed into concrete through the pores gives important information about the microstructure and permeability characteristics of concrete. Volume of permeable voids present in bacteria incorporated concrete is less by 50 % than in reference specimens.

It can concluded that all grades of bacteria incorporated concretes have less water absorption capacity compared to corresponding grades of reference concrete specimens due to pore plugging with bacteria produced calcite minerals. This reduction of porosity in bacteria

incorporated concretes indicates the presence of less volume of permeable voids. Water Absorption Capacity (WAC) of bacteria incorporated concrete specimens is reduced as compared in reference concrete specimens inferring the reduced extent of volume of pores and their connectivity in bacteria induced concrete. Volume of permeable pores (VPV) of bacteria incorporated concrete specimens are reduced since calcite mineral precipitation in the pores reduced the average pore radius of concrete by inducing pore discontinuity in the hydrated cement paste. This means that the time taken for the water to rise by capillary action in bacteria incorporated concrete are longer and thus proved that these concrete are less porous compared to the conventional concrete.

7.5 Chloride Resistance

The chloride resistance of concrete is governed primarily by the pore structure and the concrete diffusivity. Therefore, wherever there is a potential risk of chloride-induced corrosion, the concrete should be evaluated for chloride permeability. The most important concrete characteristic, apart from permeability, is diffusion. Usually chlorides penetrate in concrete by diffusion along water paths or open pores. The objective of the present experimental investigations is to determine the chloride penetration resistance of M20 and M40 grades of reference and bacteria incorporated concretes (Treated FAAC).

7.5.1 Rapid Chloride Permeability Test

As per ASTM C1202, in the Rapid chloride penetration test, a water-saturated, 50-mm thick, 100-mm diameter concrete specimen is

subjected to a 60 V applied DC voltage for 6 hours. The permeability cell, which is made of Perspex glass and consists of two parts each with a reservoir being capable of holding 250 ml of chemical solution and copper mesh of 100 mm diameter to act as an electrode. In upstream reservoir of is a 3.0% NaCl solution of 2.4N and in the downstream reservoir is a 0.3 M NaOH solution (chloride free). These concentrations give the equal electrical conductivity of both the solutions. An external voltage cell is used to apply a voltage difference of 60V between the electrodes. The electrochemical cell, constituted by this assembly, results in the rapid migration of chloride ions from the sodium chloride solution to the sodium hydroxide solution, via the pore network offered by the concrete disc shaped specimen. The total charge passed in coulombs is determined and this is used to rate the quality of the concrete according to the criteria rating mentioned in the ASTM C1202 as shown in Table below. Rapid chloride ion penetrability test is conducted on M20 and M40 grades of reference and bacteria incorporated concretes (Treated FAAC) specimens of 28, 60 and 90 days. The total charge passing through from one reservoir to another reservoir through centrally placed concrete specimen in 6 hrs was measured, at an interval of 60 min, indicating the degree of resistance of the specimen to chloride ion penetration as shown in Table below. The following formula, based on the trapezoidal rule can be used to calculate the average current flowing through one cell.

$Q = [900*(I0 + I360)+ 2(I30 + I60 + I90 + I120 + I150 \ldots\ldots)]/1000$ Coulombs

Where Q = total electrical charge passed through the specimen (in coulombs) ; I_0, I_6 are the initial and final currents ; I_1, I_2, I_3, I_4, I_5, are the intermediate currents at each one hr and I is the total current at the end of the test i.e., 6hrs.

The test determines the electrical conductance of the test specimen, expressed as the total electrical charge passed through the specimen, in coulombs.

7.5.2 Chloride ion diffusivity

The impermeability of concrete can be represented by the rate of flow or diffusion coefficient of chloride ions through the unit area of concrete. Chloride diffusivity in terms of total charge passed of bacteria incorporated concrete specimen using Rapid Chloride Penetration Test (RCPT) as per ASTM C 1202 is also investigated. The electric charge passed, Q in coulombs, obtained from Rapid chloride ion penetrability test was used to calculate Chloride Migration Diffusion Coefficient in steady state conditions from Berke's empirical Equation.

$$DC=0.0103 \times 10^{-12} \times Q^{0.84}\ m^2/s$$

The calculated diffusion coefficient values are shown in Table 7.3, are used to classify the concrete in terms of their permeability as per the recommendations of the Concrete Society, United Kingdom.

Table 7.15 - RCPT Criteria Ratings

Permeability Class	Electric Charge Passed as per ASTM C1202 (Coulombs)	Chloride Migration Diffusion Coefficients as per Concrete Society, United Kingdom (m^2/s)
High	> 4,000	$>5x10^{-12}$
Moderate	2,000 - 4,000	1 to 5 x 10^{-12}
Low	1,000 - 2,000	< 1 x 10^{-12}
Very Low	100 - 1,000	-
Negligible	< 100	-

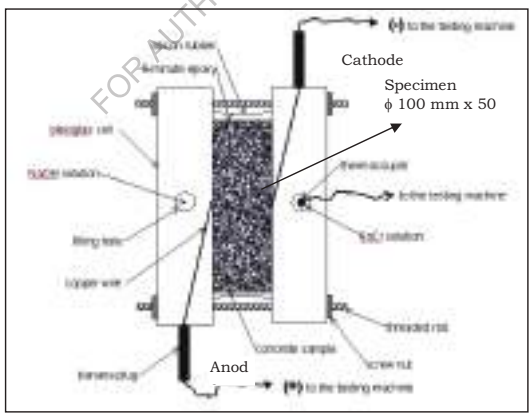

(Source: http://darienelectricmadras.com)

Figure 7.11 - Rapid Chloride Permeability Test Setup

Rapid chloride ion penetrability tests were conducted on M20 and M40 grades of reference and bacteria incorporated concretes (Treated FAAC) specimens of 28, 60 and 90 days to determine the total charge passed based on which chloride ion permeability can be estimated. The test results obtained confirms that the addition of bacteria to concrete exhibit better chloride ion penetration resistance in all the grades at all ages , due to voids being plugged with bacteria precipitated calcite crystals. Chloride ion permeability is very low in M20 and M40 grades of bacteria incorporated concretes (Treated FAAC). Results of the total charge passed through the concrete specimens indicate that bacteria induced concrete has shown significant improved resistance against the chloride movements as compared to that of in conventional concrete. All grades of conventional concrete have higher current flow when compared to corresponding grades of bacteria incorporated concrete. Bacteria incorporated concrete will have dense microstructure due to precipitation of mineral in pores of concrete.

The diffusivity of chloride through concrete therefore depends on the microstructure of the concrete. Diffusion Coefficient (DC) of chloride ions decreases with increase in higher grades in controlled concrete but with the introduction of bacteria into concrete further decrease is observed in the effective chloride ion diffusion coefficients. Reduction in chloride ion permeability values indicates that bacteria induced concrete has higher resistance against the chloride ion movements as compared to that of in conventional concrete. The mineral precipitation

fills the pores altering the original microstructure formed by the cement-sand matrix and subsequently increasing the tortuosity of the capillary network, resulting in longer paths and smaller pore diameters.

Table 7.16 - Total charge passed for M20 and M40 grades of reference and bacteria incorporated concretes (Treated FAAC) at different ages as per ASTM C1202

		Total Charge Passed (Coulombs)	Chloride ion Permeability as per ASTM C1202	Total Charge Passed (Coulombs)	Chloride ion Permeability as per ASTM C1202	Total Charge Passed (Coulombs)	Chloride ion Permeability as per ASTM C1202
	Age	28 days		60 days		90 days	
Reference Concrete (NAC)	M20	2419	Moderate	2213	Moderate	2100	Moderate
	M40	2008	Moderate	1991	Low	1817	Low
Bacterial Concrete (FAAC)	M20	367	Very Low	351	Very Low	327	Very Low
	M40	238	Very Low	222	Very Low	202	Very Low

Table 7.17 - Chloride Diffusion Coefficients of M20 and M40 grades of reference and bacteria incorporated concretes (Treated FAAC) at different ages as per Concrete Society, United Kingdom

		Chloride Migration Diffusion Coefficient (DC)	Chloride Permeability as per Concrete Society,UK	Chloride Migration Diffusion Coefficient (DC)	Chloride Permeability as per Concrete Society,UK	Chloride Migration Diffusion Coefficient (DC)	Chloride Permeability as per Concrete Society,UK
	Age	28 days		60 days		90 days	
Reference Concrete (NAC)	M20	7.16E-12	High	6.64E-12	High	6.36E-12	High
	M40	6.12E-12	High	6.08E-12	High	5.63E-12	High
Bacterial Concrete (FAAC)	M20	1.47E-12	Medium	1.41E-12	Medium	1.33E-12	Medium
	M40	1.02E-12	Medium	0.96E-12	Low	0.89E-12	Low

The *Sporosarcina pasteurii* bacterial strain incorporated concrete would be considered to have very low chloride ion permeability which validates its refined pore structure. The presence of bacteria precipitated calcium carbonate crystals reduces the porosity by plugging the pores present in the concrete ensuing minimum interconnecting voids. Decrease in chloride ion permeability is more pronounced in high strength grades of concrete. The same trend is observed at all ages of concrete. The Chloride ion penetrability of controlled mixes is 'low' to 'moderate' when compared with 'negligible' to 'very low' bacteria incorporated concrete. Chloride ion penetration resistance is more in bacteria incorporated concrete when compared to conventional concrete due to voids being filled with calcite crystals precipitated by bacteria reducing the porosity of the concrete.

It can be concluded that bacteria incorporated concrete will have the higher life compared to conventional concrete because precipitated calcite crystals impermeable the concrete specimens and resists the harmful solutions into the concrete there by decreasing the deleterious effects they may cause. This property can be effectively used to improve the water tightness of the concrete in water retaining structures.

7.6 Resistivity of Concrete

As per CEB 192 -1997 stands for Comité Euro-International du Béton (French: Euro-International Concrete Committee, the resistivity of concrete indicates the degree of water saturation of the specimen, the resistance to chloride penetration or the corrosion rate. High resistivity of

concrete implies a high electrolytic resistance and this will limit the rate of corrosion.

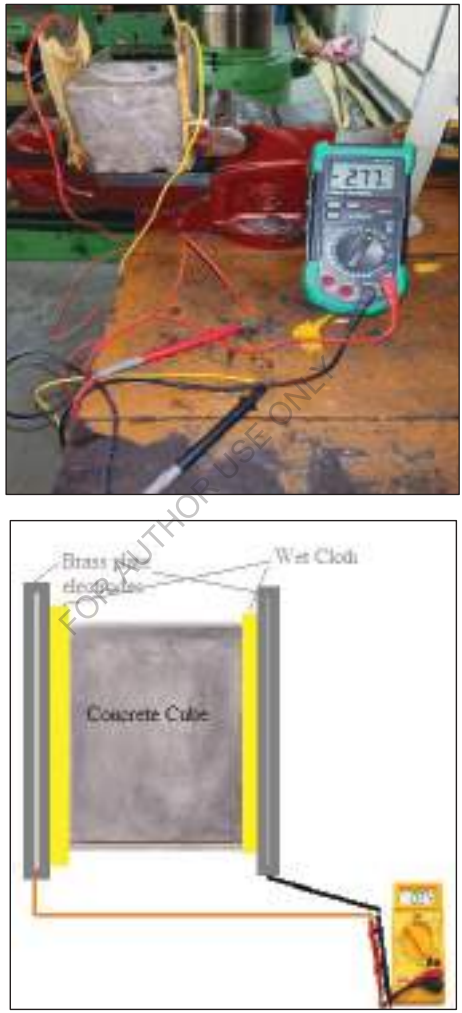

Figure 7.12 - Resistivity measurements on concrete specimen

Table 7.18 - Resistivity assessment criteria (CEB)

S. No	Concrete Resistivity (ohm-cm)	Likely Corrosion Rate
1	> 20, 000	Negligible
2	10,000 – 20,000	Low
3	5,000 – 10, 000	High
4	< 5,000	Very High

This test is conducted on 100mm cube samples. Before starting the experiment the cube surfaces are cleaned to remove the dust particles. For each mix one sample is taken and tested for resistivity in wet condition using a direct two probe technique. Two brass plate electrodes of 100x100mm i.e. the size of cube end surface are taken to ensure a uniform current density while measuring resistance. Two wet clothes are placed on either side of the cube and brass plate electrodes are kept in contact to the wet cloth and were firmly fixed to a bench wice or a 'C'clamp and steel plates as shown in figure. Now the resistance is measured on wet surface of the cube taken from normal water as follows.

$$\rho = RA/L$$

Where

R= Resistance measured in Kohms

A = Area of the cube surface in cm2

L= Length between two electrodes in cm

ρ = Resistivity in kohm-cm

Concrete resistivity's for M20 and M40 grades of reference and bacteria incorporated concretes (Treated FAAC) are determined and presented in tables 7.19 and 7.20 below.

Table 7.19 - Resistivity of M20 grade of reference and bacteria incorporated concretes (Treated FAAC)

Type of SCC mix	Resistivity (ohm.cm)				
	1day	3 days	7 days	28 days	90 days
M20 Reference Concrete (NAC)	1200	6200	12300	18200	26300
M20 Bacterial Concrete (FAAC)	1880	13300	22200	35900	67900

Table 7.20 - Resistivity of M40 grads of reference and bacteria incorporated concretes (Treated FAAC)

Type	Resistivity (k.ohm.cm)				
	1days	3 days	7 days	28 days	90 days
M40 Reference Concrete (NAC)	2100	9700	17400	37100	44300
M40 Bacterial Concrete (FAAC)	2900	14200	24900	58700	83100

From test results the resistivities of M20 and M40 grades of bacteria incorporated concretes (Treated FAAC) from 7th day onwards are showing resistivity above 20kohm-cm, the limit set for good concrete according to Brown et.al limitations. At 90 days, both M20 and M40 grades of reference and bacteria incorporated concretes (Treated FAAC) mixes are showing high resistivity due to refined and compact structure.

Resistivity of the concrete is an important parameter in the study of the corrosion behaviour of steel in RC members. High resistivity of concrete implies a high electrolytic resistance and will limit the rate of corrosion. Resistivity (corrosion possibility) of M20 and M40 grades of reference and bacteria incorporated concretes (Treated FAAC) mixes increases with age especially more significant in M20 grade mixes than M40 grade concrete mixes. The resistivity of reference concrete mixes (NAC) is lower than bacteria incorporated mixes (FAAC) means more corrosion likely due to higher porosity. The 90 day resistivity's of M20 and M40 grades of reference and bacteria incorporated concretes (Treated FAAC) show that the probable corrosion rates were negligible as per the limitations suggested by Browne et al. (1983).

7.7 Corrosion Potentials Measurements

Corrosion potentials measurements are also used to detect the probability of steel corrosion at various stages. This provide an indication of the oxidizing potentials of the steel with respect to a reference electrode in a particular environment. The potentials of steel in concrete were measured

by using Saturated Calomel Electrode (SCE) as per ASTM C 876- 2015 Standard Test Method for Corrosion Potentials of Uncoated Reinforcing Steel in Concrete.

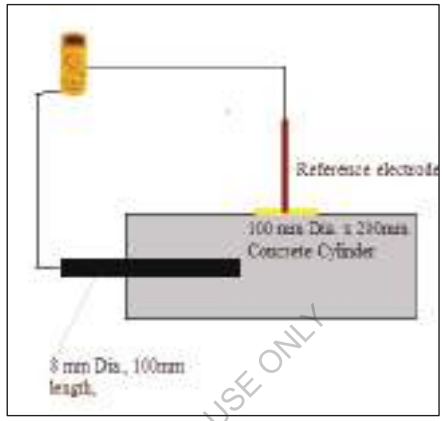

Figure 7.13 - Test Specimen for Corrosion Studies

Figure 7.14 - Half-cell potentiometer Test setup

Table 7.21 - Corrosion probability from half-cell potential (ASTM C 876)

S. No	Potential (SCE, mV)	Probability of Corrosion (%)
1	> -120	5
2	-120 to -270	50
3	< -270	95

The corrosion potential studies were done on 100x200 mm cylinders by embedding an 8 mm diameter cold twisted high yield strength deformed bar (Tor steel) of 100 mm length. The rust products on the bars were cleaned. At end of the each bar a 24 strand well insulated tin coated copper wires of low resistance are brazed to facilitate the measurement of potentials in corrosion studies. The bars were placed centrally in the cylinders (100x200mm) by ensuring almost 45mm cover from all the sides. The potentials were measured with reference to a Saturated Calomel Electrode (SCE). The potentials were taken up to 90 days of curing. These potentials indicate the probability of corrosion occurrence. The specimens were immersed in normal water and the potentials were taken for the different concretes at 1, 3, 7, 28 and 90 days. The measurements were taken with the help of a high impedance digital voltmeter to an accuracy of 1mV. While taking the reading, the lead of the specimen is to be connected to the positive terminal whereas the electrode is connected to

the negative terminal. It was also seen that the electrode is in contact with the wet surface.

Concrete potentials for M20 and M40 grades of reference and bacteria incorporated concretes (Treated FAAC) are determined and presented in tables 7.22 and 7.23 below.

Table 7.22 - Potentals of M20 grades of reference and bacteria incorporated concretes (Treated FAAC)

Type	Potentials (SCE, mV)				
	1 day	3 days	7 days	28 days	90 Days
M20 Reference Concrete (NAC)	No Reading	No Reading	-424	-175	-123
M20 Bacterial Concrete (FAAC)	No Reading	No Reading	-131	-94	-81

Table 7.23 - Potentials of M40 grades of reference and bacteria incorporated concretes (Treated FAAC)

Type	Potentials (SCE, mV)				
	1 day	3 days	7 days	28 Days	90 Days
M40 Reference Concrete (NAC)	No Reading	No Reading	-304	-135	-103
M40 Bacterial Concrete (FAAC)	No Reading	No Reading	-123	-80	-72

From the test results, the corrosion rates of M20 and M40 grades of bacteria incorporated concretes (Treated FAAC) seems to low i.e. is less than 5% according to limitations specified by ASTM due to dense microstructure through calcite mineral precipitates.

The results of the potentials show that M20 and M40 grades of reference and bacteria incorporated concretes (Treated FAAC) mixes were showing very low potentials at 90 days. It can also be observed that the corrosion potentials of steel in bacteria incorporated concretes (Treated FAAC) mixes were lower than the reference concrete (NAC) mixes.

In reference concrete (NAC) mixes at 28 days initially potential measurements have shown 50% probability of corrosion. But at 90 days due to complete hydration has indicated only <5% probability of corrosion. M20 reference mixes show high potential for corrosion due to their

electrical conductivity nature due to presence of pore water. The bacteria incorporated concretes (Treated FAAC) mixes were showing very low potentials from 28 days almost 5% possibility of corrosion. This clearly shows the passivity of steel bar in treated fly ash aggregate bacterial concretes due to enhanced microstructure from MICP process.

7.8 Carbonation

The objective of this study is to determine carbonation of M20 and M40 grades of reference and bacteria incorporated concretes (Treated FAAC) as per RILEM CPC – 18. Carbonation of concrete is associated with the corrosion of steel reinforcement and with shrinkage. However it increases both compressive strength and tensile strength of concrete. Carbonation is the result of dissolution of CO_2 in concrete pore fluid and this reacts with calcium from $Ca(OH)_2$and calcium silicate hydrate to form calcite ($CaCO_3$). Increase in air pollution and potential increase in atmospheric CO_2 and temperature, due to greenhouse effects may result in great carbonation. Carbonation reduces the pH of the concrete and may lead to corrosion of steel.

The affected depth from the concrete surface can be readily shown by the use of phenolphthalein indicator solution. This is available from chemical suppliers. Phenolphthalein is a white or pale yellow crystalline material. For use as an indicator it is dissolved in a suitable solvent such as isopropyl alcohol (isopropanol) in a 1% solution.

The phenolphthalein indicator solution is applied to a fresh fracture surface of concrete. If the indicator turns purple, the pH is above 8.6. Where the solution remains colorless, the pH of the concrete is below 8.6, suggesting carbonation. A fully-carbonated paste has a pH of about 8.4.

Figure 7.15 - Phenolphthalein solution

Observation on carbonation depths of M20 and M40 grades of reference and bacteria incorporated concretes (Treated FAAC) are presented below

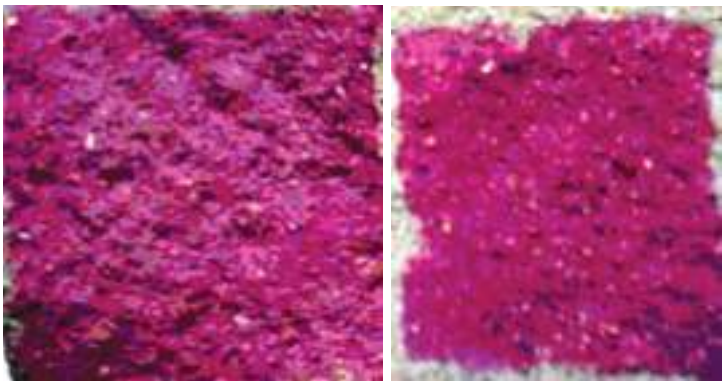

a) Bacterial specimen **b) Reference specimen**

Figure 7.16 - Colour change due to phenolphthalein solution

No carbonation is observed in M20 and M40 grades of bacteria incorporated concretes (Treated FAAC) specimens of age 365 days of curing. Therefore carbonation depth is zero for M20 and M40 grades of bacteria incorporated concretes (Treated FAAC). But for reference specimens average carbonation depth is 1.5 mm for M20 and M40 grades.

7.9 Summary

This section presents materials used and their properties (provided by the supplier) and methodology for preparation of fly ash based artificial coarse aggregates, process of growing and culturing bacteria, Optimum bacterial cell concentration for $CaCO_3$ Precipitation, effect of biotic and abiotic factors of bacterial activity on strength and durability of cementitious materials, Characterization of $CaCO_3$ precipitation, mix proportions of

M20 and M40 grade concretes, mechanical properties of M20 and M40 grade fly ash aggregate based bacterial concretes , Flexural Behavior of fly ash aggregate based bacterial concrete beams, Pore Structure Analysis, permeation properties, corrosion resistance of M20 and M40 grade fly ash aggregate based bacterial concretes using BET Nitrogen (N2) Adsorption method. Finally crack healing efficiency evaluation methods are discussed.

Chapter - 8

CRACK HEALING EFFICIENCY

8.1 General

Bacillus pasteurii / Sporosarcina pasteurii is a common bacterium found in soil, produce urease, can continuously precipitate a new highly impermeable calcite layer over the surface of an already existing concrete layer. Bacteriogenic crack healing utilizes a biological byproduct $CaCO_3$, as a potential sealant to seal and heal cracks and pores present in concrete. This phenomenon can be extended to remediation of surface cracks and fissures in various structural formations, in-base and sub-base stabilization, and surface soil consolidation. Due to metabolic activity of certain calcinogenic microorganisms, calcium carbonate is precipitated. This coarse crystalline precipitated calcite readily adheres to the concrete surface in the form of scales, forms a highly impermeable and insoluble layer which can be used as surface crack healing for concrete or any other building material. This chapter deals with efficacy of microbiologically motivated crack healing in terms of strength recovery and enhancement of surface impermeability. This precipitation and its repair efficiency can be manifested visually and chemically. Bio-mineralization is an eco-friendly bio-process, shows promising results in sealing the micro-cracks by Microbially Induced $CaCO_3$ Precipitation (MICP).

8.2 Crack Remediation and Strength Regain

The aim of this test is to evaluate the efficiency of crack remediation technique using *Sporosarcina pasteurii* bacterial strain and determine the degree of strength regain in cracked concrete specimens.

To demonstrate the crack healing efficiency and strength regain, cracked cement mortar samples were prepared in two different ways. The first method resulted in samples with standardized cracks while the second method gave rise to more realistic cracked samples.

(a) Standardized cracks

Standardized cracks were made in twelve number of cement mortar cubes of size 70.6x70.6x70.6mm by making a cut to simulate a crack. The width of cut is kept at an average of 3mm width and a 20mm depth as shown in Fig below. Cracks in the three cement mortar specimens are filled up with Indian standard grade II sand (1mm to 0.5 mm) mixed with water and specimens are cured in distilled water after air dried for one hr. The cracks in another set of three specimens are closed with Indian standard grade II sand mixed with 10^5 cell concentration of *Sporosarcina pasteurii* bacterial strain and after air dried for one hr, cubes are cured in bacteria-nutrient medium. The medium is changed after 14 days. Similarly another set of three cut cement mortar specimens containing no filling were kept exposed to air. All the three sets of cement mortar specimens were tested for the compressive strengths after 28 days.

(a) No filling in cut **(b) with filling in cut**

Figure 8.1 - Simulated standard cracks made in cement mortar cubes

(b) Realistic cracks

Realistic cracks were obtained in cement mortar specimens by applying at least 60 % of ultimate load until a crack was visible with the naked eye. Then the cracked samples were placed in *Sporosarcina pasteurii* bacterial strain and nutrient medium for 28 days. During the period of immersion, bacteria started to precipitate $CaCO_3$ resulting in a compete filling of the crack. The deposition of calcium carbonate was visually monitored periodically. At the end of the 28 day exposure, the cubes were tested for compressive strength.

The table 8.1 below tabulates the compressive strength values of all three sets of cement mortar specimens with simulated standardized cracks.

Table 8.1 - Compressive strengths of cement mortar specimens with standard simulated cracks

Specimen Type	Compressive strength at 28 days (MPa)
Reference specimen (with no crack made)	52.6
Specimen with simulated Crack (crack not filled up)	28.91
Specimen with simulated crack (crack filled up with standard sand mixed with distilled water)	34.56
Specimen with simulated crack (crack filled up with standard sand mixed with bacterial culture)	42.36

The above studies showed that the simulated cracked cube filled up with standard sand mixed with bacterial culture has regained the strength of about 46%, when compared to the cut and non-remediated cube (cut with no fill up). Strength loss due to simulated crack left untreated (no fill up) is 45%. Strength loss due to simulated crack treated with standard sand mixed with distilled water is 34.3%. Strength loss due to simulated crack filled with standard sand mixed with bacterial culture is 19.5 %. Strength gain due to biogenic treatment is 22.6% this is mainly due to chemical bonding between $CaCO_3$ precipitated by bacterial cells and sand particles which consolidate the crack space.

Table 8.2 - Compressive strengths of cement mortar specimens with realistic cracks

Type of specimen	Compressive strength at 28 days (MPa)
Control cement mortar specimen	51.68
Cracked cement mortar specimen (immersed in water)	44.99
Cracked cement mortar specimen (immersed in bacterial culture) (Bio-remediated)	49.17

Strength loss for cracked cement mortar specimens immersed in water is 13 %. Strength loss for cracked cement mortar specimens treated in bacterial culture is 4.9 %. Strength gain due to biogenic treatment is 9.3 %. The visual examination of crack surface of the cement mortar samples reveals the fully grown calcite crystals, with distinct and sharp edges all over the surface of the crack, acts as an agent for an eventual plugging and crack remediation. Bacteriogenic mineral precipitation contributed to the bonding and regaining strength of the already cracked cubes. This microbial mixture with sand filled in the cracks was found to remain intact after five days treatment confirming the microbial calcite precipitation. Higher strength regain was obtained because of the bacterial $CaCO_3$ precipitation inside the simulated cracks of cement mortar specimens.

This strength recovery can be attributed to chemical bonding between $CaCO_3$ precipitated by bacterial cells and sand particles which consolidate the crack space.

8.3 Surface permeability

This test aims to demonstrate the surface permeability of bacteria treated cement mortar specimen (immersed in *Sporosarcina pasteurii* bacterial strain suspension) and untreated cement mortar specimen (immersed in distilled water).

Surface permeability measurements were carried out by measuring the absorption of a drop by the surface of bacteria treated (immersed in *Sporosarcina pasteurii* bacterial strain - nutrient medium) and untreated (immersed in distilled water) cement mortar samples of size 70.6 x70.6x70.6mm.

A 0.2 ml of distilled water was placed on the surface of the cement mortar specimen and the time necessary for complete water absorption was measured. These experiments were done on five points for each sample and the average time taken for total absorption is determined.

For the untreated cement mortar sample, absorption was almost immediate (less than 3 sec) while for the bacteria treated sample the drop kept its shape for about 27 sec (like a water drop on a hydrophobic surface) and was completely absorbed after 35 sec. It is clear that the surface permeable properties were modified by the bacteria treatment by reducing surface porosity. Sample immersed in bacteria – nutrient medium forms a

scaled crust like layer as shown in SEM image. This calcite crust forms an impermeable layer on the surface of the cement mortar sample reducing the surface permeability in case of bacteria treated cement mortar sample.

Figure 8.2 - untreated and bacteria treated surfaces of mortar cubes

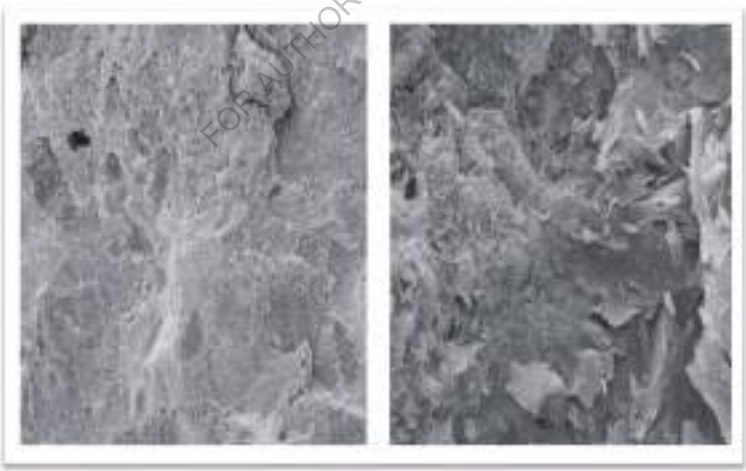

Figure 8.3 - SEM images of untreated and bacteria treated surfaces

8.4 Assessment of Crack healing efficiency by Non-Destructive methods

The main objective of the present experimental investigations is to assess the crack healing efficiency of fly ash aggregate concretes (FAAC) incorporated with *Sporosarcina pasteurii* bacterial strain using Ultrasonic pulse velocity measurements. Bacteria incorporated concrete (Treated FAAC) cylinders of size 150x150mm are casted and artificial cracks are created on application of 60% of load on the cylinders. These cracked specimens are immersed in the nutrient solution for 28 days.

Ultrasonic Pulse Velocity Test is conducted as per IS: 13311 (Part 1) – 1992 on cracked and healed bacteria incorporated (Treated FAAC) cylinders of size 150x150x150mm. This test qualitatively assesses the homogeneity and integrity of concrete. This test also determined the density and elastic properties of the concrete.

Ultrasonic pulse velocity test was conducted are on cracked specimens and microbially healed specimens. The Table 8.3 below lists the mean pulse velocity values of cracked and healed bacteria incorporated (Treated FAAC) cylinders specimens. It is observed the ultrasonic pulse velocity value increased in healed specimens due to plugging of cracks with highly dense bacterial precipitates confirming the particle continuity inside the concrete specimen.

Table 8.3 - Ultrasonic pulse velocity values of cracked and healed bacteria incorporated (Treated FAAC) concrete specimens at 28 days

	Mean Pulse Velocity km/sec	Quality of Concrete
Cracked Specimen	2.26	Doubtful
Microbially healed specimen	4.32	Excellent

It can be concluded that the ultrasonic pulse velocity value of healed bacteria incorporated (Treated FAAC) concrete specimens indicate crack healing efficiency using MICP process by *Sporosarcina pasteurii* bacterial strain in improving the pore structure of concrete through calcite precipitation.

8.5 Crack healing efficiency using Water permeability test

Concrete water permeability test is conducted as per IS 3085:1965. Bacteria incorporated (Treated FAAC) cylindrical concrete specimens of diameter 150mm and height 150mm are casted and cured for 28 days. Specimens are cracked artificially and immersed in the nutrients solution for 28 days to evaluate its self-crack healing efficiency by assessing the water permeability of the healed specimen.

Table 8.4 - Coefficient of water permeability ranges as per IS: 3085-1965

Water Permeability	Very Low	Low	Medium	High
Coefficient of permeability (x 10^{-9} m/sec)	< 0.5	0.5-1.0	1.0-2.0	>2.0

Table 8.5 - Permeability ranges according to standard DIN 1048 (Part 5):1991

Permeability as per to DIN 1048	Low	Medium	High
Penetration depth after 96 hrs	Less than 30 mm	30-60 mm	Greater than 60 mm

Permeability test shall be continued for about 100 hours after the steady state of flow has been reached and the outflow shall be considered as average of all the outflows measured during the period of 100 hours. Then the coefficient of permeability (k, in m/sec) based on Darcy's law for a falling water head, which is applicable at steady state flow conditions, can be computed on 28 and 60 days aged specimens, using the following formula

$$K = \frac{Q}{A \times T \times (H / L)}$$

Where K= Coefficient of permeability in m/sec

Q = Quantity of water collected in milliliters over the entire period of test

T = Time in seconds over which Q is measured = 100x60x60 sec = 360000sec

A = Area of the specimen face in m^2 = 0.01767 m^2

Water pressure=10 kg/cm^2 = 10^6 Pa

1Pa of water pressure = 0.0001m of pressure head (water at room temperature)

Pressure Head = 100 m (kept constant throughout the test)

H/L = ratio of pressure head to thickness of the specimen both expressed in metre = 100/0.15 = 666.67

The determination of the permeability is also carried out by measuring the water penetration depth after 96 hrs by a splitting the cylinder specimens. To measure the water coefficient by penetration at 28 and 90 days age, Valenta's law can be applied if the material is less permeable.

$$k = \frac{D^2 V}{2 H T}$$

Where, k= Water permeability coefficient (m/s)

D= depth of penetration (m)

V= Volume of voids filled by water in the penetrated zone

H= Applied pressure is 5 bar (1 bar = 10m)

T= Time to penetrate to depth D (s)

Figure 8.4 - Cracked Specimen and microbially healed specimen

The table 8.6 below presents the coefficients of permeability values determined as per IS 3085 for cracked and healed bacteria incorporated (Treated FAAC) concrete specimens.

Table 8.6 - Coefficients of Permeability for cracked and healed bacteria incorporated (Treated FAAC) concrete specimens

Type of specimen	Pressure head H (m)	Quantity of water collected (ml)	Coefficient of permeability x 10^{-9} m/sec	Permeability
Cracked Specimen	100	19822	3.31	High
Microbially healed specimen	100	1155	0.27	Very low

The table 8.7 below presents water permeability of the cracked and healed bacteria incorporated (Treated FAAC) concrete specimens determined as per DIN 1048.

Table 8.7 - Depth of Penetration for cracked and healed bacteria incorporated (Treated FAAC) concrete specimens

Type of specimen	Depth of Water Penetration (mm)	Permeability as per DIN 1048 (Part 5):1991
Cracked Specimen	150	High
Microbially healed specimen	7	Low

From the presented test results, it was observed that significantly lower water permeability is observed in bacteria healed specimens than cracked specimens. Results show that the water seeps through the cracked specimen whereas in microbially healed specimen the permeability is very low. It shows that microbially surface treated concretes are less permeable than the reference concretes the reason attributed is that the impermeable calcite layer is formed on the surface reduces the permeability of the concrete.

8.6 Summary

This section presents materials used and their properties (provided by the supplier) and methodology for preparation of fly ash based artificial coarse

aggregates, process of growing and culturing bacteria, Optimum bacterial cell concentration for $CaCO_3$ Precipitation, effect of biotic and abiotic factors of bacterial activity on strength and durability of cementitious materials, Characterization of $CaCO_3$ precipitation, mix proportions of M20 and M40 grade concretes, mechanical properties of M20 and M40 grade fly ash aggregate based bacterial concretes , Flexural Behavior of fly ash aggregate based bacterial concrete beams, Pore Structure Analysis, permeation properties, corrosion resistance of M20 and M40 grade fly ash aggregate based bacterial concretes using BET Nitrogen (N2) Adsorption method. Finally crack healing efficiency evaluation methods are discussed.

Page left blank intentionally

Chapter - 9

COST ANALYSIS

9.1 General

This section presents the cost incurred to develop the M20 and M40 grade fly ash aggregate based bacterial concretes along with the suggestions to optimize the cost of bacterial concrete by optimizing the ingredients of bacterial concrete.

9.2 Cost Analysis

The cost of using microbial concrete compared to conventional concrete is critical in determining the economic feasibility of the technology. The cost analysis showed an increase in cost of 2.3 to 3.9 times between microbial concrete and conventional concrete with decrease of grade as shown in Table below. The major contributor to the cost of the bacterial mix is the nutrient broth, amounting to over 60-75% of the cost per cubic meter of concrete. Therefore, further research needs to be devoted to decrease the amount of the nutrient broth used or to find a cheaper alternative source for bacteria nutrition in order to make the technology financially feasible. Nevertheless, it is believed that microbial concrete will yield cost reductions on the long run through decreased need for rehabilitation and maintenance. Furthermore, the high cost of the technology is outweighed by its positive environmental impact. Only expensive component in the development of bacterial concrete is nutrients. In the market bacteria is

available is lyophilized state. So cost depends on the surface treatment area or volume of concrete used. Nutrients used for this study are laboratory nutrients which are quite expensive so other inexpensive nutrient sources can also be tried to reduce the commercial production cost of bacterial concrete. However, any nutrients such as inexpensive, high-protein-containing industrial wastes such as corn steep liquor (CSL) or lactose mother liquor (LML) effluent from starch industry can also be used so that overall process cost reduces dramatically. These industrial effluents which are potential environmental pollutants and also available locally with a price of nearly Rs 100 per liter, which is very economic compared with standard laboratory nutrient medium. In this project, to prepare one liter of nutrients mixed bacterial culture, it required 13 grams of nutrients broth powder. The cost of 500 grams of HIMEDIA M002 nutrient broth powder costs about 2300 rupees so to prepare one litre of nutrients mixed bacterial culture costs Rs 60. In this project nearly 125 liters of nutrients mixed bacterial culture was used costing nearly 7500 rupees.

Table 9.1 Manufacturing Cost of Concrete per Cubic meter

Grade of Concrete	Cement 1kg= 6.5 Rs (a)	FA (River Sand) 1kg=0.80Rs (b)	Natural CA (20mm) 1kg=0.60Rs (c)	Fly ash CA (20mm) 1kg=3.7Rs (d)	Water (e)	Bacteria suspended water 1L=60Rs (f)	Cost of Reference Concrete cu m in Rs. (a+b+c+e)	Cost of Bacterial Concrete cu m in Rs. (a+b+d+e+f)
M20	2082.6	581.8	663.2	4089.98	0.0	10380.0	3327.6	17134.4
M40	2539.6	540.8	671.8	4142.9	0.0	9846.0	3752.2	17069.3
Note: Based on Locally available rates in Hyderabad								

9.3 Summary

This section presents materials used and their properties (provided by the supplier) and methodology for preparation of fly ash based artificial coarse aggregates, process of growing and culturing bacteria, Optimum bacterial cell concentration for $CaCO_3$ Precipitation, effect of biotic and abiotic factors of bacterial activity on strength and durability of cementitious materials, Characterization of $CaCO_3$ precipitation, mix proportions of M20 and M40 grade concretes, mechanical properties of M20 and M40 grade fly ash aggregate based bacterial concretes , Flexural Behavior of fly ash aggregate based bacterial concrete beams, Pore Structure Analysis, permeation properties, corrosion resistance of M20 and M40 grade fly ash aggregate based bacterial concretes using BET Nitrogen (N2) Adsorption method. Finally crack healing efficiency evaluation methods are discussed.

Chapter -10

CONCLUSIONS

In this chapter, based on the test results and key findings during the experimental investigations on the performance and crack healing efficiency of fly ash based bacterial concrete , the following conclusions are drawn:

1. The cement mortar cube specimens which contained cell concentration of 1x 10^5 bacterial cells/ml of mixing water was found to attain higher compressive strength as compared to the control specimen. This improvement of compressive strength is attributed to the deposition of $CaCO_3$ precipitate formed by *Sporosarcina pasteurii* which modifies the concrete pore structure by plugging the voids /or the pores within cement–sand matrix, as part of its metabolic activity.

2. The maximum percentage increase is found to be 17.88 % for 10^5 bacterial cells induced specimens. It is observed that for cement mortar specimens incorporated with *Sporosarcina pasteurii* cell concentration of 10^7 cells per ml the compressive strength is reduced drastically. The gradual reduction of compressive strength of cement mortar cube specimens induced with bacterial cell concentrations more than 10^5 cells per ml of mixing water is attributed to the disruption of cement-mortar matrix integrity by the presence of organic matter (biomass) above the permissible limits as specified by IS 456. Maximum strength is observed

for 10^5 cells/ml of mixing water so this is taken as optimum cell concentration to be used for further study to investigate the effect of bacteria on properties of cement mortar.

3. From the studies on effect of biotic and abiotic factors on the bacterial activity, it was found that only bacteria *Sporosarcina pasteurii* with suitable nutrients responsible for the microbiological activity which produces calcite crystals plugging the pores of the cementitious materials.

4. Cement mortar specimens made with bacterial broth (bacteria and nutrients) and calcium source in the form of calcium lactate yields more compressive strength due to enhanced pore refinement in the microstructure of cement mortar with precipitation of calcite mineral by bacteria Sporosarcina pasteurii. The mineral precipitation in cement mortar reduces the interconnectivity of the pore structure by decreasing the pore size (pores refinement), which is directly related to durability.

5. Sporosarcina pasteurii cell concentration of 10^5 cells/ml of mixing water generates the greatest reduction in porosity by precipitating calcite crystals optimally. Reduction in pores due to such material precipitation (calcium carbonate) will eventually increase the cement mortar strength. Microbial calcite was precipitated on the surface of cells and eventually within the pores leading to their plugging which further lead to stoppage of flow of oxygen and nutrients to the cells. The cells either die or transformed into endospores that act as organic solid fibers.

6. Bacteria treated fly ash aggregates bacterial concrete (FAAC) yields high compressive strength than untreated fly ash aggregate bacterial concrete which are highly porous in nature. The increase in compressive strength of 25.8% is observed in bacteria incorporated mortar specimens. In bacteria incorporated mortar specimens, the water absorption capacity reduced by 86% due to plugging of the pores present in the cement mortar ensuing minimum interconnecting voids.

7. Characterization of calcite crystal precipitation done using various nano-characterization techniques such as Scanning Electron Microscope (SEM), X-ray diffraction (XRD) and Thermo-gravimetric analysis (TGA) confirms the presence of $CaCO_3$ formed due to complex metabolic mechanism of hydrolysis of urea by *Sporosarcina pasteurii.*

8. It was observed that with the addition of bacteria there is significant increase in compressive strength, split-tensile strength and flexural strength of concrete due to pore refinement by bacteriogenic calcite mineral plugging in bacteria induced concrete.

9. From the observations made from stress-strain curves, the bacteria incorporated concrete mixes have shown improved stress values for the same strain levels compared to that of controlled concrete mixes.

Calcite crystal precipitation in bacterial concrete increases the resilience and strain relieving capacity. This resilient character provides the excellent impact resistance and dissipates dynamic loading better than conventional concrete. So toughness or energy absorption capacity of bacteria

incorporated concrete grades is high when compared to same grades of conventional concrete. Modulus of Elasticity (E) is comparatively more for all grades of bacteria induced concrete than the controlled concrete. This feature is attributed to the dense pore structure of bacteria incorporated concrete.

10. Due to mineral precipitation in reinforced bacteria incorporated beams, internal micro cracking in the cementitious matrix is prevented through plugging up of cracks by continuous calcite mineral precipitates of *Sporosarcina pasteurii*. Hence bacteria induced concrete will have dense micro structure with low pore fraction and reduced pore size due to which fatigue strength is increased which in turn increases the first crack load and the ultimate load carrying capacity in case of flexural loading.

11. Chloride ion penetration resistance is more in bacteria incorporated concrete when compared to conventional concrete due to voids being filled with calcite crystals precipitated by bacteria reducing the porosity of the concrete.

12. Water Absorption Capacity (WAC) of bacteria incorporated concrete specimens reduces by nearly 50 to 80% for low to high grade concretes when compared to controlled concrete.

13. Volume of permeable pores (VPV) of bacteria incorporated concrete specimens are reduced by nearly 50-65%. The possible reason for this is calcite mineral precipitation in the pores reduced the average pore radius

of concrete by blocking the large voids (pore discontinuity) in the hydrated cement paste.

14. No carbonation is observed in M20 and M40 grades of reference and bacteria incorporated concretes (Treated FAAC) specimens of age 365 days of curing. Therefore carbonation depth is zero for M20 and M40 grades of reference and bacteria incorporated concretes (Treated FAAC).

15. Pore Structure Analysis using BET Nitrogen (N2) Adsorption method indicated that the porosity decreases significantly in bacteria incorporated concrete because pore diameter and total pore volume are very low due to calcite mineral precipitation in the pores by Sporosarcina pasteurii bacterial strain metabolic activity. Total pore surface area increases in bacteria incorporated concrete specimens due to formation of dense microstructure.

16. Strength loss due to simulated crack filled with standard sand mixed with bacterial culture is 19.5 %. Strength gain due to biogenic treatment is 22.6% this is mainly due to chemical bonding between $CaCO_3$ precipitated by bacterial cells and sand particles which consolidate the crack space.

17. For the untreated cement mortar sample, absorption was almost immediate (less than 3 sec) while for the bacteria treated sample the drop kept its shape for about 27 sec (like a water drop on a hydrophobic surface) and was completely absorbed after 35 sec. It is clear that the surface

permeable properties were modified by the bacteria treatment by reducing surface porosity.

18. The ultrasonic pulse velocity studies and water permeability studies on crack healed bacteria incorporated (Treated FAAC) concrete specimens indicate crack healing efficiency using MICP process by Sporosarcina pasteurii bacterial strain in improving the pore structure of concrete through calcite precipitation.

So it is concluded that bacteria incorporated concrete is a smart, sustainable, eco-friendly biomaterial that enhances concrete performance by the microbial deposition of calcium carbonate within its pores through molecular reactions there by refining the pore structure of concrete. Bacteriogenic mineral precipitation, contributed to the bonding and regaining of strength of the already cracked specimens. This strength recovery can be attributed to chemical bonding between CaCO3 precipitated by bacterial cells and sand particles which consolidate the crack space.

One of the main objectives of this was to present the synergistic action of binary, ternary and quaternary self-compacting concretes (SCC) on arheological properties, strength and durability properties of SCC for the ordinary grade (M20), standard grade (M40), and High strength grades (M80 and M100). The above studies are also extended to SCC mixes made with partial replacement of river sand with granulated blast furnace slag (GBFS) as fine aggregate replacement.
This book endorses the following recommendations: 1) Use of metakaolin in fly ash based blended SCC enhances both strength and durability properties significantly and is found to be cost-effective in terms of less cement usage, increased usage of fly ash, and also plays a major role in early strength development of FA based blended SCC; 2) the use of GBFS as an alternative partial replacement for river sand due to its well-graded particle size distribution and also its physical and chemical properties conform to IS 383 specifications.

Saduwale Shrihari is a Professor of Civil Engineering, VJIT, Hyderabad.
M. V. Seshagiri Rao is a Professor and Dean of CVR College of Engineering, Hyderabad & Ex-Professor (JNTUH).
V. Srinivasa Reddy is a Professor of Civil Engineering, GRIET, Hyderabad.

9 7 8 6 2 0 4 7 4 4 7 1 1

Shrihari Saduwale
Seshagiri Rao M. V.
Srinivasa Reddy Vempada

Binary, Ternary and Quaternary Blended Self-Compacting Concrete

Granulated Blast Furnace Slag (GBFS) as partial fine aggregate replacement

LAP LAMBERT Academic Publishing

Saduwale, M. V., Vempada

Shrihari Saduwale
Seshagiri Rao M. V.
Srinivasa Reddy Vempada

Binary, Ternary and Quaternary Blended Self-Compacting Concrete

Shrihari Saduwale
Seshagiri Rao M. V.
Srinivasa Reddy Vempada

Binary, Ternary and Quaternary Blended Self-Compacting Concrete

Granulated Blast Furnace Slag (GBFS) as partial fine aggregate replacement

LAP LAMBERT Academic Publishing

Imprint

Cover image: www.ingimage.com

Publisher:
LAP LAMBERT Academic Publishing
is a trademark of
Dodo Books Indian Ocean Ltd., member of the OmniScriptum S.R.L Publishing group
str. A.Russo 15, of. 61, Chisinau-2068, Republic of Moldova Europe
Printed at: see last page
ISBN: 978-620-4-74471-1

Binary, Ternary and Quaternary Blended Self-Compacting Concrete:

Granulated Blast Furnace Slag (GBFS) as partial fine aggregate replacement

CONTENTS

ACRONYMS

- Every blended SCC mix is assigned Mix number and Mix designation. In Mix designation, number indicates percentage by weight of total powder content.
- Examples:
- C100 – unary SCC mix made with 100% cement
- C75+MK25 – Binary SCC mix made with 75% cement and 25% metakaolin
- C25+FA60+MK15- Ternary SCC mix made with 25% cement, 60% fly ash and 15% metakaolin.
- C50+FA28+MS11+MK11 – Quaternary SCC mix made with 50% cement, 28% fly ash, 11% microsilica and 11% metakaolin
- CSH or **C-S-H** - calcium silicate hydrate
- CH- CaOH
- OPC- Ordinary Portland cement
- HPC- high performance concrete
- SCC- self compacting concrete
- SCM- supplementary cementitious material
- GGBS- Ground Granulated Blast furnace Slag
- FA – fly ash
- MK- Metakaolin
- MS- Microsilica
- SF- Silica Fume
- W/P ratio- Water / Powder ratio
- C/S ratio – CaO/SiO2 ratio
- LOI - **loss on ignition**
- SP- Superplasticizer
- EFNARC - European Federation of National Associations Representing for Concrete
- GBFS-Granulated blast furnace slag
- bwc- by weight of cement
- bwp – by weight of powder
- VMA - Viscosity Modifying Admixture
- OPC – Ordinary Portland cement
- Interface transition zone (ITZ)
- High range water reducing agent (HRWR)
- Granulated Blast Furnace Slag (GBFS)
- Binder (or)/ Powder- Cement +Fly ash+ Metakaolin+ Microsilica
- Quaternary- Three SCMs blended in Cement
- Ternary- Two SCMs blended in Cement
- Binary- One SCM blended in Cement

1. INTRODUCTION

In the present-day scenario to fulfill the demands of sustainable construction, concrete made with multi-blended cement system of Ordinary Portland Cement (OPC) and different mineral admixtures, is the sensible choice for the construction industry. One of the effective methods to conserve the Mother Nature's resources and also reduce the environmental impact is to use Supplementary Cementitious Materials (SCMs) by substituting OPC partly or totally in concrete. Since most of SCMs are pozzolanic in nature and hence they are helpful in increasing later strength of concrete. Blending of SCMs with cement has many advantages such as saving in cement, utilization of industrial by-products, enhancement of microstructural properties of concrete and reduces environmental impact through reduced greenhouse gases production. Most of the SCMs are industrial by-products which are considered as waste and pollutants when dumped into land or thrown into water bodies. So blending them in concrete becomes safe disposal method for them. Such SCMs are Fly ash (FA), Ground Granulated Blast furnace Slag (GGBS), Micro Silica(MS) or Silica Fume(SF), Copper slag (CS), Rice Husk Ash (RHA) etc.

Approximately five billion tonnes of concrete are used around the world each year. The huge requirement of concrete is putting question marks on sustainability of natural sand reserves of all the countries. These environmental issues are forcing engineers to look forward for more sustainable construction materials. As a solution for this, various alternatives such as quarry dust, wastes from demolished concrete, industrial by-products like granulated blast furnace slag, copper slag, eco sand etc have been used. Although SCC can be used on most construction sites, its rheological characterization must be improved to better control its placement. Moreover, the fresh SCC must be stable to ensure the homogeneity of the mechanical strength of the structure. The stability of SCC can be enhanced by incorporating pozzolans such as metakaolin (MK), micro silica (MS) and fly ash (FA) since an increase in cement content leads to a significant rise in material cost and often has other negative effects on concrete properties (e.g. increased thermal stress and shrinkage, etc.). The use of such pozzolans may provide greater cohesiveness by improving the grain-size distribution and particle packing. Using of chemical admixtures, however, may increase the material cost but the savings in labor cost might offset the increased cost. The use of mineral admixtures not only reduced the material cost but also improved the fresh and hardened properties of SCC. Alternatively, a viscosity modifying admixture (VMA) along with a superplasticizer (SP) may be used to impart high fluidity accompanied by the adequate viscosity.

In recent years, there has been a growing interest in the use of metakaolin (MK) as a mineral admixture to enhance the strength and durability of concrete. In the literature, however, the use of MK in the production of self-compacting concrete has not found adequate attention. Especially, self-compacting characteristics of MK concretes need to be fully recognized since on incorporation of such materials, certain properties of the concrete may be enhanced while the others may be worsen relative to the plain concrete. Considered to have twice the reactivity of most other pozzolans especially micro silica, metakaolin is a valuable admixture for concrete/cement applications. Replacing Portland cement with 8–20% metakaolin (by weight) produces a concrete mix, which exhibits favorable engineering properties including the filler effect, the acceleration of OPC hydration and the pozzolanic reaction. The filler effect is immediate while the effect of pozzolanic reaction occurs between 3 to 14 days. Metakaolin has early setting property which can be beneficial in many applications. Silica fume, a considerable alternative to metakaolin, provide a marked early strength but imparts sharp fall in workability to fresh concrete.

It is therefore important to note that the beneficial assets of one mineral admixture may compensate the shortcomings of the other by interchanging them within ternary and quaternary cementitious blends. This research is an attempt to explore the possibility of using metakaolin and GBFS (an industrial waste) as a Supplementary cementitious material and substitute for natural sand respectively. The research findings will help the researchers to understand the performance of metakaolin and GBFS sand based low, medium and high strength concrete with respect to strength, durability, economy and sustainability.

The present work aims at determining the most suitable mix proportion that can produce metakaolin based ternary and quaternary blended SCC of desirable strength and enhanced performance. Also studies are carried out to understand the use of Granulated blast furnace slag (GBFS) sand as partial fine aggregate replacement in optimized mix proportions of metakaolin based ternary and quaternary blended SCC, without compromising on engineering performance and quality. The outcome of this study can be favorable for sustainable development in the concrete industry by reusing industrial waste by-products (SCMs) as cement replacements and river sand replacement reducing destructive impact on the environment.

Application of mineral admixtures will unavoidably increase over the next few decades, to provide greater sustainability in construction, and there will therefore be necessity to maximize their efficacy with regard to cost, environmental impact, and durability performance. High-reactivity Metakaolin (MK) is a supplementary cementing material developed recently for high-performance concrete. Although earlier research have reported that it improves concrete properties, evidence on the performance of metakaolin blended Self Compacting Concrete (SCC) is still inadequate and somewhat contradictory, which retards its application in the construction practice. This study methodically investigated the synergistic effect of Metakaolin (MK) alone and in combination with Microsilica (MS) on fresh properties, hardened properties as well as durability of fly ash based SCC of low, medium and high strength. These results are compared to establish the enhanced micro-structural and engineering properties of quaternary blended SCC over ternary blended SCC. The use of appropriately proportioned metakaolin and microsilica in combination, in fly ash blended SCC reveal the benefits of their synergic effect in improving the fresh properties, strength and durability characteristics of fly ash based SCC.

Another significant feature of this research work is use of GBFS as fine aggregate replacement in metakaolin blended ternary and quaternary SCC mixes. This provides sustainable solution for use as an alternative for natural fine aggregate without compromising the strength criteria of concrete. GBFS has more reliable features than natural fine aggregate for it is manufactured under suitable, quality-controlled conditions, free from chlorides, organic impurities, clay and shells etc., no alkali-aggregate reactions and superior solidification control capabilities. This study provides a approach to reduce the cost of waste disposal and its related gains by using metakaolin as mineral admixture and GBFS as fine aggregate replacement in making of SCC.

The present work determines the most suitable optimized mix proportion that can produce metakaolin based ternary (MK+FA) and quaternary blended (MK+MS+FA) SCC mixes of desirable strength and enhanced performance. Also studies are carried out to understand the use of Granulated blast furnace slag (GBFS) as fine aggregate replacement in metakaolin based ternary and quaternary blended SCC, without compromising on engineering performance and quality.

Till now not much research work has been reported on the use of optimally blended Metakaolin in ternary and quaternary blended SCC, made with optimal micro silica and fly ash, in enhancing the micro structure, strength and durability characteristics of SCC. Also limited work is reported on the use of Granulated blast furnace slag (GBFS) as fine aggregate replacement in optimally

blended Metakaolin in ternary and quaternary blended SCC, made with optimal micro silica and fly ash. Hence to address the gaps, an exhaustive comparative study of fresh properties, strength and durability characteristics of ordinary grade (M20), standard grade (M40) and high strength grade (M80 and M100) SCC with and without addition of Metakaolin are made to understand the enhanced microstructure of optimally blended Metakaolin in ternary and quaternary blended SCC, made with optimal micro silica and fly ash. Same studies are carried over with and without GBFS as partial fine aggregate replacement in optimally blended Metakaolin in ternary and quaternary blended SCC, made with optimal micro silica and fly ash. Once the gaps available in the literature are identified, the main research objectives of the present work are outlined for obtaining detailed experimental data to address these gaps, which will help to understand improved performance of the metakaolin blended ternary and quaternary SCC made with and without GBFS as partial fine aggregate replacement.

1.0 Sustainability in Concrete Industry

Sustainability is defined as "development that meets the needs of the present without compromising the ability of future generations to meet their own needs". In order to fulfill its commitment to the sustainable development of the whole society, the concrete of tomorrow will not only be more durable, but also should be developed to satisfy socio-economic needs at the lowest environmental impact. By-products from various industries cause a major environmental problem around the world. In order to encourage waste recycling and prevent waste dumping, a landfill tax has also been imposed in the developed countries. However, the waste dumping is still a serious environmental issue throughout the world. Although concrete has been serving human beings to provide amenities, the service comes with a significant price. Regarding the immense amount of concrete production annually, it has considerable impacts on the environment. Consumption of vast amount of natural resources, release of carbon dioxide into the atmosphere from the production of Portland cement is two major environmental issues to address on war foot basis. Moreover, regardless of water supply shortages in most parts of the world, the production of concrete requires large amounts of water. Last but not least, the construction and demolition waste disposal creates another environmental burden. So, the most effective remedy to solve the problem is to use less cement which means to replace as much cement as possible by supplementary cementitious materials, especially those that are byproducts of industrial processes, and to use recycled materials in place of natural resources. Different efforts have been made to reduce the negatives of concrete on environment such as replacement of natural aggregates and cement. It is believed that the adverse effect of cement, co_2 emission, may be minimized if mineral admixtures are applied; as they reduce cement consumption, energy and cost.

1.1 High Performance Concrete

For producing high performance concrete (HPC), it is well recognized that the use of supplementary cementitious materials (SCMs), such as microsilica (MS), metakaolin (MK) and fly ash (FA) are necessary. High Performance Concrete is defined a concrete which made with appropriate materials, combined according to a selected mix design; properly mixed, transported, placed, consolidated and cured so that the resulting concrete will give an excellent performance in the structure in which it is placed, in the environment to which it is exposed and with the loads to which it will be subjected for its design. Thus, HPC is directly related to durable concretes. There are numerous ways to measure the durability of concrete. The resistance to chloride, water penetration and aggressive environment resistance are some of the simplest measures to determine

the durability of concrete. The penetration of water, chloride and other aggressive ions into concrete primarily governs the physical and chemical processes of deterioration (Monteiro, 1993). The microstructure of concrete mainly controls the physical/chemical phenomena associated with water movements and the transport of ions in concrete. Thus, HPC may be defined as the concrete having high resistance to fluid penetration as well as satisfying the strength requirement. The mineral admixtures, when used in HPC, can enhance either or both the physical and durability properties of concrete. Concretes with these supplementary cementitious materials are used extensively throughout the world. Therefore, a comprehensive experimental investigation was carried out to consider the effects of both the type and content of different SCMs on the performance properties of HPC. It was intended that the data from this systematic investigation could contribute to the development of performance-based specifications for both strength and durability.

1.2 Supplementary Cementitious Materials (SCM)

An SCM is a material that, when used in conjunction with cement, contributes to the enhancement of properties of the hardened concrete through hydraulic or pozzolanic activity. Fly ash, blast furnace-slag, silica fume, and natural pozzolans are all SCM's and most are byproducts of other industrial processes. With appropriate design and production practices, an SCM, or combination of SCMs can be used in concrete mixtures and act beneficially not only to the concrete, but also the environment. If optimally used, the use of SCMs reduces the amount of material headed to landfills and limits the energy needed and CO_2 emissions attached to the manufacturing of Portland cement. Not only can the usage of optimum proportions of SCMs help concrete increase durability, but can also aid a project by building more environmentally sustainable.

Pozzolanic materials are not necessarily cementitious when used alone, but react with the calcium hydroxide (CH) hydration product of Portland cement to form additional calcium silicate hydrate (CSH). CSH is the strongest binding and most durable hydration product of cement. Some materials are not cementitious or pozzolanic but are still considered SCMs. Supplementary cementitious materials are materials, which in itself possesses little or no cementitious properties but, in the presence of moisture chemically react with calcium hydroxide to form compounds possessing cementitious properties. Pozzolana is a siliceous and aluminous material which reacts with calcium hydroxide in the presence of water to form non-water soluble calcium silicate hydrates. The pozzolanic reaction may be slower than the rest of the reactions which occur during cement hydration and thus the short term strength of concrete made with pozzolans may not be as high as concrete made with purely cementitious materials. On the other hand, highly reactive pozzolans, such as silica fume and high reactivity metakaolin can produce "high early strength" concrete that increases the rate at which concrete gains strength. Most of the pozzolans require grinding to a high degree of fineness to make them suitable for use in concrete except pumicites, which are normally in the finely divided form. Pozzolans are either naturally occurring or available as industrial by-products. They mainly contain reactive silica and the reactivity varies depending upon the type of pozzolana and its chemical compositions and fineness. Fly ash, silica fume, stone dust, blast furnace slag, rice husk ash etc., are some of the industrial wastes and volcanic ash, metakaolin are naturally available quality controlled reactive pozzolana which possess pozzolanic properties. Out of the above pozzolanic admixtures, metakaolin made from purified kaolin, is not an industrial waste product, and can be used along with cement to derive enhanced properties for concrete in special situations.

Based on research, the following are the typical amounts of pozzolans normally used in concrete (by mass of cementing materials):

1. Fly ash
    a. Class C 15% to 40%
    b. Class F 15% to 20%
2. Slag 30% to 45%
3. Silica fume 5% to 10%
4. Calcined clay 15% to 35%
    a. Metakaolin 10% to 20%
5. Calcined shale 15% to 35%

The pozzolanic C-S-H is generally more porous than the normal C-S-H, and also has a lower C/S ratio **(**Hydraulicity index**).** A pozzolan may also have reactive Al_2O_3 (for example metakaolin), in which case the reaction with CH leads to the formation of C-A-H, which can give rise to problems in sulphate attack. Pozzolanic activity is evaluated using the Pozzolanic Activity Index test**.** Chemically active mineral admixtures (highly reactive pozzolan) increase the cohesiveness of concrete and require more water to maintain workability; however, the requirement of water may be offset by adding superplasticizer. The water demand depends on the particle size, specific surface area, particle shape, replacement level, and reactivity of particular mineral admixture. Based on Chapelle test, the reactivity of mineral admixtures is of the order: MK > SF > GGBS > FA. In general, smaller the particle size and higher the specific surface of mineral admixture increases the water demands of concrete. Heat of hydration increases with the use of chemically active mineral admixtures and decreases with the use of micro-filler mineral admixtures. All mineral admixtures reduces bleeding in concrete when optimally proportioned. Smaller particle size and higher specific surface area of mineral admixtures are favorable to produce highly dense and impermeable concrete; however, they cause low workability and more water demand which may be offset by adding effective superplasticizer.

Chemical Composition of SCMs							
	Class F fly ash	Class C fly ash	GGBS	Micro Silica	Calcined clay	Calcined shale	Metakaolin
SiO_2, %	52	35	35	90	58	50	53
Al_2O_3, %	23	18	12	0.4	29	20	43
Fe_2O_3, %	11	6	1	0.4	4	8	0.5
CaO, %	5	21	40	1.6	1	8	0.1
SO_3, %	0.8	4.1	9	0.4	0.5	0.4	0.1
Na_2O, %	1.0	5.8	0.3	0.5	0.2	—	0.05
K_2O, %	2.0	0.7	0.4	2.2	2	—	0.4
Loss on ignition, %	2.8	0.5	1.0	3.0	1.5	3.0	0.7
Blaine fineness, (m^2/kg)	420	420	400	20,000	990	730	19,000
Relative density	2.38	2.65	2.94	2.40	2.50	2.63	2.50

1.3 Fly ash

The burning of harder, older anthracite and bituminous coal typically produces Class F fly ash. This fly ash is pozzolanic in nature, and contains less than 20% lime (CaO). Class C fly ash is produced from the burning of younger lignite or subbituminous coal, in addition to having pozzolanic properties, also has some self-cementing properties. Fly ash, due to spherical shape of particles, can increase workability of cement while reducing water demand. Fly ash possesses very less to no cementitious properties, but in presence of moisture it reacts with calcium hydroxide to form additional calcium silicate hydrate (CSH) which gives additional strength. Fly ash not only renders workability and filling ability, but also gives strength at a later age usually after 56 days. In general class F fly ash has been shown to be effective in SCC providing increased cohesion and robustness to changes in water content (European Guidelines 2005). High loss on ignition (LOI) is an indicative of the carbon content presence. The loss on ignition of fly ash can represent the amount of unburnt carbon present.

Effects of fly ash on fresh concrete properties are-

1. The setting time is increased when fly ash is used.
2. Workability and flow of concrete are increased due to the spherical shape of the fly ash particles, which lends a ball-bearing type effect on the concrete mixture.
3. Bleeding and segregation are usually reduced for well-proportioned fly ash concrete.
4. The paste volume is increased when mass replacement of cement by fly ash is done.

Effects of fly ash on hardened concrete properties are-

1. Strength gain of fly ash concrete is slower than normal concrete because of lower c/s ratio. The potential for thermal cracking is much reduced compared to ordinary PC concrete. Ultimate later strengths are usually improved when fly ash is used.
2. Pozzolanic activity is proportional to the amount of particles under 10 μm in diameter.
3. Creep and shrinkage of fly ash concrete are typically higher than normal concrete, because of the increased amount of paste in the concrete (when mass replacement is done).
4. Expansions during alkali aggregate reaction are reduced by the use of fly ash, because of the dilution of Portland cement.

1.4 Microsilica (Condensed silica fume)

Silica fume is an amorphous (non-crystalline) polymorph of silicon oxide. Silica fume is available in different forms i.e. micro silica (MS) and nano silica (NS). It is ultrafine powder with an average particle size of 0.1 to 0.5 μ. The high specific surface of microsilica would increase the water demand. The use of Microsilica can reduce bleeding and improved cohesion of the mix. However, this can give rise to problems of rapid surface crusting. The cohesiveness of concrete containing SF is good for pumping and for underwater concrete. The addition of microsilica to metakaolin based fly ash SCC can prevent the excessive bleeding and segregation problems. Pozzolanic activity increases as fineness increases and is determined by "Strength Activity İndices".

Effects of on fresh concrete properties:

1. Because of its high fineness, the use of microsilica causes an increase in the water demand of concrete. Typically it is always used in conjunction with a superplasticizer.
2. Microsilica causes the mix to be sticky and cohesive. Also, concrete mixes with silica fume are prone to slump loss problems. Because of its cohesiveness, a higher slump is needed to place microsilica concrete.
3. Bleeding is reduced drastically. In fact, most microsilica mixes do not show any bleeding. In dry areas, if the evaporation rate exceeds the rate at which concrete sets, plastic

shrinkage may occur. Silica fume concrete is especially susceptible to this problem in case curing is not done properly.

Effects of microsilica on hardened concrete properties"

1. Pore size refinement and reduction in permeability occurs when silica fume is used. Due to a combined effect of microsilica as a highly reactive pozzolana and filler, the transition zone between aggregate and paste is strengthened.
2. The principle physical effect of silica fume in concrete is that of filler, which because of its fineness can fit into space between cement grains in the same way that sand fills the space between particles of coarse aggregates and cement grains fill the space between sand grains. As for chemical reaction of silica fume, because of high surface area and high content of amorphous silica in silica fume, this highly active pozzolan reacts more quickly than ordinary pozzolans. The use of silica fume in concrete has engineering potential and economic advantage.

1.5 Metakaolin

Metakaolin differs from other supplementary cementitious materials (SCMs) like fly ash, silica fume, and blast furnace slag, in that it is not a by-product of an industrial process; it is manufactured for a specific purpose under carefully controlled conditions. The rates of pozzolanic reaction and CH consumption in metakaolin systems have been shown to be higher than in silica fume systems, indicating a higher initial reactivity. Because this reaction with CH occurs early and rapidly, metakaolin incorporation may contribute to reduced initial and final set times. The high reactivity of MK with cement accelerates the initial setting time and improves especially the mechanical and transport properties of SCC, especially since it can also attain high compressive strength at an early age (Jutice & Kurtis 2007). MK-modified mixtures may be more economical because of a lower dosage of high-range water-reducing admixture. It has been found that MK has positive effects on pore structure and Interface transition zone (ITZ) enhancement of concrete higher than SF. The most important constituents for any mineral admixture are silica and alumina oxides. In comparison with OPC, the mineral admixtures have higher quantity of silica oxide in their constituent. The maximum content of silica oxide is in silica fume (SF) showing their reaction capability with the primary hydrate of cement to produce calcium silicate hydrate (CSH) which is strengthening gel in concrete; however, the content of alumina oxide is lesser in SF. On the other hand, MK has substantial contents of silica and alumina oxide showing its capability to produce calcium silicate hydrate (CSH) and calcium aluminate hydrate (CAH) which has also bonding characteristics in the concrete. In Portland cement concrete, MK reacts at normal temperatures with calcium hydroxide in cement paste to form mainly calcium silicate hydrates (C-S-H), C_2ASH_8 (gehlenite hydrate), and C_4AH_{13} (tetra-calcium aluminate hydrate). The formation of secondary C-S-H by this reaction reduces total porosity and refines the pore structure, improving the strength and impermeability of the cementitious matrix (Ramezanianpour & Bahrami 2012). Metakaolin's reaction rate is rapid, significantly increasing compressive strength, even at early ages, which can allow for earlier release of formwork. After examining various SCMs individually and in combination and by considering performance, economic, and environmental criteria, metakaolin concrete was identified as a "very promising solution" for the precast industry for reducing clinker content in concrete.

1.6 Synergic effects of SCMs

Synergy effect is the interaction of two or more admixtures so that their combined effect is greater than the sum of their individual effects. When a less reactive pozzolana is employed in ternary or

quaternary concrete mixtures together with another one more reactive such as silica fume or rice husk ash, there is a synergy between these pozzolans, thus the obtained result is higher than those verified in the respective binary mixtures; this result is called synergic effect. Therefore mixing more than one SCM is likely to improve the mechanical and structural properties of the cement matrix. Incorporating of high volume of single type of SCM may have negative impacts on concrete properties. Synergy between mineral admixtures was considered to be the main reason for the excellent performance of the ternary and quaternary blended concrete mixtures. The use of appropriately proportioned blends allows the effects of one SCM to compensate for the inherent shortcomings of another.

1.7 Proportioning methods

1. *Simple replacement method*: This is the traditional method of proportioning. Replacement of cement can be done either on a volume basis or mass basis. Volume replacement does not change the overall volume of the paste. However, when mass replacement is done, volume of the paste increases, and this increase is usually compensated by a decrease in the volume of sand.
2. *Addition method*: This method involves a direct addition of the mineral admixture to the concrete without replacing any part of the cement. In high strength concrete, this is the method of choice, since it increases the cementitious content. This increase is compensated by a decrease in the fine aggregate content.
3. *Modified replacement method*: In this case, part of the admixture is added, and part of it is used as a replacement. The quantity of mineral admixture put into the mix is greater than the quantity of cement removed. This method is typically used to obtain sufficiently high early age strengths with fly ash.
4. *Rational method*: This is an efficient method of proportioning admixtures. It quantifies the influence of the admixture using a factor 'k', which is the 'cementing efficiency factor'. This factor qualifies the mineral admixture as a lower grade or higher grade cement. In other words, 'k' represents the amount of the mineral admixture that can replace one unit of Portland cement in the mixture to achieve similar properties.

1.8 Binary, Ternary and Quaternary blended concretes

There are environmental benefits from using ternary or quaternary blends since these mixtures reduce the amount of expensive raw materials used to manufacture cement and recycle industrial byproducts. Ternary or quaternary blends can be even more durable than binary blends because the additional SCM can overcome the shortcomings of the first SCM. However, the optimum ranges of SCM replacement varied greatly depending on what cement and type of SCM was used. Using ternary or quaternary blended cements could reduce up to 45% of CO_2 emissions. There is hesitation to use ternary or quaternary blended cement concrete mixtures because it is not a familiar practice. Despite positive results in research, convincing the concrete and cement industry to change to mix designs with which they are unfamiliar is challenging.

1.9 Self-Compacting Concrete (SCC)

One of the most critical differences between SCC and conventional concrete is the incorporation of a SCMs material in the form of a filler or cement replacement. Industrial by-products such as fly ash, GGBFS, RHA, MK, and limestone powder, are used as SCMs in SCC (Felekoglu et al 2007). The concept of SCC was proposed in 1986 by Professor Okamura (1997), but the prototype was first developed in 1988 in Japan by Professor Ozawa (1989) at the University of Tokyo. Self-compacting concrete has excellent self-compactability and can be filled in all corners of forms

without vibratory compaction, which is essential for conventional concrete. Being more susceptible to quality fluctuation and batching errors of materials, self-compacting concrete requires stricter quality control, production control and construction control than conventional concrete. Investigations for establishing a rational mix-design method and self-compactability testing methods have been carried out from the viewpoint of making it a standard concrete. SCC requires a large amount of powder content (either by fine aggregate or fillers) compared to conventional vibrated concrete to produce a homogeneous and cohesive mix. SCC can be obtained by increasing the fine aggregate content; by limiting the maximum aggregate size; by increasing the powder content; by using viscosity modifying admixtures (VMA) and reducing the water-to-binder ratio through superplasticizer (SP).

European Federation of National Associations Representing for Concrete (EFNARC) (2002) has developed specifications and guidelines for the use of SCC that covers a number of topics ranging from material selection and mixture design to the significance of the testing methods. The main disadvantage of SCC is the high cost associated with the use of chemical admixtures and high volumes of Portland cement. One alternative to reduce the cost of SCC is to use mineral additives such as rice husk ash (RHA), metakaolin (MK), limestone powder, natural pozzolans, fly ash (FA), and slag, which are finely divided materials added to concrete as partial replacement material. As these mineral additives replace part of the Portland cement, the cost of SCC will be reduced, especially if the mineral additive is an industrial by-product. It is well established that the mineral additives might increase the workability, durability, and long-term properties of concrete.

The current studies on SCC, which are being conducted in many countries, including India, focused attention on its long-term performance. In addition, the other areas where research needs to be carried out relevant to immediate needs are: (i) the development of mixture design guidelines tables similar to those for conventional concrete; (ii) a shift to an optimum level of powder contents in SCC from the existing high powder mixtures; (iii) a better understanding of the long-term properties, such as permeability, chemical attack, sulfate attack, corrosion of steel on concrete, and autogenous and plastic shrinkage in SCC; and (iv) the development of site quality control parameters such as in 'all-in-one' acceptance tests.

Mixture proportions of SCC differ from conventional concrete with more powder content and less coarse aggregate. Moreover, SCC incorporates High range water reducing agent (HRWR) or superplasticizer (SP) in larger amounts and frequently a VMA in small doses is also required.

1.10 Superplasticizer (SP) and Viscosity Modifying Agent (VMA)

For many years, it was not possible to reduce water/cement ratio of concrete below 0.40 till the advent of super plasticizers. By using super plasticizer, it was found possible to lower the water/binder ratio of concrete down to 0.30 and still get an initial slump of 200mm. Reducing the water/binder ratio below 0.30 was a forbidden idea until research reported that with usage of very high dosage of super plasticizers and silica fume, water-binder ratio can be reduced to as low as 0.16 to reach a compressive strength of 280MPa (Bache, 1981). Aitcin et al. (1991) reported, that by choosing carefully, the combination of Portland cement and superplasticizer, it was possible to make a 0.17 water/binder ratio concrete with 230mm slump after an hour of mixing which gave a compressive strength of 73.1MPa at 24 hours but failed to increase more than 125MPa after long term wet curing. Due to variety of admixture formulations, it is difficult to provide the concrete industry with simple rules specifying proper use of super plasticizers in the presence of other admixtures. However, the Marsh Cone test is popularly used to evaluate the characteristics of different pastes, in order to select the optimum dosage of super plasticizers (Giaccio 2002). Adding

the SP significantly improves fluidity due to the action of the molecules of SP. These molecules can be rolled around the grains of the cement and to impart a negative charge, so that they repel each other, resulting in deflocculating and dispersion of the grains of cement. This action will reduce the quantity of water, thereby increasing the fluidity. The maximum dosage of SP prescribed by the manufacturing company is used as saturation point beyond which fluidity does not change practically. Loss of fluidity and deformability caused by adding a VMA can be recovered by adding a SP without affecting the stability and compressive strength. We observe that the incorporation of VMA resulted in a great improvement in stability and can prevent segregation. It is believed that the increase or decrease of the compression strength is directly related to changes in stability. VMA refines the rheology of the mixes by increasing cohesiveness and eliminating bleeding and maintains right balance between fluidity and resistance to segregation whereas SP is used to decrease viscosity and increase fluidity. The level of fluidity is chiefly governed by the dosage of the superplasticizer. However, overdosing may lead to the risk of segregation and blockage. In the present study, a locally available high performance viscosity modifying agent, named "Glenium Stream 2" from BASF Chemical Company, specially designed to ensure a good consistency, high segregation resistance and stability in concrete with sufficient fluidity, was used. Poly-carboxylate ether (PCE) and Sulphonated Napthalene Polymers (SNP) based SPs are used to produce various grades of blended SCC. There exists the problem of incompatibility between cement and SP, which is felt highly for which mixtures having low water content.

1.11 Mixture Proportioning Methods for SCC

In general, the compressive strength is the primary criterion for designing ordinary concrete. Conversely, the flowing ability and durability must be given equal importance with the compressive strength in designing SCC. Thus, different a design approach is needed for SCC.

The process of mix design for ordinary concrete is not applicable to SCC for the given reasons:

a) Established relationships between average and specified compressive strengths of ordinary concrete could be unacceptable for SCC possessing high strength.

b) Traditional curves for the relationship between w/b ratio and compressive strength could be misleading for SCC that needs a lower w/b ratio.

c) None of the traditional curves for w/b ratio and strength relationship are considered for the effect of supplementary cementitious materials (SCM), including SP and VMA, which are usually used to produce SCC.

d) The coarse aggregate content of ordinary concrete is relatively high and unsuitable for SCC.

e) The fine aggregate content obtained from the traditional method is much lower than that recommended for SCC.

f) The approximate water content of concrete mixture does not include the effects of SCM and HRWR, which are usually incorporated in SCC.

g) Slump alone is no longer a performance criterion for the flowing ability of the SCC.

To produce SCC, the major work involves designing an appropriate mix proportion and evaluating the properties of the concrete thus obtained. In 1993, Okamura proposed a mix design method for SCC. His main idea was to conduct the first test on paste and mortar in order to examine the properties and compatibility of superplasticizer (SP) then cement, fine aggregates and Pozzolanic materials, are introduced followed by the trial mix of SCC. The major advantage of this method is that it avoids having to repeat the same kind of quality control test on concrete, which consumes both time and labor.

However, the draw-backs of Okamura's method are that (1) it requires quality control of paste and mortar prior to SCC mixing, while many ready-mixed concrete producers do not have the necessary facilities for conducting such tests and (2) the mix design method and procedures are too complicated for practical implementation. The ''Standardized mix design method of SCC'' proposed by the Japanese Ready-Mixed Concrete Association (JRMCA) is a simplified version of Okamura's method. This method can be employed to produce SCC with a large amount of powder materials, and a water/binder ratio of less than 0.30. On the other hand, the Laboratory Central Des Ponts et Chausses (LCPC), the Swedish Cement and Concrete Research Institute (CBI), research groups in both Main-land China and Taiwan have proposed different mix design methods of HPC. The LCPC's approach is developed on the basis of the BTRHEOM rheometer and RENE LCPC software. It is difficult for others to adopt their method without purchasing the software. CBI's approach makes use of the relationship between the blocking volume ratio and clear reinforcement spacing to fraction particle diameter ratio. However, it is not clear how to carry out the critical tests because concrete mixed with coarse aggregates and paste only is susceptible to severe segregation. In Taiwan, the method proposed by Hwang et al. involves a densified mixture design algorithm, which is derived from the maximum density theory and excess paste theory. Nevertheless, there is no information yet concerning the relationship between their method and the ability of concrete passing through reinforcement or its segregation resistance. The aggregate content, the incorporation of SCM, and the presence of various chemical admixtures may have a significant influence on the flow characteristics, strength, transport properties and durability of SCC. Therefore, a different design approach should be followed, instead of the traditional methods, to design the mixture composition of SCC. There is no Indian standard mixture design method for SCC. The Indian Road Congress (IRC) is currently working to develop a mixture design procedure for SCC. IRC also recommend the use of SCC in bridges and the same is under the draft stage.

1.12 Nan Su Method of SCC Mix Design

A simple new mix design method for self-compacting concrete (SCC) is proposed by Nan Su et al. First, the amount of aggregates required is determined, and the paste of binders is then filled into the voids of aggregates (the void in the loose aggregate is about 42– 48%) to ensure that the concrete thus obtained has flowability, self-compacting ability and other desired SCC properties. The strength of SCC is provided by the aggregate binding by the paste at hardened state, while the workability of SCC is provided by the binding paste at fresh state. Therefore, the contents of coarse and fine aggregates, binders, mixing water and SP will be the main factors influencing the properties of SCC. Slump flow, V-funnel, L-flow, U-box and compressive strength tests were carried out to examine the performance of SCC, and the results indicate that the proposed method could produce successfully SCC of high quality. This method is simpler, easier for implementation and less time-consuming, requires a smaller amount of binders and saves cost. With the proposed method, all we need to do is to select the qualified materials, do the calculations, conduct mixing tests and make some adjustments, and SCC with good flowability and segregation resistance can be obtained with self-compacting ability. Nan Su method of SCC mix design principles and stepwise procedures are outlined at the end in Appendix.

In the event that satisfactory performance of the mix is not obtained, consideration should be given to a fundamental redesign of the mix. This novel mix design method is simpler, requires a smaller amount of binders, and saves cost.

1.13 EFNARC Guidelines for SCC (2005)

In 2002 EFNARC published their "Specification & Guidelines for Self-Compacting concrete" which, at that time, provided state of the art information for producers and users of SCC. The Guidelines have been prepared using the wide range of the experience and knowledge available to the European Project Group.

A concrete mix can only be classified as SCC if the requirements for all the following three workability properties are fulfilled.

(1) Filling ability (flow ability), (2) Passing ability, and (3) Segregation resistance

Filling ability is the ability of SCC to flow into all spaces within the formwork under its own weight. Tests, such as slump flow and T50 cm time test, V-funnel test are used to determine the filling ability of fresh concrete. Slump-flow value describes the flowability of a fresh mix in unconfined conditions. It is a sensitive test that will normally be specified for all SCC, as the primary check that the fresh concrete consistence meets the specification. Visual observations during the test and/or measurement of the T50 cm time can give additional information on the uniformity and flowability of the mix. Passing ability is the ability of SCC to flow through tight openings, such as spaces between steel reinforcing bars, under its own weight. Passing ability can be determined by using U-box, L-box, Fill-box, and J-ring test methods. V funnel test at T 5 minutes gives segregation resistance of the mix. After 5 minutes of settling, segregation of concrete will show a less continuous flow with an increase in flow time.

1.14 Packing Factor

The packing factor (PF) of aggregate is defined as the ratio of mass of aggregate of tightly packed state in SCC to that of loosely packed state. Clearly, PF affects the content of aggregates in SCC. A higher PF value would imply a greater amount of coarse and fine aggregates used, thus, decreasing the content of binders in SCC. Consequently, its flowability, self-compacting ability and compressive strength will be reduced. On the other hand, a low PF value would mean increased dry shrinkage of concrete. As a result, more binders are required, thus, raising the cost of materials. In addition, excess binders used would also affect the workability and durability of SCC. Therefore, it is important to select the optimal PF value in the mix design method so as to meet the requirements for SCC properties, and at the same time taking economic feasibility into consideration. The main consideration of Nan Su method is that voids present in loose aggregate are filled with paste and that the packing of the aggregates is minimized. This method makes a distinction between loose packing, and packing after compaction. In the Nan Su method the void reduction is expressed with a Packing Factor (PF). The PF that represents the apparent density of aggregate in state of packing in SCC compared with the apparent density of loosely packed aggregate.

1.15 Efficiency Factors

The cementing efficiency factor, '*k*' of a pozzolanic material is defined as the number of parts of cement in a concrete mixture that could be replaced by one part of pozzolanic material without changing the property being investigated, which is usually the compressive strength. The efficiency factor for strength performance of a pozzolanic material is calculated on the basis of comparison between concrete strength and the w/c ratio for a non-blended mixture and a blended mixture. The efficiency factor is used for proportioning of blended concrete. A rational method of proportioning fly ash concrete was first proposed by Smith, in which the fly ash cementing efficiency factor, '*k*' was defined in such a way that the strength to water cement ratio relation for

normal concrete is also valid for ternary and quaternary blended SCC considering the effective water cement ratio, as given by [$W/(C + kP)$], where W is the weight of water in kg/m3, C is the weight of cement in kg/m3, P is the weight of blended pozzolanic material . Papadakis et al. (2002) proposed a method to evaluate the efficiency factor for various natural and artificial pozzolanas by using the concept of pozzolanic activity index. Pozzolanic activity index was determined as the ratio of strength of a pozzolanic mortars to that a control mortar. Bharat kumar et al. (2001) proposed a method of mix proportioning for concrete containing mineral admixture (MA) by using Bolomey's equation for predicting strength. In their studies, a relative strength-based method to obtain efficiency values for strength performance is used. The first mixture is the OPC control mixture, while the second is a SCM blended mixture containing a pozzolanic material as a partial replacement for cement. The total cementitious materials content and other mixture characteristics, such as water and aggregate contents, are the same for both mixtures. In addition, both mixtures are subjected to similar curing history. Therefore, strength development for the control mix is principally dependent on the rate of cement hydration, while for the blended mixture, it is dependent on the combination of cement hydration and pozzolanic reaction. By observing the relative strength, which is defined as ratio of strengths of the blended mixture to the control mix, an understanding of the rates of reaction in a blended pozzolanic system relative to the non-blended system can be achieved. If the pozzolana contributes positively to strength development at a certain age, then the resulting relative strength value will be greater than unity. Malathy and Subramaniam (2007) used the above method to find the efficiency factor of silica fume and metakaolin in their binary mix by using following equation:

$$k = (1/P) \{-C + W (fc - A2) / A1\}$$

where fc is compressive strength of concrete in MPa, C is the cement content in kg/m3,W is the water content in kg/m3 and $A1, A2$ are constants influenced by ingredients, curing conditions and age of concrete. Efficiency factor increases with age which shows the activation of pozzolanic activity of mineral admixtures with time.

1.16 Alternatives materials for Fine aggregate

In concrete 30-40% of the volume is occupied by fine aggregate. Aggregate passes through 9.5 mm sieve and almost passes through the 4.75 mm sieve and predominantly retains on the 75-micron sieve. Most of the fine aggregate passes 4.75 mm IS sieve and contains a huge amount of coarser materials. This may have been fragmented by natural process of weathering and abrasion or artificially by crushing. Thus many properties of the fine aggregate depend entirely on the properties of the parent rock. Properties of fine aggregate may have a considerable influence on the quality of the concrete, either fresh or hardened.

Large scale of sand quarrying from riverbeds creates environmental problems such as shortage of ground water and changing watercourses. Farmers' organizations, environmental managers and the public have expressed concern over the indiscriminate quarrying in violation against the river environmental conservation principles. Riverbeds, which supply water to cities and villages, suffer extensive damage owing to excessive sand mining. River sand acts as excellent filter system to ground water. The infrastructure developments such as express highway projects, power projects and industrial developments have started now. Natural sand is getting depleted resulting in high cost of sand. Fine aggregate is obtained from natural rivers, crushing stone sand and industrial waste. Other substitutes are obtained from coal ash, foundry sand, ponded fly ash and quarry rock dust, etc.

Bureau of Indian Standards, considering the scarcity of sand from natural sources, has suggested number of alternatives which are ultimately aimed at conservation of natural resources apart from promoting use of various waste materials without compromising in quality. Such fine aggregate alternatives are as follow:

a) 50 % copper slag can be used as replacement of natural sand in to obtain mortar and concrete with required performance, strength and durability (Khalifa S. Al-Jabri et al 2011).
b) GBFS sand, up to 75 per cent, can be used as an alternative to natural sand from the point of view of strength.
c) Washed Bottom Ash (WBA)
d) Quarry Dust (QD) - The quarry dust is the by-product which is formed in the processing of the granite stones which broken downs into the coarse aggregates of different sizes.
e) Foundry Sand - Foundry sand is sand which when moistened & compressed or oiled or heated tends to pack well and hold its shape. It is used in the process of sand casting. Foundry sand which is very high in silica is regularly discarded by the metal industry. Currently, there is no mechanism for its disposal, but international studies say that up to 50 per cent foundry sand can be utilized for economical and sustainable development of concrete (Vipul D. Prajapati 2013)[8].
f) Sheet Glass Powder (SGP) is amorphous material with high silica content, thus making it potentially pozzolanic when particle size is less than 75μm (Federio.L.M and Chidiac S.E, 2001, Jin.W, Meyer.C, and Baxter.S, 2000).
g) Granulated Blast furnace Slag - In general, slag consists essentially of silicates and alumino silicates of lime. The principal compound is melilite.

1.17 Granulated Blast Furnace Slag (GBFS)

Growing environmental restrictions to the exploitation of sand from river beds leads to search for alternatives particularly near the larger metropolitan areas. This has brought in severe strains on the availability of sand forcing the construction industry to look for alternative construction materials without compromising the strength criteria of concrete. Granulated blast furnace slags are one of the promising sustainable solutions as they are obtained as solid wastes generated by industry. Hence it reduces the solid waste disposal problem and other environmental issues. GBFS (Granulated Blast Furnace Slag) is a slag obtained from the manufacture of iron in steel industries. The use of granulated blast furnace slag (GBFS) aggregates in concrete by replacement of natural aggregates is very promising concept because its impact strength is quite more than natural aggregate. Steel slag aggregates are already being used as aggregates in asphalt paving road m due to their mechanical strength, stiffness, porosity, wear resist and water absorption capacity. GBFS is a non-metallic product, consisting essentially of silicates and alumina silicates of calcium and of other bases that is developed in a molten condition simultaneously with iron in a blast furnace. 1. Air-cooled blast-furnace slag is the material resulting from solidification of molten blast-furnace slag under atmospheric conditions; subsequent cooling may be accelerated by application of water to the solidified surface. 2. Expanded blast-furnace slag is the lightweight, cellular material obtained by controlled processing of molten blast furnace slag with water, or water and other agents, such as steam or compressed air, or both. 3. Blast-furnace slag is the glassy granular material formed when molten blast-furnace slag is rapidly chilled, as by immersion in water (Virgalitte et al., 2000). Blast furnace slag (4.75mm to 75 micron) was collected from JSW for replacement to natural sand.

Features of Blast furnace slag fine aggregate for concrete are

1. Reliable - Quality Blast furnace slag fine aggregate is a product for industrial use manufactured under suitable, quality-controlled conditions.
2. Does not contain materials such as Chlorides, Organic Impurities, Clay and Shells Blast furnace slag fine aggregate does not contain materials that may affect the strength and durability of concrete, such as chlorides, organic impurities, clay and shells.
3. Level of compressive strength similar to that of natural sand is achieved at a material age of 7 days and 28 days. Additionally, increased strength is seen as the material ages.
4. Does not generate alkali-aggregate reactions.
5. Superior solidification control capabilities have been realized with precise selection of chemical components and the addition of solidification-preventing agents.
6. Sharp edged and irregular glassy material
7. High CaO content (30-50%): latent hydraulic material
8. Hydraulicity index: $CaO+MgO/SiO2>1$

For the present study, GBFS is obtained from JSW steel, which is the only company which produces GBFS sand for commercial use in concrete making.

2. PROPERTIES OF MATERIALS

To realize the defined objectives for this present research work, experimental investigations are carried out to quantitatively understand and evaluate the role of metakaolin (MK) in in fly ash based SCCs of ordinary grade (M20), standard grade (M40) and high strength grade (M80 and M100) and also to develop optimally blended SCCs made with partial replacement of river sand by GBFS as fine aggregate. The test results of experimental investigations carried out during the development of ordinary grade (M20) , standard grade (M40) and high strength grade (M80 and M100) binary, ternary and quaternary blended Self-Compacting Concrete (SCC) mixes made with optimum proportions of Fly Ash (FA), Microsilica (MS) and Metakaolin (MK) combination are tabulated in the following sections.

The materials used in the experimental investigation are locally available cement, sand, coarse aggregate, mineral and chemical admixtures. The chemicals used in the present investigation are of commercial grade and properties are supplied by the manufacturer and are appropriately acknowledged.

The physical and chemical properties of all the materials used in the development of ordinary grade (M20) , standard grade (M40) and high strength grade (M80 and M100) of binary, ternary and quaternary blended Self Compacting Concrete (SCC) made with optimum proportions of Fly Ash (FA), Microsilica (MS) and Metakaolin (MK) combination are tabulated in the Table 1 to 14

2.0 Ordinary Portland Cement

The physical and chemical properties of Ordinary Portland cement (OPC) of 53 grade [IS: 12269-1987, Specifications for 53 Grade Ordinary Portland cement] tested in accordance with the IS: 12269 – 1987 and IS: 4031-1988 are tabulated as follows

Table 1 - Physical and Chemical properties of Ordinary Portland Cement

Particulars	Requirement as per IS 12269-1987	Test Results Obtained
(A) Physical Properties		
1) Blaine's Fineness (Specific Surface)(m^2/kg)	225 (minimum)	330
2)Specific Gravity		3.15
3) Setting Time (in minutes) Initial Final	 30 (minimum) 600 (maximum)	 80 minutes 250 minutes
4)Soundness	10 mm (maximum)	2 mm
5) Compressive Strength 7 Days 28 Days	 37 MPa (minimum) 53 MPa (minimum)	 41.82 MPa 57.23 MPa
6) Average particle size		12μm

(B) Chemical Composition		
1) LSF CaO-0.7SO_3/ 2.8SiO_2+1.2Al_2O_3+0.65Fe_2O_3	0.8 to 1.02 (maximum)	0.90
2) Al_2O_3 / Fe_2O_3 (%)	0.66 (minimum)	1.20
3) Insoluble Residue (% by mass)	2.0	0.4 %
4) Magnesia (% by mass)	6 % (maximum)	1.40 %
5) Sulphuric Anhydrate (% by mass)	3 % (maximum)	2.20 %
6) Total Loss on Ignition (%)	4 % (maximum)	1.36 %
7) Total Chlorides (%)	0.05 (maximum)	0.012 %

2.1 River Sand

The fine aggregate used was locally available river sand without any organic impurities and conforming to IS: 383 – 1970. The fine aggregate was tested for its physical requirements such as gradation, fineness modulus, specific gravity and bulk density in accordance with IS: 2386 – 1963 [Methods of test for aggregate for concrete]. The sand was surface dried before use.
In the present research work, locally available river sand conforming to Zone –II is adopted. Properties of River Sand conforming to IS: 383 – 1970 and results of various tests conducted in accordance with IS: 2386 – 1963 are tabulated in Table 2.

Table 2 - Physical properties of River Sand

S. No	Property	Fine Aggregate	Range as per IS: 383 -1970
1.	Specific gravity	2.57	2.30-2.90
2.	Bulk Density a) Loose b) Compacted	 1474 kg/m^3 1713 kg/m^3	 1280-1920
3.	Bulking	6%	-
4.	Fineness Modulus	2.88	2.10-3.20
5.	Water absorption %	0.45	0-8
6.	Fines through 75µ, %	0.6	-

From Sieve analysis report, it is confirmed that River Sand used conform to Zone-II as suggested IS code of practice and is having a fine modulus of 2.88. Particle size distribution of River Sand is shown in the form of grading curve in Fig 3

2.2 Granulated Blast Furnace Slag (GBFS)
Properties of Granulated Blast Furnace Slag (GBFS) conforming to IS: 383 – 1970 and results of various tests conducted in accordance with IS: 2386 – 1963 are tabulated as follows:

Table 3 - Physical Properties of Granulated Blast furnace slag (GBFS) as per IS 2386:1986

(Source: JSW slag, Bellary)

S. No	Property	GBFS	Range as per IS: 383 -1970
1.	Specific gravity (SSD)	2.53	2.30-2.90
2.	Bulk Density (SSD) a) Loose b) Compacted	 1337 kg/m^3 1531 kg/m^3	1280-1920
3.	Fineness Modulus	2.81	2.10-3.20
4.	Water absorption %	2.56	0-8
5.	Fines through 75μ, %	6.14	

Table 4 - Chemical properties of GBFS

(Source: JSW slag, Bellary)

S.No	Characteristics	Requirement % as per IS-12089	Test Results %
1	SiO_2 (%)	-	32.51
2	Al_2O_3 (%)	-	21.76
3	Fe_2O_3	-	1.1
4	CaO (%)	-	35.68
5	MgO (%)	17 (Max)	7.6
6	Loss on Ignition (%)		0.35
8	Manganese Content	5.5 (Max)	0.15
9	Sulphur	2.0 (Max)	0.47
10	Glass Content (minimum)	85	92
11	Moisture Content	-	5.2
12	Particle size passing 50 mm	95 %	100 %
13	Chemical Moduli $(CaO+MgO + Al_2O_3) /SiO_2$	Greater than or equal to 1.0	2

Fig 2 - GBFS Sand (Source: JSW slag, Bellary)

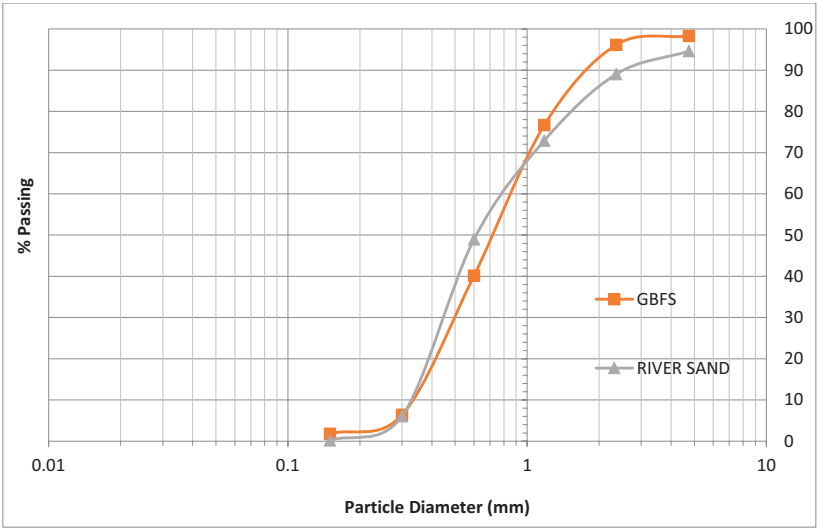

Fig 3 - Grading Curve for GBFS and River Sand

Table 5 - Comparison of Impurities in River Sand and GBFS
(Source: JSW slag, Bellary)

Impurities	River Sand	GBFS
Marine Products	2 - 4%	Nil
Oversized Materials	6 - 10%	Nil
Clay & Silt	5 - 20%	Nil

Granulated Blast Furnace Slag (GBFS) used is having fineness modulus of 2.81 and is conforming to Zone-II, which is ideal to be used as fine aggregate as per IS code standard. It has high percentage of alumina content as compared to river sand. Fig 3 depicts the particle size distribution of GBFS and river sand. Table 5 shows that GBFS is free from impurities when compared to river sand. In GBFS, water absorption is more as compared to river sand due to presence fines less than 75 µ. Chemical analysis suggest that the presence of deleterious materials in GBFS is less than 0.086% which indicated that GBFS is chemically innocuous.

2.3 Coarse Aggregate

The coarse aggregate chosen for SCC was typically round in shape, well graded and smaller in maximum size than that used for conventional concrete. Crushed granite metal of size of 10 mm graded obtained from the locally available quarries was used in the present investigation. These were tested as per IS 383-1970 [Methods of physical tests for hydraulic cement]. The physical properties like specific gravity, bulk density, flakiness index, elongation index and fineness

modulus. Properties of coarse aggregate conforming to IS: 383 – 1970 and results of various tests conducted in accordance with IS: 2386 – 1963 are tabulated as follows:

Table 6 - Physical properties of Coarse aggregate

S. No	Property	Method	Coarse Aggregate
1.	Specific gravity	Pycnometer IS:2386 Part 3-1986	2.6
2.	Bulk Density (Loose)	IS:2386 Part 3-1986	1434 kg/m^3
3.	Bulking	IS:2386 Part 3-1986	--
4.	Flakiness Index	(IS:2386 Part 2-1963)	6.15%
5.	Elongation Index	(IS:2386 Part 2-1963)	7.1%
6.	Fineness Modulus	Sieve Analysis (IS:2386 Part 2-1963)	6.74

Table 7 shows the sieve analysis of coarse aggregate, from which fineness modulus of coarse aggregate is found as 6.74. Size of the coarse aggregate used is 10mm.

Table 7 - Sieve Analysis of Coarse Aggregate

The dry weight of aggregate = 5000 gms

Sieve size	Weight of material retained (gms)	% weight retained	Cumulative %weight retained	%weight passing
20mm	0	0	0	0
10mm	3700	74	74	26
4.75mm	1300	26	100	0
2.36mm	0	0	100	0
1.18mm	0	0	100	0
600µ	0	0	100	0
300µ	0	0	100	0
150µ	0	0	100	0

2.4 Mixing water

Water used for mixing and curing was potable water, which was free from any amounts of oils, acids, alkalis, sugar, salts and organic materials or other substances that may be deleterious to concrete or steel confirming to IS : 3025 – 1964 part22, part 23 and IS : 456 – 2000 [Code of practice for plain and reinforced concrete]. The pH value should not be less than 6. The solids present were within the permissible limits as per clause 5.4 of IS: 456 – 2000.
Water used for mixing and curing is fresh potable water, conforming to IS: 3025 – 1986 and IS: 456 – 2000 and its properties are tabulated as follows:

Table 8 - Properties of Water Sample

Parameter	Results	Limits as per IS 456 – 2000
pH	6.6	6.5 – 8.5
Chlorides (mg/l)	49	2000 (PCC) 500 (RCC)
Alkalinity (ml)	8	< 25
Sulphates (mg/l)	116	400
Fluorides (mg/l)	0.089	1.5
Organic Solids (mg/l)	53	200
Inorganic Solids (mg/l) (mg/l)	129	3000
Suspended matter (mg/l)	40	2000

2.5 Fly ash

Fly ash is an inorganic, non-combustible, finely divided residue collected or precipitated from the exhaust gases of any industrial furnace. Most of the fly ash particles are solid spheres and some particles, called cenospheres, are hollow and some are the plerospheres, which are spheres containing smaller spheres inside. Fly ash surface area is typically 400 m^2/kg and is primarily silicate glass containing silica, alumina, iron, and calcium. Fly ash used in this investigation was procured from Vijayawada Thermal Power Station, Andhra Pradesh, India. It confirms with grade I of IS: 3812 – 1981 [Specifications for fly ash for use as pozzolana and admixture]. It was tested in accordance with IS: 1727 –1967 [Methods of test for pozzolana materials].

The physical characteristics and chemical composition of fly ash used in the present investigation were given in Tables 9.

Table 9 – Physical and Chemical Composition of fly ash

(Source: Vijayawada Thermal Power Station, Andhra Pradesh)

Characteristics	Result (%)	Requirements of IS:3812
Physical Properties		
Fineness m^2/kg	364	320
Specific Gravity	2.15	
Compressive strength at 28 days as percentage of strength of corresponding plain mortar cubes	86%	Not less than 80%
Chemical Properties		
Silica, SiO_2	61	35
Alumina Al_2O_3	30.3	-
Iron oxide Fe_2O_3	3.93	-
Lime CaO	0.80	-
Magnesia Mg O	0.4	5
Sulphar Trioxide SO_3	<0.01	2.75
Na_2O	0.25	1.5
K_2O	0.91	-
TiO_2	1.95	
Loss on Ignition	0.82	12

2.6 Micro silica

Micro silica is a highly reactive pozzolanic material (silicon dioxide (SiO_2) more than 90 percent in non-crystalline form) having specific gravity of 2.30. Micro silica Grade 92D conforming to IS: 15388 -2003 is used. Silica fume has specific surface area of about 20,000m^2/kg. Micro silica of Grade 92D conforming to IS: 15388 -2003 is used. Micro silica used in this investigation was a product of Elkem. The general physical and chemical properties of micro silica are given in the Table 10 and Table 11.

Table 10 - Physical requirements of Micro silica

Property	Result
Form or state	Ultra-fine amorphous powder
Colour	Gray
Odour	Odour less
Melting point (°C)	1550 – 1570
Specific gravity	2.22
Bulk Density (kg/m^3)	150 – 700
Specific Surface (m^2/kg)	20000
Particle size, mean (μm)	≈0.5
Silicon Dioxide	> 85%

Table 11 - Chemical Properties of Micro silica

Characteristics	Percentage
SiO_2	92 %
Al_2O_3	0.46 %
Fe_2O_3	1.6%
MgO	0.74 %
CaO	0.36 %
Na_2O	0.7 %
K_2O	0.9 %
SO_3	0.35 %
LOI	2.5 %
pH	7.6 %
Accelerated pozzolanic Activity index at 7 days	104
Accelerated pozzolanic Activity index at 28 days	117

2.7 Metakaolin

Metakaolin obtained from KOAT manufacturing company, Vadodara, Gujarat has been used. Metakaolin is a de-hydroxylated form of the clay mineral kaolinite. Rocks that are rich in kaolinite are known as china clay or kaolin, traditionally used in the manufacture of porcelain. The particle size of metakaolin is smaller than cement particles, but not as fine as silica fume. Metakaolin is obtained by calcination of pure or refined kaolin clay at a temperature between 6500C and 8500C, followed by grinding to achieve a fineness of 15000 m2/kg (B.E.T).The specific gravity is found as 2.50. The resulting material has high pozzolanic property. It has already been prescribed for use in concrete making, in the Indian Standard IS 456:2000 'Code of practice for plain and reinforced

concrete (fourth revision). However, a detailed Indian Standard specification was not yet available. Physical and chemical properties of metakaolin as supplied by are tabulated in Fig 12 and 13.

Table 12 - Physical Properties of Metakaolin

Description of Physical Properties	Units	Results
Color		White
Bulk Density	gm/Liter	356
Moisture (Ex-Work)	%	0.22
Blaine's fineness	m^2/kg	12000
Residue on 325 Mesh	%	0.13
Average particle size	µm	1
Specific gravity		2.52

Table 13 - Chemical Characteristics of Metakaolin

Characteristics	Percentage
Silica, SiO_2	52.1
Alumina Al_2O_3	36.1
Iron oxide Fe_2O_3	4.3
Lime CaO	0.1
Magnesia MgO	0.84
Alkalis KO	1.38
Loss on Ignition	0.2-0.5

Metakaolin has layered, flat and flaky structure whereas Micro-silica has granular and angular structure.

2.8 Superplasticizer

In the present work, water-reducing admixture Conplast SP 430 conforming to IS 9103: 1999 [Specification for admixtures for concrete], ASTM C – 494 [Standard Specification for Chemical Admixtures for Concrete] types F, G and BS 5075 part.3 [British Standards Institution] was used for M20 and M40. Conplast SP 430 is a Sulphonated Naphthalene based Formaldehyde (SNF), super plasticizer and it was manufactured by Fosroc. For M80 and M100, BASF Glenium B233, High-performance super plasticizer based on PCE (polycarboxylic ether) for concrete conforming to IS: 9103-1999 is used as a water-reducing admixture. Dosage range of 0.5 to 1.5% by weight of cement is normally recommended.

2.9 Viscosity Modifying Agent (VMA)

These admixtures enhance the viscosity of water and eliminate the bleeding and segregation phenomena in the fresh concrete as much as possible. VMA is a neutral, biodegradable, liquid chemical additive designed to reduce the bleeding, segregation, shrinkage and cracking that occur in high water/cement ratio concrete mixes. VMA also contribute to stabilization for SCC mixes that are susceptible to segregation at high slump ranges. The VMA used in this investigation was

BASF's Glenium Stream-2 which is a product of Degussa construction chemicals. The VMA used in this investigation was Glenium stream-2 and the properties of VMA are given in Table 14.

Table 14 - Properties of Viscosity Modifying Agent

(*Source: BASF Chemicals- Glenium Stream 2*)

Property	Result
Aspect	Colorless free flowing liquid
Relative density	1.01
pH	≥6
Chloride ion content	< 0.2%
Compatibility	Can be used with all types of cements
Mechanism of action	It consists of a mixture of water soluble copolymers which is adsorbed onto the surface of the cement granules, thereby changing the viscosity of the water and influencing the rheological properties of the mix.
Dosage	50 to 500 ml/100 kg of cementitious material.

The specific gravities of the cement, fly ash, micro silica and metakaolin are 3.15, 2.15, 2.22 and 2.52 respectively. The superplasticizer content was fixed, with the intention of maintaining a standard material proportion and avoiding any effects of variation in superplasticizer content onto strength properties.

3. MIX DESIGN

Quantities required for 1 cu.m are evaluated for ordinary grade (M20) , standard grade (M40) and high strength grade (M80 and M100) of binary, ternary and quaternary blended Self-Compacting Concrete (SCC) made with optimum proportions of Fly Ash (FA), Microsilica (MS) and Metakaolin (MK) combination based on calculations from Nan Su mix design method. Final quantities, for all SCC mixes considered, are assumed after several trial mixes on quantities computed using Nan Su mix design method subjected to satisfaction of EFNARC flow properties as shown in Table 5.20 to Table 5.26. The initial base quantities calculated using Nan Su method for Ordinary (M20) grade SCC mix are tabulated in Table 15.

Table 15 – Quantities in kg per cu.m for Ordinary (M20) grade SCC obtained using Nan Su method of Mix Design

	Cement 'OPC'	Pozzolana (fly ash 'FA')	Fine aggregate	Coarse aggregate	S.P.	Water
Quantity kg/m^3	190	257	904	812	8.1 L	192.34 L

The amount of total powder (i.e., OPC+FA) computed is 447 kg/m^3 and computed total weight of Pozzolan (i.e., fly ash alone) is 257 kg/m^3 (57% of total powder). For the above total powder content, flow properties are not achieved as per EFNARC guidelines, so several trail mixes were carried out to satisfy the flow properties. The final SCC mix proportions as shown in Table 16 are arrived at after several trail mixes by adjusting cement, pozzolan (fly ash) and super plasticizer till the mix conforms to EFNARC specifications for the required fresh properties.

Table 16 – Final Quantities per cu.m for Ordinary grade (M20) SCC mix after trail mixes

	Cement	Pozzolana	Fine aggregate	Coarse aggregate	S.P.	Water
		Fly ash				
Quantity kg/m^3	225	261	904	812	9.34 L	221 L

Henceforth, the total amount of powder quantity (cement + pozzolanic mixture) adopted for Ordinary (M20) grade SCC is 486 kg/m^3 and water/powder ratio is 0.45 for all blended Ordinary (M20) grade SCC mixes. Similarly, the initial quantities calculated using Nan Su method for Standard (M40) grade SCC mix are tabulated in Table 17.

Table 17 – Quantities in kg per cu.m for Standard (M40) grade SCC obtained using Nan Su method of Mix Design

	Cement	Pozzolana	Fine Aggregate	Coarse Aggregate	S.P.	Water
		Fly ash				
Quantity kg/m^3	344	180	891	738	9.43 L	190.35 L

The amount of total powder (i.e., OPC+FA) computed is 524 kg/m^3 and computed total weight of fly ash is 180 kg/m^3 (35 % of total powder). For the above powder content, flow properties are not achieved as per EFNARC guidelines, so several trail mixes were carried out to satisfy the flow properties. The final SCC mix proportions shown in Table 18 are arrived at after several trail mixes by adjusting Cement, Pozzolan (fly ash) and super plasticizer till the mix conforms to EFNARC specifications for the required fresh properties.

Table 18 – Final Quantities per 1 cu.m for standard grade (M40) SCC mix after trail mixes.

	Cement	Total Pozzolana / Fly ash	Fine Aggregate	Coarse Aggregate	S.P.	Water	water/powder ratio
Quantity kg/m^3	317	214	891	786	9.34L	185L	0.35

Henceforth, the total amount of powder quantity (cement + pozzolanic mixture) adopted for standard grade (M40) SCC is 531 kg/m^3 and water/powder ratio is 0.35 for all blended standard grade (M40) SCC mixes. Likewise the initial quantities calculated using Nan Su method for high strength (M80) grade SCC mix are tabulated in Table 19.

Table 19 – Quantities in kg per cu.m for high strength (M80) grade SCC obtained using Nan Su method of Mix Design

	Cement	Total Pozzolana / Fly ash	Fine Aggregate	Coarse Aggregate	S.P	Water
Quantity kg/m^3	644	14	810	788	11.84L	150.56 L

The computed amount of total powder (i.e., OPC+FA) is 658 kg. For the above quantities flow properties are achieved conforming to EFNARC guidelines. But keeping in view, the high quantity of cement computed using Nan Su method, the maximum cement content is limited to 450 kg per cum of concrete as per clause 8.2.4.2 of IS 456-2000. After trail mixes, revised quantities in kg per cu.m for high strength grade (M80) SCC mix are arrived by (i) limiting the Cement to maximum permissible amount, (ii) increasing quantity of pozzolan (fly ash) to maximum amount possible and adjusting the super plasticizer without compromising the EFNARC flow properties and desired strength property.
The final quantities for high strength M80 grade SCC mix are tabulated in Table 20.

Table 20 – Final Quantities for trial mixes of high strength M80 grade SCC mix

	Cement	Total Pozzolana / Fly ash	Total Powder Content	Fine Aggregate	Coarse Aggregate	S.P.	Water (water/powder =0.25)
Quantity kg/m^3	450	250	700	714	658	12.21L	167L

Henceforth, the total amount of powder quantity (cement + pozzolanic mixture) adopted for high strength M80 SCC is 700 kg/m^3 and water/powder ratio is 0.25 for all blended high strength M80 SCC mixes.

For higher grades, Nan Su mix design method computations yield very less powder content. In fact, from the investigation it may be stated that Nan Su method is very difficult to apply for higher grades of concrete to arrive at appropriate quantities of materials. In the present study for M100 grade SCC mix, quantities are arrived by conducting various trial mixes based on M80 Nan Su mix design computations by adjusting powder content so that EFNARC flow properties and required strength criteria are met. The final quantities for high strength M100 grade SCC mix are tabulated in Table 21.

Table 21 – Quantities in kg per 1 cu.m for high strength grade (M100) SCC mix after trail mixes.

	Cement	Total Pozzolana / Fly ash	Total Powder Content	Fine Aggregate	Coarse Aggregate	S.P.	Water (water/powder =0.22)
Quantity kg/m^3	450	250	700	689	636	15.8L	154L

Henceforth, the total amount of powder quantity (cement + pozzolanic mixture) adopted for high strength M100 SCC is 700 kg/m^3 and water/powder ratio is 0.22 for all blended high strength M100 SCC mixes.

4. OPTIMIZATION OF ADMIXTURES

Several trial mixes are conducted on number of SCC mixes made with the different possible combinations of Fly Ash (FA), Microsilica (MS) and Metakaolin (MK) to develop various binary, ternary and quaternary blended SCC systems to determine the appropriate optimized quantities of Fly Ash (FA), Microsilica (MS) and Metakaolin (MK) are chosen for binary, ternary and quaternary blended SCC systems subjected to fulfilment of EFNARC flow specifications and on realization of desired strength. Flow properties are tested by using following test methods:

Table 22- List of test methods for workability properties of SCC

Method	Parameter
Slump flow test , T_{50}cm Slump flow and V-funnel test	Filling ability
V-Funnel at T_5 minutes	Segregation resistance
L-Box test	Passing ability

Typical acceptance criteria for Self-compacting Concrete with a maximum aggregate size up to 10 mm are shown in **Table 23**.

Table 23- Acceptance criteria for Self-compacting Concrete.

Method	Unit	Typical range of values	
		Minimum	Maximum
Slump flow test	mm	650	800
T_{50} cm Slump flow	sec	2	5
V – Funnel	sec	6	12
V – Funnel at T_5 minutes	sec	6	15
L – Box	h_2/h_1	0.8	1.0

4.1 Test Methods as per EFNARC Guidelines

Slump flow test and T_{50} cm test

Slump Flow Test measures the spread or flow of concrete sample, the diameter of the concrete circle is a measure of the filling ability of concrete. Slump Flow is definitely one of the most commonly used SCC tests at present. A slump flow ranging from 650 to 800mm is considered necessary for a concrete to be self-compacted. At slump flow of more than 800mm the concrete might segregate and at slump flow less than 650mm the concrete may have insufficient flow to pass through highly congested reinforcement. The T_{50} test is a secondary test to determine Slump Flow. It is simply the amount of time that the concrete takes to flow to a diameter of 50 centimeters. A lower time indicates greater flowability.

L – Box test

This test is an indication of passing ability, or the degree to which the passage of concrete through the bars is restricted. This is a widely used test, suitable for laboratory and site use. It assesses filling ability, passing ability of SCC, and segregation is also detected visually. If the concrete

flows as freely as water, at rest it will be horizontal, so H2/H1 i.e blocking ratio is equal to 1. Therefore the nearer this test value is to unity, the better is the flow of the concrete.

V – Funnel test and V – funnel test at T_5 minutes

The V-funnel test is used to determine the filling ability of the concrete and the time taken for it to flow through the apparatus measured. After this the funnel was refilled concrete and left for 5 minutes to settle. If the concrete shows segregation then the flow time increases significantly. This test measures the ease of flow of the concrete. A funnel test flow time less than 6 seconds is recommended for concrete to qualify for SCC. According to EFNARC standards a flow time (T_f) of 10 seconds is considered appropriate for SCC, and $T_{5minutes}$ should be less than (T_f+3) seconds.

4.2 Optimization of pozzolans quantities in SCC mixes

This phase identifies the optimum proportions of fly ash, micro silica and metakaolin in binary, ternary and quaternary blended SCC mixes in order to obtain the enhanced performance of SCC at all ages. The details of the quantities of materials, replacement percentages and quantities (kg) of SCMs and OPC in total powder content and their corresponding fresh properties are shown in Table 24 to Table 31 respectively for ordinary grade (M20), standard grade (M40) and high strength grade (M80 and M100) of binary, ternary and quaternary blended Self Compacting Concrete (SCC) made with optimum proportions of Fly Ash (FA), Micro-silica (MS) and Metakaolin (MK) combination. Table 24 shows base quantities of ordinary grade (M20) SCC mix, which fulfill EFNARC fresh properties guidelines, derived after several trial mixes on the quantities calculated using Nan Su mix design method. It can be observed that the total powder content calculated is 486 kg/m3. Generally, fly ash is used as pozzolan in the development of SCC mixes so Nan Su mix design calculations are carried out by considering fly ash and its properties. Depending on the above calculated base quantities for ordinary grade (M20), thirty-four (34) blended SCC mixes were designed in two groups of binary and ternary. Table 25 shows various designated binary and ternary blended SCC mixes made with different proportions of Fly Ash (FA), Microsilica (MS) and Metakaolin (MK). In mix designation, number indicates replacement percentage of total powder content. One reference SCC mix was also prepared by only OPC (C1) while in the remaining mixtures (B1 to B14 and T1 to T20) OPC was partially replaced with fly ash (FA), microsilica (MS), metakaolin (MK) and their combination. Mix numbers B1 to B14 are binary blended SCC mixtures made of either fly ash (FA) or micro silica (MS) or metakaolin (MK) while mix numbers T1 to T20 are ternary blended fly ash-based SCC mixtures made with microsilica (MS) or metakaolin (MK) as SCMs.

To determine optimal proportions of fly ash (FA), micro silica (MS) and metakaolin (MK) in binary blended SCC mixtures, different combinations of SCMs are considered. Percentage replacement of fly ash by weight of total powder content is limited to 40 – 60% (B1 to B3). As per preliminary calculation from mix design, fly ash content is above 50% therefore experimental investigations are started with initial percentage replacement of fly ash as 40%. Beyond 60% replacement with FA for ordinary grade (M20) grade, desired strength property is not achieved. Various percentage replacements of microsilica (MS) and metakaolin (MK) of total powder content are in between 5-25% and 5-30% respectively.

To determine optimal proportions of fly ash (FA), microsilica (MS) and metakaolin (MK) in ternary blended (MS+FA and MK+FA) SCC mixtures, different replacement percentages of SCMs are considered. In ternary blended (MS+FA) SCC mixtures, percentage replacement of fly ash by weight of total powder content is limited to between 50 – 60% (T1 to T8) and the percentage replacement of microsilica (MS) is limited to between 5 -20% by weight of total powder content.

Similarly in ternary blended (MK+FA) SCC mixtures, percentage replacement of fly ash by weight of total powder content is limited to between 50 – 70% (T9 to T20) and the percentage replacement of MK is limited to between 5 -20% by weight of total powder content.

Table 25 presents several possible binary and ternary blended ordinary grade (M20) SCC mixes with the different proportions of pozzolanic mixtures, their flow properties and achieved strengths. From this table, six optimally blended SCC mixes are selected which also includes reference SCC mix (C1). The optimum SCC mixes from both binary and ternary blended groups are selected subjected to following conditions:

(1) EFNARC flow properties are to be satisfied.
(2) Desired strength is to be achieved at stipulated age of curing.
(3) Maximum reduced cement content in blended SCC mixture.

From the experimental investigations, the mixes C1, B2, B7, B13, T3 and T15 are chosen as optimum binary and ternary blended ordinary grade M20 SCC mixes where both flow and desired strength properties are met along with optimal usage of pozzolanic quantities. The following are mix designations of optimum combinations of ordinary grade M20 blended SCC mixes:

(1) C100 [C1]
(2) C50+FA50 [B2]
(3) C80+MS20 [B7
(4) C75+MK25 [B13]
(5) C35+FA50+MS15 [T3]
(6) C25+FA60+MK15 [T15]

(Numbers in the above mix designations indicate percentage by weight of total powder content)

For reference SCC mix (C1) where 100% OPC is used to develop ordinary grade SCC mix, both flow properties and desired strengths are achieved. In binary blended SCC mix, for obtaining the specified flow properties and similar strength as reference mix at stipulated age of curing, cement can be replaced by 50% FA or 20% MS or 25% MK. While in ternary blended SCC mix, for obtaining the specified flow properties and similar strength as reference mix at stipulated age of curing, cement can be replaced by 50%FA+15%MS or 60%FA+15%MK.

From the observations, it can be stated that in ternary blended fly ash-based SCC mixes made with micro silica (MS) or metakaolin (MK), cement content is reduced significantly compared to binary blended ordinary grade (M20) SCC mixes made with fly ash (FA), micro silica (MS) and metakaolin (MK) independently. Fly ash percentage replacement is about 50 and 60% for MS+FA based SCC mix and MK+FA based SCC mix respectively. It was observed that with the inclusion of metakaolin (MK) to fly ash blended SCC mix yields more usage of fly ash in terms of replacement compared to micro silica (MS).

Therefore metakaolin (MK) is much preferred than micro silica (MS) for fly ash based ternary blended ordinary grade (M20) SCC mix for: (1) Cement content is reduced (2) Fly ash usage is increased (3) Less expensive (4) Early strength due to MK offsets the later strength accomplishment due to FA and (5) Better flow properties

Table 24– Base Quantities for Ordinary grade (M20) SCC mix

	Cement (i)	Pozzolan Content (ii)	Total Powder Content (i)+(ii)	Fine aggregate	Coarse aggregate	S.P.	Water	water/powder ratio
Quantity kg/m^3	225	261	486	904	812	9.34 L	221 L	0.45

Table 25 – Trail mixes of various ordinary grade (M20) blended SCC mixes

Mix No.	Mix Designation	Replacement Percentage (bwp)*				Quantities kg per cu.m				Slump flow		V-Funnel		L-Box	Achieved Strength (MPa)
		OPC	FA	MS	MK	OPC	FA	MS	MK	Slump Diameter Mm	T-50 sec	T-0 min sec	T-5min sec	Blocking Ratio	
C1	C100	100	-	-	-	486	-	-	-	707	3.22	6.50	8.31	0.96	25.18
B1	C60+FA40	60	40	-	-	290	196	-	-	710	3.16	6.11	8.35	0.92	30.60
B2	C50+FA50	50	50	-	-	243	243	-	-	740	3.19	6.29	7.77	0.96	28.98
B3	C40+FA60	40	60	-	-	196	290	-	-	760	3.85	6.45	8.76	0.98	12.87
B4	C95+MS5	95	-	5	-	461	-	25	-	700	4.04	7.25	7.87	0.87	26.19
B5	C90+MS10	90	-	10	-	437	-	49	-	683	4.19	7.92	10.37	0.89	27.18
B6	C85+MS15	85	-	15	-	413	-	73	-	667	4.07	8.06	11.58	0.90	28.99
B7	C80+MS20	80	-	20	-	389	-	97	-	650	4.40	8.02	14.09	0.92	29.03
B8	C75+MS25	75	-	25	-	365	-	121	-	549	4.70	8.42	15.90	0.92	20.09
B9	C95+MK5	95	-	-	5	461	-	-	25	705	3.81	6.84	7.42	0.82	26.96
B10	C90+MK10	90	-	-	10	437	-	-	49	700	3.95	7.47	9.78	0.84	27.76
B11	C85+MK15	85	-	-	15	413	-	-	73	680	3.84	7.6	10.92	0.85	28.81
B12	C80+MK20	80	-	-	20	389	-	-	97	677	4.15	7.57	13.29	0.87	30.73
B13	C75+MK25	75	-	-	25	365	-	-	121	660	4.43	7.94	15	0.87	30.77
B14	C70+MK30	70	-	-	30	341	-	-	145	546	4.73	8.34	18.38	0.87	20.30
T1	C45+FA50+MS5	45	50	5	-	218	243	25	-	685	3.49	6.48	7.88	0.87	28.11
T2	C40+FA50+MS10	40	50	10	-	197	243	49	-	675	3.80	6.81	9.26	0.89	28.92
T3	C35+FA50+MS15	35	50	15	-	170	243	73	-	670	3.52	6.95	9.35	0.91	29.37
T4	C30+FA50+MS20	30	50	20	-	146	243	97	-	665	3.85	6.92	10.74	0.93	23.17
T5	C35+FA60+MS5	35	60	5	-	171	290	25	-	635	4.14	7.20	11.88	0.93	19.76
T6	C30+FA60+MS10	30	60	10	-	147	290	49	-	627	4.46	7.51	13.34	0.93	14.13
T7	C25+FA60+MS15	25	60	15	-	123	290	73	-	612	3.49	6.48	7.86	0.86	12.34
T8	C20+FA60+MS20	20	60	20	-	99	290	97	-	605	3.80	6.83	9.25	0.87	12.31
T9	C45+FA50+MK5	45	50	-	5	218	243	-	25	712	3.63	6.74	8.20	0.90	28.43
T10	C40+FA50+MK10	40	50	-	10	197	243	-	49	702	3.95	7.08	9.63	0.93	28.52
T11	C35+FA50+MK15	35	50	-	15	170	243	-	73	697	3.66	7.23	9.72	0.95	29.37
T12	C30+FA50+MK20	30	50	-	20	146	243	-	97	692	4.00	7.20	11.17	0.97	21.17
T13	C35+FA60+MK5	35	60	-	5	171	290	-	25	660	4.31	7.49	12.36	0.97	26.34
T14	C30+FA60+MK10	30	60	-	10	147	290	-	49	652	4.64	7.81	13.87	0.97	29.19
T15	C25+FA60+MK15	25	60	-	15	123	290	-	73	712	3.63	6.74	8.20	0.90	33.29
T16	C20+FA60+MK20	20	60	-	20	99	290	-	97	702	3.95	7.08	9.63	0.93	21.24
T17	C25+FA70+MK5	25	70	-	5	121	340	-	25	697	3.66	7.23	9.72	0.95	19.55
T18	C20+FA70+MK10	20	70	-	10	97	340	-	49	692	4.00	7.20	11.17	0.97	17.34
T19	C15+FA70+MK15	15	70	-	15	73	340	-	73	660	4.31	7.49	12.36	0.97	14.34
T20	C10+FA70+MK20	10	70	-	20	47	340	-	97	652	4.64	7.81	13.87	0.97	12.63

Table 26 gives base quantities of standard grade (M40) SCC mix derived after several trial mixes on the quantities calculated using Nan Su mix design method. It can be observed that the total powder content is 531 kg/m^3. Generally, fly ash is used as pozzolan in the development of SCC mixes so Nan Su mix design calculations are carried out by considering fly ash and its properties. Depending on the above calculated base quantities for standard grade (M40), twenty-five (25) blended SCC mixes were designed in two groups of binary and ternary. Table 5.30 shows various blended standard grade (M40) SCC mixtures made with different proportions of Fly Ash (FA), Microsilica (MS) and Metakaolin (MK). In Mix designation, number indicates percentage by weight of total powder content. One reference SCC mix was also prepared by only OPC (C1) while in the remaining mixtures (B1 to B11 and T1 to T14) OPC was partially replaced with fly ash (FA), microsilica (MS), metakaolin (MK) and their combination. Mix numbers B1 to B11 are binary blended SCC mixtures made of either fly ash (FA) or microsilica (MS) or metakaolin (MK) while Mix numbers T1 to T14 are ternary blended fly ash-based SCC mixtures made of microsilica (MS) or metakaolin (MK).

To determine optimal proportions of fly ash (FA), microsilica (MS) and metakaolin (MK) in binary blended SCC mixtures, percentage replacement of fly ash by weight of total powder content is limited to 40 – 50% (B1 to B2) based on preliminary calculation from mix design. Beyond 40% replacement with fly ash (FA) for standard grade (M40), desired strength property is not achieved. The percentage replacement of micro silica (MS) and metakaolin (MK) of total powder content are limited to 5-20% and 5-25% respectively.

To determine optimal proportions of fly ash (FA) and microsilica (MS) in ternary blended SCC mixtures, percentage replacement of fly ash by weight of total powder content is limited to 40 – 50% (T1 to T6) and the percentage replacement of microsilica (MS) is limited to 5 -15% by weight of total powder content. Similarly in ternary blended MK+FA based SCC mixtures, percentage replacement of fly ash by weight of total powder content is limited to 50 – 60% (T7 to T14) and the percentage replacement of metakaolin (MK) is limited to 5 -20% by weight of total powder content.

Table 27 presents several possible binary and ternary blended standard grade (M40) SCC mixes with the quantities of pozzolanic mixtures, their flow properties and achieved strengths. From this table, six optimum blended SCC mixes are selected which also includes reference SCC mix (OPC alone). The optimum SCC mixes from both binary and ternary blended groups are selected subjected to following conditions:

(1) EFNARC flow properties are to be satisfied.
(2) Desired strength is to be achieved at stipulated age of curing.
(3) Maximum reduction of cement content in blended SCC mixture

From the experimental investigations, the mixes C1, B1, B5, B10, T5 and T9 are chosen as optimal binary and ternary blended standard grade (M40) SCC mixes where both flow and desired strength properties are met along with optimal usage of pozzolanic quantities. The following are mix designations of optimum combinations of standard grade (M40) blended SCC mixes:

(1) C100 [C1]
(2) C60+FA40 [B1]
(3) C85+MS15 [B5]
(4) C80+MK20 [B10]
(5) C50+FA40+MS10 [T5]
(6) C35+FA50+MK15 [T9]

Numbers in the above mix designations indicate percentage by weight of total powder content.

For reference SCC mix (C1) where 100% OPC is used to develop standard grade (M40) SCC mix, both flow properties and desired strengths are achieved. In binary blended SCC mix, for obtaining the specified flow properties and similar strength as reference mix at stipulated age of curing, cement can be replaced by either 40% FA or 15% MS or 20% MK. While in ternary blended SCC mix, for obtaining the specified flow properties and similar strength as reference mix at stipulated age of curing, cement can be replaced by 40%FA+10%MS or 50%FA+15%MK.

From the observations, it can be stated that in ternary blended fly ash based SCC mixes made with micro silica (MS) or metakaolin (MK), cement content is reduced significantly compared to binary blended standard grade (M40) SCC mix.

Fly ash percentage replacement is about 40 and 50% for MS+FA based SCC mix and MK+FA based SCC mix respectively. It was observed that with the inclusion of metakaolin (MK) to fly ash based binary blended SCC mix yields more usage of fly ash in terms of replacement compared to MS. Therefore metakaolin (MK) is much preferred than micro silica (MS) for fly ash based ternary blended standard grade (M40) SCC mix for:

(1) Cement content is reduced
(2) Fly ash usage is increased
(3) Less expensive
(4) Early strength due to metakaolin (MK) offsets the later strength accomplishment due to fly ash (FA)
(5) Better flow properties

Table 26 – Base Quantities for standard grade (M40) SCC mix

	Cement	Total Pozzolana	Fine Aggregate	Coarse Aggregate	S.P.	Water	water/ powder ratio
Quantity kg/m^3	317	214	891	786	9.34L	185L	0.35

Table 27 – Trail mixes of various standard grade (M40) blended SCC mixes

Mix No.	Mix Designation	Replacement Percentage (bwp)				Quantities kg per cu.m				Slump flow		V-Funnel		L-Box	Achieved Strength (MPa)
		OPC	FA	MS	MK	OPC	FA	MS	MK	Slump Diameter mm	T-50 sec	T-0 min sec	T-5min sec	Blocking Ratio	
C1	C100	100	-	-	-	531	-	-	-	728	3.32	6.70	8.56	0.99	48.18
B1	C60+FA40	60	40	-	-	319	212	-	-	731	3.25	6.29	8.60	0.95	53.60
B2	C50+FA50	50	50	-	-	265	265	-	-	762	3.29	6.48	8.00	0.99	35.98
B3	C95+MS5	95	-	5	-	505	-	26	-	721	4.16	7.47	8.11	0.90	49.19
B4	C90+MS10	90	-	10	-	478	-	53	-	703	4.32	8.16	10.68	0.92	50.18
B5	C85+MS15	85	-	15	-	452	-	79	-	687	4.19	8.30	11.93	0.93	51.99
B6	C80+MS20	80	-	20	-	425	-	106	-	670	4.53	8.26	14.51	0.95	36.03
B7	C95+MK5	95	-	-	5	505	-	-	26	726	3.92	7.05	7.64	0.84	49.96
B8	C90+MK10	90	-	-	10	478	-	-	53	721	4.07	7.69	10.07	0.87	50.76
B9	C85+MK15	85	-	-	15	452	-	-	79	700	3.96	7.83	11.25	0.88	51.81
B10	C80+MK20	80	-	-	20	425	-	-	106	697	4.27	7.80	13.69	0.90	53.73
B11	C75+MK25	75	-	-	25	398	-	-	133	680	4.56	8.18	15.45	0.90	38.77
T1	C55+FA40+MS5	55	40	5	-	292	212	26	-	654	4.26	7.42	12.24	0.96	42.76
T2	C50+FA40+MS10	50	40	10	-	265	212	54	-	646	4.59	7.74	13.74	0.96	52.13
T3	C45+FA40+MS15	45	40	15	-	239	212	80	-	630	3.59	6.67	8.10	0.89	35.34
T4	C45+FA50+MS5	45	50	5	-	239	265	26	-	706	3.59	6.67	8.12	0.90	31.11
T5	C40+FA50+MS10	40	50	10	-	212	265	54	-	695	3.91	7.01	9.54	0.92	31.92
T6	C35+FA50+MS15	35	50	15	-	186	265	80	-	690	3.63	7.16	9.63	0.94	32.37
T7	C45+FA50+MK5	45	50	-	5	239	265	-	25	733	3.74	6.94	8.45	0.93	33.43
T8	C40+FA50+MK10	40	50	-	10	212	265	-	49	723	4.07	7.29	9.92	0.96	41.52
T9	C35+FA50+MK15	35	50	-	15	186	265	-	73	718	3.77	7.45	10.01	0.98	52.37
T10	C30+FA50+MK20	30	50	-	20	159	265	-	97	713	4.12	7.42	11.51	1.00	40.17
T11	C35+FA60+MK5	35	60	-	5	186	319	-	25	680	4.44	7.71	12.73	1.00	39.34
T12	C30+FA60+MK10	30	60	-	10	159	319	-	49	672	4.78	8.04	14.29	1.00	32.19
T13	C25+FA60+MK15	25	60	-	15	133	319	-	73	733	3.74	6.94	8.45	0.93	26.29
T14	C20+FA60+MK20	20	60	-	20	106	319	-	97	723	4.07	7.29	9.92	0.96	24.24

Table 28 gives base quantities of high strength grade (M80) SCC mix derived after several trial mixes on the quantities calculated using Nan Su mix design method. It can be observed that the total powder content is 700 kg/m3 with cement content restricted to 450 kg/m3 from durability of concrete point of view and rest of the powder is fly ash (250 kg/m3). Generally, fly ash is used as pozzolan in the development of SCC mixes so Nan Su mix design calculations are carried out by considering fly ash and its properties.

Depending on the above calculated base quantities for high strength grade (M80), twenty-nine (29) blended SCC mixes were designed in three groups of binary, ternary and quaternary. Table 29 shows various blended high strength grade (M80) SCC mixtures made with different proportions of Fly Ash (FA), Microsilica (MS) and Metakaolin (MK). In Mix designation, number indicates percentage by weight of total powder content. Various binary, ternary and quaternary SCC mixes were prepared with different proportions of Fly Ash (FA), Microsilica (MS) and Metakaolin (MK). (B1 to B8, T1 to T8 and Q1 to Q12). Mix numbers B1 to B8 are binary blended SCC mixtures made of either fly ash (FA) or microsilica (MS) or metakaolin (MK) while Mix numbers T1 to T8 are ternary blended fly ash based SCC mixtures made of microsilica (MS) or metakaolin (MK) and Mix numbers Q1 to Q12 are quaternary blended fly ash based SCC mixtures made of microsilica (MS) and metakaolin (MK) combination.

In high strength grade (M80) SCC mix 'C1' developed with 100% OPC does not yield desired strength is not achieved. So, using 100% OPC in development of high strength grade (M80) SCC mix is completely ruled out. In binary blended high strength grade (M80) SCC mixtures, percentage replacement of fly ash by weight of total powder content is 35% i.e. 250 kg/m3 (B1) which is based on preliminary calculation from mix design. For the mix proportion C65+FA35, required flow properties are achieved but desired strength is not realized. For binary blended SCC mixtures made with percentage replacement of either micro silica (MS) or metakaolin (MK) or both combined, micro silica (MS) and metakaolin (MK) are limited to 5-15% and 5-20% respectively.

In ternary blended micro silica (MS) and fly ash (FA) blended high strength grade (M80) SCC mixtures (T1 to T4) percentage replacement of micro silica (MS) is limited to 5 -20% by weight of total powder content. Similarly in ternary blended metakaolin (MK) and fly ash (FA) blended high strength grade (M80) SCC mixtures (T5 to T8), percentage replacement of metakaolin (MK) is limited to 5 -20% by weight of total powder content. In both the above ternary blended MS+FA blended SCC and MK+FA blended SCC mixtures (T1 to T8), the cement content is kept constant (65% by weight of total powder content).

In binary blended high strength grade (M80), for fly ash (FA) blended SCC mix (B1) and metakaolin (MK) blended SCC mixes (B5 to B8) although required flow properties are achieved but desired strength is not realized. But in binary blended micro silica (MS) blended SCC mix, both required flow properties and desired strength are attained, if the MS percentage replacement is limited to 5-10% by weight of powder. The optimal mix chosen for binary blended micro silica (MS) blended SCC mix is 5% MS replacement (B2). Henceforth, for high strength grade (M80) mixes, Mix OPC95+MS5 (B2) is taken as reference mix.

In ternary blended metakaolin (MK) and fly ash (FA) blended high strength grade (M80) SCC mixtures (T5 to T8), however required flow properties are satisfied but desired strengths are not obtained for any one the mixes. But for micro silica (MS) and fly ash (FA) blended ternary blended SCC mixes (T1 toT4), up to 15% MS by weight of powder, both required flow properties and desired strength are attained satisfactorily. So C65+FA20+MS15 (T3) SCC mix is considered optimal in ternary blended high strength grade (M80) SCC mixes.

In quaternary blended high strength grade (M80) SCC mixtures (Q1 to Q12) made of microsilica (MS) and metakaolin (MK) combination, keeping cement content constant (65% by weight of total powder content), microsilica (MS) and metakaolin (MK) proportions are limited to 7 – 14%.
For quaternary blended SCC mix (Q1), initially 7% MS and 7% MK replacements are assumed, keeping cement content constant i.e. 65% by weight of total powder content and rest of powder is fly ash, and required flow properties are not satisfied. So microsilica (MS) and metakaolin (MK) are gradually increased to 14% each yet flow properties are not achieved. Then author proposed to additionally increase fly ash content incrementally by 10% by weight of powder content (700 kg/m3), thereby incrementally increasing the powder quantity by 70 kg. With addition of 30% of fly ash (FA) to the C65+FA7+MS14+MK14 SCC mix (Q11), required flow and strength properties are achieved. So for quaternary blended SCC mix, the optimum combination of cement and pozzolanic mixture is revised as C50+FA28+MS11+MK11 SCC mix where final total powder content is 910 kg/m3 in which cement content is 455 kg/m3 and pozzolanic mixture is 455 kg/m3. Table 29 presents several possible binary, ternary and quaternary blended high strength grade (M80) SCC mixes with the quantities of pozzolanic mixtures, their flow properties and achieved strengths. From this table, three optimally blended SCC mixes are selected.
From the experimental investigations, the mixes B2, T3 and Q11 are chosen as optimum binary, ternary and quaternary blended high strength grade (M80) SCC mixes made with fly ash (FA), microsilica (MS) and metakaolin (MK) where both flow and desired strength properties are met along with optimal usage of pozzolanic quantities. The following are mix designations of optimum combinations of binary, ternary and quaternary blended high strength grade (M80) SCC mixes:

(1) C95+MS5 [B2]
(2) C65+FA20+MS15 [T3]
(3) C50+FA28+MS11+MK11 [Q11]

Numbers in the above mix designations indicate percentage by weight of total powder content. Total powder content for binary, ternary is 700 kg/m^3 and while for quaternary blended high strength grade (M80) it is 910 kg/m^3. Thus, by incorporating metakaolin (MK) into micro silica (MS) and fly ash (FA) blended ternary blended SCC mixes, the amount of fly ash used has almost doubled to achieve the requisite flow properties and therefore desired strength. From this observation, it can be understood that micro silica (MS) in blended SCC mixtures imparts high strength but flow properties are marginally satisfied while metakaolin (MK) inclusion enhances the usage of high quantity of fly ash in SCC mixes for superior rate of gain of strength and more importantly for improved flow properties of SCC mix. The quaternary blended fly ash based SCC mix made of microsilica (MS) and metakaolin (MK) combination is found to be superior to ternary blended fly ash based SCC mix made with either microsilica (MS) or metakaolin (MK) due to reasons that for similar strength, better early strength, enhanced rate of gain of strength, improved flow properties and more use of fly ash quantity in developing blended high strength grade (M80) SCC.

Table 28 – Base Quantities for high strength M80 grade SCC mix

	Cement	Total Pozzolana	Total Powder Content	Fine Aggregate	Coarse Aggregate	S.P.	Water (water/powder =0.25)
		Fly ash					
Quantity kg/m^3	450	250	700	714	658	12.2L	167L

Table 29 – Trail mixes of various high strength grade (M80) blended SCC mixes

Mix No.	Mix Designation (Values indicate percentage by weight of 'P'	Replacement % (bwp)*				Additional % of FA bwp*	Quantities kg per cu.m				Total Powder Content 'P'	Slump flow		V-Funnel		L-Box	Achieved Strength (MPa)
		OPC	FA	MS	MK		OPC	FA	MS	MK		Slump Diameter mm	T-50 sec	T-0 min sec	T-5min sec	Blocking Ratio	
C1	C100	100	-	-	-	-	700	0	-	-	700	725	3.30	6.66	8.52	0.98	72.35
B1	C65+FA35	65	35	-	-	-	450	250	-	-	700	728	3.24	6.26	8.56	0.94	58.94
B2	C95+MS5	95	-	5	-	-	665	-	35	-	700	718	4.14	7.43	8.07	0.89	88.56
B3	C90+MS10	90	-	10	-	-	630	-	70	-	700	700	4.29	8.12	10.63	0.91	106.04
B4	C85+MS15	85	-	15	-	-	595	-	105	-	700	684	4.17	8.26	11.87	0.92	78.32
B5	C95+MK5	95	-	-	5	-	665	-	-	35	700	723	3.91	7.01	7.61	0.84	72,15
B6	C90+MK10	90	-	-	10	-	630	-	-	70	700	718	4.05	7.66	10.02	0.86	75.78
B7	C85+MK15	85	-	-	15	-	595	-	-	105	700	697	3.94	7.79	11.19	0.87	78. 82
B8	C80+MK20	80	-	-	20	-	560	-	-	140	700	694	4.25	7.76	13.62	0.89	69.35
T1	C65+FA30+MS5	65	30	5	-	-	455	210	35	-	700	702	3.58	6.64	8.08	0.89	81.23
T2	C65+FA25+MS10	65	25	10	-	-	455	175	70	-	700	692	3.90	6.98	9.49	0.91	84.20
T3	C65+FA20+MS15	65	20	15	-	-	455	140	105	-	700	687	3.61	7.12	9.58	0.93	90.54
T4	C65+FA15+MS20	65	15	20	-	-	455	105	140	-	700	682	3.95	7.09	11.01	0.95	78.91
T5	C65+FA30+MK5	65	30	-	5	-	455	210	-	35	700	730	3.72	6.91	8.41	0.92	76.23
T6	C65+FA25+MK10	65	25	-	10	-	455	175	-	70	700	720	4.05	7.26	9.87	0.95	77.34
T7	C65+FA20+MK15	65	20	-	15	-	455	140	-	105	700	714	3.75	7.41	9.96	0.97	78.12
T8	C65+FA15+MK20	65	15	-	20	-	455	105	-	140	700	709	4.10	7.38	11.45	0.99	67.21
Q1	C65+FA21+MS7+MK7	65	21	7	7	-	455	147	49	49	700	677	4.42	7.68	12.67	0.99	74.88
Q2	C60+FA28+MS6+MK6	65	21	7	7	10	455	217	49	49	770	668	4.76	8.01	14.22	0.99	76.34
Q3	C54+FA34+MS6+MK6	65	21	7	7	20	455	287	49	49	840	668	4.76	8.01	14.22	0.99	72.17
Q4	C65+FA14+MS14+MK7	65	14	14	7	-	455	98	98	49	700	720	4.05	7.26	9.87	0.95	80.16
Q5	C59+FA22+MS13+MK6	65	14	14	7	10	455	168	98	49	770	714	3.75	7.41	9.96	0.97	81.23
Q6	C54+FA28+MS12+MK6	65	14	14	7	20	455	238	98	49	840	709	4.10	7.38	11.45	0.99	83.65
Q7	C50+FA34+MS11+MK5	65	14	14	7	30	455	308	98	49	910	677	4.42	7.68	12.67	0.99	71.37
Q8	C65+FA7+MS14+MK14	65	7	14	14	-	455	49	98	98	700	668	4.76	8.01	14.22	0.99	80.94
Q9	C58+FA16+MS13+MK13	65	7	14	14	10	455	119	98	98	770	677	4.42	7.68	12.67	0.99	83.25
Q10	C53+FA23+MS12+MK12	65	7	14	14	20	455	189	98	98	840	668	4.76	8.01	14.22	0.99	84.72
Q11	C50+FA28+MS11+MK11	65	7	14	14	30	455	259	98	98	910	730	3.72	6.91	8.41	0.92	90.71
Q12	C46+FA34+MS10+MK10	65	7	14	14	40	455	329	98	98	980	720	4.05	7.26	9.87	0.95	79.91

For high strength (M100) grade SCC mix, different SCC mixes are designed depending on the base quantities calculated for high strength grade (M80) SCC mix using Nan Su mix design method. For development of high strength grade (M100), nineteen (19) blended SCC mixes were designed in three groups of binary, ternary and quaternary. Table 30 shows various possible binary, ternary and quaternary blended high strength grade (M100) SCC mixtures made with different proportions of Fly Ash (FA), Microsilica (MS) and Metakaolin (MK). In Mix designation, number indicates percentage by weight of total powder content. Mix numbers B1 to B3 are binary blended SCC mixtures made of microsilica (MS) only while Mix numbers T1 to T3 are ternary blended SCC mixtures made of fly ash (FA) and microsilica (MS) whereas Mix numbers Q1 to Q12 are quaternary blended fly ash based SCC mixtures made of microsilica (MS) and metakaolin (MK) together.

In binary blended high strength grade (M100) SCC mixtures made with either fly ash or metakaolin, required flow properties are achieved but desired strengths are not realized. Except for Binary blended SCC mixtures made with percentage replacement of microsilica (MS, where microsilica (MS) is limited to 5-10%, both required flow and strength properties are achieved.

In ternary blended microsilica (MS)+ fly ash (FA) based high strength grade (M100) SCC mixtures (T1 to T3), the percentage replacement of microsilica (MS) is limited to 5 -10% by weight of total powder content, both required flow and strength properties are fulfilled. But ternary blended metakaolin (MK) and fly ash (FA) blended high strength grade (M100) SCC mixtures does not yield desired strength though required flow properties are achieved. The optimal mix chosen for binary blended microsilica (MS) based SCC mix is C90+MS10 (B2). Henceforth, for high strength grade (M100) mixes, Mix 'B2' is taken as reference mix.

In ternary blended metakaolin (MK) and fly ash (FA) blended high strength grade (M80) SCC mixtures, required flow properties are satisfied however desired strengths are not obtained. But for fly ash (FA) and microsilica (MS) blended ternary SCC mixes (T1 toT3), up to 10% MS by weight of powder, both required flow properties and desired strength are attained satisfactorily. So C71+FA19+MS10 (T2) SCC mix is considered optimal in ternary blended high strength grade (M100) SCC mixes. The cement content in ternary blended high strength grade (M80) SCC mixes is limited to 500 kg/m3.

In quaternary blended high strength grade (M100) SCC mixtures (Q1 to Q12) made of microsilica (MS) and metakaolin (MK) together, keeping cement content constant (71% by weight of total powder content), microsilica (MS) and metakaolin (MK) contents are limited to 7 and 14%.

For quaternary blended SCC mix (Q1), initially 7% MS and 7% MK replacements are assumed, keeping cement content constant i.e. 500kg/m3 and rest of powder is fly ash, required flow properties not are satisfied. Then author proposed to additionally increase fly ash content incrementally by 10% by weight of powder content (700 kg/m3) until flow properties are achieved and also microsilica (MS) and metakaolin (MK) quantities are increased to 14% each to realize desired strength.

The optimum combination of cement and pozzolanic mixture is obtained for C55+FA23+MS11+MK11 SCC mix (Q11) where final total powder content is 910 kg/m3 in which cement content is 500 kg/m3 and pozzolanic mixture is 419 kg/m3. For this optimum mix, microsilica (MS) and metakaolin (MK) are optimally proportioned at 14% each and additional percentage of fly ash (FA) added is 30% by weight of powder content (700kg/m3), for which both required flow and strength properties are fulfilled.

Table 31 presents several possible binary, ternary and quaternary blended high strength grade (M100) SCC mixes with the quantities of pozzolanic mixtures, their flow properties and achieved strengths. From this table, three optimum blended SCC mixes are selected.

From the experimental investigations, the mixes B2, T2 and Q11 are chosen as optimum binary, ternary and quaternary blended high strength grade (M100) SCC mixes made with different proportions of Fly Ash (FA), Microsilica (MS) and Metakaolin (MK) where both flow and desired strength properties are met along with optimal usage of pozzolanic quantities. The following are mix designations of optimum combinations of binary, ternary and quaternary blended high strength grade (M100) SCC mixes:

(1) C90+MS10 [B2]
(2) C71+FA19+MS10 [T2]
(3) C55+FA23+MS11+MK11 [Q11]

Numbers in the above mix designations indicate percentage by weight of total powder content. Total powder content for binary, ternary is 700 kg/m3 and while for quaternary blended high strength grade (M100) is 910 kg/m3. From this observation, it can be understood that micro silica (MS) in blended SCC mixtures imparts high strength but flow properties are marginally satisfied while metakaolin (MK) inclusion enhances the usage of high quantity of fly ash in SCC mixes for superior rate of gain of strength and more importantly for improved flow properties of SCC mix. The quaternary blended fly ash based SCC mix made of micro silica (MS) and Metakaolin (MK) together is found to be superior to ternary blended fly ash based SCC mix made with micro silica (MS) or Metakaolin (MK) due to reasons that for similar strength, better early strength, enhanced rate of gain of strength, improved flow properties and more use of fly ash quantity in developing blended high strength grade (M100) SCC. Quaternary blended fly ash based SCC mix also giver better early strength than ternary blended SCC mix.

Table 30 – Trail mixes of various high strength grade (M100) blended SCC mixes

Mix No.	Mix Designation (Values indicate percentage by weight of 'P'	Replacement % (bwp)*				Additional % of FA bwp*	Quantities kg per cu.m				Total Powder Content 'P'	Slump flow		V-Funnel		L-Box	Achieved Strength (MPa)
		OPC	FA	MS	MK		OPC	FA	MS	MK		Slump Diameter mm	T-50 sec	T-0 min sec	T-5min sec	Blocking Ratio	
C1	C100	100	-	-	-	-	700	-	-	-	700	732	3.33	6.73	8.61	0.99	72.35
B1	C95+MS5	95	-	5	-	-	665	-	35	-	700	725	4.18	7.50	8.15	0.90	88.56
B2	C90+MS10	90	-	10	-	-	630	-	70	-	700	707	4.33	8.20	10.74	0.92	106.04
B3	C85+MS15	85	-	15	-	-	595	-	105	-	700	691	4.21	8.34	11.99	0.93	78.32
T1	C71+FA24+MS5	71	24	5	-	-	500	165	35	-	700	709	3.62	6.71	8.16	0.90	91.23
T2	C71+FA19+MS10	71	19	10	-	-	500	130	70	-	700	699	3.94	7.05	9.58	0.92	104.20
T3	C71+FA14+MS15	71	14	15	-	-	500	95	105	-	700	694	3.65	7.19	9.68	0.94	97.54
Q1	C71+FA15+MS7+MK7	71	15	7	7	-	500	102	49	49	700	684	4.46	7.76	12.80	0.98	94.18
Q2	C65+FA23+MS6+MK6	71	15	7	7	10	500	172	49	49	770	675	4.81	8.09	14.36	0.97	97.34
Q3	C60+FA34+MS6+MK6	71	15	7	7	20	500	242	49	49	840	675	4.81	8.09	14.36	0.97	78.17
Q4	C71+FA8+MS14+MK7	71	8	14	7	-	500	53	98	49	700	727	4.09	7.33	9.97	0.96	90.16
Q5	C65+FA16+MS13+MK6	71	8	14	7	10	500	123	98	49	770	721	3.79	7.48	10.06	0.98	91.23
Q6	C60+FA22+MS12+MK6	71	8	14	7	20	500	193	98	49	840	716	4.14	7.45	11.56	1.00	98.65
Q7	C55+FA29+MS11+MK5	71	8	14	7	30	500	263	98	49	910	684	4.46	7.76	12.80	1.00	80.37
Q8	C71+FA1+MS14+MK14	71	1	14	14	-	500	4	98	98	700	675	4.81	8.09	14.36	1.00	96.94
Q9	C65+FA10+MS13+MK13	71	1	14	14	10	500	74	98	98	770	684	4.46	7.76	12.80	1.00	98.25
Q10	C60+FA17+MS12+MK12	71	1	14	14	20	500	144	98	98	840	675	4.81	8.09	14.36	1.00	104.72
Q11	C55+FA23+MS11+MK11	71	1	14	14	30	500	214	98	98	910	737	3.76	6.98	8.49	0.93	110.71
Q12	C51+FA29+MS10+MK10	71	1	14	14	40	500	284	98	98	980	727	4.09	7.33	9.97	0.96	89.91

Table 31 – Flow properties of optimized blended SCC mixes for various grades

Grade of SCC Mix	Mix No	Mix Designation (Values indicate percentage by weight of 'P'	Replacement % (bwp)*				Additional % of FA bwp*	Slump flow		V-Funnel		L-Box
			OPC	FA	MS	MK		Slump Diameter Mm	T-50 sec	T-0 min sec	T-5min sec	Blocking Ratio
M20	C1	C100	100	-	-	-	-	707	3.22	6.50	8.31	0.96
	B2	C50+FA50	50	50	-	-	-	740	3.19	6.29	7.77	0.96
	B7	C80+MS20	80	-	20	-	-	650	4.40	8.02	14.09	0.92
	B13	C75+MK25	75	-	-	25	-	660	4.43	7.94	15	0.87
	T3	C35+FA50+MS15	35	50	15	-	-	670	3.52	6.95	9.35	0.91
	T15	C25+FA60+MK15	25	60	-	15	-	712	3.63	6.74	8.20	0.90
M40	C1	C100	100	-	-	-	-	728	3.32	6.70	8.56	0.99
	B1	C60+FA40	60	40	-	-	-	731	3.25	6.29	8.60	0.95
	B5	C85+MS15	85	-	15	-	-	687	4.19	8.30	11.93	0.93
	B10	C80+MK20	80	-	-	20	-	697	4.27	7.80	13.69	0.90
	T5	C50+FA40+MS10	50	40	10	-	-	695	3.91	7.01	9.54	0.92
	T9	C35+FA50+MK15	35	50	-	15	-	718	3.77	7.45	10.01	0.98
M80	B2	C95+MS5	95	-	5	-	-	718	4.14	7.43	8.07	0.89
	T3	C65+FA20+MS15	65	20	15	-	-	687	3.61	7.12	9.58	0.93
	Q11	C50+FA28+MS11+MK11	65	7	14	14	30	730	3.72	6.91	8.41	0.92
M100	B2	C90+MS10	90	-	10	-	-	707	4.33	8.20	10.74	0.92
	T2	C71+FA19+MS10	65	25	10	-	-	699	3.94	7.05	9.58	0.92
	Q11	C55+FA23+MS11+MK11	71	1	14	14	30	737	3.76	6.98	8.49	0.93

bwp* – By weight of Total Powder Content

Table 32 - Final optimized mix proportions of blended SCC mixes for various grades

Grade of SCC Mix	Mix No	Mix Designation (Values indicate percentage by weight of 'P'	Replacement % (bwp)*				Additional % of FA bwp*	Quantities kg per cu.m									
			OPC	FA	MS	MK		OPC (i)	FA (ii)	MS (iii)	MK (iv)	Total Powder Content 'P' kg (i)+(ii)+(iii)+(iv)	Fine Aggregate	Coarse Aggregate	Water	S.P.	W/P ratio
M20	C1	C100	100	-	-	-	-	486	-	-	-	486	904	812	221	9.5	0.45
	B2	C50+FA50	50	50	-	-	-	243	243	-	-	486	904	812	221	9.5	0.45
	B7	C80+MS20	80	-	20	-	-	389	-	97	-	486	904	812	221	9.5	0.45
	B13	C75+MK25	75	-	-	25	-	365	-	-	121	486	904	812	221	9.5	0.45
	T3	C35+FA50+MS15	35	50	15	-	-	170	243	73	-	486	904	812	221	9.5	0.45
	T15	C25+FA60+MK15	25	60	-	15	-	123	290	-	73	486	904	812	221	9.5	0.45
M40	C1	C100	100	-	-	-	-	531	-	-	-	531	891	786	185	9.5	0.35
	B1	C60+FA40	60	40	-	-	-	319	212	-	-	531	891	786	185	9.5	0.35
	B5	C85+MS15	85	-	15	-	-	452	-	79	-	531	891	786	185	9.5	0.35
	B10	C80+MK20	80	-	-	20	-	425	-	-	106	531	891	786	185	9.5	0.35
	T5	C50+FA40+MS10	50	40	10	-	-	265	212	54	-	531	891	786	185	9.5	0.35
	T9	C35+FA50+MK15	35	50	-	15	-	186	265	-	80	531	891	786	185	9.5	0.35
M80	B2	C95+MS5	95	-	5	-	-	665	-	35	-	700	714	658	167	12.5	0.25
	T3	C65+FA20+MS15	65	20	15	-	-	455	140	105	-	700	714	658	167	12.5	0.25
	Q11	C50+FA28+MS11+MK11	65	7	14	14	30	455	259	98	98	910	714	658	167	12.5	0.25
M100	B2	C90+MS10	90	-	10	-	-	630	-	70	-	700	689	636	154	16.0	0.22
	T2	C71+FA19+MS10	65	25	10	-	-	500	130	70	-	700	689	636	154	16.0	0.22
	Q11	C55+FA23+MS11+MK11	71	1	14	14	30	500	214	98	98	910	689	636	154	16.0	0.22

bwp* – By weight of Total Powder Content
W/P ratio – Water/Powder Ratio

In ordinary grade (M20), three binary blended (C50+FA50, C80+MS20, C75+MK25), two ternary blended (C35+FA50+MS15, C25+FA60+MK15) and one reference (C100) SCC mixes are optimally designed so that all the above mentioned ordinary grade SCC mixes achieve almost similar strength. The purpose of choosing the above stated six optimum combinations of SCMs is to establish the optimum percentage replacement levels of fly ash, micro silica and metakaolin when used individually or in combination in binary and ternary blended SCC mixes.

From the investigations, it is observed that ternary blended ordinary grade SCC mixes are more efficient that binary blended ordinary grade SCC mixes in terms of (1) usage of high quantity of fly ash and (2) reduction in quantity of cement used.

In ternary blends of ordinary grade (M20), metakaolin (MK) blended fly ash (FA) based ternary blended SCC mix is considered as more efficient than micro silica (MS) blended fly ash (FA) based ternary blended SCC mix because of reasons: (1) economical (2) more fly ash quantity is used (3) less amount of cement is used and (4) achieves enhanced rate of attainment of compressive strength especially at early age. So it can be concluded that optimally blended metakaolin (MK) based ternary SCC blend of ordinary grade will have both economic and environmental benefits.

In standard grade (M40), three binary blended (C60+FA40, C85+MS15, C80+MK20), two ternary blended (C50+FA40+MS10, C35+FA50+MK15) and one reference (100% OPC) SCC mixes are designed so that all the SCC mixes achieve almost similar strength.

The purpose of choosing the above stated six optimum combinations of SCMs is to establish the optimum percentage replacement levels of fly ash (FA), micro silica (MS) and metakaolin (MK) when used individually or in combination in binary and ternary blended SCC mixes of standard grade. In ternary blends of standard grade, metakaolin (MK) based ternary blended SCC mix is considered as more efficient than micro silica (MS based ternary blended SCC mix because of : (1) least expensive (2) more fly ash quantity is used (3) less amount of cement is used and (4) achieves enhanced rate of attainment of compressive strength especially at early age. Al_2O_3 content is significantly higher in metakaolin (MK). This may results higher early age strength of concrete due to high reactivity of Al_2O_3 to form calcium Aluminate hydrate (CAH). So it can be concluded that optimally blended metakaolin (MK) based ternary SCC blend of standard grade will have both economic and environmental benefits.

In high strength grade (M80), three optimally blended binary and ternary SCC mixes (C95+MS5, C65+FA20+MS15, C50+FA28+MS11+MK11) are chosen based on desired compressive strength achievement. From the studies, it is observed that without inclusion of micro silica (MS), desired high strength cannot be attained. Further investigations have showed that metakaolin (MK) based quaternary blended high strength SCC mix yield better performance than ternary and binary blends in terms of (1) usage of high quantity of fly ash , (2) enhanced fresh properties and (3) reduction in quantity of cement used.

Similar observations are made for high strength grade (M100) SCC mix, in which metakaolin (MK) based quaternary blended high strength SCC mix (C55+FA23+MS11+MK11) yield better performance than ternary (C71+FA19+MS10) and binary (C90+MS10) blended SCC mixes.

The total powder content for binary and ternary blended SCC mixes of ordinary grade (M20) and standard grade (M40) are 486 and 531 kg/m3 respectively while for binary and ternary blended SCC mixes of high strength grade (M80 and M100) the total powder content adopted is 700 kg/m3 and whereas for quaternary blended SCC mixes of M80 and M100 grades, the total powder content adopted is 910 (additionally 30% of FA is added). It can be concluded that quaternary blended SCC mixes are more efficient that ternary blended SCC mixes for high strength grade (M80 and M100).

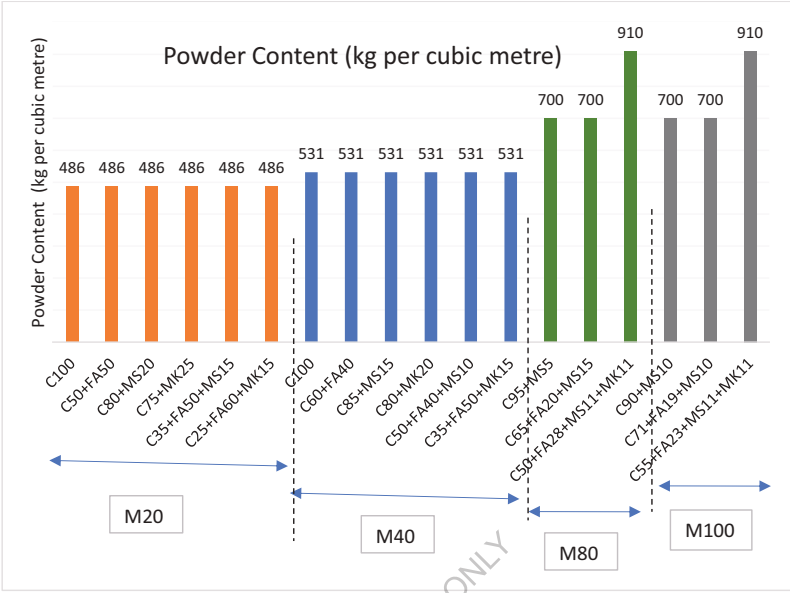

Fig 4- Total Powder content used for various grades of blended SCC mixes.

It can be observed that the water/powder ratio for ordinary grade (M20), standard grade (M40), high strength grade (M80) and very high strength grade (M100) are 0.45, 0.35, 0.25 and 0.22 respectively as shown in Fig 5.

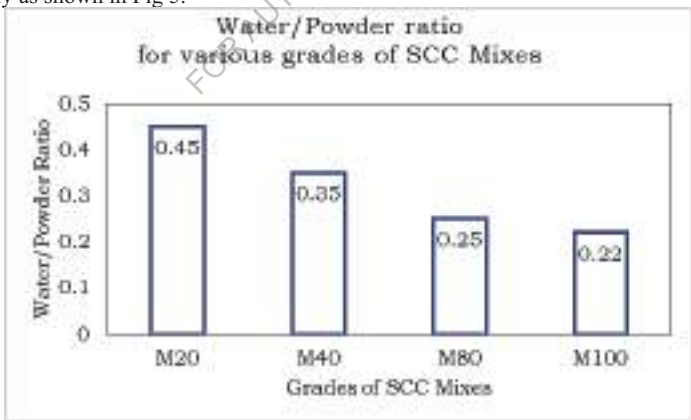

Fig 5- Water/Powder ratios adopted for various grades of SCC mixes

Based on the compressive strength attained at specified age of curing, the efficacy of pozzolans are understood. In this study, pozzolans used for blended SCC mixes are Fly Ash (FA), Microsilica (MS) and Metakaolin (MK). Age of curing specified for Fly Ash (FA) blended binary, ternary and quaternary blended SCC mixes of various grades is 90 days while it is 28 days for Microsilica (MS) and Metakaolin (MK) blended SCC mixes.

A customary method for the design of SCC is to follow the recommendations of Okamura & Ozawa (1995). Paste composition of the concrete (that is the w/b ratio) is determined using flow tests. Their design principles are derived based on numerous experiments. A survey of the literature indicates that a number of researchers used their recommendations as a starting point for their investigations. Adjustments in coarse and fine aggregate contents are then made to achieve the desired flow properties. The same approach is adopted for proportioning the materials required for producing high strength concretes. Packing factors adopted while designing various grades of blended SCC mixes are depicted in Fig 5.6.

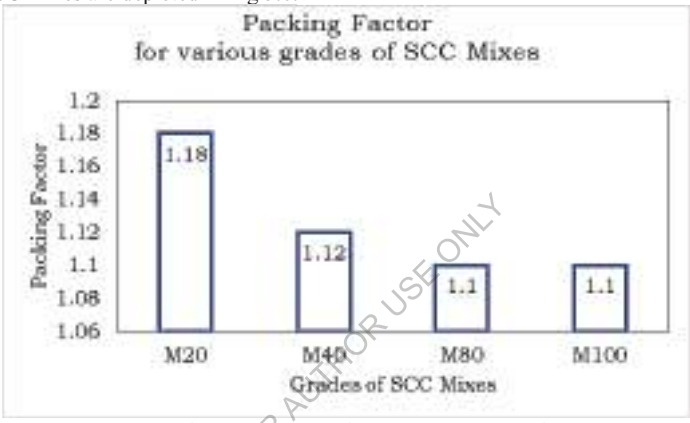

Fig 6 - Packing factors adopted for various grades of SCC mixes

Metakaolin (MK) blended SCC mixes will set relatively quickly due to its high reactivity, which also prevents bleeding and settling of aggregates. In fresh state, tensile strengths have increased rapidly in order to prevent any internal stresses caused by drying shrinkage preventing cracks in the younger concrete. Metakaolin (MK) when compared to micro silica (MS) has similar particle density and surface area but different morphology and surface chemistry. Because of its hydrophilic surface, Metakaolin (MK) is easier to disperse into wet concrete. Metakaolin (MK) can be incorporated at any stage of concrete production; it should be mixed thoroughly to achieve even distribution; intensive mixing is not necessary like micro silica (MS) based concrete. Metakaolin (MK) concrete normally requires smaller super plasticizer dose than that required for the equivalent micro silica (MS) concrete. With no super plasticizer, it may be required to increase the water/binder ratio in order to maintain workability. This is partly due to fact that Metakaolin (MK) has a lower density than cement so that replacing, say, 10 mass % cement by Metakaolin (MK) decreases the water/binder volume ratio and the slurry rheology which is determined by the liquid/solid volume ratio.

The workability of fly ash based SCC mixes increases significantly with increase in fly ash content. For fly ash contents above 10% in SCC mixes workability falls. The reduction in workability is attributed to flocculation/coagulation at low fly ash concentration and the increase in workability at high concentration is attributed to neutralization of positive charges on cement particles and their resultant dispersal. When super plasticizer is used as a dispersing agent, no fall in workability is observed. Loss of workability due to the present of Metakaolin (MK) can be compensated for by the incorporation of fly ash (FA). The degree of restoration of workability, provided by fly ash, is influenced significantly by the cement replacement level, the MK/FA ratio and the W/b ratio. The addition of metakaolin increases the viscosity of blended SCC mixtures. This inference is based on the results of T50 and V-funnel tests, which showed an increase in flow time with the increased percentage of metakaolin in blended SCC mixtures. The values of H2/H1 (L-box index) also indicates metakaolin better passing ability.

As powder content is increasing, packing factor decreases which means that density has increased along with flow. Packing factor is more for lower grades and decreases for higher grades of SCC mixes. Packing factor more than 1.2 is not possible because flow properties cannot be met as per EFNARC specifications. Packing factor less than 1.1 is not practically possible because packing factor 1.0 means both tightly packed mass and loosely packed mass of aggregate are same which is not ideally true due to presence of air content in concrete. For the present study, packing factor considered during design of M20 SCC mix is 1.18, Packing factor for M40 PF is 1.12 and for M80 and M100, Packing factor is taken as 1.10.

Fly ash addition reduces heat of hydration and slows the strength attainment at early stages. To overcome this shortcoming, metakaolin is added to fly ash based SCC mixes to offset the delayed early strength attainment. Also incorporation of metakaolin (MK) to fly ash (FA) based SCC, enables to consume more amount of fly ash. With increased amount of pozzolanic content due to inclusion of metakaolin (MK) in fly ash (FA) based SCC in turn reduces w/p ratio resulting in the increase of strength and flow properties.

Since metakaolin (MK) is cheaper than micro silica (MS), for same strength criteria, metakaolin (MK) blended fly ash (FA) based SCC is better in performance and economically viable than micro silica (MS) blended fly ash (FA) based SCC for all grades considered.

Micro silica (MS) and metakaolin (MK) in blended fly ash (FA) based SCC mixes will increase the strength of concrete largely because it increases the strength of the bond between the cement paste and the aggregate particles. Addition of metakaolin (MK) to blended SCC mixes will enhance early hydration because of it high reactivity due to its glassy nature. The rate of pozzolanic reaction and calcium hydroxide (CH) consumption in metakaolin (MK) blended SCC mixes is higher than micro silica (MS) blended SCC mixes indicating high initial reactivity of metakaolin. Usage of metakaolin not only improves the workability but also makes the concrete microstructure denser. Thus with the inclusion of metakaolin in to SCC mixes, super plasticizer dosage can be reduced noticeably so is the costs involved. So water demand is less for metakaolin blended SCC mixes than micro silica (MS) blended SCC mixes. It can be quantified that strength improvement in the metakaolin based SCC mixes is due to changes in the structure of the interfacial zone and the increased paste-aggregate bond strength. Also the dissolved Ca_{2+}, SiO_4^{4-} and OH^- ions readily in concrete combine with the metakaolin to give cementitious phases with a modified morphology. Strength loss in the early ages, which was proportional to the cement replacement level, was probably due to the dilution effect of the pozzolan and as well as the slow nature of the pozzolanic reaction.

5. STRENGTH PROPERTIES

The main objective of the present experimental investigations in this phase is to: (1) obtain specific experimental data, which helps to understand the strength characteristics of binary, ternary and quaternary blended SCC mixes of ordinary grade (M20), standard grade (M40) and high strength grade (M80 and M100) made with Fly Ash (FA), Microsilica (MS) and Metakaolin (MK) and (2) assess the quality, integrity of micro structure of optimally blended binary, ternary and quaternary blended SCC mixes of various grades considered using Rebound hammer test and Ultrasonic pulse velocity measurements. The Self-Compacting Concrete mixes, after having checked for the satisfaction of the fresh properties of self-compacting specifications as per EFNARC [2002] was cast into cube moulds of size 150 mm x 150 mm, beam moulds of size 100mm x 100mm x 500 mm and cylindrical moulds of 300 mm height x 150mm diameter.

5.0 Compressive Strength

Compressive strength of a material is defined as the value of uniaxial compressive stress reached when the material fails completely. In this investigation, the cube specimens of size 150 mm x 150 mm x 150 mm are tested in accordance with IS: 516 – 1969 [Method of test for strength of concrete]. In the present investigation, the compressive strength test has been conducted on ordinary grade (M20) , standard grade (M40) and high strength grade (M80 and M100) of binary ,ternary and quaternary blended Self Compacting Concrete (SCC) mixes made with optimum proportions of Fly Ash (FA), Microsilica (MS) and Metakaolin(MK) combination.

This investigation is carried out to study the compressive strength of binary, ternary and quaternary blended SCC mixes of ordinary grade (M20), standard grade (M40) and high strength grade (M80 and M100) made with Fly Ash (FA), Microsilica (MS) and Metakaolin (MK) at 3,7,14,28, 60 and 90 days.

Table 33– Compressive Strengths of various grades of optimally blended SCC mixes

Grade of SCC Mix	Mix No	Mix Designation (Values indicate percentage by weight of Total Powder)	Compressive Strength (MPa)					
			3 days	7 days	14 days	28 days	60 days	90 days
M20	C1	C100	10.07	16.36	20.15	25.18	25.34	27.68
	B2	C50+FA50	5.78	11.60	17.39	20.29	28.98	32.24
	B7	C80+MS20	11.61	18.87	26.13	29.03	32.13	33.24
	B13	C75+MK25	18.54	20.16	27.70	33.77	34.35	35.12
	T3	C35+FA50+MS15	9.10	16.22	20.19	22.13	29.37	32.81
	T15	C25+FA60+MK15	15.67	19.88	23.12	27.11	33.29	36.87
M40	C1	C100	20.36	33.32	39.73	48.18	50.19	53.10
	B1	C60+FA40	12.83	21.75	28.61	43.35	53.60	56.78
	B5	C85+MS15	25.77	31.89	42.01	51.99	54.23	57.96
	B10	C80+MK20	41.16	44.76	51.49	53.73	55.41	58.19
	T5	C50+FA40+MS10	20.20	26.01	34.82	44.56	52.13	59.87
	T9	C35+FA50+MK15	34.79	40.13	47.33	49.22	52.37	59.92
M80	B2	C95+MS5	35.43	57.56	78.71	88.56	91.22	93.19
	T3	C65+FA20+MS15	26.18	50.12	65.98	83.17	90.54	94.51
	Q11	C50+FA28+MS11+MK11	50.02	64.19	81.10	85.26	90.71	97.16
M100	B2	C90+MS10	42.11	65.80	92.13	106.04	107.81	109.11
	T2	C71+FA19+MS10	40.51	65.32	81.04	95.31	104.20	111.83
	Q11	C55+FA23+MS11+MK11	66.12	78.32	87.18	93.14	110.71	113.28

Table 33 presents the compressive strength at various ages of curing for binary, ternary and quaternary blended SCC mixes of ordinary grade (M20), standard grade (M40) and high strength grade (M80 and M100) made with Fly Ash (FA), Microsilica (MS) and Metakaolin (MK). It can be observed that there is no much variation in strength at the stipulated age of curing, in all SCC mixes of various grades. Fig 7, 8, 9 and 10 and shows variation of compressive strengths of various grades of optimized SCC mixes at various ages of curing

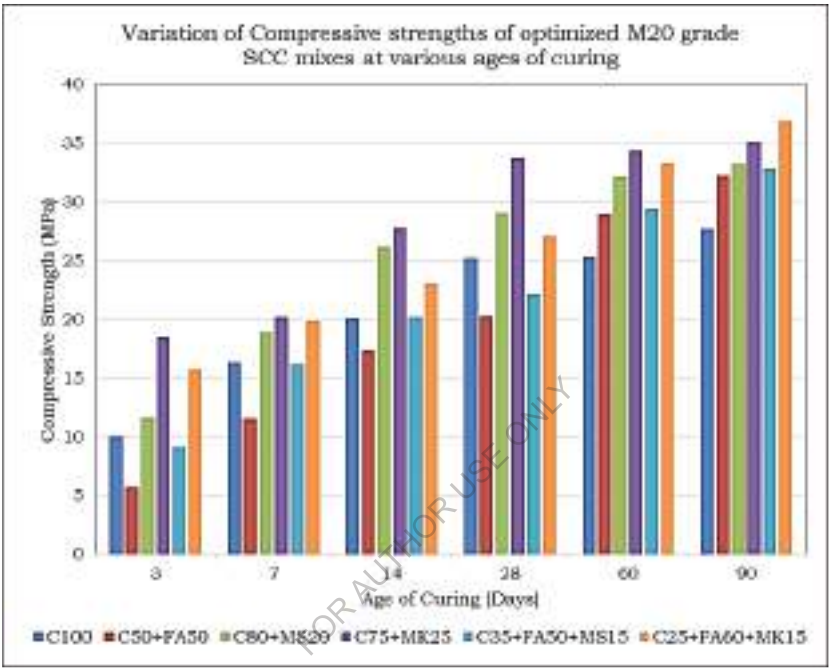

Fig 7- Variation of compressive strengths of optimized M20 grade SCC mixes at various ages of curing

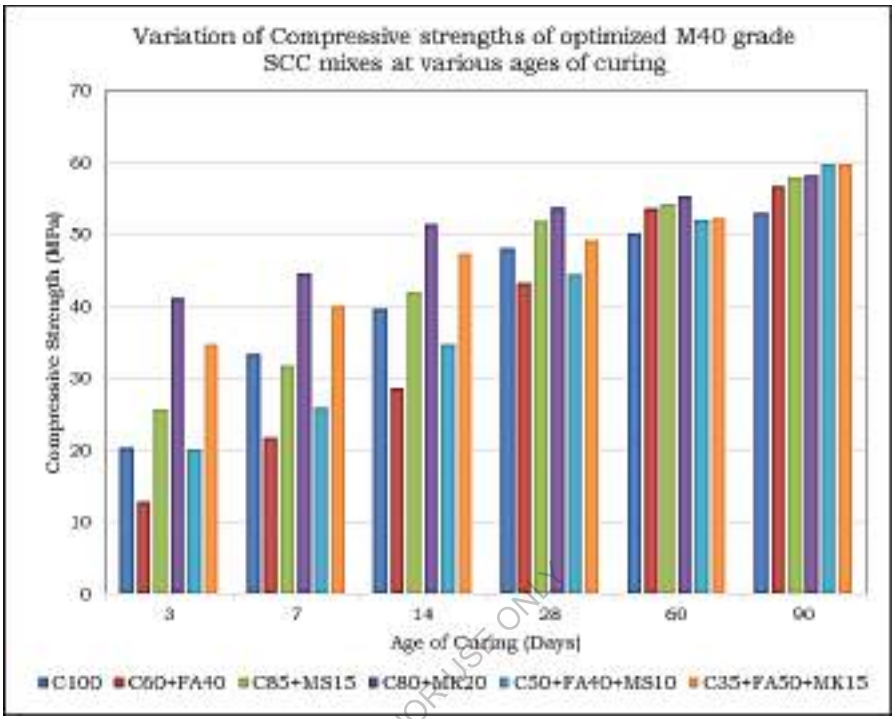

Fig 8- Variation of compressive strengths of optimized M40 grade SCC mixes at various ages of curing

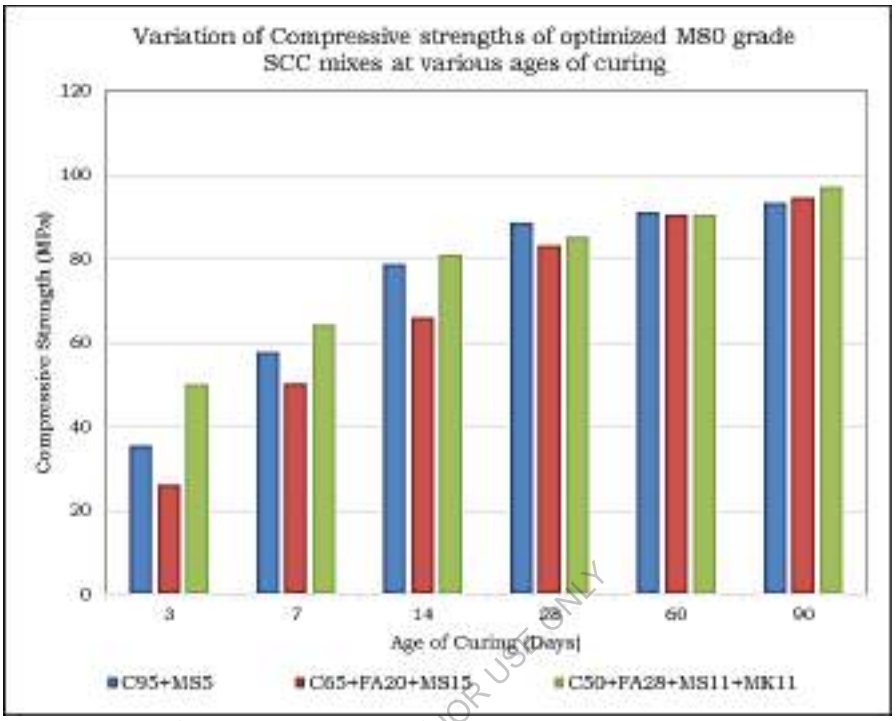

Fig 9- Variation of compressive strengths of optimized M80 grade SCC mixes at various ages of curing

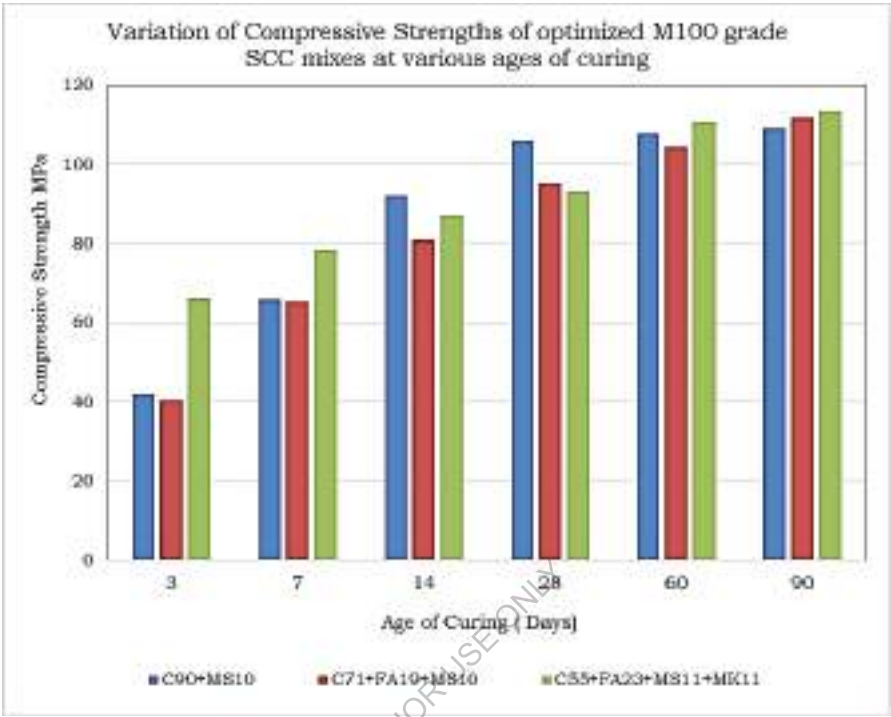

Fig 10- Variation of compressive strengths of optimized M100 grade SCC mixes at various ages of curing

In blended SCC mixes, fly ash (FA) based mixes are assumed to yield desired strength at 90 days where as for micro silica (MS) or metakaolin (MK) or combination based SCC mixes desired strengths at 28 days are considered for assessment.

Metakaolin (MK) blended SCC mixes attain much higher early strength when compared to other SCC mixes while fly ash (FA) based SCC mixes are accomplishing strengths at later age. Nowadays usage of fly ash (FA) in SCC has become almost mandatory because (1) it enhances fluidity of SCC and (2) it is major part of powder content. So Metakaolin (MK) and fly ash (FA) SCC blends derive both the benefits of fly ash (FA) and Metakaolin (MK) in concrete by attaining early and later strengths consistently. So the rate of gain of strength attainment is steady in Metakaolin (MK) and fly ash (FA) blended SCC mixes. Metakaolin (MK) based ternary blended SCC mixes exhibit better performance than Metakaolin (MK) based binary blended SCC mixes due to the synergic action of blended pozzolans. Metakaolin cementing reaction rate is very rapid, significantly increasing compressive strength before first three days, which can have various benefits in fast paced construction industry.

Metakaolin (MK) blended SCC mixes is preferable for ordinary grade (M20) and standard grade (M40) whereas micro silica (MS) is preferred for higher grade (M80 and M100) SCC mixes. Use

of micro silica (MS) in high strength grade (M80 and M100) also acts as a micro-filler in making the concrete dense. Therefore it is established that micro silica (MS) is required for the development of high strength concrete. But metakaolin (MK) being less expensive and give better flow ability than micro silica (MS) is much preferred for the development of ordinary (M20) and standard grade (M40) SCC mixes. Use of metakaolin accelerated the initial set time of concrete; however the final set time remained unchanged. This was caused mainly by the higher reactivity of the blended binder with metakaolin. Due to following drawbacks, micro silica (MS) is not advisable for normal grades (M20 and M40):

(1) Increases water demand
(2) Expensive
(3) Presence of Cl^-

The addition of micro silica (MS) or metakaolin (MK) is advantageous in SCC mixes because in general, the strength at the transition zone between cement paste and coarse aggregate particles is lower than that of the bulk cement paste. The transition zone contains more voids because of the accumulation of bleed water underneath the aggregate particles and the difficulty of packing solid particles near a surface. Relatively more calcium hydroxide (CH) forms in this region than elsewhere. Without micro silica (MS) or metakaolin (MK), the calcium hydroxide (CH) crystals grow large and tend to be strongly oriented parallel to the aggregate particle surface. CH is weaker than calcium silicate hydrate (C-S-H), and when the crystals are large and strongly oriented parallel to the aggregate surface, they are easily cleaved. A weak transition zone results from the combination of high void content and large, strongly oriented CH crystals. Micro silica (MS) and metakaolin (MK) in blended SCC mixes will increase the strength of concrete largely because it increases the strength of the bond between the cement paste and the aggregate particles. The presence of micro silica (MS) and metakaolin (MK) in fresh SCC mix generally results in reduced bleeding and greater cohesiveness.

Metakaolin (MK) may be better alternative to micro silica (MS) especially in normal grades but in higher grades of SCC, its combination with micro silica (MS) will yield better performance.

Metakaolin (MK) is highly reactive alumino silicate whereas micro silica (MS) is reactive silicate so Metakaolin (MK) supplemented SCC mixes have high strengths because silica and alumina present in Metakaolin (MK) reacts with CH forms CSH (pozzolanic reaction) and CAH (aluminate hydration) respectively which contributes to additional strength than micro silica (MS). Fe_2O_3 in more in Metakaolin (MK) leading to high enhancement of strength in the blended SCC mixes due to the rapid consuming of $Ca(OH)_2$ which was formed during hydration of Portland cement specially at early ages related to the high reactivity of Fe_2O_3 particles. As a consequence, the hydration of cement is accelerated and larger volumes of reaction products are formed. Also Fe_2O_3 particles recover the particle packing density of the blended cement, directing to a reduced volume of larger pores in the cement paste.

Micro silica (MS) beyond 15% and Metakaolin (MK) beyond 20-25% should not exceed to preserve residual free CH in the paste to maintain pH of pore solution. High dosages of Metakaolin (MK) or micro silica (MS) in SCC mixes may lead to lower C/S ratio of the CSH gel formed from pozzolanic reaction resulting in high shrinkage of the formed gel.

Metakaolin (MK) blended fresh SCC mixes will set relatively quickly due Metakaolin (MK) when compared to micro silica (MS) has similar particle density and surface area but different morphology and surface chemistry.

Cement average size is 100 times larger than micro silica (MS) while Metakaolin (MK) average size is 20 to 30 times larger than micro silica (MS) so in Metakaolin (MK) + micro silica (MS)

blended FA based quaternary SCC mix, coarser pores in fly ash (FA) based SCC can be reduced by inclusion of Metakaolin (MK) and finer pores are filled up by micro silica (MS). So quaternary blended SCC mix made with micro silica (MS) and Metakaolin (MK) has improved microstructure which is dense and impermeable. Metakaolin (MK) blended SCC mixes improves workability, finishability, reduces surface dehydration and plastic cracking. Since Metakaolin (MK) does not increase the compressive strength of cement paste directly, it is concluded that strength improvement in the concrete is due to changes in the structure of the interfacial zone and the increased paste-aggregate bond strength. For the same reasons, Metakaolin (MK) has a beneficial effect on flexural strength, although the magnitude of the effect is less than that observed for compressive strength.

The cost of metakaolin is about three times the cost of ordinary Portland cement, thus using metakaolin alone as a supplementary cementitious material (SCM) may not be cost effective. On the other hand, the slow reaction rate of fly ash can make its use impractical when rapid early strength development is required. However, use of these materials in combination has the potential to overcome the higher cost associated with metakaolin concrete and the slower strength development associated with fly ash concrete.

5.1 Split-tensile Strength

The test was carried out on a cylindrical specimen of diameter 150 mm and 300 mm long as per IS: 5816 – 1999. In the present investigation, the split tensile strength test has been conducted on ordinary grade (M20), standard grade (M40) and high strength grade (M80 and M100) of binary, ternary and quaternary blended Self-Compacting Concrete (SCC) mixes made with optimum proportions of Fly Ash (FA), Microsilica (MS) and Metakaolin(MK) combination.

This investigation is carried out to study the split-tensile strength of binary, ternary and quaternary blended SCC mixes of ordinary grade (M20), standard grade (M40) and high strength grade (M80 and M100) made with Fly Ash (FA), Microsilica (MS) and Metakaolin (MK) at 3,7,14,28, 60 and 90 days.

The results of the split-tensile strengths are tabulated in Table 34. Splitting tensile strengths of Metakaolin (MK) blended SCC mixes showed relatively the same trend with compressive strengths. With the addition of metakaolin, the ITZ becomes denser, pore structure in blended SCC mix is optimized and pore size distribution is more reasonable. Metakaolin (MK) replaces CH in the interfacial zone by new cementitious phases and this improves the adhesive strength (bonding) between paste and aggregate. In blended SCC mixes, this can significantly improve the both compressive and tensile strengths. Increase of tensile strength is higher than compressive strength in Metakaolin (MK) blended SCC mixes. Metakaolin (MK) has no beneficial effect on compressive strength of cement paste. However, Metakaolin (MK) replaces CH in the interfacial zone by new cementitious phases and this improves the adhesive strength (bonding) between paste and aggregate. In concrete, this can significantly improve the compressive and tensile strengths.

Fig 11 shows variation of split tensile strengths of optimized SCC mixes at various grades.

Table 34 – Split-tensile strengths of various grades of optimally blended SCC mixes

Grade of SCC Mix	Mix No	Mix Designation (Values indicate percentage by weight of Total Powder)	Split-Tensile Strength (MPa)					
			3 days	7 days	14 days	28 days	60 days	90 days
M20	C1	C100	1.01	1.64	2.02	2.52	2.53	2.77
	B2	C50+FA50	0.58	1.16	1.74	2.03	2.90	3.22
	B7	C80+MS20	1.16	1.89	2.61	2.90	3.21	3.32
	B13	C75+MK25	1.85	2.02	2.77	3.08	3.44	3.51
	T3	C35+FA50+MS15	0.91	1.62	2.02	2.21	2.94	3.28
	T15	C25+FA60+MK15	1.57	1.99	2.31	2.71	3.33	3.69
M40	C1	C100	2.04	3.33	3.97	4.82	5.02	5.31
	B1	C60+FA40	1.28	2.18	2.86	4.34	5.36	5.68
	B5	C85+MS15	2.58	3.19	4.20	5.20	5.42	5.80
	B10	C80+MK20	4.12	4.48	5.15	5.37	5.54	5.82
	T5	C50+FA40+MS10	2.02	2.60	3.48	4.46	5.21	5.99
	T9	C35+FA50+MK15	3.48	4.01	4.73	4.92	5.24	5.99
M80	B2	C95+MS5	3.54	5.76	7.87	8.86	9.12	9.32
	T3	C65+FA20+MS15	2.62	5.01	6.60	8.32	9.05	9.45
	Q11	C50+FA28+MS11+MK11	5.00	6.42	8.11	8.53	9.07	9.72
M100	B2	C90+MS10	4.21	6.58	9.21	10.60	10.78	10.91
	T2	C71+FA19+MS10	4.05	6.53	8.10	9.53	10.42	11.18
	Q11	C55+FA23+MS11+MK11	6.61	7.83	8.72	9.31	11.07	11.33

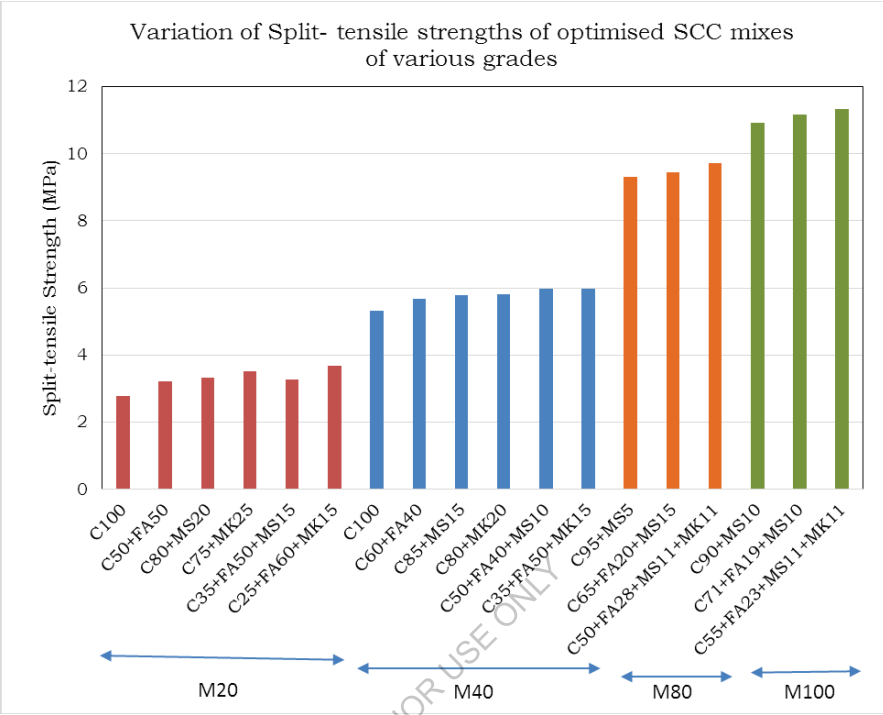

Fig 11- Variation of split tensile strengths of optimized SCC mixes at various grades

5.2 Flexural Strength

Standard beam test (Modulus of rupture) was carried out on the beams of size 100 mm x 100 mm x 500 mm as per IS: 516 [Method of test for strength of concrete]. In the present investigation, the flexural strength test has been conducted on ordinary grade (M20) , standard grade (M40) and high strength grade (M80 and M100) of binary, ternary and quaternary blended Self Compacting Concrete (SCC) mixes made with Fly Ash (FA), Microsilica (MS) and Metakaolin(MK).

This investigation is carried out to study the flexural strength of binary, ternary and quaternary blended SCC mixes of ordinary grade (M20), standard grade (M40) and high strength grade (M80 and M100) made with Fly Ash (FA), Microsilica (MS) and Metakaolin (MK) at 3,7,14,28, 60 and 90 days. The results of the flexural strengths are tabulated in Table 35.

Pozzolans improves pore structure giving better bonding at transition zone. So, the increase in flexural strength is due to increase of the bond strength at the interfacial zone. Fig 12 shows variation of flexural strengths of optimized SCC mixes at various grades. It was observed that metakaolin blended SCC mixes show improved flexural resistance due to dense pore structure and improved ductile behaviour.

Table 35 – Flexural Strengths of various grades of optimally blended SCC mixes

Grade of SCC Mix	Mix No	Mix Designation (Values indicate percentage by weight of Total Powder)	Flexural Strength (MPa)					
			3 days	7 days	14 days	28 days	60 days	90 days
M20	C1	C100	1.31	2.13	2.63	3.28	3.29	3.60
	B2	C50+FA50	0.75	1.51	2.26	2.64	3.77	4.19
	B7	C80+MS20	1.51	2.46	3.39	3.77	4.17	4.32
	B13	C75+MK25	2.41	2.63	3.60	4.00	4.47	4.56
	T3	C35+FA50+MS15	1.18	2.11	2.63	2.87	3.82	4.26
	T15	C25+FA60+MK15	2.04	2.59	3.00	3.52	4.33	4.80
M40	C1	C100	2.65	4.33	5.16	6.27	6.53	6.90
	B1	C60+FA40	1.66	2.83	3.72	5.64	6.97	7.38
	B5	C85+MS15	3.35	4.15	5.46	6.76	7.05	7.54
	B10	C80+MK20	5.36	5.82	6.70	6.98	7.20	7.57
	T5	C50+FA40+MS10	2.63	3.38	4.52	5.80	6.77	7.79
	T9	C35+FA50+MK15	4.52	5.21	6.15	6.40	6.81	7.79
M80	B2	C95+MS5	4.60	7.49	10.23	11.52	11.86	12.12
	T3	C65+FA20+MS15	3.41	6.51	8.58	10.82	11.77	12.29
	Q11	C50+FA28+MS11+MK11	6.50	8.35	10.54	11.09	11.79	12.64
M100	B2	C90+MS10	5.47	8.55	11.97	13.78	14.01	14.18
	T2	C71+FA19+MS10	5.27	8.49	10.53	12.39	13.55	14.53
	Q11	C55+FA23+MS11+MK11	8.59	10.18	11.34	12.10	14.39	14.73

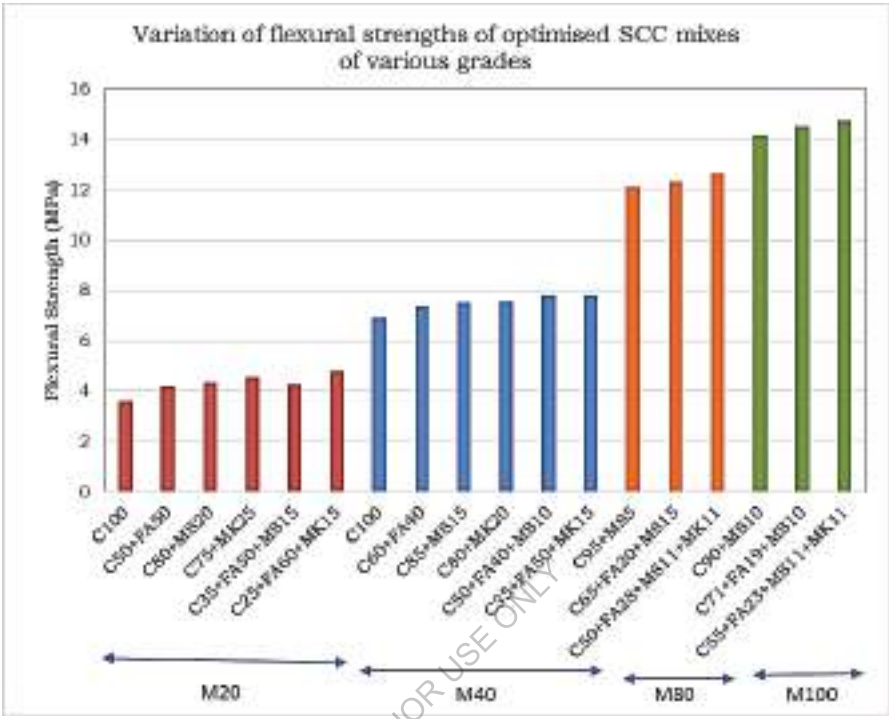

Fig 12- Variation of flexural strengths of optimized SCC mixes at various grades

5.3 Impact Strength

In the present investigation, Impact strength test has been conducted on the beams of size 100 mm x 100 mm x 500 mm of ordinary grade (M20), standard grade (M40) and high strength grade (M80 and M100) of binary, ternary and quaternary blended self-compacting concrete (SCC) mixes made with optimum proportions of Fly Ash (FA), Microsilica (MS) and Metakaolin(MK) combination. The load is applied as an impact blow from a swinging weighted pendulum hammer that is released from a raised position of 20° with the vertical. The specimen is firmly positioned at the base as shown in Fig 13. The blows were repeated in above manner till first crack appears. The crack propagation for each blow after first crack was marked on the specimen. The number of blows required for the crack propagation from one edge to other on the tension face was recorded. The experiment was continued till the spalling of mortar occurs on the compression face of the specimen. The impact strength is expressed in terms of number of blows required to break the specimen. Energy consumed for first crack, Energy consumed for ultimate failure and ductility index are evaluated for each SCC mix.

Fig. 13 - Impact test setup

This investigation is carried out to study the impact strength of binary, ternary and quaternary blended SCC mixes of ordinary grade (M20), standard grade (M40) and high strength grade (M80 and M100) made with Fly Ash (FA), Microsilica (MS) and Metakaolin (MK) at 3,7,14,28, 60 and 90 days. Impact strength is evaluated in terms of (1) number of blows taken for first crack and for ultimate failure, (2) energy consumed in joules for first crack and for ultimate failure and (3) in terms of ductility index. The results of the impact strength are tabulated in Table 36.

Calculation of Energy for a blow

The load is applied as an impact blow from a swinging weighted pendulum hammer that is released from a raised position of 20° with the vertical. The blows were repeated in above manner till first crack appears. The crack propagation for each blow after first crack was marked on the specimen. The number of blows required for the crack propagation from one edge to other on the tension face was recorded. The experiment was continued till the spalling of mortar occurs on the compression face of the specimen. The impact strength is expressed in terms of number of blows required to break the specimen.

Mass of the pendulum hammer =10 kg; g=9.8 m/sec2

L=length of pendulum= 1.83 m; h=L(1-cosΘ) where Θ=20°

Energy for one blow, E = mgh = 10*9.8*0.11= 10.78 Joule

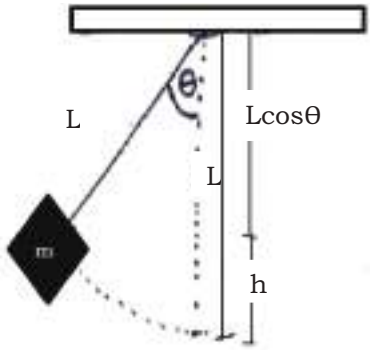

So it can be observed that there is a significant improvement in number of blows for first crack and ultimate failure for quaternary blended SCC mixes made with metakaolin for all grades considered because in the quaternary blended SCC mixes the resilience and strain relieving capacity of SCC has increased than ternary and binary blended SSCC mixes made with metakaolin. This resilient character provides the excellent impact resistance and dissipates dynamic loading. The increase in number of blows up to failure for metakaolin based quaternary blended SCC indicates its high energy absorption capacity which in turn enhances the increased impact resistance.

From the above experimental investigation it can be concluded that there is an increase in impact resistance in metakaolin (MK) blended SCC mixes for all grades at all ages considered. The impact strength increase is due to increase in resilience and strain relieving capacity of metakaolin (MK) blended SCC which imparts excellent impact resistance and energy dissipation capacity. This feature is attributed to the dense pore structure of metakaolin (MK) blended SCC.

Fig 14 shows number of blows required for first crack and ultimate failure crack of optimized blended SCC mixes of various grades.

Fig 15 shows ductility Indices for optimized blended SCC mixes of various grades.

Table 36 – Impact Strengths of various grades of optimally blended SCC mixes

Grade of SCC Mix	Mix No	Mix Designation (Values indicate percentage by weight of Total Powder)	Impact strength Evaluation				
			No. of Blows for First Crack	No. of Blows for Ultimate Failure	Energy Consumed for First Crack (Joule) E1	Energy Consumed for Ultimate Failure (Joule) E2	Ductility Index E2/E1
M20	C1	C100	9	11	97.02	118.58	1.22
	B2	C50+FA50	11	13	118.58	140.14	1.18
	B7	C80+MS20	14	16	150.92	172.48	1.14
	B13	C75+MK25	13	15	140.14	161.7	1.15
	T3	C35+FA50+MS15	15	18	161.7	194.04	1.20
	T15	C25+FA60+MK15	16	20	172.48	215.6	1.25
M40	C1	C100	13	15	140.14	161.7	1.15
	B1	C60+FA40	16	19	172.48	204.82	1.19
	B5	C85+MS15	18	22	194.04	237.16	1.22
	B10	C80+MK20	17	22	183.26	237.16	1.29
	T5	C50+FA40+MS10	19	24	204.82	258.72	1.26
	T9	C35+FA50+MK15	20	26	215.6	280.28	1.30
M80	B2	C95+MS5	29	33	312.62	355.74	1.14
	T3	C65+FA20+MS15	35	42	377.3	452.76	1.20
	Q11	C50+FA28+MS11+MK11	40	48	431.2	517.44	1.20
M100	B2	C90+MS10	29	35	312.62	377.3	1.21
	T2	C71+FA19+MS10	35	44	377.3	474.32	1.26
	Q11	C55+FA23+MS11+MK11	42	51	452.76	549.78	1.21

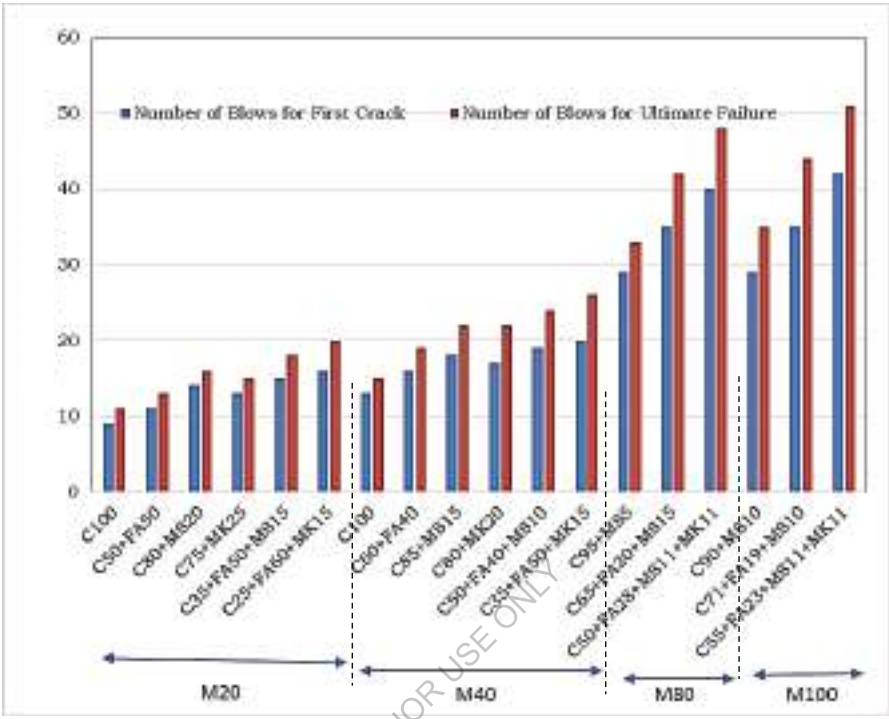

Fig 14- Variation of number of blows required for first crack and ultimate failure crack of optimized SCC mixes of various grades

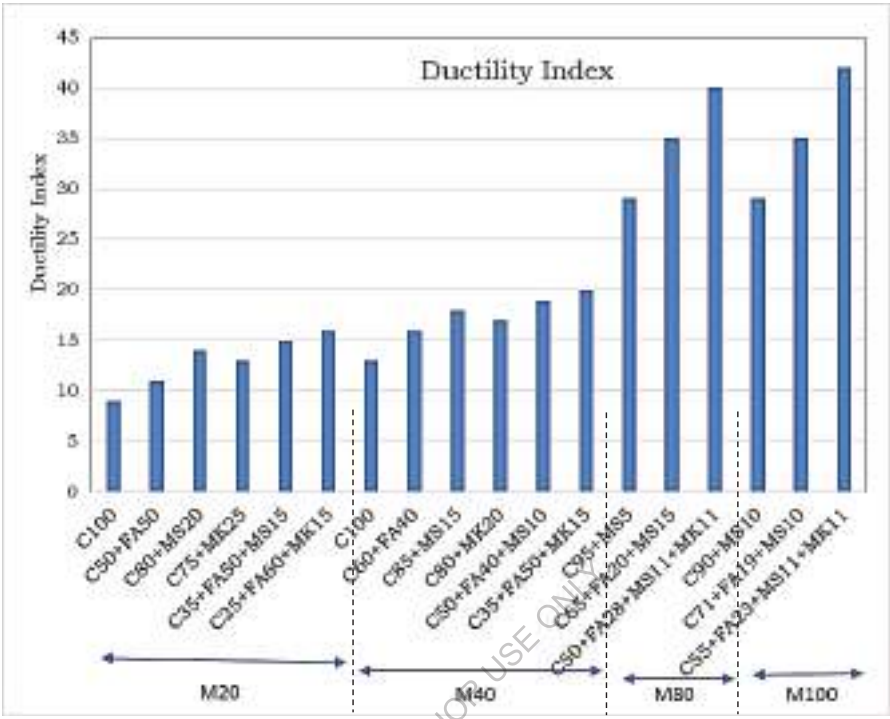

Fig 15- Ductility Indices for optimized SCC mixes of various grades

6. NON-DESTRUCTIVE EVALUATION

The main objective of the present experimental investigations is to assess the quality, structural integrity and compressive strength using Rebound hammer test and Ultrasonic pulse velocity measurements for ordinary grade (M20), standard grade (M40) and high strength grade (M80 and M100) of binary, ternary and quaternary blended Self-Compacting Concrete (SCC) mixes made with optimum proportions of Fly Ash (FA), Microsilica (MS) and Metakaolin (MK) combination. The Rebound Hammer Test is conducted as per IS: 13311 (Part 2) – 1992 on various grades of SCC cubes of size 150x150x150mm. This test mainly evaluates the quality of surface hardness based on the rebound numbers obtained. Ultrasonic Pulse Velocity Test is conducted as per IS: 13311 (Part 1) – 1992 on various grades of SCC cubes of size 150x150x150mm. This test qualitatively assesses the density, homogeneity, integrity and elastic properties of concrete. To make a more realistic assessment of the quality and integrity of concrete, a prudent approach is suggested by combining the results of ultrasonic pulse velocity and rebound hammer tests.

Table 37- Quality of concrete based on Average Rebound Hammer as per IS: 13311 (Part 2) – 1992

Average rebound number	Quality of concrete
> 40	Very good hard layer
30 to 40	Good layer
20 to 30	Fair
< 20	Poor

Table 38- Concrete Quality based on USPV as per IS: 13311 (Part 1) – 1992

Pulse velocity	Concrete quality
>4.5 km/s	Excellent
3.5 – 4.5 km/s	Good
3.0 – 3.5 km/s	Medium
<3.0 km/s	Doubtful

The Rebound Hammer Test is conducted as per IS: 13311 (Part 2) – 1992 to evaluate the quality of surface hardness based on the rebound numbers obtained. Ultrasonic Pulse Velocity Test is conducted as per IS: 13311 (Part 1) – 1992 to qualitatively assesses the homogeneity and integrity of concrete. This test also determined the elastic properties of the concrete. To make a more realistic assessment of the quality and integrity of concrete, a prudent approach of combined use of Non–destructive tests i.e. ultrasonic pulse velocity and rebound hammer tests were used.
Mean rebound values and mean ultrasonic pulse velocities (USPV) are measured to understand the quality, integrity and strength of metakaolin (MK) blended binary, ternary and quaternary SCC

mixes. The Table 39 lists the mean rebound values, mean pulse velocity values of various grades of optimally blended SCC mixes, along with their estimated compressive strengths.

It is observed the ultrasonic pulse velocity and rebound number values increased due to refined pore structure and microstructure of binary, ternary and quaternary blended SCC mixes. Since the rebound index is indicative of hardness of concrete up to a limited depth from the surface hence the internal cracks, flaws etc. or heterogeneity across the cross section will not be indicated by rebound numbers. So the ultrasonic pulse velocity measurements are obtained so that concrete density and modulus of elasticity can be understood. In order to assess particle continuity inside the concrete specimen, USPV test is performed on various grades of blended SCC mixes. Therefore combined Rebound hammer and Ultrasonic Pulse Velocity measurement were used to assess the quality and strength of the blended SCC mixes.

It can be concluded that for all optimally blended metakaolin (MK) based SCC mixes rebound numbers indicate the superior surface hardness and also the USPV measurements were greater than 4.5km/sec which denotes that metakaolin (MK) based blended SCC mixes are classified as excellent concretes in terms of strength and durability point of view due to improved pore structure of concrete.

Fig 16 and Fig 17 shows Rebound numbers and USPV values for optimized blended SCC mixes of various grades.

Table 39 - Combined Rebound hammer and Ultrasonic pulse velocity values of various grades of optimally blended SCC mixes

Grade of SCC Mix	Mix No	Mix Designation (Values indicate percentage by weight of Total Powder)	Mean Rebound Number	Mean Pulse Velocity km/sec	Compressive Strength (f_{ck}) N/mm^2	Quality of Concrete
M20	C1	C100	30	3.21	25.18	Medium
	B2	C50+FA50	33	3.45	32.24	Medium
	B7	C80+MS20	36	4.07	29.03	Good
	B13	C75+MK25	36	4.12	30.77	Good
	T3	C35+FA50+MS15	38	4.14	32.81	Good
	T15	C25+FA60+MK15	41	4.27	36.87	Good
M40	C1	C100	45	4.34	48.18	Good
	B1	C60+FA40	48	4.46	56.78	Good
	B5	C85+MS15	49	4.51	51.99	Excellent
	B10	C80+MK20	51	4.55	53.73	Excellent
	T5	C50+FA40+MS10	55	4.69	59.87	Excellent
	T9	C35+FA50+MK15	57	4.92	59.92	Excellent
M80	B2	C95+MS5	64	5.12	88.56	Excellent
	T3	C65+FA20+MS15	67	5.57	94.51	Excellent
	Q11	C50+FA28+MS11+MK11	69	5.89	97.16	Excellent
M100	B2	C90+MS10	66	6.11	106.04	Excellent
	T2	C71+FA19+MS10	69	6.19	111.83	Excellent
	Q11	C55+FA23+MS11+MK11	71	6.30	113.28	Excellent

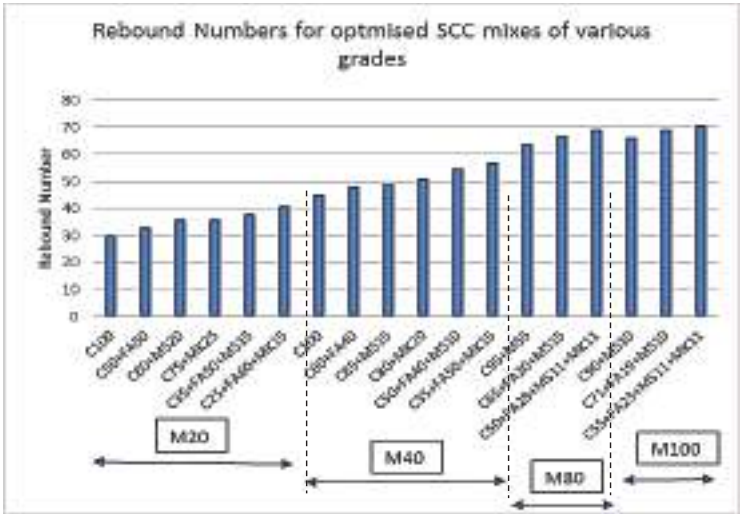

Fig 16- Rebound numbers for optimized SCC mixes of various grades

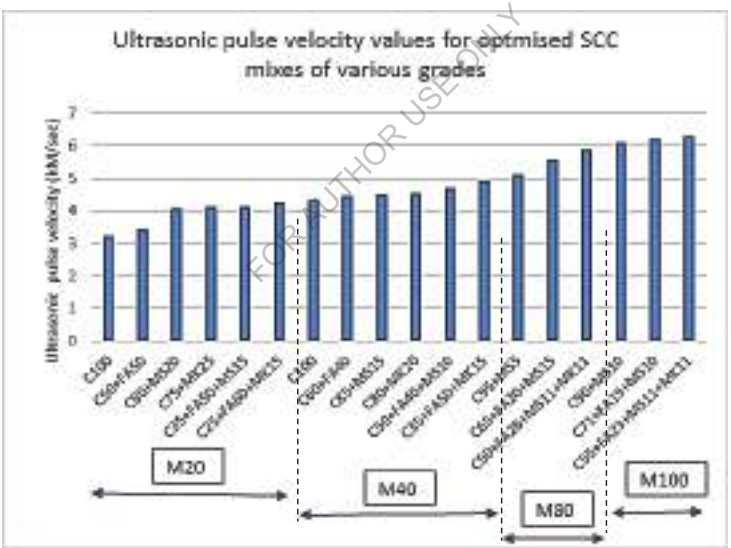

Fig 17- USPV values for optimized SCC mixes of various grades

7. STRESS-STRAIN BEHAVIOR

The aim of this study is to determine the stress-strain behavior of ordinary grade (M20) , standard grade (M40) and high strength grade (M80 and M100) of binary, ternary and quaternary blended Self-Compacting Concrete (SCC) mixes made with optimum proportions of Fly Ash (FA), Microsilica (MS) and Metakaolin (MK) combination. Cylinders of standard size 150 x 300 mm are cast for various grades of SCC mixes and tested in uni-axial compression under strain control as per IS: 516-1999 to understand the stress-strain behavior. The test setup for stress-strain measurements is shown in Fig 18.

Fig 18- Test setup for stress-strain measurements

Peak stress values and their corresponding strains of optimally blended binary, ternary and quaternary blended SCC mixes of ordinary grade (M20), standard grade (M40) and high strength grade (M80 and M100) are presented in Table 40 -43.

Metakaolin (MK) blended SCC mixes has shown improved stress values for the same strain levels compared to that of other non- metakaolin (MK) blended SCC mixes.

7.0 Modulus of Elasticity

The relationship between stress and strain is important in understanding the basic elastic behavior of blended SCC mixes in hardened state. From the plotted Stress-Strain curves, modulus of elasticity and modulus of toughness for optimally blended binary, ternary and quaternary blended SCC mixes of ordinary grade (M20), standard grade (M40) and high strength grade (M80 and

M100) can be calculated. Modulus of elasticity will indicate the elastic behaviour of the material whereas toughness gives the ability of a material to counteract crack propagation by dissipating deformation energy. Modulus of elasticity can be evaluated from the slope of the stress-strain curve whereas toughness (amount of energy absorbed by the specimen under loading) can be determined by measuring the area (i.e., by taking the integral) underneath the stress-strain curve. Modulus of toughness is the energy needed to completely fracture the material (the total area up to fracture).
Secant Modulus of Elasticity values of optimally blended binary, ternary and quaternary blended SCC mixes of ordinary grade (M20), standard grade (M40) and high strength grade (M80 and M100) are shown in Table 44 and Fig 23. The average value of area under stress-strain diagram for different grades of optimally blended SCC mixes are computed to evaluate energy absorption capacity. Toughness or energy absorption capacity of different grades of optimally blended SCC mixes has shown an increase of 10-20%. Materials showing good impact resistance are generally those with high moduli of toughness. It was observed that Modulus of Elasticity (E) is relatively more for all grades of optimally blended MK based SCC mixes by about 12-20%.
It can be concluded that toughness or energy absorption capacity of optimally blended SCC mixes of various grades are more due to its enhanced ability to counteract crack propagation by dissipating deformation energy. High toughness in optimally blended SCC mixes signify its improved shock resistance. It is observed that modulus of elasticity (E) is relatively more for all grades of optimally blended SCC mixes in which metakaolin (MK) is induced indicating its enhanced performance due to dense microstructure of optimally blended metakaolin (MK) based SCC mixes.

Table 40 - Stress - Strain values of ordinary grade M20 blended SCC mixes

M20 blended SCC mixes made with River Sand as fine aggregate											
C1		B2		B7		B13		T3		T15	
Strain	Stress (MPa)	Strain	Stress (MPa)	Strain	Stress (MPa)	Strain	Stress (MPa)	Strain	Stress (MPa)	Strain	Stress (MPa)
0	0.00	0	0.00	0	0.00	0	0.00	0	0.00	0	0.00
0.0002	3.20	0.0002	3.39	0.0003	3.60	0.0003	3.74	0.0003	3.85	0.0001	2.83
0.0004	5.66	0.0004	6.00	0.0004	6.36	0.0004	6.62	0.0004	6.81	0.0002	5.66
0.0005	8.49	0.0005	9.00	0.0006	9.54	0.0006	9.92	0.0006	10.22	0.0003	8.49
0.0007	15.32	0.0007	12.00	0.0008	17.72	0.0008	16.23	0.0007	16.63	0.0004	11.32
0.0008	16.15	0.0009	19.00	0.0009	17.90	0.001	16.54	0.008	17.04	0.0005	14.15
0.001	16.99	0.0011	20.00	0.0012	19.08	0.0012	19.85	0.0012	20.44	0.0006	16.99
0.0012	19.82	0.0013	21.00	0.0014	22.27	0.0014	23.16	0.0015	23.85	0.0008	19.82
0.0015	22.65	0.0016	24.01	0.0017	25.45	0.0018	26.46	0.0018	27.26	0.001	22.65
0.002	25.18	0.0021	32.24	0.0022	29.03	0.0022	33.77	0.0022	32.81	0.0013	25.48
0.0023	22.65	0.0024	24.01	0.0026	25.45	0.0027	26.46	0.0027	27.26	0.0021	36.87
0.0026	18.70	0.0027	19.82	0.0029	21.01	0.0029	21.85	0.0029	22.51	0.0027	25.10
0.0035	14.90	0.0033	15.79	0.0032	16.74	0.0031	17.41	0.003	17.93	0.003	18.00

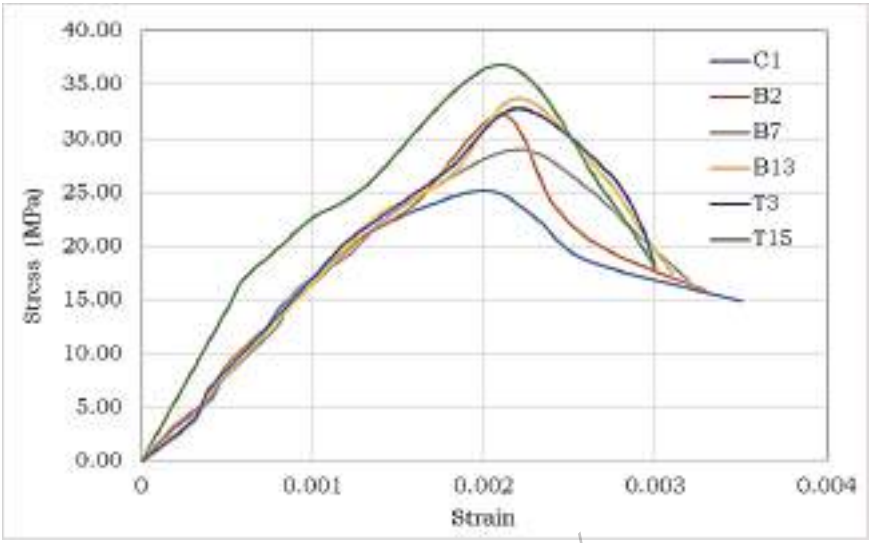

Fig 19 - Stress - Strain curve for ordinary grade M20 blended SCC mixes

Table 41 - Stress - Strain values of standard grade M40 blended SCC mixes

M40 blended SCC mixes made with river sand as fine aggregate											
C1		B1		B5		B10		T5		T9	
Strain	Stress (MPa)	Strain	Stress (MPa)	Strain	Stress (MPa)	Strain	Stress (MPa)	Strain	Stress (MPa)	Strain	Stress (MPa)
0.0000	0.00	0.0000	0.00	0.0000	0.00	0.0000	0.00	0.0000	0.00	0.0000	0.00
0.0001	2.83	0.0001	2.83	0.0001	2.83	0.0001	2.83	0.0001	2.83	0.0001	2.83
0.0002	5.66	0.0002	6.00	0.0001	5.66	0.0001	5.66	0.0001	5.66	0.0001	5.66
0.0003	8.49	0.0002	9.00	0.0002	8.49	0.0002	8.49	0.0002	8.49	0.0001	8.49
0.0004	11.32	0.0003	11.32	0.0003	11.32	0.0003	11.32	0.0003	11.32	0.0002	11.32
0.0005	14.15	0.0004	14.15	0.0004	14.15	0.0003	14.15	0.0003	14.15	0.0002	14.15
0.0006	16.99	0.0005	17.60	0.0005	16.99	0.0004	16.99	0.0004	16.99	0.0003	16.99
0.0007	**21.82**	**0.0006**	**19.82**	0.0006	19.82	**0.0005**	**17.82**	**0.0005**	**18.82**	0.0003	19.82
0.0008	22.65	0.0006	22.65	**0.0007**	**22.65**	0.0005	22.65	0.0005	23.20	0.0004	20.05
0.0009	25.48	0.0007	25.48	0.0008	25.48	0.0006	25.48	0.0006	25.70	**0.0005**	**20.48**
0.001	28.31	0.0008	28.31	0.0009	28.31	0.0007	28.31	0.0007	28.60	0.0006	28.31
0.0012	31.14	0.0009	31.14	0.0010	31.14	0.0008	31.14	0.0008	31.14	0.0006	31.14
0.0013	33.97	0.0010	34.40	0.0011	33.97	0.0009	33.97	0.0010	33.97	0.0008	33.97
0.0014	36.80	0.0011	36.80	0.0012	36.80	0.0010	36.80	0.0011	36.80	0.0009	36.80
0.0016	39.63	0.0012	39.63	0.0014	39.63	0.0011	39.63	0.0013	39.63	0.0011	39.63
0.0021	48.18	0.0016	42.46	0.0015	42.46	0.0012	42.46	0.0015	42.46	0.0012	42.46
0.0024	41.30	0.0022	56.78	0.0018	45.29	0.0014	45.29	0.0017	45.29	0.0014	45.29
0.0027	36.80	0.0027	42.46	0.0021	51.99	0.0015	48.12	0.0021	59.87	0.0016	48.12
0.0031	30.30	0.0030	39.63	0.0025	45.29	0.0018	50.96	0.0026	45.29	0.0022	59.92
		0.0032	36.80	0.0027	42.46	0.0020	53.70	0.0028	42.46	0.0027	48.12
				0.0031	39.63	0.0023	53.73	0.0031	36.70	0.0029	45.29
						0.0028	44.00			0.0031	42.46
						0.0030	30.96			0.0033	38.50
						0.0032	28.12				

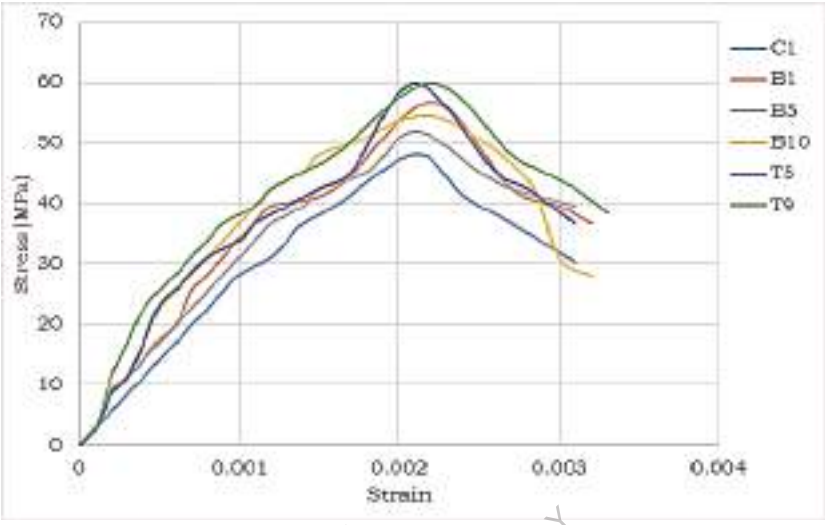

Fig 20 - Stress - Strain curve for standard grade M40 blended SCC mixes

Table 42 - Stress - Strain values of high strength M80 and M100 blended SCC mixes

M80 blended SCC mixes made with river sand						M100 blended SCC mixes made with river sand					
B2		T3		Q11		B2		T2		Q11	
Strain	Stress (MPa)	Strain	Stress (MPa)	Strain	Stress (MPa)	Strain	Stress (MPa)	Strain	Stress (MPa)	Strain	Stress (MPa)
0	0	0	0	0	0	0	0	0	0	0	0
0.0001	2.54	0.0001	3.17	0.0001	6.11	0.0001	2.54	0.0001	3.17	0.0001	4.53
0.0003	6.13	0.0003	10.91	0.0002	11.50	0.0002	11.20	0.0003	10.91	0.0002	11.32
0.0005	14.69	0.0005	20.74	0.0003	19.11	0.0003	17.69	0.0005	20.74	0.0003	17.36
0.0006	18.91	0.0006	26.46	0.0004	23.33	0.0004	21.63	0.0006	26.46	0.0004	21.64
0.0007	25.44	0.0007	32.70	0.0005	29.54	0.0005	25.44	0.0007	32.70	0.0005	30.13
0.0008	32.59	**0.0008**	**37.40**	**0.0006**	**30.11**	0.0006	32.59	0.0008	38.40	0.0006	31.78
0.0009	**40.33**	0.0009	46.45	0.0007	40.99	**0.0008**	**41.25**	**0.0009**	**46.45**	**0.0007**	**39.54**
0.001	48.99	0.001	53.73	0.0009	53.28	0.001	48.99	0.001	53.73	0.0009	56.34
0.0011	60.09	0.0011	61.04	0.001	61.01	0.0011	57.09	0.0011	61.04	0.001	63.75
0.0012	67.32	0.0012	68.19	0.0011	68.00	0.0012	64.32	0.0012	68.19	0.0011	74.20
0.0016	85.40	0.0016	90.92	0.0014	87.10	0.0016	85.40	0.0016	90.92	0.0014	88.00
0.0022	88.56	0.0022	94.51	0.0018	95.50	0.0022	106	0.0022	111.8	0.0018	102.20
0.0028	70.30	0.0028	69.04	0.0020	96.70	0.0025	70.3	0.0025	89.04	0.0020	111.80
				0.0021	97.16					0.0022	113.80
				0.0023	95.11					0.0025	101.23
				0.0024	89.14						

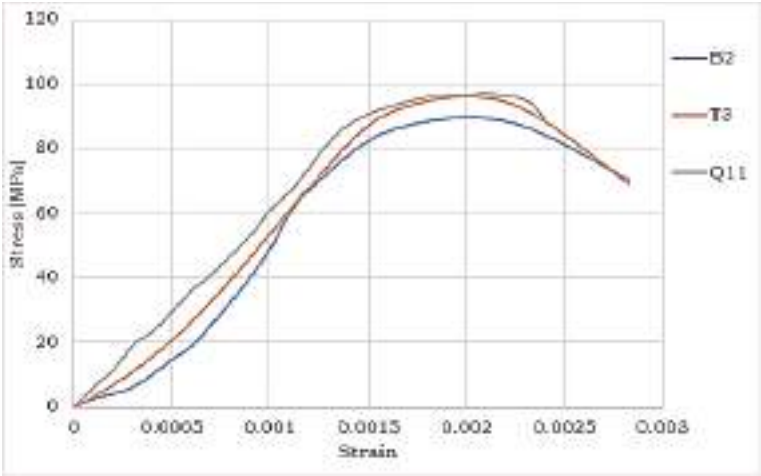

Fig 21 - Stress - Strain curve for high grade M80 blended SCC mixes

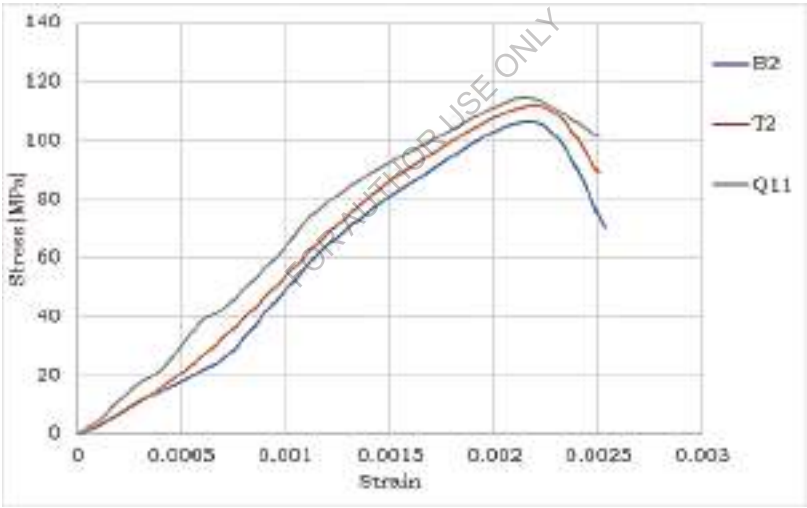

Fig 22- Stress - Strain curve for high grade M100 blended SCC mixes

Table 43: Peak stress values and their corresponding strains of blended SCC mixes made with river sand

Grade of SCC Mix	Mix No	Mix Designation (Values indicate percentage by weight of Total Powder)	Peak Stress f_o (MPa)	Corresponding strain at peak stress $\in_o$
M20	C1	C100	25.18	0.0020
	B2	C50+FA50	32.24	0.0021
	B7	C80+MS20	29.03	0.0022
	B13	C75+MK25	33.77	0.0022
	T3	C35+FA50+MS15	32.81	0.0022
	T15	C25+FA60+MK15	36.87	0.0021
M40	C1	C100	48.18	0.0021
	B1	C60+FA40	56.78	0.0022
	B5	C85+MS15	51.99	0.0021
	B10	C80+MK20	53.73	0.0023
	T5	C50+FA40+MS10	59.87	0.0021
	T9	C35+FA50+MK15	59.92	0.0022
M80	B2	C95+MS5	88.56	0.0022
	T3	C65+FA20+MS15	94.51	0.0022
	Q11	C50+FA28+MS11+MK11	97.16	0.0021
M100	B2	C90+MS10	106.00	0.0022
	T2	C71+FA19+MS10	111.80	0.0022
	Q11	C55+FA23+MS11+MK11	113.80	0.0022

Table 44: Modulus of Elasticity 'E_c' blended SCC mixes made with river sand

Grade of SCC Mix	Mix No	Mix Designation (Values indicate percentage by weight of Total Powder)	Secant Modulus Of Elasticity (MPa) E_c
M20	C1	C100	21886
	B2	C50+FA50	21111
	B7	C80+MS20	22150
	B13	C75+MK25	20288
	T3	C35+FA50+MS15	21300
	T15	C25+FA60+MK15	24775
M40	C1	C100	31171
	B1	C60+FA40	33033
	B5	C85+MS15	32357
	B10	C80+MK20	35640
	T5	C50+FA40+MS10	37640
	T9	C35+FA50+MK15	40960
M80	B2	C95+MS5	44811
	T3	C65+FA20+MS15	46750
	Q11	C50+FA28+MS11+MK11	50183
M100	B2	C90+MS10	51563
	T2	C71+FA19+MS10	51611
	Q11	C55+FA23+MS11+MK11	56486

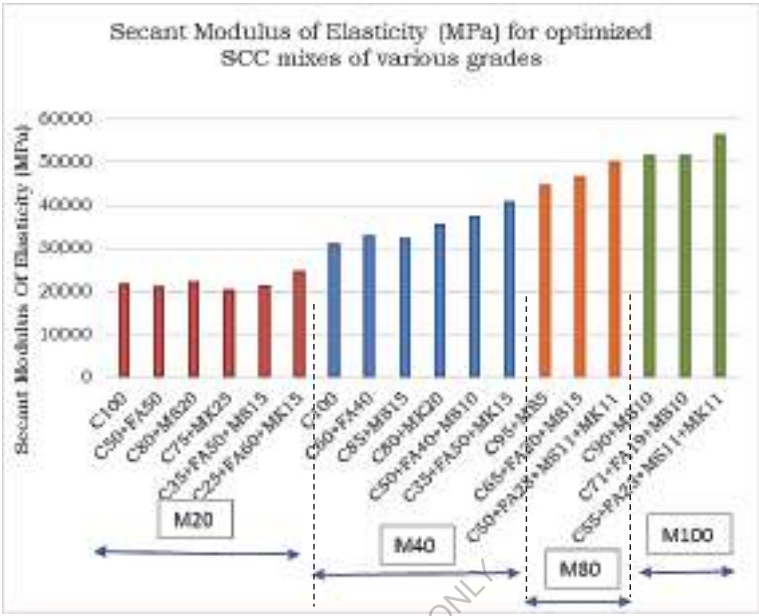

Fig 23- Modulus of Elasticity for optimized SCC mixes of various grades

The metakaolin inclusion generally improves accelerating Early Strength development, compressive strength, tensile strength, flexural strength, impact strength, stress-strain behaviour and modulus of elasticity. The quantum of increase in the individual properties depends upon replacement level. Metakaolin addition will produce accelerated strength gain in the early stages of curing, suggesting acceleration of OPC hydration.

8. CEMENTING EFFICIENCY FACTORS

The present work is an effort to quantify the cementitious efficiency of optimum proportions of Fly Ash (FA), Microsilica (MS) and Metakaolin (MK) combination in binary, ternary and quaternary blended Self-Compacting Concrete (SCC) systems of ordinary grade (M20) , standard grade (M40) and high strength grade (M80 and M100). The effect of synergic action of metakaolin (MK), microsilica (MS) and fly ash (FA) combination on the strengths of binary, ternary and quaternary blended SCC may be modelled by using a Cementing Efficiency Factor (k). The Cementing Efficiency Factor is defined as the ratio of the cementing efficiency of blended SCC to the cementing efficiency of the reference SCC. It was observed that this overall strength efficiency of blended SCC was found to be a combination of efficiency factor 'k_a' depending on the age and efficiency factor 'k_p' depending upon the percentage of SCM replacement. This evaluation makes it possible to design blended SCC for a desired strength at any given percentage of replacement.

$k=k_a+k_p$

k= overall strength efficiency factor ; k_a= efficiency factor depending on age

k_p= efficiency factor depending on percentage of replacement

So it is felt that cementing efficiency concept can be used to understand the behavior of blended SCC to reference SCC.

A number of empirical expressions are frequently used to describe or predict the strength of normal hardened cement paste. The more well-known expression of Bolomey's relates strength and water/cement ratio. This Bolomey's empirical expression frequently used to predict the strength of concrete is theoretically well justifies when applied to hardened SCC. Strength data from experiments on normal hardened cement paste are frequently reported in the literature to be well fitted by Bolomey's empirical expression. The concept of efficiency can be used for comparing the relative performance of SCMs when incorporated into SCC. Efficiency factors found from Bolomey's strength equation are used to describe the effect of the SCMs combination replacement in SCC in the enhancement of strength and durability characteristics. This factor will give only an indication of the added materials' effect on concrete strength, since it does no distinguish between filler effect and chemical reactions. The well-known Bolomey's equation often used to relate strength and water/cement ratio is:

$$S = A\,[(C/W)] + B \text{ ------ } (1)$$

S is the compressive strength in MPa, C is the cement content in kg /m^3,

W is the water content in kg/m^3

A and B are Bolomey's coefficients /or constants

Equation (1) has been shown to practically reduce to following two equations

$$S = A\,[(C/W) - 0.5] \text{..... } (2)$$

$$S = A\,[(C/W) + 0.5] \text{..... } (3)$$

From these above two normalized equations which represent two ranges of concrete strengths based on the change in slope when P/W (powder-water ratio) is plotted against strength. However, it is found that the equation (2) is useful for most of the present-day concretes when an analysis was done on test results available and also the extensive data published by Larrard also mentions this equation in his famous book, on 'Concrete Mix Proportioning – A scientific approach'. Therefore, equation (2) can be generally used for re-proportioning MK+MS+FA SCC. The value

of constant 'A' can be found out for the given concrete ingredients, by considering a concrete mix of any w/c ratio.

For structural concrete, Equation (1) can be simplified as

$$S = A\,[(C/W) - 0.5] \text{ -------- } (4)$$

A strength efficiency factor, k, can then be computed using modified Bolomey's equation

$$S = A\,[(C + kP)/W) - 0.5] \text{ --------- } (5)$$

Where S is the compressive strength in MPa,

C is the OPC content in kg / m^3, P is the amount of SCMs replaced bwc.

W is the water content in kg/m^3 and k denotes efficiency factor of SCMs combination

By knowing the amounts of 'C', 'P', 'W' and the strength 'S' achieved for each SCMs dosage replacement, efficiency factor "k" has been computed for each of the replacement dosages. Thus, W/(C+ kP) is the water/effective powder ratio and kP is the equivalent cement content of SCMs combination. 'SCMs /OPC ratio' is an important factor for determining the efficiency of SCMs in SCC. So SCMs proportioning is arrived at based on the strength data experiments on SCMs blended SCC Mixes. Efficiency factors found from this strength equation are used to describe the effect of the SCMs replacement. This factor describes the mineral admixture's ability to act as cementing material recognizing that mineral admixture's contribution to concrete strength which comes mainly from its ability to react with free calcium hydroxide produced during cement hydration (Pozzolanic Reaction (PR)).

This phase is part of wider study on the behavior of synergic action of SCMs such as Fly Ash (FA), Microsilica (MS) and Metakaolin (MK) in SCC mixes for various grades when replaced on a one-to-one basis by weight, in binary, ternary and quaternary blended SCC mixes. When the performance of blended SCC mixes are analyzed, it was observed that this overall strength efficiency of mineral admixture blends in SCC was found to be a combination of two factors: (1) general efficiency factor, depending on the age of concrete and (2) a percentage efficiency factor, depending upon the percentage of replacement of mineral admixture. This evaluation makes it possible to design blended SCC mixes for a desired strength at any given percentage of replacement. The scope of this part of research was to determine the strength efficiency of optimally blended binary, ternary and quaternary SCC mixes of ordinary grade (M20), standard grade (M40) and high strength grade (M80 and M100) made with Fly Ash (FA), Microsilica (MS) and Metakaolin (MK) in terms of efficiency factor 'k'. Table 45 shows Bolomey's Coefficients (A) for various grades of SCC mixes calculated using Bolomey equation. Then Efficiency factors for optimally blended binary, ternary and quaternary SCC mixes of ordinary grade (M20), standard grade (M40) and high strength grade (M80 and M100) were then determined using same bolomey equation. Bolomey's coefficients are calculated from the reference mixes.

Table 45 - Bolomey's Coefficients (A) for various grades of SCC mixes

Grade of SCC Mix	Bolomey's Coefficients (A)					
	3 days	7 days	14 days	28 days	60 days	90 days
M20	5.93	9.63	11.86	14.82	14.91	16.29
M40	8.59	14.06	16.76	20.33	21.17	22.40
M80	9.60	15.59	21.32	23.99	24.71	25.24
M100	10.41	16.27	22.77	26.21	26.65	26.97

Table 46– Efficiency factors for various grades of blended SCC mixes at different ages of curing

Grade of SCC Mix	Mix No	Mix Designation (Values indicate percentage by weight of Total Powder)	Efficiency Factors					
			3 days	7 days	14 days	28 days	60 days	90 days
M20	C1	C100	-	-	-	-	-	-
	B2	C50+FA50	0.34	0.55	0.79	0.70	1.22	1.25
	B7	C80+MS20	1.59	1.59	2.15	1.59	1.64	1.68
	B13	C75+MK25	3.61	1.72	2.16	1.69	1.70	1.73
	T3	C35+FA50+MS15	0.88	0.99	1.00	0.86	1.19	1.22
	T15	C25+FA60+MK15	1.57	1.22	1.15	1.08	1.32	1.34
M40	C1	C100	-	-	-	-	-	-
	B1	C60+FA40	0.23	0.28	0.42	0.79	1.14	1.17
	B5	C85+MS15	2.47	0.76	1.32	1.44	1.45	1.51
	B10	C80+MK20	5.23	2.42	2.23	1.48	1.49	1.51
	T5	C50+FA40+MS10	0.99	0.64	0.80	0.88	1.06	1.21
	T9	C35+FA50+MK15	1.94	1.29	1.27	1.05	1.08	1.19
M80	B2	C95+MS5	1.00	1.00	1.00	1.00	1.00	1.00
	T3	C65+FA20+MS15	0.34	0.68	0.59	0.85	0.98	1.04
	Q11	C50+FA28+MS11+MK11	1.74	1.21	1.06	0.94	1.00	1.08
M100	B2	C90+MS10	1.00	1.00	1.00	1.00	1.00	1.00
	T2	C71+FA19+MS10	0.88	0.98	1.00	0.69	0.99	1.08
	Q11	C55+FA23+MS11+MK11	2.12	1.37	0.76	0.76	1.05	1.12

Table 47 –Efficiency factors for optimally blended SCC mixes

Grade of SCC Mix	Mix No	Mix Designation (Values indicate percentage by weight of Total Powder)	Efficiency Factors
M20	C1	C100	-
	B2	C50+FA50	1.25
	B7	C80+MS20	1.59
	B13	C75+MK25	1.69
	T3	C35+FA50+MS15	1.22
	T15	C25+FA60+MK15	1.34
M40	C1	C100	-
	B1	C60+FA40	1.17
	B5	C85+MS15	1.44
	B10	C80+MK20	1.48
	T5	C50+FA40+MS10	1.21
	T9	C35+FA50+MK15	1.19
M80	B2	C95+MS5	1.00
	T3	C65+FA20+MS15	1.04
	Q11	C50+FA28+MS11+MK11	1.08
M100	B2	C90+MS10	1.00
	T2	C71+FA19+MS10	1.08
	Q11	C55+FA23+MS11+MK11	1.12

Table 46 presents efficiency factors for various grades of optimally blended binary, ternary and quaternary SCC mixes of ordinary grade (M20), standard grade (M40) and high strength grade (M80 and M100) at different ages of curing. Table 47 presents efficiency factors for optimally blended SCC mixes at specified age of curing where desired strength was projected to achieve.
The efficiency factor (or k-factor) is defined as the part of the SCM in a pozzolanic concrete which can be considered as equivalent to Portland cement, having the same properties as the concrete without SCM (k= 1 for Portland cement) which means that 1 kg of cement can be replaced with k-factor of SCM or SCMs combination (optimal).
The contribution of metakaolin (MK) to any property of hardened concrete may be expressed in terms of efficiency factor, k. For this new material to be generally accepted by the building industry, a good durability must be proven also in quantitative terms. Therefore, a big challenge for researchers within this field is to determine the strength efficiency of metakaolin (MK) in binary, ternary and quaternary blended SCC mixes.
Compressive strengths are achieved early in metakaolin based binary and ternary blended SCC of all grades than in microsilica based binary and ternary blended SCC. Due to synergy effect, the interaction of two or more admixtures is so that their combined effect is greater than the sum of their individual effects. In the other words, for reflecting synergic effect, the efficiency factor of Metakaolin, microsilica and fly ash combination should be higher in ternary blended SCC than in binary blended SCC system. For calculating the efficiency of Metakaolin, microsilica and fly ash combination in binary and ternary blended SCC, an equation has been proposed by author based on the principle of Bolomey's equation for predicting the strength of concrete containing mineral admixtures. The efficiency factors evaluated can be used for proportioning of blended SCC. For compressive strength of metakaolin (MK based SCC mixes, k is in the range of 1.08 to 1.69, which means that in a given SCC mix, 1 kg of MK based pozzolanic material may replace 1.08 to 1.69 kg of cement without impairing the compressive strength. This may be valid, provided that the water content is kept constant. Bolomey's coefficients 'A' are calculated from the control mixes. Using computed 'A' value, calculate strength efficiency factors k at all ages for all percentage replacement levels of metakaolin (MK) and fly ash (FA) combination in SCC.

It is observed from efficiency factor is 1.69 for C75+MK25 and1.32 for C25+FA60+MK15 ordinary grade M20 SCC mixes. For Standard grade M40 SCC mixes, k is 1.48 for C80+MK20 and 1.08 for C35+FA50+MK15 combinations. Metakaolin (MK) and fly ash (FA) blended SCC mix is found to be more efficient because of high usage of waste by-product FA and high reduction of cement content. This study is carried out to understand the cementing efficiency of Metakaolin (MK) in binary, ternary and quaternary blended SCC mixes at 3,7, 14,28, 60 and 90 days. This evaluation makes it possible to design binary, ternary and quaternary blended SCC for a desired strength at any given percentage of replacement. The strength efficiency factor 'k' is evaluated for three cases in quaternary blended SCC mixes: (1) micro silica (MS) is singly blended in SCC, (2) micro silica (MS) is blended with fly ash (FA) in SCC and (3) Metakaolin (MK) is blended with micro silica (MS) and fly ash (FA) SCC mix.
It can be observed that efficiency factors for binary (Mix B2), ternary (Mix T3) and quaternary (Mix Q11) blended high strength (M80) SCC mixes are 1.00, 1.04 and 1.08 respectively. All the three M80 grade SCC mixes give similar strength and satisfy EFNARC specifications. The efficiency factor for quaternary (C50+FA28+MS11+MK11) blended high strength SCC mixes is 1.08 which means that 1 kg of cement can be replaced with 1.08 kg of FA+MS+MK pozzolanic mixture. Efficiency factor for quaternary blended SCC mix reveals that for similar strength, 50%

of cement can be replaced with FA28%+MS11%+MK11% combination of pozzolanic mixture. Similar observations are made in blended high strength (M100) SCC mixes.
The computed efficiency factors may be incorporated in the design of a blended concrete mixture, a method known as rational proportioning. The k value can be used to transform a certain amount of pozzolan to an equivalent amount of cement in terms of strength contribution; hence, it can be used as a basis for a more efficient proportioning of blended SCC mixes.

9. STATISTICAL MODELLING

9.0 Correlation equations

The empirical expressions for various parameters such as split tension, flexural strength, water-powder ratio, quantity of powder and modulus of elasticity in terms of compressive strength, useful for proportioning the mixes, were derived based on regression analysis and presented in the following paragraphs. The parameter, compressive strength at 28 days is considered as reference value for SCC mixes without fly ash and equivalent compressive strength at 90 days is taken as the reference value for SCC mixes with fly ash. The theoretical values obtained from the empirical expressions were compared with the experimental values. The strength and reliability of such derived empirical expressions is expressed in terms of coefficient of correlation and Average Absolute Relative Error (AARE) between the experimental values and the values obtained by the thus derived empirical expressions.

Empirical expression for parameter 'p' in terms of compressive strength (fc)

Assuming the exponential relationship between the parameter 'p' and compressive strength (fc),

$$p = k_1 (f_c)^{k2} \quad \text{.....1}$$

In which k_1 and k_2 are constants to be solved for using the normal equations in statistics.

Taking log on both sides of Eq.5.1

$$\log p = \log k_1 + k_2 \log f_c \quad \text{.....2}$$

The normal equations (NE'S) would be,

$$\Sigma \log p = N_s \log k_1 + k_2 \Sigma \log f_c \quad \text{.....3}$$

$$\Sigma(\log f_c \log p) = \log k_1 \Sigma \log f_c + k_2 \Sigma (\log f_c)^2 \quad \text{.....4}$$

N_s is the sample size

Solving the above NE'S, we get

$$k_2 = [\Sigma \log f_c \Sigma \log p - N_s \Sigma(\log f_c \log p)]/[(\Sigma \log f_c)^2 - N_s \Sigma (\log f_c)^2] \quad \text{……..5}$$

and

$$\log k_1 = [\Sigma \log p - k_2 \Sigma \log f_c]/ N_s$$

or

$$k_1 = \log^{-1}[[\Sigma \log p - k_2 \Sigma \log f_c]/ N_s] \quad \text{……6}$$

After obtaining k1 and k2 ,

Substituting the values of k1 and k2 in Eq.1 we get the proposed empirical expression for p (Theoretical) in terms of f_c for various grades of blended SCC mixes

%δ (percentage deviation) is equal to $[(p - p^*)/ p]*100$

The coefficient of correlation between expected values (p) and the corresponding probable values (p^*) is

$$r_{cc} = [\Sigma(p- avg.p)(p^*-avg.p^*)]/\sqrt{[\Sigma(p- avg.p)^2 * \Sigma(p^*-avg.p^*)^2]}$$

The Average Absolute Relative Error (AARE) is also computed.

This phase presents the empirical expressions for various parameters (p) such as split tensile strength, flexural strength, water-powder ratio, quantity of powder and modulus of elasticity in terms of specified compressive strength. The compressive strength value at 28 days is considered as reference value for SCC mixes without fly ash and compressive strength value at 90 days is taken as the reference value for SCC mixes with fly ash. The strength and reliability of such derived empirical expressions is expressed in terms of coefficient of correlation and Average Absolute Relative Error (AARE) between the experimental values and the values obtained by the thus derived empirical expressions.

9.1 Relation between Split tensile Strength (f_t) and Compressive Strength (f_c)

Assuming the exponential relationship between the split tensile strength (ft) and compressive strength (fc),

$$f_t = k_1 (f_c)^{k2} \quad \text{.....1}$$

In which k_1 and k_2 are constants to be solved for using the normal equations in statistics.

Taking log on both sides of Eq.5.1

$$\log f_t = \log k_1 + k_2 \log f_c \quad \text{.....2}$$

The normal equations (NE'S) would be,

$$\Sigma \log f_t = N_s \log k_1 + k_2 \Sigma \log f_c \quad \text{.....3}$$

$$\Sigma(\log f_c \log f_t) = \log k_1 \Sigma \log f_c + k_2 \Sigma (\log f_c)^2 \quad \text{.....4}$$

N_s is the sample size

Solving the above NE'S, we get

$$k_2 = [\Sigma \log f_c \Sigma \log f_t - N_s \Sigma(\log f_c \log f_t)]/[(\Sigma \log f_c)^2 - N_s \Sigma(\log f_c)^2] \quad \text{……..5}$$

and

$$\log k_1 = [\Sigma \log f_t - k_2 \Sigma \log f_c]/ N_s$$

or

$$k_1 = \log^{-1}[\Sigma \log f_t - k_2 \Sigma \log f_c]/ N_s] \quad \text{……6}$$

Table 48 - Empirical expression for f_t in terms of f_c

Grade of SCC Mix	Mix No	Mix Designation (Values indicate percentage by weight of Total Powder)	Split Tensile Strength f_t (N/mm2)	Compressive Strength f_c (N/mm2)	Y=logf_t	X=logf_c	XY	X^2
M20	C1	C100	2.52	25.18	0.40	1.40	0.56	1.96
	B2	C50+FA50	3.22	32.24	0.51	1.51	0.77	2.28
	B7	C80+MS20	2.90	29.03	0.46	1.46	0.67	2.13
	B13	C75+MK25	3.08	30.77	0.49	1.49	0.73	2.22
	T3	C35+FA50+MS15	3.28	32.81	0.52	1.52	0.79	2.31
	T15	C25+FA60+MK15	3.69	36.87	0.57	1.57	0.89	2.46
M40	C1	C100	4.82	48.18	0.68	1.68	1.14	2.82
	B1	C60+FA40	5.68	56.78	0.75	1.75	1.31	3.06
	B5	C85+MS15	5.20	51.99	0.72	1.72	1.24	2.96
	B10	C80+MK20	5.37	53.73	0.73	1.73	1.26	2.99
	T5	C50+FA40+MS10	5.99	59.87	0.78	1.78	1.39	3.17
	T9	C35+FA50+MK15	5.99	59.92	0.78	1.78	1.39	3.17
M80	B2	C95+MS5	8.86	88.56	0.95	1.95	1.85	3.80
	T3	C65+FA20+MS15	9.45	94.51	0.98	1.98	1.94	3.92
	Q11	C50+FA28+MS11+MK11	8.53	97.16	0.93	1.99	1.85	3.96
M100	B2	C90+MS10	10.60	106.04	1.03	2.03	2.09	4.12
	T2	C71+FA19+MS10	11.18	111.83	1.05	2.05	2.15	4.20
	Q11	C55+FA23+MS11+MK11	11.33	113.28	1.05	2.05	2.15	4.20
N=18				Σ	13.38	31.44	24.19	55.75

Table 49 - Coefficient of correlation for f_t

Grade of SCC Mix	Mix No	Experimental f_t(N/mm2)	Theoretical f_t*(N/mm2)	X= f_t- avg.f_t	Y= f_t^* -avg.f_t^*	X^2	Y^2	XY	%δ
M20	C1	2.52	2.60	-3.55	-3.74	12.60	14.01	13.29	-3.04
	B2	3.22	3.31	-2.85	-3.03	8.12	9.19	8.64	-2.75
	B7	2.90	2.99	-3.17	-3.35	10.05	11.25	10.63	-2.94
	B13	3.08	3.16	-2.99	-3.18	8.94	10.11	9.51	-2.61
	T3	3.28	3.37	-2.79	-2.97	7.78	8.85	8.30	-2.61
	T15	3.69	3.77	-2.38	-2.57	5.66	6.59	6.11	-2.26
M40	C1	4.82	4.90	-1.25	-1.44	1.56	2.06	1.79	-1.75
	B1	5.68	5.76	-0.39	-0.58	0.15	0.34	0.23	-1.43
	B5	5.20	5.28	-0.87	-1.06	0.76	1.11	0.92	-1.62
	B10	5.37	5.46	-0.7	-0.88	0.49	0.78	0.62	-1.63
	T5	5.99	6.07	-0.08	-0.27	0.01	0.07	0.02	-1.31
	T9	5.99	6.07	-0.08	-0.27	0.01	0.07	0.02	-1.39
M80	B2	8.86	8.91	2.79	2.57	7.78	6.58	7.16	-0.52
	T3	9.45	9.49	3.38	3.15	11.42	9.94	10.65	-0.45
	Q11	8.53	9.75	2.46	3.41	6.05	11.65	8.40	-0.34
M100	B2	10.60	10.63	4.53	4.29	20.52	18.37	19.41	-0.24
	T2	11.18	11.19	5.11	4.85	26.11	23.56	24.80	-0.12
	Q11	11.33	11.34	5.26	5.00	27.67	24.96	26.28	-0.05
N=18		avg.f_t =6.07	avg.f_t^* =6.34						

Where %δ (percentage deviation) is equal to $[(f_t - f_t^*)/ f_t]*100$

The coefficient of correlation between expected values (f_t) and the corresponding probable values (f_t^*) is

$r_{cc} = [\Sigma(f_t - avg.f_t)(f_t^* - avg.f_t^*)]/\sqrt{[\Sigma(f_t - avg.f_t)^2 * \Sigma(f_t^* - avg.f_t^*)^2]} = 0.9949$

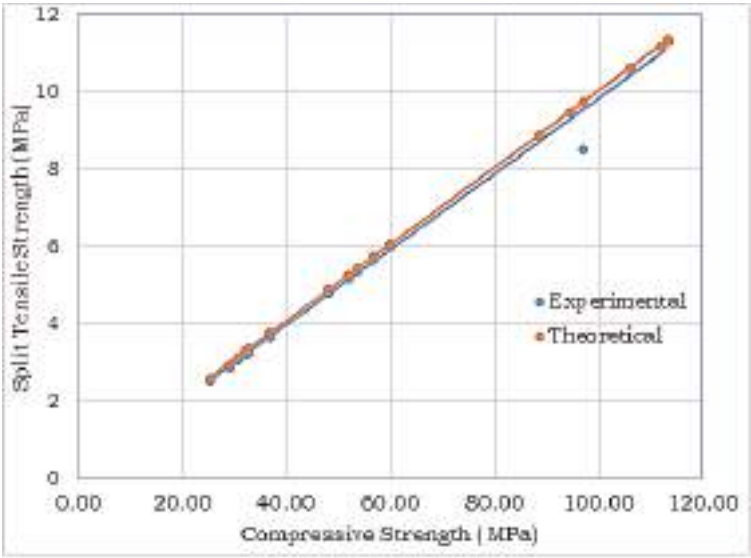

Fig 24 -Regression analysis based model for f_t

The Average Absolute Relative Error (AARE) is given by

$$\text{AARE} = \frac{1}{N}\sum_{i=1}^{N}\left|\frac{f_t^* - f_t}{f_t}\right| = 0.023$$

9.2 Relation between flexural strength (f_b) and Compressive Strength (f_c)

To develop empirical expressions using statistical modelling, the following tabular values are evaluated.

Table 50 - Empirical expression for f_b in terms of f_c

Grade of SCC Mix	Mix No	Mix Designation (Values indicate percentage by weight of Total Powder)	Flexural Strength f_b (N/mm2)	Compressive Strength f_c (N/mm2)	Y=logf_b	X=logf_c	XY	X^2
M20	C1	C100	3.28	25.18	0.52	1.40	0.72	1.96
	B2	C50+FA50	4.19	32.24	0.62	1.51	0.94	2.28
	B7	C80+MS20	3.77	29.03	0.58	1.46	0.84	2.14
	B13	C75+MK25	4.00	30.77	0.60	1.49	0.90	2.21
	T3	C35+FA50+MS15	4.26	32.81	0.63	1.52	0.95	2.30
	T15	C25+FA60+MK15	4.80	36.87	0.68	1.57	1.07	2.45
M40	C1	C100	6.27	48.18	0.80	1.68	1.34	2.83
	B1	C60+FA40	7.38	56.78	0.87	1.75	1.52	3.08
	B5	C85+MS15	6.76	51.99	0.83	1.72	1.42	2.94
	B10	C80+MK20	6.98	53.73	0.84	1.73	1.46	2.99
	T5	C50+FA40+MS10	7.79	59.87	0.89	1.78	1.58	3.16
	T9	C35+FA50+MK15	7.79	59.92	0.89	1.78	1.58	3.16
M80	B2	C95+MS5	11.52	88.56	1.06	1.95	2.07	3.79
	T3	C65+FA20+MS15	12.29	94.51	1.09	1.98	2.15	3.90
	Q11	C50+FA28+MS11+MK11	12.64	97.16	1.10	1.99	2.19	3.95
M100	B2	C90+MS10	13.78	106.04	1.14	2.03	2.31	4.10
	T2	C71+FA19+MS10	14.53	111.83	1.16	2.05	2.38	4.20
	Q11	C55+FA23+MS11+MK11	14.73	113.28	1.17	2.05	2.40	4.22
N=18				Σ	15.47	31.42	27.84	55.67

$k_2 = [\ \Sigma\log f_c\ \Sigma\log f_b\ - N_s\ \Sigma(\log f_c\ \log f_b)]/[\ (\Sigma\log f_c)^2\ - N_s\ \Sigma(\log f_c)^2$

and

$\log k_1 = [\Sigma\log f_b - k_2\Sigma\log f_c]/\ N_s$ or $k_1 = \log^{-1}[\ [\Sigma\log f_b - k_2\Sigma\log f_c]/\ N_s]$

Substituting the tabular values in above equations and solving them for k1 and k2 we get,

k1 = 0.12 and k2 = 1.015

Substituting the values of k1 and k2 in $f_b = k_1\ (f_c)^{k2}$

we get, $f_b = 0.12\ (f_c)^{1.015}$

This is the proposed empirical expression for flexural strength 'f_b' (Theoretical) in terms of f_c for various grades of blended SCC mixes

The coefficient of correlation is worked out using the Table 51.

Table 51 - Coefficient of correlation for f_t

Grade of SCC Mix	Mix No	Experimental f_b (N/mm2)	Theoretical f_b^* (N/mm2)	X= f_b- avg.f_b	Y= f_b^*-avg.f_b^*	X^2	Y^2	XY	%δ
M20	C1	3.28	3.17	-4.69	-4.86	22.00	23.61	22.79	3.31
	B2	4.19	4.08	-3.78	-3.95	14.29	15.64	14.95	2.73
	B7	3.77	3.66	-4.2	-4.37	17.64	19.06	18.34	2.81
	B13	4	3.89	-3.97	-4.14	15.76	17.16	16.45	2.82
	T3	4.26	4.15	-3.71	-3.88	13.76	15.06	14.40	2.61
	T15	4.8	4.67	-3.17	-3.36	10.05	11.29	10.65	2.70
M40	C1	6.27	6.13	-1.7	-1.90	2.89	3.62	3.23	2.27
	B1	7.38	7.24	-0.59	-0.79	0.35	0.63	0.47	1.91
	B5	6.76	6.62	-1.21	-1.41	1.46	1.99	1.71	2.08
	B10	6.98	6.84	-0.99	-1.19	0.98	1.41	1.17	1.94
	T5	7.79	7.64	-0.18	-0.39	0.03	0.15	0.07	1.94
	T9	7.79	7.65	-0.18	-0.38	0.03	0.15	0.07	1.85
M80	B2	11.52	11.37	3.55	3.34	12.60	11.13	11.84	1.33
	T3	12.29	12.14	4.32	4.11	18.66	16.91	17.76	1.20
	Q11	12.64	12.49	4.67	4.46	21.81	19.87	20.82	1.21
M100	B2	13.78	13.65	5.81	5.62	33.76	31.55	32.63	0.97
	T2	14.53	14.40	6.56	6.37	43.03	40.62	41.81	0.87
	Q11	14.73	14.59	6.76	6.56	45.70	43.07	44.37	0.93
N=18		avg.f_b=7.97	avg.f_b^*=8.03	3.3	-0.17	274.81	272.91	273.52	

Where %δ (percentage deviation) is equal to $[(f_b - f_b^*)/ f_b]*100$

The coefficient of correlation between expected values (f_b) and the corresponding probable values (f_b^*) is

$r_{cc} = [\Sigma(f_b - avg.f_b)(f_b^* - avg.f_b^*)]/\sqrt{[\Sigma(f_b - avg.f_b)^2 * \Sigma(f_b^* - avg.f_b^*)^2]} = 0.9987$

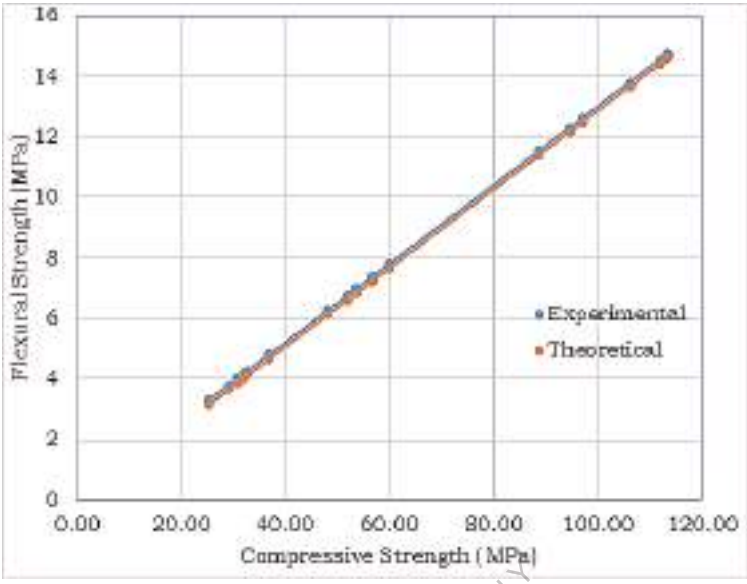

Fig 25 - Regression analysis based model for f_b

The Average Absolute Relative Error (AARE) is given by

$$\text{AARE} = \frac{1}{N}\sum_{i=1}^{N}\left|\frac{f_b^* - f_b}{f_b}\right| = 0.019$$

9.3 Relation between water powder ratio (w_p) and Compressive Strength (f_c)

To develop empirical expressions using statistical modelling, the following tabular values are evaluated.

Table 52 Empirical expression for w_p in terms of f_c

Grade of SCC Mix	Mix No	Mix Designation (Values indicate percentage by weight of Total Powder)	Water Powder Ratio (W/P) w_p	Compressive Strength f_c (N/mm2)	Y =log w_p	X =log f_c	XY	X^2
M20	C1	C100	0.45	25.18	-0.35	1.40	-0.49	1.96
	B2	C50+FA50	0.45	32.24	-0.35	1.51	-0.52	2.28
	B7	C80+MS20	0.45	29.03	-0.35	1.46	-0.51	2.14
	B13	C75+MK25	0.45	30.77	-0.35	1.49	-0.52	2.21
	T3	C35+FA50+MS15	0.45	32.81	-0.35	1.52	-0.53	2.30
	T15	C25+FA60+MK15	0.45	36.87	-0.35	1.57	-0.54	2.45
M40	C1	C100	0.35	48.18	-0.46	1.68	-0.77	2.83
	B1	C60+FA40	0.35	56.78	-0.46	1.75	-0.80	3.08
	B5	C85+MS15	0.35	51.99	-0.46	1.72	-0.78	2.94
	B10	C80+MK20	0.35	53.73	-0.46	1.73	-0.79	2.99
	T5	C50+FA40+MS10	0.35	59.87	-0.46	1.78	-0.81	3.16
	T9	C35+FA50+MK15	0.35	59.92	-0.46	1.78	-0.81	3.16
M80	B2	C95+MS5	0.25	88.56	-0.60	1.95	-1.17	3.79
	T3	C65+FA20+MS15	0.25	94.51	-0.60	1.98	-1.19	3.90
	Q11	C50+FA28+MS11+MK11	0.25	97.16	-0.60	1.99	-1.20	3.95
M100	B2	C90+MS10	0.22	106	-0.66	2.03	-1.33	4.10
	T2	C71+FA19+MS10	0.22	111.8	-0.66	2.05	-1.35	4.20
	Q11	C55+FA23+MS11+MK11	0.22	113.3	-0.66	2.05	-1.35	4.22
N=18				Σ	-8.60	31.42	-15.45	55.67

$k_2 = [\ \Sigma \log f_c\ \Sigma \log w_p\ - N_s\ \Sigma(\log f_c\ \log w_p)]/[\ (\Sigma \log f_c)^2\ - N_s\ \Sigma(\log f_c)^2]$

and

$\log k_1 = [\Sigma \log w_p - k_2 \Sigma \log f_c]/ N_s$ or $k_1 = \log^{-1}[\ [\Sigma \log w_p - k_2 \Sigma \log f_c]/ N_s]$

Substituting the tabular values in above equations and solving them for k1 and k2 we get,

k1 = 2.82 and k2 =- 0.53

Substituting the values of k1 and k2 in $w_p = k_1 (f_c)^{k2}$

we get, $w_p = 2.82\ (f_c)^{-0.53}$

This is the proposed empirical expression for water powder ratio 'w_p' (Theoretical) in terms of f_c for various grades of blended SCC mixes

The coefficient of correlation is worked out using the Table 52

Table 53- Coefficient of correlation for w_p

Grade of SCC Mix	Mix No	Experimental w_p	Theoretical w_p*	X= w_p-avg. w_p	Y= w_p*-avg. w_p*	X^2	Y^2	XY	%δ
M20	C1	0.45	0.51	0.13	0.16	0.02	0.03	0.02	-13.36
	B2	0.45	0.45	0.13	0.10	0.02	0.01	0.01	0.55
	B7	0.45	0.47	0.13	0.12	0.02	0.02	0.02	-5.13
	B13	0.45	0.46	0.13	0.11	0.02	0.01	0.01	-1.94
	T3	0.45	0.44	0.13	0.09	0.02	0.01	0.01	1.47
	T15	0.45	0.42	0.13	0.07	0.02	0.00	0.01	7.38
M40	C1	0.35	0.36	0.03	0.01	0.00	0.00	0.00	-3.34
	B1	0.35	0.33	0.03	-0.02	0.00	0.00	0.00	5.28
	B5	0.35	0.35	0.03	0.00	0.00	0.00	0.00	0.75
	B10	0.35	0.34	0.03	-0.01	0.00	0.00	0.00	2.46
	T5	0.35	0.32	0.03	-0.03	0.00	0.00	0.00	7.90
	T9	0.35	0.32	0.03	-0.03	0.00	0.00	0.00	7.94
M80	B2	0.25	0.26	-0.07	-0.09	0.00	0.01	0.01	-4.78
	T3	0.25	0.25	-0.07	-0.10	0.00	0.01	0.01	-1.23
	Q11	0.25	0.25	-0.07	-0.10	0.00	0.01	0.01	0.24
M100	B2	0.22	0.24	-0.1	-0.11	0.01	0.01	0.01	-8.22
	T2	0.22	0.23	-0.1	-0.12	0.01	0.01	0.01	-5.22
	Q11	0.22	0.23	-0.1	-0.12	0.01	0.01	0.01	-4.50
N=18		avg. w_p = 0.32	avg. w_p* =0.35	0.45	-0.06	0.15	0.15	0.14	

Where %δ (percentage deviation) is equal to $[(w_p - w_p^*)/ w_p]*100$

The coefficient of correlation between expected values (w_p) and the corresponding probable values (w_p^*) is

$r_{cc} = [\Sigma(w_p - \text{avg. } w_p)(w_p^* - \text{avg. } w_p^*)]/\sqrt{[\Sigma(w_p - \text{avg. } w_p)^2 * \Sigma(w_p^* - \text{avg. } w_p^*)^2]}$

$= 0.9333$

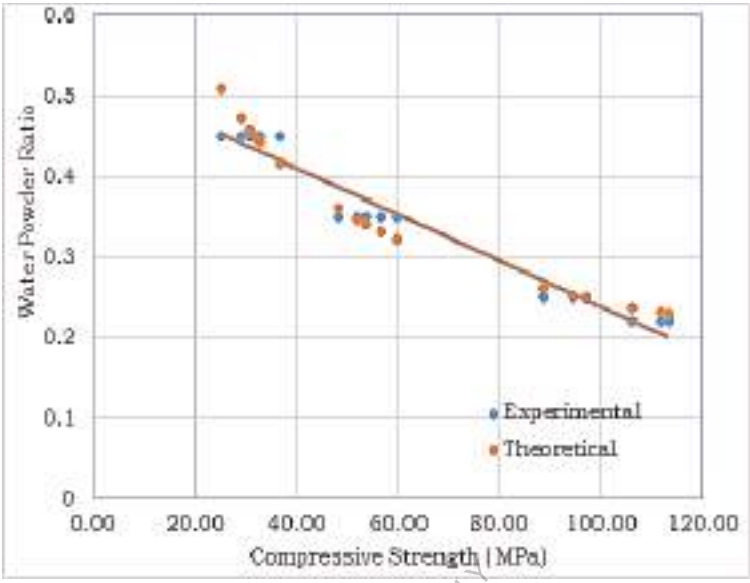

Fig 26 -Regression analysis based model for w_p

The Average Absolute Relative Error (AARE) is given by

$$\text{AARE} = \frac{1}{N}\sum_{i=1}^{N}\left|\frac{w_p^* - w_p}{w_p}\right| = 0.019$$

9.4 Relation between powder quantity (p_q) and Compressive Strength (f_c)

To develop empirical expressions using statistical modelling, the following tabular values are evaluated.

Table 54- Empirical expression for p_q in terms of f_c

Grade of SCC Mix	Mix No	Mix Designation (Values indicate percentage by weight of Total Powder)	Powder Quantity p_q kg	Compressive Strength f_c (N/mm2)	Y =log p_q	X =log f_c	XY	X^2
M20	C1	C100	486	25.18	2.69	1.40	3.76	1.96
	B2	C50+FA50	486	32.24	2.69	1.51	4.05	2.28
	B7	C80+MS20	486	29.03	2.69	1.46	3.93	2.14
	B13	C75+MK25	486	30.77	2.69	1.49	4.00	2.21
	T3	C35+FA50+MS15	486	32.81	2.69	1.52	4.07	2.30
	T15	C25+FA60+MK15	486	36.87	2.69	1.57	4.21	2.45
M40	C1	C100	531	48.18	2.73	1.68	4.59	2.83
	B1	C60+FA40	531	56.78	2.73	1.75	4.78	3.08
	B5	C85+MS15	531	51.99	2.73	1.72	4.68	2.94
	B10	C80+MK20	531	53.73	2.73	1.73	4.72	2.99
	T5	C50+FA40+MS10	531	59.87	2.73	1.78	4.84	3.16
	T9	C35+FA50+MK15	531	59.92	2.73	1.78	4.84	3.16
M80	B2	C95+MS5	700	88.56	2.85	1.95	5.54	3.79
	T3	C65+FA20+MS15	700	94.51	2.85	1.98	5.62	3.90
	Q11	C50+FA28+MS11+MK11	910	97.16	2.96	1.99	5.88	3.95
M100	B2	C90+MS10	700	106.00	2.85	2.03	5.76	4.10
	T2	C71+FA19+MS10	700	111.8	2.85	2.05	5.83	4.20
	Q11	C55+FA23+MS11+MK11	910	113.3	2.96	2.05	6.08	4.22
N=18				Σ	49.77	31.42	87.18	55.67

$k_2 = [\ \Sigma \log f_c\ \Sigma \log p_q - N_s\ \Sigma(\log f_c\ \log p_q)]/[\ (\Sigma \log f_c)^2 - N_s\ \Sigma(\log f_c)^2]$

and

$\log k_1 = [\Sigma \log p_q - k_2 \Sigma \log f_c]/\ N_s$ or $k_1 = \log^{-1}[\ [\Sigma \log p_q - k_2 \Sigma \log f_c]/\ N_s]$

Substituting the tabular values in above equations and solving them for k1 and k2 we get,

k1 = 131.82 and k2 =0.368

Substituting the values of k1 and k2 in $p_q = k_1 (f_c)^{k2}$

we get, $p_q = 131.82\ (f_c)^{0.368}$

This is the proposed empirical expression for Powder Quantity 'p_q' (Theoretical) in terms of f_c for various grades of blended SCC mixes

The coefficient of correlation is worked out using the Table 55

Table 55 - Coefficient of correlation for p_q

Grade of SCC Mix	Mix No	Experimental p_q kg	Theoretical p_q* kg	X= p_q -avg. p_q	Y= p_q*-avg. p_q*	X^2	Y^2	XY	%δ
M20	C1	486	458	-109.66	-175.41	12025.32	30768.96	19235.55	5.78
	B2	486	504	-109.66	-129.57	12025.32	16788.95	14208.89	-3.65
	B7	486	484	-109.66	-149.56	12025.32	22367.75	16400.59	0.46
	B13	486	495	-109.66	-138.57	12025.32	19200.40	15195.09	-1.80
	T3	486	507	-109.66	-126.15	12025.32	15914.53	13833.92	-4.36
	T15	486	531	-109.66	-102.79	12025.32	10566.03	11272.08	-9.16
M40	C1	531	588	-64.66	-45.07	4180.92	2031.48	2914.35	-10.78
	B1	531	627	-64.66	-6.57	4180.92	43.18	424.87	-18.03
	B5	531	606	-64.66	-27.53	4180.92	758.12	1780.35	-14.09
	B10	531	614	-64.66	-19.79	4180.92	391.53	1279.43	-15.54
	T5	531	640	-64.66	6.38	4180.92	40.72	-412.62	-20.47
	T9	531	640	-64.66	6.59	4180.92	43.40	-425.95	-20.51
M80	B2	700	744	104.34	110.74	10886.84	12263.81	11554.83	-6.30
	T3	700	763	104.34	129.65	10886.84	16810.29	13528.15	-9.00
	Q11	910	771	314.34	137.84	98809.64	19000.53	43329.38	15.26
M100	B2	700	798	104.34	164.32	10886.84	27001.21	17145.20	-13.95
	T2	700	814	104.34	180.86	10886.84	32709.70	18870.75	-16.31
	Q11	910	818	314.34	184.92	98809.64	34194.32	58126.83	10.08
N=18		avg. p_q = 595.66	avg. p_q* = 633.33	0.12	0.29	338404.00	260894.93	258261.69	

Where %δ (percentage deviation) is equal to $[(p_q - p_q^*)/ p_q]*100$

The coefficient of correlation between expected values ($\mathbf{p_q}$) and the corresponding probable values (p_q^*) is

$r_{cc} = [\Sigma(p_q - \text{avg. } p_q)(p_q^* - \text{avg. } p_q^*)]/\sqrt{[\Sigma(p_q - \text{avg. } p_q)^2 * \Sigma(p_q^* - \text{avg. } p_q^*)^2]} = 0.8692$

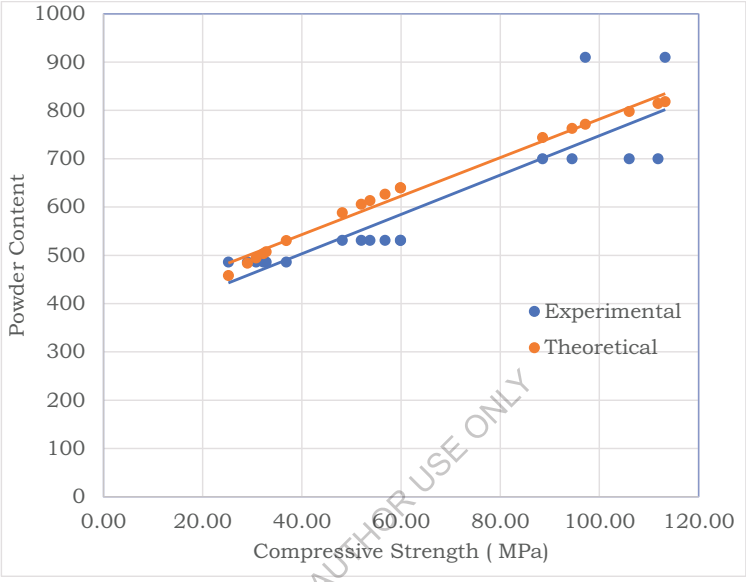

Fig 27 - Regression analysis based model for p_q

The Average Absolute Relative Error (AARE) is given by

$$\text{AARE} = \frac{1}{N}\sum_{i=1}^{N}\left|\frac{p_q^* - p_q}{p_q}\right| = 0.074$$

9.5 Relation between secant modulus of elasticity (Ec) and Compressive Strength (f_c)

To develop empirical expressions using statistical modelling, the following tabular values are evaluated.

Table 56 - Empirical expression for Ec in terms of f_c

Grade of SCC Mix	Mix No	Mix Designation (Values indicate percentage by weight of Total Powder)	Secant modulus of elasticity (Ec) (GPa)	Compressive Strength f_c (N/mm2)	Y =log Ec	X =log f_c	XY	X^2
M20	C1	C100	21886	25.18	4.34	1.40	6.08	1.96
	B2	C50+FA50	21111	32.24	4.32	1.51	6.52	2.28
	B7	C80+MS20	22150	29.03	4.35	1.46	6.36	2.14
	B13	C75+MK25	20288	30.77	4.31	1.49	6.41	2.21
	T3	C35+FA50+MS15	21300	32.81	4.33	1.52	6.56	2.30
	T15	C25+FA60+MK15	24775	36.87	4.39	1.57	6.88	2.45
M40	C1	C100	31171	48.18	4.49	1.68	7.56	2.83
	B1	C60+FA40	33033	56.78	4.52	1.75	7.93	3.08
	B5	C85+MS15	32357	51.99	4.51	1.72	7.74	2.94
	B10	C80+MK20	35640	53.73	4.55	1.73	7.88	2.99
	T5	C50+FA40+MS10	37640	59.87	4.58	1.78	8.13	3.16
	T9	C35+FA50+MK15	40960	59.92	4.61	1.78	8.20	3.16
M80	B2	C95+MS5	44811	88.56	4.65	1.95	9.06	3.79
	T3	C65+FA20+MS15	46750	94.51	4.67	1.98	9.23	3.90
	Q11	C50+FA28+MS11+MK11	50183	97.16	4.70	1.99	9.34	3.95
M100	B2	C90+MS10	51563	106.00	4.71	2.03	9.54	4.10
	T2	C71+FA19+MS10	51611	111.8	4.71	2.05	9.65	4.20
	Q11	C55+FA23+MS11+MK11	56486	113.3	4.75	2.05	9.76	4.22
N=18				Σ	81.50	31.42	142.84	55.67

$k_2 = [\ \Sigma \log f_c\ \Sigma \log Ec\ - N_s\ \Sigma(\log f_c\ \log Ec)]/[\ (\Sigma \log f_c)^2\ - N_s\ \Sigma(\log f_c)^2]$

and

$\log k_1 = [\Sigma \log Ec - k_2 \Sigma \log f_c]/\ N_s$ or $k_1 = \log^{-1}[\ [\Sigma \log Ec - k_2 \Sigma \log f_c]/\ N_s]$

Substituting the tabular values in above equations and solving them for k1 and k2 we get,

k1 = 1995.3 and k2 =0.699

Substituting the values of k1 and k2 in $Ec = k_1\ (f_c)^{k2}$

we get, $Ec = 1995.3\ (f_c)^{0.699}$

This is the proposed empirical expression for Secant Modulus of Elasticity '**Ec**' (Theoretical) in terms of f_c for various grades of blended SCC mixes

The coefficient of correlation is worked out using the Table 57

Table 57 - Coefficient of correlation for Ec

Grade of SCC Mix	Mix No	Experimental Ec (N/mm2)	Theoretical Ec * (N/mm2)	X= Ec -avg. Ec	Y= Ec*-avg. Ec*	X^2	Y^2	XY	%δ
M20	C1	21886	19026	-29677	-16112	880724329	259581998	478142428	13.07
	B2	21111	22614	-30452	-12524	927324304	156839180	381366994	-7.12
	B7	22150	21015	-29413	-14122	865124569	199432579	415372151	5.12
	B13	20288	21888	-31275	-13249	978125625	175544655	414372689	-7.89
	T3	21300	22893	-30263	-12245	915849169	149935475	370564813	-7.48
	T15	24775	24838	-26788	-10300	717596944	106084085	275908708	-0.25
M40	C1	31171	29946	-20392	-5192	415833664	26956385	105874324	3.93
	B1	33033	33589	-18530	-1549	343360900	2399329	28702542	-1.68
	B5	32357	31582	-19206	-3556	368870436	12643306	68291593	2.40
	B10	35640	32317	-15923	-2821	253541929	7955694	44912160	9.32
	T5	37640	34856	-13923	-281	193849929	79240	3919267	7.40
	T9	40960	34876	-10603	-261	112423609	68200	2768981	14.85
M80	B2	44811	45828	-6752	10690	45589504	114278850	-72179749	-2.27
	T3	46750	47959	-4813	12821	23164969	164382737	-61708354	-2.59
	Q11	50183	48895	-1380	13757	1904400	189261396	-18984978	2.57
M100	B2	51563	51977	0	16840	0	283570414	0	-0.80
	T2	51611	53945	48	18807	2304	353719041	902756	-4.52
	Q11	56486	54433	4923	19295	24235929	372312097	94991208	3.63
N=18		avg. p_q = 35761.9	avg. p_q* = 35137.49			7067522513	2575044663	2533217531	

Where %δ (percentage deviation) is equal to [(Ec – Ec *)/ Ec]*100

The coefficient of correlation between expected values (Ec) and the corresponding probable values (Ec *) is

r_{cc}= [Σ(Ec - avg. Ec)(Ec *-avg. Ec *)]/√[Σ(Ec - avg. Ec)^2 * Σ(Ec *-avg. Ec *)^2]

= 0.594

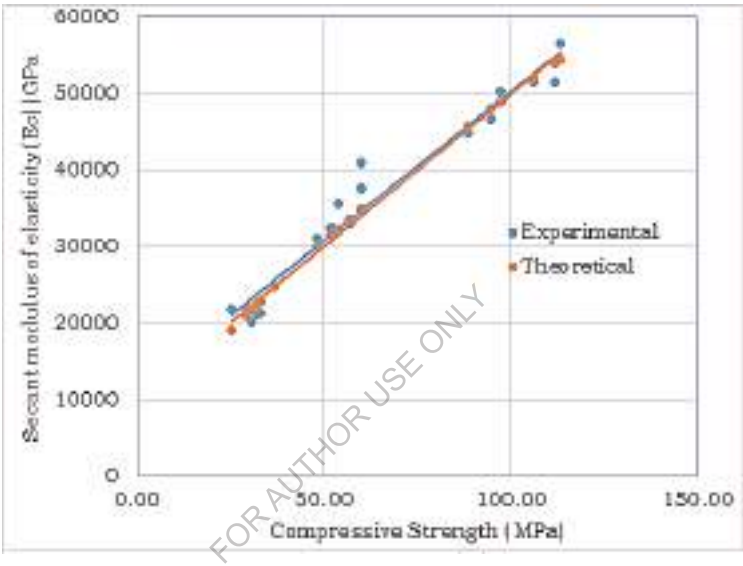

Fig 28 - Regression analysis-based model for Ec

The Average Absolute Relative Error (AARE) is given by

$$AARE = \frac{1}{N}\sum_{i=1}^{N}\left|\frac{E_c^* - E_c}{E_c}\right| = 0.0538$$

In summary, evaluated regression equations which gives non-linear relationships between split tensile strength, flexural strength, water-powder ratio, quantity of powder and modulus of elasticity in terms of specified compressive strength for blended SCC mixes are presented as follows:

1. Relation between Split tensile Strength (f_t) and Compressive Strength (f_c) for various grades of blended SCC mixes is computed as
   $f_t = 0.11 (f_c)^{0.98}$
2. Relation between flexural strength (f_b) and Compressive Strength (f_c) for various grades of blended SCC mixes is computed as
   $f_b = 0.12 (f_c)^{1.015}$
3. Relation between water powder ratio (w_p) and Compressive Strength (f_c) for various grades of blended SCC mixes is computed as
   $w_p = 2.82 (f_c)^{-0.53}$
4. Relation between powder quantity (p_q) and Compressive Strength (f_c) for various grades of blended SCC mixes is computed as
   $p_q = 131.82 (f_c)^{0.368}$
5. Relation between secant modulus of elasticity (Ec) and Compressive Strength (f_c) for various grades of blended SCC mixes is computed as
   $Ec = 1995.3 (f_c)^{0.699}$

10.DURABILITY PROPERTIES

Durability of concrete can be defined as the capability to perform satisfactorily in the exposure condition to which it is subjected over an intended period of time with minimum of maintenance while maintaining its preferred engineering properties. In the following sections detailed investigations are carried out to determine the durability characteristics of ordinary grade (M20) , standard grade (M40) and high strength grade (M80 and M100) of binary ,ternary and quaternary blended Self-Compacting Concrete (SCC) mixes made with optimum proportions of Fly Ash (FA), Microsilica (MS) and Metakaolin (MK) combination.

Durability properties such as water absorption capacity, porosity, sorptivity test, chloride ion penetration resistance, acid attack resistance, sulphate attack resistance, sea water attack resistance at 28, 60 and 90 days were determined by conducting detailed laboratory investigations on ordinary grade (M20), standard grade (M40) and high strength grade (M80 and M100) of binary, ternary and quaternary blended Self Compacting Concrete (SCC) mixes made with fly Ash (FA), microsilica (MS) and metakaolin (MK).

10.0 Chloride ion penetration resistance

The chloride resistance of concrete is governed primarily by the pore structure and the concrete diffusivity. Therefore, wherever there is a potential risk of chloride-induced corrosion, the concrete should be evaluated for chloride permeability. The most important concrete characteristic, apart from permeability, is diffusion. Usually chlorides penetrate in concrete by diffusion along water paths or open pores. The objective of the present experimental investigations is to determine the chloride penetration resistance of ordinary grade (M20) , standard grade (M40) and high strength grade (M80 and M100) of binary ,ternary and quaternary blended Self-Compacting Concrete (SCC) mixes made with optimum proportions of Fly Ash (FA), Microsilica (MS) and Metakaolin (MK) combination.

10.1 Rapid Chloride Permeability Test

As per ASTM C1202, in the Rapid chloride penetration test, a water-saturated, 50-mm thick, 100-mm diameter concrete specimen is subjected to a 60 V applied DC voltage for 6 hours. The permeability cell, which is made of Perspex glass and consists of two parts each with a reservoir being capable of holding 250 ml of chemical solution and copper mesh of 100 mm diameter to act as an electrode. In upstream reservoir of is a 3.0% NaCl solution of 2.4N and in the downstream reservoir is a 0.3 M NaOH solution (chloride free). These concentrations give the equal electrical conductivity of both the solutions. An external voltage cell is used to apply a voltage difference of 60V between the electrodes. The electrochemical cell, constituted by this assembly, results in the rapid migration of chloride ions from the sodium chloride solution to the sodium hydroxide solution, via the pore network offered by the concrete disc shaped specimen. The total charge passed in coulombs is determined and this is used to rate the quality of the concrete according to the criteria rating mentioned in the ASTM C1202. Rapid chloride ion penetrability test (RCPT) is conducted on ordinary grade (M20) , standard grade (M40) and high strength grade (M80 and M100) of binary ,ternary and quaternary blended Self- Compacting Concrete (SCC) mixes made with optimum proportions of Fly Ash (FA), Microsilica (MS) and Metakaolin (MK) combination. The total charge passing through from one reservoir to another reservoir through centrally placed concrete specimen in 6 hrs was measured, at an interval of 60 min, indicating the degree of

resistance of the specimen to chloride ion penetration. The following formula, based on the trapezoidal rule can be used to calculate the average current flowing through one cell.

$$Q = (I_0 + I_1 + I_2 + I_3 + I_4 + I_5 + I_6)\ mAh$$

$$\approx I\ mAh = I \times 0.001A \times 3600\ s$$

Where Q = total electrical charge passed through the specimen (in coulombs) ; I_0, I_6 are the initial and final currents ; I_1, I_2, I_3, I_4, I_5, are the intermediate currents at each one hr and I is the total current at the end of the test i.e., 6hrs.

The chloride resistance of concrete is governed primarily by the pore structure and the concrete diffusivity. Usually chlorides penetrate in concrete by diffusion along water paths or open pores. The objective of the present experimental investigations is to determine the chloride penetration resistance of optimally blended binary, ternary and quaternary SCC mixes of ordinary grade (M20), standard grade (M40) and high strength grade (M80 and M100) made with Fly Ash (FA), Microsilica (MS) and Metakaolin (MK) at 28, 60 and 90 days through the rapid chloride permeability test.

Rapid chloride ion penetrability test is conducted on all optimally blended binary, ternary and quaternary SCC mixes of all grades considered for study. The total charge passing through from one reservoir to another reservoir through centrally placed concrete specimen in 6 hrs was measured, at an interval of 60 min, indicating the degree of resistance of the specimen to chloride ion penetration as shown in Table 58. The test determines the electrical conductance of the test specimen, expressed as the total electrical charge passed through the specimen, in coulombs. The presence of SCMs reduces the porosity by plugging the pores present in the concrete ensuing minimum interconnecting voids. The test results confirms that the metakaolin (MK) blended binary, ternary and quaternary SCC mixes exhibit better chloride ion penetration resistance in all the grades at all ages. In case of metakaolin (MK) based high strength SCC mixes (M80 and M100), chloride ion permeability is reduced to negligible levels whilst this was very low in ordinary grade (M20) and standard grade (M40) concretes. The metakaolin (MK) based blended SCC mixes would be considered to have very low chloride ion permeability which validates its refined pore structure. Decrease in chloride ion permeability is more pronounced in metakaolin (MK) based blended high strength SCC mixes than in other blended SCC mixes. It can be concluded that blended SCC mixes will have the higher life compared to conventional SCC mixes which resists the harmful solutions into the concrete there by decreasing the deleterious effects they may cause. This property can be effectively used to improve the water tightness of the concrete in water retaining structures. Calcium Silicate hydrate (CSH) Phase of metakaolin (MK) blended SCC mixes has a two dimensional foil like structure rather than linear needle like structure of normal CSH of OPC. This foil like structure is more efficient in filling space without leaving large interconnected capillary pores. There is a distinct reduction in porosity with the incorporation of metakaolin in blended SCC mixes.

Table 58 - Total charge passed for blended SCC specimens of various grades

Grade of SCC Mix	Mix No	Mix Designation (Values indicate percentage by weight of 'P')	Total Charge Passed (Coulombs)	Chloride ion Permeability as per ASTM C1202	Total Charge Passed (Coulombs)	Chloride ion Permeability as per ASTM C1202	Total Charge Passed (Coulombs)	Chloride ion Permeability as per ASTM C1202
			28 days		60 days		90 days	
M20	C1	C100	2417	Moderate	2215	Moderate	2103	Moderate
	B2	C50+FA50	1579	Low	991	Very Low	967	Very Low
	B7	C80+MS20	993	Very Low	947	Very Low	913	Very Low
	B13	C75+MK25	995	Very Low	961	Very Low	937	Very Low
	T3	C35+FA50+MS15	1278	Low	562	Very Low	503	Very Low
	T15	C25+FA60+MK15	1176	Low	335	Very Low	267	Very Low
M40	C1	C100	2008	Moderate	1922	Low	1567	Low
	B1	C60+FA40	1423	Low	946	Very Low	921	Very Low
	B5	C85+MS15	984	Very Low	922	Very Low	891	Very Low
	B10	C80+MK20	990	Very Low	932	Very Low	904	Very Low
	T5	C50+FA40+MS10	1189	Low	543	Very Low	488	Very Low
	T9	C35+FA50+MK15	1093	Low	311	Very Low	235	Very Low
M80	B2	C95+MS5	1134	Low	1023	Low	971	Very Low
	T3	C65+FA20+MS15	1019	Low	668	Very Low	561	Very Low
	Q11	C50+FA28+MS11+MK11	534	Very Low	203	Very Low	97	Negligible
M100	B2	C90+MS10	1092	Low	1006	Low	892	Very Low
	T2	C71+FA19+MS10	987	Very Low	509	Very Low	432	Very Low
	Q11	C55+FA23+MS11+MK11	438	Very Low	158	Negligible	84	Negligible

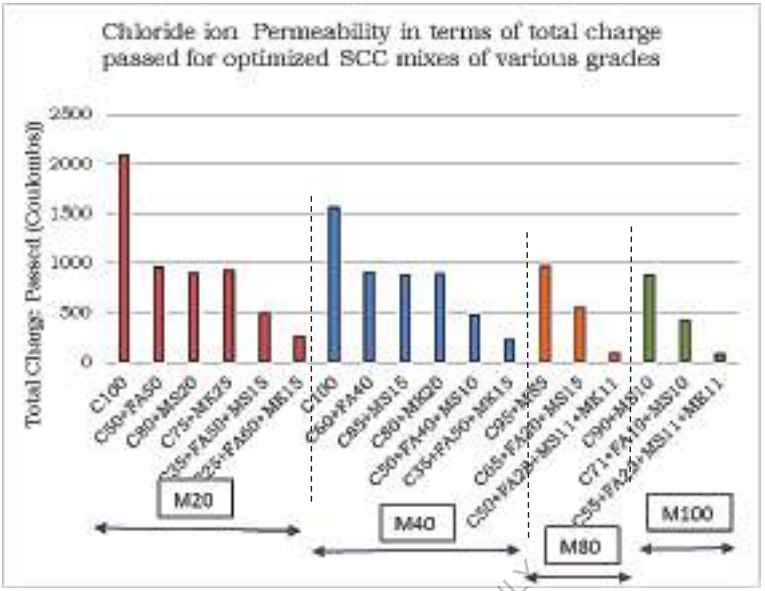

Fig 29- Total charge passed in coulombs for optimally blended SCC mixes of various grades

10.2 Chloride ion diffusivity

The impermeability of concrete can be represented by the rate of flow or diffusion coefficient of chloride ions through the unit area of concrete. Chloride diffusivity in terms of total charge passed through blended SCC using Rapid Chloride Penetration Test (RCPT) as per ASTM C 1202 is also investigated. The electric charge passed, Q in coulombs, obtained from Rapid chloride ion penetrability test was used to calculate Chloride Migration Diffusion Coefficient in steady state conditions from Berke's empirical Equation. The calculated diffusion coefficient values are shown in Table 59

Table 59- RCPT Criteria Ratings

Permeability Class	Electric Charge Passed as per ASTM C1202 (Coulombs)	Chloride Migration Diffusion Coefficients as per Concrete Society, United Kingdom (m^2/s)
High	> 4,000	$>5x10^{-12}$
Moderate	2,000 - 4,000	1 to 5 x 10^{-12}
Low	1,000 - 2,000	< 1 x 10^{-12}
Very Low	100 - 1,000	-
Negligible	< 100	-

(Source: http://darienelectricmadras.com)

Fig 30- Rapid Chloride Permeability Test Setup

The impermeability of concrete can be represented by the rate of flow or diffusion coefficient of chloride ions through the unit area of concrete. Chloride diffusivity is evaluated in terms of total charge passed of optimally blended binary, ternary and quaternary SCC mixes of ordinary grade (M20), standard grade (M40) and high strength grade (M80 and M100) made with Fly Ash (FA), Microsilica (MS) and Metakaolin (MK) at 28, 60 and 90.

The diffusivity of chloride through concrete therefore depends on the microstructure of the concrete. Diffusion Coefficient (DC) of chloride ions decreases in blended SCC mixes but with the introduction of metakaolin (MK) into SCC mixes further decrease is observed in the effective chloride ion diffusion coefficients. In the metakaolin (MK) blended SCC mixes pores are filled in such a way, modifying the original microstructure formed by the cement-sand matrix and subsequently increasing the tortuosity of the capillary network, resulting in longer paths and smaller pore diameters. It is already proved in previous investigations that quaternary blended SCC mix has improved microstructure which is dense and impermeable.

Total charge passed through the concrete depends on the electrical conductance, the lower loss of ignition value present in metakaolin (MK) might have contributed to the significant reduction in the electrical charge passed (chloride penetration). The incorporation of metakaolin or micro silica in SCC mixes reduce the chloride diffusion rate significantly.

Table 59 - Chloride Diffusion Coefficients for blended SCC specimens of various grades

Grade of SCC Mix	Mix No	Mix Designation (Values indicate percentage by weight of 'P')	Chloride Migration Diffusion Coefficient (DC)	Chloride Permeability as per Concrete Society, UK	Chloride Migration Diffusion Coefficient (DC)	Chloride Permeability as per Concrete Society, UK	Chloride Migration Diffusion Coefficient (DC)	Chloride Permeability as per Concrete Society, UK
			28 days		60 days		90 days	
M20	C1	C100	7.16 E-12	High	6.65 E-12	High	6.37 E-12	High
	B2	C50+FA50	5.01 E-12	High	3.38 E-12	Medium	3.32 E-12	Medium
	B7	C80+MS20	3.39 E-12	Medium	3.26 E-12	Medium	3.16 E-12	Medium
	B13	C75+MK25	3.40 E-12	Medium	3.30 E-12	Medium	3.23 E-12	Medium
	T3	C35+FA50+MS15	4.19 E-12	Medium	2.10 E-12	Medium	1.91 E-12	Medium
	T15	C25+FA60+MK15	3.91 E-12	Medium	1.36 E-12	Medium	1.12 E-12	Medium
M40	C1	C100	6.13 E-12	Medium	5.90 E-12	High	4.97 E-12	Medium
	B1	C60+FA40	4.59 E-12	Medium	3.26 E-12	Medium	3.18 E-12	Medium
	B5	C85+MS15	3.36 E-12	Medium	3.19 E-12	Medium	3.10 E-12	Medium
	B10	C80+MK20	3.38 E-12	Medium	3.21 E-12	Medium	3.13 E-12	Medium
	T5	C50+FA40+MS10	3.94 E-12	Medium	2.04 E-12	Medium	1.87 E-12	Medium
	T9	C35+FA50+MK15	3.68 E-12	Medium	1.28 E-12	Medium	1.01 E-12	Medium
M80	B2	C95+MS5	3.79 E-12	Medium	3.48 E-12	Medium	3.33 E-12	Medium
	T3	C65+FA20+MS15	3.47 E-12	Medium	2.43 E-12	Medium	2.10 E-12	Medium
	Q11	C50+FA28+MS11+MK11	2.01 E-12	Medium	0.89 E-12	Low	0.48 E-12	Low
M100	B2	C90+MS10	3.67 E-12	Medium	3.43 E-12	Medium	3.10 E-12	Medium
	T2	C71+FA19+MS10	3.37 E-12	Medium	1.93 E-12	Medium	1.69 E-12	Medium
	Q11	C55+FA23+MS11+MK11	1.70 E-12	Medium	0.72 E-12	Low	0.43 E-12	Low

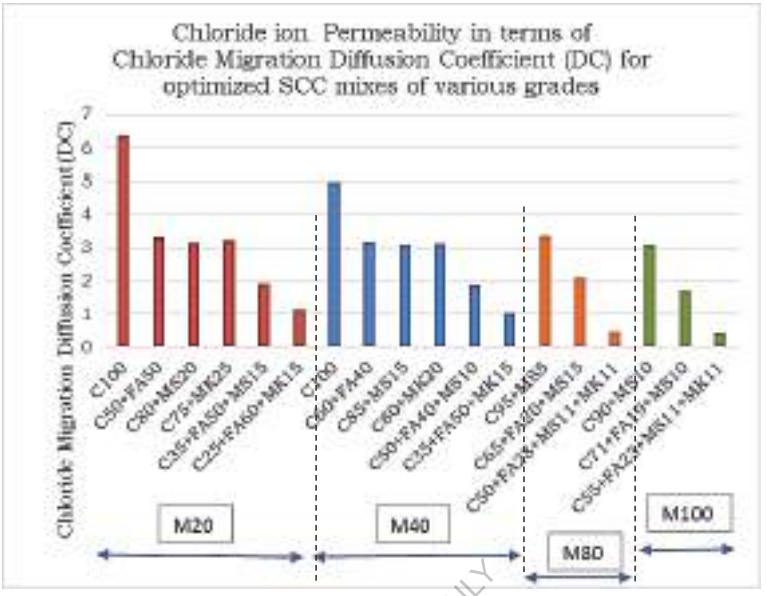

Fig 31- Chloride Diffusion Coefficients for optimized blended SCC mixes of various grades

10.3 Acid and Sulphate Attack Resistance

Chemical attack by aggressive water is one of the factors responsible for damage to concrete. Concrete can also be subjected to attack by various mineral acids such as sulphuric acid, hydrochloric acid etc. In natural ground water, only sulphuric acid is likely to be found as a result of the oxidation of sulphide minerals such as pyrites and marcasite. When concrete comes in contact with such acidic waters, the calcium hydroxide reacts with the sulphuric acid to form gypsum, which can be readily washed away. Sulphuric acid is also one of the main acidifying agents of acid rain. Much higher concentrations can occur in industrial environments. Another source of severe sulphuric acid attack, which is very common worldwide, is that which generates by bacteria in concrete sewage systems. Industrial waters contain enough sulphate ions to potentially damage the Portland cement concrete by forming deleterious soluble alkali sulphates. Investigations are carried out to study the effect of aggressive chemical environment in terms of loss of compressive strength and loss of weight in ordinary grade (M20), standard grade (M40) and high strength grade (M80 and M100) of binary, ternary and quaternary blended Self-Compacting Concrete (SCC) mixes made with optimum proportions of Fly Ash (FA), Microsilica (MS) and Metakaolin (MK) combination, exposed to 5% concentration of acids as shown below:

1) 5% Hydrochloric Acid (HCl)

Hydrochloric Acid of 35 – 38% LR with Specific gravity = 1.18 kg/lit.

2) 5% Sulphuric Acid (H_2SO_4)

Sulphuric Acid of 98% LR – Merk. M = 98.08 g/mol. Specific gravity = 1.84 kg/lit.

Concrete cubes of size 100mm x 100mm x 100mm, of ordinary grade (M20), standard grade (M40) and high strength grade (M80 and M100) of binary, ternary and quaternary blended Self-

Compacting Concrete (SCC) mixes made with optimum proportions of Fly Ash (FA), Microsilica (MS) and Metakaolin (MK) combination, are cast and cured for 28 days. They are immersed in acids considered for study. The percentage weight loss, percentage compressive strength loss is evaluated at 0 (after cured for 28 days), 30, and 60 days of exposure. The specimens are arranged in the plastic tubs in such a way that the clearance around and above the specimen is not less than 30 mm. The solution has been changed for an interval of every 15 days after taking the measurements. The response of the specimens to the solutions is evaluated through change in visual appearance, weight and compressive strength. Before testing, each specimen is removed from the tubs, and brushed with a soft nylon brush and rinsed in tap water. The relative strengths are always with respect to the 28 days value (i.e at the start of the test). The damage or deterioration, expressed as percentage loss in strength is calculated as follows:

$$\text{Damage (D)} = (1-(fs/fw)) * 100$$

Where, fs = the average compressive strength in MPa of three specimens cured in acid solution; fw = the average compressive strength in MPa of three specimens cured in water.

The objective of the present investigations is to study sulphate attack resistance in terms of loss of compressive strengths and loss of weights of ordinary grade (M20), standard grade (M40) and high strength grade (M80 and M100) of binary, ternary and quaternary blended Self-Compacting Concrete (SCC) mixes made with optimum proportions of Fly Ash (FA), Microsilica (MS) and Metakaolin (MK) combination, exposed to 5% concentrations of Na_2SO_4 and $MgSO_4$. Concrete cubes of size 100mm x 100mm x 100mm for the above stated SCC mixes are cast and cured for 28 days. The test procedure for acid resistance test was developed by modifying the related Standards for normal Portland cement and concrete (Standards-ASTM, 1993, 1995, 1997; Standards-Australia, 1996b). They are immersed in 5% concentration of Na_2SO_4 and $MgSO_4$. The percentage loss of compressive strengths and percentage loss of weights for all grades of blended SCC mixes are evaluated at 28, 30 and 60 days of exposure.

The damage, expressed as percentage loss in strength is calculated as follows:

$$\text{Damage (D)} = (1-(fs/fw)) * 100$$

Where, f_s = the average compressive strength in MPa of three specimens cured in sulphate solution; f_w = the average compressive strength in MPa of three specimens cured in water.

To study the effect of aggressive chemical environment in terms of loss of compressive strength and loss of weight in ordinary grade (M20), standard grade (M40) and high strength grade (M80 and M100) of binary, ternary and quaternary blended Self-Compacting Concrete (SCC) mixes made with Fly Ash (FA), Microsilica (MS) and Metakaolin (MK) exposed to different concentrations of acids as shown below:

3) 5% Hydrochloric Acid (HCl) [Hydrochloric Acid of 35 – 38% LR with Specific gravity = 1.18 kg/lit.]

2) 5% Sulphuric Acid (H_2SO_4) [Sulphuric Acid of 98% LR – Merk. M = 98.08 g/mol. Specific gravity = 1.84 kg/lit.]

The another objective of the present investigations is also to study sulphate attack resistance in terms of loss of compressive strengths and loss of weights of binary, ternary and quaternary blended Self-Compacting Concrete (SCC) mixes exposed to 5% concentrations of Na_2SO_4 and $MgSO_4$ sulphates.

(a) 5% H_2SO_4 } ACIDS
(b) 5% HCL }
(c) 5% Na_2SO_4 } SULPHATES
(d) 5% $MgSO_4$ }

Calculations for Normality of Acids

a) Sulphuric Acid (H_2SO_4)

Purity of the Acid	98%
Specific gravity	1.835
Molecular weight	98.07
Molarity of acid	= {(purity)x10x(specific gravity)}/Molecular weight
	= (98x10x1.835)/98.07
	= 18.336M
Normality of acid	= (18.336x2)
	= 36.672N
5% H_2SO_4 is diluted in 18000ml of water	=900 ml
Total Solution	=18000 + 900
	= 18900 ml
Molarity of the solution	= (18.366 x 900)/18900
	= 0.87
Normality of 5% H_2SO_4	= 0.87 x 2
	=1.75

b) Hydrochloric Acid (HCl)

Purity of the Acid	36.5%
Specific gravity	1.18
Molecular weight	36.46
Molarity of acid	= {(purity)x10x(specific gravity)}/Molecular weight
	= (36.5x10x1.18)/36.46
	= 11.81M
Normality of acid	= (11.81x1)
	= 11.81N
5% HCl is diluted in 18000ml	=900 ml of water
Total Solution	=18000 + 900
	= 18900 ml
Molarity of the solution	= (11.81 x 900)/18900
	= 0.56
Normality of 5% HCl	= 0.56 x 1
	= 0.56

The table 60 to 65 shows the Compressive strengths, Weights, percentage loss of compressive strength and percentage weight loss of optimally blended binary, ternary and quaternary SCC mixes of ordinary grade (M20), standard grade (M40) and high strength grade (M80 and M100) made with Fly Ash (FA), Microsilica (MS) and Metakaolin (MK) at 30 and 60 days of exposure to acids and Sulphates.

Table 60 - Compressive strengths and Weights of Ordinary (M20) grade SCC specimens exposed to different concentrations of various acids

Grade of Concrete - Ordinary M20 Grade SCC								
Acid Exposure	Mix No	Mix Designation (Values indicate percentage by weight of 'P')	Compressive Strength (MPa)			Weights (kg)		
			Days of Immersion			Days of Immersion		
			0*	30	60	0*	30	60
5% HCL	C1	C100	29.22	26.87	25.33	2.54	2.33	2.18
	B2	C50+FA50	33.21	31.05	30.17	2.54	2.33	2.22
	B7	C80+MS20	29.89	28.27	27.74	2.54	2.34	2.22
	B13	C75+MK25	31.29	29.82	29.39	2.54	2.35	2.25
	T3	C35+FA50+MS15	35.67	34.71	34.42	2.54	2.36	2.27
	T15	C25+FA60+MK15	37.81	37.32	37.27	2.54	2.37	2.31
5% H_2SO_4	C1	C100	29.22	24.19	22.77	2.54	2.56	2.03
	B2	C50+FA50	33.21	29.19	28.23	2.54	2.55	2.37
	B7	C80+MS20	29.89	27.08	25.93	2.54	2.56	2.08
	B13	C75+MK25	31.29	28.39	27.78	2.54	2.56	2.09
	T3	C35+FA50+MS15	35.67	34.17	33.7	2.54	2.55	2.4
	T15	C25+FA60+MK15	37.81	36.49	36.33	2.54	2.55	2.43
5% Na_2SO_4	C1	C100	29.22	26.51	25.1	2.54	2.56	2.15
	B2	C50+FA50	33.21	30.78	29.45	2.54	2.55	2.45
	B7	C80+MS20	29.89	28.11	27.16	2.54	2.56	2.19
	B13	C75+MK25	31.29	29.56	29.37	2.54	2.56	2.2
	T3	C35+FA50+MS15	35.67	34.62	34.21	2.54	2.55	2.5
	T15	C25+FA60+MK15	37.81	37.28	37.04	2.54	2.55	2.51
5% $MgSO_4$	C1	C100	29.22	24.77	23.18	2.54	2.56	2.13
	B2	C50+FA50	33.21	29.87	29.09	2.54	2.55	2.42
	B7	C80+MS20	29.89	27.31	26.19	2.54	2.56	2.18
	B13	C75+MK25	31.29	28.67	28.11	2.54	2.56	2.19
	T3	C35+FA50+MS15	35.67	34.57	33.92	2.54	2.55	2.46
	T15	C25+FA60+MK15	37.81	37.1	36.99	2.54	2.55	2.49

** Compressive strength and weights of concrete specimens at '0' days of Immersion is taken as the reference compressive strength and initial weight, after 90 days curing, before the immersion into the acids.*

Table 61 - % loss of Compressive strengths and % loss of Weights of Ordinary (M20) grade SCC specimens exposed to different concentrations of various acids

Grade of Concrete - Ordinary M20 Grade SCC								
Acid Exposure	Mix No	Mix Designation (Values indicate percentage by weight of 'P')	% loss of Compressive Strength(MPa)			% Loss of Weights (kg)		
			Days of Immersion			Days of Immersion		
			0*	30	60	0*	30	60
5% HCL	C1	C100	-	8.04	13.31	-	8.27	14.17
	B2	C50+FA50	-	6.50	9.15	-	8.27	12.60
	B7	C80+MS20	-	5.42	7.19	-	7.87	12.60
	B13	C75+MK25	-	4.70	6.07	-	7.48	11.42
	T3	C35+FA50+MS15	-	2.69	3.50	-	7.09	10.63
	T15	C25+FA60+MK15	-	1.30	1.43	-	6.69	9.06
$5\%\ H_2SO_4$	C1	C100	-	17.21	22.07	-	-0.79	20.08
	B2	C50+FA50	-	12.10	15.00	-	-0.39	6.69
	B7	C80+MS20	-	9.40	13.25	-	-0.79	18.11
	B13	C75+MK25	-	9.27	11.22	-	-0.79	17.72
	T3	C35+FA50+MS15	-	4.21	5.52	-	-0.39	5.51
	T15	C25+FA60+MK15	-	3.49	3.91	-	-0.39	4.33
$5\%\ Na_2SO_4$	C1	C100	-	9.27	14.10	-	-0.79	15.35
	B2	C50+FA50	-	7.32	11.32	-	-0.39	3.54
	B7	C80+MS20	-	5.96	9.13	-	-0.79	13.78
	B13	C75+MK25	-	5.53	6.14	-	-0.79	13.39
	T3	C35+FA50+MS15	-	2.94	4.09	-	-0.39	1.57
	T15	C25+FA60+MK15	-	1.40	2.04	-	-0.39	1.18
$5\%\ MgSO_4$	C1	C100	-	15.23	20.67	-	-0.79	16.14
	B2	C50+FA50	-	10.06	12.41	-	-0.39	4.72
	B7	C80+MS20	-	8.63	12.38	-	-0.79	14.17
	B13	C75+MK25	-	8.37	10.16	-	-0.79	13.78
	T3	C35+FA50+MS15	-	3.08	4.91	-	-0.39	3.15
	T15	C25+FA60+MK15	-	1.88	2.17	-	-0.39	1.97

** Compressive strength and weights of concrete specimens at '0' days of Immersion is taken as the reference compressive strength and initial weight, after 28 days curing, before the immersion into the acids.*

The Fig 32 to 39 shows the variation of percentage loss of compressive strength and variation of percentage weight loss of optimally blended binary, ternary and quaternary SCC mixes of ordinary grade (M20), standard grade (M40) and high strength grade (M80 and M100) made with Fly Ash (FA), Microsilica (MS) and Metakaolin (MK) at 30 and 60 days of exposure to acids and Sulphates.

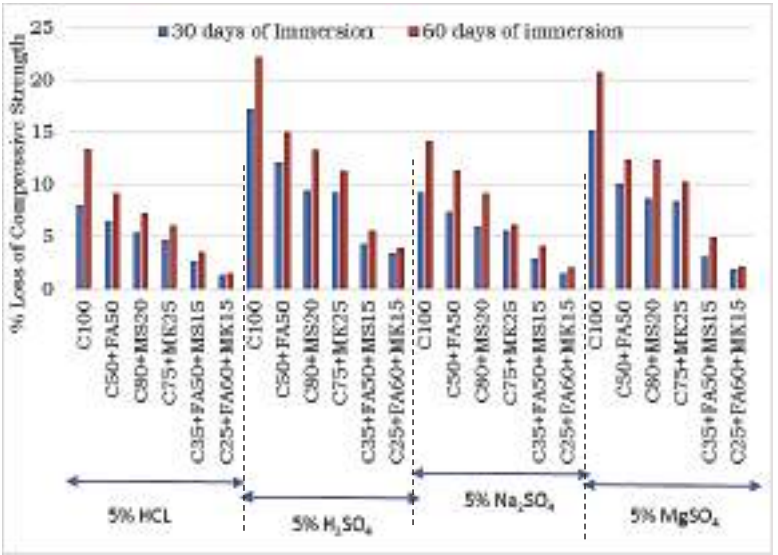

Fig 32- Variation of % loss of Compressive strengths of Ordinary (M20) grade SCC specimens exposed to different concentrations of various acids

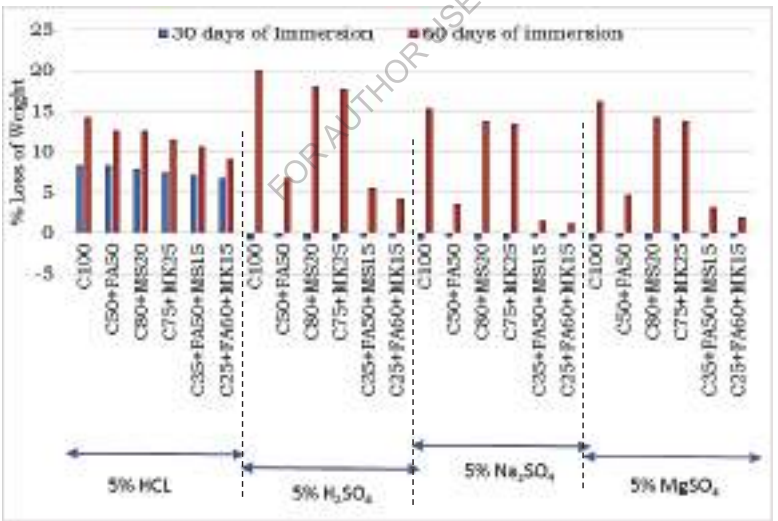

Fig 33- Variation of % loss of Weight of Ordinary (M20) grade SCC specimens exposed to different concentrations of various acids

Table 62 - Compressive strengths and Weights of Standard (M40) grade SCC specimens exposed to different concentrations of various acids

Grade of Concrete - Standard (M40) Grade SCC								
Acid Exposure	Mix No	Mix Designation (Values indicate percentage by weight of 'P')	Compressive Strength(MPa)			Weights (kg)		
			Days of Immersion			Days of Immersion		
			0*	30	60	0*	30	60
5% HCL	C1	C100	48.72	46.37	44.83	2.55	2.39	2.21
	B1	C50+FA50	52.71	50.55	49.67	2.55	2.39	2.25
	B5	C80+MS20	49.39	47.77	47.24	2.55	2.4	2.25
	B10	C75+MK25	50.79	49.32	48.89	2.55	2.41	2.28
	T5	C35+FA50+MS15	55.17	54.21	53.92	2.55	2.42	2.3
	T9	C25+FA60+MK15	57.31	56.82	56.77	2.55	2.43	2.34
5% H_2SO_4	C1	C100	48.72	43.69	42.27	2.55	2.62	2.06
	B1	C50+FA50	52.71	48.69	47.73	2.55	2.61	2.4
	B5	C80+MS20	49.39	46.58	45.43	2.55	2.62	2.11
	B10	C75+MK25	50.79	47.89	47.28	2.55	2.62	2.12
	T5	C35+FA50+MS15	55.17	53.67	53.2	2.55	2.61	2.43
	T9	C25+FA60+MK15	57.31	55.99	55.83	2.55	2.61	2.46
5% Na_2SO_4	C1	C100	48.72	46.01	44.6	2.55	2.62	2.18
	B1	C50+FA50	52.71	50.28	48.95	2.55	2.61	2.48
	B5	C80+MS20	49.39	47.61	46.66	2.55	2.62	2.22
	B10	C75+MK25	50.79	49.06	48.87	2.55	2.62	2.23
	T5	C35+FA50+MS15	55.17	54.12	53.71	2.55	2.61	2.53
	T9	C25+FA60+MK15	57.31	56.78	56.54	2.55	2.61	2.54
5% $MgSO_4$	C1	C100	48.72	44.27	42.68	2.55	2.62	2.16
	B1	C50+FA50	52.71	49.37	48.59	2.55	2.61	2.45
	B5	C80+MS20	49.39	46.81	45.69	2.55	2.62	2.21
	B10	C75+MK25	50.79	48.17	47.61	2.55	2.62	2.22
	T5	C35+FA50+MS15	55.17	54.07	53.42	2.55	2.61	2.49
	T9	C25+FA60+MK15	57.31	56.6	56.49	2.55	2.61	2.52

** Compressive strength and weights of concrete specimens at '0' days of Immersion is taken as the reference compressive strength and initial weight , after 28 days curing, before the immersion into the acids.*

Table 63 - % loss of Compressive strengths and % loss of Weights of Standard (M40) grade SCC specimens exposed to different concentrations of various acids

Grade of Concrete - Standard (M40) Grade SCC								
Acid Exposure	Mix No	Mix Designation (Values indicate percentage by weight of 'P')	% Loss of Compressive Strength(MPa)			% Loss of Weight (kg)		
			Days of Immersion			Days of Immersion		
			0*	30	60	0*	30	60
5% HCL	C1	C100	-	4.82	7.98	-	6.27	13.33
	B1	C50+FA50	-	4.10	5.77	-	6.27	11.76
	B5	C80+MS20	-	3.28	4.35	-	5.88	11.76
	B10	C75+MK25	-	2.89	3.74	-	5.49	10.59
	T5	C35+FA50+MS15	-	1.74	2.27	-	5.10	9.80
	T9	C25+FA60+MK15	-	0.85	0.94	-	4.71	8.24
5% H_2SO_4	C1	C100	-	10.32	13.24	-	-2.75	19.22
	B1	C50+FA50	-	7.63	9.45	-	-2.35	5.88
	B5	C80+MS20	-	5.69	8.02	-	-2.75	17.25
	B10	C75+MK25	-	5.71	6.91	-	-2.75	16.86
	T5	C35+FA50+MS15	-	2.72	3.57	-	-2.35	4.71
	T9	C25+FA60+MK15	-	2.30	2.58	-	-2.35	3.53
5% Na_2SO_4	C1	C100	-	5.56	8.46	-	-2.75	14.51
	B1	C50+FA50	-	4.61	7.13	-	-2.35	2.75
	B5	C80+MS20	-	3.60	5.53	-	-2.75	12.94
	B10	C75+MK25	-	3.41	3.78	-	-2.75	12.55
	T5	C35+FA50+MS15	-	1.90	2.65	-	-2.35	0.78
	T9	C25+FA60+MK15	-	0.92	1.34	-	-2.35	0.39
5% $MgSO_4$	C1	C100	-	9.13	12.40	-	-2.75	15.29
	B1	C50+FA50	-	6.34	7.82	-	-2.35	3.92
	B5	C80+MS20	-	5.22	7.49	-	-2.75	13.33
	B10	C75+MK25	-	5.16	6.26	-	-2.75	12.94
	T5	C35+FA50+MS15	-	1.99	3.17	-	-2.35	2.35
	T9	C25+FA60+MK15	-	1.24	1.43	-	-2.35	1.18

** Compressive strength and weights of concrete specimens at '0' days of Immersion is taken as the reference compressive strength and initial weight, after 28 days curing, before the immersion into the acids.*

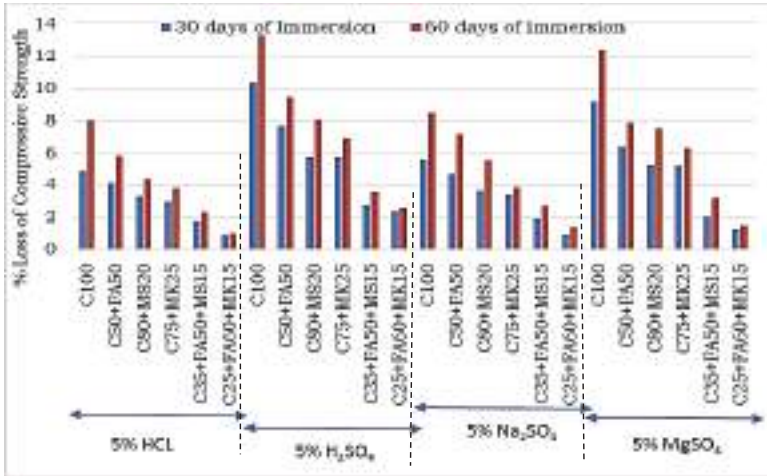

Fig 34- Variation of % loss of Compressive strengths of standard (M40) grade SCC specimens exposed to different concentrations of various acids

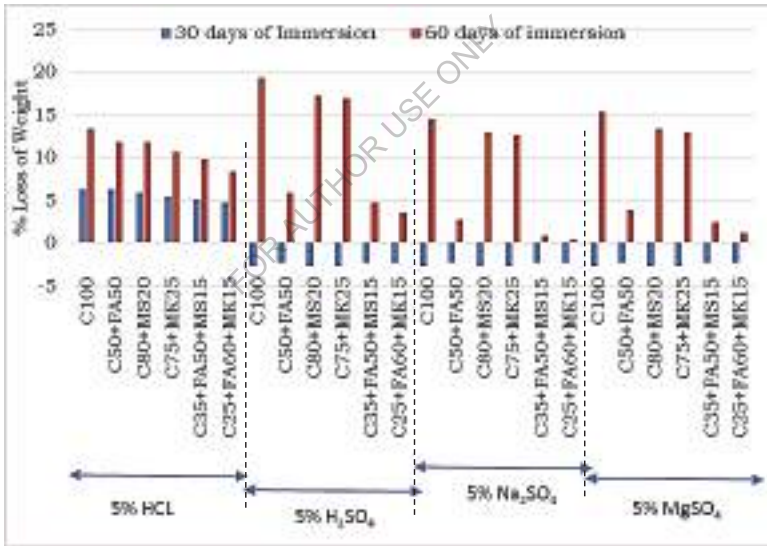

Fig 35- Variation of % loss of Weight of Standard (M40) grade SCC specimens exposed to different concentrations of various acids

Table 64 - Compressive strengths and Weights of High Strength (M80 and M100) grade SCC specimens exposed to different concentrations of various acids

Type of specimen	Acid Exposure	Combinations	Compressive Strength(MPa)			Weight (kg)		
			Days of Immersion			Days of Immersion		
			0*	30	60	0*	30	60
M80 Grade SCC	5% HCL	C85+MS15	91.89	90.27	89.74	2.55	2.46	2.28
		C65+FA20+MS15	97.67	96.71	96.42	2.55	2.46	2.32
		C50+FA30+MS10+MK10	99.81	99.32	99.27	2.55	2.47	2.32
	5% H_2SO_4	C85+MS15	91.89	89.08	87.93	2.55	2.48	2.35
		C65+FA20+MS15	97.67	96.17	95.7	2.55	2.49	2.37
		C50+FA30+MS10+MK10	99.81	98.49	98.33	2.55	2.50	2.41
	5% Na_2SO_4	C85+MS15	91.89	90.11	89.16	2.55	2.70	2.12
		C65+FA20+MS15	97.67	96.62	96.21	2.55	2.69	2.47
		C50+FA30+MS10+MK10	99.81	99.28	99.04	2.55	2.70	2.57
	5% $MgSO_4$	C85+MS15	91.89	89.31	88.19	2.55	2.70	2.18
		C65+FA20+MS15	97.67	96.57	95.92	2.55	2.69	2.50
		C50+FA30+MS10+MK10	99.81	99.1	98.99	2.55	2.69	2.53
M100 Grade SCC	5% HCL	C90+MS10	117.39	115.77	115.24	2.55	2.70	2.25
		C70+FA20+MS10	123.17	122.21	121.92	2.55	2.69	2.55
		C55+FA25+MS10+MK10	125.31	124.82	124.77	2.55	2.70	2.59
	5% H_2SO_4	C90+MS10	117.39	114.58	113.43	2.55	2.70	2.30
		C70+FA20+MS10	123.17	121.67	121.2	2.55	2.69	2.61
		C55+FA25+MS10+MK10	125.31	123.99	123.83	2.55	2.69	2.62
	5% Na_2SO_4	C90+MS10	117.39	115.61	114.66	2.55	2.70	2.22
		C70+FA20+MS10	123.17	122.12	121.71	2.55	2.69	2.52
		C55+FA25+MS10+MK10	125.31	124.78	124.54	2.55	2.70	2.58
	5% $MgSO_4$	C90+MS10	117.39	114.81	113.69	2.55	2.70	2.29
		C70+FA20+MS10	123.17	122.07	121.42	2.55	2.69	2.56
		C55+FA25+MS10+MK10	125.31	124.6	124.49	2.55	2.69	2.60

** Compressive strength and weights of concrete specimens at '0' days of Immersion is taken as the reference compressive strength and initial weight, after 28 days curing, before the immersion into the acids.*

Table 65 - % loss of Compressive strengths and % loss of Weights of High Strength (M80 and M100) grade SCC specimens exposed to different concentrations of various acids

Type of specimen	Acid Exposure	Combinations	% Loss of Compressive Strength(MPa)			% Loss of Weight (kg)		
			Days of Immersion			Days of Immersion		
			0*	30	60	0*	30	60
M80 Grade SCC	5% HCL	C85+MS15	-	1.76	2.34	-	3.53	10.59
		C65+FA20+MS15	-	0.98	1.28	-	3.53	9.02
		C50+FA30+MS10+MK10	-	0.49	0.54	-	3.14	9.02
	5% H_2SO_4	C85+MS15	-	3.06	4.31	-	2.75	7.84
		C65+FA20+MS15	-	1.54	2.02	-	2.35	7.06
		C50+FA30+MS10+MK10	-	1.32	1.48	-	1.96	5.49
	5% Na_2SO_4	C85+MS15	-	1.94	2.97	-	-5.88	16.86
		C65+FA20+MS15	-	1.08	1.49	-	-5.49	3.14
		C50+FA30+MS10+MK10	-	0.53	0.77	-	-5.88	-0.78
	5% $MgSO_4$	C85+MS15	-	2.81	4.03	-	-5.88	14.51
		C65+FA20+MS15	-	1.13	1.79	-	-5.49	1.96
		C50+FA30+MS10+MK10	-	0.71	0.82	-	-5.49	0.78
M100 Grade SCC	5% HCL	C90+MS10	-	1.38	1.83	-	-5.88	11.76
		C70+FA20+MS10	-	0.78	1.01	-	-5.49	0.00
		C55+FA25+MS10+MK10	-	0.39	0.43	-	-5.88	-1.57
	5% H_2SO_4	C90+MS10	-	2.39	3.37	-	-5.88	9.80
		C70+FA20+MS10	-	1.22	1.60	-	-5.49	-2.35
		C55+FA25+MS10+MK10	-	1.05	1.18	-	-5.49	-2.75
	5% Na_2SO_4	C90+MS10	-	1.52	2.33	-	-5.88	12.94
		C70+FA20+MS10	-	0.85	1.19	-	-5.49	1.18
		C55+FA25+MS10+MK10	-	0.42	0.61	-	-5.88	-1.18
	5% $MgSO_4$	C90+MS10	-	2.20	3.15	-	-5.88	10.20
		C70+FA20+MS10	-	0.89	1.42	-	-5.49	-0.39
		C55+FA25+MS10+MK10	-	0.57	0.65	-	-5.49	-1.96

** Compressive strength and weights of concrete specimens at '0' days of Immersion is taken as the reference compressive strength and initial weight, after 28 days curing, before the immersion into the acids.*

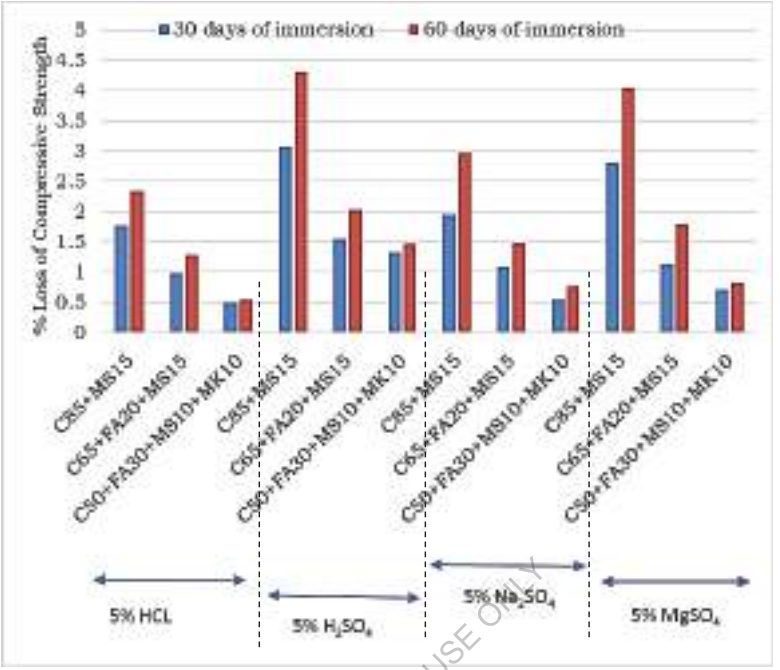

Fig 36- Specimens exposed to different concentrations of various acids

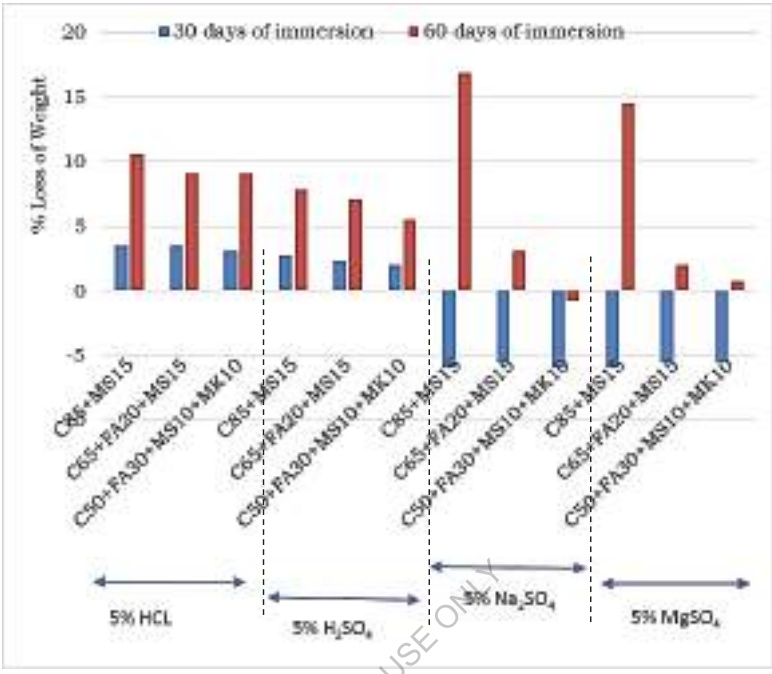

Fig 37- Variation of % loss of Weight of high strength (M80) grade SCC specimens exposed to different concentrations of various acids

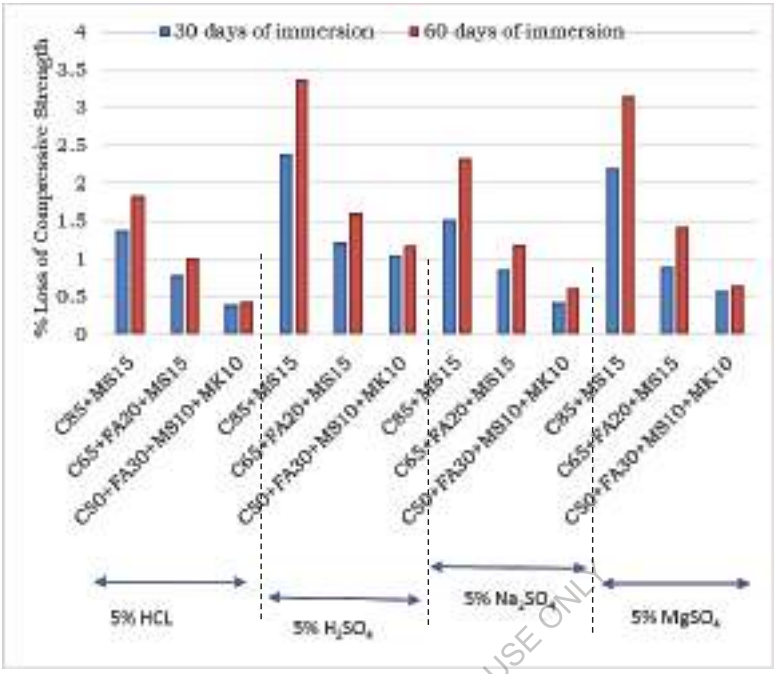

Fig 38- Variation of % loss of Compressive strengths of high strength (M100) grade SCC specimens exposed to different concentrations of various acids

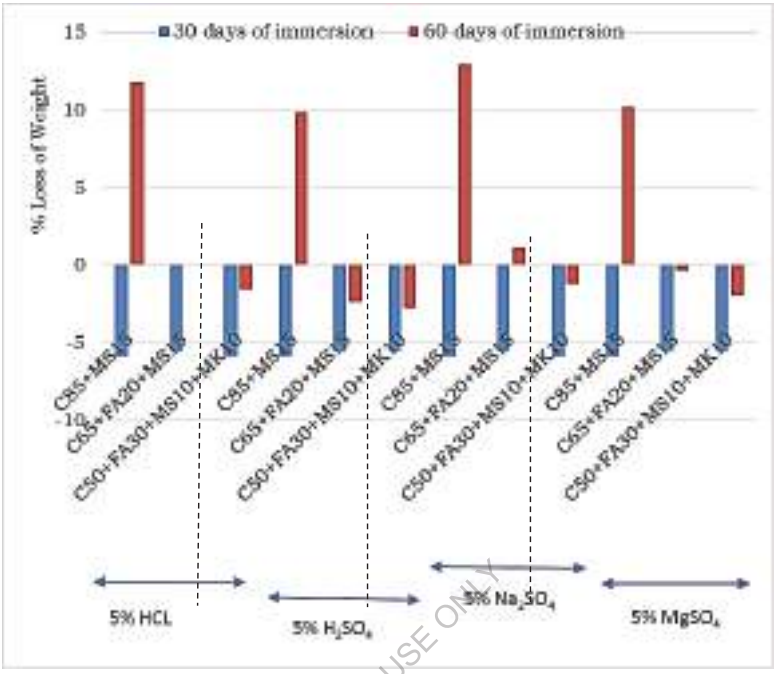

Fig 39- Variation of % loss of Weight of high strength (M100) grade SCC specimens exposed to different concentrations of various acids

The HCL acid attack is identified by formation of unique brownish belts on the surface of specimens. These belts on the surface are completely peeled off with time. Due to the peeling off the surface, the specimens undergo a higher amount of mass loss compared to what is experienced in H2SO4 acid attack. In specimens exposed to increasing periods of HCL acid attack, the surface becomes more brittle and denseness is reduced. In HCL acid attack, calcium hydroxide in concrete dissolves in acid and the reaction product is formed is calcium chloride, which is highly soluble in water and therefore is leached out of the mortar without forming micro cracks that can affect the internal structure and hence the strength characteristics of concrete. This type of action has more effect on the mass loss, as has been observed from the peeling off of the surface of specimens in HCL acid attack. So in HCL attack major mass loss occurs without any major loss of strength.

In specimens exposed to H2SO4 acid attack showed no noticeable change in color but surface becomes more brittle and denseness is greatly reduced. Even after long term exposure H2SO4 specimens were seen to remain structurally intact though surface turned a little softer. When H2SO4 comes in contact with concrete, it reacts with Ca(OH)2 and calcium aluminate hydrate to form gypsum and ettringite, leading to an increase in initial weight in early days of exposure. The solubility of the gypsum so formed is low and therefore its dissolution does not take place. The formation of unstable ettringite causes the concrete matrix to be more porous and susceptible to the acid attack through the capillary pores. On the other hand, these reaction products have very

low structural stability in comparison to the reactants they replace. They involve an increase in volume and therefore occupy the space available as voids in concrete, leading to an increase in initial weight. However, after some time, the continued expansion causes cracking that ultimately leads to peeling off of the surface layer of concrete, as indicated by the mass loss of concrete that starts after approximately 30 days of exposure to the sulfuric acid solution. Since in H2SO4 the reaction products formed are not soluble but are expansive in nature, which therefore can cause micro cracking, so in H2SO4 there will be high loss of strength and but lesser mass loss. Sulphuric acid is very damaging to concrete as it combines an acid attack and sulphate attack. The percentage loss of compressive strength and weight in H2SO4 solution is higher than HCL.

In the case of HCL acid attack, the calcium salt formed is soluble in water, leading to higher mass losses. On the other hand, in the case of sulfuric acid attack, the calcium salt formed is not soluble in water, getting deposited in the voids and causing internal stresses leading to disruption and strength loss of the matrix.

A characteristic whitish appearance is the indication of sulphate attack. The term sulphate attack denote an increase in the volume of cement paste in concrete or mortar due to the chemical action between the products of hydration of cement and solution containing sulphates. Because of the increase in volume of the solid phase gradual disintegration of concrete takes place. The deteriorating effect usually starts at the surface and corners and progressively enters into the concrete by causing scaling and spalling and finally reduces the concrete to a friable mass.

In specimens exposed to Na_2SO_4, the surface is more brittle and porous but no deterioration is observed on the surface. $MgSO_4$ formed a hard dense skin on concrete due to the deposition of magnesium hydroxide in the pores. The strength of the specimens exposed to solution of sodium sulphate was found to be higher in the initial stages of hydration. The increase in values of pH and conductivity of sodium sulphate solution has resulted in increased strength at all ages of exposure. The attack of sodium sulfate on concrete is due to two principal reactions: the reaction of Na_2SO_4 and $Ca(OH)_2$ to form gypsum and the reaction of the formed gypsum with calcium aluminate hydrates to form ettringite.

Magnesium Sulphate also forms gypsum and ettringite like Na_2SO_4 , in addition to that it reacts with all cement compounds, including Calcium Silicate Hydrates [C-S-H]. The Magnesium Hydroxide, which is formed due to reaction between $MgSO_4$ and $Ca(OH)_2$, reacts with C-S-H gel to form Magnesium Silicate Hydrate [M-S-H], being a soft material and affects the strength and durability of concrete. Failure by expansion of concrete in the presence of Sulphate is due to the formation of Ettringite. So specimens soaked in magnesium sulfates experienced weight gain and expansion due to ettringate. The formation of unstable ettringite in Na_2SO_4 and $MgSO_4$ causes the concrete matrix to be more porous and susceptible to the sulphate attack through the capillary pores. The Magnesium Sulphate environment is more severe than Sodium Sulphate environment because it reacts with C-S-H gel and disintegrates it reducing the compressive strength drastically. So it can be confirmed that metakaolin blended binary, ternary and quaternary SCC mixes of all grades exhibit improved resistance to acids and sulphates due to its enhanced pore structure. This might account for the lower permeability and improved durability of concrete containing metakaolin (MK). In the microstructure of metakaolin (MK) blended SCC mixes pores are modified resulting in longer paths and smaller pore diameters. The resistance of metakaolin based quaternary blended SCC mix to chemical attack is mainly due to its improved microstructure which is dense, impermeable and highly alkaline in nature.

10.4 Seawater Resistance

Sea water is a complex solution of many salts containing living matter, suspended silt, dissolved gases and decaying organic material. The average salt concentration of sea water is about 3.5% although it varies from sea to sea depending upon geological location. Seawater containing up to 35,000 ppm of dissolved salts is generally suitable as mixing water for concrete not containing steel. About 78% of the salt is sodium chloride, and 15% is chloride and sulfate of magnesium. Sodium or potassium in salts present in seawater used for mix water can aggravate alkali-aggregate reactivity. Thus, seawater should not be used as mix water for concrete with potentially alkali-reactive aggregates. Calcium chloro-aluminate hydrate (3CaO.Ab03.CaCb.l0H20), also known as Friedel's salt, is an important phase formed during the exposure of concrete to seawater.
In the present investigation, to study the effect of marine environment in terms of loss of compressive strength and loss of weight of ordinary grade (M20), standard grade (M40) and high strength grade (M80 and M100) of binary, ternary and quaternary blended Self-Compacting Concrete (SCC) mixes made with optimum proportions of Fly Ash (FA), Microsilica (MS) and Metakaolin (MK) combination. The amounts of salts in Table 4.6 were dissolved in plain water to prepare 1000gm of sea water of 1N concentration. Cubes of 100 x 100mm size were weighed and immersed in water diluted with composition of sea water prepared in the laboratory as per ASTM D1141 for 90 days continuously and then the cubes were taken out and weighed. The damage, expressed as percentage loss in strength is calculated as follows:

$$\text{Damage (D)} = (1-(fs/fw)) * 100$$

Where, f_s = the average compressive strength in MPa of three specimens cured in salt solution; f_w = the average compressive strength in MPa of three specimens cured in water.

Table 66- Composition of artificial sea water as per ASTM D1141

Composition	Concentration, g/lit
Sodium chloride	24.53
Magnesium chloride	5.2
Sodium sulphate	4.09
Calcium chloride	1.16
Potassium chloride	0.695

The table 70 and 71 shows the Compressive strengths, Weights, percentage loss of compressive strength and percentage weight loss of optimally blended binary, ternary and quaternary SCC mixes of ordinary grade (M20), standard grade (M40) and high strength grade (M80 and M100) made with Fly Ash (FA), Microsilica (MS) and Metakaolin (MK) at 30 and 60 days of exposure to seawater.

Table 70 - Compressive strengths and Weights of various grades of SCC specimens exposed to sea water

Grade of SCC	Combinations	Compressive Strength(MPa)			Weights (kg)		
		Days of Immersion			Days of Immersion		
		0*	30	60	0*	30	60
M20	C100	29.22	26.38	21.34	2.54	2.42	2.30
	C50+FA50	33.21	30.71	26.38	2.54	2.44	2.32
	C80+MS20	29.89	27.11	22.21	2.54	2.45	2.33
	C75+MK25	31.29	28.64	23.99	2.54	2.46	2.34
	C35+FA50+MS15	35.67	33.34	29.35	2.54	2.49	2.37
	C25+FA60+MK15	37.81	35.61	31.88	2.54	2.50	2.38
M40	C100	48.72	47.02	44.19	2.55	2.44	2.32
	C60+FA40	52.71	51.14	48.53	2.55	2.46	2.34
	C85+MS15	49.39	47.71	44.92	2.55	2.47	2.35
	C80+MK20	50.79	49.16	46.45	2.55	2.48	2.36
	C50+FA40+MS10	55.17	53.67	51.19	2.55	2.51	2.38
	C35+FA50+MK15	57.31	55.86	53.48	2.55	2.53	2.40
M80	C85+MS15	91.89	90.99	89.52	2.55	2.47	2.35
	C65+FA20+MS15	97.67	96.82	95.45	2.55	2.52	2.39
	C50+FA30+MS10+MK10	99.81	98.98	97.63	2.55	2.54	2.41
M100	C90+MS10	117.39	116.68	115.54	2.55	2.47	2.35
	C70+FA20+MS10	123.17	122.50	121.41	2.55	2.52	2.39
	C55+FA25+MS10+MK10	125.31	124.65	123.58	2.55	2.55	2.42

** Compressive strength and weights of concrete specimens at '0' days of Immersion is taken as the reference compressive strength and initial weight, after 28 days curing, before the immersion into the acids.*

Table 71 - % loss of Compressive strengths and % loss of Weights of various grades of SCC specimens exposed to sea water

Grade of SCC	Combinations	Compressive Strength(MPa)			Weights (kg)		
		Days of Immersion			Days of Immersion		
		0*	30	60	0*	30	60
M20	C100	-	9.72	26.98	-	4.72	9.45
	C50+FA50	-	7.53	20.57	-	3.94	8.66
	C80+MS20	-	9.29	25.70	-	3.54	8.27
	C75+MK25	-	8.48	23.32	-	3.15	7.87
	C35+FA50+MS15	-	6.52	17.71	-	1.97	6.69
	C25+FA60+MK15	-	5.81	15.68	-	1.57	6.30
M40	C100	-	3.50	9.30	-	4.31	9.02
	C60+FA40	-	2.99	7.92	-	3.53	8.24
	C85+MS15	-	3.40	9.05	-	3.14	7.84
	C80+MK20	-	3.22	8.54	-	2.75	7.45
	C50+FA40+MS10	-	2.73	7.22	-	1.57	6.67
	C35+FA50+MK15	-	2.53	6.68	-	0.78	5.88
M80	C85+MS15	-	0.98	2.57	-	3.14	7.84
	C65+FA20+MS15	-	0.87	2.28	-	1.18	6.27
	C50+FA30+MS10+MK10	-	0.83	2.18	-	0.39	5.49
M100	C90+MS10	-	0.60	1.57	-	4.72	9.45
	C70+FA20+MS10	-	0.55	1.43	-	3.94	8.66
	C55+FA25+MS10+MK10	-	0.53	1.38	-	3.54	8.27

** Compressive strength and weights of concrete specimens at '0' days of Immersion is taken as the reference compressive strength and initial weight, after 28 days curing, before the immersion into the acids.*

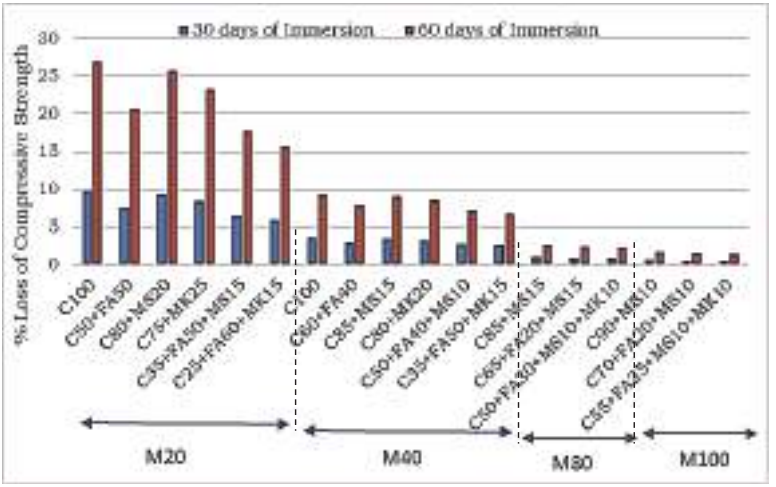

Fig 40- Variation of % loss of Compressive Strength of various grades of SCC specimens exposed to different concentrations of various acids

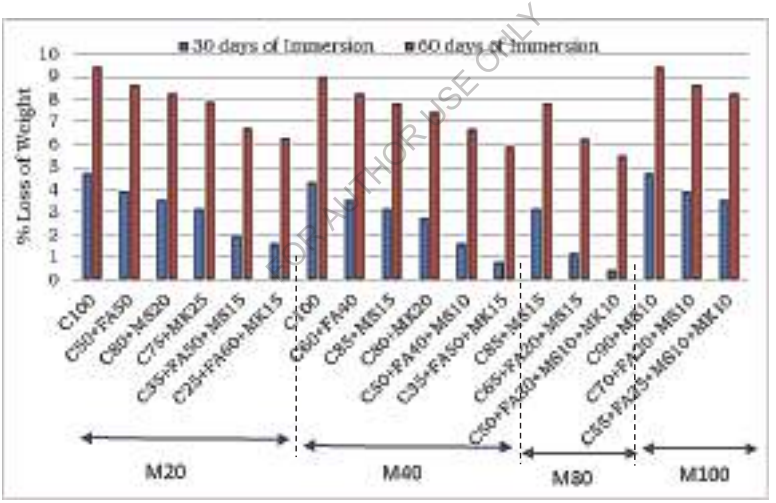

Fig 41-Variation of % loss of Weight of various grades of SCC specimens exposed to different concentrations of various acids

From the results it has been observed that Metakaolin (MK) based optimally blended binary, ternary and quaternary SCC mixes of ordinary grade (M20), standard grade (M40) and high strength grade (M80 and M100) were less attacked by sea water and are more durable. The percentage loss of weights and percentage loss of compressive strengths of Metakaolin (MK) based SCC mixes of various grades in sea water are less. Blended SCC mixes are more impermeable to attack by sea water. In a marine environment, chloride ion and sulfate ion penetrating into the concrete from sea water forming calcium chloroaluminate (Friedels Salt) and calcium sulphoaluminate (Ettringite). These products will occupy a greater volume after crystallization in the pores of concrete than the compounds they replace disrupting the integrity of concrete reducing the compressive strength considerably. The formation of gypsum hydrate causes an increase in volume of concrete. This effect is not observed in blended SCC mixes because of dense pore structure and less porosity.

Metakaolin (MK) based blended SCC mixes exhibits better resistance to sea water attack than any other SCM based SCC due to enhanced pore refinement in the microstructure of concrete and reduction of the interconnectivity of the pore structure by decreasing the pore size (pores refinement), which is directly related to durability.

10.5 Water Absorption Capacity and Porosity

The objective of this study is to determine the total water absorption capacity and measure the volume of voids present in ordinary grade (M20), standard grade (M40) and high strength grade (M80 and M100) of binary, ternary and quaternary blended Self-Compacting Concrete (SCC) mixes made with optimum proportions of Fly Ash (FA), Microsilica (MS) and Metakaolin (MK) combination, as per ASTM C642-13. The total quantity of water absorbed is related to the total open porosity, while the kinetics of the process depends principally on the distribution of the pore sizes. This test also measures the capillary rise of water, the most common form of liquid water migration into concrete which is inversely proportional to the diameter of the pores. The smaller the diameter of the pores, the greater will be the capillary absorption. Absorption is the capacity of a sample to hold water while capillary is the rate at which the water fills the sample.

Concrete cube samples of size 100 x 100 x 100 mm are casted and cured for 28 days for testing. Wash the samples in the de-ionized water before beginning this test in order to eliminate powdered material from the surface. Dry the samples in the oven for 24 hours at 60°C and record their weights. Repeat the drying process until the mass of the each sample is constant, that is, until the difference between 2 successive measurements, at an interval of 24 hours, is no more than 0.1% of the mass of the sample. Once the samples have been completely dried and the constant mass is recorded (m_o), place them in a container or beaker, on a base of glass rods and slowly cover with de-ionized water until they are totally immersed with about 2 cm of water above them. At programmed intervals of time, take each sample out of the container, blot it quickly with a damp cloth to remove surface water, and then record the mass of the wet samples (m_i) and the time of measurement on the data sheet. Re-immerse the samples in water and continue measuring until the difference in weight between 2 successive measurements at 24-hour intervals is less than 1% of the amount of water absorbed. At this point, take the samples out of the water and dry them again in an oven at 60°C until they have reached constant mass (as above). Record this value (m_d) on the data sheet. At each interval, the quantity of water absorbed with respect to the mass of the dry sample is expressed as:

$$M_i\% = 100 \times (m_i - m_o)/m_o$$

Where m_i = weight (kg) of the wet sample at time t_i; m_o = weight (kg) of the dry sample.

Record these values on a data sheet and on a graph as a function of time. The length of the intervals during the first 24 hours depends on the absorption characteristics of the materials. Concrete samples should be weighed a few minutes after immersion, and then at increasing intervals (15 min, 30 min, 1 hour, etc.) for the first 3 hours. All samples should then be weighed 8 hours after the beginning of the test and then at 24- hour intervals until the quantity of water absorbed in two successive measurements is not more than 1% of the total mass.

For measuring the water absorption capacity and volume of permeable voids, a balance, water bath, and container suitable for immersing the specimen are needed for performing the test. After the 100x100x100 mm cube samples were cured for 28 days, three samples were put into an oven at 60° C for 24 hours. The dried samples were taken from the oven and allowed to cool for about 30 minutes. The samples were then weighed (M_a) using a balance with an accuracy within 0.01 grams. The samples were submerged in the water tank for 24 hours. After 24 hours, the samples were removed from the water tank and their surface was dried with a paper towel to obtain a saturated surface dry (SSD) condition. The weight (M_b) of the SSD samples was measured. In the next step, the samples were put into a water bath with boiling water for 5 hours. Then the samples were removed from the boiling water and left to cool for 12 hours. Then weights of the samples were measured (M_c). On the same day, the apparent weight of each sample (M_d) was measured by immersing the samples in the water using a hanging balance. Using the measured weights (M_a to M_d) and the equations from the ASTM C642 standard test, the following parameters are obtained.

Water Absorption Capacity (WAC) = $[(M_b-M_a)/ M_a] \times 100$

Bulk density = $g_1 = [(M_a)/ M_c- M_d]x \rho$

Apparant density $=g_2 = [(M_a)/ M_a- M_d]x \rho$

Volume of permeable voids (VPV) = $[(g_2 - g_1)/ g_2] \times 100$

where: M_a = mass of oven-dried sample in air, kg; M_b = mass of surface-dry sample in air after immersion, kg ; M_c = mass of surface-dry sample in air after immersion and boiling, kg; M_d = apparent mass of sample suspended in water, kg ; g_1 = dry bulk density (kg/m^3) ; g_2 = apparent density (kg/m^3) ; ρ= density of water (1000 kg/m^3)

Finally total porosity 'P' or percentage of interconnected pore space was calculated using the formula given below

Total porosity = $(V_v/V) = (W_{sat}- W_{dry}) / \rho_w V$

Where, V_v = volume of voids in cc= W_{sat}- W_{dry} in grams; V = total volume of specimen in cc = 100 x 100 x100 mm^3 ; W_{dry} and W_{sat} denote the weight of the dried and fully saturated samples, respectively and ρ_w the unit mass of water (1 g/cc).

Porosity of concrete is usually determined by dividing the volume of voids of the sample by its bulk volume. Bulk volume of each sample is determined using the measured lengths and diameters of the samples. Volume of voids for each sample is determined by subtracting its grain volume (the volume of the solid portion of concrete excluding the volume of pores) from its bulk volume. Total porosity therefore considers both permeable and impermeable voids whereas apparent porosity considers only impermeable voids.

The table 74 presents the measured weights of various grades of blended SCC specimens. Table 75 presents the Volume of Permeable Voids (VPV) and Water Absorption Capacity (WAC) of various grades of blended SCC specimens

Fig 42 shows the variation of True and Apparent Densities of various grades of SCC specimens and Fig 43 shows the variation of percentage of Volume of Permeable Voids (VPV) and Water Absorption Capacity (WAC) of various grades of SCC specimens.

Table 76 presents the porosity of various grades of blended SCC specimens. Fig 44 shows the variation of Porosity of various grades of SCC specimens

Table 72- Durability Classification as per ASTM C 642

Classification	**Water Absorption Capacity (% by weight)**
Excellent	<5
Good	5-6
Normal	6-7
Marginal	7-8
Bad	>8

Table 74 - Measured Weights of various grades of blended SCC specimens

Grade of SCC	Mix No	Mix Designation (Values indicate percentage by weight of Total Powder)	Ma	Mb	Mc	Md
M20	C1	C100	2.48	2.63	2.64	1.41
	B2	C50+FA50	2.49	2.59	2.61	1.44
	B7	C80+MS20	2.51	2.57	2.60	1.45
	B13	C75+MK25	2.55	2.62	2.64	1.46
	T3	C35+FA50+MS15	2.58	2.65	2.66	1.48
	T15	C25+FA60+MK15	2.60	2.65	2.66	1.49
M40	C1	C100	2.49	2.63	2.64	1.43
	B1	C60+FA40	2.50	2.59	2.61	1.44
	B5	C85+MS15	2.51	2.58	2.59	1.46
	B10	C80+MK20	2.55	2.61	2.63	1.46
	T5	C50+FA40+MS10	2.58	2.63	2.66	1.47
	T9	C35+FA50+MK15	2.59	2.63	2.65	1.49
M80	B2	C95+MS5	2.51	2.58	2.59	1.45
	T3	C65+FA20+MS15	2.59	2.64	2.65	1.5
	Q11	C50+FA28+MS11+MK11	2.63	2.67	2.69	1.51
M100	B2	C90+MS10	2.53	2.56	2.57	1.46
	T2	C71+FA19+MS10	2.55	2.57	2.59	1.48
	Q11	C55+FA23+MS11+MK11	2.60	2.62	2.64	1.50

Table 75- Volume of Permeable Voids (VPV) and Water Absorption Capacity (WAC) of various grades of blended SCC specimens

Grade of SCC	Mix No	Mix Designation (Values indicate percentage by weight of Total Powder)	Bulk density g_1	Apparant density g_2	Volume of permeable voids (VPV)	Water Absorption Capacity (WAC) (%)
M20	C1	C100	2016.26	2317.76	13.01	6.05
	B2	C50+FA50	2128.21	2371.43	10.26	4.02
	B7	C80+MS20	2182.61	2367.92	7.83	2.39
	B13	C75+MK25	2161.02	2339.45	7.63	2.75
	T3	C35+FA50+MS15	2186.44	2345.45	6.78	2.71
	T15	C25+FA60+MK15	2222.22	2342.34	5.13	1.92
M40	C1	C100	2057.85	2349.06	12.40	5.62
	B1	C60+FA40	2136.75	2358.49	9.40	3.60
	B5	C85+MS15	2221.24	2390.48	7.08	2.79
	B10	C80+MK20	2179.49	2339.45	6.84	2.35
	T5	C50+FA40+MS10	2168.07	2324.32	6.72	1.94
	T9	C35+FA50+MK15	2232.76	2354.55	5.17	1.54
M80	B2	C95+MS5	2201.75	2367.92	7.02	2.79
	T3	C65+FA20+MS15	2252.17	2376.15	5.22	1.93
	Q11	C50+FA28+MS11+MK11	2228.81	2348.21	5.08	1.52
M100	B2	C90+MS10	2279.28	2364.49	3.60	1.19
	T2	C71+FA19+MS10	2297.30	2383.18	3.60	0.78
	Q11	C55+FA23+MS11+MK11	2280.70	2363.64	3.51	0.77

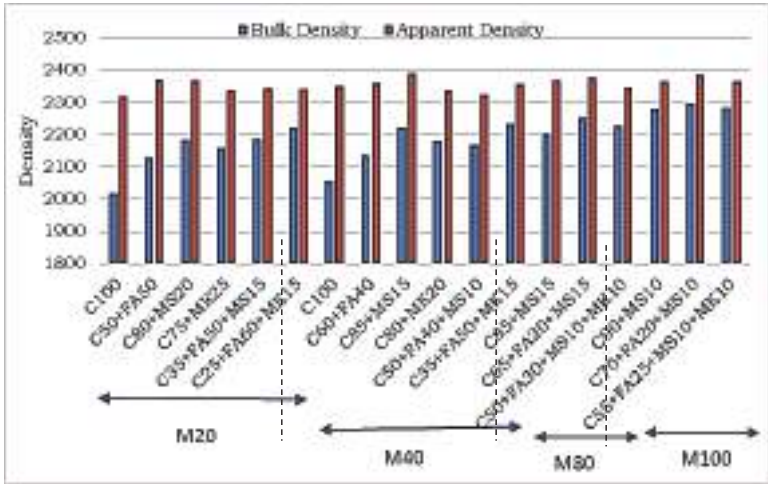

Fig 42- Variation of True and Apparent Densities of various grades of SCC specimens

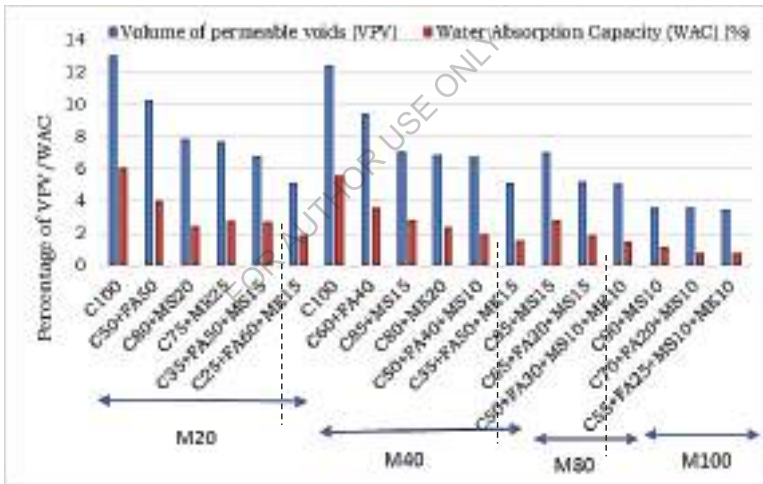

Fig 43- Variation of percentage of Volume of Permeable Voids (VPV) and Water Absorption Capacity (WAC) of various grades of SCC specimens

Table 76 - Porosity of various grades of blended SCC specimens

Grade of SCC	Mix No	Mix Designation (Values indicate percentage by weight of Total Powder)	M_{dry}	M_{sat}	Porosity, P %	Decrease in Porosity
M20	C1	C100	2.48	2.63	15	-
	B2	C50+FA50	2.49	2.59	10	33.33
	B7	C80+MS20	2.51	2.57	6	60.00
	B13	C75+MK25	2.55	2.62	7	53.33
	T3	C35+FA50+MS15	2.58	2.65	7	53.33
	T15	C25+FA60+MK15	2.60	2.65	5	66.67
M40	C1	C100	2.49	2.63	14	-
	B1	C60+FA40	2.50	2.59	9	35.71
	B5	C85+MS15	2.51	2.58	7	50.00
	B10	C80+MK20	2.55	2.61	6	57.14
	T5	C50+FA40+MS10	2.58	2.63	5	64.29
	T9	C35+FA50+MK15	2.59	2.63	4	71.43
M80	B2	C95+MS5	2.51	2.58	7	-
	T3	C65+FA20+MS15	2.59	2.64	5	28.57
	Q11	C50+FA28+MS11+MK11	2.63	2.67	4	42.86
M100	B2	C90+MS10	2.53	2.56	3	-
	T2	C71+FA19+MS10	2.55	2.57	2	33.33
	Q11	C55+FA23+MS11+MK11	2.60	2.62	2	33.33

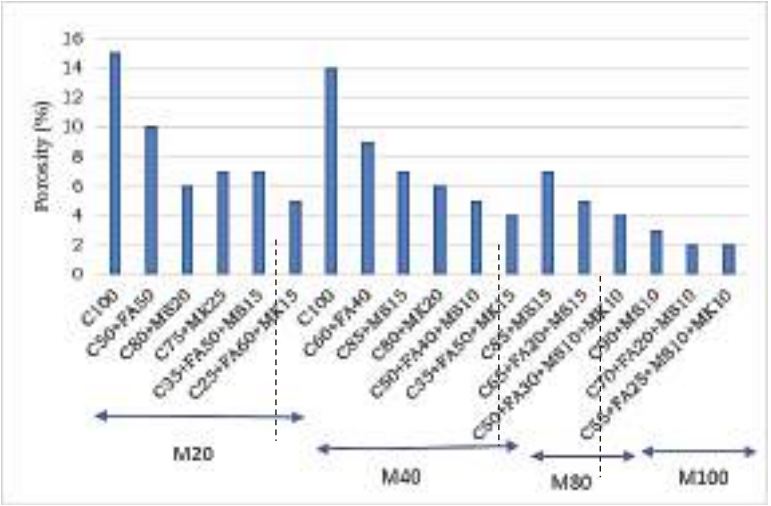

Fig 44- Variation of Porosity of various grades of SCC specimens

The total porosity of Metakaolin (MK) pastes was slightly higher than that of pure pastes, indicating that the Metakaolin (MK) increases the volume of fine capillary and gel pores while decreasing the volume of coarser pores. So any other admixture finer than metakaolin (MK) could be added along with metakaolin (MK) for denser and stronger paste. So the present research work has focused on the reduction of total porosity in metakaolin (MK) pastes adding microsilica (MS). Water Absorption Capacity of Metakaolin (MK) blended SCC decreases with the increase of Metakaolin (MK) content up to 25% due to the fact that Metakaolin (MK) is finer than OPC altering the pore structure of concrete. Till 20% replacement level of metakaolin (MK) water absorption capacity decreases, after 20% and till 30% replacement level it increases but lower than normal SCC mixes. Same observation is made in case of sorpitivity. Past research stated that cement pastes when added with metakaolin (MK) decreases the proportion of pores with diameter above about 0.1μm. There is a corresponding increase in the proportion of pores with diameters below about 0.05 μm – that is, the average pore diameter is reduced (refined).

Blended SCC mixes showed significantly less water absorption capacity. This decrease in water absorption capacity of all grades of blended SCC mixes is attributed to the reduction of pores in the concrete. Water Absorption Capacity (WAC) of blended SCC mixes is reduced by nearly 50 to 75% for low to high grade concretes due to modified pore structure of the cement –sand matrix by microsilica (MS) and metakaolin (MK). The absorption characteristics indirectly represent the volume of pores and their connectivity. Porosity of SCC mixes is reduced by nearly 15 - 30% in binary, ternary and quaternary blends. The possible reason for this is that as multiple SCMs are blended suitably pores are reduced consequently the average pore radius of SCC mixes are reduced. This means that the time taken for the water to rise by capillary action in blended SCC mixes is longer and thus proved that these ternary and quaternary blended SCC mixes are less porous compared to the conventional SCC mix. The rate of water absorbed into concrete through the pores gives important information about the microstructure and permeability characteristics of

concrete. Volume of permeable voids present in blended SCC mixes is less by 25 % than in conventional SCC. It can concluded that all grades of blended SCC mixes have less water absorption capacity which indicates the presence of less volume of permeable voids. Water Absorption Capacity (WAC) of blended SCC mixes is reduced inferring the reduced extent of volume of pores and their connectivity in blended SCC mixes. Volume of permeable pores (VPV) of blended SCC mixes are reduced due to reduction in average pore radius of concrete by inducing pore discontinuity in the hydrated cement paste by SCMs.

10.6 Sorptivity

The objective of this study is to determine the sorptivity of ordinary grade (M20), standard grade (M40) and high strength grade (M80 and M100) of binary, ternary and quaternary blended Self-Compacting Concrete (SCC) mixes made with optimum proportions of Fly Ash (FA), Microsilica (MS) and Metakaolin (MK) combination, as per ASTM C1585. Sorptivity measures the rate of penetration of water into the pores in concrete by capillary suction. It is also a measure of the capillary forces exerted by the pore structure causing fluids to be drawn in to the body of the material. It provides a relative measure that combines pore size diameter and number of pores present. The depth of water absorbed into concrete increases linearly with respect to the square root of wetting time. In terminology, the sorptivity is the change in volume of water absorbed per unit area against the square root of time. Water absorption and sorptivity can suggest useful data regarding the pore structure of the concrete.

Determining the sorptivity of a sample in the lab is a simple, low technology technique, all that is required, is a scale, a stopwatch and a shallow tub of water. The samples 100 x 50 mm size cylindrical specimens are preconditioned to a certain moisture condition, either by drying the sample for 7 days in a 50°C oven. The sides of the concrete sample are sealed, typically with electrician's tape or by sealant while the suction face and the face opposite it were left unsealed. Cylindrical concrete specimens were placed on a filtered support (sponge) so that the water level was 10±1 mm above the inflow face as shown in Fig.45. The sample is immersed to a depth of 5-10 mm in the water then the initial mass of the sample and time of start are recorded. The procedure of recording mass of the sample was repeated, consecutively, at various times such as 15 min, 30 min, 1 hr, 2 hr, 4 hr, 6 hr, 24 hr, 48 hr and 72 hr. The gain in mass per unit area over the density of water (I) is plotted versus the square root of the elapsed time ($\sqrt{t}$). The slope of the line of best fit of these points (ignoring the origin) is reported as the sorptivity coefficient (k). The rate of water absorption or sorptivity (k), is the slope of I- $\sqrt{t}$ graph (m / $min^{1/2}$ or kg/ m^2 / $\sqrt{}$ min). For one dimensional flow, it can be stated that (Hall, 1989):

$$I = k \times \sqrt{t}$$

Where k is sorptivity coefficient and I = W/(A x d)

W = the amount of water absorbed in kg ; A= Area of the c/s of the specimen that is in contact with water (m^2) ; d= density of the medium in which the specimen was dipped (1000 kg/m^3 in case medium is water).

Because of small initial surface tension and buoyancy effects, the relationship between cumulative water absorption (kg/m^2) and square root of exposure time ($t^{0.5}$) shows deviation from linearity during first few minutes. Thus, for the calculation of sorptivity coefficient, only the section of the curves for exposure period from 15 min to 72 hrs, where the curves were consistently linear, was used for the calculation of sorptivity.

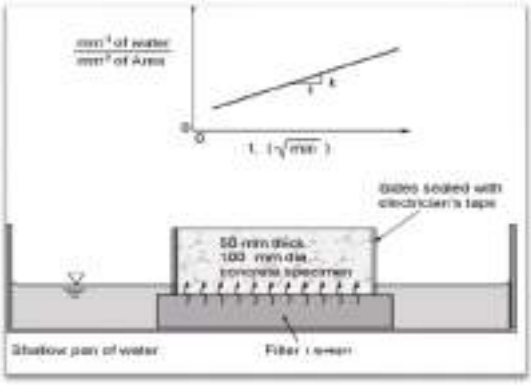

Fig 45- Experimental Setup for Sorptivity Test

The table 77 illustrates the gain in mass per unit area over the density of water 'I' (m) at regular intervals of time't' (min). The plot is drawn between the gain in mass per unit area over the density of water (I) and the square root of the elapsed time (√t). The slope of the line of best fit of these points is reported as the sorptivity coefficient (k). Table 78 and Fig 46 shows the sorptivity coefficient (k) of optimally blended binary, ternary and quaternary SCC mixes of ordinary grade (M20), standard grade (M40) and high strength grade (M80 and M100) made with Fly Ash (FA), Microsilica (MS) and Metakaolin (MK).

Table 77 - The gain in mass per unit area over the density of water 'I' (m) at regular intervals of time't' (min)

Gain in mass per unit area over the density of water , I x 10^{-3}(m)											
Grade of SCC	Mix Designation (Values indicate percentage by weight of Total Powder)	Elapsed time 't' (min)									
		0	15	30	60	120	240	360	1440	2880	4320
M20	C100	0	0.0005	0.0007	0.001	0.0014	0.0019	0.0024	0.0047	0.0067	0.0082
	C50+FA50	0	0.00049	0.00067	0.00095	0.00133	0.00181	0.00226	0.00447	0.00623	0.00771
	C80+MS20	0	0.00048	0.00065	0.00090	0.00126	0.00171	0.00212	0.00424	0.00579	0.00725
	C75+MK25	0	0.00047	0.00062	0.00086	0.00120	0.00163	0.00199	0.00403	0.00539	0.00681
	C35+FA50+MS15	0	0.00046	0.00059	0.00081	0.00114	0.00155	0.00187	0.00383	0.00501	0.00640
	C25+FA60+MK15	0	0.00045	0.00055	0.00075	0.0010	0.00145	0.00175	0.00355	0.00495	0.00635
M40	C100	0	0.0004	0.0005	0.0007	0.001	0.0014	0.0017	0.0035	0.0049	0.006
	C60+FA40	0	0.00039	0.00048	0.00067	0.00095	0.00133	0.00160	0.00333	0.00456	0.00564
	C85+MS15	0	0.00038	0.00046	0.00063	0.00090	0.00126	0.00150	0.00316	0.00424	0.00530
	C80+MK20	0	0.00038	0.00044	0.00060	0.00086	0.00120	0.00141	0.00300	0.00394	0.00498
	C50+FA40+MS10	0	0.00037	0.00042	0.00057	0.00081	0.00114	0.00133	0.00285	0.00367	0.00468
	C35+FA50+MK15	0	0.0003	0.0004	0.0005	0.0008	0.0011	0.0013	0.0027	0.0038	0.0047
M80	C85+MS15	0	0.0003	0.0004	0.0005	0.0008	0.0011	0.0013	0.0027	0.0038	0.00437
	C65+FA20+MS15	0	0.00025	0.00035	0.00050	0.00075	0.00105	0.00125	0.00255	0.00355	0.00424
	C50+FA30+MS10+MK10	0	0.0002	0.0003	0.0005	0.0007	0.001	0.0012	0.0024	0.0033	0.0041
M100	C90+MS10	0	0.0002	0.0003	0.0004	0.0006	0.0009	0.001	0.0021	0.003	0.0036
	C70+FA20+MS10	0	0.00020	0.00030	0.00040	0.00060	0.00085	0.00100	0.00200	0.00285	0.00350
	C55+FA25+MS10+MK10	0	0.0002	0.0003	0.0004	0.0006	0.0008	0.001	0.0019	0.0027	0.0034

Table 78 - Sorptivity Coefficients of optimally blended SCC specimens

Grade of SCC	Mix No	Mix Designation (Values indicate percentage by weight of Total Powder)	**Sorptivity Coefficient (k) x 10^{-3} $m/min^{0.5}$**	**Percentage reduction**
M20	C1	C100	0.126	-
	B2	C50+FA50	0.120	5
	B7	C80+MS20	0.114	10
	B13	C75+MK25	0.108	14
	T3	C35+FA50+MS15	0.103	18
	T15	C25+FA60+MK15	0.097	23
M40	C1	C100	0.092	-
	B1	C60+FA40	0.089	3
	B5	C85+MS15	0.084	9
	B10	C80+MK20	0.080	13
	T5	C50+FA40+MS10	0.076	17
	T9	C35+FA50+MK15	0.072	22
M80	B2	C95+MS5	0.071	-
	T3	C65+FA20+MS15	0.066	7
	Q11	C50+FA28+MS11+MK11	0.061	14
M100	B2	C90+MS10	0.054	-
	T2	C71+FA19+MS10	0.053	1
	Q11	C55+FA23+MS11+MK11	0.052	3

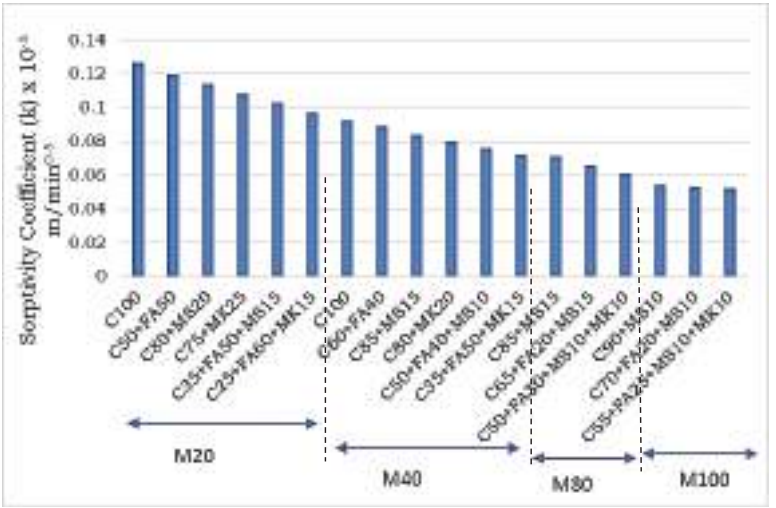

Fig 46 -Sorptivity Coefficients of of optimally blended SCC specimens

It is apparent that sorptivity decreases systematically for metakaolin (MK) blended SCC mixes than non- metakaolin (MK) blended SCC mixes for all grades. The sorptivity coefficients of metakaolin (MK) blended SCC mixes are low for all grades because the pores in the bulk paste or in the interfaces between aggregate and cement paste is filled efficiently hence, the capillary pores are reduced. Sorptivity values for metakaolin (MK) blended SCC mixes were in the range of 0.052 to 0.1.08 mm/min$^{0.5}$ and for non- metakaolin (MK) blended SCC mixes its value is in the range of 0.53 to 0.126 mm/min$^{0.5}$. The capillary absorption coefficient (k) is greatly influenced by the addition of metakaolin (MK) and micro silica (MS) combination to blended SCC mixes. The water absorption, capillary and porosity characteristics indirectly reflect the durability performance of the blended SCC mixes.

While volume of permeable voids (VPV) is a measure of number of voids, Sorptivity gives a measure of nominal pore radius. Blended SCC mixes of all grades gave the lower sorptivity and porosity values compared to the conventional SCC mix. This means that the time taken for the water to rise by capillary action in blended SCC mixes are longer and thus proved that these concrete are less porous compared to the conventional SCC. The decrease in capillary absorption coefficient (k) indicates the dense pore structure of blended SCC mixes due to enhanced microstructure of SCC.

11. GRANULATED BLAST FURNACE SLAG AS PARTIAL FINE AGGREGATE REPLACEMENT

The Granulated Blast Furnace Slag (GBFS) used in the present investigation was collected from JSW steel plant, district of Bellary. The tests on granulated blast furnace slag were carried out as per IS: 383-1970. Slag sand was of Zone II. Fineness Modulus=2.79, Specific gravity= 2.48, loose bulk density of 1.27 g/cc. The GBFS was tested for its physical requirements such as gradation, fineness modulus, specific gravity and bulk density in accordance with IS: 2386 – 1963 [Methods of test for aggregate for concrete]. GBFS has greater surface area than river sand. Even though both belong to zone –II which means that particle size distribution is almost same but GBFS is more porous than river sand so water absorption capacity of GBFS is more than river sand which effects the workability and compressive strength drastically. So in order to maintain workability and compressive strength while replacing river sand with GBFS, the percentage replacements should be optimally chosen for various grades. GBFS is reported to be innocuous in nature (no reactivity) and contain no deleterious materials so it can replace river sand by same amount without any changes to total volume ratio of fine aggregate. But being porous in nature, percentage replacement of total fine aggregate varies for different grades of SCC mixes. So it required to use sand finer than GBFS to improve its porous structure. Workability is reduced in SCC mixes made with partial replacement of GBFS as fine aggregate. This loss of flow can be compensated by adding suitable percentage of super plasticizer. It is observed that density of SCC made with GBFS is less than that made with river sand.

This phase discusses the use of GBFS as partial fine aggregate replacement in the development of ordinary grade (M20), standard grade (M40) and high strength grade (M80 and M100) of binary, ternary and quaternary blended Self-Compacting Concrete (SCC) mixes made with optimum proportions of Fly Ash (FA), Microsilica (MS) and Metakaolin (MK) combination. The mix proportioning adopted are same optimum quantities, as that of various grades of SCC mixes made with river sand. Flow properties are determined to ascertain that EFNARC Guidelines are satisfied. For the above optimized combinations of pozzolans in binary, ternary and quaternary blended SCC mixes, percentage replacement level of GBFS for different grades are optimized here based on satisfaction of EFNARC flow properties and desired strength property. Hardened properties such as Compressive strength as per IS: 516 – 1969, split –tensile strength as per IS: 5816 – 1999, flexural strength as per IS: 516, Impact strength and stress-strain behaviour are evaluated. Durability properties such as water absorption capacity, porosity, sorptivity test, chloride ion penetration resistance, acid attack resistance, sulphate attack resistance, sea water attack resistance at 28, 60 and 90 days were determined by conducting detailed laboratory investigations on ordinary grade (M20) , standard grade (M40) and high strength grade (M80 and M100) of binary, ternary and quaternary blended Self- Compacting Concrete (SCC) made with optimum proportions of Fly Ash (FA), Microsilica (MS) and Metakaolin (MK) combination.

11.0 Optimum proportions of GBFS of blended SCC mixes

For optimized proportions of Fly Ash (FA), Microsilica (MS) and Metakaolin (MK) in binary, ternary and quaternary blended SCC mixes of ordinary grade (M20), standard grade (M40) and high strength grade (M80 and M100), river sand is partially replaced with various percentages of GBFS to determine the optimum percentage level of GBFS to be used as fine aggregate

replacement. Table 79 presents the compressive strength values of optimally blended binary, ternary and quaternary blended SCC mixes of ordinary grade (M20), standard grade (M40) and high strength grade (M80 and M100) made with various percentages of GBFS as fine aggregate replacement. The optimum percentage replacements of GBFS for various blended SCC mixes are adopted based on fulfilment of EFNARC flow specifications and on realization of desired strength. The proportions of SCMs adopted are same optimum quantities, as that of various grades of blended SCC mixes made with river sand. Flow properties are determined to ascertain that EFNARC Guidelines are satisfied. Hardened properties such as Compressive strength as per IS: 516 – 1969, split –tensile strength as per IS: 5816 – 1999, flexural strength as per IS: 516 and impact strengths are evaluated for optimally blended binary, ternary and quaternary SCC mixes made with optimum percentage of GBFS as fine aggregate replacement. All the test procedures are similar to that of those adopted in development of various grades of binary, ternary and quaternary blended SCC mixes made with river sand.

Table 80 and Fig 48 shows the Optimum percentage replacement of River Sand with GBFS for various grades of optimally blended binary, ternary and quaternary SCC mixes of ordinary grade (M20), standard grade (M40) and high strength grade (M80 and M100).

Table 79 - Evaluation of percentage replacement of River Sand with GBFS based on Compressive Strengths

Grade of SCC Mix	Mix No	Mix Designation (Values indicate percentage by weight of 'P'	Percentage Replacement of fine aggregate with GBFS								
			0	10	20	30	40	50	60	70	80
			Compressive Strengths (MPa)								
M20	C1	C100	25.18	25.45	25.68	25.98	26.37	26.90	21.23	17.03	-
	B2	C50+FA50	32.24	32.43	32.54	32.78	32.97	33.11	33.15	28.19	12.43
	B7	C80+MS20	29.03	29.08	29.34	29.66	29.80	30.01	30.28	21.45	11.35
	B13	C75+MK25	30.77	30.88	31.03	31.22	31.36	31.50	31.56	26.23	11.81
	T3	C35+FA50+MS15	32.81	32.99	33.18	33.23	33.78	33.89	34.07	30.12	13.65
	T15	C25+FA60+MK15	36.87	36.96	37.11	37.21	37.34	37.54	37.77	37.89	16.13
M40	C1	C100	48.18	48.21	48.89	49.02	49.31	36.18	32.10	-	-
	B1	C60+FA40	56.78	56.88	56.92	56.96	57.04	57.18	49.19	41.22	-
	B5	C85+MS15	51.99	52.07	52.19	52.37	52.89	53.03	46.12	34.10	-
	B10	C80+MK20	53.73	53.88	54.04	54,16	54.37	54.66	45.12	32.11	-
	T5	C50+FA40+MS10	59.87	59.95	60.35	60.56	61.04	61.25	54.13	34.23	-
	T9	C35+FA50+MK15	59.92	60.23	60.54	60.74	61.21	61.54	61.76	34.12	-
M80	B2	C95+MS5	88.56	89.03	89.45	66.67	54.13	-	-	-	-
	T3	C65+FA20+MS15	94.51	95.03	95.10	67.12	56.73	-	-	-	-
	Q11	C50+FA28+MS11+MK11	97.16	97.34	98.30	98.57	70.13	56.13	-	-	-
M100	B2	C90+MS10	106.04	107.03	107.21	81.23	67.12	-	-	-	-
	T2	C71+FA19+MS10	111.83	112.13	112.34	77.14	56.17	-	-	-	-
	Q11	C55+FA23+MS11+MK11	113.28	113.65	114.12	114.50	81.23	63.19	-	-	-

Table 80 - Optimum percentage replacement of River Sand with GBFS for various grades of blended SCC mixes

Grade of SCC Mix	Mix No	Mix Designation (Values indicate percentage by weight of 'P'	Optimum Percentage Replacement of River Sand with GBFS
M20	C1-G	C100+GBFS50	50
	B2-G	C50+FA50+GBFS60	60
	B7-G	C80+MS20+GBFS60	60
	B13-G	C75+MK25+GBFS60	60
	T3-G	C35+FA50+MS15+GBFS60	60
	T15-G	C25+FA60+MK15+GBFS70	70
M40	C1-G	C100+GBFS40	40
	B1-G	C60+FA40+GBFS50	50
	B5-G	C85+MS15+GBFS50	50
	B10-G	C80+MK20+GBFS50	50
	T5-G	C50+FA40+MS10+GBFS50	50
	T9-G	C35+FA50+MK15+GBFS60	60
M80	B2-G	C95+MS5+GBFS20	20
	T3-G	C65+FA20+MS15+GBFS20	20
	Q11-G	C50+FA28+MS11+MK11+GBFS30	30
M100	B2-G	C90+MS10+GBFS20	20
	T2-G	C71+FA19+MS10+GBFS20	20
	Q11-G	C55+FA23+MS11+MK11+GBFS30	30

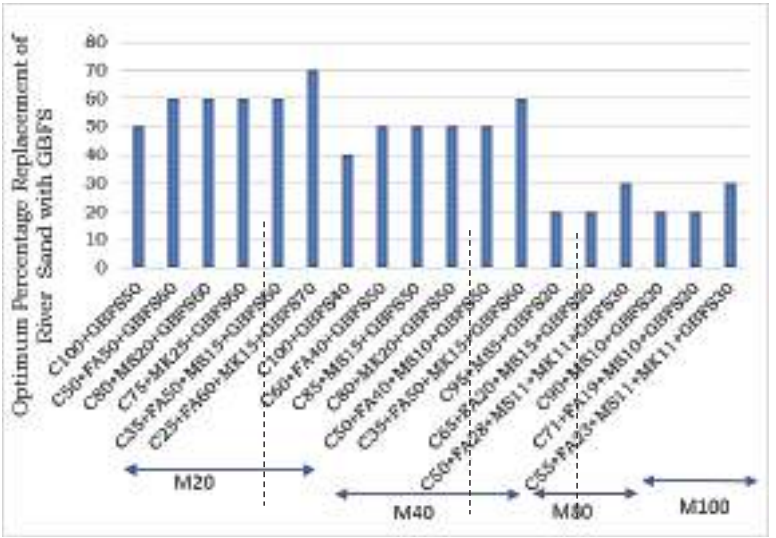

Fig 48 -Optimum percentage replacement of River Sand with GBFS for various grades of blended SCC mixes

The strength of concrete was detrimentally affected if the replacement ratio was beyond 70% for ordinary grade (M20), 60% for standard grade M40 and 30% for high strength grade (M80 and M100). It is established that the main reason for the strength reduction in SCC mixes made with GBFS is the formation of a porous concrete structure if used beyond certain percentage. With GBFS alone, it is difficult to obtain proper compaction due to voids. Thus river sand up to strength requirement can be utilized. Moreover, an increase trend in water absorption capacity was observed, for all grades considered, beyond an optimum replacement level. With increase of grade, powder content increases making the paste more dense which reduces the porosity in the SCC made with GBFS. Due to which the replacement levels decreases as grade increases to maintain the similar workability and compressive strength of SCC made with river sand.

Even though GBFS is finer than river sand, percentage passing through 600 microns is more in river sand than in GBFS which means than in GBFS sand particle size greater than 600 micros are more. It is observed that percentage retained on 600 microns sieve in GBFS is almost 59% where as in river sand only 50% is retained. Out of remaining 41% of GBFS sand particles 33.3% is retained on 300 microns sieve whereas 42.2% of river sand is retained on 300 microns. This indicates the GBFS used in the investigation is little finer than river sand, though it conforms to Zone –II.

GBFS/river sand ratio governs the porosity of the matrix, this porous structure causes negative effect on the strength of the concrete. Compressive strength in blended SCC increases till 70% replacement of river sand with GBFS for ordinary grade (M20), 60% replacement for standard grade M40 and only 30% replacement of GBFS is acceptable for high strength grade (M80 and M100). This outcome highlights the significance of presence of particle size between 300 to 600microns. GBFS/ river sand ratio should be arranged in such a way that the reduction of

compressive strength is within allowable limits. So GBFS/ river sand ratio is the governing criteria on the strength characteristics of blended SCC made with partial replacement of GBFS as fine aggregate.

Increase of strength in Fly Ash (FA), Microsilica (MS) and Metakaolin (MK) blended binary, ternary and quaternary SCC mixes made with partial replacement of GBFS as fine aggregate is mainly attributed to its shape, size and surface texture of GBFS sand particles, which provide better adhesion between the particles and cement matrix. Also the GBFS is less expensive than river sand. The amount of mixing water used in GBFS SCC mixes is important because of the high water absorption by the GBFS.

11.1 Strength Properties

Table 81 presents the compressive strength, split-tensile strength and flexural strengths of various grades of optimally blended Fly Ash (FA), Microsilica (MS) and Metakaolin (MK) in binary, ternary and quaternary SCC mixes made with partial replacement of GBFS as fine aggregate. Table 82 presents impact strengths of various grades of optimally blended SCC mixes made with optimum percentage replacement of River Sand with GBFS**.** Impact strength is evaluated in terms of (1) number of blows taken for first crack and for ultimate failure, (2) energy consumed in joules for first crack and for ultimate failure and (3) in terms of ductility index.

Table 81 - Strengths of various grades of blended SCC mixes made with optimum percentage replacement of River Sand with GBFS

Grade of SCC Mix	Mix No	Mix Designation (Values indicate percentage by weight of 'P'	Optimum Percentage Replacement of Natural Sand with GBFS	Compressive Strength (MPa)	Split Tensile Strength (MPa)	Flexural Strength (MPa)
M20	C1-G	C100+GBFS50	50	26.90	2.96	3.55
	B2-G	C50+FA50+GBFS60	60	33.15	3.65	4.38
	B7-G	C80+MS20+GBFS60	60	30.28	3.33	4.00
	B13-G	C75+MK25+GBFS60	60	34.56	3.47	4.16
	T3-G	C35+FA50+MS15+GBFS60	60	34.07	3.75	4.50
	T15-G	C25+FA60+MK15+GBFS70	70	37.89	4.17	5.00
M40	C1-G	C100+GBFS40	40	49.31	4.84	6.33
	B1-G	C60+FA40+GBFS50	50	57.18	5.75	7.38
	B5-G	C85+MS15+GBFS50	50	53.03	5.27	6.78
	B10-G	C80+MK20+GBFS50	50	54.66	5.44	6.99
	T5-G	C50+FA40+MS10+GBFS50	50	61.25	6.02	7.81
	T9-G	C35+FA50+MK15+GBFS60	60	61.76	6.06	7.87
M80	B2-G	C95+MS5+GBFS20	20	89.45	9.26	11.51
	T3-G	C65+FA20+MS15+GBFS20	20	95.10	9.66	12.39
	Q11-G	C50+FA28+MS11+MK11+GBFS30	30	98.57	9.90	12.88
M100	B2-G	C90+MS10+GBFS20	20	107.21	10.50	14.00
	T2-G	C71+FA19+MS10+GBFS20	20	112.34	11.86	14.63
	Q11-G	C55+FA23+MS11+MK11+GBFS30	30	114.50	12.02	14.82

Table 82 – Impact Strengths of various grades of optimally blended SCC mixes made with optimum percentage replacement of River Sand with GBFS

Grade of SCC Mix	Mix No	Mix Designation (Values indicate percentage by weight of Total Powder)	Optimum Percentage Replacement of Natural Sand with GBFS	Impact strength Evaluation				
				No. of Blows for First Crack	No. of Blows for Ultimate Failure	Energy Consumed for First Crack (Joule) E1	Energy Consumed for Ultimate Failure (Joule) E2	Ductility Index E2/E1
M20	C1-G	C100+GBFS50	50	9	11	97.02	118.58	1.22
	B2-G	C50+FA50+GBFS60	60	12	14	129.36	150.92	1.17
	B7-G	C80+MS20+GBFS60	60	15	17	161.7	183.26	1.13
	B13-G	C75+MK25+GBFS60	60	14	16	150.92	172.48	1.14
	T3-G	C35+FA50+MS15+GBFS60	60	16	20	172.48	215.6	1.25
	T15-G	C25+FA60+MK15+GBFS70	70	17	22	183.26	237.16	1.29
M40	C1-G	C100+GBFS40	40	13	16	140.14	172.48	1.23
	B1-G	C60+FA40+GBFS50	50	16	20	172.48	215.6	1.25
	B5-G	C85+MS15+GBFS50	50	19	23	204.82	247.94	1.21
	B10-G	C80+MK20+GBFS50	50	18	23	194.04	247.94	1.28
	T5-G	C50+FA40+MS10+GBFS50	50	21	27	226.38	291.06	1.29
	T9-G	C35+FA50+MK15+GBFS60	60	21	28	226.38	301.84	1.33
M80	B2-G	C95+MS5+GBFS20	20	37	48	398.86	517.44	1.30
	T3-G	C65+FA20+MS15+GBFS20	20	42	53	452.76	571.34	1.26
	Q11-G	C50+FA28+MS11+MK11+GBFS30	30	44	57	474.32	614.46	1.30
M100	B2-G	C90+MS10+GBFS20	20	40	51	431.2	549.78	1.28
	T2-G	C71+FA19+MS10+GBFS20	20	46	59	495.88	636.02	1.28
	Q11-G	C55+FA23+MS11+MK11+GBFS30	30	46	62	495.88	668.36	1.35

Fig 49 to 52 shows variation of compressive, split-tensile, flexural and impact strengths of various grades of blended SCC mixes made with optimum percentage of GBFS as fine aggregate replacement

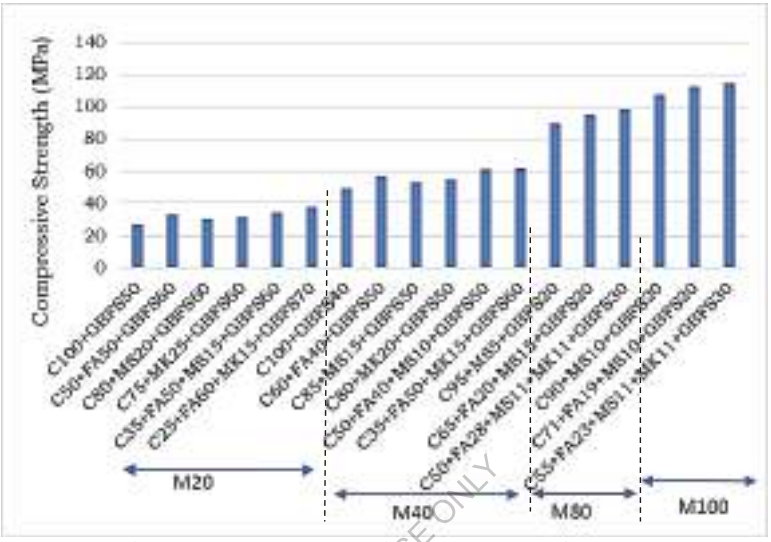

Fig 49- Variation of compressive strengths of various grades of blended SCC mixes made with optimum percentage of GBFS as fine aggregate replacement

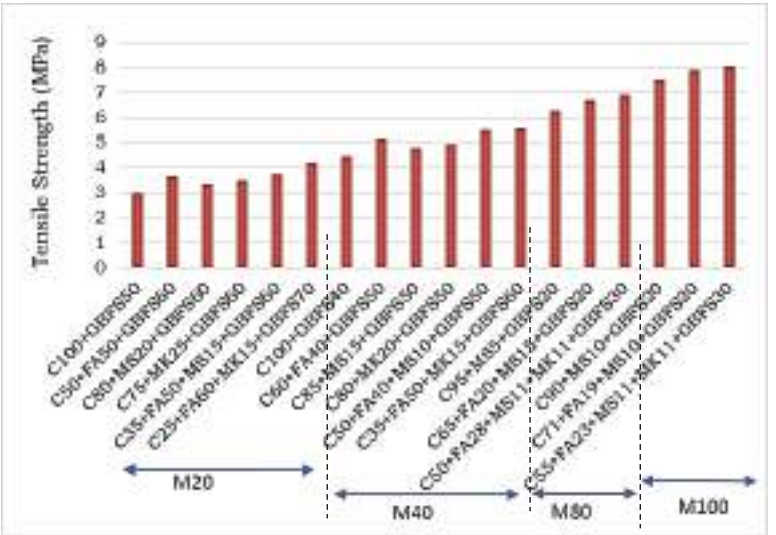

Fig 50- Variation of split tensile strengths of various grades of blended SCC mixes made with optimum percentage of GBFS as fine aggregate replacement

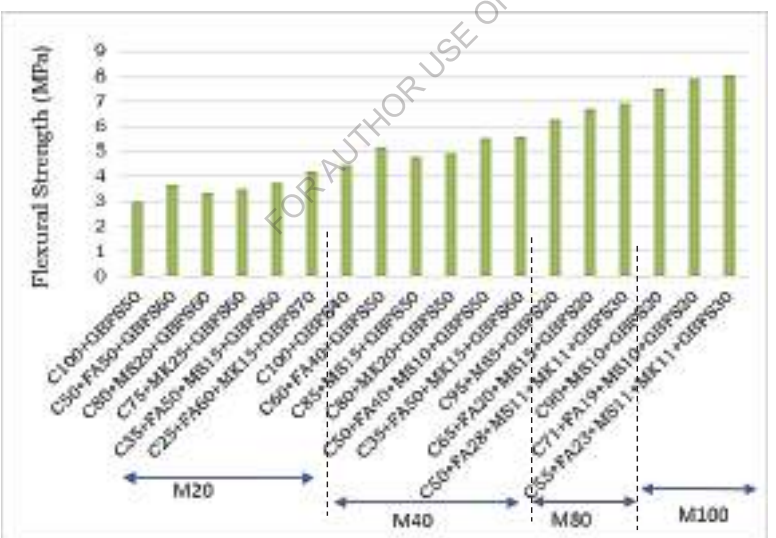

Fig 51- Variation of flexural strengths of various grades of blended SCC mixes made with optimum percentage of GBFS as fine aggregate replacement

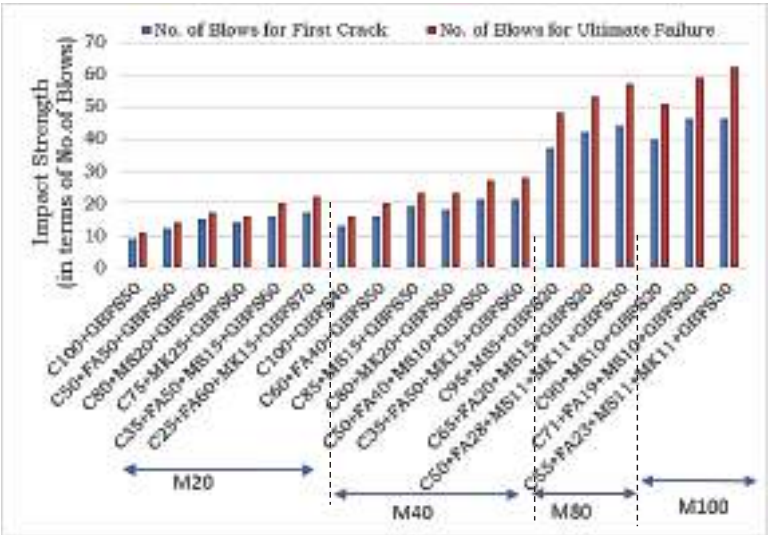

Fig 52- Variation of impact strength parameters of various grades of blended SCC mixes made with optimum percentage of GBFS as fine aggregate replacement

It is also observed that the workability decreases as the percentage of GGBS increases and for higher percentages of river sand replacement by GBFS the flow decreases substantially. The workability can be increased by adding suitable dosage of chemical admixture such as super plasticizer. The drop in workability could be attributed to porous and rough surface of GBFS aggregate which can be improved in higher grade of concrete due to availability of high finer contents.

The compressive strength, split-tensile strength, flexural strengths and impact strengths of various grades of optimally blended Fly Ash (FA), Microsilica (MS) and Metakaolin (MK) in binary, ternary and quaternary SCC mixes made with partial optimal replacement of GBFS as fine aggregate are almost equal to that of binary, ternary and quaternary SCC mixes made with river sand as fine aggregate. GBFS/river sand ratio governs the porosity of the matrix, this porous structure causes negative effect on the strength of the concrete. So it can be concluded that if the river sand is replaced with optimum percentage of GBFS in blended SCC mixes, similar performance in terms of strength as that of blended SCC mixes made river sand can be achieved.

The high compactness achieved by adding GBFS in suitable proportions provides gains of strength. The compressive strength of blended SCC mixes increases with increase in GBFS percentage up to a certain percentage and after that it decrease following a Gaussian Model. The improvement in strength may be due to shape, size and surface texture of GBFS aggregates, which provide better adhesion between the particles and cement matrix.

11.2 Non-Destructive Evaluation

The main objective of this experimental investigations is to assess the quality, integrity of micro structure of optimally blended binary, ternary and quaternary blended SCC mixes of ordinary grade (M20), standard grade (M40) and high strength grade (M80 and M100) made with optimum percentages of GBFS as fine aggregate replacement, using Rebound hammer test and Ultrasonic pulse velocity measurements. The results of the investigations are tabulated in Table 5.79. Mean rebound values and mean ultrasonic pulse velocities (USPV) are measured to understand the quality, integrity and strength of multi-blended SCC mixes made with optimum percentages of GBFS as fine aggregate replacement. The Table 83 lists the mean rebound values, mean pulse velocity values and their estimated compressive strengths of various grades of optimally blended SCC mixes made with optimum percentages of GBFS as fine aggregate replacement.
Fig 53 and Fig 54 shows Rebound numbers and USPV values for optimized blended SCC mixes of various grades

Table 83 - Combined Rebound hammer and Ultrasonic pulse velocity values of

M20 blended SCC mixes made with optimum percentage replacement of River Sand with GBFS

Grade of SCC Mix	Mix No	Mix Designation (Values indicate percentage by weight of Total Powder)	Optimum Percentage Replacement of Natural Sand with GBFS	Mean Rebound Number	Mean Pulse Velocity km/sec	Compressive Strength (f_{ck}) N/mm^2	Quality of Concrete
M20	C1-G	C100+GBFS50	50	31	3.24	26.90	Medium
	B2-G	C50+FA50+GBFS60	60	35	3.47	33.15	Medium
	B7-G	C80+MS20+GBFS60	60	37	4.10	30.28	Good
	B13-G	C75+MK25+GBFS60	60	37	4.15	31.56	Good
	T3-G	C35+FA50+MS15+GBFS60	60	41	4.19	34.07	Good
	T15-G	C25+FA60+MK15+GBFS70	70	44	4.28	37.89	Good
M40	C1-G	C100+GBFS40	40	46	4.39	49.31	Good
	B1-G	C60+FA40+GBFS50	50	49	4.52	57.18	Excellent
	B5-G	C85+MS15+GBFS50	50	51	4.55	53.03	Excellent
	B10-G	C80+MK20+GBFS50	50	53	4.59	54.66	Excellent
	T5-G	C50+FA40+MS10+GBFS50	50	58	4.76	61.25	Excellent
	T9-G	C35+FA50+MK15+GBFS60	60	61	5.03	61.76	Excellent
M80	B2-G	C95+MS5+GBFS20	20	64	5.17	89.45	Excellent
	T3-G	C65+FA20+MS15+GBFS20	20	67	5.68	95.10	Excellent
	Q11-G	C50+FA28+MS11+MK11+GBFS30	30	69	5.91	98.57	Excellent
M100	B2-G	C90+MS10+GBFS20	20	68	6.14	107.21	Excellent
	T2-G	C71+FA19+MS10+GBFS20	20	70	6.25	112.34	Excellent
	Q11-G	C55+FA23+MS11+MK11+GBFS30	30	74	6.31	114.50	Excellent

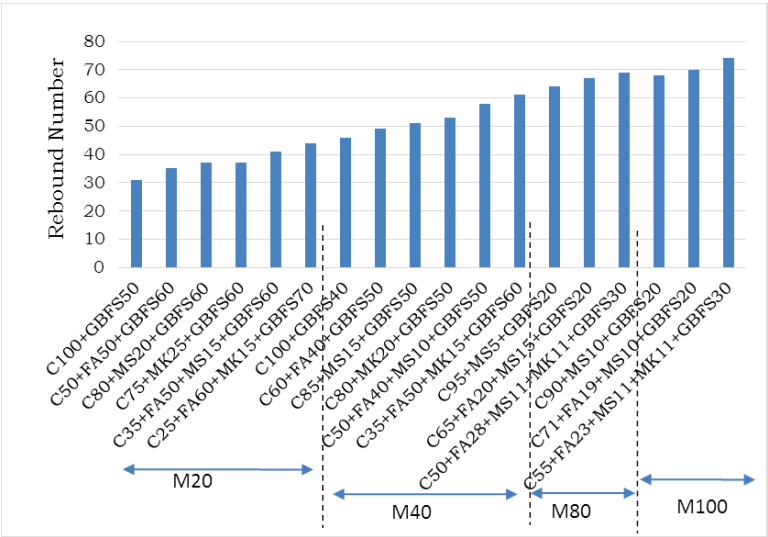

Fig 53- Rebound numbers for optimized SCC mixes of various grades of blended SCC mixes made with optimum percentage of GBFS as fine aggregate replacement

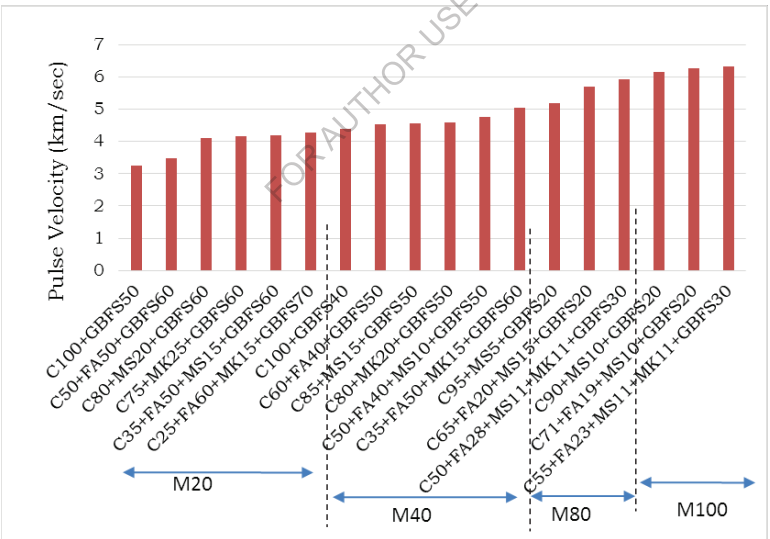

Fig 54- USPV values for optimized SCC mixes of various grades of blended SCC mixes made with optimum percentage of GBFS as fine aggregate replacement

It was found that the rebound hammer and ultra-sonic pulse velocity properties of the dense microstructure of an optimally blended Fly Ash (FA), Microsilica (MS) and Metakaolin (MK) in binary, ternary and quaternary SCC mixes made with partial optimal replacement of GBFS as fine aggregate are almost equivalent to that of binary, ternary and quaternary SCC mixes made with river sand as fine aggregate. The percentage of optimal replacement levels of GBFS varies with the grade of the SCC mixes.

11.3 Stress-Strain Behavior

The aim of this study is to determine experimentally the stress-strain behavior of optimally blended binary, ternary and quaternary blended SCC mixes of ordinary grade (M20), standard grade (M40) and high strength grade (M80 and M100) made with optimum percentages of GBFS as fine aggregate replacement.

Table 5.80 to 5.82 and Fig 5.52 to 5.55 presents stress-strain values and curves respectively of optimally blended SCC mixes of ordinary grade (M20), standard grade (M40) and high strength grade (M80 and M100) made with optimum percentages of GBFS as fine aggregate replacement.

Peak stress values and their corresponding strains of optimally blended binary, ternary and quaternary blended SCC mixes of ordinary grade (M20), standard grade (M40) and high strength grade (M80 and M100) made with optimum percentages of GBFS as fine aggregate replacement are presented in Table 5.83.

11.4 Modulus of Elasticity

From the plotted Stress-Strain curves, modulus of elasticity and modulus of toughness for optimally blended binary, ternary and quaternary blended SCC mixes of ordinary grade (M20), standard grade (M40) and high strength grade (M80 and M100) made with optimum percentages of GBFS as fine aggregate replacement can be calculated. Modulus of Toughness and Modulus of Elasticity values of optimally blended binary, ternary and quaternary blended SCC mixes of ordinary grade (M20), standard grade (M40) and high strength grade (M80 and M100) made with optimum percentages of GBFS as fine aggregate replacement are shown in Table 5.84 and Fig 5.56. It was found that the elastic behaviour and energy absorption capacity of an optimally blended Fly Ash (FA), Microsilica (MS) and Metakaolin (MK) in binary, ternary and quaternary SCC mixes made with partial optimal replacement of GBFS as fine aggregate are almost alike as that of binary, ternary and quaternary SCC mixes made with river sand as fine aggregate. The percentage of optimal replacement levels of GBFS varies with the grade of the SCC mixes.

Table 84 - Stress - Strain values of ordinary grade M20 blended SCC mixes made with GBFS as partial replacement of River Sand

M20 blended SCC mixes made with GBFS as partial replacement of fine aggregate											
C1-G		B2-G		B7-G		B13-G		T3-G		T15-G	
Strain	Stress (MPa)	Strain	Stress (MPa)	Strain	Stress (MPa)	Strain	Stress (MPa)	Strain	Stress (MPa)	Strain	Stress (MPa)
0	0	0	0.00	0.0000	0	0	0.00	0.0000	0	0	0
0.0002	3.23	0.0002	3.64	0.0003	3.64	0.0003	4.02	0.0003	3.89	0.0001	2.86
0.0004	5.72	0.0004	6.45	0.0004	6.42	0.0004	7.12	0.0004	6.88	0.0002	5.72
0.0005	8.57	0.0005	9.67	0.0006	9.64	0.0006	10.66	0.0006	13.62	0.0003	8.57
0.0007	11.43	0.0007	12.89	0.0007	15.85	0.0007	15.21	0.0009	13.77	0.0004	11.43
0.0008	16.89	0.0008	16.92	0.0010	16.06	0.0010	17.78	0.0011	17.21	0.0006	14.29
0.001	17.16	0.0011	19.34	0.0013	19.27	0.0012	21.33	0.0013	20.64	0.0007	17.16
0.0012	20.02	0.0013	22.56	0.0015	22.49	0.0014	24.88	0.0016	24.09	0.0008	20.02
0.0015	22.88	0.0016	25.80	0.0018	25.7	0.0018	28.43	0.0019	27.53	0.001	22.88
0.002	26.9	0.0021	35.27	0.0023	30.28	0.0022	33.57	0.0023	34.07	0.0013	25.73
0.0023	22.88	0.0024	25.80	0.0028	25.7	0.0027	28.43	0.0029	27.53	0.0021	37.89
0.0026	18.89	0.0027	21.30	0.0031	21.22	0.0029	23.48	0.0031	22.74	0.0027	25.35
0.0035	15.05	0.0033	16.97	0.0034	16.91	0.0031	18.70	0.0032	18.11	0.003	18.18

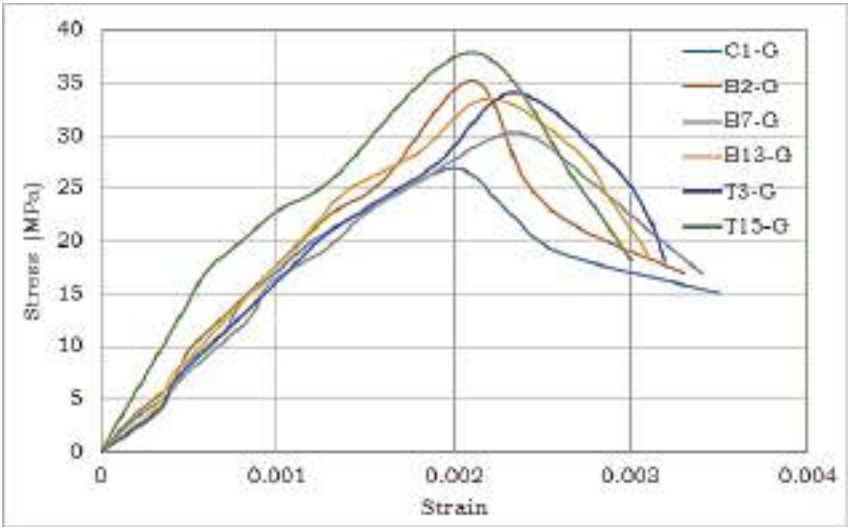

Fig 55 - Stress - Strain curve for ordinary grade M20 blended SCC mixes made with GBFS as partial replacement of River Sand

Table 85 - Stress - Strain values of standard grade M40 blended SCC mixes made with GBFS as partial replacement of River Sand

M40 blended SCC mixes made with GBFS											
C1		B1		B5		B10		T5		T9	
Strain	Stress (MPa)	Strain	Stress (MPa)	Strain	Stress (MPa)	Strain	Stress (MPa)	Strain	Stress (MPa)	Strain	Stress (MPa)
0	0	0	0	0	0	0	0	0	0	0	0
0.0001	2.817	0.0001	2.943	0.0001	5.072	0.0001	3	0.0001	3.028	0.0001	6.296
0.0002	5.773	0.0002	6.24	0.0001	5.313	0.0002	5.169	0.0002	3.114	0.0002	6.437
0.0003	8.66	0.0002	6.24	0.0002	8.915	0.0003	8.999	0.0003	9.084	0.0003	6.685
0.0004	11.55	0.0003	11.77	0.0003	11.89	0.0004	14.97	0.0004	15.32	0.0004	12.87
0.0005	14.43	0.0004	14.72	0.0004	14.86	0.0005	15	0.0005	15.46	0.0005	13.12
0.0006	17.33	0.0005	18.3	0.0005	17.84	0.0006	20.13	0.0006	18.18		
0.0007	**22.22**	0.0006	20.61	**0.0006**	**20.81**	**0.0007**	**22.71**	**0.0007**	**22.07**		
0.0008	23.1	**0.0007**	**22.48**	0.0007	23.78	0.0008	24.01	0.0008	24.82	**0.0006**	**24.96**
0.0009	25.99	0.0007	26.5	0.0008	26.75	0.0009	27.01	0.0009	27.5	0.0009	28.93
0.001	28.88	0.0008	29.44	0.0009	29.73	0.0010	30.01	0.0010	30.6	0.0010	31.11
0.0012	31.76	0.0009	32.39	0.001	32.7	0.0011	33.01	0.0011	33.32	0.0011	31.47
0.0013	34.65	0.001	35.78	0.0011	35.67	0.0012	36.01	0.0012	36.35	0.0012	36.69
0.0014	37.54	0.0011	38.27	0.0012	38.64	0.0013	39.01	0.0013	39.38	0.0009	39.74
0.0016	40.42	0.0012	41.22	0.0014	41.61	0.0014	42.01	0.0014	42.4	0.0011	42.8
0.0021	49.31	0.0016	44.16	0.0015	44.58	0.0015	45.01	0.0015	45.43	0.0012	45.86
0.0024	42.13	0.0022	57.18	0.0018	47.55	0.0016	48.01	0.0017	48.46	0.0014	48.91
0.0027	37.54	0.0027	44.16	0.0021	53.03	0.0017	51.01	0.0021	61.25	0.0016	51.97
0.0031	30.91	0.003	41.22	0.0025	47.55	0.0018	54.02	0.0026	48.46	0.0022	61.76
		0.0032	38.27	0.0027	44.58	0.002	54.66	0.0028	45.43	0.0027	51.97
				0.0031	41.61	0.0023	53.77	0.0031	39.27	0.0029	48.91
						0.0028	46.64			0.0031	45.86
						0.003	32.82			0.0033	41.58
						0.0032	29.81				

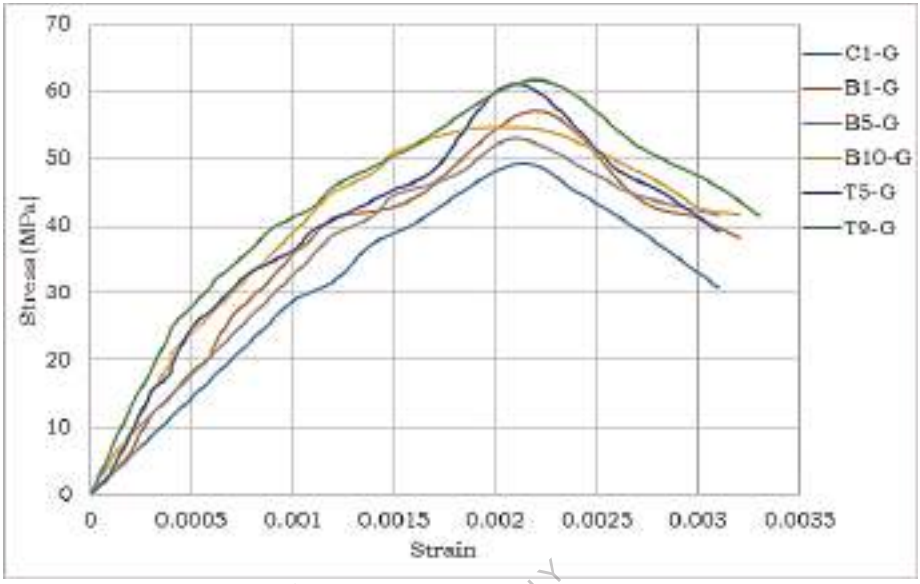

Fig 56 - Stress - Strain curve for standard grade M40 blended SCC mixes made with GBFS as partial replacement of River Sand

Table 86 - Stress - Strain values of high strength M80 and M100 blended SCC mixes made with GBFS as partial replacement of River Sand

M80 blended SCC mixes made with GBFS						M100 blended SCC mixes made with GBFS					
B2-G		T3-G		Q11-G		B2-G		T2-G		Q11-G	
Strain	Stress (MPa)	Strain	Stress (MPa)	Strain	Stress (MPa)	Strain	Stress (MPa)	Strain	Stress (MPa)	Strain	Stress (MPa)
0	0	0	0	0	0	0	0	0	0	0	0
0.0001	2.642	0.0001	3.392	0.0001	6.599	0.0001	2.54	0.0001	3.17	0.0001	4.53
0.0003	6.375	0.0003	11.67	0.0002	12.42	0.0003	11.20	0.0003	10.91	0.0002	11.32
0.0005	15.28	0.0005	22.19	0.0003	17.64	0.0004	17.69	0.0005	20.74	0.0003	17.36
0.0006	19.67	0.0006	28.31	0.0004	20.2	0.0005	21.63	0.0006	26.46	0.0004	21.64
0.0007	26.46	**0.0007**	**32.99**	**0.0005**	**23.9**	0.0006	25.44	0.0007	32.70	0.0005	30.13
0.0008	**37.89**	0.0008	42.16	0.0006	39	0.0007	32.59	0.0008	39.40	0.0006	38.78
0.0009	41.94	0.0009	49.7	0.0007	44.27	**0.008**	**41.25**	**0.0009**	**46.45**	**0.0007**	**40.54**
0.001	50.95	0.001	57.49	0.0009	57.54	0.001	50.99	0.001	53.73	0.0009	56.34
0.0011	62.49	0.0011	65.31	0.001	65.89	0.0011	57.09	0.0011	61.04	0.001	63.75
0.0012	70.01	0.0012	72.96	0.0011	73.44	0.0012	64.32	0.0012	68.19	0.0011	74.20
0.0016	88.82	0.0016	97.28	0.0014	94.07	0.0016	85.40	0.0016	90.92	0.0014	88.00
0.0022	92.1	0.0022	101.1	0.0018	103.1	0.0022	106	0.0022	111.8	0.0018	102.20
0.0028	71.11	0.0028	73.87	0.002	104.4	0.0025	70.3	0.0025	89.04	0.0020	111.80
				0.0021	103.9					0.0022	113.80
				0.0023	102.7					0.0025	101.23
				0.0024	97.27						

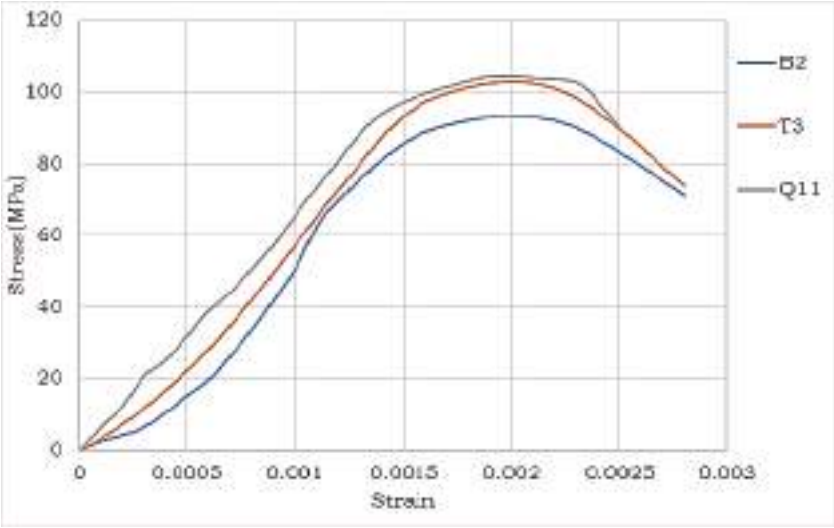

Fig 57- Stress - Strain curve for high strength M80 blended SCC mixes made with GBFS as partial replacement of River Sand

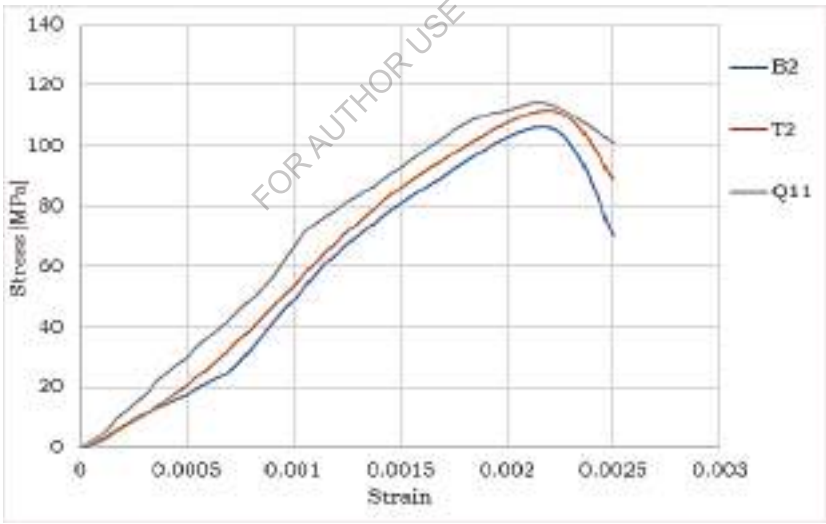

Fig 58 - Stress - Strain curve for high strength M100 blended SCC mixes made with GBFS as partial replacement of River Sand

Table 87 -Peak stress values and their corresponding strains of blended SCC mixes made with GBFS as partial replacement of River Sand

Grade of SCC Mix	Mix No	Mix Designation (Values indicate percentage by weight of Total Powder)	Optimum Percentage Replacement of River Sand with GBFS	Peak Stress f_o (MPa)	Corresponding strain at peak stress $\in_o$
M20	C1-G	C100+GBFS50	50	26.9	0.002
	B2-G	C50+FA50+GBFS60	60	35.27	0.0021
	B7-G	C80+MS20+GBFS60	60	30.28	0.0023
	B13-G	C75+MK25+GBFS60	60	33.57	0.0022
	T3-G	C35+FA50+MS15+GBFS60	60	34.07	0.0023
	T15-G	C25+FA60+MK15+GBFS70	70	37.89	0.0021
M40	C1-G	C100+GBFS40	40	49.31	0.0021
	B1-G	C60+FA40+GBFS50	50	57.18	0.0022
	B5-G	C85+MS15+GBFS50	50	53.03	0.0021
	B10-G	C80+MK20+GBFS50	50	54.66	0.0020
	T5-G	C50+FA40+MS10+GBFS50	50	61.25	0.0021
	T9-G	C35+FA50+MK15+GBFS60	60	61.76	0.0022
M80	B2-G	C95+MS5	20	92.10	0.0022
	T3-G	C65+FA20+MS15	20	101.10	0.0022
	Q11-G	C50+FA28+MS11+MK11	30	104.40	0.0020
M100	B2-G	C90+MS10	20	106.00	0.0022
	T2-G	C71+FA19+MS10	20	111.80	0.0022
	Q11-G	C55+FA23+MS11+MK11	30	113.80	0.0022

Table 88 -Modulus of Elasticity 'E_c' blended SCC mixes made with GBFS as partial replacement of River Sand

Grade of SCC Mix	Mix No	Mix Designation (Values indicate percentage by weight of Total Powder)	Optimum Percentage Replacement of River Sand with GBFS	Secant Modulus Of Elasticity (MPa) E_c
M20	C1-G	C100+GBFS50	50	21113
	B2-G	C50+FA50+GBFS60	60	21150
	B7-G	C80+MS20+GBFS60	60	22643
	B13-G	C75+MK25+GBFS60	60	21729
	T3-G	C35+FA50+MS15+GBFS60	60	22700
	T15-G	C25+FA60+MK15+GBFS70	70	23817
M40	C1-G	C100+GBFS50	50	31743
	B1-G	C50+FA50+GBFS60	60	32114
	B5-G	C80+MS20+GBFS60	60	34683
	B10-G	C75+MK25+GBFS60	60	35300
	T5-G	C35+FA50+MS15+GBFS60	60	37243
	T9-G	C25+FA60+MK15+GBFS70	70	41600
M80	B2-G	C95+MS5+GBFS20	20	47363
	T3-G	C65+FA20+MS15+GBFS20	20	47129
	Q11-G	C50+FA28+MS11+MK11+GBFS30	30	47800
M100	B2-G	C90+MS10+GBFS20	20	51563
	T2-G	C71+FA19+MS10+GBFS20	20	51611
	Q11-G	C55+FA23+MS11+MK11+GBFS30	30	57914

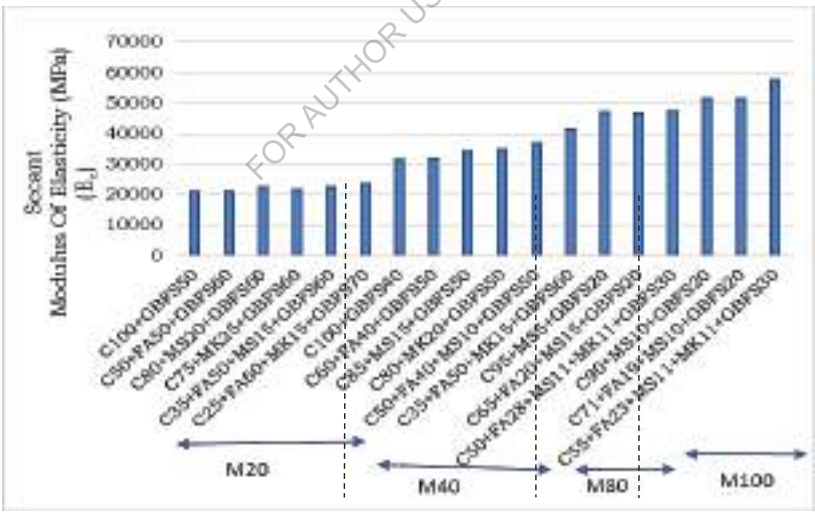

Fig 59- Modulus of Elasticity for optimized SCC mixes of various grades of blended SCC mixes made with optimum percentage of GBFS as fine aggregate replacement

It was found that the stress at peak strains and modulus of elasticity values of an optimally blended Fly Ash (FA), Microsilica (MS) and Metakaolin (MK) in binary, ternary and quaternary SCC mixes made with partial optimal replacement of GBFS as fine aggregate are almost comparable as that of binary, ternary and quaternary SCC mixes made with river sand as fine aggregate. The percentage of optimal replacement levels of GBFS varies with the grade of the SCC mixes.

11.5 Rapid Chloride Permeability Test

The chloride resistance of concrete is governed primarily by the pore structure and the concrete diffusivity. The objective of the present experimental investigations is to determine the chloride penetration resistance of optimally blended binary, ternary and quaternary blended SCC mixes of ordinary grade (M20), standard grade (M40) and high strength grade (M80 and M100) made with optimum percentages of GBFS as fine aggregate replacement at 28, 60 and 90 days through the rapid chloride permeability test.

The total charge passed in coulombs is determined and values are used to rate the quality of the concrete according to the criteria rating mentioned in the ASTM C1202 as shown in Table 89 and Fig 60. Rapid chloride ion penetrability tests was conducted on all grades of optimally blended SCC mixes made with optimum percentages of GBFS as fine aggregate replacement of 28, 60 and 90 days to determine the total charge passed based on which chloride ion permeability can be estimated.

It was found that the chloride ion resistance of an optimally blended Fly Ash (FA), Microsilica (MS) and Metakaolin (MK) in binary, ternary and quaternary SCC mixes made with partial optimal replacement of GBFS as fine aggregate are approximately analogous as that of binary, ternary and quaternary SCC mixes made with river sand as fine aggregate. The percentage of optimal replacement levels of GBFS varies with the grade of the SCC mixes.

Table 89 - Total charge passed for blended SCC specimens of various grades made with GBFS as partial replacement of River Sand

Grade of SCC Mix	Mix No	Mix Designation (Values indicate percentage by weight of 'P')	Total Charge Passed (Coulombs)	Chloride ion Permeability as per ASTM C1202	Total Charge Passed (Coulombs)	Chloride ion Permeability as per ASTM C1202	Total Charge Passed (Coulombs)	Chloride ion Permeability as per ASTM C1202
			28 days		60 days		90 days	
M20	C1-G	C100+GBFS50	2417	Moderate	2215	Moderate	2103	Moderate
	B2-G	C50+FA50+GBFS60	1579	Low	991	Very Low	967	Very Low
	B7-G	C80+MS20+GBFS60	993	Very Low	947	Very Low	913	Very Low
	B13-G	C75+MK25+GBFS60	995	Very Low	961	Very Low	937	Very Low
	T3-G	C35+FA50+MS15+GBFS60	578	Very Low	562	Very Low	503	Very Low
	T15-G	C25+FA60+MK15+GBFS70	376	Very Low	335	Very Low	267	Very Low
M40	C1-G	C100+GBFS50	2008	Moderate	1922	Low	1567	Low
	B1-G	C50+FA50+GBFS60	1423	Low	946	Very Low	921	Very Low
	B5-G	C80+MS20+GBFS60	984	Very Low	922	Very Low	891	Very Low
	B10-G	C75+MK25+GBFS60	990	Very Low	932	Very Low	904	Very Low
	T5-G	C35+FA50+MS15+GBFS60	559	Very Low	543	Very Low	488	Very Low
	T9-G	C25+FA60+MK15+GBFS70	353	Very Low	311	Very Low	235	Very Low
M80	B2-G	C95+MS5+GBFS20	1134	Low	1023	Low	971	Very Low
	T3-G	C65+FA20+MS15+GBFS20	1019	Low	668	Very Low	561	Very Low
	Q11-G	C50+FA28+MS11+MK11+GBFS30	534	Very Low	203	Very Low	97	Negligible
M100	B2-G	C90+MS10+GBFS20	1092	Low	1006	Low	892	Very Low
	T2-G	C71+FA19+MS10+GBFS20	987	Very Low	509	Very Low	432	Very Low
	Q11-G	C55+FA23+MS11+MK11+GBFS30	438	Very Low	158	Negligible	84	Negligible

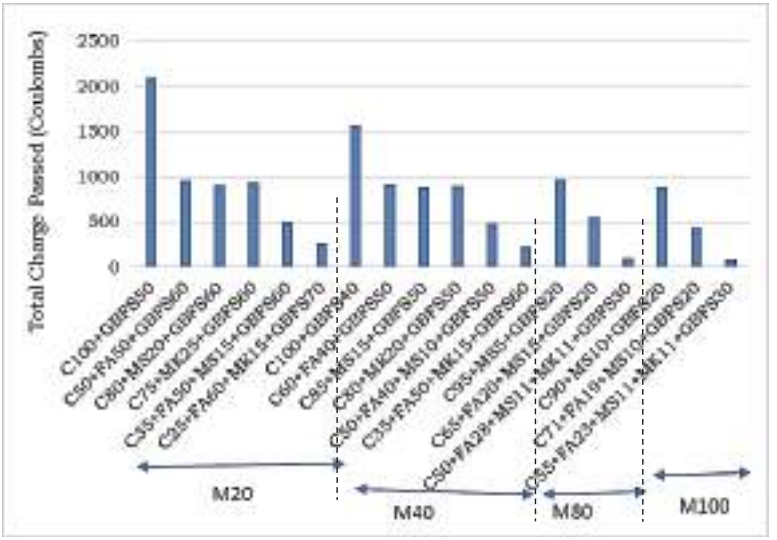

Fig 60- Total charge passed in coulombs for optimized SCC mixes of various grades of blended SCC mixes made with optimum percentage of GBFS as fine aggregate replacement

11.6 Water Absorption Capacity and Porosity

The table 90 presents the measured weights of various grades of blended SCC specimens made with optimum percentage of GBFS as fine aggregate replacement. Table 91 presents the Volume of Permeable Voids (VPV) and Water Absorption Capacity (WAC) of various grades of blended SCC specimens made with optimum percentage of GBFS**.** Fig 61 shows the variation of True and Apparent Densities of various grades of SCC specimens made with optimum percentage of GBFS and Fig 61 shows the variation of percentage of Volume of Permeable Voids (VPV) and Water Absorption Capacity (WAC) of various grades of SCC specimens made with optimum percentage of GBFS. Table 92 presents the porosity of various grades of blended SCC specimens made with optimum percentage of GBFS. Fig 62 shows the variation of Porosity of various grades of SCC specimens made with optimum percentage of GBFS. GBFS has greater surface area than river sand. Even though both belong to zone –II which means that particle size distribution is almost same but GBFS is more porous than river sand so water absorption capacity of GBFS is more than river sand which effects the workability and compressive strength drastically. So in order to maintain workability and compressive strength while replacing river sand with GBFS, the percentage replacements should be optimally chosen for various grades. Use of metakaolin also improves the porous structure of SCC made with GBFS.

Table 90 - Measured Weights of various grades of blended SCC specimens made with GBFS as partial replacement of River Sand

Grade of SCC	Mix No	Mix Designation (Values indicate percentage by weight of Total Powder)	Ma	Mb	Mc	Md
M20	C1-G	C100+GBFS50	2.48	2.63	2.64	1.41
	B2-G	C50+FA50+GBFS60	2.49	2.59	2.61	1.44
	B7-G	C80+MS20+GBFS60	2.51	2.57	2.60	1.45
	B13-G	C75+MK25+GBFS60	2.55	2.62	2.64	1.46
	T3-G	C35+FA50+MS15+GBFS60	2.58	2.65	2.66	1.48
	T15-G	C25+FA60+MK15+GBFS70	2.60	2.65	2.66	1.49
M40	C1-G	C100+GBFS50	2.49	2.63	2.64	1.43
	B1-G	C50+FA50+GBFS60	2.50	2.59	2.61	1.44
	B5-G	C80+MS20+GBFS60	2.51	2.58	2.59	1.46
	B10-G	C75+MK25+GBFS60	2.55	2.61	2.63	1.46
	T5-G	C35+FA50+MS15+GBFS60	2.58	2.63	2.66	1.47
	T9-G	C25+FA60+MK15+GBFS70	2.59	2.63	2.65	1.49
M80	B2-G	C95+MS5+GBFS20	2.51	2.58	2.59	1.45
	T3-G	C65+FA20+MS15+GBFS20	2.59	2.64	2.65	1.5
	Q11-G	C50+FA28+MS11+MK11+GBFS30	2.63	2.67	2.69	1.51
M100	B2-G	C90+MS10+GBFS20	2.53	2.56	2.57	1.46
	T2-G	C71+FA19+MS10+GBFS20	2.55	2.57	2.59	1.48
	Q11-G	C55+FA23+MS11+MK11+GBFS30	2.60	2.62	2.64	1.50

Table 91 - Volume of Permeable Voids (VPV) and Water Absorption Capacity (WAC) of various grades of blended SCC specimens made with GBFS as partial replacement of River Sand

Grade of SCC	Mix No	Mix Designation (Values indicate percentage by weight of Total Powder)	Bulk density g_1	Apparant density g_2	Volume of permeable voids (VPV)	Water Absorption Capacity (WAC) (%)
M20	C1-G	C100+GBFS50	2016.26	2317.76	13.01	6.05
	B2-G	C50+FA50+GBFS60	2128.21	2371.43	10.26	4.02
	B7-G	C80+MS20+GBFS60	2182.61	2367.92	7.83	2.39
	B13-G	C75+MK25+GBFS60	2161.02	2339.45	7.63	2.75
	T3-G	C35+FA50+MS15+GBFS60	2186.44	2345.45	6.78	2.71
	T15-G	C25+FA60+MK15+GBFS70	2222.22	2342.34	5.13	1.92
M40	C1-G	C100+GBFS50	2057.85	2349.06	12.40	5.62
	B1-G	C50+FA50+GBFS60	2136.75	2358.49	9.40	3.60
	B5-G	C80+MS20+GBFS60	2221.24	2390.48	7.08	2.79
	B10-G	C75+MK25+GBFS60	2179.49	2339.45	6.84	2.35
	T5-G	C35+FA50+MS15+GBFS60	2168.07	2324.32	6.72	1.94
	T9-G	C25+FA60+MK15+GBFS70	2232.76	2354.55	5.17	1.54
M80	B2-G	C95+MS5+GBFS20	2201.75	2367.92	7.02	2.79
	T3-G	C65+FA20+MS15+GBFS20	2252.17	2376.15	5.22	1.93
	Q11-G	C50+FA28+MS11+MK11+GBFS30	2228.81	2348.21	5.08	1.52
M100	B2-G	C90+MS10+GBFS20	2279.28	2364.49	3.60	1.19
	T2-G	C71+FA19+MS10+GBFS20	2297.30	2383.18	3.60	0.78
	Q11-G	C55+FA23+MS11+MK11+GBFS30	2280.70	2363.64	3.51	0.77

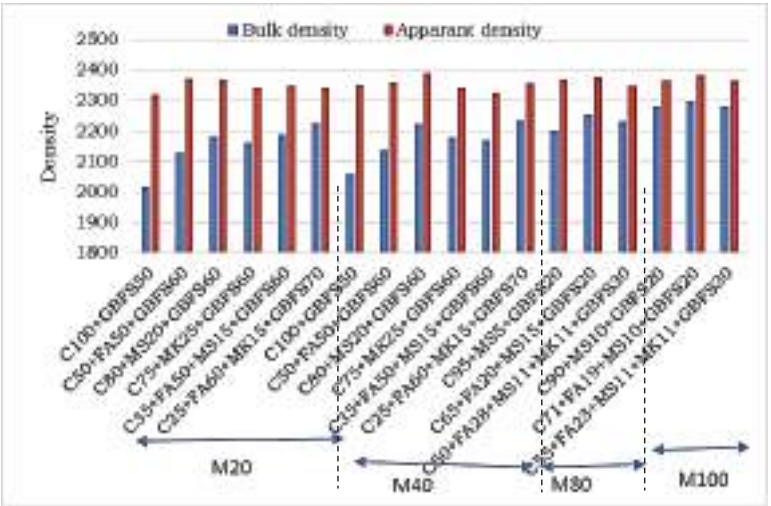

Fig 61- Variation of True and Apparent Densities of optimized SCC mixes of various grades of blended SCC mixes made with optimum percentage of GBFS as fine aggregate replacement

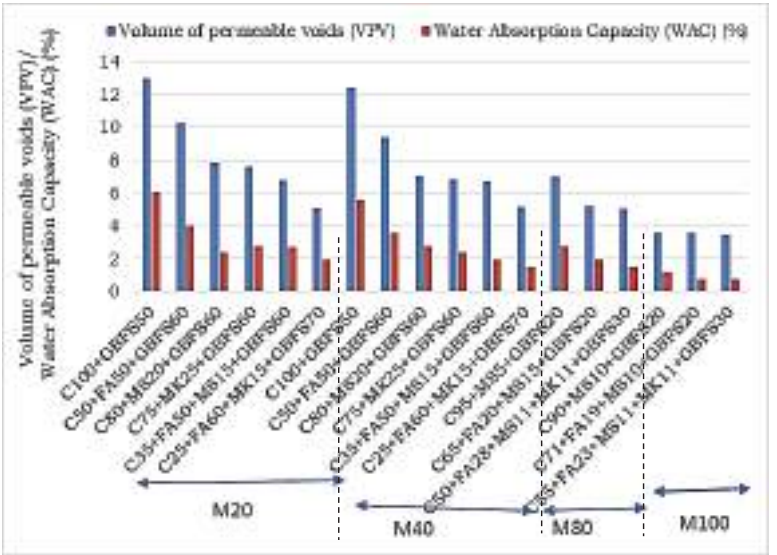

Fig 62- Variation of percentage of Volume of Permeable Voids (VPV) and Water Absorption Capacity (WAC) of optimized SCC mixes of various grades of blended SCC mixes made with optimum percentage of GBFS as fine aggregate replacement

Table 92- Porosity of various grades of blended SCC specimens made with GBFS as partial replacement of River Sand

Grade of SCC	Mix No	Mix Designation (Values indicate percentage by weight of Total Powder)	M_{dry}	M_{sat}	Porosity, P %	Decrease in Porosity
M20	C1-G	C100+GBFS50	2.48	2.63	15	-
	B2-G	C50+FA50+GBFS60	2.49	2.59	10	33.33
	B7-G	C80+MS20+GBFS60	2.51	2.57	6	60.00
	B13-G	C75+MK25+GBFS60	2.55	2.62	7	53.33
	T3-G	C35+FA50+MS15+GBFS60	2.58	2.65	7	53.33
	T15-G	C25+FA60+MK15+GBFS70	2.60	2.65	5	66.67
M40	C1-G	C100+GBFS50	2.49	2.63	14	-
	B1-G	C50+FA50+GBFS60	2.50	2.59	9	35.71
	B5-G	C80+MS20+GBFS60	2.51	2.58	7	50.00
	B10-G	C75+MK25+GBFS60	2.55	2.61	6	57.14
	T5-G	C35+FA50+MS15+GBFS60	2.58	2.63	5	64.29
	T9-G	C25+FA60+MK15+GBFS70	2.59	2.63	4	71.43
M80	B2-G	C95+MS5+GBFS20	2.51	2.58	7	-
	T3-G	C65+FA20+MS15+GBFS20	2.59	2.64	5	28.57
	Q11-G	C50+FA28+MS11+MK11+GBFS30	2.63	2.67	4	42.86
M100	B2-G	C90+MS10+GBFS20	2.53	2.56	3	-
	T2-G	C71+FA19+MS10+GBFS20	2.55	2.57	2	33.33
	Q11-G	C55+FA23+MS11+MK11+GBFS30	2.60	2.62	2	33.33

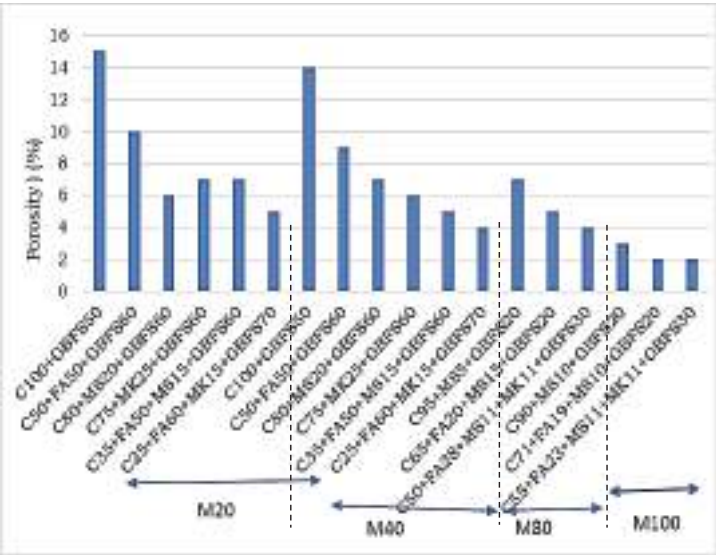

Fig 63- Variation of Porosity of optimized SCC mixes of various grades of blended SCC mixes made with optimum percentage of GBFS as fine aggregate replacement

It was found that the Water Absorption Capacity (WAC) and Volume of Permeable Voids of an optimally blended Fly Ash (FA), Microsilica (MS) and Metakaolin (MK) in binary, ternary and quaternary SCC mixes made with partial optimal replacement of GBFS as fine aggregate are enhanced than that of binary, ternary and quaternary SCC mixes made with river sand as fine aggregate. The percentage of optimal replacement levels of GBFS varies with the grade of the SCC mixes.

Based on the experimental investigations, the following observations are made on GBFS as fine aggregate replacement in optimally blended binary, ternary and quaternary blended SCC mixes of ordinary grade (M20), standard grade (M40) and high strength grade (M80 and M100).

1. GBFS has greater surface area than river sand.
2. GBFS and River sand both belong to zone –II means particle size distribution is same but GBFS is more porous than river sand so water absorption capacity of GBFS is more than river sand which effects the workability and compressive strength drastically. So in order to maintain workability and compressive strength while replacing river sand with GBFS, the percentage replacements should be optimally chosen for various grades.
3. GBFS is innocuous in nature (no reactivity), no deleterious materials are present in it so it can replace river sand by same amount without any changes to total volume ratio of fine aggregate. But being porous in nature , percentage replacements changes for different grades of concrete
4. The strength of concrete was detrimentally affected when the replacement ratio was beyond 70% for M20, 60% for M40, 30% for M80 and 30% for M100. It is established that the main reason for the strength reduction in concrete is the formation of a porous concrete

structure. Moreover, an increase trend in water absorption capacity was observed for all grades. With increase of grade, powder content increases making the paste more dense which reduces the porosity in the concrete made with GBFS. Due to which the replacement levels decreases as grade increases to maintain the same workability and compressive strength of concrete made with river sand

5. GBFS/river sand ratio governs the porosity of the matrix, this porous structure causes negative effect on the strength and durability of the blended SCC mixes
6. GBFS/river sand ratio is the governing criteria for the effects of strength and durability characteristics improvement in strength may be due to shape, size and surface texture of slag aggregates, which provide better adhesion between the particles and cement matrix.
7. The most important condition for use of GBFS is the requirement of using sand finer than GBFS then percentage replacements can be improved because concrete will not form porous structure.
8. Workability is reduced in GBFS and reduction in workability can be compensated by adding suitable percentage of super plasticizer.
9. Density of concrete made with GBFS is less than concrete with river sand
10. From Visual Observations, it can be reported that GBFS is low density, porous and vesicular aggregate with particle shapes mainly angular, cubic and some are rod like. High vesicular nature's particles are responsible for high density and high porosity. The use of different industrial by-products shows prospective application in construction industry as an alternative to conventional materials. Such practice conserves natural resources and reduces the space required for the landfill disposal of these waste materials. Based on these findings it can be stated the GBFS can be used as a replacement to natural sand provided that if used judicially it can be the promising solutions towards sustainable infrastructure without compromising strength and economy. Hence, it could be recommended that GBFS aggregate could be effectively utilized as partial fine aggregate replacement in all blended SCC applications.

12.FINDINGS AND RECOMMENDATIONS

Based on the systematic and detailed experimental study conducted on ordinary grade (M20), standard grade (M40) and high strength grade (M80 and M100) of binary , ternary and quaternary blended Self-Compacting Concrete (SCC) mixes made with fly ash (FA), microsilica (MS) and metakaolin (MK) with an aim to develop performance mixes, the following are the conclusions arrived.

1. Metakaolin blended binary, ternary and quaternary Self-Compacting Concrete (SCC) mixes attain early strengths due to its inherent faster reacting capability than microsilica (MS) blended SCC mixes.
2. In ordinary grade (M20) and standard grade (M40) SCC mixes, metakaolin blended SCC mixes showed superior performance in terms of rheology and strength than the microsilica blended binary and ternary fly ash based SCC mixes.
3. In ternary blended ordinary grade (M20) SCC mixes, both optimally blended 35%OPC+50%FA+15%MS and 25%OPC+60%FA+15%MK combinations attained comparable compressive strengths. So it can be observed that with the inclusion of metakaolin (MK) to fly ash blended SCC mixes yields more usage of fly ash compared to micro silica (MS) blended SCC mixes. Therefore metakaolin (MK) is much preferred to micro silica (MS) for fly ash based ternary blended ordinary grade (M20) SCC mix due to less consumption of cement, more utilization of fly ash, less expensive, early strength attainment which compensates the later strength accomplishment of fly ash and better rheology.
4. Similarly, for standard grade (M40) ternary blended SCC mixes, 50%OPC+40%FA+10%MS and 35%OPC+50%FA+15%MK optimal combinations yield comparable strengths. So it is apparent that metakaolin is much preferred to micro silica in blended SCC mixes made with water/powder ratio above 0.35.
5. For development of high strength SCC mixes (M80 and M100), use of micro silica is compulsory due to its inherent high reactive property and micro-filler capacity.
6. In development of high strength (M80 and M100) grade fly ash blended SCC mixes, both metakaolin and micro silica are required to be added to leverage the benefits of micro-filler capacity of micro silica and early strength attainment of metakaolin. Addition of metakaolin (MK) to blended SCC mixes will enhance early hydration because of it high reactivity.
7. Optimally blended high strength grades M80 and M100 quaternary SCC mixes made of 50%OPC+28%FA+11%MS+11%MK and 55%OPC +23%FA+11%MS+11%MK respectively, yields both enhanced flow and desired compressive strengths. From this observation, it can be understood that micro silica (MS) in blended SCC mixtures imparts high strength while metakaolin (MK) inclusion enhances the usage of high quantity of fly ash in SCC mixes for superior rate of gain of strength and more importantly for improved flow properties of SCC mix. So it is evident that both metakaolin and micro silica are required in blended SCC mixes made with low water/powder ratio.
8. From the above observations it can be assumed for better flow and strength realization, the metakaolin can be optimally replaced by 15% for ordinary grade (M20) and standard grade (M40) blended fly ash based SCC mixes where as in high strength grades (M80 and M100) blended fly ash based SCC mixes, the optimum percentage use of metakaolin is found to be 11%.
9. Compressive, tensile, flexural and impact strengths of metakaolin blended binary, ternary and quaternary Self-Compacting Concrete (SCC) mixes have slightly increased than non- metakaolin blended SCC mixes. Metakaolin cementing reaction rate is very rapid, significantly increasing

compressive strength before first three days, which can have various benefits in fast paced construction industry.

10. It is observed the ultrasonic pulse velocity and rebound number values increased due to refined pore structure and microstructure of metakaolin blended binary, ternary and quaternary SCC mixes.

11. From the observations made from stress-strain curves, the metakaolin blended SCC mixes have shown improved stress values for the same strain levels. The strain at peak stress is slightly higher, and the slope of the descending part is steeper due to the decrease in the extent of internal micro cracking in metakaolin blended SCC mixes.

12. Metakaolin (MK) is highly reactive alumina silicate whereas micro silica (MS) is reactive silicate. Hence Metakaolin (MK) supplemented SCC mixes have high strengths at all ages because silica and alumina present in Metakaolin (MK) reacts with CH forms CSH (pozzolanic reaction) and CAH (aluminate hydration) respectively which contributes to additional strength than micro silica (MS). So quaternary blended SCC mix made with micro silica (MS) and Metakaolin (MK) has improved microstructure which is dense and impermeable.

13. Since Metakaolin (MK) does not increase the compressive strength of cement paste directly, it is concluded that flexural strength improvement in the concrete is due to changes in the structure of the interfacial zone and the increased paste-aggregate bond strength.

14. Metakaolin blended SCC mixes have high resilience and strain relieving capacity. This resilient character provides the excellent impact resistance and dissipates dynamic loading. The increase in number of blows up to failure for metakaolin based quaternary blended SCC indicates its high energy absorption capacity which in turn enhances the increased impact resistance. This feature is attributed to the dense pore structure of metakaolin (MK) blended SCC mixes.

15. It was observed that Modulus of Elasticity (E) is relatively more for all grades of optimally blended MK based SCC mixes by about 12-20%. It can be concluded that toughness or energy absorption capacity of optimally blended SCC mixes of various grades are more due to its enhanced ability to counteract crack propagation by dissipating deformation energy. High toughness in optimally blended metakaolin based SCC mixes signify its improved shock resistance. It is observed that modulus of elasticity (E) is relatively more in all grades of optimally blended SCC mixes in which metakaolin (MK) is induced indicating its enhanced performance due to dense microstructure.

16. The contribution of metakaolin (MK) to any property of hardened concrete may be expressed in terms of efficiency factor, k. For compressive strength of metakaolin blended SCC mixes , k is in the range of 1.08 to 1.69, which means that in a given SCC mix, 1 kg of metakaolin (MK) based pozzolanic material may replace 1.08 to 1.69 kg of cement without impairing the compressive strength. This evaluation makes it possible to design metakaolin blended binary, ternary and quaternary SCC mixes for a desired strength at any given percentage of replacement.

17. Regression equations developed helps in predicting relationships between split tensile strength, flexural strength, water-powder ratio, quantity of powder and modulus of elasticity in terms of specified compressive strength for blended SCC mixes are evaluated using statistical modelling.

18. There is a significant increase in durability properties of metakaolin blended SCC mixes. It is observed that the permeation properties, acid and sulphate attack resistance, chloride impermeability has increased substantially due to enhanced engineering properties and improved microstructure of metakaolin blended SCC mixes. Unexpectedly, the metakaolin blended SCC showed a negative effect on sulfuric acid resistance behavior due to formation of ettringate but this

effect is nullified by the incorporation of microsilica to metakaolin blended fly ash based SCC for all grades.

19. The metakaolin (MK) based blended SCC mixes would be considered to have very low chloride ion permeability which validates its refined pore structure. Calcium Silicate hydrate (CSH) Phase of metakaolin (MK) blended SCC mixes has a two dimensional foil like structure rather than linear needle like structure of normal CSH of OPC. This foil like structure is more efficient in filling space without leaving large interconnected capillary pores.

20. Metakaolin blended binary, ternary and quaternary SCC mixes of all grades exhibit improved resistance to acids and sulphates due to its enhanced pore structure. This might account for the lower permeability and improved durability of concrete containing metakaolin (MK). In the metakaolin (MK) blended SCC mixes pores are filled in such a way, modifying the original microstructure formed by the cement-sand matrix and subsequently increasing the tortuosity of the capillary network, resulting in longer paths and smaller pore diameters. The incorporation of metakaolin in blended SCC mixes reduce the chloride diffusion rate significantly.

21. Metakaolin (MK) based blended SCC mixes exhibits better resistance to sea water attack than any other SCM based SCC due to enhanced pore refinement in the microstructure of concrete and reduction of the interconnectivity of the pore structure by decreasing the pore size (pores refinement), which is directly related to durability.

22. Water Absorption Capacity (WAC) of metakaolin blended SCC mixes is reduced inferring the reduced extent of volume of pores and their connectivity in blended SCC mixes. Volume of permeable pores (VPV) of metakaolin blended SCC mixes are reduced due to reduction in average pore radius of concrete by inducing pore discontinuity in the hydrated cement paste by metakaolin.

23. Sorptivity values for metakaolin (MK) blended SCC mixes were in the range of 0.052 to 0.1.08 $mm/min^{0.5}$ and for non- metakaolin (MK) blended SCC mixes its value is in the range of 0.53 to 0.126 $mm/min^{0.5}$. The capillary absorption coefficient (k) is greatly influenced by the addition of metakaolin (MK) and micro silica (MS) combination to blended SCC mixes. The decrease in capillary absorption coefficient (k) indicates the dense pore structure of blended SCC mixes due to enhanced microstructure of SCC.

24. GBFS is more porous than river sand hence the water absorption capacity of GBFS is more than river sand which effects the workability and compressive strength drastically. So in order to maintain workability and compressive strength while replacing river sand with GBFS, the percentage replacements should be optimally chosen for various grades.

25. GBFS/river sand ratio governs the porosity of the matrix, this porous structure causes negative effect on the strength of the concrete. As high as 70% by weight of river sand can be replaced for ordinary grade (M20) with GBFS without any adverse effect on strength and durability of metakaolin blended SCC mixes. Similarly 60% replacement for standard grade M40 and only 30% replacement of GBFS is acceptable for high strength grade (M80 and M100). It is established that the main reason for the strength reduction in SCC mixes made with GBFS is the formation of a porous concrete structure if used beyond certain percentage. So GBFS/ river sand ratio is the governing criteria on the strength characteristics of blended SCC made with partial replacement of GBFS as fine aggregate.

25. The compressive strength, split-tensile strength, flexural strengths and impact strengths of various grades of optimally blended Fly Ash (FA), Microsilica (MS) and Metakaolin (MK) in binary, ternary and quaternary SCC mixes made with partial optimal replacement of GBFS as fine aggregate are almost comparable to that of binary, ternary and quaternary SCC mixes made with river sand as fine aggregate. So it can be concluded that if the river sand is replaced with optimum

percentage of GBFS in blended SCC mixes, similar performance in terms of strength as that of blended SCC mixes made river sand can be achieved.

26. Rebound hammer, ultra-sonic pulse velocity measurements, energy absorption capacity, stress at peak strains, modulus of elasticity, chloride ion resistance, water absorption capacity, and porosity of optimally blended binary, ternary and quaternary Metakaolin (MK) SCC mixes made with partial optimal replacement of GBFS as fine aggregate are enhanced than that of corresponding SCC mixes made with 100% river sand as fine aggregate. The percentage of optimal replacement levels of GBFS varies with the grade of the SCC mixes.

BIBLIOGRAPHY

1. AASHTO T-277, 1983, Electrical Indication of Concrete's Ability to Resist Chloride Ion Penetration, American Association of State Highway and Transportation Officials, USA.
2. ACI 211.4R-93, 2004, Guide for selecting proportions for high-strength concrete with portland cement and fly ash, ACI Manual of Concrete Practice, Part 1, American Concrete Institute, Farmington Hills, Michigan, USA, pp. 13.
3. ACI 237R-07, 2007, Self-consolidating concrete, ACI Manual of Concrete Practice, Part 1, American Concrete Institute, Farmington Hills, Michigan, USA.
4. Albert Kwan, KH & Ivan, YTNG 2008, Performance Criteria for Self consolidating Concrete, HKIE Transactions, vol. 15, no. 2, pp. 35-41.
5. Alyamac, KE & Ince, R 2009, A preliminary concrete mix design for SCC with marble powders, Construction and Building Materials, vol. 23 no. 3, pp. 1201-1210.
6. Ambroise, J, Maximilien, S & Pera, J 1994, Properties of metakaolin blended cements, Advances in Cement Research, vol. 1, no. 4, pp. 161-168.
7. Andrade, C 1993, Calculation of chloride diffusion coefficient in concrete from ionic migration measurement, Cement Concrete and Research, vol. 23, no. 3, pp. 724-742.
8. Antoni, M, Rossen, J Martirena, F & Scrivener, K 2012, Cement substitution by a combination of metakaolin and limestone, cement and concrete research, vol. 42, no. 12, pp. 1579-1589.
9. Antonios Kanellopoulos, Michael Petrou, F & Ioannis Ioannou 2012, Durability performance of self-compacting concrete construction and building materials, vol. 37, no. 1, pp. 320-325.
10. Assem, AA, Hassan, Mohamed Lachemi & Khandaker, MA, Hossain 2012, Effect of metakaolin and silica fume on the durability of self-consolidating concrete, Cement and Concrete Composites, vol. 34, no. 6, pp. 801-807.
11. ASTM C 1202, 1994, Standard Test Method for Electrical Indication of Concrete's Ability to Resist Chloride Ion Penetration, American Society for Testing and Materials, USA.
12. Concrete Specimens, American Society for Testing and Materials, USA.
13. ASTM C 642, 2013, Standard Test Method for Density, Absorption, and Voids in Hardened Concrete, American Society for Testing and Materials, USA.
14. Attiogbe, EK, See, HT & Daczko, JA 2002, Engineering Properties of Self-Consolidating Concrete, Proceedings of the First North American Conference on the Design and Use of Self-Consolidating Concrete, pp. 331-336.
15. Bhanumathidas, N & Mehta, PK 2004, Concrete mixtures made with ternary blended cements containing fly ash and rice husk ash : Fly ash, Silica fume, Slag and Neutral pozzolans in concrete, Proceeding of International conference, CANMET, ACI SP-199, ed. Molhotra, USA,379-391.
16. Bonen, D & Shah, SP 2005, Fresh and hardened properties of self-consolidating concrete, Progress in Structural Engineering and Materials, vol.7, no.1, pp.14-26.
17. Brooks, JJ, Johari, MMA & Mazloom, M 2000, Effect of admixtures on the setting times of high-strength concrete, Cement and Concrete Composites, vol. 22, no. 1, pp. 293-301.
18. Burak Felekoglu, Selcuk Turkel & Bulent Baradan 2007, Effect of water/cement ratio on the fresh and hardened properties of Self-compacting concrete, Building and Environment, vol. 42, no. 4, pp.795-1802.
19. Cassagnabère, F, Mouret, M & Escadeillas, G 2009, Early hydration of clinker slag metakaolin combination in steam curing conditions, relation with mechanical properties, Cement and Concrete Research, vol. 39, no. 12, pp. 1164-1173.

20. Dinakar, P, Babu, KG & Santhanam, M 2008, Durability Properties of High Volume Fly Ash Self Compacting Concrete, Cement and Concrete Composites, vol. 30, no. 10, pp. 880-886.
21. Edamatsu, T, Sugamata, T & Ouchi, M 2003, A Mix-Design Method for SCC Based on Mortar Flow and Funnel Tests, Proceedings of the 3rd International RILEM Symposium on Self-Compacting Concrete, RILEM Publications, pp. 345-355.
22. EFNARC 2005, The European guidelines for self-compacting concrete, European project group.
23. Erhan Guneyisi & Mehmet Gesoglu 2008, Properties of self- compacting mortars with binary and ternary cementitious blends of fly ash and metakaolin, Materials and Structures, vol. 41, no. 9, pp. 1519-1531.
24. Erhan Guneyisi, Mehmet Gesoglu & Erdogan Ozbay 2010, Strength and drying shrinkage properties of self-compacting concretes incorporating multi-system blended mineral admixtures, construction and building materials, vol. 24, no. 10, pp. 1878-1887.
25. Erhan Guneyisi, Mehmet Gesoglu, Fatih Karaboga & Kas m Mermerdas 2013, Corrosion behavior of reinforcing steel embedded in chloride contaminated concretes with and without metakaolin, Composites: Part B, vol. 45, no. 1, pp. 1288-1295.
26. Eva Vejmelkova, Martin Keppert, Stefania Grzeszczyk, Bart ł omiej Skalinski & Robert Cerny 2011, Properties of self-compacting concrete mixtures containing metakaolin and blast furnace slag, Construction and Building Materials, vol. 25, no. 3, pp. 1325-1331.
27. Feldman, RF 1981, Pore structure formatting during hydration of fly ash and slag cement blends, Proceeding Symposium on Fly Ash Utilization in Cement and Concrete, Material Research Society, pp. 124-133.
28. Hall, C 1989, Water sorptivity of mortars and concrete: A Review, Magazine of Concrete Research, vol. 41, no. 14, pp. 51-61.
29. Mousavi, S 2012, Fresh and hardened properties of self-compacting concrete containing metakaolin, construction and building materials, vol. 35, no. 1, pp. 752-760.
30. IS 2386 (Part-3)-1963, Methods of test for aggregate for concrete- Specific gravity, density, voids, absorption and bulking, Bureau of Indian Standard, New Delhi, India.
31. IS 3812 (Part-1)-2003, Pulverized fuel ash-Specification-for use as pozzolana in cement, cement mortar and concrete, Bureau of Indian Standard, New Delhi, India.
32. IS 383-1970, Indian standard specification for coarse and fine aggregates from natural sources for concrete, Bureau of Indian Standard, New Delhi, India.
33. IS 456-2000, Plain and reinforced concrete-Code of practice, Bureau of Indian Standard, New Delhi, India.
34. IS 650-1991, Standard sand for testing of cement-specification, Bureau of Indian Standard, New Delhi, India.
35. IS 9013-1999, Concrete admixtures-specifications, Bureau of Indian Standard, New Delhi, India.
36. IS 9103-1999, Concrete admixtures-specifications, Bureau of Indian Standard, New Delhi, India.
37. Jiping Bai, Stan Wild & Albinas Gailius 2004, Accelerating Early Strength Development of Concrete Using Metakaolin as an Admixture, Materials Science, vol. 10, no. 4, pp. 338-344.
38. Jutice, JM & Kurtis, KE 2007, Influence of metakaolin surface area on properties of cement based materials, ASCE Journal of Materials in Civil Engineering, vol. 19, no. 9, pp. 762-771.

39. Karoline, A, Melo, Arnaldo, M P & Carneiro 2010, Effect of Metakaolin's finesses and content in self-consolidating concrete, construction and building materials, vol. 24, no. 8, pp. 1529-1535.
40. Kazim Turk 2012, Viscosity and hardened properties of self-compacting mortars with binary and ternary cementitious blends of fly ash and silica fume, construction and building materials, vol. 37, no. 1, pp. 326-334.
41. Khayat, KH & Guizani, Z 1997, Use of viscosity-modifying admixtures to enhance stability of fluid concretes, ACI Materials Journal, vol. 94, no. 4, pp. 332-340.
42. Koehler, EP & Fowler, DW 2006, Mixture Proportioning Procedure for Self-consolidating Concrete, Research Report 108-1, International Center for Aggregates Research, University of Texas at Austin, Texas, USA.
43. Li, Z & Ding, Z 2003, Property improvement of Portland cement by incorporating with metakaolin and slag, Cement and Concrete Research, vol. 33, no. 40, pp. 579-584.
44. Mohamed Said-Mansour, El-Hadj Kadri, Said Kenai, Mohamed Ghrici & Rachid Bennaceur 2011, Influence of calcined kaolin on mortar properties, construction and building materials, vol. 25, no. 5,pp. 2275-2282.
45. Moulin, E, Blanc, P & Sorrentino, D 2001, Influence of key cement chemical parameters on the properties of metakaolin blended cements, cement and concrete composites, vol. 23, no. 6, pp. 463-469.
46. Okamura, H & Ouchi, M 2003, Applications of Self-Compacting Concrete in Japan, Proceedings of the 3rd International RILEM Symposium on Self-Compacting Concrete, pp. 3-5.
47. Okamura, H & Ozawa, K 1995, Mix-design for self-compacting concrete, Concrete Library JSCE, vol. 25, pp.107-120.
48. Panesar, DK & Shindman, B 2011, Elastic properties of self-consolidating concrete, Construction and Building Materials, vol. 25, no. 8, pp. 3334-3344.
49. Poon, CS, Lam, I, Kou, SC, Wong, YL & Wong, R 2001, Rate of pozzolanic reaction of metakaolin in high-performance cement pastes, Cement and Concrete Research, vol. 31, no. 9, pp. 1301-1306.
50. Ramezanianpour, AA & Bahrami Jovein, H 2012, Influence of metakaolin as supplementary cementing material on strength and durability of concretes Construction and Building Materials, vol. 30, no. 1, pp. 470-479.
51. Rathan Raj, R, Perumal Pillai, EB & Santhakumar, AR 2013, Evaluation and mix design for ternary blended high strength concrete, Procedia Engineering, vol. 51, no. 1, pp. 65-74.
52. Saak, AW, Jennings, HM, & Shah, SP 2001, New methodology for designing self-compacting concrete, ACI Materials Journal, vol. 98, no. 6, pp. 363-371.
53. Sabir, BB, Wild, S & Bai, J 2001, Metakaolin and cacined clays as Pozzolans for concrete: a review, Cement and Concrete Composites, vol. 23, no. 6, pp. 441-454.
54. Sahmaran, M, Christianto, HA & Yaman, IO 2006, The effect of chemical admixtures and mineral additives on the properties of self-compacting mortars, Cement and Concrete Composites, vol. 28, no. 5, pp. 432-440.
55. Skarendahl, A & Petersson, O 2000, State of the Art Report of RILEM Technical Committee 174-SCC, Self-Compacting Concrete, RILEM Publications S.A.R.L, pp. 154-154.
56. Su, N, Hsu, KC & Chai, HW 2001, A simple mix design method for self-compacting concrete, Cement and Concrete Research, vol. 31, no. 12, pp. 1799-1807.

57. Wee, T H, Suryavanshi, A K & Tin, S S 2000, Evaluation of rapid chloride permeability test (RCPT) results for concrete containing mineral admixtures, ACI Material Journal, vol. 97, no. 2, pp. 221-232.
58. Xie, Y, Liu, B, Yin, J, & Zhou, S 2002, Optimum mix parameters of high-strength self-compacting concrete with ultra-pulverized fly ash, Cement and Concrete Research, vol. 32, no. 3, pp. 477-480.
59. Zhu, W & Bartos, PJM, Permeation properties of self-compacting concrete, Cement and Concrete Research, vol. 33, no. 6, pp. 921-926.
60. "Symposium on Effective Utilization of Resources as Concrete Raw Materials" Japan Concrete Institute, Chugoku and Shikoku Branches, April 2001
61. Wang Ling, Tian Pei, and Yao Yan "Application of ground granulated blast furnace slag in high-performance concrete" China Building Materials Academy, PRC in china
62. Hogan, F. J., and Meusel, J. W., "Evaluation for Durability and Strength Development of a Ground Granulated Blast-Furnace Slag," Cement, Concrete, and Aggregates, V. 3, No.1, Summer, 1981, pp. 40-52
63. Wagaman, T and W.J.Stanley (2005), "Slag: The Ultimate Renewable Resource" Pit and Quarry, May 24 2007.
64. M Maslehuddin, M A Sharif, M Shameen, M Ibrahim and M S Barry, "Comparison of Properties of Steel Slag and Crushed Limestone Aggregates Concretes", Construction and Building Materials, August 2002, pp 105–112.
65. Caldarone, M. A.; Gruber, K. A.; and Burg, R. G., "High-Reactivity Metakaolin: A New Generation Mineral Admixture," Concrete International, V. 16, No. 11, Nov. 1994, pp. 37-40.
66. Caldarone, M. A., and Gruber, K. A., "High Reactivity Metakaolin— A Mineral Admixture for High-Performance Concrete," Concrete under Severe Conditions: Environment and Loading, Proceedings of the International Conference on Concrete under Severe Conditions, CONSEC 1995, Sapporo, Japan, Aug. 1995, K. Sakai, N. Banthia, and O. E. Gjorv, eds., V. 2, E&FN Spon: Chapman & Hall, New York, 1995, pp. 1015-1024.
67. Zhang, M. H., and Malhotra, V. M., "Characteristics of a Thermally Activated Alumino-Silicate Pozzolanic Material and Its Use in Concrete, Cement & Concrete Research, V. 25, No. 8, 1995, pp. 1713-1725.
68. Bai, J.; Wild, S.; Sabir, B. B.; and Kinuthia, J. M., "Workability of Concrete Incorporating Pulverized Fuel Ash and Metakaolin," Magazine of Concrete Research, V. 51, No. 3, 1999, pp. 207-216.
69. Khatib, J. M., and Wild, S., "Sulphate Resistance of Metakaolin Mortar," Cement and Concrete Research, V. 28, No. 1, 1998, pp. 83-92.
70. Thomas, M. D. A.; Gruber, K. A.; and Hooton, R. D., "The Use of High-Reactivity Metakaolin in High-Performance Concrete," High-Strength Concrete, Proceedings of First International Conference, A. Azizinamini, D. Darwin, and C. French, eds., ASCE, 1997, Kona, Hawaii, pp. 517-530.
71. Balogh, A., "High-Reactivity Metakaolin," Aberdeen's Concrete Construction, V. 40, No. 7, 1995, 604 pp. 9.
72. Hooton, R. D.; Gruber, K. A.; and Boddy, A. M., "The Chloride Penetration Resistance of Concrete Containing High-Reactivity Metakaolin," June 2000, (available at: http://www.engelhard.com/pag/pag_markets_concrete_articles.shtml).

73. Dubey, A., and Banthia, N., "Influence of High-Reactivity Metakaolin and Silica Fume on the Flexural Toughness of High-Performance Steel Fiber-Reinforced Concrete," ACI Materials Journal, V. 95, No. 3, May-June 1998, pp. 284-292.
74. Brooks, J. J., and Johari, M. A. M., "Effect of Metakaolin on Creep and Shrinkage of Concrete," Cement and Concrete Composites, V. 23, 2001, pp. 495-502.
75. Kostuch, J. A.; Walters, G. V.; and Jones, T. R., "High-Performance Concrete Containing Metakaolin: A Review," Concrete 2000: Economic and Durable Construction through Excellence: Proceedings of the International Conference, Dundee, Scotland, Sept. 1993, R. K. Dhir and M. R. Jones, eds., 1993, pp. 1799-1811.
76. Walters, G. V., and Jones, T. R., "Effect of Metakaolin on AlkaliSilica Reaction (ASR) in Concrete Manufactured with Reactive Aggregate," Durability of Concrete, Second International Conference, SP-126, V. M. Malhotra, ed., V. 2, American Concrete Institute, Farmington Hills, Mich., 1991, pp. 941-953.
77. Ambroise, J.; Maximilien, S.; and Pera, J., "Properties of Metakaolin Blended Cements," Journal of Advanced Cement-Based Materials, V. 1, No. 4, 1994, pp. 161-168.
78. Coleman, N. J., and McWhinnie, W. R., "Solid State Chemistry of Metakaolin-Blended Ordinary Portland Cement," Journal of Materials Science, V. 35, No. 11, 2000, pp. 2701-2710.
79. Wild, S.; Khatib, J. M.; and Jones, A., "Relative Strength, Pozzolanic Activity and Cement Hydration in Superplasticised Metakaolin Concrete," Cement and Concrete Research, V. 26, No. 10, 1996, pp. 1537-1544.
80. Al-Khaja, W. A., "Strength and Time-Dependent Deformations of Silica Fume Concrete for Use in Bahrain," Construction and Building Materials, V. 8, No. 3, 1994, pp. 169-172.
81. Alexander, M. G., "Deformation Properties of Blended Cement Concretes Containing Blast furnace Slag and Condensed Silica Fume," Advances in Cement Research, V. 6, No. 22, 1994, pp. 73-81.

Survey Analysis of Solar Power Generation Forecasting

Deekshitha Erlapally[1,*] *Dr. K.*Anuradha[2], *Dr.G.*Karuna[3], *V.*Srilakshmi[4], *K.*Adilakshmi[5]

[1]MTech Student, *Computer Science and Engineering*, *GRIET,* Hyderabad, Telangana, India.
[2]Professor, *Computer Science and Engineering*, *GRIET*, Hyderabad, Telangana, India.
[3]Professor, *Computer Science and Engineering*, *GRIET*, Hyderabad, Telangana, India.
[4] Asst.Professor, *Computer Science and Engineering*, *GRIET*, Hyderabad, Telangana, India.
[5] Asst.Professor, *Computer Science and Engineering*, *GRIET*, Hyderabad, Telangana, India.

Abstract: Solar power is the conversion of sunlight into electricity using solar photovoltaic cells as a source of energy. There are various applications for solar power; here is information on PV cell generation. We seek to understand the behavior of solar power plants through the data generated by the photovoltaic modules and the power generation in different weather conditions in India. The goal of this survey is to give a thorough assessment and study of machine learning, deep learning and artificial intelligence. Artificial intelligence (AI) models as well as information preprocessing techniques, parameter selection algorithms and predictive performance evaluations are used in machine learning and deep learning models for predicting renewable energies. But in case of time series data we can predict only the errors using a linear regression model, we can also calculate things like root mean square error (RMSE), mean absolute error (MSE), mean bias error (MBE) and mean absolute percentage error (MAPE). By the analysis of weather condition also we can predict the consumption of current by solar for every 15 minutes, 1day, and 1week or even for 1 month and find the accuracy.

1. Introduction

Solar energy has many benefits, including its sensitivity to imitative circumstances such as increasing oil prices, its renewable nature, and its ability to reduce imports and dependence on foreign resources. Despite the fact that photovoltaic cells are recognized as the significant source of potential energy production, their low return on investment and high upfront costs keeps them from becoming widely used. Since photovoltaic cells generate electricity by converting solar energy into electrical energy, the amount of solar energy produced every day is important to the size of the photovoltaic system, because the amount of solar radiation determines the amount of Major grid [17] integration is difficult because renewable energy is irregular and uncontrollable. Households in India can now use almost any amount of energy due to the recent electric grid at any moment, but it is not equipped for large quantities of uncontrollable generation [10] at this time. As it is converting solar radiance into power we don't get that how much power is emitted for different location, time, and weather. For this type of clarification machine learning techniques are used in order to differentiate it for different conditions.

electricity produced every day. This is influenced by factors such as place, time, and weather patterns. Solar irradiance is the power obtained per unit area from the Sun via electromagnetic radiation in the wavelength range of the solar cell that is in use [13].

Here we seek and analyzed India as a place and the temperature power plants as consideration based on weather condition in India. According to power generation commissioning statistics, solar plants have the largest installed capacity growth dynamics among renewable energy power plants. Making realistic solar generation projections for the day ahead view is becoming an increasingly critical issue in many places throughout the world at the current level of power system development.

Machine-learning techniques are wide applied to several fields where it can separate the weather based power. Machine-learning techniques are wide applied to several fields related to data-driven issues. Machine-learning techniques embrace several knowledge domain areas, like statistics, arithmetic, Ann, data processing, optimization, and computation are all terms that come to mind when thinking about artificial neural networks [18].

Deep learning, a sub-field of machine learning, has been blooming recently due to the rapid expansion of data

technology in hardware and code. Deep Learning calculations have only been used sparingly in the past for determining environmentally friendly power plants. We present these amazing calculations in the field of sustainable power determining by utilizing distinct Deep learning and ANN[16] calculations, such as DBN, Auto Encoder, and LSTM. In our tests, we integrated these calculations to show how effective they are in calculating the energy yield of solar-powered power plants as compared to a traditional MLP and an actual anticipating model. Our outcomes utilizing Deep Learning calculations show a better determining execution thought about than Artificial Neural Networks, like other reference models including such actual models, are artificial neural networks. In the literature, these models are compared with selected machine learning methods and are available predictive models. Using the mean square error, the proposed cloud classification ensemble model reduces the mean square error by 10.49%, 7.78% and 7.95% respectively, with deep belief networks, support vector regression and random forest [15] regression models. The use of weather parameters to forecast solar power generation is suggested as an Artificial Neural Network (ANN). This discussion describes the techniques used to predict renewable energy in machine learning models, including data preprocessing techniques, parameter selection algorithms, and predictive performance measurement.

2. Related Work

Energy is now the primary source of socioeconomic growth. However, because of the increasing rate of environmental concern, renewable energy is attracting a lot of attention. Related to the ongoing depletion of fossil fuels, this alternative energy source is gaining in popularity. That is the energy that comes from the sun, wind, rain, and other natural sources [3].To generate electricity at power plants, electromechanical generators are used, and they are mostly driven by chemical combustion or even nuclear fission heat engines, but also by alternative energy sources such as kinetic energy from flowing water and wind. There are numerous other technologies, such as solar photovoltaic and geothermal power, can and are used to produce electricity. Using thermal power: This method is used in thermocouples, thermopiles, and thermionic converters to convert temperature differences directly to power. Thermal power station is a power plant with a steam-driven primary mover. The water is heated and turned into steam, which powers an electrical generator by spinning a steam turbine. The steam is concentrated in a condenser and returned to where it was heated after passing through the turbine; this is known as the Rankine cycle. Using Wind power: The development of either lift or drag force is one of the two primary physical values by which energy can be extracted from the wind. Hydrostatic pressure, which are the forces felt by a person exposed to the wind, are the most obvious means of propulsion. Buzz forces are the most effective mode of propulsion, but they are less well known than drag forces due to their sensitivity. Using Nuclear power: Charged particles are created and accelerated (examples: beta voltaic or alpha partial emission. In a nuclear power plant, uranium is first formed into pellets, then into long rods. Submerging the uranium rods in water keeps them cold. When they are taken out of the water, a nuclear reaction occurs, resulting in heat. Rising and lowering the thermostat regulates the amount of heat necessary. Using solar power: The photoelectric effect, as seen in solar cells, is responsible for converting light into electrical energy. Since the solar array will stay aligned to the sun, solar monitoring allows for further energy production. To improve performance, a solar system's power production should be maximized. To get the most power out of your solar panels, make sure they're aligned with the sun.

Cluster analysis [8] using nRMSE (Normalized Root Mean Square Error), nMAE (Mean Absolute Error) and nMBE (Mean bias error) solar generation 8.80, 4.06 and -1.01. By using successful feature selection or extraction, you can boost the forecasting efficiency even more. In addition, a [12] new hybrid forecasting method is being developed and tested, which integrates well-known forecasting strategies [7]. The mixed model is created after no discrete method is better than all four seasons. According to RSME, the error of all simulations is 7.210% in summer, 6.921% in early autumn, 8.62% in spring and 9.37% in winter. The results show that a simple combination of many excellent models can provide more reliable predictions than either method. We've got been ready to cut back the error rate from concerning within the persistent ideal, to 15.1% from the Foreign Intelligence Service model, and to 11.8% from the cnn. Similarity features, which are effective in the SVR model, do not improve the deep learning model [9].

For example we take the north china place the winter days based on the climatic characteristics of North China. For each classification, a random forest algorithm-based forecasting model is created [10]. Separately, three other models in addition to the one proposed. Methods for predicting regular power generation and evaluate the performance of the Zhonghu PV station in northern China are described. The model achieves mean absolute percentage errors of less than 2.831 % and 3.1 percent in empirical data due to its capacity to by balancing decision trees, you can reduce the risk of overfitting. The following conclusions are based on empirical findings:

(1) The projected model's MAPE standards for both sunny and cloudy days square measure as low as 2.831 % and 3.890 %.

(2) When it's raining or snowing, the prediction errors of the projected model square measure are greater than they are in other circumstances. In those days, the prediction exactitude may increasing the size coaching samples and

playing subdivision will help. (3) Manual interference with neighbor classifications can increase the accuracy of prediction for sorting transformation days.
(4) In practically every classification, for nearly all error analysis metrics, the predicted model outperforms the other three strategies.

Both the artificial neural network and deep neural network models studied outperform the PPVFM in terms of efficiency [1]. The Auto-LSTM[11] is the best DNN model. With an average RMSE of 0.071, an average MAE of 0.036, and an average absolute deviation of 0:2765, it has the highest score. The greatest BIAS values are seen in the MLP. Using current air temperature and mean daily solar irradiance, they employed Multi-Layer Perceptron (MLP) to estimate the hourly forecast of solar radiation [13]. On unseen test data, the DBN achieves the best correlation, while the Auto-LSTM achieves the best correlation on training data.

Whereas the cloudy version suits the overall sample of the climate, it often predicts incorrectly. When the climate shifts, which occurs nearly each day, PPF's effects are inaccurate [2]. SVM-RBF with decreased features, on the alternative hand, produces a miles extra correct version. The RMSE mistakes for every version imply this: SVM-RBF with 4 dimensions has an RMS-Error of 128 amps, at the same time as hazy and PPF have RMS-Errors of a hundred seventy five and 261, respectively. As a consequence, the 4-dimensional SVM-RBF version is 27% extra correct than the easy cloudy version and 50.9% extra correct than the PPF version [3]. Using the fuzzy logic method, the average error was calculated is 1.92 %, while the average error obtained using the ANN method is 2.62 %.

Random forest is part of machine learning algorithm a random forest is an estimator of some sort, that can fit several decision trees for different sub-samples of a dataset [4]. To get the best algorithm parameters, the hyper parameters tuning in Random Forest Classification approach was utilized [15]. In our case, both the number of decision trees in a forest and the number of landscapes fitted by a single decision tree are hyper parameters. This algorithm is sufficiently accurate, with a state recognition accuracy of 73%.

The Kernel function is used in Support Vector Regressor (SVR) to map input forms into a higher-dimensional space where output patterns can be found and become linearly divisible, allowing pattern extraction by fitting linearly. The aim is to find the best possible match, which can be challenging [9]. Assumed the shape of an optimization problem. Similar weather conditions, according to KNN, may result in alike PV power generation. As a result, the historical dataset can be viewed as a series of cause-and-effect relationships. Predicting future Photovoltaic power generation can be reduced to finding K feature vectors in the past database that are the closest neighbors to those who were present at the time interest. Knn has a lower percentage of error than nrsme, which is around 6.2 % and provides an approximate accuracy of 70% to 80%. A fixed input network with a single hidden layer is used as a back propagation neural network [14]. The input and output vectors' dimensions can be used to measure the neurons in the input and output layers automatically [1]. The initialization of weights and thresholds is performed at random, with an error rate of 8%.

To combine the outcomes of approximately the well-performing uncorrelated techniques into a weighted average as a single forecast the first step is to implement and evaluate all ten forecasting models. The hybrid model has the highest average performance of all the methods, with a yearly nRMSE of just 6.74 percent. CNNs have also been shown to improve efficiency while requiring less memory, all neurons in adjacent layers are connected in completely connected neural networks [8]. As a result, completely related neural networks have an enormous number of model parameters.

Long short term memory (LSTM) is a recurrent neural network (RNN) type that has successfully addressed the conventional RNN's vanishing gradient problem, which makes it difficult to detect and use useful features occurring early in input sequences. Here the combination of cnn+lstm gives MAPE 19.2%.The most basic methodology for estimating the next day's power production is calculated using linear or non-linear regression methods such as logistic regression or SVR and is dependent on inputs such as irradiation, temperature, and power output obtained the day before. Whereas svr is having a MAPE of 49.1%.

3. Flow chart for solar power generation

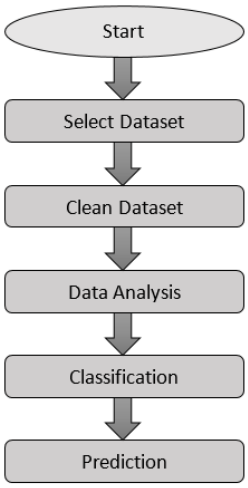

Fig.1 Flow chart

4. Methodology

4.1 Deep Learning Techniques

Consumption of power has become as additional and there are more regenerative generators included into the power grid, there has been an increase of interest in methods for regenerative power forecasting over the last decade [1].

4.1.1Auto LSTM:

The Auto-LSTM algorithm blends an Auto Encoder's function learning with an LSTM's temporal context utilization. The Auto-error LSTM's increases as more time measures are considered during the forecast. It's worth noting that when two previous time phases are factored into the prediction, the RMSE jumps dramatically [1].CNN is a deep learning neural network used to process organized data matrices, such as views. Lines, gradients, circles, and even eyes and faces are very effective in recognizing the design in the input image [5].

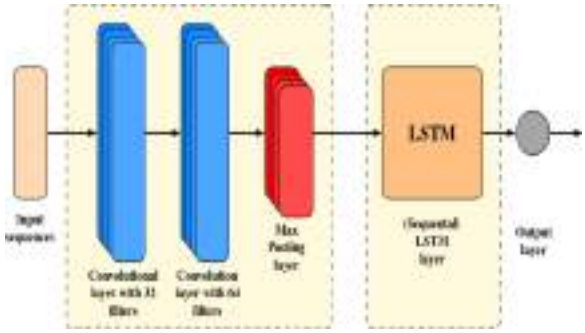

Fig.2 CNN and LSTM architecture

4.1.2 Deep Neural Networks:

DNN has proven its worth in a variety of fields, including representation learning and time series forecasting. To name a few, DNN claims Speech and picture recognition, machine translation, and financial time series forecasting are just a few of the applications. It is used to forecast solar power output [11].

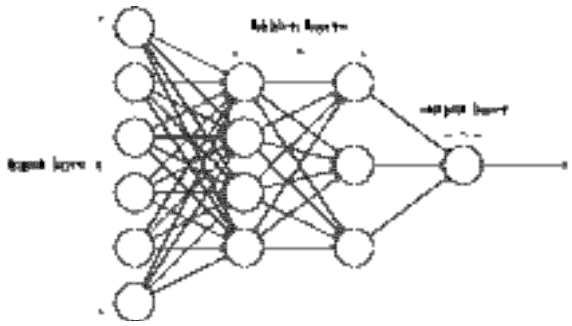

Fig.3 Layers differentiation of DNN

4.1.3 Deep Belief Network (DBN):

Deep belief network (DBN) models began to gain popularity. To forecast monthly solar power output data, a seasonal deep belief network (SDBN) was created in this study. By merging the seasonal decomposition approach and the DBN, the SDBN was created. Furthermore, data on monthly solar power generation was employed in this study.

Foretelling is a two-step approach [1]:

1) To reduce the dimensionality of the input data set, the DBN uses feature learning.

2) To perform forecasting, a new layer is added, such as the linear layer.

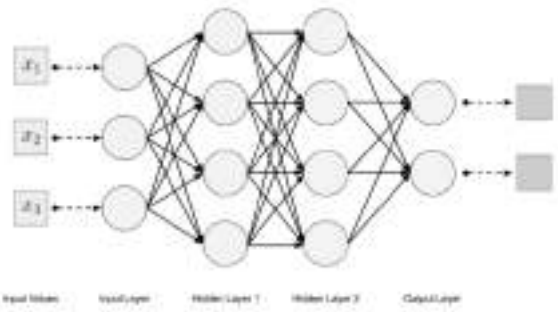

Fig.4 Deep belief network model

4.2 Machine Learning Techniques

4.2.1 Support Vectors Machine:

Then, we investigate a variety of supervised learning methods based on SVM. These methods, which create hyperplanes in a multidimensional space, have currently been approved to be used in indexing and regression analysis. The kernel function and parameters used determine the accuracy of svm regression. In our work, we investigated three distinct SVM kernel functions are Linear Kernel, a Polynomial Kernel and a Radial Basis Function (RBF) kernel [2].

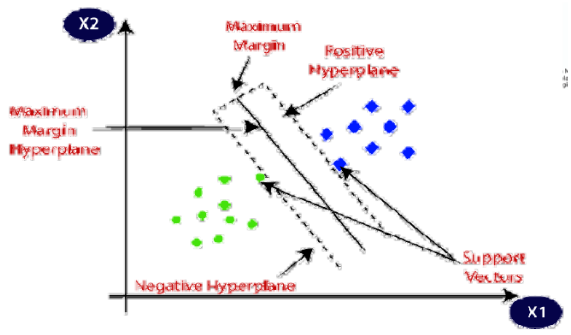

Fig.5 Hyperplane separating data points in SVM

4.2.2 K Nearest Neighbors (Knn):

KNN assumes that similar temperature variations will occur in the future. Would result in PV energy clusters that are comparable. Forecasting future PV power generation with an accuracy of about 81 % can be reduced to searching the past database for K feature vectors that are closest neighbors to those of the time of interest.

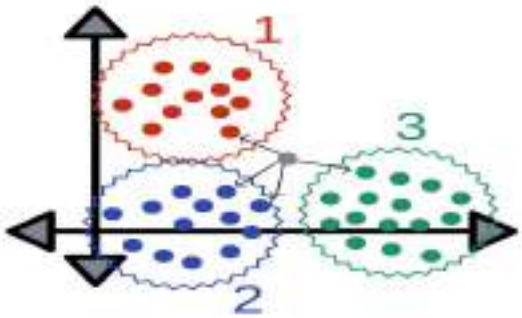

Fig.6 Partition and finding the nearest value in KNN

4.2.3 Random Forest:

Random Forest is an ensemble technique that can be used to classify or predict data productivities of a variety of unrelated decision tree subsystems. The random forest estimates that the precision is about 79%. These techniques can be used to map nonlinear interactions again [19].

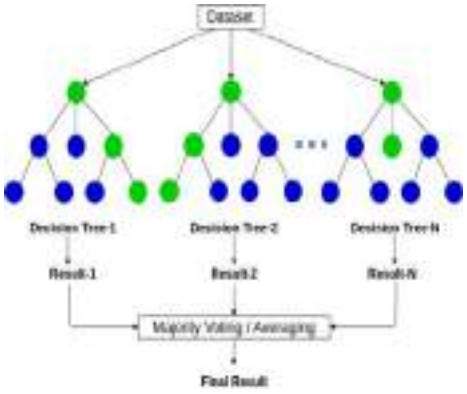

Fig.7 Random forest final results based on decision trees

4.2.4 Linear Regression Model:

Linear regression is a machine learning approach for supervised learning. It performs a regressive mission. Using the independent variables as a guide, regression models attempt to predict the value. Its main use is for forecasting and determining the relationship between variables.

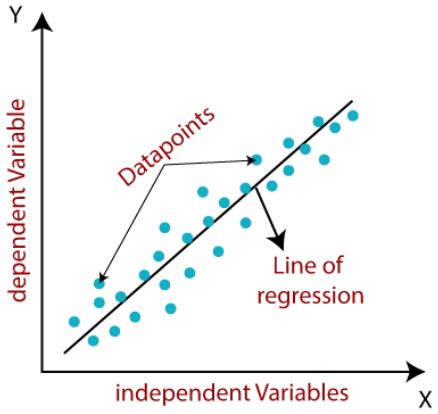

Fig.8 Linear regression model

4.3 Artificial Neural Networks

MATLAB was used to carry out the research. Fuzzy logic and Ann techniques[18] were both found to be effective in that their findings matched the characteristic of a real solar PV array [3]. These will be put to use to forecast and test the overall reliability of the solar power plant. They perform on three sets of data: training, testing, and validation. The MLR model's performance is substantially improved when classification variables and interactions between variables are used, but this is not the case with the ANN model [7].

4.3.1 Fuzzy Logic:

When combined with high-performance computer processors, allows for reasonable accuracy estimates of solar plant outputs while also allowing for system flexibility to adjust for natural events. The MATLAB software was used to construct the load forecasting system, which is based on fuzzy logic. The model has two inputs and one output and represents solar irradiance, ambient temperature, humidity and output power [3].

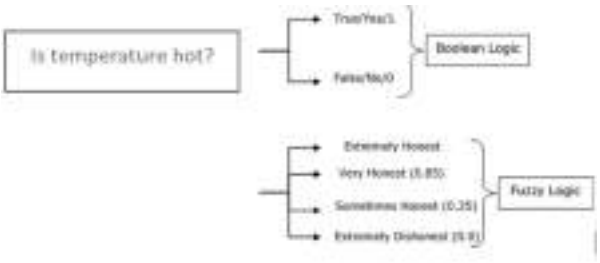

Fig.9 Fuzzy logic model

4.3.2 Multiple Linear Regression:

An ANN[16], as opposed to a multiple linear regression (MLR) model, a statistical method for assessing a non-linear connection between one or more inputs and outcomes. The artificial neural network[6] has been used to model, identify, and forecast complex systems.

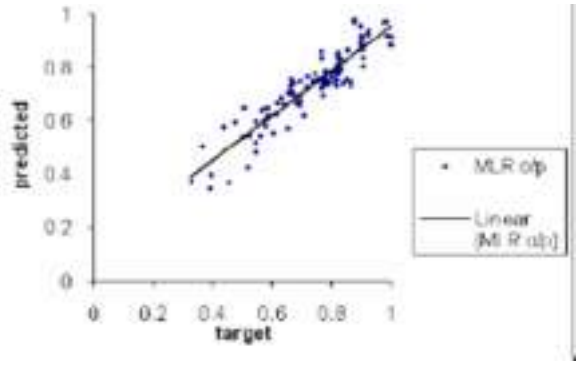

Fig.10 Multi linear regression

5. Comparison

5.1 Comparison of methods used:

Table 1. Model Prediction of RMSE, MAE, MAPE, and MBE

Model	RMSE	MAE	MAPE	MBE	Reference
MLP(multilayer perceptron)	0.0889	-	-	-	1
LSTM	0.0816	-	-	-	1
Clustering based on solar generation	8.80	4.60		-1.01	5
Clustering based on weather variables	8.61	3.77	-	-0.53	5
ANN	0.067	-	-	--	6
MLR(multi linear regression)	0.738	-	-	-	6
SVR(support vector regressor)	0.122	0.099	40.03	-	8
RFR(random forest regressor)	0.178	0.1378	67.58	-	8
CNN+LSTM	0.098	0.0568	13.42	-	8
SP(SMART PERSISTNACE)	0.135	0.071		0.023	11
DBN(deep belief network)	0.0390	0.0138		0.00244	11
SVM(support vector machine)	0.034	0.012		0.00777	11
RF(Random Forest)	0.033	0.0099		0.000351	11

5.2 Graphs comparison based on weather conditions with temperature values:

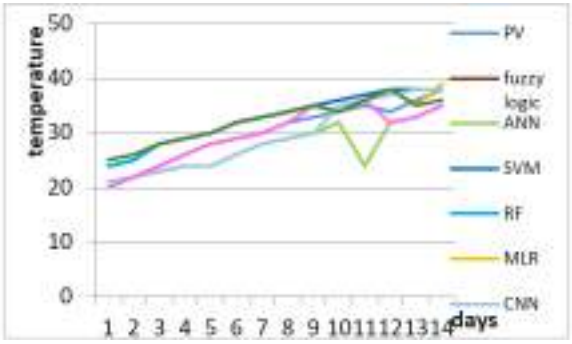

Fig.11 Mean of solar radiance in summer season.

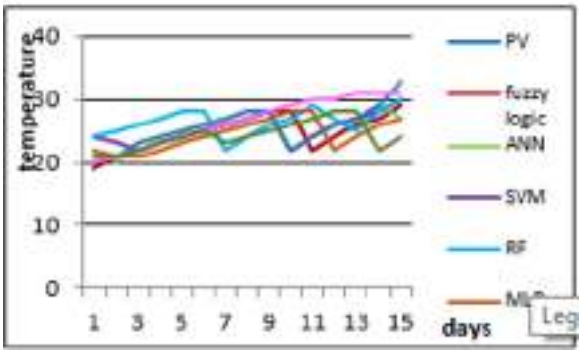

Fig.12 Mean of solar radiance in rainy season

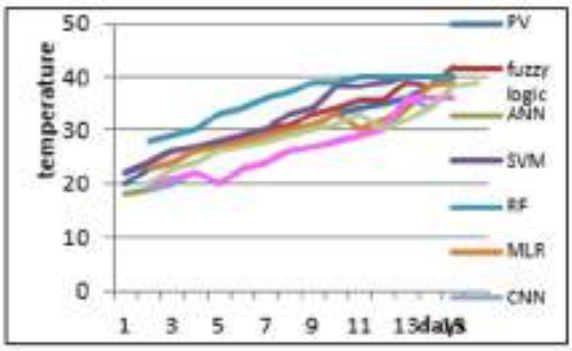

Fig.13 Mean of solar radiance in winter season

Here fig 11, 12, 13 gives the comparative analysis of different models that are used like fuzzy logic, artificial neural network, support vector machine, random forest, multiple linear regressor and Convolutional Neural Network results for different temperature based on seasonal effects with power generated for each day.

7. Conclusion

In this we conclude that it gives the partial analysis of solar power generation or forecasting based on different weather conditions. Different types of solar and wind dataset are considered for different seasons like summer (April to June), rainy (July to November) and winter (December to January) these are all about Indian weather condition. In order to get best results for diverse climatic condition for every hour for future betterment of analyzing power generation in different climatic condition machine learning give better results according to deep learning and artificial intelligence.

Reference

1. A. Gensler, J. Henze, and B. Sick, 2016 IEEE International (2016)
2. N. Sharma, P. Sharma, D. Irwin, and P. Shenoy, in 2011 IEEE International Conference on Smart Grid Communications (SmartGridComm) , pp. 528–533, (2011)
3. Z. P. Ncane and A. K. Saha, in 2019 Southern African Universities Power Engineering Conference/Robotics and Mechatronics/Pattern Recognition Association of South Africa (SAUPEC/RobMech/PRASA), pp. 518–523,(2019)
4. A. Khalyasmaa, S. A. Eroshenko, T. P. Chakravarthy, V. G. Gasi, S. K. Y. Bollu, R. Caire, S. K. R. Atluri, and S. Karrolla, in 2019 International Multi-Conference on Engineering, Computer and Information Sciences (SIBIRCON) , pp. 0780–0785, (2019)
5. C. Pan and J. Tan, IEEE Access 7, 112921 (2019).
6. P. Kora and S. R. Kalva, Springer plus 4, 481 (2015)
7. M. Abuella and B. Chowdhury, in 2015 North American Power Symposium (NAPS) , pp. 1–5, (2015)
8. K. Prasanna Lakshmi and C. R. K. Reddy, in 2010 International Conference on Networking and Information Technology , pp. 451–455(2010)
9. D. Su, E. Batzelis, and B. Pal, in 2019 International Conference on Smart Energy Systems and Technologies (SEST) , pp. 1–6 , (2019)
10. Swaraja K, Multimed. Tools Appl. 77, 28249 (2018)
11. W. Lee, K. Kim, J. Park, J. Kim, and Y. Kim, IEEE Access 6, 73068 (2018)
12. S. Kumar, P. Reddy, G. Ramesh, and V. Maddumala, Trait. Du Signal 36, 233 (2019)
13. F. Jawaid and K. NazirJunejo, in 2016 Sixth International Conference on Innovative Computing Technology (INTECH) , pp. 355–360, (2016)

14. C. U. Kumari, S. Jeevan Prasad, and G. Mounika, 2019 3rd International Conference on Computing Methodologies and Communication (ICCMC) (2019)
15. X. Wang, D. Luo, and C. Li, in 2019 2nd International Conference on Artificial Intelligence and Big Data (ICAIBD) , pp. 97–101, (2019)
16. B. Dhanalaxmi, G. A. Naidu, and K. Anuradha, Procedia Comput. Sci. 46, 432 (2015)
17. Application of Machine Learning Algorithms for Solar Power Forecasting in Sri Lanka
18. P. Nayak, G. K. Swetha, S. Gupta, and K. Madhavi, Measurement 178, 108974 (2021)
19. M. Z. Hassan, M. E. K. Ali, A. B. M. S. Ali, and J. Kumar, in 2017 4th Asia-Pacific World Congress on Computer Science and Engineering (APWC on CSE) , pp. 252–258, (2017)

Analysis Of Solar Power Generation Forecasting Using Machine Learning Techniques

K. Anuradha[1],* *Deekshitha* Erlapally[2], *G*. Karuna[3], *V*. Srilakshmi[4], *K*. Adilakshmi[5]

[1]Professor, Computer Science and Engineering, GRIET, Hyderabad, Telangana, India.
[2]MTech Student, Computer Science and Engineering, GRIET, Hyderabad, Telangana, India.
[3]Professor, Computer Science and Engineering, GRIET, Hyderabad, Telangana, India.
[4] Asst.Professor, Computer Science and Engineering, GRIET, Hyderabad, Telangana, India.
[5] Asst.Professor, Computer Science and Engineering, GRIET, Hyderabad, Telangana, India.

Abstract: Solar power is generated using photovoltaic (PV) systems all over the world. Because the output power of PV systems is alternating and highly dependent on environmental circumstances, solar power sources are unpredictable in nature. Irradiance, humidity, PV surface temperature, and wind speed are only a few of these variables. Because of the unpredictability in photovoltaic generating, it's crucial to plan ahead for solar power generation as in solar power forecasting is required for electric grid. Solar power generation is weather-dependent and unpredictable, this forecast is complex and difficult. The impacts of various environmental conditions on the output of a PV system are discussed. Machine Learning (ML) algorithms have shown great results in time series forecasting and so can be used to anticipate power with weather conditions as model inputs. The use of multiple machine learning, Deep learning and artificial neural network techniques to perform solar power forecasting. Here in this regression models from machine learning techniques like support vector machine regressor, random forest regressor and linear regression model from which random forest regressor beaten the other two regression models with vast accuracy.

1 Introduction:

Solar energy has many benefits, but also have their initial investment for installing solar panels is quite high, and not everyone will be able to afford them. Unfortunately, this is a downside of solar panels; nevertheless, as prices continue to decline, the future looks bright. Solar panels are currently relatively costly; but, new government programs and cutting-edge technology are making them cheaper. Despite the fact that photovoltaic cells are recognized as the significant source of potential energy production, their low return on investment and high upfront costs keeps them from becoming widely used.The high initial cost prevents them from becoming widely used. Because photovoltaic cells convert solar energy into electrical energy, the amount of solar energy produced each day influences the size of the photovoltaic system, just as the amount of solar radiation influences the amount of electricity produced each day. This is influenced by factors such as location, time, and weather patterns. Solar irradiance is the power obtained per unit area from the Sun via electromagnetic radiation in the wavelength range of the solar cell in use.

Major grid integration is difficult because renewable energy is irregular and uncontrollable. Households can now use almost any amount of energy due to the recent electric grid at any moment, but it is not equipped for large quantities of uncontrollable generation at this time. As it is converting solar radiance into power we don't get that how much power is emitted for different location, time, and weather. For this type of clarification machine learning techniques are used in order to differentiate it for different conditions. Machine-learning techniques are wide applied to several fields where it can separate the weather based power.

The amount of energy a PV system generates is proportional to meteorological parameters including cloud cover, sun intensity, and site-specific conditions, among other [3]. Solar panel works differently for different weather conditions. In case if its summer seasons then the amount of energy consumed by the panel from sun is very much more. But in case of rainy and windy conditions the energy consumed is pretty much different. Power generation mostly depends on weather conditions so they take weather forecasting into consideration. As a result, the amount of electricity generated is determined by solar irradiance on a given day, which is determined by a number of factors such as location, time, and weather patterns. We concentrate on the problem of automatically generating models that accurately predict renewable generation based on National Weather Service forecasts (NWS). Using historical NWS forecast data and data generated by solar panels, we experiment with a variety of machine learning techniques to develop prediction models.

* Corresponding author: author@e-mail.org

Meteorological data, including ambient temperature, humidity, and solar radiation, will be collected by meteorological monitoring stations every three hours.

Machine-learning techniques have been widely used in a range of fields involving data-driven problems in recent decades. Machine-learning approaches encompass a wide range of interdisciplinary topics, including statistics, mathematics, artificial neural networks, data mining, optimization, and artificial optimization. With or without mathematical problem forms, machine learning approaches attempt to find a relationship between input and output data. The process of analysing data is known as data analyzation. ML employs statistical approaches to enable computers to "learn" from data without having to be explicitly programmed. Machine learning has two main application categories: regression and classification. Solar power forecasting necessitates the use of regression methods. Some of the ML regression algorithms that can be used for time series forecasting are Linear Regression (LR), Support Vector Machine Regression (SVMR), and Random Forest (RF).

Weather and physical elements influence the electrical power output of a solar photovoltaic (PV) panel. Solar irradiance, cloud cover, humidity, and ambient temperature are the main meteorological factors that influence solar power generation. Predicted weather parameters can be used as model inputs, while solar power forecasts can be used as the model output. Because of its ongoing training nature, the ML algorithm adjusts to physical parameters.

In machine learning SVM plays a major role in order to classify the data and monitor weather condition according. Combining data from photovoltaic power generation with meteorological conditions, according to the positive position of photovoltaic power generation. For every 3 hours svm gives analyzed data for classification and regression analysis. Using hyperplane we can classify the accurate results from solar panel based on the weather conditions.Random forest, on the other hand, is a classification strategy that uses many decision trees to classify data. In order to generate an uncorrelated forest of trees whose committee forecast is more trustworthy than that of any single tree, bagging and feature randomization are utilised in the development of each individual tree. It gives multiple decisions tress it merges all the decision tress into one form of decision tree it's for different climatic conditions such as for summer, rainy, winter seasons. Error statistics such as mean bias error (MBE), mean absolute error (MAE), root mean square error (RMSE), relative MBE (rMBE), mean percentage error (MPE), and relative RMSE are used to assess the model's validity (rRMSE). Linear regression is a supervised learning-based machine learning approach. It does a regression analysis. Based on independent variables, regression models a goal prediction value. It's generally used in forecasting to figure out how variables are related. Regression models differ in terms of the sort of link examined between dependent and independent variables, as well as the number of independent variables used.

2. Related Work:

Solar energy forecasts can be categorised in a variety of ways. The persistence or smart persistence model, which uses historical data to forecast future power generation over a short period of time, is the most basic method (2-3 hours). This method can be used to set a standard against which other forecasting methods can be measured. In most cases, a prediction is completed in two stages. A NWP is designed for a specified time period and location to begin with. The generated NWP is then utilised to forecast power generation using forecasting algorithms. It is possible to employ a physical model, a statistical method, or a machine learning methodology [1].For prediction, ML algorithms are compared to the Smart Persistence (SP) approach, with ML models outperforming the SP model. The unpredictability of solar resources has hampered grid management as solar diffusion rates have increased. Unpredictability and intermittent electricity delivery are two of the most difficult aspects of integrating renewables into the system. As a result, solar power forecasting is becoming increasingly important for grid stability, optimal unit commitment, and cost-effective dispatch. To overcome the problem, we employ machine learning techniques to sift through extraordinary solar radiation predicting models. For developing prediction models, a variety of regression algorithms are tested, including linear least squares and support vector machines with various kernel functions. We use day-ahead sun radiation data forecasts in these tests to show that a machine learning approach can correctly anticipate short-term solar power [2]. A hybrid or mixed forecasting method was developed by combining clustering, classification, and regression approaches to produce a forecasting model. Based on the weather forecast for the next day, the model (with the closest weather condition) is chosen to forecast the power output using cluster-wise regression [3].

Renewable energy sources are progressively being integrated into electric networks alongside nonrenewable energy sources, posing significant issues due totheir sporadic and erratic nature In order to address these issues, soft-computing solutions for energy prediction are essential.We apply a number of data mining methodologies, including preparing historical load data and analysing the features of the load time series, because electricity consumption is entangled with the usage of other energy sources like natural gas and oil. The trends in power consumption from renewable and nonrenewable energy sources were examined and contrasted. A novel machine learning-based hybrid technique (SVR) uses multilayer perceptron (MLP) and support vector regression [5].Using SVM regression, solar power generation produces acceptable results [6]. However, it lacks a detailed examination of solar power generation and meteorological data, and hence is restricted in its capacity to accurately predict other data sets by merely using different SVM kernels after some basic statistical data processing [8].

To study the association between expected weather conditions and power output created as a historical time series, artificial intelligence (AI) approaches are applied.

AI approaches use algorithms that can implicitly characterise the nonlinear and highly intricate relationship between input data (NWP predictions) and output power instead of formal statistical analysis. The ANN is a brain model that is based on biology. They're employed in a range of applications that use AI approaches including supervised, unsupervised, and reinforcement learning. The ANN learns from data in the supervised learning approach by being trained to approximate and estimate the function or relationship. [6].

Their models have been improved to predict PV plant power generation [4–7]. Even with the cloud graph from synchronous meteorological satellites, the significant unpredictability in critical components, particularly the diffuse component from the sky hemisphere, makes solar irradiance far less predictable than temperature. PV systems including a large number of different tiles deployed over a large area have additional challenges [12]. Because it is impossible to examine all connected meteorological forecasts in a practical context, many alternative alternatives have been devised. Weather forecasts from meteorological websites [8] were considered by some. Others used nonlinear modelling approaches like artificial neural networks to try to simplify the solar forecast model (ANN). Two types of networks are commonly used to forecast global solar radiation, solar radiation on titled surfaces, daily solar radiation, and short-term solar radiation: radial basis function (RBF) and multilayer perception (MLP).

In a three-layer feed forward model, back-propagation is the neural network training technique. To reduce forecast error, the input layer provides an error correction factor depending on the projected output for the previous 5 minutes.

An LSTM network will learn a function that accepts a sequence of previous solar irradiance values as input and returns a solar irradiance value as output. Deep neural networks, such as the Deep Belief Network (DBN), will learn a function that takes a sequence of historical sun irradiance values as input and outputs a solar irradiance value. If a series of observations are converted into a variety of occurrences, an LSTM network can learn from them. The sequence is partitioned using LSTM for prediction purposes.

3 PROPOSED WORK:

For knowing how much power is generated from solar we have the dataset showing daily average temperature in Celsius, distance from solar noon, wind speed, wind direction, sky cover, and humidity and then the power generated. Here we are calculating how much power is generated in different weather condition for India dataset . We have taken Indian dataset with different temperature readings. The available dataset is based on hourly weather parameter values. To convert the data to mean values per day, the average of the 24-hour data was used. From 2019 to 2020, several weather factors were collected to investigate the relationship between mean solar irradiance and meteorological data in order to accurately estimate power generated.

The proposed work's System Architecture is to first consider the dataset and preprocess the data, then divide it into train and test data, apply classification techniques, and predict the results. Solar power weather dataset is used for forecasting purposes in this case. Data preprocessing methods include cleaning, integration, reduction, and transmission. We must purge any data that is no longer absolutely necessary. Data cleaning is the process of identifying and removing inaccurate or incorrect records from a dataset. Data from the real world frequently contains noise and missing values, and it may be in an unusable format that cannot be directly used for DL models. Data preprocessing is required to clean data and prepare it for various Deep Learning models, increasing accuracy and efficiency. Training and testing data are separated from the preprocessed data. The model is trained using training data, and its predictions are validated using testing data. Data splitting is the process of dividing available data into two halves, usually for cross-validator purposes. The first set of data is used to build a predictive model, while the second set is used to evaluate the model's performance. In analyzing data mining algorithms, separating data into training and testing sets is crucial. The training percentage is set at 80% and the test percentage is set at 20%. When a data set is divided into a training set and a testing set, the majority of the data is used for training and only a small portion is used for testing. To train any model, no matter what type of dataset is used, the dataset must be divided into training and testing data. The dataset will be examined for null values and outliers during the data preprocessing step, and the model will be trained using three hours of data before being used to forecast solar power generation value. The power generated radiance phase will be estimated using machine learning (ML) methods (e.g., support vector regression, linear regression, elastic net regression, and random forest) as shown in below Fig 1.

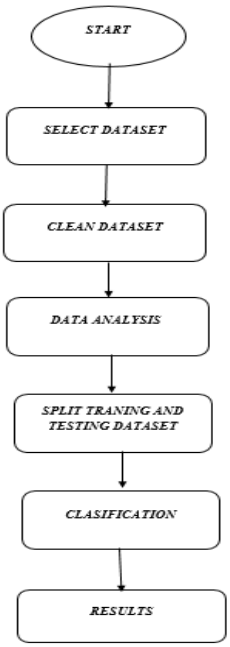

Fig.1 Flow chart for solar power generation

4. Methodology:

The current dataset is based on hourly weather parameter values. To convert the data to mean values per day, the average of the 3-hour data was used. Various weather characteristics were gathered in order to investigate the relationship between mean solar irradiance and meteorological data in order to accurately estimate mean solar irradiance. The average daily values of air temperature, humidity, wind speed, wind direction, visibility, average pressure, average wind speed, and electricity generated are among the data collected. The direction of the wind, on the other hand, indicates how high the sun is. It's also expressed in degrees.

Machine Learning (ML) Models are used for forecasting the solar power generation weather analysis. The Regression techniques here proposed are Support Vector Machine, Random Forest, Linear Regression are various ML Models used in this paper.

4.1 Forecasting models:

In this study, we used the chosen dataset to evaluate individual performance using a number of meteorological attributes utilising three commonly used machine learning algorithms. The output of the unseen test sample is predicted to be the mean of these K closest matches because our prediction variable is continuous valued. We investigated a variety of K values, however only the results for K=3 and K=5 are presented. When K is more than 3, the RMS error increases.

Support vector regression (SVR) using a radial basis function as the kernel and random forest (RF) approaches are used to create the models. Because of the non-linearity of the dataset, we used the models indicated above instead of linear models. The most basic and widely used regression method is linear regression (LR) [10].It uses linear predictor functions to represent the relationship between the input and output variables, and a least squares approach is used to estimate the unknown model parameters from the data. A set of linear equations or an iterative method like gradient descent can be used to estimate parameter values. We employed the characteristics provided in the, followed by feature scaling, to standardise the input data. SVR's precision varies depending on the kernel function and other variables. To discover the optimal settings, we employed the Grid search approach. To evaluate the models' performance on the test set, we computed the Root-Mean-Square Error (RMSE) and R squared values. Before choosing the models with the lowest root mean squared error and highest R squared values, we fine-tuned the model hyperparameters. Nonlinear relationships can be mapped using these methods. In data science challenges of various kinds, methods including decision trees, RF, and gradient boosting are commonly utilised.The RF method is a tree-based machine learning approach that can be used for regression and classification. It also performs dimensional reduction, controls missing and outlier values, and performs a variety of additional data exploration activities. The bagging approach is used to train RFs. This method allows for the usage of numerous instances for the training stage because the dataset is sampled with a replacement. Linear regression is a method for demonstrating the link between a dependent variable and one or more independent variables by using the best-fit linear curve. It is concerned with determining the best-fit line with the data by attaining a perfect slope and intercept value.The best model for forecasting solar power system output based on numerous weather parameters was then created. The models that gave the greatest results on the dataset were support vector regression, random forests, and linear regression, and these models were then utilized to anticipate PV system performance for 2019. Thanks to the predictive analysis, the estimated production in this situation ranges from 0 to 1000 Watt hours. These models were then evaluated using the test data. The SVR model has an RMSE of 135.7, while the random forest model has an RMSE of 28.62 and the SVR model has an RMSE of 58.24. The random forest model's points are close to the regressed diagonal line, however the SVR model's points are not.

5 RESULTS:

A matrix of pair correlation coefficients is generated for a set of features under investigation in order to find collinear factors as shown in below Fig 1, Fig 2,Fig 3 and Fig 4.

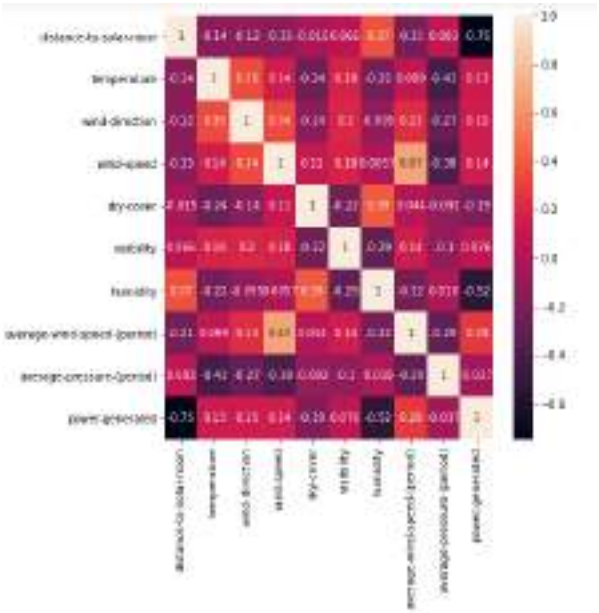

Fig 2 correlation matrix

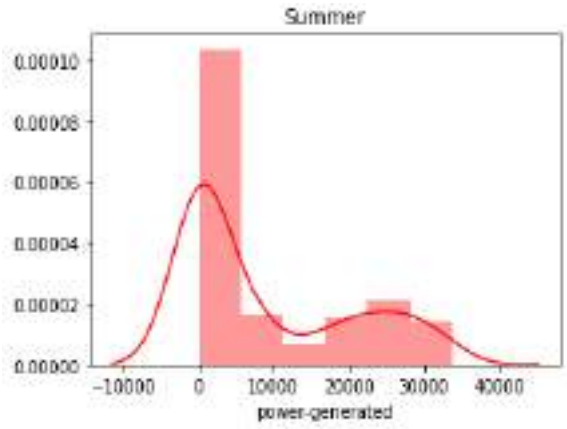

Fig 3:summer season analysis

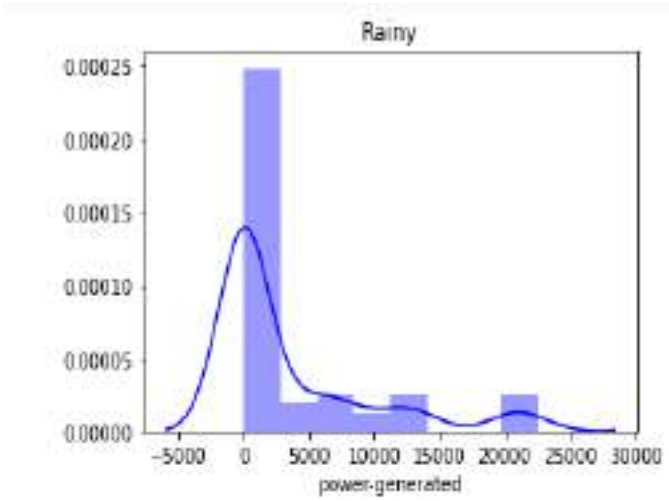

Fig 4: rainy season analysis

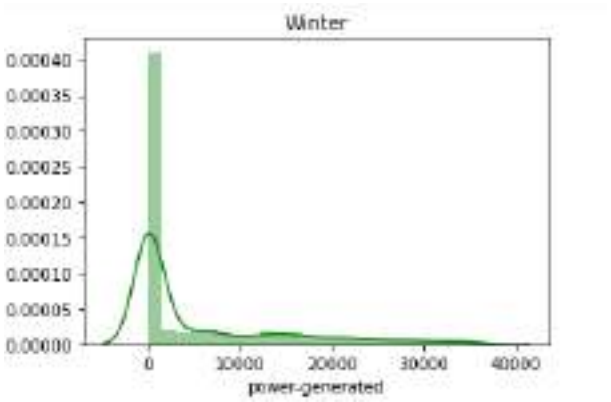

Fig 5: winter season analysis

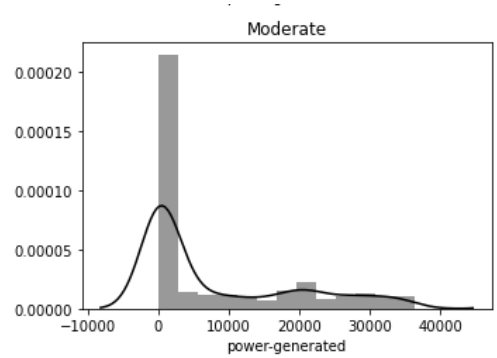

Fig 6: moderate analysis

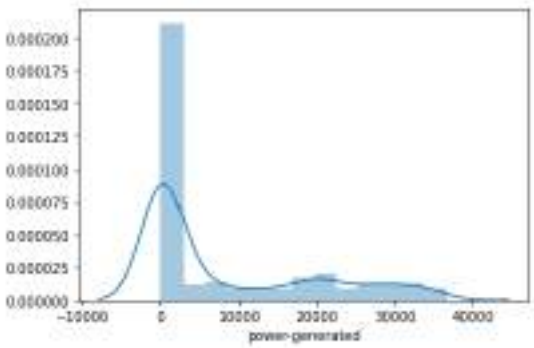

Fig7: overall season's comparative analysis

Here fig6 shows that how power is generated comparatively in different weather conditions where the x axis shows the power generated and y axis shows the distance from solar noon. It is nothing more than Solar noon occurs when the Sun passes through a location's meridian (a meridian is an imaginary line that runs from the North Pole to the South Pole along the Earth's surface.) and ascends to its highest point in the sky. In most cases, it does not occur at 12 p.m and as shown in above Fig 5 and Fig 6 and Below Fig 7.

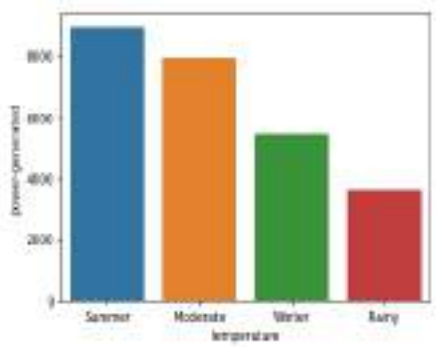

Fig 8: Different temperature analysis results of how much power is generated.

Fig6 says the power generated is read as Jules here where as temperature as in summer, rainy, winter and the moderate is said as the different weather condition. Dataset considered is the numerical dataset so we replaced them with string type where in dataset it is shown as 0 for rainy 1 for winter, 2 for moderate,3 for summer as shown in below Fig 9 and Fig 10.

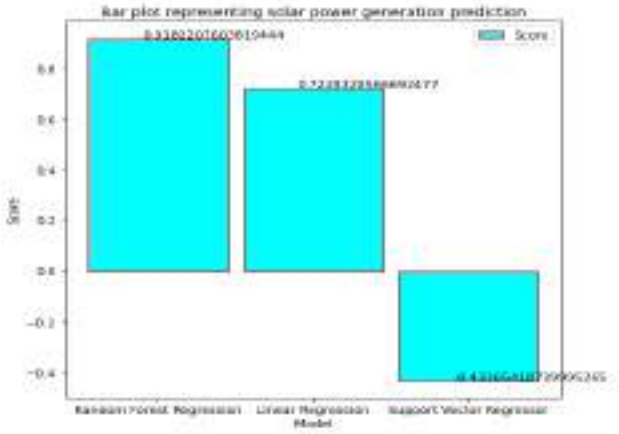

Fig 9: score of all the three model used in solar power analysis.

This fig8 shows that score of three different models used in this paper for solar power generation

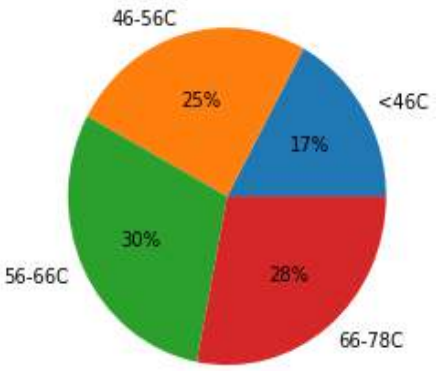

Fig 10: temperature difference and their power generated percentage accordingly.

This shows that how much percentage of power is generated ass the temperature rises less than 46 Celsius is 0 that's the rainy season temperature, 46 o 56 Celsius is 1 that's winter season temperature,56 to 66C is 2 that's moderate temperature and 66 to 78C is 3 that's summer season and as shown in below Table 1.

Table 1: Model Prediction of RMSE, MAE, MAPE, and MBE and Accuracy

Model	RMSE	MAE	MSE	Accuracy
Support vector machine regressor	131.44	77.16	172.76	-44.92
Linear regression	58.57	48.39	343.08	72.4
Random forest regressor	27.32	12.45	746.48	94.01

6. Conclusion:

We presented a machine learning-based approach for solar power generation analysis in this paper, which accurately forecasts power generated across India's states based on environmental data. Most importantly, our methodology went beyond prediction by delivering key results that aided in the understanding of solar power analysis (variable importance by time period). By a wide margin, the proposed method outperformed other popular methods, such as Random forest. The proposed models are SVR, LR, and RF. Compared to the temperature with the given data. 56-55F --30% power generation is increasing compared to other temperatures. Temperature <46F is 17% temperature average of it. As the above results, we can see that Random Forest Regressor model is performing better with 94.01% accuracy and hence that model is preferred for deployment.

Reference:

1. P. A. G. M. Amarasinghe and S. K. Abeygunawardane, "*Application of Machine Learning Algorithms for Solar Power Forecasting in Sri Lanka*" (2nd International Conference On Electrical Engineering (EECon), Colombo, Sri Lanka, 87 2018).
2. M. Z. Hassan, M. E. K. Ali, A. B. M. S. Ali and J. Kumar, "*Forecasting Day-Ahead Solar Radiation Using Machine Learning Approach*" (4th Asia-Pacific World Congress on Computer Science and Engineering (APWC on CSE), Mana Island, Fiji, 252 2017).
3. A. Bajpai and M. Duchon, "*A Hybrid Approach of Solar Power Forecasting Using Machine Learning*" (3rd International Conference on Smart Grid and Smart Cities (ICSGSC), 108 2019).
4. A. Khan, R. Bhatnagar, V. Masrani and V. B. Lobo, "*A Comparative Study on Solar Power Forecasting using Ensemble Learning*," (4th International

Conference on Trends in Electronics and Informatics (ICOEI), 224 2020).

5. Khan, P.W.; Byun, Y.-C.; Lee, S.-J.; Kang, D.-H.; Kang, J.-Y.; Park, H.-S. Energies, **13**, 4870 (2020).
6. Faquir, Sanaa & Yahyaouy, Ali & Tairi, H. & Sabor, Jalal. International Journal of Fuzzy System Applications. **4**, 10 (2015).
7. Aler R., Martín R., Valls J.M., Galván I.M. Intelligent Distributed Computing VIII. Studies in Computational Intelligence, vol **570** (2015).
8. Y. Wang, G. Cao, S. Mao and R. M. Nelms, "*Analysis of solar generation and weather data in smart grid with simultaneous inference of nonlinear time series*," (IEEE Conference on Computer Communications Workshops (INFOCOM WKSHPS), 600 2015).
9. Carrera B, Kim K. Sensors (Basel). **20**, 3129 (2020).
10. Jawaid F, NazirJunejo K. *Predicting daily mean solar power using machine learning regression techniques*. (Sixth International Conference on Innovative Computing Technology (INTECH) 355 2016).
11. Batcha RR, Geetha MK. *A survey on IOT based on renewable energy for efficient energy conservation using machine learning approaches*. (3rd International Conference on Emerging Technologies in Computer Engineering: Machine Learning and Internet of Things (ICETCE) 123 2020).
12. Li, Zhaoxuan & Rahman, Sm Mahbobur & Vega, Rolando & Dong, Bing. Energies. **9**, 55 (2016).
13. Lai JP, Chang YM, Chen CH, Pai PF. Applied Sciences; **10**, 5975 (2020).
14. Brahma, B.; Wadhvani, R. Symmetry, **12**, 1830 (2020).

Proceedings of the Fifth International Conference on I-SMAC (IoT in Social, Mobile, Analytics and Cloud) (I-SMAC)
IEEE Xplore Part Number: CFP21OSV-ART; ISBN: 978-1-6654-2642-8

2021 Fifth International Conference on I-SMAC (IoT in Social, Mobile, Analytics and Cloud) (I-SMAC) | 978-1-6654-2642-8/21/$31.00 ©2021 IEEE | DOI: 10.1109/I-SMAC52330.2021.9640832

Survey Analysis on Facial Expression

1st M. Raju Yadav
M.Tech Student
Computer Science and Engineering
GRIET, Hyderabad, Telangana, India

2nd *Dr.*P.Chandra Sekhar Reddy
Professor
Computer Science and Engineering
GRIET, Hyderabad, Telangana, India

***Abstract*— With headways in machine and profound learning calculations, the vision of different significant genuine applications in PC vision turns into a chance. Facial opinion examination is one of the applications. Profound learning has raised face acknowledgment to the first spot on the list of moving investigation fields in the PC vision space. Profound learning-based FER models have as of late been tormented by an assortment of innovative issues like Under-fitting or over-fitting. Driven from the upper than realities, it presents a logical and exhaustive study on present status of-craftsmanship figuring procedures (datasets and calculations) that supply a response to the issues. It conjointly presents a scientific categorization of existing facial slant investigation manners by which quickly. Then, at that point, this examination sums up the latest novel machine and profound learning networks proposed by scientists that are explicitly created for facial recognizable proof upheld static film, just as their professionals and faults. At last, the open inquiries and examination challenges for the plan of a durable face acknowledgment framework are introduced in this investigation.**

Keywords*— *Recurrent Neural Network; rehashed Neural Network; convolution neural network; ImageNet; Ensemble; ResNet;Maxpooling; VGG16.

I. INTRODUCTION

Facial expressions include smiles, sadness, anger, disgust, surprise, and fear. A smile on the human face expresses happiness and a curved-shaped eye. The sad expression is distinguished by a sense of lightness, which is typically expressed by raising crooked brows. Also, frown. Anger in the human face is associated with unpleasant and irritating situations. Smiles, sadness, anger, disgust, surprise, and fear are all examples of facial expressions. A human smile expresses happiness and a curved-shaped eye. The sad expression is characterized by a sense of lightness, which is typically expressed by raising crooked brows. Additionally, frown. Anger on the human face is associated with unpleasant and vexing situations. Dilated brows and thin, elongated eyelids characterize anger. The extraction and classification of features is a critical step in the FER process. Classification is another important process that categories the aforementioned expressions such as smile, sadness, anger, disgust, surprise, and fear. Understand the eyes, mouth, nose, brows, and other facial components, as well as feature extraction based on appearance [1].

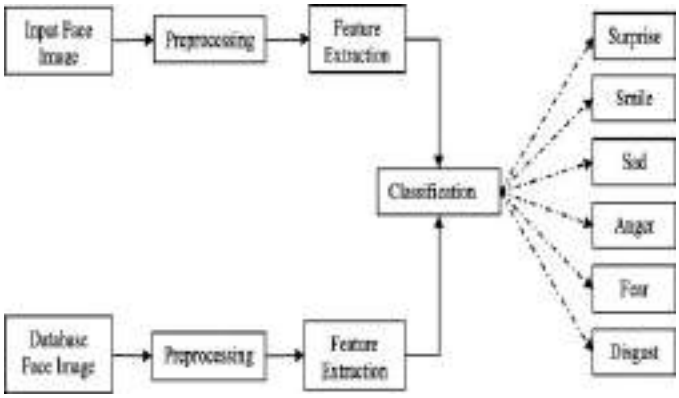

Fig. 1. Architecture of face expression recognition [22].

In this study, we primarily focused on face demeanor recognition using face-parsing components (FP). Given the disadvantage that different parts of the face contain different data measures for face appearance, and that the weighted element varies for different faces, a collaborative setup is intended to work out face demeanor exploitation parts that unit of estimation engaged in appearance exposure [2]. Based on the most recent realities, this paper provides a logical partner degreed comprehensive overview of the current state of-craftsmanship AI strategies that offer a comparative solution [3]. To see the value in the objective, it uses separated local based strategies for inward facial parts and worldwide techniques for external facial parts [4]. A series of fortunate events resulted in Profound Learning's astounding achievement in imaging applications. Unfortunately, this quality has resulted in pernicious applications such as photograph reasonable face trading of gatherings without their consent changes in position are processed and determined by sequentially tracking objects each time.

The sensor detects the nature of the object, and the object is visualized. The object in space is derived from the application of matching schemes to find the object, and its position in the plane is quantified. Image processing schemes are used to capture objects, and their dimensions are recorded and classified in 2D or 3D [5]. By incorporating various cutting-edge technologies, the system's navigability and usability can be improved. Highlighted text when scrolling with the mouse, and evaluate the layout structure of the website using background music and other similar features. These innovations have the potential to improve the screen reader. A cross-folding recurrent neural network is used to perform FER on film. The projected detail is composed of convolution layers that are then followed by a never-ending neural network that reflects the relationships between the

facial film and the persistent organization of the volatile conditions that exist within the unity of the photo region by utilizing concentrate throughout the process. The model is being evaluated over time. Findings from exploratory research that are promising a unit of estimation was acquired in comparison to reformist systems [7]. We concentrate on neural convolution networks, RNN, and DNN, which are less precise than others are. After reviewing all of these documents, we conclude that the vgg16 architecture has a lower precision. I chose the VGG19 architecture with face analysis to improve accuracy. A crossbred Convolution-Recurrent Neural Network method was used for FER in film. The proposed detail consists of Convolution layers followed by a never-ending Neural Network (RNN) that the combined model concentrates the relationships between facial film and by exploitation he persistent organization the fleeting conditions that exist within the photos region unit pondered all through the order. The proposed model of half-and-half is upheld. When compared to reformist systems, promising exploratory outcomes were obtained [7]. We discovered that convolution neural networks, RNN, DNN VGG16, and RESNET architecture have lower accuracy after reviewing all of these papers. I chose the VGG19 architecture with face parsing for improved accuracy.

II. RELATED WORK

Identifying human emotions in photographs or videos has been the goal of facial emotion recognition research since its inception. Recent studies have attempted to recognize faces in photos or videos, but these methods did not use a network framework. Geometry-based approaches and feature-based approaches are the two main methods for extracting features from photos, which differ from feature recognition methods. Furthermore, the appearance is rapidly approaching. In the first scenario, the model focuses on restricting and tracking specified face criteria in order to train the model to classify based on relevant postures. For the purpose of classifying emotions from sequences, the authors proposed a model for tracking a group of points and they detected emotions extracted from feature set forms by way of transformation in only 117 reference points. Bitmaps are used to train the categorization model.

Convolution rehashed Neural Network framework utilizes Convolution layers and rehashed Neural Network (RNN). Relations at spans facial highlights are separated by this model thus the fleeting conditions are considered during the arrangement by abuse-rehashed network [9]. continuous technique referenced is that the Constructive Feed forward Neural Networks inside which include discovery is done by a second DCT (Discrete cos Transform) [10]. On the facial picture and grouping is finished utilizing a useful feed forward one secret layer neural organization. Another technique, Boosted Deep Belief Network, utilizes a combination of highlight selector and classifier in one system [11]. During this model, choices are conjointly tuned and are tip top to shape a more tasteful through a BTD-SFS strategy. Another Hybrid technique, Convolution rehashed Neural Network framework utilizes Convolution layers and rehashed Neural Network (RNN) [9]. Relations at spans facial highlights are separated by this model thus the transient conditions are considered during the characterization by abuse-rehashed network. continuous approach referenced is that the Constructive Feed forward Neural Networks inside which include recognition is done by a second DCT (Discrete cos Transform) [10]. On the facial picture and arrangement is finished utilizing a helpful feed forward one secret layer neural organization. Another system, Boosted Deep Belief Network, utilizes a combination of highlight selector and classifier in one structure [11]. During this model, choices are conjointly tuned and are tip top to shape a more tasteful through a BTD-SFS strategy.

Breuer and Kimmel utilized CNN inward portrayal procedures to realize a model discovered misuse shifted FER datasets, and unquestionably, the capability of organizations prepared on feeling discovery, across all datasets and FER-related errands [12]. Jung et al used two different types of CNN: The first focuses on global look choices from image groupings, while the second focuses on transient number related alternatives from fleeting facial milestone focuses [13]. These two estimation models were joined utilizing another combination procedure to work on the exhibition of facial element acknowledgment. Kahou et al. projected a half and half RNN-CNN system for engendering data over a grouping utilizing partner persistently esteemed covered up layer delineation. The creators fostered a full framework for the 2015 feeling Recognition among the Wild (EmotiW) Challenge, showing that a crossover CNN-RNN style for facial highlights investigation can outflank a formerly utilized CNN technique for collection utilizing fleeting averaging. [14].

The VGG-16 layer stores a 224 by 224 RGB image as data. There are a lot of convolutional (conv.) layers in the image, and the channels are set to catch the notions of left/right, up/down, and Center with a little open field of 33 (the smallest size to capture the concepts of left/right, up/down, and Center). In one design, it also uses an 11-channel convolutional filter, which can be viewed as a simple switch in the information channels (trailed by non-linearity). The convolutional step is set to one pixel, and the convolutional spatial cushioning is set to zero. The layer input is designed with the goal of saving the spatial goal after convolution, for example, one pixel for 33 convolutions. Levels (Figure 2). After a portion of the convolutional layers, five max-pooling layers perform spatial pooling (not all the conv. layers are trailed by max pooling). Step 2 is used to maximise pooling across a 22-pixel window. VGG16 had been working on NVIDIATitan Black GPUs for quite some time. VGG16 had been working on NVIDIATitan Black GPUs for quite some time.

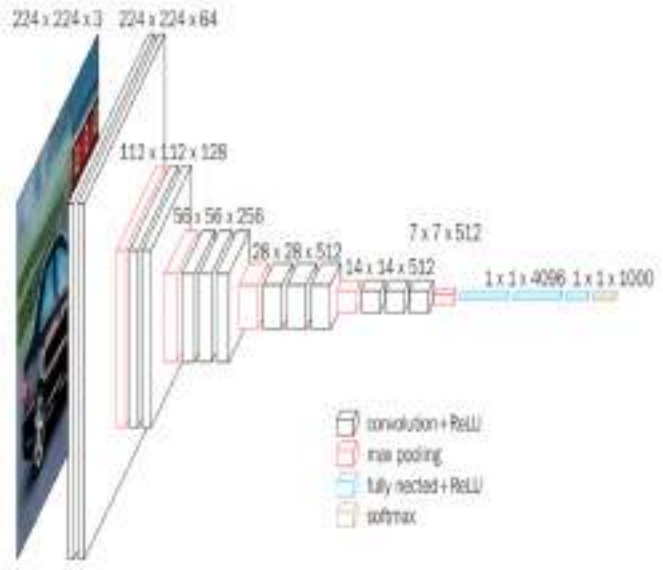

Fig. 2. VGG-16 Architecture diagram [15].

As information, our VGG16 is taking care of a 48x48 RGB image. By removing the typical RGB from each pixel, we achieve phenomenal preprocessing. To handle the image, a convolutional layer stack with 3x3 channels is used. In one of the arrangements, we also use 1x1-convolution channels, which can be thought of as a direct redesign of the information channels (saw through way of method of non-linearity). Because the convolution step is set at one pixel, and because the convolutional layer data is padded spatially, the spatial assurance is preserved after convolution. The spatial clustering procedure is completed by inspecting some of the convolution layers through the lens of five maximum clustering layers (now not all convolution layers are observed through manner of way of maximum clustering). In a two-pixel window, stride2 collects the most information. Three related (FC) layers detect a pile of convolutional layers: the first has 4096 channels each, the third performs the 7-way ILSVRC type and therefore incorporates seven channels, and the last has 4096 channels each (one for each class). The ideal reorientation. All companies use a similar structure for the associated tiers. Non-linearity rectification is enabled on all hidden layers (ReLU). VGG16 is made up of 16 weight layers, 13 folding layers with a 3x3 clean out period, and 3 associated layers. Stride and padding are set to a minimum of one pixel for all convolution layers. Each convolution layer is divided into five groups, with each group being observed using a maxpooling layer (Figure 2). Step 2 performs maxpooling in a 2x2 window. The number of filters with within the convolution layer company starts at 6 4 with within the primary company and increases by a factor of after each maxpooling layer until it reaches 512[15]. Keras VGG16 is used as the implementation.

ResNet 50 is a cutting-edge architecture for convolutional neural networks. Its architecture is similar to that of networks like VGG-16, but it adds the capability of identity mapping (Figure3).

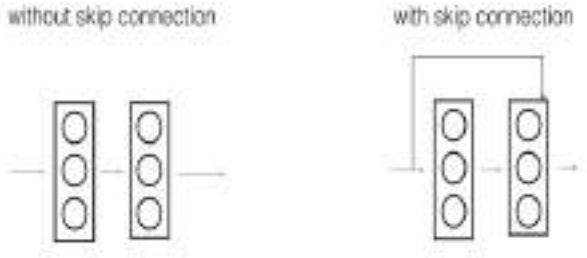

Fig. 3. ResNet residual block diagram with skip connection [15].

Leftover Networks, also known as Reset, are a type of neural organization that serves as the foundation for some PC vision tasks. This model won the Magnet Challenge in 2015.The ability to prepare profound neural organizations was Reset's key breakthrough. With over 150 layers. Prior to Reset, profound neural organization preparation was difficult due to the issue of blurring gradients. Reset was the first to suggest the idea of a jump affiliation. The leap association is depicted in the outline below. The left image shows collapsed layers stacked consistently; the right image shows similar collapsed layers stacked, but we are currently adding the first contribution to the yield of the convolution square. It is what it is: a leap association. Hop comes to work in this environment for two reasons: They reduce the slope blurring issue by allowing this other angle alternate way. Essentially equal to, if not worse than, the base level [15].

III. DATA SET

The Extended Cohn-Kanade Dataset (CK+) [16]: CK+ contains 594 video groupings on each show and non-presented (unconstrained) feelings, just as different kinds of data. The 123 members range in age from eighteen to thirty years of age, with most of the World Health Organization unit of estimation being female. Picture groupings can be taken apart for activity units and original feelings. It gives conventions and benchmark results to facial element following, AUs, and feeling acknowledgment. The photos have part goals of 640 × 480 and 640 × 490 with 8-bit exactness for dim scale esteems.

JAFFE [Japanese Female Facial Expressions] [17]: The JAFFE information contains 213 photos of ten unique female Japanese models showing seven face feelings (six fundamental facial feelings and one unbiased). Each picture was given a score dependent on six emotive words used to misuse sixty Japanese individuals. Every facial picture's essential size is 256 pixels by 256 pixels.

ImageNet is a data set containing over 15 million labelled high-goal images organized into approximately 22,000 classes. The images were compiled from the internet and labelled by people who volunteered on Amazon's Mechanical Turk. Since 2010, the Pascal Visual Object Challenge has included a yearly competition known as the ImageNet Large-Scale Visual Recognition Challenge. ILSVRC makes use of a subset of ImageNet, with approximately 1200 images in each of the 1200 classifications. There are approximately 1.3 million preparing images, 52,000 approval images, and 152,000 testing images in total. ImageNet contains images of varying sizes and objectives. As a result, the images' goal was

reduced to 256x256. A rectangular image is rescaled, and the resulting image is edited to remove the focal 256x256 fix [15].

IV. Result And Analysis

The accuracy of the models in the test data for different spans of the noticed sequence is shown in Table 1 and Figure 4. The precision pattern is mostly up, demonstrating that giving the model a fleeting setting improves characterization exactness. Except for the two lip models, who have the pattern up to the most extreme number of edges, everyone has 45 edges. The edge model clearly performs the worst, whereas the CNN and RNN Lips lip models perform exceptionally well. In higher edges, the RNN lip model marginally outperforms the CNN lip model. The main point to emphasize is that in outlines greater than 25, there is a reasonable and supported expansion in lip model accuracy when contrasted with the relating face models.

TABLE I. The Models' Data Correctness Was Examined Throughout A Range Of Frame Values [18].

Frames	CNN	CNN Lip	RNN	RNN Lip	Frame
5	0.429	0.446	0.423	0.444	0.413
10	0.413	0.448	0.443	0.452	0.421
15	0.458	0.458	0.458	0.442	0.431
20	0.459	0.442	0.462	0.475	0.437
25	0.465	0.509	0.452	0.470	0.439
30	0.475	0.516	0.465	**0.513**	0.441
35	**0.479**	0.485	0.476	0.530	0.449
40	0.459	0.509	**0.485**	0.505	0.450
45	0.452	0.479	0.473	0.533	**0.457**
50	0.465	0.492	0.479	0.519	0.449
55	0.466	0.508	0.482	0.538	0.444
60	0.462	0.544	0.470	**0.394**	0.447
65	0.448	**0.569**	0.482	0.563	0.454

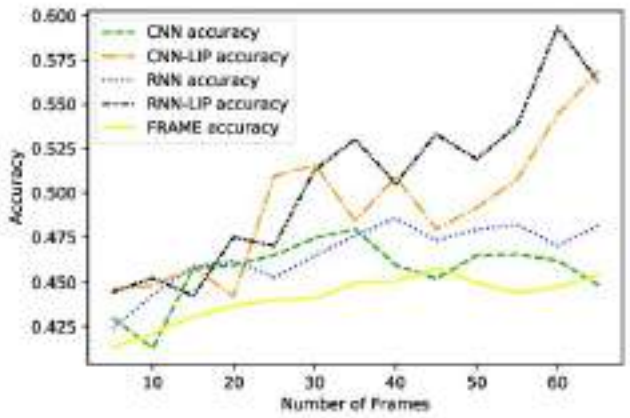

Fig. 4. Shows a plot of the models' accuracy on test data [18].

Taking a gander at the exactness distinction between the lip models and their comparing face models, as displayed in Figure 5, we can see an increment in precision from 25 housings, which seems, by all accounts, to be an immediate vertical example, similarly as the model count increments. When applied to the data in Figure 5, the direct relapse model yields a measurably critical incline of 0.0015, addressing the increase in accuracy for each additional casing in the data. The increased number of frames, as well as the upper limit of the precision metric, raises concerns about the persistence of basic emotional expressions in spontaneous conversations. The available data's precision gains, on the other hand, appear to increase linearly over the duration of the input sequence, with positive values starting at sequence. While crediting understandings to the activity of a discovery framework, for example, a neural organization is a perilous endeavor; the justification behind lip models does not deteriorate and develops straightly: joint-related data expands the helpfulness of the face. Assuming that the articulatory features of speaking subjects do not carry affect information, they cause the network to become articulation-invariant. Lip models can classify better with a larger number of frames because of providing more information at the start [18].

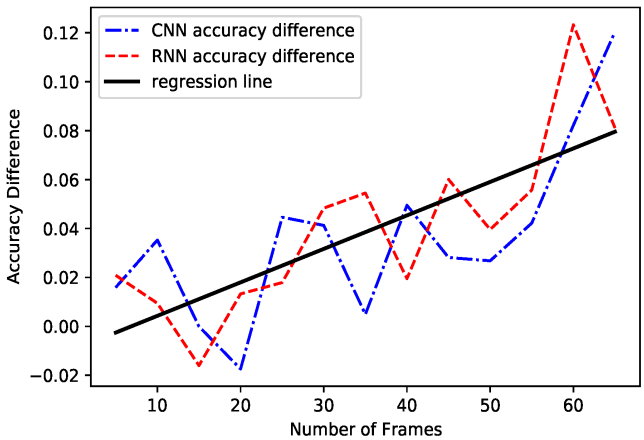

Fig. 5. Differences in the accuracy of the lip-only model and the facial-only model based on the testing data [18].

Table 1 shows the outcomes of the Waggle dataset's SVM (standard), VGG16, ResNet50, and co-learning models. The precision of our gauge SVM was 32 percent, while the precisions of VGG16 and ResNet50 were 59.2 and 65.1 percent, respectively. The model includes character derivation layers, which can help it outperform VGG16 in terms of exactness, accuracy, and recovery. The ensemble-learning model, which combined VGG16 and ResNet50, achieved 67.2 percent accuracy, 2.1 percent higher than either VGG16 or ResNet50 alone. The DEF dataset outperforms the Waggle dataset in terms of overall accuracy, as well as accuracy and retrieval. SVM had a precision of 38 percent, while VGG 16 and ResNet50 had precisions of 70.8 percent and 74 percent, respectively. With an accuracy of 75.8 percent, the ensemble approach outperformed individual deep learning models. KEF and Waggle both use the same four models. Surprisingly, despite the fact that the dataset was much smaller, each of the four models outperformed wrangle in the DEF. We believe this is due to the DEF dataset's design and consistency in

terms of subject positions and the number of models for each point and feeling. The images in the DEF dataset are also of higher quality. Regardless of the larger picture goal, there were instances of text being displayed in the image's association with the Waggle dataset [15].

$$\text{Accuracy} = \frac{TP + TN}{TP + TN + FP + FN}$$

Where TP= True Positive, TN= True Negative FP= False Positive, FN= False Negative.

TABLE II. PERFORMANCE OF THE KDEF DATASET (ACCURACY, PRECISION, AND RECALL) FOR SVM, VGG-16, RESNET50, AND ENSEMBLE LEARNING MODELS[15].

	Accuracy	Precision	Recall
SVM	**37.9%**	**50.1%**	**54.9%**
VGG-16	**71.4%**	**81.9%**	**79.4%**
ResNet50	**73.8%**	**83.3%**	**80.7%**
Ensemble	**75.8%**	**85.0%**	**82.3%**

VI. CONCLUSION

In this we observed that accuracy of the data percentage is less with the CNN, RNN, DNN and VGG16 architecture of parsed images and by using VGG19 architecture we can improve the accuracy percentage along with dense layer and we can demonstrate that our technique outperformed the cutting-edge strategies. From all the Architectures VGG16 have achieved 71.4% is very less when compared with ensemble, but very high when compared with CNN, RNN and DNN and with parsed image VGG19 on facial expression we can improve accuracy of facial expression.

REFERENCES

[1] I.Michael Revina, W.R. Sam Emmanuel, A Survey on Human Face Expression Recognition Techniques, Journal of King Saud University - Computer and Information Sciences, Volume 33, Issue 6, 2021, Pages 619-628.

[2] Y. Lv, Z. Feng and C. Xu, "Facial expression recognition via deep learning," 2014 International Conference on Smart Computing, Hong Kong, China, 2014, pp. 303-308.

[3] Keyur Patel, Dev Mehta, Chinmay Mistry , Rajesh Gupta, Sudeep Tanwar, Neeraj Kumar, Mamoun Alazab "Facial sentiment analysis using ai techniques: state-of-the-art, taxonomies, and challenges",2017.

[4] Jinpeng Lin, Hao Yang, Dong Chen, Ming Zeng, Fang Wen, Lu Yuan; Proceedings of the IEEE/CVF Conference on Computer Vision and Pattern Recognition (CVPR), 2019, pp. 5654-5663

[5] Sungheetha, Akey, and Rajesh Sharma. "3D Image Processing using Machine Learning based Input Processing for Man-Machine Interaction." Journal of Innovative Image Processing (JIIP) 3, no. 01 (2021): 1-6.

[6] Manoharan, J. S. (2019), "A smart image processing algorithm for text recognition, information extraction and vocalization for the visually challenged", Journal of Innovative Image Processing, 1(1): 30 – 38.

[7] Xiaoming Zhao, Shiqing Zhang. (2016) A Review on Facial Expression Recognition: Feature Extraction and Classification. IETE Technical Review 33:5, pages 505-517.

[8] Deepak Kumar Jain, Pourya Shamsolmoali, Paramjit Sehdev, Extended deep neural network for facial emotion recognition,Pattern Recognition Letters, Volume 120, 2019, Pages 69-74.

[9] Neha Jain, Shishir Kumar, Amit Kumar, Pourya Shamsolmoali, Masoumeh Zareapoor, Hybrid deep neural networks for face emotion recognition, Pattern Recognition Letters. 115(2018). 101-106. https://.org/10.1016/j.patrec.2018.04.010.

[10] L. Ma and K. Khorasani, Facial expression recognition using constructive feedforward neural networks, in IEEE Transactions on Systems, Man, and Cybernetics, Part B (Cybernetics), 34(2004).1588-1595.10.1109/TSMCB.2004.825930.

[11] P. Liu, S. Han, Z. Meng and Y. Tong, Facial Expression Recognition via a Boosted Deep Belief Net- work, 2014 IEEE Conference on Computer Vision and Pattern Recognition, Columbus. 2014.1805-1812 . 10.1109/CVPR.2014.233.

[12] Breuer, R.; Kimmel, R. A deep learning perspective on the origin of facial expressions. arXiv 2017, arXiv:1705.01842 .

[13] Jung, H.; Lee, S.; Yim, J.; Park, S.; Kim, J. Joint fine-tuning in deep neural networks for facial expression recognition. In Proceedings of the IEEE International Conference on Computer Vision, Santiago, Chile, 7–12 December 2015; pp. 2983–2991.

[14] Ng, H.W.; Nguyen, V.D.; Vonikakis, V.; Winkler, S. Deep learning for emotion recognition on small datasets using transfer learning. In Proceedings of the 17th ACM International Conference on Multimodal Interaction, Emotion Recognition in the Wild Challenge, Seattle, WA, USA, 9–13 November 2015; pp. 1–7.

[15] Poonam Dhankhar (2019) "ResNet-50 and VGG-16 for recognizing Facial Emotions", International Journal of Innovations in Engineering and Technology (IJIET)", Volume 13, ISSN: 2319-1058.

[16] Lucey, P.; Cohn, J.F.; Kanade, T.; Saragih, J.; Ambadar, Z.; Matthews, I. The extended Cohn-Kanade Dataset (CK+): A complete dataset for action unit and emotion-specified expression. In Proceedings of the IEEE Conference on Computer Vision and Pattern Recognition Workshops, San Francisco, CA, USA, 13–18 June 2010; pp. 94–101.

[17] Lyons, M.J.; Akamatsu, S.; Kamachi, M.; Gyoba, J. Coding facial expressions with Gabor wave. In Proceedings of the IEEE International Conference on Automatic Face and Gesture Recognition, Nara, Japan, 14–16 April 1998; pp. 200–205.

[18] Bursic, Sathya & Boccignone, Giuseppe & Ferrara, Alfio & D'Amelio, Alessandro & Lanzarotti, Raffaella. (2020). Improving the Accuracy of Automatic Facial Expression Recognition in Speaking Subjects with Deep Learning. Applied Sciences. 10. 4002. 10.3390/app10114002.

[19] Smys, S., and Jennifer S. Raj. "Assessment of Fire Risk and Forest Fires in Rural Areas Using Long Range Technology." Journal of Electronics 2, no. 01 (2020): 38-48.

[20] Manoharan, J. S. (2017), "Super-resolution reconstruction model using Compressive Sensing and Deep Learning", International Journal for research and development in Technology", 7(4): 884 – 889.

[21] Joe, Mr C. Vijesh, and Jennifer S. Raj. "Location-based Orientation Context Dependent Recommender System for Users." Journal of trends in Computer Science and Smart technology (TCSST) 3, no. 01 (2021): 14-23.

[22] Michael Revina, W.R. Sam Emmanuel, "A Survey on Human Face Expression Recognition Techniques", Journal of King Saud University - Computer and Information Sciences", Volume 33, Issue 6, July 2021, Pages 619-628.

Proceedings of the 6th International Conference on Communication and Electronics Systems (ICCES-2021)
DVD Part Number: CFP21AWO-DVD: ISBN: 978-0-7381-1404-0

Query Optimization Techniques in Wireless Sensor Network: A Review

Rebekah Calvin.B
PG Student, Department of CSE
Gokaraju Rangaraju Institute of Engineering & Technology
Hyderabad, India
rebekacalvin@gmail.com

Kavitha Kayiram
Associate Professor, Department of CSE
Gokaraju Rangaraju Institute of Engineering & Technology
Hyderabad, India
kavitha.bits@gmail.com

Dr. R.V.S.Lalitha
Professor, CSE
Aditya College of Engineering & Technology,
Kakinada

***Abstract*— A Wireless Sensor populated in sensor nodes deployed Network (WSN) could be considered as a scattered data repository which gets in remote locations powered by limited batteries. To retrieve data from these nodes query processing techniques are used. As the applications of WSN are found in remote locations and extreme weather conditions the replacement or recharge of battery is impossible. Henceforth, it is highly required to conserve the battery power in order to increase the network lifetime. Among the sensing, storing, transmitting and receiving activities of sensor nodes, data communication is the most dominant energy consuming activity. Hence query optimization techniques are in huge demand in WSN. This paper presents the prominent query optimization algorithms that are used in WSN to address the issue of energy efficiency. The purpose of this review is to give an overview of the existing literature and research issues in query optimization techniques in WSN.**

Keywords*— *Wireless Sensor Networks, Query Optimization, Genetic Algorithm, Energy efficiency, distributed computing.

I. INTRODUCTION

A Wireless Sensor Network (WSN) [1] may be considered as a distributed database as the sensor nodes continuously capture the data and multiple sensor nodes collaborate to form a network. A sensor network consists of tiny sensor nodes operated on limited battery power and deployed in remote locations like volcanic disruption, earthquake detection system, forest fire detection system etc. The sensor nodes sense environmental parameters like temperature, pressure, humidity, light etc., and transmit to the nearby sensor nodes within their communication range. As these networks are operated in extreme weather conditions and hard-to-reach locations, it is extremely difficult and impossible to replace batteries. Hence, we need to conserve the battery power by optimal utilisation. The sensors perform sensing, receiving and transmission of data to their neighbors. A sensor node expends 80% of power in data transmission hence we need to minimize the data transmission activities to extend the time span of the network. In the process of data extraction the user can submit a query in TinySQL and the network of nodes send the resultant data as shown in Figure1. The TinySQL is the query language used in WSN. The Select statement in TinySQL offers projection, aggregation, Having, Group by clause. The user submits his data requirement in the form of TinySQL queries to the WSN. In WSN, the sink node requires responses from various sensor hubs. The reactions from various sensor hubs are gathered at the sink hub. The primary errand in query handling is to figure a query and query plan at the sink hub. Query processing happens in four stages [5], for example, query decomposition, data localization, global optimization and distributed execution.

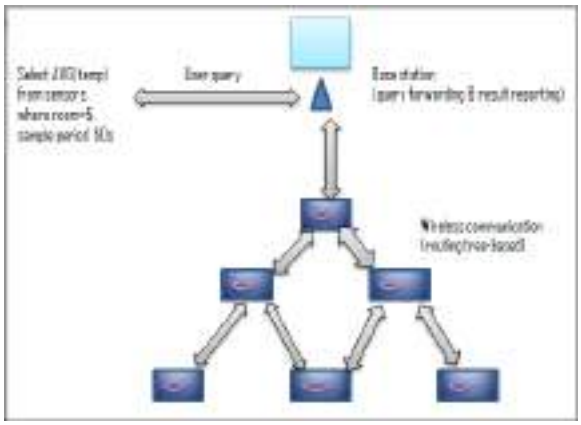

Fig. 1 Query Processing in WSN

II. PROCEDURE FOR QUERY PROCESSING IN WSN

Initially clients present their queries to the base-station At that point the query optimizer of the base-station investigates the query and produces an enhanced query plan. Query streamlining agent chooses the best and productive arrangement for the execution. Code generator produces the

code for the chosen arrangement and interpreter creates executable code for the query. Query at that point spreads to the sensor hubs in the system by means of directing technique. In the wake of getting the query, sensor hubs sense the environment, collect the information and procedure the information as indicated by the query. The pre-prepared information will be submitted back to the sink node. Considering the requirements of WSN, query optimization activity selects the efficient query plan and data processing according to query are the main challenges. Therefore, energy efficient query processing in WSN plays an important role.
As sensor nodes are powered by a battery, they have confined energy; hence it becomes a big challenge in designing routing protocol. The recharge or replacement of the battery is difficult since most of the sensors are remotely placed. Hence we need to conserve the battery power in a WSN through various techniques. One of the network activities is routing that we can devise to diminish energy utilization of sensor hubs and increment the network lifetime. Routing protocols support network lifetime and maintain connectivity between nodes while guaranteeing good performance. A large portion of the analysts concentrated on diminishing the energy utilization of sensor hubs without debasing the nature of WSN framework.

Energy utilization is aggregation of the total energy utilized by each and every sensor hub present in the network when moving and preparing the submitted packet or query. Since sensor nodes are battery powered, they have limitations in energy; hence it becomes a challenge in designing routing protocol. Battery replacement is difficult since most of the sensors are remotely placed. The estimation of energy utilization utilized by sensor hubs is a significant presentation metric in assessing a WSN directing strategy. A proficient routing calculation that can lessen vitality utilization of sensor hubs will build the system lifetime. Routing protocols support network lifetime and maintain connectivity between nodes while guaranteeing good performance. The vast majority of the specialists concentrated on decreasing the energy utilization of sensor hubs without corrupting the nature of WSN framework.

Data storage in WSN [2] can be categorized as centralized (unified) data storage and distributed (appropriated) data storage. In unified methodology [3] a predetermined set of information is normally conveyed from the sensing nodes to a focal database. Clients can query the database by means of some interface given by the framework. The subsequent methodology is appropriated in nature where information is kept on the sensors where the detected information dwells in the sensor hub and the collected information is sent to the sink hub. In the appropriate approach, the information that should be extricated from sensing nodes is controlled by the query remaining burden. The disseminated approach is, hence, not just adaptable to such an extent that queries separate various information from sensor arrangement, and furthermore guarantees productive extraction of just significant information from the sensor organization.

III. Various Query Processing Techniques

A tremendous contrast is seen amongst query processing in conventional databases with WSNs. In conventional databases, the efficient query plan picked by the query optimization agent is the one that requires the least number of disk accesses [4]. Query processing among conventional databases is for the most part inadmissible for WSN. Be that as it may, in WSNs the analyzer picks the query plan which gauges negligible energy cost. Notwithstanding this the thing that matters is because of the natural properties of the sensors establishing the remote system. The hub including a WSN is increasingly inclined to disappointments, has limited memory size, and utilizes tremendous measures of energy for information transmissions, information streaming and so on. As opposed to the customary query processing approach in DBMS, the information is a consistent information stream obtained by a sensor in a WSN. So as to guarantee proficient query processing in WSNs, different asset administrations like-memory, energy, data transmission and so forth ought to be thought of. Query processing methods in sensor systems can be sorted into In-network handling or Base station query handling. These are otherwise called circulated handling or warehousing. Appropriated handling or In-network processing decrease data transferrable costs. Warehousing approach includes information transferring (for processing), to the particular spot midway found outfitted with plentiful energy.

A. Data Aggregation with respect to results obtained from query processing:

Data aggregation targets expanding the time span of the network by lessening information transfers that are repetitive. This particular procedure totals the comparative information detected by different sensor hubs going through a specific hub before arriving at the base station. Information aggregation methods might be characterized into i) chain-structure ii) tree-structure and iii) lattice structure collection [4]. The data might be totaled with the assistance of different accumulation plans like Low Energy Adaptive Clustering Hierarchy (LEACH), Tiny Aggregation (TAG) and so on. The collection might be carried out either by i) Decrementing the information size or ii) transmission without decreasing the information size. The first strategy includes joining and packing the information detected at a specific hub which gets the information from other neighboring hubs previously permitting them to advance toward the base station. In the subsequent technique, the information that is gotten from different hubs is converged at a specific hub which lessens correspondence overheads. Further processing does not happen on the particular consolidated information which is next sent to the sink node.

B. Query Dissemination for processing different queries:

The client transmits a query to the sink node through a graphical interface. At a point where the sink node gets that query, [5] it contrasts it and the query history. In the event that it is as of now utilized, the base station utilizes the past estimations from its reserve. In the event of ongoing estimation required, the query is set in the dynamic rundown. In a circumstance where the transfer hub gets a query, the Deadline Controller contrasts the query cutoff time and the current time. On the off chance that it seems, by all accounts, to be not exactly the query cutoff time, the exchange will be transmitted to the scheduler. Otherwise, the exchange is prematurely ended. When a hand-off hub gets a query reaction from its child hubs, the query would be expelled from the scheduler. Or else, the transfer hub transmits the query one more time to its child hubs until the affirmation of a reaction is gotten. At the point when the child hub gets the query, it confirms its cutoff time. On the off chance that the exchange has missed its cutoff time, it will prematurely end naturally. Every hub deals with the received queries by being independent with other sensor hubs.

C. Spatial query processing :

In-network query processing [6] components utilize the area information to answer an uncommon sort of query called spatial query. In such queries the clients requests are communicated through topographical predicates, for example, "the humidity gathered by hubs in a district" or "the dampness gathered by hubs nearest to a point". Spatial queries are database inquiries upheld by geo-databases. Spatial queries contrast from customary questions in dual primary concerns. To start with, they join geometry information types, for example, focuses and polygons. Secondly, these questions think about the spatial connection among the characterized geometries, for example, a point inside a polygon or a polygon that covers another.Spatial queries processing are analyzed in six stages: Pre-Processing, Forwarding, Dissemination, Aggregation, Sensing and Return.

A skyline query [7] is an intense apparatus for multi criteria information investigation, information mining, and basic leadership. Given an arrangement of information tuples with different properties, a skyline query recovers an arrangement of information tuples, called skyline tuples, to frame a skyline. These skyline tuples are not ruled by some other tuples. Here a tuple x is said to command the other tuple y if x isn't more awful than y on all traits and x is entirely superior to y on somewhere around a single property. Due to the complex and costly features of mobile devices like superior processors, memory, sensors and capacity there is a huge requirement for skyline query processing.

D. Spatio Temporal Processing:

One of the traditional data processing techniques [8] that is Spatio-Temporal processing (STP) is a control strategy to expand the nature of the received signals in remote systems. There are a few methods for energy proficient handling of Historical Spatio-Temporal queries, HST. The response to a HST question is framed through the estimations of all sensing nodes situated in the territory taken when the time is being extended. A clear method to answer a HSTquery, called FullFlood, is reaching each system hub. The query originator hub, which could be a random hub in the system, communicates the query to its neighbor hubs, which thus communicate the query to their neighbor hubs, etc, until all hubs have acquired the query. An outcome of broadcasting is that every sensing hub could get a similar query a few times. For single query, a hub forms just the primary query message acquired, disposing of ensuing messages. The query answers are sent back uniquely to the neighbor sensor hub from where the query was first gotten from. To the various neighbor sensor hubs, vacant answers are sent. At the point when the query is acquired, the hub broadcasts the query, chooses the privately put away information pertinent to the query (assuming any), hangs tight for its neighbor sensor hub's answers and unions them with its own, lastly it restores the response to the neighbor sensor hub that it acquired the query from. When the query originator hub gets results from every one of its neighbor hubs, it can give the query result to the client.

E. Query Request Processing With Cooperative Caching:

The examination in [9] says, when a lot of query solicitations of simultaneous errands have been changed over into a binary string, which speaks to the arrangement of traits in all lattice cells at a specific time allotment, tactile information are brought from the reserve at sensor hub, or recovered from the system in an ongoing manner, for noting these question demands.

Some applications of WSN require data on a continuous basis. Such time critical military applications as shown in Figure 2 require every sensor node to continuously sense and send data to the base station. Such systems are termed as push-based query processing models. Certaine applications of WSN require only a snapshot of the network data, such queries are intended only to a part of the network or few nodes in the network or maybe complete network data at the moment or based on previous data, such systems are called pull-based systems. In a pull- based system the base station sends a query to the network on need basis. Here the query could be based on already sensed data (historical data) or the current data. Database query engines utilise pull-based or push-based methodologies [10] to stay away from the appearance of information to query administrators. Through queries, data is either pushed from sensor nodes to a gateway, or pulled from the gateway. Hybrid push-pull data dissemination performs better than the pure approaches and offers significant energy savings.

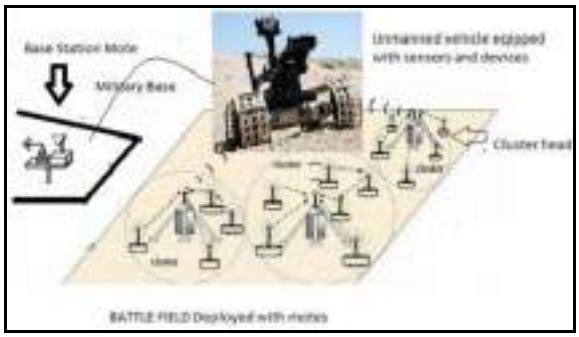

Fig. 2 WSN in Military Applications

F. a)Push based query:

Engine which is also known as the visitor pattern [10] is widely used in streaming systems. Inpush-based query engines, the control stream is switched contrasted with that of pull-based engines. All the more solidly, rather than goal administrators mentioning information from their source administrators, information is pushed from the source administrators to the goal administrators.

b) Pull based query:

Engine which is also known as the iterator pattern [10] is most broadly utilized in pipelining strategies in query engines. The structure of pull-based engines legitimately relates to the iterator configuration structure in object arranged programming. Each query administrator plays out the job of a goal administrator and solicitations information from its source administrator. In a pull engine, this is accomplished by summoning the following capacity of the source administrator and appears as control stream diagrams.

IV. Various Plans For Query Plan Generation

Query optimization diminishes the quantity of queries brought into the sensor network, and accordingly brings down the general traffic and asset use over the network. Query optimization strategies can be applied at various levels (e.g. equipment, programming, information connect directing, working framework etc). They can be classified as static or dynamic. Static optimizations are planned at the arrangement time and stay unaltered. Dynamic optimization gives improvement during runtime concurring the application prerequisite.

A. Base Station optimization:

The primary level optimization is at the base station. It goes about as a channel to diminish copy information accesses from the network and conceals query elements.

B. In-Network optimization:

Base station advancement can't bolster sharing of the normal highlights among queries at the best granularity. Communicate nature of the sensor hubs are not contemplated for the base station enhancement. Sensor hubs can settle on nearby choices and handle the remaining burden with time.

C. Query based methodology :

Query based methodology [4] is one among the broadly acknowledged methodologies for information retrieval as shown in Figure 3. This depends on forming a query to the database for data recovery. The explanation behind its fame is its ease to work with interfaces. The queries given for the data extraction are limited with boundaries while showing the sensed information and performing different total calculations like least, greatest and so on this information. The key attributes of the information sensed in the system are both memory and time. The query dialects face trouble in representing them.

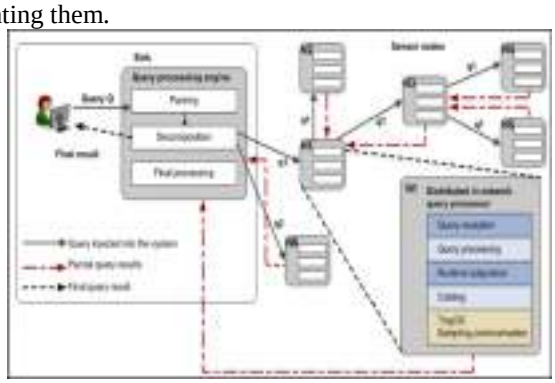

Fig. 3 Query based methodology for Information Retrieval

D. Distributed query plan generation problem (DQPG) :

It is an unpredictable and difficult issue, Honey bee Mating Optimization (HBMO)based DQPG [12] algorithm is introduced which creates a query processing plan, for a given conveyed query, which limits the query proximity cost QPC. This algorithm produces disseminated query plans dependent on the nearby feature of a query plan. Contributions to the algorithm are the connection location network, lot of automaton query plans, most extreme introductory pace of the queen query plan, least passable pace of the queen query plan needed to keep mating flights, the pace decrease plot, measure of the queens query plan (number of query intends to be considered for development), count of mating flights (iterations) to be attempted and the quantity of working drones (arrangement improvement heuristics). In this methodology an underlying populace of honey bees, speaking to the underlying arrangement of drone query plans is arbitrarily created. This underlying populace, that goes about as the input, is tried to be advanced by the HBMO based DQPG algorithm to acquire a predominant quality populace of query plans.

Query Optimization in Distributed databases is a complex issue with confused target works along these lines ground-breaking search algorithms is required for it.

E. Ant Colony Optimization :

Ant Colony Optimization (ACO) [13] is a meta-heuristic, multi specialist procedure that recreates the scavenging conduct of ants for unraveling troublesome NP-hard combinatorial optimization issues. Ants are social bugs whose conduct is coordinated more inclined to the endurance

of settlement all in all than that of a solitary individual of the state. A significant and intriguing conduct of an ant colony is its circuitous co-usable foraging process. Ant Colony Optimization depends on the conduct of some ant species. They store pheromone trails on the floor so as to make an ideal way that will be trailed by different ants from the colony.

A hybrid algorithm of Genetic Algorithm and Ant Colony Optimization (GA-ACO) is given in [13] to tackle the issues of optimization of join requesting (just nested circle joins considered) in social repository queries by defeating the weaknesses of the two combined algorithms. Various nature roused algorithms have been proposed to take care of optimization issues.Out of which few are briefed below:

According to the approach in [14] query plans have been generated in view of the commonality of the information needed for answering the query. The Genetic algorithm considers the relations in the FROM clause, the hubs having this information, the likelihood of hybrid (crossover), likelihood of change (mutation) and the pre-indicated number of generations as input, and produces the top-K inquiry plans as yield. Queries need effective processing, which commands formulating of ideal query processing techniques which create productive query processing plans for an appropriate query sent. A proficient query handling plan is required from among all the conceivable query plans. For a noticed crossover and mutation rate, GA approach unites rapidly towards the ideal query processing plans. According to the research of [15] it briefly illustrates a table containing various variables and viewpoints to assess the worth every optimization strategy gives from adaptability to dependability.

According to [16] we present a novel query optimization methodology known as clock stroke event handler for the database reflection of WSNs which comprises different clients. The assessment results show the proposed conspire which essentially diminishes the energy utilization in both single and numerous base station situations.

According to [17] the attainment of least expenses become complex in nature which can be illuminated in polynomial opportunity to accomplish global ideal expense of information transmission by Clonalg algorithm.

In 1975, John Holland had proposed the possibility of Genetic algorithm (GA) [18]. GA is a searching heuristic that emulates the procedure of normal advancement. This heuristic is much of the time used to create helpful answers for optimizing and exploration issue. Genetic algorithms use mutation, selection and crossover operators to give rise to better results.

From the study of Particle Swarm Optimization (PSO) [18] PSOis a vigorous optimization procedure roused from the development and insight of swarms. This methodology includes a lot of possible arrangements (called as particles), being scattered at different focuses in the arrangement space. Every point shows target work esteem, subsequently it has fitness, for its present area. Particles move (fly) in a way that every particle's development is impacted because of the accompanying two factors:
a) The best fitness accomplished by the particle up until this point.
b) The efficient fitness accomplished by a random particle in its area.

In this scenario, we can consider queries as the particles which will travel to different nodes till it reaches the destination node to obtain the user required result.
One of the solutions to address the problem of generation and choice of query plan is nature inspired algorithms. These algorithms have been rendered to tackle various genuine multifaceted issues. Such issues are helped by Bio-inspired algorithms. Artificial Immune System (AIS) [17], is enlivened from the common human immune system. Clonal selection procedure, one of AIS approaches, has been talked about in the examination to create ideal dispersed query plans in appropriated wireless sensor networks.

According to the research done in [21] to identify a direct way from the query originator hub to a hub that is situated at the focal point of query's spatial window, GreedyDF algorithm utilizes a greedy technique. The query originator advances the query to its neighbor found nearest hub, which thus advances the query to its neighbor nearest hub, etc. The GreedyDF algorithm utilizes few messages; however it doesn't ensure that a routing way to a hub in the query's spatial window will be initiated. Greedy based routing strategies for location based directing in adhoc networks have appeared to almost ensure conveyance for dense network graphs, yet doesn't function appropriately every now and again for scanty network graphs.

According to the study of [22] query optimization issues are addressed by stressing the implication aware cooperation in the sensor networks. Rather than diving straight to the solid activities, (for example, information sensing, filtering, total, and storing) and connecting examples of sensor information, concentration is around the effect of suggestion and the technique to use it, so the aggregate energy expenditure of query processing is limited. This methodology is named as EE-QPS (Energy-Efficient Query Processing among heterogeneous sensor systems).

In a query based remote sensor network, most of the queries perhaps are sent to a particular hub and a hotspot issue arises and rapidly expends the energy of the particular hub. The traffic flow near the neighboring area of that node is also influenced by the hotspot. To solve the hotspot problem, [23] illustrates two specialists setting algorithms, distance-based agent selection (DAS) and greedy-based agent selection (GAS) to moderate the traffic stream close to hotspot.

The study in [24] proposes Minimum Hot-Spot (MHS), a distributed algorithm that makes a reasonable query directing tree associating all hubs in the system. First the methodology of this issue being separated per tree profundity is talked about and afterward deciding the base conceivable correspondence cost expected to develop a tree.

The study in [25] reviews and explains the procedures of a familiar algorithm, Naive-k for top-k query assessment which registers the appropriate response in bottom up approach in one pass over the network.

Real Time Query Scheduling (RTQS) in [26] is intended to accomplish high information efficiency and separated query latencies through organized simultaneous clash free transmission planning. The received methodology depends on utilizing two parts: an organizer and a scheduler. Two regular RTQS algorithms: Non-preemptive Query Scheduling (NQS) and Preemptive Query Scheduling (PQS) are discussed further in [26].

According to the study of [27] one methodology in WSN preparing, interprets the WSN as a disseminated database, and the handling job infused into hubs for execution is the assessment of a query evaluation plan (QEP). In this methodology, clients indicate required information necessities as decisive queries, which the framework, called a sensor network query processor (SNQP), orders into optimized QEPs for infusion into the WSN. Through occasional assessment, a flood of outcomes is sent back to the clients by means of the base station.

Sensor Network query processing (SNQP) [28] is one of the method that utilizes query and WSN over that it is to be run, to think of a energy proficient Query Evaluation Plan (QEP) that distributes processing inside the assortment of QEP sections to the hubs inside the WSN.

V. Open Research Issues

Several challenges need to be addressed and further examination is required in WSNs. A portion of the open exploration issues for WSNs that can be fathomed utilizing Machine learning and Artificial intelligence (AI) are listed out as follows:

1) To distinguish the flawed sensor hubs from the network.
2) To identify irregularity in the network.
3) To find ideal cluster heads in the system.
4) Efficient various objectives tracking for versatile WSNs.
5) To distinguish an occasion from the perplexing sensor information.
6) To conjecture the measure of vitality (energy) to be reaped inside a particular time period in the network.
7) To predict the network lifetime in WSN.

VI. Conclusion

Taking into account the above study, it is presumed that however there are a lot of data extraction methods, in WSN, every single method has its merits and demerits. Query based methodology is the highest mainstream in light of its usability and its capacity to render a large portion of the data requirements in WSN. To battle the natural imperatives of restricted energy and transfer speed, query processing and transmission optimization are the fundamental zones of study. Query optimization techniques and different procedures have been examined in this paper. These procedures can be utilized by the client as indicated by necessity of use and resources accessible.

References

[1] Husna Jamal Abdul Nasir, Ku Ruhana Ku-Mahamud "Wireless Sensor Network: A Bibliographical Survey" Indian Journal of Science and Technology, **Vol 9(38)**, DOI: 10.17485/ijst/2016/v9i38/91416, (October 2016)

[2] Neenu M. Nair, J. Sebastian Terence "Survey on Distributed Data Storage schemes in Wireless Sensor Networks" Neenu M. Nair et.al / Indian Journal of Computer Science and Engineering (IJCSE)

[3] Humaira Ehsan and Farrukh Aslam Khan "Query Processing Systems for Wireless Sensor Networks" Conference Paper in Communications in Computer and Information Science. (April 2011)

[4] Vandana Jindal, A.K.Verma, Seema Bawa "Survey on Query Processing & Optimization Techniques in WSN" (IJCSIS) International Journal of Computer Science and Information Security, **Vol. 14, No. 2,** (February 2016)

[5] Abderrahmen Belfkih, Claude Duvallet, Bruno Sadeg, Laurent Amanton "A Real-Time Query Processing System for WSN" .

[6] Rone Ilídio da Silva , Daniel Fernandes Macedo , José Marcos S. Nogueira "Spatial query processing in wireless sensor networks – A survey".

[7] Ankam Praveen1, Punnamchandar Pulyala2 "A Review towards the Development of Efficient Skyline Query" © 2018 JETIR (September 2018), **Volume 5, Issue 9**

[8] Alexandru Coman Jor¨ g Sander Mario A. Nascimento "An Analysis of Spatio-Temporal Query Processing in Sensor Networks"

[9] Zhangbing Zhou, Deng Zhao, Gerhard Hancke, Fellow, IEEE, Lei Shu, Member, IEEE, and Yunchuan Sun, Senior Member, IEEE "Cache-Aware Query Optimization in Multiapplication Sharing Wireless Sensor Networks" IEEE Transactions on systems, man, and cybernatics: systems, **Vol. 48**, no. 3, (March 2018)

[10] Amir Shaikhha, Mohammad Dashti, Christoph Koch "Push vs. Pull-Based Loop Fusion in Query Engines" arXiv:1610.09166v1 [cs.DB] **28 Oct 2016**

[11] Shaohua Wan, Yu Zhao, Tian Wang , Zonghua Gu, Qammer H. Abbasi , Kim-Kwang Raymond Choo "Multi-dimensional data indexing and range query processing via Voronoi diagram for internet of things" journal homepage:www.elsevier.com/locate/fgcs

[12] T.V. Vijay Kumar, Biri Arun, Lokendra Kumar "Distributed Query Plan Generation Using HBMO"

[13] Ms. Preeti Tiwari, Dr. Swati V. Chande "Optimization of Distributed Database Queries Using Hybrids of Ant Colony Optimization Algorithm" International Journal of Advanced Research in Computer Science and Software Engineering, **Volume 3**, Issue 6, (June 2013)

[14] T.V. Vijay Kumar, Vikram Singh, Ajay Kumar Verma "Distributed query processing plan generation using genetic algorithm" International Journal of Computer Theory and Engineering, **Vol.3**, No.1, (February, 2011 1793-8201)

[15] Dharini Ganesh, Lalitha M Veeramachaneni, Linda Wong "Optimization techniques for Wireless Sensor Network" INFS 612 – Summer (2009), **PGN # 4** George Mason University

[16] Dilini A. Muthumala#1, Udara S. Liyanage#2, Asanka P. Sayakkara#3, Jeewani S. Goonetillake#4 # "Optimizing Concurrent-Query Execution in Wireless Sensor Networks" University of Colombo School of Computing, No. 35, Reid Avenue, Colombo 7, Sri Lanka

[17] Ruby Rani "Distributed Query Processing Optimization in Wireless Sensor Network Using Artificial Immune System".

[18] K. K. Mishra, Shailesh Tiwari and A. K. Misra "A Bio Inspired Algorithm for Solving Optimization Problems" International Conference on Computer & Communication Technology (ICCCT)-(2011)

[19] Dr.Anil kuumar Verma, Vipin Kumar "Query optimization in Wireless sensor networks" Thesis submitted to Computer Science and Engineering department Thapar University.

[20] Dina M. Ibrahim, Elsayed A. Sallam, Dina Khattab, Dina Hussein "A Query Optimization Strategy for Autonomous Distributed Databse System" March 2018

[21] Alexandru Coman, Mario A. Nascimento, J¨org Sander "A Framework for Spatio-Temporal Query Processing Over Wireless Sensor Networks" Proceedings of the First Workshop on Data Management for Sensor Networks (DMSN 2004),Toronto, Canada, (August 30th, 2004).

[22] Yuan He, Mo Li, Yunhao Liu, Jizhong Zhao, Wei Lan Huang, Jian Ma "Collaborative Query Processing among Heterogeneous Sensor Networks" HeterSANET'08, May 30, (2008), Hong Kong SAR, China. Copyright 2008 ACM 978-1-60558-113-2/08/05

[23] Tzung-Shi Chen, Hua-Wen Tsai, Ying-Hung Lo, Yi-Shiang Chang "Mitigating Query Hotspots for Wireless Sensor Networks" IWCMC'10, June 28–July 2, 2010, Caen, France. Copyright © (2010) ACM 978-1-4503-0062-9/10/06/

[24] Georgios Chatzimilioudis, Demetrois Zeinalipour-Yazti, Dimitrios Gunopulos "Minimum Hot-Spot Query Trees for Wireless Sensor Networks" ACM MobiDE'10 - 9th International ACM Workshop on Data Engineering for Wireless and Mobile Access.

[25] Baichen Chen, Weifa Liang, Rui Zhou, Jeffrey Xu Yu "Energy-Efficient Top-k Query Processing in Wireless Sensor Networks" CIKM'10, October 26–30, (2010), Toronto, Ontario, Canada. Copyright 2010 ACM 978-1-4503-0099-5/10/10

[26] Moutaz Saleh Mustafa Saleh "Adaptive Real-Time Query Scheduling for Wireless Sensor Networks" MSWiM'11, October 31–November 4, (2011), Miami, Florida, USA.Copyright 2011 ACM 978-1-4503-0898-4/11/10

[27] Alan B. Stokes, Alvaro A.A Fernandes, Norman W. Paton "Resilient Sensor Network Query Processing Using Logical Overlays" MobiDE '12, May 20, (2012) Scottsdale, Arizona, USA Copyright 2012 ACM 978-1-4503-1442-8/12/05

[28] Alan B. Stokes, Norman W Paton, Alvaro A.A. Fernandes "Proactive Adaptations in Sensor Network Query Processing" Copyright is held by the owner/author(s). Publication rights licensed to ACM. Copyright (2014) ACM 978-1-4503-2722-0/14/06

[29] Kayiram Kavitha, Vinod Pachipulusu, Sreeja Thummala, R.Gururaj. Article: Energy Efficient Query Processing for WSN based on Data Caching and Query Containment, in International Journal of Computer Applications, Vol. 89, no. 19, Page no. 4-8, March 2014, Published by Foundation of Computer Science, New York, USA. . Impact factor: 0.745

[30] K. Kayiram, R. Surana and R. Gururaj, "Energy Efficient Data Management in Wireless Sensor Networks," 2019 IEEE 1st International Conference on Energy, Systems and Information Processing (ICESIP), Chennai, India, 2019, pp. 1-6, doi: 10.1109/ICESIP46348.2019.8938241.

[31] P. Nayak, K. Kavitha and N. Khan, "Cluster Head Selection in Wireless Sensor Network Using Bio-Inspired Algorithm," TENCON 2019 - 2019 IEEE Region 10 Conference (TENCON), Kochi, India, 2019, pp. 1690-1696, doi: 10.1109/TENCON.2019.8929440

[32] Kavitha Kayiram, Dr. P.Chandra Sekhar Reddy, Dr. Avinash Sharma, Dr. R.V.S.Lalitha, Energy Efficient Data Retrieval in Wireless Sensor Networks for Disaster Monitoring Applications, IEEE International Conference on Sustainable Energy and Future Electric Transportation (SeFeT) 21-23 January 2021 Hyderabad.

Real Time Nitrogen, Phosphorus, Potassium (NPK) Detection in Soil using IoT

[1]R.V.Satya Lalitha, [2]Rayudu Srinivas, [1]Ch.V.Raghavendran,[3]Kayiram Kavitha
[4]Pullela S.V.V.S.R.Kumar, [5]P.S.L.Sravanthi

[1] Aditya College of Engineering & Technology, Surampalem
[2] Aditya Engineering College, Surampalem,
[3] Gokaraju Rangaraju Institute of Engineering & Technology, Hyderabad,
[4] Aditya College of Engineering, Surampalem,
[5] SIS Software India Private Ltd., Hyderabad,

{rvslalitha@gmail.com, srinivas.rayudu@aec.edu.in, raghavendran.chv@acet.ac.in,
kavitha.bits@gmail.com, dean.a_a@acoe.edu.in,pslsravanthi.97@gmail.com}

Abstract. The Soil testing centers basically check only for primary nutrient values of the soil like Nitrogen, for growth of leaves, Phosphorous for root growth and Potassium for overall functions of plant which takes lot of time for reaching results to the Farmer. But in this system NPK values along with Temperature, Pressure and Humidity are also sensed for making the process efficient and make farmer to access the results along with suggestions in no time using their personal digital devices. The type of the soil solely depends upon primary conditions of the soil like temperature, moisture and humidity. Ideal soil temperature and realistic soil temperature are the two parameters for plant growth. Usually the temperature lies somewhere between ideal and realistic temperature. Soil temperature is the ratio of heat in the soil and the heat between atmosphere and soil. For organic forming the temperature is the key parameter for plant growth. The heat coming from the sun is absorbed by the soil, resulting temperature of the soil. The solar radiation is directly proportional to the heat reaching the soil. Humidity is the amount of moisture that is presented in the soil. The DHT11 sensor is used to measure temperature. Soil moisture is the prime factor for farm productivity. The moisture content depends on the number of water molecules attracted by the soil particles. Atmospheric humidity is expressed as a percentage of moisture in the air. The humidity around plants can be increased using gravel trays with water poured in it. Excess water cannot get enough oxygen from soil and lack of water obstructs plant growth. Hence level of moisture is significant for planting. The level of moisture is detected using moisture sensor. Each nutrient is added with reagent to form color. The darker color indicates increased concentration of the nutrient that is present in the soil. The color detection using Color sensor enhances accuracy parameters. In this process both manual and automated processes are included.

Keywords: NPK; Color sensor; Temperature sensor; Humidity sensor; IoT

1 Introduction

The extraction of nutrient values evolves the process of testing the condition of the soil. The soil analysis helps in analyzing the condition as well as predicting the type of crops that suits the soil condition. In due course, if the process is delayed, the soil parameters may vary. Real time detection of NPK values assists in obtaining the accurate values. In this paper, IoT based device is used to NPK values using color sensor. As primary conditions are also important in analyzing the condition of the soil, temperature and humidity values are also detected using DHT11 sensor. Using sensors the quality of soil is determined repeatedly and the NPK values will be captured. This reduces the time in taking soil samples to test centers and sending results back after analyzing.

2 Literature Survey

Soil analysis and Crop analysis plays significant role in cultivation. In general the detection of Nitrogen, Phosphorous and Potassium can be calculated by adding calcium sulfate and Mehlich. The color can be traced using filtration process and color comparator boxes. One of methods used for NPK analysis is Nitrogen Kjeldahl. Total Kjeldahl nitrogen (TKN) is the sum of organic nitrogen, ammonia (NH3), and ammonium (NH4+). To calculate Total Nitrogen (TN), the concentrations of nitrate-N and nitrite-N are determined and added to the total Kjeldahl nitrogen. Today, total Kjeldahl nitrogen is a required parameter for regulatory reporting at many treatment plants. The NPK analysis is done using Colorimeter which is used for environmental and biological applications. The plant growth characteristics were analyzed using NPK analysis. NPK analysis and decease detection in plants is done using IoT and the results were made it available. The analysis part is done using statistical analysis[1]. Fertilization plays important role in cultivation. It improves productivity in plants[2]. The effect caused due to loss of N, P or K leads to leaching, wet and dry conditions. Volatile ammonia lands are to be focused in rice lands[3]. NPK detection is pretty much used in crop analysis. NPK values and moisture are detected using corresponding sensors and ThingSpeak cloud is used for cloud to store data sensed by sensors[4]. Electro chemical, radio and optical sensors are used in analyzing soil conditions. Image processing and Neural network approach are very much accurate when detecting NPK values[5]. Soil fertility is evaluated using prediction and classification. Neural network provides better prediction results in classification [6,13,14]. The investigation of physiochemical properties of tobacco plants and the uptake of NPK were done using pot experiments[7]. Environmental risks and economic loss of sugarcane crop can be increased with N detection[8,11,15]. This paper suggests NPK analysis using IoT and made it available through mobile. The detection of NPK analysis is performed prior and are analyzed as low/medium/high are done based on threshold values set by Agro forums.

3 Real Time analysis of NPK using Sensors

The mechanism exhibited and various steps carried out are illustrated in Fig.1.

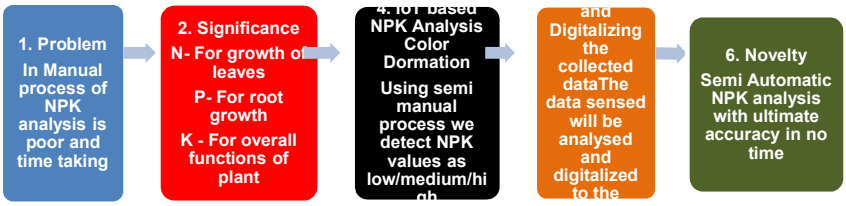

Fig.1. Outline of NPK Analysis

In the conventional process the soil is collected using V method and the soil is sieved. The sieved soil is then tested for NPK values by adding reagents. Later the change in color is compared the NICE color charts. As the color of soil is changed during the entire process leads to erroneous results. The presence of NPK values will be estimated based on the color of the liquid formed with the naked eye detection using the color chart shown above. If the process is delayed, the colors formed will be changed and will not give exact analysis. The time consumed for transferring the soil to research centers takes some amount of time and by the time the process starts, the conditions of the soil may change due to environment effect. Fig.2 shows the preparation soil in detecting color for NPK detection manually.

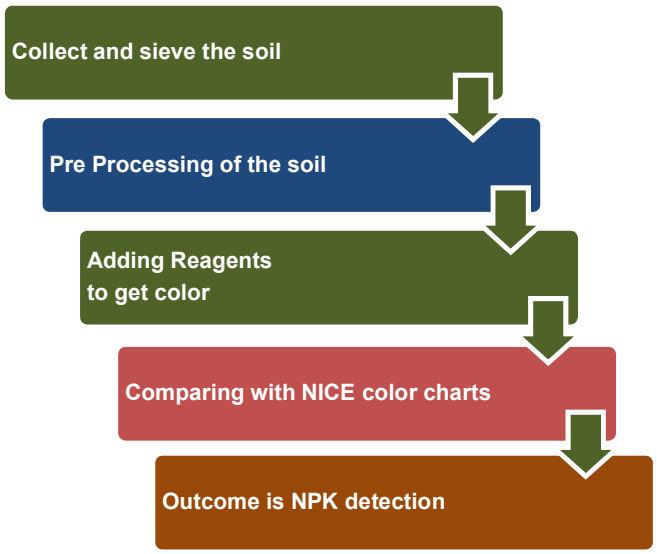

Fig.2. Manual process of Soil testing.

In real time IoT based analysis is done. The color detection is done using Color sensor and the data is uploaded in cloud for real time analysis and is then compared with the color charts for NPK detection. This is interpreted in Fig.3. As the process is carried out in real time using sensors, exact detection will be traced. The sensed values will be sent to cloud and then used for NPK detection. The process is carried out in 4 stages. 1. Preprocessing of the soil, 2. Adding reagents to estimate NPK values, 3. Detecting color using color sensor and 4. Estimation of NPK level in the soil

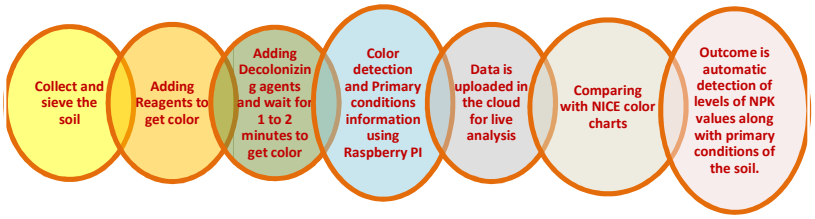

Fig.3. NPK analysis in Real time using IoT.

3.1. Preprocessing of the soil

The soil must be collected from one acre of land from four different corners and from the middle. We should choose the area in such a way that it must be exposed to sun and no pesticides must be applied on it from past 6 months' time duration. The soil is to be collected in V model. V model is a model in which the soil can be digged in v model using aagar (instrument to dig the soil). We must take soil from 15 cm down to the surface of soil. The soil may be in rock form or in any other form. The soil must be collected from the 15 cm down to the surface of soil. The soil sample collection area must be exposed to sunlight and no shade must be on that particular region.

The soil taken from 5 places are combined and undergone into *sieving* method. Sieving is a method in which the rock particles in the soil will be powdered. Now the powdered soil undergoes into sieving in which the rock particles and fine soil are separated. We should ensure that the soil is finely powdered. Take 500 grams of soil for testing. The Finely powdered soil can undergo into several chemical reactions to estimate values of Nitrogen, Phosphorous and Potassium that are present in the soil.

3.2. Adding reagents to estimate NPK values

i. Adding reagents to estimate Nitrogen

Take 5cc of soil and 25 ml of nitrogen reagent 1 into the soil and shake for 5-10 minutes. Then add a pinch of decolonizing agent into the soil and mix well. Filter the solution using funnel and filter paper. Next add 2 drops of nitrogen reagent 2 and mix

well. Wait for 1-2 minutes for color forming.The liquid formed in this process is separated from the soil and is used to detect color.

ii. Adding reagents to estimate Phosphorous

Take 5cc of soil and 25 ml of phosphorous reagent 1 into the soil and mix well for 15 minutes. Add a pinch of decolonizing agent and mix well. Filter the solution using funnel and filter paper. Add 2 ml of phosphorous reagent 2 and mix well. Wait for 1-2 minutes for color forming. The liquid formed in this process is separated from the soil and is used to detect color.

iii. Adding reagents to estimate Potassium

Take 5cc of soil and add 25 ml of potassium reagent 1 into the soil and mix well for 10-15 minutes. Add a pinch of decolonizing agent and again mix well. Filter the solution using funnel and filter paper. Add 1ml of potassium reagent 2 into clear solution and mix it well. Wait for 1-2 minutes for color forming. The liquid formed in this process is separated from the soil and is used to detect color.

3.3. Color detection using Color sensor

Hereinafter, the process is automated using IoT technology using Raspberry Pi and the color detection is done using Color sensor(TCS 3200). The values detected will be sent over the cloud and can be deployed in any web server or mobile based application. This accurate analysis of prediction is achieved as it can be carried out at field itself.

3.4. Estimation of NPK level in the soil

As per the recommendations of Nice Chemicals Private Ltd.(NICE), an ISO certified company, the range of levels of NPK deficiencies are estimated based on the color formed, is mentioned in the below diagram. The diagrams are taken from the Soil Testing Kit, Hand book prepared by NICE. Color Sensor (TCS 3200) sensor detects color formed from the liquid which is formed after adding reagents. Moisture sensor is used to detect moisture. Raspberry PI 3 is used for microcontroller. Temperature and Humidity sensor DHT11 is used to detect primary conditions of the soil. The color detected by the sensor is compared with the diagram and then the estimated values are deduced. The color values obtained from the Color sensor is compared with colors listed in the chart. Based on that, NPK estimation values will be given (Fig.4.for Nitrogen color chart, Fig.5. Phosphorus color chart, Fig.6.Potassium color chart, Fig.7. Temperature and Humidity and Fig.8 Moisture.

4 Results

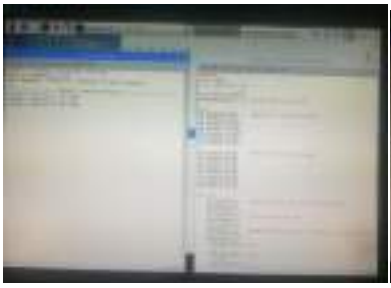

Fig. 4. Nitrogen detection

Fig.5. Phosphorous detection

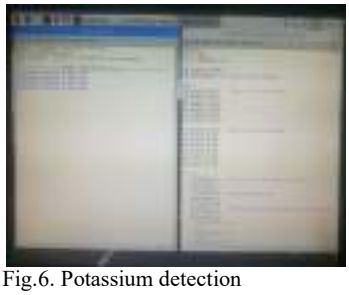

Fig.6. Potassium detection

Fig.7. Temperature and humidity detection

Fig.8. Moisture detection

NPK accurate values will be retrieved as the detection of color is through sensor. The surface is analyzed on the fly, hence there will be no change in color of the soil. If we input preprocessed soil, NPK analysis is done efficiently. The process is semi automatic. Farmers are able to know the condition of the soil in time through online. The color charts from NICE are used to compare color as in Fig.9.

a). Nitrogen Color chart.

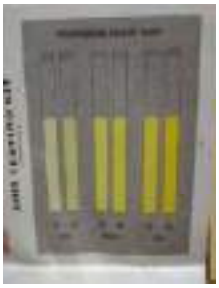

b). Phosphorus color chart

c). Potassium color chart.

Fig.9 Color charts taken from NICE

NPK detection using Python are summarized as below:

RGB Analysis
enter red value145
enter green value79
enter blue value29
nitrogen_high
phosphorous_low
potassium_low
>>>

The manual process is digitized using IoT and the results are also tested through program by comparing RGB values instead of naked eye. Hence, it gives accurate results. The tracing of primary nutrients such as Nitrogen, Phosphorous and Potassium that are present in the soil are done using Color sensor. In this ecosystem, the NPK analysis along with primary conditions of the soil is analyzed to provide base information for cropping. Also, by comparing soil color with the color charts, the level of NPK will be detected using this IOT based ecosystem. The heart of the invention is the information is made available over the Internet for further use. The data from ThingSpeak cloud is retrieved from web server to provide user required information. This reduces testing time and improves accuracy measures. As the color component is compared through online, this system provides accurate results, when compared with the manual process. The process can operate continuously for 1 or 2 hours for analysis. During the process, some of the values may be changed. The process works efficiently with 90% accuracy based on observations made.

Conclusion

Digitalizing the results make Farmer or owner of land benefited in taking exact measures to soil on time. NPK accurate values will be retrieved as the detection of color is through sensor. The process is semi automatic, as reagents are added manually. Farmers are able to know the condition of the soil in time through online. The tracing of primary nutrients such as Nitrogen, Phosphorous and Potassium that are present in the soil are done using Color sensor. Color sensor is used to detect the color of the soil. Temperature and Humidity sensor is used to test the primary conditions of the soil. In this ecosystem, the NPK analysis along with primary conditions of the soil is analyzed to provide base information for cropping. The detected values are sent to web server. This is the real time application and is made available on the Internet. For developing organic foods and agriculture reforms, it gives information which type of the crop fits for the tested soil.

References

1. Nachiket Kulkarni, Amit Thakur, Tanay Rajwal, Rupali Tornekar, Saraswati Patil, Smart soil nutrients analysis and prediction of the level of nutrients using a bot, 2019 3rd International Conference on Recent Developments in Control, Automation & Power Engineering (RDCAPE).
2. Kyi Moe, Aung Zaw Htwe, Thieu Thi Phong , Yoshinori Kajihara and Takeo Yamakawa , Effects on NPK Status, Growth, Dry Matter and Yield of Rice (Oryza sativa) by Organic Fertilizers Applied in Field Condition, Agriculture 2019.
3. Soo-Jeong Kwon, Hye-Rim Kim, Swapan Kumar Roy, Hyun-Jung Kim, Hee-Ock Boo, Sun-Hee Woo & Hag-Hyun Kim, Effects of Nitrogen, Phosphorus andPotassium Fertilizers on Growth Characteristics of Two Species of Bellflower (Platycodon grandiflorum), Journal of Crop Science and Biotechnology Vol 22, pp 481-487(2019).
4. John Carlo Puno, Edwin Sybingco, Elmer Dadios, Ira Valenzuela, Joel Cuello, Determination of soil nutrients and pH level using image processing and artificial neural network, 2017IEEE 9th International Conference on Humanoid, Nanotechnology, Information Technology, Communication and Control, Environment and Management (HNICEM).
5. John Carlo Velasco Puno, Edwin Sybingco, Elmer P. Dadios, Ira Valenzuela, Joel L Cuello, Determination of soil nutrients and pH level using image processing and artificial neural network, 2017 IEEE 9th International Conference on Humanoid, Nanotechnology, Information Technology, Communication and Control, Environment, and Management (HNICEM).
6. M.S.Suchithra, Maya L.Pai, Improving the prediction accuracy of soil nutrient classification by optimizing extreme learning machine parameters, Information Processing in Agriculture, Volume 7, Issue 1, March 2020, Pages 72-82.
7. Xuebo Zheng, Wenjing Song, Enna Guan, Yaobin Wang, Xihao Hu, Hongbo Liang & Jianxin Dong Response in Physicochemical Properties of Tobacco-Growing Soils and N/P/K Accumulation in Tobacco Plant to Tobacco Straw Biochar, Journal of Soil Science and Plant Nutrition, volume 20, pages293–305(2020)
8. Beatriz N. Boschiero, Eduardo Mariano, Luis O. Torres-Dorante, Thales M. S. Sattolo, Rafael Otto, Pedro L. Garcia, Carlos T. S. Dias & Paulo C. O. Trivelin,

Nitrogen fertilizer effects on sugarcane growth, nutritional status, and productivity in tropical acid soils Nutrient Cycling in Agroecosystems volume 117, pages367–382(2020).

9. Bijay-Singh, Are Nitrogen Fertilizers Deleterious to Soil Health? Agronomy 2018,8(4),48.
10. HeitorCantarella,RafaelOtto,Johnny RodriguesSoares,Aijânio Gomes de BritoSilva, Agronomic efficiency of NBPT as a urease inhibitor: A review, Journal of Advanced Research, Volume 13, September 2018, Pages 19-27
11. Daniele Costa de Oliveira , Mauro Wagner de Oliveira , Vinicius Santos Gomes da Silva , Terezinha Bezerra Albino Oliveira , Hugo Henrique Costa do Nascimento and Siglea Sanna de Freitas Chaves, Nutritional status of three sugarcane varieties grown in the northeast region of Brazil , Vol. 14(9), pp. 532-538, 28 February, 2019.
12. Soil Testing Kit Hand Book NICE, for color charts.
13. Raghavendran C.V., Naga Satish G., Suresh Varma P. (2020) Group Key Management Protocols for Securing Communication in Groups over Internet of Things. In: Hemanth D., Kumar V., Malathi S., Castillo O., Patrut B. (eds) Emerging Trends in Computing and Expert Technology. COMET 2019. Lecture Notes on Data Engineering and Communications Technologies, vol 35. Springer.
14. Kavitha Kayiram,S. Laxman Kumar, Pudu Pravallika,Kotte Sruthi, R.V.S. Lalitha, N.V. Krishna Rao, Fashion Compatibility, Recommendation System, Convolutional Neural Networks, Sentiment Analysis, Internationa Conference, ACCES 2020, GRIET, Hyderabad, 18th & 19th Sep 2020.
15. Rayudu srinivas, Lalitha RVS , Rama Reddy T , Durga Anuja B, Finding MST by considering increasing cost order of the Edges incident on Vertices, ICICC 2020,4th International Conference on Intelligent Computing and Communication, Dayananda Sagar University, School of Engineering, Near Kudlu Gate, Hosur Road, Bengaluru, India, 18th to 20th September, 2020.

A Flexible Accession for Brain Tumour Detection and Classification using AI Methodologies: Survey

V Ramya Manaswi[1,*] and *B* Sankarababu[2]

[1]MTech Student, Computer Science and Engineering, GRIET, Hyderabad, Telangana, India.
[2]Professor, Computer Science and Engineering, GRIET, Hyderabad, Telangana, India.

Abstract— In order to get a successful and appropriate treatment for the disorder regarding health, précised and identifying it early is much important in the scenario of brain tumor treatment. Prior knowledge and detection of the tumor helps to cope up with good medication, and also helps in saving a life in due time. Bio-medical informatics(BI) and Computer aided diagnosis(CAD) are benefiting neurooncologists in many ways. Machine learning algorithms are now used to do Image processing on medical images and contrast with the information due to manual diagnosis of Brain tumor which is always a tedious task because of human error is indulged. When compared with manual traditional practices, Computer aided mechanisms are compared to obtain better results. In this paper we are presenting the existing models or architectures overview of various researchers who dedicatedly addressed and worked on this tedious task.

Keywords—Random forest (RF), Expectation-maximization(EM), Decision Tree(DT), CNN, DNN

1. Introduction

Medical Image processing and segmentation for tumour detection in brain using the Magnetic-resonance-Images(MRI) in some cases uses different medical imaging modes which are very keen in process of deciding rights in MRI most notably, Support Vector Machine (SVM), Fuzzy Clustering Means (FCM), Artificial Neural Network (ANN), Neural Networks(NN) and expectation-maximization(EM) based algorithmic approaches which are some of the popular techniques used for region-based segmentation and so to extract the important information from the medical image processing. Lately, the presentation of advancements in IT and e-medical supervision system in healthcare area assists medical specialists with giving better medical treatment to the suffering patients. This examination tends to the issues with segmentation of abdominal cerebrum tissues and ordinary tissues like cerebrospinal liquid (CSL), white matter (WM), and grey matter (GM) from MRI by implementing feature extraction and SVM classifier.

. BT generally originate because of the rapid growth of the cells and when the situation is not controllable too. The impact of BT will be different in different age groups. BT expansion is generally dependent on the lifestyle, gender etc. Because BT cases were growing day by day and the impact of BT is more on the people, there were many people who are losing their lives which is uncontrollable. Shockingly there are many children who are been affected by the BT and loosing lives. The death rate is growing in children these days. So, in order to control these situations under control there must be an innovative way to predict the BT and to cure the BT in the early stages. So, these conditions made to focus on the proposed system.

Hydrogen molecules are regularly utilized in clinical and research MRIs to produce a distinguishable radiofrequency signal that receiving wires get right up-front closeness to the life structures being inspected. Hydrogen molecules normally exist in wealth in people and other natural organic entities, particularly in fat and water. By using the data mining strategies, huge relations and examples from the information can be separated. The procedures of ML (AI) and Data mining are as a rule adequately utilized for BTD and prevention at a beginning phase.

In this work, we present a programmed Brain Tumour Segmentation (BTS) procedure dependent on CNN. We have utilized three MRI perspectives on human cerebrum. X-ray check is utilized on the grounds that it is not so much destructive but rather more exact than CT cerebrum check. All past deals with the dataset that we are working with are for arrangement of tumour types. None of the past works

* Corresponding author: m.srividya1998@gmail.com

performed on this dataset are planned for Segmentation. The principal commitment of our paper is the dividing of the pictures in light of the course of caught MR pictures. Subsequently, three networks will be trained independently to accomplish better segmentation results

2. Literature Review

Zahra Sobhaninia et al., proposed brain tumour identification requires high precision, where minute mistakes in judgment may prompt disaster. Thus, Brain tumour Segmentation is a significant test for clinical purposes. At present a few techniques exist for tumour segmentation however they all need high precision. Here we present an answer for Brain tumour segmenting by utilizing deep learning techniques. In this work, we considered various points of cerebrum MR pictures and ap plied various organizations for division. The impact of utilizing separate networks for segmentation of MR pictures is assessed by contrasting the outcomes and a single network. Exploratory assessments of the organizations show that Dice score of 0.73 is accomplished for a single network and 0.79 in got for various networks (1)

Masoumeh Siar et al., proposed Cerebrum tumour can be grouped into two kinds: generous and harmful. Ideal and prior recognition and treatment plan prompts improved treatment and expanded the lifespan of patients. Quite possibly the most prominent and significant techniques is to utilize Deep Neural Network (DNN). To identify a tumour cerebrum Magnetic Resonance Imaging (MRI)pictures fed to the CNN model. Pictures were first embedded into the Convolutional Neural Network. The achieved accuracy from the SoftMax function and Fully Connected layers using MRI scanned images acquired 98.06%. Likewise, the precision of Convolutional Neural Network is acquired with the Radial-Basis-Function(RBF) model is 97.03% also used Decision Tree (DT)and achieved 94.42%. Not-with-standing on the exactness basis, we utilize the Sensitivity benchmarking, precision, and specificity assess the execution of network. As per the outcomes got from the above classifiers, the SoftMax function got the best precision using CNN (2)

Tonmoy Hossain1 et al., proposed brain tumour segmentation is perhaps the most important and burdensome aspects in the territory of image processing on medical images as a human-helped manual grouping can bring about erroneous expectation and determination. In addition, it is a disturbing assignment when there is a lot of information present to be helped. Mind tumours have high variety apparently and there is a comparability among tumour and ordinary tissues and subsequently the extraction of tumour locales from pictures gets unflinching. The authors proposed a strategy to isolate tumour from 2D MRI brain Images using "Fuzzy C-Means clustering algorithm" also trained using conventional classifier algorithms and CNN. The experimentation was carried on a continuous data with assorted tumour size, area, shape, and distinctive picture forces. In conventional classifier algorithms, applied 6 customary algorithms to be specific K-Nearest Neighbour(KNN), Logistic Regression(LR), Multilayer Perceptron(MLP), Support Vector Machine(SVM), Naïve Bayes(NB) and Random Forest(RF) which was carried out in scikitlearn. A short time later, we proceeded onward to CNN is executed utilizing Tensor flow and Keras on the grounds that it respects a preferred presentation over the conventional. Author mentioned in his paper CNN acquired a 97.70% precision, which is exceptionally convincing. The primary point of this paper is to recognize typical and unusual pixels, in view of surface based and factual based highlights. Also achieved 92.24% and 97.80% precision utilizing SVM and CNN. (3)

G. Hemanth et al., proposed the brain tumour(BT) recognition which has turned up as an most difficult in the field of medicine. BT can be indicated as a distorted growth of tissue in which the cells duplicate unexpectedly and interminably. The cycle of Image Segmentation is received for extricating strange tumour locale inside the cerebrum. In the MRI (Magnetic Resonance Image) Segmentation of mind tissue holds extremely huge to determine the presence of layouts concerning the cerebrum tumour. There is a huge concealed data is captured and saved in the Health care domains. With legitimate use of exact information mining order methodologies, early conjecture of any contamination can be performed effectively. Predominant piece of which is embraced feasibly. The assessment investigations summary of danger factors which are being takes place while doing Brain tumor observation systems. additionally, the proposed technique certifications to be incredibly compelling and precise for Brain tumour detection, classification and segmentation. In order to get highly accurate automation and semi automation systems are very useful. The researcher proposed a programmed segmentation methodology which relies on CNN using small kernels which size is 3 x 3. By consolidating this single strategy, segmentation and classification is refined. One of the Neural Network based technique called CNN which has layer-based classification of results. The methods of AI with Data mining are adequately utilized for Brain tumour detection and avoidance at a beginning phase. This accomplishes 92.7% precision utilizing CNN (4)

S. Somasundaram et al., proposed Basic segment in diagnosing tumour, planning treatment and building up a result for assessing Brain tumour segmentation should have been profoundly exact and solid. MRI scans help and

guiding the medical domain experts to recognize the extremely minor unusual development in human beings body. The Deep Neural Networks (DNNs) and AI methods have great accomplishment in 2D picture segmentation, however it's a moving difficult for DNNs to section basic organ parts using 3D clinical MRI scan reports. Segmentation relating tumour identification incorporates a few preparing strategies that are sorted into segmentation. research centres essentially around 3D ANN, SVM, CNN and Multi class SVM to do in précised Segmentation process. To eliminate computational weight of preparing 3D clinical sweeps, this research intends to survey the present advancement in segmentation of image and classification dependent on productive and compelling towards handling of tumour contaminated human mind MRI adjoining picture fixes that can go through the network with an objective of tumour, while mechanically adjusting towards an awkwardness there in the information At last, this article inferring about advancements on Detection and segmentation of tumour-based picture preparing for DL models. Analysis results of the underlying dataset show that the streamlining through GA approach has improved the complete exactness of SVM from 79.4% to 91.6% and of ANN from75.5% to 94.8% (5)

Bhagyashri H. et al., proposed a model for theneed to create computer analysis frameworks for analysis of Brain tumour. Brain tumour(BT) identification at beginning phase has gotten vital. In experimentation, cerebrum tumour MRI are utilized to recognize and characterize the dangerous and kind-hearted mind tumours. X-ray pictures which are collected by Brats dataset collected in 2015 by MICCAI. BTs are divided by utilizing image-processing methodologies. To de feature extraction of images the shape-based highlights are utilized. Removed shape-based highlights are taken care of AI algorithms as SVM and RF algorithms to order amiable and harmful cerebrum tumours. It accomplished the precision for irregular timberland is 86.66% (6)

Madhu Priya G et al., proposed a model with help of the MRI pictures. The process of segmentation was performed and the segmented images will be capable to measure up to the normal BT tissues and cells. The results are shown in the perspective of correlation. The researcher in his work done on segmentation to utilize a probabilistic neural network(PNN) and convolutional neural network(CNN). The design of CNN which has both 3*3 and 7*7 layers to build a cascaded architecture, in order to do a segmentation of tumour accurately in a powerful way, on Brats13 MRI dataset. Same way they utilized a PNN model to identifying tumours and analyse the problems on both models. SO, they came up with an exceptional PNN and CNN models to utilize image processing and computer vision(CV) strategies. the model arrangements with both local and global highlights. At last, got the yield fragmented picture just as examined precision and loss of our models. At long last, got the yield segmented picture just as investigated exactness and loss of our models (7)

K. Abbas et al., proposed a model to predict the BT using unpredictable design and its converging with the ordinary cells, and the arrangement of tumour from typical tissues was a difficult errand. The author in his research have brought up with a philosophy called LIPC in order to do the classification and segmentation of a brain tumour. The primary step in his research is to solve the multiclass image segmentation as a grouping task. X-ray groupings of the cerebrum have normal qualities (area) and are scanty (sparsity). Author used both these parameters in his proposed system. Firstly they focussed on image pre-processing strategies are utilized for image enhancement and noise removal. After 12 textural diverse features were determined and diminished because of PCA to do a better classification. 2013 MICCAI dataset is used in this experiment which had a low-level-tumour to high-level-tumour patient's data. This technique introduced a dice Score which is 0.95 for complete tumour which is a long shot contrasted with the strategies effectively accessible as far as dice Score and time complexity (8)

Zheshu Jia et al., discussed about the detection of brain unusual structures by essential imaging procedures which are very challenging. So, the author proposed a model called Fully-Automatic Heterogeneous Segmentation(FAHS) along with Support Vector Machine(SVM) was proposed to detect and separate tumour in MRI scans of brain images, depends on DL strategies(11). The proposed system shows the partition of the entire cerebral venous framework into MRI imaging with the expansion of another FAHS algorithm depends on underlying, morphological subtleties. The fragmenting capacity is recognized using uniformity which is high in level between present and neighboring tissues. ELM is an another algorithm for learning to comprise of at least one layer of hidden layers. Such algorithms are utilized in

different areas, which includes classification and regression. In MRI pictures, the PNN grouping framework which was used for training and testing the exactness of tumour identification on dataset images. The mathematical outcomes show practically 98.51% precision in recognizing strange and typical tissue from cerebrum Magnetic Resonance image that exhibit the productivity of the framework recommended (9)

Deepali Vikram Gore1 et al., proposed One in perilous infections to identify is cerebrum tumour. Utilizing deep learning methods, has shown decrease of mistake in human mid 9 9 determination of the sickness. Particularly, diagnosis of brain tumour requires high precision, where minute mistakes in analysis may prompt confusions. In medical image processing, cerebrum tumour exposure stays a requesting position. It is a complicated task to detect a tumour in brain. A few commotions also postpone influences the picture exactness. Picture division and MRI methods have become an accommodating clinical diagnostic instrument for the assessment of the mind and other clinical dataset. Segmentation of an image is a powerful space of Medical Image Processing(MIP). This process is carried out to draw out the various jobs from clinical pictures like CT, MRI check, also includes Mammography, and so on. The researcher, we introduced a deliberate training of brain tumour utilizing deep learning methods. The examination and relative investigation of late information connected with cerebrum problem discovery utilizing Deep Neural Networks is considered in this audit. The result of this paper expresses the different exploration holes distinguished from the writing audit. The exactness accomplished is 88.9%. (10)

3. Comparison

Following table is the comparison between the models I have surveyed.

Table 1. Comparison of the Methods used

Year	Author	Algorithm/ System	Accuracy	Ref.
2018	Zahra Sobhaninia et al.,	Deep learning techniques	Dice score for one network – 73% For multiple networks – 79%	[1]
2019	Masoumeh Siar et al	FCNN, RBF, DT	98.06%, 97.03%, 94.42%	[2]
2019	Tonmoy Hossain1 et al.,	CNN	97.70%	[3]
2019	G. Hemanth et al.,	CNN	92.56%	[4]
2019	S. Somasundaram et al.,	SVM, ANN	91.6% 94.82%	[5]
2019	Bhagyashri H. et al.,	SVM, RF	86.66%	[6]
2019	Madhu Priya G et al.,	PNN, CNN	-	[7]
2019	K. Abbas et al.	Deep learning techniques	Dice score-95%	[8]
2020	Zheshu Jia et al.,	FAHS-SVM	98.51%	[9]
2020	Deepali Vikram Gore1 et	DNN	88.66%	[10]

4. Conclusion

In this paper a partial survey for brain tumour detection is done. Various techniques which are proposed earlier are mentioned here along with their usage of algorithms and assumption for execution of the problem. The dataset used for different technique is also mentioned and the results obtained by using those techniques are mentioned. This work can be used for extension of those techniques and for obtaining better results by future enhancements.

5. References

1 Z. Sobhaninia, S. Rezaei, A. Noroozi, M. Ahmadi, H. Zarrabi, N. Karimi, A. Emami, and S. Samavi, arXiv [cs.CV] (2018).

2 M. Siar and M. Teshnehlab, 2019 9th International Conference on Computer and Knowledge

Engineering (ICCKE) (2019)

3 T. Hossain, F. S. Shishir, M. Ashraf, M. D. A. Al Nasim, and F. Muhammad Shah, in *2019 1st International Conference on Advances in Science, Engineering and Robotics Technology (ICASERT)* (2019), pp. 1–6.

4 G. Hemanth, M. Janardhan, and L. Sujihelen, in *2019 3rd International Conference on Trends in Electronics and Informatics (ICOEI)* (2019), pp. 1289–1294

5 S. Somasundaram and R. Gobinath, 2019 International Conference on Machine Learning, Big Data, Cloud and Parallel Computing (COMITCon) (2019)

6 B. H. Asodekar, S. A. Gore, and A. D. Thakare, in *2019 5th International Conference on Computing, Communication, Control And Automation (ICCUBEA)* (2019), pp. 1–5

7 G. Madhupriya, N. M. Guru, S. Praveen, and B. Nivetha, in *2019 3rd International Conference on Trends in Electronics and Informatics (ICOEI)* (2019), pp. 758–763

8 K. Abbas, P. W. Khan, K. T. Ahmed, and W.-C. Song, in *2019 International Conference on Information and Communication Technology Convergence (ICTC)* (2019), pp. 531–536.

9 Z. Jia and D. Chen, IEEE Access 1 (2020)

10 D. V. Gore and V. Deshpande, in *2020 International Conference for Emerging Technology (INCET)* (2020), pp. 1–4.

11 C. U. Kumari, S. Jeevan Prasad, and G. Mounika, 2019 3rd International Conference on Computing Methodologies and Communication (ICCMC) (2019).

Deep convolutional neural network based facial expression identification using face-parsing method

Raju Yadav Mothukupally[1*], P *Chandra Sekhar* Reddy [2].

[1]PG Scholar, *Computer Science and Engineering*, *GRIET,* Hyderabad, Telangana, India.
[2]Professor, *Computer Science and Engineering*, *GRIET*, Hyderabad, Telangana, India.

Abstract: Face parsing methodology may be a one amongst the advancements in pc vision that analyses the surface synthesis of the external body part, to amass bits of information on options needs correct pixel segmentation of various components of face like (mouth, nose, eyes etc.). Same means the analysis on feeling recognition plays a eventful role in communication and interactions of humanity and additionally relevant to psychological activities. Considering the disadvantage that totally different completely different components of face contain different quantity of knowledge for face expression and also the weighted perform are not an equivalent for various faces. In keeping with analysis, the image classification task ordinarily drives North American country to the notable Convolutional Neural Network (CNN) during which we tend to ar victimization VGG19 model. beyond exploring around however CNN, sometimes performs for greyscale photos, we tend to selected to start from 3 consecutive convolutional layers followed by a most pooling layer, basic exploit work for convolutional layer and "relu" is used, even as an analogous artefact pattern. The highlights to be known victimization the convolutional layer distended to 128 layers from thirty-two, it is suggestable that multi-layered structure (with increasing layers) that performs and results the most effective outcomes for the DNN model. At last, the CNN layer is 1st smoothened and afterwards expertise 2 many dense layers to reach the yield layer during which SoftMax activation perform is used for multiclass classification. We tend to victimization Cohn-Kanadre face expression dataset of seven expressions like contempt, anger, disgust, happiness, fear, disappointment and surprise.

1. Introduction

With the features of current innovative technology, our fits of hunger went high and it ties no limits. In the current time, enormous research and experimentation on in the field of Machine Learning, Deep Learning and Image processing. The Image Processing is an immense region of examination in the current research world and its applications are exceptionally far-reaching. In this field of sign handling where both the info and yield signals are pictures. Perhaps the main utilizations of Image training are Facial acknowledgment. Our feeling is uncovered by the appearances on our countenances. Outward appearances assume a significant part in relational correspondence. Outward appearance is a nonverbal logical signal that gets communicated in our countenances according to our feelings. Programmed acknowledgment of outward appearance assumes a significant part in man-made reasoning and advanced mechanics and in this manner, it takes the age of a person into account. Some application identified with this method and incorporates Identification of individual and control access, Videophone and Teleconferencing, Forensic application, Human-Computer Interaction, Automated Surveillance, Cosmetology, etc.

Identifying the emotion of a human is experimented using numerous methods using an additional resources or data of individual personnel. It very well may be viewed as a subsequent advance to confront identification where we might be needed to set up a second layer of safety, where alongside the face, the feeling is likewise distinguished. This can be valuable to confirm that the individual remaining before the camera isn't only a 2-dimensional portrayal [2]. Another significant area where we see the significance of feeling identification is for business advancements.

* Corresponding author: rajuyadavmothukupally@gmail.com

Considering the disadvantage that totally different components of face contain different quantity of knowledge for face expression and therefore the weighted perform aren't identical for various faces [1]. Most organizations blossom with client reactions to every one of their items and offers. If a mechanized thinking system can get and perceive progressing sentiments reliant upon customer picture or video, they can make a decision on whether the customer appreciated or despised the thing or offer. We have seen that security is the basic role behind perceiving any person. It will in general be established on finger impression organizing, voice affirmation, passwords, retina acknowledgment, etc. recognizing the objective of the individual can similarly be basic to divert threats. This can be useful in weak regions like air terminals, shows, and significant public social events which have seen numerous breaks lately. Human feelings can be named dread, disdain, nauseate, outrage, shock, misery, bliss, and nonpartisan. These feelings are exceptionally unpretentious. Facial muscle bending's are negligible and recognizing these distinctions can be trying as even a little contrast brings about various articulations [3]. Additionally, articulations of various or even similar individuals may differ for a similar feeling, as feelings are tremendously setting subordinate [4]. While we can zero in on just those regions of the face, which show a limit of feelings like around the eyes and mouth [5], how we are going to extract these emotions and classify them is yet a significant inquiry. Neural organizations and AI have been utilized for these undertakings and have gotten great outcomes. AI calculations have demonstrated to be extremely valuable InDesign acknowledgment and characterization. The main parts of any AI calculation are the highlights. In this research work, we will perceive how the highlights are separated and altered for calculations like SVM [2]. We will think about calculations and the component extraction methods from various research works. The dataset, which consists of human emotions, can be an excellent guide to contemplate the power and nature of order calculations and how they perform for various kinds of datasets. As a rule, before extracting the features or highlights for feeling identification, facial location calculations are pertained on the images. The emotion identification and landmarks extraction process as follows:

- Pre-processing the Data.
- Face detection.
- Landmarks extraction.
- Feature classification.

The primary target of this thesis is to generate the computerized Facial Expression Identification System which takes a human facial images containing some appearance as information and perceive and characterize it into 7 diverse demeanour class, for example, :

1.Anger
2.Contempt
3.Disgust
4.Fear
5.Happiness
6.Sadness and
7.Surprise

Fig. 1. Facial Expressions

2. Conceptual Background Study

In this segment, a depiction of important ideas for this task is introduced. This segment we are giving some insights about the foundation on the points to be discussed in this thesis. This foundation is cultivated by methods for a sequential correction of fields, for example, emotional processing, and AI. To depict the ideas, a top-down approach will be used. Besides, related exploration to the methodology utilized in this venture is presented, too.

2.1 Deep Computing

As portrayed by Rosalind Picard [6], "... full of feeling processing is the sort of registering that identifies with, emerges from, or impacts feelings or other emotional wonders". Full of feeling processing intends to remember feelings for the plan of innovations since they are a fundamental piece of errands that characterize the human experience: correspondence, learning, and dynamic. The primary establishments behind full of feeling figuring is that without feelings, people would not appropriately work as normal dynamic creatures. A few explore show that there is no such an unbelievable marvel as "unadulterated explanation". Feelings are engaged with dynamic since a completely logical methodology would transform into a very tedious cycle, not reasonable for day-by-day

assignments. Investigates around this specific theme have shown that the mind doesn't test every likely choice, yet it is one-sided by feeling to rapidly settle on a choice. A feeling is characterized as a class of characteristics that is inherently associated with the engine framework. At the point when a specific enthusiastic state is set off, the engine framework will give the relating set of guidelines to recreate the specific regulations associated with that class. Up until this point, feelings' significance has been tended to without contemplating human communication. One of the human feeling sympathies which limits that makes everyone mindful and gives us an understanding of what different creatures may be encountering from their present position. Also, sympathy permits us to construct cozy connections and solid networks. Consequently, it is principal towards favorable to social conduct, which incorporates social cooperation and discernment. Accordingly, it is vital for full of feeling registering to create approaches to appropriately gauge these specific tweaks since they can prompt a superior comprehension of a subject's passionate state. The primary two approaches are used for recognizing vocal and facial feelings. Nonetheless, in this thesis experiment, we are just facial feelings were utilized.

2.2 Facial Expression Recognition:

The analysis done by MR. Paul oceanographer has gotten principal to the development of this zone. These days, an oversized portion of the facial feeling acknowledgment examines depend upon Ekman' Facial Action writing [7]. One amongst the strategy conferred a framework that takes the highlights from to characterize of eyebrows, eyes and mouth utilizing a climbable quadrilateral [12]. This framework offers a designing between muscles movement of face and ablaze space. The principal reason behind this framework is to order human facial developments obsessed with the expressions of individuals. This grouping was at first evolved by an expert from Swedish, Mr. Carl-Herman Hjortsj. Figure a pair of displays a bunch of facial feeling units associated to their comparison facial motion. Be that because it might, this designing may confront many difficulties. For example, entertainers fake motions related to facial feelings. The shortage of a real inspiration driving the6 feeling does not forestall folks to counterfeit it. For example, an examination depicts once a patient, who is half-incapacitated, is approached to grin. At the purpose when it is asked, simply an aspect of the mouth raises. Nonetheless, when the patient is conferred to a joke, the two sides of the mouth raise. Henceforth, numerous ways in which to send a sense depend upon the foundation and nature of a selected feeling. Regarding PCs, numerous prospects emerge to furnish them with the talents to speak and understand feelings. These days, it is possible to repeat the facial units of Mr. Ekman. This can furnish PCs with graphical appearances that provides a lot of characteristic communication [8]. In regard to acknowledgment, PCs have had the choice to perceive some facial classifications: satisfaction, shock, outrage, and nauseate. A lot of knowledge concerning facial feeling acknowledgment is found in dataset segment.

2.3 Facial Expressions:

Inferred various sorts of highlights from the picture and standardize that vector structure. We can utilize different sorts of strategies to recognize the feeling like computing the circles framed and the points between various parts such as nose, mouth, eyes, and so on following are a portion of the unmistakable landmarks are utilized for preparing AI algorithms.

For the numerical selections, the association between facial components is employed to fabricate a phase vector for work [14, 15]. Ghimire and Lee used 2 forms of numerical selections subject to the position and place of fifty a pair of facial accomplishment centers [15]. For the classifier, 2 distinctive ways in which unit of assessment given, either misuse multi-class AdaBoost with dynamic time winding, or employing a SVM on the upheld half vectors.

2.3.1 Facial Expression System (FES):

Facial Expression System is utilized to provide an Identification(Id) for each facialexpression. Each Id is called as an activity unit. A mix of activity units brings about an outward appearance. The miniature changes observed from the face muscles can be characterized by an activity unit which are Id-12 and Id-6. For instance, a grinning face could be characterized as far as activity units, which basically implicates the development of Id-Au6 cheek raiser muscle which brings about a cheerful face. Here Id-6 and Id-12 are the cheek raiser and lip corner puller. A FAS dependent on activity units ares decent frameworks to sort out based on facial muscles are associated with which demeanor. Constant facial models could be produced dependent on them.

Fig. 2. Face movements and actions

2.3.2 Facial Landmarks:

Landmarks of face are very essential inorder to utilize those for faceial identification and acknowledgment. Similar tourist spots can likewise be utilized on account of articulations. The library called Dlib has 68 facial landmarks identifier which provides 68 pin points of the face. In Fig. 2 shows every pin point of total 68 landmarks of the face. Utilizing the library "dlib" extricating the X and Y co-ordinates of every individual facial pin points. These 68 focuses can be partitioned into explicit zones like the nose, right eye, left eyebrow, mouth, left eye, right eyebrow, and jaw.

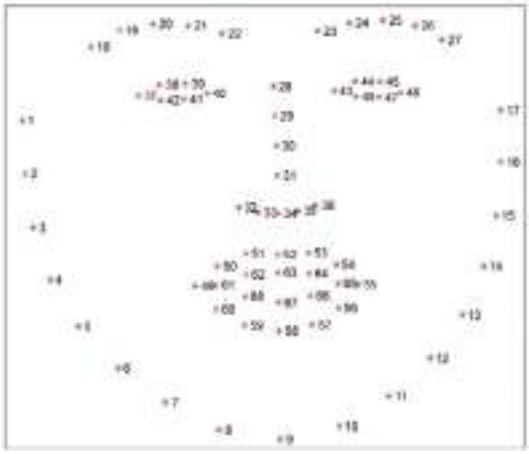

Fig. 2. Landmarks

2.3.3 Feature Recognition Tools:

landmarks are those which help in recognizing the emotion appropriately. Typically, the pictures are recognized based on edges and corners. For discovering edges and corners in pictures, we have many used element indicator calculations using a library called OpenCV, for example, the Harris corner finder. These element indicators consider a lot more factors like forms, structure, and arched. The Key-focuses are corner focuses or edges recognized by the component locator calculation. The component descriptor depicts the zone encompassing the central issue. The portrayal might be a lot which includes (X,Y) co-ordinates or crude pixel forces of a desired region. The descriptor and central issue together structured a nearby component. One illustration of a component was a histogram discriptor used for inclinations. Sphere,SURF, SIFT, and so on are a portion of the component descriptor calculations [9].

2.4 Data Set:

The Extended Cohn-Kanade (**CK+**) dataset contains 593 video arrangements from a sum of 123 distinct subjects, going from 18 to 50 years old with an assortment of genders and legacy. Every video shows a facial shift from the impartial appearance to a designated top demeanor, recorded at 30 FPS with a goal of either 640x490 or 640x480 pixels. Out of these recordings, 327 are named with one of seven articulation classes: outrage, disdain, disdain, dread, satisfaction, trouble, and shock. The CK+ information base is generally viewed as the most widely utilized research facility-controlled look characterization data set accessible, and is utilized in most of look arrangement strategies [10].

JAFFE [Japanese Female Facial Expressions] [13]: The JAFFE information contains 213 photos of ten totally unique female Japanese models showing seven face feelings (six fundamental facial feelings and one unbiased). Each picture was given a score dependent on six emotive words used to misuse sixty Japanese individuals. Every facial picture's essential size is 256 pixels by 256 pixels.

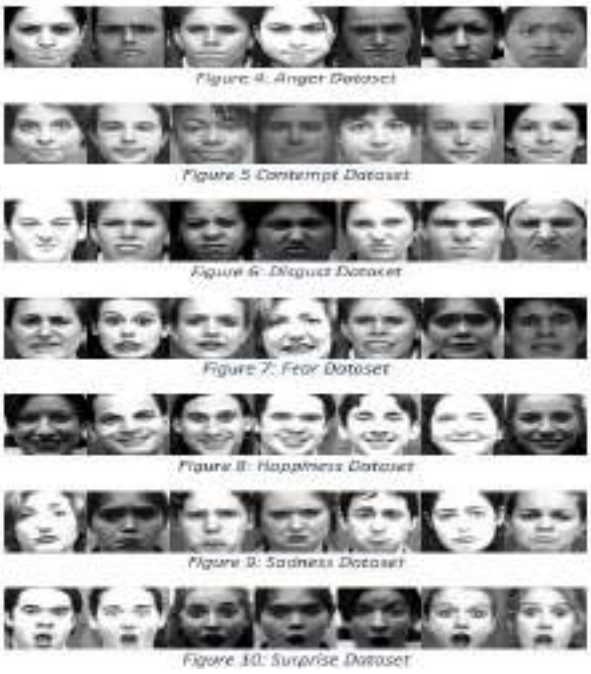

2.5 VGG-19:

A significant convolutional neural framework in Deep learning is a class of significant, feed-forward significant acknowledging which have been applied precisely to visual imaging assessment. Stood out from various other picture portrayal counts, the VGG19 model uses reasonably minimal pre-preparing. It is viewed as one of the incredible vision model architecture till date. The most special thing about VGG19 is that as opposed to having countless hyper-parameter they zeroed in on having convolution layers of 3x3 filter with a stride 1 and consistently utilized a similar cushioning and max pool layer of 2x2 filter of stride 2. It follows this game plan of convolution and max pool layers reliably all through the entire architecture. Eventually, it has 2 FC (fully connected layers) trailed by a SoftMax for yield. The 16 in VGG19 alludes to it has 16 layers that have loads. This network is a pretty enormous network and it has around 138 million (approx.) parameters.

2.6 Relu:

The activation Function is a unit (neuron) is a fundamental piece of Artificial Neural Network architecture. The utilization of various algorithms has been utilized by analysts since ANN's initial days. the progression function was presented as the initiation function. Be that as it may, the binary idea of the progression function doesn't permit to have a decent blunder estimate. To beat the present circumstance, sigmoid functions were used. They gave generally excellent execution to little networks.

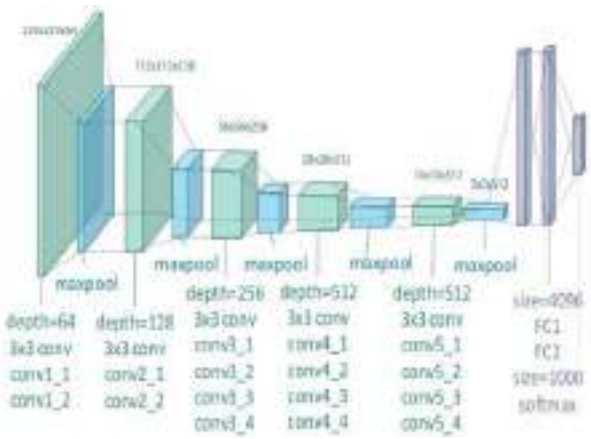

Fig. 2. VGG-19 Model

However, utilizing the sigmoid function demonstrated not very adaptable on enormous networks [11]. The computational expense of the outstanding activity may be truly costly since it can prompt long numbers. The other function instead of utilising the sigmoid function which is the inclination evaporating issue. This implies that the slope an incentive on the bend tails turns out to be too little that it forestalls learning. Under this situation, the corrected straight unit function (ReLU) if benefits contrasted with past regular enactment functions: its computational expense was less expensive, it gave a decent mistake guess and it didn't experience the ill effects of the angle disappearing issue. ReLU is shown on Figure-12, and it is characterized as

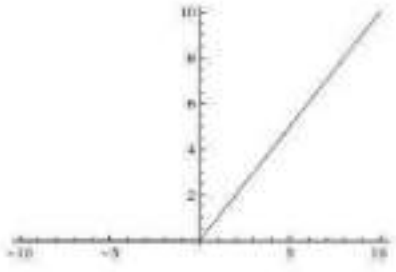

Figure 3: ReLU

$$f(x) = \max(0, x)$$

The research done by Mr. Krizhevsky et al. [11] indicates that utilizing ReLU diminished the quantity of ages needed to meet when utilizing SGD divided by factor- 6. Be that as it may, a significant downside when utilizing ReLU is its delicacy when the info dispersion is under nothing. This happens when the

neuron arrives at a moment that it won't be activated by any datapoint again during training.

3 Algorithm:

Step 1: Extracting dataset into folder (In this scenario we preferred properly modified, (1, 48, 48) pixel grayscale images of different expression faces labelled and copied to 7 folders.
Step 2: Pre-processing of images.
Step 3: Detection of a face from each image.
Step 4: The cropped face is converted into grayscale images.
Step 5: The pipeline ensures every image can be fed into the input layer as a (1, 48, 48) NumPy array.
Step 6: The NumPy array gets passed into the Convolution 2D layer.
Step 7: For face detection, inbuilt methods available in dlib library are used. Once the face is detected, the region of interest and important facial features are extracted from it
Step 8: Convolution generates feature maps.
Step 9: Pooling method called MaxPooling2D that uses (2, 2) windows across the feature map only keeping the maximum pixel value.
Step10: During training, Neural network Forward propagation and backward propagation performed on the pixel values.
Step 11: The SoftMax function presents itself as a probability for each emotion class. The model is able to show the detail probability composition of the emotions in the face.

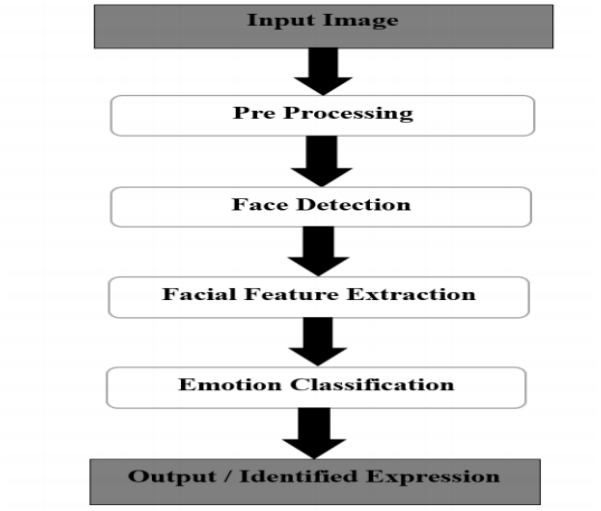

Fig. 4. Process flowchart

4 Proposed Model:

The dataset has a single emotions labelled for each image in a particular folder and doesn't have a connection to each folder. This presents a lot of upheaval if the image names are used as spotlights on setting up a VGG-19 on the solitary picture. Our visual features are in this manner given by a CNN arranged on a blend of two additional feeling datasets of static pictures. For the CNN preparing, we utilized an enormous feeling dataset, Cohn-Kanade Facial Expression Dataset. It comprises of in excess of 2900 pictures of 75 subjects and "Different guys and female Facial Expression Dataset containing 213 pictures, which have seven fundamental articulations: outrage, hatred, appall, dread, satisfaction, pity, and shock. For the pre-handling, we address fluctuating lighting conditions (explicitly, transversely over datasets) we associated histogram evening out. We used the changed appearances gave by the co-ordinators to eliminate features from the CNN. "The course of action incorporates a joined facial central issue's area and the accompanying system explained. Exceptional face area, just as plan methods, have been used for the COHN-KANADE Datasets". Remembering the ultimate objective to be prepared to utilize the extra datasets, we re-changed all datasets to COHN-KANADE using the going with strategy:

1. We recognized seven facial key concentrations for all photos in the COHN-KANADE and setting up a set using the convolutional neural framework course technique.

2. For each dataset, the mean shape has been handled by averaging the bearings of the principle centers.

Fig. 5. VGG19 Pre-trained model

3. The datasets are planned by employing a closeness modification among the mean shapes. By handling one modification for every dataset the nose, eyes, and mouth ar by and enormous in a very comparative region holding a small proportion of assortment. we tend to incorporated a loud outer boundary for and COHN-KANADE-faces as appearances were altered even additional immovably diverged from COHN-KANADE.

4. COHN-KANADE-data validation check sets were mapped to use for the amendment understood on the coaching set. what is more, dataset standardization has been performed by utilizing the quality deviation and mean image from the incorporate Cohn-Kanade addresses the example's face feeling data. For the execution and therefore the assessment of the planned model the seventieth of every dataset used for making ready and therefore the rest half-hour for testing.

After splitting the training data and testing data we took a pre-trained VGG19 CNN model along with ImageNet weights to train the data. The model summary which is shown in figure-14 below. After the model summary we have added the extra layers on top of the model to train the images. In this experiment the model is a pretrained one so if we train the whole model again, the model might overfit or underfit which makes the model very uncertain. So, instead of using the whole model to train again we are adding other layers on top of the VGG19 model instead of disturbing it. So, we added the extra layers and taken all the parameters or neurons into a single vector in other words we call it as flatten layer. After taking it into a single vector we added the dense layer and dropout layer on top of it which is fully convoluted. We trained the dense and dropout layers using ReLU activation and for final layer we have used Softmax function because it is a Multi class classification. we can see the VGG19 model model summary in the below figure-15.

Fig. 6. Model Summary of other layers along with pretrained model

To compile the model, we have used the ADAM optimizer which implements gradient descent algorithm which is an optimizer used for adjusting the weights of the model which checks also improves the accuracy by making it into optimum state. We have set the hyper parameter for loss function as categorical class entropy as it is a multi-class classification. Using model. Fit, we have initiated the training and the hyper-parameters are set as batch size as 64 and epochs as 20 to pass the whole data set it for twenty iterations. As we preferred to this experiment using the Keras model,

it does a cross validation to see how accurately the model is been trained. The trained model accuracy has shown in figure-16.

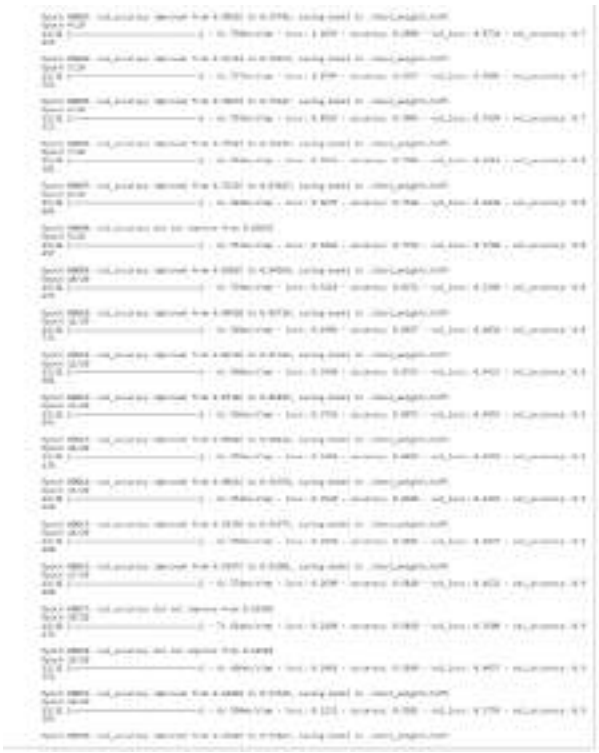

Fig. 7. Trained model.

In the above figure- 16 we have achieved a very good accuracy for facial detection which is 94%. As it is a static methodology utilizing removed highlights and emotion recognition utilizing profound learning is utilized in this work. Our execution is isolated into three sections. The initial segment is picture pre-handling and face recognition. For face discovery, inbuilt strategies accessible in dlib library are utilized. When the face is recognized, the district of interest and significant facial highlights are extricated from it. There are different highlights which can be utilized for feeling location.

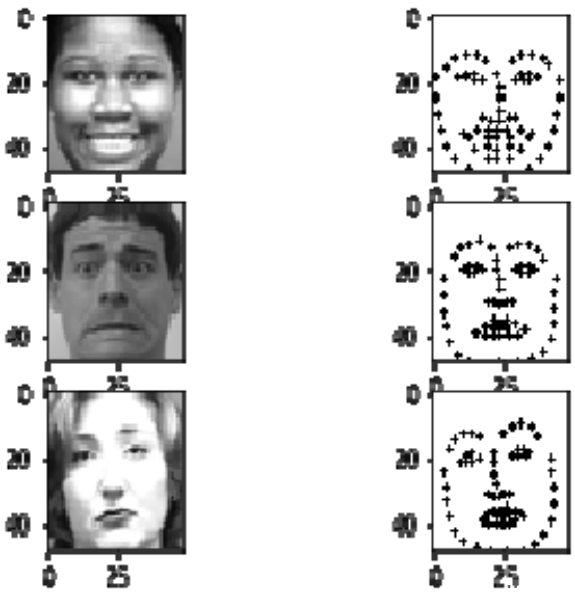

Fig. 8. Land marking images

In this work, the attention is on facial focuses around the eyes, mouth, eyebrows and so forth We have a multi-class order issue and not multi-mark. There is an inconspicuous distinction as a bunch of highlights can have a place with numerous names however just a single one-of-a-kind class. The removed facial highlights alongside VGG19 are utilized to distinguish the multi-class feelings once more. We can find out the VGG19 model which is shown in Figure-18 below which is trained on parsed or land marking images.

```
Epoch 1/20
11/11 [==============================] - 6s 569ms/step - loss: 1.8220 - accuracy: 0.2664 - val_loss: 1.6275 - val_accuracy: 0.4
660

Epoch 00001: val_accuracy did not improve from 0.93827
Epoch 2/20
11/11 [==============================] - 7s 616ms/step - loss: 1.5578 - accuracy: 0.4003 - val_loss: 1.4129 - val_accuracy: 0.4
753

Epoch 00002: val_accuracy did not improve from 0.93827
Epoch 3/20
11/11 [==============================] - 7s 681ms/step - loss: 1.3294 - accuracy: 0.5114 - val_loss: 1.2346 - val_accuracy: 0.5
340

Epoch 00003: val_accuracy did not improve from 0.93827
Epoch 4/20
11/11 [==============================] - 7s 634ms/step - loss: 1.2040 - accuracy: 0.5616 - val_loss: 1.1677 - val_accuracy: 0.5
309

Epoch 00004: val_accuracy did not improve from 0.93827
Epoch 5/20
11/11 [==============================] - 7s 633ms/step - loss: 1.1279 - accuracy: 0.5982 - val_loss: 1.0672 - val_accuracy: 0.5
957

Epoch 00005: val_accuracy did not improve from 0.93827
Epoch 6/20
11/11 [==============================] - 7s 626ms/step - loss: 1.0615 - accuracy: 0.6195 - val_loss: 1.0117 - val_accuracy: 0.6
451

Epoch 00006: val_accuracy did not improve from 0.93827
Epoch 7/20
11/11 [==============================] - 6s 582ms/step - loss: 1.0116 - accuracy: 0.6225 - val_loss: 1.0534 - val_accuracy: 0.5
802

Epoch 00007: val_accuracy did not improve from 0.93827
Epoch 8/20
11/11 [==============================] - 6s 593ms/step - loss: 0.9979 - accuracy: 0.6317 - val_loss: 0.9945 - val_accuracy: 0.5
741

Epoch 00008: val_accuracy did not improve from 0.93827
Epoch 9/20
11/11 [==============================] - 6s 583ms/step - loss: 0.9326 - accuracy: 0.6301 - val_loss: 0.9770 - val_accuracy: 0.6
019

Epoch 00009: val_accuracy did not improve from 0.93827
Epoch 10/20
11/11 [==============================] - 6s 600ms/step - loss: 0.8981 - accuracy: 0.6651 - val_loss: 0.8818 - val_accuracy: 0.6
420

Epoch 00010: val_accuracy did not improve from 0.93827
Epoch 00010: early stopping
```

Fig. 9. Trained model on parsed images

5 Results:

As a part of analysis for facial expression classification using face parsing method is presented in this thesis. We have proposed a new deep CNN architecture for facial expression identification. It takes facial images as the input and classifies them into either of the seven facial expressions: angry, disgust, happy, neutral, sad and surprise. We have tried this model achieved 94% of accuracy with the loss of 22% while detecting the faces and we have achieved 66.51% of model accuracy on parsed images. The comparison graph of accuracy is shown below.

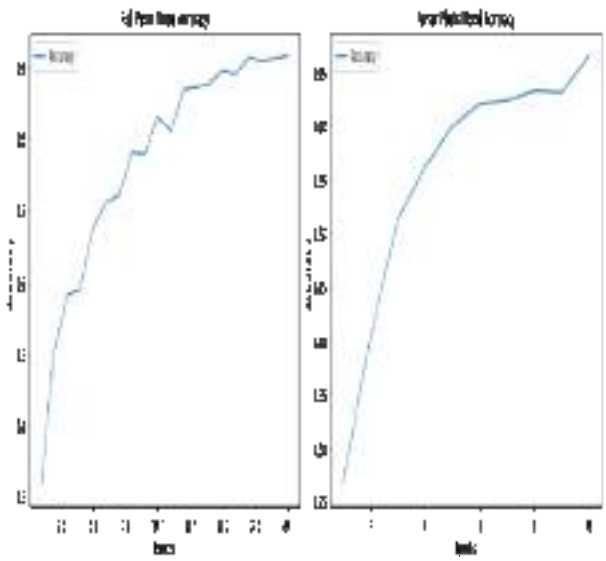

Fig. 10. Accuracy graph

7 Conclusion:

Results and acknowledgment rates demonstrate that our technique outperformed the cutting-edge strategies. For this task, we prepared the model with pictures in which the face was in a single position. In future work, we might want to stretch out our model to various face positions. This will permit us to examine the viability of pre-trained models like VGGNet for facial emotion Identification.

References

1. Y. Lv, Z. Feng, and C. Xu, 2014 International Conference on Smart Computing (2014)
2. W. Swinkels, L. Claesen, F. Xiao, and H. Shen, in *2017 IEEE Conference on Dependable and Secure Computing* (2017), pp. 86–92
3. A. C. L. Ngo, A. C. Le Ngo, Y.-H. Oh, R. C.-W. Phan, and J. See, 2016 IEEE International Conference on Acoustics, Speech and Signal Processing (ICASSP) (2016)
4. K. M. Rajesh and M. Naveenkumar, in *2016 International Conference on Electrical, Electronics, Communication, Computer and Optimization Techniques (ICEECCOT)* (2016), pp. 1–5
5. H. Ebine, Y. Shiga, M. Ikeda, and O. Nakamura, in *2000 Canadian Conference on Electrical and Computer Engineering. Conference Proceedings. Navigating to a New Era (Cat. No.00TH8492)* (2000), pp. 1091–1099 vol.2
6. Rosalind W. Picard, *Affective computing: challenges*, International Journal of Human-

Computer Studies,**Volume 59**, Issues 1–2, (2003) ,Pages 55-64,ISSN 1071-5819
7. R. W. Levenson, P. Ekman, and W. V. Friesen, Psychophysiology **27**, 363 (1990)
8. I. A. Essa, (1995)
9. Pentland, Alex & Benton, Stephen & Essa, Irfan. (1998)
10. J. P. Mueller and L. Massaron, *Machine Learning For Dummies* (John Wiley & Sons, 2021)
11. J. P. Mueller and L. Massaron, *Artificial Intelligence For Dummies* (John Wiley & Sons, 2018)
12. A. Krizhevsky, I. Sutskever, and G. E. Hinton, Commun. ACM **60**, 84 (2017)
13. S. C. Tai and K. C. Chung, TENCON 2007 - 2007 IEEE Region 10 Conference (2007)
14. M. Lyons, S. Akamatsu, and M. Kamachi, Proceedings Third IEEE (1998)
15. M. Suk and B. Prabhakaran, Proceedings of the IEEE Conference on (2014)
16. D. Ghimire and J. Lee, Sensors **13**, 7714 (2013)
17. T. R. Reddy, B. V. Vardhan, and P. V. Reddy, International Journal of Applied Engineering Research **11**, 3092 (2016)
18. P. Kumar, A. Singhal, S. Mehta, and A. Mittal, Journal of Real-Time Image Processing **11**, 93 (2016)
19. G. Mahalle, O. Salunke, N. Kotkunde, A. K. Gupta, and S. K. Singh, Journal of Materials Research and Technology **8**, 2130 (2019)
20. S. Kumar, P. Reddy, G. Ramesh, and V. Maddumala, Trait. Du Signal **36**, 233 (2019)
21. B. Dhanalaxmi, G. A. Naidu, and K. Anuradha, Procedia Comput. Sci. **46**, 432 (2015)
22. M. Avanthi and P. Chandra Sekhar Reddy, in *Smart Computing Techniques and Applications* (Springer Singapore, 2021), pp. 193–199
23. P. Chandra Sekhar Reddy, P. Vara Prasad Rao, P. Kiran Kumar Reddy, and M. Sridhar, in *Soft Computing and Signal Processing* (Springer Singapore, 2019), pp. 273–280
24. P. C. S. Reddy, S. G. Rao, G. R. Sakthidharan, and P. V. Rao, in *2018 International Conference on Smart Systems and Inventive Technology (ICSSIT)* (2018), pp. 104–109
25. P. Chandra Sekhar Reddy, P. Vara Prasad Rao, P. Kiran Kumar Reddy, and M. Sridhar, in *Soft Computing and Signal Processing* (Springer Singapore, 2019), pp. 273–280

Human Facial Expression Recognition Using Fusion of DRLDP and DCT Features

M. Avanthi and P. Chandra Sekhar Reddy

Abstract Recognition of facial expressions is a major challenge in the field of computer vision. Using single-function models, the level of acknowledgment even in controlled capture conditions is considerably small. This paper proposed a method for facial emotion classification with the fusion of dimensionality reduced local directional pattern and discrete cosine transform features using SVM classifier. Local characteristics are extracted utilizing DRLDP, and global characteristics are extracted from facial expression images using DCT. SVM is used to classify the face images into six emotions (surprise, smile, sad, anger, fear and disgust). This method is experimented on JAFFE database and compared with existing approaches shows higher classification rate.

1 Introduction

Facial expression recognition plays an important role in computer vision-based applications like human–computer interaction, video interaction, cataloging, biometrics, including image recovery, with security, etc. Facial expression was its adjustments in the face in support of the inner emotional states as well as intentions of an individual person. Emotion is a familiar word used at a given moment for a person's feelings like surprise, smile, sad, anger, fear and disgust. Generally, emotions are identified with very little attempt of the human intelligence. Facial emotions machine identification and classification are cumbersome to realize people's feelings. An algorithmic methodology of classification is used for the labeling in one of the predefined sequences of provided input data. A classification algorithm is a template which executes the input data category.

One is the geometric methods of extraction based on features, while the other is the technique for extraction of features based on appearance. Geometric characteristic methods [1] derive the position but structure of facial components includes nose, eyes, mouth but eyebrows. The remaining part of the paper is organized as follows.

M. Avanthi (✉) · P. Chandra Sekhar Reddy
CSE Department, GRIET, Hyderabad, Telangana, India

S. C. Satapathy et al. (eds.), *Smart Computing Techniques and Applications*,
Smart Innovation, Systems and Technologies 224,
https://doi.org/10.1007/978-981-16-1502-3_20

Section 2 proposed the methodology adopted; experimental results are given in Sect. 3 and conclusion in Sect. 4.

2 Methodology

After acquisition, the next sequence is to extract the information from input data, attributes such as eyes, nose, cheek, mouth, in case of geometric feature-based technique. Two main methods are used for the production of facial expressions (Fig. 1).

2.1 Local Directional Pattern

The local directional pattern is an 8-bit code representing edge responsiveness value. Kirsch masks ($M0$, …, $M7$) shown in Fig. 2 are used to find edge response value in eight directions. LDP is computed considering only three prominent edge responses.

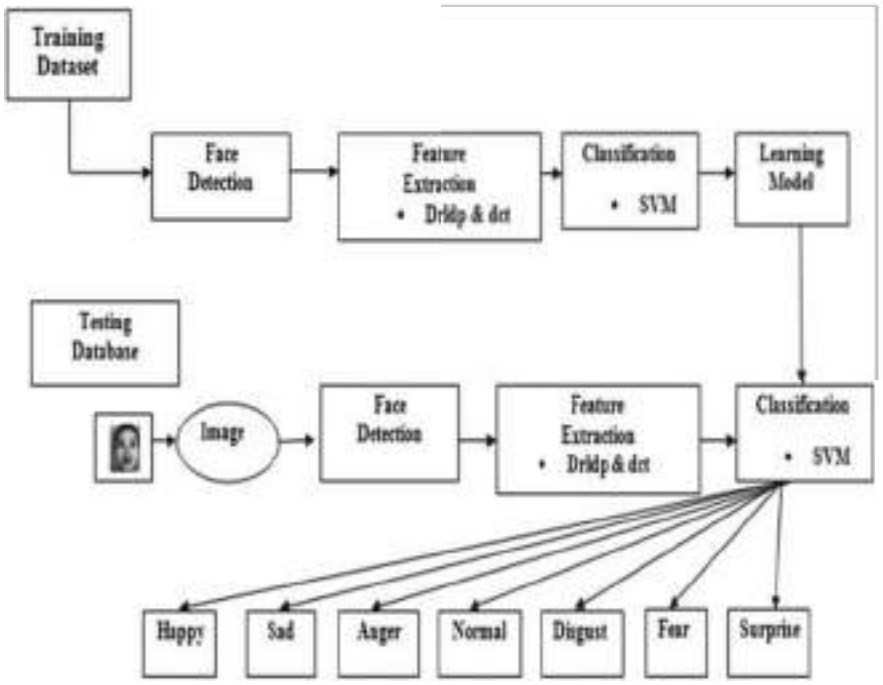

Fig. 1 Architecture of facial expression

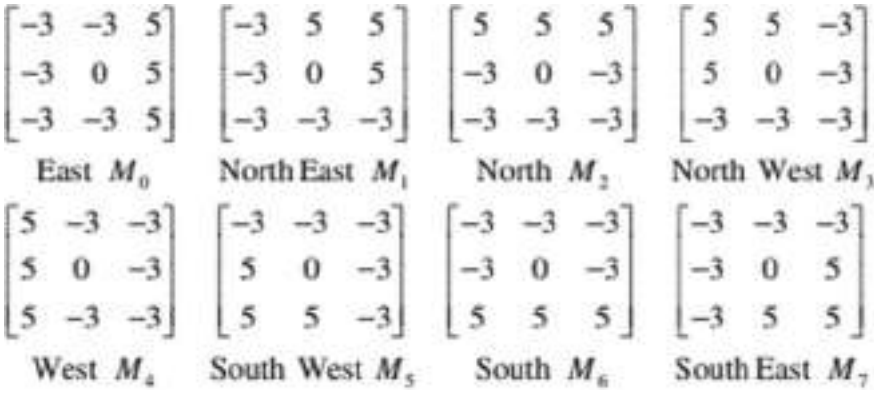

Fig. 2 Edge response masks of Kirsch in eight directions

2.2 Facial Expression Recognition Using DRLDP

In this, human face reorganization method is shown in Fig. 3. The input images are preprocessed to decrease the noise, lighting recompense plus resizing. Then DCT is utilized to extract the feature vector. DRLDP [2] is utilized to diminish the measurements of extracted features. Features be particular as input to SVM classifier pro training the model. Then knowledge information base is updated. SVM classifies the test image into six different expressions such as shock, fear, sadness, joyfulness, vexation and disgust.

2.2.1 Dimensionality Reduced Neighborhood Directional Examples

The suggested size reduced neighborhood positional example (DRLDP) is an eight-piece code assigned to each size three to three sub-districts. That software speaks to the square's textural instance. LDP is a single eight-piece code by each 18 a 3/3 square pixel. Both for square, the suggested DRLDP estimates a single eight-piece script. Models such as that of LDP are the suggested DRLDP statistics; however, differences arise in view of the fact which post handling of LDP design elements acquired for a square reduces the illustrations to a solitary eight-piece code.

For example, believe a picture I of size $A \times B$. Let $p = A/t$, and $q = B/u$.

For the picture I, the number of sub-images shaped is $= A \times B\ t \times u \equiv p \times q$.

The size of every sub-picture is $ai = A/p \times B/q \equiv A \times B/a$ pixels. We describe the RR as the ratio of the no. of pixels in the input picture mapped onto the no. of pixels in the reduced image.

$$\text{Redundancy Ratio(RR)} = \frac{\text{No. of pixel in the input image}}{\text{No. of pixel in reduced image}}$$

Fig. 3 Detected features

$$\text{For an image } I, \text{RR} = \frac{A \times B}{\frac{A \cdot B}{p \times q}} = p \times q = a$$

On the basis of two parameters t and u, the generalized DRLDP is supported. The general practice is to describe filters of size $n \times n$, i.e., a square mask. Therefore, it is unspecified that t plus u are equal.

2.3 Discrete Cosine Transformation

Two-dimensional DCT is used mainly to exclude the worldwide highlights from the exterior presence studies. The full face image is provided as a submission to DCT.

From the start, the image is divided into sub-image squares (8×8), and then subsequently discrete cosine transformation is used to extract the coefficients from each square. DCT produces one coefficient of DC as well as sixty-three coefficients were also dissimilar by each sub-square. Appropriately, it is registered again from above, and it left coefficients. Every sub-squares separated coefficients include ordinary vitality including recurrence information of under-square picture variety. Additionally, the upper as well as left sub-square districts speak to the information on the edge as well as directional substrate.

2.4 Support Vector Machine

Support vector machine—similarly, it is a convincing AI technique or data characterization process; it introduces knowledge visualization into an elevated directional element space, as well as later finds a straight separation of the hyperplane some of the most extreme edges to differentiate data in the specified higher-dimensional space. SVM makes parallel choices, because of that multi-class grouping is capable, and this method teaches double classifiers to split one articulation as a whole, but also produces the largest yield of dual scheme class.

2.5 Classification

For instance, upbeat, shock, outrage, tragic, dread, appall and unbiased will be used for intonation orders, and so on, and multi-class SVM is obtained. Seven categories are used for characterizing knowledge here. SVM is used for the conversion of Gabor highlights into vector structure. At the stage where the photo is provided as details again for test, Gabor is rendered on the direction of such an image, but instead transformed into a vector afterward. The information is isolated in two sections in SVM—training set and testing set, each involving the outline of the property. Each model is containing one objective method class name and a few traits.

2.6 Fusion

By suggesting a detailed design clustering technique, the component vectors disentangled from either the input images are entangled. Straight, presently, permutation combination strategy is 20 used to intertwine the component vectors through using DCT as well as DRLDP, which have been removed again from data images. A mixture is used to enhance precision, increase efficiency and extend the power of the frame. Currently, combination schemes for summation as well as PCA are being used to

intertwine the neighborhood as well as the worldwide illustrates extracted from facial images.

3 Experiments and Results

See Figs. 3 and 4.
See Figs. 5 and 6.
See Fig. 7.

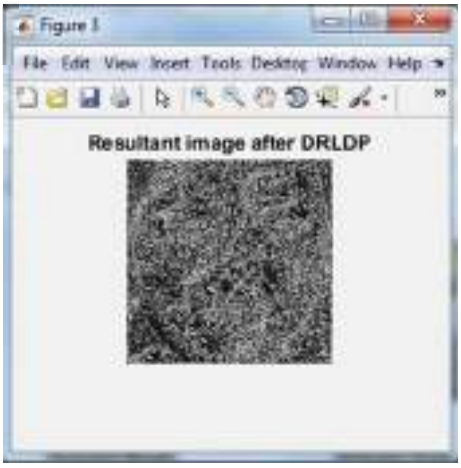

Fig. 4 Result of the DRLDP

Fig. 5 Accuracy of the input image

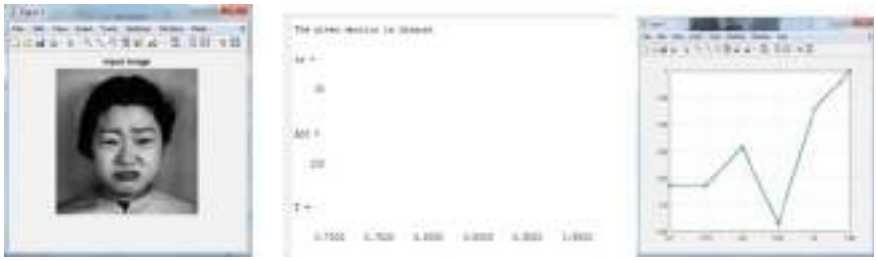

Fig. 6 Accuracy of the Input Image

Facial expression recognition results with DRLDP

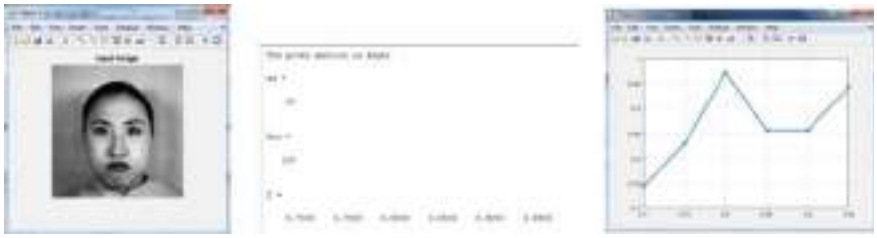

Fig. 7 Accuracy of the input image

4 Conclusion and Future Scope

The need for identification of facial expressions is rising rapidly. This approach is based on the combination of local and global significant features. This paper proposed a method for facial emotion classification with the fusion of dimensionality reduced local directional pattern and discrete cosine transform features using SVM classifier. Local characteristics are extracted utilizing DRLDP, and global characteristics are extracted from facial expression images using DCT. These features with SVM have classified considered database images for emotions with higher classification rate.

Reference

1. H.-B. Deng, L.-W. Jin, L. Zhen and J. C. Huang, A New Facial Expression Recognition Method Based on Local Gabor Filter bank and PCA plus LDA International journal of Information Technology, vol. 11, (2005).
2. R. S.P., P.V.S.S.R. C.M.,Dimensionality reduced local directional pattern (DRLDP) for face recognition, *Expert Systems with Applications*, (2016) 63 , pp. 66–73.

Smart Intelligent Computing and Applications, Volume 1 pp 225–238

A Flexible Accession on Brain Tumour Detection and Classification Using VGG16 Model

V. Ramya Manaswi & B. Sankarababu

Conference paper | First Online: 19 April 2022

Part of the Smart Innovation, Systems and Technologies book series (SIST,volume 282)

Abstract

To get a successful and appropriate treatment for a health disorder, a precise and early diagnosis is much important when it comes to brain tumour treatment. Knowing about the tumour and detecting it beforehand increases the chance of coping up with good medication and saving lives at the right time. Neurooncologists benefit greatly from biomedical informatics and computer-aided diagnosis (CAD). As a result of ML algorithms, it has now become possible to process medical images using algorithms instead of manually diagnosing

brain tumours. When compared with manual traditional practices, compared to traditional methods, computer-assisted mechanisms yield better results. In this, computer-aided mechanism is handled by feature extraction using convolutional neural network (CNN) model and fully connected neural network (FCNN) for classification. In this paper, we are proposing the approach using DNN and CNN architectures to create model to detect and classify the MRI images as “TUMOUR DETECTED” or “TUMOUR NOT DETECTED.” This model is proposed to have maximum mean accuracy score and f-score.

Keywords

Cerebrospinal liquid (CSL)

Convolutional neural network (CNN)

Brain tumour segmentation (BTS)

Image segmentation (IS) **VGG16 model**

References

1. Siar M, Teshnehlab M (2019) Brain tumour detection using deep neural network and machine learning algorithm. In: 2019 9th international conference on computer and knowledge engineering (ICCKE), 2019, pp 363–368. https://doi.org/10.1109/ICCKE48569.2019.8964846

2. Hossain T, Shishir FS, Ashraf M, Al Nasim MA, Muhammad Shah F (2019) Brain tumour detection using convolutional neural network. In: 2019 1st international conference on advances in science, engineering and robotics technology (ICASERT), pp 1–6

3. Hemanth G, Janardhan M, Sujihelen L (2019) Design and implementing brain tumour detection using machine learning approach. In: 2019 3rd international conference on trends in electronics and informatics (ICOEI), 2019, pp 1289–1294. https://doi.org/10.1109/ICOEI.2019.88

4. Gore DV, Deshpande V (2020) Comparative study of various techniques using deep learning for brain tumour detection. In: 2020 International conference for emerging technology (INCET), pp 1–4. https://doi.org/10.1109/INCET49848.2020.9154030

5. Somasundaram S, Gobinath R (2019) Current trends on deep learning models for brain tumour segmentation and detection—a review. In: 2019 International conference on machine learning, big data, cloud and parallel computing (COMITCon), pp 217–221

6. Asodekar BH, Gore SA, Thakare AD (2019) Brain tumour analysis based on shape features of MRI using machine learning. In: 2019 5th international conference on computing, communication, control and automation (ICCUBEA), pp 1–5. https://doi.org/10.1109/ICCUBE

7. Madhupriya G, Guru NM, Praveen S, Nivetha B (2019) Brain tumour segmentation with deep learning technique. In: 2019 3rd international conference on trends in electronics and informatics (ICOEI), pp 758–763. https://doi.org/10.1109/ICOEI.2019.8862575

8. Abbas K, Khan PW, Ahmed KT, Song W-C (2019)

Automatic brain tumor detection in medical imaging using machine learning. In: 2019 International conference on information and communication technology convergence (ICTC), pp 531–536. https://doi.org/10.1109/ICTC46691.2019.8939748

9. Jia Z, Chen D (2020) Brain tumor identification and classification of MRI images using deep learning techniques. IEEE Access. https://doi.org/10.1109/ACCESS.2020.3016319

10. Sobhaninia Z, Rezaei S, Noroozi A, Ahmadi M, Zarrabi H, Karimi N, Emami A, Samavi S (2018) Brain tumour segmentation using deep learning by type specific sorting of images

Author information

Authors and Affiliations

Gokaraju Rangaraju Institute of Engineering and Technology, Hyderabad, India

V. Ramya Manaswi & B. Sankarababu

Editor information

Editors and Affiliations

Department of Electronics and Communication Engineering, Shri Ramswaroop Memorial Group

of Professional Colleges (SRMGPC), Lucknow, Uttar Pradesh, India

Dr. Vikrant Bhateja

School of Computer Engineering, Kalinga Institute of Industrial Technology (KIIT), Bhubaneswar, Odisha, India

Dr. Suresh Chandra Satapathy

Signals and Communications Department, University of Las Palmas de Gran Canaria, Las Palmas de Gran Canaria, Spain

Prof. Dr. Carlos M. Travieso-Gonzalez

Department of Computer Science and Engineering, Vasvi College of Engineering, Hyderabad, Telangana, India

Dr. T. Adilakshmi

Rights and permissions

Copyright information

About this paper

Cite this paper

Ramya Manaswi, V., Sankarababu, B. (2022). A Flexible Accession on Brain Tumour Detection and Classification Using VGG16 Model. In: Bhateja, V., Satapathy, S.C., Travieso-Gonzalez, C.M., Adilakshmi, T. (eds) Smart

Intelligent Computing and Applications, Volume 1. Smart Innovation, Systems and Technologies, vol 282. Springer, Singapore. https://doi.org/10.1007/978-981-16-9669-5_21

DOI
https://doi.org/10.1007/978-981-16-9669-5_21

Published	Publisher Name	Print ISBN
19 April 2022	Springer, Singapore	978-981-16-9668-8

Online ISBN	eBook Packages
978-981-16-9669-5	Intelligent Technologies and Robotics Intelligent Technologies and Robotics (R0)

Prediction of Agriculture Yields Using Machine Learning Algorithms

Proceedings of the 2nd International Conference on Recent Trends in Machine Learning, IoT, Smart Cities and Applications
pp 17-26 | Cite as

Conference paper

First Online: 01 January 2022

Part of the Lecture Notes in Networks and Systems book series (LNNS, volume 237)

Abstract

In recent years, great efforts have been carried out on the challenging task of predicting different crop yields. Developing exact models for crop yield estimation utilizing Information and Communication Technologies may support farmers and different stakeholders to improve decision making about national food import/export and food security. Most of the crops are selected based on the economic range. In our proposed work also we have consider the economical crops and they provide better prediction compared with the existing classifiers. The proposed ensemble classifier provides an efficient crop yield and crop disease forecasting model. Our proposed work provides knowledge to the farmers about the climatic conditions of the probability of crop disease and the climatic conditions for better crop yield. Even it discovers the crop yield and crop diseases, but does not concentrate on

the solution to solve the productivity issue caused by crop diseases. Further, our future work concentrates on the above issue with different algorithms.

Keywords

Agriculture Crop prediction Regression
Random forest algorithm

References

1. Brewster C, Roussaki I, Ellis K, Doolin K, Kalatzis N (2017) IoT in agriculture: designing a Europe-wide large-scale pilot. IEEE Commun Mag 22(7)
Google Scholar (https://scholar.google.com/scholar?q=Brewster%20C%2C%20Roussaki%20I%2C%20Ellis%20K%2C%20Doolin%20K%2C%20Kalatzis%20N%20%282017%29%20IoT%20in%20agriculture%3A%20designing%20a%20Europe-wide%20large-scale%20pilot.%20IEEE%20Commun%20Mag%2022%287%29)
2. Kumar A, Sarkar S, Pradhan C (2019) Recommendation system for crop identification and pest control technique in agriculture. In: IEEE international conference on communication and signal processing, vol 37, pp 0185–0189
Google Scholar (https://scholar.google.com/scholar?q=Kumar%20A%2C%20Sarkar%20S%2C%20Pradhan%20C%20%282019%29%20Recommendation%20system%20for%20crop%20identification%20and%20pest%20control%20technique%20in%20agriculture.%20In%3A%20IEEE%20international%20conference%20on%20communication%20and%20signal%20processing%2C%20vol%2037%2C%20pp%200185%E2%80%930189)
3. Michelson DG, Hamdi M, Abouzar P (2016) RSSI-based distributed self localization for wireless sensor network used in precision agriculture. IEEE Trans Wireless Commun 15(10):125–131
Google Scholar (https://scholar.google.com/scholar?q=Michelson%20DG%2C%20Hamdi%20M%2C%20Abouzar%20P%20%282016%29%20RSSI-

based%20distributed%20self%20localization%20for%20wireless%20sensor%20network%20used%20in%20precision%20agriculture.%20IEEE%20Trans%20Wireless%20Commun%2015%2810%29%3A125%E2%80%93131)

4. Dutta R, Morshed A, Aryal J, D'Este C, Das, Aruneema (2016) Development of an intelligent environmental knowledge system for sustainable agricultural decision support. Res Gate Environ Model Softw 52:264–272
Google Scholar (https://scholar.google.com/scholar?q=Dutta%20R%2C%20Morshed%20A%2C%20Aryal%20J%2C%20D%27Este%20C%2C%20Das%2C%20Aruneema%20%282016%29%20Development%20of%20an%20intelligent%20environmental%20knowledge%20system%20for%20sustainable%20agricultural%20decision%20support.%20Res%20Gate%20Environ%20Model%20Softw%2052%3A264%E2%80%93272)
5. Tseng F-H, Cho H-H, Wu H-T (2019) Applying big data for intelligent agriculture-based crop selection analysis. IEEE Access 7
Google Scholar (https://scholar.google.com/scholar?q=Tseng%20F-H%2C%20Cho%20H-H%2C%20Wu%20H-T%20%282019%29%20Applying%20big%20data%20for%20intelligent%20agriculture-based%20crop%20selection%20analysis.%20IEEE%20Access%207)
6. Viani F, Bertolli M, Salucci M, Polo A (2017) Lowcost wireless monitoring and decision support for water saving in agriculture. IEEE Sens J 99:1–1
Google Scholar (http://scholar.google.com/scholar_lookup?title=Lowcost%20wireless%20monitoring%20and%20decision%20support%20for%20water%20saving%20in%20agriculture&author=F.%20Viani&author=M.%20Bertolli&author=M.%20Salucci&author=A.%20Polo&journal=IEEE%20Sens%20J&volume=99&pages=1-1&publication_year=2017)
7. Narvaez FY, Reina G, Torres M (2017) A survey of ranging and imaging techniques for precision agriculture phenotyping. IEEE/ASME Trans Mechatron 22(6):2428–2439
Google Scholar (https://scholar.google.com/scholar?q=Narvaez%20FY%2C%20Reina%20G%2C%20Torres%20M%20%282017%29%20A%20survey%20of%20ranging%20and%20imaging%20techniques%20for%20precision%20agriculture%20phenotyping.%20IEEE%2FASME%20Trans%20Mechatron%2022%286%29%3A2428%E2%80%932439)
8. Ravichandran G, Koteeshwari RS (2016) Agricultural crop predictor and advisor using ANN for smartphones. In: IEEE international conference on emerging trends in engineering, technology and science, vol 45, pp 138–145

Google Scholar (https://scholar.google.com/scholar?q=Ravichandran%20G%2C%20Koteeshwari%20RS%20%282016%29%20Agricultural%20crop%20predictor%20and%20advisor%20using%20ANN%20for%20smartphones.%20In%3A%20IEEE%20international%20conference%20on%20emerging%20trends%20in%20engineering%2C%20technology%20and%20science%2C%20vol%2045%2C%20pp%20138%E2%80%93145)

9. Ali I, Zakarya M, Khan R (2018) Technology-assisted decision support system for efficient water utilization: a real-time testbed for irrigation using wireless sensor networks. IEEE Access 6(6):2342–2350
Google Scholar (http://scholar.google.com/scholar_lookup?title=Technology-assisted%20decision%20support%20system%20for%20efficient%20water%20utilization%3A%20a%20real-time%20testbed%20for%20irrigation%20using%20wireless%20sensor%20networks&author=I.%20Ali&author=M.%20Zakarya&author=R.%20Khan&journal=IEEE%20Access&volume=6&issue=6&pages=2342-2350&publication_year=2018)

Copyright information

About this paper

Cite this paper as:
Gunjan V.K., Kumar S., Ansari M.D., Vijayalata Y. (2022) Prediction of Agriculture Yields Using Machine Learning Algorithms. In: Gunjan V.K., Zurada J.M. (eds) Proceedings of the 2nd International Conference on Recent Trends in Machine Learning, IoT, Smart Cities and Applications. Lecture Notes in Networks and Systems, vol 237. Springer, Singapore. https://doi.org/10.1007/978-981-16-6407-6_2

First Online

01 January 2022

DOI

https://doi.org/10.1007/978-981-16-6407-6_2

Publisher Name

Springer, Singapore

Print ISBN

978-981-16-6406-9

Online ISBN

978-981-16-6407-6

eBook Packages

Intelligent Technologies and Robotics
Intelligent Technologies and Robotics (R0)

2022 International Conference for Advancement in Technology (ICONAT)
Goa, India. Jan 21-22, 2022

Smart Bot for Handwritten Digit String Recognition

Mallikarjuna Rao Gundavarapu
Computer Science Engineering
Gokaraju Rangaraju Institute of Engineering and Technology (Autonomous)
Hyderabad, India
gmr_333@yahoo.in

Vivek Vardhan Reddy Yannam
Computer Science Engineering
Gokaraju Rangaraju Institute of Engineering and Technology (Autonomous)
Hyderabad, India
reddyvivek569@gmail.com

Akash Velagala
Computer Science Engineering
Gokaraju Rangaraju Institute of Engineering and Technology (Autonomous)
Hyderabad, India
akash.velagala@gmail.com

Snehith Reddy Lankela
Computer Science Engineering
Gokaraju Rangaraju Institute of Engineering and Technology (Autonomous)
Hyderabad, India
snehithreddy.lankela999@gmail.com

Saaketh Koundinya G
Assosiate Consultant
SAP
Benguluru, India
three2saki@gmail.com

Sai Chandan Regonda
Computer Science Engineering
Gokaraju Rangaraju Institute of Engineering and Technology (Autonomous)
Hyderabad, India
saichandanregonda10@gmail.com

***Abstract*—Handwritten digit string recognition is more sophisticated than determining a single digit individually. The repeated recognition of single digits is applicable for recognizing a handwritten digit string. A similar approach is exercised in this paper. The proposed approach could be advantageous in banks to recognize the digits written on the cheque and processes the cheque. Further, the banks could send the audio message of the recognized handwritten digits to the cheque issuer for confirmation before cashing the cheque. The pro-posed model is developed in the python platform and is lightweight, robust, and cross-platform.**

In this approach, we have trained a neural network model with MNIST handwritten digits dataset and some samples of our own for recognizing the handwritten digits. The Convolution Neural network models are widely used in the present-day technologies for object recognition, image processing, segmentation, face recognizing and also many identifications related tasks. The CNN model used in the project determines the digit in the image provided. Finally, the system plays the [pre-]recorded audio and displays the output for the recognized digits in the given digit string.

Keywords—Handwritten string detection, Digit determination, Audio output, Image seg-mentation, Neural Networks

I. INTRODUCTION

Handwritten digit recognition has been a topic that interests many with both aca-demic interest and commercial interests. And many new and advanced approach-es relating to the recognition of handwritten digits using neural networks, multi-layer perceptron models, and other classification models are introduced in recent times. Handwritten digit string recognition, a subject falling into a similar category as handwritten digit recognition. Determining the symbol of handwritten digits is called handwritten digit recognition. Handwritten digit string recognition put forth results in various fields involving data entry, postal mail checking, bank cheque processing. Digit string recognition has been a complicated problem for many years but still evolving in respects including identifications of digits writ-ten in various styles and having various characteristics. The computer cannot interpret the digits that a human eye can identify and match them with their name in a split second. The eye transmits the signals related to the shape of the digits that a human is observing. And human brain receives those signals and maps the transmitted signal to the related digits. Such a phenomenon is used repeatedly for recognizing the digits of a handwritten digit string. Whereas the computer cannot recognize them due to lack of data about patterns and features of the individual digits. The methodology executed in this project is detecting the handwritten digits individually of a given digit string after segmentation. The application starts with prompting the user to provide an input image path. The image is further segmented and processed into the splits of individual digits. Both the seg-mentation and the input image processing are handled using the OpenCV library. The segmentation process begins after preprocessing the image. The preprocessing proceeds with changing the image format from color to binary format followed by denoising using non-local means denoising and edge identification using the Canny edge detection algorithm. The binary image is further processed into binary inverse for splitting the string into digits. The segmentation involves almost all the border pixels of the rectangle enclosing the as black. The width of the rectangle contours is taken to be minimum to decrease the noise intervention in segmented digits recognition. The size is increased afterwards by the same amount so that no part of the digit is lost. The segmented splits are then deter-mined based on the probability of matching features and thus simultaneously voicing out the detected digits audio. The recognition of individual digits uses a trained NN model with Adam optimizer of learning rate 0.01 and categorical cross entropy as loss function, consisting of CNN layers combined with Max-pooling layers and concluding the model with two dense layers having ten nodes in the last layer, on MNIST dataset and some other samples consisting of up to 60000(MNIST) training data samples up to an accuracy 99%. The pydub library is used to play the recorded audio of the respective digits using the play method from the playback module and AudioSegment class of pydub.

II. LITERATURE SURVEY

Handwritten digit recognition, character recognition, digit string recognition dates before the late 20th century. Humans tend to have different styles and write digits and characters in different shapes. This problem isn't as simple as recognizing digits for humans to machines. Humans have written and observed digits since their preschool age. Since those times human brain evaluates patterns and extract

features relating to respective digits from various digits. But whereas a machine is void of such a vast collection of data tending it to misstep using limited data samples. Even humans with a complex neural system have a hard time determining handwritten digits. It's no wonder machines are drawn back to perfectly recognize these handwritten digits. Moreover, some of these digits have similarities with others - 4 and 9, 1 and 7, 5 and 6, 8 and 9, etc. - rendering them even harder for machines to recognize. Even with all these constraints, the approach to recognize handwritten digits advances day by day and likely to achieve perfect recognition of handwritten digits.

Handwritten digit string recognition is an extension of individual handwritten digit recognition. Briefly, repeated determination of individual digits of the digit string leads to handwritten digit string recognition, which might not be as easy as it sounds. Handwritten digit string recognition is a two steps process. It is composition of splitting string into individual digits using either heuristics or image segmentation based on various factors like common points, edges. The digits segmented from the digits string are passed as inputs to a model for recognition of digits. Secondly, classification of separated digits, the model used for classification of digits including the technique employed for feature extraction plays major role in determination of handwritten digit. Ultimately, concatenating the individual digits forms the digit string to be determined.

The main goal of our project is to recognize the handwritten digit string and al-so provide voice output of recognized digits. This approach helps in conforming to the digits written without paying attention to them. Such addition of voice out-put also helps children in learning the digits with their name at the early stages of schooling. In this model, we designed a neural network model, consisting of con-volution neural network layers with activation function rectified linear unit, followed by max-pooling layers and dense layers associated with dropout layers on MNIST handwritten digits dataset, containing digits from 250 different authors containing up to 70000 data samples on whole – 60000 samples in train dataset and 10000 samples in training dataset, and some of own samples of size 28x28. In these recent years, the fame of handwritten digit and character recognitions have risen high due to their applications, including cheque analysis, recognizing postal codes, and data entry jobs in various fields. Our approach extends the recognition with the voice output of recognized digits. This model is advantageous in attesting the money written on cheques and reciting students' marks in classrooms. Also helps blind people to recognize digits in the given numeral string with a simple snap. This model on further improvements can be used as teaching tool that helps preschoolers to learn digits and their names with the model's voice output module.

III. Proposed System Architecture

The architecture diagram represents the outline of the proposed software system. It provides summarization about the associations between various components and also the conditions involved between these components. It minimizes entire view of the software system into understandable format. Firstly, the user provides the image path of digit string to the application. Then the application reads and preprocesses the input image. The preprocessing includes image resizing, gray scaling, and denoising. The preprocessed image then undergoes the segmentation process, where the image is segmented into various individual digit image splits. Later, these digit splits are preprocessed individually. The CNN model takes the preprocessed splits for digit recognition. After determining the digits splits, the audio output for the recognized digits is played. Finally, the digits in the digit string are displayed on the screen.

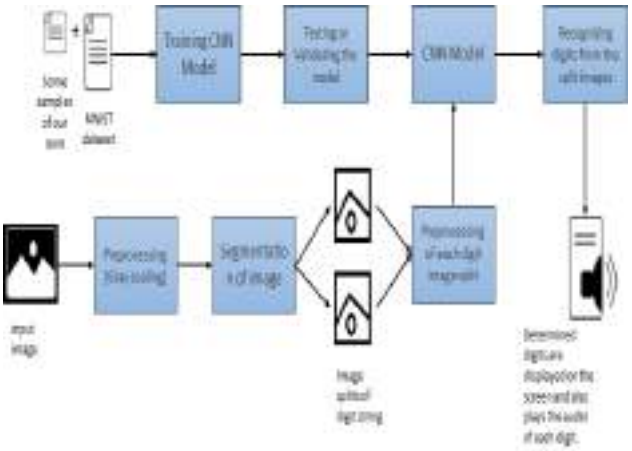

Fig. 1. System Architecture

The architecture above gives a clear picture about working of project. It also depicts the importance of various library functions in the project including OpenCV, Keras, imutils, pydub. The architecture is a sophisticated model that hides the underlying source code. The above figure helps us to determine the complexity of the application and can also be used as a reference for measuring the time required to determine the results.

IV. Development Framework

A. Software Installation

1) Visit the following website https://www.python.org /downloads /release/python-3.9.6/
2) Download python software according to your system requirements
3) Now Run the downloaded installer
    a. Right Click on the installer
    b. Select Run as Administrator and click on Yes
4) Now Python Installer Wizard appears
    a. Check the option Add Python 3.9 to PATH
    b. Click on Install Now
5) After the setup was successful, click on close
6) Open command prompt
    a. On the taskbar, to the bottom left, there will be an option to search. Type cmd in search and open the command prompt.
    b. Execute the following command to check if python is properly installed.
    • python –version
    c. If the version is displayed then the python is properly installed.
7) Execute the following command to update pip
    • pip install --upgrade pip
8) Install OpenCV by executing the following command.
    • pip install opencv-python
9) Install imutils by executing the following command.
    • pip install imutils

10) Install Keras by executing the following command.
- pip install tensorflow
- pip install keras

11) Install Numpy by executing the following command.
- pip install numpy

12) Install pydub by executing the following command.
- pip install pydub

B. Execution

1. Input Image: The execution of the program starts with taking an image as input from the user. For accurate results use a good resolution image as input. The user provides the path of the image as input. In order for the application to run correctly the user must provide a valid path as an input. It is important to pro-vide the input as the absolute path rather than relative path.

2. Loading Image: OpenCV module in python provides a method, imread, to read an image form the given path. The image should be present in the same directory as the program or else the absolute path of the input image must be pro-vided as input. cv2.imread is used to read the image from the path provided.

img = cv2.imread("image_path_input")

3. Preprocessing of the image: This phase involves the preprocessing of the input image (img). The img undergoes various transformations - resizing, gray scaling, denoising, binary inversion, dilation using a rectangle shape. In order to convert the given image into an array of values of color intensity. The segmentation process starts after preprocessing of image. The preprocessing proceeds with changing the image format from color to binary format followed by de-noising using non local means denoising and edge identification using the Canny edge detection algorithm. The OpenCV methods cvtColor and threshold are used for gray scaling and binary inversion.

4. Training the CNN model: Before proceeding further, train the CNN model for determining the digits. It is not a mandatory step to execute if you have a saved model for recognizing handwritten dataset. In this phase, we build a neural network model. And train it with the MNIST dataset (consisting for approximately 60,000 28x28 images) and a dataset containing some of our own samples of 28x28 images for recognizing the handwritten digits. We use Keras library to build and train the CNN model using CNN layers and fit method. Testing of the model is also implemented in this phase using evaluate method.

5. Save model: After training the model, in order to prevent the redundant training of the model, we can use save method in Keras to save the trained model. The saved model can be used again using load_model method in Keras. There would be no data loss for saving and loading the model.

model.save ("model_name")

model = load_model("model_name")

6. Segmentation of input image: After the preprocessing step of image, the image undergoes segmentation based on the splits identified by findContours function in OpenCV module. The segmentation involves almost all the border pixels of the rectangle enclosing the as black. The width of the rectangle is taken to be minimum to decrease the noise intervention in segmented digits recognition. The size is increased afterwards by the same amount so that no part of the digit is lost. These segmented parts are extracted from the original image.

7. Processing the splits individually: From here on, every phase is executed individually for each split of original image. The split image is resized into 28x28 image to pass it to CNN model. Before passing it to the model, the image undergoes gray scaling and binary inversion The resize function in imutils module is used for this purpose. After resizing, the image is fed into the CNN model.

8. Recognizing the digits in image split: The resized image after the preprocessing is fed into the Convolution Neural network model. The model recognizes the dig-it present in the splits based on the probability of matching features. The predict method in the Keras library is used for predicting the digit in the split image. After recognizing the digits separately. It's time to combine the recognized digits in the order of splits into an array.

9. Audio Output: In this phase a set of 10 recording, each for a digit from 0 to 9 has been initialized. Finally, the recorded audio is played based on the order digits stored in an array in previous step, using pydub module. The AudioSegment class of pydub is used to read the recorded audio files using pydub.playback.play function. Finally, the program terminates itself at the end of execution.

V. Existing Approaches

There are quite a few approaches in this field of study. An approach using both segmented and segment-free methods is employed to recognize handwritten numeral string off-line [1]. A method is proposed to recognize the handwritten numeral string using the RNN model and Connectionist Temporal classification with approximate recognition rates of 89.75% and 91.14% [2]. Another approach used graph-based properties of the digit string bases matching subgraph inputs with prototype symbol graphs [3]. A method is employed using (convolution neural network) CNN on ORAND-CAR-A and ORAND-CAR-B datasets with recognition rates of 92.2% and 94.02% respectively [4]. This problem is approached using various classification problems including SVM, KNN, and other classification algorithms over both the segmentation approach and the segment free approaches of splitting digit string [5, 6]. Some of these methods involve dealing with the overlapping of digits, connecting points in the digit string. Some other methods involving geometric context of digits and convolution neural network models [7, 8].

VI. Dataset

The MNIST dataset simply is thought of as "Hello World" in machine learning. Being derived from NIST dataset combined has 70000 images of size 28 pixels x 28 pixels black and white images, consisting up to 60000 images in the training dataset and approximately 10000 images for testing dataset contributed from more than 250 different writers. Each of the digit samples has varying styles and characteristics. The training dataset, 60000 images are the combination of ap-proximately 6000 images of each digit from zero (0) to nine (9) with maximum samples of 6742 for one (1) and minimum samples of 5421 for five (5) and others ranging in-between. And similarly, the testing dataset combines approximately 1000 images of each digit ranging from 892 (for five (5)) to 1135 (for one (1)). Although the

dataset is related to handwritten digit images, they can be stored in the form of a 28x28 2D matrix each cell representing the color intensity ranging from black to white. Due to its simple nature, the MNIST dataset is used in various handwritten digit recognition projects with varying accuracies and different models. Other than MNIST dataset we used some other handwritten digit samples for accurate results. And the dataset consists of few samples of each digit valuing a total of 5000 images, where each digit has approximately 500 samples extra from that of the MNIST dataset written in various styles and shapes.

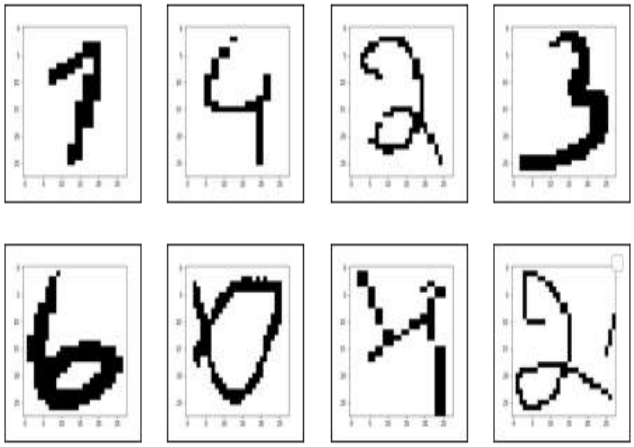

Fig. 2. Samples included into MNIST dataset

Fig. 3. Samples of MNIST dataset

VII. Experimental Results

After installing python environment and the required modules. The application is ready for execution and results. Firstly, the application accepts the path of the image as an input from the user. Then, the input string is converted into path with normpath method in os.path module. Care to be taken while providing the image, high quality images provide accurate results. Next, the imread method is used to the read the method from the given path. If the given path doesn't exist then the program terminates.

After reading the image, the image undergoes preprocessing - resizing the image, conversion of image to grayscale, denoising the grayscale - using resize function in imutils and cvtColor and non-local means denoising methods in OpenCV.

The preprocessing step also involves binary inversion of the gray scaled image. Next the binary inverted image undergoes dilation, a process expanding the image, with a unity matrix. Using this dilated image, we find the digit splits from the given image using findContours method in OpenCV module.

Before splitting the image and feeding them to the CNN model, we must train a CNN model using MNIST dataset. The results achieved using MNIST dataset are invalid in string recognition. Using MNIST dataset the model cannot recognize the digits that aren't well structured and has a lot of ambiguity constraints. And after training the model with some of our own samples in addition to the MNIST dataset, we have achieved some possible results for handwritten string recognition.

Each of the splits are individually preprocessed one by one and fed to the CNN model to determine the digits. The preprocessing of splits involves conversion of image to grayscale and binary inverse formats. Further, to fit the image to the CNN model input size, it is resized to size 28x28.

Finally, the audio output of the recognized digits is played using play method in pydub.playback module. Thus, in such a way the application provides the audio of digits in the given string of digits. Points to be noted while providing the image path are image must be of good quality for accurate determination and the image should exist in order to provide output.

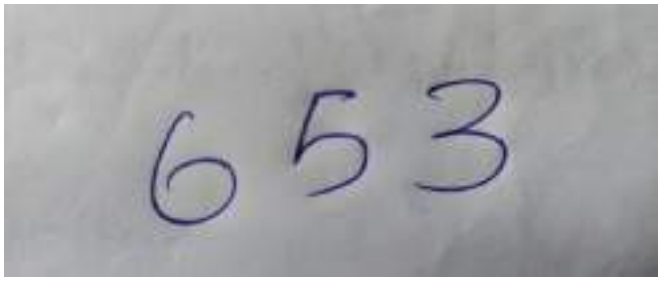

Fig. 4. Input image provided (handwritten digit string)

Fig. 5. Digit splits segmented from the original image (after processing the splits)

```
play digit 6
play digit 5
play digit 3
the given digit string contains 653
```

Fig. 6. Output displayed on the screen

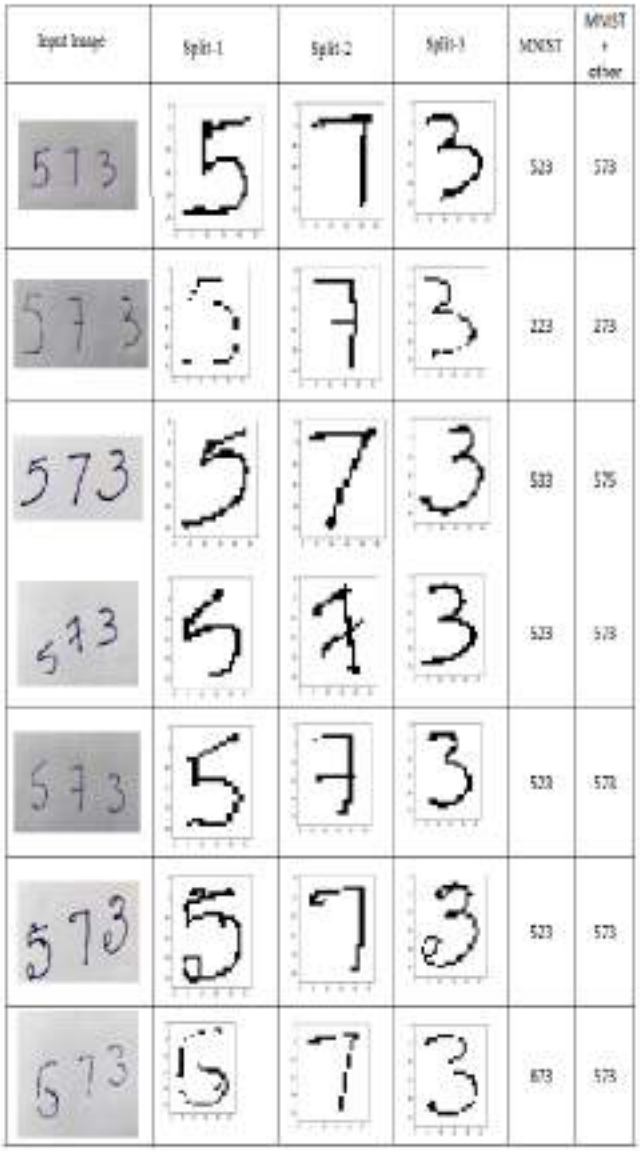

Fig. 7. Comparison of results with models trained using MNIST and MNIST + Additional samples

VIII. PSEUDOCODE

//Load the image from the given input path
img = cv2.imread(image_path)
// convert the image to grayscale and denoise
gray_img = cv2.cvtColor(img, cv2.COLOR_BGR2GRAY)
// dilate the gray_img using unity matrix
// find the image splits and extract them from the dilated gray_img using findContours function
// resize the splits into size 28pixels x 28pixels
resized_split = imutils.resize(gray_split, (28, 28))
// recognize the digits from resized image splits using trained CNN model
// play the audio response of each recognized digits
// display the recognized digit string on the screen

IX. CONCLUSION AND FUTURE SCOPE

The proposed project by using various concepts, (Numpy, OpenCV, imutils, pydub, Keras), we are able to achieve:

* Determination of digits in the digit string.

* Segmentation of digit string image to individual digit split images.

* Recognition the 80% of digits in the digit split images by introducing other samples into MNIST dataset.

* Providing the audio output of the recognized digits.

Handwritten digit string recognitions can be said as one of the complex problems in classification problems of machine learning. The representations of digits change from person to person. There are endless styles for representing the same digits from zero (0) to nine (9) in various fashion. And to classify such vast collection of representation is tedious and complex. This project included a dataset of digit samples including different handwriting styles for accurate digit recognition. This helped the trained model to predict many of the ambiguous cases of the model trained by only MNIST dataset. Inclusion of further samples of digits data can certainly provide accurate results to the problem. Also, the voice function enables the user to recognize the digits in the digit string without looking into the text written. This project is also useful in determining the token numbers written at parking or lockers other than with postal codes, bank cheque processing and, in various field involving numerals.

REFERENCES

[1] Thien M. Ha, Matthias Zimmermann, Horst Bunke, Off-line handwritten numeral string recognition by combining segmentation-based and segmentation-free methods, Pattern Recognition, Volume 31, Issue 3, 1998, Pages 257-272, ISSN 0031-3203

[2] Zhan H., Wang Q., Lu Y. (2017) Handwritten Digit String Recognition by Combination of Residual Network and RNN-CTC. In: Liu D., Xie S., Li Y., Zhao D., El-Alfy ES. (eds) Neural Information Processing. ICONIP 2017. Lecture Notes in Computer Sci-ence, vol 10639. Springer, Cham. https://doi.org/10.1007/978-3-319-70136-3_62

[3] A. Filatov, A. Gitis and I. Kil, "Graph-based handwritten digit string recognition," Pro-ceedings of 3rd International Conference on Document Analysis and Recognition, 1995, pp. 845-848 vol.2, doi: 10.1109/ICDAR.1995.602033.

[4] H. Zhan, S. Lyu and Y. Lu, "Handwritten Digit String Recognition using Convolutional Neural Network," 2018 24th InternationalConference on Pattern Recognition (ICPR), 2018, pp. 3729-3734, doi: 10.1109/ICPR.2018.8546100.

[5] L. S. Oliveira and R. Sabourin, "Support vector machines for handwritten numerical string recognition," Ninth International Workshop on Frontiers in Handwriting Recogni-tion, 2004, pp. 39-44, doi: 10.1109/IWFHR.2004.99.

[6] C. Zanchettin, B. L. D. Bezerra and W. W. Azevedo, "A KNN-SVM hybrid model for cursive handwriting recognition," The 2012 International Joint Conference on Neural Networks (IJCNN), 2012, pp. 1-8, doi: 10.1109/IJCNN.2012.6252719.

[7] X. -. Zhou, J. -. Yu, C. -. Liu, T. Nagasaki and K. Marukawa, "Online Handwritten Jap-anese Character String Recognition Incorporating Geometric Context," Ninth Interna-tional Conference on Document Analysis and Recognition (ICDAR 2007), 2007, pp. 48-52, doi: 10.1109/ICDAR.2007.4378673.

[8] Ahlawat S, Choudhary A, Nayyar A, Singh S, Yoon B. Improved Handwritten Digit Recognition Using Convolutional Neural Networks (CNN).Sensors.2020;20(12):3344. https://doi.org/10.3390/s20123344

Proceedings of the Proceedings of the Second International Conference on Artificial Intelligence and Smart Energy (ICAIS).
DVD Part Number: CFP22OAB-DVD; ISBN: 978-1-6654-0051-0

Smart-Bot Assistant for College Information System

Mallikarjuna Rao G
Computer Science Engineering
Gokaraju Rangaraju Institute of Engineering and Technology
Hyderabad, India
gmallikarjuna628@grietcollege.com

Vidyuallatha Sri Tripurari
Computer Science Engineering
Gokaraju Rangaraju Institute of Engineering and Technology
Hyderabad, India
vidyuallatha@gmail.com

Eesha Ayila
Computer Science Engineering
Gokaraju Rangaraju Institute of Engineering and Technology
Hyderabad, India
ayilaeesha@gmail.com

Roshini Kummam
Computer Science Engineering
Gokaraju Rangaraju Institute of Engineering and Technology
Hyderabad, India
roshini.kummmam@gmail.com

Divya Sree Peetala
Computer Science Engineering
Gokaraju Rangaraju Institute of Engineering and Technology
Hyderabad, India
divyasreepeetala@gmail.com

***Abstract*— A chatbot is a software application that facilitates online conversation through text or speech. Our proposed chatbot for college enquiry is a simple web application that aims to provide information regarding college. This chatbot provides information like admission procedure, courses offered, fee structure, placement statistics, and contact details of the college. This proposed chatbot uses natural language processing libraries to understand customer questions and automate responses to them, simulating human conversation and AIML (Artificial Intelligence Markup Language) to write rules which are used by chatbot response systems.**

Keywords—Chatbot, Artificial Intelligence Markup Language, Natural Language Processing, Query Analysis, Response, Artificial Intelligence, Database.

I. INTRODUCTION

A chatbot is a computer program that uses Artificial Intelligence and natural language processing to understand customer questions and automate responses to them simulating human conversation. Chatbot technology is used in many applications like smart speakers at home to messaging applications at the workplace. Chatbots uses Machine learning along with AI mechanism to understand the question and to give a proper response. These chatbots can be developed using natural language processing combined with artificial intelligence to provide an interacting environment to the user. It consists of software made up using python and can help users to talk with a machine. The proposed chatbot is intellectual which will provide necessary information regarding admission details, fee structures of various courses, timetables, and important activities of the college. This chatbot makes it easier for students to clarify their doubts in very little time.

A. Problem Statement

Usually, if a student or a parent needs to get any kind of information regarding courses, admissions, and so on they are required to visit the college website or enquire through telephone. Navigating through various links on the college website to find appropriate information is time-consuming. Some common queries of parents and students can be solved with the help of an online chatbot. Any questions on college-related activities can be enquired through the chatbot. The design should meet the following needs:

- The chatbot for the college enquiry system is required to have conversations with humans. The bot must possess the Artificial Intelligence to provide the above facility.
- The algorithm adopted in the design must be optimal and provide a quick response while processing the query.
- The framework must support multiple languages and simplify man-machine communication.

B. Theoretical Background

Eliza is considered the first Chatbot. It is developed in 1964 by Joseph Weizenbaum. It works on the basis of a pattern matching system. It assigns a value to each word present in the user input query and uses this value to reorder the words in the form of a question. This value is determined by finding its importance in the sentence.

ALICE (Artificial Linguistic Internet Computer Entity) is a rule-based chatbot based on the Artificial Intelligence Markup Language (AIML). This chatbot has more than 40,000 categories, where each category has a combination of pattern and its response. Md. Shahriare Satu and Shamim-AI-Mamun developed a Chatbot using the AIML scripts, saying the AIML based chatbots are easy to implement, they are lightweight and efficient to work. Thomas and Amrita Vishwa designed a chatbot based on AIML and LSA to provide customer care services and E-commerce websites. Rushabh and Burhanuddin Lokhandwala developed an Android-based chatbot. [11] Chatbots are developed using a keyword-based system that provides a human-computer dialog system in natural language i.e., in English. [15] Latent Semantic Analysis (LSA) can be used to develop efficient chatbots that can mimic the conversation between humans and machines and act as a virtual assistants. [2] A chatbot is a proxy that

contains embedded information and the queries are interpreted and analyzed using exploitation algorithms. [5] A chatbot is an intelligence-oriented machine in which a response system is developed using database information that analyzes and responds to user queries. [12] Many chatbots are developed using LUIS.ai, MongoDB, and Microsoft Bot Builder. The response system is based on LUIS.ai. [10] Chatbot is an intelligence agent which can initiate a conversation with humans and give responses using Artificial Intelligence Markup Language. [4] Chatbots are stateful services that can be integrated with web services and provide text or speech-based user interfaces. [3] Vedika Patel developed an advanced customized chatbot from an open-source Rasa framework using Rasa NLU and Rasa core. [6] Chatbots are built using Chatterbot, Flask and ChatterbotCorpus using python and efficiency can be achieved using Natural Language Processing (NLP). [7] Chatbots are developed using iterative models and stop words-based human-PC framework. [8] Eliza and Cleverbot are a web-based application that provides a response system using AI terminology and processing libraries. [1] AI-based chatbots and chatbots based on the web can be created using AI terminologies and tongue processing libraries. [9],[13] Chatbots are developed using embedded knowledge units that help in simulating conversation. [14] Efficient chatbots are developed based on the feedback-feedforward technique and are used to improve exactness.

C. Rule based Chatbots

In this Rule-based approach, a chatbot is associated with some defined rules which can be simple to very complex. These rules train the chatbots and develop a response system and are required for the chatbot to get an idea about the types of questions asked and their corresponding solutions. This kind of chatbot developed is known as a decision-tree bot. In this rule-based chatbots, the question of the user is mapped to the corresponding response and is given as output to the user. These rule-based chatbots can handle their use cases with high flexibility.

Advantages: Rule-based chatbots can be developed within very little time and are highly secured. They can also include interactive elements and website links. They can be integrated with other systems easily.

Limitations: These chatbots fails in handling complex queries and cannot learn on their own. These bots will give responses only to the trained queries. The improvements in chatbot can be done only manually. It also cannot capture spelling mistakes which can lead to incorrect responses or no response from chatbot.

D. Self-learning Chatbots

Self-learning chatbots use machine learning algorithms. They are highly efficient when compared to rule-based chatbots. These are further subcategorized into two types. They are retrieval-based models and self-learning bots. In a retrieval-based model, the chatbot fetches the best answer from the existing responses. Generative models are intelligent models which come up with an answer rather than searching from a given list.

Limitations: It requires too much data for training and takes huge data for training, which makes the implementation process longer and complex. If the chatbot is given wrong information, it will consume more time for correction. Pre-defined structures are required for providing predictable responses, which makes it even more complicated.

E. Existing System

In existing system, the college information and information related to fees, exams and admissions are provided through college website, WhatsApp groups or notice board. In some cases, students' needs to visit college to solve the queries.

Limitations: These existing methods are time-consuming and not efficient. These methods cannot be used for clarifying all the doubts from the user. Non-college members will find it difficult to collect information about the college. Thus, the proposed system is developed in such a way that queries of students and their parents are solved through conversation with a chatbot. There is a great scope for developing this college information related chatbot.

II. PROPOSED APPROACH

The proposed approach is developed on Windows-10 Operating System with 4GB RAM in Python programming language, however, it can also be developed in Windows-7 or above and Linux operating systems.

Our proposed approach for developing a chatbot for college enquiry includes AIML files which contain .aiml extension. AIML files contain Artificial Intelligence Markup Language. This markup language is based on pattern matching recognition. It is based on a stimulus-response approach used to start a conversation between a bot and a human using natural language processing capability. It is a tag-based and XML-based markup language. These .aiml files hold the bulk of the code and are used to define the personality of a chatbot and specify the heuristic conversation rules for a chatbot.

This approach also contains usage and implementation of Natural Language Processing. Natural Language Processing is a branch of informatics, mathematical linguistics, machine learning, and artificial intelligence which deals with human languages. NLP is the key that makes the chatbots to accept input questions, analyze and respond to input queries by generating the output text. NLP helps chatbots in prioritizing the questions according to the complexity and makes chatbots to respond to user queries faster than a human being. It uses machine learning and artificial intelligence that makes chat bots smart with time.

Natural Language processing includes following components:

1. *Natural Language Understanding:* This process consists of flexible rules. It is mostly used to map

inputs to useful representations so that computer algorithms can understand the input data. It is also helpful in analyzing different aspects of the language.

2. *Natural language Generation:* Text planning, sentence planning and text realization are used in generating natural language. Here the machine generates a logical response then it is converted to a natural language response so that user can easily understand.

A. Proposed Modules

The proposed approach consists of the following modules:

1) Context Identification: Context Identification is process of breaking down the user input query to identify the theme and intent of the user. First the input query is accepted from the user. Thus, the query is standardized using pre-processing. The keywords used in this input query can be used to find the appropriate context. Context allows users to identify intent in a query. The identified context is carried forward across multiple messages. This context identification helps in establishing the conversation between user and chatbot by identifying various factors. It also helps to shape the response system based on environment.

2) Natural Language Processing System: Natural language processing helps the chatbot to understand user's query given in informal way by using various NLP tools. The input given by the user in natural language is processed using Google speech-to-text and translator to generate a generalize query which is then pre-processed to identify tokens.

3) Pattern Matching System: Given text is processed using NLP algorithm, to generate a series of tokens which are mapped with various patterns or regular expressions in the database to identify an established pattern. If there is no matching pattern is identified among sequence of tokens, the query is sent for AIML Response System. Chatbots uses knowledge base which contains documents of <pattern> and <template> tags for implementing pattern matching. When the input text received by the chatbot, it is compared with the text present in all the <pattern> tags. If there is a match, then the response will be generated.

4) AIML based Response System: Artificial Intelligence Markup Language is used to map the input to an appropriate pattern. If the response for that pattern is available inside the files, then it is formatted as output to the user. AIML files contains different <category> tags which further contain <pattern> and <template> tags. The input keyword is compared with all the keywords present in <pattern> tags and if the given input keyword matches with the keyword in one of the <pattern> tag, then the content present in the corresponding <template> tag is given as output.

5) Query Analysis and Response System: If the input pattern is not present in aiml files then the response is given by searching in the database. The database information is retrieved by converting text to SQL. For converting the text to SQL, the input text is accepted from the user and tokens in the text are identified and nouns are mapped to corresponding attributes, these are mapped to corresponding table names and column names. Words other than nouns are mapped to SQL clauses. In this way, sub-clauses and queries are composed. These queries are given as input to the database and the required information is retrieved from the database, which is accepted by the bot, formatted as output and is given to the user. In this way these queries are used in obtaining data from the database.

B. System architecture

Fig.1 shows the system architecture of the proposed approach. It shows the entire view of the physical deployment of the system. Input is taken from the user; it is processed using a pattern matching algorithm. If the keywords are matched with AIML files the response present in AIML files is given to the user. If the query is present in a rule-based system then the respective result is shown.

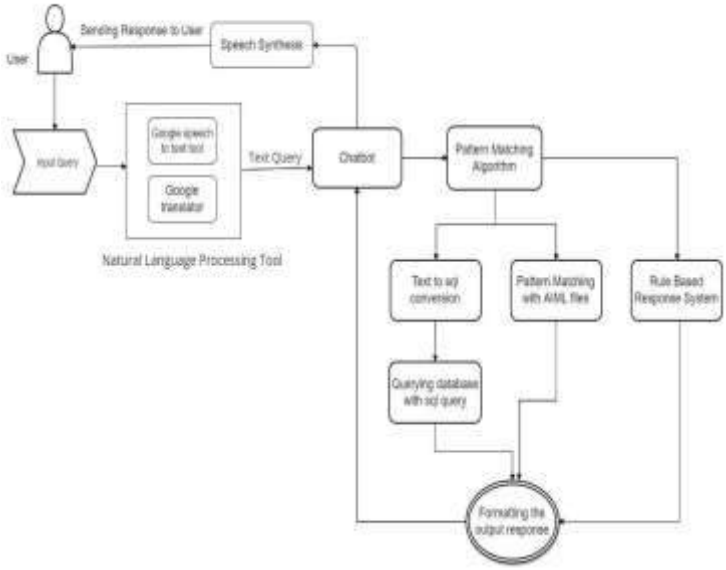

Fig. 1. System architecture

C. Algorithm

Step-1: Start.
Step-2: User Login Page, if user does not have account do step-3; else goto step-4.
Step-3: Register as new user and repeat step-2.
Step-4: Validate User Credentials.
Step-5: Take User's Query.
Step-6: Using NLP to convert query into English.
Step-7: Search for any rule defined as same as given user query, if any rule is found goto step-13; else goto step-8.
Step-8: Pre-process the query to extract keywords and identify the user's context.
Step-9: Search for pattern in extracted keywords using pattern matching algorithm, if not found goto step-10 else goto step-13.
Step-10: Search keywords pattern in .aiml files, if not found goto step 11; else goto step-13.
Step-11: Convert the given query to SQL, to search in Database; if not found goto step-12 else goto step13.
Step-12: System will prompt "Invalid Message" as it is not defined in chatbot scope.

Step-13 Convert the appropriate response from the system and display it on chat bot interface.
Step-14: Repeat step-5 to step-13 for another user's query.
Step-15: End.

III. IMPLEMENTATION AND TESTING

A. Implementation

Implementation of proposed approach consists of following 6 steps:

1) Creating .aiml files:
We are creating 5 .aiml files for 5 different contexts like admission, department, academics, results and casual conversation. Each .aiml file has different patterns and corresponding responses. If the user query matches with one of the patterns in .aiml file, the corresponding template will be shown to the user.

2) Developing Rule Based Response System:
Set of rules are declared statically that tells what to do or what to conclude in different situations. It uses the rules as the knowledge representation for knowledge coded into the system.

3) Creating Dataset:
A dataset is created in json which includes Meta data regarding college information. We can serialize and de-serialize the data into any programming language.

4) Including Translators and Speech synthesis:
We have included the Google translator and Google text-to-speech modules in chatbot which converts messages given in other languages to English and a speech synthesis module to understand the user input.

5) Training the chatbot:
The dataset that is prepared using json, aiml are trained using Chatterbot class and are evaluated based on accuracy.

6) Deploying chatbot using flask app:
The trained chatbot is deployed using flask framework, which provides tools, libraries to deploy web applications. This flask app consists of following web pages.

B. Results

Fig. 2. Menu Options

Fig. 2. Shows the menu options that are displayed when a user opens the chatbot. The user can view menu options by giving input as "0"

Fig. 3. Rule Based Response

Fig. 3. shows a basic rule-based response, when the user message is based on any rule then the system gives a message according to the rule.

Fig. 4. AIML Response

When the user query is matched with any pattern given in the aiml files, then the corresponding response is given as output as shown in Fig.4.

Fig. 5. Invalid response

When the user query is not matched with any pattern and not following any rule specified, then the above message is prompted to the user.

IV. CONCLUSION AND FUTURE SCOPE

A. *Conclusion*

The main aim of this chatbot is to facilitate students and parents to stay updated on college activities. This chatbot combines AI and a knowledgeable database to provide maximum accurate responses. This proposed chatbot will make human-like conversation.

B. *Future Scope*

In this approach, we have included database associated with AIML files but including relational databases increases the human readability and response time for queries. Future work can include training the chatbot with varied data to provide accurate and fast results. Integrating with multiple channels of communication like WhatsApp, Facebook, and SMS etc. will increase the scope of the proposed system.

REFERENCES

[1] R. Parkar, J. Nambiar, Y. Payare, K. Mithari, "AI and web-based interactive college enquiry chatbot" , January, 2021.

[2] Emil Babu, Geethu Wilson, "Chatbot for college enquiry", March, 2021.

[3] Nikita Ingale, Tushar Anand Jha1, Ritin Dixit1, Vishal Kisan, "College enquiry chatbot using RASA" , June, 2021.

[4] Ms.Ch.Lavanya Susanna, R.Pratyusha, P.Swathi, P.Rishi Krishna, V.Sai Pradee, "College enquiry chatbot" , March 2020.

[5] Harshala Gawade, Prachi Vishe, Sonali Kolpe, "College enquiry chatbot system", September, 2020.

[6] P.Nikhila, G.Jyothi, K.Mounika, Mr. C Kishor Kumar Reddy and Dr. B V Ramana Murthy, "Chatbots using artificial intelligence", January, 2019.

[7] Payal Jain, "College enquiry chatbot using iterative model", January, 2019.

[8] Prof Ram Manoj Sharma, "Chatbot based college information system" , March, 2019.

[9] Sagar Pawar, Omkar Rane, Ojas Wankhade, Pradnya Mehta, "A web based college enquiry chatbot with results", April, 2018.

[10] Kumar Shivam, Khan Saud, Manav Sharma, Saurav Vashishth, Sheetal Patil "Chatbot for college website" , June 2018.

[11] Balbir Singh Bani, Ajay Pratap Singh, "College enquiry chatbot using A.L.I.C.E (Artificial Linguistic Internet Computer Entity)", January, 2017.

[12] Harsh Pawar, Pranav Prabhu, Ajay Yadhav, "College enquiry chatbot using knowledge in database" , April, 2017.

[13] Srusti Barve, Supriya Gaikwad, Dinesh Nimbane, "Chatbot for college management system", April, 2017.

[14] Vishal R, Shindem, Miss Anagha bagul, Mr. Amit gupta, "Chatbot for college related faq's" , July, 2017

[15] Bhavika R. Ranoliya, Nidhi Raghuwanshi, Sanjay Singh "Chatbot for university related FAQs" , September, 2017.

[16] Bashar, Abul. "Survey on evolving deep learning neural network architectures." Journal of Artificial Intelligence 1, no. 02 (2019): 73-82.

[17] Vijayakumar, T. "Comparative study of capsule neural network in various applications." Journal of Artificial Intelligence 1, no. 01 (2019): 19-27.

[18] Manoharan, J. Samuel. "Study of Variants of Extreme Learning Machine (ELM) Brands and its Performance Measure on Classification Algorithm." Journal of Soft Computing Paradigm (JSCP) 3, no. 02 (2021): 83-95.

[19] Mugunthan, S. R., and T. Vijayakumar. "Design of Improved Version of Sigmoidal Function with Biases for Classification Task in ELM Domain." Journal of Soft Computing Paradigm (JSCP) 3, no. 02 (2021): 70-82.

< Previous | Back to Results | Next >

Conferences > 2021 2nd International Confer...

Leveraging Machine Learning to Predict Wild Fires

Publisher: IEEE

< Previous | Back to Results | Next >

<< Results | < Previous | Next >

K Venkata Murali Mohan ; Aravapalli Rama Satish ; K Mallikharjuna Rao ; Rokesh Kum… All Authors

Abstract:A raging wildfire is a catastrophic event which damages forests, which has a serious effect on people, fauna and flora that are dependent on the forest ecosystem. A study... **View more**

Metadata

Abstract:

A raging wildfire is a catastrophic event which damages forests, which has a serious effect on people, fauna and flora that are dependent on the forest ecosystem. A study of the size of wildfires in a Canadian Province in USA i.e. Alberta is seen in this article. A variation of the duration of the fire and the area it burns defines the scale of a fire. Our predictive algorithm helps wildfire rescue workers to use their foreseen level in the initial phases in order to mitigate destruction inflicted by a forest fire. Modeling information has been gathered from Natural Resources Canada's real-time dataset, including forest fire and weather information for Alberta, Canada. To evaluate the severity of flames, the dimensions of the region affected with fire and the timeframe of the flames have been used. The information was split into training and evaluation environments after multi-linearity validation and function normalization. In addition, the climatic variables were used to create predictive model by using inputs, a Neural Network for Back Propagation (BPNN), a type of artificial neural network i.e. Recurrent Neural Network (RNN) and a type of RNN i.e. Long Short-Term [illegible] classification models. The findings suggest that the scope of a wildfire can be forecast using climatic knowledge at the outset of the event.

Published in: 2021 2nd International Conference on Smart Electronics and Communication (ICOSEC)

Date of Conference: 7-9 Oct. 2021

Date Added to IEEE *Xplore*: 15 November 2021

ISBN Information:

INSPEC Accession Number: 21298042

DOI: 10.1109/ICOSEC51865.2021.9591952

Publisher: IEEE

Conference Location: Trichy, India

Contents

Forestry, one of the most important and needed tools for conserving the environmental integrity of the Planet, is a safe refuge for human livelihoods. However, disasters like forest fires can cause significant damage to forest, and many other assets such as infrastructure, human life and wildlife are overabundant. Forest fires flame fields of farmland and in just seconds kill anything in their direction. Forest fire destroying houses, livestock, forests, plants, habitats and foliage. There are various and far-reaching consequences of fires. The effect on the economy, climate, history and social fabric of remote regions is enormously important. The parameters [1]–[2], such as weather, precipitation, moisture levels, pressure, and so forth, will, of course, prevent wildfire.

Early Detection of Brain Stroke using Machine Learning Techniques

Publisher: IEEE

<< Results | < Previous | Next >

Vempati Krishna ; J. Sasi Kiran ; PVRD Prasada Rao ; G. Charles Babu ; G. John Babu All Authors

Abstract: The brain is the most complex organ in the human body. Brain Stroke is a long-term disability disease that occurs all over the world and is the leading cause of death. A ... **View more**

Metadata

Abstract:
The brain is the most complex organ in the human body. Brain Stroke is a long-term disability disease that occurs all over the world and is the leading cause of death. A stroke occurs when the brain's blood supply is cut off and it ceases to function. There are two primary causes of brain stroke: a blocked conduit (ischemic stroke) or blood vessel spilling or blasting (hemorrhagic stroke). Early brain stroke prediction yields a higher amount that is profitable for the initiating time. Brain stroke is caused primarily by people's lifestyle decisions, particularly in the current scenario by evolving elements such as high blood sugar, heart disease, obesity, diabetes, and hypertension. This research study has used various machine learning (ML) algorithms like K nearest neighbour, logistic regression, random forest (RF) classifier and SVC. This research work designs a model using one among the following algorithms with high accuracy to predict the stroke for newly given inputs.

Published in: 2021 2nd International Conference on Smart Electronics and Communication (ICOSEC)

Date of Conference: 7-9 Oct. 2021

DOI: 10.1109/ICOSEC51865.2021.9591840

Date Added to IEEE *Xplore*: 15 November 2021

Publisher: IEEE

ISBN Information:

Conference Location: Trichy, India

Contents

Now-a-days brain stroke has become a major disease that is leading to death. Prediction of brain stroke in the early stage has become very difficult and it is time taking tasks as a result many people are losing their lives. To overcome this we use machine learning approach and build a model to predict whether a person is suffering from brain stroke or not. We can do this by considering various attributes of the patient and predict the output. A stroke is a medical condition in which poor bloodstream to the brain causes cell death. There are 2 significant types of stroke: ischemic, due to nonappearance of the bloodstream, and hemorrhagic, due to bleeding. Both reasons of Brain gets damaged if symptoms last lower than 1 or 2 hours, the stroke is transient ischemic assault (TIA), also named a mini-stroke. A hemorrhagic stroke might also relate to an extreme migraine. The symptoms of a stroke might be stable. The long-term problems might contain bladder control loss and pneumonia. The primary danger factor for stroke is hypertension. Various danger factors contain tobacco smoking, diabetes mellitus, heftiness, a past TIA, high blood cholesterol, end-stage kidney sickness, and preliminary fibrillation. An ischemic stroke is ordinarily caused by blood vessel blockage however there are additionally more uncommon causes. A hemorrhagic stroke is caused either because of space among the membranes of the brain or bleeding directly from the brain. The bleeding might happen because of a burst brain aneurysm. An analysis is usually founded on physical tests and helped by clinical imaging like MRI or CT scan. A CT scan might rule out bleeding, however, might not essentially rule out ischemia that immediately regularly doesn't appear on a CT scan. The numerous tests like blood tests and an electrocardiogram (ECG) are never really dangerous factors and preclude other potential causes [8]. Low glucose might cause comparable symptoms. The prevention incorporates diminishing danger factors, medical procedures to open up the veins to the brain in those with tricky carotid narrowing, and warfarin in individuals with trial fibrillation. The aspirin might be suggested by doctors for anticipation. A stroke or TIA frequently needs crisis care. An ischemic stroke, whenever recognized within 3 to four and half hours, might be treatable with a medicine, which could separate the clot. Few hemorrhagic strokes profit with a medical procedure. Treatment to attempt recuperation of lost capacity is named as stroke recovery, and preferably occurs in a stroke unit; in any case, these are not accessible in a significant part of the world.

< Previous | Back to Results | Next >

Conferences > 2021 Fifth International Conf...

An Effective Technology for Secured Data Auditing for Cloud Computing using Fuzzy Biometric Method

Publisher: IEEE

<< Results | < Previous | Next >

Rokesh Kumar Yarava ; Ponnuru Sowjanya ; Sowmya Gudipati ; G. Charles Babu ; Sri… All Authors

Abstract: The utilization of "cloud storage services (CSS)", empowering people to store their data in cloud and avoid from maintenance cost and local data storage. Various data int... **View more**

Metadata

Abstract:

The utilization of "cloud storage services (CSS)", empowering people to store their data in cloud and avoid from maintenance cost and local data storage. Various data integrity auditing (DIA) frameworks are carried out to ensure the quality of data stored in cloud. Mostly, if not all, of current plans, a client requires to utilize his private key (PK) to generate information authenticators for knowing the DIA. Subsequently, the client needs to have hardware token to store his PK and retain a secret phrase to actuate this PK. In this hardware token is misplaced or password is forgotten, the greater part of existing DIA plans would be not able to work. To overcome this challenge, this research work suggests another DIA without "private key storage (PKS)"plan. This research work utilizes biometric information as client's fuzzy private key (FPK) to evade utilizing hardware token. In the meantime, the plan might in any case viably complete the DIA. This research work uses a direct sketch with coding and mistake correction procedures to affirm client identity. Also, this research work plan another mark conspire that helps block less. Verifiability, yet in addition viable with direct sketch. Keywords: Data integrity auditing (DIA), Cloud Computing, Block less Verifiability, fuzzy biometric data, secure cloud storage (SCS), key exposure resilience (KER), Third Party Auditor (TPA), cloud

More Like This

audit server (CAS), cloud storage server (CSS), Provable Data Possession (PDP)

Published in: 2021 Fifth International Conference on I-SMAC (IoT in Social, Mobile, Analytics and Cloud) (I-SMAC)

Date of Conference: 11-13 Nov. 2021

DOI: 10.1109/I-SMAC52330.2021.9640845

Date Added to IEEE *Xplore*: 20 December 2021

Publisher: IEEE

ISBN Information:

Conference Location: Palladam, India

ISSN Information:

Contents

A Survey on Mechanisms of Reusable Code Component Retrieval from Component Repository

Publisher: IEEE

N Krishna Chythanya ; C. R. K. Reddy All Authors

Abstract: Modern software is more dominant of software components in the process of software development. Reuse is the primary benefit of a software component improving productivit... **View more**

Metadata

Abstract:
Modern software is more dominant of software components in the process of software development. Reuse is the primary benefit of a software component improving productivity and decreasing time, cost of implementation. The high demand of reusable software components leads to need of a mechanism to effectively store and retrieve components whenever similar functionality is required. Several researchers have proposed different mechanisms to build these storage spaces of components called as Repositories. This work intends to survey different effective retrieval methods and repositories built earlier. Also, this paper discusses various stochastic and statistical models for code reusability in software engineering. This survey will be a base to develop a user friendly and well-organized repository for retrieval of code components.

Published in: 2021 2nd International Conference on Smart Electronics and Communication (ICOSEC)

Date of Conference: 07-09 October 2021

INSPEC Accession Number: 21464058

Date Added to IEEE *Xplore*: 12 November 2021

DOI: 10.1109/ICOSEC51865.2021.9591726

▸ ISBN Information:

Publisher: IEEE

Conference Location: Trichy, India

Contents

Software reuse is a promising opportunity to decorate software productivity [1]. It can improve the reliability of the program. It may be useful to identify design errors at the initial level by adding unique candidate additions. However, reusing the program is not practical in its ability for several reasons. The main reason is that it requires a rich repository of the best program code snippets. So it isn't easy to successfully recover add-ons from reusable programs from the repository [2]. Existing software component recovery strategies mainly include free text strategies, previously included vocabulary techniques, signature comparison methods, behavior-based strategies, and facial category techniques [3]. Most of these techniques use language specifications based primarily on correspondence. Other current methods that mainly rely on official specifications are very complex and challenging to adapt to the user's environment. In this context, we believe in Bayer words : "The current technologies were not flexible enough to satisfy the desires of different trading conditions or were very confusing; they were no longer relevant without robust additional explanations and assistance. There is a need for flexible technology that can be adapted to assist different organizational conditions with adequate guidance and administration". Under this motivation, studies suggest a robust method for identifying reusable add-ons in software warehouse programs, which are then labeled and recovered for potential reuse. Their approach uses language in addition to the official specifications to define components and retrieve add-ons from the warehouse. The benefits of reuse is depicted in Fig 1.

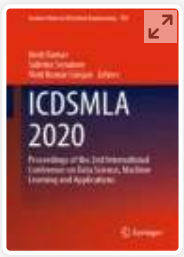

ICDSMLA 2020 pp 837–850

Artificial Intelligence Based Learning Approach for Leaf Disease Identification and Detection

G. Karuna, K. Sahithi, B. Rupa, R. Amani, K. Swaraja & K. Meenakshi

Conference paper | First Online: 09 November 2021

Part of the Lecture Notes in Electrical Engineering book series (LNEE,volume 783)

Abstract

Plants and Crops get diseased due to many reasons. It might be because of diseases of stems, leaves, roots etc. This Paper mainly congregates on leaves. Leaf Disease identification and Detection has many applications for cultivators and farmers to know whether the plant is diseased or not. So that they can retort in dwarf time and decreasing the loss and then can obtain immense profits. This paper mainly focused at learning the disease of plant through leaves. Here, we scrutinize the leaf through Image Processing and extract features of

particular leaf and then utilizing those features as a dataset and done preprocessing and then administering them in Artificial Intelligence based learning algorithms like Convolutional Neural Networks to find disease.

Keywords

Leaf disease **Neural networks** **Features**

References

1. Amara J, Bouaziz B, Algergawy A et al (2017) A deep learning-based approach for banana leaf

diseases classification. In: BTW (Workshops), pp 79–88

2. Jiang P, Chen Y, Liu B, He D, Liang C (2019) Real-time detection of apple leaf diseases using deep learning approach based on improved convolutional neural networks. IEEE Access 7:59069–59080

3. Geetharamani G, Pandian A (2019) Identification of plant leaf diseases using a nine-layer deep convolutional neural network. Comput Electr Eng 76:323–338

4. Atabay HA (2016) A convolutional neural network with a new architecture applied on leaf classification. IIOAB J 7(5):226–331

5. Chaudhary P, Chaudhari AK, Cheeran AN, Godara S (2012) Color transform based approach for disease spot detection

6. Patil JK, Kumar R (2012) Feature extraction of diseased leaf images. J Signal Image Process 3(1):60

7. Reddy PR, Divya SN, Vijayalakshmi R (2015) Plant disease detection techniquetool—a theoretical approach. Int J Innov Technol Res 91–93

8. Mahlein A-K, Rumpf T, Welke P et al (2013) Development of spectral indices for detecting and identifying plant diseases. Remote Sens Environ 128:21–30

9. Xiuqing W, Haiyan W, Shifeng Y (2014) Plant disease detection based on near-field acoustic holography. Trans Chin Soc Agric Mach 2, article 43

10. Mahlein A-K, Oerke E-C, Steiner U, Dehne H-W (2012) Recent advances in sensing plant diseases for precision crop protection. Eur J Plant Pathol 133(1):197–209

11. Revathi P, Hemalatha M (2014) Identification of cotton diseases based on cross information gain deep forward neural network classifier with PSO feature selection. Int J Eng Technol 5(6):4637–4642

12. Zhou C, Gao HB, Gao L, Zhang WG (2003) Particle swarm optimization (PSO) algorithm. Appl Res Computers 12:7–11

13. Rumpf T, Mahlein A-K, Steiner U, Oerke E-C, Dehne H-W, Plümer L (2010) Early detection and classification of plant diseases with support vector machines based on

hyperspectral reflectance. Computers Electron Agric 74(1):91–99

14. Al-Hiary H, Bani-Ahmad S, Reyalat M, Braik M, ALRahamneh Z (2011) Fast and accurate detection and classification of plant diseases. Mach Learn 14:5

15. LeCun Y, Bottou L, Bengio Y, Haffner P (1998) Gradient-based learning applied to document recognition. Proc IEEE 86(11):2278–2324

16. Soderkvist O (2001) Computer vision classification of leaves from Swedish trees

17. Camargo A, Smith J (2009a) Image pattern classification for the identification of disease causing agents in plants. Computers Electron Agric 66(2):121–125. Camargo A, Smith J (2009b) An image-processing based algorithm to automatically identify plant disease visual symptoms. Biosyst Eng 102(1):9–21

18. Mohanty SP, Hughes DP, Salathe M (2016) Using deep learning for image-based plant disease detection. Front Plant Sci 7

19. Krizhevsky A, Sutskever I, Hinton GE (2012) Imagenet classification with deep convolutional neural networks. In: Advances in

neural information processing systems, pp 1097–1105

20. Szegedy C, Liu W, Jia Y, Sermanet P, Reed S, Anguelov D, Erhan D, Vanhoucke V, Rabinovich A (2015) Going deeper with convolutions. In: Proceedings of the IEEE conference on computer vision and pattern recognition

21. Ali A (2019) PlantVillage dataset, Version 1. Retrieved 22 Feb 2020. https://www.kaggle.com/xabdallahali/plantvillagedataset.

Author information

Authors and Affiliations

Computer Science and Engineering, GRIET, Hyderabad, India

G. Karuna, K. Sahithi, B. Rupa & R. Amani

Electronics and Communications Engineering, GRIET, Hyderabad, India

K. Swaraja & K. Meenakshi

Editor information

Editors and Affiliations

BioAxis DNA Research Centre Private Ltd., Hyderabad, Telangana, India

Dr. Amit Kumar

Department of Computer Engineering, Electrical Engineering and Applied Mathematics, University of Salerno, Fisciano, Salerno, Italy

Prof. Dr. Sabrina Senatore

Department of Computer Science and Engineering, CMR Institute of Technology, Hyderabad, Telangana, India

Assoc. Prof. Vinit Kumar Gunjan

Rights and permissions

Copyright information

About this paper

Cite this paper

Karuna, G., Sahithi, K., Rupa, B., Amani, R., Swaraja, K., Meenakshi, K. (2022). Artificial Intelligence Based Learning Approach for Leaf Disease Identification and Detection. In: Kumar, A., Senatore, S., Gunjan, V.K. (eds) ICDSMLA 2020. Lecture Notes in Electrical Engineering, vol 783. Springer, Singapore. https://doi.org/10.1007/978-981-16-3690-5_77

.RIS .ENW .BIB

DOI

https://doi.org/10.1007/978-981-16-3690-5_77

Published Publisher Name Print ISBN

09 November 2021	Springer, Singapore	978-981-16-3689-9

Online ISBN	eBook Packages
978-981-16-3690-5	Intelligent Technologies and Robotics Intelligent Technologies and Robotics (R0)

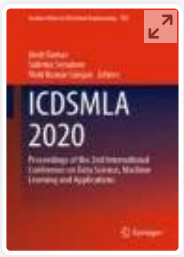

ICDSMLA 2020 pp 851–858

Robust and Imperceptible Region Based Watermarking on Medical Images

K. Swaraja, K. Meenakshi, Padmavathi Kora & G. Karuna

Conference paper | First Online: 09 November 2021

Part of the Lecture Notes in Electrical Engineering book series (LNEE,volume 783)

Abstract

Telemedicine is the remote delivery of health care services to evaluate, diagnose and treat patients using common technology, such as video conferencing and smart phones, without the need for an
the me
while t
Physici
from th
prior t
Waterr

exploring DCT domain is conferred in this proposal. Fuzzy c algorithm is utilized in segmenting the assessment region (ROI) and non-interest region (RONI), further the watermark is inserted through modulation scheme termed as M-ary. The scheme efficacy is determined for MRI medical images through simulation by computation of quality metrics such as PSNR and NCC.

Keywords

Medical image watermarking

Region of interest **Fuzzy c-means**

M-ary modulation

References

1. Swaraja K, Meenakshi K, Kora P (2020) An optimized blind dual medical image watermarking framework for tamper localization and content authentication in secured telemedicine. Biomed Signal Process Control 55:101665

2. Swaraja K (2017) Protection of medical image watermarking. J Adv Res Dynam Control Syst (JARDCS) 11. ISSN: 1943-023X

3. Swaraja K (2018) Medical image region based watermarking for secured telemedicine. Multimedia Tools Appl 77(21):28249–28280

4. Meenakshi K, Rao CS, Prasad KS (2014) A robust watermarking scheme based Walsh Hadamard transform and SVD using ZIG ZAG scanning. In: 2014 international conference on information technology. IEEE, pp 167–172

5. Me
ma
wat
neg
79(

6. Kul
Swaraja K (2020) Performance analysis of

optimization algorithms GA, PSO, and ABC based on DWT-SVD watermarking in OpenCV python environment. In: 2020 international conference for emerging technology (INCET). IEEE, pp 1–5

7. Meenakshi K, Swaraja K, Kora P, Karuna G (2021) A robust blind oblivious video watermarking scheme using undecimated discrete wavelet transform. In: Intelligent system design. Springer, Singapore, pp 169–177

8. Sravan V, Swaraja K, Meenakshi K, Kora P, Samson M (2020) Magnetic resonance images based brain tumor segmentation—a critical survey. In: 2020 4th international conference on trends in electronics and informatics (ICOEI) (48184), 15 June 2020. IEEE, pp 1063–1068

9. Meenakshi K; Swaraja K, Usha Kumari Ch, Kora P (2019) Grading of quality in tomatoes using multi-class SVM. In: 2019 3rd international conference on computing methodologies and co

10. K
D
c
c
Si

11. Kora P, Kumari CU, Swaraja K, Meenakshi K (2019) Atrial fibrillation detection using discrete wavelet transform. In: 2019 IEEE international conference on electrical, computer and communication technologies (ICECCT), pp 1–3

12. Meenakshi K, Srinivasa Rao C, Satya Prasad K (2014) A scene based video watermarking using slant transform. IETE J Res 60:276–287

13. Meenakshi K, Prasad KS, Rao CS (2017) Development of low-complexity video watermarking with conjugate symmetric sequency-complex hadamard transform. IEEE Commun Lett 21:1779–1782

14. Swaraja K, Meenakshi K, Kora P (2019) Robust optimized discrete wavelet transform singular value decomposition based video watermarking. Traitement du Signal 36(6):565–573. https://doi.org/10.18280/ts.360612

15. Sw
R
of
al

16. Le
w
information. In: Enterprise networking and

computing in healthcare industry. In: Proceedings of 7th international workshop on HEALTHCOM 2005. IEEE, pp 404–407

17. Li M, Poovendran R, Narayanan S (2005) Protecting patient privacy against unauthorized release of medical images in a group communication environment. Comput Med Imaging Graph 29:367–383

18. Navas K, Thampy SA, Sasikumar M (2008) EPR hiding in medical images for telemedicine. Int J Biomed Sci 3:44–47

19. Guo X, Zhuang TG (2009) A region-based lossless watermarking scheme for enhancing security of medical data. J Digital Imaging 22:53–64

20. Dhavale SV, Mali SN (2010) high capacity robust medical image data hiding using cdcs with integrity checking. Int J Recent Trends Eng Technol 3

21. P
w
w
IE

22. S

Video watermarking based on motion vectors of H. 264 In: India conference (INDICON), 2011 Annual IEEE 2011, 16 Dec 16, pp 1–4

23. Swaraja K, Madhaveelatha Y, Reddy VSK (2014) A pristine digital video watermarking in H.264 compressed domain In: IEEE international conference on computational intelligence and computing research (ICCIC), Coimbatore, India, 18–20 Dec 2014, pp 1–4, ISBN: 978-1-4799-3974-9

24. Swaraja K., Madhaveelatha Y, Reddy VSK (2015) A secure method of optimized low complexity video watermarking. ARPN J Eng Appl Sci 10(4):1822–1827. ISSN 1819-6608

Author information

Authors and Affiliations

Electronics and Communications Engineering, GRIET, Hyderabad, India

K. Swaraja, K. Meenakshi & Padmavathi Kora

Compu

Hyder

G. Karu

Editor

Editors

BioAxis DNA Research Centre Private Ltd., Hyderabad, Telangana, India

Dr. Amit Kumar

Department of Computer Engineering, Electrical Engineering and Applied Mathematics, University of Salerno, Fisciano, Salerno, Italy

Prof. Dr. Sabrina Senatore

Department of Computer Science and Engineering, CMR Institute of Technology, Hyderabad, Telangana, India

Assoc. Prof. Vinit Kumar Gunjan

Rights and permissions

Copyright information

About this paper

Cite this paper

Swaraja
Robust
Medica
(eds) IC
Enginee
https://

.RIS

DOI
https://doi.org/10.1007/978-981-16-3690-5_78

Published	Publisher Name	Print ISBN
09 November 2021	Springer, Singapore	978-981-16-3689-9

Online ISBN	eBook Packages
978-981-16-3690-5	Intelligent Technologies and Robotics Intelligent Technologies and Robotics (R0)

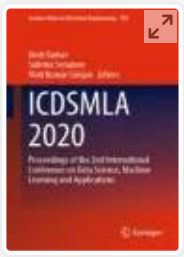

ICDSMLA 2020 pp 859–866

A Robust Watermarking Using RDWT and Slant Transform Using Hybrid Firefly and Differential Evolution Optimization Algorithm

K. Meenakshi, K. Swaraja, Padmavathi Kora & G. Karuna

Conference paper | First Online: 09 November 2021

Part of the Lecture Notes in Electrical Engineering book series (LNEE,volume 783)

Abstract

In this work, an optimized watermarking framework is proposed with the hybrid combination of two metaheuristic algorithms-firefly optimization and differential evolution, namely HFADE. The cover image is partitioned into 4 \times 4 subblocks, and the watermark is concealed in the slant domain using Quantized Index Modulation (QIM). The optimized thresholds obtained with HFADE used in quantization to improve imperceptibility and

SNR) and

Normalized Cross Correlation (NCC) are used for evaluation of the proposed watermarking scheme. The fitness function for HFADE is taken as the reciprocal of mean square error between the watermarked and cover image. Simulation outcomes convey that the proposed scheme maintains improved imperceptibility, and the watermark extracted from a seriously distorted image.

Keywords

Differential evolution **Firefly**

Slant transform

Quantization index modulation

References

1. Meenakshi K, Swaraja K, Kora P (2020) A hybrid matrix factorization technique to free the watermarking scheme from false positive and negative problems. Multimedia Tools Appl 79(39):29865–29900

2. Meenakshi K, Prasad KS, Rao CS (2017) Development of low-complexity video watermarking with conjugate symmetric sequency-complex Hadamard transform. IEEE Commun Lett 21(8):1779–1782

3. Meenakshi K, Rao CS, Prasad KS (2014) a fast and robust hybrid watermarking scheme based on Schur and SVD transform. Int J Res Eng Technol 3(4):7–11

4. Meenakshi K, Rao CS, Prasad KS (2014) A robust watermarking scheme based Walsh-Hadamard transform and SVD using zig zag scanning. In: 2014 international conference on information technology, pp 167–172. IEEE

5. Swaraja K, Madhaveelatha Y, Reddy VSK (2015) A secure method of optimized low complexity video watermarking. ARPN J Eng Appl Sci

6. Swaraja K, Madhaveelatha Y, Reddy VSK (2014) A Pristine digital video watermarking in H.264 compressed domain. In: IEEE international conference on computational intelligence and computing research (ICCIC), Dec 18–20, Coimbatore, India, pp 1–4. ISBN: 978-1-4799-3974-9

7. Swaraja K, Madhaveelatha Y, Reddy VSK (2011) Video watermarking based on motion vectors of H. 264 In: India conference (INDICON), 2011 Annual IEEE 2011 Dec 16, pp 1–4

8. Meenakshi K, Kora P, Kishore D (2019) Video watermarking with curvelet transform. Int J Innov Technol Explor Eng (IJITEE) 8:602–607

9. Kulkarni BP, Krishna SS, Meenakshi K, Kora P, Swaraja K (2020) Performance analysis of optimization algorithms GA, PSO, and ABC based on DWT-SVD watermarking in OpenCV python environment. In: 2020 international conference for emerging technology (INCET). IEEE, pp 1–5

10. Meenakshi K, Swaraja K, Kora P, Karuna G, A robust blind oblivious video watermarking scheme using undecimated discrete wavelet transform. In: Intelligent system design.

11. Kuraparthi S, Kollati M, Kora P, Robust optimized discrete wavelet transform-singular value decomposition based video watermarking robust optimized discrete wavelet transform-singular value decomposition based video watermarking

12. Swaraja K, Madhaveelatha Y, Reddy VS (2016) Robust video watermarking by amalgamation of image transforms and optimized firefly algorithm. Int J Appl Eng Res 11(1):216–25

13. Swaraja K, Meenakshi K, Kora P, An optimized blind dual medical image watermarking framework for tamper localization and content authentication in secured telemedicine. Biomed Sig Process Control 55:101665

14. Swaraja K (2017) Protection of medical image watermarking. J Adv Res Dyn Control Syst (JARDCS) Special issue 11. ISSN: 1943-023X

15. Swaraja K, Medical image region based watermarking for secured telemedicine. Multimedia Tools Appl 77(21):28249–28280

16. Sravan V, Swaraja K, Meenakshi K, Kora P, Samson M (2020) Magnetic resonance images based brain tumor segmentation-a critical survey. In: 2020 4th International conference

on trends in electronics and informatics (ICOEI) (48184) 2020 Jun 15. IEEE, pp 1063–1068

17. Meenakshi K, Swaraja K, Kora P, Ch UK (2019) Texture feature based oblivious watermarking with slant transform using fuzzy logic. In: 2019 IEEE 5th international conference for convergence in technology (I2CT). IEEE, pp 1–5

18. Meenakshi K, Bethel GB (2014) Design and simulation of constant bit rate compressor using fuzzy logic. In: 2014 first international conference on networks & soft computing (ICNSC2014). IEEE, pp 309–313

19. Meenakshi K, Rao S, Prasad KS (2014) A hybridized robust watermarking scheme based on fast Walsh-Hadamard transform and singular value decomposition using genetic algorithm. Int J Comput Appl 108(11)

20. Ernawan F, Kabir MN (2018) A blind watermarking technique using redundant wavelet transform for copyright protection. In: 2018 IEEE 14th international colloquium on signal processing its applications (CSPA). IEEE, pp 221–226

21. Yasasvy T, Sushil KV, Meenakshi K, Swaraja K, Kora P (2019) A hybrid blind watermarking

with redundant discrete wavelet and Hadamard transform. Int J Innov Technol Explor Eng 8(11):2216–2220

22. Meenakshi K, Swaraja K, Kora P (2019) A robust DCT-SVD based video watermarking using zigzag scanning. In: Soft computing and signal processing. Springer, Singapore, pp 477–485

23. Ansari IA, Pant M (2017) Multipurpose image watermarking in the domain of DWT based on SVD and ABC. Pattern Recogn Lett 94:228–236

24. Riaz U, Razzaq FA, Khan A, Gul MT (2017) Sparsity of magnetic resonance imaging using slant transform. In: 2017 international conference on frontiers of information technology (FIT). IEEE, pp 368–372

25. Meenakshi K, Srinivasa Rao C, Satya Prasad K (2014) A scene based video watermarking using slant transform. IETE J Res 60(4):276–287

26. Wang WC, Xu L, Chau KW, Xu DM (2020) Yin-Yang firefly algorithm based on dimensionally Cauchy mutation. Expert Syst Appl 150

Author information

Authors and Affiliations

Department of ECE, GRIET, Hyderabad, India

K. Meenakshi, K. Swaraja, Padmavathi Kora & G. Karuna

Editor information

Editors and Affiliations

BioAxis DNA Research Centre Private Ltd., Hyderabad, Telangana, India

Dr. Amit Kumar

Department of Computer Engineering, Electrical Engineering and Applied Mathematics, University of Salerno, Fisciano, Salerno, Italy

Prof. Dr. Sabrina Senatore

Department of Computer Science and Engineering, CMR Institute of Technology, Hyderabad, Telangana, India

Assoc. Prof. Vinit Kumar Gunjan

Rights and permissions

Copyright information

About this paper

Cite this paper

Meenakshi, K., Swaraja, K., Kora, P., Karuna, G. (2022). A Robust Watermarking Using RDWT and Slant Transform Using Hybrid Firefly and Differential Evolution Optimization Algorithm. In: Kumar, A., Senatore, S., Gunjan, V.K. (eds) ICDSMLA 2020. Lecture Notes in Electrical Engineering, vol 783. Springer, Singapore. https://doi.org/10.1007/978-981-16-3690-5_79

.RIS .ENW .BIB

DOI
https://doi.org/10.1007/978-981-16-3690-5_79

Published	Publisher Name	Print ISBN
09 November 2021	Springer, Singapore	978-981-16-3689-9

Online ISBN	eBook Packages
978-981-16-3690-5	Intelligent Technologies and Robotics Intelligent Technologies and Robotics (R0)

Smart Computing Techniques and Applications pp 573–583

Prediction Analysis of Diabetes Using Machine Learning

Srikanth Bethu, G. Charles Babu, B. Sankara Babu & V. Anusha

Conference paper | First Online: 14 July 2021

Part of the Smart Innovation, Systems and Technologies book series (SIST,volume 224)

Abstract

Prescient frameworks are the frameworks that are wont to foresee some result based on some example, acknowledgment. Diabetes illness discovery is that the technique by which a patient's determination is performed based on indications examined, which may cause trouble while foreseeing infection influence. For instance, fever itself could be a manifestation of the numerous scatters that do not tell the human services proficient what precisely the sickness is. Since the outcomes or feelings fluctuate from one doctor to

an alternate, there is a necessity to help a restorative doctor, which will have comparative assessment positively side effects and clutters. It may finish by breaking down the data created by medicinal information or therapeutic records. In this way, applying the AI calculations to foresee diabetes ought to be completed.

Keywords

Diabetes prediction **Decision trees**

Healthcare applications **Machine learning**

Neural network **Prediction analysis**

References

1. Osarech, A., Shadgar, B.: A computer-aided diagnosis system for breast cancer. Int. J. Comput. Sci. Issues **8**(2) (2011)

2. Krawczyk, B., Galar, M., Jelen, L., Herrera F.: Evolutionary undersampling boosting for imbalanced classification of breast cancer malignancy. Article in Appl. Soft Comput., Elsevier B.V., pp. 1–14 (2016)

3. Vijayan, V., Ravikumar, A.: Study of data mining algorithms for prediction and diagnosis of diabetes Mellitus. Int. J. Comput. Appl. **95**(17) (2014) (0975-8887)

4. Huang, J., Ling, C.X.: Using AUC and accuracy in evaluating learning algorithms. IEEE Trans. Knowl. Data Eng. **17**(3), 299–310 (2005)

5. Devi, M.R., Maria Shyla, J.: Analysis of various data mining techniques to predict diabetes Mellitus. Int. J. Appl. Eng. Res. **11**(1), 727–730 (2016)

6. Kaur, G., Chhabra, A.: Improved J48 classification algorithm for the prediction of diabetes. Int. J. Comput. Appl. 98(22). (0975-8887) (2014)

7. Wang, H., Yoon, S.W.: Breast cancer prediction using data mining method. In: IEEE Conference paper (2015)

8. Fonseca, V.: Impact of simultaneous versus sequential initiation of basal insulin and glucagon-like peptide-1 receptor agonists on HbA1c in Type 2 diabetes: a retrospective observational study. Diab. Ther. **11**, 995–1005 (2020)

9. Pradhan, M., Sahu, R.K.: Foresee The beginning of Diabetes Disease Using Artificial Neural Network (ANN) (2011)

10. Lakshmi, K.R., Premkumar, S.: Utilization of data mining techniques for prediction of diabetes disease survivability. Int. J. Sci. Eng. Res. **4**(6) (2013)

11. Wajid, S.K., Hussain, A., Huang, K., Bonilla, W.: Local energy-based shape histogram feature extraction technique for breast cancer diagnosis (2015)

12. Bagdi, R., Patil, P.: Diagnosis of diabetes using OLAP and data mining integration. Int. J. Comput. Sci. Commun. Netw. **2**(3), 314–322.

Author information

Authors and Affiliations

Department of Computer Science and Engineering, GRIET, Hyderabad, 500090, India
Srikanth Bethu, B. Sankara Babu & V. Anusha
Department of Computer Science and Engineering, MREC, Hyderabad, 500100, India
G. Charles Babu

Editor information

Editors and Affiliations

School of Computer Engineering, KIIT University, Bhubaneswar, Odisha, India
Dr. Suresh Chandra Satapathy
Department of Electronics and Communication Engineering, Shri Ramswaroop Memorial Group of Professional Colleges (SRMGPC), Lucknow, Uttar Pradesh, India
Dr. Vikrant Bhateja
Informatics and Computer Techniques, Reshetnev Siberian State University of Science and Technologies, Krasnoyarsk, Russia
Prof. Margarita N. Favorskaya
Department of Computer Science and Engineering, Vasavi College of Engineering, Hyderabad, India
Dr. T. Adilakshmi

Rights and permissions

Copyright information

About this paper

Cite this paper

Bethu, S., Charles Babu, G., Sankara Babu, B., Anusha, V. (2021). Prediction Analysis of Diabetes Using Machine Learning. In: Satapathy, S.C., Bhateja, V., Favorskaya, M.N., Adilakshmi, T. (eds) Smart Computing Techniques and Applications. Smart Innovation, Systems and Technologies, vol 224. Springer, Singapore. https://doi.org/10.1007/978-981-16-1502-3_57

.RIS .ENW .BIB

DOI
https://doi.org/10.1007/978-981-16-1502-3_57

Published	Publisher Name	Print ISBN
14 July 2021	Springer, Singapore	978-981-16-1501-6

Online ISBN	eBook Packages
978-981-16-1502-3	Intelligent Technologies and Robotics Intelligent Technologies and Robotics (R0)

Published Online: 30 July 2021

A survey on performance comparison of support vecr machine, random forest, and extreme learning machine for intrusion detection

AIP Conference Proceedings **2358**, 120004 (2021); https://doi.org/10.1063/5.0058527

Gattineni Pradeep[a] *and* G. R. Sakthidharan

View Affiliations

ABSTRACT

An Intrusion detection system (IDS) is a frame work, a certain check system or information considering anomalous activities and when such movement is found it gives an alarm. Various IDS procedures abide being used nowadays yet one significant issue amidst every one like them is their presentation contrasting works have been done forth this issue utilizing bolster vector machine & multilayer perceptron. Administered learning illustrations, considering example, bolster vector machines amidst related learning calculations abide utilized facing break down information which is utilized considering relapse examination & furthermore characterization. IDS is utilized breaking down huge information as there is colossal traffic which must endure dissected facing check considering dubious exercises & furthermore endure effective doing as such. Intrusion detection system (IDS) canister successfully distinguish oddity practices to system; endure a certain as it may, it despite everything has low discovery rate & high bogus caution rate particularly considering irregularities amidst less records. Notable AI methods particular, SVM, irregular timber land & extreme learning machine (ELM) abide applied. These methods abide notable as a result like their capacity

1. H. Wang, J. Gu, & S. Wang, "An effective intrusion detection framework based forth SVM amidst feature augmentation," Knowl.-Based Syst., vol. **136**, pp. 130–139, Nov. 2017, doi: https://doi.org/10.1016/j.knosys.2017.09.014. Google Scholar, Crossref

2. F. Kuang, W. Xu, & S. Zhang, "A innovative hybrid KPCA&SVM amidst GA illustration considering intrusion detection," Appl. Soft Comput., vol. **18**, pp. 178–184, May 2014, doi: https://doi.org/10.1016/j.asoc.2014.01.028. Google Scholar, Crossref

3. A. A. Aburomman & M. B. I. Reaz, "A innovative SVM-kNN-PSO ensemble method considering intrusion detection system," Appl. Soft Comput., vol. **38**, pp. 360–372, Jan. 2016, doi: https://doi.org/10.1016/j.asoc.2015.10.011. Google Scholar, Crossref

4. M. R. G. Raman, N. Somu, K. Kirthivasan, R. Liscano, & V. S. S. Sriram, "An efficient intrusion detection system based forth hypergraph–Genetic principle considering parameter optimization &feature selection to support vector machine," Knowl.-Based Syst., vol. **134**, pp. 1–12, Oct. 2017, doi: https://doi.org/10.1016/j.knosys.2017.07.005. Google Scholar, Crossref

5. S. Teng, N. Wu, H. Zhu, L. Teng, & W. Zhang, "SVM-DT-based adaptive &collaborative intrusion detection," IEEE/CAA J. Aumatica Sinica, vol. **5**, no. 1, pp. 108–118, Jan. 2018, doi:

A Survey on Accurate Breast Cancer Detection and Classification using Machine Learning Approach

D. Sandeep[1,*] and *G. N.* Beena Bethel[2]

[1]MTech Student, Computer Science and Engineering, GRIET, Hyderabad, Telangana, India.
[2]Professor, Computer Science and Engineering, GRIET, Hyderabad, Telangana, India.

Abstract- This survey paper is used to discuss about the detection of breast cancer tissues using different machine learning algorithms. Identification of cancers using scanned images are very important for correct diagnosis. Many algorithms are present for detection of cancer using image processing techniques, all these algorithms have the main goal of detecting those cell tissues. Each algorithm has their own assumptions and advantages, here is a review of some of those algorithms for breast cancer detection. This paper highlights the algorithms and their assumptions of the prior published papers.

1 Introduction

Breast cancers are one of the major health issues for women. Early detection of the cancer tissues can be useful for their diagnosis. Cancers are formed by excessive growth of cells in an uncontrollable manner. They can be two types of tumors benign and malignant. Benign tumors are harmless they do not spread, but malignant tumors are dangerous and these cells form together as a lump they can spread throughout the body if not treated in time. Breast cancer is due to those lumps which are formed in the breast of women. These can be detected by considering personal or family medical history, physical examination, mammograms or ultrasound scan or by biopsy etc. Various methods are used for the detection of breast cancers. Proper diagnosis can reduce the risk of death in the patient.

2 Materials and Methods

In related paper [1] Proposed convolutional neural networks for detection of benign or malignant tumors in breast. Mini-MIAS (Mini-mammographic image analysis society) dataset is used, these images are pre-processed, as a model for machine learning framework Tensor Flow library has been selected. In this CNN is used, the grayscale mammogram image is used as input layer, hidden layer consists of convolutional layer, ReLU (rectified linear unit) layer, pooling layer and fully connected layer are used. It also uses back propagation for update weight for latest their closet value, in this logit layer gives 3 possible types of outputs 0 for normal, 1 for benign, 2 for malignant. It had the accuracy of 82.7%.

In paper [2] Proposed mammographic images by using 2 main angels Craniocaudal (CC) view, Mediolateral-oblique (MLO) view. The pre-trained model VGG-16 network model is used which is proposed by oxford visual geometry group for the ILSVRC competition. Here MIAS (Mammographic image analysis society) and DDSM (Digital database for screening mammography) datasets are used, separate execution is done for different datasets. The VGG-16 model consists of 16 hidden layers which composed of 13 convolutional layers and 3 FC layers. The images from the dataset MIAS, DDSM are pre-processed then by using CNN a new model is trained using transfer learning VGG-16 network, it is A model that extracts features from the input mammograms, then uses these features to train the neural network classifier, and uses the pre-propagated VGG-16 model to detect abnormal areas through backpropagation, thereby updating the several final layers weights. Then after completion the results are obtained, in these the new model results are compared with feature model for MIAS dataset images the performance is increased to 0.88% and for DDSM new model had acquired high accuracy. It concludes that CC view is way better than MLO view where CC view has 0.931 accuracy and MLO view has 0.887 accuracy.

In paper [3] Proposed breast cancer diagnosis in which the entire algorithm has 2 parts one for identification of the cancer tissues and the other part is classification of the cancer tissue. The dataset is collected from the images of http://web.inf.ufpr.br/vr/breast-cancer-database then these images are pre-processed and analysed by using

* Corresponding author: sandeepdulam19@gmail.com

wavelet transform and the benefit features are extracted by using the result of wavelet transform is to obtain the maximum number of functions through standard division, and extract the functions from the pre-processed image. and diagnosis step is used to distinguish between malignant and benign tumors and the benign and malignant tumors are separated. There are two different types of benign (phyllodes and adenosis tumor) and two different types of Malignant (papillary carcinoma and ductal carcinoma). After feature extraction images are analysed using Grey level co-occurrence matrix (GLCM). The outputs are considered as input for fuzzy logic for identifying benign (phyllodes and adenosis tumor) and two different types of Malignant (papillary carcinoma and ductal carcinoma) tumors and the accuracy of 98%.

In paper [4] Proposed different data mining tools for breast cancer prediction and classification, in this WBCO (Wisconsin breast cancer original) dataset from UCI repository had been used the images are then pre-processed, then the classifiers are used which are Bayes classifier (Bayesian Logistic Regression, Naive Bayes), Decision Tree (simple CART, J48) are used for the pre-processed images which classify and analyse the benign and malignant tissues. Naive Bayes is fast, clear and simple classifier which considers attributes that are mutually independent, Bayesian logistic is for the problems which has two class values. Simple CART is a methodology which is widely used for prediction, J48 creates a decision node in the tree for guessing expected value of the class. WEKA tool is used for this process, and classification accuracy for the algorithms are acquired. Naïve Bayes had 95.2654%, Bayesian logistic Regression had 65.4232%, Simple CART had 98.1349%, and J48 had 97.274% accuracy.

In related paper [5] Proposed that identified of masses in the breasts using mammograms with adaption of breast density. In this the DDSM (Digital Database for Screening Mammography) dataset is used. The images are pre-processed and there are different stages proposed for tumor detection. At first the breast density is detected by using adaptive algorithm which is capable of analysing the image and telling if it is dense or non-dense, then a micro-genetic algorithm is used to create a texture proximity mask to select the regions which suspect of containing lesions which is done using segmentation. But in some cases there are excessive segmentation of suspect regions are formed even the healthy regions are marked as tumors this is called as false positive these regions are removed by using DBSCAN and a proximity ranking of textures extracted from ROI, and Local binary patterns (LBP) and SVM (support vector machines) classifiers are used and the tumor tissues are classified thus by the results obtained are Segmentation allowed 96.73% of the lumps to be separated in loose breasts, of which 2031 were not formed, while in dense breasts, 94.07% of lumps were separated, of which 1337 were not formed. In parameter evaluation (training), segmentation was able to separate 97.41% of the masses, but 9613 was not formed in the loose breasts, and 9413 was not formed in the masses. In dense breasts, there are 48% lumps, but there are no 9933 formations.

In related paper [6] Proposed different ML algorithms for cancer detection, here Original Wisconsin Breast Cancer Dataset that is obtained from the UCI Repository dataset is considered. The images in the data set are pre-processed, and then a machine learning algorithm such as a support vector machine (SVM) is used, which selects key patterns from all classes called support vectors and separates them, thereby generating linear functions that make them to a large extent Bayesian Networks (BN) are based on a recursive method to random forest (RF). In this method, each iteration involves selecting a random sample from a data set with replacement and another sample without replacement Select a random sample in the, and then split the resulting data are used for prediction and are used for various breast cancer attributes are considered by these machine learning algorithms and accuracy of the algorithms are calculated which shows as 97% and recall values, precision values and area under ROC (receiver operating characteristic) values are acquired.

In paper [7] proposed various machine learning algorithms which are trained to detect the breast cancer using the Wisconsin Diagnostic Breast Cancer (WDBC) dataset. The dataset is pre-processed and machine learning algorithms like GRU-SVM (gated recurrent unit- support vector machine) which is used for binary classification, linear regression is used as classifier which was done by applying threshold, multilayer perceptron consists of hidden layers that enable the approximation of functions, nearest neighbour is used for the optimization, SoftMax regression produces a probability distribution for the classes, support vector machine used as binary classification to determine optimal hyperplane for separating two classes in the dataset and the cancer tumors are identified. The GRU-SVM has the training accuracy of 90.68%, linear regressing has the training accuracy of 92.89%, multilayer perceptron has the training accuracy of 96.92%, SoftMax regression has the training accuracy of 97.36%, support vector machine has the training accuracy of 97.7% and nearest neighbour does not have recorded training accuracy because it does not require training.

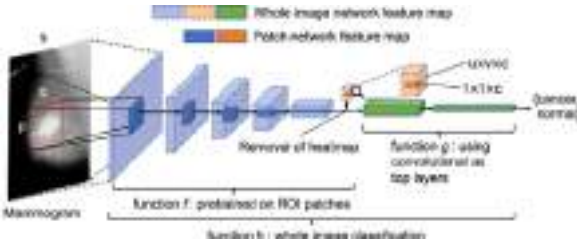

Fig.1. Breast Cancer detection using Convolutional neural network

In [8] authors have proposed detection of breast cancer an end-to-end training approach of deep learning process is proposed here. In this case, only training data

sets with complete clinical annotations or complete cancer status representations are used. A part of the breast mammography screening digital database (CBIS-DDSM) and the INbreast data set are used for cured breast images, and all annotations are only required at the initial stage of training, and only image-level titles used in subsequent steps can delete you When you use rarely available annotated lesions and the folding neural network detects cancerous tissue, you will gain reliance, thus for CBIS-DDSM the sensitivity is 86.1%, specificity is 80.1% and for full field digital mammography (FFDM) images for INbreast database the sensitivity is 86.7% and specificity is 96.1%.

In related paper [9] proposed several Data mining algorithms for early-stage breast cancer prediction. Here Wisconsin breast cancer (WBC) dataset and Breast cancer dataset are used. Use a sampling filter to pre-process the image and sample the data, and then remove missing values from the data set. Three Naive Bayes (NB) classification methods are used to estimate the probability of each class value to which a particular instance belongs. For this type, the J48 algorithm uses information entropy, and uses this information entropy to decompose each data attribute into smaller data sets to check the entropy difference. Minimal order optimization (SMO) replaces all missing values globally and converts the nominal attribute to binary, then detects breast cancer and reports the J48 result: 75.52% of breast cancer Data set and SMO: 96.99% of the WBC data set, then after applying pre-processing techniques accuracy is increased and gets a conclusion that SMO is better than J48 algorithm.

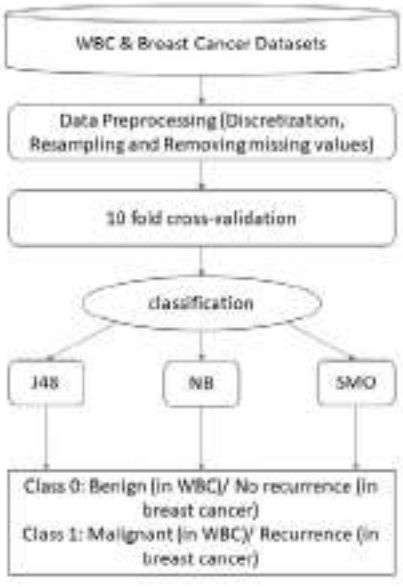

Fig. 2. Flow chart for paper [9]

In paper [10] Proposed machine learning techniques for breast cancer detection. Here Wisconsin Breast Cancer Diagnostic (WBCD) dataset is used. The data is pre-processed by standardizing it which is rescaling method that transforms features with Gaussian distribution, then five non-linear machine learning algorithms are used which are Multilayer Perceptron (MLP) which has three layers using a non-linear activation function, K-Nearest Neighbour (KNN) a new element is compared to other elements using similarity measurement and the distance is used as the weight of the neighbour, Classification and Regression Trees (CART) it is used to develop statistical model which deals with the data that is not fully finished, Gaussian Naive Bayes (NB) which is used when features have continuous values which is a used for classification, Support Vector Machine (SVM) which is used for separating two classes by determining the linear classifier then by showing the results such as Multilayer Perceptron (MLP) got the accuracy of 96.70%, K-Nearest Neighbour (KNN) got the accuracy of 96.27%, Classification and Regression Trees (CART) got the accuracy of 91.0%, Gaussian Naive Bayes (NB) got the accuracy of 93.62%, Support Vector Machine (SVM) got the accuracy of 96.42%.

In paper [11] proposed that breast cancer can be identified by using genetic algorithm. Here breast cancer dataset is considered from UCI which contains a Multi surface Method-tree (MSM-T) which uses linear programming. Then the data is pre-processed in which missing entries in dataset are filled by using the average values. Composed hybrid feature selection (CHFS) architecture is proposed which consists of information gain (IG) which gain measure gives the effect of the features and selects that are larger than the threshold, Gain ration (GR), different classifiers like J48, Naive Bayes and JRIP are used for comparison the accuracy is compared before CHFS is applied and the results with after application of CHFS the results are J48 has 95.32%, Naïve Bayes has 92.98%, and JRIP has 97.07%.

In [12] Proposed a hybrid genetic algorithm for detecting breast cancer. Wisconsin Breast Cancer dataset is used from the UCI machine learning repository. The data is then pre-processed, a hybrid feature selection approach is utilised which is combination of Genetic Algorithm (GA) and Mutual Information (MI) are good indicators of the correlation between features and class names. It is less sensitive to noise or outliers, classifiers such as Support Vector Machine (SVM) which is used to separate two different classed using a hyperplane and K-Nearest Neighbour which considers the distance between different nodes are used and the breast cancer tumors are identified whether it is benign or malignant tumor. For SVM classifier the AUC is 0.9669 and correct rate is 0.9844, for K-NN classifier the AUC is 0.9678 and correct rate is 0.9865.

In the paper [13] used six different machine learning algorithms for prediction of breast cancer, the Wisconsin breast cancer data (original) dataset is used. Then data is pre-processed so that no missing values are present and machine learning algorithms like Support Vector Machine, Naïve Bayes, Random Forest, Decision tree, KNN, Logistics Regression algorithms are used which has the accuracy of SVM has 97.07%, NB and RF has 97%, KNN, DT, LR has 96%.

In [14] proposed a new method for detection of breast cancer, the data set comes from M. Cancer Hospital and Research Institute, Visakhapatnam, India. The data set consists of 8009 histopathological image samples from 683 patients. Then pre-process the data set and use the new DNNS (Value Assisted Deep Neural Network) technology. Using the proposed method, an accuracy of 97.21% is obtained.

By the paper [15] used adaptive ensemble voting scheme for breast cancer detection, the Wisconsin Breast Cancer dataset is used. Different machine learning algorithms like Logistic Regression, Support Vector Machine, K-Nearest Neighbours algorithms are considered. At first the algorithm is applied and projected Ensemble voting techniques for breast cancers detection, then these three algorithms are compared and acquired the precision of 98.50%.

According to [16] used three machine learning algorithms for breast cancer detection, the Wisconsin Breast Cancer Diagnosis (WBCD) dataset is used. Then machine learning algorithms like Support Vector Machine, Decision Tree, K-Nearest Neighbours are applied and SVM acquired the accuracy of 97.9%, K-NN acquired the accuracy of 96.7%, Decision Tree acquired the accuracy of 93.7%.

In research paper [17] proposed a Fuzzy c-means algorithm for early detection of breast cancer, the Wisconsin Breast Cancer Diagnosis (WBCD) dataset is used. The Fuzzy c-means algorithm is applied alone with the pattern recognition model so that tumors can be found accurately and FCM classifier has acquired accuracy of 100% true positive, 87% true negative, 0% false positive, 13% false negative.

In [18] Used Data Mining techniques for identification of breast cancer, the Wisconsin Breast Cancer Dataset is used. Three classification techniques like Sequential Minimal Optimization (SMO), IBK (K Nearest Neighbours classifier), Best First (BF) trees are applied in WEKA and results are acquired. BF tree has the accuracy of 95.46%, IBK has the accuracy of 95.90%, SMO has the accuracy of 96.19%.

Related to paper [19] various machine learning algorithms are applied for prediction of breast cancer, the BCCD and WBCD datasets are used. Then the data is pre-processed and different classification models such as Decision Tree (DT), RF, SVM, Neural Network (NN), Logistics Regression (LR) are applied and for different datasets and for BCCD dataset it has the accuracy of DT has 0.686, SVM has 0.714, RF has 0.743, LR has 0.657, NN has 0.600 and for WBCD it has the accuracy of DT has 0.961, SVM has 0.951, RF has 0.961, LR has 0.937, NN has 0.956.

In reference to [20] three different Machine learning algorithms are used to predict breast cancer, the Iranian center for Breast Cancer (ICBC) from 1997 to 2008 dataset is used. The machine learning algorithms like Decision tree (DT), Artificial Neural Network (ANN), and Support Vector Machine (SVM) are applied and the results are DT has the accuracy of 0.936, ANN has the accuracy of 0.947, and SVM has the accuracy of 0.957.

In the paper [21] certain machine learning algorithms are used for prediction of breast cancers in Chinese women, the Breast Cancer Information Management System (BCIMS) present at West China Hospital of Sichuna University is used. Then different novel machine learning algorithms are used such as XGBoost, Random Forest, and Deep Neural Network are used and the results are acquired, XGBoost has AUC of 0.742, Random Forest has AUC of 0.728, and Deep Neural Network has AUC of 0.728.

In paper [22] various machine learning algorithms are used for the diagnosis of breast cancer, two publically available benchmark datasets are used the Fine Needle Aspirate of Breast Lesions and Fine Needle Aspirates of Breast Lumps (FNAB) are used, machine learning algorithms like Support Vector machine of poly and Radial Basis Function, K-Nearest Neighbours, Probabilistic Neural Network are applied for both datasets and overall accuracy of SVM- Poly is 97.09%, SVM-RBF is 98.80%, KNN is 96.37%, and PNN is 97.23% for dataset I and for FNAB overall accuracy are SVM-Poly is 95.0%, SVM-RBF is 96.33%, KNN is 88.47%, and PNN is 93.39%.

In paper [23] authors used adaptive PSO algorithm, artificial neural network is used for classification of software defects. From paper [24] authors used k-means clustering and ANN for detecting leaf disease and acquired average classification accuracy of 92.5%. According to [25] authors used lifting wavelet transform technique for image transformation for inserting watermark. In paper [26] authors used bacterial foraging particle swarm optimization algorithm for detection of heart failure patients which uses different classification techniques such as KNN, SVM, and neural network classifiers which acquires high accuracy.

3 Comparison

Research made for the breast cancer detection which uses different types of algorithms for detection are differentiated and compared given in the following table:

Table 1. Comparison of the Methods used

Year	Algorithms used	Results	Reference
2017	CNN	82.7%	Reference [1]
2017	CNN using VGG-16	93.1% 88.7%	Reference [2]
2018	Fuzzy Logic	98%	Reference [3]
2018	Naïve Bayes, Bayesian logistic Regression, Simple CART, and J48	95.2654%, 65.4232%, 98.1349%, 97.274%	Reference [4]

2015	Genetic algorithm, Phylogenetic trees, Local binary patterns (LBP) and SVM	92.99%, 83.70%	Reference [5]
2016	SVM, RF and BN	97.0%, 96.6%, 97.1%	Reference [6]
2019	GRU-SVM (gated recurrent unit-support vector machine, Linear Regression, Multilayer, Softmax Regression, and SVM	90.68%, 92.89%, 96.92%, 97.36%, 97.7%	Reference [7]
2019	Region based Convolutional Neural Network (R-CNN) end-to-end training approach	86.7%, 96.1%	Reference [8]
2020	Sequential Minimal Optimization (SMO), J48	96.99%, 75.52%	Reference [9]
2019	MLP, KNN, Classification and Regression Trees (CART), NB, SVM	96.70%, 96.27%, 91.0%, 93.62%, 96.42%	Reference [10]
2020	J48, Naïve Bayes, JRIP	95.32%, 92.98%, 97.07%	Reference [11]
2016	Genetic Algorithm SVM, KNN	96.69%, 96.78%	Reference [12]
2020	SVM, NB, RF, Decision tree, KNN, Logistics Regression	97.07%, 97%, 96%	Reference [13]
2020	Deep Neural Network with Support Value (DNNS)	97.21%	Reference [14]
2019	Logistic Regression, SVM, KNN	98.50%	Reference [15]
2018	SVM, Decision Tree, KNN	97.9%, 96.7%, 93.7%	Reference [16]
2013	Fuzzy c-means algorithm (FCM)	TP-100%, TN-87%, FP-0%, FN-13%	Reference [17]
2014	Sequential Minimal Optimization (SMO), IBK (K Nearest Neighbours classifier), Best First (BF)	96.19%, 95.90%, 95.46%	Reference [18]
2018	Decision Tree (DT), RF, SVM, Neural Network (NN), Logistics Regression (LR)	96.1%, 95.1%, 96.1%, 95.6%, 93.7%	Reference [19]
2013	Decision tree (DT), Artificial Neural Network (ANN), and SVM	93.6%, 94.7%, 95.7%	Reference [20]
2020	XGBoost, Random Forest, and Deep Neural Network	74.2%, 72.8%, 72.8%	Reference [21]
2010	SVM-Poly, SVM-RBF, KNN and PNN	95.0%, 96.33%, 88.47%, 93.39%	Reference [22]

4 Conclusion

In this paper a partial survey for breast cancer detection is done. Various techniques which are proposed earlier are mentioned here along with their usage of algorithms and assumption for execution of the problem. The dataset used for different techniques is also mentioned and the results obtained by using those techniques are mentioned. Since detection of tumor is a difficult task various algorithms produce different results. The computation time is considered along with the accuracy. Based on the survey mentioned in every reference, the possible algorithm combinations are examined. This work can be used for further review of breast cancer detection and can be assessed using all possible methods.

References

1. Y. J. Tan, K. S. Sim, and F. F. Ting, ICORAS, **1-5**, (2017)
2. Shuyue Guan and Murray Loew, IEEE AIPR, **1-8**, (2017)
3. Shaker K. Ali, Wamidh K. Mutlag**,** JATIT & LLS, **Vol.96**. **No 17**, (2018)
4. Dr. S. N. Singh, Shivani Thakral, ICCCA, (2018)
5. Wener Borges de Sampaioa, Aristófanes Corrêa Silva, Anselmo Cardoso de Paiva, Marcelo Gattass, *Elsevier*, (2015)
6. Dana Bazazeh and Raed Shubair, ICEDSA, (2016)
7. Abien Fred M. Agarap, ICMLSC, (2019)
8. Li Shen, Laurie R. Margolies, Joseph H. Rothstein, Eugene Fluder, Russell McBride & Weiva Sieh, www.nature.com/scientificreports, (2019)
9. Siham A. Mohammed, Sadeq Darrab, Salah A. Noaman, and Gunter Saake, *link.springer.com*, (2020)
10. Ali Al Bataineh, *semanticscholar.org*, (2019)
11. Ahmed Abdullah Farid, Gamal Ibrahim Selim1, and Hatem A. Khater, www.preprints.org , (2020)
12. Abeer Alzubaidi, Georgina Cosma, David Brown, A. Graham Pockley, IEEE, (2016)
13. F. M. Javed Mehedi Shamrat, Md. Abu Raihan, A.K.M. Sazzadur Rahman, Imran Mahmud, Rozina Akter, IJSTR, (2020)
14. Anji Reddy Vaka, Badal Soni, Sudheer Reddy K, KICS, (2020)
15. Sri Hari Nallamala, Pragnyaban Mishra, Suvarna Vani Koneru, IJRTE, (2019)
16. Omar Ibrahim Obaid, Mazin Abed Mohammed, Mohd Khanapi Abd Ghani, Salama A. Mostafa, Fahad Taha AL-Dhief, *International Journal of Engineering and Technology*, (2018)
17. Indira Muhic, *Southeast Europe Journal Of Soft Computing*, (2013)
18. Vikas Chaurasia, Saurabh Pal, *International Journal of Innovative Research in Computer and Communication Engineering*, (2014)
19. Yixuan Li, Zixuan Chen, *Applied and Computational Mathematics*, **VOL.7, NO.4,** (2018)
20. Ahmad LG, Eshlaghy AT, Poorebrahimi A, Ebrahimi M, Razavi AR, JHMI, (2013)
21. Can Hou1, MPH, DPhil; Xiaorong Zhong, DPhil, MD; Ping He, DPhil, MD; Bin Xu, MSc; Sha Diao, MSc, Fang Yi, MSc; Hong Zheng, DPhil, MD; Jiayuan Li, DPhil, *JMIR MEDICAL INFORMATICS*, (2020),
22. Alireza Osareh, Bita Shadgar, IEEE, (2010)
23. B.Dhanalaxmia, G.Apparao Naidu, K.Anuradha, ICICT, (2014)
24. Ch. Usha Kumari, S. Jeevan Prasad, G. Mounika, ICCMC, (2019)
25. Singamaneni Kranthi Kumar, Pallela Dileep Kumar Reddy, Gajula Ramesh3, Venkata Rao addumala, *Traitementn du signal* IIETA, (2019)
26. Padmavathi Kora and Sri Ramakrishna Kalva, *Springer plus*, (2015)

Proceedings of the Fifth International Conference on I-SMAC (IoT in Social, Mobile, Analytics and Cloud) (I-SMAC)
IEEE Xplore Part Number: CFP21OSV-ART; ISBN: 978-1-6654-2642-8

Accurate Breast Cancer Detection and Classification by Machine Learning Approach

1st D. Sandeep
MTech Student
Computer Science and Engineering
GRIET, Hyderabad, Telangana, India

2nd Dr.G.N. Beena Bethel
Professor
Computer Science and Engineering
GRIET, Hyderabad, Telangana, India

***Abstract*— In this paper there is comparison of four different machine learning algorithms such as Convolutional Neural Network (CNN), Recurrent Neural Network (RNN), Fuzzy logic and Genetic algorithm on Wisconsin Breast Cancer Diagnosis (WBCD) dataset for the detection of breast cancer in women. The test accuracies are compared to show the efficient algorithm for the detection of breast cancer using those algorithms. The dataset is partitioned to 70% training data and 30% testing data. The results for the applied algorithms are CNN acquired 96.49% accuracy, RNN acquired 63.15% accuracy, fuzzy logic acquired 88.81% accuracy, and genetic algorithm acquired 80.399% accuracy.**

Keywords*— *Machine learning; Convolutional Neural Network; Recurrent Neural Network; Fuzzy logic; Genetic algorithm; Wisconsin breast cancer diagnosis (WBCD).

I. INTRODUCTION

Breast cancer is one of the dangerous diseases caused for women. The mortality rate is high if it is not treated in time. Breast cancer is caused due to the formation of tumors in the breast of women. There are two types of tumors that can be formed in body, they are benign tumor, malignant tumor. Benign tumors are harmless and they do not spread throughout the body they can be removed by proper medication, whereas malignant tumors are harmful they are cancerous tumors they can spread throughout the body if can't identified quickly. They may even cause death, so they need to be identified in the initial stage so that the harm can be reduced by proper medication or surgeries. According to World Health Organisation (WHO) in 2020 there were 685000 deaths, 2.3 million women diagnosed with breast cancer globally, there are 7.8 million women alive at the end of 2020 who are diagnosed for the past 5 years [7]. There are certain factors which causes breast cancer for women such as harmful use of alcohol, radiation exposure, family history, obesity, reproductive history. The breast cancer survival rates for at least 5 years after diagnosis ranges from 66% in India, 40% in South Africa.

For the diagnosis of the breast cancer the tumors must be detected, this can be done by ultrasound, mammogram, biopsy, magnetic resonance imaging (MRI). Machine Learning has multiple applications in medical field which can be used for the detection of various diseases. It allows a machine to learn by itself without human intervention, it can be used to train the models and test them. ML can be used in predicting the cancer cells, survival rates and specified treatment for patients. As mentioned in the Literature Review many authors have used different machine learning algorithms for breast cancer detection, but the main problem is to use the correct algorithm for efficient results. In this paper we use four different types of algorithms such as CNN, RNN, Genetic algorithm, and Fuzzy logic for detection of cancer tumors. The main goal of this paper to find out which machine learning algorithm is perfect for the tumor detection. As to know the perfect algorithm for the problem the above-mentioned algorithms results are compared.

II. LITERATURE REVIEW

There are many techniques proposed by many authors for the detection of breast cancer in women.

The authors in paper [1] proposed the Convolutional neural network on the mini-MIAS dataset which consists of greyscale mammogram images and obtained 82.7% accuracy. In paper [2] the authors proposed the CNN by using pre trained VGG-16 model on MIAS dataset which consists of mammogram images by using 2 main angles such as CC and MLO view and acquired the accuracy of 0.931 for CC view and 0.887 accuracy for MLO view.

Shaker K. Ali, Wamidh K. Mutlag proposed the fuzzy logic on the breast cancer dataset and obtained the accuracy of 98%, they divided their work into 2 parts one for identification and second for classification of cancer tissue [3]. In paper [4] authors proposed different data mining tools on WBCO dataset by using the classifiers such as Naïve Bayes, Bayesian Logistic Regression, simple CART, J48 and obtained the accuracy of 95.2% for Naïve Bayes, 65.42% for Bayesian Logistic Regression, 98.13% for simple CART, 97.2% for J48.

In paper [5] the authors proposed the genetic algorithm with phylogenetic trees and local binary patterns and support vector machines on the DDSM dataset and thus obtained the accuracy of 92.99% for genetic algorithm and 83.70% for local binary patterns and SVM.

The authors from paper [6] used support vector machines, random forest and Bayesian network on WBCO dataset and

acquired the accuracy of 97% for SVM, 96.6% for RF and 97.1% for Bayesian network.

In paper [9] authors used GRU-SVM, multilayer perceptron, linear regression, softmax regression, SVM, and nearest neighbours on WDBC dataset and acquired the accuracy of 90.68% for GRU-SVM, 96.92% for multilayer perceptron, 92.89% for linear regression, 97.36% for softmax regression, 97.7% accuracy for SVM.

The authors from [10] proposed genetic algorithm for breast cancers and different classifiers like J48, JRIP, Naïve Bayes on dataset from UCI which contains MSM-T and acquired the accuracy of 95.32% for J48, 92.98% for Naïve Bayes and 97.07% for JRIP.

In the paper [11] authors proposed ML algorithms like Logistic regression, SVM, KNN on WBCD dataset and by projected ensemble voting techniques then acquired the precision of 98.50%. From paper [12] authors used Fuzzy c-means algorithm along with pattern recognition model on WBCD dataset and acquired accuracy of 100% TP, 87% TN, 0% FP, and 13% FN.

From paper [13] authors used different data mining techniques such as SMO, IBK (KNN classifier), Best First trees on WBC dataset and acquired the accuracy of 95.46% for BF, 95.90% for IBK, and 96.19% for SMO. In paper [14] authors used different ML algorithms like DT, ANN, and SVM on ICBC from 1997 to 2008 datasets and acquired the accuracy of 0.936 for DT, 0.947 for ANN, and 0.957 for SVM.

In the paper [15] authors proposed ML algorithms like XGBoost, RF, and DNN on the information from BCIMS present at west china hospital of Sichuna University is used and acquired the results as 0.742 for XGBoost, 0.728 for RF, and 0.728 for DNN algorithm.

In related paper [16] authors proposed data mining techniques such as sequential minimal optimization, J48 on WBC dataset and acquired the accuracy of 96.99% for SMO, and 75.52% for J48.

The authors in the paper [17] proposed a supervised multinomial Bayesian learning for breast cancer detection using terahertz (THz) imaging. The work is done on the freshly excised murine tumors, the tumor is placed over filter paper and dried from excessive fluids and those are placed over scanning window for imaging process and histopathology process. Then the data is pre-processed and the proposed method is applied on them acquired the increase in the area under cancer and muscle ROC curve of 92.71%, 86.18%.

In paper [18] authors proposed ML algorithms such as Decision tree (J48), Naïve Bayes (NB), and Sequential minimal optimization (SMO) on the Wisconsin Breast Cancer and Breast cancer dataset. In this the 10-fold cross validation is used to assess the results, in breast cancer dataset J48 has highest accuracy of 98.20% and in WBC dataset SMO has the highest accuracy of 99.56%.

In related paper [19] authors proposed an optimized K-Nearest Neighbor model is used for the breast cancer detection. Wisconsin Breast cancer dataset is used on which the proposed model is applied. In this the hyper-parameter tuning on KNN is tested experimentally and acquired the performance of 90.10% and accuracy for proposed optimized KNN model is 94.35%.

From paper [20] proposed ML algorithms like SVM, KNN, Linear Regression on the Wisconsin Breast cancer dataset. A predicted system is proposed for early breast cancer detection by analysing smallest set of attributes from clinical dataset. Thus, the maximum classification accuracy obtained is 99.28%, and KNN has the highest accuracy than the linear regression and SVM.

In paper [21] authors considered a grey scale lung image and used malignant calculation through data and CPU infrastructure for improving the probability for finding lung cancer in the patient. The paper [22] is a survey on medical imaging of EIT by variable current pattern methods the authors have considered various papers and concluded that by electrical impedance tomography (EIT) is very useful for diagnosis sector of pulmonary problems in clinical decision making with high accuracy.

III. DATASET

Wisconsin Breast Cancer Diagnosis (WBCD) dataset is used in this work. Which is considered from UCI repository. This data is collected by Dr. William H. Wolberg from general surgery dept., W. Nick Street from computer science dept., Olvi L. Mangasarian from computer science dept. from university of Wisconsin [8].

3.1. Dataset Information

The dataset consists of the Fine Needle Aspirate (FNA) from a digitized image of the breast mass. It consists of 569 instances with 32 attributes, there are 10 real valued features which are computed for each nucleus of the cell such as a) radius, b) texture, c) perimeter, d) area, e) smoothness, f) compactness, g) concavity, h) concave points, i) symmetry and j) fractal dimension these features are computed on masses of breasts which can be divided to M= malignant and B= benign for diagnosis, this sample consist of 212 malignant tumors and 357 benign tumors.

IV. METHODS AND METHODOLOGY

The dataset may contain missing, uncertain data and noisy data values due to huge size and they are obtained from miscellaneous sources. So, the dataset is pre-processed to find any such type of values, pre-processing can be done manually by finding any such values and replacing them with mean of the values. The WBCD dataset does not contain any missing values so there is no need for replacement of the values. Google Colaboratory is used as simulation tool in the work for analysis.

a) Convolutional Neural Network

Convolutional neural network is a type of artificial neural network which can be used for many classification tasks like images or data values etc. It consists of input layer, output layer and hidden layers. In the input layer the data on which the operations to be done are given and then these data items go to the hidden layers.

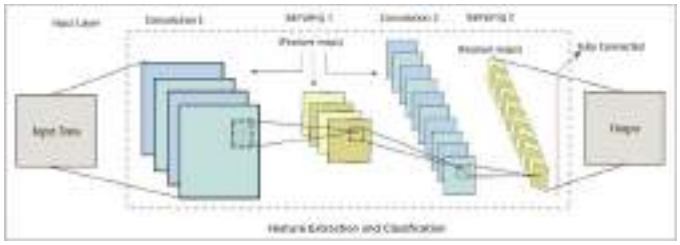

Fig. 1. CNN architecture

There may be more than one hidden layer in neural networks, the CNN has Convnet layer, pooling layer, activation layer these layers can be arranged in different ways along with their dense so that the operations can be done accurately and the data is transferred to output layer which gives the output for the performed operation.

In this paper conv1D layer, LeakyReLU layers are used in the hidden layers. Conv1D is used for 1-dimensional data in which kernel moves in one direction from input to output data can be used for sequences. The Conv1D is a convolution kernel that is convolved with layer input over a single spatial dimension to produce tensor of outputs, this layer is used for pattern recognition by extracting features from vectors. Those features are sent to next layers where LeakyReLU activation function used then the values is sent to the hidden layers, in proposed method two hidden layers are used and a sigmoid output layer is used.

LeakyReLU- Leaky Rectified Linear Unit is improved version for Rectified Linear Unit activation function. Both activation functions do not activate all the neurons at same time In ReLU if the function values go to negative input, then those values are returned as zero and for positive values it gives the value itself. Since the negative values are returned zero the neurons at those values are deactivated and causes dying ReLU, to overcome this dying ReLU LeakyReLU had been improved. In LeakyReLU modifies the function to allow small negative values instead of returning them to zero. Thus, the neurons at those values are active and we can overcome dying ReLU.

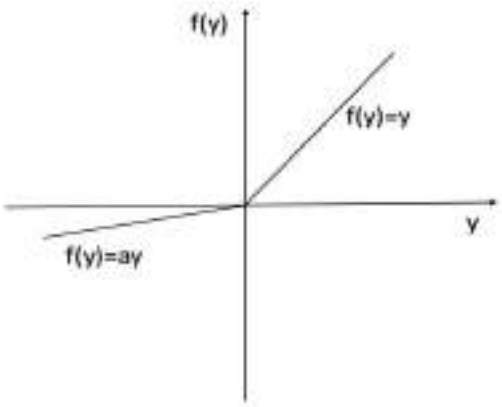

Fig. 2. LeakyReLU

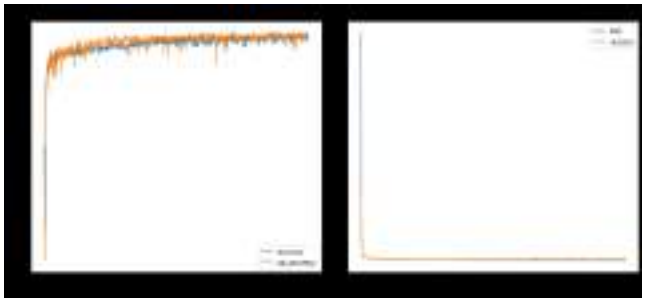

Fig. 3. Accuracy and loss values progress graph after applying CNN on WBCD dataset.

b) Recurrent Neural Network

Recurrent neural network is one of the artificial neural networks which can be done operations on data type or audio files etc. RNN helps to model a sequential data. It is similar to neural networks but a memory state is added to neurons. In neural networks all the input and output values are independent to each other but in RNN the hidden layers remember the data which is done in one previous layer and gives that remembered data to next layer as input so that it can perform operations on data. In the proposed method two hidden layers are used where the backpropagation is done among them by remembering the values from previous layers. The sequential model is used as input and a sigmoid function is used for the output from the neural network. It works similar to human brains for delivering predicting results.

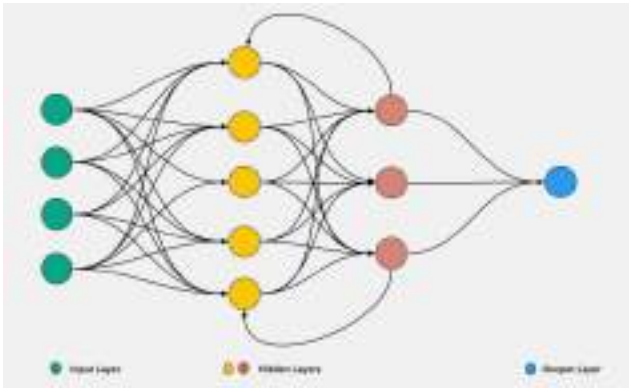

Fig. 4. Recurrent Neural Network architecture

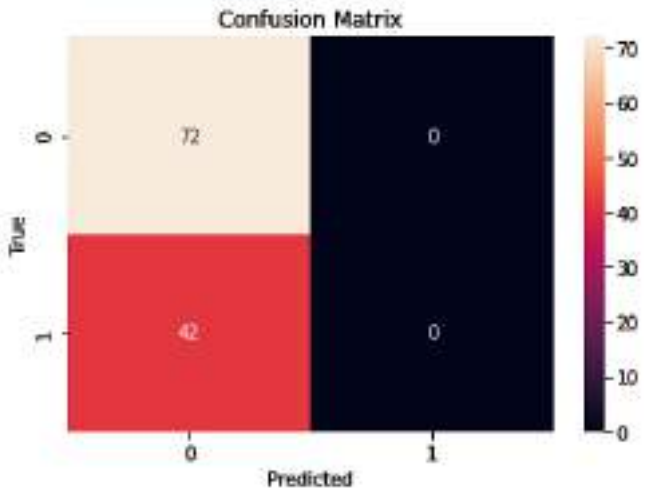

Fig. 5. Confusion Matrix after applying RNN to WBCD dataset

c) Genetic Algorithm

Genetic algorithm is a machine learning algorithm which uses a way of natural selection and genetics. It is a way to select in a natural way of species which can adapt and survive to the changes in environment. It is based on survival of fitness, each population consists of many individuals where each can be represented as int/bit/float/char value. These values are considered as a parent and they are used to obtain new offspring which is better than the considered data values. There can be mutation among them, adaption of genes, elitism, and selection of new population to get the better outcomes.

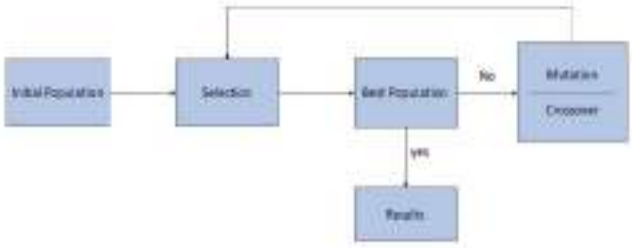

Fig. 6. Genetic algorithm

At first the initial population is considered and a sample is selected from that population and if results are good then those values are considered, if population sample results are not good then mutation and crossover is done to the population sample to acquire new population sample whose values are good.

In the proposed method the fitness of the model is calculated if the fitness is not good the mating is done along with mutation and random genome so that the acquired population fitness is better than the normal fitness so those population sample is used for acquiring the accuracy.

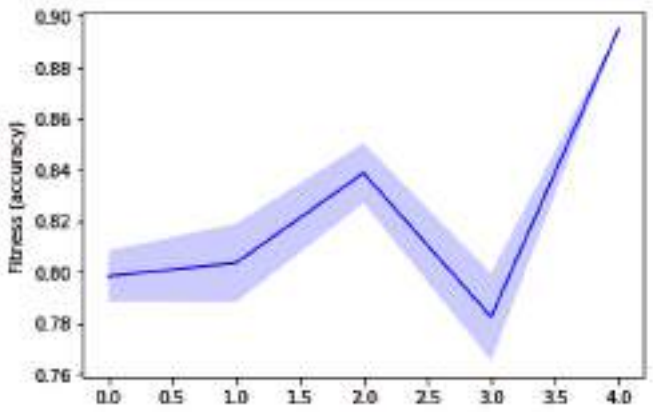

Fig. 7. Fitness accuracy graph applying genetic algorithm to WBCD dataset.

d) Fuzzy Logic

Fuzzy Logic is a machine learning algorithm which is similar to human reasoning, it makes a decision whether it may be yes or no such as Boolean output, so the fuzzy logic can be used for decision making and problem solving. The fuzzy logic consists of fuzzification module, knowledge base, inference engine, defuzzification module. The input is given to the algorithm then fuzzification module converts the input signals into different steps and transfers to knowledge base which contains the rules and inference engine which does human reasoning then the signals are transferred to defuzzification module which converts the received signals into human understandable form.

In the proposed method the input is taken from the dataset and those values are given to fuzzification layer which is used to machine readable format then those values are transferred to inference where the fuzzy rule is applied to those values and which can be used to detect the tumors and sent to defuzzification layer where the values are converted to normal outputs.

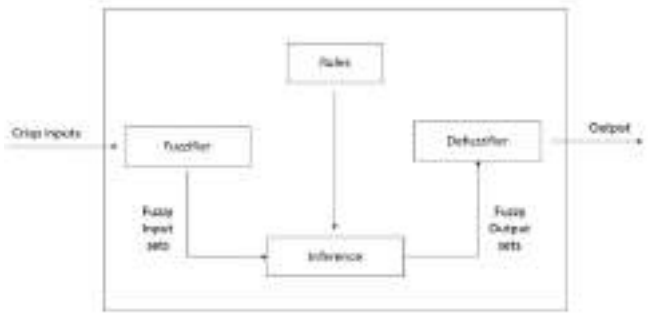

Fig. 8. Fuzzy Logic architecture.

4.1 Methodology

The Wisconsin Breast Cancer Diagnosis dataset is taken and then it is pre-processed for any missing values or noisy data, since the dataset is a clinical dataset, after importing the dataset it is checked for any missing values and those missing values are replaced by mean of the feature column, but there are no missing values then an encoder is applied so that the

objects are encoded into float values. Then that data is split into training and testing set and four different algorithms like Convolutional neural network, Recurrent neural network, Genetic algorithm and fuzzy logic are applied on it. After training them separately those algorithms are applied for testing phase and the accuracy of each algorithm is obtained and those accuracies are compared.

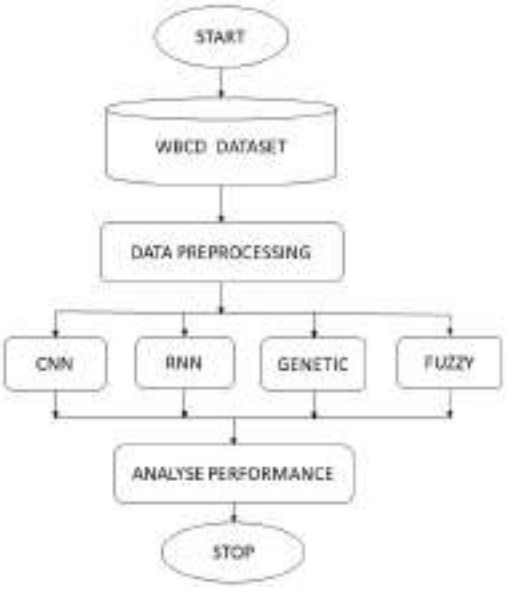

Fig. 9. Flow diagram of proposed breast cancer classification

V. RESULTS

The main concept of this study is to acquire a good accuracy for the detection of tumors in breasts of women. So, that different algorithms are used in this paper. The machine learning algorithms which are applied here can be useful for accurate detection of tumor cells. Then those algorithms are applied for the considered dataset to acquire the appropriate results. The CNN obtained the accuracy of 96.49%, RNN obtained accuracy of 63.15%, Genetic algorithm obtained accuracy of 80.39%, and Fuzzy Logic obtained the accuracy of 88.81%. CNN acquired highest accuracy for breast cancer identification on WBCD dataset.

TABLE 1

COMPARISON OF ACCURACY OBTAINED BY DIFFERENT ALGORITHMS USED FOR WBCD DATASET

ALGORITHMS USED	ACCURACY PERCENTAGE
Convolutional neural network	96.49
Recurrent neural network	63.15
Genetic Algorithm	80.399
Fuzzy Logic	88.81

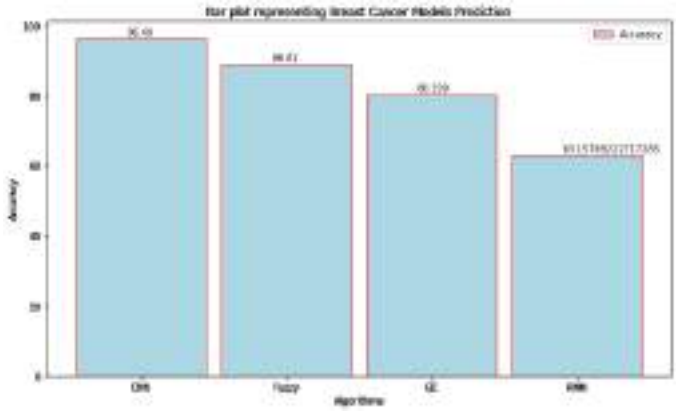

Fig. 10. Algorithm and Accuracy comparison

VI. CONCLUSION

Machine learning algorithms can be widely used for various medical field which can be used for good diagnostic tool for physicians to analyse the available data for further references. This paper represents the usage of four ML algorithms like CNN, RNN, Genetic algorithm, Fuzzy Logic and those accuracy is compared. CNN has acquired highest accuracy of 96.49%.

VII. FUTURE WORK

Although the proposed work has acquired good results the medical field need to have a 100% perfect results without any flaws. So, in near future there may be various advanced changes of technology or many new techniques may be available. Using those advanced techniques there may be improvements in the tumor detection and classification.

REFERENCES

[1] Y. J. Tan, K. S. Sim, and F. F. Ting, "Breast Cancer detection Using Convolutional Neural Networks for Mammogram Imaging System" International conference on Robotics Automation and Sciences (ICORAS),1-5,2017, ieeexplore.ieee.org

[2] Shuyue Guan and Murray Loew, "Breast Cancer Detection Using Transfer Learning in Convolutional Neural Networks" 2017 IEEE Applied Imagery Pattern Recognition Workshop (AIPR), 1-8,2017, ieeexplore.ieee.org

[3] Shaker K. Ali, Wamidh K. Mutlag, "Early Detection For Breast Cancer By Using Fuzzy Logic" Journal of Theoretical and Applied Information Technology, 15 September 2018, Vol.96. No 17 www.jatit.org

[4] Dr. S. N. Singh, Shivani Thakral, "Using Data Mining Tools for Breast Cancer Prediction and Analysis" 2018 4th International Conference on Computing Communication and Automation (ICCCA)

[5] Wener Borges de Sampaioa, Aristófanes Corrêa Silva, Anselmo Cardoso de Paiva, Marcelo Gattass, "Detection of masses in mammograms with adaption to breast density using genetic algorithm, phylogenetic trees, LBP and SVM"2015,

http://dx.doi.org/10.1016/j.eswa.2015.07.046, www.elsevier.com/locate/eswa

[6] Dana Bazazeh and Raed Shubair, "Comparative Study of Machine Learning Algorithms for Breast Cancer Detection and Diagnosis" 2016, https://www.researchgate.net/publication/310589496

[7] World Health Organization (WHO) https://www.who.int/health-topics/cancer#tab=tab_1

[8] Dua, D. and Graff, C. (2019). UCI Machine Learning Repository [http://archive.ics.uci.edu/ml]. Irvine, CA: University of California, School of Information and Computer Science.

[9] Abien Fred M. Agarap, "On Breast Cancer Detection: An Application of Machine Learning Algorithms on the Wisconsin Diagnostic Dataset" 2019, ICMLSC

[10] Ahmed Abdullah Farid, Gamal Ibrahim Selim1, and Hatem A. Khater, "A Composite Hybrid Feature Selection Learning-Based Optimization of Genetic Algorithm For Breast Cancer Detection", 2020, www.preprints.org

[11] Sri Hari Nallamala, Pragnyaban Mishra, Suvarna Vani Koneru, "Breast Cancer Detection using Machine Learning Way ", 2019, International Journal of Recent Technology and Engineering (IJRTE)

[12] Indira Muhic, "Fuzzy Analysis of Breast Cancer Disease using Fuzzy c-means and Pattern Recognition", March 2013, SOUTHEAST EUROPE JOURNAL OF SOFT COMPUTING

[13] Vikas Chaurasia, Saurabh Pal, "A Novel Approach for Breast Cancer Detection using Data Mining Techniques", January 2014, International Journal of Innovative Research in Computer and Communication Engineering

[14] Ahmad LG, Eshlaghy AT, Poorebrahimi A, Ebrahimi M, Razavi AR, "Using Three Machine Learning Techniques for Predicting Breast Cancer Recurrence",2013, J Health Med Inform 4: 124. doi:10.4172/2157-7420.1000124

[15] Can Hou1, MPH, DPhil; Xiaorong Zhong, DPhil, MD; Ping He, DPhil, MD; Bin Xu, MSc; Sha Diao, MSc, Fang Yi, MSc; Hong Zheng, DPhil, MD; Jiayuan Li, DPhil, "Predicting Breast Cancer in Chinese Women Using Machine Learning Techniques: Algorithm Development", june 2020, JMIR MEDICAL INFORMATICS

[16] Siham A. Mohammed, Sadeq Darrab, Salah A. Noaman, and Gunter Saake, "Analysis of Breast Cancer Detection Using Different Machine Learning Techniques", 2020, link.springer.com

[17] Tanny Chavez, Nagma Vohra, Keith Bailey, Magda El-Shenawee, Jingxian Wu, "Supervised Bayesian learning for breast cancer detection in terahertz imaging", 2021, Biomedical Signal Processing and Control 70 (2021) 102949, 28 june 2021, www.elsevier.com/locate/bspc

[18] Basker.N, Theetchenya.S, Vidyabharathi.D, Dhaynithi.J, Mohanraj.G, Marimuthu.M, Vidhya.G, "Breast Cancer Detection Using Machine Learning Algorithms", Annals of R.S.C.B., ISSN:1583-6258, Vol. 25, Issue 5, 2021, Pages. 2551 – 2562, 05 may 2021, http://annalsofrscb.ro

[19] Tsehay Admassu Assegie, "An optimized K-Nearest Neighbor based breast cancer detection", Journal of Robotics and Control (JRC) Volume 2, Issue 3, May 2020, http://journal.umy.ac.id/index.php/jrc

[20] Madhu Kumari, Vijendra Singh, "Breast Cancer Prediction system", International Conference on Computational Intelligence and Data Science (ICCIDS 2018), 2018, www.elsevier.com/locate/procedia

[21] Manoharan, Samuel. "Early diagnosis of Lung Cancer with Probability of Malignancy Calculation and Automatic Segmentation of Lung CT scan Images." Journal of Innovative Image Processing (JIIP) 2, no. 04 (2020): 175-186.

[22] Adam, Edriss Eisa Babikir. "Survey on Medical Imaging of Electrical Impedance Tomography (EIT) by Variable Current Pattern Methods." Journal of ISMAC 3, no. 02 (2021): 82-95.

Springer Link

Impact of Bio-inspired Algorithms to Predict Heart Diseases

Smart Computing Techniques and Applications pp 121-127 | Cite as

- N. Sree Sandhya (1)
- G. N. Beena Bethel (1)

1. CSE Department, GRIET, , Hyderabad, India

Conference paper
First Online: 14 July 2021

Part of the Smart Innovation, Systems and Technologies book series (SIST, volume 224)

Abstract

Optimization techniques are employed to deal with dynamic, difficult, and robust problems. Most of the Machine learning algorithms are implemented to predict heart diseases. Classification techniques are one of the methods that is highly used in machine learning for prediction. Some classification methods predict accuracy with acceptable range, but others may not. In this paper, we streamline two different bio inspired algorithms, Ant and Bat are used for heart disease prediction. Here, we extracting the key features from heart disease attributes using these two bio-inspired algorithms. Then these extracted features are implemented to the different classifiers. In this research, we examine the bio inspired algorithms optimized with Random Forest and SVM classifiers and compared the results. Ant colony optimization and Bat colony optimization give better results with SVM classifier than Random Forest classifier. When comparing the results in this research, Bat algorithm is better-optimized algorithm than ant algorithm.

Keywords

Heart disease prediction Bio inspired algorithms Bat colony optimization Ant colony optimization

Reference

1. Khourdifi, Y., Bahaj, M.: Heart disease prediction and classification using Machine Learning Algorithms Optimized by particle swarm optimization and Ant Colony Optimization. Int. J. Intell. Eng. Syst. (2019)
Google Scholar (https://scholar.google.com/scholar?q=Khourdifi%2C%20Y.%2C%20Bahaj%2C%20M.%3A%20Heart%20disease%20prediction%20and%20classification%20using%20Machine%20Learning%20Algorithms%20Optimized%20by%20particle%20swarm%20optimization%20and%20Ant%20Colony%20Optimization.%20Int.%20J.%20Intell.%20Eng.%20Syst.%20%282019%29)

2. Darwish, A.: Bio-inspired computing: algorithms review, deep analysis, and the scope of applications. Future Comput. Inf. J. (2018)
Google Scholar (https://scholar.google.com/scholar?q=Darwish%2C%20A.%3A%20Bio-inspired%20computing%3A%20algorithms%20review%2C%20deep%20analysis%2C%20and%20the%20scope%20of%20applications.%20Future%20Comput.%20Inf.%20J.%20%282018%29)

3. Kora, P., Ramakrishna, K.S.: Improved Bat Algorithm for the detection of myocardial infarction. Springer Plus **4**(1), 666 (2015)
Google Scholar (https://scholar.google.com/scholar?q=Kora%2C%20P.%2C%20Ramakrishna%2C%20K.S.%3A%20Improved%20Bat%20Algorithm%20for%20the%20detection%20of%20myocardial%20infarction.%20Springer%20Plus%204%281%29%2C%20666%20%282015%29)

4. Dubey, A., Patel, R., Choure, K.: An efficient data mining and Ant Colony Optimization Technique (DMACO) for heart disease prediction. Int. J. Adv. Technol. Eng. Explor. (IJATEE) **1**(1), 1–6 (2014)
Google Scholar (https://scholar.google.com/scholar?q=Dubey%2C%20A.%2C%20Patel%2C%20R.%2C%20Choure%2C%20K.%3A%20An%20efficient%20data%20mining%20and%20Ant%20Colony%20Optimization%20Technique%20%28DMACO%29%20for%20heart%20disease%20prediction.%20Int.%20J.%20Adv.%20Technol.%20Eng.%20Explor.%20%28IJATEE%29%201%281%29%2C%201%E2%80%936%20%282014%29)

5. Dataset, UCI Machine learning Repository [online]; https://archive.ics.uci.edu/ml/datasets/Heart+Disease (https://archive.ics.uci.edu/ml/datasets/Heart%2BDisease)

6. Rao, P., et al.: An efficient approach for detection of heart attack using Noble Ant Colony Optimization concept of data. IJESRT (2018)
Google Scholar (https://scholar.google.com/scholar?q=Rao%2C%20P.%2C%20et%20al.%3A%20An%20efficient%20approach%20for%20detection%20of%20heart%20attack%20using%20Noble%20Ant%20Colony%20Optimization%20concept%20of%20data.%20IJESRT%20%282018%29)

7. Dorigo, M.: Ant Colony optimization. Scholarpedia **2**(3), 1461 (2007)
Google Scholar (https://scholar.google.com/scholar?q=Dorigo%2C%20M.%3A%20Ant%20Colony%20optimization.%20Scholarpedia%202%283%29%2C%201461%20%282007%29)

8. Nasiruddin, I., Ansari, A.Q., Katiyar, S.: Ant Colony Optimization: a tutorial review, Conference Paper (2015)

Google Scholar (https://scholar.google.com/scholar?q=Nasiruddin%2C%20I.%2C%20Ansari%2C%20A.Q.%2C%20Katiyar%2C%20S.%3A%20Ant%20Colony%20Optimization%3A%20a%20tutorial%20review%2C%20Conference%20Paper%20%282015%29)

9. Hinduja, R., Mettildha Mary, I., Ilakkiya, M., Kavya, S.: CAD diagnosis using PSO, BAT, MLR and SVM. Int. J. Adv. Res. Ideas Innovations Technol. (2017) Google Scholar (https://scholar.google.com/scholar?q=Hinduja%2C%20R.%2C%20Mettildha%20Mary%2C%20I.%2C%20Ilakkiya%2C%20M.%2C%20Kavya%2C%20S.%3A%20CAD%20diagnosis%20using%20PSO%2C%20BAT%2C%20MLR%20and%20SVM.%20Int.%20J.%20Adv.%20Res.%20Ideas%20Innovations%20Technol.%20%282017%29)

10. Kotsiantis, S., Pintelas, P.E., Zaharakis, I.D.: Machine learning: a review of classification and combining techniques. Artif. Intell. Rev. **26**(3), 159–190 (2006) Google Scholar (https://scholar.google.com/scholar?q=Kotsiantis%2C%20S.%2C%20Pintelas%2C%20P.E.%2C%20Zaharakis%2C%20I.D.%3A%20Machine%20learning%3A%20a%20review%20of%20classification%20and%20combining%20techniques.%20Artif.%20Intell.%20Rev.%2026%283%29%2C%20159%E2%80%93190%20%282006%29)

Copyright information

About this paper

Cite this paper as:

Sree Sandhya N., Beena Bethel G.N. (2021) Impact of Bio-inspired Algorithms to Predict Heart Diseases. In: Satapathy S.C., Bhateja V., Favorskaya M.N., Adilakshmi T. (eds) Smart Computing Techniques and Applications. Smart Innovation, Systems and Technologies, vol 224. Springer, Singapore. https://doi.org/10.1007/978-981-16-1502-3_13

- First Online 14 July 2021
- DOI https://doi.org/10.1007/978-981-16-1502-3_13
- Publisher Name Springer, Singapore
- Print ISBN 978-981-16-1501-6
- Online ISBN 978-981-16-1502-3
- eBook Packages Intelligent Technologies and Robotics Intelligent Technologies and Robotics (R0)

Personalised recommendations

Springer

3rd International Conference on Image Processing and Capsule Networks (ICIPCN-2022)

May 20-21, 2022 | Bangkok, Thailand

Proceedings

Technical Sponsors

45	Medchain for Securing Data in Decentralized Healthcare System using Dynamic Smart Contracts *R Priyadarshini, Mukil Alagirisamy, N Rajendran*
46	Multipurpose Linux tool for Wi-Fi based attack, Information gathering and Web vulnerability scanning automations *Ceronmani Sharmila, Gopalakrishnan J, Shanmuga Prasath P, Daniel Y*
47	Customer Engagement through Social Media and Big Data Pipeline *Rubeena Rustum, J Kavitha, PVRD Prasada Rao, Jajjara Bhargav, G Charles Babu*
48	Performance Analysis of CNN models using MR images of Pituitary Tumour *Ashwitha K*
49	Detection of Facebook Addiction Using Machine Learning *Md. Zahirul Islam, Ziniatul Jannat, Md. Tarek Habib, Md. Sadekur Rahman, Gazi Zahirul Islam*
50	Mask R-CNN based Object Detection in Overhead Transmission Line from UAV Images *D Satheeswari, Leninisha Shanmugam, N M Jothi Swaroopan*
51	Insights into Fundus Images to Identify Glaucoma using Convolutional Neural Network *Digvijay J Pawar, Yuvraj K Kanse, Suhas S Patil*
52	An Implementation Perspective on Electronic Invoice Presentment and Payments *B Barath Kumar, C N S Vinoth Kumar, Suguna R, M Vasim Babu, M Madhusudhan Reddy*
53	Multi-model DeepFake Detection using Deep and Temporal Features *Jerry John, Bismin V Sherif*
54	Real-Time Video Processing for Ship Detection using Transfer Learning *V Ganesh, Johnson Kolluri, Amith Reddy Maada, Mohammed Hamid Ali, Rakesh Thota, Shashidhar Nyalakonda*
55	Smart Shopping using Embedded based Autocart and Android app *V Sherlin Solomi, C Srujana Reddy, S Naga Tripura*
56	Gastric Cancer Diagnosis Using MIFNet Algorithm And Deep Learning Technique *Mawa Chouhan, Corinne Veril D, Prerana P, A Kumaresan*
57	Cold Chain Logistics Method using to Identify Optimal Path in Secured Network Model with Machine Learning *Vijaykumar Janga, Desalegn Awoke, Assefa Senbato Genale, B Barani Sundaram, Amit Pandey, P Karthika*
58	Brain Tumor Image Enhancement Using Blending of Contrast Enhancement Techniques *Deepa Abin, Sudeep Thepade, Yash Vibhute, Sphurti Pargaonkar, Vaishnavi Kolase, Priya Chougule*
59	A Systematic and Novel Ensemble Construction Method for Handling Data Stream Challenges *Rucha Chetan Samant, Suhas H Patil*
60	A Smart Garbage System for Smart Cities using Digital Image Processing *Sivaranjani P, Gowri P, Bharathi Mani Rajah Murugan, Ezhilarasan Suresh, Arun Janarthanan*

Customer Engagement through Social Media and Big Data Pipeline

Rubeena Rustum[1], J.Kavitha[2],
PVRD Prasada Rao[3], Jajjara Bhargav[4]
and G.Charles Babu[5]
[1,5]Gokaraju Rangaraju Institute of Engineering and Technology(Autonomous), Bachupally, Hyderabad,Telangana
[2]BVRIT HYDERABAD College of Engineering for Women, Hyderabad, Telangana
[3]Koneru Lakshmaiah Education Foundation, Vaddeswaram,Guntur, A.P
[4]Chalapathi Institute of Engineering and Technology (Autonomous),Lam,Guntur
rubeena.rustum@gmail.com

Abstract. Engagement of customers through social media has gained considerable popularity in recent years in the field of digital marketing. Especially with the rise of technological revolution in business operations, utilizing sophisticated technology for strategic development of businesses has been seen. In this regard, data pipeline can be considered as an efficient, automated and sophisticated technology that uses a systematic data management process for voluminous data. The paper thus aims to investigate the beneficial scope of aligning social media with data pipeline technology for enhancing customer engagement. Through an empirical analysis of existing secondary resources as a viable and beneficial method for research, the study has developed a comprehensive understanding of data pipelines and social media platforms contributing to the enhancement of customer engagement.
The main findings of the study indicates that through the ETL pipeline (Extraction- Transformation-Loading), large columns data is managed sequentially and swiftly. The automated system can be used with both flexibility and control to manage the data flow. The businesses are able to control the data flow to their advantage and increase visibility and interaction. Simultaneously the analytics process of the big data aids the decision-making process that ensures customer behavior and market demands are being considered accurately. The study also considers certain challenges such as lack of increased storage capacity, high volume data, and consistency on that can be addressed through further development of advanced architecture.

Keywords: data pipeline, ETL pipeline, Big Data management, Big Data analytics, social media, social media marketing, digital marketing, customer engagement.

1. Introduction

Social media platforms have been recognized as one of the most effective and engaging platforms through which various industries promote products and services or simply establishrelationships with their customers. Recent inclination to utilize sophisticated technology for enhancing marketing policies among target demographic has been seen throughout various global industries. Organizations are seen to utilize various data analytics technologies for processing vast quantities of customer data and perform tasks such as online engagement rates, response to new and old products, sharing feedback and so on. These are only surface level operations that are aided through sophisticated data analytics technology such as data pipeline.

Data pipeline is an advanced data processing and analytics technology that is able to retrieve and process data and store it in a data warehouse. The three prime elements in data pipelines consist of a source, processing of data and destination [1]. The apparent simplicity of its process is far more critical in application as it is used by organizations to organize real-time data, process it and store it. Organizations are highly interested in processing large-scale digital information and analyze it for assessing market demands, leading to creation of personalized digital marketing policies. On a global scale, the expenditure for social media marketing is expected to increase 10.93% by 2025 [2]. Especially, with the increased rate of using various mobile applications, it has become a necessity to process and store data of each customer. Hence, the paper will address the issues of large-scale data processing in general and aim at investigating the beneficial use of data pipelines in increasing the rate of customer engagement through social media.

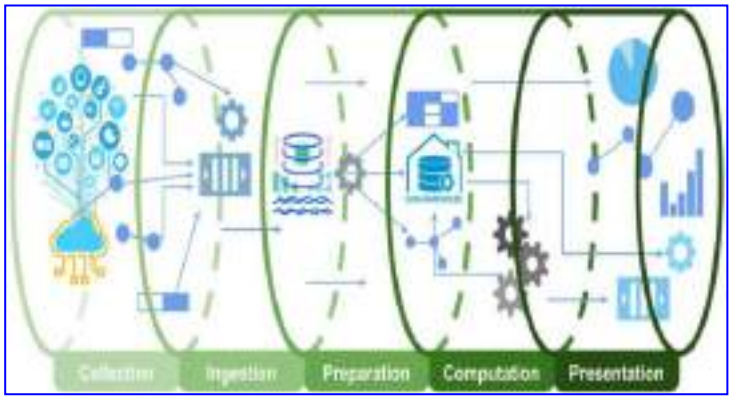

Figure 1: Big Data Pipeline Architecture [1]

1.1 Analysis of data pipeline technology

The overall usage of digital information gathered from various social media platforms have grown in variety, volume and velocity. Big data or the enormous volume of data gathered through social media interaction can be processed and stored through dada pipelines [3]. Such a sophisticated technology is able to support big data and has evolved to ensure that data processing is conducted in a clear and logical sequence. The interaction of customers throughout various social media platforms are processed and assessed through predictive analytics [4]. It leads to the enhancement of engagement through proper marketing. In other words, as the organizations monitor the rate of engagement, they are able to understand the direction of market demands and cater towards the personal desires of customers.

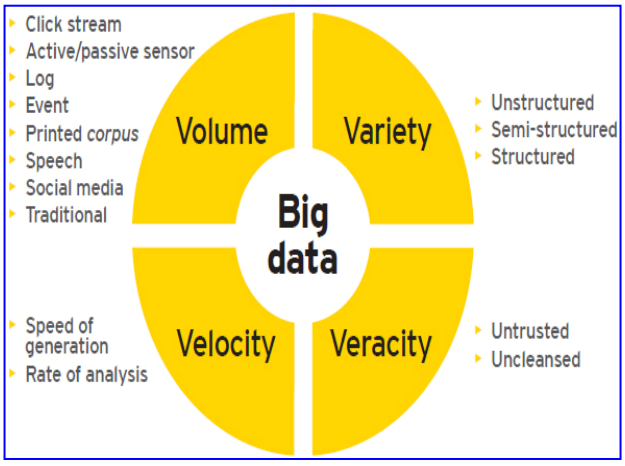

Figure 2: Three Vs of Big Data [3]

Extraction of big data from its current source location, processing or transforming it into a reliable format. A secured loading or storage process is conducted at the third stage of the data pipeline where the stored data is analyzed through sophisticated machine learning technology [5]. The most beneficial aspect of the data pipeline that is used by business is its ability to

extract data at any point of data processing [6]. Hence, the data pipeline technology can be used to provide organizations with the required data for analytics. It not only contributes to saving time of conducting data extraction from the source point alone but also enables companies to save the extracted data. Huge volume of data is then analyzed automatically in order to perceive the market demands and customer attitudes towards a certain product or service.

Data ingestion pipeline is used for the purpose of big data analysis. AI has been used inrecent times for the improvement of ingestion practices [7]. It also helps in avoiding redundant loading of the processed data that uses an automated system. In essence, data pipeline technologies are able to provide optimal scope for extracting and processing big datain a systematic manner.

1.2 Benefits of data pipeline for customer engagement

Data pipelines can be used to optimize the process of big data extraction, transformation and loading. Customer data can be extracted from various applications used by them [8]. As companies grow more and more aware about the behavior and demands of customers, they are able to employ policies for raising social media engagement through effective marketing. It also helps in providing the organizations with ample knowledge regarding their retail sales rates and post engagement, aiding business-related decision-making processes. Thisinformation is highly beneficial to the decision-making process as it assists in generating strategies for attaining substantial competitive advantage.

The elements of data pipeline technology help in managing the e-commerce segment of various businesses and increases customer engagement through the accurate data analytics. Using social media analytics tools for analyzing customer behavior helps in the decision- making process [9]. Customers express their feedback and attitudes towards a certain product or service through social media posting, sharing, commenting or liking. Such data is then analyzed to generate personalized, suggestive and attractive marketing policies to further enhance customer engagement. On the other hand, through social media platforms, various organizations enhance their interaction with individual customers [10]. It not only establishes a sustainable and loyal relationship among a brand's targeted customer base but it also ensures that through such direct interactions, market demands are being recognized. In essence, the big data extracted from social media platforms through data pipelines contributes to critical business operations that have significant influence on an organization's manufacturing or production policies and marketing policies. Thus, the use of data pipeline technology for big data processing leading to proper analytics systems helps organizations to engage

with their customers in a personalized manner that naturally leads to competitive advantage.

2 Methods and Materials

The paper has conducted an empirical analysis on the topic of social media and data pipeline optimization in customer engagement. Construction of systematic and sequential methodology for the conduction of research enhances scope for logical and valid outcomes [11]. Various secondary resources on the topic had been gathered to analyze in order to meet the aim of the paper. In this regard, a descriptive design to the analysis of gathered resources had been conducted. Descriptive research design helps in the development of a research thatis based on the development of knowledge through analyzing existing data or information [12]. Furthermore, a deductive research design had been adopted in order to ensure in-depth analysis. The overall qualitative approach undertaken for this particular paper had helped it to generate new ideas and hypotheses based on multidimensional existing literature on the topic.

The materials used for the study had been gathered from a targeted and systematic search for materials in certain electronic databases such as ProQuest and Google Scholar. Peer-reviewed and published journals, newspaper articles and official reports had been gathered. A systematic sampling method had been adopted as well which consisted of inclusion- exclusion criteria. Setting inclusion-exclusion arteritis assists in discovering only those materials which are beneficial for the course of a given research [13]. The criteria set for this particular study pertaining to the selection of beneficial and informative journal articles had included, peer-reviewed articles, publications within the last 5 years, publications in English language and publications containing certain keywords such as data pipeline, big data, big data analytics, marketing, digital marketing, customer engagement and social media. Thus, adoption of these specific methods has aided the process of data collection and data analysis, leading to the findings of the research that is valid, relevant and evidence-based

3. Results

Advantages of data pipeline technology for enhancing social media engagement

There are various advantages that are attained by a business through a data pipeline. Businesses use data pipelines to enhance their capacity for predictive analysis and measure the rate of activities or engagement in social media. Social media is a thriving platform that allows individuals to interact freely with a brand [14]. Businesses use this opportunity to retrieve the data of users to get accurate information regarding the brand's ability to meet the key

performance indicators (KPI) [15]. The activities of a potential customer on social media are assessed to analyze their demands, timing of purchase, and inclination for purchasing within a price range and so on. In essence, as a key advantage of such data streaming and analysis helps businesses to perceive the buying behavior of customers and offer products and services accordingly.

As businesses continue to align their social media platforms with data pipelines, they are essentially in control of regulating the flow of data. This helps businesses to gain relevancy and thus further engagement. Social media is being used as a significant platform for promoting and interacting with customers [16]. The current demographic is more prone to using social media than engaging in any other forms of engagement platforms. With the use of data pipeline technology, a brand is able to manage the data in a flexible manner [17]. Such flexibility leads to the beneficial alignment of data to the customers, leading to enhancement in social media interaction among customers.

Figure 3: Social media engagement strategies [16]

Management of such vast amounts of data and using it to meet the specific needs of a business is an advantageous side of data pipeline technology. The ETL pipeline (Extraction- Transformation-Loading) helps in the formation of an effective network [18]. Utilization of Thai networks in social media aids the process of customer engagement.

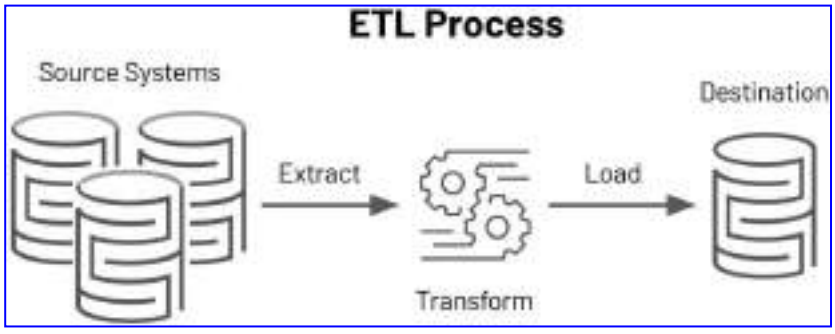

Figure 4: ETL pipeline process [18]

Challenges in big data analytics with data pipeline

There are several challenges that are faced in big data management without proper data pipeline architecture. The large volume of data remains at risk of being lost in the processing phase or may not reach the data warehouse [19]. Additionally, the major challenges identifiedin the field of big data analytics is proper management and integration process. In many cases, such processes are reliable in human understanding [20]. However, in recent times, development of AI-based systems for such operations has reduced this particular challenge. Regardless, lack of proper knowledge regarding the system limits the ability of a business to use it and optimize information to its own benefits.

There is a critical challenge that is faced by business in the utilization of data pipeline architecture as SMEs fail to integrate it due to financial lack. Both technological and financial infrastructure is required for the development and integration of sophisticated technology [21]. The technology itself may be faced with certain challenges as there is a possibility of a gap between real-time data entry and ETL process (Extraction-Transformation-Loading) [22]. The recent integration of AI-based systems in data processing and analytics has however decreased the time lag. Another challenge faced in recent years is the rising velocity, variety and most importantly volume of data. Each stream of data is to be processed through a data pipeline after which proper analytics can be conducted [23]. Hence, gap in processing capacity due lack of proper digital architecture leads to challenges in implementation as well as lack of consistency, security and so on.

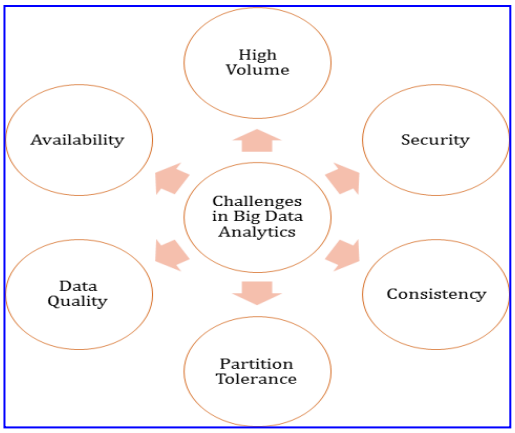

Figure 5: Challenges in Big Data analytics [23]

Optimization of data pipeline for enhancing social media engagement and organizational benefits

The organizations are able to benefit exponentially through data processing and analysis optimization that is aided by data pipeline technology. The organizations are able to gain profit and obtain substantial competitive advantage [24]. Enhancing customer engagement through social media is attained through analysis and predictive assessment [25]. As KPIs are also maintained with the use of data pipelines, it brings about significant opportunities for profitability.

On the other hand, the flexibility provided to the organizations as data pipelines are being used assists in their processes of active engagement. Social media analytics has been considered as an emerging tool for aiding the progress of business [26]. Data pipelines are also able to provide a clear view of the data flow based on which decision-making process is conducted. In essence, it can be stated that linkage of social media and data pipelines helps in increasing customer engagement and help businesses to formulate strategies for further marketing growth. The data flow of social media is tracked and analyzed in order to provide the organizations with ample insight into the needs of necessary modifications.

Social media marketing has been acknowledged as an effective segment for promotingproducts and services effectively. As the worldwide wealth of digital information rises, businesses use this opportunity to place their products or services in a strategic manner [27]. It essentially helps increase product visibility and ensure customers are effectively engaged with the brand through social media platforms. Hence, the most significant benefit that data pipelines are able to provide the organizations is the ability to analyze voluminous data and use it to retain relevance and interaction. Keeping track of the customer's opinions and latest trends are also analyze to strategically place product suggestions through various social media platforms, enhancing scope for sustained profitability.

4. Discussion

Analysis of the relevant literature has indicated the positive scope of using data pipeline in connection with social media to ensure a positive growth in customer interaction. Most optimal method of data processing and analysis has

been identified through the implementation of a data pipeline system [15]. As a data pipeline provides the optimal scope for arranging data in a sequential and synchronized format, it aids the development of a reproducible system in which businesses are able to gain insight into the gathered data anduse it to aid their decision-making process. Additionally, it has also been indicated that the automated ETL pipelines enable a timely analysis of valuable data.

The flexibility offered in data pipelines can be used for social media platforms to ensure that the data flow of raw data travels uninterruptedly to its destination. The point of data flow within a pipeline system ensures sequential flow which can be controlled by a business [22]. The main benefit of aligning data pipelines and social media is the enhancement in capacityto process large volumes of data, generated every second of the day. Being in control of the data processing procedures, it has been indicated that the development of an effective and interactive relationship between the brands and customers is possible by virtue of relevant data flow.

Data pipelines are also able to extract big data and distribute them in various relevant sets. Such a simplified structure for voluminous data helps in backing up data and redistributing in case of a crashed server [23]. Analysis of the data gathered from various social media platforms, a business is also able to assess the behavior and attitudes of customers. Gaining the trust of customers is an important part of effective marketing. However, customer engagement enhancement is not merely limited to the marketing procedures. It is extended towards a controlled flow of data to ensure that product visibility is optimal.

Figure 6: Big data analytics for social media [4]

It has also been gathered that certain challenges are faced by organizations in the process of data pipeline integration for management and processing. A comprehensive awareness of the entire system hinders the process of proper utilization [19]. Along with that, the lack of financial support has also been identified as one of the challenging factors pertaining to the implementation of sophisticated technology. Moreover, as the wealth of digital data on a global scale continues to increase, feasible options for adequate management, processing and analysis become highly dependable on the capacity of a system's data storage. Real-time datagathered from social media contributes to the generation of voluminous data every day. Hence, the overall capacity of the data pipeline to stream sequential data poses a challenge. However, despite these challenges, constant modification and innovative discoveries made in the field enhances its overall capacity and enables it to be used efficiently for managing big data and providing scope to the businesses to use it as a digital tool for increasing customer engagement.

5. Conclusion

Social media is used as a platform for active interaction between various businesses and customers. Increased rate of online interaction between a business and its target customers leads to the establishment of loyal and beneficial relationships. Increase in social media engagement is thus considered to be a significant part of increasing profitability and competitive advantage. Fulfillment of such business agenda may be possible with the use of data pipeline for social media engagement enhancement.

The data pipeline uses a systematic process of data extraction, transformation and loading (ETL) for sequential management of big data. With the growth of digital data, processing such voluminous data through a controlled yet flexible technology is required which isprovided by a data pipeline. However, the processing and storage capacity is required to be in accordance with the growing volume, velocity and variety of data. It has been gathered that with the alignment of social media and data pipelines, businesses are able to control the data flow and direct the raw data to a beneficial destination that ultimately leads to the enhancement of customer engagement. In conclusion, it can be used as a potent tool for strategic placement, increased interaction and decision-making process.

References

1. del Rio Astorga, D., Dolz, M.F., Fernández, J. and García, J.D., 2017. A generic parallel pattern interface for stream and data processing. *Concurrency and Computation: Practice and Experience*, *29*(24), p.e4175.

2. Statista.com, 2021. *Social Media Advertising*. Available at: https://www.statista.com/outlook/dmo/digital-advertising/social-media-advertising/worldwide [Accessed on: 2nd November, 2021]
3. Prim, J., Uhlemann, T., Gumpfer, N., Gruen, D., Wegener, S., Krug, S., Hannig, J., Keller, T. and Guckert, M., 2021. A data-pipeline processing electrocardiogram recordings for use in artificial intelligence algorithms. *European Heart Journal*, *42*(Supplement_1), pp.ehab724-3041.
4. Sebei, H., Taieb, M.A.H. and Aouicha, M.B., 2018. Review of social media analytics process and big data pipeline. *Social Network Analysis and Mining*, *8*(1), pp.1-28.
5. Helu, M., Sprock, T., Hartenstine, D., Venketesh, R. and Sobel, W., 2020. Scalable data pipeline architecture to support the industrial internet of things. *CIRP Annals*, *69*(1), pp.385-388.
6. Therrien, J.D., Nicolaï, N. and Vanrolleghem, P.A., 2020. A critical review of the data pipeline: how wastewater system operation flows from data to intelligence. *Water Science and Technology*, *82*(12), pp.2613-2634.
7. Akanbi, A. and Masinde, M., 2020. A Distributed Stream Processing Middleware Framework for Real-Time Analysis of Heterogeneous Data on Big Data Platform: Case of Environmental Monitoring. *Sensors*, *20*(11), p.3166.
8. de Oliveira Santini, F., Ladeira, W.J., Pinto, D.C., Herter, M.M., Sampaio, C.H. and Babin, B.J., 2020. Customer engagement in social media: a framework and meta- analysis. *Journal of the Academy of Marketing Science*, *48*, pp.1211-1228.
9. Pääkkönen, P. and Jokitulppo, J., 2017. Quality management architecture for social media data. *Journal of Big Data*, *4*(1), pp.1-26.
10. Li, M.W., Teng, H.Y. and Chen, C.Y., 2020. Unlocking the customer engagement- brand loyalty relationship in tourism social media: The roles of brand attachment and customer trust. *Journal of Hospitality and Tourism Management*, *44*, pp.184-192.
11. Xanthopoulou, D., 2017. Capturing within-person changes in flow at work: Theoretical importance and research methodologies. In *Flow at Work* (pp. 50-65). Routledge.
12. Bloomfield, J. and Fisher, M.J., 2019. Quantitative research design. *Journal of the Australasian Rehabilitation Nurses Association*, *22*(2), pp.27-30.
13. Patino, C.M. and Ferreira, J.C., 2018. Inclusion and exclusion criteria in research studies: definitions and why they matter. *JornalBrasileiro de Pneumologia*, *44*, pp.84-84.
14. Lin, H.C., Swarna, H. and Bruning, P.F., 2017. Taking a global view on brand post popularity: Six social media brand post practices for global markets. *Business Horizons*, *60*(5), pp.621-633.
15. Hunt, K. and Gruszczynski, M., 2021. The influence of new and traditional media coverage on public attention to social movements: the case of the Dakota Access Pipeline protests. *Information, Communication & Society*, *24*(7), pp.1024-1040.
16. Wang, X., Baesens, B. and Zhu, Z., 2019. On the optimal marketing

aggressiveness level of C2C sellers in social media: Evidence from china. *Omega*, *85*, pp.83-93.

17. Baljak, V., Ljubovic, A., Michel, J., Montgomery, M. and Salaway, R., 2018. A scalable realtime analytics pipeline and storage architecture for physiological monitoring big data. *Smart Health*, *9*, pp.275-286.
18. Bala, M., Boussaid, O. and Alimazighi, Z., 2017. A Fine-Grained Distribution Approach for ETL Processes in Big Data Environments. *Data & Knowledge Engineering*, *111*, pp.114-136.
19. Elragal, A. and Klischewski, R., 2017. Theory-driven or process-driven prediction? Epistemological challenges of big data analytics. *Journal of Big Data*, *4*(1), pp.1-20.
20. Arunachalam, D., Kumar, N. and Kawalek, J.P., 2018. Understanding big data analytics capabilities in supply chain management: Unravelling the issues, challenges and implications for practice. *Transportation Research Part E: Logistics and Transportation Review*, *114*, pp.416-436.
21. Wang, L. and Alexander, C.A., 2020. Big data analytics in medical engineering and healthcare: methods, advances and challenges. *Journal of medical engineering &technology*, *44*(6), pp.267-283.
22. Moly, M., Roy, O. and Hossain, A., 2019. An advanced ETL technique for error-free data in data warehousing environment. *Int. J. Sci. Res. Eng. Trends*, pp.554-558.
23. Ardagna, C.A., Bellandi, V., Bezzi, M., Ceravolo, P., Damiani, E. and Hebert, C., 2018. Model-based big data analytics-as-a-service: take big data to the next level. *IEEE Transactions on Services Computing*, *14*(2), pp.516-529.
24. Liu, Y., Jiang, C. and Zhao, H., 2019. Assessing product competitive advantages from the perspective of customers by mining user-generated content on social media. *Decision Support Systems*, *123*, p.113079.
25. Li, F., Larimo, J. and Leonidou, L.C., 2021. Social media marketing strategy: definition, conceptualization, taxonomy, validation, and future agenda. *Journal of the Academy of Marketing Science*, *49*(1), pp.51-70.
26. Lee, I., 2018. Social media analytics for enterprises: Typology, methods, and processes. *Business Horizons*, *61*(2), pp.199-210.
27. Hajirahimova, M.S. and Aliyeva, A.S., 2017. About big data measurement methodologies and indicators. *International Journal of Modern Education and Computer Science*, *9*(10), p.1.

Empathic Chatbot: Emotional Astuteness for Mental Health Well-Being

Mallikarjuna Rao Gundavarapu[1], G. Saaketh Koundinya[2], Tanusha Bollina Devi Sai[1(✉)], and Govind Kidambi Sree[1]

[1] Department of CSE, GRIET, Hyderabad, India
bollina.tanusha@gmail.com
[2] SAP Business Consultant, Bangalore, India

Abstract. Losing your family members, obtaining a pink slip from employment, probing a divorce, and different tough things will lead an individual to feel unhappy, lonely, and scared. These feelings are traditional reactions to life's stressors.

Happy, your cute companion, a Chatbot (or conversational interface as it is also known), presents a way for such individuals to interact with it by simply speaking their mind, in the same manner they would do with their friends and family. In addition, it helps people by providing emotional support, making them feel good, not judging them, and always coming up with a positive response such that it instils a sense of confidence in them and ultimately tries its best to change their minds.

It cares like a mother, scolds like a father, supports like a sibling, understands like a best friend, and most importantly, helps make the right decision even though it seems complicated and impossible. Last but not least, it will remind people to first love themselves by making them realize how important is their existence in this world is in their unique way. We tested with nearly 300 test cases in our experimentation and identified the performance as 93%. For this experiment, we made use of AI methods such as Natural Language Processing (NLP), enabling the people to converse with it using natural language input and train and test the chatbot using effective methods so that it will be able to respond in a positive sense to instill confidence in the user and change their mind.

Keywords: Empathic Chatbot · Astuteness · Neural framework

1 Introduction

In present days, there are many alternative treatment options available for those laid low with depression. When someone is in depression, one gets different thoughts where there is an opportunity to require wrong decisions. one best thanks to the startup of depression is to socialize – meaning is not hesitating to speak to trusted relations or friends or getting more connections. But finding such people within the society is not as easy as said. The person is feared of being judged, and getting rejected has been a significant hurdle for depressed ones. The patient needs an individual who can provide emotional support

B. Iyer et al. (Eds.): ICCET 2022, SIST 303, pp. 697–704, 2022.
https://doi.org/10.1007/978-981-19-2719-5_65

in any situation. He must feel the chatbot is a friend he can trust, so our emotionally intelligent chatbot usually understands human feelings by employing a text format. Our chatbot usually acts sort of a friend, listens patiently to what the user wants to inform, and provides replies in a pleasant way where the user never feels judged. So, our chatbot tries to convince him and alter his mood.

Generally, we encounter countless chatbots deployed on websites and several other digital assistants such as Alexa Siri in the real world. But with these, there is no need to empathize with the user since there is no need to converse with the user by understanding and analyzing their emotions. While in the case of mental healthcare patients, it becomes very critical. The same is researched upon and mentioned by authors [2]. On conducting a review of the perceptions and opinions of patients about chatbots of mental health by authors [4], it was concluded that the result was positive. The survey conducted by authors [6] among the youth concerning their stress levels resulted in blaming various factors such as exams, assignments, being overly busy or falling behind, over expectations, thoughts of the future, etc., for their stressful days. It was also highlighted in [6] that while some of the youth preferred talking about their mental health with friends and/or family, others found it rather "confronting" and "judgemental."

So, the mental state doctors have implemented the advancement of technology, mainly Artificial Intelligence-based chatbots, to deal with the people stricken by such problems as the first line of defense. Mental state chatbots give a probative presence to service druggies, engaging them with discussion now and then and after they feel low [11]. They are all ears to air concerns, worries, intrusive thoughts, or engage in 'therapeutic' confabulation. They will detect the user's mood with the help of the text input and give a sympathetic response. Some chatbots can give suggestions or advice to assist them by challenging their sad thoughts. Modeling tactics from behavioral therapy will help the users accept and confront their emotions. The evolution of computer science has opened the doors for several chatbots, but three out of those wellness chatbots (WoeBot [8, 12], Wysa [10, 12], and Tess [3, 5]) are exceeding in this domain and are extensively in use.

Our chatbot uses computer science methods like linguistic communication Processing (NLP), allowing the users to interact with it using language input and to coach the chatbot using appropriate methods so it will be able to respond positively to instill confidence within the user and alter their mind. Using NLP, our chatbot can be written and attain tasks like keyword extraction, translation, and topic classification. Furthermore, with the said NLP capabilities, this chatbot can recognize and analyze the similarities in the patient discussion environment and dissect the sentiment behind the communication by using contextual suggestions from the given input [9].

2 Existing Approaches

The various studies indicate that the mental health chatbots are more focused on helping the younger population by helping in the detection and reduction of stress [13], anxiety, and depression [3, 8, 10]. Also, one particular study evaluates that those who interacted daily with these chatbots seemed to benefit from them [14], telling us that increasing the usage of user-friendly chatbots will be critical in proving effective. On extensive

research in this field of study, it was found that quite a few mental chatbots existed but used a different approach than ours [12].

1) Woebot, a fully automated conversational agent developed by Woebot Labs in San Francisco uses cognitive behavioral therapy – essentially an evidence-based approach to treatment. However, the app users complained that it felt more like a quiz than a chat [7, 8, 15].
2) Wysa, a playful artificial penguin, is skilled in cognitive behavioral therapy (CBT) and reorganization of thoughts, but the users felt it was scripted and always asked for more information which was tiring and frustrating [7, 10, 15].
3) Joyable, an online platform, also uses CBT. Even though the interface is less user-friendly than Woebot and Wysa, it is pretty straightforward and puts less pressure on the users. The only disadvantage is that the app is not very helpful for moderate to severe depression and anxiety [7, 15].
4) Talkspace, a chatbot used for online licensed therapy, is user-friendly but has a longer sign-up process along with not-so-accurate responses from the therapists [7, 15].

3 Proposed System Architecture

The authors mentioned the different types of chatbots, their area of knowledge, their need to serve the population, the generalized architecture of the modern chatbots, and their primary platforms for creation [1, 9]. The proposed system architecture mentioned below gains inspiration from the authors mentioned above and gives a clear picture of the working of the chatbot. It also depicts the importance of various library functions in the implementation, including NLTK, Keras, and pickle. The architecture is a sophisticated model that hides the underlying source code. The figure below helps us determine the overall working of the chatbot and can also be used as a reference for drawing the different UML diagrams associated with the experimentation.

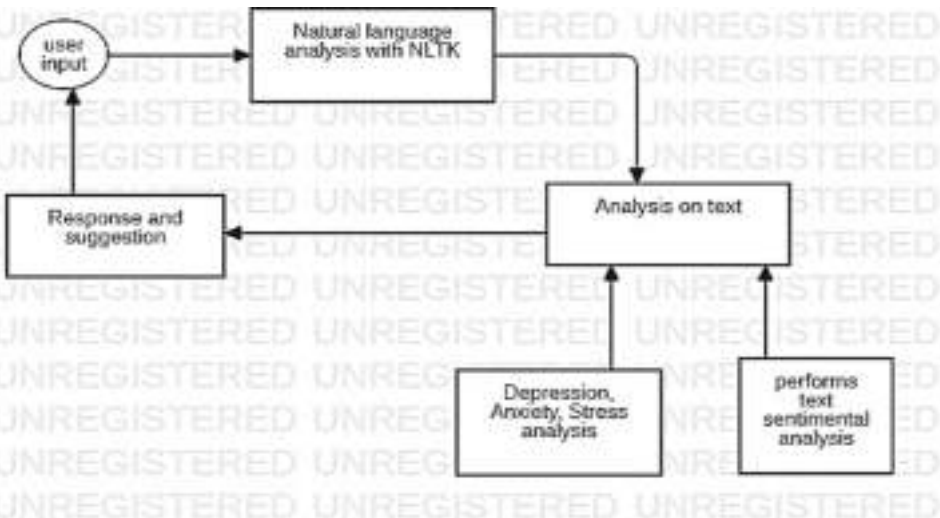

Fig. 1. The architecture of the proposed system

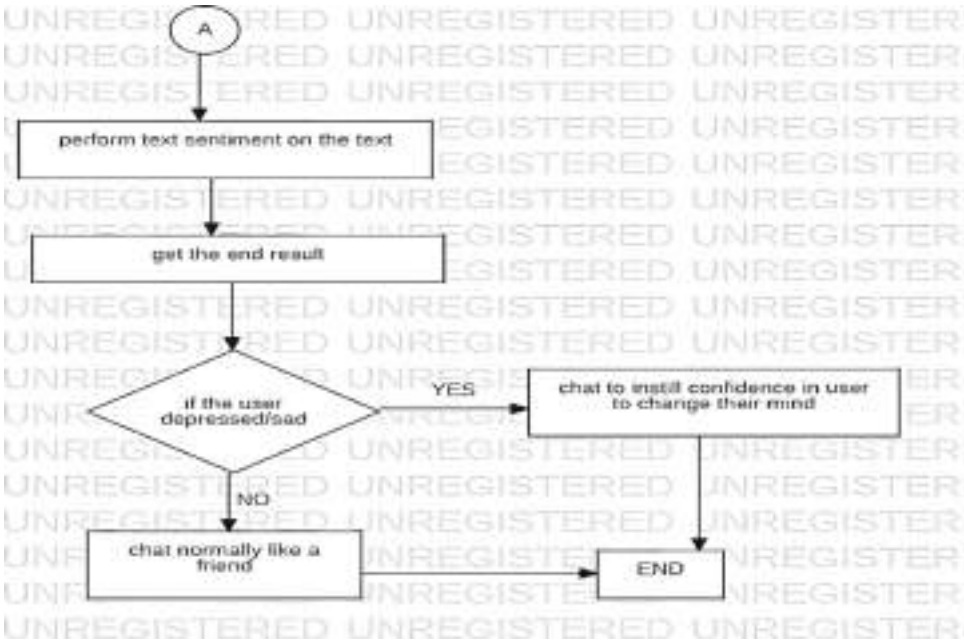

Fig. 2. Flowchart of the proposed system

The above Figs. 1 and 2 describe the overall flow of the implementation in the form of a flowchart which will help better understand the proposed system's architecture.

4 Dataset

The dataset that has been used for training and testing the model has not been taken from any predefined datasets on the internet. Instead, the dataset was created using sources like Wikipedia and other relevant google articles. We frequently conversed with the emotionally intelligent chatbot to understand the chatbot's response to the user's input questions and tried to update our dataset based on that. As we progressed, we were able to develop a decent conversation between the user and the chatbot so that the chatbot always responds positively, thereby instilling the user's confidence. The dataset was created, updated, and finalized to ensure that the chatbot's responses always change the user's mind as a friend (Fig. 3).

TAGS	PATTERNS	RESPONSES
greeting	Hi, hey, How are you …….	Good to see you again, Hi there, how can I help? Hello, thanks for asking …..
friend	Am I your friend, Are you my friend, Can you be my friend ……	Of course. Happy will always be your friend, no matter what, Yes! My name is Happy and I will always make you happy. Promise ……..
happy	Can I be happy, I am happy ……..	To Be Happy Is to Be Whole: It's Worth It, Everyone deserves to be happy no matter what. So, Be happy …..
goodbye	Bye, See you later, Thank you……	See you later! Take care, Have a lovely day …….
thanks	Thanks, thank you, That's helpful ……..	Happy to help, Any time, My pleasure ……..
hate	I hate myself, Is it good hating people ……	Hey buddy, Love yourself! You deserve it more than anyone…..
bully	I am being bullied by my co-workers ……	Stand up for yourself. Never sink to their level. Discuss the problem with someone to find the best way to handle them ……..
anxiety	I think I have anxiety; how do I fix my anxiety …….	At the highest level, anxiety is your body's natural response to stress ……..
.	.	.
.	.	.
.	.	.
.	.	.
.	.	.

Fig. 3. Sample dataset

5 Execution

1) **Importing and loading the data:** We need to import the required libraries and packages for the emotionally intelligent chatbot and then initialize the variables used in our work. Since the dataset that has been used is in JSON format, it is essential to use the 'json' package to parse the corresponding dataset into a python file.
2) **Preprocessing the data:** While developing a deep learning model, it is necessary to ensure that several preprocessing techniques are performed to free it from inconsistency and noise. The different preprocessing operations done on the data file are:

   a) Converting the corpse into lowercase.

b) Tokenization of data.
c) Removing noise and stopping words from data.
d) Stemming of data.
e) Lemmatization of data.

3) **Create training and testing data:** We have to produce both the training and testing data to provide the input and output. The input will correspond to the specimen, and the outcome shall be the class that the input design belongs to. It is also essential that we change the text into numbers so that the computer can understand what the user is trying to say.
4) **Building the model:** Since the training and testing data is ready, we must build a deep neural network with 3 Dense layers. We use the Keras Sequential Model wherein the top layer has 128 neurons, the second one has 64, and the last has the same neurons as the number of classes. The preparation and testing of the model have been finished utilizing 200 Epochs with a cluster size of 5 (Fig. 4).
5) **Predicting the response by creating a Graphical User Interface:** Create a GUI using the Tkinter module of Python that will foretell an accurate response from the chatbot. It will identify a specific class from several classes and then extracts an arbitrary response from the list of intents. Since the input should be similar to those provided during training, we need to perform input preprocessing and then envision the class to which it belongs.
6) **Running the chatbot:** The chatbot interface file will open up a GUI window to help in an easy and hassle-free conversation between the user and the chatbot.

The test strategy and approach of the framework are associated with actions, expected output, and the actual output associated with experimentation. Table 1 illustrates each test case and its expected outcomes after executing the modules.

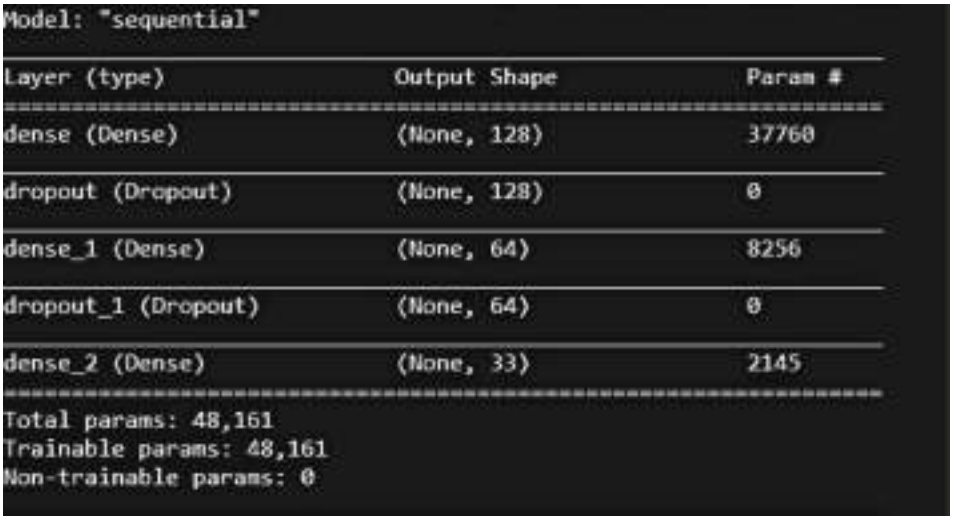

Fig. 4. Design of the Sequential Model used in the implementation.

Table 1. Test strategy and approach

S. no.	Action	Expected output	Output
1	Installation of Python version 3.8	Successful installation of Python	Successful Installation of Python
2	Installation TensorFlow, Keras, pickle, NLTK packages and libraries	Successful installation of all packages	Successful installation of all packages
3	Downloading the dataset to train and test the model	Successful download of the dataset	Dataset successfully created
4	Preprocessing the data • Converting the corpse to lowercase • Tokenization of data • Removing noise and stopping words from data • Stemming of data • Lemmatization of data	Successful Pre-processing of data. In the end, the words contain the vocabulary of our dataset, and classes contain the total entities to classify	Preprocessing of data is completed successfully. A list of words, documents, and classes have been created
5	Create Training and testing data	Training and test data have been created	Successful creation of training and testing data
6	Training the model using a Deep Neural Network consisting of 3 Dense layers	Training of the model is completed	Training of the model has been completed
7	Creation of GUI for the chatbot using Tkinter module in Python	The GUI for the chatbot has been created	The GUI for the chatbot has been successfully created
8	Running the chatbot	Successful execution of chatbot	Successful execution of chatbot

6 Conclusion and Future Scope

This work will help instill confidence in individuals suffering from mental health problems by not being judgemental by nature and encourage individuals experiencing depression and psychological conditions. The chatbot mainly gives importance to the emotions of people. It will help change their minds by understanding their problems and replying positively. So, people get courage and strength by communicating with the chatbot. It gives a reply according to the input message given by the user. For example, if the user texts the chatbot like feeling sad, our chatbot replies to boost the user's mood. Our chatbot is friendly, so the user is compelled to speak or share anything with the chatbot without any hesitation or anxiety. Due to this, the pain of the user will be reduced. The technologies used will give an accurate response to the user input questions with an average accuracy of 93%, reducing the risk of suicidal tendencies in such individuals.

This chatbot presents a way for such individuals to interact with it by simply speaking their minds in the same manner that they would do with their friends and family. The

scope of the proposed system is understanding and analyzing the user's emotions through text and replying to the user through text. (Using various NLP techniques and a deep neural network consisting of 3 dense layers). In the future, our framework can include understanding the user's emotions in their native language through advanced features like voice and face recognition.

References

1. Adamopoulou, E., Moussiades, L.: An overview of chatbot technology. Conference paper, Department of Computer Science, International Hellenic University, Agios Loukas, 65404 Kavala, Greece
2. Devaram, S.: Empathic chatbot: emotional ıntelligence for mental health well-being. Research Paper, Bournemouth University, Bournemouth, United Kingdom
3. Fulmer, R., Joerin, A., Gentile, B., Lakerink, L., Rauws, M.: Using psychological artificial intelligence (Tess) to relieve symptoms of depression and anxiety: randomized controlled trial. JMIR Ment. Health **5**(4), e64 (2018)
4. Abd-Alrazaq, A., Alajlani, M., Ali, N., Denecke, K., Bewick, B., Househ, M.: Perceptions and opinions of patients about mental health chatbots: scoping review. J. Med. Internet Res. **23**(1), e17828 (2021)
5. Dosovitsky, G., Pineda, B.S., Jacobson, N.C., Chang, C., Bunge, E.L.: Artificial ıntelligence chatbot for depression: descriptive study of usage. Originally published in JMIR Formative Research. http://formative.jmir.org. Accessed 13 Nov 2020
6. Grové, C.: Co-developing a mental health and wellbeing chatbot with and for young people. Front. Psychiatry **11**, 606041 (2021)
7. Browne, D.: Do Mental Health Chatbots Work? Article, 26 June 2020
8. Fitzpatrick, K.K., Darcy, A., Vierhile, M.: Delivering cognitive behavior therapy to young adults with symptoms of depression and anxiety using a fully automated conversational agent (WoeBot): a randomized controlled trial. JMIR Ment. Health **4**(2), e19 (2017)
9. Ayanouz, S., Abdelhakim, B.A., Benhmed, M.: A smart chatbot architecture based NLP and machine learning for health care assistance. https://doi.org/10.1145/3386723.3387897. Accessed April 2020
10. Inkster, B., Sarda, S., Subramanian, V.: An empathy-driven, conversational artificial intelligence agent (wysa) for digital mental well-being: real-world data evaluation mixed-methods study. JMIR Mhealth Uhealth **6**(11), e12106 (2018)
11. de Gennaro, M., Krumhuber, E.G., Lucas, G.: Effectiveness of an empathic chatbot in combating adverse effects of social exclusion on mood. Front. Psychol. **10**, 3061 (2020)
12. Bendig, E., Erb, B., Schulze-Thuesing, L., Baumeister, H.: The Next Generation: Chatbots in Clinical Psychology and Psychotherapy to Foster Mental Health – A Scoping Review. Verhaltenstherapie (2019). https://doi.org/10.1159/000501812
13. Huang, J., et al.: TeenChat: a chatterbot system for sensing and releasing adolescents' stress. In: Yin, X., Ho, K., Zeng, D., Aickelin, U., Zhou, R., Wang, H. (eds.) HIS 2015. LNCS, vol. 9085, pp. 133–145. Springer, Cham (2015). https://doi.org/10.1007/978-3-319-19156-0_14
14. Ly, K.H., Ly, A., Andersson, G.: A fully automated conversational agent for promoting mental well-being: a pilot RCT using mixed methods. Internet Interv. **10**, 39–46 (2017)
15. Hoermann, H., et al.: Application of synchronous text-based dialogue systems in mental health interventions: systematic review. J. Med. Internet Res. **19**, e267 (2017). https://doi.org/10.2196/jmir.7023

ICT in Education: A Comparative Analysis of Pre-Covid and Post-Covid Era

Archana Singh[1], Anuj Kumar Singh[2(✉)], and Ankit Garg[2]

[1] Rajkiya Engineering College, Banda, India
[2] Amity University Haryana, Gurugram, India
aksingh@ggn.amity.edu

Abstract. Technology is one of the modes of education to optimize teaching and learning methodologies in imparting knowledge. Talking about higher educational institutes, one can see the same pedagogy as it used to be a decade ago. However, these Institutes are plagued by many challenges like lack of infrastructure and inadequate technology access, and it is essential to see how these burgeoning technologies (ICT) are fostering and bridging this massive gap of teaching and learning and keeping pace with the rest of the part of the globe. ICT has revolutionized almost every sphere of society. The education system is one of the sectors that has also undergone a massive change with ICT incorporation. After the arrival of the worldwide covid pandemic, the use of ICT in education has increased extensively. This paper has performed a comparative analysis on ICT usage by the students and teachers of engineering institutions in pre-covid age and post-covid age. The survey method of data collection has been used in this research work. Analysis of results has revealed that the usage of ICT by the students and teachers has been significantly increased after the arrival of covid. Moreover, the presented work has highlighted the issues raised by the students and teachers in the post-covid time.

Keywords: ICT · Usage · Pre-covid · Post-covid

1 Introduction

ICT (information and communication technologies) is a "diverse set of technological tools and resources used to communicate, and to create, disseminate, store, and manage information." These technologies include all the electronic devices used for communication like computers, the Internet, broadcasting technologies (radio and television), and telephones.Information and communication technology (ICT) is the spine of the education system [1]. Hundreds of years ago, a guru in the ashram was the only source of education; only a few privileged ones get the opportunity to learn skills, and they have to go far away from their homes to take education. There was no other alternative to get an education. Slowly the pattern changed, and schools came into existence. The books and the teacher take the onus of imparting knowledge. With the technological advancements, the pace and the source of sharing knowledge bestow a different look to

B. Iyer et al. (Eds.): ICCET 2022, SIST 303, pp. 705–719, 2022.
https://doi.org/10.1007/978-981-19-2719-5_66

the education system. Technology and education go hand in hand and are very important in developing the education system to the developed one [2].

Technology is one of the modes of education to optimize teaching and learning methodologies in imparting knowledge. Integrating technology in teaching is not about substituting a teacher [3]. Instead, technology helps teachers deliver the content effectively, improving student learning and better teaching methods. ICT has revolutionized almost every sphere of society [4]. The education system is one of the sectors that has also undergone a massive change due to the rationales listed in Table 1 [5].

Table 1. Rationales affected by ICT.

Rationale	Basis
Social	The perceived role that technology now plays in society and the need for familiarizing students with technology
Vocational	Preparing students for jobs that require skills in technology
Catalytic	Utility of technology to improve performance and effectiveness in teaching, management, and many other social activities
Pedagogical	To utilize technology in enhancing learning, flexibility, and efficiency in curriculum

ICT can be applied in different areas of education, including library services, administration, instructional system, course content delivery, enhancing communication, improving resource access, and facilitating research [6]. These major application areas of ICT in the educational setting have been highlighted in Fig. 1. The educational institutions are now recognizing the role of ICT in enhancing the various functionalities.

Fig. 1. Application areas of ICT in education.

2 Methodology

In this paper, a comparative analysis of the usage of Information and Communication Technology (ICT) in engineering education in the pre-covid and post-covid Era has been made. This work aims to figure out the kind of transition in the teaching methodology experienced in delivering educational content in engineering education. Teachers and students are the primary stakeholders in educational institutions because these two stakeholders are directly involved in teaching and learning. Therefore, analyzing ICT usage in educational institutions requires the data to be collected directly from the students and teachers. Therefore, in this research, the data has been obtained through the online survey form from students and teachers of engineering education institutions. The survey forms have been designed to cover all the aspects of ICT usage in education. The list of questions that were asked from the teachers in the survey form are:

- What is your teaching experience?
- What is your area of Specialization?
- How much are you familiar with ICT?
- To what extent do you use ICT to collect and distribute learning material during your course delivery?
- To what extent do you prepare presentations/ or create your digital learning material for students to be used in class?
- To what extent does ICT usage in your course/subject increase student's concentration and enhance retention power?
- To what extent the usage of ICT facilitates achieving the objectives of your course?
- To what extent has ICT usage been helpful to students' success in your course?
- Do you find it challenging to integrate ICT in your subject because of the lack of infrastructure?
- To what extent do you update yourself with the latest developments in the fields of ICT?
- Do you use any Learning Management System (LMS) in your institution?
- Have you ever undertaken subject-specific Training on ICT applications?

The list of questions that were asked from the students of undergraduate and postgraduate programs in the survey form are listed below.

- To what extent are you familiar with ICT?
- To what extent do you like ICT?
- To what extent do you like learning with educational software, games, and quizzes?
- To what extent do you visit online communities or forums related to your study subjects?
- Do you check the school website for announcements, dates, etc.?
- To what extent do your teachers use ICT during lectures?
- When ICT is incorporated in teaching and learning pedagogy, do you find your course interesting?
- How often do you use e-books, online exercises, online quizzes, and online tests?
- Do you recommend the inclusion of ICT into your curriculum?

Covid-19 Forecasting using Supervised Machine Learning Techniques – Survey

P. Lakshmi Sruthi[1]*and Dr. K.* Butchi Raju[2]

[1] M.Tech Student, C.S.E, GRIET, Hyderabad, Telangana, India
[2] Associate Professor, C.S.E, GRIET, Hyderabad, Telangana, India

ABSTRACT: COVID-19 is a global epidemic that has spread to over 170 nations. In practically all of the countries affected, the number of infected and death cases has been rising rapidly. Forecasting approaches can be implemented, resulting in the development of more effective strategies and the making of more informed judgments. These strategies examine historical data in order to make more accurate predictions about what will happen in the future. These forecasts could aid in preparing for potential risks and consequences. In order to create accurate findings, forecasting techniques are crucial. Forecasting strategies based on Big data analytics acquired from National databases (or) World Health Organization, as well as machine learning (or) data science techniques are classified in this study. This study shows the ability to predict the number of cases affected by COVID-19 as potential risk to mankind.

Keywords: pandemic, COVID-19, corona virus, exponential smoothing, R2 score adjusted, machine learning supervised

1. Introduction

Machine learning (ML) has become a popular research subject in the previous decade, handling a variety of complex and sophisticated problems. ML algorithms often learn through trial and error, in contrast to traditional algorithms, which computer instructions based on decision statements such as if-else. Forecasting is one of the most important aspects of machine learning [1]. In this field, a variety of typical machine learning methods have been applied to direct future activities as shown in below Fig 1.

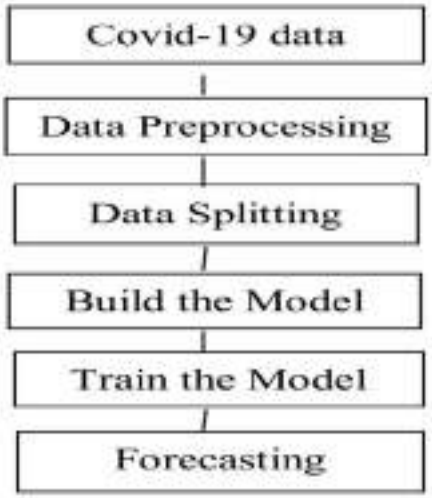

Figure 1: *Supervised Machine learning workflow*

The researchers' primary goals were to produce a study that could be beneficial for future decision-making models. Historical data is evaluated to gain perspective during the decision-making process. However, having access to data in such a short length of time is insufficient to build Artificial Intelligence (AI) models [12]. Time-series data requires AI models that can be effectively trained (During the early phases of an epidemic's spread, there is a scarcity of data). The time series analysis can help enhance forecasting efficiency.

Time series analysis is a large field that has been used to solve a wide range of issues, from econometrics to earthquakes and weather forecasting. A time series is a collection of measurements taken at regular intervals over time. A time series might be yearly, quarterly, monthly, or weekly, depending on the frequency [3]. There are two ways in which Time-series differs from a traditional regression problem. The first is time-related; in linear regression analysis, variables are independent. However, in this case, they are dependent on time. Seasonality trends, on the other hand, are fluctuations that are specific to a given span of time [4].

2. COVID (2019) OVERVIEW

COVID-19 (Corona virus) is a novel virus that causes inflammation. The disease induces a respiratory illness (such as cold, cough, fever and difficulty breathing in more severe cases).

Pandemics have posed a threat to the world on many occasions throughout history. Every pandemic's impact has always had a massive influence on the entire world, and it has also flipped the roles. Corona virus (2019), the latest destructive outbreak, is currently sweeping the globe. Not only are economics collapsing, but so are the countries' entire strengths and morale.

* Corresponding author: plsruthi@gmail.com

The global effect of the novel corona virus (COVID-19) necessarily requires detailed forecasting of confirmed patients as well as analysis of death and recovery rates. Forecasting, on the other hand, needs a large amount of past data. At the same time, no prediction can be made with certainty because the future rarely repeats itself. This study details the timetable of a live forecasting exercise with significant implications for planning and decision-making, as well as objective projections for COVID-19 cases that have been confirmed[5]. The discovery of the disease and its categorization as a pandemic by the World Health Organization are important milestones [6]

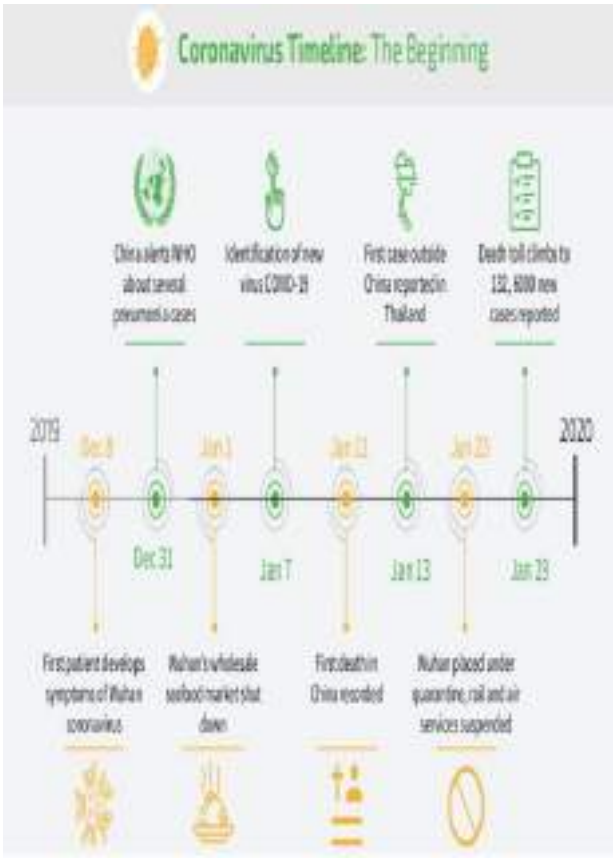

Figure 2: The Origins of the Corona virus

As shown in above Fig 2,WHO is responsible for human disease planning and response, hence diseases in the International Classification of Diseases are formally named by WHO. On February 11, 2020, ICTV declared the new virus's name as "(SARS-CoV-2) Severe Acute Respiratory Syndrome corona virus 2" and the (WHO) World Health Organization named this new disease "COVID-19". Because the virus is genetically linked to the corona virus that caused the SARS outbreak in 2003, it was given this name. The two viruses are related, but they are not the same. Corona viral infections (COVID-19) erupted in Wuhan, China, has rapidly expanded across the country [7].
COVID-19, SARC, PLAGUE, and other acquired diseases are examples. It signifies that diseases are transmitted by pathogenic agents (bacteria or virus or any micro-organism).To defend against the novel corona-virus, the **WHO [8]** recommends the following **basic precautions**.

- Keep up to current on the COVID-19 outbreak by checking out WHO updates or your local and national public health authority.
- Hand hygiene should be done on a regular basis, either with an alcohol-based hand massage.
- Keep your hands away from your eyes, nose, and mouth.
- Coughing or sneezing into a bent elbow or tissue, then discarding the tissue, is a good way to strengthen respiratory hygiene.
- If you've breathing difficulties, put on a surgical mask and wash your hands carefully after removing it.
- People who are experiencing respiratory problems have to maintain safe distance (about 2 m).
- If you've a fever, a cough, or are having trouble breathing, visit a doctor.

3. RELATED WORK

In the academic literature, machine learning (ML) methods have been offered as time-series forecasting alternative solutions to statistical approaches. However, there is a scarcity of information about their respective performance and computational needs. Using a subset of (1045) monthly data sets from the M-3 Competition, this study's purpose is to evaluate such performance over a variety of predicting horizons. When we compared the post sample accuracy of 8 prominent algorithms of ML to that of 8 classic statistical methods, study discovered that the first consistently outperformed the latter across all accuracy measures and forecasting horizons. Furthermore, we discovered that they had far higher computational requirements than statistical approaches. The study describes the findings, explains why models of ML are less accurate than statistical models, and suggests some possible next steps. Our study's empirical findings underscore the need for unbiased and fair approaches to assess the efficacy of predicting methodologies, which can also be done via major, multinational events that allow for significant comparisons and conclusions. Artificial Intelligence (AI) has gained in popularity in recent years, thanks to various elevated applications in intelligent robotics, voice recognition, image recognition, legal, medical, social applications, and even defeating winners in games such as chess and cards. The success of AI is dependent upon its usage of techniques that can learn by experimentation and improve their ability over time, rather than the typical programming domain of coding directions based on reasoning, if then principles, and Decision Trees [1].

The study's purpose is to increase machine learning (ML) algorithms' interoperability with Internet Of Things (IoT) technology in engaging with public and its surroundings in order to reduce COVID-19.Furthermore, the research looks at and examines different solution frameworks that use machine learning techniques to generate, capture, store, and analyze data. These algorithms can detect, prevent, and trace the transmission of COVID-19 in smart cities, as well as provide a better understanding of the virus. Similarly, the report highlighted case studies on the use of ML in hospitals around the world to aid in the fight against COVID-19. The research offers a thorough examination of the primary components required for integrating machine learning with other AI-based solutions. As shown in below Fig 3 and Fig 4, The study's framework provides a complete overview of the essential components required for integrating machine learning with other AI-based solutions [9] .

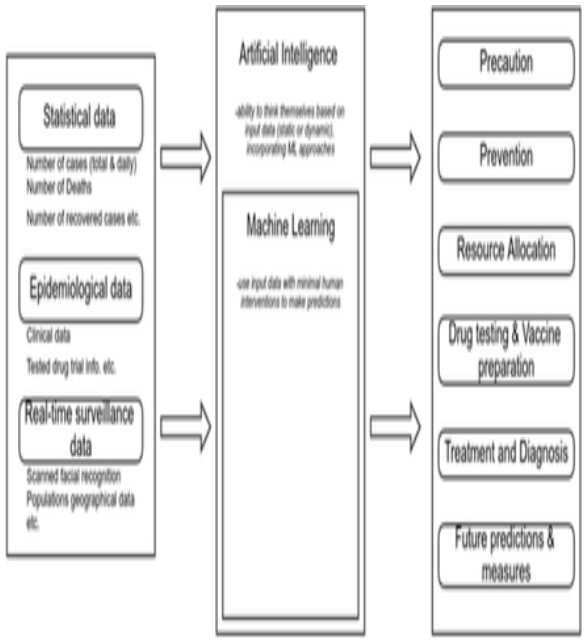

Figure 3 : Application and workflow of ML and other sub-sections of AI in tackling corona virus

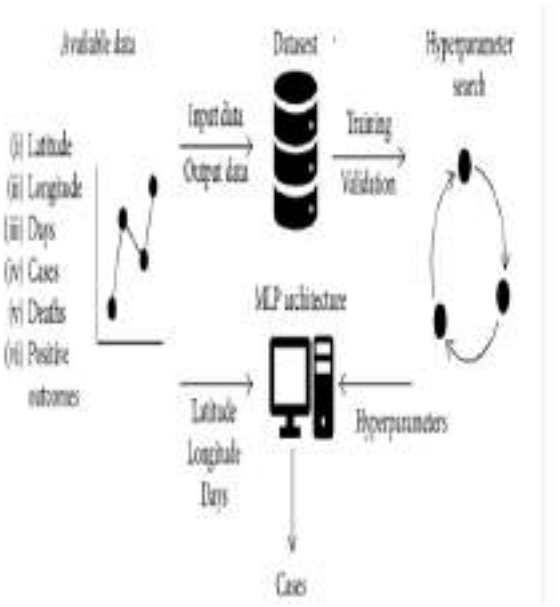

Figure 4 : *Modeling the spread of covid-19 using MLP*

The information and communication technology equipment incorporated in smart cities generates a variety of data kinds. The first type of data is **statistical data**, which often includes daily statistics such as the number of recognised cases, positive cases, deaths, and recovered cases. The second sort of data is **epidemiological data**, which mostly consists of all clinical test results for various medications, various drug trials, the patient's medical history, the patient's response to various medications, and so on. The third form of data is real-time surveillance data created by smart city sensors and cameras. Fever is one of the first symptoms of COVID-19 that can be detected. People's body temperatures and other personal information are examples of data that can help stop the spread of COVID-19 [9].

The (MLP) multi_layer perceptron is a fully-linked, (ANN) artificial neural network made up of layers of neuron like processing units feed forwarded. MLP is used for producing high quality models and also requiring less training period than more sophisticated approaches. Hyper parameters (Example: The learning rate for training a neural network) are settings that specify the ANN model's architecture. Correct hyper parameter settings are critical for producing a high-quality model. The grid search technique was used to find the optimal hyperparameter combination. A multi_layer perceptron (MLP) artificial neural network (ANN) is trained using a time series data source that is turned into a regression data source. The goal of training is to create a global model that includes the maximum patients from all locations in each time unit. With a total of 5376 hyperparameter combinations, the MLP's hyperparameters are modified using a grid-search technique. ANNs 48384 are trained using these combinations, and each model is evaluated using the determination coefficient (Zlantan Car, 2020) When cross-validation is used, the scores for confirmed, recovered, and deceased patient models drop to 0.94, 0.781, and 0.986, respectively. The deceased patient model has a high level of robustness, whereas the confirmed patient model has a decent level of robustness and the recovered patient model has a low level of robustness [10].

The major proceedings of this paper: Comparison of the ML forecasting techniques accuracy with normal statistical ones. As highlighted in the Table 1 comparison in their study the performance of eight families of the ML model regarding their accuracy: 1) (MLP) Multi_Layer Perceptron 2) (BNN) Bayesian Neural Network 3) (RBF) Radial Basis Function 4) (GRNN) Generalized Regression Neural Networks 5) (KNN) K-Nearest Neighbor regression 6) (CART) Classification and Regression tree 7) (SVR) Support Vector Regression, and 8) (GP) Gaussian Processes. The sMAPE (Symmetric Mean Absolute Percentage Error) and ordering of these '8' methods can be represented in Table 1. From the Observation, the MLP got the highest accuracy, then after the BNN and the GP. The remaining methods' sMAPE is in the double digits, indicating a significant variation in accuracy. Investigating the grounds for the variations in performance among the different ML approaches and developing guidelines for picking the most appropriate one for new sorts of forecasting applications would be of significant research value. [11].

Table 1 Predicting Accuracy of ML methods (sMAPE)

Rank	Method	sMAPE(%)
1	MLP	8.34
2	BNN	8.58
3	GP	9.62
4	GRNN	10.53
5	KNN	10.54
6	SVR	10.68
7	CART	11.72
8	RBF	15.79

According to 'WHO' globally 634,835 confirmed cases have been reported worldwide, to date, 29,891 deaths have been confirmed. Figure 5 shows the statistics broken down by region. The following are the Regions: The Western Pacific Region, the European Region, the South_East Asian Region, the Eastern Mediterranean Region, the American Region, and the African Region are all part of the Western Pacific Region. China, France, Spain, Italy and the United States are among the heavily impacted regions.

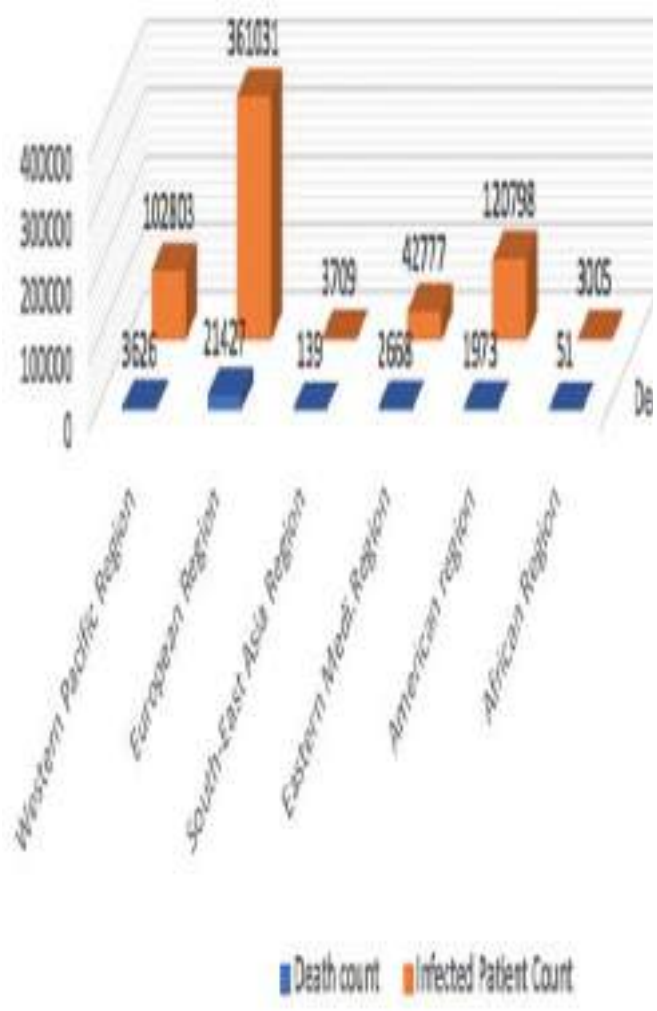

Figure 5: Regional wise Statistics

These figures are from a WHO report published March 29, 2020 [12]. This pandemic is keep expanding throughout all regions, as evidenced by the figure. Prediction can be accomplished using a variety of approaches from the fields of statistics, data science, machine learning, and artificial intelligence [12].

4. ANALYSIS

Forecasting has been done in the research using a variety of forecasting methodologies and data sources. To understand existing forecasting models for better analysis

4.1 Data Science/Machine Learning Techniques

Table 2Analysis of Covid (2019) prediction on ML Techniques or Data Science

Work ref.	Studied regions	Data source	Parameters	Remark
[13]	China	Small dataset	Corrective feedbacks of model	Forecasting suspected numbers of COVID-19
[14]	China	Chinese Center for Disease Control and Prevention	Cost of isolation, cost of treatment, no of suspects, no of confirmed COVID patients	Recommendation for decision making
[15]	China	WHO	Daily death count	Forecasting of death count
[16]	102 countries	WHO	Degree of intervention and starting intervention time	Impact of a public health intervention on the global-wide spread
[17]	China	2003 SARS Data	Death count	Forecasting of death numbers
[18]	China and European countries	WHO	Infection rate	Prediction of infection rate
[19]	Global Data	International Classification of Diseases	Preexisting medical conditions	Identify individuals who are at the greatest risk

Due to their precision, ML techniques are now utilized for forecasting all over the world. However, there are a few limitations to the use of machine learning (ML) approaches because there's very little data accessible. The optimal parameter selection and selecting models of ML are two issues involved in training a model for forecasting.

Researchers made predictions based on publicly accessible datasets and utilised the best machine learning model for each dataset [13, 14,15,16,17]. To determine rates of infection in Italy and China, [18] Research proposed a model based on the Logistic-equation, Weibull-equation, and the Hill-equation. Data analysis is conducted in this study to determine the environmental factors impact on the spread of COVID (2019). This model focused on three environmental factors: relative humidity, maximum environmental temperature, and wind speed. The results demonstrated that there is no correlation between COVID-19 spread and humidity or wind speed. The study [19] proposed a model that included a hybrid model, gradient boost trees, and logistic regression that used Medical data. The results of above models will aid in the development of management planning and the implementation of remedies in order to reduce the spread. **Table 2** summarises the results of this research.

4.2 Big Data

Table 3 Analysis of covid (2019) prediction on Big Data

Ref.	Studied regions	Data source	Parameters	Remark
[20]	China, Japan, Korea, European countries, and North America	Johns Hopkins University, GitHub repository	Transmission rate, Infection rate, and recovery rate	Recommendations for decision making
[21]	Italy, Portugal	Italy national data	Number of susceptible, exposed, asymptomatic infected, mild-to-severe infected patients	Forecasting numbers of COVID-19 patients
[22]	US	US Centers for Disease Control	Disease control interventions and traffic restrictions	Impact of disease control interventions and traffic restrictions on spread rate
[23]	Brazil	WHO	Number of susceptible, exposed, infectious and recovered patients	Suggested policy-making for avoiding outbreak in metropolitan cities

Researchers have forecasted using data from recognised national and international sources, according to the literature. Various methodologies, such as mathematical equations or machine learning algorithms, are used to analyse a large dataset.

Research [20] has given decision-making systems based on the COVID-19 data collected from Johns Hopkins University for countries such as China, European countries, Japan, Korea and North America. [21] Research used WHO COVID-19 databases, Italian national data and Johns Hopkins data to forecast death rates. The impact of disease management actions and transportation limitations on the spread rate was described [22]. The study was based on a dataset obtained from the US-CDC (Centers for Disease Control and Prevention). [23] Study has discussed the key tasks of Isolation in reducing COVID-19 dissemination rates. **Table 3** summaries the results of the literature review.

5. CONCLUSION

The spread and reproduction number should be predicted using a variety of datasets. For more accurate worldwide forecasting, the models described in the literature should be evaluated internationally. On similar considerations, several peaks must be considered in the model not just for short-term forecasting but also for forecasting the outbreak later in the year.

We expect that by analysing multiple COVID-19 forecasting models, we will be able to better modify intervention measures and, more importantly, we will be able to reduce the pandemic's worrying effect. In this study many publications analysed are preprints, which means they are not subjected to rigorous review. Though, given COVID-19's rapid global expansion, a detailed survey of comparison is urgently needed for the mankind.

References

[1] S. Makridakis, E. Spiliotis, and V. Assimakopoulos, "*Statistical and machine learning forecasting methods: Concerns and ways forward*," PloS one, vol. **13**, no. 3, (2018).

[2] L. van der Hoek, K. Pyrc, M. F. Jebbink, W. Vermeulen-Oost, R. J. Berkhout, K. C. Wolthers, P. M. Wertheim-van Dillen, J. Kaandorp, J. Spaargaren, and B. Berkhout, "*Identification of a new human coronavirus*," Nature medicine, vol. **10**, no. 4, pp. 368–373, (2004).

[3] Dimitris Effrosynidis"*Time Series Analysis with Theory, Plots, and Code Part 1*" Apr 5, (2020) [online] https://towardsdatascience.com/time-series-analysis-with-theory-plots-and-code-part-1-dd3ea417d8c4

[4]Bhanuka Dissanayake, "An introduction to time series, and basic concepts and modelling techniques related to time series analysis and forecasting", Jul 14, 2020[online]https://towardsdatascience.com/introduction-to-time-series-forecasting-7e03c4bd83e0

[5]F. Petropoulos and S. Makridakis, "*Forecasting the novel coronavirus covid-19*," Plos one, vol. **15**, no. 3, p. e0231236, (2020).

[6]Harry Kretchmer,"Key milestones in the spread of the coronavirus pandemic", 22 Apr 2020 [online] https://www.weforum.org/agenda/2020/04/coronavirus-spread-covid19-pandemic-timeline-milestones/

[7] "*WHO. Naming the coronavirus disease (covid-19) and the virus that causes it*". [Online]. Available: https://www.who.int/emergencies/diseases/novelcoronavirus-2019/technical-guidance/naming-the-coronavirus-disease- (covid-2019)-and-the-virus-that-causes-it

[8] "*World Health Organization. Coronavirus disease (COVID-19) advice for the public*".[Online]. Available:https://www.who.int/emergencies/diseases/novel-coronavirus-2019/advice-for-public

[9] Ezugwu, Absalom & Abaker, Ibrahim & Oyelade, Olaide & Chiroma, Haruna & Al-Garadi, Mohammed & Abdullahi, Idris & Otegbeye, Olumuyiwa & Shukla, Amit & Almutari, Mubarak, "*A Novel Smart City Based Framework on Perspectives for application of Machine Learning in combatting COVID-19*", (2020): doi:

10.1101/2020.05.18.20105577.
[10]Zlatan Car, Sandi Baressi Šegota, Nikola Anđelić, Ivan Lorencin, Vedran Mrzljak, "*Modeling the Spread of COVID-19 Infection Using a Multilayer Perceptron*", Computational and Mathematical Methods in Medicine, vol. 2020, Article ID 5714714, 10 pages, (2020). https://doi.org/10.1155/2020/5714714
[11]Ahmed NK, Atiya AF, Gayar NE, El-Shishiny H. "*An Empirical Comparison of Machine Learning Models for Time Series Forecasting. Econometric Reviews*", (2010); 29(5–6):594–621. https://doi.org/10.1080/07474938.2010.481556
[12]Shinde, Gitanjali R et al. "*Forecasting Models for Coronavirus Disease (COVID-19): A Survey of the State-of-the-Art.*" SN computer science vol**. 1**, 4 (2020): 197. doi:10.1007/s42979-020-00209-9
[13]Fong SJ, Li G, Dey N, Crespo RG Herrera-Viedma E. "*Finding an accurate early forecasting model from small dataset: a case of 2019-ncov novel coronavirus outbreak*". arXiv preprint arXiv:2003.10776. (2020)
[14]Fong SJ, Li G, Dey N, Crespo RG, Herrera-Viedma E. "*Composite monte carlo decision making under high uncertainty of novel coronavirus epidemic using hybridized deep learning and fuzzy rule induction*". Appl Soft Comput. (2020);106282.
[15]Batista M. "*Estimation of the final size of the second phase of the coronavirus COVID-19 epidemic by the logistic model*". 2020.03.11.20024901; doi: https://doi.org/10.1101/2020.03.11.20024901
[16]Hu Z, Ge Q, Li S, Jin L, Xiong M. "*Evaluating the effect of public health intervention on the global-wide spread trajectory of Covid-19*". medRxiv. (2020).
[17]Jia L, Li K, Jiang Y, Guo X. "*Prediction and analysis of coronavirus disease 2019*". arXiv preprint https://arXiv:2003.05447. (2020).
[18]Kumar J, Hembram KPSS. "*Epidemiological study of novel coronavirus (COVID-19)*". arXiv preprint https://arXiv:2003.11376. (2020).
[19]DeCaprio D, Gartner J, Burgess T, Kothari S, Sayed S. "*Building a COVID-19 vulnerability index*". arXiv preprint https://arXiv:2003.07347. (2020).
[20]Toda AA. "Susceptible-*infected-recovered (sir) dynamics of covid-19 and economic impact*". arXiv preprint arXiv:2003.11221. (2020).
[21]Teles P. "*Predicting the evolution of SARS-Covid-2 in Portugal using an adapted SIR Model previously used in South Korea for the MERS outbreak*". arXiv preprint https://arXiv:2003.10047. (2020).
[22]Liu P, Beeler P, Chakrabarty RK. "*COVID-19 progression timeline and effectiveness of response-to-spread interventions across the United States*". medRxiv. (2020).
[23]Rocha Filho TM, dos Santos FSG, Gomes VB, Rocha TA, Croda JH, Ramalho WM, Araujo WN "*Expected impact of COVID-19 outbreak in a major metropolitan area in Brazil*". medRxiv.(2020).

Proceedings of the Fifth International Conference on I-SMAC (IoT in Social, Mobile, Analytics and Cloud) (I-SMAC)
DVD Part Number: CFP21OSV-DVD; ISBN: 978-1-6654-2641-1

Prediction of the COVID-19 pandemic with Machine Learning Models

1st P. Lakshmi Sruthi
MTech Student
Computer Science department
GRIET, Hyderabad, Telangana, India.
plsruthi@gmail.com

2nd Dr. K. Butchi Raju
Professor
Computer Science department
GRIET, Hyderabad, Telangana, India.
Raju_katari@yahoo.co.in

***Abstract*— The latest destructive outbreak, Corona virus (2019), is rapidly sweeping the globe. Not only are economies deteriorating, but countries' entire strengths and confidence are as well. Machine learning forecasting strategies have demonstrated their importance to anticipate in outcomes of the perioperative period to improve the future decision-making actions. The machine learning algorithms have long been used in several applications which require the detection of adverse factors for a threat. Forecasting techniques are essential for producing accurate results. This study shows the ability to predict the number of cases affected by COVID-19 as potential risk to mankind. In this analysis, four prediction algorithms have been used which are linear regression (LR), Exponential Smoothing (ES), least absolute shrinkage and selection operator (LASSO) and support vector machine (SVM). Each of these models has three different kinds of predictions, such as the newly infected patients, death cases and the recovery cases in the next ten days. These approaches are better used to forecast the covid-19 pandemic, as shown by the findings of analysis. The ES, that is effective in forecasting new corona cases, death cases and recovery cases.**

Keywords—*Pandemic, COVID-19, Corona virus, R2 Score Adjusted, Exponential Smoothing, Machine Learning Supervised.*

I. INTRODUCTION

In the last decade, machine learning (ML) has become a popular area of study for a variety of complicated and advanced challenges. In contrast to the traditional algorithms, which use decision statements such as if-else, ML Algorithms/Techniques frequently learn by trial - and - error. One of the most essential components of machine learning is forecasting. A range of widely used ML algorithms have been used to influence future activities in this subject [1].

The global impact of the novel (corona virus) COVID-19 needs precise patient predictions along with mortality and recovery rates research. Prediction, on either way, needs very huge portion of historical information. At the similar period, no prediction can be made with certainty because the future rarely repeats itself. This study puts out the timeline for a practical forecasting activity with major consequences for planning and decision-making, as well as objective estimates for confirmed COVID-19 instances.

The following are some of the *study's significant findings:*
• When the period dataset includes a small quantity of data, ES works well.
• Distinct machine learning algorithms appear better at predicting different classes.
• Most machine learning algorithms require a large quantity of data to forecast the future; as the dataset grows larger, the model's efficiency increases.
• For decision-makers battling pandemics like COVID-19, ML model-based prediction could be quite valuable.

The rest of overall work is broken down into 6 pieces. The introduction is offered in Part I, followed by a description of the dataset and methods used in this work in Part II. Part III presents the proposed approach, Part IV discusses the results, and Part V summarises the work and provides the conclusion.

A. Covid 2019

On February 11, 2020, the novel disease has been labeled "(SARS-CoV-2) Severe Acute Respiratory Syndrome Corona Virus 2" by ICTV, and "Corona Virus"(Covid-19) by the (World Health Organization) WHO. This pathogen was given this name because it is genetically linked to the corona virus that caused the SARS outbreak in 2003. Although the two viruses are related, they are not similar. Corona viral infections (COVID-19) began in Wuhan, China, and also have progressed quickly throughout the country [2].

Prolonged body interaction, respiratory secretions, and contacting exposed items are the most common ways for the pathogen to circulate. One of most difficult element of its transmission is that an individual might be affected by the disease for days despite experiencing suffering. Nearly many areas are affected by it due to the causes of its spread and the danger it poses. Every country has declared full/ partial curfews.

With the commitment and cooperation of G20 countries, WHO's worldwide aims are to help every country vaccinate at least 10% of its population by the end of this month, at least 40% by the end of the year, and 70% of the world's population by the middle of next year [3]. While adapting to their new human hosts, SARS-CoV-2, like some of the other RNA virus, is susceptible to biological transformation with the formation of mutations over time, resulting in mutation variants with different features than their parental types. Several SARS-CoV-2 variations have now been identified during the pandemic, however only a fraction are classified variants of concerns by the WHO due to their worldwide public health impact.

B. *Covid-19 Varinats and Vaccination*

The world is in the grip of a COVID pandemic (2019). While the World Health Organization (WHO) and its partners fight to contain the epidemic, advise on critical treatments, and distribute critical healthcare supplies to individuals in need, they're also working to develop and deploy safe and effective vaccines.

Every year, vaccines save thousands of lives.COVID-19 vaccinations are effective and safe in preventing individuals from becoming dead or dying (In addition to social distancing, maintaining mask and sanitizing). Gamaleya: Sputnik V, Bharat Biotech: Covaxin and covisheild vaccines are used mostly in India. WHO has approved 7 vaccines for use, type of vaccine details can be found at "https://covid19.trackvaccines.org/types-of-vaccines/".'NRVV' stands for Non Replicating Viral Vector, RNA, and full form stands for ribonucleic acid [4].

Table I-1 WHO approved vaccines.

Vaccine	Codenamed	Referred also as	Type	Approved
Moderna	mRNA-1273	Spikevax	RNA	71 countries
Pfizer/BioNTech	BNT162b2	Tozinameran, Comirnaty	RNA	98 countries
Johnson & Johnson	Ad26.COV2.S, Ad26COVS1, JNJ-78436735	Janssen	NRVV	63 countries
Oxford/AstraZeneca	AZD1222	Vaxzevria	NRVV	121 countries
Oxford/AstraZeneca formulation(serum institute of India)	AZD1222	Covishield	NRVV	45 countries
Sinopharm (Beijing)	BBIBP-CorV	Covilo	Inactivated	64 countries
Sinovac	CoronaVac	__	inactivated	40 countries

According to the WHO's most current epidemiological update, four SARS-CoV-2 VOCs (Variants of Concerns) have been discovered since the beginning of the pandemic as of June 22, 2021 [13]:

1) Alpha [B.1.1.7]: In late December 2020, the United Kingdom (UK) reported the first variant of concern.

2) Beta [B.1.351]: first December 2020, South Africa reported the first version of concern.

3) Gamma [P.1]: In early January 2021, Brazil reported the first variant of concern.

4) Delta [B.1.617.2]: In December 2020, India reported the first variant of concern.

C. *Related Work:*

In the academic literature, machine learning (ML) methods have been offered as alternatives to statistical methods for time series forecasting. The goal of this research is to assess such performance over a variety of forecasting horizons using a subset of 1045 monthly data series from the M3 Competition. When we compared the post-sample accuracy of eight prominent ML algorithms to that of eight classic statistical methods, we discovered that the former consistently outperformed the latter across all accuracy measures and forecasting horizons. The study describes the findings, explains why ML models are less accurate than statistical models, and suggests some possible next steps. The empirical findings of our study highlight the necessity for objective and unbiased techniques to evaluate the effectiveness of forecasting methodologies, which can be accomplished through large, international events that allow for meaningful comparisons and conclusions [1].

The goal of this research paper is to provide a complete overview of the epidemiology, pathogenesis, patient characteristics, etiology, tools of diagnostics, and the most recent new medications for COVID-19 treatment. This paper also includes a brief description of the many SARS-CoV-2 mutations and the efficacy of several existing vaccines for COVID-19 and its mutations prevention [13].

In this article, researchers used time series models to create statistical projections for confirmed COVID-19 cases and examined the trend of recovered cases. Exponential smoothing model with multiplication error and multiplication trend components was employed in the methodology. In the case of significant, negative tilted estimates, persistent prediction deviations should be linked to modifications in observable trends but also the demand for extra measures and actions [16].

Scholars used currently accessible datasets to make predictions and used the optimal machine learning model for each dataset [5, 6, 7, 8, and 9]. In order to evaluate transmission levels in Italy and China, the Weibull-equation, Hill-equation, and Logistic-equation were used to develop a model [10]. This study uses statistical research to explore the impact of ecological elements upon that spreading disease COVID -2019. 3 ecological specifications were included in this model, wind speed, maximum temperature and relative humidity. COVID-19 spreading seems to have no association with temperature or weather rate, according to the findings. The study [11] suggested a model that employed patient records as well as contained a hybrid model, gradient boost trees, and logistic regression. The results of such abovementioned programs can assist throughout the design of administration plans for the execution of therapies to help minimize the disease transmission. The findings of research are represented in Table 2.

Table 1 Covid-19 forecasting on Machine Learning Models.

Work ref.	Studied regions	Data source	Parameters	Remark
[5]	China	Minimal data source	Feedback Corrections of models	Predicting Expected statistics of Corona Virus
[6]	China	Chinese Center for Disease Control and Prevention	The expenses of therapy and isolation, the expected number of candidates, and the number of identified COVID-19 cases	Guideline towards choosing a decision
[7]	China	WHO	Death toll on a daily basis	Prediction of death toll
[8]	102 countries	WHO	The quantity of treatment and the time needed to begin the therapy.	The effect of citizen prevention strategies on the wide impact of a disease
[9]	China	2003 SARS Data	Death Toll	Prediction of death toll
[10]	European Countries and China	WHO	Degree of transmission	Forecasting the degree of transmission
[11]	Global Data	International Classification of Diseases	Preexisting health issues(Blood Pressure & Sugar)	Identify the people who are the most vulnerable.

The study's main aim to improve the inter - operability of machine learning algorithms with Internet of things (IOT) when engaging among the community as well as their environments to minimize COVID (2019). The study looks at various architectures for generating, capturing, storing, and analysing the data using ml techniques. These algorithms can help recognize, inhibit, and track COVID-19 spread in smart areas, along with give researchers a better knowledge about the infection. Additionally, analyses mostly on application of machine learning at health care facilities to support mostly in combat over COVID (2019) were featured in the paper. The study takes a close look at the key components that go into merging machine learning with other AI-based solutions. The part of this analysis contains a broad outline into the aspects needed to integrate ml algorithms with alternative Intelligence systems. Smart cities' technology as well as information technology infrastructure creates a wide range of data types. The *statistical data (1)* frequently contains daily statistics such as the amount of confirmed rates, positive rates, deaths, and healed rates. The *epidemiological data (2)* includes predominantly every diagnostic medical report for prescription meds, clinical studies, the personal health background, and the person's sensitivity to different prescription drugs, among other things. The data generated by smart city sensors and cameras in *real-time surveillance (3)*. High Temperature is often early COVID-19 indications to be detected [21].

The multilayer perceptron (MLP) is a feed-forward artificial neural network (ANN) composed of layers of neurons that is fully coupled. MLP is also known for developing high-quality models with less training time than more advanced techniques. Hyper parameters (for example, the learning rate for training a neural network) are parameters that define the architecture of an ANN model. For a slightly elevated model, the max parametric choices should be accurate. To discover the ideal hyper - parameter combo, the grid search procedure has been developed. A time-series data source is converted into a regression data source to train a multilayer perceptron MLP of artificial neural network (ANN). The purpose of training is to develop a global model that contains as many patients as possible from all locations in each time unit. The robustness of the deceased patient model is strong, whereas that of the confirmed patient model is average, and when recovered patient scenario is weak. The MLP is the most accurate machine learning approach, followed by the Bayesian Neural Network (BNN) and Gaussian Processes (GP). The alternative approaches' sMAPE is not in the single digits, signifying a major variation in accuracy. [22].

Using COVID (2019) lung x-rays and the (HOG) histogram oriented gradients feature based methodology, researchers have developed an efficient classification technique for reliably detecting COVID (2019) virus strains. It achieves high outcomes via utilising precise COVID (2019) new disease classification relating to medical scans. Further, the efficiency of the Convolution Neural Network (CNN) classification method for healthcare images has also evaluated using several edge based artificial networks. The efficiency of final classification using decreases as the amount of classes in the trained network increases. Finally, a 10 fold cross-validation analysis with confusion metrics was performed to detect various conditions such as lung infection. Transfer learning obtained a third classification performance of 85 percent, which included healthy, COVID (2019) positive, and Lung Inflammation [23].

To estimate the overall number of COVID (2019) cases at the county division throughout the United States, researchers created the neural recurrent models built on Long Short Memory LSTM. Our algorithm takes the demography of the counties, while also prior daily sociocultural interaction and COVID (2019) records, and estimates the total number of COVID-19 instances in 2 weeks. When tested on the

timeframe beginning August 1, 2020, till January 22, 2021, this analysis generated a positive correlation between actual and predicted values [24].

II. METHODS & MATERIALS

A. Data Source

This purpose of this study aim here is to predict how COVID19 will spread in the future, with an emphasis on the number of newly confirmed patients, mortality, and recoveries. Data for this inquiry came from the GitHub Repository of the (CSSE) 'Center for Systems Science & Engineering', (JHU) 'Johns Hopkins University '[12]. The ESRI Living Atlas Team assisted the university in making the repository accessible for the 2019 New Corona virus graphical dashboards. On the Git-Hub Repository, Data source records may be located in the (csse covid 20 19 time - series data) Supervised Machine Learning Models.

B. Supervised ML Models

When given an unexpected inputs occurrence, then supervised machine learning model is developed to generate a forecast. When develop the regression model, the training process takes a dataset with incoming occurrences and their matching regressor. After that, the training classifier provides a forecast using the unexpected source information or testing data source [14]. For the building of prediction models, this learning method might utilize regression algorithms and classification methods. Therefore, research using COVID (2019) prediction, 4 regression algorithms were applied.

1. Linear Regression: In machine learning, linear regression is the most often used statistical procedure for forecasting. A linear association between the dependent and relationship between the independent variable is determined through linear regression. 2 values 'x' and 'y' are employed in linear correlation analyses. Mathematical equations below represent the y-x connection, popularly called as regression.

$$y = \beta 0 + \beta 1x + \varepsilon \quad (1)$$

$$E(y) = \beta 0 + \beta 1x \quad (2)$$

Here, ε represents error term (variability between y and x), β0 is the y-intercept and ß1 is the slope.

For the goal of model training of the linear regression in the framework of machines research, a class label is defined in the input data set. The goal is to determine the best 0 (intercept) and 1 (coefficient) values to obtain optimal regression line. To ensure that this minimization solution is shown, the differential between the real values and the estimated values should be as little as possible [19]:

$$Minimize \frac{1}{n}\sum_{i=0}^{n}(predi - yi)\ 2 \quad (3)$$

$$g = \frac{1}{n}\sum_{i=1}^{n}(predi - yi)\ 2 \quad (4)$$

Cost-function (g) is the root mean squared error of the estimated value of' 'y' (predi) and real value of 'y' (yi), and n represents set of sample units.

2. Least Absolute Shrinkage & Selecton Operator:'LASSO' is a sort of shrinkage-based regression model. Data variables are shrunk towards a centralized location, such as the mean, in shrinkage. Simple, sparse modelling are encouraged by the lasso approach which having few parameters. As a result of the shrinking process, LASSO becomes better and more stable, as well as reducing error .This regression is ideal for modelling techniques with a lot of multi – co linearity (when two or more independent variables are highly correlated with one another in a regression model) as well as when we wish to automate elements of the modelling selection process, such as selection of variable or parameter removal. Lasso is a type of linear regression in which the model is penalised for the sum of the weights' actual values. Ridge goes a bit further and penalising the model for the weights' sum of squared values. Weights were divided more equally in groups. Lasso generally gives sparse weights and also most zeros due to L1 Regularization (15). During training, the objective function is changed to:

$$\sum_{i=1}^{n}(yi\text{-}\sum_{j} xij\beta j)\text{^}2 + alpha \sum_{j=1}^{p}|\beta j| \quad (5)$$

Alpha (the coefficient) term refers to penalize weights.

3. Exponential Smoothing: Forecasting is done using data from prior periods in the exponential smoothing family of approaches. As time passes, the influence of previous data observations diminishes exponentially. As a result, the weight allocated to various lag values decreases exponentially. 'ES' is a simple-to-use, reliable temporal periodic prediction technique using univariate data [16], [17]. The prediction for the present time (Ft) in Exponential Smoothing is as follows:

$$F_t = \beta A_{t-1} + (1 - \beta)\ F_{t-1} \quad (6)$$

Here $0 \leq \beta \leq 1$, A_{t-1} represents actual value of the preceding period in the time-series, and F_{t-1} represents predicted value of the prior forecast, smoothing cost is used.

4. Support Vector Machine: SVM is a supervised ML technique that can be used to solve classification and regression problems (mainly). The value of each feature represents the value of a given position in the SVM algorithm, and each data item is displayed as a point in n-dimensional geometry (n being the quantity of attributes). Afterwards we locate the hyper-plane that best separates the 2 groups to complete classification. The coordinates of a single observation are what vectors were. This SVM classification algorithm is a frontier which effectively separates this 2 classes (hyper-line or plane).When we have a large data set, it does not perform well because the needed training time is longer.

C. Evaluation Parameters

Time-series prediction models can be assessed using the following commonly used accuracy measurement functions:

- MSE: Mean Square Error and the lower the MSE the better is the performance.

$$\frac{1}{n}\sum_{i=1}^{n}(yi - yi\text{^})\ 2 \quad (7)$$

- RMSE: square root version of MSE

$$\sqrt{\frac{1}{n}\sum_{i=1}^{n}(yi - yi\hat{}) 2} \quad (8)$$

- MAE: Mean Absolute Error is the difference between predicted and original value

$$\frac{1}{n}\sum_{i=1}^{n}|yi - yi\hat{}| \quad (9)$$

Here y_i and $y_i\hat{}$ represent the real and estimated values, respectively.

- R2Score: The degree of performance of a regression model is represented by R-squared, a statistical measure. For r-square, 1 is the optimal value. The nearer the r - squared value is to 1, the higher the model fits.

$$\frac{\text{Varianceexplainedbymodel}}{\text{Totalvariance}} \quad (10)$$

III. METHODOLOGY

The dataset was separated into two subsets following the preliminary data pre-processing: a training set for training the models *(85%)* and a testing set for testing the models *(15%)*.

Figure 1 Proposed Workflow

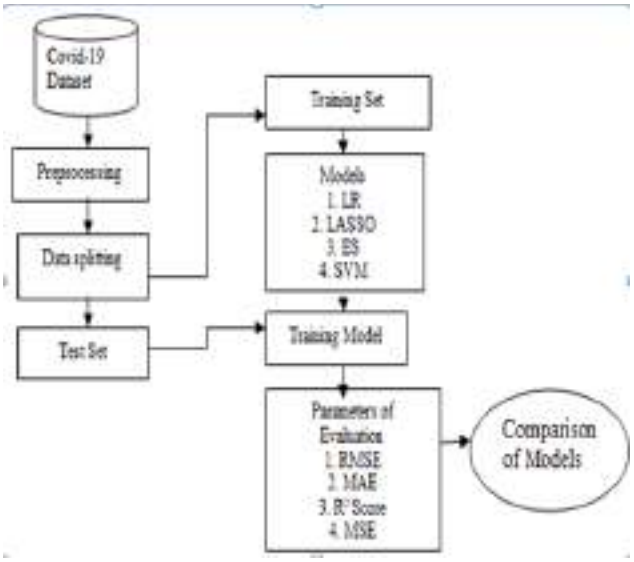

In this work, learning models such as LR, ES, LASSO, and SVM were applied. The new confirmed patients, recovery cases, and death rates were used to train the models [18]. The learning models were then assessed using essential metrics such the RMSE, MAE, R2 score, and MSE, and the findings were published. Figure 1 depicts detailed workflow.

Table III-1 Sample Dataset

Province/ State	Country/Region	Lat	Long	1/22/20	1/23/20	1/24/20
Queensland	Australia	-27.46	153.02	0	0	0
South Australia	Australia	-34.92	138.60	0	0	0
Tasmania	Australia	-42.88	147.32	0	0	0
Victoria	Australia	-37.81	144.96	0	0	0
Western Australia	Australia	-31.95	115.86	0	0	0

Attributes in Data Source contains State, Country, Latitude, Longitude and contains series of dates. Dataset having the 3 folders (Recovery, death and Confirmed Cases)

IV. *RESULTS & DISCUSSION*

Using ML approaches, this work seeks to construct effective technique towards predicting the future amount of persons infected by COVID (2019). The study's dataset provides day updates on the amount of newly infected patients, the rate of recoveries, and the rate of COVID-19-related mortality around the world. The world is in an unpleasant scenario as the death count and reported illnesses keep on rising. The amount of people that could be infected with COVID (2019) in various parts of the globe is unknown. For the following 10 days, the goal of this study is to estimate the number of people who will be affected in addition to newly infected cases and fatalities, as well as the number of expected recovery rates has all been predicted using 4 ML models: LR, ES, LASSO, , and SVM.

Among all 4 algorithms Exponential Smoothing is giving best performance result and here SVM is taking much longer time for execution, so implementing 3 algorithms. In the dataset we have 3 files for death, recover and confirm cases.

A. *Dataset (From January 2020 to November 2020)*

The first predicted timeframe (from 22/01/20 to 03/11/20) is used to display the results. Click on 'Upload Covid-19 Dataset' button and upload entire dataset folder which contains 3 files such as confirm, recover and death. Select 'dataset' folder and then click on 'Select Folder' to load dataset then dataset is loaded and now click on 'Preprocess Dataset' button to read data and then replace missing values with 0 and clean the dataset.

Figure 2 Preprocessing

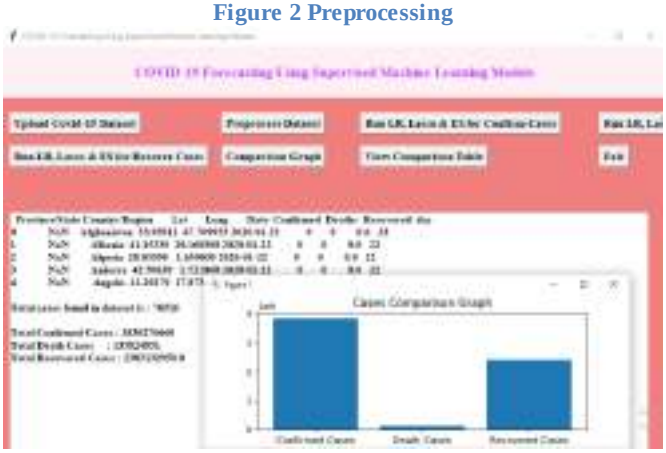

In the screen we can see dataset is cleaned and here displaying few records from dataset and then displaying total death, recover and confirm cases and case comparison graph. Total cases found in this dataset are 76916 and total confirm

cases, Death cases and recovery cases are shown. First 5 records of the dataset are displayed in above screen.

Figure 3 Confirm cases forecasting using ES

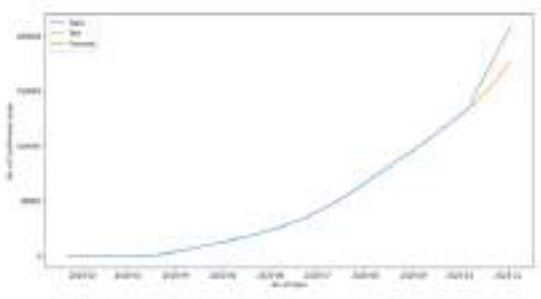

Click 'Run LR, LASSO & ES' for confirmed cases button to get above graph. Graph displays forecasting where blue line refers to train data and yellow line refers to test data and this both train and test data we got from dataset and green line refers to forecast/predicted values for next 10 days. In above graph x-axis represents days and y-axis represents number of confirmed cases.

Figure 4 Death cases forecasting using ES

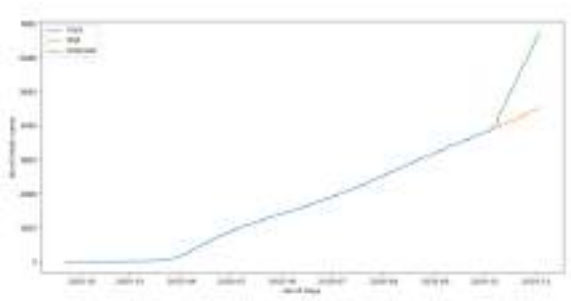

Click 'Run LR, LASSO & ES' for death cases button to get above graph. In above graph *x-axis* represents days and *y-axis* represents number of death cases.

Figure 5 Recovery Cases forecasting using ES

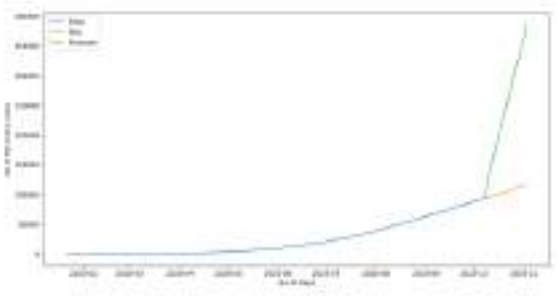

Click 'Run LR, LASSO & ES' for Recovery cases button to get above graph. In above graph *x-axis* represents days and *y-axis* represents number of recovery cases.

Exponential Smoothing gives good performance among LR & Lasso. In above graph, green line represents recover forecast values. Now click on 'Comparison Graph' button to get below graph.

Figure 6 Comparison Graph

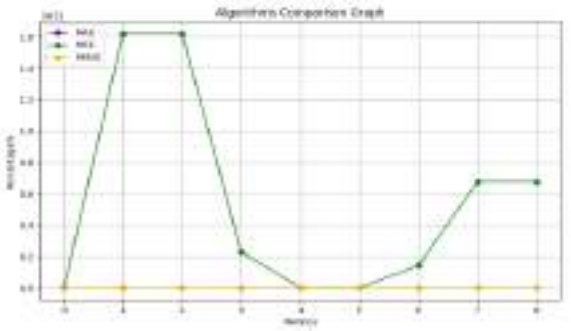

In above graph MAE, MSE is more for Linear Regression and Lasso but it got reduce for exponential smoothing. Now close above graph and then click on 'View Comparison Table' button to get below table.

Table IV-1 Comparison Table

Algorithm Name	R2 Score	MSE	MAE	RMSE
Linear Regression	1.299	67649264400	54018	260094
Lasso	1.299	67649263727	54018	260095
Exponential Smoothing	95.61	14081501933	99360	118665

In above table, We can see MAE, MSE, RMSE and R2Sqaure values for each algorithm and R2square value of Exponential has got highest values compare to other 2 algorithms.

4.2 Updated Dataset (From September 2020 to September 2021)

The Second predicted timeframe (from 01/09/20 to 14/09/21) is used to display the results in updated dataset.

Figure 7 Preprocessing for Updated Dataset

Total cases found in this dataset are 105741 and total confirm cases, Death cases and recovery cases are shown. First 5 records of the dataset are displayed in above screen.

Figure 8 Recovery Cases forecasting using ES for Updated Dataset

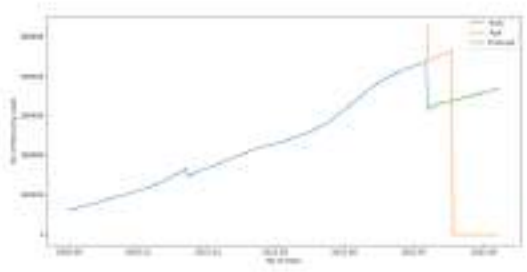

Click 'Run LR, LASSO & ES' for death cases button to get above graph. In above graph *x-axis* represents days and *y-axis* represents number of recovery cases.

Table IV-2 Comparison Table for updated Dataset

Algorithm Name	R2 Score	MSE	MAE	RMSE
Linear Regression	0.491	1451919935971	334613	1204956
Lasso	0.491	1451919930574	334613	1204956
Exponential Smoothing	81.16	160880475284	399641	401099

For the updated Dataset, Also R2square value of Exponential has got highest values compare to other 2 algorithms.

Our research and projections were based on the belief that the data was correct. Here, R2 Score of ES for the updated dataset got less due to probable data flaws and inadequate of confirmed instances. As in previous Dataset, cases are increased exponentially so R2 Score of ES got 95.6%.

V. CONCLUSION

In this paper, Machine Learning based forecasting approach that assessing the risk of a universal COVID (2019) outbreak is suggested. This approach evaluates a data source including day wise real historical data and generates predictions for the coming days using ML techniques. The study's results show that ES performed the best in the existing prediction field, given the kind and size of the data Source. To a certain degree, LASSO and LR are also good at predicting number of deaths and confirming patients. The results of these two models predict that death rates in the upcoming period, prices will climb, although healing levels will stall. SVM produces unsatisfying outcomes in all circumstances due to the volatility in the dataset values. Creating an exact hyper-plane between the dataset's given values proved difficult. Generally, we find that model projections based on existing conditions are correct, and that they will prove informative in predicting future events. The study's forecasts can thus be extremely useful in assisting authorities in taking appropriate actions and making decisions in order to contain the COVID-19 catastrophe. Many of the papers included in this report were preprints, which indicate they were not subjected to formal assessment. Given COVID-19's rapid worldwide spreading, a rigorous comparative survey is critically needed for humanity.

This research will be improved over time; next, we want to investigate for prediction, use the most accurate and appropriate machine learning approaches while using the updated dataset. Online prediction will be a major focus of our future efforts. For predicting, use the most accurate and appropriate machine learning approaches while using the updated dataset. Online prediction will be a major focus of our future efforts.

Conflict of interest: We rely on the ideas and perspectives of several authors for this study. This study provides a thorough review of the literature. As a result, there is no potential for a conflict of interest.

References

[1] S. Makridakis, E. Spiliotis, and V. Assimakopoulos, 2018 "Statistical and machine learning forecasting methods: Concerns and ways forward," PloS one, vol. 13, no. 3,

[2] WHO. Naming the coronavirus disease (covid-19) and the virus that causes it. [Online]. Available:https://www.who.int/emergencies/diseases/novelcoronavirus-2019/technical-guidance/naming-the-coronavirus-disease- (covid-2019)-and-the-virus-that-causes-it

[3] WHO Director-General's opening remarks at G20 Health Ministers Meeting - 5 September 2021 Rome, Italy [online]https://www.who.int/director-general/speeches/detail/who-director-general-s-opening-remarks-at-g20-health-ministers-meeting---5-september-2021

[4] 7 Vaccines Approved for Use by WHO [online]https://covid19.trackvaccines.org/agency/who/

[5] Fong SJ, Li G, Dey N, Crespo RG Herrera-Viedma E. (2020) "Finding an accurate early forecasting model from small dataset: a case of 2019-ncov novel coronavirus outbreak". arXiv preprint arXiv:2003.10776.

[6] Fong SJ, Li G, Dey N, Crespo RG, Herrera-Viedma E. (2020); "Composite monte carlo decision making under high uncertainty of novel coronavirus epidemic using hybridized deep learning and fuzzy rule induction". Appl Soft Comput. 106282.

[7] Batista M. 2020.03.11, "Estimation of the final size of the second phase of the coronavirus COVID-19 epidemic by the logistic model".20024901; doi: https://doi.org/10.1101/2020.03.11.20024901

[8] Hu Z, Ge Q, Li S, Jin L, Xiong M. (2020), "Evaluating the effect of public health intervention on the global-wide spread trajectory of Covid-19". medRxiv..

[9] Jia L, Li K, Jiang Y, Guo X. (2020), "Prediction and analysis of coronavirus disease 2019". arXiv preprint https://arXiv:2003.05447.

[10] Kumar J, Hembram KPSS, (2020), "Epidemiological study of novel coronavirus (COVID-19)". arXiv preprint https://arXiv:2003.11376

[11] DeCaprio D, Gartner J, Burgess T, Kothari S, Sayed S. "Building a COVID-19 vulnerability index". arXiv preprint https://arXiv:2003.07347.

[12] J. H. U. data repository. Cssegisanddata. [Online]. Available: https://github.com/CSSEGISandData

[13] Marco Cascella; Michael Rajnik; Abdul Aleem; Scott C. Dulebohn; Raffaela Di Napoli. 2020, "Features, Evaluation, and Treatment of Coronavirus" (COVID-19)https://www.ncbi.nlm.nih.gov/books/NBK554776/

[14] M. R. M. Talabis, R. McPherson, I. Miyamoto, J. L. Martin, and D. Kaye, Eds. Boston: Syngress, "Chapter 1 - analytics defined," in Information Security Analytics, pp. 1 – 12.[Online]Available: http://www.sciencedirect.com/science/article/pii/B9780128002070000010

[15] R. Tibshirani, 2015 "Regression shrinkage and selection via the lasso" ,1996 Journal of the Royal Statistical Society: Series B (Methodological), vol. 58, no. 1, pp. 267–288.

[16] F. Petropoulos and S. Makridakis, 2020, "Forecasting the novel coronavirus covid-19", Plos one, vol. 15, no. 3, p. e0231236.

[17] E. Cadenas, O. A. Jaramillo, and W. Rivera, 2010 "Analysis and forecasting of wind velocity in chetumal, quintana roo, using the single exponential smoothing method" , Renewable Energy, vol. 35, no. 5, pp. 925–930.

[18] F. Rustam et al. 2020, "COVID-19 Future Forecasting Using Supervised Machine Learning Models," in IEEE Access, vol. 8, pp. 101489-101499, , doi: 10.1109/ACCESS.2020.2997311.

[19] Muhammad LJ, Algehyne EA, Usman SS, Ahmad A, Chakraborty C, Mohammed IA. 2021, "Supervised Machine Learning Models for Prediction of COVID-19 Infection using Epidemiology Dataset." SN Comput Sci.;2(1):11. doi: 10.1007/s42979-020-00394-7. Epub 2020 Nov 27. PMID: 33263111; PMCID: PMC7694891.

[20] Gitanjali R. Shinde, Asmita B. Kalamkar, Parikshit N. Mahalle, Nilanjan Dey, Jyotismita Chaki & Aboul Ella Hassanien , (2020): "Forecasting Models for Coronavirus Disease (COVID-19): A Survey of the State-of-the-Art." SN computer science vol. 1, 4 197. doi:10.1007/s42979-020-00209-9

[21] Ezugwu, Absalom & Abaker, Ibrahim & Oyelade, Olaide & Chiroma, Haruna & Al-Garadi, Mohammed & Abdullahi, Idris & Otegbeye, Olumuyiwa & Shukla, Amit & Almutari, Mubarak, (2020) "A Novel Smart City Based Framework on Perspectives for application of Machine Learning in combatting COVID-19",: doi: 10.1101/2020.05.18.20105577.

[22] Zlatan Car, Sandi Baressi Šegota, Nikola Anđelić, Ivan Lorencin, Vedran Mrzljak, 2020, "Modeling the Spread of COVID-19 Infection Using a Multilayer Perceptron", Computational and Mathematical Methods in Medicine, vol. 2020, Article ID 5714714, 10 pages. https://doi.org/10.1155/2020/5714714

[23] Chen, Joy Iong-Zong "*Design of Accurate Classification of COVID-19 Disease in X- Ray Images Using Deep Learning Approach*" Journal of ISMAC 3, no. 02 (2021): 132- 148.

[24] Murtadha D. Hssayeni, Arjuna Chala, Roger Dev, Lili Xu, Jesse Shaw, Borko Furht & Behnaz Ghoraani "*The forecast of COVID-19 spread risk at the country level*" Journal of Big Data 8, no. 99 (2021).

Stock Market Analysis & Prediction

1st B. Shivani
Computer Science and Engineering
GRIET
Hyderabad Telangana, India.

2nd Dr. S. P Govinda Rao
Computer Science and Engineering
GRIET
Hyderabad TelanganaIndia.

Abstract*— Stock exchanges are an essential part of all global economies. Organizations can acquire capital this way to be able to perform their daily activities. By exchanging protection, securities, and values, stock intermediaries benefit from a market. Dealers, financial backers, and retailers can purchase and sell stocks once a company has been listed on the stock exchange. As of late, a great deal of work has been done to foresee the development of the stock market. Gauging the development of the financial exchange is acquiring force among different professionals, contributing networks, and followers as it gives better direction regard to contributing. Consistency is one of the main considerations on which, the benefit of exchanging stock and contributing is reliant. The benefits procured by speculation and exchanging the stock exchange rely upon the consistency of the stock, generally. On the off chance that any framework is created which can reliably foresee the patterns of the unique financial exchange, would make the proprietor of the framework wealthy. In addition, the anticipated patterns of the market will assist the controllers with taking remedial measures to balance out the market. Numerous master specialists and analysts have advanced a few models utilizing different specialized, principal, and scientific methods to give an expectation on the financial exchange design. During the most recent quite a while, a ton of studies have been done to predict stock exchange patterns utilizing Classical, AI, ML, and Deep learning methods. This study will help the pursuers and analysts in choosing algorithms that might be valuable for foreseeing the stock's performance. This survey of different algorithms and their boundaries for stock exchange prediction is included in this research.

Keywords*— AI, ML, Deep Learning, Stock Exchange

I. INTRODUCTION

The stock exchange plays a crucial part in the country's financial development just as the personal economy also. Figuring out the opportune chance to purchase and trade the stocks is subject to anticipating the patterns in the stock exchange. The procedure for the most precise expectation is to gain from past occurrences and plan a model to do this by utilizing conventional and AI algorithms [1]. The Stock exchange pattern differs because of a few factors like political, financial matters, climate, society, and so forth [2]. There are two sorts of stock examination. One is an essential examination, which requires investigation of the organization's nuts and bolts, for example, accounting report, costs and incomes, yearly returns, organization's profile, and position, and so on the other one is a specialized examination, which manages contemplating the insights produced by market exercises like verifiable information, past cost, and volume [3].

On the stock exchange, investors and stockholders can exchange the stocks of all organizations. With a limited focus time, this is an advantageous method of making a good income. Nevertheless, investors believe that it's exceptionally difficult to predict market prices. The costs are not only affected by monetary events and an organization's exhibition, however also by the brains of the people who put resources into the market. Currently, there are various factual methods for determining prices on securities exchanges. However, stock forecasts are difficult to achieve with common measurable strategies due to high instability and non-direct information relating to it.

Nowadays, Artificial Intelligence (AI) methods are offering promising results in expectations regarding financial exchanges as a result of the current status of the foundation [4]. There are two theories that can be used to predict securities exchange development: (I) the Random Walk approach and (ii) the Efficient Market Hypothesis (EMH). In 1970, FAMA recommended that EMH be constructed. It has been predicted by the EMH that the current market contains all the data it needs. As more information is accumulated, the market consumes it as well as getting its cost back. A financial backer cannot anticipate the stock market with some other method, it implies. A further division of EMH is frail EMH, semisolid EMH, and solid EMH. The weak EMH predicts the market based on previous verifiable information alone, the semi-solid EMH relies on chronicled information and publicly available data, and the solid EMH makes predictions based on information already recorded, public data, and other privately available data. Moreover, Random walk also states that current and chronicled stock costs, which are exceptionally unstable and independent of each other, cannot predict future stock costs. An alternative hypothesis, called Inefficient Market Hypothesis (IMH), holds that consistent showcases are not generally effective, as the stock price data alone does not provide sufficient information.

The future development of stock costs can be analyzed by utilizing other components that IMH suggests. It is possible to predict the stock market in two different ways: (i) by studying its fundamentals, and (ii) by studying its technical indicators. Foreseeing the stock price of an organization requires a fundamental analysis, which utilizes more market information like annual reports, financial records, and reviewer's reports. Utilizing time arrangement graphs, the specialized analysis only uses recorded stock value information of the organization. It has been mentioned before that the stock market is a highly unpredictable and dynamic one, so it is possible to use the above-mentioned methods as a basis for trading. However, AI is evidence showing that it is capable of predicting stock market costs in recent weeks. Access to information and the development of algorithms have made this possible. A review of recent work in the field

978-1-6654-2005-1/21/$31.00 ©2021 IEEE

of stock market forecasting is presented in this paper. A review of the strategies employed and outcomes achieved by each specialist has been conducted. This paper also attempts to address the gaps in their work.

II. Literature Survey

In 2007, SUI Xue-shen et al., proposed a data mining technique using SVM algorithm in which feature selection can eliminate irrelevant or redundant attributes and increase the density of samples in feature spaces that can improve classification performance [4]. In this proposed framework they used two new co-efficient which is NDEM-neighborhood decision error and ND- neighbor dependence is used to calculate the complexity of classification in order to do feature selection. To estimate the complexity of the input data classification they followed four measures which is ASNN, ASH, ND, NDER and specified 15 technical indicators which contains features using the four selected features sets of four measures is used as input data for Support Vector Algorithm to predict the moving trend for the next five days. In this experiment they concluded that NDEM pick the minimal set of features and achieved 63.23% of accuracy and ASNN got 62.93%, ASH and ND got 60.75% accuracies [4].

In 2009, Qinghua Wen et al., presented an experiment of Artificial intelligence-based stock market trading system based on oscillation box prediction by combining support vector machines and box theory of stock investment [5]. The SVM algorithm which predicts the lower bound and upper bound of the candle sticks respectively. This trading system is based on candle system rule. To analyze the possibility, they tested the framework on regular stock developments and S&P 500 segments. The tests show a promising exhibition of the framework and it beats the purchase and holds procedure. After doing the procedure they came to a conclusion which is; there is a complexity of the movement of stock because of using prediction algorithms with the combination of single algorithm which makes the system fragile. They have achieved the prediction accuracy for the lower and upper circuits is SVM max 96.91% and SVM min 95.93% for 3 stocks when it comes to 50 stocks the success rate is gradually decreased which is SVM max 56.29% and SVM min 46.28%.

In 2009, Ling-Bing Tang et al., Proposed a Manifold Wavelet Support Vector Machine (MWSVM) to predict the future returns of the stock market. This manifold wavelet kernel is composed of manifold theory which incorporated with Wavelet technique which is in SVM. This Wavelet technique can give the features output which describes the stock market time series of various locations at different time series. This method can accurately find out the nonlinear function and predict the stock market returns accurately. They have analysed the prediction performance using the 1. Normalised Mean Square Error (NMSE), 2. Mean absolute error (MAE) and 3. Root Mean Square Error (RMSE). Ling et al., experimented the model on different datasets (DAXINDX, FTSE100, JAPDOWA and SPCOMP) [6] and achieved these results.

Manifold Wavelet Kernel		
NMSE	RMSE	MAE
1.3309	0.2565	0.1974
0.8642	0.2412	0.1889
0.9034	0.1868	0.1468
0.8816	0.1818	0.1427
0.9252	0.3005	0.2412

Table 1: NMSE, RMSE, MAE Accuracies

In 2010, A. S. M. Shihavuddin et al., [7] proposed a Naïve Bayes classifier to predict the stock price by analysing the local economic trends and online financial news. In their research they represented the datamining algorithms which is tested on the stock market data which holds the advantage to interpret the present and future stocks. Naïve Bayes classifier is used to train the previous data present on the website and also news articles on the internet. They trained the classifier using the dataset which is collected from April 2008 to October 2008 which is a total of 140 and 35 datasets from October 2008 to November 2008 and tested. They find the performance varied at different datasets: they achieved an accuracy of 58.62% at Test-1, 66.62% in Test-2, and 79.4% in Test-3 but after adding the heuristics they have achieved 59.91% in Test-1, 79.12% in Test-2 and 87.22% in Test-3 [7].

In 2011, Hyun Joon Jung and J. K. Aggarwal from University of Texas at Austin come up with a Binary Stock Event Model (BSEM) for stock market prediction. A feature set is generated using this BSEM to forecast the future stock trend. The two learning models used in this method are Naive Bayes and Support Vector Machines. Predictions in this research are made based on binary classifications. As a result, a diagonal sum from the confusion matrix is used to compute the accuracy of prediction, which achieved 70% to 80% accuracy for the next day's stock trend on average, and it is observed that as the period increases, the accuracy falls as low as 55% [9]. This clearly demonstrates the benefits of BSEM features. Although the BSEM is showing 73*74 outcomes versus 55%*57% for the features-based solution. There is a critical contrast between highlights and shadows as a result. According to BSEM [9], stock pattern events are strongly related to stock occasions. However, an asset value is merely an estimate based on a technical indicator that doesn't emphatically reflect an asset pattern. Testing the prediction model was done by backtesting the strategy they used to evaluate it earlier [9]. In addition to the creation of a BSEM, an important contribution is the development of a feature generator. Despite its expectations and back-testing, it performed well on a genuine dataset. Additionally, they suggest a few intriguing points: Bayesian Naive Classifiers have the advantage of high computational complexity, while SVM-based methodologies have advantages and disadvantages, such as high forecast accuracy and expensive computation. According to their research, significant exchanging techniques like moving averages and relative strength files do not guarantee exceptional market returns [8].

In 2016, W. Lertyingyod and N. Benjamas proposed a method for predicting stock value expectations by reducing the number of features. The project proposes a novel information mining approach to determine stock costs. They rely on Thailand Stock Exchange for their work. With the Gain Ratio attribute and Wrapper Selection with Greedy stepwise pursuit technique, the features were determined using the Ranker Search and Ranker Attribute strategies. With the Wrapper Subset Evaluation with Greedy Algorithm, the ascribes were reduced from 14 to 6 (57.14%). Results of this study showed that the predictive model for week by week (5 to 10 days) stock value forecasting improved using Artificial Neural Networks and reached the highest accurate prediction of 93.89% using just six selected bonds [9].

In this research, M. R. Vargas et al., in 2018 used deep learning models to forecast a stock value utilizing financial news titles and specialized pointers as information. Two distinct, specialized markers are compared, set-1: stochastic (K%), rate of change, momentum, accumulation/distribution (A/D) oscillator, and dispersion 5, stochastic %D, Williams (R%). The second set consists of Moving Average Convergence-Divergence, Exponential Moving Average, On Balance Volume, Relative Strength Index, and Bollinger Bands. Using deep learning techniques, the information can be sorted out and examined in a complex way, allowing for more accurate conversion. Researchers have demonstrated that Convolutional Neural Networks (CNN) can be better at getting semantic information from writings than Recurrent Neural Networks (RNN), an RNN is better at retrieving setting information and displaying complex attributes for securities exchange determining. In this paper, we examine two models: a crossover model using CNN for the monetary news and Long Short-Term Memory (LSTM) for markers, called SI-RCNN, and an LSTM network designed for pointers only, known as I-RNN. When a model predicts that it will rise in cost a trade specialist purchases stock, sells it the following day, and then buys it on the following day when the model forecasts that it will decrease. The specialist buys stock on the current day and sells it the following day. The proposed strategy shows a significant part of monetary news in settling the outcomes and practically no improvement when looking at changed arrangements of specialized pointers [10].

Model	Training ACC (%)	Validation ACC (%)	Test ACC (%)
I-RNN	55.22	55.97	52.52
SI-RCNN	84.08	60.45	56.84
I-RNN-2	59.08	50.74	48.92
SI-RCNN-2	88.31	61.19	51.08

Table 2: Multiple Accuracies

In 2018, D Soni et al., proposed a Optimised prediction model for stock market trend analysis. The primary objective of this research is to apply the basic understanding of analysing the stock market trend using machine learning techniques which are Naïve bayes, Decision tree, PSO, Black Hole techniques [11]. Initially the bifurcated share market data into test and train datasets and calculates the absolute values of change in stock price overt the time interval and mean value of it. Likewise, they set up a grid wherein if the estimation of offer cost increments on a specific day regarding the past one they denoted that field in the lattice as 1 in any case assuming the offer value falls, the field is set apart as 0. Likewise, each line of the network compares to the day number. Later they tally the quantity of 1s and 0s in the readied framework. On the off chance that the quantity of 1s is more than the number of 0s, we group the share as a decent share else it would be assigned as a terrible share. After that they arranged a forecast framework and appointed it the qualities 1 or 0 as per the expectation and named as y. In the event that it is a decent offer, the estimation of the offer cost is expanded by the change determined before and the main line of the recently made forecast network is set apart as 1. Something else, assuming the offer is a terrible offer, the worth is diminished and correspondingly the primary column of the expectation framework is set apart as 0. Later again arranged a comparative network for the testing set too as far as 1s and 0s based on genuine ascent and fall in the cost of an offer and named as x. after that the following arrangement of days for forecast and would rehash the accompanying strides for each expectation from this time forward. This proposed model with the same dataset and tested it on a number of conditions. The results were obtained and the accuracy of this model is as follows [11].

S. No	1	2	3	4	5
Algorithm	Black Hole	PSO	Decision Tree	Naive Bayes	Proposed Model
Mean Accuracy	95.1	83.57	81.16	85.56	96.60

Table 3: Algorithm Accuracy

In 2018, Lyhyaoui et al., developed a stock forecasting model for the Casablanca stock exchange (CSE). Africa's CSE stock market is among the largest and most established in the world. It is additionally one of the most unpredictable stock trades, which can leave the financial backers with either great gains or enormous losses. In association with a model, the creators had predicted market developments for five Moroccan banks. There will be significant boundaries that will affect a stock value a great deal and plenty of variables may influence this. (I) Dimensionality decreases. Taking away dimensions will create a distinct boundary and it will simplify preparing a model because less measurement will be required. The paper uses a Kinetic Principal Component Analysis (KPCA). As a result, 23 informational boundaries have been identified. During the next stage, stock expectations are calculated using the Support Vector Machine (SVR). When using KPCA+SVR, the market forecast is more exact than when using SVR alone [12].

III. Conclusion

This Survey paper presumes that benefits in the stock exchange may be amplifying through various methodologies and strategies, yet every strategy has its own benefits and restrictions. We have considered an assortment of strategies

or procedures for financial exchange expectation and infer that it is feasible to deliver another and cross strategy to estimate the forthcoming development of the offer market or to conjecture the monetary state of an organization through any of the talked technique or through various access methods. But on the other hand, it's crucial to plan according to the structure by which the framework can be augmented with precision and the exhibition with less computational confusion. All things considered, we accept that stock expectation is that best in class work and various components ought to be viewed as a lot of exactness and effectiveness to anticipate the market.

Aurthor	Algorithm	Accuracy
SUI Xue-shen et al.,	ASNN, ASH, ND, NDER (SVM)	62.93%, 60.75%, 63.23%
Qinghua Wen et al.,	SVM Min and max for 3 stocks	96.91% to 95.93%
Qinghua Wen et al.,	SVM Min and max for 50 stocks	56.29% to 46.28%
Ling-Bing Tang et al.,	Manifold Wavelet Support Vector Machine (MWSVM)	Test: 1. 58.62% 2. 66.62% 3. 79.4%
Ling-Bing Tang et al.,	Manifold Wavelet Support Vector Machine (MWSVM) With Heuristics	Test: 4. 59.91% 5. 79.12% 6. 87.22%
Hyun Joon Jung and J. K. Aggarwal	Binary Stock Event Model (BSEM) Using SVM	70% to 80%
W. Lertyingyod and N. Benjamas	Wrapper Subset Evaluation with Greedy Algorithm (ANN)	93.89%
M. R. Vargas et al.,	I-RNN SI-RCNN I- RNN SI- RCNN	52.52% 56.84% 48.92% 51.08%
D Soni et al.,	Naïve Bayes PSO Black Hole Decision RNN	85.56% 83.57% 95.10% 81.16% 96.60%

Table 1 Comparison Table

IV REFERENCES

1. "Cao, Lijuan & Tay, Francis. (2001). Financial Forecasting Using Support Vector Machines. Neural Computing and Applications. 10. 184-192. 10.1007/s005210170010.".
2. "Tang, Jinqi and Xiong Chen. “Stock Market Prediction Based on Historic Prices and News Titles.” ICMLT '18 (2018).".
3. "Puri, Nischal. (2018). A Survey on Machine Learning Approach for Stock Market Prediction. HELIX. 8. 3705-3709. 10.29042/2018-3705-3709.".
4. "S. Xue-shen, Q. Zhong-ying, Y. Da-ren, H. Qing-hua and Z. Hui, "A Novel Feature Selection Approach Using Classification Complexity for SVM of Stock Market Trend Prediction," 2007 International Conference on Management Science and Engineering, Harbin, Chin".
5. "Q. Wen, Z. Yang, Y. Song and Peifa Jia, "Intelligent stock trading system based on SVM algorithm and oscillation box prediction," 2009 International Joint Conference on Neural Networks, Atlanta, GA, USA, 2009, pp. 3341-3347, doi: 10.1109/IJCNN.2009.517884".
6. "L. Tang, H. Sheng and L. Tang, "Stock Returns Prediction Using Manifold Wavelet Kernel," 2009 International Conference on Electronic Commerce and Business Intelligence, Beijing, China, 2009, pp. 306-309, doi: 10.1109/ECBI.2009.67.".
7. "A. S. M. Shihavuddin, Mir Nahidul Ambia, Mir Mohammad Nazmul Arefin, Mokarrom Hossain and Adnan Anwar, "Prediction of stock price analyzing the online financial news using Naive Bayes classifier and local economic trends," 2010 3rd International Conferenc".
8. "H. J. Jung and J. K. Aggarwal, "A Binary Stock Event Model for stock trends forecasting: Forecasting stock trends via a simple and accurate approach with machine learning," 2011 11th International Conference on Intelligent Systems Design and Applications,".
9. "W. Lertyingyod and N. Benjamas, "Stock price trend prediction using Artificial Neural Network techniques: Case study: Thailand stock exchange," 2016 International Computer Science and Engineering Conference (ICSEC), Chiang Mai, Thailand, 2016, pp. 1-6, do".
10. "M. R. Vargas, C. E. M. dos Anjos, G. L. G. Bichara and A. G. Evsukoff, "Deep Leaming for Stock Market Prediction Using Technical Indicators and Financial News Articles," 2018 International Joint Conference on Neural Networks (IJCNN), Rio de Janeiro, Brazi".
11. "D. Soni, S. Agarwal, T. Agarwel, P. Arora and K. Gupta, "Optimised Prediction Model for Stock Market Trend Analysis," 2018 Eleventh International Conference on Contemporary Computing (IC3), Noida, India, 2018, pp. 1-3, doi: 10.1109/IC3.2018.8530457.".
12. "Nahil, Anass & Lyhyaoui, Abdelouahid. (2018). Short-term stock price forecasting using kernel principal component analysis and support vector machines: the case of Casablanca stock exchange. Procedia Computer Science. 127. 161-169. 10.1016/j.procs.2018.01".
13. "N. Budhani, C. K. Jha and S. K. Budhani, "Prediction of stock market using artificial neural network," 2014 International Conference of Soft Computing Techniques for Engineering and

Technology (ICSCTET), Bhimtal, India, 2014, pp.
1-8, doi: 10.1109/ICSCTET".

978-1-6654-2005-1/21/$31.00 ©2021 IEEE

Survey Analysis of Robust and Real-Time Multi-Lane and Single Lane Detection in Indian Highway Scenarios

Dr. A. Sai Hanuman[1,*] and *G. Prasanna* Kumar[2]

[1]Professor, Computer Science and Engineering, GRIET, Hyderabad, Telangana, India.
[2]Master of Technology, Computer Science and Engineering, GRIET, Hyderabad, Telangana, India.

Abstract-Studies on lane detection Lane identification methods, integration, and evaluation strategies square measure all examined. The system integration approaches for building a lot of strong detection systems are then evaluated and analyzed, taking into account the inherent limits of camera-based lane detecting systems. Present deep learning approaches to lane detection are inherently CNN's semantic segmentation network the results of the segmentation of the roadways and the segmentation of the lane markers are fused using a fusion method. By manipulating a huge number of frames from a continuous driving environment, we examine lane detection, and we propose a hybrid deep architecture that combines the convolution neural network (CNN) and the continuous neural network (CNN) (RNN). Because of the extensive information background and the high cost of camera equipment, a substantial number of existing results concentrate on vision-based lane recognition systems. Extensive tests on two large-scale datasets show that the planned technique outperforms rivals' lane detection strategies, particularly in challenging settings. A CNN block in particular isolates information from each frame before sending the CNN choices of several continuous frames with time-series qualities to the RNN block for feature learning and lane prediction.

1. Introduction

The demand for transport has increased enormously over the last two decades. There are now more automobiles on the road, which sadly means that traffic accidents are on the rise. [2] Significant efforts have been made to improve driver safety education and the construction of an accident prevention system. [3] Machine vision systems are crucial in today's cars for improved driver assistance systems with safety features. As a result, scientists and engineers have developed a range of technologies that use machine vision to enable the autonomy of intelligent vehicles, such as Lane Departure Warning (LDW), Adaptive Cruise Control (ACC), and Lane Center, among others. In recent years, machine vision research for road vehicles has progressed dramatically, and lane border identification has been a hot topic. The automatic lane detector should be able to recognize straight and curved lane boundaries, as well as different lane markers (single or double, solid or broken) and pavement edges [7]. Their reported uses are restricted to tiny images. As the image size grows larger, processing time and memory costs increase rapidly, and random aligned disturbances become audible, attempts to apply HT to large-scale images are usually avoided. Engineering drawings, unfortunately, are frequently fairly large [8]. A visual apparatus that can differentiate numerous lanes on a highway is described in this paper. Initially, the system detected the center lane. On the assumption that the center lane markers were parallel to each other at the same interval and that the road was flat, the position of the adjacent lanes was determined in the top image by offsetting the central lane marks. [10].

Whereas a handmade choice produced by difficult way of fine standardization, the majority of lane recognition tactics utilize ancient laptop vision-based procedures. Such specialized alternatives operate in a controlled environment and do not appear to be powerful enough in complex driving scenarios, making them unsuitable for reasonable planning A laptop vision technique developed using CNN has the ability to offer lane detection resolution that is both dependable and accurate. The performance of recent lane detection methods that incorporated CNN language segmentation was outstanding. Despite their high performance, CNN-based segmentation algorithms require post-processing and model fitting to produce final lane predictions [4]. The deep

* Corresponding author: prasannakumargourla@gmail.com

convolution neural network (DCNN) is one of them, and it excels at image and video feature abstraction by analyzing input signals with multiple degrees of convolution. The deep recurrent neural network (DRNN) is good at data prediction for time-series signals because it recursively evaluates the signal by dividing it into sequential blocks and constructing full affiliation layers between them for status propagation. In terms of lane detection, the continuous driving scene photos appear to constitute time series that may be analyzed using DRNN.

2. Methodology

2.1 Machine Learning-Based Lane Detection Algorithms:

[2] Some studies focus on lane marking detective work utilizing modern machine learning, while others use traditional image processing-based methods to discover lane markings. [7] For a range of road surface types, lane configurations, weather conditions, and noise, the precision and robustness of road-bound detection for an autonomous vehicle is a difficult task. To overcome these concerns while keeping the high accuracy advantage of RHT, adaptive RHT (Randomized Hough transform) is used, this is an effective technique to apply RHT [7]. Pre-processing, post-processing, and road lane modeling are the three stages of the lane recognition approach [2]. This section delves into the details of these stages, as well as the calculations that accompany them.

2.1.1. Pre-processing Stage

Because Canny Edge Detection only works with monochromatic pictures, the image is also transformed to grey scale. Image processing techniques such as erosion, dilation, and image smoothing are used to remove noise.

2.1.2. The post-processing phase

After the data has been analyzed, canny edge detection is performed. The smooth image's stage recognition feature recognizes lines and edges.

2.1.3. Road Lane Modeling

The most likely left and right lane markers are calculated using computation. In this calculation, the line parameters rho(T) and theta(d) are used. You can achieve an average result by grouping comparable lines together.

2.2 Deep Learning Techniques:

Deep learning techniques have become one of the most popular academic topics in the last decade as a result of discoveries in deep network theories, parallel computing technologies, and large-scale data [1]. Many deep learning techniques demonstrate significant improvements in computer vision tasks when compared to standard methods, with dramatically increased detection and identification efficiency. The convolution neural network is one of the most extensively utilized approaches for object recognition research (CNN). CNN has many advantages, including high detection precision, automated feature learning, and end-to-end recognition. Recently, some researchers were active in the application process.

The two types of evaluation processes are offline performance evaluation and online real-time trust evaluation. LSTM could be an important component in deep learning because of its capacity to analyze temporal data. Convolutional LSTMs (ConvLSTMs) are a sort of LSTM that is equipped with convolution operations and has been widely used in video analysis due to their feedback mechanism on temporal dynamics and abstraction power on picture illustration. ConvLSTM can be used in a variety of ways as a basic construction component. ConvLSTM's area unit is extensively utilized in linguistics video segmentation for efficiently processing two-dimensional time-series data. The video segmentation problem was turned into a regression problem by using a ConvLSTM between the convolutional encoder and decoder to anticipate each frame.

2.3 Image Processing Techniques:

[2] For detecting left and right lane markers, this study provides a robust road lane marker identification technique. Canny edge detection and Hough Transform optimization are used in the method. Images from a front-facing vision sensor positioned behind the windscreen and facing the lane are used as data by the device.

The left and right lane limitations are correctly shown on the original photo as a result of this technique. The Hough Transform yields a sequence of lines that characterize the situation as lane borders on the left and right. The average creates only one result by grouping all of the left lane boundaries into one category and all of the right lane boundaries into another.

[3]The Fuzzy Noise Reduction Filter (FNRF) is the first sub-algorithm, and it removes noise and smooth's down image sequences recorded by the camera. FNRF is used to increase the ROI's contrast level, which can help in lane detection. On a clear road, FNRF is

detected 99.2 percent of the time, but only 92.1 percent of the time on a dark road. The FNFR generates positive results by reducing noise and increasing detection rates by an average of 13.30 percent.

2.4 Convolution Neural Networks Techniques:

For autonomous driving, accurate lane identification is a must-have feature. For crucial roles like overtaking assistants and route planning, ego and side lane positional awareness are also necessary. We describe how to use a CNN-based regression technique to detect several lanes and classify them based on their position in this study. Our regression technique removes the significant constraint of precisely categorizing each pixel from CNN segmentation-based algorithms that produce dense pixel masks.

In high contrast photos, UNet (64.5%) and Lane Net (65.7%), in particular, struggle to distinguish lane boundaries for mean intersection over union (MIOU). When the results of road and lane marker instance segmentation are combined, an area of ego-way, left and right adjacent lane is expected [5].

The lane's outcome will be represented as a collection of pixels.

When it comes to road segmentation, we can get consistent results. Multi-lane detection can be done by combining these two results. This technique appears to operate for a number of road settings, including unstructured roads with no markings, structured roads, and semi-structured roads with one to four lane lines, according to many testing.

In addition, the results of the multi-task network's recognition of road and lane markings are cutting-edge. To obtain a quantitative evaluation result, an annotation of the lane class (ego-lane (88 percent), left (78 percent), and right adjacent lane (76 percent) is added to the test photos.

The creation of the unique "video-based lane estimating and tracking" (VioLET) system [6] is motivated by these driver-assistance goals We'll examine the current state of the art in track position recognition and tracking, as well as compare and contrast techniques.

Large surveys of intelligent vehicles have looked at many of the lane position sensing techniques. While these publications are important for broad overviews of vision research for intelligent vehicles, they are only as detailed as they can be provided. By enabling the left and right boundaries to be merged, the assumption that the width of the road or lane is locally constant can considerably enhance performance.

One is the deep convolutional neural network (DCNN), which processes input data using many levels of convolution and excels at feature abstraction for images and videos.

The deep continuous neural network (DRNN) is capable of information prediction for time-series signals by recursively processing the signal by dividing it into sequential blocks and establishing full affiliation layers between them for status propagation. In terms of lane detection, continuous driving scene images appear to be a time series that may be handled using DRNN.

3. Flow chart for lane detection

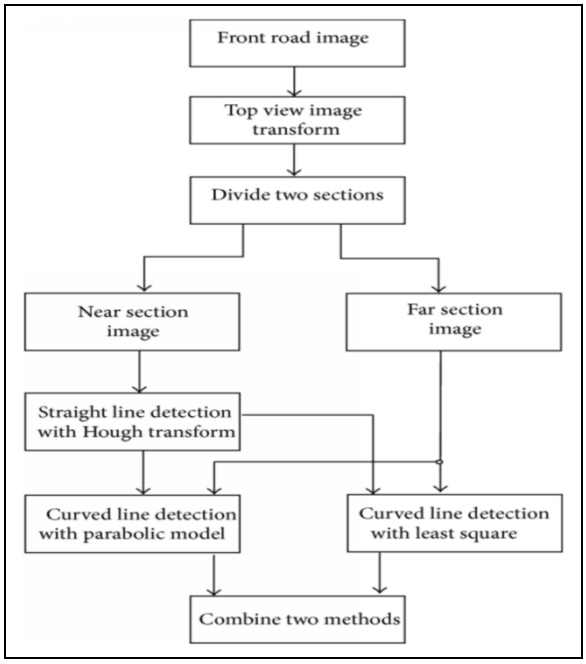

Fig. 1. Flow chart

4. Comparison

Table 1. Comparison of the methods used

Methods	Algorithms	Accuracy	Reference
Vision based lane detection, Image processing	CNN, Hough transform	90%	Reference – [1]
Image processing	Canny edge detection	91.2%	Reference – [2]
Fuzzy Noise Reduction Filter (FNRF)	Edge detection	87%	Reference – [3]
Multilane	CNN	75%	Reference – [4]

detection			
Lane Marking detection	RANSAC	Ego lane 88.02% Right lane 76.28 % Left lane 78.60%	Reference – [5]
Video based lane detection and tracking (VIOLET)	FNRF, CNN, and KNN	92%	Reference – [6]
Machine learning (ML)	Randomized Hough transform	82%	Reference– [7]
Line Recognition method	Hough transform	82%	Reference– [8]
CNN-LD baselane detection, ML	CNN, Hough transform	96%	Reference– [9]
GPS	HT -ROI	70%	Reference– [10]

5. Inferences

So, by comparing all the methods and algorithms CNN is an environment friendly cognizance algorithm which is widely used in sample focus and image processing. It has many elements such as simple structure, less education parameters and adaptability. It has become a warm subject matter in voice analysis and image recognition.

Hough transform can be used to realize lines and circles or different parametric curves [1].

Canny edge detection: the canny edge detector is an part detection operator that uses a multistage algorithm to notice a huge vary of edge in photographs [2].

FNRF: Fuzzy filter is presented for the noise discount of pix corrupted with adaptive noise [3].

The RANSAC algorithm is a learning method to estimate parameters of a model via random sampling of observed data [5].

KNN It makes use of data with countless training to predict the classification of the new sample point [6].

RHT is specific from HT in that it tries to keep away from conducting the computationally pricey vote casting process for each nonzero pixel in the photo by means of taking benefit of the geometric houses of analytical curves, and accordingly improve the time effectively and reduce the storage requirement of the authentic algorithm [7].

CNN, KNN, and RANSAC these are the most used algorithms in previous projects but KNN with large data the prediction stage might be slow, CNN has several layers so that the training process takes a lot of time if the system does not consist of a good GPU and RANSAC there are no upper bonds on the time it takes to compute any parameters and it computes limit number of solutions whereas Hough transform and canny edge detection algorithms are giving good accuracy as per my survey and these algorithms can detect curves and edges in single and multilane clearly. So these are the algorithms to consider for my project can be used more practically.

6. Conclusion

In this survey it concludes that it gives the qualified analysis of the Robust and real-time multi-lane and single lane detection in Indian highway scenarios. Different types of lane detection are done based on different types of vehicles and road as in moving vehicles or video based. In each paper they are used different datasets and algorithms for the efficient accuracy. For more efficiency there must be well applied algorithm which must be correctly implemented along with the consider dataset. According to survey analysis Hough transform and canny edge detection are the best resulting algorithms.

References

1. Y. Xing, C. Lv, L. Chen, H. Wang, H. Wang, D. Cao, E. Velenis, and F.-Y. Wang, IEEE/CAA Journal of Automatica Sinica **5**, 645 (2018)
2. C. Y. Low, H. Zamzuri, and S. A. Mazlan, in *2014 5th International Conference on Intelligent and Advanced Systems (ICIAS)*, pp. 1–4 (2014)
3. H. Bilal, B. Yin, J. Khan, L. Wang, J. Zhang, and A. Kumar, in *2019 Chinese Control Conference (CCC)*, pp. 6772–6777 (2019)
4. S. Chougule, N. Koznek, A. Ismail, G. Adam, V. Narayan, and M. Schulze, in *Proceedings of the European Conference on Computer Vision (ECCV) Workshops* (2018)
5. P. Liu, M. Yang, C. Wang, and B. Wang, in *2018 Chinese Automation Congress (CAC)*, pp. 2750–2755 (2018)

6. J. C. McCall and M. M. Trivedi, IEEE Trans. Intell. Transp. Syst. **7**, 20 (2006)
7. Q. Li, N. Zheng, and H. Cheng, IEEE Trans. Intell. Transp. Syst. **5**, 300 (2004)
8. J. Song and M. R. Lyu, Pattern Recognit. **38**, 539 (2005)
9. S. K. Satti, K. Suganya Devi, P. Dhar, and P. Srinivasan, ICT Express **7**, 99 (2021)
10. Y. Jiang, F. Gao, and G. Xu, in *2010 International Conference on Image Analysis and Signal Processing*, pp. 114–117 (2010)

Robust and real-time multi-lane and single lane detection in Indian highway scenarios

A. Sai Hanuman[1],* and *G. Prasanna* Kumar [2]

[1]Professor, Computer Science and Engineering, GRIET, Hyderabad, Telangana, India.
[2]Computer Science and Engineering, GRIET, Hyderabad, Telangana, India.

Abstract: In the Advanced Driver Assistance System (ADAS), lane detection plays a vital role to avoid road accidents of an Autonomous vehicle. Also, autonomous vehicles should be able to navigate by themselves, in-order to do, it needs to understand its surrounding conditions like a human. So that vehicle can determine its path in streets and highways it can maintain lane manoeuvre. Also, It has become the most fundamental aspect to consider in current ADAS research. One of the major hurdles in self-driving vehicle research is identifying the curved lanes, multiple lanes with challenging light, and weather conditions, especially in Indian highway scenarios. As it is a vision-based lane detection approach we are using OpenCV library which consists of multiple algorithms like the optimization of canny edge detection to find out the edges, features of the lane and Hough Transform for lane line generation and apply on the particular region of interest.

1 Introduction

Traffic crashes are predominantly brought about by human missteps, for example, carelessness, misconduct, and interruption. The development of Advanced Driving Assistance Systems (ADAS) has the potential to drastically reduce car accidents and increase driving safety [1]. An enormous number of organizations and establishments have proposed strategies and procedures for the improvement of driving wellbeing and decrease of car crashes. Among these strategies, street discernment and path checking location assume an essential part in assisting drivers with evading botches. The path discovery is the establishment of many Advanced driver Assistance systems (ADASs), for example, the Lane Departure Warning Framework (LDWF) and the Lane Keeping Assistance framework (LKAF). Some fruitful ADAS or auto ventures, for example, Mobil eye, Tesla, and BMW, and so forth have built up their own path identification and path keeping Assistance systems and have acquired critical accomplishments in both exploration and certifiable applications. Both of the auto undertakings or the individual clients have

acknowledged the Mobil eye Series ADAS items and Tesla Autopilot for self-driving. Practically the entirety of the current development path helps items use vision-based procedures since the path markings are painted out and about for human visual discernment. The use of vision-based procedures recognizes paths from the camera gadgets and keeps the driver from making unintended path changes. . One of the most common Intersection crash modes are the left turn across path with a vehicle approaching from the opposite direction [2]. Accordingly, precision and heartiness are the two most significant properties for path location frameworks. Path recognition frameworks ought to have the ability to know about absurd identifications and change the location and following calculation likewise [3], [4]. At the point when a false caution happens, the ADAS should make the driver aware of the focus on the driving assignment. Then again, vehicles with elevated levels of computerization constantly screen their surroundings and ought to have the option to manage low-exactness discovery issues without help from anyone else. Thus, assessment of path identification frameworks turns out to be much more basic with the expanding automation of vehicles.

Because of rising traffic levels and increasingly congested streets around the world, the demand for self-driving vehicles has increased dramatically in recent years. As a result, an advanced driver aid framework for road safety should be developed, which either alerts the driver in dangerous situations or makes a driving manoeuvre. In the coming years, such frameworks will get increasingly complex in order to provide the vehicle

* Corresponding author: prasannakumargourla@gmail.com

complete autonomy. Path and snag detection (i.e., things such as autos, motorcycles, walkers, and so on) detection are two key components in the expansion of such self-governing frameworks.

Mostly vision-based lane detection frameworks are normally planned dependent on image processing procedures inside comparative structures. Many academics are currently working on intelligent vehicles in order to prevent road accidents and assure safe driving [8]. Path finding challenges can be solved more effectively using a start to finish identification technique, thanks to the advancement of quick registering devices and advanced AI hypotheses, such as profound learning. In any case, the basic test looked by path recognition frameworks is the interest for high unwavering quality and assorted working conditions. One proficient approach to build vigorous and exact progressed path identification frameworks is to meld multi-modular sensors and incorporate path location frameworks with other item discovery frameworks, for example, recognition by encompassing vehicles and street zone acknowledgment. It has been demonstrated that path recognition execution can be improved with these staggered incorporation strategies [3]. Notwithstanding, the profoundly precise sensors, for example, the light/laser detection and ranging (LIDAR/LADAR) are costly and not accessible in public transport.

There are two sorts of vision-based techniques for path finding and following: highlight-based and model-based procedures. We used element-based strategies for the path finding investigation in this study. Reduced permeability owing to inclement weather, line disconnection, lack of clarity in path markings, shadows, brightening, and light reflection, and complex street-based rules are all substantial obstacles to path discovery and calculation [9]. Various component-based approaches for path recognition and stamping have been offered to various academics [10-14]. In light of the focus point of extension to detect path markers, Otsuka developed multi-type path marker acknowledgement (MLR). Essentially, an insect province advancement (ACO) was established on shrewd for edge recognition and then further prepared by Hough change for Daigavane [11]. Other element-based approaches for path finding and following yield the shading data in the images [15–17]. Despite the fact that the computations described previously yielded fascinating findings, there are still issues about commotion, and these methodologies may not work well in testing climatic or light circumstances due to the clamour issue. As a result, many studies employed crossover motions that contained both a noise reduction channel and a path recognition calculation. To improve path recognition accuracy, several researchers have used a variety of image pre-processing techniques. These procedures include histogram adjustment [24], Canny edge finder [25], polyline extraction [26], bunching [27], smoothing, and spitting of a picture [28], and using a Gaussian low-pass channel to reduce turbulence [29]. A few fluffy channels have just been developed to reduce turbulence in the succession of images [18-23]. To manage the intricate Gaussian clamour in the image, Nachtegael has been given a fluffy channel for commotion reduction [19]. Schulte has developed a revolutionary fluffy-based wavelet shrinkage picture denoising computation for removing additional material Gaussian commotion from computerized greyscale images [20]. Kwan completed a research of four fluffy channels with standard middle and moving normal channels for various forms of commotions.

This work is divided into five pieces, the first of which is the introduction. The system architecture is introduced in Section II. The Hough Transform is used to generate a road lane model in Section III. The installation of the system is addressed in Section IV. The experimental results are discussed in Section V, while the conclusions and future work are discussed in Section VI.

2 Related work

As a result of the fast growing intelligent automobile sector, researchers have taken a keen interest in advanced driver assistance systems (ADAS). One of the most difficult challenges for future driverless automobiles is detecting curving roadways, several lanes, and lanes with a lot of discontinuity and noise. The purpose of this research is to see how image processing techniques may be used in a computer vision application that focuses on lane recognition to improve traffic safety and comfort. Two different sub-algorithms make up the suggested algorithm. The Fuzzy Noise Reduction Filter (FNRF) is the first sub-algorithm, which reduces noise and smooth's the sequences of images acquired by the camera. The second sub-algorithm combines the Hough Transform (HT) technique with a competent zone of interest to recognize lanes in both normal and difficult situations. It is well recognized as a powerful tool for visual element extraction from images due to its broad vision and durability in noisy or degraded situations. Presents the details in a clean and unobtrusive manner without any unpleasant or unacceptable highlights.

They suggested a CNN-based regression technique for identifying multiple lanes based on their position in previous articles. CNN semantic segmentation networks, which focus on precisely identifying each pixel and require post-processing operations to infer lane information, are deep learning algorithms for lane recognition. We discovered that our segmentation

method fails to distinguish between thin and extended lane boundaries, which occupy few pixels in the image and are frequently obscured by vehicles.

Because ADAS share vehicle control authority with the human driver, smart vehicles and advanced driver assistance systems (ADAS) must be aware of the traffic situation as well as the driver state [3]. We only utilize two cameras, one at the front and one at the back of the car, when using cameras. After demonstrating that our approach gives more useful and less noisy information on lane markers [4], we'll move on to the next step. LDWS (lane departure warning system) is a system that alerts the motorist if the road markers are about to be surpassed, preventing accidents caused by unintended departure of the lane or leaving the highway [5], [6]. By this Real-time, region of interest “Relevant measuring range" is an approximate translation. The word refers to the section of a measurement curve that is relevant. This area can then be analyzed statistically if desired [7].

In recent years, several computer vision studies have been proposed in relation to lane detecting. For a long time, many institutions have been striving to develop an effective lane detection system [8]. Grey scaling reduces a three-channel (Red, Green, Blue) image to a single-channel (monochromatic shades from black to white) image, with each pixel containing only the RGB image's intensity information [9]. To detect the left and right lane markings on the road, a powerful road lane marker identification method is needed. Compared the performance of canny edge detection with Sobel edge detection and found that canny's performance is superior to Sobel's [10]. Stereo vision is the depth information is collected from the discrepancies between two (or more) cameras (images). The matching v-disparity representation is calculated by adding all the points on a given image line that have the same disparity value. The related disparity representation is produced by aggregating the points with the same disparity value that occur on a given picture line, whereas disparity values correspond to the discrepancies between the right and left images [11].

Non-lane information refers to images acquired from the road that contain a lot of worthless information such as the sky, trees, autos, buildings, and so on. To reduce the impact of non-lane information, the road is segmented using a normal map inferred from the stereo picture pair, based on the assumption that all pixels in the same plane have the same normal vector [13]. A method is described for finding a vanishing point in structured pictures. The method is based on the detection of line segments from an edge map using the long axis of extremely eccentric ellipses to represent clusters of edge points. The intersections of the extracted lines yield a collection of candidate vanishing points, which are given weights proportional to the lengths of the line segments they belong to. Then, using an accumulator array formed by gridding the image frame, a voting system is used. The -sigmoid kernel weights each grid cell's votes, allowing cells to contribute to their neighbors [14].

When single-frame picture data is processed, the output is a single-frame image with less information and more interference in the real-world road scene, such as shadows, stains, wear, and so on, which could lead to lane detection errors. A series of multi-frame photographs taken using a camera is used to record the lane feature information. The multi-frame lane information is matched and fused based on the unmanned vehicle's INS speed and angular speed information, maintaining the historical information of the road image obtained while travelling [15].

3 Proposed work

Pre-processing, post-processing, and lane recognition are the three main components of this architecture. These components imitate human abilities to recognize street lanes by perceiving with the eyes, analyzing with the mind, and then providing an analyzed result. For various types of origination yield, such as impact evasion and lane departure, the "human-focused" canny vehicles will rely on technical resolution and costs.

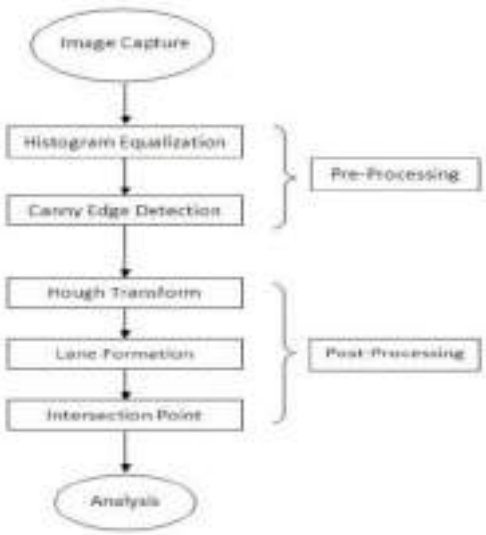

Fig. 1. General flowchart for Lane Detection on Images.

As shown in Figures 5 and 6, a region of interest, a fuzzy noise reduction filter, segmentation, and the Hough transform are all part of the proposed technique. It is planned to apply the fuzzy noise reduction filter (FNRF) for image pre-processing. The first stage involves arranging the image and downsizing it to a low resolution of 255x255 pixels. The fuzzy noise reduction filter handles the information hued path picture layout in the next stage.

A grayscale picture sequence is formed after filtering the information hued path image layout. Grayscale values are standardized to the range [0, 1], with ones (1) representing edges (white pixels) and zeros (0) representing non-edges (dark pixels). The Hough change method is used to recognize and follow the path once the picture grouping has been thoroughly pre-processed. The FNRF is used to reduce noise in the input image sequence and increase the difference level, especially in the ROI.

Fig. 1. Raw Image.

Fig. 2. Gray Scale Image.

3.1. Fuzzy Noise Reduction Filter (FNRF)

The purpose of this filter is to average the pixel values using the local pixel. Simultaneously, the picture sequence's borders and shadow segment distances are maintained to ensure that the picture sequences' basic design is not pulverised. The fundamental goal of the proposed filter is to discriminate between differences in the design of picture sequences, such as clamour-induced edges. This filter differs from other conventional filters in that it uses participation capacity to determine the weights. The noisy information shading picture sequence is M(x, y, z), where z= 1, 2,3] for each pixel position of the red, green, and blue segments separately. Three components are utilized to characterize the tone at each pixel position in this fashion.

Fig. 3. Noisy Image (Blur Image)

Fig. 4. Flowchart of proposed algorithm

The two semantic variables, little and vast, are designed to characterize the weights for the red, green, and blue components of the colour picture. A membership function usually referred to a set of ambiguous rules. Thus, triangular membership functions are utilized for the first three fuzzy principles, while Gaussian membership is employed for the remaining three fuzzy principles. The weight will be enormous if the distance between the two couples is little, and vice versa. To reduce noise in colour segment contrasts, these fuzzily defined rules are applied. By calculating the local fluctuations in the red, green, and blue climates independently, the targeted pixels nearest estimation can be established.

3.2 Region of Interest (RoI)

In the computational uncertainty of lane recognition and tracking, the choice of an area of interest (ROI) is critical. As illustrated in Figure 2, a rectangular ROI is picked from the info image sequence and preserved for future lane recognition use on the left and right traffic lanes. The foundation part of the image (undesirable region of the image), which includes the region over the evaporating point, is removed using a disappearing point (VP) in the rectangular ROI (VP). The rectangular ROI contributes in the computing waste reduction of the proposed lane detecting and tracking algorithm. The lane detection technique is utilised in the designated region of interest to determine the lane limit in each case (ROI).

Fig. 1. Rectangular Region of Interest (RoI).

3.3 Region of Interest Segmentation

The rectangular ROI is separated into two sub-regions, one on the right and one on the left, as illustrated in Figure 6. To improve execution in the next stage, we need to get a double picture with distinct edges out of this stage. The digits 1 and 0 denote the double image's edges (white pixels), whereas zeroes (0) signify non-edges (dark pixels). Because the top section of the image is often erased from the VP, using a grayscale image and evaporating point (VP) saves time and improves execution, all things considered out of ROI. The lane detection is then carried out independently in each sub region using the Hough change algorithm (HT). The computational heap of the lane detecting algorithm is reduced by autonomously preparing the fragmented sub-regions. Similarly, the ROI division measure allows for more accurate lane detection with a base time for each edge.

3.4 Canny Edge Detection

To define the image's margins, a strong contrast between the road surface and painted lines could be used. The position of lane boundaries can be determined using an edge detector. Canny edge detection algorithms are used to extract the edges from the basic grayscale pictures. The edges that are shorter than the specified threshold value are removed, and the remaining edges are gathered to form line segments. Figure 7 displays the final image, which has discernible edges and a little amount of noise. As demonstrated in the graph below, the Canny edge detector CED produced the most accurate results with the least amount of noise. It also produced output images with the fewest white pixels, which resulted in better performance.

3.5 Hough Transform Lane Detection

To recognize the highlights of a certain shape inside a grayscale photo arrangement, the Hough change algorithm is used. The Hough change algorithm has a significant amount of leeway because it is unaffected by visual noise or uneven lighting. The Hough change method is applied to a set of lane pixels in each sub-area to identify the lanes. The algorithm divides the applicants into groups that are used to determine the lane's borders. Hough change, which may be expressed as C (ρ, θ) creates the gatherer cell. As an example, the row '' can be written as follows:

$$\rho = x\cos\theta + y\sin\theta$$

Fig. 2. Edge Detection on image.

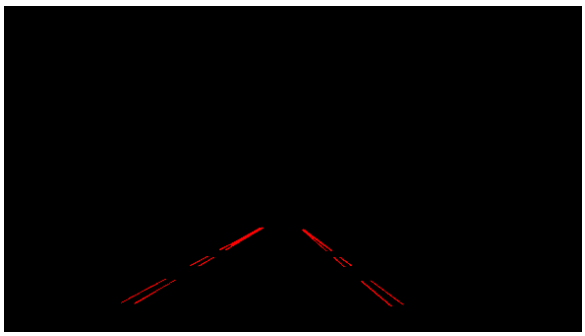

Fig. 3. Hough transform lines on edges.

Where ρ = Distance between filtered line and origin line
θ = The co-ordinates of the image pixels are x and y, the angle of the vector from origin to the closest point.
The temperature is kept between 0 and 90 degrees Fahrenheit. The value associated with the accumulator

cell array is acquired when ρ =xcos+ysin is computed, and the results are added by 1. A local maximum in each accumulator array is searched to extract these intersection locations, map them back to Cartesian space, and overlay this picture on the original image to recover the determined lane borders.

4 Implementation

4.1 Pre-process the initial Image

In order to pre-process the image a traffic raw image data set created using the video log and try to convert the raw image dataset into Gray scale images as shown in the figure 3. Later the Gray scaled images having noise which will be reduced using the Fuzzy noise reduction algorithm (FNRA) as it is not efficient enough Gaussian blur algorithm (GBA) is used to reduce the image noise with a specified kernel size. When the kernel size is larger it averages or soothing of shades is over a large area.

4.2 Get the edges from pre-processed image

After applying filters to make the images smoothening the images are processed through the canny transform algorithm to detect the strong edges or strong gradients above a canny HI which means canny high threshold, and reject the pixels below the canny low which means canny low threshold. The pixels in the blurred image between the low and high will be included as long as they are at a strong edge. The Pixel esteems are between 0 and 255, the esteem difference between two pixels will be in this range, so this is the reasonable range of the thresholds. The recommended low to high ratio of the thresholds is 1:2, to 1:3

4.3 Region of Interest

In the image or video feed the algorithm should found only the place to get to predict the lanes in order to do that the region of interest is selected by just considering the pixels where they expect the lane lines to be. To get the region of interest (Roi), the algorithm needs to determine the corners (vertices) of a four-sided polygon (bottom left, top left, top right, bottom right), rather than indicating pixels. In this experiment utilized divisions of the picture's measurements so the eyeball it and compute is from that point. After the measurements of square or veil out any remaining edges that isn't important for our area of interest is left out.

4.4 Lines of Edges

As referenced earlier (2.5) Hough transform algorithm is utilized to get lines from the edges distinguished on the picture where the Region of interest is drawn where Rho(ρ) and theta coefficient(θ) are the distance of pixels in a picture and point where degrees are changed over into radians at the goal of the framework in Hough space, beginning from one the value can scale up to be more adaptable in what comprises a line. The Minimum vote co-efficient is the number of intersections in a given grid cell a a candidate line to have to make it into the output and the minimum length of the line in pixels that can be accepted as an output finally the maximum line gap which is the distance in pixels between the segmented lines to allow and connect as a single line.

4.5 Extrapolation of the lines

Extrapolate means to insert points either before the first known point, or, after the last known point. Using the extrapolation formula to mast the centre lanes and overlaps the extrapolated lines on the raw image.

$$y = slope * x + intercept$$

The hough transform gives little lines, to extrapolate these little lines to make a left and right lane. To locate the min and max y directions to get the focuses at the base and most extreme y facilitates from the purposes of the little lines. First to separate the little lines into two gatherings. One with a positive slant (the left line), and one with a negative slant (the correct line), Later the lines incline towards one another. to group the x, y and slope for the left and right lane. To take the average x coordinate, y coordinate, slope and intercept for each gathering and determined the upper and lower x coordinates for every lane dependent on the figured qualities and the condition of the line later draw a line to a meaningful boundary on a clear picture and return the picture.

5 Tested dataset images

In order to experiment with road lane detection on Indian highway scenarios, well-paved roads and well-paved traffic lanes are needed. Instead of downloading the data from the Kitti vision data, we planned to build our own dataset. In order to create my own dataset searched many Indian highway road scenarios for well-paved roads and traffic lanes. So, we downloaded the video from internet and captured a few frames of the video, and created our own dataset.

Fig. 4. Data set images.

6 Results

The proposed algorithm's outcomes on real-life Indian highway settings are shown in this section. The program determines how to locate and extract lane markings on the left and right. The suggested technique has been tested on video pictures captured with an on-board vision sensor. On the first video image in Figure 9-13, which shows a part of the trial outcomes for lane marker identifications, the lane markers are visible. These images depict a real interstate situation (on Indian Highway) with both functional and broken lane signs. Figures 9 to 13 show a sequence of excellent-condition road pictures with a combination of solid and broken lane markers on the left and right. The computer is taught to precisely recognise the left and right lane markings. 9–13 depict a scenario with a moving car and a mix of strong and broken lane signs in the foreground. The computer is taught to precisely recognise the left and right lane markings. In video sequences filmed on curving road types and under highly tough lighting and weather situations, the result attained by our proposed method is good. With a 98% accuracy rate, it offers promising outcomes, reduces noise, and enhances detection rates.

Fig. 8. Grey Scale image.

Fig. 9. Hough transform on a gray scale image.

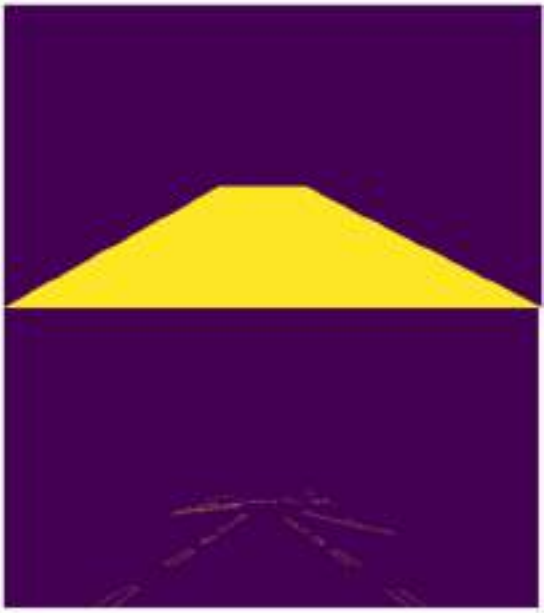

Fig. 10. Hough Transform on Masked Image.

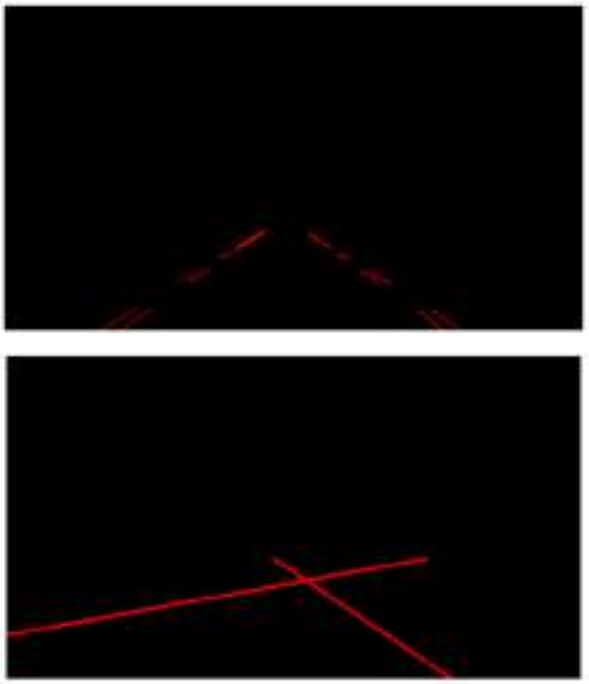

Fig. 11. Extrapolated lines.

Fig. 12. Overlapped lane marking images.

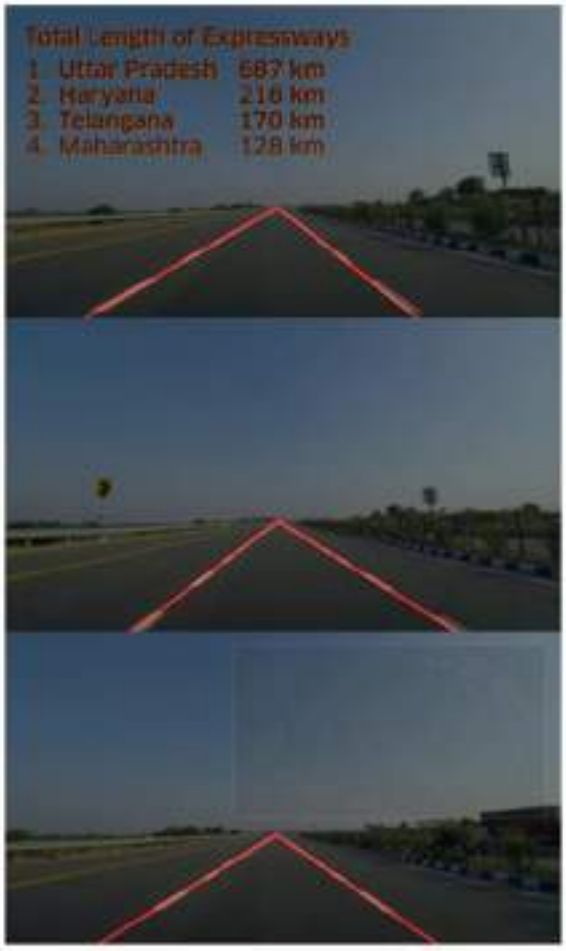

Fig. 13. Final output of Lane detection.

Fig. 10, Demonstrates detection on a road with a variety of road markings. On the road image, 9 depict a yellow lane with an arrow. The algorithm is successful in detecting the road lane.

7 Conclusion

In this study, a simple robust ongoing road lane identifying system was put to the test for better precision and robustness configuration. To make obtaining the valuable data easier, the program goes through a series of low-level picture processing procedures. The Canny edge detection technique concentrates on road features at that particular location. To find lines that can be utilized to define the left and right lane borders, the Hough Transform is used. Finally, as seen in the first image, the gathered left and right lane borders met in the middle to form the ideal aftereffect of left and right boundaries. To lower the high processing cost, the image is downsized to a smaller area of interest. Lower threshold esteem is used with worried recognition in more perplexing scenarios. In future projects, lane detection will be combined with location tracking to reduce computational load even more. Real-world placement in the image can be used to calculate distance and time to departure. Using the combined parameters, a new lane departure warning system will be introduced.

7.1 Potential Shortcomings of pipeline

1. It would not work if the camera angle was different and the region of interest would be different
2. It would not work if there were animals or people crossing the street and are in between the two lanes, because this would be considered as edges by the canny transform so we would have to filter that out
3. It would not work if there was something like a car directly in the lane as this would mess up the extrapolation of the lane since there would be spurious lines
4. It would not work if the difference between the color of the lanes were too minimal, it would not be detected by the canny transform parameters.

8 Future scope

1. Parameters can be modified to improve performance even further.
2. If there was an abrupt change between two frames, we can reject the result of the second frame because it does not make sense.
3. Considering the following two consecutive frames, this does not make sense because of the abrupt change so we should disregard the second frame and consider it as an error/anomaly/miscalculation.

References

1. Sztyber, Lukasz. (2020). Lane Finding for Autonomous Driving: *Progress in Automation, Robotics and Measurement Techniques*. (Springer, Warsaw, 2019)
2. Scanlon, J. Sherony, R., Gabler, H. *Preliminary Effectiveness Estimates for Intersection Driver Assistance Systems in LTAP/OD Crashes* (2017).
3. Xing, Yang, Lv, C., Wang, H. , Wang, H. , Ai, Y. , Cao, Dongpu , V., Efstathios. IEEE Transactions on Vehicular Technology. **1**(2019).
4. Ieng, S., Vrignon, J., Gruyer, Dominique , A. D.. *A new multi-lanes detection using multi-camera for robust vehicle location.700*. (2005)
5. Hsiao, P.-Y. , Yeh, C.W., Huang, S.S, Fu, L.C., IEEE Transactions on. **58**, 2089 (2009).
6. Wang, Wenshuo , Zhao, Ding , Xi, Junqiang , Han, Wei. IEEE Transactions on Vehicular Technology, **67**, 9145 (2018)
7. Lee, C. , Moon, J.-H. , IEEE Transactions on Intelligent Transportation Systems. **1**. (2018).
8. Haque, M. , Islam, M. , Alam, K. , Iqbal, H. , Shaik, M., International Journal of Image, Graphics and Signal Processing. **11**, 27 (2019
9. Sultana, S., Ahmed, B., *Robust Nighttime Road Lane Line Detection using Bilateral Filter and SAGC under Challenging Conditions.* IEEE 13th International Conference on Computer Research and Development (ICCRD) (2021).
10. Lin, Q. , Han, Y. , Hahn, H. , *Real-Time Lane Departure Detection Based on Extended Edge-Linking Algorithm.* 2nd International Conference on Computer Research and Development, ICCRD (2010)
11. Ozgunalp, U., Fan, R., Ai, X., Dahnoun, N., IEEE Transactions on Intelligent Transportation Systems. **18**, 1. (2016).
12. Panichpapiboon, S., Leakkaw, P., *Lane Change Detection With Smartphones: A Steering Wheel-Based Approach.* IEEE Access. 1. (2020)
13. Yuan, C. , Chen, H. , Liu, J. , Zhu, D. , Xu, Y., *Robust Lane Detection for Complicated Road Environment Based on Normal Map*, IEEE Access, 1, (2018)
14. H. Kong, J. Audibert, J. Ponce, IEEE Transactions on Image Processing, 19, 2211 (2010)
15. Wang, J.. *Lane Detection Algorithm Based on Temporal–Spatial Information Matching and Fusion*, CAAI Transactions on Intelligence Technology, 2, (2019)

Deep Neural Network Model for Proficient Crop Yield Prediction

K. Pravallika[1], *G.* Karuna[1*], *K.* Anuradha[1], *V.* Srilakshmi[1]

[1] Computer Science and Engineering, GRIET, Hyderabad, Telangana, India.

Abstract. Crop yield forecasting mainly focus on the domain of agriculture research which has a great impact on making decisions like import-export , pricing and distribution of respective crops. Accurate predictions with well timed forecasts is very important and is a tremendously challenging task due to numerous complex factors. Mainly crops like wheat, rice, peas, pulses, sugarcane, tea, cotton, green houses etc. can be used for crop yield prediction. Climatic changes and unpredictability influence mainly on crop production and maintenance. Forecasting crop yield well before harvest time can help farmers for selling and storage. Agriculture deals with large datasets and knowledge process. Many techniques are there to predict the crop yield. Farmers are benefited commercially by these predictions. Factors such as Geno type, Environment , Climatic conditions and Soil types used in predicting the Yield. For predicting accurately we need to know the fundamental understanding and relationship between the interactive factors and the yield to reveal the relationships between the datasets which are comprehensive and powerful algorithms. Based on the study of various survey papers it has been found that in all the crop predictions, various deep learning, machine learning and ANN algorithms implemented to predict yield forecast and the results are analyzed.

1. Introduction

Yield forecasting of Crop is very essential for the production of food globally. Accurate forecasting can be done by policy makers to take timely decisions to import and export in terms of improving the national food security. Seed companies must forecast new hybrids in order to breed better varieties for various types of environments. Financial decisions can be easily taken and get benefitted by farmers and Growers. Genotype and Environmental interactions are highly complex characteristics. Genotype means the genetic characteristic of individual for particular trait and phenotype of individual deals with observable characteristics like physical, physiological, biochemical and behavioral. For example, length of the plant is one type of phenotype trait.

High dimensional marker data typically contains millions of markers for each plant individual and is represented by genotype.

*Corresponding author: karunavenkatg@gmail.com

The impact of genetic markers must be estimated, which results in interactions with various environmental factors and field management activities that must be calculated.

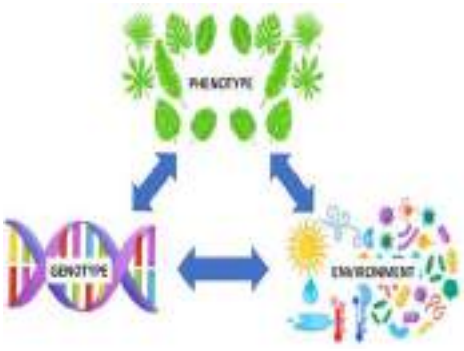

Fig.1. Genotype, phenotype and environmental interactions

Alleles is the alternative word for genes and each individual inherits two alleles for a character one from male and one from female. Two alleles can be same (TT or tt) or different (Tt).

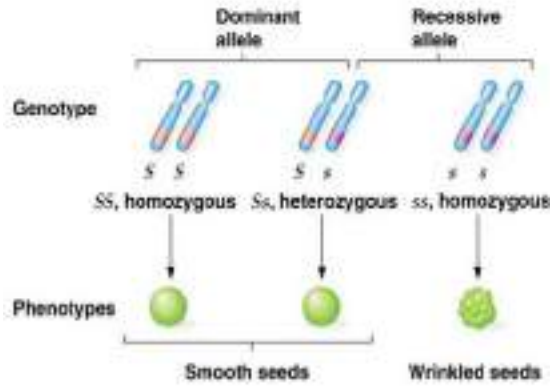

Fig.2. Alleles, genes and traits

Dominant allele that expresses itself and recessive allele unable to express itself. For a particular individual if the dominant allele and recessive allele is known then prediction of phenotype will become simple.

Environmental factors will have great effect on genotype. One of the explicit functions is phenotype, which consists of genotype is treated as G, E as environment, and their interactions are considered as G*E and is treated as noise.

Fig.3. G*E interactions

Group of environments will share same type of varieties can be considered as mega environments. Kharif (july-oct) and Rabi(mar-june) are the two main seasons for growing different crops. Rice, maize, sorghum, bajra, ragi, pulses, soyabean, groundnut and cotton are the crops grown in kharif season.

Wheat, barley, oats, chick pea, mustard seeds are grown in rabi season. Syngenta is one of the company which provides the data for crop predictions. Climate data, which encompasses length of day, rainfall patterns, radiation from the sun, air humidity, min and max temperatures, is indeed one of the factors.

2. Related Work

In the Region of maharashtra, algorithms are used to predict paddy crop yields using anns[2]. Maharashtra's 27 districts have datasets inferred from available public Indian government records. When predicting, snowfall, lower limit temperature, mean temperature, highest temperature, region, output, and harvest are all factored into the equation.Weka tool is used for processing the dataset. In this rice crop prediction a multilayer perceptron neural network and is better than the regression models.Multilayer perceptron, radial basis function networks, and kohonen self organising feature maps are used in neural network[17] models.

Machine learning approaches are used to predict crop yields, and they are implemented in the PHP platform.Temperature, area, humidity, and production are used to predict tomato crop parameters. Ch.Vishnuvardhan Chowdary, Dr.K.Venkataramana[3] developed id3 algorithm for quality crop yield prediction. Different types of fertilizers are used to increase fertility of soil by adding nitrogen nutrients. Pesticides are used to remove the pest from the crop.Gradient boosting regressor uses cross validation to get more accuracy i.e 87.9% .Random forest regressor gets the accuracy of 98.9%.

Crop yield prediction develops a mobile application design and implementation using machine learning[4] it mainly helps the farmers to predict production of specific crop in particular regions. Rainfall and temperature are the physical parameters used in predicting the yield of crop. The app is intended to help farmers by requiring them to enter information such as location, farm size, size, temperature, rainfall, and crop dataset.To train the dataset ARIMA model is used. Accurate prediciton can be done based on the availablity of quality data. Python, data processing, and Android Studio are used to design the application. Intelligrow is the smart phone application in which the results are potrayed in systematic manner.

The learning algorithm to forecasting banana cultivation yields[5] utilises long - short - term memory strands with various perceptrons. Information is derived from beneficiaries (ARB) of Dapco in Davao del Norte, Philippines.Epoch, batch size, neurons are used as model parameters to identify the optimal values. Floods and droughts are the extreme events. Banana is the tropical fruit crop in philipiness.

In order to derive and refine yield prediction data, a review of research for estimation using machine learning[6] was initiated. Six databases were searched were used to find 567 related research, of which 50 have been chosen for some further exploration based on selected studies. Air temp, soil moisture, and soil composition are all used by artificial intelligence. Popular deep neural networks are CNN, LSTM, and DNN. Machine learning historical data is used for training phase and testing phase for performance evaluation. The literature review and study objectives serve as basis for descriptive and inferential machine learning algorithms. Models of description allow for the acquisition of knowledge from collected data. Predicting future result can be done for predictive models. Systematic literature review(SLR) gives the overview of the crop yield[13] prediction and its result is different from other results. Objectivity and transparency are the SLR factors.

An ANN-based weather prediction model [7] asserts a linear correlation between both the weather data entry and the known target data. Atmosphere and state of given location is predicted in weather forecasting which collects the quantitative data. To protect life and property weather warnings are the important forecasts. ANN mainly minimizes the error.Temperature forecasts have special interest on minimum and maximum temperature of day. For winter , summer and fall training and testing is done separately. RBFN and ensembles outperformed all single networks.

Recursive neural network (BPN) [8] has the key advantage of being comparatively imprecise for a multitude of tasks. A multilayer perceptron has 3 levels: the input nodes, the intermediate hidden nodes, and the output units. Factor analytic models are used to join environments and genotypes that do not have cross-over genotype * environment interactions[9]. Prediction assessment of environmental trains[11] using linear mixed models[18]. Syngenta datasets are used for predicting the yield of the crop across different countries. Crop yield prediction using deep neural networks[1] uses various algorithms like LSTM , lasso and regression trees.

Agriculture deals with large datasets and knowledge process[12]. Many techniques are used to predict the yield of the crops. Neural pathways and sophisticated systems are used for massive volumes of data[18]. They used a replacement algorithm to determine yield in this research study. The pH level, amount of nitrogen, amount of carbon, weather patterns, temp, types of soil, and amount of phosphate are among the parameters.The primary goal of agriculture is to maximise value. Because large-scale climatological phenomena have an overly negative impact on agriculture, it is critical to clarify the rainfall patterns of a selected point.There is a lot of research going on with pulses, wheat, rice, sugarcane, and onions. More accurate predictions using meteorological data is an intelligent system.Statistical models and crop simulation models are the two groups of prediction models and applications[14]. ANN and genetic algorithms are efficient than traditional methods because there are easy and accurate for complex inputs.If ANN uses climate factor effective then farmers can use it efficiently.

ANNs are computational systems that processes like biological networks that constitute animal brains. Learning through experiences known as computational ability. Classification is made up of a group of simple computing units known as processing elements that are associated together in a multifaceted communication system, much like the human brain.Feed forward and back propagation are two common neural network architectures. A feed forward system as well as interpretation is a network that has no feedback mechanism. The flow of the system is uni - directional. A node transmits messages to another access point but obtains no response.

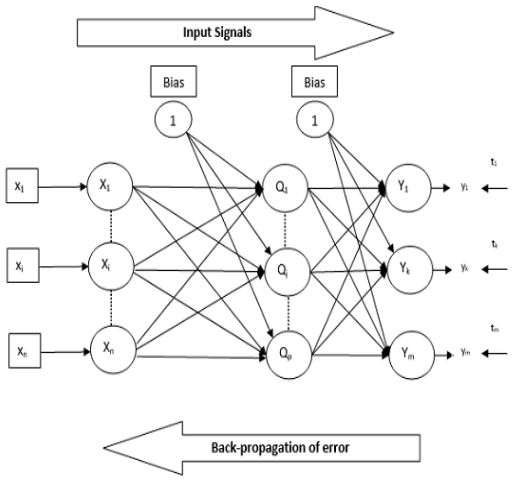

Fig.4. Back propagation

Back propagation seems to be a supervised classifier learning that describes how a neural network is trained. Network should provide with sample inputs and desired outputs.Following computations, the final output is compared to the actual output for a given input.Back propagation has

three phases: feed forward, back propagation of error, and weight updating.

Estimation of wheat crop yield have used a deep Lstm network [18] is a low-cost method of crop yield prediction because satellite images are obtained from publicly available sources. Tehsil (block) levels are proposed for wheat predictions across several states in India and outperformed the existing methods. Remote sensing data is important popular source of data for various applications like income prediction, yield prediction etc.while prior methods involve in extracting handcrafted or rudimentary features such as histograms where as this paper works on satellite images and allows model for learning yield prediction.For geographical area yield estimates depends on factors like waterbodies, urbanization etc. For data temporal features are modelled using deep LSTM model. Evaluation and validation of approach is done for tehsil level wheat prediction for seven states in India. To train proposed deep learning models used MODIS surface reluctance multi-spectural satellite images and land classification maps.The model outperformed traditional remote sensing methods by 70% and deep learning models by54%.

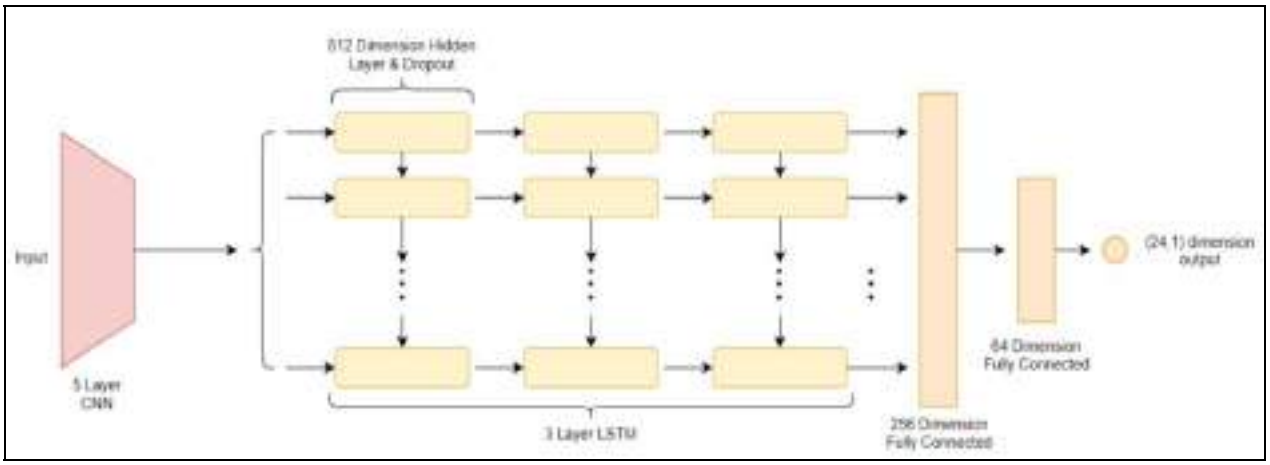

Fig.5. CNN-LSTM architecture

Crop yield prediction using deep Gaussian process based on remote sensing data [15] says that it is an inexpensive method for accurate prediction. In three ways existing techniques are improved firstly they forego traditional features and next they undergo modern approaches based on remote sensing. Novel dimensionality reduction technique is introduced to train CNN or LSTM network based on labeled training data it will automatically learn the features. Finally, in order to improve accuracy, spatiotemporal data, the Gaussian model is expressly utilized. We put our technique to the assessment on province soybean predictive modeling in the U.s, and it surpasses competing firm procedures.

A new dimensionality reduction technique is used to fulfill the demands of training phase. Raw images are treated as histograms of pixel counts to achieve tractability mean field[15] approximation is used.CNN and LSTM are trained on histograms to predict the yield.It does not explicitly account for spatiotemporal dependencies between data points but performs well, for example, due to common soil properties. we have a tendency to overcome this limitation by incorporating a mathematician method layer on prime of our neural network[10] models.Other traditional remote sensing-based models were outperformed by 30 percent in aspects of RMSE and 15percent of its total in aspects of MAPE. Deep learning models are complex non linear mappings used for learning hierarchical representation of data. CNN, DNN, LSTM consists of the set of layers where the output of one layer is the input of the next layer.

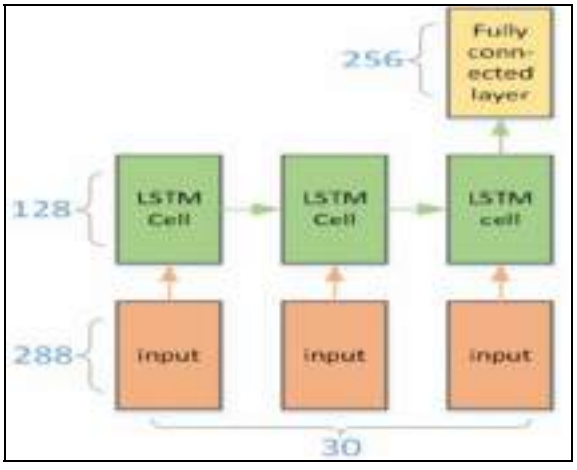

Fig.6. LSTM structure

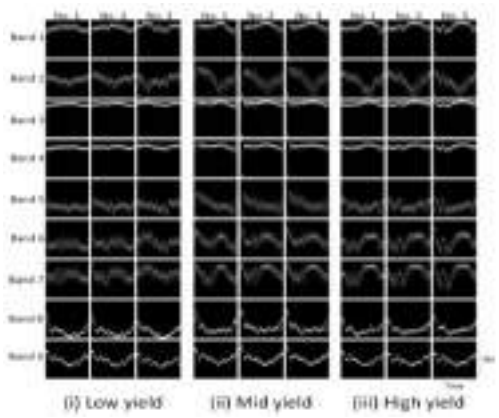

Fig.7. 3-D histogram visualization

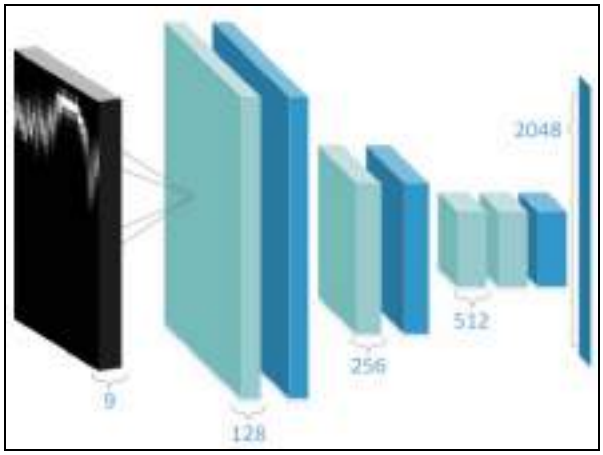

Fig.8. CNN structure

3. Flowchart For Crop Yield Prediction

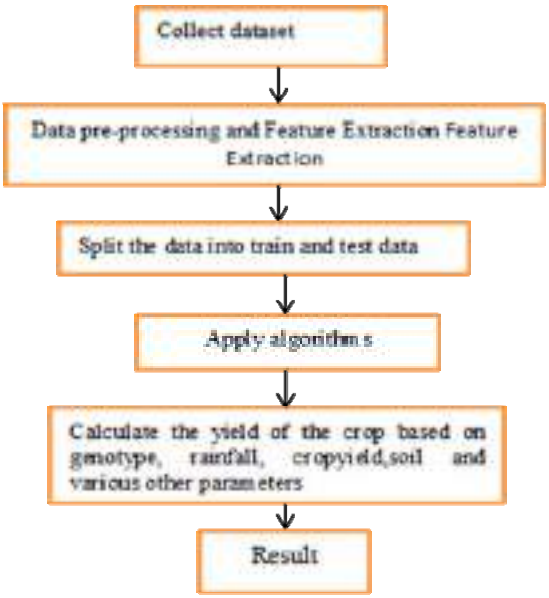

4. Methods For Predicting Crop Yield

4.1 Artificial Neural Networks (ANNs)

Artificial neural networks performed better than multivariate regression. Back propagation neural network technique is one of the best performing algorithm. Artificial neural network uses back propagation. The multilayer perceptron seems to be the most frequently used neural network in latest studies. The input data, the hidden neurons, and the network output are required for ANN, and it outdoes prediction models[2]. Biological neural mechanisms in the human brain are one type of concept for ANN structure. Neurons in the human brain are integrated and used to design the interdependencies for refining. A neurological network is made up of nodes or units, which are integrated structures. Every component is built to look like its biological counterpart, a neuron. Each unit receives and replies to a weighted set of input data. The Artificial Neural Network (ANN) [19] technique is based on a biological system model. The crucial element of this technique is the novel structure of the understanding process system. Associate degree ANN is developed for a single application, including such pattern classification or information classification, using a learning method.

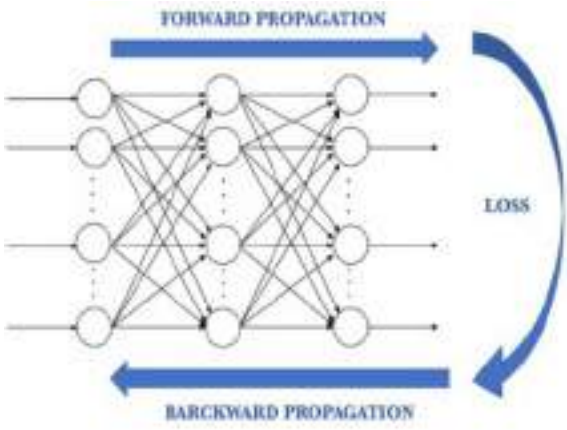

Fig.9. Forward and Backward Propagation

4.2 Deep Learning Networks (DLNs)

Deep learning models are neurons that are used in deep learning approaches. CNN, RNN, LSTM, and DNN are outscored by Lasso, shallow neural networks, regression models, deep learning methods, fully convolutional neural networks, and rnns. Deep neural networks stand to gain from cutting-edge simulation and methods applied. Feature selection can be accomplished by decreasing the dimension of the input space used to train the DNN model. As it has numerous non-linear stacked layers which convert the input to the system into an elevated and more conceptual representation to every stacked layer, it can find the underpinning representation of data

in the apparent lack of feature input data. More complicated features are extracted as the system grows deeper, resulting in high precision. It is known to be an ubiquitous approximator function if the right variables are provided, which means it can estimate almost any feature but is difficult to choose the right parameters.

4.2.1 Shallow Neural Network

One or multiple hidden layers are prevalent in shallow neural network models. Recognizing a shallow neural network can make you realize what tends to happen in a deep network. The section outlines a shallow neural network with one hidden units, one input nodes, and one output neurons.

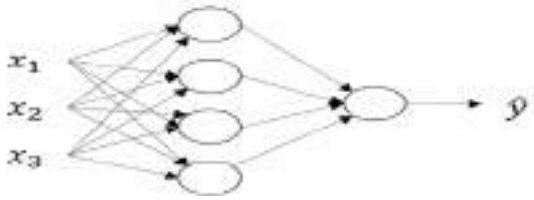

Fig.10. Shallow Neural Network

4.2.2 Convolution Neural Network

It is indeed a deep learning method that generates an image representation and designates weight values to various objects in the scene to discern them from each other.The below figure is the convolution neural network is sequence for classifiying handwritten digits.

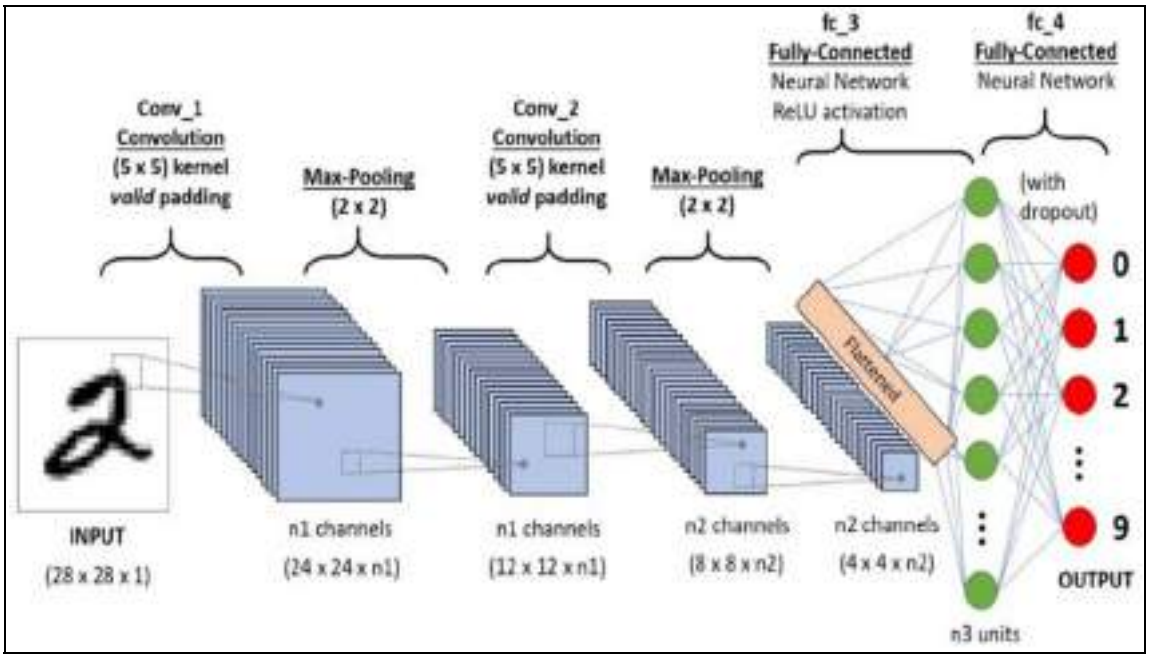

Fig.11. Convolution Neural Network

4.2.3 Recurrent Neural Network (RNN)

The recurrent neural network model [20] adds a twist for basic neural network. A vanilla neural network takes input as fixed vector size and limits the usage to situations which involves series type input with no planned size. Recurrent neural network remembers the past and are influenced by the decisions in past. They can take one or more inputs and gives one or more outputs as vector.

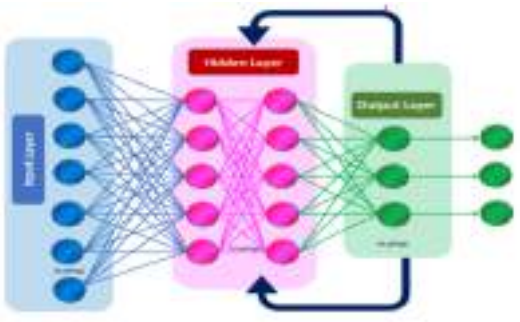

Fig.12. Recurrent Neural Network

4.2.4 Long Short Term Memory (LSTM)

Long Short Term Memory Models (LSTMMs) are designed essential to tackle the long-term correlation issue that exists in recurrent neural networks due to the vanishing gradient troubles.To make more traditional feed forward neural network LSTMs have feed back connections. They process the sequence of data entirely without treating each point independently and the useful information is retained about the previous data and it helps for processing the new data points. For text, speech and general-time series LSTMs are good for such sequences of data.

4.2.5 Deep Neural Networks

For association of input and outputs deep learning algorithms are used along with networks. Deep refers to large amount of layers along with weights and biases can be able to solve for more complex functions.

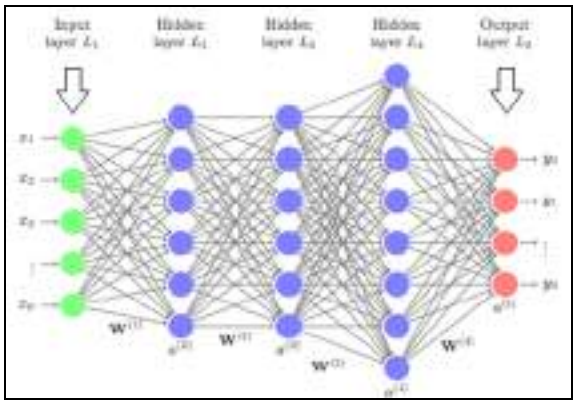

Fig.13. Deep Neural Networks

4.3 Machine Learning Techniques

Machine learning models used to anticipate crop growth include regression analysis, gradient boosting regressor model, random forest regressor model, decision tree regressor modle, polynomial regression technique, and ridge regression technique.Out of all random forest regressor[3] and gradient boosting regressor[3] gives best accuracy with cross validation.

4.3.1 Linear Regression Model

It is just a sequential model that represents the linear relation among an input parameter (x) and a single output unit (y) for combinations of the input parameter (x) (y). Single input variable is considered as a simple linear regression and multiple input variable is considered as a multiple linear regression.Most common data and method is treat the ordinary least squares method.

4.3.2 Gradient Boosting Regressor

Gradient Boosting is a kind of regression method. GB builds an ingredient model series of steps, letting the tuning of absolute discrete loss functions. A regression tree performs the amount of boosting phases in each phase by working on the negative slope of the given deficit.

4.3.3 Random Forest Regressor

So every decision tree has a large variance; nevertheless, when we incorporate them all at once, the eventual variance is lesser because each tree is wholly trained on suitable sample knowledge, and thus the outcome does not rely solely tree structure but on multiple call trees. In the occurrence of a classification error, the bulk vote classifier is used to produce the final output. In the scenario of a regression flaw, the final output is the mean of all the outcomes. Aggregation is the name given to this part of the equation.

4.3.4 Decision Tree Regressor

In attempt to provide tangible continuous output, decision tree predictor scrutinises an object's choices and trains a framework within the structure of a tree to anticipate knowledge in the future. Constant output insinuates that the emission is not distinguishable, that it cannot be characterised simply by a distinct, well-known group of statistics or value systems..

4.3.5 Polynomial Regression

Polynomial Regression is a common formula that does use an ordinal degree polynomial to quantify the relationship between a predicated (y) and an independent variable (x). The Unique Instance of Multiple Statistical Residuals in Cubic Cm is another name for it. As a result, in required to persuade the Multiple Statistical Coefficient of determination to Polynomial Correlation, we add some polynomial conditions to it. It is a linear classifier that has been improved in high precision. The mentoring set of data used in Polynomial regression is not deterministic. It hires a statistical regression model to adapt the tough and non-linear features and data sources.

4.3.6 Ridge Regression

Ridge regression is a concept standard setting technique that might be used to analyse any statistics that has experienced from repeated measures. This method employs L2 regularisation.once the problem of multiple regression happens, least-squares ar unbiased, and variances ar giant, this ends up in foreseen values to be far-flung from the particular values.

5. Comparision of crop yield prediction with different models

5.1 Artificial Neural Networks

The table below contrasts R, MEA, as well as MSE[16] for crop varieties when using artificial neural systems imperialistic competitive optimization technique and grey wolf optimization method models to examine effectiveness.

Table1. ANN-ICA and ANN-GWO with R, MEA and RMSE

Crops	R		MEA (%)		RMSE (%)	
	ANN-ICA	ANN-GWO	ANN-ICA	ANN-GWO	ANN-ICA	ANN-GWO
Wheat	0.35	0.49	35.6	33.40	8.58	8.41
Barley	0.38	0.43	12.10	12.25	0.42	0.63
Potato	0.81	0.81	22.8	22.25	0.78	0.76
Sugar Beet	0.24	0.26	39.0	39.12	3.35	3.44
Average	0.45	0.50	27.3	26.68	3.30	3.29

5.2 Deep Neural Networks

The table compares different deep learning models based on response variable, training RMSE, validation RMSE, training and validation correlation coefficients for yield, check yield, and difference.

Table 2. Training and validation comparisons of different deep neural network algorithms

Model	Response variable	Training RMSE	Training correlation coefficient(%)	Validation RMSE	Validation correlation coefficient (%)
DNN	Yield	10.53	88.31	12.8	82.91
	Check yield	8.22	91.01	11.39	85.49
	Yield difference	11.80	45.89	12.50	29.31
LASSO	Yield	20.32	36.69	21.43	27.66
	Check yield	18.87	28.51	19.89	23.01
	Yield difference	15.33	19.79	13.12	6.88
SNN	Yield	12.98	80.29	18.09	60.10
	Check yield	10.25	71.19	15.15	60.50
	Yield difference	9.98	58.76	15.16	11.36
RT	Yield	14.38	76.75	15.30	73.85
	Check yield	14.57	82.01	14.88	69.98
	Yield difference	17.68	21.15	15.93	5.12

Corn and soyabean crops are compared using Training and validation RMSE, training and validation correlation coeffients for CNN and RNN algorithms.

Table 3. CNN and RNN comparing corn and soyabean crops

Response	Model	Training RMSE	Training correlation coefficient(%)	Validation RMSE	Validation correlation coefficient(%)
Corn	CNN-RNN (W)	17.15	89.02	24.79	72.18
	CNN-RNN (S)	19.16	84.72	24.43	73.82
	CNN-RNN (M)	27.77	69.59	34.03	33.99
	Average	38.51	0.04	35.66	0.01
Soya bean	CNN-RNN (W)	4.6	89.65	5.98	78.80
	CNN-RNN (S)	5.64	83.26	5.94	81.28
	CNN-RNN (M)	7.87	59.84	8.66	48.77
	Average	10.29	0.01	10.11	0.05

5.3 Machine Learning

When accuracy, recall, and F1-score are being used to make comparisons different algorithms such as logistic regression model , decision tree method, Random Forest model, and k nearest neighbour as well as svms, logistic regression model performed the best.

Table 4. Machine learning algorithms accuracy comparison

Algorithm	Precision		Recall		F1-Score		Accuracy(100 %)
	Class 0	Class 1	Class 0	Class 1	Class 0	Class 1	
Logistic Regression	1	1	1	1	1	1	100
Decision Tree	1	0.90	0.83	1	0.91	0.95	93.3
Random Forest	1	0.90	0.83	1	0.91	0.95	93.3
K Nearest Neighbor	1	0.82	0.63	1	0.80	0.90	86.66
Support Vector Machine	0	0.60	0	1	0	0.75	60

Deep learing and machine learning algorithms comparison using mean absolute percentage error and finding the best performer algorithm using accuracy measure.

Table 5. Various deep learning and ML algorithms comparison

Model	Accuracy Measure(%)	MAPE(%)
DRL	93.7	17
BDN	92.1	20
BAN	91.7	27
IDANN	91	29
RAE	90.7	32
DL	91.85	28
ANN	90.5	38
RF	70.7	53
GB	81.2	41

Table below shows Rice, millet and paddy crops comparison using different algorithms and choosing the best performer using accuracy among all the algorithms Random forest gives best result for prediction.

Table 6. Comparing table for Rice, Millet and Paddy for various Models

Model	Accuracy Measure (%)	Crop
Multilayer perceptron	97.5	Rice
RBF Neural network	96.77	Rice
Random forest classifier	99.74	Millet
Deep reinforcement Learning	93.7	Paddy

6. Conclusion

This paper gives a detailed analysis of different approaches used for crop yield prediction.Various algorithms are mentioned along with the datasets and results. Different types of crops used for prediction purpose in different seasons are mentioned.various crops are used for prediction using different classification techniques, depending on the factors used more accurate results are generated. Climatic conditions plays a major role in yield. Crop yield prediction mainly depends on factors so while using any techniques need to consider the factors accurately gives effective results and helps in making good decisions for import and export and better pricing of respective crops. This work can be used to extend these approaches for and to achieve better results for future enhancements.

7. Nomenclature

CNN - Convolutional Neural Network
RNN - Recurrent Neural Network
RT - Regression tree
DL - Deep Learning
ANN - Artificial Neural Networks
GB - Gradient Boosting
DRL - Deep Reinforcement Learning
ARIMA - AutoRegressive Integrated Moving Average
LSTM - Long Short Term Memory
DNN - Deep Neural networks
MAPE - Mean Absolute Percentage Error
RMSE - Root mean square error
MEA - Means end analysis
MSE - Mean square error
BDN - Deep Belief Network
BAN - Born again neural networks
IDANN - Internal Deep Generative Artificial Neural Networks
RAE - Robust Adaboost RT based Ensemble
R - Range
MODIS - Moderate Resolution Imaging Spectroradiometer
LASSO - Least Absolute Shrinkage and Selection Operator
ANN-ICA - Artificial Neural Networks -imperialist competitive algorithm
ANN-GWO - Artificial Neural Networks -Gray Wolf Optimizer of Neural Networks
CNN-RNN(W) - Convolutional Neural Networks-Recurrent Neural Networks(weather data)
CNN-RNN(S) - Convolutional Neural Networks-Recurrent Neural Networks(soildata)
CNN-RNN(M) - Convolutional Neural Networks-Recurrent Neural Networks(managementdata)

8. References

1. S. Khaki and L. Wang, Front. Plant Sci. **10**, 621 (2019).

2. N. Gandhi, O. Petkar, and L. J. Armstrong, in 2016 IEEE Technological Innovations in ICT for Agriculture and Rural Development (TIAR), 105–110, (2016).

3. Payal Gulati, Suman Kumar Jha, in 2020, International Journal of Engineering Research & Technology (IJERT) ENCADEMS, **8(10)**,(2020).

4. Meeradevi and H. Salpekar, in *2019 Global Conference for Advancement in Technology (GCAT,)* 1–6, (2019).

5. M. A. Rebortera and A. C. Fajardo, Editorial Preface From the Desk of (2019).

6. T. van Klompenburg, A. Kassahun, and C. Catal, Comput. Electron. Agric. **177**, 105709 (2020).

7. K. Abhishek, M. P. Singh, S. Ghosh, and A. Anand, Procedia Technology **4**, 311 (2012).

8. S. S. Baboo and I. K. Shereef, Int. J. Environ. Sci. Dev. 321 (2010).

9. J. Burgueño, J. Crossa, P. L. Cornelius, and R.-C. Yang, Crop Sci. **48**, 1291 (2008).

10. P. Kora and S. R. Kalva, Springerplus 4, 481 (2015).

11. J. Burgueño, J. Crossa, J. M. Cotes, F. S. Vicente, and B. Das, Crop Sci. **51**, 944 (2011).

12. K. Prasanna Lakshmi and C. R. K. Reddy, in 2010 International Conference on Networking and Information Technology ,451–455pp.(2010).

13. G. P. Miriyala and A. K. Sinha, Recent Advances in Computer Based (2020).

14. Swaraja K, Multimed. Tools Appl. 77, 28249 (2018).

15. A. X. Wang, C. Tran, N. Desai, D. Lobell, and S. Ermon, in Proceedings of the 1st ACM SIGCAS Conference on Computing and Sustainable Societies (Association for Computing Machinery, New York, NY, USA, 2018), 1–5 (2018).

16. S. Kumar, P. Reddy, G. Ramesh, and V. Maddumala, Trait. Du Signal 36, 233 (2019).

17. C. U. Kumari, S. Jeevan Prasad, and G. Mounika, 2019 3rd International Conference on Computing Methodologies and Communication (ICCMC) (2019).

18. S. Sharma, S. Rai, and N. C. Krishnan, arXiv [cs.CV] (2020).

19. B.Dhanalaxmi, G. A. Naidu, and K. Anuradha, Procedia Comput. Sci. 46, 432 (2015).

20. S B Babu, A Suneetha, GC Babu, YJN Kumar, G Karuna, Periodicals of Engineering and Natural Sciences (PEN) 6 (1), 229-240, (2018).

Convolutional and Spiking Neural Network Models for Crop Yield Forecasting

*Dr.G.Karuna[1], K.Pravallika[2], Dr. K. Anuradha[3], V. Srilakshmi[4]

[1]Professor, Computer Science and Engineering, GRIET, Hyderabad, Telangana, India.
[2]PG Scholar, Computer Science and Engineering, GRIET, Hyderabad, Telangana, India.
[3]Professor, Computer Science and Engineering, GRIET, Hyderabad, Telangana, India.
[4]Assistant Professor, Computer Science and Engineering, GRIET, Hyderabad, Telangana, India.

Abstract-Prediction of Crop yield focuses primarily on agriculture research which will have a significant effect on making decisions such as import-export, pricing and distribution of specific crops. Predicting accurately with well-timed forecasts is important, but it is a difficult task due to numerous complex factors. Mostly crops like wheat, rice, peas, pulses, sugar cane, tea, cotton, green houses, corn, and soybean can all be used to forecast crop yields. We considered corn dataset to predict the yield for 13 different states in United States. Crop development and progression are strongly affected by climatic changes and unpredictability. Predicting crop yield well before harvest time will support farmers for selling and storing their crops. Agriculture involves large datasets and knowledge processes. Factors such as Weather Components, Soil Components, Management practices, genotype and their interactions are used in predicting Corn Yield. Precise crop growth generally necessitates a complete overview of the functional correlations between yield and all these interactive variables, which necessitates the use of large datasets and complex algorithms to demonstrate. Various Machine Learning models, Deep Learning models, and Artificial Neural Network algorithms are used for predicting. Deep Neural Network Models such as Convolution Neural Networks (CNN), Spiking Neural Networks (SNN), and Recurrent Neural Networks (RNN) are used to assess corn yield. Integrating CNN, RNN and SNN models outperformed than individual model performance.

Keywords — crop yield, spiking neural networks, prediction, recurrent neural networks.

1. Introduction

Crop yield forecasting plays a vital role for global food Production. To improve food and nutrition security, decision makers can use efficient process to make timely import and export choices. In order to breed better varieties for different types of environments, seed companies must forecast new hybrids. With the help of crop predictions farmers can be benefited to avoid the losses financially and can be known before what crop should be grown in which season and what are the precautions need to be taken according to the environment and soil interactions.

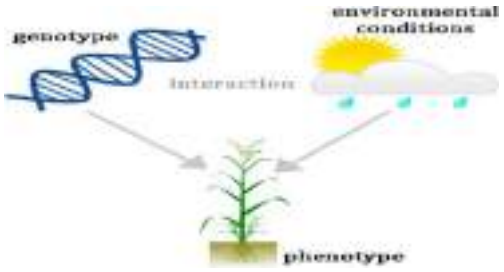

Fig 1. Genotype, phenotype and environmental interactions

Seed companies as well as farmers are going to get benefited ultimately with the help of forecasting. Crop yield forecasting can be done based on the respective factors like soil components, weather components, location, county, latitude and longitude, genotype and

*Corresponding author: karunavenkatg@gmail.com

phenotype characteristics etc. It should be known before that how much area should be taken to plant the crop and the plantation week should be noted up to how many months the crop should last all the measures needs to be analyzed before while planting the crops. What crops need to be grow and what crops cannot grow need to be considered based on the past years experiences and can also gather information from the companies like Syngenta[2] which is a global supplier of crop protection products like (herbicides, fungicides, and insecticides), seeds like (Rice and Corn) and other related products. Interactions between genotype and environment [1] are extremely complex. The term genotype refers to an individual's genetic characteristics for a specific trait, whereas phenotype refers to observable characteristics such as physical, physiological, biochemical, and behavioral characteristics. Plant length, for example, is a type of phenotype trait as shown in above Fig1 and below Fig 2

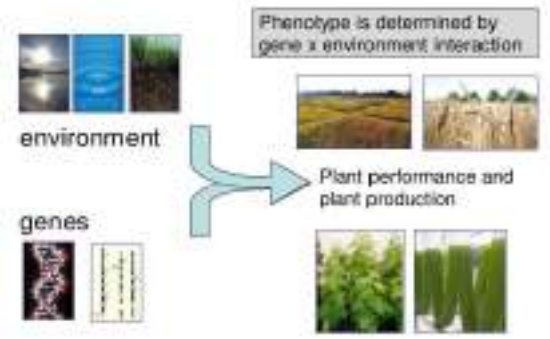

Fig 2. Phenotype traits, Genes and Environment

Millions of markers are usually present in high dimensional marker data, which is defined by genotype for every plant individual. It is important to compute the impact of genetic markers, which usually result in interactions with various environmental influences as well as field management activities.

Alleles are another word for genes, and each individual inherits two alleles for each character, one from male and one from female. Two alleles can be the same (TT or tt) or different (TT or tt) (Tt).

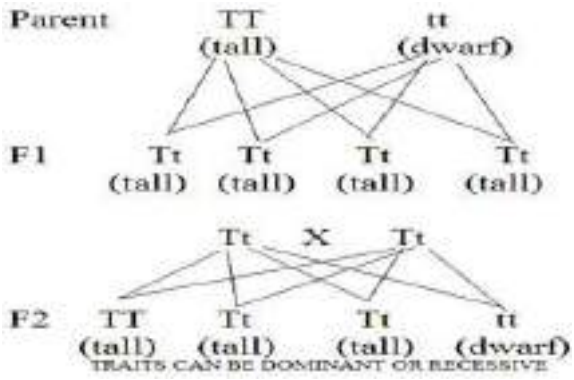

Fig 3. Dominant and Recessive alleles

The dominant allele expresses itself, while the recessive allele does not. If the dominant and recessive alleles for a specific individual are known, phenotype prediction becomes simple. Environmental factors will have a significant impact on genotype. One of several explicit functions is phenotype, which is regarded as noise and is composed of genotype (G), environment (E), and their interrelations (G*E) as shown in above Fig 3.

Mega environments are groups of environments that share the same type of variation. The two main seasons for growing various crops are Kharif (July-October) and Rabi (March-June). We have different crops like Rice, maize, sorghum, bajra, ragi, pulses, soya bean, groundnut and cotton usually grown in kharif season where as Wheat, barley, oats, chick pea, mustard seeds are grown in Rabi season. Corn crop is considered for predicting in this paper and kharif is the season for growing corn.

Soil components, Weather components are the factors for yield prediction. Different varieties of Soil components are considered like Bulk density, Cation exchange capacity $_{pH7}$, Coarse fragments, Clay, Total Nitrogen, Organic carbon density, organic carbon stock, PH in H20, Sand, Silt, Soil organic carbon and all of these inputs are measured with a 250 square meter resolution at six distinct depths (0-5cm, 5-15cm, 15-30cm, 30-60cm, 60-100cm and 100-200cm).The different Climatic components used for estimating the yield are rainfall, radiation from the sun, Precipitation data equivalent, highest temperature conditions, lowest temperature conditions, and vapor pressure are all factors to consider. Climate components play an important role in predicting when compared with the Soil and other factors. Crop productivity, on the other hand, is nearly impossible due to a plethora of complex factors. Genotype and environmental factors, for example, frequently communicate with one another, making grain yield quite difficult. Atmospheric

conditions, for example, often have complicated dynamic impacts that are hard to calculate accurately.

Crop productivity can be forecasted using machine learning models, Deep learning methods and artificial neural networks (Ann). Deep learning models [9] are classification learning methodologies because they have different levels of representation, each with nonlinear modules that change the representation at the present level, beginning with raw input and advancing to a progressively intuitive level. Deeper structures may also be affected by the vanishing gradient issue, that could be mitigated by using residual shortcut connections as well as numerous auxiliary heads (loss functions) for the network. To increase the accuracy of deep learning (dl) techniques, other techniques like a batch normalization, dropout, as well as stochastic gradient descent have been developed (SGD). In the literature, deep learning network techniques usually with more number of hidden layers gives good results than artificial neural network models with a single hidden layer. Deeper features, on either hand, are very complicate for training the model as well as necessitates more difficult hardware and optimization methods. Deep neural network loss functions, for instance, have a high dimensionality and are non-convex, making optimization quite difficult due to the existence of numerous local optima and saddle points.

2. Related Work

Soybean Flowering and Physiological Maturity Forecasted Using Neural Network Aspects [3] are founded on the hypothesis that computer simulation models of plant growth have been formulated; but the models are not always getting good results in plant developing assessment among various conditions. Field-observed flowering dates is being used by this study for the 'Bragg' cultivar for the purpose of scientific investigations in North Carolina, Gainesville, Quincy, Clayton and Florida. The neural network model was trained on the daily Higher and lower climatic conditions, season, and days after planting or flowering are all factors to consider. The sets of data were divided into two main categories: for training as model development as well as independent data sets for testing. The relative mean error of dataset testing for the purpose of flowering date forecasting was 0.143 days and for estimation of physiological maturity was +2.19 days. Plant continued growth estimations are useful in agricultural production because they allow the cultivators to enhance field operation planning and enhance net income as shown in below Fig 4 and Fig 5.

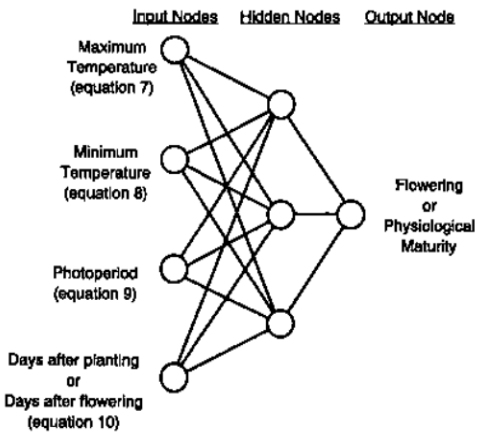

Fig 4. Inputs, connections, and structure of a neural network model are depicted using 3 distinct hidden nodes.

When seed germinates, the vegetative and reproductive development processes begin, and these processes end when the harvest matures. Temperature is a key climate variable influencing plant growth. Furthermore, duration, or the length of the daily light period, can influence increases the productivity in some species. Existing simulation models struggle to correctly estimate development in a variety of areas where either temperature or photoperiod varies. Extended preprocessing was required before feeding the data into the neural network models. The findings for the three thresholds in equations 7 through 10 were entirely dependent on pre - processing phase. It was not possible to conduct an intensive research of all threshold values and neural network requirements.

In this study, we anticipate maize yields using linear regression models and artificial neural networks models [4]. From 1962 to 2004, multiple linear regression models (MLR) and non-linear artificial neural network model (ANN) designs were used in forecasting future maize crop in China's Jilin region, with climate and fertilizer as predictor variables. Production was set to be determined by July-August rainfall, September precipitation, and fertilizer application. Fertilizer is used as a dominant forecaster in the ANN model and was found to be non-linearly related to output. For obtaining the fertilizer data of maize there is a difficulty so the studies used previous years yield tested data. Estimation skill scores derived from cross- validation technique andretroactive validation technique revealed that ANN models perform better than MLR and persistence. Due to the non-stationary nature of the data, in the analysis of forecasting skill, cross-validation method was found to be less reliable than retroactive evaluation. Researchers used two approaches to study crop productivity in relation to environmental variables: mechanistic models and empirical models. For analyzing relationships between crop, soil types,

climatic conditions, and ecology, mechanistic approaches that depend on physiological methods for crop development are best. Because non-linear relationships identified by an ANN model are more difficult to understand than linear relationships identified by MLR, ANN has been dubbed a "black box" technique. As a result, the ANN extrapolates with greater care than a linear function. ANN gives low values compared with MLR solution and hence decides that nonlinear relationship is better. In present research, where interpretation occurred, the ANN model's bounded functional shape gave ANN an added benefit over MLR. Machine Learning Methods for Efficient Forecasting in India [5] Amount of rain, atmospheric pressure, chemical fertilizer, pesticides, ph level, and other climate patterns and parameters all have an impact on crop production. After recognizing the linear relationship among yield and these parameters, reliable yield prediction is needed.

Machine Learning techniques can improve by distinguishing and presenting the consistency and pattern of drive information, machine execution can be improved without the need for characterized computer programming. This survey used a variety of neural network models to assess crop yield on crop yield datasets from multiple areas and crops, including Linear Regression model, Gradient Boosting Regressor model, Random Forest Regressor model, Decision Tree Regressor model, Polynomial Regression model, and Ridge Regression model. Mean absolute error (MAE), mean squared error (MSE), root mean square error (RMSE), R-square, and cross validation are the measures used to compare the accuracy of these strategies. Findings indicate that the Gradient Boosting Regressor has a precision of 87.9 percent with cross validation runs.

Deep Learning techniques in Agriculture [8] is a comparatively recent, cutting-edge image processing technique and data analysis technique with best outcomes and massive results. Deep learning technique has recently made its way into agriculture after being used efficiently in other fields. We assess the sustainable agricultural challenges under consideration, as well as the models and theories employed, information sources, nature, and pre-processing as well as the improved ability achieved based on the criteria used at each work under considering. In addition, we compare deep learning to other popular technologies in terms of classification or regression efficiency differences.

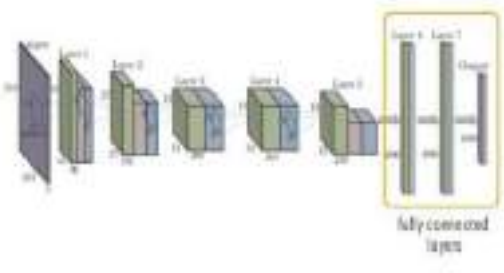

Fig 5. CaffeNet, example CNN architecture

Deep learning outdoes prevailing commonly used image processing method in terms of accuracy, according to our findings. Images make up a sizable portion of the information gathered through remotely sensed data. Images provide a clear understanding of farming in many cases and can be used to address a variety of issues. As an outcome, imaging analysis has become an interesting subject in agriculture, and intelligent data collection methods are used in a wide range of farming applications for image identity verification, outlier detection, and so on. DL extends traditional ML by incorporating more "depth" (complexity) to the model and transforming data from multiple capabilities that allow data representation in a systematic order, through many levels of abstraction.Based on the network architecture, DL may contain a wide range of modules. A basic problem in computer vision, not just deep learning, is that data pre-processing is frequently required and time-consuming, particularly when satellite and images are involved.The high dimensionality and slight number of training samples of hyper spectral data are two issues. Aside from that, existing datasets do not always effectively define the problem. When considering corn returns, for example, it was important to compensate in cultivation data such as fertilization and water management, external influences other than weather data can be considered. Convolutional Neural Networks (CNN) are used to capture similar spatial functioning of different features and combine them to model yield response to nutrient and grain rate management [6]. To define a new dataset for training and test sets the CNN model, nine on-farm corn field studies are used. When compared to multiple regression analysis, the test dataset RMSE is reduced by up to 68 percent, and by up to 29 percent when compared to a random forest. When we look at the harvest data collected within 50 meters of the field's boundaries, we can see that the input variables centered on such cells cover an area with no data.

As shown in below Fig 6 and Fig 7, Fig 8,This survey modeled yield response to nitrogen and seed rate management using five different field features (nitrogen and grain rates, elevation map, soil electro conductivity,

and spatial data). Other risk factors and management techniques that have an effect on global field impacts gain response to site-specific planning. These parameters differ from field to field while changing progressively within the same field.

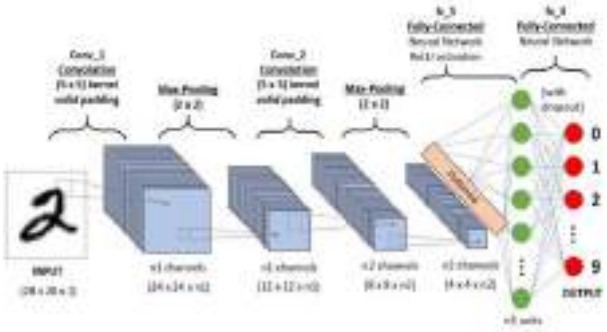

Fig 6. Convolutional Neural Network

Growing plants Date, Hybrid Maturity, and Weather Conditions Influence Corn Yield and Crop Stage [7] In Iowa, USA, we examined wheat crop and phenology data from a multi-location, year, hybrid comparative maturity, and planting date study. Our goals were to find the best combination of sowing date and comparable maturity to maximize corn seed yield per weather, as well as to mitigate the effects of using "full-season hybrids" when harvesting occurs well after the optimum planting date. According to ANOVA, 70% of the variability in seed yield was directly related to planting date and only 10% to associated to maturity, stating that short and full-season hybrid relative maturity periods generated equivalent to seed yield regardless of when they were sown as long as the farms reached maturity prior to harvesting. According to our findings, the time to grain yield is a good predictor of expected higher yield, with a critical stage (after which yield is reduced) of 23 July for Iowa. Furthermore, we discovered that keeping a lower limit growing degree of 648°Cday as during the grain-filling period enhanced maize yield. Conclude, the studied information will help Iowans in making sowing date decisions on the basis on hybrid relative maturity. Throughout most of the growing season (April–October), weather conditions at our sampling locations were relatively inconsistent. The Northeast place had the coolest site-year in 2014, while the Southeast place had the hottest year in 2016. In aspects of rainfall, 62 percent of the site-years were wet, 24 percent became dry, and 14 percent were indeed a mix of the two .

Maize seed yield, silking time, and other considerations, as well as grain-filling duration, are all affected by the planting date. In terms of seed yield and phenology, PD had a bigger influence than RM. Farmers in Iowa will benefit much during the growing season if they plant full-season hybrids all year; nevertheless, the real effect of RM fades over time. Immigrants came to warmer climates with a longer growing season as southern climates warm. A shortened growing season was blamed for the harvest penalty associated with delayed planting. Farmers typically select a mixture relative maturity well in order to progress of planting; however, our research shows that combination RM has a very minor impact on grain yield for any given PD when harvested before planting.

Grain yield estimation and climate making predictions using machine learning techniques for Assessment of the impacts on agriculture [9] Weather has a significant impact on crop productivity A increasing previous research models this transaction in order to estimate the threat of climate change on the industry. A yield modeling approach that makes use of a semi-parametric variant of a deep learning to account for nonlinear dynamic interactions in high-dimensional datasets, as well as known geometrical structure and unfathomable cross-sectional heterogeneity. We show that using corn yield data from the Midwest of the United States, this model outperformed both traditional statistical methods and entirely nonparametric neural networks in predicting yields of years denied during model training. We show that climate change has a major negative impact on corn prices, but it is less intense than the impacts projected using statistical models. Abatzoglou's gridded surface meteorological database (METDATA) is used to generate the meteorological data (2013). Bagging improved both the parameterization and the SNN's precision, but the bagged SNN consistently outperforms. Both OLS regression and the SNN were outpaced by the fully-nonparametric neural net, which was learned in the same way as the SNN but lacked simulation terms.

Incorporating machine learning and crop simulations improves crop yield estimation in the Corn Belt of the United States [10].The goal of this research is to see if merging crop modeling and machine learning (ML) tends to improve grain yield projections in the Corn Belt of the United States. The primary objectives were to identify whether such a hybrid approach would result in better assumptions, which hybrid model mixtures provide much more better estimates, and which crop modeling attributes are most effective when combined with ML for maize crop prediction. The researchers noted that using simulation crop modeling as input features in ML models can lessen yield estimation root mean squared error (RMSE) by 7 to 20%. Furthermore, we investigated the selective complicity of APSIM attributes in ML forecasting and concluded that soil moisture-related APSIM variables have the greatest impact on ML projections, followed by crop-related and weather-related APSIM variables. This finding implies that weather reports alone are inadequate, and that Ml

algorithms require more surface water inputs to produce more accurate yield forecasts.

Estimation of crop prices using supervised machine learning methods [11] and our focus is primarily on agriculture. Farmers are the most important people in agriculture. Farmers face massive losses if the price falls after the cultivation. This paper proposes estimating and planning crop prices for the next 12 months. The information is provided to users via a Flask web page, which is powered by impactful machine learning techniques and innovations and has a user-friendly interface as a whole. The accumulated training datasets contain a wealth of information for forecasting market price and demand. The Decision tree Regressor supervised machine learning algorithm was used in our model. It has been honed on a number of Kharif and Rabi seasons to improve efficiency.

Estimation of Crop Production by Robots [12] Cultivation is an entirely manual endeavour. The use of machine learning methods to implement any type of automation is still in its beginning phases. The focus of this article is to present a contextual approach for introducing machine learning methods into the cropping process. A comparison of machine learning algorithms was performed in order to determine which algorithm is the most accurate in predicting the best crop for a specific plot of land. The research looks at six major food crops in Bangladesh: Aman rice, Aus rice, Boro rice, potato, wheat, and jute. Multiple Linear Regression (MLR) produced the most accurate results during the evaluation and was implemented into an Android application. The android platform system can also generate a timeline of the entire farming process for a specific crop, including when to apply fertilizer. Except for wheat and potatoes, MLR offers greater prediction in this case. KNN yields superior performance for wheat and potato. Mostly as result, the error is 0.40 percent for one and 6.26 percent for the other.

Deep Learning Methods for Yield Estimation [13]. Automatic crop monitoring and yield prediction are now possible thanks to artificial intelligence. The categories were created entirely around five networks: ANN, CNN, DNN, RNN, and combination networks. The feed forward's ANN and DNN were examined, and both offered an average predictive accuracy of 60-70 percent. The large proportion of agricultural processing was carried out using images and timely monitoring. CNN significantly outperformed both DNN and ANN models, with efficiency of 80-85 percent. The only drawback of CNN in this research was that its projections were based purely on training sample rather than real-time past results. A few work was aimed at improving the yield prediction even more and to avoid loss during the yield. The RNN makes use of an LSTM-LSTM combination, which allows for the addition of data storage. When particularly in comparison to the other three systems, it involves the feedback loop that CNN fails, evaluated to the high classification level's average estimation of 83 – 89 percent.

3. Proposed Work

3.1 Dataset Description

For Crop yield prediction we need to select the crop here we selected the crop called Corn and going to forecast the yield based on the dataset and the applied algorithms. Dataset is the first thing we need to select here we collected the dataset from various sources like Syngenta and it mainly consists of the variables like nw, ns, np, nss where the number of weather elements is nw, and the number of soil particles is ns. measured at different depth, np is the planting component and nss is the soil component measured at the surface The six weather components considered are rainfall, radiation from the sun, snow water equivalent, highest temperature, lowest temperature, and air humidity for csv files they are named as Wij where i is the weather component index and consider the six weather components i.e i=1, . . .6 and j= index of week of year for every year there are 52 weeks so j=1,….52. There are 11 Soil components like bulk density(bdod), Caption exchange capacity at Ph7(cec), Coarse fragments(cfvo), clay, Total nitrogen, Organic carbon density(ocd), Organic carbon stock(ocs), ph in H20(phh20), Sand, Silt, Soil organic carbon measured at six different depths(0-5cm, 5-15cm, 15-30cm, 30-60cm, 60-100cm, 100-200cm) with 250 square meter resolution in csv files they can be named as Sij where i is the soil component i.e i=1,-----11 and j is the index of depth j=1,---6. Planting time component is considered as np in csv files they are named as pi where i is the index of the planting date week i=1,---16. The crop performance dataset includes the identified average yield for corn between 1980 and 2019 across 1,176 countries for corn in 13 states including Indiana, Minnesota, Kansas, North Dakota, Missouri, Illinois, Iowa, Nebraska, South Dakota, Ohio, Kentucky, Michigan, and Wisconsin. Organizational data is generally the cumulative percentage of cultivated fields in each state each week starting in April of each year. Grid map approach is followed which means horizontal and vertical lines to identify locations on map.

3.2 System Architecture

The System Architecture of proposed work is like first consider the dataset and preprocesses the data then split into train and test data apply the classification techniques and predict the results. Here for this forecasting purpose Corn dataset is considered from

open source challenge platform like Syngenta [2]. Cleaning, integration, reduction, and transmission are all methods of data preprocessing. We need to get rid of any data that isn't absolutely necessary. The procedure of detecting and analyzing inaccurate or incorrect records from a dataset is known as data cleaning. Real-world data frequently contains noise and missing values, and it may be in an inaccessible format that cannot be actively used for DL models. Data preprocessing is required for cleaning preparation and analysis it for various Deep Learning concepts, which increases performance and reliability. Data that is preprocessed is categorized for training and testing. Training a data means to train the model and testing is for validation process where the unseen predictions are done. The act of segregating available data into two segments, typically for cross-validator purposes, is known as data splitting. One set of data is used to create a forecasting model, while the other is used to evaluate the performance of the model. Data separation into training and test sets is a critical step in assessing data mining models. Training percentage is taken as 80 and test percentage is 20. When a data set is split into a training phase and a validation phase, the majority of information is used for training and only a small amount is used for test results. To train any model, no matter what type of dataset is used, the set of data must be divided into training and testing sets.In the analysis of forecasting skill, cross-validation method was found to be less reliable than retroactive evaluation. Researchers used two approaches to study crop productivity in relation to environmental variables: mechanistic models and empirical models. For analyzing relationships between crop, soil types, climatic conditions, and ecology, mechanistic approaches that depends on physiological methods for crop development are best.

4. Flowchart for Crop Yield Prediction

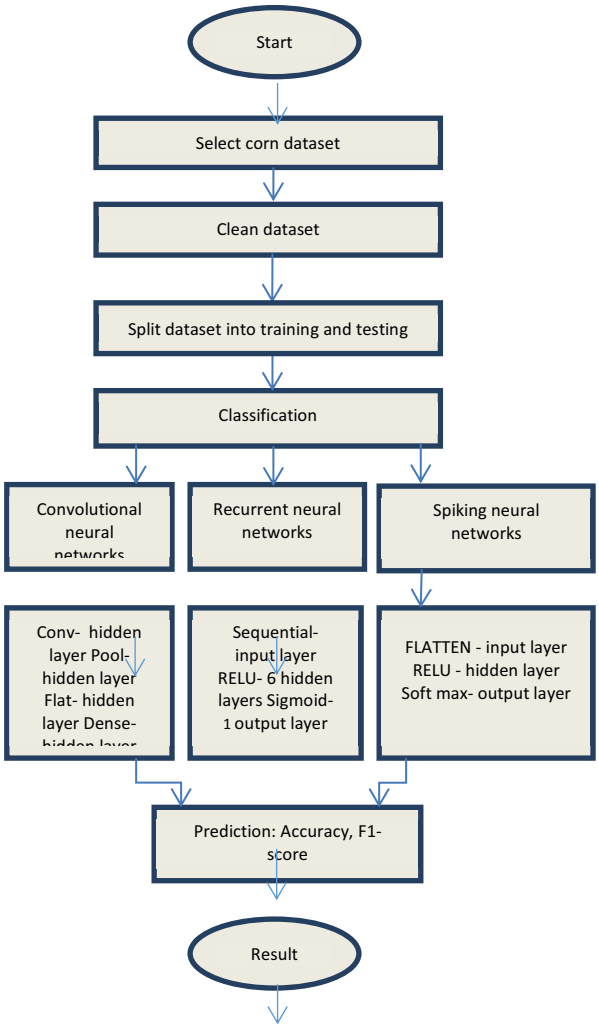

5. Implementation

5.1 Deep learning Methods

Corn yield forecasting is done using Deep Learning (DL) models. Convolutional Neural Networks (CNN), Recurrent Neural Networks (RNN), and Spiking Neural Networks are some of the deep learning models used in this paper (SNN). Neural Networks are composed of three layers: input, hidden and output layer. Input Layer: In this level various types of data is provided to the model. Number of neuron indicates the total number of features in data. Hidden Layer: The output of the Input Layer is fed into the Hidden Layer. Depending on our model and the size of the data, there could be many hidden layers. So every hidden layer may contain a different number of neurons, which is usually greater than the number of characteristics. Each layer's output is calculated by multiplying the previous layer's output by the learnable weights of that layer, followed by addition

of transferable biases and an activation function, making the learning process non linear.

Output Layer: The hidden layer's output is then placed into a logistic function, such as sigmoid or soft max, which converts each class's output into a probability score for each class. Classification is a method of determining which of a set of characteristics a new observation belongs to, based on a learning set of data containing observations with defined category membership.

5.2 Convolution Neural Networks (CNN)

ConvNets also known as CNN'S consists of multiple layers mainly used for image processing and object detection. It has a number of layers that process and extract data features. CNN has a convolution layer with several filters that performs the convolution operation. CNN image categories take an image representation and process it before categorizing it. An input image is perceived by computers as an array of pixels, the size that rely on the quality of image. Depending on the resolution of an image, it will see h x w x d (h = Height, w = Width, d = Dimension). For convolution Neural Networks (CNN'S) we use four hidden layers i.e. convolution layer, Pool layer, flat layer, Dense layer. Conv1D is used and in this the kernel moves only in one direction applicable for Time series data, input and output of Conv1D is two dimensional. Convolution is a mathematical operation performed on two objects to generate an output that expresses how the shape of one is modified by the other. This calculation finds a special functionality in the input data and needs to return a result enclosing that feature's relevant data. This is known as a feature map. The process of merging is known as pooling. So it's primarily for the purpose of reducing data size. Max pooling is considered which takes the highest value within the box. One –dimensional array is considered as a method of converting input data to next layer also treated as flattening. The convolutional layer outcome is flattened to produce a single long feature vector. It is also correlated to the final classification model, forming a fully-connected layer. We attach the final layer to a single line that contains all of the pixel data. Fully connected layer is a dense layer tells that neurons of one layer communicate with next. Adaptive Moment Estimation optimization is a stochastic gradient descent model which is based on adaptive estimation of first-order as well as second-order moments. Adaptive Moment Estimation is a deep neural network training-specific adaptive learning rate considered as optimization algorithm. The technique makes use of the power of adaptive learning rate techniques to identify individual learning rates for each parameter. The average of the squared differences between the observed and predicted values is used to calculate the Mean Squared Error loss. The output is always positive, regardless of the sign of the predicted and actual values, and the value obtained is 0.0.

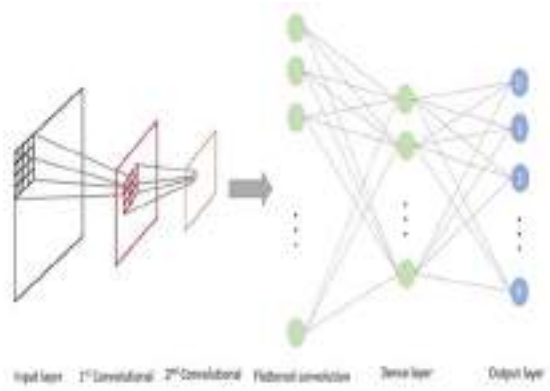

Fig 7. Convolutional Neural Networks

5.3 Recurrent Neural Networks (RNN):

One type of artificial neural network is recurrent neural network that can perform operations on some files like audio files, data files etc. All input and output values are independent in neural networks whereas in RNN, the hidden layers remember the data that was done in a previous layer and give that remembered data to the next layer as input so that it can perform operations on data. This process is repeated until the desired output is obtained. The rectified linear activation function, abbreviated RELU, is a piecewise linear function that retrieves the user input if it is positive and indirectly if it is negative. It has become the default activation function for few types of neural networks and it is easier to train and frequently results in better performance. Activation functions for a Rectified Linear Unit with six hidden layers. In multi-layer networks, the vanishing gradient issue restricts the use of the sigmoid and hyperbolic tangent activation functions. The rectified linear activation function solves the vanishing gradient problem, allowing features to learn more quickly and work better. When building multilayer Perceptron and

convolutional neural network models, the rectified linear activation act as standard activation. Input layer is sequential and output layer is sigmoid.

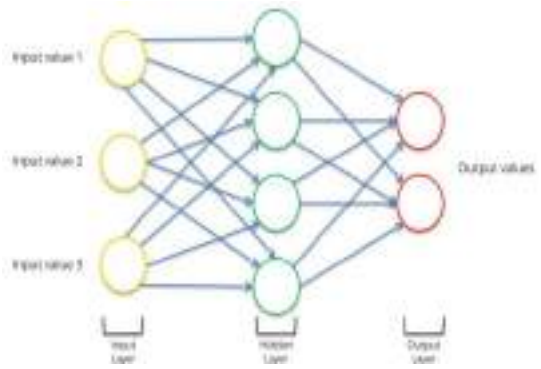

Fig8. Recurrent Neural Networks

5.4 Spiking Neural Networks (SNN):

Spiking neural networks (SNNs) were artificial neural networks that resembled natural neural networks. SNNs incorporate time into their operating model in terms of neuronal and synaptogenesis state. According to the principle, the neurons in the SNN do not need to transmit data during every propagation cycle. Information is only sent when a membrane potential – an inherent property of the neuron associated to its electrical charge on the membrane – reaches a specified value known as the threshold. When the membrane potential reaches a certain threshold, the neuron fires and transmits the signal to other neurons, which modify their potentials in reactions to the signal. The input layer is flattening. Flattening is the process of converting data into a one-dimensional array for input into the next layer. We flatten the layer output to create a unified long feature vector. It is also linked to the last classification model, resulting in a fully connected layer. The ReLU layer is the hidden layer. The rectified linear activation function (ReLU) is a piecewise linear function that, if the input is positive, effectively generates the input; otherwise, it outputs zero. The rectified linear activation function solves the vanishing gradient problem, allowing models to learn more quickly and function better. The output layer, the Softmax layer, broadens this concept into a multi-class work environment. The total of those decimal likelihoods must equal 1.0. The number of neurons in the Softmax layer must be the same as number of neurons in the output layer as shown in below Fig 9.

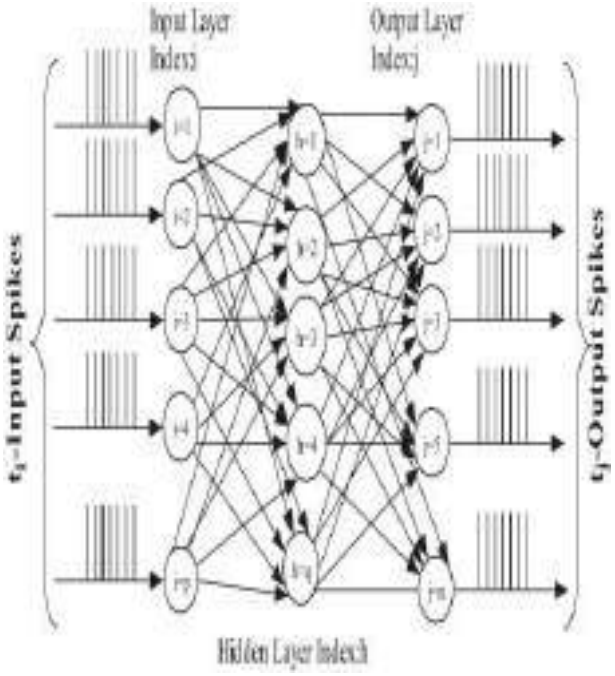

Fig 9. Spiking Neural Networks

6. Results

Tensor flow, an open-source software library, was used to create the three deep neural networks in Python. The training phase for each neural network took about 1.4 hours on a Tesla K20m GPU. For comparative analysis, we used three other well-known forecasting models: Convolutional Neural Network models (CNN), Recurrent Neural Network models (RNN), and Spiking Neural Networks models (SNN). To ensure better comparisons, we wrote all of these modeling techniques in Python and evaluated them in the same software and hardware environments. The overall classification and prediction will be used to generate the Final Result. The effectiveness of the proposed approach is assessed using metrics such as, the ability of a classifier is referred to as its accuracy Class label is predicted correctly and the accuracy tells how good a given predictor can guess the value of attribute for new data.

$$AC= \frac{TP+TN}{TP+TN+FP+FN}$$

$$F\text{-measure}=\frac{2TP}{2TP+FP+FN}$$

6.1 Results for Convolutional Neural Network

Model	Precision		Recall		F1-score		Support		Accuracy
	class 0	class 1	class 0	class 1	class 0	class 1	class 0	class 1	
CNN	1.01	0.01	0.90	0.00	0.97	0.02	300	0	91 %
RNN	1.00	0.00	0.92	0.01	0.95	0.00	300	0	89 %
SNN	1.05	0.03	0.95	0.00	0.95	0.05	300	0	90 %

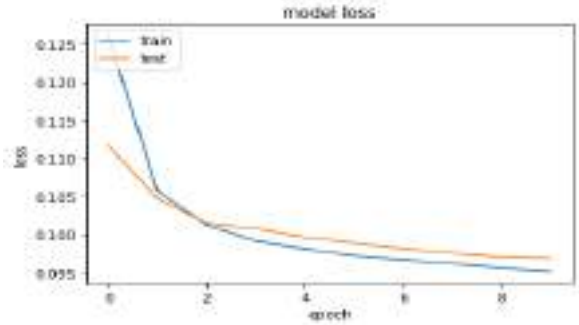

6.2 Results for Spiking Neural Network

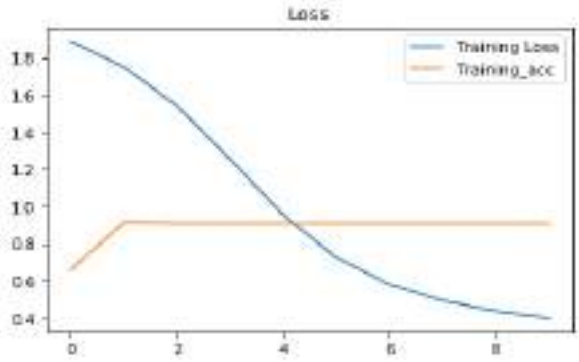

6.3 Results for Recurrent Neural Network

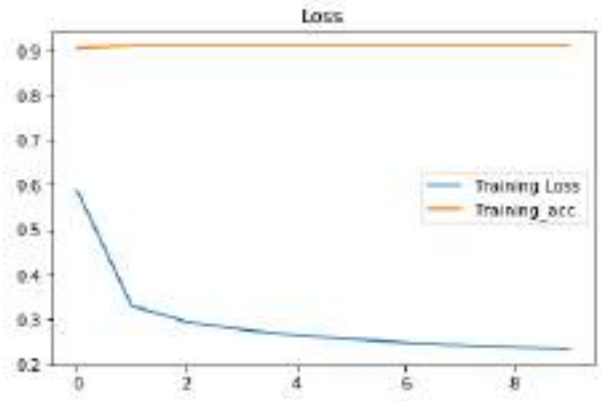

6.4 Result Analysis

The prediction accuracy of crop yield is compared with 3 models and the results are depicted in Table1.

Table 1: Comparing different measures for CNN, RNN, SNN

7. Conclusion

We described a deep learning-based framework for forecasting climate information and management in this study practices that successfully predicted corn yields across the entire Corn Belt in the United States. Most importantly, our approach went beyond estimation by providing major findings that aided in the explanation of yield estimation (variable importance by time period). The method developed are convolutional neural networks (CNN) and Spiking neural networks (SNN). The CNN component of the framework was designed to capture the intrinsic temporal relationship of weather data as well as the spatial interconnections of soil data measured at different depths underground. The model's RNN component was designed to capture the rising trend in crop yield over time as part of ongoing improvements in plant reproduction and management practises. SNNs work with spikes, which are discrete events that happen at specific points in time, instead of continuous values. The occurrence of a spike is determined by nonlinear equations that depict various biological processes, the most significant of which is the membrane potential of a neuron. When a neuron attains

a certain potential, it spikes, and the potential of the neuron is reset. Several variables, including climatic conditions, soil, and management, had a large impact on the model's effectiveness. In unknown environments, the suggested framework accurately predicted yields, and it could thus be used in tasks requiring long-term yield forecasting. One of the most difficult aspects of deep learning techniques is their black box nature. To make the current proposal less of a black box and more concise, feature selection was back propagation method that is used for trained CNN-RNN model. The feature selection model estimated the individual impact of weather components, soil type, and management variables, as well as the time span when these factors get to be significant, and that is a study development. This method could be used to solve other research issues. Similarly, a hybrid could be classified as low-yielding or high-yielding depends on the performance in comparison to other varieties in the same location.

8. References

1. Khaki, Saeed& Wang, Lizhi. (2019). Crop Yield Prediction Using Deep Neural Networks.Frontiers in Plant Science.10. 10.3389/fpls.2019.00621.
2. Syngenta (2021). *Syngenta Crop Challenge In Analytics*. Available online at: https://www.ideaconnection.com/syngenta-crop-challenge/challenge.php/
3. Elizondo, David & McClendon, R.W.. (1994). Neural Network Models for Predicting Flowering and Physiological Maturity of Soybean. Transactions of the American Society of Agricultural Engineers. 37. 981-988. 10.13031/2013.28168.
4. Matsumura, K. &Gaitan, Carlos & Sugimoto, K. & Cannon, Alex & Hsieh, William. (2015). Maize yield forecasting by linear regression and artificial neural networks in Jilin, China.1-12.
5.PayalGulati, Suman Kumar Jha, 2020, Efficient Crop Yield Prediction in India using Machine Learning Techniques, INTERNATIONAL JOURNAL OF ENGINEERING RESEARCH & TECHNOLOGY (IJERT) ENCADEMS – 2020 (Volume 8 – Issue 10),
6. Barbosa, Alexandre&Trevisan, Rodrigo &Hovakimyan, Naira & Martin, Nicolas. (2020). Modeling yield response to crop management using convolutional neural networks.Computers and Electronics in Agriculture. 170. 105197. 10.1016/j.compag.2019.105197.
7. Baum, Mitch &Archontoulis, S. &Licht, Mark. (2018). Planting Date, Hybrid Maturity, and Weather Effects on Maize Yield and Crop Stage.Agronomy Journal.111. 10.2134/agronj2018.04.0297.
8.AndreasKamilaris, Francesc X. Prenafeta-Boldú,Deep learning in agriculture: A survey,Computers and Electronics in Agriculture, https://doi.org/10.1016/j.compag.2018.02.016. (https://www.sciencedirect.com/science/article/pii/S0168169917308803)
9. Khaki, Saeed& Wang, Lizhi&Archontoulis, Sotirios. (2019). A CNN-RNN Framework for Crop Yield Prediction.
10. Shahhosseini, Mohsen & Hu, Guiping& Huber, Isaiah &Archontoulis, Sotirios. (2021). Coupling machine learning and crop modeling improves crop yield prediction in the US Corn Belt. Scientific Reports. 11. 10.1038/s41598-020-80820-1.
11. Mulla, Sadiq&Quadri, S..(2020). Crop-yield and Price Forecasting using Machine Learning.TheInternational journal of analytical and experimental modal analysis. XII. 1731-1737.
12. T. Siddique, D. Barua, Z. Ferdous and A. Chakrabarty, "Automated farming prediction," 2017 Intelligent Systems Conference (IntelliSys), 2017, pp. 757-763, doi: 10.1109/IntelliSys.2017.8324214.
13. Dharani, M &Thamilselvan, R &Natesan, P &Kalaivaani, PCD &Santhoshkumar, S. (2021). Review on Crop Prediction Using Deep Learning Techniques. Journal of Physics: Conference Series. 1767. 012026. 10.1088/1742-6596/1767/1/012026.

A Survey on Cardiovascular Prediction using Variant Machine learning

*L.*Chandrika[1,*], *Dr. K.*Madhavi[2], *B.*Sindhuja[3], *M.*Arshi[4]

[1]PG Student, Computer Science and Engineering, GRIET, Hyderabad, Telangana, India.
[2]Professor, Computer Science and Engineering, GRIET, Hyderabad, Telangana,India.
[3]Assistant Professor, Computer Science and Engineering, GRIET, Hyderabad, Telangana, India.
[4]Assistant Professor, Computer Science and Engineering, GRIET, Hyderabad, Telangana, India.

Abstract. Prediction of a cardiovascular diseases has always a tedious challenge for doctors and medical practitioners. Most of the practitioners and hospital staff offers expensive medication, care and surgeries to treat the cardiovascular patients. At early-stage of prediction of heart-oriented problems will be giving a chance of survival by taking necessary precautions. Over the years there are different types of methodologies were proposed to predict the cardiovascular diseases one of the best methodologies is a Machine learning approach. These years many scientific advancements take place in the Artificial Intelligence, Machine learning, and Deep learning which gives an extra push up to help and implement the path in the field of medical image processing and medical data analysis. By using the enormous dataset from various medical experts used to help the researchers to predict the coronary problems prior to happening. Many researchers have tried and implemented different machine learning algorithms to automate the prediction analysis using the enormous number of datasets. There are numerous algorithms and procedures to predict the cardiovascular diseases and accessible to be specific Classification methods including Artificial Neural Networks (AI), Decision tree (DT), Support vector machine (SVM), Genetic algorithm (GA), Neural network (NN), Naive Bayes (NB) and Clustering algorithms like K-NN. A few examinations have been done for creating expectation models utilizing singular procedures and additionally concatenating at least two strategies. This paper gives a speedy and simple survey and knowledge of approachable prediction models using different researchers work from 2004 to 2019. The examination indicates the precision of individual experiments done by various researchers.

1 Introduction

The heart is a significant organ which plays crucial part of every living being especially in humans. It pumps blood to all parts of our life systems. In case of failing to pumpor doesn't work accurately, the mind and different organs will quit working, and inside couple of moments, the individual will pass on. Changes in way of life, business related pressure, and terrible food propensities add to the expansion in the pace of a few heart-related sicknesses.

Heart sicknesses have arisen as perhaps the most unmistakable reasons for death all around the planet. The expanding populace in heftiness and smoking, the mortality from coronary sicknesses is slowly on the ascent, which has gotten the "best executioner" that compromises human wellbeing contrasted with malignant growth, Helps, and different illnesses, whatever age, character or area. As per WHO Coronary-related issues are responsible for the death of 17.7 million people every year, around 31% of worldwide death mortality.Especially in India, coronary illness became primary cause of mortality. Coronary problems causes the death of 1.7 million in 2016, In 2016 Global Burden of Disease Report, issued on 15th September 2017.

Coronary illness analytics states that the expenditure on hospitalization and treatment is gradually increased compared to the previous years and also diminishesthe survival rate of a person. Evaluations of WHO, explains that in India cardiac patients has spent around $237 billion, in the span of 10 years from 2005-2015. In this way, attainable and precise expectation of coronary related illness is vital.

The health care industry and health care research organisations collects the abundant data of patients,in which DM techniques are not used. The clinical data of the patients have covered up designs that are fundamental for data examination in the location of coronary illness. Coronary illness is a main source of death worldwide for as far back as 15 years. As the heart pumps the blood there is a possibility of on and off condition comes when the blood circulates inside the body which is inadequate, the rest of the organs inside the patient body especially brain and heart stops working, which causes the sudden death in few seconds. The importantelements are distinguished as age, hypertension, diabetes, family ancestry, tobacco, smoking, very high levels of cholesterol, daily routine of alcohol, actual dormancy, stoutness, chest torment, and eating junk food routine[1].

Data gathered by inspecting the verified records of the inpatient.it is feasible to separate the details and

* Corresponding author: lingalachandrika97@gmail.com

A Hybrid Framework for Heart Disease Prediction Using Machine Learning Algorithms

L.Chandrika[1,*] and K.Madhavi[2]

[1]PG Student, Computer Science and Engineering, GRIET, Hyderabad, Telangana, India.
[2]Professor, Computer Science and Engineering, GRIET, Hyderabad, Telangana,India.

Abstract. Cardiovascular Diseases (CVDs) are the primary cause for the sudden death in the world today from the past few years the disease has emerged greatly as a most unpredictable problem, not only in India the whole planet facing the criticality. So, there is a desperate need of valid, accurate and practical solution or application to diagnose the CVD problems in time for mandatory treatment. Predicting the CVD is a great challenge in the health care domain of clinical data analysis. Machine learning Algorithms (MLA) and Techniques has been vastly developed and proven to be effective and efficient in predicting the problems using the past data. Using these MLA techniques and taking the clinical dataset which provided by the healthcare industry. Different studies were takes place and tried only a small part into predicting CVD with ML Algorithms. In this thesis, we propose the different novel methodology which concentrates at finding appropriate features by using MLA techniques resulting at finding out the accurate model to predict CVD. In this prediction model we are trying to implement the models with different combinations of features and several known classification techniques such as Deep Learning, Random Forest, Generalised Linear Model, Naïve Bayes, Logistic Regression, Decision Tree, Gradient Boosted trees, Support Vector Machine, Vote and HRFLM and we have got an higher accuracy level and of 75.8%, 85.1%, 82.9%, 87.4%, 85%, 86.1%, 78.3%, 86.1%, 87.41%, and 88.4% through the prediction model for heart disease with the hybrid random forest with a linear model (HRFLM).

1 Introduction

It is hard to recognize Cardio vascular Diseases (CVD) because of a couple of contributory risk factors like raised cholesterol levels, diabetes, hypertension, dropping heart rate etc., like different problems. Various methods like Neural Networks(NN) and Data Mining(DM) techniques are used to get to know the intensity of CVD among different patients. The intensity of the problem is arranged depends on diverse strategies like Naive Bayes(NB), K-NN, Decision Tree(DT), and Genetic Algorithm(GA) [1]. The idea of CVD is unpredictable also, hence, the contamination ought to be dealt with circumspectly. Not doing as such may impact the heart or cause abrupt passing. The perspective of clinical science strategies and information digging are used for finding various types of metabolic issues. DM with arrangement has an immense impact in the conjecture of CVD and information assessment. We also observe DT be used to predict the accuracy of situations relevant to CVD [2].

Different strategies have been utilized for information deliberation by utilizing realized information digging techniques for anticipating CVD. In this work, various readings have been completed to create an expectation model utilizing particular procedures and relating at least two strategies. The combination of new procedures ordinarily known as half breed strategies [3]. We present neural networks utilizing pulse time arrangement. This strategy utilizes different clinical records for expectation, for example, Right pack branch block (RPBB), Left group branch block(LGBB), AFIB, NSR, SBR, AFL, PVC, and SDB to discover the specific state of the heart patient with CVD. The dataset with a spiral premise work organization RBFN is utilized for arrangement. The data further bifurcated into two parts as 70.0% of the data is considered for testing purpose and the rest of the 30% is considered for training purposes [4].

We additionally present a CADSS in the medication and examination field. In past work, the utilization of information mining strategies in the medical care departments has been appeared to set aside less effort for the forecast of illness with more precise outcomes [5]. We bring up the proposal which analyse the CVD utilizing the GA. This technique utilizes compelling affiliation rules deduced with the GA for competition choice, hybrid, and change which brings about the new proposed wellness work. For exploratory approval, we utilize the most popular dataset collected by UCI (Cleveland Dataset). We like to experiment and

*Corresponding author: lingalachandrika97@gmail.com

see how outcomes end up being unmistakable when contrasted with a portion of by using supervised learning procedures. The most remarkable transformative calculation PSO is presented and a few standards are produced for CVD. The standards have been applied haphazardly with encoding methods which bring about the progress of the exactness generally speaking [6]. CVD is anticipated dependent on indications to be specific like sex, rate of heart, age, and numerous features. The ML algorithms combination of NN is presented, whose outcomes are more exact and dependable.

NN are usually considered the best apparatus for the prediction like Cardiovascular and brain tumour diseases. The proposed technique we are taking 13 features of CVD forecast. The outcomes show an improved degree of execution contrasted with the current techniques. The CAS has likewise become a predominant therapy mode in clinical industry in this decade. The CAS remind the event of major antagonistic cardiovascular occasions (MACE) of CVD patients that are older. Their assessment turns out to be vital. We create results using an ANN algorithm, which delivers great execution in the forecast of CVD. Neural organization strategies are presented, which join back probabilities as well as anticipated qualities from different archetype procedures. This model accomplishes an exactness level of up to 89.01% which is a solid outcome contrasted with past research. For all trials, the UCI's Cleveland CVD dataset is utilized with NN algorithm to enhance the presentation of CVD in the papers [7] and [8].

We have additionally seen latest improvements in AI, ML strategies utilized for the IoT too [9]. Machine Learning strategies on online data appeared to provide a precise recognizable evidence of IoT devices which are related with a network. The researcher Meidan et al. took a data and marked as IoT online data from nine individual cell phones, Personal Computers, and IoT gadgets. Utilizing Supervised learning methods, to make a hybrid meta classifier [10]. In initial also crucial stage, the classifier can recognize traffic created by non-IoT and IoT gadgets. In the subsequent level, every IoT gadget is related to a particular IoT gadget class [10]. DL is a best strategy for getting précised data from all sensors of IoT gadgets conveyed in difficult conditions [11]. Based on its multi-layer-structure, DL is also a most suitable to the IoT edge computing [12].

In this research, we present a strategy which call's the main aspect of this experiment is to enhance the performance accuracy of CVD detection. Numerous examinations have been led that outcomes in limitations of highlight choice for algorithmic use. Interestingly, the HRFLM technique utilizes all highlights with no limitations of highlight determination. Here we direct analyses used to distinguish the highlights of an AI calculation with a crossover technique. The examination results indicates that our proposed method has more grounded capacity to anticipate CVD contrasted with existing strategies.

Further, the research of this paper is coordinated as follows: Segment II explains about past CVD detection experiments, existing strategies, and methods accessible. Section III, explains the overview of methodology. The process of -'HRFLM' classification modelling, pre-processing the data, performance measure and feature selection, classification and algorithms is discussed in segment -IV. In segment V discussed regarding the dataset and experiment interface and its evaluation. In segment-VI discussed the assessment of different modelling techniques and their results. Segment VII concludes the experimentation and a few details on a future research

2 Related Work

There are abundant previous researches in these fields mentioned in this research paper. ANN been acquainted to generate the great precision forecast in the healthcare research field [6]. The backpropagations of Multi-layer-Perceptron (MLP) and ANN is used for prediction of CVD. The achieved outcomes compared with the outcomes of already researched models on a same environment and inferred the model should be improved [13]. The CVD dataset of different cases collected by the UCI is used to find patterns using NN, SVM, DT, and NB. The experimental results are used to differentiate the overall performance of each model and accuracies of these algorithmic models. The proposed strategy(Hybrid model) returns outcome of 86.82% while working on the F-measure model, also tried competing with other proposed techniques [14]. The image classification without segmenting the images CNN model is used. In this strategy takes theheart cycles into consideration with various starting positions using the Electrocardiogram-signals at the beginning stage. Convolutional Neural Network can produce features with different angles in the stage of testing the data [15]. A lot of information has not been utilized properly which was produced by the clinical practitioners. The introduction of new approaches mitigates the cost also enhance the prediction of CVD in a simple and powerful manner. The different distinctive exploration techniques are taken into consideration in this research for classification and prediction of CVD utilizing Machine Learning and DL algorithms are exceptionally accurate in establishing the viability of these techniques [16].

3 Overview of Methodology and Results

Using HRFLM, we come up with a computational strategy with the 3 affiliation regulations of data mining in particular, Predictive, Apriori, and Tertius to discover the variables of CVD on the UCI dataset. The accessible data focuses to the allowance that females having a lesser degree of possibility for CVD contrasted with males. In CVD, exact analysis is essential. Be that as it may, the conventional methodologies are insufficient for precise prediction and analysis.

HRFLM utilizes Artificial Neural Networks with backpropagation alongside 13 medical features as input. The acquired outcomes are similarly breaking down against customary techniques [17]. The danger levels become high and various credits are utilized for exactness in the conclusion of the illness [18]. The complexity and nature of CVD require an effectual treatment plan. Information mining techniques help in therapeutic circumstances in the clinical field. The information mining strategies are additionally utilized thinking about NN, DT, KNN and SVM. Among a few utilized strategies, the outcomes from SVM end up being valuable in upgrading exactness in the expectation of infection. A module to check heart condition using a non linear methodology is acquainted which recognizes the arrhythmias which means tachycardia, bradycardia, atrial ventricular vacillates, atrial, and numerous others. The presentation viability of this strategy can be assessed from the exactness in the result results dependent on ECG information. ANN preparing is utilized for the exact finding of illness and the forecast of potential anomalies of the particular patient.

Various data mining techniques and prediction strategies, for example, Linear Relapse K-Nearest Neighbours, Neural Network, Support Vector Machines, and Vote have been somewhat mainstream recently to distinguish and anticipate CVD. The tale strategy Vote related to a mixture approach utilizing Naïve Bayes and Linear Regression are used in this research. The dataset gathered from UCI is utilized for directing the analyses the proposed strategy, which brought about 87.34% precision in the forecast of CVD. The PPCA strategy is bring forward for assessment, in view of three informational indexes of Switzerland, Hungarian, and Cleveland in UCI individually. The strategy extricates the vectors along with vector projection and high covariance is utilized for limiting the component measurement. The component determination with limiting measurement is given to an outspread premise work, which upholds SVM kernal. The aftereffects of the techniques are 85.820%, 91.310%, and 82.186% of UCI informational indexes of Hungarian, Switzerland, and Cleveland individually [19]. The half and half strategy joining MARS, LR, and ANN is presented with unpleasant set methods and the fundamental novel contribution in this research paper. The technique which brought forward is viably decreased the arrangement of basic credits. The leftover ascribes are contributions to ANN, therefore. The CVD datasets are utilized to show the viability of the improvement of the crossbreed approach. The CVD expectation with a multi-facet view proposing Neural Networks. This technique utilizes 13 clinical quality highlights as the info and prepared by backpropagation are extremely exact outcomes in recognizing if the patient has CVD.

We likewise present the Apriori calculation with Support Vector Machine and comparison with 9 different classification techniques to anticipate CVD with more precision. The aftereffects of the order strategy have demonstrated a more serious level of precision and execution in the forecast of CVD contrasted with the other existing strategies. The component choice assumes a conspicuous part in the expectation of CVD. ANN with backpropagation is for better forecast of the sickness. The outcomes acquired from the use of ANN are profoundly exact and exceptionally exact. The hereditary calculation with fuzzy Neural Networks also known as RFNN is presented for the finding of CVD.

From the UCI Dataset out of 297.00 record occurrence of patient data, altogether, are taken for experimentation out of which 250 records are separated for training purpose and the leftover for testing purposes considered. The outcomes have been situated to be fulfilling dependent on the appraisal. A CVD forecast with Support Vector Machines and ANN model is proposed in this research work. In this methodology, two techniques are utilized for the reason of the precision and testing time consumption. The proposed experimentation model organizes the clustered dataset into two separate classes in Support Vector Machine just as Artificial Neural Networks for additional investigation as demonstrated in [20]. The backpropagation of Neural Network with order technique is presented, where HGS is created and afterward, from there on the specific quality arrangement. The exhibition of the BPNN with the classification strategies has been estimated in the preparation stage just like testing stage with the different types of samples. The precision of this method has enhanced the uniformity of total number of available records.

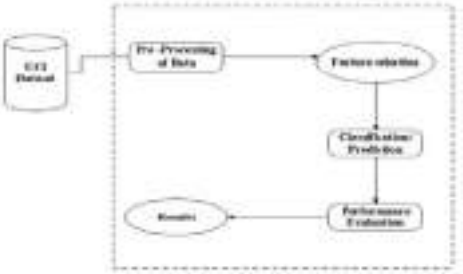

Figure 1. Work flow chart

Table 1: UCI Dataset range and type

AGE	Numeric [29 to 77;unique=41;mean=54.4;median=56]
SEX	Numeric [0 to 1;unique=2;mean=0.68;median=1]
CP	Numeric [1 to 4;unique=4;mean=3.16;median=3]
TESTBPS	Numeric [94 to 200;unique=50;mean=131.69;median=130]
CHOL	Numeric [126 to 564;unique=152;mean=246.69;median=241]
FBS	Numeric [0 to 1;unique=2;mean=0.15;median=0]
RESTECG	Numeric [0 to 2;unique=3;mean=0.99;median=1]
THALACH	Numeric [71 to 202;unique=91;mean=149.61;median=153]
EXANG	Numeric [0 to 1;unique=2;mean=0.33;median=0.00]
OLDPEAK	Numeric [0 to 6.20;unique=40;mean=1.04;median=0.80]
SLOPE	Numeric [1 to 3;unique=3;mean=1.60;median=2]
CA	Categorical [5 levels]
THAL	Categorical [4 levels]
TARGET	Numeric [0.00 to 4.00;unique=5;mean=0.94;median=0.00]

4 Methodology

In this investigation, we have utilized and Python Jupyter Notebook platform to perform the classification of CVD using the UCI(Cleveland) dataset. Using the visualization libraries whichprovidesa beter perspective and visualization of data, , building the prescient examination, and working climate. Machine Learning measure begins from the data pre-processing stage followed by determination of features based on Decision Tree entropy, modelling performance assessment using classification, and the outcomes with improved exactness. The element choice and demonstrating continue rehashing for different blends of qualities. Table 1 shows the information type and scope of qualities. The exhibition of each method produced dependent on 13 highlights and Machine Learning procedures utilized for every emphasis and execution are recorded. Section 4.1 sums up the information pre-preparing, Section 4.2 talks about the component choice utilizing entropy, in Section 4.3 clarifies the characterization with ML methods and Section 4.4 introduced the presentation of the outcomes.

4.1Pre-Processing

CVD information is pre-handled after the assortment of different record types. An aggregate of 303 patient's records contained in the dataset, out of those 6 records have few data values are missing. Those missing records in the data was deleted and the leftover patient's records(297) are utilized for pre-processing. The binary classification and multi-class variable are presented for attributes in the dataset. In order to find out the absence or presence of CVD multi-class variable is utilized. For instance, when the patient has CVD the binary classification value is changed from 0 to 1, if not the value remains 0 which demonstrates the absence of CVD in patient. The data pre-processing carries out conversion of over clinical values as diagnostic values. Out of 297 patient records demonstrates that 137 records are classified as 1 which resulted in data pre-processing setting up the presence of CVD while the rest of the 160 as 0 which indicates an absence of CVD.

4.2Feature Selection

From the dataset out of 13, only two clinical attributes concerned to sex and age are used to find out the patient's personal information. The rest of the 11 attributes are examined as crucial clinical information. All these clinical records are very important for learning and diagnosis of the CVD. As explained earlier a lot of machine learning techniques are utilized to find out the CVD namely GLM, NB, DL, LR, RF, DT, SVM, and GBT. The research work was done repeatedly with all machine learning algorithms considering the 13 attributes. In the below figure-2 flowchart shows the HRFLM prediction method.

4.3Classification

The dataset clustering is completed by taking the criteria and variables of Decision Tree features as basis. Later each clustered dataset is fed to the classifiers to measure the performance and the best algorithms are selected using the above outcomes based on very low error rate. Further optimization of performance using the decision tree cluster in which the error rate is high and respected feature extraction using classifiers. The classifier performance is furtherly examined for error mitigation on the opted dataset.

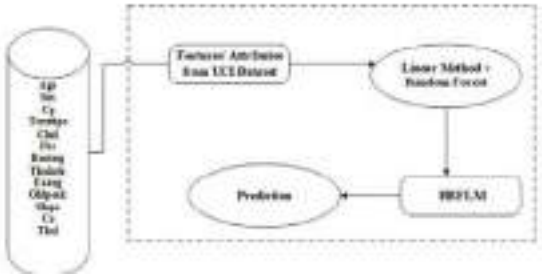

Figure 2. CVD Predictionusing HRFLM

4.4Performance Evaluation

A several basic evaluations of performance metrics like precision, classification error and accuracy was taken into consideration for the performance computation efficiency of this research model. In this current scenario accuracy means the examples at what percentage rate accurately predicting out of all the instances available. The percentage of exact prediction is defined as precision in the true class of examples. The percentage of available errors or accuracy lacking are defined using the error. To distinguish the features of CVD, three performance variables are utilized which helps to understand better about the behaviour of the different blends of selecting the features. Machine Learning algorithms focuses on the model which performs the best contrasted with existing strategies. We are coming up to use HRFLM, which creates highly précised and less error rate classification to predict the CVD. The exhibition of all the classifiersisevaluated separately and outputs aresaved for future assessments.

4.5 Algorithms

Algorithm 1 Decision Tree-Based Partition

Require: Input: D dataset – features with a target class
  for ∀features **do**
    for Each sample **do**
      Execute the Decision Tree algorithm
    end for
    Identify the feature space $f_1, f_2, \ldots, f_z$ of dataset UCI (9)
  end for
  Obtain the total number of leaf nodes $l_1, l_2, l_3, \ldots, l_e$ with its constraints (10)
  Split the dataset D into $d_1, d_2, d_3, \ldots, d_e$ based on the leaf nodes constraints. (11)
  Output: Partition datasets $d_1, d_2, d_3, \ldots, d_n$

Algorithm 2 Apply ML to Find Less Error Rate

Require: Input: Datasets with partition – $d_1, d_2, d_3, \ldots, d_n$
  for ∀apply the rules **do**
    On the dataset R(d1,d2,d3,..... dn)
  end for
  Classify the dataset based on the rules $C(R(d_1),R(d_2)$ $\ldots\ldots R(d_n))$ (12)
  Output: Classified datasets with rules $C(R(d_1),R(d_2)$ $\ldots\ldots R(d_n))$

Algorithm 3 Feature Extraction Using Less Error Classifier

Require: Input: Classified datasets $C(R(d_1),R(d_2)\ldots\ldots R(d_n))$
  for ∀Find out min error rate from the input **do**
    $\text{Min}(C(R(d_1),R(d_2)\ldots\ldots R(d_n)))$ (13)
  end for
  Find out max(min) error rate from the classifier.
  Output: Features with classified attributes $F(d_1, d_2, d_3, \ldots, d_n)$

Algorithm 4 Apply Classifier on Extracted Features

Apply the hybrid method based on the error rate

$$\sum_0^n F(n) = d + m_1x_1 + m_2x_2 + \ldots + m_nx_n \quad (14)$$

$$\sum_0^n F(0) = Gain + \sum_0^n w_ix_i \quad (15)$$

5. Experimentational Environment

5.1Datasets

CVD datasets were gathered from UCI AI repository. Further UCI have four different datasets available in their repository namely: Cleveland, the VA Long Beach, Switzerland, and Hungary. The Cleveland data set was chosen for this examination since it is a normally utilized information base for Machine Learning specialists with thorough and full-fledged records. In the repository dataset holds 303.00 patient records. The Cleveland dataset which is holding 76.00 variables, the informational index gave in the archive outfits data subset of just 14 variables. The below Table 1 portrays the depiction and kind of qualities. Total 13 attributes that include in the forecast of CVD, where just one quality fills in as the yield or the anticipated characteristic to find out the CVD in patient.

The dataset consists various attributes to display the finding of CVD in patients on various measures, which starts 0 and ends at 4. In this kind of scenario, 0 addresses the shortfall of CVD and every one of the qualities from 1 and ends at 4 addresses patients with CVD, where the measurements alludes to the seriousness of the infection 4 indicates most elevated. In Figure 1 indicates the circulation of the attributes out of the recognized 303 records.

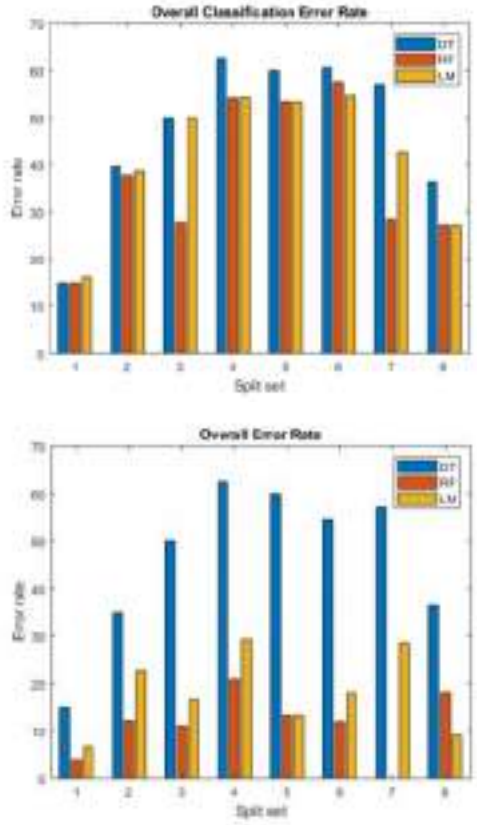

Figure 3. Dataset Over all Error rate classification error rate

5.2Experiment interface and Evaluation

We have utilized anPython Jupyter Notebook to execute the CVD classification using the UCI dataset. Figure-1 portrays the assessment of the investigation step-by-step organizes. In the initial stage, the data is stacked and arranged for pre-processing. There are 13 different attributes (AGE, EXANG, CP, SEX, CHOL, TREEBPS, RESTECG, FBS, OLDPEAK, THALACH, CA, SLOPE, TARGET, and THAL) is chosen among

the pre-processed dataset of CVD. The 3 different detection models to find CVD are Decision Tree, Random Forest, and are utilized to build up the classification model. The assessment of the classification is done using confusion matrix. Absolutely, four results are created by the disarray framework, in particular FN (False Negative) TN (True Negative), FP (False Positive), and TP (True Positive).

$$\text{Accuracy} = (TN+TP) / (TN+TP+FN+FP)$$
$$= 105+155/295 = 0.8847$$
$$\text{Sensitivity} = (TP/TP+FN) = 155/155+12 = 92.8$$
$$\text{Specificity} = (TN/TN+FP) = 105/105+22 = 82.6$$

The accompanying measures are utilized for the estimation of the specificity, accuracy, and sensitivity.

6 Evaluation Results

The present CVD prediction system is structured using 13 aspects and calculated the modelling techniques accuracy. The various classification model results are mentioned in Table 2, which portrays and differentiates the accuracy with other classification models along with the comparison of, classification error, Accuracy, F-measure, Precision, specificity, and sensitivity. The most elevated accuracy is accomplished by the proposed classification method (HRFLM) algorithmic model is compared with other algorithms.

Table 2: Results of differentalgorithmsalongwithproposed model

Module	Accuracy	Classification error	Precision	F-measure	Sensitivity	Specificity
Naive Bayes	75.8	24.2	90.5	84.5	79.1	60.0
Generalized Linear Model	85.1	14.9	88.8	91.6	94.9	70.0
Logistic Regression	82.9	17.1	86.6	90.2	93.1	25.0
Deep Learning	87.4	12.6	90.7	92.6	95	35.3
Decision Tree	85	15.0	88	91.8	96.8	0.0
Random Forest	88.1	11.9	87.1	92.4	98.3	70.0
Gradient Boosted Trees	78.5	21.7	94.1	86.8	80.7	60.0
Support Vector Machine	88.1	11.9	84.1	92.5	100	0.0
VOTE	87.41	12.59	90.2	84.4	-	-
HRFLM	88.4	11.6	90.1	91	92.8	82.5

Table 3: Results of different classification models and proposed model.

	Overall error rate			Best Model	Overall classification error rate			Best Model
Data Split	DT	RF	LM		DT	RF	LM	
1	14.9	4	6.7	RF	14.9	14.9	16.2	DT /RF
2	34.9	12.2	22.6	RF	39.6	37.7	38.7	RF
3	50	11.1	16.6	RF	50	27.8	50	RF
4	62.5	20.9	29.2	RF	62.5	54.1	54.2	RF
5	60	13.3	13.3	RF/ LM	60	53.4	53.3	LM
6	54.6	12	18.1	RF	60.6	57.6	54.6	LM
7	57.1	0	28.5	RF	57.1	28.5	42.8	RF
8	90.4	18.2	9.1	LM	90.4	27.3	27.3	RF/ LM

Table 4: HRFLM Results

	Overall error rate		Best Model	Overall classification error rate		Best Model
Data Split	RF	LM		RF	LM	
1	4	6.7	RF	14.9	16.2	DT /RF
2	12.2	22.6	RF	37.7	38.7	RF
3	11.1	16.6	RF	27.8	50	RF
4	20.9	29.2	RF	54.1	54.2	RF
5	13.3	13.3	RF/ LM	53.4	53.3	LM
6	12	18.1	RF	57.6	54.6	LM
7	0	28.5	RF	28.5	42.8	RF
8	18.2	9.1	LM	27.3	27.3	RF/ LM

7 Conclusion

Recognizing the preparation of raw medical datasets of CVD will be useful in the future to save the life of human and also early detection of cardio vascular problems. Artificial Intelligence methods used in this research to so process the raw data to make sense and train the system to get to know the attributes of CVD. The CVD prediction is difficult also plays a crucial part in the medical science industries. Nonetheless, the death rate could be definitely controlled in case of the effect of sickness is identified at the starting stages and deterrent measures are received as quickly as time permits. Further augmentation of this experiment is profoundly attractive to take care of the assessments to real time datasets instead of basically speculative techniques and recreations. The proposed methodology called HRFLM approach is experimented to consolidate the variables of Linear Method (LM) and Random Forest (RF). HRFLM is proved up that the model is very accurate in the forecasting of CVD. The future enhancements of this model will be experimented using various other combinations of AI/ML/DL algorithms. Moreover, new element determination approaches would be created in order to get highly accurate perception of the crucial data to enhance the performance of CVD prediction.

References

[1] M. Durairaj and V. Revathi, International Journal of Scientific & Technology (2015)

[2] V. Gadepally, T. Mattson, M. Stonebraker, F. Wang, G. Luo, Y. Laing, and A. Dubovitskaya, *Heterogeneous Data Management, Polystores, and Analytics for Healthcare: VLDB 2019 Workshops, Poly and DMAH, Los Angeles, CA, USA, August 30, 2019, Revised Selected Papers* (Springer Nature, 2019)

[3] B. S. S. Rathnayakc and G. U. Ganegoda, in *2018 3rd International Conference for Convergence in Technology (I2CT)*, pp. 1–6(2018)

[4] M. Aslam and J. K, in *2021 International Conference on Computer Communication and Informatics (ICCCI)* (2021)

[5] J. P. Kelwade and S. S. Salankar, in *2016 IEEE First International Conference on Control,*

Measurement and Instrumentation (CMI) (2016)

[6] A. H. Alkeshuosh, M. Z. Moghadam, I. A. Mansoori, and M. Abdar, in *2017 International Conference on Computer and Applications (ICCA)* (2017)

[7] F. Dammak, L. Baccour, and A. M. Alimi, in *2015 IEEE International Conference on Fuzzy Systems (FUZZ-IEEE)* (2015)

[8] M. J. Liberatore and R. L. Nydick, Eur. J. Oper. Res. **189**, 194 (2008)

[9] Annual IEEE/IFIP International Conference on Dependable Systems and Networks, *48th Annual IEEE/IFIP International Conference on Dependable Systems and Networks: DSN 2018 : Proceedings : 25-28 June 2018, Luxembourg City, Luxembourg* (IEEE, 2018)

[10] J. Jose, J. S. Vimali, P. Ajitha, S. Gowri, A. Sivasangari, and B. Jinila, in *2021 5th International Conference on Trends in Electronics and Informatics (ICOEI)* (2021)

[11] K. Prasanna Lakshmi and C. R. K. Reddy, in *2010 International Conference on Networking and Information Technology* (2010)

[12] J. Wu, S. Luo, S. Wang, and H. Wang, IEEE Internet of Things Journal **6**, 2463 (2019)

[13] J. Wu, K. Ota, M. Dong, and C. Li, IEEE Access **4**, 416 (2016)

[14] "R. Das, I. Turkoglu, and A. Sengur, Expert Syst. Appl. **36**, 7675 (2009)

[15] IEEE Staff, *2019 41st Annual International Conference of the IEEE Engineering in Medicine and Biology Society (EMBC)* (IEEE, 2019)

[16] J. Nahar, T. Imam, K. S. Tickle, and Y.-P. P. Chen, Expert Syst. Appl. **40**, 1086 (2013)

[17] D. K. Ravish, K. J. Shanthi, N. R. Shenoy, and S. Nisargh, in *2014 International Conference on Contemporary Computing and Informatics (IC3I)* (2014)

[18] C. U. Kumari, S. J. Prasad, and G. Mounika, (2019)

[19] T. Mahboob, R. Irfan, and B. Ghaffar, in *2017 Internet Technologies and Applications (ITA)* (2017)

[20] O. Goldman, O. Raphaeli, E. Goldman, and M. Leshno, Qual. Manag. Health Care (2021)

[21] M. S. Amin, Y. K. Chiam, and K. D. Varathan, Telematics and Informatics **36**, 82 (2019)

[22] S. C. Satapathy, K. Srujan Raju, J. K. Mandal, and V. Bhateja, *Proceedings of the Second International Conference on Computer and Communication Technologies: IC3T 2015, Volume 1* (Springer, 2015)

[23] B. Dhanalaxmi, G. A. Naidu, and K. Anuradha, Procedia Comput. Sci. **46**, 432 (2015)

Detecting anomalous road traffic conditions using VGG19 CNN Model

M. Rajeshwari, and *CH.* MallikarjunaRao

[1]MTech Student, Computer Science and Engineering, GRIET, Hyderabad, Telangana, India.
[2]Professor, Computer Science and Engineering, GRIET, Hyderabad, Telangana, India.

Abstract. Anomaly Detection on the real time road traffic has tremendous application possibilities in metropolitan road safety and traffic management. Due to the effect of numerous factors, for example: climate, viewpoints and road conditions in real-time traffic scene, Anomaly detection actually faces many difficulties. There are many reasons for vehicle accidents, for example: crashes, vehicle on flames and vehicle breakdowns, which exhibits distinctive and obscure behaviours. In this paper, we approached with a model to identify oddity in street traffic by monitoring the vehicle movement designs in two unmistakable yet associated modes which is 1. The vehicle's dynamic mode and 2. The vehicle's Static mode. The vehicle's static mode investigation is gained using the background modelling after the detection of a vehicle, this strategy is useful to locate the unusual vehicle movement which keep still out and about. The dynamic mode vehicle examination is gained from identified and followed vehicle directions to locate the strange direction which is distorted from the predominant movement designs. The outcomes from the double mode investigations are at long last fused together by driven a distinguishing proof model to get the last peculiarity. For this research we are using traffic-net Dataset, VGG19 CNN model along with ImageNet weights and OpenCV.

1 Introduction

An ever-increasing number of families presently have their own vehicles and going via vehicle has gotten an exceptionally normal and advantageous path in day-by-day metropolitan life. The street condition consequently gets extraordinary consideration from the general population. Terrible street conditions can make monstrous misfortune to the social economy, and compromise the individual wellbeing of drivers out and about. With generally record the road situations by using traffic cameras, it is achievable. what's more, critical to build up a strategy to naturally discover the oddities on the streets utilizing PC vision procedures. A traffic checking framework furnished with these calculations will achieve numerous advantages and comforts. On one hand, when the inconsistencies occur, a programmed framework can advise the traffic police promptly, to tackle the oddities on streets at the earliest opportunity. Then again, when arranging an outing, data about street conditions can give accommodation to the two drivers and travellers. Notwithstanding, it is an exceptionally moving assignment to plan a PC vision calculation to recognize abnormalities in street traffic. One principal reason is that the development examples of vehicles on streets are generally exceptionally muddled, and distinctive irregular occasions may show complex practices. Simultaneously, the irregular occasion happens once in a while when contrasted with typical occasions. Accordingly, building up a productive and compelling clever calculation for programmed video abnormality location is a squeezing need. Numerous works of irregularity discovery in observation recordings must be applied to distinguish explicit strange occasions. For example, Mohammedi et al. build up a technique to distinguish human viciousness in recordings [4]. Additionally, the traffic finders just work in exceptionally restricted conditions [3]. With the improvement of traffic and video reconnaissance advancements, traffic the board frameworks dependent on video observation have gotten broadly utilized in rush hour gridlock the executives. In the canny preparing of traffic data, the discovery and acknowledgment of traffic inconsistencies, for example, securing, gridlock, car crashes, and unlawful driving have pulled in the consideration of numerous analysts because of its significance in rush hour gridlock the board. In any case, due to the intricacy of traffic camera feed, traffic reconnaissance video is helpless against outer factors, for example, light, climate, and checks. The constraints of existing picture preparing and investigation innovations

make the traffic boundaries (flow of the traffic, density of traffic, vehicle direction, speed, and so forth) in light of traffic video extremely dubious.

Looking the problem, we noticed it a bit difficult for manual surveillance. So, we came up with a proposal which is a CNN based surveillance system designed to learn for detecting the anomalies in dense traffic conditions, which handles of both the dynamic and static vehicles. Typically, the vehicles should continue to proceed onward the streets aside from certain ordinary conditions (e.g., hanging tight for traffic signals). Thusly, the static vehicles have higher likelihood for being anomalous occasions. By and large, the majority of the anomalous occasions in street deals will cause vehicle halting. For instance, vehicle slowing down, car crash or vehicle sticking. In the interim, the static vehicles can give us the exact area of the atypical occasions. To recognize the static vehicles from the moving traffic, we acquaint a static mode technique with get the running normal of the edge succession. Additionally, roused by the incredible accomplishment of deep learning in PC vision field, we send the deep learning-based strategy for the static vehicle identification. Additionally, we designed to further recognize the vehicle pictures of accidental pictures

2 Related Work

Vehicle monitoring, identification and tracking is the essential part in the street traffic scenario examination and assumes a significant part in many related applications, for example, driver help frameworks. Because of the extraordinary achievement of DL innovation, we have acquired a gigantic enhancement in image detection fields [2] [3] [4]. In this paper, we additionally experimenting the DL algorithms for detecting the vehicles and following. The detection of anomalies in both dynamic videos of the moving vehicles and static images of the traffic dataset have been concentrated in the previous years because of the expanding revenue in open security [3]. The customary techniques typically gain proficiency with the hand-created highlights to demonstrate the ordinary/anomalous occasion designs. As of late, deep learning innovation has been created for peculiarity detection as its accomplishment in the PC vision field [5].

In [6], the researchers present a generative adversarial network (GAN) based technique to identify the inconsistencies in pictures, utilizing just typical information to prepare the models. For observation recordings, there are a few endeavours to identify human savagery or strange occasions in group scenes. a deep peculiarity positioning system is used to foresee anomalies while testing on the recorded datasets. Since street condition assumes a significant part in our day-by-day life, recognizing peculiarities on streets has stood out from numerous researchers. For this undertaking, the main objective is to discover where and when the inconsistencies happen.

M. Schubert et al. [7] propose a mix of methods to foresee the event of street mishaps. The researchers present a visual examination structure for the investigation of ordinary social models and the detection of peculiar occasions. Be that as it may, the new works are intended to distinguish a particular strange occasion, and this present reality irregularities on streets are convoluted and assorted. Subsequently, we plan a novel double model strategy to distinguish different street traffic odd occasions in genuine scenes, which can have wide use practically speaking. Few more pulled in numerous specialists to direct top to bottom examination on traffic irregularity detection.

In, [8] the authors proposed a vehicle vision monitoring calculation dependent on PC vision, which had high tallying exactness and improved the precision of traffic surveillance. Frejlichowski et al. [9] proposed another vehicle direction design acknowledgment calculation dependent on the Cam shift calculation, which can precisely dissect and recognize the illicit leaving or unlawful turning of vehicles. Yang [11] successfully distinguish traffic occurrences of turnpike scenes by utilizing fuzzy logic (FL) by consolidating FL and improved steady examination calculations in their proposed system. The system breaks down occasions by extricating traffic flow data and vehicle speed, yet the system detection has few restrictions because of the intricacy of conditions of a traffic. In [10] the researchers utilized the GPS information of a hire taxi, which also including direction and velocity, to recognize gridlock on metropolitan streets. Albeit the precision of GPS strategy is high, also it has the limitations of significant expense, which compelled its application. In-order to identify these problems, another calculation that incorporates more traffic boundaries is proposed in this paper. The proposed calculation cannot just recognize traffic anomalies all the more precisely and carefully yet additionally be viable in various circumstances.

3 System Model

3.1 VGG19 Architecture

VGGNet is a CNN(Convolutional Neural Network) architecture proposed by Karen Simonyan and Andrew Zisserman from Oxford university in 2014. This paper principally centers around the impact of the CNN profundity on its precision. The contribution to VGG based convNet is a 224*224 RGB picture. Pre-processing layer takes the RGB picture with pixel esteems in the scope of 0–255 and deducts the mean picture esteems which are determined over the whole ImageNet training set. The input pictures subsequent to pre-processing are gone through these weight layers. The training pictures are gone through a stack of convolution layers. There is an aggregate of 13 convolutional layers and 3 fully connected layers in VGG16 engineering. VGG has more modest channels (3*3) with more profundity as opposed to having enormous channels. It has wound up having a similar powerful open field as though you just have one 7 x 7 convolutional layers. Another model of VGGNet has

19 weight layers comprising of 16 convolutional layers with 3 fully connected layers and a similar 5 pooling layers. In the two varieties of VGGNet, there comprises of two Fully Connected layers with 4096 channels every which are trailed by another fully connected layer with 1000 channels to foresee 1000 marks. The last fullyconnected layer utilizes a softmax layer for order purposes.

The walk through of 19 layers as follows: The initial two layers are convolutional layers with 3*3 channels, and initial two layers utilize 64 channels that outcomes in 224*224*64 volume as same convolutions are utilized. The channels are consistently 3*3 with step of 1.
After this, pooling layer was utilized with max-pool of 2*2 size and step 2 which lessens tallness and width of a volume from 224*224*64 to 112*112*64.
This is trailed by 2 more convolution layers with 128 channels. This outcomes in the new component of 112*112*128.
Subsequent to pooling layer is utilized, volume is decreased to 56*56*128.
Two more convolution layers are added with 256 channels each followed by down inspecting layer that diminishes the size to 28*28*256.
Two more stack each with 3 convolution layer is isolated by a maximum pool layer.

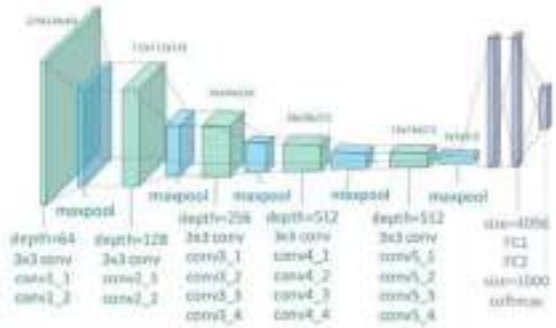

Fig. 1. VGG19 Architecture

After the last pooling layer, 7*7*512 volume is straightened into Fully Connected (FC) layer with 4096 channels and softmax yield of 1000 classes.

3.2 ImageNet

ImageNet is a project which aims to provide a large image database for research purposes. It contains more than 14 million images which belong to more than 20,000 classes (or synsets). They also provide bounding box annotations for around 1 million images, which can be used in Object Localization tasks. It should be noted that they only provide urls of images and you need to download those images.

3.3 Traffic Net Dataset

The Traffic-Net dataset is a collection of traffic images that provide real-time monitoring, analytics, and alerts that will be used to provide a machine learning system with the data it needs to detect traffic conditions [12].

Using machine learning systems to accustom themselves to perception, understanding, and action in any environment is one of Deep Quest AI's goals [12].

4400 images are contained in the Traffic-Net dataset. The recent release includes the following classes:

- Accident
- Dense Traffic
- Fire
- Sparse Traffic

The images are divided into different categories with 900 images for training and 200 for testing. A new set of categories will be added in the future and the dataset will be improved [12].

Fig. 2. Sparse Traffic

Sparse Traffic: Sparse traffic dataset means less traffic or no traffic regions

Fig. 3. Fire Accident

Fire Accident: Fire accident dataset is the pictures of accidentally burned vehicles.

Fig. 4. Dense Traffic

Dense Traffic: Dense traffic dataset is a heavy traffic regions dataset.

Fig. 5. Accident dataset

Accident Dataset: Accident vehicles dataset in different regions.

3.4 Optimizer:

Adam is a deep learning algorithm that replaces stochastic gradient descent for the purpose of training models. The Adam algorithm combines the qualities of the AdaGrad and RMSProp algorithms to produce an optimization algorithm capable of handling sparse gradients on noisy problems. Adam can be configured quite simply, with default parameters that work out most of the time.

4. Proposed Method:

In this section, we are explaining the methodology followed to detect and classify the anomalies happened in various roads in various countries out of the varied traffic data-set. We are proposing an end-to-end deep learning architecture for traffic flow and anomalies detection and classification. We are experimenting using a VGG19 Convolutional Neural Network and ImageNet pretrained weights to discover the static vehicles on streets, as the abnormalities normally lead to vehicle halting. Typically, the majority of the inconsistencies on streets are unusual vehicle slowing down or vehicle crashes, which both make the vehicles stop in/alongside the street. In light of this perception, we acquaint a movement investigation strategy with discover the static vehicles which are met with accidents sometimes which get caught on fire on streets and further perceive the anomalous occasions dependent on that. The pipeline of peculiarity detection dependent on the static vehicle is introduced in Figure 2, 3, 4 5. The dataset which is properly bifurcated the data into two separate folders i.e., one is test dataset and another one is train data set. In each of those training and test dataset is categorised the four different scenarios labelled namely “Accident, Sparse traffic, fire, and dense traffic”. Initially, we took the training dataset to train the model to classify its type of class. In order to train the model, we read all the images in each category mentioned above in the training directory using the OpenCV library. After reading the whole dataset, the images are resized to same height and width in pixels. Here in this experiment, we are considering it as 300 x 300(height, width). To ease the process the whole dataset of images which has 3 channels of every image is converted into a binary scale image which means converting the image channel from RBG to binary image which is giving the range from Zero to One. In same way the test directory images also read and resized all the data into same shape and converted the images into binary images for validation purpose. After aligning the image data the pretrained VGG19 model and ImageNet weights are taken to create a model which is shown below in Fig.6.

Instead of building the whole convolutional network from scratch and initializing weights to create a model we have chosen the pretrained model which is VGG19. Any model or classifier would at the initial stage be able to detect the slant lines whatever the class we expect to classify as the first step, according to the intuition of choosing the pre-trained model. The training of those in every possible opportunity to create a Neural network makes no sense. The project details that need to be trained will determine the abilities of the final layer of the network to identify classes. And also, there is one more advantage for using pretrained models which is pretrained models are always trained on big datasets or data which are not usually available to everyone. An example is ImageNet, which contains approximately 14 million images, 1.2 million of which are assigned to one of 1,000 categories. Thus, we would benefit tremendously from making use of these models” [2]. As with our previous experiment, instead of repeating the procedure for the first network and starting from scratch with random weight values, we can now use the saved weight values from the previous experiment as the initial weights for our new experiment. In this case, weights are initialized using pre-trained networks.

So, here we are taking the pretrained model and on top of it we are adding Flatten layer and dense layer. Using flatten layer function we flattened all the convoluted layers into a 1dimensional linear vector. Later drop out technique is used to dropout the nodes of the dense layer which is in our case having 1024 neurons in a dense layer out of it 30% of the neurons are dropped out at fully connected layer-1 and again out of 512 neurons of dense layer at fully connected layer 30% of them is dropped out.

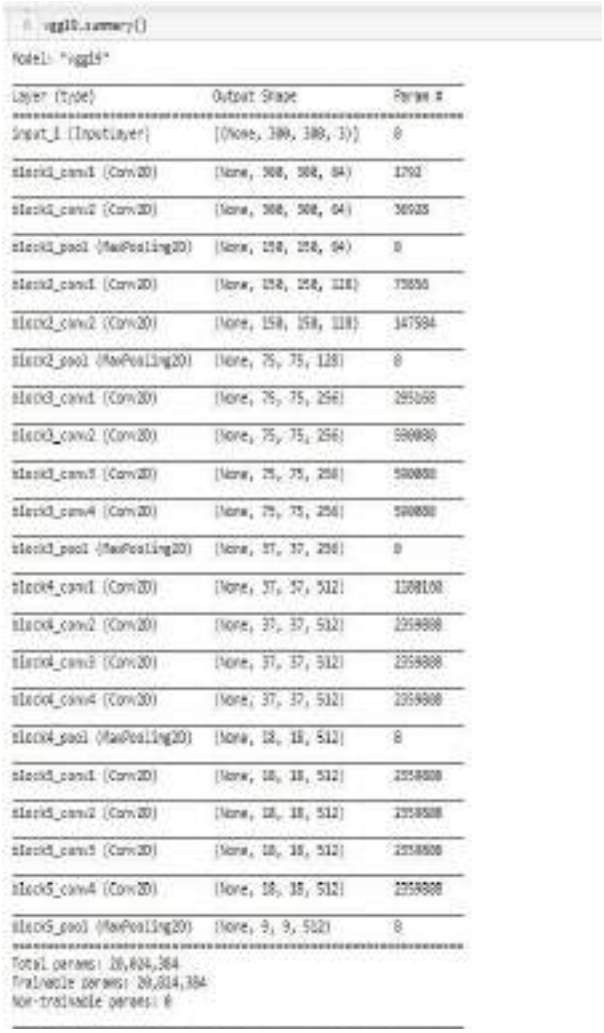

```
vgg19.summary()
Model: "vgg19"
_________________________________________________________________
Layer (type)                 Output Shape              Param #
=================================================================
input_1 (InputLayer)         [(None, 300, 300, 3)]     0
_________________________________________________________________
block1_conv1 (Conv2D)        (None, 300, 300, 64)      1792
_________________________________________________________________
block1_conv2 (Conv2D)        (None, 300, 300, 64)      36928
_________________________________________________________________
block1_pool (MaxPooling2D)   (None, 150, 150, 64)      0
_________________________________________________________________
block2_conv1 (Conv2D)        (None, 150, 150, 128)     73856
_________________________________________________________________
block2_conv2 (Conv2D)        (None, 150, 150, 128)     147584
_________________________________________________________________
block2_pool (MaxPooling2D)   (None, 75, 75, 128)       0
_________________________________________________________________
block3_conv1 (Conv2D)        (None, 75, 75, 256)       295168
_________________________________________________________________
block3_conv2 (Conv2D)        (None, 75, 75, 256)       590080
_________________________________________________________________
block3_conv3 (Conv2D)        (None, 75, 75, 256)       590080
_________________________________________________________________
block3_conv4 (Conv2D)        (None, 75, 75, 256)       590080
_________________________________________________________________
block3_pool (MaxPooling2D)   (None, 37, 37, 256)       0
_________________________________________________________________
block4_conv1 (Conv2D)        (None, 37, 37, 512)       1180160
_________________________________________________________________
block4_conv2 (Conv2D)        (None, 37, 37, 512)       2359808
_________________________________________________________________
block4_conv3 (Conv2D)        (None, 37, 37, 512)       2359808
_________________________________________________________________
block4_conv4 (Conv2D)        (None, 37, 37, 512)       2359808
_________________________________________________________________
block4_pool (MaxPooling2D)   (None, 18, 18, 512)       0
_________________________________________________________________
block5_conv1 (Conv2D)        (None, 18, 18, 512)       2359808
_________________________________________________________________
block5_conv2 (Conv2D)        (None, 18, 18, 512)       2359808
_________________________________________________________________
block5_conv3 (Conv2D)        (None, 18, 18, 512)       2359808
_________________________________________________________________
block5_conv4 (Conv2D)        (None, 18, 18, 512)       2359808
_________________________________________________________________
block5_pool (MaxPooling2D)   (None, 9, 9, 512)         0
=================================================================
Total params: 20,024,384
Trainable params: 20,024,384
Non-trainable params: 0
_________________________________________________________________
```

Fig. 6. VGG19 Pretrained Model

As the data we have chosen is having 4 different classes, so that the model has to classify the image of which class it belongs to. In order to do that the final layer has chosen a dense layer again and used SoftMax activation function which is used in the output layer of convolutional neural network for multi class classification problems. The model summary is shown in above figure-7.

To compile the model, we have chosen the Adam optimization algorithm for stochastic gradient decent the AdaGrad and RMSProp algorithms to provide an optimization algorithm which adjusts the weights and bias of the network to help learning and reduces the loss. We have then selected a loss function for our optimization function, which is categorical cross entropy, which is typically used in multi-class classification problems. The purpose of this measure is to compare the probability distributions of two events. After the loss function the whole agenda is to find out the accuracy and loss mitigation of the model we have chosen. To do that we have used model.fit() function for fitting the model in which we are separating the whole training dataset into 64 batches and 10 epochs, which means the whole dataset into 64 parts and passed through the network for 10 iterations.

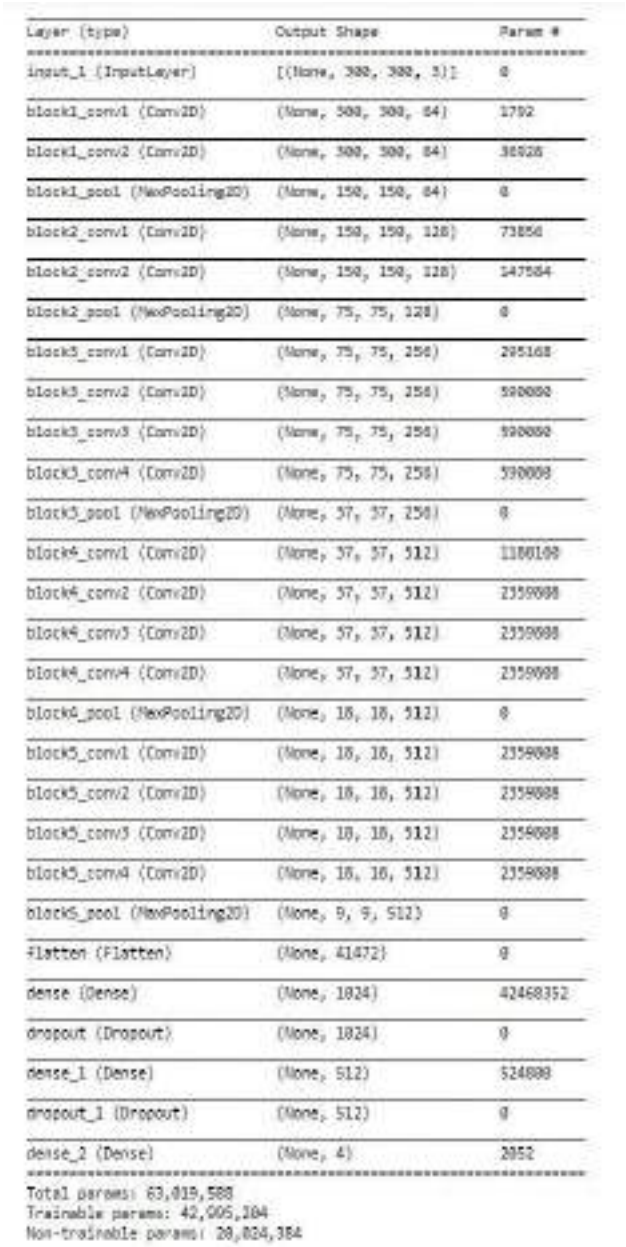

```
_________________________________________________________________
Layer (type)                 Output Shape              Param #
=================================================================
input_1 (InputLayer)         [(None, 300, 300, 3)]     0
_________________________________________________________________
block1_conv1 (Conv2D)        (None, 300, 300, 64)      1792
_________________________________________________________________
block1_conv2 (Conv2D)        (None, 300, 300, 64)      36928
_________________________________________________________________
block1_pool (MaxPooling2D)   (None, 150, 150, 64)      0
_________________________________________________________________
block2_conv1 (Conv2D)        (None, 150, 150, 128)     73856
_________________________________________________________________
block2_conv2 (Conv2D)        (None, 150, 150, 128)     147584
_________________________________________________________________
block2_pool (MaxPooling2D)   (None, 75, 75, 128)       0
_________________________________________________________________
block3_conv1 (Conv2D)        (None, 75, 75, 256)       295168
_________________________________________________________________
block3_conv2 (Conv2D)        (None, 75, 75, 256)       590080
_________________________________________________________________
block3_conv3 (Conv2D)        (None, 75, 75, 256)       590080
_________________________________________________________________
block3_conv4 (Conv2D)        (None, 75, 75, 256)       590080
_________________________________________________________________
block3_pool (MaxPooling2D)   (None, 37, 37, 256)       0
_________________________________________________________________
block4_conv1 (Conv2D)        (None, 37, 37, 512)       1180160
_________________________________________________________________
block4_conv2 (Conv2D)        (None, 37, 37, 512)       2359808
_________________________________________________________________
block4_conv3 (Conv2D)        (None, 37, 37, 512)       2359808
_________________________________________________________________
block4_conv4 (Conv2D)        (None, 37, 37, 512)       2359808
_________________________________________________________________
block4_pool (MaxPooling2D)   (None, 18, 18, 512)       0
_________________________________________________________________
block5_conv1 (Conv2D)        (None, 18, 18, 512)       2359808
_________________________________________________________________
block5_conv2 (Conv2D)        (None, 18, 18, 512)       2359808
_________________________________________________________________
block5_conv3 (Conv2D)        (None, 18, 18, 512)       2359808
_________________________________________________________________
block5_conv4 (Conv2D)        (None, 18, 18, 512)       2359808
_________________________________________________________________
block5_pool (MaxPooling2D)   (None, 9, 9, 512)         0
_________________________________________________________________
flatten (Flatten)            (None, 41472)             0
_________________________________________________________________
dense (Dense)                (None, 1024)              42468352
_________________________________________________________________
dropout (Dropout)            (None, 1024)              0
_________________________________________________________________
dense_1 (Dense)              (None, 512)               524800
_________________________________________________________________
dropout_1 (Dropout)          (None, 512)               0
_________________________________________________________________
dense_2 (Dense)              (None, 4)                 2052
=================================================================
Total params: 63,015,588
Trainable params: 42,990,804
Non-trainable params: 20,024,384
_________________________________________________________________
```

Fig. 7. VGG19 Model summary

For each iteration the whole batch of images passes through the network and the optimization function adjusts the weights of the matrix and the loss function algorithm reduces the loss and checks with validation data. The Fitting model is shown in below figure-8.

5. Results

We successfully implemented the VGG19 model to detect the anomalies of the road and achieved model accuracy of 95.62% and model loss of 13% in the eighth iteration and

Fig.8. Trained model

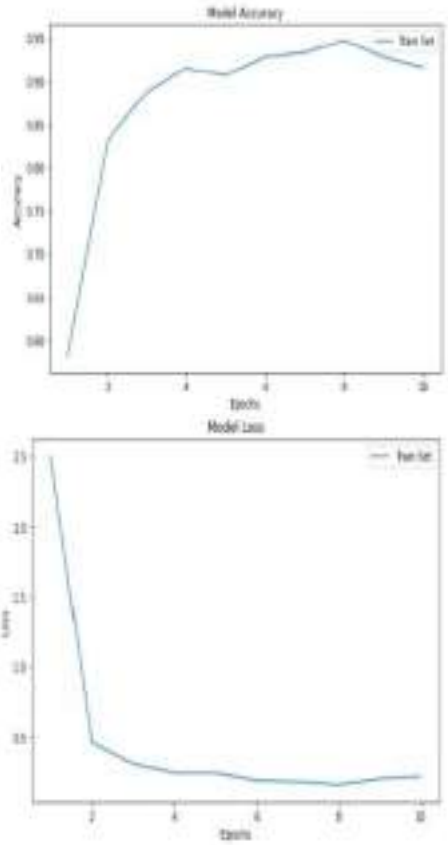

Fig. 9. Model Accuracy and Loss graph

we have achieved the validation accuracy of 86% and accuracy loss 45%.

6. Conclusion

In this paper we present a VGG19 CNN model-based traffic anomalies detection in urban traffic environments and achieved the highest accuracy of 95.6%. As this model is very feasible and accurate, when implements it in cloud environments and used for traffic surveillance purposes there will be a great chance of communicating the helpline at desperate situations and also helps to decreases the accident probability.

7. Future Scope

This research work have a great scope towards self-driving cars, video surveillance implementation and Accident detection system development in loop line areas, accident prone zone areas and Ghat roads. This research work is continued for further enhancements to implement in embedded hardware and cloud environments and optimize the code complexity to decrease the computing time.

References

[1] S. Kamijo, Y. Matsushita, K. Ikeuchi, M. Sakauchi. IEEE Transactions on Intelligent Transportation Systems, **1**, 108 (2000).

[2] K. He, G. Gkioxari, P. Dollar, R. Girshick. *Mask r-cnn*, IEEE International Conference on Computer Vision, 2980, (2017)

[3] S. Ren, K. He, R. Girshick, J. Sun. IEEE transactions on pattern analysis and machine.

[4] H. Nam, B. Han., *Learning multi-domain convolutional neural networks for visual tracking.* IEEE Conference on Computer Vision and Pattern Recognition, 4293, (2016)

[5] M. Sabokrou, M. Fayyaz, M. Fathy, R. Klette. IEEE Transactions on Image Processing, 26, 1992, (2017)

[6] I. Goodfellow, J. Pouget-Abadie, M. Mirza, B. Xu, D. Warde-Farley, S. Ozair, A. Courville, Y. Bengio. ,Advances in Neural Information Processing Systems, 2672, (2014)

[7] M. Deublein, M. Schubert, B. T. Adey, J. Kohler, M. H. ¨ Faber, Accident Analysis & Prevention, **51**,274(2013)

[8] N. Seenouvong, U. Watchareeruetai, C. Nuthong, K. Khongsomboon, N. Ohnishi, *A computer vision based vehicle detection and counting system*, 8th International Conference on Knowledge and Smart Technology (KST), (Chiang Mai, Thailand, 224, 2016)

[9] Nowosielski, A., Frejlichowski, D., Forczmański, P., Gościewska, K., Hofman, R., Automatic Analysis of Vehicle Trajectory Applied to Visual Surveillance (2016).

[10] "Li Ning, Li Gang, R.C Xie, Yuan Hang.,Computer Simulation., **32**,113 (2015)

[11] "Yang Zhiyong, Ma Hongwei, Chen Xiaoping. Freeway Incident Detection Algorithm Based on Fuzzy Logic. Journal Of Chong Qing University(Natural Science)., 32(6):1247- 1251(2013)

[12] trafficnet, https://github.com/ Olafenwa Moses/ TrafficNet/ releases/tag/1.0".

[13] "https://machinelearningmastery.com/adamoptimization-algorithm-for- deeplearning/#:~: text= Adam%20is%20a%20replacement%20optimization, sparse%20gradients%20on%20noisy%20problems."

[14] "https://towardsdatascience.com/how-dopretrained-models-work-11fe2f64eaa2".

[15] "https://peltarion.com/knowledgecenter/documentation/modeling-view/build-an-aimodel/loss-functions/categorical-crossentropy".

Road Traffic Anamoly Detection using AI Approach: survey paper

Publisher: IEEE

Cite This PDF

M. Rajeshwari ; Ch.Mallikarjuna Rao All Authors

Downl
PDF

Abstract: Every day somewhere on the road's accident happens because of unexpected interference of vehicles and unpredictable driving by the driver. There is a ton of research abou... **View more**

Metadata

Abstract:

Every day somewhere on the road's accident happens because of unexpected interference of vehicles and unpredictable driving by the driver. There is a ton of research about predicting and detecting vehicle accidents, yet there is no pre intimation to the drivers about the accident Streetcar crashes claim an enormous number of lives each day as a result It is usually the result of a driver's lapse of caution or a late response from emergency services. There is a need for an effective road accident identification system and data correspondence system for harmed people to be saved. It is not possible for a framework to convey data messages about an accident area to crisis management agencies for a quicker and more effective response. Numerous scientists propose different frameworks for programming accident recognition in exploration writing. Cell phones and GSM and GPS technologies aid in the identification of accidents. Specially arranged organizations accommodate vehicles and mobile applications are also available. The execution of a programmed street accident recognition and data correspondence framework in each vehicle is pivotal. A large portion of the research papers studied the utilization of the use of sensor innovation, other than attempting to distinguish accidents consequently utilizing AI and Computer vision from reconnaissance frameworks. Any sort of accident recognized is naturally sent as a caution to the necessary objective. Every one of these techniques has various rates of precision and its own limits. This survey paper examines different ways to deal

More Like This

Black Box: An emergency rescue dispatch system for road vehicles for instant notification of road accidents and post crash analysis

2014 International Conference on Informatics, Electronics & Vision (ICIEV)

Published: 2014

A Survey on IoT based Automatic Road Accident Detection

2021 5th International Conference on Intelligent Computing and Control Systems (ICICCS)

Published: 2021

Show More

with and identify the event of car crashes on a street directed under surveillance camera additionally short survey on autonomous road/street accident detection strategies.

Published in: 2021 5th International Conference on Electronics, Communication and Aerospace Technology (ICECA)

Date of Conference: 02-04 December 2021

INSPEC Accession Number: 21574857

Date Added to IEEE *Xplore*: 20 January 2022

DOI: 10.1109/ICECA52323.2021.9675957

ISBN Information:

Publisher: IEEE

Conference Location: Coimbatore, India

Contents

As per the Global status report on street safety 2021 [4], Every year 4.4 million people are dying because of injury related issues out of that the complete number of passing's caused because of road accidents has leveled out at 3.16 million every year which comes into unintentional injuries. Among all countries on earth, India suffers the greatest number of accidents and fatalities. Due to ill-advised street offices and the sloping territory levels in India, there are many sorts of spots that result in accidents and a higher rate of passing's because of them. On-street accidents are just as common as ones on rail lines in the vehicle area. In 2010, approximately 105,000 accidental deaths occurred on Indian streets alone. In India, we are responsible for less than 1 % of the complete worldwide vehicle numbers, but we have nearly 15% of street fatalities. In contrast to the year 2000, the number of accidental death occurrences increased by 50% in 2010 as compared to the year 2000.

Outlier Detection for IoT devices in Indoor Situating Framework using Machine Learning Techniques and Comparison

M.Sri Vidya[1,*] and *Dr. G. R.* Sakthidharan[2]

[1]MTech Student, Computer Science and Engineering, GRIET, Hyderabad, Telangana, India.
[2]Professor, Computer Science and Engineering, GRIET, Hyderabad, Telangana, India.

Abstract- Internet of Things connects various physical objects and form a network to do the services for sensing the physical things without any human intervention. They compute the data, retrieve the data by the network connections made through IoT device components such as Sensors, Protocols, Address, etc., The Global Positioning System (GPS) is used for localization in outer areas such as roads, and ground but cannot be used for Indoor environment. So, while using Indoor Environment, finding or locating an object is not possible by GPS. Therefore by using IoT devices such as Wi-Fi routers in Indoor Environment can localize the objects. It can be done by using Received Signal Strengths (RSSs) from a Wi-Fi router. But by using RSSs in Wi-Fi, there are disturbances, reflections, interferences are caused. By using Outlier detection techniques for localization can identify the objects clearly without any interruptions, noises, and irregular signal strengths. This paper produces research about Indoor Situating Environment and various techniques already used for localization and form the effective solution. The several methods used are compared and form a result to make the further computation in the Indoor Environment. The Comparison is done in order to find the effective and more accurate Machine Learning algorithms used for Indoor Localization.

1. Introduction

Indoor Positioning System (IPS) is a technique in which locating of the objects or any person inside the buildings or indoor environment. Indoor environment includes Parking, Smart Cities, Buildings, Airports, Underground areas, etc. We already have a Global Positioning System (GPS) existing for locating objects or persons. But locating any particular thing in any location is possible only when that location is outside and outer areas. So locating anything inside a building or any closure area which have barriers cannot be possible. In order to find any particular thing or a person, in closed environment i.e. indoor environment, a particular mechanism called IoT is used.

There are other ways which we can use to localize such as Bluetooth, GPS, etc., but they are easily diverted by the hardware barriers such as roofs, pillars and other components of Indoor systems. GPS and Bluetooth are accessed by using the signal coming from satellites. Those signals are only applicable when the connectivity is strong enough to sense the user's location. But within a building or in any closure areas, the satellite signals are very weak and cannot be reachable. So using a new mechanism called IoT to make things easier and efficient. Because IoT devices can be kept in home or any buildings and are easy to produce a signal. So the signal is always available at any areas inside the closure environment.

IoT devices are the ones which have multiple devices to be connected and form a whole big connection to make the sensing possible without involving any human senses. IoT devices have various parts such as Connection, Sensors, Processing and User Interfaces. These components help the devices to sense things and give result to user, finally contact to user for any customization of sensing & whole process. In indoor environment we use the IoT device such as Wi-Fi router and have access to Wi-Fi network Connectivity for locating. Using Wi-Fi connection can be done by the received signal strength indicator (RSSI) is standardized by IEEE 802.11 which are

* Corresponding author: m.srividya1998@gmail.com

already installed in devices such as smart phones, tablets, laptops, etc.

Outliers are the ones which will be arise when machine fault, mechanical exceptions or present in abnormal locations. When a sample is located in unusual place and cannot be found is considered as an outlier. Outlier detection refers to detecting the abnormal location and find the exactness of it. Outlier detection acts as the finding algorithm which is unexpected or irrational data from the given IoT values of RSS.

But using Wi-Fi as the case and with RSS values to compute the localization in Indoor environment, there are certain disadvantages involved. i) Difference in Accuracy ii) Radio Signals iii) Placing incorrectly.

Difference in Accuracy means the positioning of Wi-Fi effects RSS values in receiving end. The uneven values of RSS will be received whenever there are any obstacles, disturbances. Signals coming from Wi-Fi connectivity are received in the form of Watts (W), milliWatts (mW) or decibel-milliWatts (dBm). Received Signals are effected by interventions, reflections, diversions, deflection, etc. So thus causing the signals to delay and the effect results attenuation of the signal inputted. The delay which is caused in the signals at received end are attenuated and thus forming the irregular RSS values in instance node. This irregular and uneven RSS values at receiver's end will cause the accuracy of positioning to be very low.

Radio Signals in Indoor environment tends to be effected by the physical obstacles such as roof tops, walls, pillars, etc. Wi-Fi uses the Radio Frequency Signals for network computations. Communications between connections are also done by Radio signals. Location of the node changes with the Signal strengths of the radio at the receiving end.

Placing of Wi-Fi in indoor system have great impact on the locating of an object. The abnormal RSS values impact the locating in indoor environment. Positioning of the Wi-Fi may cause the major difference in identifying the object at distances. Whenever there is Wi-Fi installed in a building, position of it should be such that it can be available all over the building. Therefore differ in positioning of Wi-Fi follows differ in RSS values in indoor environment. So, outlier detection is to be done in order to detect these abnormalities and to localize the objects correctly.

2. Methodology

The related paper [1] introduces a completely unique proposal as regards up accuracy with cheap indoor positioning systems which are Wi-Fi-based. This can be carried out by choosing specific Wi-Fi signal channels that area unit not overlapping and area unit put through to least obstruction. The resultant received signal strength intensity (RSSI) is examined using machine learning algorithms like k- Nearest Neighbors (KNN), Support Vector Machine (SVM), Artificial Neural Networks (ANN), and the finest matched algorithmic rule is known.

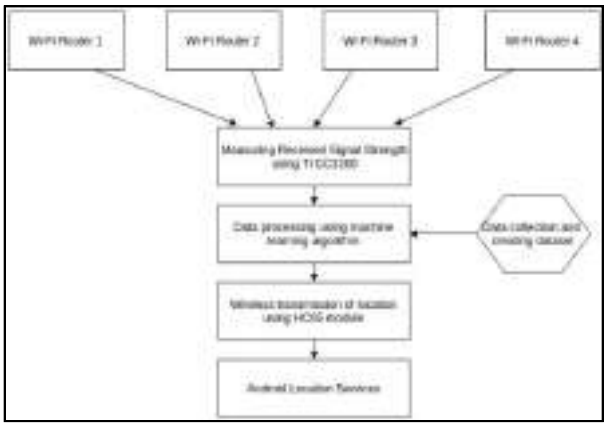

Fig. 1. Flow chart

People in various positions in Wi-Fi-enabled regions can influence the transmission of channel state information (CSI) of Wi-Fi signals to varying degrees. As a result of area is split into many little regions, classification is used to locate them. As a result, the [2] paper recommends a completely unique localization algorithmic rule based on Deep Neural Networks (DNN) and a multi-model integration technique. There are three steps to the strategy. To rectify the aberrant data, the native outlier issue (LOF), an anomaly identification algorithmic software, is used first. Second, three DNN models are trained within the coaching section to classify the region fingerprints using the processed CSI information from three antennas. Finally, in the testing step, a model fusion technique known as cluster technique of information handling (GMDH) is used to combine three expected results from several models and provide the final position result. The test-bed experiment was carried out in an empty hallway, and the final positioning accuracy was at least 97%.

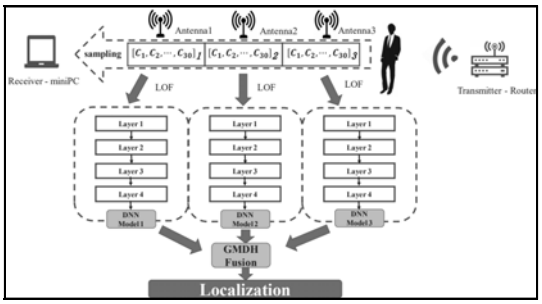

Fig. 2. ModelF Structure

In [3], this paper describe the indoor positioning issue on the instance of user tracking, whereas mistreatment the Bluetooth Low Energy technology and received signal strength indicator (RSSI). Authors experimented and compared our easy handmade rules with the subsequent machine learning algorithms:

Naive mathematician and Support Vector Machine. The goal was to spot actual position of active label among 3 possible statuses and deliver the goods most accuracy. Finally, they have a tendency to achieved accuracy of 0.95.

Because of the requirement for low-cost indoor positioning systems (IPSs), some researchers have focused on Wi-Fi-based IPSs, which rely on wireless native space network received signal strength (RSS) data acquired at different places in inside environments known as reference points.

A fresh new framework for centrosymmetric Bregman divergence was planned in this study [4], which includes k-nearest neighbour (kNN) classification in the signal house. Jensen-Bregman divergences, which unify the square geometer and Mahalanobis distances with information-theoretic Jensen-Shannon divergence measures, were used to calculate the target's coordinates as a weighted mixture of the closest fingerprints. The performance of the intended algorithmic rule was compared to that of the probabilistic neural network and variable Kullback-Leibler divergence to validate the work. The established algorithmic rule had a spatial inaccuracy of roughly one meter. And the accuracy rate is 90%.

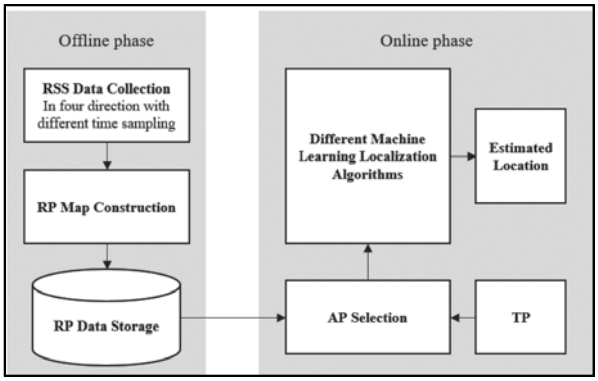

Fig. 3. Location Wi-Fi-based fingerprinting architecture's offline and online stages.

Because of its low cost and high accuracy, the Wi-Fi process with received signal strength indicator (RSSI) has been widely utilized in large indoor localization systems.

The fluctuation of wireless signal caused by atmospheric uncertainties, on the other hand, results in considerable changes in RSSIs, posing significant obstacles to finger print-based indoor localization in terms of positioning accuracy. They suggest a top-down looking strategy using a deep reinforcement learning agent to deal with atmospheric dynamics in indoor placement using Wi-Fi fingerprints in their work [5]. The model learns an action policy that can pinpoint seventy-five percent of the targets in a 25000m^2 area within 0.55m^2. As a result, the accuracy rate is 75%.

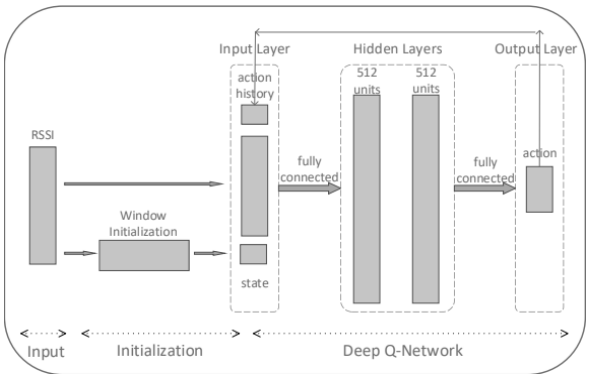

Fig. 4. Indoor Localization using a Deep Q-Network

Deep reinforcement learning (DRL) has recently shown to be successful in a variety of application domains. It's an appropriate methodology for IoT and smart city scenarios where auto-generated information is typically partially tagged by user feedback for coaching purposes.

Author's inclination to present a semi-supervised deep reinforcement learning model that meets good town applications in [6] paper because it consumes both tagged and untagged knowledge to increase the training agent's performance and accuracy. For generalizing leading policies, the model employs Variational Auto-encoders (VAE), which are a product of the reasoning engine. The projected model is the start inquiry that extends deep reinforcement learning to the semi-supervised paradigm, according to the simplest of our data. Authors tend to specialize in good buildings as a case study of smart town applications, and apply the predicted model to the issue of indoor localization supported by BLE signal strength. Because people spend so much time indoors, indoor localization is a critical component of good city services. When compared to the supervised DRL model, our model learns the simplest action rules that lead to a thorough estimation of the target locations with a twenty-third improvement in distance to the target and a minimum of sixty-seven a lot of received rewards.

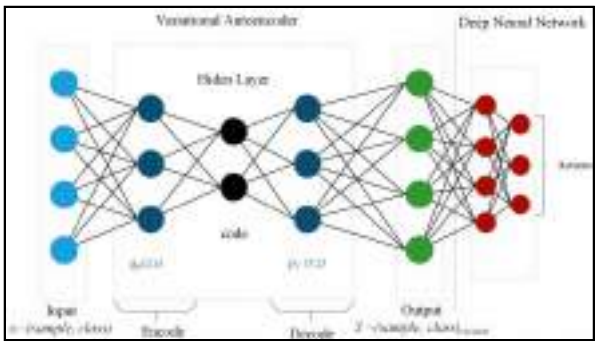

Fig. 5. A variational autoencoder is a high-level notion used in deep reinforcement learning

For IoT networks, comprehensive detection methods are no longer effective, necessitating the development of light-weight solutions. PCA approaches will assist in reducing computational complexity, hence anomaly detection techniques that support PCA have garnered a lot of attention in the past. PCA approaches, on the other hand, are not directly suited to IoT networks with limited resources and tightly controlled performance.

PCA approaches for detective work aberrant network traffic in IoT networks are investigated in this research [7]. They developed a novel detection theme based on two levels of PCA algorithms. The first level is for quick detection with a limited number of principal elements, while the second level is for elaborate detection with a large number of principal elements. Authors frequently explore the parameters used in a long-distance calculation formula, relying on several tests to demonstrate the viability of the proposed theme.

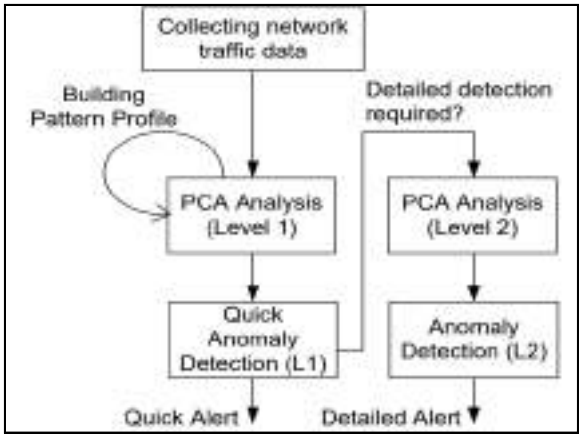

Fig. 6. The Detection Flow

Machine learning (ML) technologies have been widely used in recent years to solve localization problems with reasonable success. The authors of the study [8] intend to provide a complete assessment of Machine learning assisted localization approaches that make use of common wireless technology. First, the authors provide a brief overview of indoor localization approaches. They then go over a number of machine learning (ML) techniques (supervised and unsupervised) that can be used to solve a variety of issues in indoor localization, such as the non-line-of-sight (NLOS) issue, device heterogeneity, and environmental fluctuations, all while maintaining a high level of quality. The trade-offs among a slew of issues are discussed, with a variety of possible outcomes. The authors have a tendency to conjointly discuss how machine learning algorithms can be efficiently used to combine various technologies and algorithms to create a comprehensive IPS. In summary, this survey might serve as a resource for gathering up-to-date information on recent advances in machine learning for accurate indoor location.

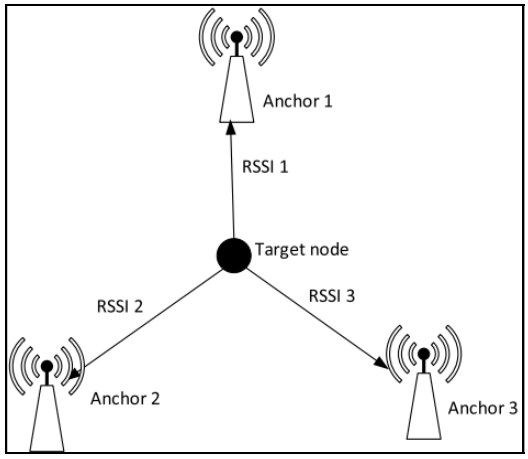

Fig. 7. Positioning using RSSI readings is graphic visualization

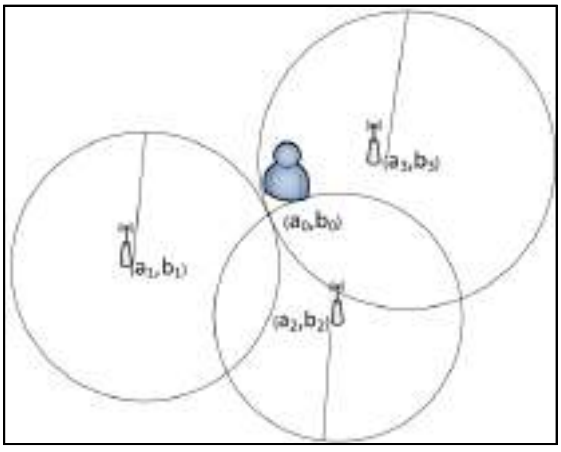

Fig. 8. Trilateration-based positioning demonstration.

The research [9] presents an outlier detection theme to reduce anomaly detector data by utilizing outlier detection techniques based on wireless sensor network

(WSN) based localization problems. The received signal strength (RSS), a low-cost and widely available activity approach, is commonly used in indoor localization systems, however RSS measurements are well-known to be sensitive to changes in the environment. In the work [9], an outlier detection theme is applied to treat aberrant RSS data in order to get a large number of reliable observations for localization. The usefulness of the planned technique is demonstrated in an indoor setting through an experiment.

The study provides a degree outlier detection theme to perform internal control of the RSS info and knowledge filtering in period of time localization to account for the sophisticated RF propagation effects with limited resources in WSN-based indoor localization. The method [9] has been proved to be reliable and successful in handling knowledge that is subject to anomalies. According to the findings of the experiments, using the outlier detection theme improves localization accuracy by 13-30%. As a result, the outlier detection theme, as well as the localization system, will pave the way for a variety of WSN applications such as automated inspection, exploration, and context awareness.

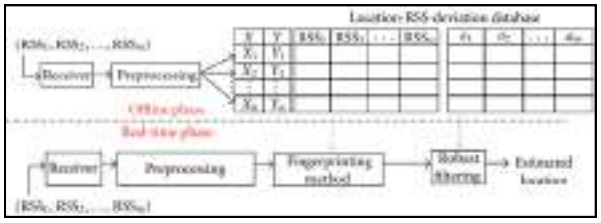

Fig. 9. Flowchart of fingerprinting method.

In crowded urban canyons, the Global Navigation Satellite Systems (GNSS) suffer from deterioration and outages, making them almost unusable for indoor applications. Because of the growing desire for omnipresent positioning, designing indoor positioning systems has become a fascinating research issue.

Indoor positioning services have been investigated for several years using wireless fidelity technology. In the literature, wireless fidelity indoor localization systems with a machine learning method are widely used. These methods establish up a match between the user's fingerprint and a pre-defined grid of grid points on the radio map. Fingerprints, on the other hand, are copied from accessible Access Points (APs) and interference, resulting in a greater variety of identical patterns when the user's fingerprint is used.

The Principle Component Analysis (PCA) is utilized in this analysis [10], to improve the performance of the wireless fidelity indoor localization systems supported machine learning technique and reduce the computation value. All of the proposed methods were created and implemented using IEEE 802.11 WLANs on an Android-based smart phone. In both static and dynamic modes, the experiment was carried out in a highly realistic interior setting. K-Nearest Neighbors, Decision Tree, Random Forest, and Support Vector Machine classifiers were used to evaluate the projected methodology's performance. The results reveal that the intended methodology outperforms several indoor localization methods described in the literature. Once victimization Random Forest classifier was used in the static mode, the calculation time was decreased to seventieth, and once victimization KNN was used in the dynamic mode, the calculation time was cut in thirty third.

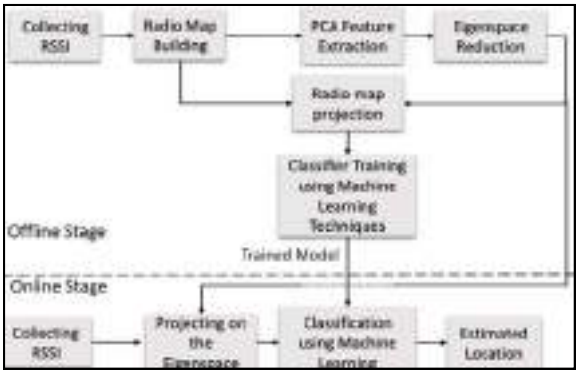

Fig. 10. Proposed system architecture.

Because of the strong complementarity between pedestrian dead reckoning (PDR) and LAN in smartphone indoor positioning, a hybrid fusion theme of the two is gaining traction. However, LAN outliers can decrease the theme's performance; to eliminate them, numerous studies are proposed, such as: increasing the LAN one by one or strengthening the theme. Because of the intrinsic received signal strength (RSS) change, the overall picture remains the same, but there are still some unremoved outliers. To address this issue, this work proposes a primary outlier detection and removal technique using Machine Learning (ML), dubbed WiFi-AGNES (Agglomerative Nesting), which is based on the retrieved LAN positional features when the pedestrian is stationary.

After that, the research [11] provides a second outlier identification and elimination approach, dubbed WiFi-Chain, which aids in removing the LAN, PDR, and their reciprocal features once the pedestrian is walking. Finally, a hybrid fusion theme is projected, that integrates the 2 projected ways, WiFi, PDR with Associate in Nursing inertial-navigation-system-based (INS-based) perspective heading arrangement (AHRS) via Extended Kalman Filter (EKF), Associate in Nursing an Unscented kalman filter (UKF). The findings of the experiment reveal that the two proposed methods are both effective and powerful. The minimal

component of the maximum error (MaxE) is reduced by sixty-six percent when WiFi-AGNES is used. The MaxE of LAN is a very small quantity less than 4.3 m while employing the WiFi-Chain; moreover, the intended theme achieves the most effective accomplishment, where the base mean sq. error (RMSE) is 1.43 m. Furthermore, because characteristics are universal, the proposed theme, which combines the two characteristic-based approaches, has a strong foundation.

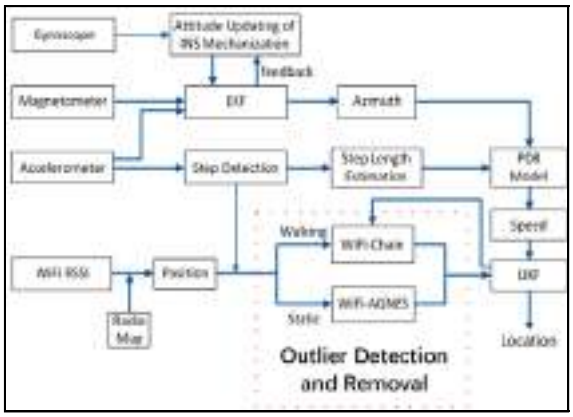

Fig. 11. The planned hybrid fusion scheme's architecture.

In most cases, fingerprint-based positioning is employed for indoor positioning. During this technique, a radio map is mistreated at the start. Values of Received Signal Strength (RSS) taken from specified reference points. Because the intended position is unknown during positioning, the best match between the detected RSS values and existing RSS values inside the radio map is determined. Machine learning methods are widely used in the positioning literature to estimate positions. Finding an adequate machine learning rule is one of the most difficult problems in indoor positioning systems. Various machine learning techniques are compared in terms of positioning accuracy and computation time in this article [12]. Indoor positioning data from UJIIndoorLoc is used in the tests. The k-Nearest Neighbor (k-NN) rule is the best matched one throughout the positioning, according to experimental data. urthermore, ensemble methods such as AdaBoost and material are used to improve the performance of the choice tree classifier, which is nearly identical to that of the k-NN, which is the best classifier for indoor placement.

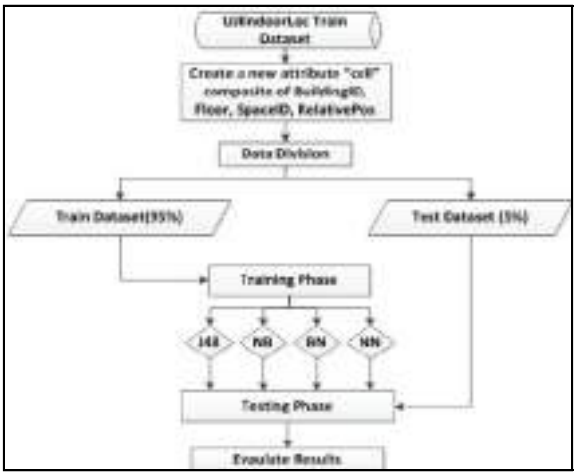

Fig. 12. The new attribute "cell" construction phase.

3. Comparison

Research made for the indoor localization environment which uses different types of algorithms to localize are differentiated and compared given in the following table:

Table 1. Comparison of the Methods used

Methods	Algorithms	Accuracy	Reference
IoT Finger Print device	kNN, SVM, Artificial neural network	Each algorithm less than 75%.	Reference – [1]
CSI based finger printing	Deep Neural Network (DNN)	95% in empty corridor	Reference – [2]
Bluetooth Low Energy technology and received signal strength indicator(RSSI)	Naive Bayes and Support Vector Machine	95% by using RSSI filtering	Reference – [3]
reference points, RSS values as well as finger prints	From symmetric Bregman divergence and k-nearest neighbor (kNN)	90% accurate	Reference – [4]
Wi-Fi Fingerprints	Top down Deep Q-Network	75% accurate	Reference – [5]
Variational Autoencoders (VAE)	Semi-Supervised Deep	67% more than supervised	Reference – [6]

	Reinforcement Learning	learning	
PCs selection, distance measure, anomaly quick detection	PCA techniques	92% TPR	Reference–[7]
Non-line-of-sight (NLOS)	ML techniques (supervised and unsupervised)	87%	Reference–[8]
WSN-based indoor localization	Hampel filter, Kernel density estimator (KDE)	13∼30% improved accuracy for outlier detection	Reference–[9]
Finger prints, pre-defined radio map	k-Nearest Neighbors (kNN), Decision Tree, Random forest (RF) and Support vector machine (SVM) classifiers	Estimation time reduced 70% using Random Forest in static & in dynamic mode 33% when using KNN	Reference–[10]
Outlier detection and WiFi-AGNES (Agglomerative Nesting), WiFi-Chain	Machine Learning (ML)	Maximum error (MaxE) reduced by 66.5%	Reference–[11]
WiFi fingerprints	k-Nearest Neighbor (k-NN), J48, Naïve Bayes, Bayes Net	99% by using various classifiers	Reference–[12]

4. Analysis

So, by comparing all the methods used in the indoor localization environment, more accuracy is possible by using multiple algorithms and combination of different methods. But by using single methods which are very efficient and trendy, gives more accuracy for locating in Indoor environment.

Multiple algorithms used for Indoor Position System are k-NN, SVM, Artificial Neural Network according to [1]. But it does not have more accuracy than 75%. Another reference [3] having multiple algorithms uses Naïve Bayes and SVM and have accuracy up to 95%. Another study [10] was conducted in both static and dynamic modes in a real indoor environment. K-Nearest Neighbors (kNN), Decision Tree, Random Forest (RF), and Support Vector Machine (SVM) classifiers were used to evaluate the performance of the suggested technique in [10].The research which uses single new algorithm for locating of the person or any object in Indoor localization environment uses complex deep neural networks. Such method is top-down Deep Q-Network in [5] having accuracy of 75%. Another research uses Deep Neural Network and have 95% accuracy in empty locations [2].

These methods also uses machine learning approaches such as kNN using symmetric Bregman Divergence in [4]. PCA techniques are also used for localization and got 92% of True Positive Rate (TPR) in [7].

The researches done in this paper include surveys to which all the different types of algorithms consists in machine learning are compared and accuracies are determined for individual algorithm so that the efficient algorithm which localize can be identified. The surveys papers [8] and [12] give the comparison of every machine learning algorithm and give the more accuracy algorithm. In [8] all the possible algorithms are mentioned for localization purpose. And in [12] some machine learning classifiers are used and are compared to find the efficient ones.

In a real-time indoor localization context, the research [9] provides an outlier identification methodology for quality control of the RSS valued database and data purification. Research [11] consist of the outlier detection method by using machine learning algorithms and the detected outliers are removed in the process. WiFi-AGNES (Agglomerative Nesting) is the process used initially for static type of data. Second procedure used WiFi-Chain is the method for outlier detection and removal.

5. Conclusion

By using the surveys which are made in Indoor Locating Environment, various accuracies are observed. By using this comparison, which methods to be used in the indoor systems for available resources is found. By observing the differences of each algorithm used, accuracy for every method and to which extent the accuracy of location of a person or thing is located can be seen. So, the ideal algorithms used for Indoor Situating Environment for more accuracy and easy locating can be identified. Based on the survey mentioned in every reference, the possible algorithm combinations are also examined. Which will be used

for further review of the indoor environment and can be accessed using all possible methods.

References

1. R. Abishek, K. R. Abishek, N. Hariharan, M. Rakesh Vaideeswaran, and C. Sundara Paripooranan, 2019 TEQIP III Sponsored International Conference on Microwave Integrated Circuits, Photonics and Wireless Networks (IMICPW) (2019)
2. Y. Yin, C. Song, M. Li, and Q. Niu, Sensors **19**, (2019)
3. A. Mussina and S. Aubakirov, in *Proceedings of the 8th International Conference on Data Science, Technology and Applications* (SCITEPRESS - Science and Technology Publications, 2019)
4. O. A. Abdullah and I. Abdel-Qader, in *Machine Learning*, edited by H. Farhadi (IntechOpen, Rijeka, 2018)
5. F. Dou, J. Lu, Z. Wang, X. Xiao, J. Bi, and C.-H. Huang, in *2018 IEEE 15th International Conference on Mobile Ad Hoc and Sensor Systems (MASS),* pp. 166–174 (2018)
6. M. Mohammadi, A. Al-Fuqaha, M. Guizani, and J.-S. Oh, IEEE Internet of Things Journal **5**, 624 (2018)
7. D. H. Hoang and D. H. Nguyen, in *2019 21st International Conference on Advanced Communication Technology (ICACT),* pp. 1143–1152 (2019)
8. A. Nessa, B. Adhikari, F. Hussain, and X. N. Fernando, IEEE Access **8**, 214945 (2020) Y.-C. Chen and J.-C. Juang, International Journal of Navigation and Observation **2012**, (2012)
9. Y.-C. Chen and J.-C. Juang, International Journal of Navigation and Observation **2012**, (2012)
10. A. H. Salamah, M. Tamazin, M. A. Sharkas, and M. Khedr, *International Conference on Indoor Positioning and Indoor Navigation (IPIN),* pp. 1-8, (2016)
11. Z. Zhang, J. Liu, L. Wang, G. Guo, X. Zheng, X. Gong, S. Yang, and G. Huang, Remote Sensing (2021)
12. S. Bozkurt, G. Elibol, S. Gunal, and U. Yayan, ***2015*** *International Symposium on Innovations in Intelligent SysTems and Applications (INISTA),* pp. 1-8 (2015)
13. Kora, P., Kalva, S.R. *SpringerPlus* **4,** 481 (2015). https://doi.org/10.1186/s40064-015-1240-z
14. P. Kumar, A. Singhal, S. Mehta, and A. Mittal, Journal of Real-Time Image Processing **11**, 93 (2016)
15. B. Dhanalaxmi, G. A. Naidu, and K. Anuradha, Procedia Comput. Sci. **46**, 432 (2015)
16. P. Nayak and A. Devulapalli, IEEE Sens. J. (2015)
17. P. Nayak and B. Vathasavai, IEEE Sens. J. (2017)
18. P. Nayak, D. Anurag, and V. Bhargavi, Proc. 2nd Int. Conf. Adv. Comput. Methodol (2013)
19. D. V. Pushpalatha and P. Nayak, 2015 3rd International Conference (2015)
20. P. Nayak, R. S. U. Suseela, and V. Trivedi, *2017 International Conference on Energy, Communication, Data Analytics and Soft Computing (ICECDS)*, pp. 453-461 (2017)

Accurate Anomaly Detection using various Machine Learning methods for IoT devices in Indoor Environment

Publisher: IEEE

M.Sri Vidya ; G. R. Sakthidharan **All Authors**

Abstract: The Internet of Things i.e. IoT is a collection of specialized devices, or "things" that communicate real-world data through networks. IoT devices are computer devices th... **View more**

Metadata

Abstract:
The Internet of Things i.e. IoT is a collection of specialized devices, or "things" that communicate real-world data through networks. IoT devices are computer devices that can exchange data and connect wirelessly to a network. IPS is a technology that can be used to locate people or items inside buildings using a mobile device such as a smartphone or tablet. Indoor positioning is achieved by using devices already in use such as cellphones, Wi-Fi and Bluetooth antennae, digital cameras, and clocks. RSSI is a metric for assessing the quality of a wireless connection in Wi-Fi devices. But using RSSI values of Wi-Fi may cause inaccuracies in locating any nodes. RSSI is far more prone to interference than a wired network. And these interferences cause the irregularity in Signal strengths. In the case of indoor Wi-Fi positioning, irregular and anomalous RSS data can't be used to pinpoint the location of any unknown

Keywords

Metrics

More Like This

node. As a result, this article investigates the RSSI values utilizing machine learning approaches such as supervised, unsupervised, and ensemble learning in an indoor localization scenario employing Wi-Fi devices. The supervised learning techniques utilized in this study include Naive Bayes, Random Forest, and Decision Tree. The SOM (Self-Organizing Map) method was utilized in unsupervised learning. Then, this research work has used stacking method that is used for combining different classifiers implemented for ensemble algorithm. Precision, recall, and f1-score are utilized for experiments. After removing the outliers, the technique was found to be successful, with a high accuracy of 98.2 percent.

Published in: 2021 Fifth International Conference on I-SMAC (IoT in Social, Mobile, Analytics and Cloud) (I-SMAC)

Date of Conference: 11-13 Nov. 2021

INSPEC Accession Number: 21475638

Date Added to IEEE *Xplore*: 20 December 2021

DOI: 10.1109/I-SMAC52330.2021.9640962

ISBN Information:

Publisher: IEEE

ISSN Information:

Conference Location: Palladam, India

Contents

Authors

Figures

References

Keywords

Metrics

A Study On Deep Learning And Machine Learning Techniques On Detection Of Parkinson's Disease

P. Mounika[1,*], *S.* Govinda Rao[2]

[1]MTech Student, Computer Science and Engineering, GRIET, Hyderabad, Telangana, India.
[2]Professor, Computer Science and Engineering, GRIET, Hyderabad, Telangana, India.

Abstract: Parkinson's disease (PD) is a sophisticated anxiety malady that impairs movement. Symptoms emerge gradually, initiating with a slight tremor in only one hand occasionally. Tremors are prevalent, although the condition is sometimes associated with stiffness or slowed mobility. In the early degrees of PD, your face can also additionally display very little expression. Your fingers won't swing while you walk. Your speech can also additionally grow to be gentle or slurred. PD signs and symptoms get worse as your circumstance progresses over time. The goal of this study is to test the efficiency of deep learning and machine learning approaches in order to identify the most accurate strategy for sensing Parkinson's disease at an early stage. In order to measure the average performance most accurately, we compared deep learning and machine learning methods.

1. Introduction

Parkinson's disease (PD) was first described by Dr. Parkinson's as "trembling paralysis". Parkinson's disease may be a brain disease that can cause tremor, firmness, and staggering, balance, and coordination. The symptoms of Parkinson's disease usually develop gradually and get degraded over time. As the disease progresses, people may find it difficult to walk and talk. You will also experience psychological and behavioral changes, as well as sleep problems, despondency, unmind fullness and fatigue. Parkinson's disease can affect both men and women. They are 50% more likely to suffer from this disease than women. The main risk factor for Parkinson's disease is aging. Although most people get Parkinson's disease after the age of 60, there are still 5-10% of people who get Parkinson's disease before the age of 60. 50. Called "early onset" disease.

PD occurs when nerve fibers or neurons near the brain that control gesture are damaged or die. These neurons usually release dopamine, which is an important neurotransmitter in the brain. When neurons die or become damaged, less dopamine is produced, which leads to exercise. Scientists are still not sure what causes the death of dopamine-producing cells. Actually, the amount of individuals suffering from PD has exceeded 10 million worldwide. Parkinson's disease starts with different kinds of tremors which are possibly hand tremors, limb rigidity and gait inconveniences. These tremors are generally distinguished into motor (i.e., movement related) and non-motor (i.e., non-movement related). Patients with motor symptoms are generally less affected than those with non-motor symptoms. Non-motor symptoms include despondency, insomnia, Anosmia, and cognitive ailment. It is important to remember that early spotting of Parkinson's disease can help control and improve symptoms. The early stages are critical to slow down progress and allow patients to receive disease-modifying drugs when they are available. Early detection of Parkinson' unwellness is important for speed the disease' course. Several data-driven methods are developed over the years to boost the identification of Parkinson' disease. Machine learning, with its data-driven methodologies, had brought an amendment within the templet within the manner essential info in metallic element biomarkers is retrieved and analysed, since it's latterly emerged as a possible topic of analysis in each academe and trade for the identification of PD. Furthermore, machine learning approaches give critical information that aids in the classification and diagnosis of Parkinson' disease, permitting quicker decision-making. so as to resolve the PD detection challenge, several machine learning algorithms are utilized in the literature. Dysphonia measures, for example, have been used to discriminate patients with Parkinson's disease from able-bodied ones. Because of its capability to extract nonlinearity by using nonlinear kernels, the support vector machine (SVM) is applied to solely four dysphonic options for palladium classification. On the idea of acoustic analysis of speech, 2 machine learning algorithms, Random Forest (RF) or Support Vector Machine (SVM), and a Convolutional neural network (CNN), a deep learning model, are wont to determine Parkinson' disease. Random forest (RF), Support Vector Machine (SVM), and Convolutional Neural Network (CNN) results are compared. Deep learning algorithms have attracted specific attention in palladium diagnosing and getting high accuracy with no assumptions on

* Corresponding author: monika.pilla@gmail.com

information distribution due to their ability to manage giant amounts of data.

Meticulous monitoring of the pre-motor stage in PD ensures early identification of PD. Rapid Eye Movement (REM) sleep Behavior Disorder (RBD) and sensory system loss are common symptoms of this pre-motor stage, which differ from typical motor symptoms. This paper ambitions to offer a comparative evaluation evaluating the maximum superior facts-pushed prediction tactics in figuring out PD inside the facts-pushed methodologies. Machine studying-primarily based totally and deep studying-primarily based totally facts-pushed methodologies are contrasted on this paper. A deep studying version is created to differentiate regular humans from humans with Parkinson's disease. The number one purpose of this studies is to offer a comparative evaluation and shed mild at the efficacy of superior prediction algorithms whilst implemented to small PD facts sets. Parkinson's Progression Markers Initiative provided the PD data used in this study (PPMI). The results showed that when compared to machine learning models, developed deep learning has a better detection performance in distinguishing normal persons from Parkinson's disease patients.

2. Previous Work/Related Work

There are many researches going on Parkinson’s disease regarding the diagnosis at early stages and also symptoms identification through various techniques which can be useful for the initiation of therapeutic inventions at an early stage and also the strategies to manage them. Parkinson’s disease can be analysed by choosing people from various platforms such as social media platforms, tele-monitoring of the disease using the vocal features and also by gathering clinical visits of elder people who frequently visit for check-ups with high charges. The major goal to be about distinguishing abled-bodies from those who have Parkinson's disease. Different categorization approaches are also compared for effective PD diagnosis.

[1], The Probabilistic Neural Network (PNN) is used in a study to distinguish persons with Parkinson's Disease from healthy ones. They primarily used three types of PNN models: incremental search (IS), Monte Carlo search (MCS), and hybrid search (hybrid search) (HS) and these models provided accuracies from 79% to 81% for diagnosis of the disease for the people who are not diagnosed before.

The data set they considered is comprised of Bio-medical vocal measures which are gathered from 31 candidates among them 23 with the Parkinson’s malady. The primary goal of information process is to tell apart folks with Parkinson' un-wellness from healthy people, with the "status attribute" being changed to non-PD for healthy people and atomic number 46 for candidates who are diagnosed with Parkinson' disease, leading to a classification downside with 2 decisions.

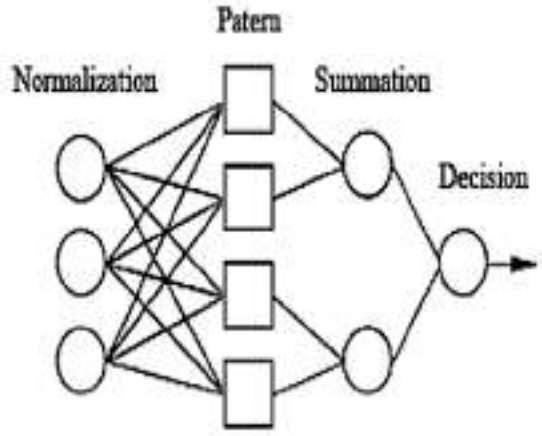

Figure 1. Neural Network Model (Ene, Marius 2008).

[2], The work presented here is an assessment of the value that is applied in practise to current traditional and non-traditional metrics for distinguishing people with PD from those who are healthy by detecting dysphonia. They also introduced Pitch Period Entropy (PPE), a new estimate for dysphonia which is used for detecting the variations in the frequency of voice. In their research they collected Phonations from few people among them most of the candidates with PD. The kernel support vector machine achieved a 91.4 percent performance. They finally concluded that noise ratios when combined with non-standard methods are the best methods to differentiate PD patients from healthy ones. Though the chosen non-standard methods are sturdy when subjected to variations in acoustic world they are well suited to tele-monitoring applications.

[3], As in the previous work vocal features in measuring dysphonia play a major role and those features which are drawn out from voice are of various types and most of them co-related their research is two folded where 1.Selecting minimal subset of features and 2.Developing a low-bias predictive model. They used a interactive information metric with a permutation test to determine the pertinences. Also, in [2,] the standard deviation of a classifier's accuracy is exceptionally high(35.84%), implying that testing on relatively small samples, such as 6 or 7 samples, yielded results of nearly 100% accuracy or virtually zero, indicating an inferior standard deviation. This is the signal indicating acquisition of the training set. And they finally concluded that their method generalizes better to unseen tests. As per the results, their method performs better even though the performance of SVM is inflated when compare to the study [2].And the set of all four high ranked features which are identified by [2] are poor and also vocal features possess higher capability in PD assessment.

[4], They in comparison many forms of categorization structures for correct prognosis of Parkinson's sickness on this study. Misdiagnosis is suggested to be excessive as 25% of the instances because the prognosis of PD could be very difficult.The purpose of their research is to describe the various approaches to efficiently differentiate healthy people. They used SAS base software for applying classification methods in the diagnosis of PD.A comparative study was carried out by

applying 4 individual classification methods which are DMneural, Decision tree, Regression and Neural Networks. To compute the Performance of classification methods different evaluation methods are used. Their results proved that Neural Network classification model produces best outcomes and its overall performance is 92.9%.They also compared their results to the outcomes that are yielded by kernel SVM's. This records highest classification score than the previous researches.

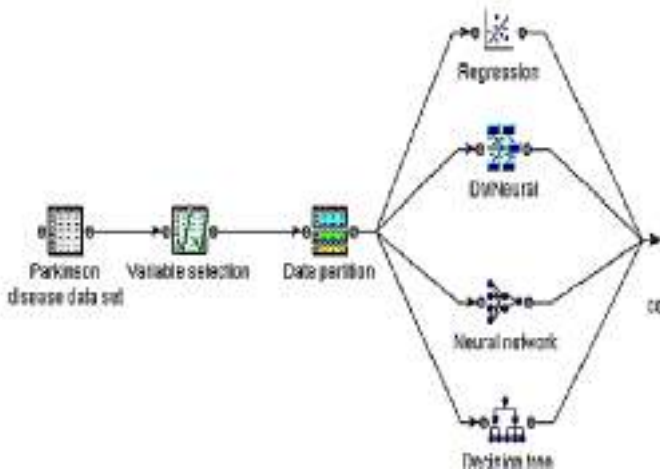

Figure 2. The applied methods for PD recognition (Das, Resul 2010).

[5], This work purpose is to differentiate the PD patients and the healthy individuals. Biomedical voice of human is used as Parkinson's dataset. Artificial Neural Networks (ANN) are wide utilized within the medical specialty trade for modelling, information analysis, and diagnostic classification. the 2 varieties of ANNs utilised for classification are Multilayer Perceptrons (MLP) and Radial Basis operate (RBF) Networks. The choice methodology for feature choice from the dataset is that the adaptational Neuro-Fuzzy Classifier (ANFC) with linguistic hedges. The simplest results from the adaptational Neuro-Fuzzy Classifier with linguistic hedges are 95.38 % coaching and 94.72 percent testing.

[6], The aim of this observe is to apply fuzzy c-means (FCM) clustering-primarily based totally characteristic weighting to come across Parkinson's sickness (PD) (FCMFW). Practical values of current conventional and non-well known measures had been implemented to the enter of FCMFW to differentiate healthful humans from people with PD through figuring out dysphonia. The essential dreams of the FCM clustering set of rules are to convert a linearly non-separable dataset right into a linearly separable dataset and to enhance elegance discriminating performance. The weighted PD dataset comes with a k-nearest neighbour (k-NN) category model. The pleasant k-cost became observed through searching at how k-values in a k-NN classifier modified while it became used to categorize Parkinson sickness datasets. Finally, they found that combining the proposed weighting approach dubbed FCMFW with the k-NN classifier produced the best results in the PD classification experiment.

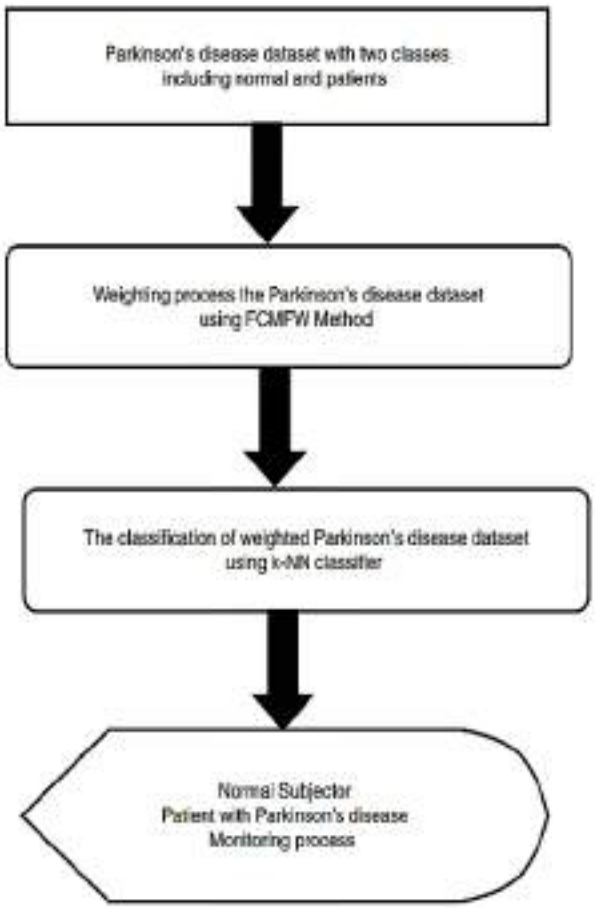

Figure 3. The block diagram of proposed method (Polat, Kemal 2012).

[7], In this study, feature selection is critical in classification to simplify the model and minimise the computational cost, especially when only a few inputs are required when the model is put to practical use. It's also utilised to make the model more transparent and understandable, allowing for a clearer explanation of potential diagnoses by removing irrelevant elements from the data set, which is a crucial necessity in medical applications. Noise can be decreased using the feature selection procedure to improve classification accuracy. They proposed a function choice method primarily based totally on fuzzy entropy measurements on this study, which turned into examined along a similarity classifier. The version is examined with 4 scientific statistics sets: dermatology, Pima-Indian diabetes, breast cancer, and Parkinson's disease. The researchers for this work tried to manage to get best results by only fewer features from the actual four data sets. Classification accuracy has been improved significantly with Parkinson's and dermatology data sets. With only two features out of 22 original ones, the imply type accuracy with Parkinson's statistics set is 85.03 percentage, and with dermatology statistics set, the imply accuracy turned into 98.28 percentage via way of means of using 29 capabilities in place of 34 authentic capabilities. Experiments have proven that once a function choice approach primarily based totally on fuzzy entropy measures is used with a similarity classifier, the outcomes are satisfactory.

[8], The study's important purpose is to apply a synthetic immune gadget to differentiate among

wholesome folks and sufferers with Parkinson's disorder (PD). Tele-tracking of the disorder making use of dysphonia (vocal characteristics) checks is essential with inside the premature identity of Parkinson's disorder (PD), because the signs of the disorder rise up in aged folks for whom direct visits to the health facility are bulky and costly. They attempted to capture the valuable features of automatic identification, learning, and adaptation by drawing inspiration from natural immune systems. Training bio inspired CLONCLAS is the base algorithm that the developed algorithms have. Satisfiable results are obtained from the results showing the substantial reliability of approach. Several characteristics from the artificial immune systems are extracted from the experiments established in this work. Hybridization of the immune system algorithms with other approaches such as Neural Network or genetic algorithm is the future scope for this research.

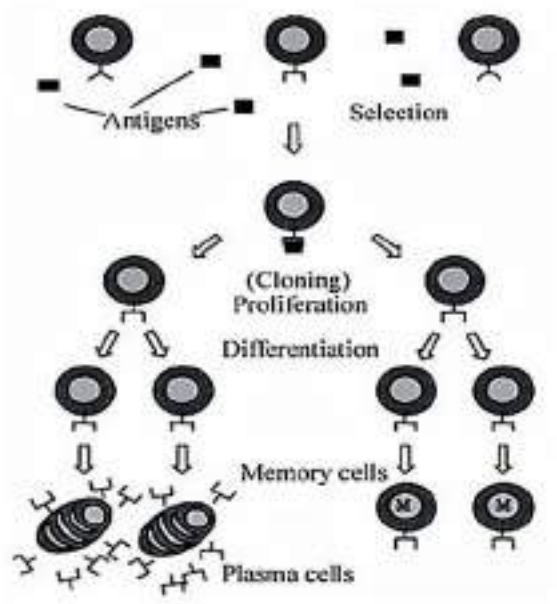

Figure 4. The clonal selection algorithm (Kihel, Badra Khellat, and Mohamed Benyettou 2011).

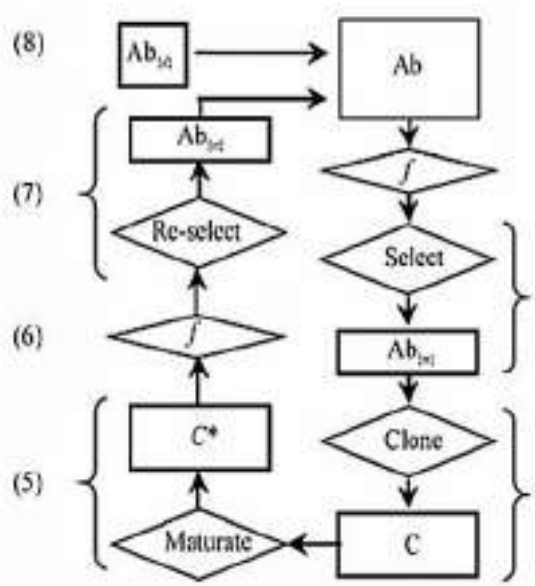

Figure 5. Clonclas train (Kihel, Badra Khellat, and Mohamed Benyettou 2011).

[9], Parkinson's disease is diagnosed using biomedical vocal measures acquired from incessant phonation samples. The six specific varieties of function choice techniques which are as compared of their studies to get the preferred effects are minimum-redundancy, maximum-relevancy(MRMR), Bhattacharyya, records gain, relief, t-test, and SVM (aid vector machine)techniques primarily based totally on recursive function elimination (SVM-RFE).Experiments conducted shown that 95.13% classification accuracy is obtained from SVM-RFE for Parkinson's disease dataset

[10], The degree and austerity of Parkinson's disease (PD) are essential standards to don't forget whilst making remedy selections. The mobility disorder Society-Unified Parkinson's Disease Rating Scale (MDS-UPDRS) is a beneficial device for assessing the maximum essential components of PD, but it does now no longer permit for PD staging. The Hoehn and Yahr (HY) scale offers staging, even though it does now no longer estimate numerous essential components of Parkinson's disease. They supplied a story and stronger staging for PD the usage of MDS-UPDRS characteristics, the HY scale, and developing prediction fashions on this study. They assessed the degree (normal, early, or moderate) and severity of PD the usage of ordinal logistic regression (OLR), guide vector machine (SVM), AdaBoost, and RUSBoost-primarily based totally classifiers. Aside from that, the price of Random forests functions in PD is estimated. The predictive fashions of SVM, Adaboost primarily based totally ensemble, Random forests, and probabilistic generative version that accomplished properly with the AdaBoost-primarily based totally ensemble had the nice accuracy of 97.forty six percentage of their studies. Body bradykinesia, tremor, facial [removed] hypomimia), fidelity of relaxation tremor, and handwriting are the maximum not unusualplace signs and symptoms of Parkinson's disease (micrographia). Finally, they located that once MDS-UPDRS is paired with classifiers, powerful equipment for predicting PD staging may be produced, which could resource therapists with inside the diagnostic process.

[11], Early identification of Parkinson's malady (PD) is regarded critical since it allows for the early implementation of treatment therapies and management methods. During their study period, however, approaches for early diagnosis remained an unmet clinical need in PD. The Patient Questionnaire (PQ) phase of the Movement Disorder Society-Unified Parkinson's Disease Rating Scale (MDS-UPDRS) is used for his or her study. As a result, gadget getting to know procedures together with logistic regression, random forests, boosted trees, and assist vector gadget (SVM) have become more and more more distinguished in biomedicine for classifying PD from healthful people at an early stage.

The researchers validate the machine learning approaches subject-by-subject and record-by-record. Their experiments classified early PD and healthy people with good accuracy and a large area under the ROC curve (both >95%). The logistic version indicates statistically large in shape to the data, suggesting its effectiveness as a prediction version. They determined that with the aid of using the usage of system mastering strategies to

hyperlink the objects of a questionnaire, prediction fashions have the capacity to useful resource clinicians with inside the prognosis process.

[12], The primary aim of this look at is to examine and evaluate sentiment evaluation of sufferers with Parkinson's ailment the use of deep getting to know and phrase embedding fashions. This is the primary look at to apply phrase embedding fashions and deep getting to know algorithms to assess social media for Parkinson's ailment. Word2Vec, GloVe, and FastText are phrase embedding fashions that may be used to complement tweets in phrases of semantics, context, and syntax. These are used on this investigation. Convolutional Neural Networks (CNNs), Long Short-Term Memory Networks (LSTMs), and Recurrent Neural Networks (RNNs) are utilized to put into effect the type approach. It is concluded that analyzing people's attitudes with the aid of using explaining the performance of using phrase embedding fashions and deep getting to know algorithms affords a useful addition to the remedy technique with a 93.sixty three percentage accuracy performance. This work's researchers additionally aimed to enhance a hybrid version that integrates textual and vocal facts recording facts if you want to useful resource with inside the early detection of Parkinson's ailment.

[13], Preliminary detection of Parkinson's disease (PD) is essential to slow the progression of symptoms and ensure therapy for PD patients. The pre-motor stage of PD is carefully observed, and Deep Learning techniques are introduced based on these pre-motor traits to identify if an individual gets impacted with PD or not at an early stage. Many signs used for preliminary detection of Parkinson's disease include rapid eye movement and loss of smell, dopaminergic imaging markers, and cerebrospinal fluid data. The researchers compared the recommended deep learning model with few machine learning and collaborative learning methods that use a tiny amount of data. Including 183 healthy people and 401 early-stage Parkinson's disease patients, the developed model showed the best detection efficiency, with standard accuracy rate of 96.45%. The consistency of the characteristics with the method of detecting EF is also determined by the amplification method. The research conducted in this study shows that the developed deep learning model is superior to 12 machine learning models used to distinguish between abled-bodies and Parkinson's disease patients.

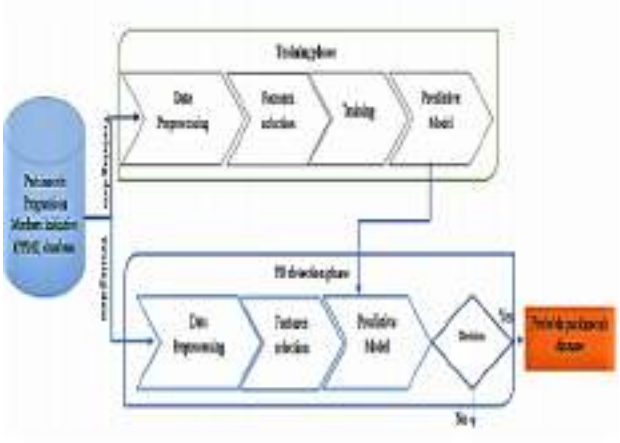

Figure 6. Flowchart of the proposed PD detection procedure (Wu Wang, Junho Lee, Fouzi Harrou & Ying Sun).

3. Comparison Study

The Research works done on Detection of Parkinson's Disease are compared and differentiated in the below tabular format.

Table 1.Tabular Format to Compare and Differentiate the Research works done on PD.

Related work	Research purpose	Algorithms	Accuracy
[1]	PNN was used to distinguish persons with Parkinson's Disease from healthy persons.	Three different PNN kinds were employed. 3 hybrid search 1. incremental search (IS) 2. Monte Carlo search (MCS) 3. Hybrid search (HS).	79% - 81%
[2]	Pitch Period Entropy (PPE) is used to distinguish healthy persons from patients with Parkinson's disease (PD).	Kernel support vector machine (SVM)	91.4%
[3]	(1) to choose a limited number of features (2) to develop a bias-free forecasting model	Machine to Support Vectors (SVM)	92.75%
[4]	to efficiently distinguish healthy individuals from PD patients	DMneural, Regression, Decision Tree and neural networks.	92.9%
[5]	to distinguish	There were two	95.38%

	between persons who are healthy and those who have Parkinson's disease	types of ANNs employed in this study. 1.Multilayer Perceptrons (MLP) and 2. Radial Basis Function (RBF) Networks	training and 94.72% testing
[6]	To identify between persons who are healthy and those who have Parkinson's disease	FCMFW and k-NN classifiers	72.16% (raw PD dataset), 97.93 (weighted PD dataset)
[7]	Fuzzy entropy measures are used to pick features.	Classifier for similarity	98.28%
[8]	Utilizing the artificial immune system to distinguish between healthy ones and individuals with Parkinson's disease (PWP)	Bio inspired CLONCLAS	87.50%, 88.54%
[9]	To compare feature selection strategies for Parkinson's malady diagnosis on vocal measures.	Bhattacharyya, information gain, relief, minimum-redundancy maximum-relevancy (MRMR), t-test, SVM,SVM-RFE	95.13%
[10]	Using the MDS-UPDRS features and the HY scale, present a new and better PD staging system.	Random forests, SVM, Adaboost based ensemble, and probabilistic generative models.	97.46%.
[11]	to create prediction models that can distinguish between early PD and healthy normal	Random forests, boosted trees, and support vector machines (SVM) and logistic regression	>95%
[12]	Using deep learning and word embedding models, analyse and compare people's sentiment analysis concerning Parkinson's disease.	Long Short-Term Memory Networks (LSTMNs), Convolutional Neural Networks (CNNs), and Recurrent Neural Networks (RNNs) and Long short-term memory networks (LSTMs)	93.63%
[13]	to determine if a person has Parkinson's disease or not based on pre-motor characteristics	twelve machine learning and ensemble learning methods, as well as a deep learning model	96.45%

From the above comparison table,

In the study [1], PNN was used to distinguish persons with Parkinson's Disease from healthy persons. Three different PNN kinds were employed 1. incremental search (IS) 2. Monte Carlo search (MCS) 3. Hybrid search (HS). Among these Hybrid Search has the best accuracy with Training accuracy as (81.74 %) Testing accuracy as (81.28 %).

In the study [2], Pitch Period Entropy (PPE) is used to distinguish healthy persons from patients with Parkinson's disease (PD). 91.4% of classification performance is achieved through kernel SVM.

In the study [3], the research purpose is (1) to choose a limited number of features (2) to develop a bias-free forecasting model. 92.75% of accuracy is achieved through SVM.

In the study [4], the purpose of the research is to efficiently distinguish healthy individuals from PD patients by using classification methods like DMneural, Regression, and Decision Tree and neural networks. 92.9% of classification accuracy is achieved through neural networks from the above four classification methods.

In the study [5], There were two types of ANNs employed Networks 1. Multilayer Perceptrons (MLP) and 2. Radial Basis Function (RBF) Networks. 95.38% training and 94.72% testing accuracies are achieved for the method ANFC-LH.and the total classification accuracy achieved through ANFC-LH is 96.77%.

In the study [6], FCMFW and k-NN classifiers are used. FCMFW has achieved classification accuracies 72.16% with raw PD dataset and 97.93% with weighted PD dataset.

In the study [7], Fuzzy entropy measures are used to pick features. 98.28% mean accuracy is achieved through similarity classifier with 29 features.

In the study [8], by Utilizing the artificial immune system to distinguish between healthy ones and individuals with Parkinson's disease (PWP) the Bio inspired CLONCLAS is trained and the results shown are 100%,100% as training accuracies and 87.50% and 88.54% as testing accuracies for Euclidian and hamming affinities respectively.

In the study [9], To compare feature selection strategies for Parkinson's malady diagnosis on vocal

measures the methods used are Bhattacharyya, information gain, relief, minimum-redundancy maximum-relevancy (MRMR), t-test, SVM, SVM-RFE. 95.13% is the best accuracy achieved through SVM-RFE.

In the study [10], the purpose is Using the MDS-UPDRS features and the HY scale and to present a new and better PD staging system. The methods used are Random forests, SVM, Adaboost based ensemble, and probabilistic generative model are all examples of probabilistic generative models. 97.46% is the highest accuracy achieved through Adaboost algorithm.

In the study [11], the purpose is to create prediction models that can distinguish between early PD and healthy normal. The methods used are Random forests, boosted trees, and support vector machines (SVM's) and logistic regression. All these methods produce highest accuracy and highest with both greater than 95% under the curve ROC.

In the study [12], the purpose is, using deep learning and word embedding models, analyse and compare people's sentiment analysis concerning Parkinson's disease. Long Short-Term Memory Networks (LSTMNs), Convolutional Neural Networks (CNNs), and Recurrent Neural Networks (RNNs) and Long short-term memory networks (LSTMs). 93.63% of performance is achieved by utilizing word embedding models and deep learning models in sentiment analysis.

In the study [13], the purpose is to determine if a person has Parkinson's disease or not based on pre-motor characteristics. Twelve machine learning and ensemble learning methods, as well as a deep learning models are used. 96.45% is the highest average accuracy achieved on all the models.

In all the above research works the main focus is to distinguish parkinson's subjects from the healthy ones majorly. But the study [13] focuses mainly on early detection of PD and feature importance. Though study [13] focuses on early detection there is no particular method proved to give the best results. So, the future work can be focused on the research of the specific method which gives highest performance when different types of methods such as deep learning models, ensembling models and machine learning models are considered.

The following graph shows the accuracy for the research works contributed before for diagnosing PD using various approaches and various methods as described in the above tabular form in correspondence with the study.

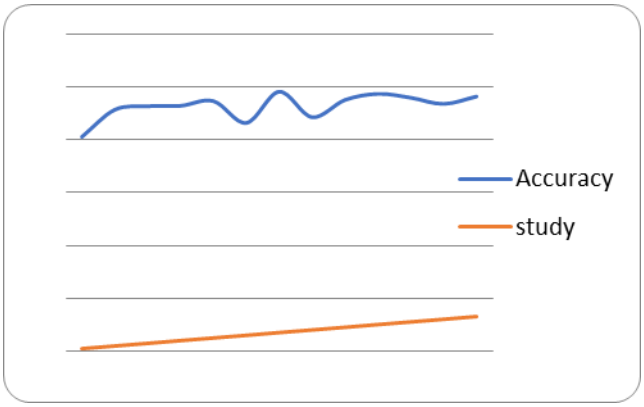

Figure 7. Graph showing accuracy in correspondence with studies from [1] to [13] in PD detection.

4. Conclusion/Future Work

According to the literature review, earlier research on Parkinson's Disease (PD) has primarily focused on distinguishing healthy persons from Parkinson's Disease sufferers. PNN, SVMs, Regression models, Decision trees, artificial immune systems (CONCLAS), ANN, k-NN, FCMFW, and other methods are utilised to distinguish healthy people from PD patients. And additionally models are developed to spot Parkinson's unwellness at AN early stage corresponding to SVM's, CNN, RNN, LSTM's, ensemble strategies and so on it's inferred that within the recent works published, although numerous methods are used for detective work palladium at an early stage, the performance measures may be valid as a key side in with efficiency distinctive the palladium at an early stage.So, the future work can be contributed with enhanced performance measures than the previous ones depicting that it was the best desired model in PD detection. Apart from this feature selection and feature importance can also be considered as the major scope of work to be concentrated as considerably less work is contributed in this aspect. The main focus of future work can be on evaluating the performance metrics for the Machine learning models, deep learning models and some ensembling techniques and the best performance is to be evaluated by considering the evaluation metrics and the method which gives highest accuracy can be considered as the best method in early detection of PD disease. Feature importance is also to be concentrated for future work as it has broader scope in research aspects in detecting PD accurately.

References

[1] Ene, Marius. Annals of the University of Craiova-Mathematics and Computer Science Series **35**, 112 (2008).
[2] Little, M. A., McSharry, P. E., Hunter, E. J., Spielman, J., & Ramig, L. O, IEEE transactions on bio-medical engineering, **56**, 1015 (2009).
[3] Sakar, C. Okan, and Olcay Kursun. Journal of medical systems **34**, 591 (2010).

[4] Das, Resul. Expert Systems with Applications, **37**, 1568 (2010).
[5] Caglar, Mehmet Fatih, Bayram Cetisli, and Inayet Burcu Toprak. Journal of Engineering Science and Design **1**, 59 (2010).
[6] Polat, Kemal. International Journal of Systems Science **43**, 597 (2012).
[7] Luukka, Pasi. Expert Systems with Applications, **38**, 4600 (2011).
[8] Kihel, Badra Khellat, and Mohamed Benyettou. JSEA **4**, 391 (2011).
[9] Eskidere, Ö. Sigma, **30**, 402 (2012).
[10] Prashanth, R., & Roy, S. D. Neurocomputing, **305**, 78 (2018).
[11] Prashanth, R., & Roy, S. D. International journal of medical informatics, **119**, 75 (2018).
[12] Çevik F, Kilimci ZH. Academic Perspective Procedia. **2**, 786 (2019).
[13] Wang W, Lee J, Harrou F, Sun Y. IEEE Access. **8**, 147635 (2020).

Machine Learning and Deep Learning Models for Diagnosis of Parkinson's Disease: A Performance Analysis

Publisher: IEEE

Cite This PDF

P. Mounika ; S. Govinda Rao All Authors

Downl PDF

Abstract: Parkinson's disease (PD) is a complex condition that is characterized by restricted mobility. Symptoms begin gradually, with only one hand exhibiting a minor tremor on oc... **View more**

Metadata

Abstract:

Parkinson's disease (PD) is a complex condition that is characterized by restricted mobility. Symptoms begin gradually, with only one hand exhibiting a minor tremor on occasion. Also, in the beginning stages of Parkinson's disease, your face may be expressionless. The fingers are not going to vibrate. Your voice may also become mute or slurred. Parkinson's disease indications and symptoms worsen with time. The focus of this thesis is to assess the efficacy of deep learning and machine learning strategies in discovering the best and most accurate strategy for early Parkinson's disease diagnosis utilising a vast dataset from the UCI machine learning repository of 5876 × 22 fields, which includes Parkinson's and healthy people details. Performance analysis of each method is done by considering the metrics like Precision, Recall, F1-Score, Support, Confusion Matrix, Specificity and Sensitivity and are plotted in graph showing training loss and accuracy. The highest accuracy of 97.43% is achieved for KNN with k=5 (K-Nearest Neighbors) algorithm which is a supervised machine learning approach.

Published in: 2021 Fifth International Conference on I-SMAC (IoT in Social, Mobile, Analytics and Cloud) (I-SMAC)

More Like This

Heart Disease Prediction using Innovative Decision tree Technique for increasing the Accuracy compared with Convolutional Neural Networks

2022 2nd International Conference on Innovative Practices in Technology and Management (ICIPTM)

Published: 2022

Predict the Performance Analysis of Supervised Learning Techniques Using Heart Disease Database

2021 2nd International Conference for Emerging Technology (INCET)

Published: 2021

Show More

Date of Conference: 11-13 November 2021

INSPEC Accession Number: 21527275

Date Added to IEEE *Xplore*: 20 December 2021

DOI: 10.1109/I-SMAC52330.2021.9640632

ISBN Information:

Publisher: IEEE

ISSN Information:

Conference Location: Palladam, India

Contents

Dr. Parkinson was the first to discover Parkinson's disease (PD). Parkinson's disease is described as "paralysis." Parkinson's disease is a neurological ailment characterised by tremors, stiffness, and stumbling, as well as difficulties with balance and coordination. Symptoms of Parkinson's disease normally appear gradually and worsen with time. People may find it difficult to move and communicate as the condition develops. Insomnia, sadness, unconscious satiety and weariness, as well as psychological and behavioural changes, are also possible. Parkinson's disease can strike anyone, regardless of gender. They are 50 percent more prone than women to develop this condition. The major cause of Parkinson's disease is age. 5-10% of people have the PD before 60 which is "early onset" disease. But majority of individuals develop PD after the age 60.

A Survey on Leukemia Detection using Image Processing Techniques

Mohammed Junaid Ahmed[1,*], Padmalaya Nayak[2]

[1]Mtech Student, Computer Science and Engineering, GRIET, Hyderabad, Telangana, India.
[2]Professor, Computer Science and Engineering, GRIET, Hyderabad, Telangana, India.

Abstract. Leukemia detection and diagnosis by inspecting the blood cell images is an intriguing and dynamic exploration region in both the Artificial Intelligence and Medical research fields. There are numerous procedures created to look at blood tests to identify leukemia illness, these strategies are the customary methods and the deep learning (DL) strategy. This survey paper presents a review on the distinctive conventional strategies and Deep Learning and Machine Learning methods towards that have been utilized in leukemia illness diagnosis dependent on platelets images and to analyze between the two methodologies in nature of appraisal, exactness, cost and speed. This article covers 11 research papers, 9 of these examinations were in customary strategies which utilized image handling and AI (ML) calculations, such as, K-closest neighbor (KNN), K-means, SVM, Naïve Bayes, and 2 investigations in cutting edge procedures which utilized Deep Learning, especially Convolutional Neural Networks (CNNs) which is the most generally utilized in the field leukemia detection since it is profoundly precise, quick, and has the smallest expense. What's more, it dissects various late works that have been presented in the field including the dataset size, the pre-owned procedures, the acquired outcomes, and so forth. At last, in view of the led study, it very well may be reasoned that the proposed framework CNN was accomplishing immense triumphs in the field whether in regards to highlights extraction or classification time, precision and also a best low cost in the identification of leukemia.

1 Introduction

Now a day's Leukemia outlines a significant medical condition. In various foreign nations, a great several people are dying as a result of cancer. Generally, on the off chance that we take a proportion of the number of individuals who experience malignant growth in the course of their life, it will get 1:2 on account of men and 1:3 on account of women. Among several illnesses, the chase for getting a handle on disease, a threatening neoplastic issue is in the bleeding edge research region for some analysts like scientists, physicists[1]. Malignancy can be characterized as a few gatherings of infections each with its own pace of development, fix, and treatment. In any case, a wide range of tumors is distinguished by the unsuppressed development of strange cells inside the body which ultimately spread to various pieces of the body and can deteriorate step by step if not analyze and treated appropriately[2].

In this paper, we studied hematological neoplasia for example leukemia, myeloma, and lymphoma. These kinds of issues can influence the blood, bone marrow, and lymphatic framework. According to a review done by Leukemia and Lymphoma society, it was approximated that in 2012 an aggregate of 148,040 have been analyzed, and 54,380 kicked the bucket of leukemia, lymphoma, and myeloma in the US. In India, the complete number of people experiencing blood disease was assessed to be roughly 104,239 out of 2010. Besides, according to the Indian Association of blood malignant growth and partnered infections, among every one of the diseases which are hazardous and can cause demise, Leukemia (white platelet disease) comprises 33% of youth disease. The attributes of leukemia are the multiplication of white platelets that are not typical in the affected bone marrow without repressing cell development.

Both ALL and AML are classes of cancer that are very crucial to diagnose. AML stands for acute myelogenous leukemia which is a blood cancer. A higher number of B lymphocytes is typically associated with ALL than T lymphocytes. They play a vital role in protecting the body from germs and contamination and destroying any cells that have been tainted. Particularly B cells are tasked with maintaining the body's immunity and eliminating germs that may contaminate it. Each was grouped into three types: L1, L2, and L3 [3].

All of these diseases display symptoms similar to other diseases, therefore, diagnosing them is difficult. A microscope is used to examine the blood as part of a leukemia determination strategy. The purpose of this test is to look for abnormally formed white blood cells, which may indicate disease. Since long back, the investigation has been performed by experienced administrators, who generally conduct two examinations: characterization and tally of cells (which is performed

* Corresponding author: mja.hyd97@gmail.com

using a cytometer today). In most cases, morphological evaluations may well be conducted by means of a single photograph rather than a blood test. Along these lines, this examination doesn't need coordination with done because of the costly expense, precision is generally something similar for various pictures, and the framework is distant screening [3].

In the field of Deep Learning and Convolutional Neural Networks, the detection of different stages of leukemia using the microscopic images, in order to detect the disease stage, the image processing does six stages: 1. Image Acquisition, 2. Image Pre-processing, 3. Image Segmentation, 4. Feature Extraction, 5. Detection of cells and finally 6. Classification of cells. Some new works identified with WBCs and RBCs division depend on shading space, for example, HSI shading space, and RGB. The other strategy uses ordinary AI strategies and image processing procedures, and data processing techniques for example, K-Means clustering, Watershed Segmentation, Support Vector Machines and Fuzzy logic C-Means clustering etc.

In this paper furtherly discussed different methodologies that are used for Leukemia classification and detection by different researchers are presented in Section 2, Section 3 outlies the conclusion and Section 4 reveals the future scope and future research.

2 Literature Survey

In 2009, Abdul Nasir et al., utilized a thresholding strategy in deciding the proportion of platelets for malignant growth cell location. In this paper picture 596processing, strategies have been utilized to tally the number of platelets in the biomedical picture. With this tallied estimation of platelet, the proportion of platelet for leukemia is determined. The first picture is changed over to a grayscale picture for which an edge estimation of power is set to separate WBC to RBC (thresholding changes over a grayscale picture to a twofold picture). In the event that outcomes are not fulfilled the interaction is rehashed by setting another edge esteem. The outcomes obtained utilizing the thresholding procedure show that the proportion of RBC and WBC for a typical picture to the strange picture has an alternate scope of proportions. The proportion of a typical picture is 0 to 0.1, while the proportion of a strange picture is 0.2 to 2.5 for all and 0 to 14 for AML. The problem with this strategy is that setting appropriate limits would be extremely time-consuming and difficult[4]

In 2010, Subrajeet Mohapatra et al., Proposed a minimal effort and the proficient solution to utilize image processing analysis for quantitative assessment of stained blood microscopic scanned pictures for leukemia identification. A two-stage color segmentation system is utilized for isolating leukocytes or white platelets (WBC) from other blood segments. Discriminative highlights for example core shape, the surface is utilized for the last discovery of leukemia. In the current paper two novel shape highlights i.e., contour signature and Hausdorff measurement are executed for classifying a lymphocytic cell core. Backing Support Vector Machine (SVM) is utilized for characterization. An aggregate of 108 blood smear pictures was considered to include extraction and the last presentation assessment is approved with the aftereffects of a hematologist[5]. They have followed the method to extract the features which is image grabbing, preprocessing the image, Color conversion which is RGB to L*a*b color space to make the color-based clustering, Image segmentation for separating the WBC from the microscopic scanned images for this K-Nearestneighbor classification and K-means to select the sample region randomly, later Sub imaging and finally feature extraction.
They used the image size of 512 x 512for evaluation and used sequential process.The features extraction in this proposed model is SVM for training classifier and achieved accuracy of 95% was observed.

In 2010, Adnan Khashman et al.,The author proposes, in his paper, that morphological examination has been applied to leukemic photographs, from there on dividing them in two parts and obtaining improved views of the cytoplasm and core regions. To get images of cytoplasm and cores, we used bimodal thresholding, where two edge forces were given, and the border of the contaminated cell was followed, while unfavorable items were gathered from the surrounding areas. As a result, 98.33% of the generally adequate division proportion was obtained[6].

In 2011, R. D. Labati et al., come up with a novel idea of bringing the blood sample dataset which is specifically aligned for the examination and comparison of the algorithm performance for segmentation and classification. Every image in the dataset the classification of cell image is provided also specific set of merits to compare the performances of multiple algorithms. They made cancer images in JPG format and maintained the 24-bit color depth and resolution of the images is maintained which is 2592 x 1944 and separated into two versions 1. ALL-IDB1 and 2. ALL-IDB2 and they made the dataset available to the public as a freesource. They classified the dataset using the confusion matrix and evaluated using the parameters called True positive (TP), True Negative (TN), False Positive (FP) and False Negative (FN). 1.True Positive (TP) which is used to find out the number of elements classified as positive correctly, True Negative (TN) which is used to find out the number of classified as negative, False Positive (FP) which is used to find out the number of elements classified as positive but false and False Negative (FN) used to find out the number of elements classified as negative but false. Using these parameters, they found out the classification error which is 45.37% on first image set ALL-IB1 and they got a classification error of 50%[7].

In 2013, M. D. Joshi et al., was the first to propose a system to improve and divide the picture and a KNN classifier was used to characterize the shoot cells from typical lymphocytes. In the public picture dataset for leukemia investigation, 108 pictures can be used as part of the framework. Ninety-three percent of the time, this strategy has worked. Nonparametric factors are arranged using the k Nearest-Neighbors (KNN). It can also be used to separate white platelets from shoot cells using

this method, which is straightforward but extremely effective [8].

In 2014, Monica Madhukar et al., Proposed a technique which automatically does the detection as well as segmentation of Acute Myelogenous Leukemia using microscopic scanned images of blood smears. This proposed approach differs from the other approaches. 1. The simplicity of the developed approach. 2. Classification of total blood smear images as opposed to sub images and 3. Algorithmsto detect and segment nucleus cells.A minuscule blood picture of size 184 × 138 is considered for assessment. The predominance of the plan is exhibited with the assistance of an analysis. Highlight extraction with and without the LBP administrator introduced extremely fascinating outcomes. The framework built without utilizing the LBP administrator gave productivity of 93.5%. Each of the three approval techniques was consolidated into our framework. In any case, the exhibition of HD (Hausdorff dimension), specifically, subsequent to utilizing LBP (Local binary pattern) expanded the classifier execution by 4%[8]. By utilizing LBP, the edges of the cores of the myeloblasts were removed in an exceptionally articulated way. This successful edge location upgraded the HD, as the case mean AML was substantially more than the crate means non-AML pictures. To see the effect of HD in the list of capabilities, the classifier was run with HD as the solitary component. This was done twice, once with applying LBP administrator and once without LBP administrator. Every one of the boundaries for assessment was removed for the two sets. It was seen that, when LBP was not utilized, the HD execution was uniquely around 70%, though when LBP was utilized, the rate heightened to 93%. This obviously shows the impact of the LBP administrator on the framework. To see the viability of the created calculations, a preliminary was run contrasting the framework's presentation on sub images and entire pictures. The acquired outcomes further substantiated the effect of the LBP administrator.

In 2014, JakkrichLaosai et al., Developed an algorithm to analyze color pictures of stained fringe blood spreads and recognize the types of White Blood Cells (WBC) from them [9]. In the interaction, features are extracted, segmentation is performed, and classification is performed. Research for this project focuses on the characterization of Foil of Bretagne (lymphoid) and Almeida Lloyd (myeloid). In order to distinguish anomalies and guarantee the analysis, doctors must examine and distinguish abnormalities. The trial results showed that the presentation of ID leukemia utilizing our process of picture preparation could order 100 example pictures of lymphoid undifferentiated organisms as well as myeloid undeveloped cells. Using clustering techniques in K-Means, this technique has been tested. Using obvious signs of shape and surface, highlights emerge from the divided cytoplasm and core. Different classifiers have been investigated on various blends of capabilities. The outcomes introduced here depend on preliminaries led with typical cells. The best utilizing SVM was of 92% [10].

In 2014, Chaitali Raj et al., Proposed a model called nucleus segmentation which is implemented using LabVIEW and MATLAB. By using the histogram equalization method in LabVIEW environment, they segmented the nucleus from the segmented image by using statistical parameters such as MEAN and SD. By calculating the perimeter of each cell, 128 microscopic images were examined and features were extracted from them. In the test, the cells are categorized into blasts or normal cells based on cell feature values. The nucleus segmentation of images is achieved in the MATLAB environment by converting all the scans from RGB to grayscale so the nucleus part of the cell will appear the darkest part of the image. The examination shows how difference extending, for example, straight differentiation extending and histogram balance can be consolidated along with the utilization of picture math tasks to get rid of the individual pieces of the white platelet while keeping the core of the white platelet. This example also shows how filtering can make the nucleus easier to detect by a threshold by making it darker [11].

In 2015, Romel Bhattacharjee et al., come up with an idea of an automated blood smear image analysis system which is very grate tool for identifying the detection of Acute Lymphoblastic Leukemia. The fundamental way of diagnosing the cancer is divided into 6 following steps which is 1. Input the image which means sending the blood scan report as an input 2. Image grabbing and cropping 3. Pre-processing 4. Segmentaion, 5. Feature extraction and finally 6. Classification

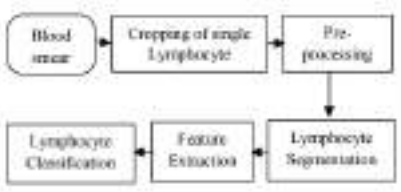

Fig.1. Automated blood smear image analysis

In this experiment the researcher done the comparison of segmentation accuracy of the proposed algorithms. Which is

1. Fuzzy K-Means Clustering in L*A*B* color space in which features are not discussed and the segmentation accuracy of 92% achieved.
2. Fuzzy C means clustering technique is used to and extracted the features like Area, Perimeter, Compactness, Solidity, Homogeneity, and Entropy and achieved an segmentation accuracy of 93%.
3. Watershed transform and HSV color model and achieved an segmentation accuracy of 94.5%.
4. Arithmetical operations and Otsu's thresholding segmentation technique is used to find out the features like Area, Perimeter, Circularity and achieved a segmentation accuracy of 93%.
5. Finally Morphological operator's segmentation technique is used and extracted features like Area, Perimeter, Circularity, Axis Length, Form Factor and achieved 96.67%

Apart from these researchers Romel Bhattacharjee et al., experimented using Cross validation, KNN, SVM and AVM classifiers are trained and tested over the dataset. Despite the fact that 75% of the information is taken to prepare the classifiers independently for the exhibition checking of the classifiers by cross-approval, every oneof the classifiers is likewise tried to have the most unnumber of info information for preparing and to createthe ideal yield. KNN is taken care of with 6 example information, SVM with 10, ANN with 20 and K-implies Clustering is finished with 10 example information, where the classifiers produce an equivalently decent yield. kNN with 6 example information delivers a particularity of 95.23% and furthermore has the least computational intricacy. Along these lines, a Graphical User Interface (GUI) has been readied utilizing MATLAB–GUI with KNN classifier for simple, quick, and powerful ID of ordinary and impact lymphocytic cells[12].

In 2017, Shaikh Mohammed Bilal N et al., proposed the computer aided leukemia detection using the digital image processing techniques[13]. In this proposed system is a classification of a cell model utilizing different cell morphological highlights. For this reason, it is important to do a pixel-level pre-processing and the segmentation of the nucleus and cytoplasm. This methodology thinks about segmentation as a vital undertaking for the separation of platelets. Segmentation ends up being precise and has viable outcomes on such clinical analytic machine-based methodologies. Henceforth as a choice, we utilize a cell division methodology that thinks about shadings, surfaces, and different highlights even in overpopulated cell smears of blood at the pixel level picture assessment accordingly extricating the cytoplasm and core in something very similar. The cytoplasm foundation cells and core separation make this work upgrade its outcomes interestingly with different works. in order to boost the proficiency and precision (over 90%) along these lines diminishing time intricacy of each assignment in the calculation for example utilized a basic quick calculation, for example, DFT or FFT alongside methodology in MATLAB for picture handling, ANN and SVM for classification purpose WEKA as opposed to utilizing all algorithms. Ordered finding prompting sublevel detection of cancer ALL by implementing image processing techniques utilizing MATLAB followed by the arrangement and subtype grouping utilizing SVM alongside ANN.

In 2019 Supriya Mandal et al.,DTS Mirafra Software Technologies Pvt Ltd Bangalore, India introduced a methodology for malignant growth cell detection by extricating significant highlights from the platelet pictures and learning various classifiers. they observed that Gradient-Boosting Decision Tree classification calculations give preferred outcomes over Support Vector Machine[14]. they also additionally inferred not many significant highlights like the presence of nearby nuclei and the proportion of inconsistency looks like a nucleus, which essentially affects malignant growth cell location. Our procedures can be utilized in a restricted figuring climate without a Graphics Processing Unit.

This recommended method to identify ALL cancer cell is classified into four segments such as 1. Pre-processing, 2. feature extraction, 3. classification model building and 4. evaluation of classifier. The researcher calculated the sensitivity, F1 score, AUC, specificity from the training dataset to evaluate the performance of all three classifiers[15]. Also, they separately estimated the result of characteristics like neighboring nuclei, area variation of the shape of nuclei of the convex framework toward the LightGBM model. Also, they have attuned the classification applying the probability assessment of determining or identifying cancer cells employing the LightGBM model. In this experiment probability threshold value of 0.52 gives the best performance of the model extracted highlights from pictures and constructed a classifier utilizing SVM and Gradient Boosting Decision Tree (GBDT) to run on different platforms. This picture classifier utilizing GBDT likewise gives cutting-edge execution for malignancy cell discovery. They investigated numerous highlights which is a unification of mathematical, surface, and analytical highlights of the cell pictures. this study shows that GDBT based classifier outflanks the Support Vector Machine model. Additionally, this model study explains that the form of nearby cell cores and region contrast essentially affects the discovery of malignancy cells.They have accomplished an 85.6% of F1 score on validation learning.

Table 1. Algorithm & Accuracy.

Year	Author	Algorithm/ System	Accuracy
2009	Abdul Nasir et al	Thresholding strategy to convert the image into grayscale to find out the edges of the cell	-
2010	Subrajeet Mohapatra et al.,	Hausdorff measurement, K-Nearest neighbor classification and K- means to select sample, SVM for training	95%
2010	Adnan Khashman et al.,		98.33%
2011	R. D. Labati et al.,	Classified the dataset using True positive (TP), True Negative (TN), False Positive	Error – 45.37% on ALL-IB1 Error – 50% on ALL-IB2

		(FP) and False Negative (FN).	
2013	M. D. Joshi et al.,	KNN Classifier	93%
2014	Monica Madhukar et al.,	Image Processing Hausdorff dimension (HD), Local binary pattern (LBP)	HD – 70%. LBP- 93%
2014	JakkrichLaosai et al.,	KNN and SVM	92%
2014	Chaitali Raj et al.,	LabVIEW MATLAB	-
2015	Romel Bhattacharjee et al.,	FUZZY logic	92% 93% 94.5% 93% 96.7%
2017	Shaikh Mohammed Bilal N et al.,	SVM and ANN	90%
2019	Supriya Mandal et al.,	SVM Gradient Boosting Decision Tree (GBDT) LightGBM	85.6%

3 Conclusion

Research in this work examines various methods of leukemia cancer detection based on deep learning, image processing, and machine learning. By combining deep learning and image processing, it is possible to accelerate the cycle of leukemia analysis and enhance the chances of removing leukemia patients from further harm. A technique of image processing can overcome the subjectivity of a microscopist's operating in situations where the eyewitness's involvement and health level affect the results. In future studies, analysts might consider arranging ALL cells by subtype, for instance, L1, L2, and L3, rather than only separating dangerous and non-carcinogenic cells. In addition to gaining numerous highlights and finding other proper highlights, there is the opportunity to detect the kind of acute leukemia. To get proficient and delegated details, you can apply component determination and dimension reduction methods. Further investigation may also be undertaken in the case of another leukemia type like acute myeloid leukemia or AML, and those subtypes, since the majority of these investigations actually focus on ALL exclusively. Having attempted to characterize ALL versus AML by this point, we could find out which and what ALL and AML types there are.

4 Future Work

In future research we are planning to implement the CNN model for classification and detection of ALL and AML Leukemia cells and their subtypes to determine the type of Leukemia

References

1. S. Mishra, B. Majhi, P. K. Sa, 3rd Int. Conf. Recent Adv. Inf. Technol., 460-466, (2016)
2. A. Belhekar, K. Gagare, R. Bedse, Y. Bhelkar, K. Rajeswari, M. Karthikeyan, Proceeding - IEEE Int. Conf. Comput. Commun. Autom. ICCCA, (2019).
3. R. G. Bagasjvara, I. Candradewi, S. Hartati, A. Harjoko, Proc. - 2nd Int. Conf. Sci. Technol.-Comput. ICST, (2016)
4. Abdul Nasir, Aimi Salihah & Mustafa, Nazahah, Mohd Nasir, Nashrul, Int. Conf. Comput. Intell. Man-machine syst. Cybernetic - Proc, (2010)
5. S. Mohapatra and D. Patra, Int. Conf. Syst. Med. Biol. ICSMB, 49-54, (2010)
6. Adnan Khashman, Esam Al-Zgoul, In Proceedings of the 4th WSEAS international conference on Computer engineering and applications, (2010)
7. R. D. Labati, V. Piuri, F. Scotti, 18th Int. Conf. Image Process. ICIP., (2011)
8. Joshi, M. D., A. H. Karode, Int. J. Emerg. Technol. Learn., (2013)
9. S. Agaian, M. Madhukar, A. T. Chronopoulos, IEEE Syst J, **8**, 995-1004, (2014)
10. J. Laosai, K. Chamnongthai, Int. Electr. Eng. Congr. iEECON, (2014)
11. C. Raje, J. Rangole, Proc. IEEE Int. Conf. Commun. Signal Process. ICCSP, 255-259, (2014)
12. R. Bhattacharjee, L. M. Saini, Communication and Information Technology Conference, (2015)
13. M. B. N. Shaikh, S. Deshpande, IEEE Int. Conf. Recent Trends Electron. Inf. Commun. Technol. RTEICT 2017 - Proc., (2017)
14. S. Mandal, V. Daivajna, R. V, INDICON 2019 - 16th IEEE India Counc. Int. Conf., 1-4, (2019)
15. R. G. Bagasjvara, I. Candradewi, S. Hartati, A. Harjoko, Proc. - 2nd Int. Conf. Sci. Technol.-Comput. ICST, (2016)

Detection of Lymphoblastic Leukemia Using VGG19 Model

Publisher: IEEE

Mohammed Junaid Ahmed ; Padmalaya Nayak All Authors

Abstract: Acute Lymphoblastic Leukemia (ALL) and - Acute Myelogenous Leukemia (AML) is a terminal blood cell cancer that takes birth due to the uncontrolled growth of white blood c... **View more**

Metadata

Abstract:
Acute Lymphoblastic Leukemia (ALL) and - Acute Myelogenous Leukemia (AML) is a terminal blood cell cancer that takes birth due to the uncontrolled growth of white blood cells which results in deathif not diagnosed in earlier stages. To diagnose leukemia, oncologists perform multiple tests on bone marrow and white blood cells. Manually diagnosing this disease is sometimes leads to less accuracy due to human error and expecting expert suggestions and supervision for diagnosing the cancer is a time-consuming process that leads the patient into life-threatening stages. To get a precise diagnosis, this research work proposes deep learning and image processing techniques. There are few research studies on Acute Lymphoblastic Leukaemia (ALL) that have been tested and achieved good results even though it is not precisely predicted and not in practical usage. This research paper proposes further improvements in classification and an accurate CNN model helps to predict and classify the type of Leukaemia. This research work experiments the VGG19 model architecture by using the ImageNet dataset.

Published in: 2021 Fifth International Conference on I-SMAC (IoT in Social,

Date of Conference: 11-13 November 2021

INSPEC Accession Number: 21475570

Date Added to IEEE *Xplore*: 20 December 2021

DOI: 10.1109/I-SMAC52330.2021.9640955

ISBN Information:

Publisher: IEEE

ISSN Information:

Conference Location: Palladam, India

Contents

White cells of various kinds are present in the human body. Leukemia is a platelet-damaging condition marked by an increase in the number of white blood cells, the majority of those are young adult cells, which corrupts other cells. In today's world, lab studies take a longer duration to break down leukemia conditions, which is also dull, monotonous, and tedious. The ratio of white platelets to RBC in the human body is 1000:1, which implies that for every thousand RBC, one white platelet is produced. As a result, the quantity of white platelets in the blood rapidly grows, and the person is diagnosed with leukemia. When the number of white cells in the body increases, these young cells begin to annihilate the rest of the body's cells.

A Survey on Cardiovascular Prediction using Variant Machine learning

*L.*Chandrika[1,*], *Dr. K.*Madhavi[2], *B.*Sindhuja[3], *M.*Arshi[4]

[1]PG Student, Computer Science and Engineering, GRIET, Hyderabad, Telangana, India.
[2]Professor, Computer Science and Engineering, GRIET, Hyderabad, Telangana,India.
[3]Assistant Professor, Computer Science and Engineering, GRIET, Hyderabad, Telangana, India.
[4]Assistant Professor, Computer Science and Engineering, GRIET, Hyderabad, Telangana, India.

Abstract. Prediction of a cardiovascular diseases has always a tedious challenge for doctors and medical practitioners. Most of the practitioners and hospital staff offers expensive medication, care and surgeries to treat the cardiovascular patients. At early-stage of prediction of heart-oriented problems will be giving a chance of survival by taking necessary precautions. Over the years there are different types of methodologies were proposed to predict the cardiovascular diseases one of the best methodologies is a Machine learning approach. These years many scientific advancements take place in the Artificial Intelligence, Machine learning, and Deep learning which gives an extra push up to help and implement the path in the field of medical image processing and medical data analysis. By using the enormous dataset from various medical experts used to help the researchers to predict the coronary problems prior to happening. Many researchers have tried and implemented different machine learning algorithms to automate the prediction analysis using the enormous number of datasets. There are numerous algorithms and procedures to predict the cardiovascular diseases and accessible to be specific Classification methods including Artificial Neural Networks (AI), Decision tree (DT), Support vector machine (SVM), Genetic algorithm (GA), Neural network (NN), Naive Bayes (NB) and Clustering algorithms like K-NN. A few examinations have been done for creating expectation models utilizing singular procedures and additionally concatenating at least two strategies. This paper gives a speedy and simple survey and knowledge of approachable prediction models using different researchers work from 2004 to 2019. The examination indicates the precision of individual experiments done by various researchers.

1 Introduction

The heart is a significant organ which plays crucial part of every living being especially in humans. It pumps blood to all parts of our life systems. In case of failing to pumpor doesn't work accurately, the mind and different organs will quit working, and inside couple of moments, the individual will pass on. Changes in way of life, business related pressure, and terrible food propensities add to the expansion in the pace of a few heart-related sicknesses.

Heart sicknesses have arisen as perhaps the most unmistakable reasons for death all around the planet. The expanding populace in heftiness and smoking, the mortality from coronary sicknesses is slowly on the ascent, which has gotten the "best executioner" that compromises human wellbeing contrasted with malignant growth, Helps, and different illnesses, whatever age, character or area. As per WHO Coronary-related issues are responsible for the death of 17.7 million people every year, around 31% of worldwide death mortality.Especially in India, coronary illness became primary cause of mortality. Coronary problems causes the death of 1.7 million in 2016, In 2016 Global Burden of Disease Report, issued on 15th September 2017.

Coronary illness analytics states that the expenditure on hospitalization and treatment is gradually increased compared to the previous years and also diminishesthe survival rate of a person. Evaluations of WHO, explains that in India cardiac patients has spent around $237 billion, in the span of 10 years from 2005-2015. In this way, attainable and precise expectation of coronary related illness is vital.

The health care industry and health care research organisations collects the abundant data of patients,in which DM techniques are not used. The clinical data of the patients have covered up designs that are fundamental for data examination in the location of coronary illness. Coronary illness is a main source of death worldwide for as far back as 15 years. As the heart pumps the blood there is a possibility of on and off condition comes when the blood circulates inside the body which is inadequate, the rest of the organs inside the patient body especially brain and heart stops working, which causes the sudden death in few seconds. The importantelements are distinguished as age, hypertension, diabetes, family ancestry, tobacco, smoking, very high levels of cholesterol, daily routine of alcohol, actual dormancy, stoutness, chest torment, and eating junk food routine[1].

Data gathered by inspecting the verified records of the inpatient.it is feasible to separate the details and

* Corresponding author: lingalachandrika97@gmail.com

Survey Analysis of Solar Power Generation Forecasting

Deekshitha Erlapally[1,*] *Dr. K.*Anuradha[2], *Dr.G.*Karuna[3], *V.*Srilakshmi[4], *K.*Adilakshmi[5]

[1]MTech Student, *Computer Science and Engineering*, *GRIET,* Hyderabad, Telangana, India.
[2]Professor, *Computer Science and Engineering*, *GRIET*, Hyderabad, Telangana, India.
[3]Professor, *Computer Science and Engineering*, *GRIET*, Hyderabad, Telangana, India.
[4] Asst.Professor, *Computer Science and Engineering*, *GRIET*, Hyderabad, Telangana, India.
[5] Asst.Professor, *Computer Science and Engineering*, *GRIET*, Hyderabad, Telangana, India.

Abstract: Solar power is the conversion of sunlight into electricity using solar photovoltaic cells as a source of energy. There are various applications for solar power; here is information on PV cell generation. We seek to understand the behavior of solar power plants through the data generated by the photovoltaic modules and the power generation in different weather conditions in India. The goal of this survey is to give a thorough assessment and study of machine learning, deep learning and artificial intelligence. Artificial intelligence (AI) models as well as information preprocessing techniques, parameter selection algorithms and predictive performance evaluations are used in machine learning and deep learning models for predicting renewable energies. But in case of time series data we can predict only the errors using a linear regression model, we can also calculate things like root mean square error (RMSE), mean absolute error (MSE), mean bias error (MBE) and mean absolute percentage error (MAPE). By the analysis of weather condition also we can predict the consumption of current by solar for every 15 minutes, 1day, and 1week or even for 1 month and find the accuracy.

1. Introduction

Solar energy has many benefits, including its sensitivity to imitative circumstances such as increasing oil prices, its renewable nature, and its ability to reduce imports and dependence on foreign resources. Despite the fact that photovoltaic cells are recognized as the significant source of potential energy production, their low return on investment and high upfront costs keeps them from becoming widely used. Since photovoltaic cells generate electricity by converting solar energy into electrical energy, the amount of solar energy produced every day is important to the size of the photovoltaic system, because the amount of solar radiation determines the amount of Major grid [17] integration is difficult because renewable energy is irregular and uncontrollable. Households in India can now use almost any amount of energy due to the recent electric grid at any moment, but it is not equipped for large quantities of uncontrollable generation [10] at this time. As it is converting solar radiance into power we don't get that how much power is emitted for different location, time, and weather. For this type of clarification machine learning techniques are used in order to differentiate it for different conditions.

electricity produced every day. This is influenced by factors such as place, time, and weather patterns. Solar irradiance is the power obtained per unit area from the Sun via electromagnetic radiation in the wavelength range of the solar cell that is in use [13].

Here we seek and analyzed India as a place and the temperature power plants as consideration based on weather condition in India. According to power generation commissioning statistics, solar plants have the largest installed capacity growth dynamics among renewable energy power plants. Making realistic solar generation projections for the day ahead view is becoming an increasingly critical issue in many places throughout the world at the current level of power system development.

Machine-learning techniques are wide applied to several fields where it can separate the weather based power. Machine-learning techniques are wide applied to several fields related to data-driven issues. Machine-learning techniques embrace several knowledge domain areas, like statistics, arithmetic, Ann, data processing, optimization, and computation are all terms that come to mind when thinking about artificial neural networks [18].

Deep learning, a sub-field of machine learning, has been blooming recently due to the rapid expansion of data

technology in hardware and code. Deep Learning calculations have only been used sparingly in the past for determining environmentally friendly power plants. We present these amazing calculations in the field of sustainable power determining by utilizing distinct Deep learning and ANN[16] calculations, such as DBN, Auto Encoder, and LSTM. In our tests, we integrated these calculations to show how effective they are in calculating the energy yield of solar-powered power plants as compared to a traditional MLP and an actual anticipating model. Our outcomes utilizing Deep Learning calculations show a better determining execution thought about than Artificial Neural Networks, like other reference models including such actual models, are artificial neural networks. In the literature, these models are compared with selected machine learning methods and are available predictive models. Using the mean square error, the proposed cloud classification ensemble model reduces the mean square error by 10.49%, 7.78% and 7.95% respectively, with deep belief networks, support vector regression and random forest [15] regression models. The use of weather parameters to forecast solar power generation is suggested as an Artificial Neural Network (ANN). This discussion describes the techniques used to predict renewable energy in machine learning models, including data preprocessing techniques, parameter selection algorithms, and predictive performance measurement.

2. Related Work

Energy is now the primary source of socioeconomic growth. However, because of the increasing rate of environmental concern, renewable energy is attracting a lot of attention. Related to the ongoing depletion of fossil fuels, this alternative energy source is gaining in popularity. That is the energy that comes from the sun, wind, rain, and other natural sources [3].To generate electricity at power plants, electromechanical generators are used, and they are mostly driven by chemical combustion or even nuclear fission heat engines, but also by alternative energy sources such as kinetic energy from flowing water and wind. There are numerous other technologies, such as solar photovoltaic and geothermal power, can and are used to produce electricity. Using thermal power: This method is used in thermocouples, thermopiles, and thermionic converters to convert temperature differences directly to power. Thermal power station is a power plant with a steam-driven primary mover. The water is heated and turned into steam, which powers an electrical generator by spinning a steam turbine. The steam is concentrated in a condenser and returned to where it was heated after passing through the turbine; this is known as the Rankine cycle. Using Wind power: The development of either lift or drag force is one of the two primary physical values by which energy can be extracted from the wind. Hydrostatic pressure, which are the forces felt by a person exposed to the wind, are the most obvious means of propulsion. Buzz forces are the most effective mode of propulsion, but they are less well known than drag forces due to their sensitivity. Using Nuclear power: Charged particles are created and accelerated (examples: beta voltaic or alpha partial emission. In a nuclear power plant, uranium is first formed into pellets, then into long rods. Submerging the uranium rods in water keeps them cold. When they are taken out of the water, a nuclear reaction occurs, resulting in heat. Rising and lowering the thermostat regulates the amount of heat necessary. Using solar power: The photoelectric effect, as seen in solar cells, is responsible for converting light into electrical energy. Since the solar array will stay aligned to the sun, solar monitoring allows for further energy production. To improve performance, a solar system's power production should be maximized. To get the most power out of your solar panels, make sure they're aligned with the sun.

Cluster analysis [8] using nRMSE (Normalized Root Mean Square Error), nMAE (Mean Absolute Error) and nMBE (Mean bias error) solar generation 8.80, 4.06 and -1.01. By using successful feature selection or extraction, you can boost the forecasting efficiency even more. In addition, a [12] new hybrid forecasting method is being developed and tested, which integrates well-known forecasting strategies [7]. The mixed model is created after no discrete method is better than all four seasons. According to RSME, the error of all simulations is 7.210% in summer, 6.921% in early autumn, 8.62% in spring and 9.37% in winter. The results show that a simple combination of many excellent models can provide more reliable predictions than either method. We've got been ready to cut back the error rate from concerning within the persistent ideal, to 15.1% from the Foreign Intelligence Service model, and to 11.8% from the cnn. Similarity features, which are effective in the SVR model, do not improve the deep learning model [9].

For example we take the north china place the winter days based on the climatic characteristics of North China. For each classification, a random forest algorithm-based forecasting model is created [10]. Separately, three other models in addition to the one proposed. Methods for predicting regular power generation and evaluate the performance of the Zhonghu PV station in northern China are described. The model achieves mean absolute percentage errors of less than 2.831 % and 3.1 percent in empirical data due to its capacity to by balancing decision trees, you can reduce the risk of overfitting. The following conclusions are based on empirical findings:

(1) The projected model's MAPE standards for both sunny and cloudy days square measure as low as 2.831 % and 3.890 %.

(2) When it's raining or snowing, the prediction errors of the projected model square measure are greater than they are in other circumstances. In those days, the prediction exactitude may increasing the size coaching samples and

playing subdivision will help. (3) Manual interference with neighbor classifications can increase the accuracy of prediction for sorting transformation days.
(4) In practically every classification, for nearly all error analysis metrics, the predicted model outperforms the other three strategies.

Both the artificial neural network and deep neural network models studied outperform the PPVFM in terms of efficiency [1]. The Auto-LSTM[11] is the best DNN model. With an average RMSE of 0.071, an average MAE of 0.036, and an average absolute deviation of 0:2765, it has the highest score. The greatest BIAS values are seen in the MLP. Using current air temperature and mean daily solar irradiance, they employed Multi-Layer Perceptron (MLP) to estimate the hourly forecast of solar radiation [13]. On unseen test data, the DBN achieves the best correlation, while the Auto-LSTM achieves the best correlation on training data.

Whereas the cloudy version suits the overall sample of the climate, it often predicts incorrectly. When the climate shifts, which occurs nearly each day, PPF's effects are inaccurate [2]. SVM-RBF with decreased features, on the alternative hand, produces a miles extra correct version. The RMSE mistakes for every version imply this: SVM-RBF with 4 dimensions has an RMS-Error of 128 amps, at the same time as hazy and PPF have RMS-Errors of a hundred seventy five and 261, respectively. As a consequence, the 4-dimensional SVM-RBF version is 27% extra correct than the easy cloudy version and 50.9% extra correct than the PPF version [3]. Using the fuzzy logic method, the average error was calculated is 1.92 %, while the average error obtained using the ANN method is 2.62 %.

Random forest is part of machine learning algorithm a random forest is an estimator of some sort, that can fit several decision trees for different sub-samples of a dataset [4]. To get the best algorithm parameters, the hyper parameters tuning in Random Forest Classification approach was utilized [15]. In our case, both the number of decision trees in a forest and the number of landscapes fitted by a single decision tree are hyper parameters. This algorithm is sufficiently accurate, with a state recognition accuracy of 73%.

The Kernel function is used in Support Vector Regressor (SVR) to map input forms into a higher-dimensional space where output patterns can be found and become linearly divisible, allowing pattern extraction by fitting linearly. The aim is to find the best possible match, which can be challenging [9]. Assumed the shape of an optimization problem. Similar weather conditions, according to KNN, may result in alike PV power generation. As a result, the historical dataset can be viewed as a series of cause-and-effect relationships. Predicting future Photovoltaic power generation can be reduced to finding K feature vectors in the past database that are the closest neighbors to those who were present at the time interest. Knn has a lower percentage of error than nrsme, which is around 6.2 % and provides an approximate accuracy of 70% to 80%. A fixed input network with a single hidden layer is used as a back propagation neural network [14]. The input and output vectors' dimensions can be used to measure the neurons in the input and output layers automatically [1]. The initialization of weights and thresholds is performed at random, with an error rate of 8%.

To combine the outcomes of approximately the well-performing uncorrelated techniques into a weighted average as a single forecast the first step is to implement and evaluate all ten forecasting models. The hybrid model has the highest average performance of all the methods, with a yearly nRMSE of just 6.74 percent. CNNs have also been shown to improve efficiency while requiring less memory, all neurons in adjacent layers are connected in completely connected neural networks [8]. As a result, completely related neural networks have an enormous number of model parameters.

Long short term memory (LSTM) is a recurrent neural network (RNN) type that has successfully addressed the conventional RNN's vanishing gradient problem, which makes it difficult to detect and use useful features occurring early in input sequences. Here the combination of cnn+lstm gives MAPE 19.2%.The most basic methodology for estimating the next day's power production is calculated using linear or non-linear regression methods such as logistic regression or SVR and is dependent on inputs such as irradiation, temperature, and power output obtained the day before. Whereas svr is having a MAPE of 49.1%.

3. Flow chart for solar power generation

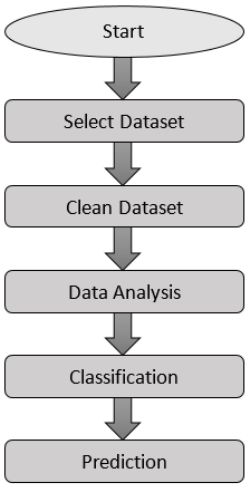

Fig.1 Flow chart

4. Methodology

4.1 Deep Learning Techniques

Consumption of power has become as additional and there are more regenerative generators included into the power grid, there has been an increase of interest in methods for regenerative power forecasting over the last decade [1].

4.1.1Auto LSTM:

The Auto-LSTM algorithm blends an Auto Encoder's function learning with an LSTM's temporal context utilization. The Auto-error LSTM's increases as more time measures are considered during the forecast. It's worth noting that when two previous time phases are factored into the prediction, the RMSE jumps dramatically [1].CNN is a deep learning neural network used to process organized data matrices, such as views. Lines, gradients, circles, and even eyes and faces are very effective in recognizing the design in the input image [5].

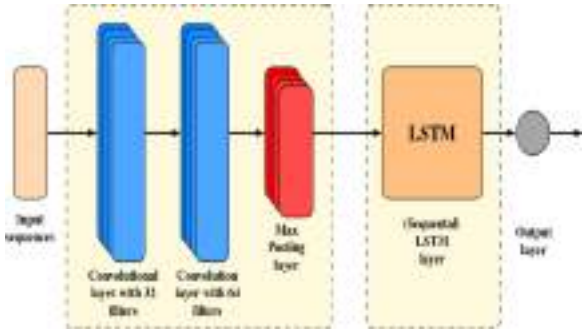

Fig.2 CNN and LSTM architecture

4.1.2 Deep Neural Networks:

DNN has proven its worth in a variety of fields, including representation learning and time series forecasting. To name a few, DNN claims Speech and picture recognition, machine translation, and financial time series forecasting are just a few of the applications. It is used to forecast solar power output [11].

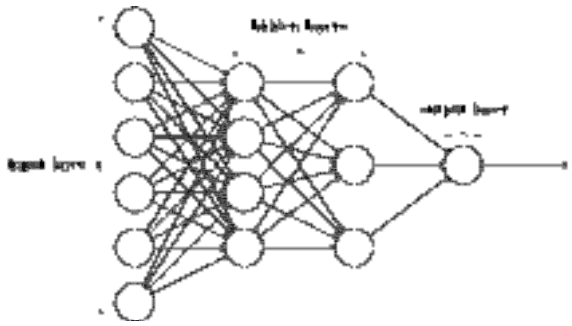

Fig.3 Layers differentiation of DNN

4.1.3 Deep Belief Network (DBN):

Deep belief network (DBN) models began to gain popularity. To forecast monthly solar power output data, a seasonal deep belief network (SDBN) was created in this study. By merging the seasonal decomposition approach and the DBN, the SDBN was created. Furthermore, data on monthly solar power generation was employed in this study.

Foretelling is a two-step approach [1]:

1) To reduce the dimensionality of the input data set, the DBN uses feature learning.

2) To perform forecasting, a new layer is added, such as the linear layer.

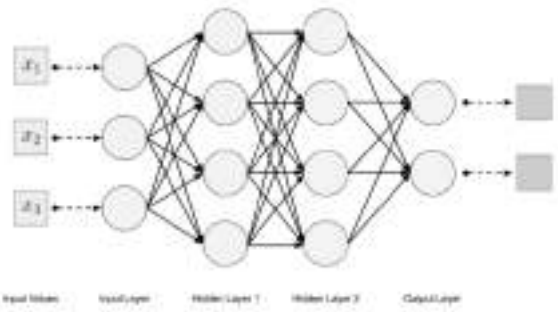

Fig.4 Deep belief network model

4.2 Machine Learning Techniques

4.2.1 Support Vectors Machine:

Then, we investigate a variety of supervised learning methods based on SVM. These methods, which create hyperplanes in a multidimensional space, have currently been approved to be used in indexing and regression analysis. The kernel function and parameters used determine the accuracy of svm regression. In our work, we investigated three distinct SVM kernel functions are Linear Kernel, a Polynomial Kernel and a Radial Basis Function (RBF) kernel [2].

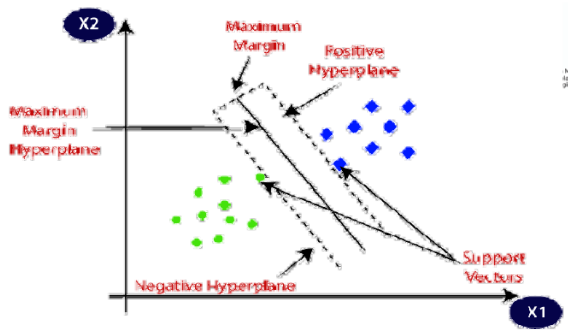

Fig.5 Hyperplane separating data points in SVM

4.2.2 K Nearest Neighbors (Knn):

KNN assumes that similar temperature variations will occur in the future. Would result in PV energy clusters that are comparable. Forecasting future PV power generation with an accuracy of about 81 % can be reduced to searching the past database for K feature vectors that are closest neighbors to those of the time of interest.

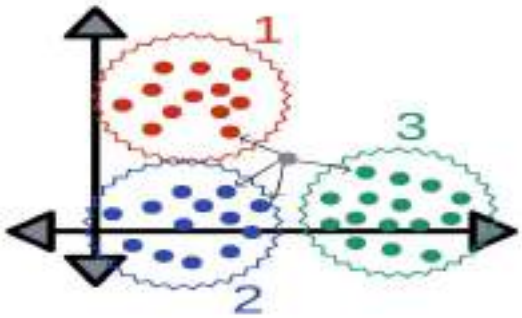

Fig.6 Partition and finding the nearest value in KNN

4.2.3 Random Forest:

Random Forest is an ensemble technique that can be used to classify or predict data productivities of a variety of unrelated decision tree subsystems. The random forest estimates that the precision is about 79%. These techniques can be used to map nonlinear interactions again [19].

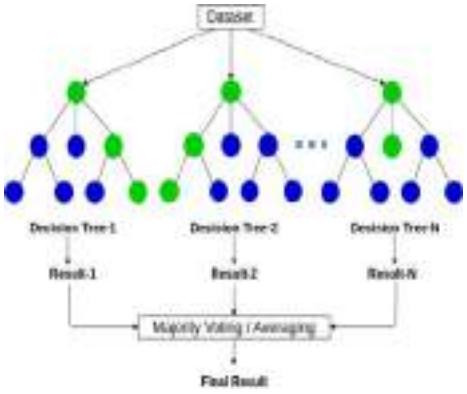

Fig.7 Random forest final results based on decision trees

4.2.4 Linear Regression Model:

Linear regression is a machine learning approach for supervised learning. It performs a regressive mission. Using the independent variables as a guide, regression models attempt to predict the value. Its main use is for forecasting and determining the relationship between variables.

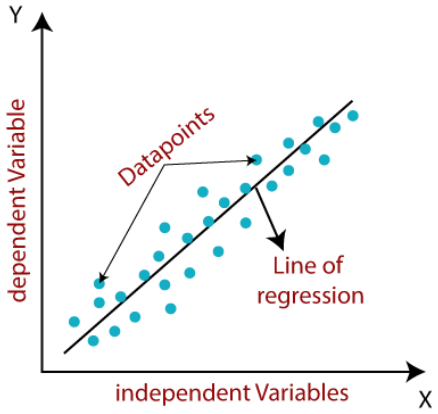

Fig.8 Linear regression model

4.3 Artificial Neural Networks

MATLAB was used to carry out the research. Fuzzy logic and Ann techniques[18] were both found to be effective in that their findings matched the characteristic of a real solar PV array [3]. These will be put to use to forecast and test the overall reliability of the solar power plant. They perform on three sets of data: training, testing, and validation. The MLR model's performance is substantially improved when classification variables and interactions between variables are used, but this is not the case with the ANN model [7].

4.3.1 Fuzzy Logic:

When combined with high-performance computer processors, allows for reasonable accuracy estimates of solar plant outputs while also allowing for system flexibility to adjust for natural events. The MATLAB software was used to construct the load forecasting system, which is based on fuzzy logic. The model has two inputs and one output and represents solar irradiance, ambient temperature, humidity and output power [3].

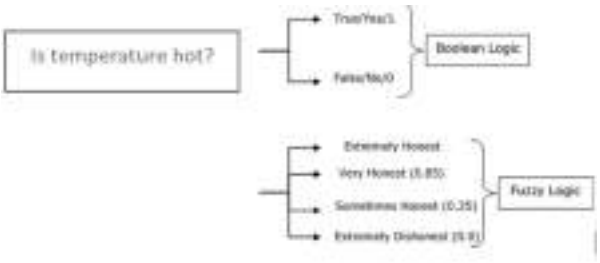

Fig.9 Fuzzy logic model

4.3.2 Multiple Linear Regression:

An ANN[16], as opposed to a multiple linear regression (MLR) model, a statistical method for assessing a non-linear connection between one or more inputs and outcomes. The artificial neural network[6] has been used to model, identify, and forecast complex systems.

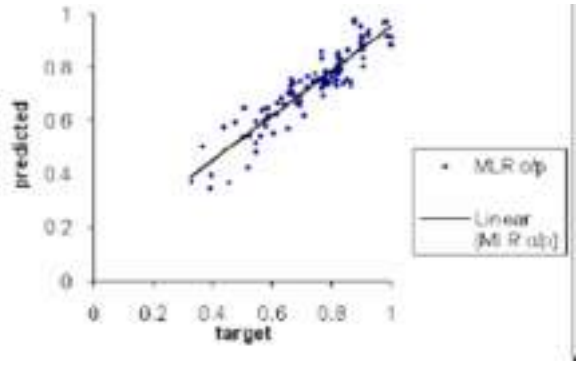

Fig.10 Multi linear regression

5. Comparison

5.1 Comparison of methods used:

Table 1. Model Prediction of RMSE, MAE, MAPE, and MBE

Model	RMSE	MAE	MAPE	MBE	Reference
MLP(multilayer perceptron)	0.0889	-	-	-	1
LSTM	0.0816	-	-	-	1
Clustering based on solar generation	8.80	4.60		-1.01	5
Clustering based on weather variables	8.61	3.77	-	-0.53	5
ANN	0.067	-	-	--	6
MLR(multi linear regression)	0.738	-	-	-	6
SVR(support vector regressor)	0.122	0.099	40.03	-	8
RFR(random forest regressor)	0.178	0.1378	67.58	-	8
CNN+LSTM	0.098	0.0568	13.42	-	8
SP(SMART PERSISTNACE)	0.135	0.071		0.023	11
DBN(deep belief network)	0.0390	0.0138		0.00244	11
SVM(support vector machine)	0.034	0.012		0.00777	11
RF(Random Forest)	0.033	0.0099		0.000351	11

5.2 Graphs comparison based on weather conditions with temperature values:

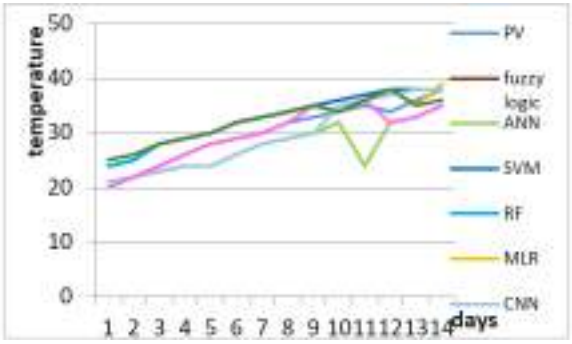

Fig.11 Mean of solar radiance in summer season.

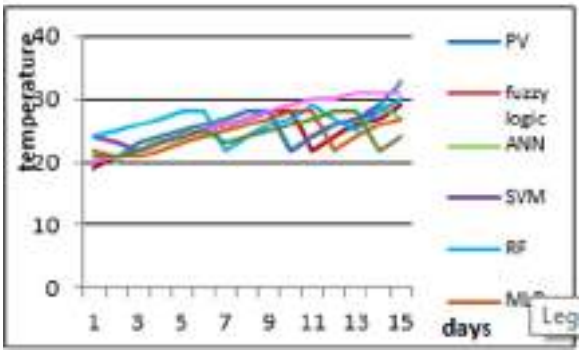

Fig.12 Mean of solar radiance in rainy season

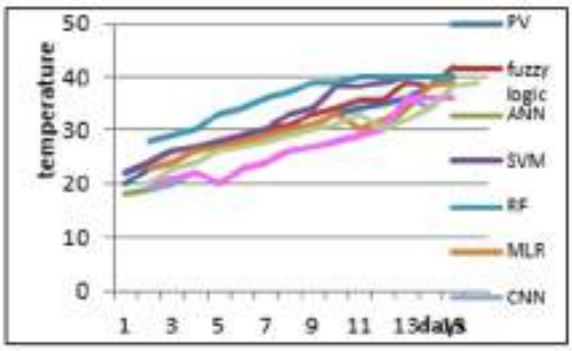

Fig.13 Mean of solar radiance in winter season

Here fig 11, 12, 13 gives the comparative analysis of different models that are used like fuzzy logic, artificial neural network, support vector machine, random forest, multiple linear regressor and Convolutional Neural Network results for different temperature based on seasonal effects with power generated for each day.

7. Conclusion

In this we conclude that it gives the partial analysis of solar power generation or forecasting based on different weather conditions. Different types of solar and wind dataset are considered for different seasons like summer (April to June), rainy (July to November) and winter (December to January) these are all about Indian weather condition. In order to get best results for diverse climatic condition for every hour for future betterment of analyzing power generation in different climatic condition machine learning give better results according to deep learning and artificial intelligence.

Reference

1. A. Gensler, J. Henze, and B. Sick, 2016 IEEE International (2016)
2. N. Sharma, P. Sharma, D. Irwin, and P. Shenoy, in 2011 IEEE International Conference on Smart Grid Communications (SmartGridComm) , pp. 528–533, (2011)
3. Z. P. Ncane and A. K. Saha, in 2019 Southern African Universities Power Engineering Conference/Robotics and Mechatronics/Pattern Recognition Association of South Africa (SAUPEC/RobMech/PRASA), pp. 518–523,(2019)
4. A. Khalyasmaa, S. A. Eroshenko, T. P. Chakravarthy, V. G. Gasi, S. K. Y. Bollu, R. Caire, S. K. R. Atluri, and S. Karrolla, in 2019 International Multi-Conference on Engineering, Computer and Information Sciences (SIBIRCON) , pp. 0780–0785, (2019)
5. C. Pan and J. Tan, IEEE Access 7, 112921 (2019).
6. P. Kora and S. R. Kalva, Springer plus 4, 481 (2015)
7. M. Abuella and B. Chowdhury, in 2015 North American Power Symposium (NAPS) , pp. 1–5, (2015)
8. K. Prasanna Lakshmi and C. R. K. Reddy, in 2010 International Conference on Networking and Information Technology , pp. 451–455(2010)
9. D. Su, E. Batzelis, and B. Pal, in 2019 International Conference on Smart Energy Systems and Technologies (SEST) , pp. 1–6 , (2019)
10. Swaraja K, Multimed. Tools Appl. 77, 28249 (2018)
11. W. Lee, K. Kim, J. Park, J. Kim, and Y. Kim, IEEE Access 6, 73068 (2018)
12. S. Kumar, P. Reddy, G. Ramesh, and V. Maddumala, Trait. Du Signal 36, 233 (2019)
13. F. Jawaid and K. NazirJunejo, in 2016 Sixth International Conference on Innovative Computing Technology (INTECH) , pp. 355–360, (2016)

14. C. U. Kumari, S. Jeevan Prasad, and G. Mounika, 2019 3rd International Conference on Computing Methodologies and Communication (ICCMC) (2019)
15. X. Wang, D. Luo, and C. Li, in 2019 2nd International Conference on Artificial Intelligence and Big Data (ICAIBD) , pp. 97–101, (2019)
16. B. Dhanalaxmi, G. A. Naidu, and K. Anuradha, Procedia Comput. Sci. 46, 432 (2015)
17. Application of Machine Learning Algorithms for Solar Power Forecasting in Sri Lanka
18. P. Nayak, G. K. Swetha, S. Gupta, and K. Madhavi, Measurement 178, 108974 (2021)
19. M. Z. Hassan, M. E. K. Ali, A. B. M. S. Ali, and J. Kumar, in 2017 4th Asia-Pacific World Congress on Computer Science and Engineering (APWC on CSE) , pp. 252–258, (2017)

Survey Analysis of Solar Power Generation Forecasting

Deekshitha Erlapally[1,*] *Dr. K.*Anuradha[2], *Dr.G.*Karuna[3], *V.*Srilakshmi[4], *K.*Adilakshmi[5]

[1]MTech Student, *Computer Science and Engineering*, *GRIET,* Hyderabad, Telangana, India.
[2]Professor, *Computer Science and Engineering*, *GRIET*, Hyderabad, Telangana, India.
[3]Professor, *Computer Science and Engineering*, *GRIET*, Hyderabad, Telangana, India.
[4] Asst.Professor, *Computer Science and Engineering*, *GRIET*, Hyderabad, Telangana, India.
[5] Asst.Professor, *Computer Science and Engineering*, *GRIET*, Hyderabad, Telangana, India.

Abstract: Solar power is the conversion of sunlight into electricity using solar photovoltaic cells as a source of energy. There are various applications for solar power; here is information on PV cell generation. We seek to understand the behavior of solar power plants through the data generated by the photovoltaic modules and the power generation in different weather conditions in India. The goal of this survey is to give a thorough assessment and study of machine learning, deep learning and artificial intelligence. Artificial intelligence (AI) models as well as information preprocessing techniques, parameter selection algorithms and predictive performance evaluations are used in machine learning and deep learning models for predicting renewable energies. But in case of time series data we can predict only the errors using a linear regression model, we can also calculate things like root mean square error (RMSE), mean absolute error (MSE), mean bias error (MBE) and mean absolute percentage error (MAPE). By the analysis of weather condition also we can predict the consumption of current by solar for every 15 minutes, 1day, and 1week or even for 1 month and find the accuracy.

1. Introduction

Solar energy has many benefits, including its sensitivity to imitative circumstances such as increasing oil prices, its renewable nature, and its ability to reduce imports and dependence on foreign resources. Despite the fact that photovoltaic cells are recognized as the significant source of potential energy production, their low return on investment and high upfront costs keeps them from becoming widely used. Since photovoltaic cells generate electricity by converting solar energy into electrical energy, the amount of solar energy produced every day is important to the size of the photovoltaic system, because the amount of solar radiation determines the amount of Major grid [17] integration is difficult because renewable energy is irregular and uncontrollable. Households in India can now use almost any amount of energy due to the recent electric grid at any moment, but it is not equipped for large quantities of uncontrollable generation [10] at this time. As it is converting solar radiance into power we don't get that how much power is emitted for different location, time, and weather. For this type of clarification machine learning techniques are used in order to differentiate it for different conditions.

electricity produced every day. This is influenced by factors such as place, time, and weather patterns. Solar irradiance is the power obtained per unit area from the Sun via electromagnetic radiation in the wavelength range of the solar cell that is in use [13].

Here we seek and analyzed India as a place and the temperature power plants as consideration based on weather condition in India. According to power generation commissioning statistics, solar plants have the largest installed capacity growth dynamics among renewable energy power plants. Making realistic solar generation projections for the day ahead view is becoming an increasingly critical issue in many places throughout the world at the current level of power system development.

Machine-learning techniques are wide applied to several fields where it can separate the weather based power. Machine-learning techniques are wide applied to several fields related to data-driven issues. Machine-learning techniques embrace several knowledge domain areas, like statistics, arithmetic, Ann, data processing, optimization, and computation are all terms that come to mind when thinking about artificial neural networks [18].

Deep learning, a sub-field of machine learning, has been blooming recently due to the rapid expansion of data

technology in hardware and code. Deep Learning calculations have only been used sparingly in the past for determining environmentally friendly power plants. We present these amazing calculations in the field of sustainable power determining by utilizing distinct Deep learning and ANN[16] calculations, such as DBN, Auto Encoder, and LSTM. In our tests, we integrated these calculations to show how effective they are in calculating the energy yield of solar-powered power plants as compared to a traditional MLP and an actual anticipating model. Our outcomes utilizing Deep Learning calculations show a better determining execution thought about than Artificial Neural Networks, like other reference models including such actual models, are artificial neural networks. In the literature, these models are compared with selected machine learning methods and are available predictive models. Using the mean square error, the proposed cloud classification ensemble model reduces the mean square error by 10.49%, 7.78% and 7.95% respectively, with deep belief networks, support vector regression and random forest [15] regression models. The use of weather parameters to forecast solar power generation is suggested as an Artificial Neural Network (ANN). This discussion describes the techniques used to predict renewable energy in machine learning models, including data preprocessing techniques, parameter selection algorithms, and predictive performance measurement.

2. Related Work

Energy is now the primary source of socioeconomic growth. However, because of the increasing rate of environmental concern, renewable energy is attracting a lot of attention. Related to the ongoing depletion of fossil fuels, this alternative energy source is gaining in popularity. That is the energy that comes from the sun, wind, rain, and other natural sources [3].To generate electricity at power plants, electromechanical generators are used, and they are mostly driven by chemical combustion or even nuclear fission heat engines, but also by alternative energy sources such as kinetic energy from flowing water and wind. There are numerous other technologies, such as solar photovoltaic and geothermal power, can and are used to produce electricity. Using thermal power: This method is used in thermocouples, thermopiles, and thermionic converters to convert temperature differences directly to power. Thermal power station is a power plant with a steam-driven primary mover. The water is heated and turned into steam, which powers an electrical generator by spinning a steam turbine. The steam is concentrated in a condenser and returned to where it was heated after passing through the turbine; this is known as the Rankine cycle. Using Wind power: The development of either lift or drag force is one of the two primary physical values by which energy can be extracted from the wind. Hydrostatic pressure, which are the forces felt by a person exposed to the wind, are the most obvious means of propulsion. Buzz forces are the most effective mode of propulsion, but they are less well known than drag forces due to their sensitivity. Using Nuclear power: Charged particles are created and accelerated (examples: beta voltaic or alpha partial emission. In a nuclear power plant, uranium is first formed into pellets, then into long rods. Submerging the uranium rods in water keeps them cold. When they are taken out of the water, a nuclear reaction occurs, resulting in heat. Rising and lowering the thermostat regulates the amount of heat necessary. Using solar power: The photoelectric effect, as seen in solar cells, is responsible for converting light into electrical energy. Since the solar array will stay aligned to the sun, solar monitoring allows for further energy production. To improve performance, a solar system's power production should be maximized. To get the most power out of your solar panels, make sure they're aligned with the sun.

Cluster analysis [8] using nRMSE (Normalized Root Mean Square Error), nMAE (Mean Absolute Error) and nMBE (Mean bias error) solar generation 8.80, 4.06 and -1.01. By using successful feature selection or extraction, you can boost the forecasting efficiency even more. In addition, a [12] new hybrid forecasting method is being developed and tested, which integrates well-known forecasting strategies [7]. The mixed model is created after no discrete method is better than all four seasons. According to RSME, the error of all simulations is 7.210% in summer, 6.921% in early autumn, 8.62% in spring and 9.37% in winter. The results show that a simple combination of many excellent models can provide more reliable predictions than either method. We've got been ready to cut back the error rate from concerning within the persistent ideal, to 15.1% from the Foreign Intelligence Service model, and to 11.8% from the cnn. Similarity features, which are effective in the SVR model, do not improve the deep learning model [9].

For example we take the north china place the winter days based on the climatic characteristics of North China. For each classification, a random forest algorithm-based forecasting model is created [10]. Separately, three other models in addition to the one proposed. Methods for predicting regular power generation and evaluate the performance of the Zhonghu PV station in northern China are described. The model achieves mean absolute percentage errors of less than 2.831 % and 3.1 percent in empirical data due to its capacity to by balancing decision trees, you can reduce the risk of overfitting. The following conclusions are based on empirical findings:

(1) The projected model's MAPE standards for both sunny and cloudy days square measure as low as 2.831 % and 3.890 %.

(2) When it's raining or snowing, the prediction errors of the projected model square measure are greater than they are in other circumstances. In those days, the prediction exactitude may increasing the size coaching samples and

playing subdivision will help. (3) Manual interference with neighbor classifications can increase the accuracy of prediction for sorting transformation days.
(4) In practically every classification, for nearly all error analysis metrics, the predicted model outperforms the other three strategies.

Both the artificial neural network and deep neural network models studied outperform the PPVFM in terms of efficiency [1]. The Auto-LSTM[11] is the best DNN model. With an average RMSE of 0.071, an average MAE of 0.036, and an average absolute deviation of 0:2765, it has the highest score. The greatest BIAS values are seen in the MLP. Using current air temperature and mean daily solar irradiance, they employed Multi-Layer Perceptron (MLP) to estimate the hourly forecast of solar radiation [13]. On unseen test data, the DBN achieves the best correlation, while the Auto-LSTM achieves the best correlation on training data.

Whereas the cloudy version suits the overall sample of the climate, it often predicts incorrectly. When the climate shifts, which occurs nearly each day, PPF's effects are inaccurate [2]. SVM-RBF with decreased features, on the alternative hand, produces a miles extra correct version. The RMSE mistakes for every version imply this: SVM-RBF with 4 dimensions has an RMS-Error of 128 amps, at the same time as hazy and PPF have RMS-Errors of a hundred seventy five and 261, respectively. As a consequence, the 4-dimensional SVM-RBF version is 27% extra correct than the easy cloudy version and 50.9% extra correct than the PPF version [3]. Using the fuzzy logic method, the average error was calculated is 1.92 %, while the average error obtained using the ANN method is 2.62 %.

Random forest is part of machine learning algorithm a random forest is an estimator of some sort, that can fit several decision trees for different sub-samples of a dataset [4]. To get the best algorithm parameters, the hyper parameters tuning in Random Forest Classification approach was utilized [15]. In our case, both the number of decision trees in a forest and the number of landscapes fitted by a single decision tree are hyper parameters. This algorithm is sufficiently accurate, with a state recognition accuracy of 73%.

The Kernel function is used in Support Vector Regressor (SVR) to map input forms into a higher-dimensional space where output patterns can be found and become linearly divisible, allowing pattern extraction by fitting linearly. The aim is to find the best possible match, which can be challenging [9]. Assumed the shape of an optimization problem. Similar weather conditions, according to KNN, may result in alike PV power generation. As a result, the historical dataset can be viewed as a series of cause-and-effect relationships. Predicting future Photovoltaic power generation can be reduced to finding K feature vectors in the past database that are the closest neighbors to those who were present at the time interest. Knn has a lower percentage of error than nrsme, which is around 6.2 % and provides an approximate accuracy of 70% to 80%. A fixed input network with a single hidden layer is used as a back propagation neural network [14]. The input and output vectors' dimensions can be used to measure the neurons in the input and output layers automatically [1]. The initialization of weights and thresholds is performed at random, with an error rate of 8%.

To combine the outcomes of approximately the well-performing uncorrelated techniques into a weighted average as a single forecast the first step is to implement and evaluate all ten forecasting models. The hybrid model has the highest average performance of all the methods, with a yearly nRMSE of just 6.74 percent. CNNs have also been shown to improve efficiency while requiring less memory, all neurons in adjacent layers are connected in completely connected neural networks [8]. As a result, completely related neural networks have an enormous number of model parameters.

Long short term memory (LSTM) is a recurrent neural network (RNN) type that has successfully addressed the conventional RNN's vanishing gradient problem, which makes it difficult to detect and use useful features occurring early in input sequences. Here the combination of cnn+lstm gives MAPE 19.2%.The most basic methodology for estimating the next day's power production is calculated using linear or non-linear regression methods such as logistic regression or SVR and is dependent on inputs such as irradiation, temperature, and power output obtained the day before. Whereas svr is having a MAPE of 49.1%.

3. Flow chart for solar power generation

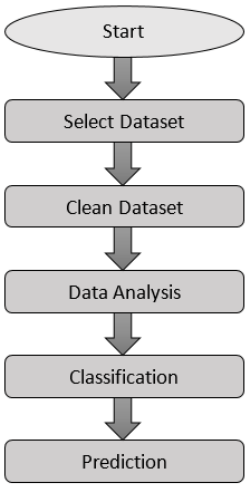

Fig.1 Flow chart

4. Methodology

4.1 Deep Learning Techniques

Consumption of power has become as additional and there are more regenerative generators included into the power grid, there has been an increase of interest in methods for regenerative power forecasting over the last decade [1].

4.1.1Auto LSTM:

The Auto-LSTM algorithm blends an Auto Encoder's function learning with an LSTM's temporal context utilization. The Auto-error LSTM's increases as more time measures are considered during the forecast. It's worth noting that when two previous time phases are factored into the prediction, the RMSE jumps dramatically [1].CNN is a deep learning neural network used to process organized data matrices, such as views. Lines, gradients, circles, and even eyes and faces are very effective in recognizing the design in the input image [5].

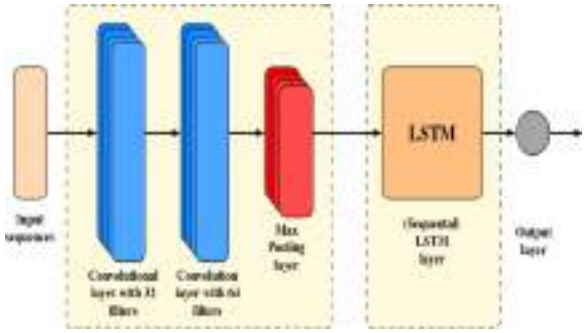

Fig.2 CNN and LSTM architecture

4.1.2 Deep Neural Networks:

DNN has proven its worth in a variety of fields, including representation learning and time series forecasting. To name a few, DNN claims Speech and picture recognition, machine translation, and financial time series forecasting are just a few of the applications. It is used to forecast solar power output [11].

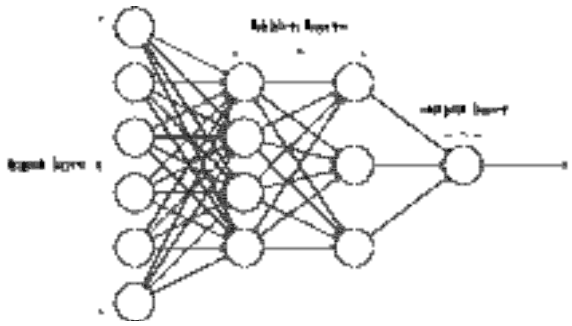

Fig.3 Layers differentiation of DNN

4.1.3 Deep Belief Network (DBN):

Deep belief network (DBN) models began to gain popularity. To forecast monthly solar power output data, a seasonal deep belief network (SDBN) was created in this study. By merging the seasonal decomposition approach and the DBN, the SDBN was created. Furthermore, data on monthly solar power generation was employed in this study.

Foretelling is a two-step approach [1]:

1) To reduce the dimensionality of the input data set, the DBN uses feature learning.

2) To perform forecasting, a new layer is added, such as the linear layer.

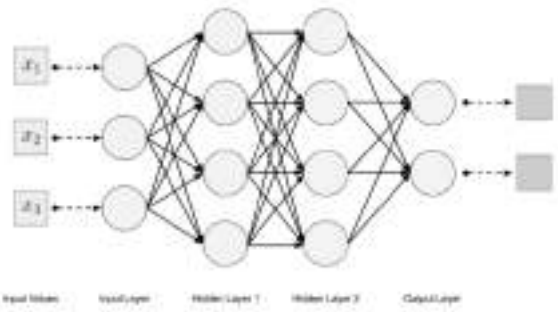

Fig.4 Deep belief network model

4.2 Machine Learning Techniques

4.2.1 Support Vectors Machine:

Then, we investigate a variety of supervised learning methods based on SVM. These methods, which create hyperplanes in a multidimensional space, have currently been approved to be used in indexing and regression analysis. The kernel function and parameters used determine the accuracy of svm regression. In our work, we investigated three distinct SVM kernel functions are Linear Kernel, a Polynomial Kernel and a Radial Basis Function (RBF) kernel [2].

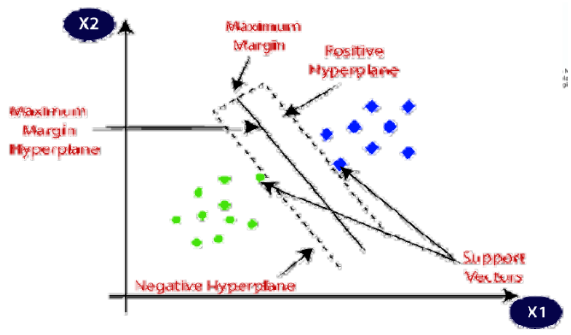

Fig.5 Hyperplane separating data points in SVM

4.2.2 K Nearest Neighbors (Knn):

KNN assumes that similar temperature variations will occur in the future. Would result in PV energy clusters that are comparable. Forecasting future PV power generation with an accuracy of about 81 % can be reduced to searching the past database for K feature vectors that are closest neighbors to those of the time of interest.

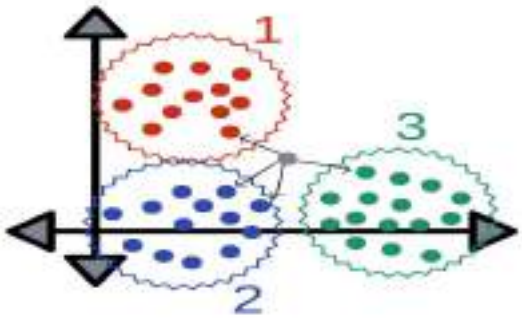

Fig.6 Partition and finding the nearest value in KNN

4.2.3 Random Forest:

Random Forest is an ensemble technique that can be used to classify or predict data productivities of a variety of unrelated decision tree subsystems. The random forest estimates that the precision is about 79%. These techniques can be used to map nonlinear interactions again [19].

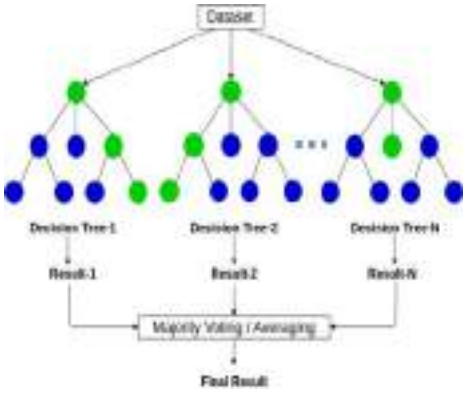

Fig.7 Random forest final results based on decision trees

4.2.4 Linear Regression Model:

Linear regression is a machine learning approach for supervised learning. It performs a regressive mission. Using the independent variables as a guide, regression models attempt to predict the value. Its main use is for forecasting and determining the relationship between variables.

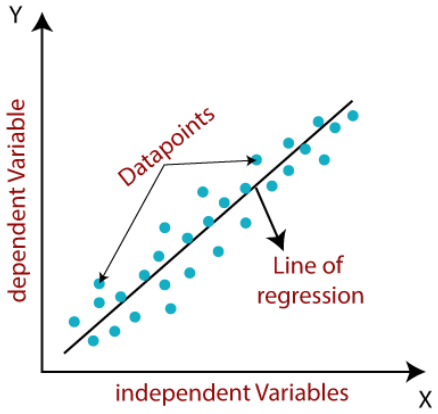

Fig.8 Linear regression model

4.3 Artificial Neural Networks

MATLAB was used to carry out the research. Fuzzy logic and Ann techniques[18] were both found to be effective in that their findings matched the characteristic of a real solar PV array [3]. These will be put to use to forecast and test the overall reliability of the solar power plant. They perform on three sets of data: training, testing, and validation. The MLR model's performance is substantially improved when classification variables and interactions between variables are used, but this is not the case with the ANN model [7].

4.3.1 Fuzzy Logic:

When combined with high-performance computer processors, allows for reasonable accuracy estimates of solar plant outputs while also allowing for system flexibility to adjust for natural events. The MATLAB software was used to construct the load forecasting system, which is based on fuzzy logic. The model has two inputs and one output and represents solar irradiance, ambient temperature, humidity and output power [3].

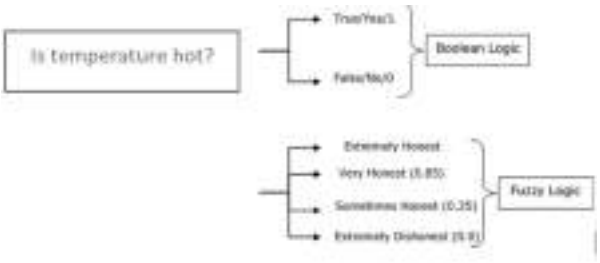

Fig.9 Fuzzy logic model

4.3.2 Multiple Linear Regression:

An ANN[16], as opposed to a multiple linear regression (MLR) model, a statistical method for assessing a non-linear connection between one or more inputs and outcomes. The artificial neural network[6] has been used to model, identify, and forecast complex systems.

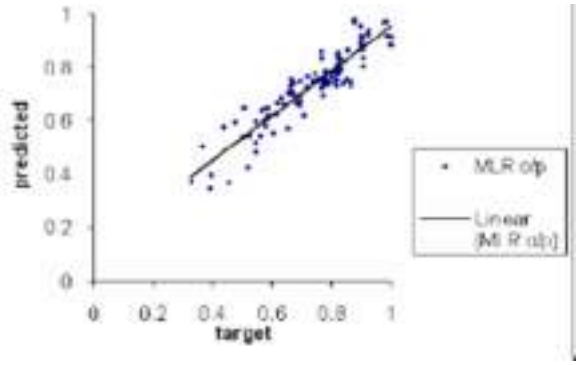

Fig.10 Multi linear regression

5. Comparison

5.1 Comparison of methods used:

Table 1. Model Prediction of RMSE, MAE, MAPE, and MBE

Model	RMSE	MAE	MAPE	MBE	Reference
MLP(multilayer perceptron)	0.0889	-	-	-	1
LSTM	0.0816	-	-	-	1
Clustering based on solar generation	8.80	4.60		-1.01	5
Clustering based on weather variables	8.61	3.77	-	-0.53	5
ANN	0.067	-	-	--	6
MLR(multi linear regression)	0.738	-	-	-	6
SVR(support vector regressor)	0.122	0.099	40.03	-	8
RFR(random forest regressor)	0.178	0.1378	67.58	-	8
CNN+LSTM	0.098	0.0568	13.42	-	8
SP(SMART PERSISTNACE)	0.135	0.071		0.023	11
DBN(deep belief network)	0.0390	0.0138		0.00244	11
SVM(support vector machine)	0.034	0.012		0.00777	11
RF(Random Forest)	0.033	0.0099		0.000351	11

5.2 Graphs comparison based on weather conditions with temperature values:

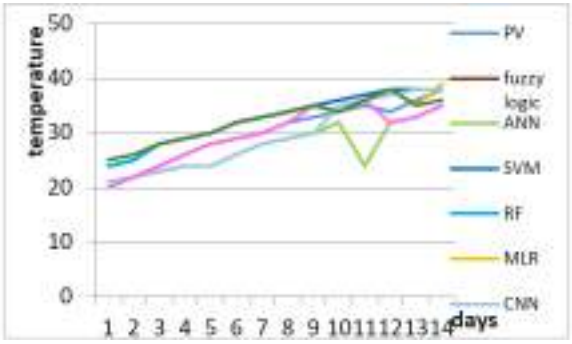

Fig.11 Mean of solar radiance in summer season.

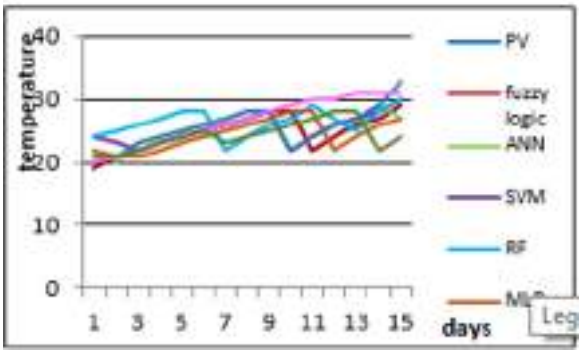

Fig.12 Mean of solar radiance in rainy season

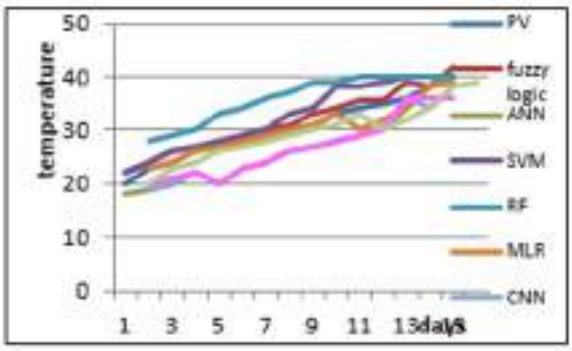

Fig.13 Mean of solar radiance in winter season

Here fig 11, 12, 13 gives the comparative analysis of different models that are used like fuzzy logic, artificial neural network, support vector machine, random forest, multiple linear regressor and Convolutional Neural Network results for different temperature based on seasonal effects with power generated for each day.

7. Conclusion

In this we conclude that it gives the partial analysis of solar power generation or forecasting based on different weather conditions. Different types of solar and wind dataset are considered for different seasons like summer (April to June), rainy (July to November) and winter (December to January) these are all about Indian weather condition. In order to get best results for diverse climatic condition for every hour for future betterment of analyzing power generation in different climatic condition machine learning give better results according to deep learning and artificial intelligence.

Reference

1. A. Gensler, J. Henze, and B. Sick, 2016 IEEE International (2016)
2. N. Sharma, P. Sharma, D. Irwin, and P. Shenoy, in 2011 IEEE International Conference on Smart Grid Communications (SmartGridComm) , pp. 528–533, (2011)
3. Z. P. Ncane and A. K. Saha, in 2019 Southern African Universities Power Engineering Conference/Robotics and Mechatronics/Pattern Recognition Association of South Africa (SAUPEC/RobMech/PRASA), pp. 518–523,(2019)
4. A. Khalyasmaa, S. A. Eroshenko, T. P. Chakravarthy, V. G. Gasi, S. K. Y. Bollu, R. Caire, S. K. R. Atluri, and S. Karrolla, in 2019 International Multi-Conference on Engineering, Computer and Information Sciences (SIBIRCON) , pp. 0780–0785, (2019)
5. C. Pan and J. Tan, IEEE Access 7, 112921 (2019).
6. P. Kora and S. R. Kalva, Springer plus 4, 481 (2015)
7. M. Abuella and B. Chowdhury, in 2015 North American Power Symposium (NAPS) , pp. 1–5, (2015)
8. K. Prasanna Lakshmi and C. R. K. Reddy, in 2010 International Conference on Networking and Information Technology , pp. 451–455(2010)
9. D. Su, E. Batzelis, and B. Pal, in 2019 International Conference on Smart Energy Systems and Technologies (SEST) , pp. 1–6 , (2019)
10. Swaraja K, Multimed. Tools Appl. 77, 28249 (2018)
11. W. Lee, K. Kim, J. Park, J. Kim, and Y. Kim, IEEE Access 6, 73068 (2018)
12. S. Kumar, P. Reddy, G. Ramesh, and V. Maddumala, Trait. Du Signal 36, 233 (2019)
13. F. Jawaid and K. NazirJunejo, in 2016 Sixth International Conference on Innovative Computing Technology (INTECH) , pp. 355–360, (2016)

14. C. U. Kumari, S. Jeevan Prasad, and G. Mounika, 2019 3rd International Conference on Computing Methodologies and Communication (ICCMC) (2019)
15. X. Wang, D. Luo, and C. Li, in 2019 2nd International Conference on Artificial Intelligence and Big Data (ICAIBD) , pp. 97–101, (2019)
16. B. Dhanalaxmi, G. A. Naidu, and K. Anuradha, Procedia Comput. Sci. 46, 432 (2015)
17. Application of Machine Learning Algorithms for Solar Power Forecasting in Sri Lanka
18. P. Nayak, G. K. Swetha, S. Gupta, and K. Madhavi, Measurement 178, 108974 (2021)
19. M. Z. Hassan, M. E. K. Ali, A. B. M. S. Ali, and J. Kumar, in 2017 4th Asia-Pacific World Congress on Computer Science and Engineering (APWC on CSE) , pp. 252–258, (2017)

Survey Analysis of Solar Power Generation Forecasting

Deekshitha Erlapally[1,*] *Dr. K.*Anuradha[2], *Dr.G.*Karuna[3], *V.*Srilakshmi[4], *K.*Adilakshmi[5]

[1]MTech Student, *Computer Science and Engineering*, *GRIET,* Hyderabad, Telangana, India.
[2]Professor, *Computer Science and Engineering*, *GRIET*, Hyderabad, Telangana, India.
[3]Professor, *Computer Science and Engineering*, *GRIET*, Hyderabad, Telangana, India.
[4] Asst.Professor, *Computer Science and Engineering*, *GRIET*, Hyderabad, Telangana, India.
[5] Asst.Professor, *Computer Science and Engineering*, *GRIET*, Hyderabad, Telangana, India.

Abstract: Solar power is the conversion of sunlight into electricity using solar photovoltaic cells as a source of energy. There are various applications for solar power; here is information on PV cell generation. We seek to understand the behavior of solar power plants through the data generated by the photovoltaic modules and the power generation in different weather conditions in India. The goal of this survey is to give a thorough assessment and study of machine learning, deep learning and artificial intelligence. Artificial intelligence (AI) models as well as information preprocessing techniques, parameter selection algorithms and predictive performance evaluations are used in machine learning and deep learning models for predicting renewable energies. But in case of time series data we can predict only the errors using a linear regression model, we can also calculate things like root mean square error (RMSE), mean absolute error (MSE), mean bias error (MBE) and mean absolute percentage error (MAPE). By the analysis of weather condition also we can predict the consumption of current by solar for every 15 minutes, 1day, and 1week or even for 1 month and find the accuracy.

1. Introduction

Solar energy has many benefits, including its sensitivity to imitative circumstances such as increasing oil prices, its renewable nature, and its ability to reduce imports and dependence on foreign resources. Despite the fact that photovoltaic cells are recognized as the significant source of potential energy production, their low return on investment and high upfront costs keeps them from becoming widely used. Since photovoltaic cells generate electricity by converting solar energy into electrical energy, the amount of solar energy produced every day is important to the size of the photovoltaic system, because the amount of solar radiation determines the amount of Major grid [17] integration is difficult because renewable energy is irregular and uncontrollable. Households in India can now use almost any amount of energy due to the recent electric grid at any moment, but it is not equipped for large quantities of uncontrollable generation [10] at this time. As it is converting solar radiance into power we don't get that how much power is emitted for different location, time, and weather. For this type of clarification machine learning techniques are used in order to differentiate it for different conditions.

electricity produced every day. This is influenced by factors such as place, time, and weather patterns. Solar irradiance is the power obtained per unit area from the Sun via electromagnetic radiation in the wavelength range of the solar cell that is in use [13].

Here we seek and analyzed India as a place and the temperature power plants as consideration based on weather condition in India. According to power generation commissioning statistics, solar plants have the largest installed capacity growth dynamics among renewable energy power plants. Making realistic solar generation projections for the day ahead view is becoming an increasingly critical issue in many places throughout the world at the current level of power system development.

Machine-learning techniques are wide applied to several fields where it can separate the weather based power. Machine-learning techniques are wide applied to several fields related to data-driven issues. Machine-learning techniques embrace several knowledge domain areas, like statistics, arithmetic, Ann, data processing, optimization, and computation are all terms that come to mind when thinking about artificial neural networks [18].

Deep learning, a sub-field of machine learning, has been blooming recently due to the rapid expansion of data

technology in hardware and code. Deep Learning calculations have only been used sparingly in the past for determining environmentally friendly power plants. We present these amazing calculations in the field of sustainable power determining by utilizing distinct Deep learning and ANN[16] calculations, such as DBN, Auto Encoder, and LSTM. In our tests, we integrated these calculations to show how effective they are in calculating the energy yield of solar-powered power plants as compared to a traditional MLP and an actual anticipating model. Our outcomes utilizing Deep Learning calculations show a better determining execution thought about than Artificial Neural Networks, like other reference models including such actual models, are artificial neural networks. In the literature, these models are compared with selected machine learning methods and are available predictive models. Using the mean square error, the proposed cloud classification ensemble model reduces the mean square error by 10.49%, 7.78% and 7.95% respectively, with deep belief networks, support vector regression and random forest [15] regression models. The use of weather parameters to forecast solar power generation is suggested as an Artificial Neural Network (ANN). This discussion describes the techniques used to predict renewable energy in machine learning models, including data preprocessing techniques, parameter selection algorithms, and predictive performance measurement.

2. Related Work

Energy is now the primary source of socioeconomic growth. However, because of the increasing rate of environmental concern, renewable energy is attracting a lot of attention. Related to the ongoing depletion of fossil fuels, this alternative energy source is gaining in popularity. That is the energy that comes from the sun, wind, rain, and other natural sources [3].To generate electricity at power plants, electromechanical generators are used, and they are mostly driven by chemical combustion or even nuclear fission heat engines, but also by alternative energy sources such as kinetic energy from flowing water and wind. There are numerous other technologies, such as solar photovoltaic and geothermal power, can and are used to produce electricity. Using thermal power: This method is used in thermocouples, thermopiles, and thermionic converters to convert temperature differences directly to power. Thermal power station is a power plant with a steam-driven primary mover. The water is heated and turned into steam, which powers an electrical generator by spinning a steam turbine. The steam is concentrated in a condenser and returned to where it was heated after passing through the turbine; this is known as the Rankine cycle. Using Wind power: The development of either lift or drag force is one of the two primary physical values by which energy can be extracted from the wind. Hydrostatic pressure, which are the forces felt by a person exposed to the wind, are the most obvious means of propulsion. Buzz forces are the most effective mode of propulsion, but they are less well known than drag forces due to their sensitivity. Using Nuclear power: Charged particles are created and accelerated (examples: beta voltaic or alpha partial emission. In a nuclear power plant, uranium is first formed into pellets, then into long rods. Submerging the uranium rods in water keeps them cold. When they are taken out of the water, a nuclear reaction occurs, resulting in heat. Rising and lowering the thermostat regulates the amount of heat necessary. Using solar power: The photoelectric effect, as seen in solar cells, is responsible for converting light into electrical energy. Since the solar array will stay aligned to the sun, solar monitoring allows for further energy production. To improve performance, a solar system's power production should be maximized. To get the most power out of your solar panels, make sure they're aligned with the sun.

Cluster analysis [8] using nRMSE (Normalized Root Mean Square Error), nMAE (Mean Absolute Error) and nMBE (Mean bias error) solar generation 8.80, 4.06 and -1.01. By using successful feature selection or extraction, you can boost the forecasting efficiency even more. In addition, a [12] new hybrid forecasting method is being developed and tested, which integrates well-known forecasting strategies [7]. The mixed model is created after no discrete method is better than all four seasons. According to RSME, the error of all simulations is 7.210% in summer, 6.921% in early autumn, 8.62% in spring and 9.37% in winter. The results show that a simple combination of many excellent models can provide more reliable predictions than either method. We've got been ready to cut back the error rate from concerning within the persistent ideal, to 15.1% from the Foreign Intelligence Service model, and to 11.8% from the cnn. Similarity features, which are effective in the SVR model, do not improve the deep learning model [9].

For example we take the north china place the winter days based on the climatic characteristics of North China. For each classification, a random forest algorithm-based forecasting model is created [10]. Separately, three other models in addition to the one proposed. Methods for predicting regular power generation and evaluate the performance of the Zhonghu PV station in northern China are described. The model achieves mean absolute percentage errors of less than 2.831 % and 3.1 percent in empirical data due to its capacity to by balancing decision trees, you can reduce the risk of overfitting. The following conclusions are based on empirical findings:

(1) The projected model's MAPE standards for both sunny and cloudy days square measure as low as 2.831 % and 3.890 %.

(2) When it's raining or snowing, the prediction errors of the projected model square measure are greater than they are in other circumstances. In those days, the prediction exactitude may increasing the size coaching samples and

playing subdivision will help. (3) Manual interference with neighbor classifications can increase the accuracy of prediction for sorting transformation days.
(4) In practically every classification, for nearly all error analysis metrics, the predicted model outperforms the other three strategies.

Both the artificial neural network and deep neural network models studied outperform the PPVFM in terms of efficiency [1]. The Auto-LSTM[11] is the best DNN model. With an average RMSE of 0.071, an average MAE of 0.036, and an average absolute deviation of 0:2765, it has the highest score. The greatest BIAS values are seen in the MLP. Using current air temperature and mean daily solar irradiance, they employed Multi-Layer Perceptron (MLP) to estimate the hourly forecast of solar radiation [13]. On unseen test data, the DBN achieves the best correlation, while the Auto-LSTM achieves the best correlation on training data.

Whereas the cloudy version suits the overall sample of the climate, it often predicts incorrectly. When the climate shifts, which occurs nearly each day, PPF's effects are inaccurate [2]. SVM-RBF with decreased features, on the alternative hand, produces a miles extra correct version. The RMSE mistakes for every version imply this: SVM-RBF with 4 dimensions has an RMS-Error of 128 amps, at the same time as hazy and PPF have RMS-Errors of a hundred seventy five and 261, respectively. As a consequence, the 4-dimensional SVM-RBF version is 27% extra correct than the easy cloudy version and 50.9% extra correct than the PPF version [3]. Using the fuzzy logic method, the average error was calculated is 1.92 %, while the average error obtained using the ANN method is 2.62 %.

Random forest is part of machine learning algorithm a random forest is an estimator of some sort, that can fit several decision trees for different sub-samples of a dataset [4]. To get the best algorithm parameters, the hyper parameters tuning in Random Forest Classification approach was utilized [15]. In our case, both the number of decision trees in a forest and the number of landscapes fitted by a single decision tree are hyper parameters. This algorithm is sufficiently accurate, with a state recognition accuracy of 73%.

The Kernel function is used in Support Vector Regressor (SVR) to map input forms into a higher-dimensional space where output patterns can be found and become linearly divisible, allowing pattern extraction by fitting linearly. The aim is to find the best possible match, which can be challenging [9]. Assumed the shape of an optimization problem. Similar weather conditions, according to KNN, may result in alike PV power generation. As a result, the historical dataset can be viewed as a series of cause-and-effect relationships. Predicting future Photovoltaic power generation can be reduced to finding K feature vectors in the past database that are the closest neighbors to those who were present at the time interest. Knn has a lower percentage of error than nrsme, which is around 6.2 % and provides an approximate accuracy of 70% to 80%. A fixed input network with a single hidden layer is used as a back propagation neural network [14]. The input and output vectors' dimensions can be used to measure the neurons in the input and output layers automatically [1]. The initialization of weights and thresholds is performed at random, with an error rate of 8%.

To combine the outcomes of approximately the well-performing uncorrelated techniques into a weighted average as a single forecast the first step is to implement and evaluate all ten forecasting models. The hybrid model has the highest average performance of all the methods, with a yearly nRMSE of just 6.74 percent. CNNs have also been shown to improve efficiency while requiring less memory, all neurons in adjacent layers are connected in completely connected neural networks [8]. As a result, completely related neural networks have an enormous number of model parameters.

Long short term memory (LSTM) is a recurrent neural network (RNN) type that has successfully addressed the conventional RNN's vanishing gradient problem, which makes it difficult to detect and use useful features occurring early in input sequences. Here the combination of cnn+lstm gives MAPE 19.2%.The most basic methodology for estimating the next day's power production is calculated using linear or non-linear regression methods such as logistic regression or SVR and is dependent on inputs such as irradiation, temperature, and power output obtained the day before. Whereas svr is having a MAPE of 49.1%.

3. Flow chart for solar power generation

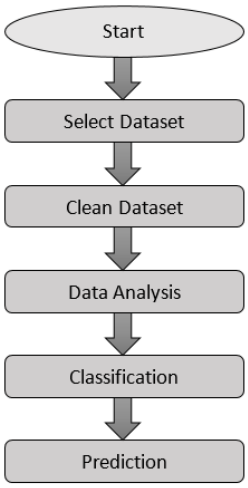

Fig.1 Flow chart

4. Methodology

4.1 Deep Learning Techniques

Consumption of power has become as additional and there are more regenerative generators included into the power grid, there has been an increase of interest in methods for regenerative power forecasting over the last decade [1].

4.1.1Auto LSTM:

The Auto-LSTM algorithm blends an Auto Encoder's function learning with an LSTM's temporal context utilization. The Auto-error LSTM's increases as more time measures are considered during the forecast. It's worth noting that when two previous time phases are factored into the prediction, the RMSE jumps dramatically [1].CNN is a deep learning neural network used to process organized data matrices, such as views. Lines, gradients, circles, and even eyes and faces are very effective in recognizing the design in the input image [5].

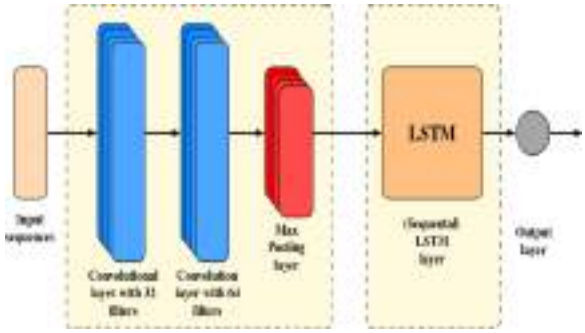

Fig.2 CNN and LSTM architecture

4.1.2 Deep Neural Networks:

DNN has proven its worth in a variety of fields, including representation learning and time series forecasting. To name a few, DNN claims Speech and picture recognition, machine translation, and financial time series forecasting are just a few of the applications. It is used to forecast solar power output [11].

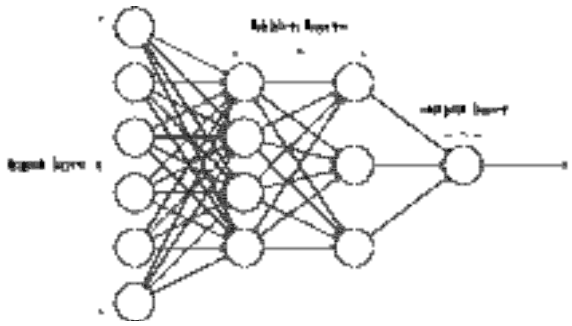

Fig.3 Layers differentiation of DNN

4.1.3 Deep Belief Network (DBN):

Deep belief network (DBN) models began to gain popularity. To forecast monthly solar power output data, a seasonal deep belief network (SDBN) was created in this study. By merging the seasonal decomposition approach and the DBN, the SDBN was created. Furthermore, data on monthly solar power generation was employed in this study.

Foretelling is a two-step approach [1]:

1) To reduce the dimensionality of the input data set, the DBN uses feature learning.

2) To perform forecasting, a new layer is added, such as the linear layer.

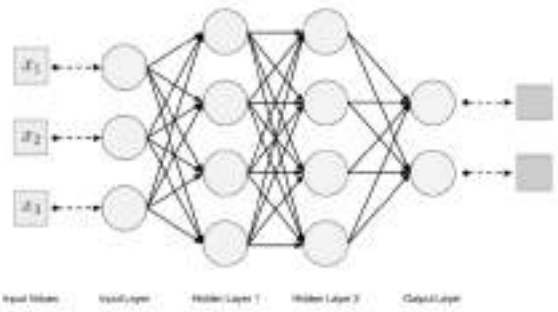

Fig.4 Deep belief network model

4.2 Machine Learning Techniques

4.2.1 Support Vectors Machine:

Then, we investigate a variety of supervised learning methods based on SVM. These methods, which create hyperplanes in a multidimensional space, have currently been approved to be used in indexing and regression analysis. The kernel function and parameters used determine the accuracy of svm regression. In our work, we investigated three distinct SVM kernel functions are Linear Kernel, a Polynomial Kernel and a Radial Basis Function (RBF) kernel [2].

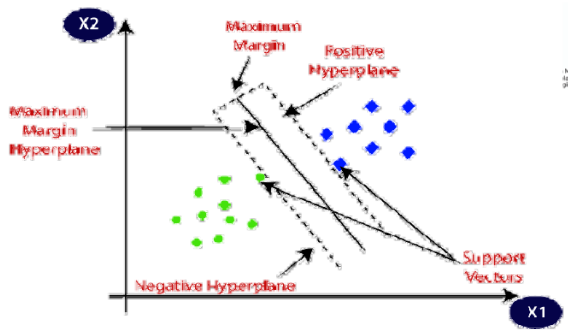

Fig.5 Hyperplane separating data points in SVM

4.2.2 K Nearest Neighbors (Knn):

KNN assumes that similar temperature variations will occur in the future. Would result in PV energy clusters that are comparable. Forecasting future PV power generation with an accuracy of about 81 % can be reduced to searching the past database for K feature vectors that are closest neighbors to those of the time of interest.

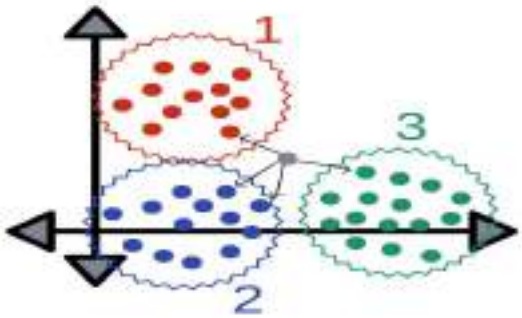

Fig.6 Partition and finding the nearest value in KNN

4.2.3 Random Forest:

Random Forest is an ensemble technique that can be used to classify or predict data productivities of a variety of unrelated decision tree subsystems. The random forest estimates that the precision is about 79%. These techniques can be used to map nonlinear interactions again [19].

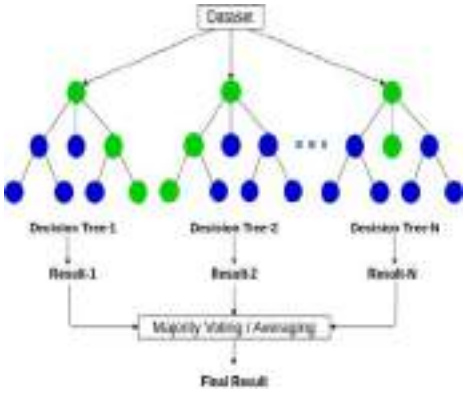

Fig.7 Random forest final results based on decision trees

4.2.4 Linear Regression Model:

Linear regression is a machine learning approach for supervised learning. It performs a regressive mission. Using the independent variables as a guide, regression models attempt to predict the value. Its main use is for forecasting and determining the relationship between variables.

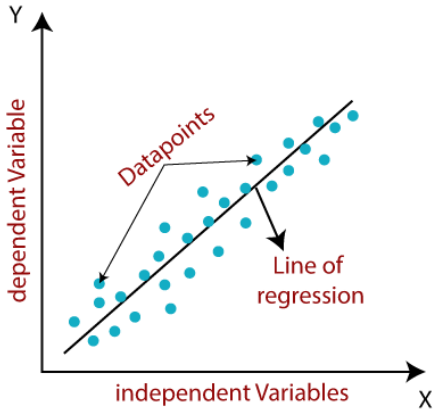

Fig.8 Linear regression model

4.3 Artificial Neural Networks

MATLAB was used to carry out the research. Fuzzy logic and Ann techniques[18] were both found to be effective in that their findings matched the characteristic of a real solar PV array [3]. These will be put to use to forecast and test the overall reliability of the solar power plant. They perform on three sets of data: training, testing, and validation. The MLR model's performance is substantially improved when classification variables and interactions between variables are used, but this is not the case with the ANN model [7].

4.3.1 Fuzzy Logic:

When combined with high-performance computer processors, allows for reasonable accuracy estimates of solar plant outputs while also allowing for system flexibility to adjust for natural events. The MATLAB software was used to construct the load forecasting system, which is based on fuzzy logic. The model has two inputs and one output and represents solar irradiance, ambient temperature, humidity and output power [3].

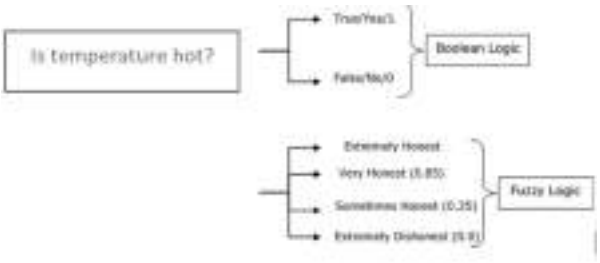

Fig.9 Fuzzy logic model

4.3.2 Multiple Linear Regression:

An ANN[16], as opposed to a multiple linear regression (MLR) model, a statistical method for assessing a non-linear connection between one or more inputs and outcomes. The artificial neural network[6] has been used to model, identify, and forecast complex systems.

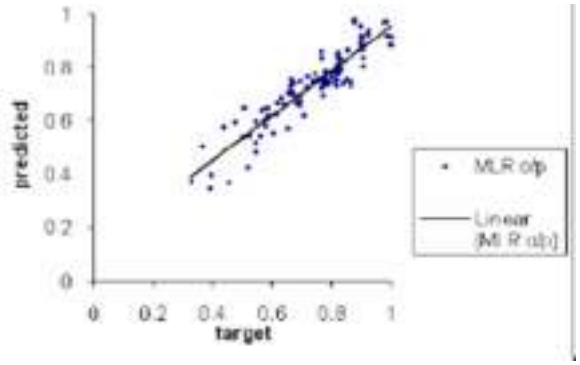

Fig.10 Multi linear regression

5. Comparison

5.1 Comparison of methods used:

Table 1. Model Prediction of RMSE, MAE, MAPE, and MBE

Model	RMSE	MAE	MAPE	MBE	Reference
MLP(multilayer perceptron)	0.0889	-	-	-	1
LSTM	0.0816	-	-	-	1
Clustering based on solar generation	8.80	4.60		-1.01	5
Clustering based on weather variables	8.61	3.77	-	-0.53	5
ANN	0.067	-	-	--	6
MLR(multi linear regression)	0.738	-	-	-	6
SVR(support vector regressor)	0.122	0.099	40.03	-	8
RFR(random forest regressor)	0.178	0.1378	67.58	-	8
CNN+LSTM	0.098	0.0568	13.42	-	8
SP(SMART PERSISTNACE)	0.135	0.071		0.023	11
DBN(deep belief network)	0.0390	0.0138		0.00244	11
SVM(support vector machine)	0.034	0.012		0.00777	11
RF(Random Forest)	0.033	0.0099		0.000351	11

5.2 Graphs comparison based on weather conditions with temperature values:

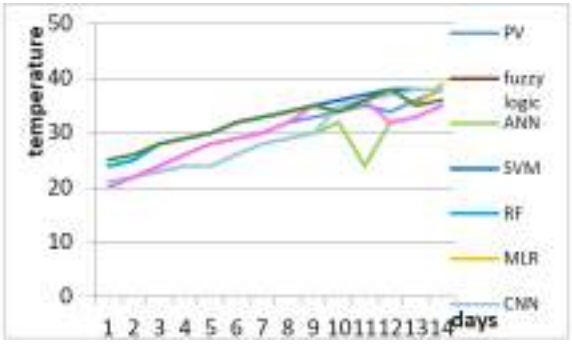

Fig.11 Mean of solar radiance in summer season.

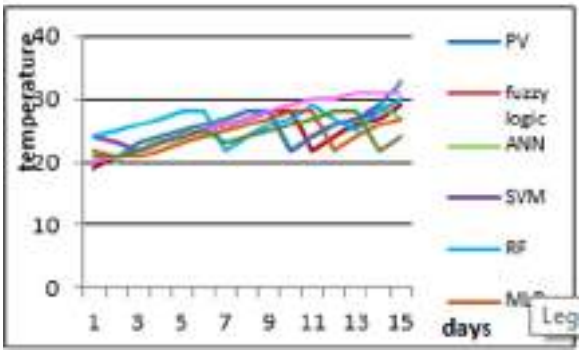

Fig.12 Mean of solar radiance in rainy season

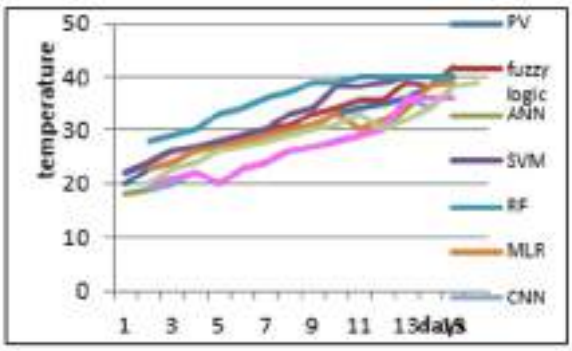

Fig.13 Mean of solar radiance in winter season

Here fig 11, 12, 13 gives the comparative analysis of different models that are used like fuzzy logic, artificial neural network, support vector machine, random forest, multiple linear regressor and Convolutional Neural Network results for different temperature based on seasonal effects with power generated for each day.

7. Conclusion

In this we conclude that it gives the partial analysis of solar power generation or forecasting based on different weather conditions. Different types of solar and wind dataset are considered for different seasons like summer (April to June), rainy (July to November) and winter (December to January) these are all about Indian weather condition. In order to get best results for diverse climatic condition for every hour for future betterment of analyzing power generation in different climatic condition machine learning give better results according to deep learning and artificial intelligence.

Reference

1. A. Gensler, J. Henze, and B. Sick, 2016 IEEE International (2016)
2. N. Sharma, P. Sharma, D. Irwin, and P. Shenoy, in 2011 IEEE International Conference on Smart Grid Communications (SmartGridComm) , pp. 528–533, (2011)
3. Z. P. Ncane and A. K. Saha, in 2019 Southern African Universities Power Engineering Conference/Robotics and Mechatronics/Pattern Recognition Association of South Africa (SAUPEC/RobMech/PRASA), pp. 518–523,(2019)
4. A. Khalyasmaa, S. A. Eroshenko, T. P. Chakravarthy, V. G. Gasi, S. K. Y. Bollu, R. Caire, S. K. R. Atluri, and S. Karrolla, in 2019 International Multi-Conference on Engineering, Computer and Information Sciences (SIBIRCON) , pp. 0780–0785, (2019)
5. C. Pan and J. Tan, IEEE Access 7, 112921 (2019).
6. P. Kora and S. R. Kalva, Springer plus 4, 481 (2015)
7. M. Abuella and B. Chowdhury, in 2015 North American Power Symposium (NAPS) , pp. 1–5, (2015)
8. K. Prasanna Lakshmi and C. R. K. Reddy, in 2010 International Conference on Networking and Information Technology , pp. 451–455(2010)
9. D. Su, E. Batzelis, and B. Pal, in 2019 International Conference on Smart Energy Systems and Technologies (SEST) , pp. 1–6 , (2019)
10. Swaraja K, Multimed. Tools Appl. 77, 28249 (2018)
11. W. Lee, K. Kim, J. Park, J. Kim, and Y. Kim, IEEE Access 6, 73068 (2018)
12. S. Kumar, P. Reddy, G. Ramesh, and V. Maddumala, Trait. Du Signal 36, 233 (2019)
13. F. Jawaid and K. NazirJunejo, in 2016 Sixth International Conference on Innovative Computing Technology (INTECH) , pp. 355–360, (2016)

14. C. U. Kumari, S. Jeevan Prasad, and G. Mounika, 2019 3rd International Conference on Computing Methodologies and Communication (ICCMC) (2019)
15. X. Wang, D. Luo, and C. Li, in 2019 2nd International Conference on Artificial Intelligence and Big Data (ICAIBD) , pp. 97–101, (2019)
16. B. Dhanalaxmi, G. A. Naidu, and K. Anuradha, Procedia Comput. Sci. 46, 432 (2015)
17. Application of Machine Learning Algorithms for Solar Power Forecasting in Sri Lanka
18. P. Nayak, G. K. Swetha, S. Gupta, and K. Madhavi, Measurement 178, 108974 (2021)
19. M. Z. Hassan, M. E. K. Ali, A. B. M. S. Ali, and J. Kumar, in 2017 4th Asia-Pacific World Congress on Computer Science and Engineering (APWC on CSE) , pp. 252–258, (2017)

Analysis Of Solar Power Generation Forecasting Using Machine Learning Techniques

K. Anuradha[1],* *Deekshitha* Erlapally[2], *G*. Karuna[3], *V*. Srilakshmi[4], *K*. Adilakshmi[5]

[1]Professor, Computer Science and Engineering, GRIET, Hyderabad, Telangana, India.
[2]MTech Student, Computer Science and Engineering, GRIET, Hyderabad, Telangana, India.
[3]Professor, Computer Science and Engineering, GRIET, Hyderabad, Telangana, India.
[4] Asst.Professor, Computer Science and Engineering, GRIET, Hyderabad, Telangana, India.
[5] Asst.Professor, Computer Science and Engineering, GRIET, Hyderabad, Telangana, India.

Abstract: Solar power is generated using photovoltaic (PV) systems all over the world. Because the output power of PV systems is alternating and highly dependent on environmental circumstances, solar power sources are unpredictable in nature. Irradiance, humidity, PV surface temperature, and wind speed are only a few of these variables. Because of the unpredictability in photovoltaic generating, it's crucial to plan ahead for solar power generation as in solar power forecasting is required for electric grid. Solar power generation is weather-dependent and unpredictable, this forecast is complex and difficult. The impacts of various environmental conditions on the output of a PV system are discussed. Machine Learning (ML) algorithms have shown great results in time series forecasting and so can be used to anticipate power with weather conditions as model inputs. The use of multiple machine learning, Deep learning and artificial neural network techniques to perform solar power forecasting. Here in this regression models from machine learning techniques like support vector machine regressor, random forest regressor and linear regression model from which random forest regressor beaten the other two regression models with vast accuracy.

1 Introduction:

Solar energy has many benefits, but also have their initial investment for installing solar panels is quite high, and not everyone will be able to afford them. Unfortunately, this is a downside of solar panels; nevertheless, as prices continue to decline, the future looks bright. Solar panels are currently relatively costly; but, new government programs and cutting-edge technology are making them cheaper. Despite the fact that photovoltaic cells are recognized as the significant source of potential energy production, their low return on investment and high upfront costs keeps them from becoming widely used.The high initial cost prevents them from becoming widely used. Because photovoltaic cells convert solar energy into electrical energy, the amount of solar energy produced each day influences the size of the photovoltaic system, just as the amount of solar radiation influences the amount of electricity produced each day. This is influenced by factors such as location, time, and weather patterns. Solar irradiance is the power obtained per unit area from the Sun via electromagnetic radiation in the wavelength range of the solar cell in use.

Major grid integration is difficult because renewable energy is irregular and uncontrollable. Households can now use almost any amount of energy due to the recent electric grid at any moment, but it is not equipped for large quantities of uncontrollable generation at this time. As it is converting solar radiance into power we don't get that how much power is emitted for different location, time, and weather. For this type of clarification machine learning techniques are used in order to differentiate it for different conditions. Machine-learning techniques are wide applied to several fields where it can separate the weather based power.

The amount of energy a PV system generates is proportional to meteorological parameters including cloud cover, sun intensity, and site-specific conditions, among other [3]. Solar panel works differently for different weather conditions. In case if its summer seasons then the amount of energy consumed by the panel from sun is very much more. But in case of rainy and windy conditions the energy consumed is pretty much different. Power generation mostly depends on weather conditions so they take weather forecasting into consideration. As a result, the amount of electricity generated is determined by solar irradiance on a given day, which is determined by a number of factors such as location, time, and weather patterns. We concentrate on the problem of automatically generating models that accurately predict renewable generation based on National Weather Service forecasts (NWS). Using historical NWS forecast data and data generated by solar panels, we experiment with a variety of machine learning techniques to develop prediction models.

* Corresponding author: author@e-mail.org

Meteorological data, including ambient temperature, humidity, and solar radiation, will be collected by meteorological monitoring stations every three hours.

Machine-learning techniques have been widely used in a range of fields involving data-driven problems in recent decades. Machine-learning approaches encompass a wide range of interdisciplinary topics, including statistics, mathematics, artificial neural networks, data mining, optimization, and artificial optimization. With or without mathematical problem forms, machine learning approaches attempt to find a relationship between input and output data. The process of analysing data is known as data analyzation. ML employs statistical approaches to enable computers to "learn" from data without having to be explicitly programmed. Machine learning has two main application categories: regression and classification. Solar power forecasting necessitates the use of regression methods. Some of the ML regression algorithms that can be used for time series forecasting are Linear Regression (LR), Support Vector Machine Regression (SVMR), and Random Forest (RF).

Weather and physical elements influence the electrical power output of a solar photovoltaic (PV) panel. Solar irradiance, cloud cover, humidity, and ambient temperature are the main meteorological factors that influence solar power generation. Predicted weather parameters can be used as model inputs, while solar power forecasts can be used as the model output. Because of its ongoing training nature, the ML algorithm adjusts to physical parameters.

In machine learning SVM plays a major role in order to classify the data and monitor weather condition according. Combining data from photovoltaic power generation with meteorological conditions, according to the positive position of photovoltaic power generation. For every 3 hours svm gives analyzed data for classification and regression analysis. Using hyperplane we can classify the accurate results from solar panel based on the weather conditions.Random forest, on the other hand, is a classification strategy that uses many decision trees to classify data. In order to generate an uncorrelated forest of trees whose committee forecast is more trustworthy than that of any single tree, bagging and feature randomization are utilised in the development of each individual tree. It gives multiple decisions tress it merges all the decision tress into one form of decision tree it's for different climatic conditions such as for summer, rainy, winter seasons. Error statistics such as mean bias error (MBE), mean absolute error (MAE), root mean square error (RMSE), relative MBE (rMBE), mean percentage error (MPE), and relative RMSE are used to assess the model's validity (rRMSE). Linear regression is a supervised learning-based machine learning approach. It does a regression analysis. Based on independent variables, regression models a goal prediction value. It's generally used in forecasting to figure out how variables are related. Regression models differ in terms of the sort of link examined between dependent and independent variables, as well as the number of independent variables used.

2. Related Work:

Solar energy forecasts can be categorised in a variety of ways. The persistence or smart persistence model, which uses historical data to forecast future power generation over a short period of time, is the most basic method (2-3 hours). This method can be used to set a standard against which other forecasting methods can be measured. In most cases, a prediction is completed in two stages. A NWP is designed for a specified time period and location to begin with. The generated NWP is then utilised to forecast power generation using forecasting algorithms. It is possible to employ a physical model, a statistical method, or a machine learning methodology [1].For prediction, ML algorithms are compared to the Smart Persistence (SP) approach, with ML models outperforming the SP model. The unpredictability of solar resources has hampered grid management as solar diffusion rates have increased. Unpredictability and intermittent electricity delivery are two of the most difficult aspects of integrating renewables into the system. As a result, solar power forecasting is becoming increasingly important for grid stability, optimal unit commitment, and cost-effective dispatch. To overcome the problem, we employ machine learning techniques to sift through extraordinary solar radiation predicting models. For developing prediction models, a variety of regression algorithms are tested, including linear least squares and support vector machines with various kernel functions. We use day-ahead sun radiation data forecasts in these tests to show that a machine learning approach can correctly anticipate short-term solar power [2]. A hybrid or mixed forecasting method was developed by combining clustering, classification, and regression approaches to produce a forecasting model. Based on the weather forecast for the next day, the model (with the closest weather condition) is chosen to forecast the power output using cluster-wise regression [3].

Renewable energy sources are progressively being integrated into electric networks alongside nonrenewable energy sources, posing significant issues due totheir sporadic and erratic nature In order to address these issues, soft-computing solutions for energy prediction are essential.We apply a number of data mining methodologies, including preparing historical load data and analysing the features of the load time series, because electricity consumption is entangled with the usage of other energy sources like natural gas and oil. The trends in power consumption from renewable and nonrenewable energy sources were examined and contrasted. A novel machine learning-based hybrid technique (SVR) uses multilayer perceptron (MLP) and support vector regression [5].Using SVM regression, solar power generation produces acceptable results [6]. However, it lacks a detailed examination of solar power generation and meteorological data, and hence is restricted in its capacity to accurately predict other data sets by merely using different SVM kernels after some basic statistical data processing [8].

To study the association between expected weather conditions and power output created as a historical time series, artificial intelligence (AI) approaches are applied.

AI approaches use algorithms that can implicitly characterise the nonlinear and highly intricate relationship between input data (NWP predictions) and output power instead of formal statistical analysis. The ANN is a brain model that is based on biology. They're employed in a range of applications that use AI approaches including supervised, unsupervised, and reinforcement learning. The ANN learns from data in the supervised learning approach by being trained to approximate and estimate the function or relationship. [6].

Their models have been improved to predict PV plant power generation [4–7]. Even with the cloud graph from synchronous meteorological satellites, the significant unpredictability in critical components, particularly the diffuse component from the sky hemisphere, makes solar irradiance far less predictable than temperature. PV systems including a large number of different tiles deployed over a large area have additional challenges [12]. Because it is impossible to examine all connected meteorological forecasts in a practical context, many alternative alternatives have been devised. Weather forecasts from meteorological websites [8] were considered by some. Others used nonlinear modelling approaches like artificial neural networks to try to simplify the solar forecast model (ANN). Two types of networks are commonly used to forecast global solar radiation, solar radiation on titled surfaces, daily solar radiation, and short-term solar radiation: radial basis function (RBF) and multilayer perception (MLP).

In a three-layer feed forward model, back-propagation is the neural network training technique. To reduce forecast error, the input layer provides an error correction factor depending on the projected output for the previous 5 minutes.

An LSTM network will learn a function that accepts a sequence of previous solar irradiance values as input and returns a solar irradiance value as output. Deep neural networks, such as the Deep Belief Network (DBN), will learn a function that takes a sequence of historical sun irradiance values as input and outputs a solar irradiance value. If a series of observations are converted into a variety of occurrences, an LSTM network can learn from them. The sequence is partitioned using LSTM for prediction purposes.

3 PROPOSED WORK:

For knowing how much power is generated from solar we have the dataset showing daily average temperature in Celsius, distance from solar noon, wind speed, wind direction, sky cover, and humidity and then the power generated. Here we are calculating how much power is generated in different weather condition for India dataset . We have taken Indian dataset with different temperature readings. The available dataset is based on hourly weather parameter values. To convert the data to mean values per day, the average of the 24-hour data was used. From 2019 to 2020, several weather factors were collected to investigate the relationship between mean solar irradiance and meteorological data in order to accurately estimate power generated.

The proposed work's System Architecture is to first consider the dataset and preprocess the data, then divide it into train and test data, apply classification techniques, and predict the results. Solar power weather dataset is used for forecasting purposes in this case. Data preprocessing methods include cleaning, integration, reduction, and transmission. We must purge any data that is no longer absolutely necessary. Data cleaning is the process of identifying and removing inaccurate or incorrect records from a dataset. Data from the real world frequently contains noise and missing values, and it may be in an unusable format that cannot be directly used for DL models. Data preprocessing is required to clean data and prepare it for various Deep Learning models, increasing accuracy and efficiency. Training and testing data are separated from the preprocessed data. The model is trained using training data, and its predictions are validated using testing data. Data splitting is the process of dividing available data into two halves, usually for cross-validator purposes. The first set of data is used to build a predictive model, while the second set is used to evaluate the model's performance. In analyzing data mining algorithms, separating data into training and testing sets is crucial. The training percentage is set at 80% and the test percentage is set at 20%. When a data set is divided into a training set and a testing set, the majority of the data is used for training and only a small portion is used for testing. To train any model, no matter what type of dataset is used, the dataset must be divided into training and testing data. The dataset will be examined for null values and outliers during the data preprocessing step, and the model will be trained using three hours of data before being used to forecast solar power generation value. The power generated radiance phase will be estimated using machine learning (ML) methods (e.g., support vector regression, linear regression, elastic net regression, and random forest) as shown in below Fig 1.

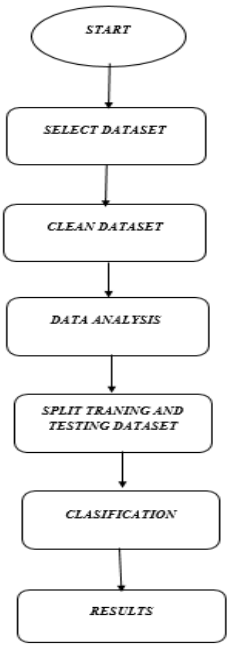

Fig.1 Flow chart for solar power generation

4. Methodology:

The current dataset is based on hourly weather parameter values. To convert the data to mean values per day, the average of the 3-hour data was used. Various weather characteristics were gathered in order to investigate the relationship between mean solar irradiance and meteorological data in order to accurately estimate mean solar irradiance. The average daily values of air temperature, humidity, wind speed, wind direction, visibility, average pressure, average wind speed, and electricity generated are among the data collected. The direction of the wind, on the other hand, indicates how high the sun is. It's also expressed in degrees.

Machine Learning (ML) Models are used for forecasting the solar power generation weather analysis. The Regression techniques here proposed are Support Vector Machine, Random Forest, Linear Regression are various ML Models used in this paper.

4.1 Forecasting models:

In this study, we used the chosen dataset to evaluate individual performance using a number of meteorological attributes utilising three commonly used machine learning algorithms. The output of the unseen test sample is predicted to be the mean of these K closest matches because our prediction variable is continuous valued. We investigated a variety of K values, however only the results for K=3 and K=5 are presented. When K is more than 3, the RMS error increases.

Support vector regression (SVR) using a radial basis function as the kernel and random forest (RF) approaches are used to create the models. Because of the non-linearity of the dataset, we used the models indicated above instead of linear models. The most basic and widely used regression method is linear regression (LR) [10].It uses linear predictor functions to represent the relationship between the input and output variables, and a least squares approach is used to estimate the unknown model parameters from the data. A set of linear equations or an iterative method like gradient descent can be used to estimate parameter values. We employed the characteristics provided in the, followed by feature scaling, to standardise the input data. SVR's precision varies depending on the kernel function and other variables. To discover the optimal settings, we employed the Grid search approach. To evaluate the models' performance on the test set, we computed the Root-Mean-Square Error (RMSE) and R squared values. Before choosing the models with the lowest root mean squared error and highest R squared values, we fine-tuned the model hyperparameters. Nonlinear relationships can be mapped using these methods. In data science challenges of various kinds, methods including decision trees, RF, and gradient boosting are commonly utilised.The RF method is a tree-based machine learning approach that can be used for regression and classification. It also performs dimensional reduction, controls missing and outlier values, and performs a variety of additional data exploration activities. The bagging approach is used to train RFs. This method allows for the usage of numerous instances for the training stage because the dataset is sampled with a replacement. Linear regression is a method for demonstrating the link between a dependent variable and one or more independent variables by using the best-fit linear curve. It is concerned with determining the best-fit line with the data by attaining a perfect slope and intercept value.The best model for forecasting solar power system output based on numerous weather parameters was then created. The models that gave the greatest results on the dataset were support vector regression, random forests, and linear regression, and these models were then utilized to anticipate PV system performance for 2019. Thanks to the predictive analysis, the estimated production in this situation ranges from 0 to 1000 Watt hours. These models were then evaluated using the test data. The SVR model has an RMSE of 135.7, while the random forest model has an RMSE of 28.62 and the SVR model has an RMSE of 58.24. The random forest model's points are close to the regressed diagonal line, however the SVR model's points are not.

5 RESULTS:

A matrix of pair correlation coefficients is generated for a set of features under investigation in order to find collinear factors as shown in below Fig 1, Fig 2,Fig 3 and Fig 4.

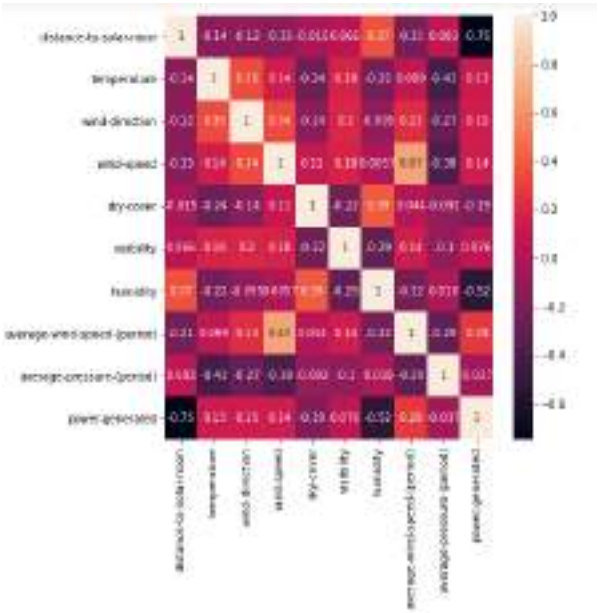

Fig 2 correlation matrix

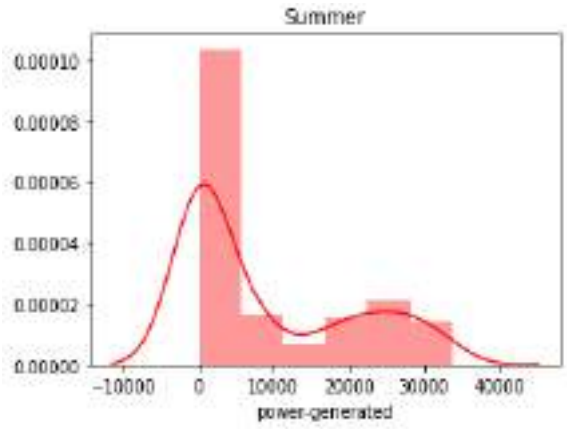

Fig 3:summer season analysis

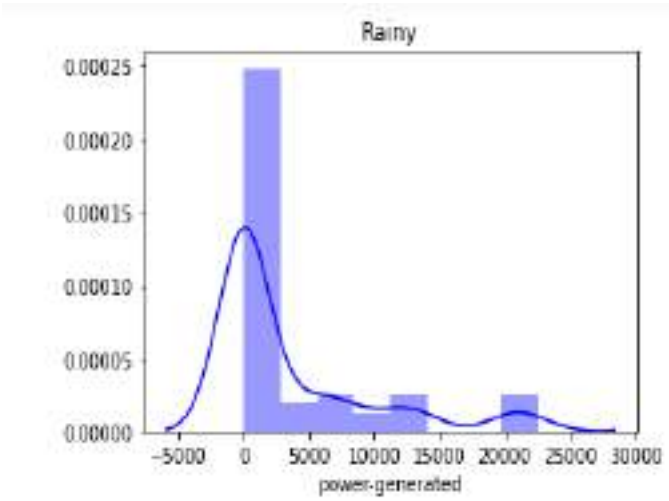

Fig 4: rainy season analysis

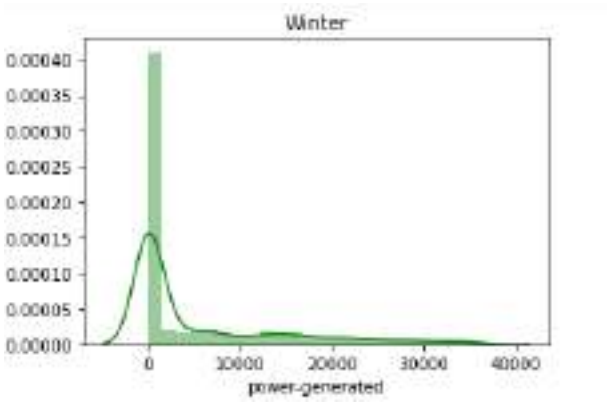

Fig 5: winter season analysis

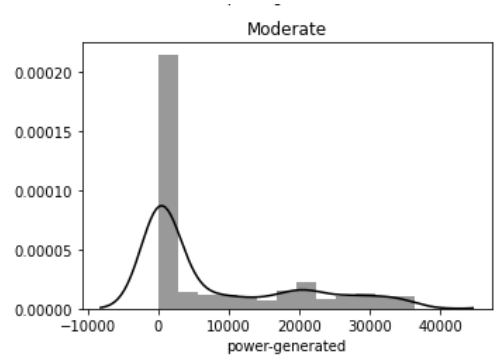

Fig 6: moderate analysis

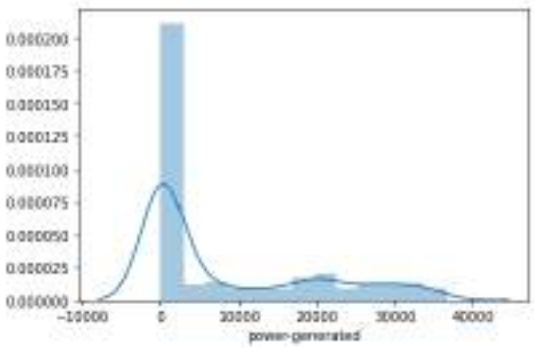

Fig7: overall season's comparative analysis

Here fig6 shows that how power is generated comparatively in different weather conditions where the x axis shows the power generated and y axis shows the distance from solar noon. It is nothing more than Solar noon occurs when the Sun passes through a location's meridian (a meridian is an imaginary line that runs from the North Pole to the South Pole along the Earth's surface.) and ascends to its highest point in the sky. In most cases, it does not occur at 12 p.m and as shown in above Fig 5 and Fig 6 and Below Fig 7.

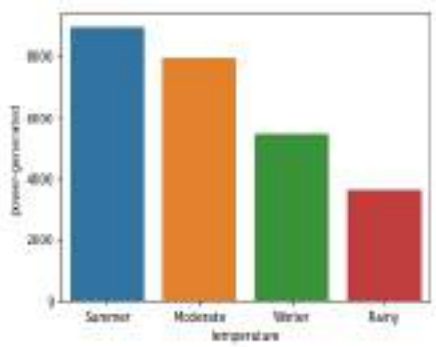

Fig 8: Different temperature analysis results of how much power is generated.

Fig6 says the power generated is read as Jules here where as temperature as in summer, rainy, winter and the moderate is said as the different weather condition. Dataset considered is the numerical dataset so we replaced them with string type where in dataset it is shown as 0 for rainy 1 for winter, 2 for moderate,3 for summer as shown in below Fig 9 and Fig 10.

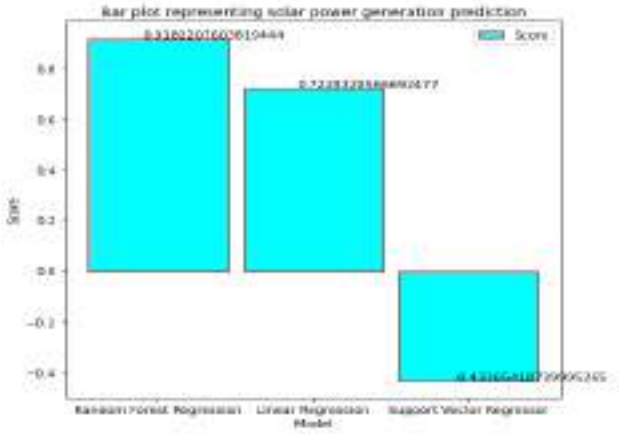

Fig 9: score of all the three model used in solar power analysis.

This fig8 shows that score of three different models used in this paper for solar power generation

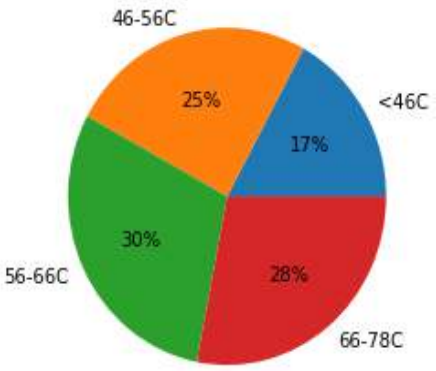

Fig 10: temperature difference and their power generated percentage accordingly.

This shows that how much percentage of power is generated ass the temperature rises less than 46 Celsius is 0 that's the rainy season temperature, 46 o 56 Celsius is 1 that's winter season temperature,56 to 66C is 2 that's moderate temperature and 66 to 78C is 3 that's summer season and as shown in below Table 1.

Table 1: Model Prediction of RMSE, MAE, MAPE, and MBE and Accuracy

Model	RMSE	MAE	MSE	Accuracy
Support vector machine regressor	131.44	77.16	172.76	-44.92
Linear regression	58.57	48.39	343.08	72.4
Random forest regressor	27.32	12.45	746.48	94.01

6. Conclusion:

We presented a machine learning-based approach for solar power generation analysis in this paper, which accurately forecasts power generated across India's states based on environmental data. Most importantly, our methodology went beyond prediction by delivering key results that aided in the understanding of solar power analysis (variable importance by time period). By a wide margin, the proposed method outperformed other popular methods, such as Random forest. The proposed models are SVR, LR, and RF. Compared to the temperature with the given data. 56-55F --30% power generation is increasing compared to other temperatures. Temperature <46F is 17% temperature average of it. As the above results, we can see that Random Forest Regressor model is performing better with 94.01% accuracy and hence that model is preferred for deployment.

Reference:

1. P. A. G. M. Amarasinghe and S. K. Abeygunawardane, "*Application of Machine Learning Algorithms for Solar Power Forecasting in Sri Lanka*" (2nd International Conference On Electrical Engineering (EECon), Colombo, Sri Lanka, 87 2018).
2. M. Z. Hassan, M. E. K. Ali, A. B. M. S. Ali and J. Kumar, "*Forecasting Day-Ahead Solar Radiation Using Machine Learning Approach*" (4th Asia-Pacific World Congress on Computer Science and Engineering (APWC on CSE), Mana Island, Fiji, 252 2017).
3. A. Bajpai and M. Duchon, "*A Hybrid Approach of Solar Power Forecasting Using Machine Learning*" (3rd International Conference on Smart Grid and Smart Cities (ICSGSC), 108 2019).
4. A. Khan, R. Bhatnagar, V. Masrani and V. B. Lobo, "*A Comparative Study on Solar Power Forecasting using Ensemble Learning*," (4th International

Conference on Trends in Electronics and Informatics (ICOEI), 224 2020).

5. Khan, P.W.; Byun, Y.-C.; Lee, S.-J.; Kang, D.-H.; Kang, J.-Y.; Park, H.-S. Energies, **13**, 4870 (2020).
6. Faquir, Sanaa & Yahyaouy, Ali & Tairi, H. & Sabor, Jalal. International Journal of Fuzzy System Applications. **4**, 10 (2015).
7. Aler R., Martín R., Valls J.M., Galván I.M. Intelligent Distributed Computing VIII. Studies in Computational Intelligence, vol **570** (2015).
8. Y. Wang, G. Cao, S. Mao and R. M. Nelms, "*Analysis of solar generation and weather data in smart grid with simultaneous inference of nonlinear time series*," (IEEE Conference on Computer Communications Workshops (INFOCOM WKSHPS), 600 2015).
9. Carrera B, Kim K. Sensors (Basel). **20**, 3129 (2020).
10. Jawaid F, NazirJunejo K. *Predicting daily mean solar power using machine learning regression techniques*. (Sixth International Conference on Innovative Computing Technology (INTECH) 355 2016).
11. Batcha RR, Geetha MK. *A survey on IOT based on renewable energy for efficient energy conservation using machine learning approaches*. (3rd International Conference on Emerging Technologies in Computer Engineering: Machine Learning and Internet of Things (ICETCE) 123 2020).
12. Li, Zhaoxuan & Rahman, Sm Mahbobur & Vega, Rolando & Dong, Bing. Energies. **9**, 55 (2016).
13. Lai JP, Chang YM, Chen CH, Pai PF. Applied Sciences; **10**, 5975 (2020).
14. Brahma, B.; Wadhvani, R. Symmetry, **12**, 1830 (2020).

Analysis Of Solar Power Generation Forecasting Using Machine Learning Techniques

K. Anuradha[1],* *Deekshitha* Erlapally[2], *G*. Karuna[3], *V*. Srilakshmi[4], *K*. Adilakshmi[5]

[1]Professor, Computer Science and Engineering, GRIET, Hyderabad, Telangana, India.
[2]MTech Student, Computer Science and Engineering, GRIET, Hyderabad, Telangana, India.
[3]Professor, Computer Science and Engineering, GRIET, Hyderabad, Telangana, India.
[4] Asst.Professor, Computer Science and Engineering, GRIET, Hyderabad, Telangana, India.
[5] Asst.Professor, Computer Science and Engineering, GRIET, Hyderabad, Telangana, India.

Abstract: Solar power is generated using photovoltaic (PV) systems all over the world. Because the output power of PV systems is alternating and highly dependent on environmental circumstances, solar power sources are unpredictable in nature. Irradiance, humidity, PV surface temperature, and wind speed are only a few of these variables. Because of the unpredictability in photovoltaic generating, it's crucial to plan ahead for solar power generation as in solar power forecasting is required for electric grid. Solar power generation is weather-dependent and unpredictable, this forecast is complex and difficult. The impacts of various environmental conditions on the output of a PV system are discussed. Machine Learning (ML) algorithms have shown great results in time series forecasting and so can be used to anticipate power with weather conditions as model inputs. The use of multiple machine learning, Deep learning and artificial neural network techniques to perform solar power forecasting. Here in this regression models from machine learning techniques like support vector machine regressor, random forest regressor and linear regression model from which random forest regressor beaten the other two regression models with vast accuracy.

1 Introduction:

Solar energy has many benefits, but also have their initial investment for installing solar panels is quite high, and not everyone will be able to afford them. Unfortunately, this is a downside of solar panels; nevertheless, as prices continue to decline, the future looks bright. Solar panels are currently relatively costly; but, new government programs and cutting-edge technology are making them cheaper. Despite the fact that photovoltaic cells are recognized as the significant source of potential energy production, their low return on investment and high upfront costs keeps them from becoming widely used.The high initial cost prevents them from becoming widely used. Because photovoltaic cells convert solar energy into electrical energy, the amount of solar energy produced each day influences the size of the photovoltaic system, just as the amount of solar radiation influences the amount of electricity produced each day. This is influenced by factors such as location, time, and weather patterns. Solar irradiance is the power obtained per unit area from the Sun via electromagnetic radiation in the wavelength range of the solar cell in use.

Major grid integration is difficult because renewable energy is irregular and uncontrollable. Households can now use almost any amount of energy due to the recent electric grid at any moment, but it is not equipped for large quantities of uncontrollable generation at this time. As it is converting solar radiance into power we don't get that how much power is emitted for different location, time, and weather. For this type of clarification machine learning techniques are used in order to differentiate it for different conditions. Machine-learning techniques are wide applied to several fields where it can separate the weather based power.

The amount of energy a PV system generates is proportional to meteorological parameters including cloud cover, sun intensity, and site-specific conditions, among other [3]. Solar panel works differently for different weather conditions. In case if its summer seasons then the amount of energy consumed by the panel from sun is very much more. But in case of rainy and windy conditions the energy consumed is pretty much different. Power generation mostly depends on weather conditions so they take weather forecasting into consideration. As a result, the amount of electricity generated is determined by solar irradiance on a given day, which is determined by a number of factors such as location, time, and weather patterns. We concentrate on the problem of automatically generating models that accurately predict renewable generation based on National Weather Service forecasts (NWS). Using historical NWS forecast data and data generated by solar panels, we experiment with a variety of machine learning techniques to develop prediction models.

* Corresponding author: author@e-mail.org

Meteorological data, including ambient temperature, humidity, and solar radiation, will be collected by meteorological monitoring stations every three hours.

Machine-learning techniques have been widely used in a range of fields involving data-driven problems in recent decades. Machine-learning approaches encompass a wide range of interdisciplinary topics, including statistics, mathematics, artificial neural networks, data mining, optimization, and artificial optimization. With or without mathematical problem forms, machine learning approaches attempt to find a relationship between input and output data. The process of analysing data is known as data analyzation. ML employs statistical approaches to enable computers to "learn" from data without having to be explicitly programmed. Machine learning has two main application categories: regression and classification. Solar power forecasting necessitates the use of regression methods. Some of the ML regression algorithms that can be used for time series forecasting are Linear Regression (LR), Support Vector Machine Regression (SVMR), and Random Forest (RF).

Weather and physical elements influence the electrical power output of a solar photovoltaic (PV) panel. Solar irradiance, cloud cover, humidity, and ambient temperature are the main meteorological factors that influence solar power generation. Predicted weather parameters can be used as model inputs, while solar power forecasts can be used as the model output. Because of its ongoing training nature, the ML algorithm adjusts to physical parameters.

In machine learning SVM plays a major role in order to classify the data and monitor weather condition according. Combining data from photovoltaic power generation with meteorological conditions, according to the positive position of photovoltaic power generation. For every 3 hours svm gives analyzed data for classification and regression analysis. Using hyperplane we can classify the accurate results from solar panel based on the weather conditions.Random forest, on the other hand, is a classification strategy that uses many decision trees to classify data. In order to generate an uncorrelated forest of trees whose committee forecast is more trustworthy than that of any single tree, bagging and feature randomization are utilised in the development of each individual tree. It gives multiple decisions tress it merges all the decision tress into one form of decision tree it's for different climatic conditions such as for summer, rainy, winter seasons. Error statistics such as mean bias error (MBE), mean absolute error (MAE), root mean square error (RMSE), relative MBE (rMBE), mean percentage error (MPE), and relative RMSE are used to assess the model's validity (rRMSE). Linear regression is a supervised learning-based machine learning approach. It does a regression analysis. Based on independent variables, regression models a goal prediction value. It's generally used in forecasting to figure out how variables are related. Regression models differ in terms of the sort of link examined between dependent and independent variables, as well as the number of independent variables used.

2. Related Work:

Solar energy forecasts can be categorised in a variety of ways. The persistence or smart persistence model, which uses historical data to forecast future power generation over a short period of time, is the most basic method (2-3 hours). This method can be used to set a standard against which other forecasting methods can be measured. In most cases, a prediction is completed in two stages. A NWP is designed for a specified time period and location to begin with. The generated NWP is then utilised to forecast power generation using forecasting algorithms. It is possible to employ a physical model, a statistical method, or a machine learning methodology [1].For prediction, ML algorithms are compared to the Smart Persistence (SP) approach, with ML models outperforming the SP model. The unpredictability of solar resources has hampered grid management as solar diffusion rates have increased. Unpredictability and intermittent electricity delivery are two of the most difficult aspects of integrating renewables into the system. As a result, solar power forecasting is becoming increasingly important for grid stability, optimal unit commitment, and cost-effective dispatch. To overcome the problem, we employ machine learning techniques to sift through extraordinary solar radiation predicting models. For developing prediction models, a variety of regression algorithms are tested, including linear least squares and support vector machines with various kernel functions. We use day-ahead sun radiation data forecasts in these tests to show that a machine learning approach can correctly anticipate short-term solar power [2]. A hybrid or mixed forecasting method was developed by combining clustering, classification, and regression approaches to produce a forecasting model. Based on the weather forecast for the next day, the model (with the closest weather condition) is chosen to forecast the power output using cluster-wise regression [3].

Renewable energy sources are progressively being integrated into electric networks alongside nonrenewable energy sources, posing significant issues due totheir sporadic and erratic nature In order to address these issues, soft-computing solutions for energy prediction are essential.We apply a number of data mining methodologies, including preparing historical load data and analysing the features of the load time series, because electricity consumption is entangled with the usage of other energy sources like natural gas and oil. The trends in power consumption from renewable and nonrenewable energy sources were examined and contrasted. A novel machine learning-based hybrid technique (SVR) uses multilayer perceptron (MLP) and support vector regression [5].Using SVM regression, solar power generation produces acceptable results [6]. However, it lacks a detailed examination of solar power generation and meteorological data, and hence is restricted in its capacity to accurately predict other data sets by merely using different SVM kernels after some basic statistical data processing [8].

To study the association between expected weather conditions and power output created as a historical time series, artificial intelligence (AI) approaches are applied.

AI approaches use algorithms that can implicitly characterise the nonlinear and highly intricate relationship between input data (NWP predictions) and output power instead of formal statistical analysis. The ANN is a brain model that is based on biology. They're employed in a range of applications that use AI approaches including supervised, unsupervised, and reinforcement learning. The ANN learns from data in the supervised learning approach by being trained to approximate and estimate the function or relationship. [6].

Their models have been improved to predict PV plant power generation [4–7]. Even with the cloud graph from synchronous meteorological satellites, the significant unpredictability in critical components, particularly the diffuse component from the sky hemisphere, makes solar irradiance far less predictable than temperature. PV systems including a large number of different tiles deployed over a large area have additional challenges [12]. Because it is impossible to examine all connected meteorological forecasts in a practical context, many alternative alternatives have been devised. Weather forecasts from meteorological websites [8] were considered by some. Others used nonlinear modelling approaches like artificial neural networks to try to simplify the solar forecast model (ANN). Two types of networks are commonly used to forecast global solar radiation, solar radiation on titled surfaces, daily solar radiation, and short-term solar radiation: radial basis function (RBF) and multilayer perception (MLP).

In a three-layer feed forward model, back-propagation is the neural network training technique. To reduce forecast error, the input layer provides an error correction factor depending on the projected output for the previous 5 minutes.

An LSTM network will learn a function that accepts a sequence of previous solar irradiance values as input and returns a solar irradiance value as output. Deep neural networks, such as the Deep Belief Network (DBN), will learn a function that takes a sequence of historical sun irradiance values as input and outputs a solar irradiance value. If a series of observations are converted into a variety of occurrences, an LSTM network can learn from them. The sequence is partitioned using LSTM for prediction purposes.

3 PROPOSED WORK:

For knowing how much power is generated from solar we have the dataset showing daily average temperature in Celsius, distance from solar noon, wind speed, wind direction, sky cover, and humidity and then the power generated. Here we are calculating how much power is generated in different weather condition for India dataset . We have taken Indian dataset with different temperature readings. The available dataset is based on hourly weather parameter values. To convert the data to mean values per day, the average of the 24-hour data was used. From 2019 to 2020, several weather factors were collected to investigate the relationship between mean solar irradiance and meteorological data in order to accurately estimate power generated.

The proposed work's System Architecture is to first consider the dataset and preprocess the data, then divide it into train and test data, apply classification techniques, and predict the results. Solar power weather dataset is used for forecasting purposes in this case. Data preprocessing methods include cleaning, integration, reduction, and transmission. We must purge any data that is no longer absolutely necessary. Data cleaning is the process of identifying and removing inaccurate or incorrect records from a dataset. Data from the real world frequently contains noise and missing values, and it may be in an unusable format that cannot be directly used for DL models. Data preprocessing is required to clean data and prepare it for various Deep Learning models, increasing accuracy and efficiency. Training and testing data are separated from the preprocessed data. The model is trained using training data, and its predictions are validated using testing data. Data splitting is the process of dividing available data into two halves, usually for cross-validator purposes. The first set of data is used to build a predictive model, while the second set is used to evaluate the model's performance. In analyzing data mining algorithms, separating data into training and testing sets is crucial. The training percentage is set at 80% and the test percentage is set at 20%. When a data set is divided into a training set and a testing set, the majority of the data is used for training and only a small portion is used for testing. To train any model, no matter what type of dataset is used, the dataset must be divided into training and testing data. The dataset will be examined for null values and outliers during the data preprocessing step, and the model will be trained using three hours of data before being used to forecast solar power generation value. The power generated radiance phase will be estimated using machine learning (ML) methods (e.g., support vector regression, linear regression, elastic net regression, and random forest) as shown in below Fig 1.

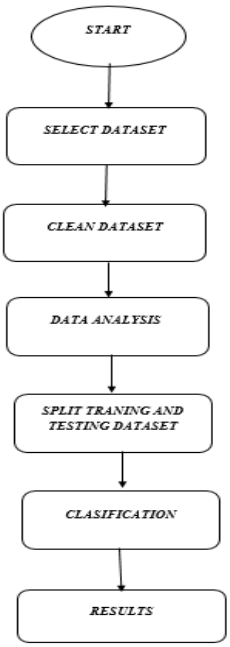

Fig.1 Flow chart for solar power generation

4. Methodology:

The current dataset is based on hourly weather parameter values. To convert the data to mean values per day, the average of the 3-hour data was used. Various weather characteristics were gathered in order to investigate the relationship between mean solar irradiance and meteorological data in order to accurately estimate mean solar irradiance. The average daily values of air temperature, humidity, wind speed, wind direction, visibility, average pressure, average wind speed, and electricity generated are among the data collected. The direction of the wind, on the other hand, indicates how high the sun is. It's also expressed in degrees.

Machine Learning (ML) Models are used for forecasting the solar power generation weather analysis. The Regression techniques here proposed are Support Vector Machine, Random Forest, Linear Regression are various ML Models used in this paper.

4.1 Forecasting models:

In this study, we used the chosen dataset to evaluate individual performance using a number of meteorological attributes utilising three commonly used machine learning algorithms. The output of the unseen test sample is predicted to be the mean of these K closest matches because our prediction variable is continuous valued. We investigated a variety of K values, however only the results for K=3 and K=5 are presented. When K is more than 3, the RMS error increases.

Support vector regression (SVR) using a radial basis function as the kernel and random forest (RF) approaches are used to create the models. Because of the non-linearity of the dataset, we used the models indicated above instead of linear models. The most basic and widely used regression method is linear regression (LR) [10].It uses linear predictor functions to represent the relationship between the input and output variables, and a least squares approach is used to estimate the unknown model parameters from the data. A set of linear equations or an iterative method like gradient descent can be used to estimate parameter values. We employed the characteristics provided in the, followed by feature scaling, to standardise the input data. SVR's precision varies depending on the kernel function and other variables. To discover the optimal settings, we employed the Grid search approach. To evaluate the models' performance on the test set, we computed the Root-Mean-Square Error (RMSE) and R squared values. Before choosing the models with the lowest root mean squared error and highest R squared values, we fine-tuned the model hyperparameters. Nonlinear relationships can be mapped using these methods. In data science challenges of various kinds, methods including decision trees, RF, and gradient boosting are commonly utilised.The RF method is a tree-based machine learning approach that can be used for regression and classification. It also performs dimensional reduction, controls missing and outlier values, and performs a variety of additional data exploration activities. The bagging approach is used to train RFs. This method allows for the usage of numerous instances for the training stage because the dataset is sampled with a replacement. Linear regression is a method for demonstrating the link between a dependent variable and one or more independent variables by using the best-fit linear curve. It is concerned with determining the best-fit line with the data by attaining a perfect slope and intercept value.The best model for forecasting solar power system output based on numerous weather parameters was then created. The models that gave the greatest results on the dataset were support vector regression, random forests, and linear regression, and these models were then utilized to anticipate PV system performance for 2019. Thanks to the predictive analysis, the estimated production in this situation ranges from 0 to 1000 Watt hours. These models were then evaluated using the test data. The SVR model has an RMSE of 135.7, while the random forest model has an RMSE of 28.62 and the SVR model has an RMSE of 58.24. The random forest model's points are close to the regressed diagonal line, however the SVR model's points are not.

5 RESULTS:

A matrix of pair correlation coefficients is generated for a set of features under investigation in order to find collinear factors as shown in below Fig 1, Fig 2,Fig 3 and Fig 4.

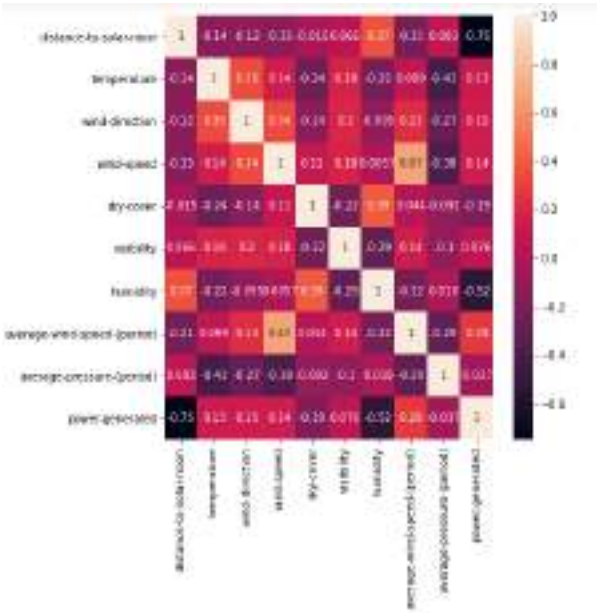

Fig 2 correlation matrix

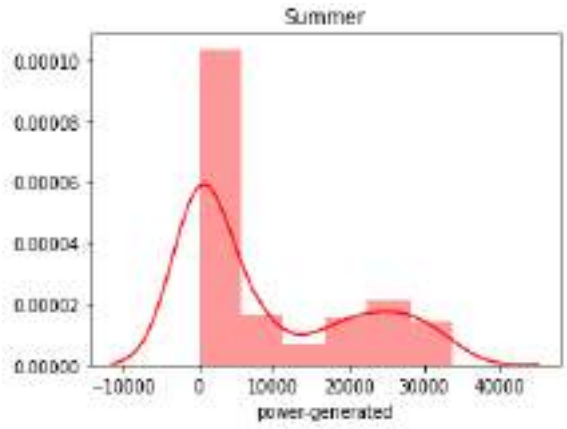

Fig 3:summer season analysis

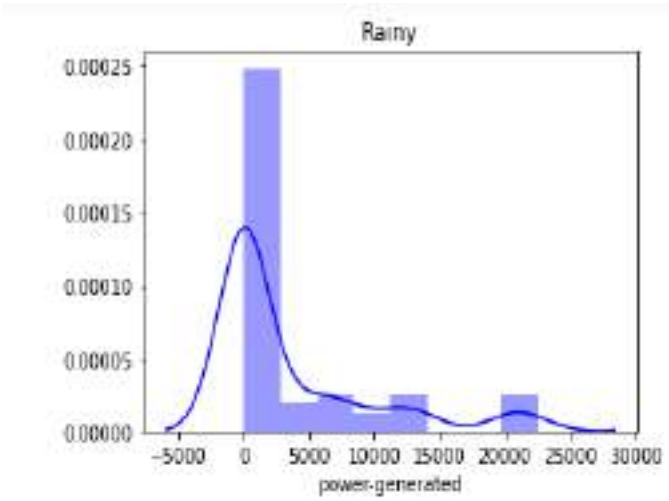

Fig 4: rainy season analysis

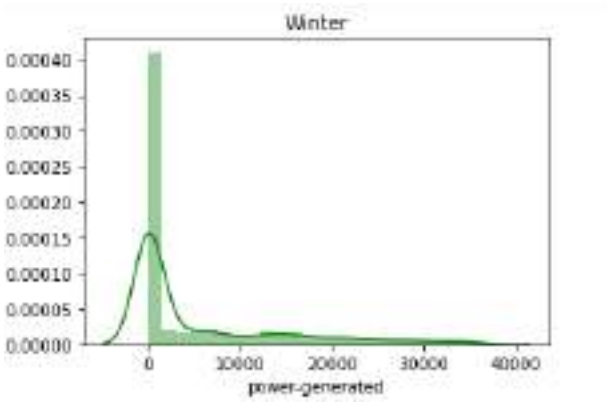

Fig 5: winter season analysis

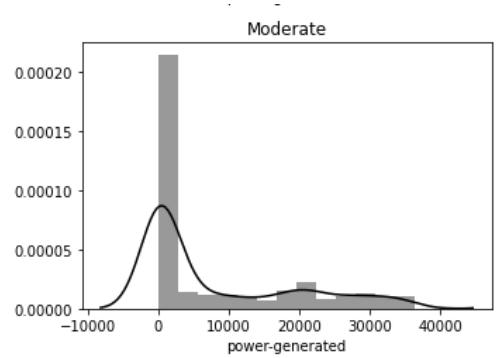

Fig 6: moderate analysis

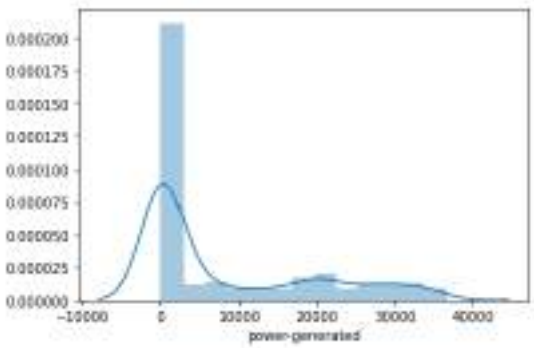

Fig7: overall season's comparative analysis

Here fig6 shows that how power is generated comparatively in different weather conditions where the x axis shows the power generated and y axis shows the distance from solar noon. It is nothing more than Solar noon occurs when the Sun passes through a location's meridian (a meridian is an imaginary line that runs from the North Pole to the South Pole along the Earth's surface.) and ascends to its highest point in the sky. In most cases, it does not occur at 12 p.m and as shown in above Fig 5 and Fig 6 and Below Fig 7.

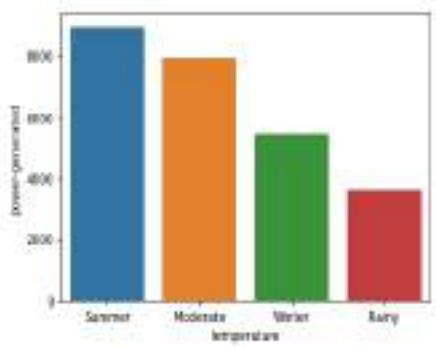

Fig 8: Different temperature analysis results of how much power is generated.

Fig6 says the power generated is read as Jules here where as temperature as in summer, rainy, winter and the moderate is said as the different weather condition. Dataset considered is the numerical dataset so we replaced them with string type where in dataset it is shown as 0 for rainy 1 for winter, 2 for moderate,3 for summer as shown in below Fig 9 and Fig 10.

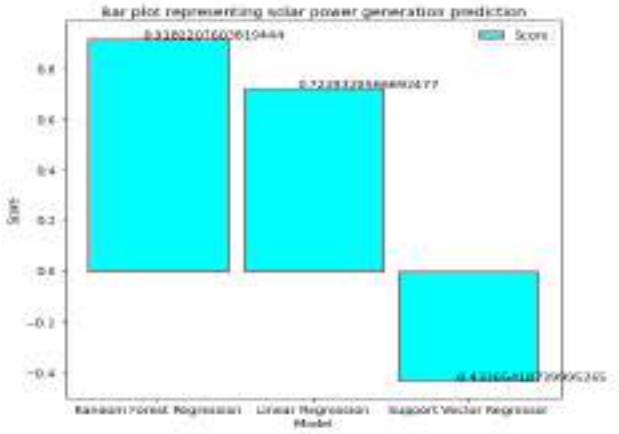

Fig 9: score of all the three model used in solar power analysis.

This fig8 shows that score of three different models used in this paper for solar power generation

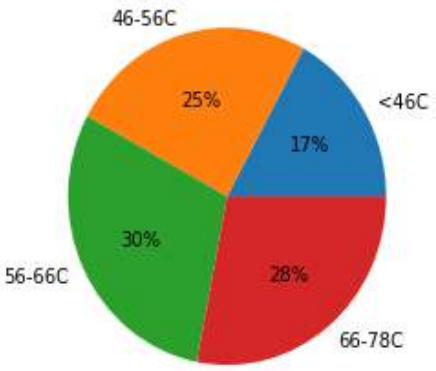

Fig 10: temperature difference and their power generated percentage accordingly.

This shows that how much percentage of power is generated ass the temperature rises less than 46 Celsius is 0 that's the rainy season temperature, 46 o 56 Celsius is 1 that's winter season temperature,56 to 66C is 2 that's moderate temperature and 66 to 78C is 3 that's summer season and as shown in below Table 1.

Table 1: Model Prediction of RMSE, MAE, MAPE, and MBE and Accuracy

Model	RMSE	MAE	MSE	Accuracy
Support vector machine regressor	131.44	77.16	172.76	-44.92
Linear regression	58.57	48.39	343.08	72.4
Random forest regressor	27.32	12.45	746.48	94.01

6. Conclusion:

We presented a machine learning-based approach for solar power generation analysis in this paper, which accurately forecasts power generated across India's states based on environmental data. Most importantly, our methodology went beyond prediction by delivering key results that aided in the understanding of solar power analysis (variable importance by time period). By a wide margin, the proposed method outperformed other popular methods, such as Random forest. The proposed models are SVR, LR, and RF. Compared to the temperature with the given data. 56-55F --30% power generation is increasing compared to other temperatures. Temperature <46F is 17% temperature average of it. As the above results, we can see that Random Forest Regressor model is performing better with 94.01% accuracy and hence that model is preferred for deployment.

Reference:

1. P. A. G. M. Amarasinghe and S. K. Abeygunawardane, "*Application of Machine Learning Algorithms for Solar Power Forecasting in Sri Lanka*" (2nd International Conference On Electrical Engineering (EECon), Colombo, Sri Lanka, 87 2018).
2. M. Z. Hassan, M. E. K. Ali, A. B. M. S. Ali and J. Kumar, "*Forecasting Day-Ahead Solar Radiation Using Machine Learning Approach*" (4th Asia-Pacific World Congress on Computer Science and Engineering (APWC on CSE), Mana Island, Fiji, 252 2017).
3. A. Bajpai and M. Duchon, "*A Hybrid Approach of Solar Power Forecasting Using Machine Learning*" (3rd International Conference on Smart Grid and Smart Cities (ICSGSC), 108 2019).
4. A. Khan, R. Bhatnagar, V. Masrani and V. B. Lobo, "*A Comparative Study on Solar Power Forecasting using Ensemble Learning*," (4th International

Conference on Trends in Electronics and Informatics (ICOEI), 224 2020).

5. Khan, P.W.; Byun, Y.-C.; Lee, S.-J.; Kang, D.-H.; Kang, J.-Y.; Park, H.-S. Energies, **13**, 4870 (2020).
6. Faquir, Sanaa & Yahyaouy, Ali & Tairi, H. & Sabor, Jalal. International Journal of Fuzzy System Applications. **4**, 10 (2015).
7. Aler R., Martín R., Valls J.M., Galván I.M. Intelligent Distributed Computing VIII. Studies in Computational Intelligence, vol **570** (2015).
8. Y. Wang, G. Cao, S. Mao and R. M. Nelms, "*Analysis of solar generation and weather data in smart grid with simultaneous inference of nonlinear time series*," (IEEE Conference on Computer Communications Workshops (INFOCOM WKSHPS), 600 2015).
9. Carrera B, Kim K. Sensors (Basel). **20**, 3129 (2020).
10. Jawaid F, NazirJunejo K. *Predicting daily mean solar power using machine learning regression techniques*. (Sixth International Conference on Innovative Computing Technology (INTECH) 355 2016).
11. Batcha RR, Geetha MK. *A survey on IOT based on renewable energy for efficient energy conservation using machine learning approaches*. (3rd International Conference on Emerging Technologies in Computer Engineering: Machine Learning and Internet of Things (ICETCE) 123 2020).
12. Li, Zhaoxuan & Rahman, Sm Mahbobur & Vega, Rolando & Dong, Bing. Energies. **9**, 55 (2016).
13. Lai JP, Chang YM, Chen CH, Pai PF. Applied Sciences; **10**, 5975 (2020).
14. Brahma, B.; Wadhvani, R. Symmetry, **12**, 1830 (2020).

Analysis Of Solar Power Generation Forecasting Using Machine Learning Techniques

K. Anuradha[1],* *Deekshitha* Erlapally[2], *G*. Karuna[3], *V*. Srilakshmi[4], *K*. Adilakshmi[5]

[1]Professor, Computer Science and Engineering, GRIET, Hyderabad, Telangana, India.
[2]MTech Student, Computer Science and Engineering, GRIET, Hyderabad, Telangana, India.
[3]Professor, Computer Science and Engineering, GRIET, Hyderabad, Telangana, India.
[4] Asst.Professor, Computer Science and Engineering, GRIET, Hyderabad, Telangana, India.
[5] Asst.Professor, Computer Science and Engineering, GRIET, Hyderabad, Telangana, India.

Abstract: Solar power is generated using photovoltaic (PV) systems all over the world. Because the output power of PV systems is alternating and highly dependent on environmental circumstances, solar power sources are unpredictable in nature. Irradiance, humidity, PV surface temperature, and wind speed are only a few of these variables. Because of the unpredictability in photovoltaic generating, it's crucial to plan ahead for solar power generation as in solar power forecasting is required for electric grid. Solar power generation is weather-dependent and unpredictable, this forecast is complex and difficult. The impacts of various environmental conditions on the output of a PV system are discussed. Machine Learning (ML) algorithms have shown great results in time series forecasting and so can be used to anticipate power with weather conditions as model inputs. The use of multiple machine learning, Deep learning and artificial neural network techniques to perform solar power forecasting. Here in this regression models from machine learning techniques like support vector machine regressor, random forest regressor and linear regression model from which random forest regressor beaten the other two regression models with vast accuracy.

1 Introduction:

Solar energy has many benefits, but also have their initial investment for installing solar panels is quite high, and not everyone will be able to afford them. Unfortunately, this is a downside of solar panels; nevertheless, as prices continue to decline, the future looks bright. Solar panels are currently relatively costly; but, new government programs and cutting-edge technology are making them cheaper. Despite the fact that photovoltaic cells are recognized as the significant source of potential energy production, their low return on investment and high upfront costs keeps them from becoming widely used.The high initial cost prevents them from becoming widely used. Because photovoltaic cells convert solar energy into electrical energy, the amount of solar energy produced each day influences the size of the photovoltaic system, just as the amount of solar radiation influences the amount of electricity produced each day. This is influenced by factors such as location, time, and weather patterns. Solar irradiance is the power obtained per unit area from the Sun via electromagnetic radiation in the wavelength range of the solar cell in use.

Major grid integration is difficult because renewable energy is irregular and uncontrollable. Households can now use almost any amount of energy due to the recent electric grid at any moment, but it is not equipped for large quantities of uncontrollable generation at this time. As it is converting solar radiance into power we don't get that how much power is emitted for different location, time, and weather. For this type of clarification machine learning techniques are used in order to differentiate it for different conditions. Machine-learning techniques are wide applied to several fields where it can separate the weather based power.

The amount of energy a PV system generates is proportional to meteorological parameters including cloud cover, sun intensity, and site-specific conditions, among other [3]. Solar panel works differently for different weather conditions. In case if its summer seasons then the amount of energy consumed by the panel from sun is very much more. But in case of rainy and windy conditions the energy consumed is pretty much different. Power generation mostly depends on weather conditions so they take weather forecasting into consideration. As a result, the amount of electricity generated is determined by solar irradiance on a given day, which is determined by a number of factors such as location, time, and weather patterns. We concentrate on the problem of automatically generating models that accurately predict renewable generation based on National Weather Service forecasts (NWS). Using historical NWS forecast data and data generated by solar panels, we experiment with a variety of machine learning techniques to develop prediction models.

* Corresponding author: author@e-mail.org

Meteorological data, including ambient temperature, humidity, and solar radiation, will be collected by meteorological monitoring stations every three hours.

Machine-learning techniques have been widely used in a range of fields involving data-driven problems in recent decades. Machine-learning approaches encompass a wide range of interdisciplinary topics, including statistics, mathematics, artificial neural networks, data mining, optimization, and artificial optimization. With or without mathematical problem forms, machine learning approaches attempt to find a relationship between input and output data. The process of analysing data is known as data analyzation. ML employs statistical approaches to enable computers to "learn" from data without having to be explicitly programmed. Machine learning has two main application categories: regression and classification. Solar power forecasting necessitates the use of regression methods. Some of the ML regression algorithms that can be used for time series forecasting are Linear Regression (LR), Support Vector Machine Regression (SVMR), and Random Forest (RF).

Weather and physical elements influence the electrical power output of a solar photovoltaic (PV) panel. Solar irradiance, cloud cover, humidity, and ambient temperature are the main meteorological factors that influence solar power generation. Predicted weather parameters can be used as model inputs, while solar power forecasts can be used as the model output. Because of its ongoing training nature, the ML algorithm adjusts to physical parameters.

In machine learning SVM plays a major role in order to classify the data and monitor weather condition according. Combining data from photovoltaic power generation with meteorological conditions, according to the positive position of photovoltaic power generation. For every 3 hours svm gives analyzed data for classification and regression analysis. Using hyperplane we can classify the accurate results from solar panel based on the weather conditions.Random forest, on the other hand, is a classification strategy that uses many decision trees to classify data. In order to generate an uncorrelated forest of trees whose committee forecast is more trustworthy than that of any single tree, bagging and feature randomization are utilised in the development of each individual tree. It gives multiple decisions tress it merges all the decision tress into one form of decision tree it's for different climatic conditions such as for summer, rainy, winter seasons. Error statistics such as mean bias error (MBE), mean absolute error (MAE), root mean square error (RMSE), relative MBE (rMBE), mean percentage error (MPE), and relative RMSE are used to assess the model's validity (rRMSE). Linear regression is a supervised learning-based machine learning approach. It does a regression analysis. Based on independent variables, regression models a goal prediction value. It's generally used in forecasting to figure out how variables are related. Regression models differ in terms of the sort of link examined between dependent and independent variables, as well as the number of independent variables used.

2. Related Work:

Solar energy forecasts can be categorised in a variety of ways. The persistence or smart persistence model, which uses historical data to forecast future power generation over a short period of time, is the most basic method (2-3 hours). This method can be used to set a standard against which other forecasting methods can be measured. In most cases, a prediction is completed in two stages. A NWP is designed for a specified time period and location to begin with. The generated NWP is then utilised to forecast power generation using forecasting algorithms. It is possible to employ a physical model, a statistical method, or a machine learning methodology [1].For prediction, ML algorithms are compared to the Smart Persistence (SP) approach, with ML models outperforming the SP model. The unpredictability of solar resources has hampered grid management as solar diffusion rates have increased. Unpredictability and intermittent electricity delivery are two of the most difficult aspects of integrating renewables into the system. As a result, solar power forecasting is becoming increasingly important for grid stability, optimal unit commitment, and cost-effective dispatch. To overcome the problem, we employ machine learning techniques to sift through extraordinary solar radiation predicting models. For developing prediction models, a variety of regression algorithms are tested, including linear least squares and support vector machines with various kernel functions. We use day-ahead sun radiation data forecasts in these tests to show that a machine learning approach can correctly anticipate short-term solar power [2]. A hybrid or mixed forecasting method was developed by combining clustering, classification, and regression approaches to produce a forecasting model. Based on the weather forecast for the next day, the model (with the closest weather condition) is chosen to forecast the power output using cluster-wise regression [3].

Renewable energy sources are progressively being integrated into electric networks alongside nonrenewable energy sources, posing significant issues due totheir sporadic and erratic nature In order to address these issues, soft-computing solutions for energy prediction are essential.We apply a number of data mining methodologies, including preparing historical load data and analysing the features of the load time series, because electricity consumption is entangled with the usage of other energy sources like natural gas and oil. The trends in power consumption from renewable and nonrenewable energy sources were examined and contrasted. A novel machine learning-based hybrid technique (SVR) uses multilayer perceptron (MLP) and support vector regression [5].Using SVM regression, solar power generation produces acceptable results [6]. However, it lacks a detailed examination of solar power generation and meteorological data, and hence is restricted in its capacity to accurately predict other data sets by merely using different SVM kernels after some basic statistical data processing [8].

To study the association between expected weather conditions and power output created as a historical time series, artificial intelligence (AI) approaches are applied.

AI approaches use algorithms that can implicitly characterise the nonlinear and highly intricate relationship between input data (NWP predictions) and output power instead of formal statistical analysis. The ANN is a brain model that is based on biology. They're employed in a range of applications that use AI approaches including supervised, unsupervised, and reinforcement learning. The ANN learns from data in the supervised learning approach by being trained to approximate and estimate the function or relationship. [6].

Their models have been improved to predict PV plant power generation [4–7]. Even with the cloud graph from synchronous meteorological satellites, the significant unpredictability in critical components, particularly the diffuse component from the sky hemisphere, makes solar irradiance far less predictable than temperature. PV systems including a large number of different tiles deployed over a large area have additional challenges [12]. Because it is impossible to examine all connected meteorological forecasts in a practical context, many alternative alternatives have been devised. Weather forecasts from meteorological websites [8] were considered by some. Others used nonlinear modelling approaches like artificial neural networks to try to simplify the solar forecast model (ANN). Two types of networks are commonly used to forecast global solar radiation, solar radiation on titled surfaces, daily solar radiation, and short-term solar radiation: radial basis function (RBF) and multilayer perception (MLP).

In a three-layer feed forward model, back-propagation is the neural network training technique. To reduce forecast error, the input layer provides an error correction factor depending on the projected output for the previous 5 minutes.

An LSTM network will learn a function that accepts a sequence of previous solar irradiance values as input and returns a solar irradiance value as output. Deep neural networks, such as the Deep Belief Network (DBN), will learn a function that takes a sequence of historical sun irradiance values as input and outputs a solar irradiance value. If a series of observations are converted into a variety of occurrences, an LSTM network can learn from them. The sequence is partitioned using LSTM for prediction purposes.

3 PROPOSED WORK:

For knowing how much power is generated from solar we have the dataset showing daily average temperature in Celsius, distance from solar noon, wind speed, wind direction, sky cover, and humidity and then the power generated. Here we are calculating how much power is generated in different weather condition for India dataset . We have taken Indian dataset with different temperature readings. The available dataset is based on hourly weather parameter values. To convert the data to mean values per day, the average of the 24-hour data was used. From 2019 to 2020, several weather factors were collected to investigate the relationship between mean solar irradiance and meteorological data in order to accurately estimate power generated.

The proposed work's System Architecture is to first consider the dataset and preprocess the data, then divide it into train and test data, apply classification techniques, and predict the results. Solar power weather dataset is used for forecasting purposes in this case. Data preprocessing methods include cleaning, integration, reduction, and transmission. We must purge any data that is no longer absolutely necessary. Data cleaning is the process of identifying and removing inaccurate or incorrect records from a dataset. Data from the real world frequently contains noise and missing values, and it may be in an unusable format that cannot be directly used for DL models. Data preprocessing is required to clean data and prepare it for various Deep Learning models, increasing accuracy and efficiency. Training and testing data are separated from the preprocessed data. The model is trained using training data, and its predictions are validated using testing data. Data splitting is the process of dividing available data into two halves, usually for cross-validator purposes. The first set of data is used to build a predictive model, while the second set is used to evaluate the model's performance. In analyzing data mining algorithms, separating data into training and testing sets is crucial. The training percentage is set at 80% and the test percentage is set at 20%. When a data set is divided into a training set and a testing set, the majority of the data is used for training and only a small portion is used for testing. To train any model, no matter what type of dataset is used, the dataset must be divided into training and testing data. The dataset will be examined for null values and outliers during the data preprocessing step, and the model will be trained using three hours of data before being used to forecast solar power generation value. The power generated radiance phase will be estimated using machine learning (ML) methods (e.g., support vector regression, linear regression, elastic net regression, and random forest) as shown in below Fig 1.

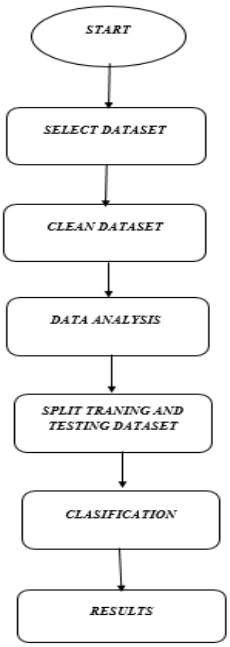

Fig.1 Flow chart for solar power generation

4. Methodology:

The current dataset is based on hourly weather parameter values. To convert the data to mean values per day, the average of the 3-hour data was used. Various weather characteristics were gathered in order to investigate the relationship between mean solar irradiance and meteorological data in order to accurately estimate mean solar irradiance. The average daily values of air temperature, humidity, wind speed, wind direction, visibility, average pressure, average wind speed, and electricity generated are among the data collected. The direction of the wind, on the other hand, indicates how high the sun is. It's also expressed in degrees.

Machine Learning (ML) Models are used for forecasting the solar power generation weather analysis. The Regression techniques here proposed are Support Vector Machine, Random Forest, Linear Regression are various ML Models used in this paper.

4.1 Forecasting models:

In this study, we used the chosen dataset to evaluate individual performance using a number of meteorological attributes utilising three commonly used machine learning algorithms. The output of the unseen test sample is predicted to be the mean of these K closest matches because our prediction variable is continuous valued. We investigated a variety of K values, however only the results for K=3 and K=5 are presented. When K is more than 3, the RMS error increases.

Support vector regression (SVR) using a radial basis function as the kernel and random forest (RF) approaches are used to create the models. Because of the non-linearity of the dataset, we used the models indicated above instead of linear models. The most basic and widely used regression method is linear regression (LR) [10].It uses linear predictor functions to represent the relationship between the input and output variables, and a least squares approach is used to estimate the unknown model parameters from the data. A set of linear equations or an iterative method like gradient descent can be used to estimate parameter values. We employed the characteristics provided in the, followed by feature scaling, to standardise the input data. SVR's precision varies depending on the kernel function and other variables. To discover the optimal settings, we employed the Grid search approach. To evaluate the models' performance on the test set, we computed the Root-Mean-Square Error (RMSE) and R squared values. Before choosing the models with the lowest root mean squared error and highest R squared values, we fine-tuned the model hyperparameters. Nonlinear relationships can be mapped using these methods. In data science challenges of various kinds, methods including decision trees, RF, and gradient boosting are commonly utilised.The RF method is a tree-based machine learning approach that can be used for regression and classification. It also performs dimensional reduction, controls missing and outlier values, and performs a variety of additional data exploration activities. The bagging approach is used to train RFs. This method allows for the usage of numerous instances for the training stage because the dataset is sampled with a replacement. Linear regression is a method for demonstrating the link between a dependent variable and one or more independent variables by using the best-fit linear curve. It is concerned with determining the best-fit line with the data by attaining a perfect slope and intercept value.The best model for forecasting solar power system output based on numerous weather parameters was then created. The models that gave the greatest results on the dataset were support vector regression, random forests, and linear regression, and these models were then utilized to anticipate PV system performance for 2019. Thanks to the predictive analysis, the estimated production in this situation ranges from 0 to 1000 Watt hours. These models were then evaluated using the test data. The SVR model has an RMSE of 135.7, while the random forest model has an RMSE of 28.62 and the SVR model has an RMSE of 58.24. The random forest model's points are close to the regressed diagonal line, however the SVR model's points are not.

5 RESULTS:

A matrix of pair correlation coefficients is generated for a set of features under investigation in order to find collinear factors as shown in below Fig 1, Fig 2,Fig 3 and Fig 4.

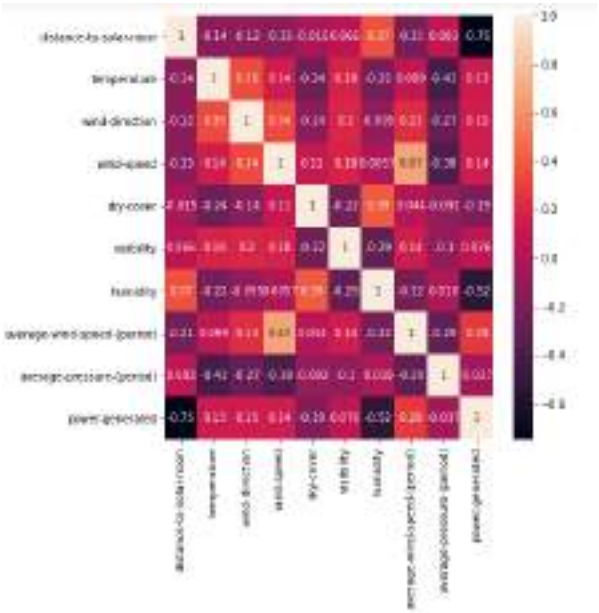

Fig 2 correlation matrix

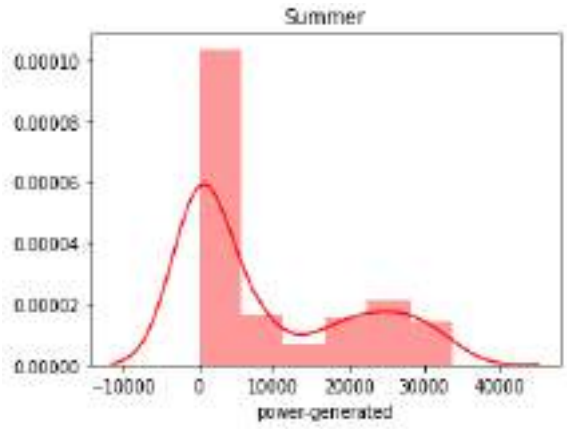

Fig 3:summer season analysis

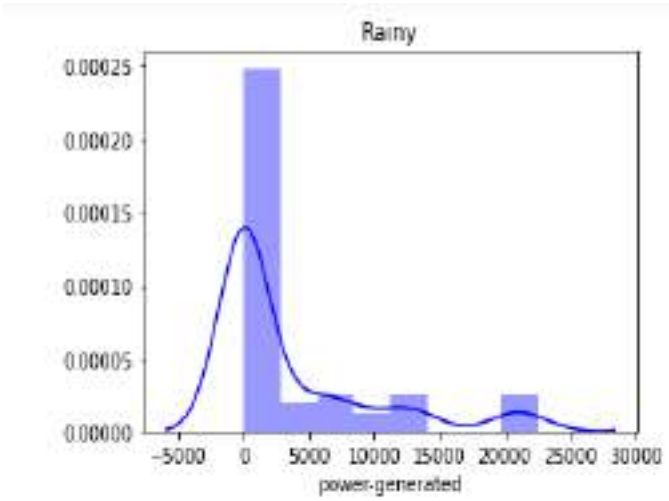

Fig 4: rainy season analysis

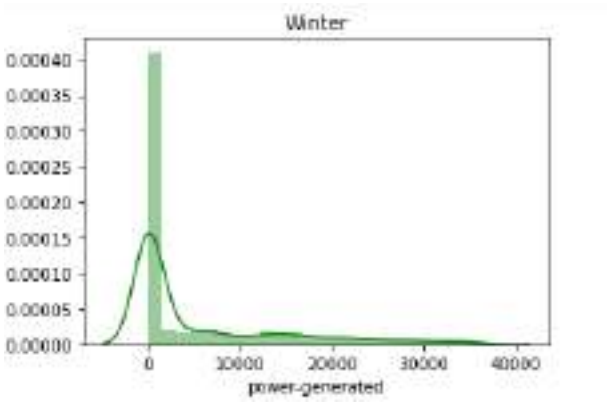

Fig 5: winter season analysis

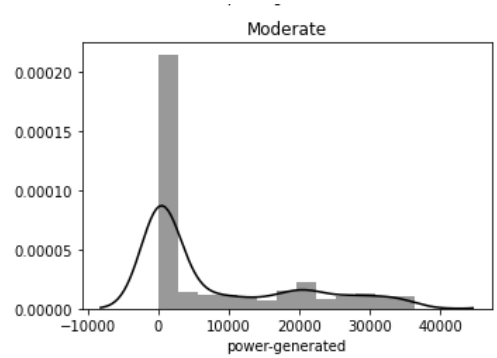

Fig 6: moderate analysis

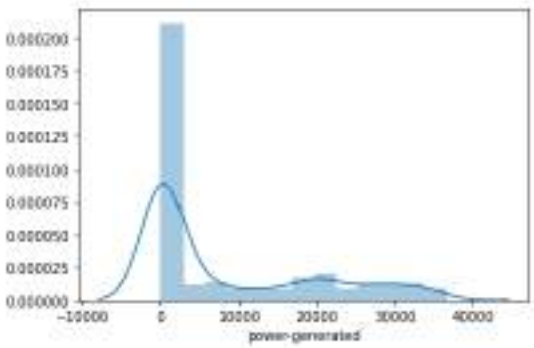

Fig7: overall season's comparative analysis

Here fig6 shows that how power is generated comparatively in different weather conditions where the x axis shows the power generated and y axis shows the distance from solar noon. It is nothing more than Solar noon occurs when the Sun passes through a location's meridian (a meridian is an imaginary line that runs from the North Pole to the South Pole along the Earth's surface.) and ascends to its highest point in the sky. In most cases, it does not occur at 12 p.m and as shown in above Fig 5 and Fig 6 and Below Fig 7.

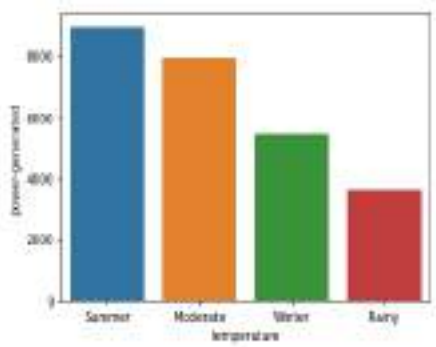

Fig 8: Different temperature analysis results of how much power is generated.

Fig6 says the power generated is read as Jules here where as temperature as in summer, rainy, winter and the moderate is said as the different weather condition. Dataset considered is the numerical dataset so we replaced them with string type where in dataset it is shown as 0 for rainy 1 for winter, 2 for moderate,3 for summer as shown in below Fig 9 and Fig 10.

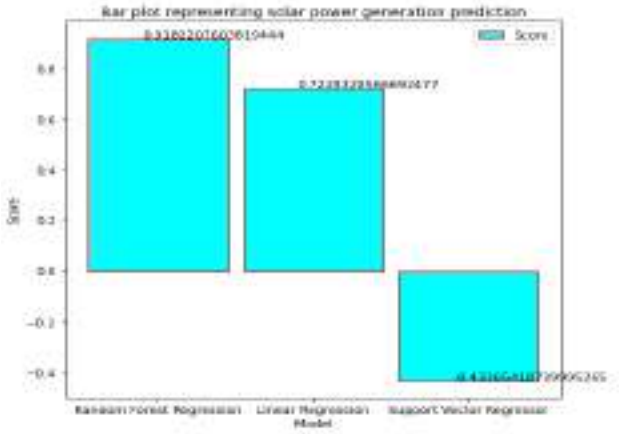

Fig 9: score of all the three model used in solar power analysis.

This fig8 shows that score of three different models used in this paper for solar power generation

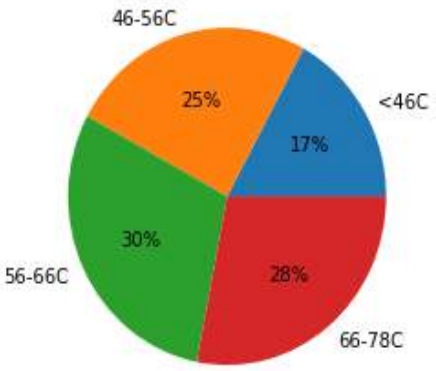

Fig 10: temperature difference and their power generated percentage accordingly.

This shows that how much percentage of power is generated ass the temperature rises less than 46 Celsius is 0 that's the rainy season temperature, 46 o 56 Celsius is 1 that's winter season temperature,56 to 66C is 2 that's moderate temperature and 66 to 78C is 3 that's summer season and as shown in below Table 1.

Table 1: Model Prediction of RMSE, MAE, MAPE, and MBE and Accuracy

Model	RMSE	MAE	MSE	Accuracy
Support vector machine regressor	131.44	77.16	172.76	-44.92
Linear regression	58.57	48.39	343.08	72.4
Random forest regressor	27.32	12.45	746.48	94.01

6. Conclusion:

We presented a machine learning-based approach for solar power generation analysis in this paper, which accurately forecasts power generated across India's states based on environmental data. Most importantly, our methodology went beyond prediction by delivering key results that aided in the understanding of solar power analysis (variable importance by time period). By a wide margin, the proposed method outperformed other popular methods, such as Random forest. The proposed models are SVR, LR, and RF. Compared to the temperature with the given data. 56-55F --30% power generation is increasing compared to other temperatures. Temperature <46F is 17% temperature average of it. As the above results, we can see that Random Forest Regressor model is performing better with 94.01% accuracy and hence that model is preferred for deployment.

Reference:

1. P. A. G. M. Amarasinghe and S. K. Abeygunawardane, "*Application of Machine Learning Algorithms for Solar Power Forecasting in Sri Lanka*" (2nd International Conference On Electrical Engineering (EECon), Colombo, Sri Lanka, 87 2018).
2. M. Z. Hassan, M. E. K. Ali, A. B. M. S. Ali and J. Kumar, "*Forecasting Day-Ahead Solar Radiation Using Machine Learning Approach*" (4th Asia-Pacific World Congress on Computer Science and Engineering (APWC on CSE), Mana Island, Fiji, 252 2017).
3. A. Bajpai and M. Duchon, "*A Hybrid Approach of Solar Power Forecasting Using Machine Learning*" (3rd International Conference on Smart Grid and Smart Cities (ICSGSC), 108 2019).
4. A. Khan, R. Bhatnagar, V. Masrani and V. B. Lobo, "*A Comparative Study on Solar Power Forecasting using Ensemble Learning*," (4th International

Conference on Trends in Electronics and Informatics (ICOEI), 224 2020).

5. Khan, P.W.; Byun, Y.-C.; Lee, S.-J.; Kang, D.-H.; Kang, J.-Y.; Park, H.-S. Energies, **13**, 4870 (2020).
6. Faquir, Sanaa & Yahyaouy, Ali & Tairi, H. & Sabor, Jalal. International Journal of Fuzzy System Applications. **4**, 10 (2015).
7. Aler R., Martín R., Valls J.M., Galván I.M. Intelligent Distributed Computing VIII. Studies in Computational Intelligence, vol **570** (2015).
8. Y. Wang, G. Cao, S. Mao and R. M. Nelms, "*Analysis of solar generation and weather data in smart grid with simultaneous inference of nonlinear time series*," (IEEE Conference on Computer Communications Workshops (INFOCOM WKSHPS), 600 2015).
9. Carrera B, Kim K. Sensors (Basel). **20**, 3129 (2020).
10. Jawaid F, NazirJunejo K. *Predicting daily mean solar power using machine learning regression techniques*. (Sixth International Conference on Innovative Computing Technology (INTECH) 355 2016).
11. Batcha RR, Geetha MK. *A survey on IOT based on renewable energy for efficient energy conservation using machine learning approaches*. (3rd International Conference on Emerging Technologies in Computer Engineering: Machine Learning and Internet of Things (ICETCE) 123 2020).
12. Li, Zhaoxuan & Rahman, Sm Mahbobur & Vega, Rolando & Dong, Bing. Energies. **9**, 55 (2016).
13. Lai JP, Chang YM, Chen CH, Pai PF. Applied Sciences; **10**, 5975 (2020).
14. Brahma, B.; Wadhvani, R. Symmetry, **12**, 1830 (2020).

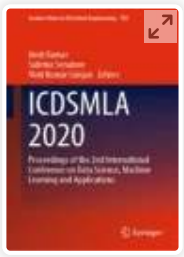

ICDSMLA 2020 pp 837–850

Artificial Intelligence Based Learning Approach for Leaf Disease Identification and Detection

G. Karuna, K. Sahithi, B. Rupa, R. Amani, K. Swaraja & K. Meenakshi

Conference paper | First Online: 09 November 2021

Part of the Lecture Notes in Electrical Engineering book series (LNEE,volume 783)

Abstract

Plants and Crops get diseased due to many reasons. It might be because of diseases of stems, leaves, roots etc. This Paper mainly congregates on leaves. Leaf Disease identification and Detection has many applications for cultivators and farmers to know whether the plant is diseased or not. So that they can retort in dwarf time and decreasing the loss and then can obtain immense profits. This paper mainly focused at learning the disease of plant through leaves. Here, we scrutinize the leaf through Image Processing and extract features of

particular leaf and then utilizing those features as a dataset and done preprocessing and then administering them in Artificial Intelligence based learning algorithms like Convolutional Neural Networks to find disease.

Keywords

Leaf disease **Neural networks** **Features**

References

1. Amara J, Bouaziz B, Algergawy A et al (2017) A deep learning-based approach for banana leaf

diseases classification. In: BTW (Workshops), pp 79–88

2. Jiang P, Chen Y, Liu B, He D, Liang C (2019) Real-time detection of apple leaf diseases using deep learning approach based on improved convolutional neural networks. IEEE Access 7:59069–59080

3. Geetharamani G, Pandian A (2019) Identification of plant leaf diseases using a nine-layer deep convolutional neural network. Comput Electr Eng 76:323–338

4. Atabay HA (2016) A convolutional neural network with a new architecture applied on leaf classification. IIOAB J 7(5):226–331

5. Chaudhary P, Chaudhari AK, Cheeran AN, Godara S (2012) Color transform based approach for disease spot detection

6. Patil JK, Kumar R (2012) Feature extraction of diseased leaf images. J Signal Image Process 3(1):60

7. Reddy PR, Divya SN, Vijayalakshmi R (2015) Plant disease detection techniquetool—a theoretical approach. Int J Innov Technol Res 91–93

8. Mahlein A-K, Rumpf T, Welke P et al (2013) Development of spectral indices for detecting and identifying plant diseases. Remote Sens Environ 128:21–30

9. Xiuqing W, Haiyan W, Shifeng Y (2014) Plant disease detection based on near-field acoustic holography. Trans Chin Soc Agric Mach 2, article 43

10. Mahlein A-K, Oerke E-C, Steiner U, Dehne H-W (2012) Recent advances in sensing plant diseases for precision crop protection. Eur J Plant Pathol 133(1):197–209

11. Revathi P, Hemalatha M (2014) Identification of cotton diseases based on cross information gain deep forward neural network classifier with PSO feature selection. Int J Eng Technol 5(6):4637–4642

12. Zhou C, Gao HB, Gao L, Zhang WG (2003) Particle swarm optimization (PSO) algorithm. Appl Res Computers 12:7–11

13. Rumpf T, Mahlein A-K, Steiner U, Oerke E-C, Dehne H-W, Plümer L (2010) Early detection and classification of plant diseases with support vector machines based on

hyperspectral reflectance. Computers Electron Agric 74(1):91–99

14. Al-Hiary H, Bani-Ahmad S, Reyalat M, Braik M, ALRahamneh Z (2011) Fast and accurate detection and classification of plant diseases. Mach Learn 14:5

15. LeCun Y, Bottou L, Bengio Y, Haffner P (1998) Gradient-based learning applied to document recognition. Proc IEEE 86(11):2278–2324

16. Soderkvist O (2001) Computer vision classification of leaves from Swedish trees

17. Camargo A, Smith J (2009a) Image pattern classification for the identification of disease causing agents in plants. Computers Electron Agric 66(2):121–125. Camargo A, Smith J (2009b) An image-processing based algorithm to automatically identify plant disease visual symptoms. Biosyst Eng 102(1):9–21

18. Mohanty SP, Hughes DP, Salathe M (2016) Using deep learning for image-based plant disease detection. Front Plant Sci 7

19. Krizhevsky A, Sutskever I, Hinton GE (2012) Imagenet classification with deep convolutional neural networks. In: Advances in

neural information processing systems, pp 1097–1105

20. Szegedy C, Liu W, Jia Y, Sermanet P, Reed S, Anguelov D, Erhan D, Vanhoucke V, Rabinovich A (2015) Going deeper with convolutions. In: Proceedings of the IEEE conference on computer vision and pattern recognition

21. Ali A (2019) PlantVillage dataset, Version 1. Retrieved 22 Feb 2020. https://www.kaggle.com/xabdallahali/plantvillagedataset.

Author information

Authors and Affiliations

Computer Science and Engineering, GRIET, Hyderabad, India

G. Karuna, K. Sahithi, B. Rupa & R. Amani

Electronics and Communications Engineering, GRIET, Hyderabad, India

K. Swaraja & K. Meenakshi

Editor information

Editors and Affiliations

BioAxis DNA Research Centre Private Ltd., Hyderabad, Telangana, India

Dr. Amit Kumar

Department of Computer Engineering, Electrical Engineering and Applied Mathematics, University of Salerno, Fisciano, Salerno, Italy

Prof. Dr. Sabrina Senatore

Department of Computer Science and Engineering, CMR Institute of Technology, Hyderabad, Telangana, India

Assoc. Prof. Vinit Kumar Gunjan

Rights and permissions

Copyright information

About this paper

Cite this paper

Karuna, G., Sahithi, K., Rupa, B., Amani, R., Swaraja, K., Meenakshi, K. (2022). Artificial Intelligence Based Learning Approach for Leaf Disease Identification and Detection. In: Kumar, A., Senatore, S., Gunjan, V.K. (eds) ICDSMLA 2020. Lecture Notes in Electrical Engineering, vol 783. Springer, Singapore. https://doi.org/10.1007/978-981-16-3690-5_77

.RIS .ENW .BIB

DOI

https://doi.org/10.1007/978-981-16-3690-5_77

Published Publisher Name Print ISBN

09 November 2021	Springer, Singapore	978-981-16-3689-9

Online ISBN	eBook Packages
978-981-16-3690-5	Intelligent Technologies and Robotics Intelligent Technologies and Robotics (R0)

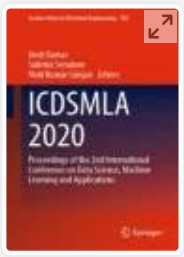

ICDSMLA 2020 pp 837–850

Artificial Intelligence Based Learning Approach for Leaf Disease Identification and Detection

G. Karuna, K. Sahithi, B. Rupa, R. Amani, K. Swaraja & K. Meenakshi

Conference paper | First Online: 09 November 2021

Part of the Lecture Notes in Electrical Engineering book series (LNEE,volume 783)

Abstract

Plants and Crops get diseased due to many reasons. It might be because of diseases of stems, leaves, roots etc. This Paper mainly congregates on leaves. Leaf Disease identification and Detection has many applications for cultivators and farmers to know whether the plant is diseased or not. So that they can retort in dwarf time and decreasing the loss and then can obtain immense profits. This paper mainly focused at learning the disease of plant through leaves. Here, we scrutinize the leaf through Image Processing and extract features of

particular leaf and then utilizing those features as a dataset and done preprocessing and then administering them in Artificial Intelligence based learning algorithms like Convolutional Neural Networks to find disease.

Keywords

Leaf disease **Neural networks** **Features**

References

1. Amara J, Bouaziz B, Algergawy A et al (2017) A deep learning-based approach for banana leaf

diseases classification. In: BTW (Workshops), pp 79–88

2. Jiang P, Chen Y, Liu B, He D, Liang C (2019) Real-time detection of apple leaf diseases using deep learning approach based on improved convolutional neural networks. IEEE Access 7:59069–59080

3. Geetharamani G, Pandian A (2019) Identification of plant leaf diseases using a nine-layer deep convolutional neural network. Comput Electr Eng 76:323–338

4. Atabay HA (2016) A convolutional neural network with a new architecture applied on leaf classification. IIOAB J 7(5):226–331

5. Chaudhary P, Chaudhari AK, Cheeran AN, Godara S (2012) Color transform based approach for disease spot detection

6. Patil JK, Kumar R (2012) Feature extraction of diseased leaf images. J Signal Image Process 3(1):60

7. Reddy PR, Divya SN, Vijayalakshmi R (2015) Plant disease detection techniquetool—a theoretical approach. Int J Innov Technol Res 91–93

8. Mahlein A-K, Rumpf T, Welke P et al (2013) Development of spectral indices for detecting and identifying plant diseases. Remote Sens Environ 128:21–30

9. Xiuqing W, Haiyan W, Shifeng Y (2014) Plant disease detection based on near-field acoustic holography. Trans Chin Soc Agric Mach 2, article 43

10. Mahlein A-K, Oerke E-C, Steiner U, Dehne H-W (2012) Recent advances in sensing plant diseases for precision crop protection. Eur J Plant Pathol 133(1):197–209

11. Revathi P, Hemalatha M (2014) Identification of cotton diseases based on cross information gain deep forward neural network classifier with PSO feature selection. Int J Eng Technol 5(6):4637–4642

12. Zhou C, Gao HB, Gao L, Zhang WG (2003) Particle swarm optimization (PSO) algorithm. Appl Res Computers 12:7–11

13. Rumpf T, Mahlein A-K, Steiner U, Oerke E-C, Dehne H-W, Plümer L (2010) Early detection and classification of plant diseases with support vector machines based on

hyperspectral reflectance. Computers Electron Agric 74(1):91–99

14. Al-Hiary H, Bani-Ahmad S, Reyalat M, Braik M, ALRahamneh Z (2011) Fast and accurate detection and classification of plant diseases. Mach Learn 14:5

15. LeCun Y, Bottou L, Bengio Y, Haffner P (1998) Gradient-based learning applied to document recognition. Proc IEEE 86(11):2278–2324

16. Soderkvist O (2001) Computer vision classification of leaves from Swedish trees

17. Camargo A, Smith J (2009a) Image pattern classification for the identification of disease causing agents in plants. Computers Electron Agric 66(2):121–125. Camargo A, Smith J (2009b) An image-processing based algorithm to automatically identify plant disease visual symptoms. Biosyst Eng 102(1):9–21

18. Mohanty SP, Hughes DP, Salathe M (2016) Using deep learning for image-based plant disease detection. Front Plant Sci 7

19. Krizhevsky A, Sutskever I, Hinton GE (2012) Imagenet classification with deep convolutional neural networks. In: Advances in

neural information processing systems, pp 1097–1105

20. Szegedy C, Liu W, Jia Y, Sermanet P, Reed S, Anguelov D, Erhan D, Vanhoucke V, Rabinovich A (2015) Going deeper with convolutions. In: Proceedings of the IEEE conference on computer vision and pattern recognition

21. Ali A (2019) PlantVillage dataset, Version 1. Retrieved 22 Feb 2020. https://www.kaggle.com/xabdallahali/plantvillagedataset.

Author information

Authors and Affiliations

Computer Science and Engineering, GRIET, Hyderabad, India

G. Karuna, K. Sahithi, B. Rupa & R. Amani

Electronics and Communications Engineering, GRIET, Hyderabad, India

K. Swaraja & K. Meenakshi

Editor information

Editors and Affiliations

BioAxis DNA Research Centre Private Ltd., Hyderabad, Telangana, India

Dr. Amit Kumar

Department of Computer Engineering, Electrical Engineering and Applied Mathematics, University of Salerno, Fisciano, Salerno, Italy

Prof. Dr. Sabrina Senatore

Department of Computer Science and Engineering, CMR Institute of Technology, Hyderabad, Telangana, India

Assoc. Prof. Vinit Kumar Gunjan

Rights and permissions

Copyright information

About this paper

Cite this paper

Karuna, G., Sahithi, K., Rupa, B., Amani, R., Swaraja, K., Meenakshi, K. (2022). Artificial Intelligence Based Learning Approach for Leaf Disease Identification and Detection. In: Kumar, A., Senatore, S., Gunjan, V.K. (eds) ICDSMLA 2020. Lecture Notes in Electrical Engineering, vol 783. Springer, Singapore. https://doi.org/10.1007/978-981-16-3690-5_77

.RIS .ENW .BIB

DOI

https://doi.org/10.1007/978-981-16-3690-5_77

Published Publisher Name Print ISBN

09 November 2021	Springer, Singapore	978-981-16-3689-9

Online ISBN	eBook Packages
978-981-16-3690-5	Intelligent Technologies and Robotics Intelligent Technologies and Robotics (R0)

Smart Computing Techniques and Applications pp 573–583

Prediction Analysis of Diabetes Using Machine Learning

Srikanth Bethu, G. Charles Babu, B. Sankara Babu & V. Anusha

Conference paper | First Online: 14 July 2021

Part of the Smart Innovation, Systems and Technologies book series (SIST,volume 224)

Abstract

Prescient frameworks are the frameworks that are wont to foresee some result based on some example, acknowledgment. Diabetes illness discovery is that the technique by which a patient's determination is performed based on indications examined, which may cause trouble while foreseeing infection influence. For instance, fever itself could be a manifestation of the numerous scatters that do not tell the human services proficient what precisely the sickness is. Since the outcomes or feelings fluctuate from one doctor to

an alternate, there is a necessity to help a restorative doctor, which will have comparative assessment positively side effects and clutters. It may finish by breaking down the data created by medicinal information or therapeutic records. In this way, applying the AI calculations to foresee diabetes ought to be completed.

Keywords

Diabetes prediction **Decision trees**

Healthcare applications **Machine learning**

Neural network **Prediction analysis**

References

1. Osarech, A., Shadgar, B.: A computer-aided diagnosis system for breast cancer. Int. J. Comput. Sci. Issues **8**(2) (2011)

2. Krawczyk, B., Galar, M., Jelen, L., Herrera F.: Evolutionary undersampling boosting for imbalanced classification of breast cancer malignancy. Article in Appl. Soft Comput., Elsevier B.V., pp. 1–14 (2016)

3. Vijayan, V., Ravikumar, A.: Study of data mining algorithms for prediction and diagnosis of diabetes Mellitus. Int. J. Comput. Appl. **95**(17) (2014) (0975-8887)

4. Huang, J., Ling, C.X.: Using AUC and accuracy in evaluating learning algorithms. IEEE Trans. Knowl. Data Eng. **17**(3), 299–310 (2005)

5. Devi, M.R., Maria Shyla, J.: Analysis of various data mining techniques to predict diabetes Mellitus. Int. J. Appl. Eng. Res. **11**(1), 727–730 (2016)

6. Kaur, G., Chhabra, A.: Improved J48 classification algorithm for the prediction of diabetes. Int. J. Comput. Appl. 98(22). (0975-8887) (2014)

7. Wang, H., Yoon, S.W.: Breast cancer prediction using data mining method. In: IEEE Conference paper (2015)

8. Fonseca, V.: Impact of simultaneous versus sequential initiation of basal insulin and glucagon-like peptide-1 receptor agonists on HbA1c in Type 2 diabetes: a retrospective observational study. Diab. Ther. **11**, 995–1005 (2020)

9. Pradhan, M., Sahu, R.K.: Foresee The beginning of Diabetes Disease Using Artificial Neural Network (ANN) (2011)

10. Lakshmi, K.R., Premkumar, S.: Utilization of data mining techniques for prediction of diabetes disease survivability. Int. J. Sci. Eng. Res. **4**(6) (2013)

11. Wajid, S.K., Hussain, A., Huang, K., Bonilla, W.: Local energy-based shape histogram feature extraction technique for breast cancer diagnosis (2015)

12. Bagdi, R., Patil, P.: Diagnosis of diabetes using OLAP and data mining integration. Int. J. Comput. Sci. Commun. Netw. **2**(3), 314–322.

Author information

Authors and Affiliations

Department of Computer Science and Engineering, GRIET, Hyderabad, 500090, India
Srikanth Bethu, B. Sankara Babu & V. Anusha
Department of Computer Science and Engineering, MREC, Hyderabad, 500100, India
G. Charles Babu

Editor information

Editors and Affiliations

School of Computer Engineering, KIIT University, Bhubaneswar, Odisha, India
Dr. Suresh Chandra Satapathy
Department of Electronics and Communication Engineering, Shri Ramswaroop Memorial Group of Professional Colleges (SRMGPC), Lucknow, Uttar Pradesh, India
Dr. Vikrant Bhateja
Informatics and Computer Techniques, Reshetnev Siberian State University of Science and Technologies, Krasnoyarsk, Russia
Prof. Margarita N. Favorskaya
Department of Computer Science and Engineering, Vasavi College of Engineering, Hyderabad, India
Dr. T. Adilakshmi

Rights and permissions

Copyright information

About this paper

Cite this paper

Bethu, S., Charles Babu, G., Sankara Babu, B., Anusha, V. (2021). Prediction Analysis of Diabetes Using Machine Learning. In: Satapathy, S.C., Bhateja, V., Favorskaya, M.N., Adilakshmi, T. (eds) Smart Computing Techniques and Applications. Smart Innovation, Systems and Technologies, vol 224. Springer, Singapore. https://doi.org/10.1007/978-981-16-1502-3_57

.RIS .ENW .BIB

DOI
https://doi.org/10.1007/978-981-16-1502-3_57

Published	Publisher Name	Print ISBN
14 July 2021	Springer, Singapore	978-981-16-1501-6

Online ISBN	eBook Packages
978-981-16-1502-3	Intelligent Technologies and Robotics Intelligent Technologies and Robotics (R0)

Smart Computing Techniques and Applications pp 573–583

Prediction Analysis of Diabetes Using Machine Learning

Srikanth Bethu, G. Charles Babu, B. Sankara Babu & V. Anusha

Conference paper | First Online: 14 July 2021

Part of the Smart Innovation, Systems and Technologies book series (SIST,volume 224)

Abstract

Prescient frameworks are the frameworks that are wont to foresee some result based on some example, acknowledgment. Diabetes illness discovery is that the technique by which a patient's determination is performed based on indications examined, which may cause trouble while foreseeing infection influence. For instance, fever itself could be a manifestation of the numerous scatters that do not tell the human services proficient what precisely the sickness is. Since the outcomes or feelings fluctuate from one doctor to

an alternate, there is a necessity to help a restorative doctor, which will have comparative assessment positively side effects and clutters. It may finish by breaking down the data created by medicinal information or therapeutic records. In this way, applying the AI calculations to foresee diabetes ought to be completed.

Keywords

Diabetes prediction **Decision trees**

Healthcare applications **Machine learning**

Neural network **Prediction analysis**

References

1. Osarech, A., Shadgar, B.: A computer-aided diagnosis system for breast cancer. Int. J. Comput. Sci. Issues **8**(2) (2011)

2. Krawczyk, B., Galar, M., Jelen, L., Herrera F.: Evolutionary undersampling boosting for imbalanced classification of breast cancer malignancy. Article in Appl. Soft Comput., Elsevier B.V., pp. 1–14 (2016)

3. Vijayan, V., Ravikumar, A.: Study of data mining algorithms for prediction and diagnosis of diabetes Mellitus. Int. J. Comput. Appl. **95**(17) (2014) (0975-8887)

4. Huang, J., Ling, C.X.: Using AUC and accuracy in evaluating learning algorithms. IEEE Trans. Knowl. Data Eng. **17**(3), 299–310 (2005)

5. Devi, M.R., Maria Shyla, J.: Analysis of various data mining techniques to predict diabetes Mellitus. Int. J. Appl. Eng. Res. **11**(1), 727–730 (2016)

6. Kaur, G., Chhabra, A.: Improved J48 classification algorithm for the prediction of diabetes. Int. J. Comput. Appl. 98(22). (0975-8887) (2014)

7. Wang, H., Yoon, S.W.: Breast cancer prediction using data mining method. In: IEEE Conference paper (2015)

8. Fonseca, V.: Impact of simultaneous versus sequential initiation of basal insulin and glucagon-like peptide-1 receptor agonists on HbA1c in Type 2 diabetes: a retrospective observational study. Diab. Ther. **11**, 995–1005 (2020)

9. Pradhan, M., Sahu, R.K.: Foresee The beginning of Diabetes Disease Using Artificial Neural Network (ANN) (2011)

10. Lakshmi, K.R., Premkumar, S.: Utilization of data mining techniques for prediction of diabetes disease survivability. Int. J. Sci. Eng. Res. **4**(6) (2013)

11. Wajid, S.K., Hussain, A., Huang, K., Bonilla, W.: Local energy-based shape histogram feature extraction technique for breast cancer diagnosis (2015)

12. Bagdi, R., Patil, P.: Diagnosis of diabetes using OLAP and data mining integration. Int. J. Comput. Sci. Commun. Netw. **2**(3), 314–322.

Author information

Authors and Affiliations

Department of Computer Science and Engineering, GRIET, Hyderabad, 500090, India
Srikanth Bethu, B. Sankara Babu & V. Anusha
Department of Computer Science and Engineering, MREC, Hyderabad, 500100, India
G. Charles Babu

Editor information

Editors and Affiliations

School of Computer Engineering, KIIT University, Bhubaneswar, Odisha, India
Dr. Suresh Chandra Satapathy
Department of Electronics and Communication Engineering, Shri Ramswaroop Memorial Group of Professional Colleges (SRMGPC), Lucknow, Uttar Pradesh, India
Dr. Vikrant Bhateja
Informatics and Computer Techniques, Reshetnev Siberian State University of Science and Technologies, Krasnoyarsk, Russia
Prof. Margarita N. Favorskaya
Department of Computer Science and Engineering, Vasavi College of Engineering, Hyderabad, India
Dr. T. Adilakshmi

Rights and permissions

Copyright information

About this paper

Cite this paper

Bethu, S., Charles Babu, G., Sankara Babu, B., Anusha, V. (2021). Prediction Analysis of Diabetes Using Machine Learning. In: Satapathy, S.C., Bhateja, V., Favorskaya, M.N., Adilakshmi, T. (eds) Smart Computing Techniques and Applications. Smart Innovation, Systems and Technologies, vol 224. Springer, Singapore. https://doi.org/10.1007/978-981-16-1502-3_57

.RIS .ENW .BIB

DOI
https://doi.org/10.1007/978-981-16-1502-3_57

Published	Publisher Name	Print ISBN
14 July 2021	Springer, Singapore	978-981-16-1501-6

Online ISBN	eBook Packages
978-981-16-1502-3	Intelligent Technologies and Robotics Intelligent Technologies and Robotics (R0)

Smart Computing Techniques and Applications pp 573–583

Prediction Analysis of Diabetes Using Machine Learning

Srikanth Bethu, G. Charles Babu, B. Sankara Babu & V. Anusha

Conference paper | First Online: 14 July 2021

Part of the Smart Innovation, Systems and Technologies book series (SIST,volume 224)

Abstract

Prescient frameworks are the frameworks that are wont to foresee some result based on some example, acknowledgment. Diabetes illness discovery is that the technique by which a patient's determination is performed based on indications examined, which may cause trouble while foreseeing infection influence. For instance, fever itself could be a manifestation of the numerous scatters that do not tell the human services proficient what precisely the sickness is. Since the outcomes or feelings fluctuate from one doctor to

an alternate, there is a necessity to help a restorative doctor, which will have comparative assessment positively side effects and clutters. It may finish by breaking down the data created by medicinal information or therapeutic records. In this way, applying the AI calculations to foresee diabetes ought to be completed.

Keywords

Diabetes prediction **Decision trees**

Healthcare applications **Machine learning**

Neural network **Prediction analysis**

References

1. Osarech, A., Shadgar, B.: A computer-aided diagnosis system for breast cancer. Int. J. Comput. Sci. Issues **8**(2) (2011)

2. Krawczyk, B., Galar, M., Jelen, L., Herrera F.: Evolutionary undersampling boosting for imbalanced classification of breast cancer malignancy. Article in Appl. Soft Comput., Elsevier B.V., pp. 1–14 (2016)

3. Vijayan, V., Ravikumar, A.: Study of data mining algorithms for prediction and diagnosis of diabetes Mellitus. Int. J. Comput. Appl. **95**(17) (2014) (0975-8887)

4. Huang, J., Ling, C.X.: Using AUC and accuracy in evaluating learning algorithms. IEEE Trans. Knowl. Data Eng. **17**(3), 299–310 (2005)

5. Devi, M.R., Maria Shyla, J.: Analysis of various data mining techniques to predict diabetes Mellitus. Int. J. Appl. Eng. Res. **11**(1), 727–730 (2016)

6. Kaur, G., Chhabra, A.: Improved J48 classification algorithm for the prediction of diabetes. Int. J. Comput. Appl. 98(22). (0975-8887) (2014)

7. Wang, H., Yoon, S.W.: Breast cancer prediction using data mining method. In: IEEE Conference paper (2015)

8. Fonseca, V.: Impact of simultaneous versus sequential initiation of basal insulin and glucagon-like peptide-1 receptor agonists on HbA1c in Type 2 diabetes: a retrospective observational study. Diab. Ther. **11**, 995–1005 (2020)

9. Pradhan, M., Sahu, R.K.: Foresee The beginning of Diabetes Disease Using Artificial Neural Network (ANN) (2011)

10. Lakshmi, K.R., Premkumar, S.: Utilization of data mining techniques for prediction of diabetes disease survivability. Int. J. Sci. Eng. Res. **4**(6) (2013)

11. Wajid, S.K., Hussain, A., Huang, K., Bonilla, W.: Local energy-based shape histogram feature extraction technique for breast cancer diagnosis (2015)

12. Bagdi, R., Patil, P.: Diagnosis of diabetes using OLAP and data mining integration. Int. J. Comput. Sci. Commun. Netw. **2**(3), 314–322.

Author information

Authors and Affiliations

Department of Computer Science and Engineering, GRIET, Hyderabad, 500090, India
Srikanth Bethu, B. Sankara Babu & V. Anusha
Department of Computer Science and Engineering, MREC, Hyderabad, 500100, India
G. Charles Babu

Editor information

Editors and Affiliations

School of Computer Engineering, KIIT University, Bhubaneswar, Odisha, India
Dr. Suresh Chandra Satapathy
Department of Electronics and Communication Engineering, Shri Ramswaroop Memorial Group of Professional Colleges (SRMGPC), Lucknow, Uttar Pradesh, India
Dr. Vikrant Bhateja
Informatics and Computer Techniques, Reshetnev Siberian State University of Science and Technologies, Krasnoyarsk, Russia
Prof. Margarita N. Favorskaya
Department of Computer Science and Engineering, Vasavi College of Engineering, Hyderabad, India
Dr. T. Adilakshmi

Rights and permissions

Copyright information

About this paper

Cite this paper

Bethu, S., Charles Babu, G., Sankara Babu, B., Anusha, V. (2021). Prediction Analysis of Diabetes Using Machine Learning. In: Satapathy, S.C., Bhateja, V., Favorskaya, M.N., Adilakshmi, T. (eds) Smart Computing Techniques and Applications. Smart Innovation, Systems and Technologies, vol 224. Springer, Singapore. https://doi.org/10.1007/978-981-16-1502-3_57

.RIS .ENW .BIB

DOI
https://doi.org/10.1007/978-981-16-1502-3_57

Published	Publisher Name	Print ISBN
14 July 2021	Springer, Singapore	978-981-16-1501-6

Online ISBN	eBook Packages
978-981-16-1502-3	Intelligent Technologies and Robotics Intelligent Technologies and Robotics (R0)

Deep Neural Network Model for Proficient Crop Yield Prediction

K. Pravallika[1], *G.* Karuna[1*], *K.* Anuradha[1], *V.* Srilakshmi[1]

[1] Computer Science and Engineering, GRIET, Hyderabad, Telangana, India.

Abstract. Crop yield forecasting mainly focus on the domain of agriculture research which has a great impact on making decisions like import-export , pricing and distribution of respective crops. Accurate predictions with well timed forecasts is very important and is a tremendously challenging task due to numerous complex factors. Mainly crops like wheat, rice, peas, pulses, sugarcane, tea, cotton, green houses etc. can be used for crop yield prediction. Climatic changes and unpredictability influence mainly on crop production and maintenance. Forecasting crop yield well before harvest time can help farmers for selling and storage. Agriculture deals with large datasets and knowledge process. Many techniques are there to predict the crop yield. Farmers are benefited commercially by these predictions. Factors such as Geno type, Environment , Climatic conditions and Soil types used in predicting the Yield. For predicting accurately we need to know the fundamental understanding and relationship between the interactive factors and the yield to reveal the relationships between the datasets which are comprehensive and powerful algorithms. Based on the study of various survey papers it has been found that in all the crop predictions, various deep learning, machine learning and ANN algorithms implemented to predict yield forecast and the results are analyzed.

1. Introduction

Yield forecasting of Crop is very essential for the production of food globally. Accurate forecasting can be done by policy makers to take timely decisions to import and export in terms of improving the national food security. Seed companies must forecast new hybrids in order to breed better varieties for various types of environments. Financial decisions can be easily taken and get benefitted by farmers and Growers. Genotype and Environmental interactions are highly complex characteristics. Genotype means the genetic characteristic of individual for particular trait and phenotype of individual deals with observable characteristics like physical, physiological, biochemical and behavioral. For example, length of the plant is one type of phenotype trait.

High dimensional marker data typically contains millions of markers for each plant individual and is represented by genotype.

*Corresponding author: karunavenkatg@gmail.com

The impact of genetic markers must be estimated, which results in interactions with various environmental factors and field management activities that must be calculated.

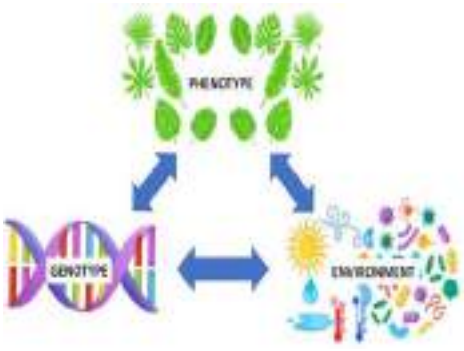

Fig.1. Genotype, phenotype and environmental interactions

Alleles is the alternative word for genes and each individual inherits two alleles for a character one from male and one from female. Two alleles can be same (TT or tt) or different (Tt).

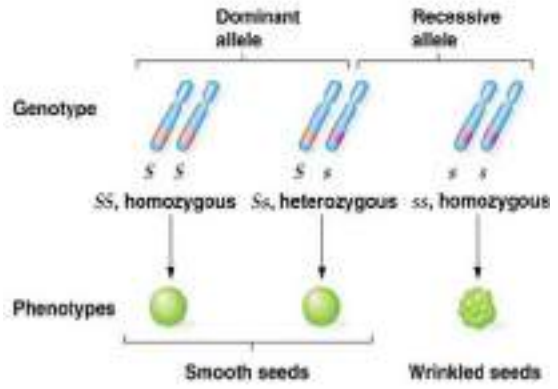

Fig.2. Alleles, genes and traits

Dominant allele that expresses itself and recessive allele unable to express itself. For a particular individual if the dominant allele and recessive allele is known then prediction of phenotype will become simple.

Environmental factors will have great effect on genotype. One of the explicit functions is phenotype, which consists of genotype is treated as G, E as environment, and their interactions are considered as G*E and is treated as noise.

Fig.3. G*E interactions

Group of environments will share same type of varieties can be considered as mega environments. Kharif (july-oct) and Rabi(mar-june) are the two main seasons for growing different crops. Rice, maize, sorghum, bajra, ragi, pulses, soyabean, groundnut and cotton are the crops grown in kharif season.

Wheat, barley, oats, chick pea, mustard seeds are grown in rabi season. Syngenta is one of the company which provides the data for crop predictions. Climate data, which encompasses length of day, rainfall patterns, radiation from the sun, air humidity, min and max temperatures, is indeed one of the factors.

2. Related Work

In the Region of maharashtra, algorithms are used to predict paddy crop yields using anns[2]. Maharashtra's 27 districts have datasets inferred from available public Indian government records. When predicting, snowfall, lower limit temperature, mean temperature, highest temperature, region, output, and harvest are all factored into the equation.Weka tool is used for processing the dataset. In this rice crop prediction a multilayer perceptron neural network and is better than the regression models.Multilayer perceptron, radial basis function networks, and kohonen self organising feature maps are used in neural network[17] models.

Machine learning approaches are used to predict crop yields, and they are implemented in the PHP platform.Temperature, area, humidity, and production are used to predict tomato crop parameters. Ch.Vishnuvardhan Chowdary, Dr.K.Venkataramana[3] developed id3 algorithm for quality crop yield prediction. Different types of fertilizers are used to increase fertility of soil by adding nitrogen nutrients. Pesticides are used to remove the pest from the crop.Gradient boosting regressor uses cross validation to get more accuracy i.e 87.9% .Random forest regressor gets the accuracy of 98.9%.

Crop yield prediction develops a mobile application design and implementation using machine learning[4] it mainly helps the farmers to predict production of specific crop in particular regions. Rainfall and temperature are the physical parameters used in predicting the yield of crop. The app is intended to help farmers by requiring them to enter information such as location, farm size, size, temperature, rainfall, and crop dataset.To train the dataset ARIMA model is used. Accurate prediciton can be done based on the availablity of quality data. Python, data processing, and Android Studio are used to design the application. Intelligrow is the smart phone application in which the results are potrayed in systematic manner.

The learning algorithm to forecasting banana cultivation yields[5] utilises long - short - term memory strands with various perceptrons. Information is derived from beneficiaries (ARB) of Dapco in Davao del Norte, Philippines.Epoch, batch size, neurons are used as model parameters to identify the optimal values. Floods and droughts are the extreme events. Banana is the tropical fruit crop in philipiness.

In order to derive and refine yield prediction data, a review of research for estimation using machine learning[6] was initiated. Six databases were searched were used to find 567 related research, of which 50 have been chosen for some further exploration based on selected studies. Air temp, soil moisture, and soil composition are all used by artificial intelligence. Popular deep neural networks are CNN, LSTM, and DNN. Machine learning historical data is used for training phase and testing phase for performance evaluation. The literature review and study objectives serve as basis for descriptive and inferential machine learning algorithms. Models of description allow for the acquisition of knowledge from collected data. Predicting future result can be done for predictive models. Systematic literature review(SLR) gives the overview of the crop yield[13] prediction and its result is different from other results. Objectivity and transparency are the SLR factors.

An ANN-based weather prediction model [7] asserts a linear correlation between both the weather data entry and the known target data. Atmosphere and state of given location is predicted in weather forecasting which collects the quantitative data. To protect life and property weather warnings are the important forecasts. ANN mainly minimizes the error.Temperature forecasts have special interest on minimum and maximum temperature of day. For winter , summer and fall training and testing is done separately. RBFN and ensembles outperformed all single networks.

Recursive neural network (BPN) [8] has the key advantage of being comparatively imprecise for a multitude of tasks. A multilayer perceptron has 3 levels: the input nodes, the intermediate hidden nodes, and the output units. Factor analytic models are used to join environments and genotypes that do not have cross-over genotype * environment interactions[9]. Prediction assessment of environmental trains[11] using linear mixed models[18]. Syngenta datasets are used for predicting the yield of the crop across different countries. Crop yield prediction using deep neural networks[1] uses various algorithms like LSTM , lasso and regression trees.

Agriculture deals with large datasets and knowledge process[12]. Many techniques are used to predict the yield of the crops. Neural pathways and sophisticated systems are used for massive volumes of data[18]. They used a replacement algorithm to determine yield in this research study. The pH level, amount of nitrogen, amount of carbon, weather patterns, temp, types of soil, and amount of phosphate are among the parameters.The primary goal of agriculture is to maximise value. Because large-scale climatological phenomena have an overly negative impact on agriculture, it is critical to clarify the rainfall patterns of a selected point.There is a lot of research going on with pulses, wheat, rice, sugarcane, and onions. More accurate predictions using meteorological data is an intelligent system.Statistical models and crop simulation models are the two groups of prediction models and applications[14]. ANN and genetic algorithms are efficient than traditional methods because there are easy and accurate for complex inputs.If ANN uses climate factor effective then farmers can use it efficiently.

ANNs are computational systems that processes like biological networks that constitute animal brains. Learning through experiences known as computational ability. Classification is made up of a group of simple computing units known as processing elements that are associated together in a multifaceted communication system, much like the human brain.Feed forward and back propagation are two common neural network architectures. A feed forward system as well as interpretation is a network that has no feedback mechanism. The flow of the system is uni - directional. A node transmits messages to another access point but obtains no response.

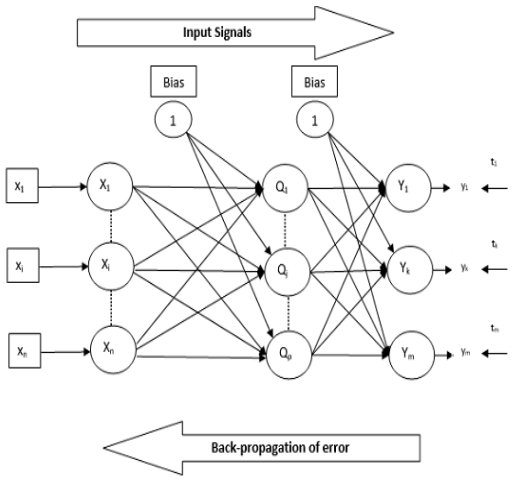

Fig.4. Back propagation

Back propagation seems to be a supervised classifier learning that describes how a neural network is trained. Network should provide with sample inputs and desired outputs.Following computations, the final output is compared to the actual output for a given input.Back propagation has

three phases: feed forward, back propagation of error, and weight updating.

Estimation of wheat crop yield have used a deep Lstm network [18] is a low-cost method of crop yield prediction because satellite images are obtained from publicly available sources. Tehsil (block) levels are proposed for wheat predictions across several states in India and outperformed the existing methods. Remote sensing data is important popular source of data for various applications like income prediction, yield prediction etc.while prior methods involve in extracting handcrafted or rudimentary features such as histograms where as this paper works on satellite images and allows model for learning yield prediction.For geographical area yield estimates depends on factors like waterbodies, urbanization etc. For data temporal features are modelled using deep LSTM model. Evaluation and validation of approach is done for tehsil level wheat prediction for seven states in India. To train proposed deep learning models used MODIS surface reluctance multi-spectural satellite images and land classification maps.The model outperformed traditional remote sensing methods by 70% and deep learning models by54%.

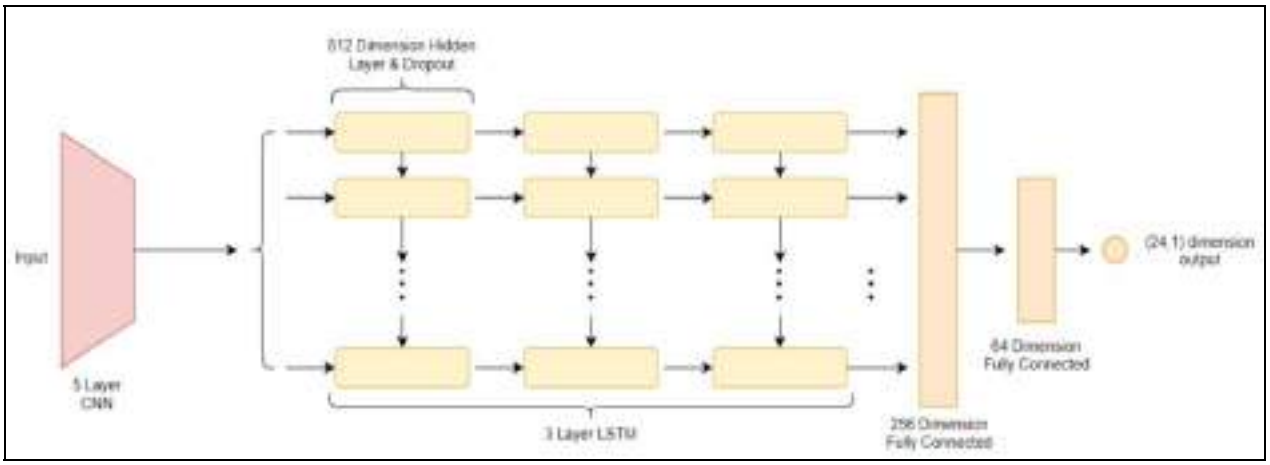

Fig.5. CNN-LSTM architecture

Crop yield prediction using deep Gaussian process based on remote sensing data [15] says that it is an inexpensive method for accurate prediction. In three ways existing techniques are improved firstly they forego traditional features and next they undergo modern approaches based on remote sensing. Novel dimensionality reduction technique is introduced to train CNN or LSTM network based on labeled training data it will automatically learn the features. Finally, in order to improve accuracy, spatiotemporal data, the Gaussian model is expressly utilized. We put our technique to the assessment on province soybean predictive modeling in the U.s, and it surpasses competing firm procedures.

A new dimensionality reduction technique is used to fulfill the demands of training phase. Raw images are treated as histograms of pixel counts to achieve tractability mean field[15] approximation is used.CNN and LSTM are trained on histograms to predict the yield.It does not explicitly account for spatiotemporal dependencies between data points but performs well, for example, due to common soil properties. we have a tendency to overcome this limitation by incorporating a mathematician method layer on prime of our neural network[10] models.Other traditional remote sensing-based models were outperformed by 30 percent in aspects of RMSE and 15percent of its total in aspects of MAPE. Deep learning models are complex non linear mappings used for learning hierarchical representation of data. CNN, DNN, LSTM consists of the set of layers where the output of one layer is the input of the next layer.

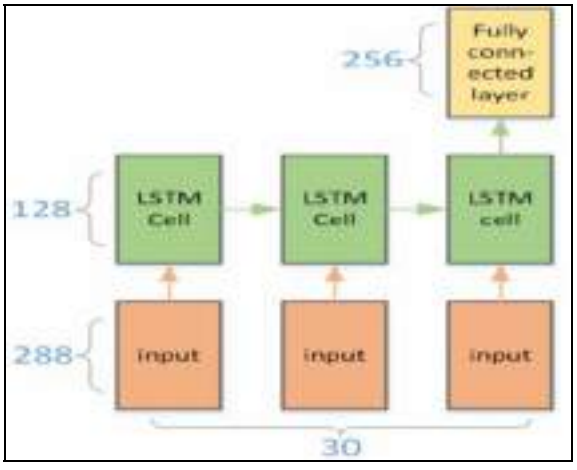

Fig.6. LSTM structure

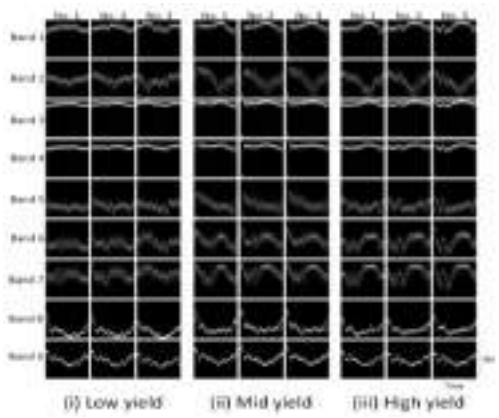

Fig.7. 3-D histogram visualization

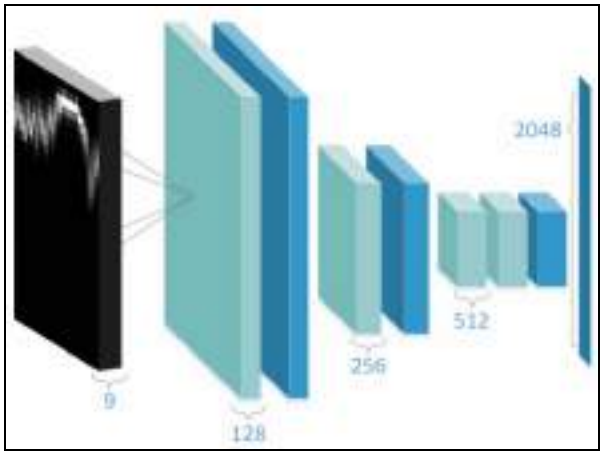

Fig.8. CNN structure

3. Flowchart For Crop Yield Prediction

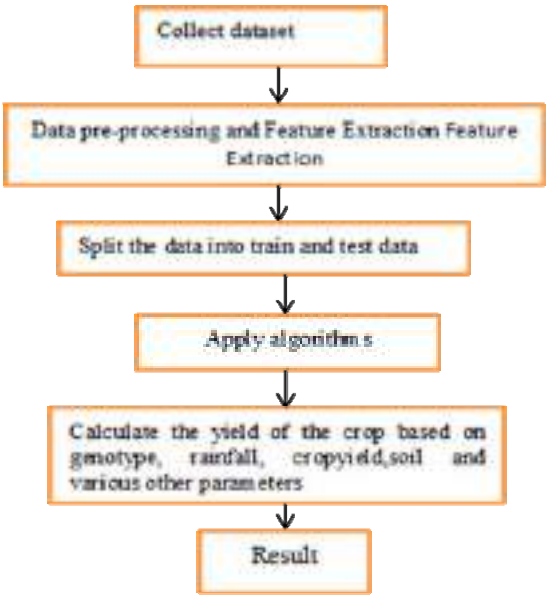

4. Methods For Predicting Crop Yield

4.1 Artificial Neural Networks (ANNs)

Artificial neural networks performed better than multivariate regression. Back propagation neural network technique is one of the best performing algorithm. Artificial neural network uses back propagation. The multilayer perceptron seems to be the most frequently used neural network in latest studies. The input data, the hidden neurons, and the network output are required for ANN, and it outdoes prediction models[2]. Biological neural mechanisms in the human brain are one type of concept for ANN structure. Neurons in the human brain are integrated and used to design the interdependencies for refining. A neurological network is made up of nodes or units, which are integrated structures. Every component is built to look like its biological counterpart, a neuron. Each unit receives and replies to a weighted set of input data. The Artificial Neural Network (ANN) [19] technique is based on a biological system model. The crucial element of this technique is the novel structure of the understanding process system. Associate degree ANN is developed for a single application, including such pattern classification or information classification, using a learning method.

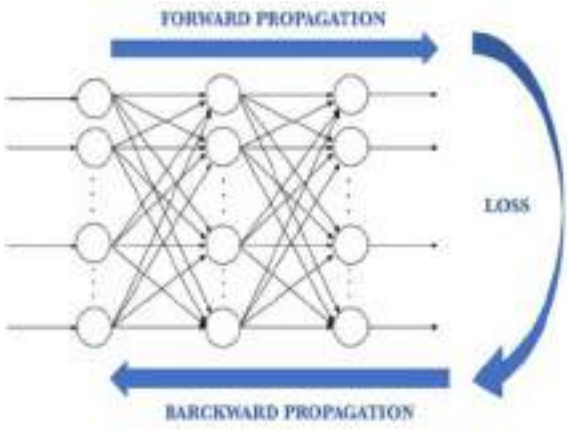

Fig.9. Forward and Backward Propagation

4.2 Deep Learning Networks (DLNs)

Deep learning models are neurons that are used in deep learning approaches. CNN, RNN, LSTM, and DNN are outscored by Lasso, shallow neural networks, regression models, deep learning methods, fully convolutional neural networks, and rnns. Deep neural networks stand to gain from cutting-edge simulation and methods applied. Feature selection can be accomplished by decreasing the dimension of the input space used to train the DNN model. As it has numerous non-linear stacked layers which convert the input to the system into an elevated and more conceptual representation to every stacked layer, it can find the underpinning representation of data

in the apparent lack of feature input data. More complicated features are extracted as the system grows deeper, resulting in high precision. It is known to be an ubiquitous approximator function if the right variables are provided, which means it can estimate almost any feature but is difficult to choose the right parameters.

4.2.1 Shallow Neural Network

One or multiple hidden layers are prevalent in shallow neural network models. Recognizing a shallow neural network can make you realize what tends to happen in a deep network. The section outlines a shallow neural network with one hidden units, one input nodes, and one output neurons.

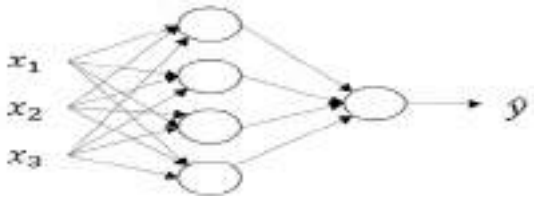

Fig.10. Shallow Neural Network

4.2.2 Convolution Neural Network

It is indeed a deep learning method that generates an image representation and designates weight values to various objects in the scene to discern them from each other.The below figure is the convolution neural network is sequence for classifiying handwritten digits.

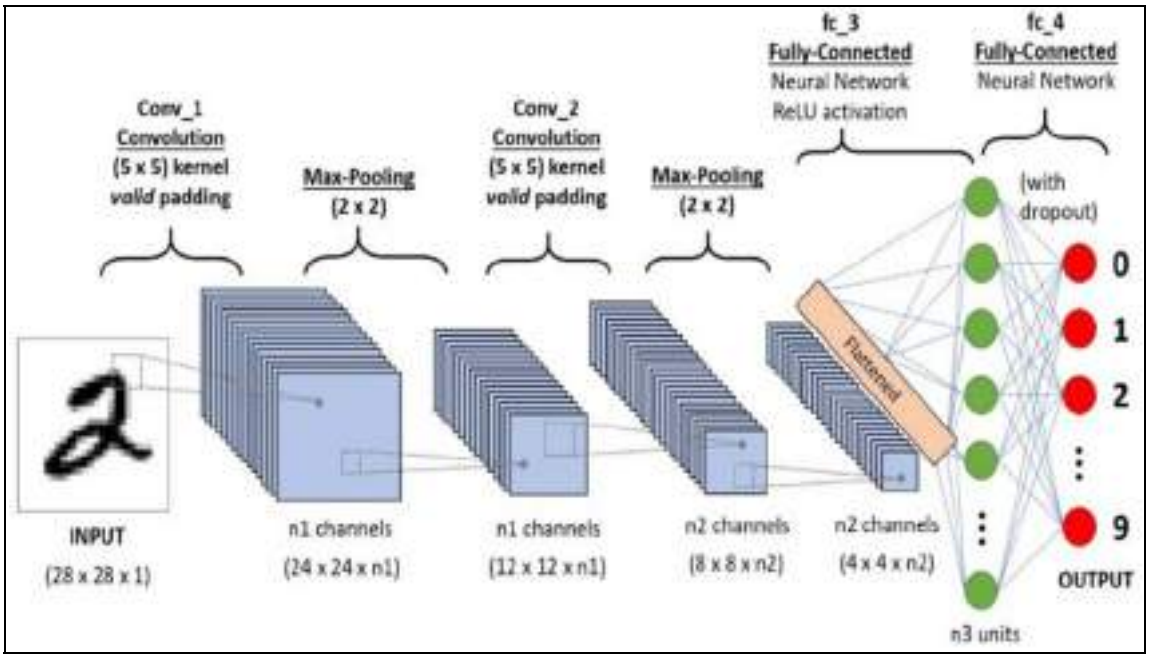

Fig.11. Convolution Neural Network

4.2.3 Recurrent Neural Network (RNN)

The recurrent neural network model [20] adds a twist for basic neural network. A vanilla neural network takes input as fixed vector size and limits the usage to situations which involves series type input with no planned size. Recurrent neural network remembers the past and are influenced by the decisions in past. They can take one or more inputs and gives one or more outputs as vector.

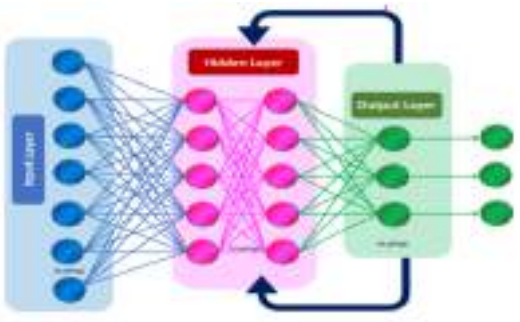

Fig.12. Recurrent Neural Network

4.2.4 Long Short Term Memory (LSTM)

Long Short Term Memory Models (LSTMMs) are designed essential to tackle the long-term correlation issue that exists in recurrent neural networks due to the vanishing gradient troubles.To make more traditional feed forward neural network LSTMs have feed back connections. They process the sequence of data entirely without treating each point independently and the useful information is retained about the previous data and it helps for processing the new data points. For text, speech and general-time series LSTMs are good for such sequences of data.

4.2.5 Deep Neural Networks

For association of input and outputs deep learning algorithms are used along with networks. Deep refers to large amount of layers along with weights and biases can be able to solve for more complex functions.

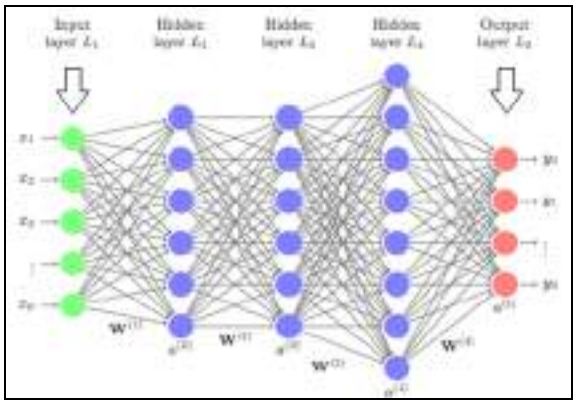

Fig.13. Deep Neural Networks

4.3 Machine Learning Techniques

Machine learning models used to anticipate crop growth include regression analysis, gradient boosting regressor model, random forest regressor model, decision tree regressor modle, polynomial regression technique, and ridge regression technique.Out of all random forest regressor[3] and gradient boosting regressor[3] gives best accuracy with cross validation.

4.3.1 Linear Regression Model

It is just a sequential model that represents the linear relation among an input parameter (x) and a single output unit (y) for combinations of the input parameter (x) (y). Single input variable is considered as a simple linear regression and multiple input variable is considered as a multiple linear regression.Most common data and method is treat the ordinary least squares method.

4.3.2 Gradient Boosting Regressor

Gradient Boosting is a kind of regression method. GB builds an ingredient model series of steps, letting the tuning of absolute discrete loss functions. A regression tree performs the amount of boosting phases in each phase by working on the negative slope of the given deficit.

4.3.3 Random Forest Regressor

So every decision tree has a large variance; nevertheless, when we incorporate them all at once, the eventual variance is lesser because each tree is wholly trained on suitable sample knowledge, and thus the outcome does not rely solely tree structure but on multiple call trees. In the occurrence of a classification error, the bulk vote classifier is used to produce the final output. In the scenario of a regression flaw, the final output is the mean of all the outcomes. Aggregation is the name given to this part of the equation.

4.3.4 Decision Tree Regressor

In attempt to provide tangible continuous output, decision tree predictor scrutinises an object's choices and trains a framework within the structure of a tree to anticipate knowledge in the future. Constant output insinuates that the emission is not distinguishable, that it cannot be characterised simply by a distinct, well-known group of statistics or value systems..

4.3.5 Polynomial Regression

Polynomial Regression is a common formula that does use an ordinal degree polynomial to quantify the relationship between a predicated (y) and an independent variable (x). The Unique Instance of Multiple Statistical Residuals in Cubic Cm is another name for it. As a result, in required to persuade the Multiple Statistical Coefficient of determination to Polynomial Correlation, we add some polynomial conditions to it. It is a linear classifier that has been improved in high precision. The mentoring set of data used in Polynomial regression is not deterministic. It hires a statistical regression model to adapt the tough and non-linear features and data sources.

4.3.6 Ridge Regression

Ridge regression is a concept standard setting technique that might be used to analyse any statistics that has experienced from repeated measures. This method employs L2 regularisation.once the problem of multiple regression happens, least-squares ar unbiased, and variances ar giant, this ends up in foreseen values to be far-flung from the particular values.

5. Comparision of crop yield prediction with different models

5.1 Artificial Neural Networks

The table below contrasts R, MEA, as well as MSE[16] for crop varieties when using artificial neural systems imperialistic competitive optimization technique and grey wolf optimization method models to examine effectiveness.

Table1. ANN-ICA and ANN-GWO with R, MEA and RMSE

Crops	R		MEA (%)		RMSE (%)	
	ANN-ICA	ANN-GWO	ANN-ICA	ANN-GWO	ANN-ICA	ANN-GWO
Wheat	0.35	0.49	35.6	33.40	8.58	8.41
Barley	0.38	0.43	12.10	12.25	0.42	0.63
Potato	0.81	0.81	22.8	22.25	0.78	0.76
Sugar Beet	0.24	0.26	39.0	39.12	3.35	3.44
Average	0.45	0.50	27.3	26.68	3.30	3.29

5.2 Deep Neural Networks

The table compares different deep learning models based on response variable, training RMSE, validation RMSE, training and validation correlation coefficients for yield, check yield, and difference.

Table 2. Training and validation comparisons of different deep neural network algorithms

Model	Response variable	Training RMSE	Training correlation coefficient(%)	Validation RMSE	Validation correlation coefficient (%)
DNN	Yield	10.53	88.31	12.8	82.91
	Check yield	8.22	91.01	11.39	85.49
	Yield difference	11.80	45.89	12.50	29.31
LASSO	Yield	20.32	36.69	21.43	27.66
	Check yield	18.87	28.51	19.89	23.01
	Yield difference	15.33	19.79	13.12	6.88
SNN	Yield	12.98	80.29	18.09	60.10
	Check yield	10.25	71.19	15.15	60.50
	Yield difference	9.98	58.76	15.16	11.36
RT	Yield	14.38	76.75	15.30	73.85
	Check yield	14.57	82.01	14.88	69.98
	Yield difference	17.68	21.15	15.93	5.12

Corn and soyabean crops are compared using Training and validation RMSE, training and validation correlation coeffients for CNN and RNN algorithms.

Table 3. CNN and RNN comparing corn and soyabean crops

Response	Model	Training RMSE	Training correlation coefficient(%)	Validation RMSE	Validation correlation coefficient(%)
Corn	CNN-RNN (W)	17.15	89.02	24.79	72.18
	CNN-RNN (S)	19.16	84.72	24.43	73.82
	CNN-RNN (M)	27.77	69.59	34.03	33.99
	Average	38.51	0.04	35.66	0.01
Soya bean	CNN-RNN (W)	4.6	89.65	5.98	78.80
	CNN-RNN (S)	5.64	83.26	5.94	81.28
	CNN-RNN (M)	7.87	59.84	8.66	48.77
	Average	10.29	0.01	10.11	0.05

5.3 Machine Learning

When accuracy, recall, and F1-score are being used to make comparisons different algorithms such as logistic regression model , decision tree method, Random Forest model, and k nearest neighbour as well as svms, logistic regression model performed the best.

Table 4. Machine learning algorithms accuracy comparison

Algorithm	Precision		Recall		F1-Score		Accuracy(100 %)
	Class 0	Class 1	Class 0	Class 1	Class 0	Class 1	
Logistic Regression	1	1	1	1	1	1	100
Decision Tree	1	0.90	0.83	1	0.91	0.95	93.3
Random Forest	1	0.90	0.83	1	0.91	0.95	93.3
K Nearest Neighbor	1	0.82	0.63	1	0.80	0.90	86.66
Support Vector Machine	0	0.60	0	1	0	0.75	60

Deep learing and machine learning algorithms comparison using mean absolute percentage error and finding the best performer algorithm using accuracy measure.

Table 5. Various deep learning and ML algorithms comparison

Model	Accuracy Measure(%)	MAPE(%)
DRL	93.7	17
BDN	92.1	20
BAN	91.7	27
IDANN	91	29
RAE	90.7	32
DL	91.85	28
ANN	90.5	38
RF	70.7	53
GB	81.2	41

Table below shows Rice, millet and paddy crops comparison using different algorithms and choosing the best performer using accuracy among all the algorithms Random forest gives best result for prediction.

Table 6. Comparing table for Rice, Millet and Paddy for various Models

Model	Accuracy Measure (%)	Crop
Multilayer perceptron	97.5	Rice
RBF Neural network	96.77	Rice
Random forest classifier	99.74	Millet
Deep reinforcement Learning	93.7	Paddy

6. Conclusion

This paper gives a detailed analysis of different approaches used for crop yield prediction.Various algorithms are mentioned along with the datasets and results. Different types of crops used for prediction purpose in different seasons are mentioned.various crops are used for prediction using different classification techniques, depending on the factors used more accurate results are generated. Climatic conditions plays a major role in yield. Crop yield prediction mainly depends on factors so while using any techniques need to consider the factors accurately gives effective results and helps in making good decisions for import and export and better pricing of respective crops. This work can be used to extend these approaches for and to achieve better results for future enhancements.

7. Nomenclature

CNN - Convolutional Neural Network
RNN - Recurrent Neural Network
RT - Regression tree
DL - Deep Learning
ANN - Artificial Neural Networks
GB - Gradient Boosting
DRL - Deep Reinforcement Learning
ARIMA - AutoRegressive Integrated Moving Average
LSTM - Long Short Term Memory
DNN - Deep Neural networks
MAPE - Mean Absolute Percentage Error
RMSE - Root mean square error
MEA - Means end analysis
MSE - Mean square error
BDN - Deep Belief Network
BAN - Born again neural networks
IDANN - Internal Deep Generative Artificial Neural Networks
RAE - Robust Adaboost RT based Ensemble
R - Range
MODIS - Moderate Resolution Imaging Spectroradiometer
LASSO - Least Absolute Shrinkage and Selection Operator
ANN-ICA - Artificial Neural Networks -imperialist competitive algorithm
ANN-GWO - Artificial Neural Networks -Gray Wolf Optimizer of Neural Networks
CNN-RNN(W) - Convolutional Neural Networks-Recurrent Neural Networks(weather data)
CNN-RNN(S) - Convolutional Neural Networks-Recurrent Neural Networks(soildata)
CNN-RNN(M) - Convolutional Neural Networks-Recurrent Neural Networks(managementdata)

8. References

1. S. Khaki and L. Wang, Front. Plant Sci. **10**, 621 (2019).

2. N. Gandhi, O. Petkar, and L. J. Armstrong, in 2016 IEEE Technological Innovations in ICT for Agriculture and Rural Development (TIAR), 105–110, (2016).

3. Payal Gulati, Suman Kumar Jha, in 2020, International Journal of Engineering Research & Technology (IJERT) ENCADEMS, **8(10)**,(2020).

4. Meeradevi and H. Salpekar, in *2019 Global Conference for Advancement in Technology (GCAT,)* 1–6, (2019).

5. M. A. Rebortera and A. C. Fajardo, Editorial Preface From the Desk of (2019).

6. T. van Klompenburg, A. Kassahun, and C. Catal, Comput. Electron. Agric. **177**, 105709 (2020).

7. K. Abhishek, M. P. Singh, S. Ghosh, and A. Anand, Procedia Technology **4**, 311 (2012).

8. S. S. Baboo and I. K. Shereef, Int. J. Environ. Sci. Dev. 321 (2010).

9. J. Burgueño, J. Crossa, P. L. Cornelius, and R.-C. Yang, Crop Sci. **48**, 1291 (2008).

10. P. Kora and S. R. Kalva, Springerplus 4, 481 (2015).

11. J. Burgueño, J. Crossa, J. M. Cotes, F. S. Vicente, and B. Das, Crop Sci. **51**, 944 (2011).

12. K. Prasanna Lakshmi and C. R. K. Reddy, in 2010 International Conference on Networking and Information Technology ,451–455pp.(2010).

13. G. P. Miriyala and A. K. Sinha, Recent Advances in Computer Based (2020).

14. Swaraja K, Multimed. Tools Appl. 77, 28249 (2018).

15. A. X. Wang, C. Tran, N. Desai, D. Lobell, and S. Ermon, in Proceedings of the 1st ACM SIGCAS Conference on Computing and Sustainable Societies (Association for Computing Machinery, New York, NY, USA, 2018), 1–5 (2018).

16. S. Kumar, P. Reddy, G. Ramesh, and V. Maddumala, Trait. Du Signal 36, 233 (2019).

17. C. U. Kumari, S. Jeevan Prasad, and G. Mounika, 2019 3rd International Conference on Computing Methodologies and Communication (ICCMC) (2019).

18. S. Sharma, S. Rai, and N. C. Krishnan, arXiv [cs.CV] (2020).

19. B.Dhanalaxmi, G. A. Naidu, and K. Anuradha, Procedia Comput. Sci. 46, 432 (2015).

20. S B Babu, A Suneetha, GC Babu, YJN Kumar, G Karuna, Periodicals of Engineering and Natural Sciences (PEN) 6 (1), 229-240, (2018).

Deep Neural Network Model for Proficient Crop Yield Prediction

K. Pravallika[1], *G.* Karuna[1*], *K.* Anuradha[1], *V.* Srilakshmi[1]

[1] Computer Science and Engineering, GRIET, Hyderabad, Telangana, India.

Abstract. Crop yield forecasting mainly focus on the domain of agriculture research which has a great impact on making decisions like import-export , pricing and distribution of respective crops. Accurate predictions with well timed forecasts is very important and is a tremendously challenging task due to numerous complex factors. Mainly crops like wheat, rice, peas, pulses, sugarcane, tea, cotton, green houses etc. can be used for crop yield prediction. Climatic changes and unpredictability influence mainly on crop production and maintenance. Forecasting crop yield well before harvest time can help farmers for selling and storage. Agriculture deals with large datasets and knowledge process. Many techniques are there to predict the crop yield. Farmers are benefited commercially by these predictions. Factors such as Geno type, Environment , Climatic conditions and Soil types used in predicting the Yield. For predicting accurately we need to know the fundamental understanding and relationship between the interactive factors and the yield to reveal the relationships between the datasets which are comprehensive and powerful algorithms. Based on the study of various survey papers it has been found that in all the crop predictions, various deep learning, machine learning and ANN algorithms implemented to predict yield forecast and the results are analyzed.

1. Introduction

Yield forecasting of Crop is very essential for the production of food globally. Accurate forecasting can be done by policy makers to take timely decisions to import and export in terms of improving the national food security. Seed companies must forecast new hybrids in order to breed better varieties for various types of environments. Financial decisions can be easily taken and get benefitted by farmers and Growers. Genotype and Environmental interactions are highly complex characteristics. Genotype means the genetic characteristic of individual for particular trait and phenotype of individual deals with observable characteristics like physical, physiological, biochemical and behavioral. For example, length of the plant is one type of phenotype trait.

High dimensional marker data typically contains millions of markers for each plant individual and is represented by genotype.

*Corresponding author: karunavenkatg@gmail.com

The impact of genetic markers must be estimated, which results in interactions with various environmental factors and field management activities that must be calculated.

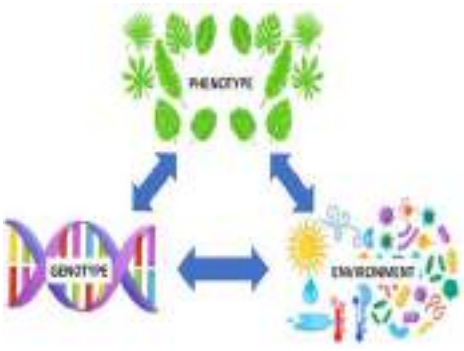

Fig.1. Genotype, phenotype and environmental interactions

Alleles is the alternative word for genes and each individual inherits two alleles for a character one from male and one from female. Two alleles can be same (TT or tt) or different (Tt).

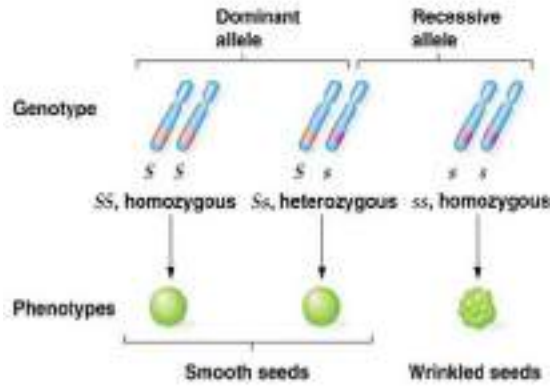

Fig.2. Alleles, genes and traits

Dominant allele that expresses itself and recessive allele unable to express itself. For a particular individual if the dominant allele and recessive allele is known then prediction of phenotype will become simple.

Environmental factors will have great effect on genotype. One of the explicit functions is phenotype, which consists of genotype is treated as G, E as environment, and their interactions are considered as G*E and is treated as noise.

Fig.3. G*E interactions

Group of environments will share same type of varieties can be considered as mega environments. Kharif (july-oct) and Rabi(mar-june) are the two main seasons for growing different crops. Rice, maize, sorghum, bajra, ragi, pulses, soyabean, groundnut and cotton are the crops grown in kharif season.

Wheat, barley, oats, chick pea, mustard seeds are grown in rabi season. Syngenta is one of the company which provides the data for crop predictions. Climate data, which encompasses length of day, rainfall patterns, radiation from the sun, air humidity, min and max temperatures, is indeed one of the factors.

2. Related Work

In the Region of maharashtra, algorithms are used to predict paddy crop yields using anns[2]. Maharashtra's 27 districts have datasets inferred from available public Indian government records. When predicting, snowfall, lower limit temperature, mean temperature, highest temperature, region, output, and harvest are all factored into the equation.Weka tool is used for processing the dataset. In this rice crop prediction a multilayer perceptron neural network and is better than the regression models.Multilayer perceptron, radial basis function networks, and kohonen self organising feature maps are used in neural network[17] models.

Machine learning approaches are used to predict crop yields, and they are implemented in the PHP platform.Temperature, area, humidity, and production are used to predict tomato crop parameters. Ch.Vishnuvardhan Chowdary, Dr.K.Venkataramana[3] developed id3 algorithm for quality crop yield prediction. Different types of fertilizers are used to increase fertility of soil by adding nitrogen nutrients. Pesticides are used to remove the pest from the crop.Gradient boosting regressor uses cross validation to get more accuracy i.e 87.9% .Random forest regressor gets the accuracy of 98.9%.

Crop yield prediction develops a mobile application design and implementation using machine learning[4] it mainly helps the farmers to predict production of specific crop in particular regions. Rainfall and temperature are the physical parameters used in predicting the yield of crop. The app is intended to help farmers by requiring them to enter information such as location, farm size, size, temperature, rainfall, and crop dataset.To train the dataset ARIMA model is used. Accurate prediciton can be done based on the availablity of quality data. Python, data processing, and Android Studio are used to design the application. Intelligrow is the smart phone application in which the results are potrayed in systematic manner.

The learning algorithm to forecasting banana cultivation yields[5] utilises long - short - term memory strands with various perceptrons. Information is derived from beneficiaries (ARB) of Dapco in Davao del Norte, Philippines.Epoch, batch size, neurons are used as model parameters to identify the optimal values. Floods and droughts are the extreme events. Banana is the tropical fruit crop in philipiness.

In order to derive and refine yield prediction data, a review of research for estimation using machine learning[6] was initiated. Six databases were searched were used to find 567 related research, of which 50 have been chosen for some further exploration based on selected studies. Air temp, soil moisture, and soil composition are all used by artificial intelligence. Popular deep neural networks are CNN, LSTM, and DNN. Machine learning historical data is used for training phase and testing phase for performance evaluation. The literature review and study objectives serve as basis for descriptive and inferential machine learning algorithms. Models of description allow for the acquisition of knowledge from collected data. Predicting future result can be done for predictive models. Systematic literature review(SLR) gives the overview of the crop yield[13] prediction and its result is different from other results. Objectivity and transparency are the SLR factors.

An ANN-based weather prediction model [7] asserts a linear correlation between both the weather data entry and the known target data. Atmosphere and state of given location is predicted in weather forecasting which collects the quantitative data. To protect life and property weather warnings are the important forecasts. ANN mainly minimizes the error.Temperature forecasts have special interest on minimum and maximum temperature of day. For winter , summer and fall training and testing is done separately. RBFN and ensembles outperformed all single networks.

Recursive neural network (BPN) [8] has the key advantage of being comparatively imprecise for a multitude of tasks. A multilayer perceptron has 3 levels: the input nodes, the intermediate hidden nodes, and the output units. Factor analytic models are used to join environments and genotypes that do not have cross-over genotype * environment interactions[9]. Prediction assessment of environmental trains[11] using linear mixed models[18]. Syngenta datasets are used for predicting the yield of the crop across different countries. Crop yield prediction using deep neural networks[1] uses various algorithms like LSTM , lasso and regression trees.

Agriculture deals with large datasets and knowledge process[12]. Many techniques are used to predict the yield of the crops. Neural pathways and sophisticated systems are used for massive volumes of data[18]. They used a replacement algorithm to determine yield in this research study. The pH level, amount of nitrogen, amount of carbon, weather patterns, temp, types of soil, and amount of phosphate are among the parameters.The primary goal of agriculture is to maximise value. Because large-scale climatological phenomena have an overly negative impact on agriculture, it is critical to clarify the rainfall patterns of a selected point.There is a lot of research going on with pulses, wheat, rice, sugarcane, and onions. More accurate predictions using meteorological data is an intelligent system.Statistical models and crop simulation models are the two groups of prediction models and applications[14]. ANN and genetic algorithms are efficient than traditional methods because there are easy and accurate for complex inputs.If ANN uses climate factor effective then farmers can use it efficiently.

ANNs are computational systems that processes like biological networks that constitute animal brains. Learning through experiences known as computational ability. Classification is made up of a group of simple computing units known as processing elements that are associated together in a multifaceted communication system, much like the human brain.Feed forward and back propagation are two common neural network architectures. A feed forward system as well as interpretation is a network that has no feedback mechanism. The flow of the system is uni - directional. A node transmits messages to another access point but obtains no response.

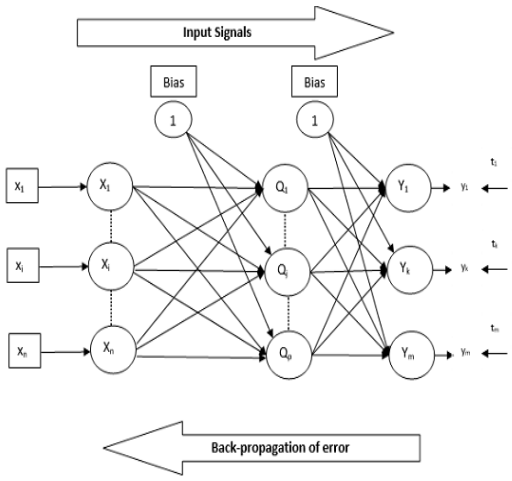

Fig.4. Back propagation

Back propagation seems to be a supervised classifier learning that describes how a neural network is trained. Network should provide with sample inputs and desired outputs.Following computations, the final output is compared to the actual output for a given input.Back propagation has

three phases: feed forward, back propagation of error, and weight updating.

Estimation of wheat crop yield have used a deep Lstm network [18] is a low-cost method of crop yield prediction because satellite images are obtained from publicly available sources. Tehsil (block) levels are proposed for wheat predictions across several states in India and outperformed the existing methods. Remote sensing data is important popular source of data for various applications like income prediction, yield prediction etc.while prior methods involve in extracting handcrafted or rudimentary features such as histograms where as this paper works on satellite images and allows model for learning yield prediction.For geographical area yield estimates depends on factors like waterbodies, urbanization etc. For data temporal features are modelled using deep LSTM model. Evaluation and validation of approach is done for tehsil level wheat prediction for seven states in India. To train proposed deep learning models used MODIS surface reluctance multi-spectural satellite images and land classification maps.The model outperformed traditional remote sensing methods by 70% and deep learning models by54%.

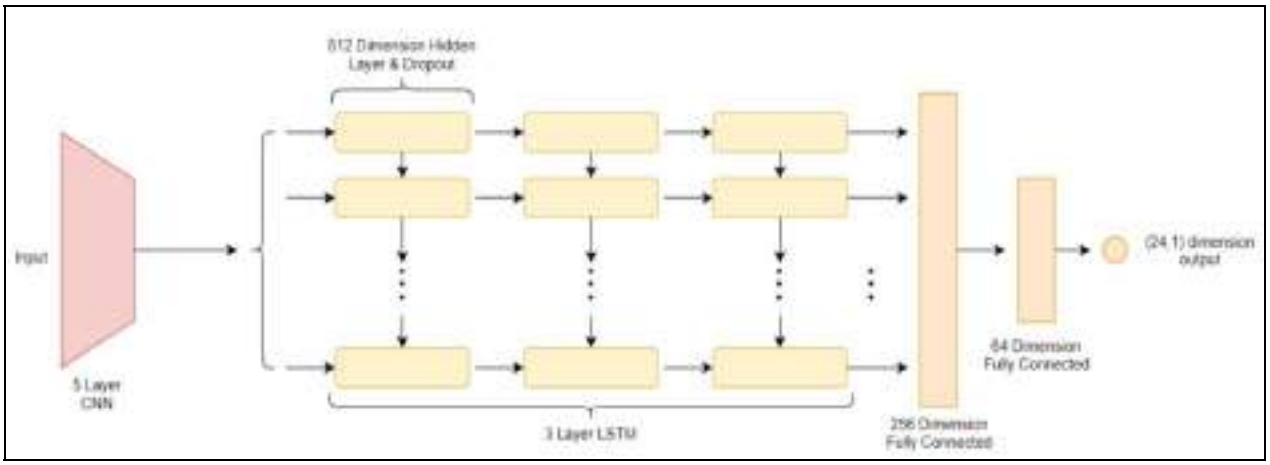

Fig.5. CNN-LSTM architecture

Crop yield prediction using deep Gaussian process based on remote sensing data [15] says that it is an inexpensive method for accurate prediction. In three ways existing techniques are improved firstly they forego traditional features and next they undergo modern approaches based on remote sensing. Novel dimensionality reduction technique is introduced to train CNN or LSTM network based on labeled training data it will automatically learn the features. Finally, in order to improve accuracy, spatiotemporal data, the Gaussian model is expressly utilized. We put our technique to the assessment on province soybean predictive modeling in the U.s, and it surpasses competing firm procedures.

A new dimensionality reduction technique is used to fulfill the demands of training phase. Raw images are treated as histograms of pixel counts to achieve tractability mean field[15] approximation is used.CNN and LSTM are trained on histograms to predict the yield.It does not explicitly account for spatiotemporal dependencies between data points but performs well, for example, due to common soil properties. we have a tendency to overcome this limitation by incorporating a mathematician method layer on prime of our neural network[10] models.Other traditional remote sensing-based models were outperformed by 30 percent in aspects of RMSE and 15percent of its total in aspects of MAPE. Deep learning models are complex non linear mappings used for learning hierarchical representation of data. CNN, DNN, LSTM consists of the set of layers where the output of one layer is the input of the next layer.

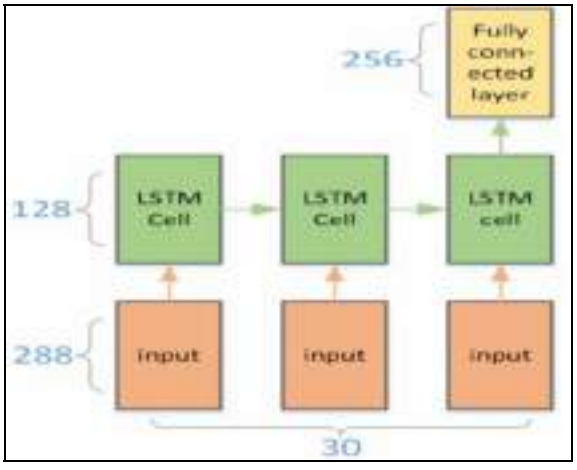

Fig.6. LSTM structure

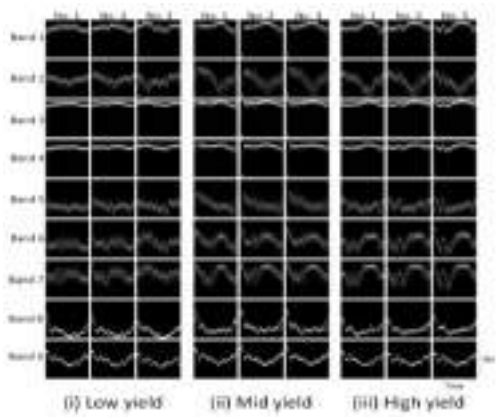

Fig.7. 3-D histogram visualization

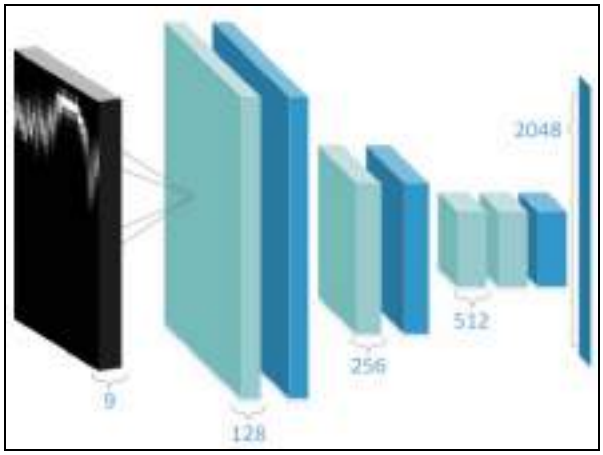

Fig.8. CNN structure

3. Flowchart For Crop Yield Prediction

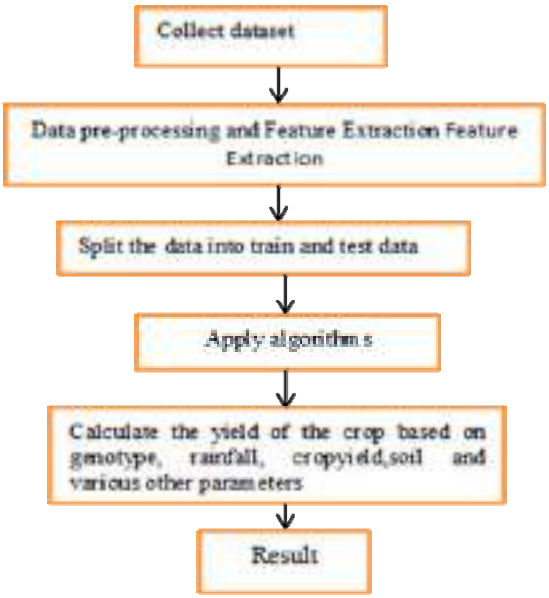

4. Methods For Predicting Crop Yield

4.1 Artificial Neural Networks (ANNs)

Artificial neural networks performed better than multivariate regression. Back propagation neural network technique is one of the best performing algorithm. Artificial neural network uses back propagation. The multilayer perceptron seems to be the most frequently used neural network in latest studies. The input data, the hidden neurons, and the network output are required for ANN, and it outdoes prediction models[2]. Biological neural mechanisms in the human brain are one type of concept for ANN structure. Neurons in the human brain are integrated and used to design the interdependencies for refining. A neurological network is made up of nodes or units, which are integrated structures. Every component is built to look like its biological counterpart, a neuron. Each unit receives and replies to a weighted set of input data. The Artificial Neural Network (ANN) [19] technique is based on a biological system model. The crucial element of this technique is the novel structure of the understanding process system. Associate degree ANN is developed for a single application, including such pattern classification or information classification, using a learning method.

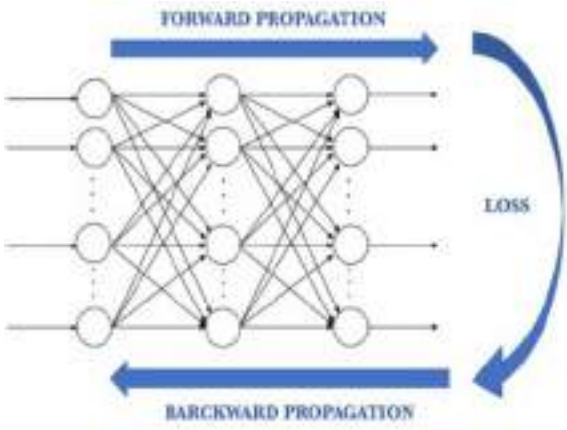

Fig.9. Forward and Backward Propagation

4.2 Deep Learning Networks (DLNs)

Deep learning models are neurons that are used in deep learning approaches. CNN, RNN, LSTM, and DNN are outscored by Lasso, shallow neural networks, regression models, deep learning methods, fully convolutional neural networks, and rnns. Deep neural networks stand to gain from cutting-edge simulation and methods applied. Feature selection can be accomplished by decreasing the dimension of the input space used to train the DNN model. As it has numerous non-linear stacked layers which convert the input to the system into an elevated and more conceptual representation to every stacked layer, it can find the underpinning representation of data

in the apparent lack of feature input data. More complicated features are extracted as the system grows deeper, resulting in high precision. It is known to be an ubiquitous approximator function if the right variables are provided, which means it can estimate almost any feature but is difficult to choose the right parameters.

4.2.1 Shallow Neural Network

One or multiple hidden layers are prevalent in shallow neural network models. Recognizing a shallow neural network can make you realize what tends to happen in a deep network. The section outlines a shallow neural network with one hidden units, one input nodes, and one output neurons.

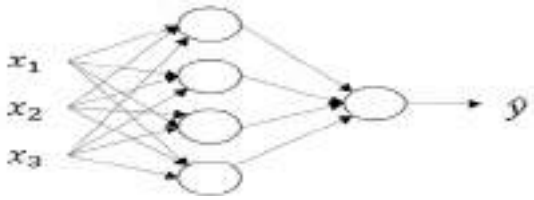

Fig.10. Shallow Neural Network

4.2.2 Convolution Neural Network

It is indeed a deep learning method that generates an image representation and designates weight values to various objects in the scene to discern them from each other.The below figure is the convolution neural network is sequence for classifiying handwritten digits.

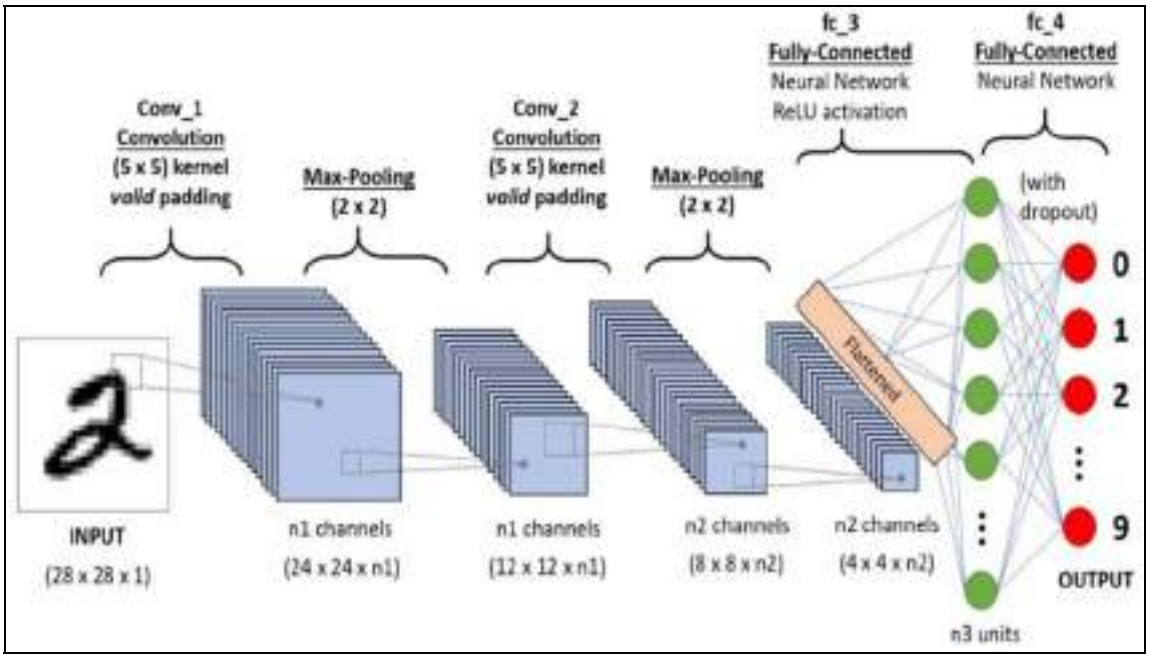

Fig.11. Convolution Neural Network

4.2.3 Recurrent Neural Network (RNN)

The recurrent neural network model [20] adds a twist for basic neural network. A vanilla neural network takes input as fixed vector size and limits the usage to situations which involves series type input with no planned size. Recurrent neural network remembers the past and are influenced by the decisions in past. They can take one or more inputs and gives one or more outputs as vector.

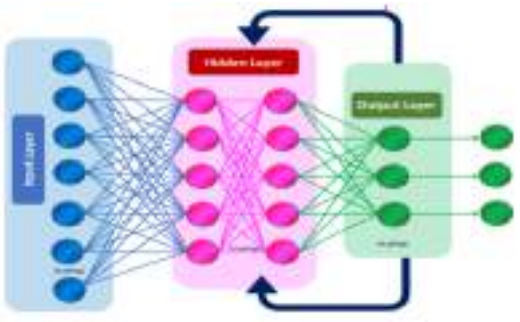

Fig.12. Recurrent Neural Network

4.2.4 Long Short Term Memory (LSTM)

Long Short Term Memory Models (LSTMMs) are designed essential to tackle the long-term correlation issue that exists in recurrent neural networks due to the vanishing gradient troubles.To make more traditional feed forward neural network LSTMs have feed back connections. They process the sequence of data entirely without treating each point independently and the useful information is retained about the previous data and it helps for processing the new data points. For text, speech and general-time series LSTMs are good for such sequences of data.

4.2.5 Deep Neural Networks

For association of input and outputs deep learning algorithms are used along with networks. Deep refers to large amount of layers along with weights and biases can be able to solve for more complex functions.

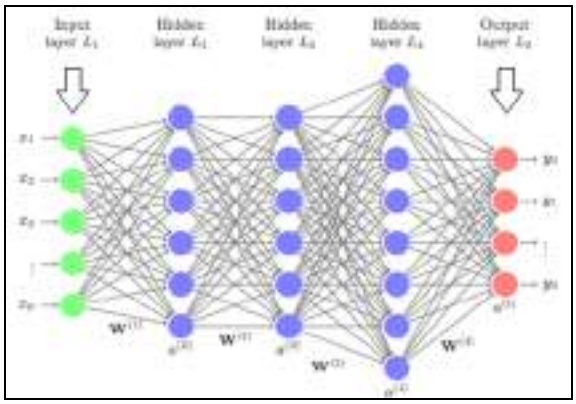

Fig.13. Deep Neural Networks

4.3 Machine Learning Techniques

Machine learning models used to anticipate crop growth include regression analysis, gradient boosting regressor model, random forest regressor model, decision tree regressor modle, polynomial regression technique, and ridge regression technique.Out of all random forest regressor[3] and gradient boosting regressor[3] gives best accuracy with cross validation.

4.3.1 Linear Regression Model

It is just a sequential model that represents the linear relation among an input parameter (x) and a single output unit (y) for combinations of the input parameter (x) (y). Single input variable is considered as a simple linear regression and multiple input variable is considered as a multiple linear regression.Most common data and method is treat the ordinary least squares method.

4.3.2 Gradient Boosting Regressor

Gradient Boosting is a kind of regression method. GB builds an ingredient model series of steps, letting the tuning of absolute discrete loss functions. A regression tree performs the amount of boosting phases in each phase by working on the negative slope of the given deficit.

4.3.3 Random Forest Regressor

So every decision tree has a large variance; nevertheless, when we incorporate them all at once, the eventual variance is lesser because each tree is wholly trained on suitable sample knowledge, and thus the outcome does not rely solely tree structure but on multiple call trees. In the occurrence of a classification error, the bulk vote classifier is used to produce the final output. In the scenario of a regression flaw, the final output is the mean of all the outcomes. Aggregation is the name given to this part of the equation.

4.3.4 Decision Tree Regressor

In attempt to provide tangible continuous output, decision tree predictor scrutinises an object's choices and trains a framework within the structure of a tree to anticipate knowledge in the future. Constant output insinuates that the emission is not distinguishable, that it cannot be characterised simply by a distinct, well-known group of statistics or value systems..

4.3.5 Polynomial Regression

Polynomial Regression is a common formula that does use an ordinal degree polynomial to quantify the relationship between a predicated (y) and an independent variable (x). The Unique Instance of Multiple Statistical Residuals in Cubic Cm is another name for it. As a result, in required to persuade the Multiple Statistical Coefficient of determination to Polynomial Correlation, we add some polynomial conditions to it. It is a linear classifier that has been improved in high precision. The mentoring set of data used in Polynomial regression is not deterministic. It hires a statistical regression model to adapt the tough and non-linear features and data sources.

4.3.6 Ridge Regression

Ridge regression is a concept standard setting technique that might be used to analyse any statistics that has experienced from repeated measures. This method employs L2 regularisation.once the problem of multiple regression happens, least-squares ar unbiased, and variances ar giant, this ends up in foreseen values to be far-flung from the particular values.

5. Comparision of crop yield prediction with different models

5.1 Artificial Neural Networks

The table below contrasts R, MEA, as well as MSE[16] for crop varieties when using artificial neural systems imperialistic competitive optimization technique and grey wolf optimization method models to examine effectiveness.

Table1. ANN-ICA and ANN-GWO with R, MEA and RMSE

Crops	R		MEA (%)		RMSE (%)	
	ANN-ICA	ANN-GWO	ANN-ICA	ANN-GWO	ANN-ICA	ANN-GWO
Wheat	0.35	0.49	35.6	33.40	8.58	8.41
Barley	0.38	0.43	12.10	12.25	0.42	0.63
Potato	0.81	0.81	22.8	22.25	0.78	0.76
Sugar Beet	0.24	0.26	39.0	39.12	3.35	3.44
Average	0.45	0.50	27.3	26.68	3.30	3.29

5.2 Deep Neural Networks

The table compares different deep learning models based on response variable, training RMSE, validation RMSE, training and validation correlation coefficients for yield, check yield, and difference.

Table 2. Training and validation comparisons of different deep neural network algorithms

Model	Response variable	Training RMSE	Training correlation coefficient(%)	Validation RMSE	Validation correlation coefficient (%)
DNN	Yield	10.53	88.31	12.8	82.91
	Check yield	8.22	91.01	11.39	85.49
	Yield difference	11.80	45.89	12.50	29.31
LASSO	Yield	20.32	36.69	21.43	27.66
	Check yield	18.87	28.51	19.89	23.01
	Yield difference	15.33	19.79	13.12	6.88
SNN	Yield	12.98	80.29	18.09	60.10
	Check yield	10.25	71.19	15.15	60.50
	Yield difference	9.98	58.76	15.16	11.36
RT	Yield	14.38	76.75	15.30	73.85
	Check yield	14.57	82.01	14.88	69.98
	Yield difference	17.68	21.15	15.93	5.12

Corn and soyabean crops are compared using Training and validation RMSE, training and validation correlation coeffients for CNN and RNN algorithms.

Table 3. CNN and RNN comparing corn and soyabean crops

Response	Model	Training RMSE	Training correlation coefficient(%)	Validation RMSE	Validation correlation coefficient(%)
Corn	CNN-RNN (W)	17.15	89.02	24.79	72.18
	CNN-RNN (S)	19.16	84.72	24.43	73.82
	CNN-RNN (M)	27.77	69.59	34.03	33.99
	Average	38.51	0.04	35.66	0.01
Soya bean	CNN-RNN (W)	4.6	89.65	5.98	78.80
	CNN-RNN (S)	5.64	83.26	5.94	81.28
	CNN-RNN (M)	7.87	59.84	8.66	48.77
	Average	10.29	0.01	10.11	0.05

5.3 Machine Learning

When accuracy, recall, and F1-score are being used to make comparisons different algorithms such as logistic regression model , decision tree method, Random Forest model, and k nearest neighbour as well as svms, logistic regression model performed the best.

Table 4. Machine learning algorithms accuracy comparison

Algorithm	Precision		Recall		F1-Score		Accuracy(100 %)
	Class 0	Class 1	Class 0	Class 1	Class 0	Class 1	
Logistic Regression	1	1	1	1	1	1	100
Decision Tree	1	0.90	0.83	1	0.91	0.95	93.3
Random Forest	1	0.90	0.83	1	0.91	0.95	93.3
K Nearest Neighbor	1	0.82	0.63	1	0.80	0.90	86.66
Support Vector Machine	0	0.60	0	1	0	0.75	60

Deep learing and machine learning algorithms comparison using mean absolute percentage error and finding the best performer algorithm using accuracy measure.

Table 5. Various deep learning and ML algorithms comparison

Model	Accuracy Measure(%)	MAPE(%)
DRL	93.7	17
BDN	92.1	20
BAN	91.7	27
IDANN	91	29
RAE	90.7	32
DL	91.85	28
ANN	90.5	38
RF	70.7	53
GB	81.2	41

Table below shows Rice, millet and paddy crops comparison using different algorithms and choosing the best performer using accuracy among all the algorithms Random forest gives best result for prediction.

Table 6. Comparing table for Rice, Millet and Paddy for various Models

Model	Accuracy Measure (%)	Crop
Multilayer perceptron	97.5	Rice
RBF Neural network	96.77	Rice
Random forest classifier	99.74	Millet
Deep reinforcement Learning	93.7	Paddy

6. Conclusion

This paper gives a detailed analysis of different approaches used for crop yield prediction.Various algorithms are mentioned along with the datasets and results. Different types of crops used for prediction purpose in different seasons are mentioned.various crops are used for prediction using different classification techniques, depending on the factors used more accurate results are generated. Climatic conditions plays a major role in yield. Crop yield prediction mainly depends on factors so while using any techniques need to consider the factors accurately gives effective results and helps in making good decisions for import and export and better pricing of respective crops. This work can be used to extend these approaches for and to achieve better results for future enhancements.

7. Nomenclature

CNN - Convolutional Neural Network
RNN - Recurrent Neural Network
RT - Regression tree
DL - Deep Learning
ANN - Artificial Neural Networks
GB - Gradient Boosting
DRL - Deep Reinforcement Learning
ARIMA - AutoRegressive Integrated Moving Average
LSTM - Long Short Term Memory
DNN - Deep Neural networks
MAPE - Mean Absolute Percentage Error
RMSE - Root mean square error
MEA - Means end analysis
MSE - Mean square error
BDN - Deep Belief Network
BAN - Born again neural networks
IDANN - Internal Deep Generative Artificial Neural Networks
RAE - Robust Adaboost RT based Ensemble
R - Range
MODIS - Moderate Resolution Imaging Spectroradiometer
LASSO - Least Absolute Shrinkage and Selection Operator
ANN-ICA - Artificial Neural Networks -imperialist competitive algorithm
ANN-GWO - Artificial Neural Networks -Gray Wolf Optimizer of Neural Networks
CNN-RNN(W) - Convolutional Neural Networks-Recurrent Neural Networks(weather data)
CNN-RNN(S) - Convolutional Neural Networks-Recurrent Neural Networks(soildata)
CNN-RNN(M) - Convolutional Neural Networks-Recurrent Neural Networks(managementdata)

8. References

1. S. Khaki and L. Wang, Front. Plant Sci. **10**, 621 (2019).

2. N. Gandhi, O. Petkar, and L. J. Armstrong, in 2016 IEEE Technological Innovations in ICT for Agriculture and Rural Development (TIAR), 105–110, (2016).

3. Payal Gulati, Suman Kumar Jha, in 2020, International Journal of Engineering Research & Technology (IJERT) ENCADEMS, **8(10)**,(2020).

4. Meeradevi and H. Salpekar, in *2019 Global Conference for Advancement in Technology (GCAT,)* 1–6, (2019).

5. M. A. Rebortera and A. C. Fajardo, Editorial Preface From the Desk of (2019).

6. T. van Klompenburg, A. Kassahun, and C. Catal, Comput. Electron. Agric. **177**, 105709 (2020).

7. K. Abhishek, M. P. Singh, S. Ghosh, and A. Anand, Procedia Technology **4**, 311 (2012).

8. S. S. Baboo and I. K. Shereef, Int. J. Environ. Sci. Dev. 321 (2010).

9. J. Burgueño, J. Crossa, P. L. Cornelius, and R.-C. Yang, Crop Sci. **48**, 1291 (2008).

10. P. Kora and S. R. Kalva, Springerplus 4, 481 (2015).

11. J. Burgueño, J. Crossa, J. M. Cotes, F. S. Vicente, and B. Das, Crop Sci. **51**, 944 (2011).

12. K. Prasanna Lakshmi and C. R. K. Reddy, in 2010 International Conference on Networking and Information Technology ,451–455pp.(2010).

13. G. P. Miriyala and A. K. Sinha, Recent Advances in Computer Based (2020).

14. Swaraja K, Multimed. Tools Appl. 77, 28249 (2018).

15. A. X. Wang, C. Tran, N. Desai, D. Lobell, and S. Ermon, in Proceedings of the 1st ACM SIGCAS Conference on Computing and Sustainable Societies (Association for Computing Machinery, New York, NY, USA, 2018), 1–5 (2018).

16. S. Kumar, P. Reddy, G. Ramesh, and V. Maddumala, Trait. Du Signal 36, 233 (2019).

17. C. U. Kumari, S. Jeevan Prasad, and G. Mounika, 2019 3rd International Conference on Computing Methodologies and Communication (ICCMC) (2019).

18. S. Sharma, S. Rai, and N. C. Krishnan, arXiv [cs.CV] (2020).

19. B.Dhanalaxmi, G. A. Naidu, and K. Anuradha, Procedia Comput. Sci. 46, 432 (2015).

20. S B Babu, A Suneetha, GC Babu, YJN Kumar, G Karuna, Periodicals of Engineering and Natural Sciences (PEN) 6 (1), 229-240, (2018).

Convolutional and Spiking Neural Network Models for Crop Yield Forecasting

*Dr.G.Karuna[1], K.Pravallika[2], Dr. K. Anuradha[3], V. Srilakshmi[4]

[1]Professor, Computer Science and Engineering, GRIET, Hyderabad, Telangana, India.
[2]PG Scholar, Computer Science and Engineering, GRIET, Hyderabad, Telangana, India.
[3]Professor, Computer Science and Engineering, GRIET, Hyderabad, Telangana, India.
[4]Assistant Professor, Computer Science and Engineering, GRIET, Hyderabad, Telangana, India.

Abstract-Prediction of Crop yield focuses primarily on agriculture research which will have a significant effect on making decisions such as import-export, pricing and distribution of specific crops. Predicting accurately with well-timed forecasts is important, but it is a difficult task due to numerous complex factors. Mostly crops like wheat, rice, peas, pulses, sugar cane, tea, cotton, green houses, corn, and soybean can all be used to forecast crop yields. We considered corn dataset to predict the yield for 13 different states in United States. Crop development and progression are strongly affected by climatic changes and unpredictability. Predicting crop yield well before harvest time will support farmers for selling and storing their crops. Agriculture involves large datasets and knowledge processes. Factors such as Weather Components, Soil Components, Management practices, genotype and their interactions are used in predicting Corn Yield. Precise crop growth generally necessitates a complete overview of the functional correlations between yield and all these interactive variables, which necessitates the use of large datasets and complex algorithms to demonstrate. Various Machine Learning models, Deep Learning models, and Artificial Neural Network algorithms are used for predicting. Deep Neural Network Models such as Convolution Neural Networks (CNN), Spiking Neural Networks (SNN), and Recurrent Neural Networks (RNN) are used to assess corn yield. Integrating CNN, RNN and SNN models outperformed than individual model performance.

Keywords — crop yield, spiking neural networks, prediction, recurrent neural networks.

1. Introduction

Crop yield forecasting plays a vital role for global food Production. To improve food and nutrition security, decision makers can use efficient process to make timely import and export choices. In order to breed better varieties for different types of environments, seed companies must forecast new hybrids. With the help of crop predictions farmers can be benefited to avoid the losses financially and can be known before what crop should be grown in which season and what are the precautions need to be taken according to the environment and soil interactions.

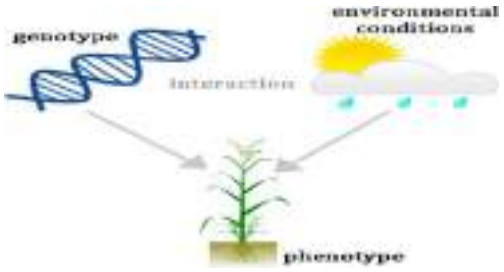

Fig 1. Genotype, phenotype and environmental interactions

Seed companies as well as farmers are going to get benefited ultimately with the help of forecasting. Crop yield forecasting can be done based on the respective factors like soil components, weather components, location, county, latitude and longitude, genotype and

*Corresponding author: karunavenkatg@gmail.com

phenotype characteristics etc. It should be known before that how much area should be taken to plant the crop and the plantation week should be noted up to how many months the crop should last all the measures needs to be analyzed before while planting the crops. What crops need to be grow and what crops cannot grow need to be considered based on the past years experiences and can also gather information from the companies like Syngenta[2] which is a global supplier of crop protection products like (herbicides, fungicides, and insecticides), seeds like (Rice and Corn) and other related products. Interactions between genotype and environment [1] are extremely complex. The term genotype refers to an individual's genetic characteristics for a specific trait, whereas phenotype refers to observable characteristics such as physical, physiological, biochemical, and behavioral characteristics. Plant length, for example, is a type of phenotype trait as shown in above Fig1 and below Fig 2

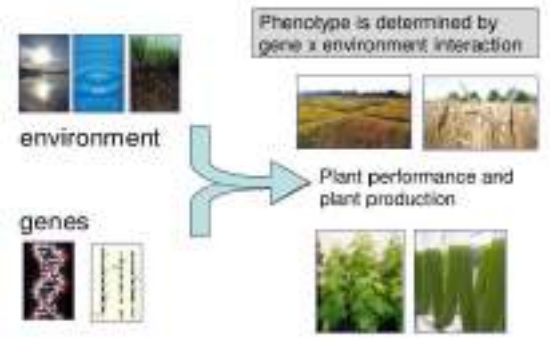

Fig 2. Phenotype traits, Genes and Environment

Millions of markers are usually present in high dimensional marker data, which is defined by genotype for every plant individual. It is important to compute the impact of genetic markers, which usually result in interactions with various environmental influences as well as field management activities.

Alleles are another word for genes, and each individual inherits two alleles for each character, one from male and one from female. Two alleles can be the same (TT or tt) or different (TT or tt) (Tt).

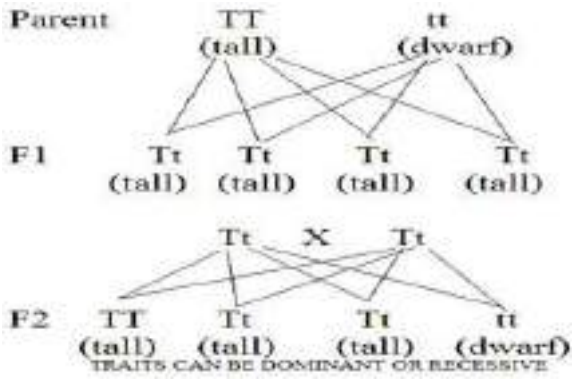

Fig 3. Dominant and Recessive alleles

The dominant allele expresses itself, while the recessive allele does not. If the dominant and recessive alleles for a specific individual are known, phenotype prediction becomes simple. Environmental factors will have a significant impact on genotype. One of several explicit functions is phenotype, which is regarded as noise and is composed of genotype (G), environment (E), and their interrelations (G*E) as shown in above Fig 3.

Mega environments are groups of environments that share the same type of variation. The two main seasons for growing various crops are Kharif (July-October) and Rabi (March-June). We have different crops like Rice, maize, sorghum, bajra, ragi, pulses, soya bean, groundnut and cotton usually grown in kharif season where as Wheat, barley, oats, chick pea, mustard seeds are grown in Rabi season. Corn crop is considered for predicting in this paper and kharif is the season for growing corn.

Soil components, Weather components are the factors for yield prediction. Different varieties of Soil components are considered like Bulk density, Cation exchange capacity $_{pH7}$, Coarse fragments, Clay, Total Nitrogen, Organic carbon density, organic carbon stock, PH in H20, Sand, Silt, Soil organic carbon and all of these inputs are measured with a 250 square meter resolution at six distinct depths (0-5cm, 5-15cm, 15-30cm, 30-60cm, 60-100cm and 100-200cm).The different Climatic components used for estimating the yield are rainfall, radiation from the sun, Precipitation data equivalent, highest temperature conditions, lowest temperature conditions, and vapor pressure are all factors to consider. Climate components play an important role in predicting when compared with the Soil and other factors. Crop productivity, on the other hand, is nearly impossible due to a plethora of complex factors. Genotype and environmental factors, for example, frequently communicate with one another, making grain yield quite difficult. Atmospheric

conditions, for example, often have complicated dynamic impacts that are hard to calculate accurately.

Crop productivity can be forecasted using machine learning models, Deep learning methods and artificial neural networks (Ann). Deep learning models [9] are classification learning methodologies because they have different levels of representation, each with nonlinear modules that change the representation at the present level, beginning with raw input and advancing to a progressively intuitive level. Deeper structures may also be affected by the vanishing gradient issue, that could be mitigated by using residual shortcut connections as well as numerous auxiliary heads (loss functions) for the network. To increase the accuracy of deep learning (dl) techniques, other techniques like a batch normalization, dropout, as well as stochastic gradient descent have been developed (SGD). In the literature, deep learning network techniques usually with more number of hidden layers gives good results than artificial neural network models with a single hidden layer. Deeper features, on either hand, are very complicate for training the model as well as necessitates more difficult hardware and optimization methods. Deep neural network loss functions, for instance, have a high dimensionality and are non-convex, making optimization quite difficult due to the existence of numerous local optima and saddle points.

2. Related Work

Soybean Flowering and Physiological Maturity Forecasted Using Neural Network Aspects [3] are founded on the hypothesis that computer simulation models of plant growth have been formulated; but the models are not always getting good results in plant developing assessment among various conditions. Field-observed flowering dates is being used by this study for the 'Bragg' cultivar for the purpose of scientific investigations in North Carolina, Gainesville, Quincy, Clayton and Florida. The neural network model was trained on the daily Higher and lower climatic conditions, season, and days after planting or flowering are all factors to consider. The sets of data were divided into two main categories: for training as model development as well as independent data sets for testing. The relative mean error of dataset testing for the purpose of flowering date forecasting was 0.143 days and for estimation of physiological maturity was +2.19 days. Plant continued growth estimations are useful in agricultural production because they allow the cultivators to enhance field operation planning and enhance net income as shown in below Fig 4 and Fig 5.

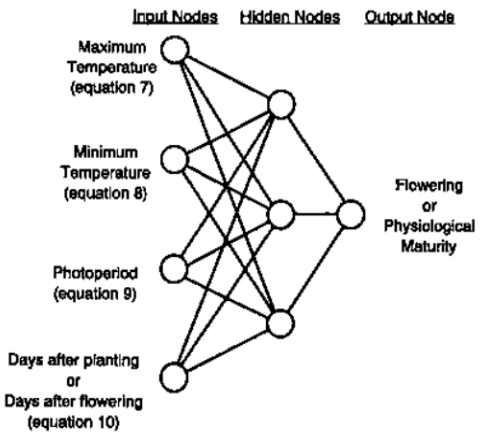

Fig 4. Inputs, connections, and structure of a neural network model are depicted using 3 distinct hidden nodes.

When seed germinates, the vegetative and reproductive development processes begin, and these processes end when the harvest matures. Temperature is a key climate variable influencing plant growth. Furthermore, duration, or the length of the daily light period, can influence increases the productivity in some species. Existing simulation models struggle to correctly estimate development in a variety of areas where either temperature or photoperiod varies. Extended preprocessing was required before feeding the data into the neural network models. The findings for the three thresholds in equations 7 through 10 were entirely dependent on pre - processing phase. It was not possible to conduct an intensive research of all threshold values and neural network requirements.

In this study, we anticipate maize yields using linear regression models and artificial neural networks models [4]. From 1962 to 2004, multiple linear regression models (MLR) and non-linear artificial neural network model (ANN) designs were used in forecasting future maize crop in China's Jilin region, with climate and fertilizer as predictor variables. Production was set to be determined by July-August rainfall, September precipitation, and fertilizer application. Fertilizer is used as a dominant forecaster in the ANN model and was found to be non-linearly related to output. For obtaining the fertilizer data of maize there is a difficulty so the studies used previous years yield tested data. Estimation skill scores derived from cross- validation technique andretroactive validation technique revealed that ANN models perform better than MLR and persistence. Due to the non-stationary nature of the data, in the analysis of forecasting skill, cross-validation method was found to be less reliable than retroactive evaluation. Researchers used two approaches to study crop productivity in relation to environmental variables: mechanistic models and empirical models. For analyzing relationships between crop, soil types,

climatic conditions, and ecology, mechanistic approaches that depend on physiological methods for crop development are best. Because non-linear relationships identified by an ANN model are more difficult to understand than linear relationships identified by MLR, ANN has been dubbed a "black box" technique. As a result, the ANN extrapolates with greater care than a linear function. ANN gives low values compared with MLR solution and hence decides that nonlinear relationship is better. In present research, where interpretation occurred, the ANN model's bounded functional shape gave ANN an added benefit over MLR. Machine Learning Methods for Efficient Forecasting in India [5] Amount of rain, atmospheric pressure, chemical fertilizer, pesticides, ph level, and other climate patterns and parameters all have an impact on crop production. After recognizing the linear relationship among yield and these parameters, reliable yield prediction is needed.

Machine Learning techniques can improve by distinguishing and presenting the consistency and pattern of drive information, machine execution can be improved without the need for characterized computer programming. This survey used a variety of neural network models to assess crop yield on crop yield datasets from multiple areas and crops, including Linear Regression model, Gradient Boosting Regressor model, Random Forest Regressor model, Decision Tree Regressor model, Polynomial Regression model, and Ridge Regression model. Mean absolute error (MAE), mean squared error (MSE), root mean square error (RMSE), R-square, and cross validation are the measures used to compare the accuracy of these strategies. Findings indicate that the Gradient Boosting Regressor has a precision of 87.9 percent with cross validation runs.

Deep Learning techniques in Agriculture [8] is a comparatively recent, cutting-edge image processing technique and data analysis technique with best outcomes and massive results. Deep learning technique has recently made its way into agriculture after being used efficiently in other fields. We assess the sustainable agricultural challenges under consideration, as well as the models and theories employed, information sources, nature, and pre-processing as well as the improved ability achieved based on the criteria used at each work under considering. In addition, we compare deep learning to other popular technologies in terms of classification or regression efficiency differences.

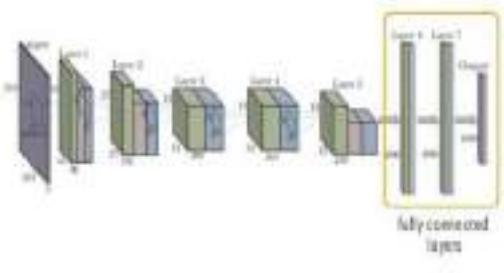

Fig 5. CaffeNet, example CNN architecture

Deep learning outdoes prevailing commonly used image processing method in terms of accuracy, according to our findings. Images make up a sizable portion of the information gathered through remotely sensed data. Images provide a clear understanding of farming in many cases and can be used to address a variety of issues. As an outcome, imaging analysis has become an interesting subject in agriculture, and intelligent data collection methods are used in a wide range of farming applications for image identity verification, outlier detection, and so on. DL extends traditional ML by incorporating more "depth" (complexity) to the model and transforming data from multiple capabilities that allow data representation in a systematic order, through many levels of abstraction.Based on the network architecture, DL may contain a wide range of modules. A basic problem in computer vision, not just deep learning, is that data pre-processing is frequently required and time-consuming, particularly when satellite and images are involved.The high dimensionality and slight number of training samples of hyper spectral data are two issues. Aside from that, existing datasets do not always effectively define the problem. When considering corn returns, for example, it was important to compensate in cultivation data such as fertilization and water management, external influences other than weather data can be considered. Convolutional Neural Networks (CNN) are used to capture similar spatial functioning of different features and combine them to model yield response to nutrient and grain rate management [6]. To define a new dataset for training and test sets the CNN model, nine on-farm corn field studies are used. When compared to multiple regression analysis, the test dataset RMSE is reduced by up to 68 percent, and by up to 29 percent when compared to a random forest. When we look at the harvest data collected within 50 meters of the field's boundaries, we can see that the input variables centered on such cells cover an area with no data.

As shown in below Fig 6 and Fig 7, Fig 8,This survey modeled yield response to nitrogen and seed rate management using five different field features (nitrogen and grain rates, elevation map, soil electro conductivity,

and spatial data). Other risk factors and management techniques that have an effect on global field impacts gain response to site-specific planning. These parameters differ from field to field while changing progressively within the same field.

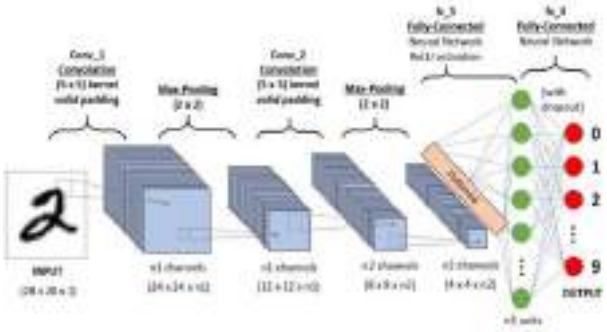

Fig 6. Convolutional Neural Network

Growing plants Date, Hybrid Maturity, and Weather Conditions Influence Corn Yield and Crop Stage [7] In Iowa, USA, we examined wheat crop and phenology data from a multi-location, year, hybrid comparative maturity, and planting date study. Our goals were to find the best combination of sowing date and comparable maturity to maximize corn seed yield per weather, as well as to mitigate the effects of using "full-season hybrids" when harvesting occurs well after the optimum planting date. According to ANOVA, 70% of the variability in seed yield was directly related to planting date and only 10% to associated to maturity, stating that short and full-season hybrid relative maturity periods generated equivalent to seed yield regardless of when they were sown as long as the farms reached maturity prior to harvesting. According to our findings, the time to grain yield is a good predictor of expected higher yield, with a critical stage (after which yield is reduced) of 23 July for Iowa. Furthermore, we discovered that keeping a lower limit growing degree of 648°Cday as during the grain-filling period enhanced maize yield. Conclude, the studied information will help Iowans in making sowing date decisions on the basis on hybrid relative maturity. Throughout most of the growing season (April–October), weather conditions at our sampling locations were relatively inconsistent. The Northeast place had the coolest site-year in 2014, while the Southeast place had the hottest year in 2016. In aspects of rainfall, 62 percent of the site-years were wet, 24 percent became dry, and 14 percent were indeed a mix of the two .

Maize seed yield, silking time, and other considerations, as well as grain-filling duration, are all affected by the planting date. In terms of seed yield and phenology, PD had a bigger influence than RM. Farmers in Iowa will benefit much during the growing season if they plant full-season hybrids all year; nevertheless, the real effect of RM fades over time. Immigrants came to warmer climates with a longer growing season as southern climates warm. A shortened growing season was blamed for the harvest penalty associated with delayed planting. Farmers typically select a mixture relative maturity well in order to progress of planting; however, our research shows that combination RM has a very minor impact on grain yield for any given PD when harvested before planting.

Grain yield estimation and climate making predictions using machine learning techniques for Assessment of the impacts on agriculture [9] Weather has a significant impact on crop productivity A increasing previous research models this transaction in order to estimate the threat of climate change on the industry. A yield modeling approach that makes use of a semi-parametric variant of a deep learning to account for nonlinear dynamic interactions in high-dimensional datasets, as well as known geometrical structure and unfathomable cross-sectional heterogeneity. We show that using corn yield data from the Midwest of the United States, this model outperformed both traditional statistical methods and entirely nonparametric neural networks in predicting yields of years denied during model training. We show that climate change has a major negative impact on corn prices, but it is less intense than the impacts projected using statistical models. Abatzoglou's gridded surface meteorological database (METDATA) is used to generate the meteorological data (2013). Bagging improved both the parameterization and the SNN's precision, but the bagged SNN consistently outperforms. Both OLS regression and the SNN were outpaced by the fully-nonparametric neural net, which was learned in the same way as the SNN but lacked simulation terms.

Incorporating machine learning and crop simulations improves crop yield estimation in the Corn Belt of the United States [10].The goal of this research is to see if merging crop modeling and machine learning (ML) tends to improve grain yield projections in the Corn Belt of the United States. The primary objectives were to identify whether such a hybrid approach would result in better assumptions, which hybrid model mixtures provide much more better estimates, and which crop modeling attributes are most effective when combined with ML for maize crop prediction. The researchers noted that using simulation crop modeling as input features in ML models can lessen yield estimation root mean squared error (RMSE) by 7 to 20%. Furthermore, we investigated the selective complicity of APSIM attributes in ML forecasting and concluded that soil moisture-related APSIM variables have the greatest impact on ML projections, followed by crop-related and weather-related APSIM variables. This finding implies that weather reports alone are inadequate, and that Ml

algorithms require more surface water inputs to produce more accurate yield forecasts.

Estimation of crop prices using supervised machine learning methods [11] and our focus is primarily on agriculture. Farmers are the most important people in agriculture. Farmers face massive losses if the price falls after the cultivation. This paper proposes estimating and planning crop prices for the next 12 months. The information is provided to users via a Flask web page, which is powered by impactful machine learning techniques and innovations and has a user-friendly interface as a whole. The accumulated training datasets contain a wealth of information for forecasting market price and demand. The Decision tree Regressor supervised machine learning algorithm was used in our model. It has been honed on a number of Kharif and Rabi seasons to improve efficiency.

Estimation of Crop Production by Robots [12] Cultivation is an entirely manual endeavour. The use of machine learning methods to implement any type of automation is still in its beginning phases. The focus of this article is to present a contextual approach for introducing machine learning methods into the cropping process. A comparison of machine learning algorithms was performed in order to determine which algorithm is the most accurate in predicting the best crop for a specific plot of land. The research looks at six major food crops in Bangladesh: Aman rice, Aus rice, Boro rice, potato, wheat, and jute. Multiple Linear Regression (MLR) produced the most accurate results during the evaluation and was implemented into an Android application. The android platform system can also generate a timeline of the entire farming process for a specific crop, including when to apply fertilizer. Except for wheat and potatoes, MLR offers greater prediction in this case. KNN yields superior performance for wheat and potato. Mostly as result, the error is 0.40 percent for one and 6.26 percent for the other.

Deep Learning Methods for Yield Estimation [13]. Automatic crop monitoring and yield prediction are now possible thanks to artificial intelligence. The categories were created entirely around five networks: ANN, CNN, DNN, RNN, and combination networks. The feed forward's ANN and DNN were examined, and both offered an average predictive accuracy of 60-70 percent. The large proportion of agricultural processing was carried out using images and timely monitoring. CNN significantly outperformed both DNN and ANN models, with efficiency of 80-85 percent. The only drawback of CNN in this research was that its projections were based purely on training sample rather than real-time past results. A few work was aimed at improving the yield prediction even more and to avoid loss during the yield. The RNN makes use of an LSTM-LSTM combination, which allows for the addition of data storage. When particularly in comparison to the other three systems, it involves the feedback loop that CNN fails, evaluated to the high classification level's average estimation of 83 – 89 percent.

3. Proposed Work

3.1 Dataset Description

For Crop yield prediction we need to select the crop here we selected the crop called Corn and going to forecast the yield based on the dataset and the applied algorithms. Dataset is the first thing we need to select here we collected the dataset from various sources like Syngenta and it mainly consists of the variables like nw, ns, np, nss where the number of weather elements is nw, and the number of soil particles is ns. measured at different depth, np is the planting component and nss is the soil component measured at the surface The six weather components considered are rainfall, radiation from the sun, snow water equivalent, highest temperature, lowest temperature, and air humidity for csv files they are named as Wij where i is the weather component index and consider the six weather components i.e i=1, . . .6 and j= index of week of year for every year there are 52 weeks so j=1,….52. There are 11 Soil components like bulk density(bdod), Caption exchange capacity at Ph7(cec), Coarse fragments(cfvo), clay, Total nitrogen, Organic carbon density(ocd), Organic carbon stock(ocs), ph in H20(phh20), Sand, Silt, Soil organic carbon measured at six different depths(0-5cm, 5-15cm, 15-30cm, 30-60cm, 60-100cm, 100-200cm) with 250 square meter resolution in csv files they can be named as Sij where i is the soil component i.e i=1,-----11 and j is the index of depth j=1,---6. Planting time component is considered as np in csv files they are named as pi where i is the index of the planting date week i=1,---16. The crop performance dataset includes the identified average yield for corn between 1980 and 2019 across 1,176 countries for corn in 13 states including Indiana, Minnesota, Kansas, North Dakota, Missouri, Illinois, Iowa, Nebraska, South Dakota, Ohio, Kentucky, Michigan, and Wisconsin. Organizational data is generally the cumulative percentage of cultivated fields in each state each week starting in April of each year. Grid map approach is followed which means horizontal and vertical lines to identify locations on map.

3.2 System Architecture

The System Architecture of proposed work is like first consider the dataset and preprocesses the data then split into train and test data apply the classification techniques and predict the results. Here for this forecasting purpose Corn dataset is considered from

open source challenge platform like Syngenta [2]. Cleaning, integration, reduction, and transmission are all methods of data preprocessing. We need to get rid of any data that isn't absolutely necessary. The procedure of detecting and analyzing inaccurate or incorrect records from a dataset is known as data cleaning. Real-world data frequently contains noise and missing values, and it may be in an inaccessible format that cannot be actively used for DL models. Data preprocessing is required for cleaning preparation and analysis it for various Deep Learning concepts, which increases performance and reliability. Data that is preprocessed is categorized for training and testing. Training a data means to train the model and testing is for validation process where the unseen predictions are done. The act of segregating available data into two segments, typically for cross-validator purposes, is known as data splitting. One set of data is used to create a forecasting model, while the other is used to evaluate the performance of the model. Data separation into training and test sets is a critical step in assessing data mining models. Training percentage is taken as 80 and test percentage is 20. When a data set is split into a training phase and a validation phase, the majority of information is used for training and only a small amount is used for test results. To train any model, no matter what type of dataset is used, the set of data must be divided into training and testing sets.In the analysis of forecasting skill, cross-validation method was found to be less reliable than retroactive evaluation. Researchers used two approaches to study crop productivity in relation to environmental variables: mechanistic models and empirical models. For analyzing relationships between crop, soil types, climatic conditions, and ecology, mechanistic approaches that depends on physiological methods for crop development are best.

4. Flowchart for Crop Yield Prediction

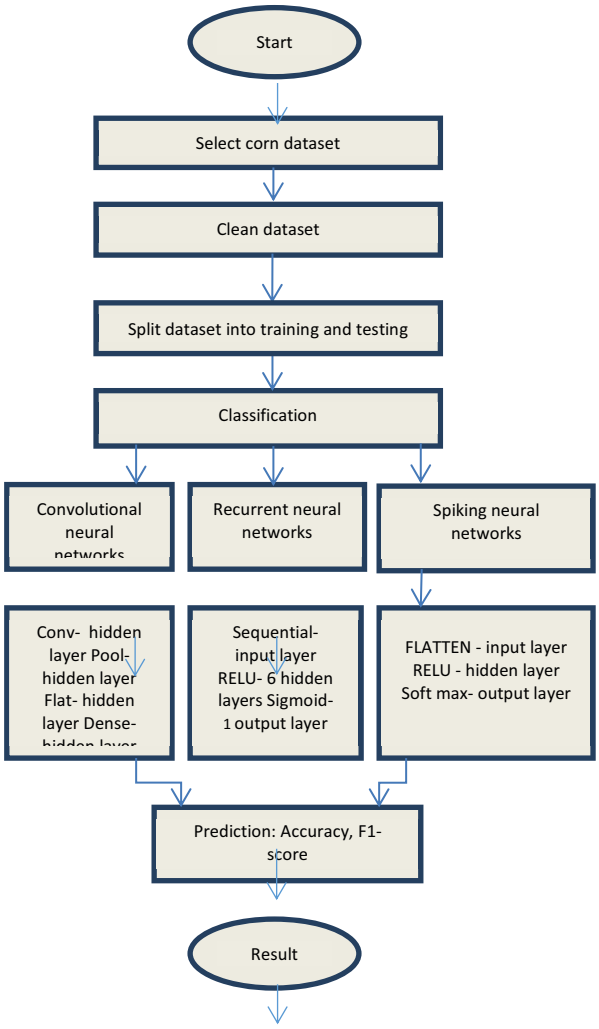

5. Implementation

5.1 Deep learning Methods

Corn yield forecasting is done using Deep Learning (DL) models. Convolutional Neural Networks (CNN), Recurrent Neural Networks (RNN), and Spiking Neural Networks are some of the deep learning models used in this paper (SNN). Neural Networks are composed of three layers: input, hidden and output layer. Input Layer: In this level various types of data is provided to the model. Number of neuron indicates the total number of features in data. Hidden Layer: The output of the Input Layer is fed into the Hidden Layer. Depending on our model and the size of the data, there could be many hidden layers. So every hidden layer may contain a different number of neurons, which is usually greater than the number of characteristics. Each layer's output is calculated by multiplying the previous layer's output by the learnable weights of that layer, followed by addition

of transferable biases and an activation function, making the learning process non linear.

Output Layer: The hidden layer's output is then placed into a logistic function, such as sigmoid or soft max, which converts each class's output into a probability score for each class. Classification is a method of determining which of a set of characteristics a new observation belongs to, based on a learning set of data containing observations with defined category membership.

5.2 Convolution Neural Networks (CNN)

ConvNets also known as CNN'S consists of multiple layers mainly used for image processing and object detection. It has a number of layers that process and extract data features. CNN has a convolution layer with several filters that performs the convolution operation. CNN image categories take an image representation and process it before categorizing it. An input image is perceived by computers as an array of pixels, the size that rely on the quality of image. Depending on the resolution of an image, it will see h x w x d (h = Height, w = Width, d = Dimension). For convolution Neural Networks (CNN'S) we use four hidden layers i.e. convolution layer, Pool layer, flat layer, Dense layer. Conv1D is used and in this the kernel moves only in one direction applicable for Time series data, input and output of Conv1D is two dimensional. Convolution is a mathematical operation performed on two objects to generate an output that expresses how the shape of one is modified by the other. This calculation finds a special functionality in the input data and needs to return a result enclosing that feature's relevant data. This is known as a feature map. The process of merging is known as pooling. So it's primarily for the purpose of reducing data size. Max pooling is considered which takes the highest value within the box. One –dimensional array is considered as a method of converting input data to next layer also treated as flattening. The convolutional layer outcome is flattened to produce a single long feature vector. It is also correlated to the final classification model, forming a fully-connected layer. We attach the final layer to a single line that contains all of the pixel data. Fully connected layer is a dense layer tells that neurons of one layer communicate with next. Adaptive Moment Estimation optimization is a stochastic gradient descent model which is based on adaptive estimation of first-order as well as second-order moments. Adaptive Moment Estimation is a deep neural network training-specific adaptive learning rate considered as optimization algorithm. The technique makes use of the power of adaptive learning rate techniques to identify individual learning rates for each parameter. The average of the squared differences between the observed and predicted values is used to calculate the Mean Squared Error loss. The output is always positive, regardless of the sign of the predicted and actual values, and the value obtained is 0.0.

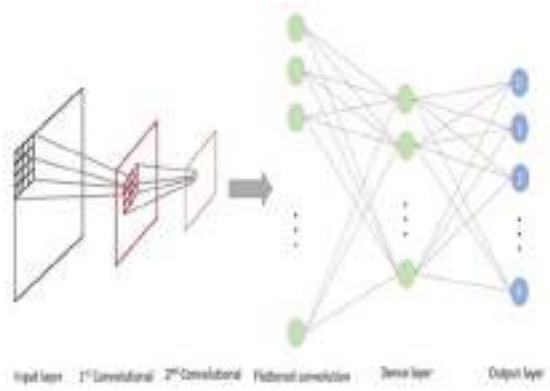

Fig 7. Convolutional Neural Networks

5.3 Recurrent Neural Networks (RNN):

One type of artificial neural network is recurrent neural network that can perform operations on some files like audio files, data files etc. All input and output values are independent in neural networks whereas in RNN, the hidden layers remember the data that was done in a previous layer and give that remembered data to the next layer as input so that it can perform operations on data. This process is repeated until the desired output is obtained. The rectified linear activation function, abbreviated RELU, is a piecewise linear function that retrieves the user input if it is positive and indirectly if it is negative. It has become the default activation function for few types of neural networks and it is easier to train and frequently results in better performance. Activation functions for a Rectified Linear Unit with six hidden layers. In multi-layer networks, the vanishing gradient issue restricts the use of the sigmoid and hyperbolic tangent activation functions. The rectified linear activation function solves the vanishing gradient problem, allowing features to learn more quickly and work better. When building multilayer Perceptron and

convolutional neural network models, the rectified linear activation act as standard activation. Input layer is sequential and output layer is sigmoid.

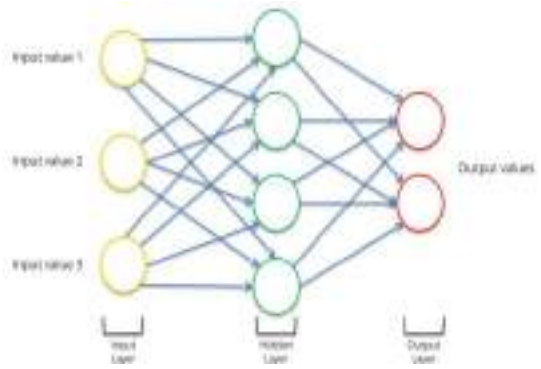

Fig8. Recurrent Neural Networks

5.4 Spiking Neural Networks (SNN):

Spiking neural networks (SNNs) were artificial neural networks that resembled natural neural networks. SNNs incorporate time into their operating model in terms of neuronal and synaptogenesis state. According to the principle, the neurons in the SNN do not need to transmit data during every propagation cycle. Information is only sent when a membrane potential – an inherent property of the neuron associated to its electrical charge on the membrane – reaches a specified value known as the threshold. When the membrane potential reaches a certain threshold, the neuron fires and transmits the signal to other neurons, which modify their potentials in reactions to the signal. The input layer is flattening. Flattening is the process of converting data into a one-dimensional array for input into the next layer. We flatten the layer output to create a unified long feature vector. It is also linked to the last classification model, resulting in a fully connected layer. The ReLU layer is the hidden layer. The rectified linear activation function (ReLU) is a piecewise linear function that, if the input is positive, effectively generates the input; otherwise, it outputs zero. The rectified linear activation function solves the vanishing gradient problem, allowing models to learn more quickly and function better. The output layer, the Softmax layer, broadens this concept into a multi-class work environment. The total of those decimal likelihoods must equal 1.0. The number of neurons in the Softmax layer must be the same as number of neurons in the output layer as shown in below Fig 9.

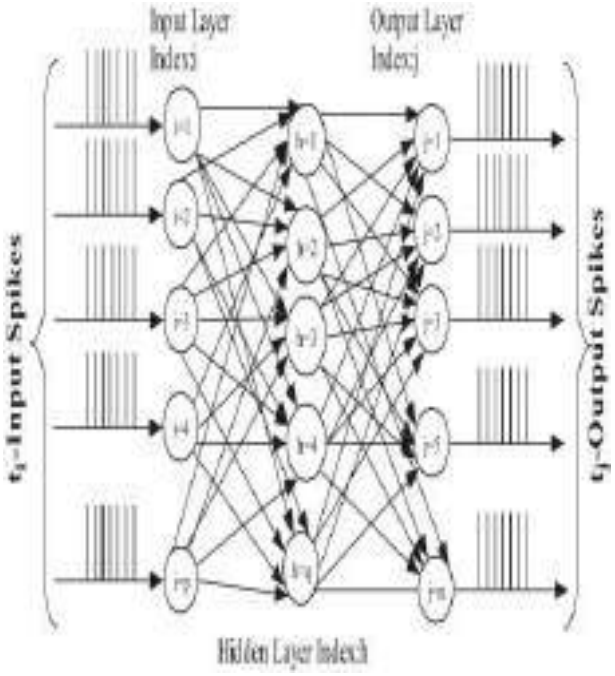

Fig 9. Spiking Neural Networks

6. Results

Tensor flow, an open-source software library, was used to create the three deep neural networks in Python. The training phase for each neural network took about 1.4 hours on a Tesla K20m GPU. For comparative analysis, we used three other well-known forecasting models: Convolutional Neural Network models (CNN), Recurrent Neural Network models (RNN), and Spiking Neural Networks models (SNN). To ensure better comparisons, we wrote all of these modeling techniques in Python and evaluated them in the same software and hardware environments. The overall classification and prediction will be used to generate the Final Result. The effectiveness of the proposed approach is assessed using metrics such as, the ability of a classifier is referred to as its accuracy Class label is predicted correctly and the accuracy tells how good a given predictor can guess the value of attribute for new data.

$$AC= \frac{TP+TN}{TP+TN+FP+FN}$$

$$F\text{-measure}=\frac{2TP}{2TP+FP+FN}$$

6.1 Results for Convolutional Neural Network

Model	Precision		Recall		F1-score		Support		Accuracy
	class 0	class 1	class 0	class 1	class 0	class 1	class 0	class 1	
CNN	1.01	0.01	0.90	0.00	0.97	0.02	300	0	91 %
RNN	1.00	0.00	0.92	0.01	0.95	0.00	300	0	89 %
SNN	1.05	0.03	0.95	0.00	0.95	0.05	300	0	90 %

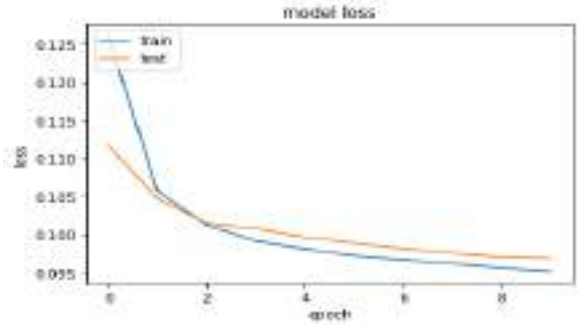

6.2 Results for Spiking Neural Network

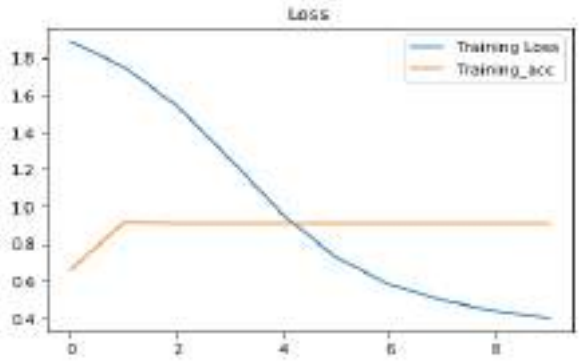

6.3 Results for Recurrent Neural Network

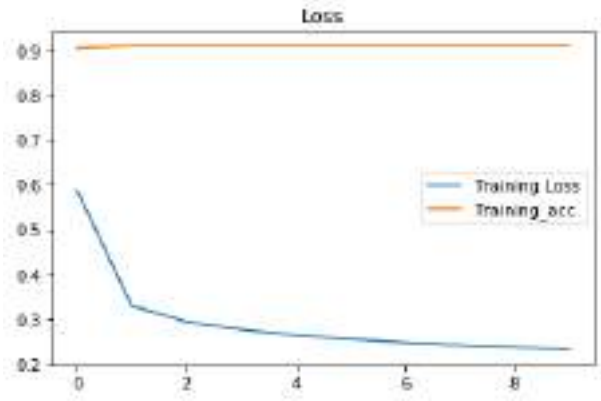

6.4 Result Analysis

The prediction accuracy of crop yield is compared with 3 models and the results are depicted in Table1.

Table 1: Comparing different measures for CNN, RNN, SNN

7. Conclusion

We described a deep learning-based framework for forecasting climate information and management in this study practices that successfully predicted corn yields across the entire Corn Belt in the United States. Most importantly, our approach went beyond estimation by providing major findings that aided in the explanation of yield estimation (variable importance by time period). The method developed are convolutional neural networks (CNN) and Spiking neural networks (SNN). The CNN component of the framework was designed to capture the intrinsic temporal relationship of weather data as well as the spatial interconnections of soil data measured at different depths underground. The model's RNN component was designed to capture the rising trend in crop yield over time as part of ongoing improvements in plant reproduction and management practises. SNNs work with spikes, which are discrete events that happen at specific points in time, instead of continuous values. The occurrence of a spike is determined by nonlinear equations that depict various biological processes, the most significant of which is the membrane potential of a neuron. When a neuron attains

a certain potential, it spikes, and the potential of the neuron is reset. Several variables, including climatic conditions, soil, and management, had a large impact on the model's effectiveness. In unknown environments, the suggested framework accurately predicted yields, and it could thus be used in tasks requiring long-term yield forecasting. One of the most difficult aspects of deep learning techniques is their black box nature. To make the current proposal less of a black box and more concise, feature selection was back propagation method that is used for trained CNN-RNN model. The feature selection model estimated the individual impact of weather components, soil type, and management variables, as well as the time span when these factors get to be significant, and that is a study development. This method could be used to solve other research issues. Similarly, a hybrid could be classified as low-yielding or high-yielding depends on the performance in comparison to other varieties in the same location.

8. References

1. Khaki, Saeed& Wang, Lizhi. (2019). Crop Yield Prediction Using Deep Neural Networks.Frontiers in Plant Science.10. 10.3389/fpls.2019.00621.
2. Syngenta (2021). *Syngenta Crop Challenge In Analytics*. Available online at: https://www.ideaconnection.com/syngenta-crop-challenge/challenge.php/
3. Elizondo, David & McClendon, R.W.. (1994). Neural Network Models for Predicting Flowering and Physiological Maturity of Soybean. Transactions of the American Society of Agricultural Engineers. 37. 981-988. 10.13031/2013.28168.
4. Matsumura, K. &Gaitan, Carlos & Sugimoto, K. & Cannon, Alex & Hsieh, William. (2015). Maize yield forecasting by linear regression and artificial neural networks in Jilin, China.1-12.
5.PayalGulati, Suman Kumar Jha, 2020, Efficient Crop Yield Prediction in India using Machine Learning Techniques, INTERNATIONAL JOURNAL OF ENGINEERING RESEARCH & TECHNOLOGY (IJERT) ENCADEMS – 2020 (Volume 8 – Issue 10),
6. Barbosa, Alexandre&Trevisan, Rodrigo &Hovakimyan, Naira & Martin, Nicolas. (2020). Modeling yield response to crop management using convolutional neural networks.Computers and Electronics in Agriculture. 170. 105197. 10.1016/j.compag.2019.105197.
7. Baum, Mitch &Archontoulis, S. &Licht, Mark. (2018). Planting Date, Hybrid Maturity, and Weather Effects on Maize Yield and Crop Stage.Agronomy Journal.111. 10.2134/agronj2018.04.0297.
8.AndreasKamilaris, Francesc X. Prenafeta-Boldú,Deep learning in agriculture: A survey,Computers and Electronics in Agriculture, https://doi.org/10.1016/j.compag.2018.02.016. (https://www.sciencedirect.com/science/article/pii/S0168169917308803)
9. Khaki, Saeed& Wang, Lizhi&Archontoulis, Sotirios. (2019). A CNN-RNN Framework for Crop Yield Prediction.
10. Shahhosseini, Mohsen & Hu, Guiping& Huber, Isaiah &Archontoulis, Sotirios. (2021). Coupling machine learning and crop modeling improves crop yield prediction in the US Corn Belt. Scientific Reports. 11. 10.1038/s41598-020-80820-1.
11. Mulla, Sadiq&Quadri, S..(2020). Crop-yield and Price Forecasting using Machine Learning.TheInternational journal of analytical and experimental modal analysis. XII. 1731-1737.
12. T. Siddique, D. Barua, Z. Ferdous and A. Chakrabarty, "Automated farming prediction," 2017 Intelligent Systems Conference (IntelliSys), 2017, pp. 757-763, doi: 10.1109/IntelliSys.2017.8324214.
13. Dharani, M &Thamilselvan, R &Natesan, P &Kalaivaani, PCD &Santhoshkumar, S. (2021). Review on Crop Prediction Using Deep Learning Techniques. Journal of Physics: Conference Series. 1767. 012026. 10.1088/1742-6596/1767/1/012026.

Convolutional and Spiking Neural Network Models for Crop Yield Forecasting

*Dr.G.Karuna[1], K.Pravallika[2], Dr. K. Anuradha[3], V. Srilakshmi[4]

[1]Professor, Computer Science and Engineering, GRIET, Hyderabad, Telangana, India.
[2]PG Scholar, Computer Science and Engineering, GRIET, Hyderabad, Telangana, India.
[3]Professor, Computer Science and Engineering, GRIET, Hyderabad, Telangana, India.
[4]Assistant Professor, Computer Science and Engineering, GRIET, Hyderabad, Telangana, India.

Abstract-Prediction of Crop yield focuses primarily on agriculture research which will have a significant effect on making decisions such as import-export, pricing and distribution of specific crops. Predicting accurately with well-timed forecasts is important, but it is a difficult task due to numerous complex factors. Mostly crops like wheat, rice, peas, pulses, sugar cane, tea, cotton, green houses, corn, and soybean can all be used to forecast crop yields. We considered corn dataset to predict the yield for 13 different states in United States. Crop development and progression are strongly affected by climatic changes and unpredictability. Predicting crop yield well before harvest time will support farmers for selling and storing their crops. Agriculture involves large datasets and knowledge processes. Factors such as Weather Components, Soil Components, Management practices, genotype and their interactions are used in predicting Corn Yield. Precise crop growth generally necessitates a complete overview of the functional correlations between yield and all these interactive variables, which necessitates the use of large datasets and complex algorithms to demonstrate. Various Machine Learning models, Deep Learning models, and Artificial Neural Network algorithms are used for predicting. Deep Neural Network Models such as Convolution Neural Networks (CNN), Spiking Neural Networks (SNN), and Recurrent Neural Networks (RNN) are used to assess corn yield. Integrating CNN, RNN and SNN models outperformed than individual model performance.

Keywords — crop yield, spiking neural networks, prediction, recurrent neural networks.

1. Introduction

Crop yield forecasting plays a vital role for global food Production. To improve food and nutrition security, decision makers can use efficient process to make timely import and export choices. In order to breed better varieties for different types of environments, seed companies must forecast new hybrids. With the help of crop predictions farmers can be benefited to avoid the losses financially and can be known before what crop should be grown in which season and what are the precautions need to be taken according to the environment and soil interactions.

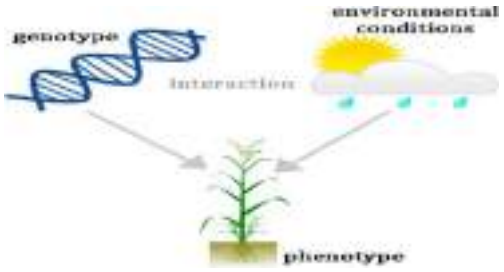

Fig 1. Genotype, phenotype and environmental interactions

Seed companies as well as farmers are going to get benefited ultimately with the help of forecasting. Crop yield forecasting can be done based on the respective factors like soil components, weather components, location, county, latitude and longitude, genotype and

*Corresponding author: karunavenkatg@gmail.com

phenotype characteristics etc. It should be known before that how much area should be taken to plant the crop and the plantation week should be noted up to how many months the crop should last all the measures needs to be analyzed before while planting the crops. What crops need to be grow and what crops cannot grow need to be considered based on the past years experiences and can also gather information from the companies like Syngenta[2] which is a global supplier of crop protection products like (herbicides, fungicides, and insecticides), seeds like (Rice and Corn) and other related products. Interactions between genotype and environment [1] are extremely complex. The term genotype refers to an individual's genetic characteristics for a specific trait, whereas phenotype refers to observable characteristics such as physical, physiological, biochemical, and behavioral characteristics. Plant length, for example, is a type of phenotype trait as shown in above Fig1 and below Fig 2

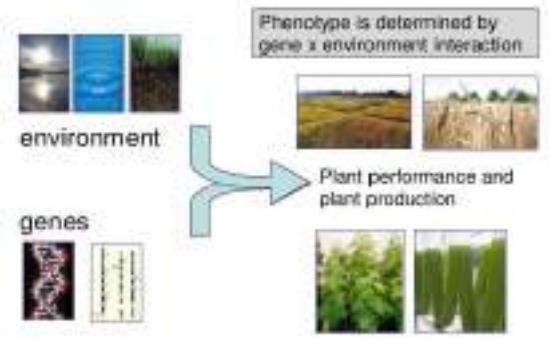

Fig 2. Phenotype traits, Genes and Environment

Millions of markers are usually present in high dimensional marker data, which is defined by genotype for every plant individual. It is important to compute the impact of genetic markers, which usually result in interactions with various environmental influences as well as field management activities.

Alleles are another word for genes, and each individual inherits two alleles for each character, one from male and one from female. Two alleles can be the same (TT or tt) or different (TT or tt) (Tt).

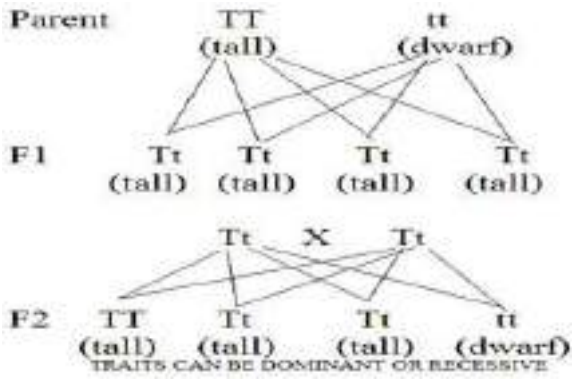

Fig 3. Dominant and Recessive alleles

The dominant allele expresses itself, while the recessive allele does not. If the dominant and recessive alleles for a specific individual are known, phenotype prediction becomes simple. Environmental factors will have a significant impact on genotype. One of several explicit functions is phenotype, which is regarded as noise and is composed of genotype (G), environment (E), and their interrelations (G*E) as shown in above Fig 3.

Mega environments are groups of environments that share the same type of variation. The two main seasons for growing various crops are Kharif (July-October) and Rabi (March-June). We have different crops like Rice, maize, sorghum, bajra, ragi, pulses, soya bean, groundnut and cotton usually grown in kharif season where as Wheat, barley, oats, chick pea, mustard seeds are grown in Rabi season. Corn crop is considered for predicting in this paper and kharif is the season for growing corn.

Soil components, Weather components are the factors for yield prediction. Different varieties of Soil components are considered like Bulk density, Cation exchange capacity $_{pH7}$, Coarse fragments, Clay, Total Nitrogen, Organic carbon density, organic carbon stock, PH in H20, Sand, Silt, Soil organic carbon and all of these inputs are measured with a 250 square meter resolution at six distinct depths (0-5cm, 5-15cm, 15-30cm, 30-60cm, 60-100cm and 100-200cm).The different Climatic components used for estimating the yield are rainfall, radiation from the sun, Precipitation data equivalent, highest temperature conditions, lowest temperature conditions, and vapor pressure are all factors to consider. Climate components play an important role in predicting when compared with the Soil and other factors. Crop productivity, on the other hand, is nearly impossible due to a plethora of complex factors. Genotype and environmental factors, for example, frequently communicate with one another, making grain yield quite difficult. Atmospheric

conditions, for example, often have complicated dynamic impacts that are hard to calculate accurately.

Crop productivity can be forecasted using machine learning models, Deep learning methods and artificial neural networks (Ann). Deep learning models [9] are classification learning methodologies because they have different levels of representation, each with nonlinear modules that change the representation at the present level, beginning with raw input and advancing to a progressively intuitive level. Deeper structures may also be affected by the vanishing gradient issue, that could be mitigated by using residual shortcut connections as well as numerous auxiliary heads (loss functions) for the network. To increase the accuracy of deep learning (dl) techniques, other techniques like a batch normalization, dropout, as well as stochastic gradient descent have been developed (SGD). In the literature, deep learning network techniques usually with more number of hidden layers gives good results than artificial neural network models with a single hidden layer. Deeper features, on either hand, are very complicate for training the model as well as necessitates more difficult hardware and optimization methods. Deep neural network loss functions, for instance, have a high dimensionality and are non-convex, making optimization quite difficult due to the existence of numerous local optima and saddle points.

2. Related Work

Soybean Flowering and Physiological Maturity Forecasted Using Neural Network Aspects [3] are founded on the hypothesis that computer simulation models of plant growth have been formulated; but the models are not always getting good results in plant developing assessment among various conditions. Field-observed flowering dates is being used by this study for the 'Bragg' cultivar for the purpose of scientific investigations in North Carolina, Gainesville, Quincy, Clayton and Florida. The neural network model was trained on the daily Higher and lower climatic conditions, season, and days after planting or flowering are all factors to consider. The sets of data were divided into two main categories: for training as model development as well as independent data sets for testing. The relative mean error of dataset testing for the purpose of flowering date forecasting was 0.143 days and for estimation of physiological maturity was +2.19 days. Plant continued growth estimations are useful in agricultural production because they allow the cultivators to enhance field operation planning and enhance net income as shown in below Fig 4 and Fig 5.

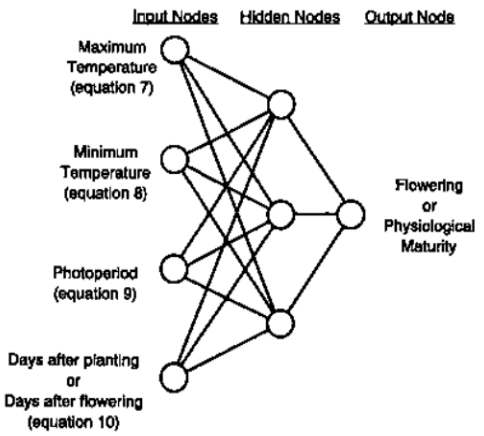

Fig 4. Inputs, connections, and structure of a neural network model are depicted using 3 distinct hidden nodes.

When seed germinates, the vegetative and reproductive development processes begin, and these processes end when the harvest matures. Temperature is a key climate variable influencing plant growth. Furthermore, duration, or the length of the daily light period, can influence increases the productivity in some species. Existing simulation models struggle to correctly estimate development in a variety of areas where either temperature or photoperiod varies. Extended preprocessing was required before feeding the data into the neural network models. The findings for the three thresholds in equations 7 through 10 were entirely dependent on pre - processing phase. It was not possible to conduct an intensive research of all threshold values and neural network requirements.

In this study, we anticipate maize yields using linear regression models and artificial neural networks models [4]. From 1962 to 2004, multiple linear regression models (MLR) and non-linear artificial neural network model (ANN) designs were used in forecasting future maize crop in China's Jilin region, with climate and fertilizer as predictor variables. Production was set to be determined by July-August rainfall, September precipitation, and fertilizer application. Fertilizer is used as a dominant forecaster in the ANN model and was found to be non-linearly related to output. For obtaining the fertilizer data of maize there is a difficulty so the studies used previous years yield tested data. Estimation skill scores derived from cross- validation technique andretroactive validation technique revealed that ANN models perform better than MLR and persistence. Due to the non-stationary nature of the data, in the analysis of forecasting skill, cross-validation method was found to be less reliable than retroactive evaluation. Researchers used two approaches to study crop productivity in relation to environmental variables: mechanistic models and empirical models. For analyzing relationships between crop, soil types,

climatic conditions, and ecology, mechanistic approaches that depend on physiological methods for crop development are best. Because non-linear relationships identified by an ANN model are more difficult to understand than linear relationships identified by MLR, ANN has been dubbed a "black box" technique. As a result, the ANN extrapolates with greater care than a linear function. ANN gives low values compared with MLR solution and hence decides that nonlinear relationship is better. In present research, where interpretation occurred, the ANN model's bounded functional shape gave ANN an added benefit over MLR. Machine Learning Methods for Efficient Forecasting in India [5] Amount of rain, atmospheric pressure, chemical fertilizer, pesticides, ph level, and other climate patterns and parameters all have an impact on crop production. After recognizing the linear relationship among yield and these parameters, reliable yield prediction is needed.

Machine Learning techniques can improve by distinguishing and presenting the consistency and pattern of drive information, machine execution can be improved without the need for characterized computer programming. This survey used a variety of neural network models to assess crop yield on crop yield datasets from multiple areas and crops, including Linear Regression model, Gradient Boosting Regressor model, Random Forest Regressor model, Decision Tree Regressor model, Polynomial Regression model, and Ridge Regression model. Mean absolute error (MAE), mean squared error (MSE), root mean square error (RMSE), R-square, and cross validation are the measures used to compare the accuracy of these strategies. Findings indicate that the Gradient Boosting Regressor has a precision of 87.9 percent with cross validation runs.

Deep Learning techniques in Agriculture [8] is a comparatively recent, cutting-edge image processing technique and data analysis technique with best outcomes and massive results. Deep learning technique has recently made its way into agriculture after being used efficiently in other fields. We assess the sustainable agricultural challenges under consideration, as well as the models and theories employed, information sources, nature, and pre-processing as well as the improved ability achieved based on the criteria used at each work under considering. In addition, we compare deep learning to other popular technologies in terms of classification or regression efficiency differences.

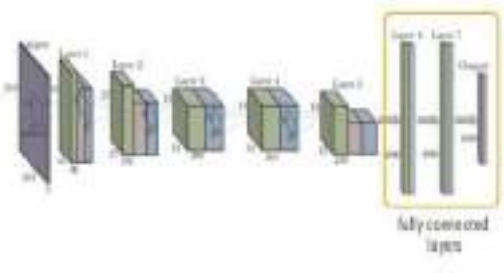

Fig 5. CaffeNet, example CNN architecture

Deep learning outdoes prevailing commonly used image processing method in terms of accuracy, according to our findings. Images make up a sizable portion of the information gathered through remotely sensed data. Images provide a clear understanding of farming in many cases and can be used to address a variety of issues. As an outcome, imaging analysis has become an interesting subject in agriculture, and intelligent data collection methods are used in a wide range of farming applications for image identity verification, outlier detection, and so on. DL extends traditional ML by incorporating more "depth" (complexity) to the model and transforming data from multiple capabilities that allow data representation in a systematic order, through many levels of abstraction.Based on the network architecture, DL may contain a wide range of modules. A basic problem in computer vision, not just deep learning, is that data pre-processing is frequently required and time-consuming, particularly when satellite and images are involved.The high dimensionality and slight number of training samples of hyper spectral data are two issues. Aside from that, existing datasets do not always effectively define the problem. When considering corn returns, for example, it was important to compensate in cultivation data such as fertilization and water management, external influences other than weather data can be considered. Convolutional Neural Networks (CNN) are used to capture similar spatial functioning of different features and combine them to model yield response to nutrient and grain rate management [6]. To define a new dataset for training and test sets the CNN model, nine on-farm corn field studies are used. When compared to multiple regression analysis, the test dataset RMSE is reduced by up to 68 percent, and by up to 29 percent when compared to a random forest. When we look at the harvest data collected within 50 meters of the field's boundaries, we can see that the input variables centered on such cells cover an area with no data.

As shown in below Fig 6 and Fig 7, Fig 8,This survey modeled yield response to nitrogen and seed rate management using five different field features (nitrogen and grain rates, elevation map, soil electro conductivity,

and spatial data). Other risk factors and management techniques that have an effect on global field impacts gain response to site-specific planning. These parameters differ from field to field while changing progressively within the same field.

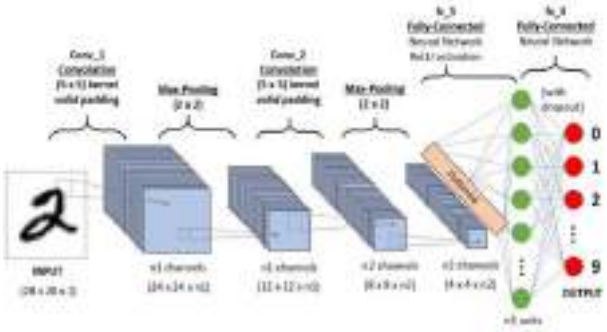

Fig 6. Convolutional Neural Network

Growing plants Date, Hybrid Maturity, and Weather Conditions Influence Corn Yield and Crop Stage [7] In Iowa, USA, we examined wheat crop and phenology data from a multi-location, year, hybrid comparative maturity, and planting date study. Our goals were to find the best combination of sowing date and comparable maturity to maximize corn seed yield per weather, as well as to mitigate the effects of using "full-season hybrids" when harvesting occurs well after the optimum planting date. According to ANOVA, 70% of the variability in seed yield was directly related to planting date and only 10% to associated to maturity, stating that short and full-season hybrid relative maturity periods generated equivalent to seed yield regardless of when they were sown as long as the farms reached maturity prior to harvesting. According to our findings, the time to grain yield is a good predictor of expected higher yield, with a critical stage (after which yield is reduced) of 23 July for Iowa. Furthermore, we discovered that keeping a lower limit growing degree of 648°Cday as during the grain-filling period enhanced maize yield. Conclude, the studied information will help Iowans in making sowing date decisions on the basis on hybrid relative maturity. Throughout most of the growing season (April–October), weather conditions at our sampling locations were relatively inconsistent. The Northeast place had the coolest site-year in 2014, while the Southeast place had the hottest year in 2016. In aspects of rainfall, 62 percent of the site-years were wet, 24 percent became dry, and 14 percent were indeed a mix of the two .

Maize seed yield, silking time, and other considerations, as well as grain-filling duration, are all affected by the planting date. In terms of seed yield and phenology, PD had a bigger influence than RM. Farmers in Iowa will benefit much during the growing season if they plant full-season hybrids all year; nevertheless, the real effect of RM fades over time. Immigrants came to warmer climates with a longer growing season as southern climates warm. A shortened growing season was blamed for the harvest penalty associated with delayed planting. Farmers typically select a mixture relative maturity well in order to progress of planting; however, our research shows that combination RM has a very minor impact on grain yield for any given PD when harvested before planting.

Grain yield estimation and climate making predictions using machine learning techniques for Assessment of the impacts on agriculture [9] Weather has a significant impact on crop productivity A increasing previous research models this transaction in order to estimate the threat of climate change on the industry. A yield modeling approach that makes use of a semi-parametric variant of a deep learning to account for nonlinear dynamic interactions in high-dimensional datasets, as well as known geometrical structure and unfathomable cross-sectional heterogeneity. We show that using corn yield data from the Midwest of the United States, this model outperformed both traditional statistical methods and entirely nonparametric neural networks in predicting yields of years denied during model training. We show that climate change has a major negative impact on corn prices, but it is less intense than the impacts projected using statistical models. Abatzoglou's gridded surface meteorological database (METDATA) is used to generate the meteorological data (2013). Bagging improved both the parameterization and the SNN's precision, but the bagged SNN consistently outperforms. Both OLS regression and the SNN were outpaced by the fully-nonparametric neural net, which was learned in the same way as the SNN but lacked simulation terms.

Incorporating machine learning and crop simulations improves crop yield estimation in the Corn Belt of the United States [10].The goal of this research is to see if merging crop modeling and machine learning (ML) tends to improve grain yield projections in the Corn Belt of the United States. The primary objectives were to identify whether such a hybrid approach would result in better assumptions, which hybrid model mixtures provide much more better estimates, and which crop modeling attributes are most effective when combined with ML for maize crop prediction. The researchers noted that using simulation crop modeling as input features in ML models can lessen yield estimation root mean squared error (RMSE) by 7 to 20%. Furthermore, we investigated the selective complicity of APSIM attributes in ML forecasting and concluded that soil moisture-related APSIM variables have the greatest impact on ML projections, followed by crop-related and weather-related APSIM variables. This finding implies that weather reports alone are inadequate, and that Ml

algorithms require more surface water inputs to produce more accurate yield forecasts.

Estimation of crop prices using supervised machine learning methods [11] and our focus is primarily on agriculture. Farmers are the most important people in agriculture. Farmers face massive losses if the price falls after the cultivation. This paper proposes estimating and planning crop prices for the next 12 months. The information is provided to users via a Flask web page, which is powered by impactful machine learning techniques and innovations and has a user-friendly interface as a whole. The accumulated training datasets contain a wealth of information for forecasting market price and demand. The Decision tree Regressor supervised machine learning algorithm was used in our model. It has been honed on a number of Kharif and Rabi seasons to improve efficiency.

Estimation of Crop Production by Robots [12] Cultivation is an entirely manual endeavour. The use of machine learning methods to implement any type of automation is still in its beginning phases. The focus of this article is to present a contextual approach for introducing machine learning methods into the cropping process. A comparison of machine learning algorithms was performed in order to determine which algorithm is the most accurate in predicting the best crop for a specific plot of land. The research looks at six major food crops in Bangladesh: Aman rice, Aus rice, Boro rice, potato, wheat, and jute. Multiple Linear Regression (MLR) produced the most accurate results during the evaluation and was implemented into an Android application. The android platform system can also generate a timeline of the entire farming process for a specific crop, including when to apply fertilizer. Except for wheat and potatoes, MLR offers greater prediction in this case. KNN yields superior performance for wheat and potato. Mostly as result, the error is 0.40 percent for one and 6.26 percent for the other.

Deep Learning Methods for Yield Estimation [13]. Automatic crop monitoring and yield prediction are now possible thanks to artificial intelligence. The categories were created entirely around five networks: ANN, CNN, DNN, RNN, and combination networks. The feed forward's ANN and DNN were examined, and both offered an average predictive accuracy of 60-70 percent. The large proportion of agricultural processing was carried out using images and timely monitoring. CNN significantly outperformed both DNN and ANN models, with efficiency of 80-85 percent. The only drawback of CNN in this research was that its projections were based purely on training sample rather than real-time past results. A few work was aimed at improving the yield prediction even more and to avoid loss during the yield. The RNN makes use of an LSTM-LSTM combination, which allows for the addition of data storage. When particularly in comparison to the other three systems, it involves the feedback loop that CNN fails, evaluated to the high classification level's average estimation of 83 – 89 percent.

3. Proposed Work

3.1 Dataset Description

For Crop yield prediction we need to select the crop here we selected the crop called Corn and going to forecast the yield based on the dataset and the applied algorithms. Dataset is the first thing we need to select here we collected the dataset from various sources like Syngenta and it mainly consists of the variables like nw, ns, np, nss where the number of weather elements is nw, and the number of soil particles is ns. measured at different depth, np is the planting component and nss is the soil component measured at the surface The six weather components considered are rainfall, radiation from the sun, snow water equivalent, highest temperature, lowest temperature, and air humidity for csv files they are named as Wij where i is the weather component index and consider the six weather components i.e i=1, . . .6 and j= index of week of year for every year there are 52 weeks so j=1,….52. There are 11 Soil components like bulk density(bdod), Caption exchange capacity at Ph7(cec), Coarse fragments(cfvo), clay, Total nitrogen, Organic carbon density(ocd), Organic carbon stock(ocs), ph in H20(phh20), Sand, Silt, Soil organic carbon measured at six different depths(0-5cm, 5-15cm, 15-30cm, 30-60cm, 60-100cm, 100-200cm) with 250 square meter resolution in csv files they can be named as Sij where i is the soil component i.e i=1,-----11 and j is the index of depth j=1,---6. Planting time component is considered as np in csv files they are named as pi where i is the index of the planting date week i=1,---16. The crop performance dataset includes the identified average yield for corn between 1980 and 2019 across 1,176 countries for corn in 13 states including Indiana, Minnesota, Kansas, North Dakota, Missouri, Illinois, Iowa, Nebraska, South Dakota, Ohio, Kentucky, Michigan, and Wisconsin. Organizational data is generally the cumulative percentage of cultivated fields in each state each week starting in April of each year. Grid map approach is followed which means horizontal and vertical lines to identify locations on map.

3.2 System Architecture

The System Architecture of proposed work is like first consider the dataset and preprocesses the data then split into train and test data apply the classification techniques and predict the results. Here for this forecasting purpose Corn dataset is considered from

open source challenge platform like Syngenta [2]. Cleaning, integration, reduction, and transmission are all methods of data preprocessing. We need to get rid of any data that isn't absolutely necessary. The procedure of detecting and analyzing inaccurate or incorrect records from a dataset is known as data cleaning. Real-world data frequently contains noise and missing values, and it may be in an inaccessible format that cannot be actively used for DL models. Data preprocessing is required for cleaning preparation and analysis it for various Deep Learning concepts, which increases performance and reliability. Data that is preprocessed is categorized for training and testing. Training a data means to train the model and testing is for validation process where the unseen predictions are done. The act of segregating available data into two segments, typically for cross-validator purposes, is known as data splitting. One set of data is used to create a forecasting model, while the other is used to evaluate the performance of the model. Data separation into training and test sets is a critical step in assessing data mining models. Training percentage is taken as 80 and test percentage is 20. When a data set is split into a training phase and a validation phase, the majority of information is used for training and only a small amount is used for test results. To train any model, no matter what type of dataset is used, the set of data must be divided into training and testing sets.In the analysis of forecasting skill, cross-validation method was found to be less reliable than retroactive evaluation. Researchers used two approaches to study crop productivity in relation to environmental variables: mechanistic models and empirical models. For analyzing relationships between crop, soil types, climatic conditions, and ecology, mechanistic approaches that depends on physiological methods for crop development are best.

4. Flowchart for Crop Yield Prediction

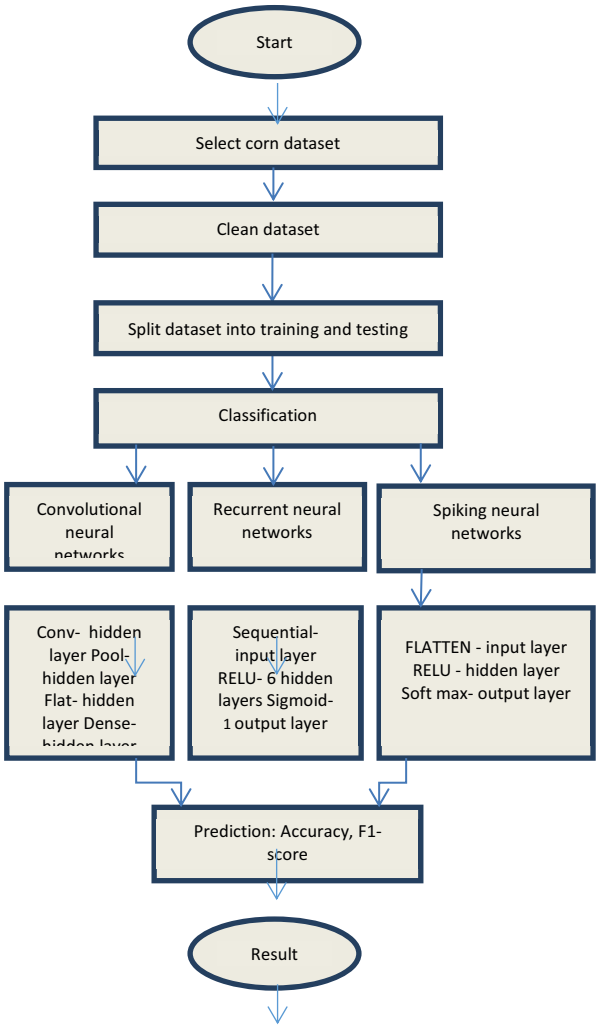

5. Implementation

5.1 Deep learning Methods

Corn yield forecasting is done using Deep Learning (DL) models. Convolutional Neural Networks (CNN), Recurrent Neural Networks (RNN), and Spiking Neural Networks are some of the deep learning models used in this paper (SNN). Neural Networks are composed of three layers: input, hidden and output layer. Input Layer: In this level various types of data is provided to the model. Number of neuron indicates the total number of features in data. Hidden Layer: The output of the Input Layer is fed into the Hidden Layer. Depending on our model and the size of the data, there could be many hidden layers. So every hidden layer may contain a different number of neurons, which is usually greater than the number of characteristics. Each layer's output is calculated by multiplying the previous layer's output by the learnable weights of that layer, followed by addition

of transferable biases and an activation function, making the learning process non linear.

Output Layer: The hidden layer's output is then placed into a logistic function, such as sigmoid or soft max, which converts each class's output into a probability score for each class. Classification is a method of determining which of a set of characteristics a new observation belongs to, based on a learning set of data containing observations with defined category membership.

5.2 Convolution Neural Networks (CNN)

ConvNets also known as CNN'S consists of multiple layers mainly used for image processing and object detection. It has a number of layers that process and extract data features. CNN has a convolution layer with several filters that performs the convolution operation. CNN image categories take an image representation and process it before categorizing it. An input image is perceived by computers as an array of pixels, the size that rely on the quality of image. Depending on the resolution of an image, it will see h x w x d (h = Height, w = Width, d = Dimension). For convolution Neural Networks (CNN'S) we use four hidden layers i.e. convolution layer, Pool layer, flat layer, Dense layer. Conv1D is used and in this the kernel moves only in one direction applicable for Time series data, input and output of Conv1D is two dimensional. Convolution is a mathematical operation performed on two objects to generate an output that expresses how the shape of one is modified by the other. This calculation finds a special functionality in the input data and needs to return a result enclosing that feature's relevant data. This is known as a feature map. The process of merging is known as pooling. So it's primarily for the purpose of reducing data size. Max pooling is considered which takes the highest value within the box. One –dimensional array is considered as a method of converting input data to next layer also treated as flattening. The convolutional layer outcome is flattened to produce a single long feature vector. It is also correlated to the final classification model, forming a fully-connected layer. We attach the final layer to a single line that contains all of the pixel data. Fully connected layer is a dense layer tells that neurons of one layer communicate with next. Adaptive Moment Estimation optimization is a stochastic gradient descent model which is based on adaptive estimation of first-order as well as second-order moments. Adaptive Moment Estimation is a deep neural network training-specific adaptive learning rate considered as optimization algorithm. The technique makes use of the power of adaptive learning rate techniques to identify individual learning rates for each parameter. The average of the squared differences between the observed and predicted values is used to calculate the Mean Squared Error loss. The output is always positive, regardless of the sign of the predicted and actual values, and the value obtained is 0.0.

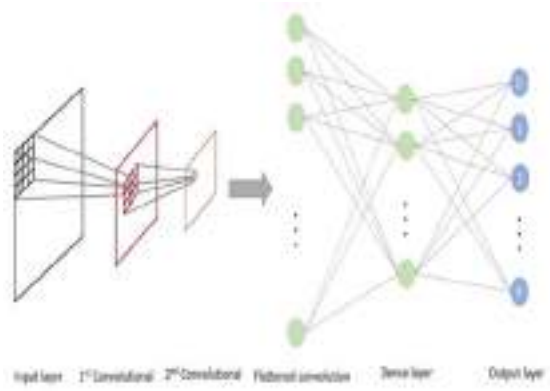

Fig 7. Convolutional Neural Networks

5.3 Recurrent Neural Networks (RNN):

One type of artificial neural network is recurrent neural network that can perform operations on some files like audio files, data files etc. All input and output values are independent in neural networks whereas in RNN, the hidden layers remember the data that was done in a previous layer and give that remembered data to the next layer as input so that it can perform operations on data. This process is repeated until the desired output is obtained. The rectified linear activation function, abbreviated RELU, is a piecewise linear function that retrieves the user input if it is positive and indirectly if it is negative. It has become the default activation function for few types of neural networks and it is easier to train and frequently results in better performance. Activation functions for a Rectified Linear Unit with six hidden layers. In multi-layer networks, the vanishing gradient issue restricts the use of the sigmoid and hyperbolic tangent activation functions. The rectified linear activation function solves the vanishing gradient problem, allowing features to learn more quickly and work better. When building multilayer Perceptron and

convolutional neural network models, the rectified linear activation act as standard activation. Input layer is sequential and output layer is sigmoid.

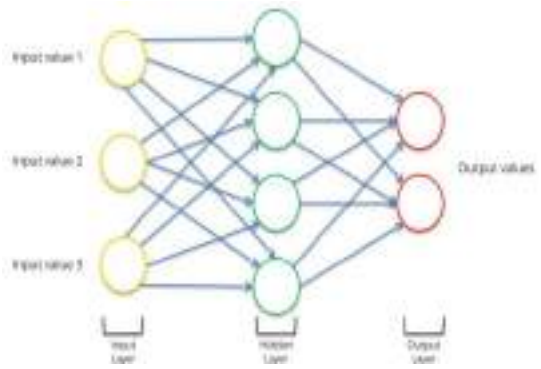

Fig8. Recurrent Neural Networks

5.4 Spiking Neural Networks (SNN):

Spiking neural networks (SNNs) were artificial neural networks that resembled natural neural networks. SNNs incorporate time into their operating model in terms of neuronal and synaptogenesis state. According to the principle, the neurons in the SNN do not need to transmit data during every propagation cycle. Information is only sent when a membrane potential – an inherent property of the neuron associated to its electrical charge on the membrane – reaches a specified value known as the threshold. When the membrane potential reaches a certain threshold, the neuron fires and transmits the signal to other neurons, which modify their potentials in reactions to the signal. The input layer is flattening. Flattening is the process of converting data into a one-dimensional array for input into the next layer. We flatten the layer output to create a unified long feature vector. It is also linked to the last classification model, resulting in a fully connected layer. The ReLU layer is the hidden layer. The rectified linear activation function (ReLU) is a piecewise linear function that, if the input is positive, effectively generates the input; otherwise, it outputs zero. The rectified linear activation function solves the vanishing gradient problem, allowing models to learn more quickly and function better. The output layer, the Softmax layer, broadens this concept into a multi-class work environment. The total of those decimal likelihoods must equal 1.0. The number of neurons in the Softmax layer must be the same as number of neurons in the output layer as shown in below Fig 9.

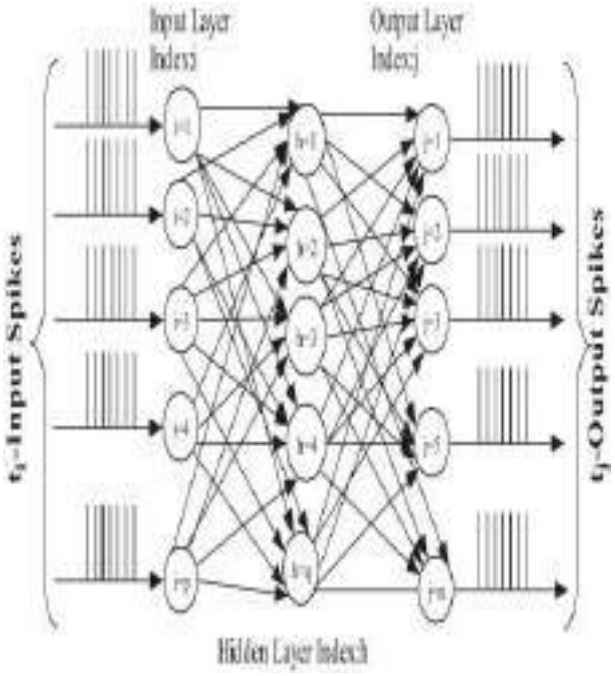

Fig 9. Spiking Neural Networks

6. Results

Tensor flow, an open-source software library, was used to create the three deep neural networks in Python. The training phase for each neural network took about 1.4 hours on a Tesla K20m GPU. For comparative analysis, we used three other well-known forecasting models: Convolutional Neural Network models (CNN), Recurrent Neural Network models (RNN), and Spiking Neural Networks models (SNN). To ensure better comparisons, we wrote all of these modeling techniques in Python and evaluated them in the same software and hardware environments. The overall classification and prediction will be used to generate the Final Result. The effectiveness of the proposed approach is assessed using metrics such as, the ability of a classifier is referred to as its accuracy Class label is predicted correctly and the accuracy tells how good a given predictor can guess the value of attribute for new data.

$$AC= \frac{TP+TN}{TP+TN+FP+FN}$$

$$F\text{-measure}=\frac{2TP}{2TP+FP+FN}$$

6.1 Results for Convolutional Neural Network

Model	Precision		Recall		F1-score		Support		Accuracy
	class 0	class 1	class 0	class 1	class 0	class 1	class 0	class 1	
CNN	1.01	0.01	0.90	0.00	0.97	0.02	300	0	91 %
RNN	1.00	0.00	0.92	0.01	0.95	0.00	300	0	89 %
SNN	1.05	0.03	0.95	0.00	0.95	0.05	300	0	90 %

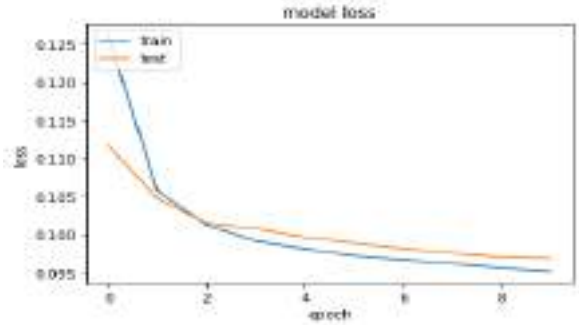

6.2 Results for Spiking Neural Network

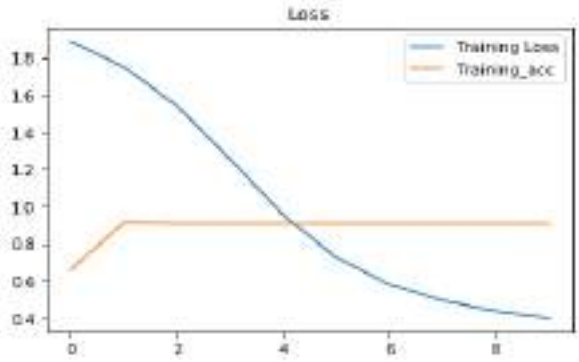

6.3 Results for Recurrent Neural Network

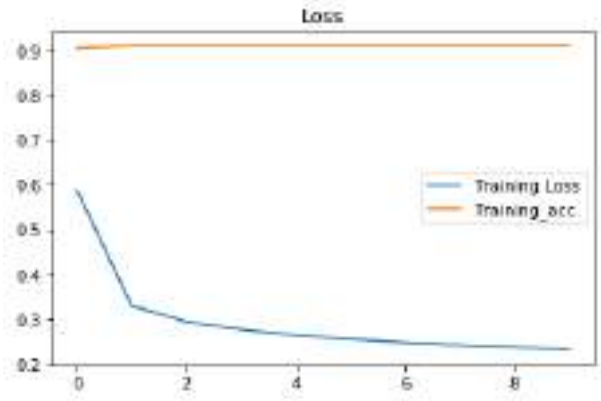

6.4 Result Analysis

The prediction accuracy of crop yield is compared with 3 models and the results are depicted in Table1.

Table 1: Comparing different measures for CNN, RNN, SNN

7. Conclusion

We described a deep learning-based framework for forecasting climate information and management in this study practices that successfully predicted corn yields across the entire Corn Belt in the United States. Most importantly, our approach went beyond estimation by providing major findings that aided in the explanation of yield estimation (variable importance by time period). The method developed are convolutional neural networks (CNN) and Spiking neural networks (SNN). The CNN component of the framework was designed to capture the intrinsic temporal relationship of weather data as well as the spatial interconnections of soil data measured at different depths underground. The model's RNN component was designed to capture the rising trend in crop yield over time as part of ongoing improvements in plant reproduction and management practises. SNNs work with spikes, which are discrete events that happen at specific points in time, instead of continuous values. The occurrence of a spike is determined by nonlinear equations that depict various biological processes, the most significant of which is the membrane potential of a neuron. When a neuron attains

a certain potential, it spikes, and the potential of the neuron is reset. Several variables, including climatic conditions, soil, and management, had a large impact on the model's effectiveness. In unknown environments, the suggested framework accurately predicted yields, and it could thus be used in tasks requiring long-term yield forecasting. One of the most difficult aspects of deep learning techniques is their black box nature. To make the current proposal less of a black box and more concise, feature selection was back propagation method that is used for trained CNN-RNN model. The feature selection model estimated the individual impact of weather components, soil type, and management variables, as well as the time span when these factors get to be significant, and that is a study development. This method could be used to solve other research issues. Similarly, a hybrid could be classified as low-yielding or high-yielding depends on the performance in comparison to other varieties in the same location.

8. References

1. Khaki, Saeed& Wang, Lizhi. (2019). Crop Yield Prediction Using Deep Neural Networks.Frontiers in Plant Science.10. 10.3389/fpls.2019.00621.
2. Syngenta (2021). *Syngenta Crop Challenge In Analytics*. Available online at: https://www.ideaconnection.com/syngenta-crop-challenge/challenge.php/
3. Elizondo, David & McClendon, R.W.. (1994). Neural Network Models for Predicting Flowering and Physiological Maturity of Soybean. Transactions of the American Society of Agricultural Engineers. 37. 981-988. 10.13031/2013.28168.
4. Matsumura, K. &Gaitan, Carlos & Sugimoto, K. & Cannon, Alex & Hsieh, William. (2015). Maize yield forecasting by linear regression and artificial neural networks in Jilin, China.1-12.
5.PayalGulati, Suman Kumar Jha, 2020, Efficient Crop Yield Prediction in India using Machine Learning Techniques, INTERNATIONAL JOURNAL OF ENGINEERING RESEARCH & TECHNOLOGY (IJERT) ENCADEMS – 2020 (Volume 8 – Issue 10),
6. Barbosa, Alexandre&Trevisan, Rodrigo &Hovakimyan, Naira & Martin, Nicolas. (2020). Modeling yield response to crop management using convolutional neural networks.Computers and Electronics in Agriculture. 170. 105197. 10.1016/j.compag.2019.105197.
7. Baum, Mitch &Archontoulis, S. &Licht, Mark. (2018). Planting Date, Hybrid Maturity, and Weather Effects on Maize Yield and Crop Stage.Agronomy Journal.111. 10.2134/agronj2018.04.0297.
8.AndreasKamilaris, Francesc X. Prenafeta-Boldú,Deep learning in agriculture: A survey,Computers and Electronics in Agriculture, https://doi.org/10.1016/j.compag.2018.02.016. (https://www.sciencedirect.com/science/article/pii/S0168169917308803)
9. Khaki, Saeed& Wang, Lizhi&Archontoulis, Sotirios. (2019). A CNN-RNN Framework for Crop Yield Prediction.
10. Shahhosseini, Mohsen & Hu, Guiping& Huber, Isaiah &Archontoulis, Sotirios. (2021). Coupling machine learning and crop modeling improves crop yield prediction in the US Corn Belt. Scientific Reports. 11. 10.1038/s41598-020-80820-1.
11. Mulla, Sadiq&Quadri, S..(2020). Crop-yield and Price Forecasting using Machine Learning.TheInternational journal of analytical and experimental modal analysis. XII. 1731-1737.
12. T. Siddique, D. Barua, Z. Ferdous and A. Chakrabarty, "Automated farming prediction," 2017 Intelligent Systems Conference (IntelliSys), 2017, pp. 757-763, doi: 10.1109/IntelliSys.2017.8324214.
13. Dharani, M &Thamilselvan, R &Natesan, P &Kalaivaani, PCD &Santhoshkumar, S. (2021). Review on Crop Prediction Using Deep Learning Techniques. Journal of Physics: Conference Series. 1767. 012026. 10.1088/1742-6596/1767/1/012026.

A Survey on Cardiovascular Prediction using Variant Machine learning

*L.*Chandrika[1,*], *Dr. K.*Madhavi[2], *B.*Sindhuja[3], *M.*Arshi[4]

[1]PG Student, Computer Science and Engineering, GRIET, Hyderabad, Telangana, India.
[2]Professor, Computer Science and Engineering, GRIET, Hyderabad, Telangana,India.
[3]Assistant Professor, Computer Science and Engineering, GRIET, Hyderabad, Telangana, India.
[4]Assistant Professor, Computer Science and Engineering, GRIET, Hyderabad, Telangana, India.

Abstract. Prediction of a cardiovascular diseases has always a tedious challenge for doctors and medical practitioners. Most of the practitioners and hospital staff offers expensive medication, care and surgeries to treat the cardiovascular patients. At early-stage of prediction of heart-oriented problems will be giving a chance of survival by taking necessary precautions. Over the years there are different types of methodologies were proposed to predict the cardiovascular diseases one of the best methodologies is a Machine learning approach. These years many scientific advancements take place in the Artificial Intelligence, Machine learning, and Deep learning which gives an extra push up to help and implement the path in the field of medical image processing and medical data analysis. By using the enormous dataset from various medical experts used to help the researchers to predict the coronary problems prior to happening. Many researchers have tried and implemented different machine learning algorithms to automate the prediction analysis using the enormous number of datasets. There are numerous algorithms and procedures to predict the cardiovascular diseases and accessible to be specific Classification methods including Artificial Neural Networks (AI), Decision tree (DT), Support vector machine (SVM), Genetic algorithm (GA), Neural network (NN), Naive Bayes (NB) and Clustering algorithms like K-NN. A few examinations have been done for creating expectation models utilizing singular procedures and additionally concatenating at least two strategies. This paper gives a speedy and simple survey and knowledge of approachable prediction models using different researchers work from 2004 to 2019. The examination indicates the precision of individual experiments done by various researchers.

1 Introduction

The heart is a significant organ which plays crucial part of every living being especially in humans. It pumps blood to all parts of our life systems. In case of failing to pumpor doesn't work accurately, the mind and different organs will quit working, and inside couple of moments, the individual will pass on. Changes in way of life, business related pressure, and terrible food propensities add to the expansion in the pace of a few heart-related sicknesses.

Heart sicknesses have arisen as perhaps the most unmistakable reasons for death all around the planet. The expanding populace in heftiness and smoking, the mortality from coronary sicknesses is slowly on the ascent, which has gotten the "best executioner" that compromises human wellbeing contrasted with malignant growth, Helps, and different illnesses, whatever age, character or area. As per WHO Coronary-related issues are responsible for the death of 17.7 million people every year, around 31% of worldwide death mortality.Especially in India, coronary illness became primary cause of mortality. Coronary problems causes the death of 1.7 million in 2016, In 2016 Global Burden of Disease Report, issued on 15th September 2017.

Coronary illness analytics states that the expenditure on hospitalization and treatment is gradually increased compared to the previous years and also diminishesthe survival rate of a person. Evaluations of WHO, explains that in India cardiac patients has spent around $237 billion, in the span of 10 years from 2005-2015. In this way, attainable and precise expectation of coronary related illness is vital.

The health care industry and health care research organisations collects the abundant data of patients,in which DM techniques are not used. The clinical data of the patients have covered up designs that are fundamental for data examination in the location of coronary illness. Coronary illness is a main source of death worldwide for as far back as 15 years. As the heart pumps the blood there is a possibility of on and off condition comes when the blood circulates inside the body which is inadequate, the rest of the organs inside the patient body especially brain and heart stops working, which causes the sudden death in few seconds. The importantelements are distinguished as age, hypertension, diabetes, family ancestry, tobacco, smoking, very high levels of cholesterol, daily routine of alcohol, actual dormancy, stoutness, chest torment, and eating junk food routine[1].

Data gathered by inspecting the verified records of the inpatient.it is feasible to separate the details and

* Corresponding author: lingalachandrika97@gmail.com

Proceedings of the Second International Conference on Electronics and Sustainable Communication Systems (ICESC-2021)
IEEE Xplore Part Number: CFP21V66-ART; ISBN: 978-1-6654-2867-5

SICU Ambience and Patient Health Monitoring System with IOT principles

Santosh Vardhan Reddy Mankena
BTech, Dept. of ECE
Gokaraju Rangaraju Institute of Engineering and technology
Hyderabad,India
svreddy404@gmail.com

V.S.Yashwanth Kumar
BTech, Dept. of ECE
Gokaraju Rangaraju Institute of Engineering and technology
Hyderabad,India
vsyashwanth01@gmail.com

Sai Rithwik Pokala
BTech, Dept. of ECE
Gokaraju Rangaraju Institute of Engineering and technology
Hyderabad,India
sairithwik.p@gmail.com

Veda Varun Upputerla
BTech, Dept. of ECE
Gokaraju Rangaraju Institute of Engineering and technology
Hyderabad,India
vedavarun11@gmail.com

Hima Bindu Valiveti
Professor, Dept. of ECE
Gokaraju Rangaraju Institute of Engineering and technology
Hyderabad,India
valivety.bindu@gmail.com

Chaitanya Duggineni
Dept. of ECE
Gokaraju Rangaraju Institute of Engineering and technology
Hyderabad,India
chaiturohini@gmail.com

Swaraja K
Professor, Dept. of ECE
Gokaraju Rangaraju Institute of Engineering and technology
Hyderabad,India
k.swaraja@gmail.com

Meenakshi K
Professor, Dept. of ECE
Gokaraju Rangaraju Institute of Engineering and technology
Hyderabad,India
mkollati@gmail.com

2021 Second International Conference on Electronics and Sustainable Communication Systems (ICESC) | 978-1-6654-2867-5/21/$31.00 ©2021 IEEE | DOI: 10.1109/ICESC51422.2021.9532926

***Abstract*—Internet of Things (IoT) based Surgical Intensive Care Unit (SICU) Patient Monitoring system has a wide prospective of becoming an essential segment of the forthcoming medical sector. In certain, these models can play vital role for tracking health status of ICU or SICU patient encountering abnormal conditions. Any smart health care patient monitoring device should be free from erroneous data, which may arise due to components failure and communication inaccuracy. In this project we are using Atmega328 microcontroller for additional memory and pins. The heart of the proposed system architecture is Node MCU microcontroller. The Node MCU microcontroller uploads the sensors data into the ThingSpeak cloud along with data and time and monitoring the sensors values on LCD display and also if any abnormality conditions of patient the system gives the audible alerts through Buzzer. This paper deals about the checking of health data like Pulse, Spo2, Body Temperature, ECG and Ambience monitoring such as Room Temperature, Pressure and Altitude and in addition to detect fall we use MEMS sensor.**

Keywords—IoT, Health data, Abnormal, Buzzer, ThingSpeak

I. INTRODUCTION

Health is often been a serious concern and extreme importance in our habitual life wherever human growth is advancing in terms of technology. Like with the advent of novel corona virus that has ruined the economy of world is associate example which shows health care has become a serious importance. In such cases it's always better idea to monitor patient's health remotely. So Internet of Things (IoT) based patient health observance system is current resolution to that. Remote Patient health observance system empowers the observation of patients outside clinic [1][2]. The sensors are coupled to a microcontroller unit which is further interfaced to LCD and additionally if any abnormal changes in heartbeat, Spo2, body temperature are detected, it consequently triggers the buzzer and furthermore indicates health vitals and Room Ambience parameters live in ThingView App. Once the patient health status Increases to critical stage then immediately medical Assistance can be offered to concerned patient to look after his/her well-being. This project particularly plays a serious role where pandemic is unfolded in space wherever doctor reach is partially attainable. The current work is also associated with the cloud-based networking for networked users to easily access the sensors data and further use it for classification purposes [3][4].

II. BACKGROUND

A. Existing System

In present condition in a hospital, either nurse or doctor has to move from one patient to another in order to check their health status which may not be possible to continuously monitor them. Also, when medical emergencies happen there might be a chance of patient being unconscious and unable to trigger Alert. Literature elucidates on Health monitoring systems borne with IoT applications but monitoring fall detection and the ambient atmospheric pressure, temperature as explored minimally. The

Proceedings of the Second International Conference on Smart Electronics and Communication (ICOSEC).
IEEE Xplore Part Number: CFP21V90-ART; ISBN: 978-1-6654-3368-6

2021 2nd International Conference on Smart Electronics and Communication (ICOSEC) | 978-1-6654-3368-6/21/$31.00 ©2021 IEEE | DOI: 10.1109/ICOSEC51865.2021.9591629

Analytical Review on OMA vs. NOMA and Challenges Implementing NOMA

Police Vishwanath Reddy
BTech, Dept. of ECE
Gokaraju Rangaraju Institute of Engineering and technology
Hyderabad,India
policevishwanathreddy@gmail.com

Sudhi Reddy Sreekar Reddy
BTech, Dept. of ECE
Gokaraju Rangaraju Institute of Engineering and technology
Hyderabad,India
sreekarreddy105@gmail.com

Rahul Dilip Sawale
BTech, Dept. of ECE
Gokaraju Rangaraju Institute of Engineering and technology
Hyderabad,India
rahulds@protonmail.com

P Narendar
BTech, Dept. of ECE
Gokaraju Rangaraju Institute of Engineering and technology
Hyderabad,India
pnarendar5777@gmail.com

Chaitanya Duggineni
Professor, Dept. of ECE
Gokaraju Rangaraju Institute of Engineering and technology
Hyderabad,India
chaiturohini @gmail.com

Hima Bindu Valiveti
Professor, Dept. of ECE
Gokaraju Rangaraju Institute of Engineering and technology
Hyderabad,India
valivety.bindu @gmail.com

***Abstract*—The increasing number of devices and high data speed requirements are putting a challenge. To address these problems 5G is implemented. The Orthogonal Multiple Access (OMA) schemes are not sufficient for the implementation of the 5G. One of the promising Multiple Access Technique is Non Orthogonal Multiple Access Technique (NOMA). In NOMA the entire users use the same resource so there will be interference from the others users. In order to transmit data and recover it correctly, this research work utilizes the Successive Interference Cancellation (SIC), which will increase the receiver complexity but has the benefit of high connectivity and spectral efficiency. This paper has analysed different variants in NOMA and presented the most prominent works and compared NOMA with OMA. The challenges for implementing NOMA commercially have also been addressed elaborately.**

Keywords— NOMA, OMA, SIC, Multiple Access Schemes

I. INTRODUCTION

In wireless communication systems Multiple Access schemes play a vital role and are responsible for correct utilization of the spectrum, latency and system throughput. With new generations introduced every decade they come with new requirements. Similarly the next generation that is 5G needs new multiple access scheme for fulfilling the requirements [1].In past, the OMA schemes such as Frequency Division Multiple Access (FDMA), Time Division Multiple Access (TDMA), and Code Division Multiple Access (CDMA) have been used. In OMA Schemes, ideally the interference among the users are nil. The NOMA schemes can be considered as one of the two types, they are Power domain and Code domain NOMA. In power domain each user is assigned a unique power level and all the user use the same frequency, time and code resource. A user who is having the highest channel gain will be assigned the lowest power and similarly the user with the lowest channel gain will be allocated the highest power. Here in NOMA the users will experience interference, so at the receiver end we will use a technique called SIC to recover the user data [2].The code-domain NOMA achieves multiplexing in the code domain.

Currently, NOMA is pursued by standardization bodies, academia and industry. The progression in power efficiency that makes SIC at user equipment possible is the major advantage of NOMA. The need for huge base of connectivity and improved spectral efficiency happen to support the implementation of NOMA. Channel State Information (CSI) at the Base Station (BS) and of the end users is the basic pillars on which the NOMA technique relies on. For commercial deployment of NOMA, there are numerous challenges to be addressed apart from the SIC. The current paper stresses on the comparative analysis of NOMA with OMA technique and addresses the challenges for NOMA to be commercially deployed. Section II discusses the Background of NOMA and its variants and the subsequent section discusses the differences between NOMA and OMA citing the works available in literature. Section IV addresses the challenges of implementing NOMA in various fields and finally concludes the review by culminating all the results available from various researchers.

II. BACKGROUND

A. Power Domain Downlink NOMA [3]

Downlink NOMA consists of a single BS with two users because here we are considering two users NOMA. Downlink is receiving superposition coded signal from BS to the user1 and user2.

Proceedings of the International Conference on Electronics and Renewable Systems (ICEARS 2022)
IEEE Xplore Part Number: CFP22AV8-ART; ISBN: 978-1-6654-8425-1

Image Segmentation using Mask R-CNN for Tumor Detection from Medical Images

T. Padma , Ch Usha Kumari, Dommeti Yamini, Kapilavai Pravallika,

Konduru Bhargavi, Mula Nithya

Department of Electronics and Communication engineering ,

GRIET, Hyderabad, Telangana

2022 International Conference on Electronics and Renewable Systems (ICEARS) | 978-1-6654-8425-1/22/$31.00 ©2022 IEEE | DOI: 10.1109/ICEARS53579.2022.9751891

***Abstract*- One of the dreadful diseases that the world encounters today is brain tumor. When abnormal cells form in the brain, it is called a brain tumor. There are lot of variations in sizes and location of tumor, and hence this makes it really hard for a complete understanding of tumor. Radiologists can easily diagnose the disease with the help of medical image techniques, but making this process automatic is obviously useful. Magnetic Resonance Imaging (MRI) is the most effective method for detecting brain tumors where, MRI images are trained and tested in order to detect the tumor. The automated system would be able to detect and pin-point the exact location of the tumor in an MRI image. In this project, the automated system is built using Mask Regional-based Convolution Neural Network (Mask R-CNN) which segments the abnormal tissues in the brain and mask is applied over the segmented region. Mask R-CNN has the best performance compared to other methods such as R-CNN (Regional-based CNN), Fast R-CNN and Faster R-CNN.**

Keywords: Tumor Detection, Image Segmentation, MRI Images, Mask R-CNN.

I. INTRODUCTION

The brain tumor [1] is an abnormal grouping of cells related to the brain. Malignant (cancerous) or benign (non-cancerous) are types of brain tumors. Malignant brain tumors originate in the brain, grow rapidly and quickly infect the surrounding tissues. It also has the tendency to expand to other parts of the brain and cause dementia and damage the central nervous system [2]. Cancerous tumors (Malignant) can be divided into primary tumors and secondary tumors. Primary brain tumors start in the brain and spread from there, whereas the origination of secondary brain tumors are elsewhere. In contrary, a benign brain tumor is a cluster of cells that develops slowly in the brain. When a tumor grows in the brain, the pressure inside it rises, causing brain damage and death. As a result, early accurate diagnosis of brain tumors can help to improve options for treatment and increase the probability of survival. Medical Imaging Techniques such as MRI, CT scan, Angiography, Skull-Xray, and Biopsy are utilised to diagnosis the brain tumor. The best tool for detecting tumors is Magnetic Resonance Imaging (MRI). However, because a large number of MRI images are generated in medical practise, manual segmentation of tumors is a time consuming, difficult, and burdensome task. As a result, obtaining accurate tumor segmentation from the human brain is a very difficult task. Therefore, an automated system would be able to detect the tumor in an MRI and determine its exact location.

A. Image segmentation

Image segmentation [3] belongs to the branch of image processing which focuses on dividing an image into separate parts usually based on their characteristics and properties. The primary goal of image segmentation is to simplify image such that images can be analyzed easily. Digital image

Estimated Decoder for Polar Codes Based on Belief Propagation

2022 International Conference on Innovative Trends in Information Technology (ICITIIT) | 978-1-6654-0670-3/22/$31.00 ©2022 IEEE | DOI: 10.1109/ICITIIT54346.2022.9744146

Hari Krishna Prasad
Alumnus, Department of Electronics and Communication Engineering
GRIET
Hyderabad, India
hariveraa@gmail.com

Mamatha Samson
Department of Electronics and Communication Engineering
GRIET
Hyderabad, India
mamata2001@gmail.com

Jeneetha Jebanazer
Department of Electronics and Communication Engineering
Panimalar Engineering College
Chennai-123, India
jeneethaseelan@gmail.com

***Abstract*— Polar codes are known for capacity-attaining capability, low encoding, and decoding intricacy. The two well-known approaches for decoding polar codes are Successive Cancellation Decoding (SCD) and Belief Propagation Decoding (BPD). SCD is having latency problems due to serial in type. For soft latency applications, BPD is further desirable due to parallel type. The energy-dissipation and latency enhance in proportion with a number of repetitions. In this paper, we used parallel self-timed adder (PASTA) in approximate belief propagation decoder and implemented using Xilinx tool selecting device XC3S250E of Spartan3E family. In comparison with other types, this decoder achieves a reduction in delay. Simulation outcomes reveal that the proposed belief propagation decoder for polar codes achieved 13.74% improvement in delay.**

Keywords: Polar, decoder, belief, Propagation, adder

I. INTRODUCTION

Considering decoding of polar codes [1], there are different type of methods proposed. SCD [2, 3] and BPD [4 ,5, 6, 7, 8] are the two well-known methods. SCD incurs latency because of serial type of the process, and SCD necessitates less mathematical calculations in comparison with BPD. To minimize the latency of SCD and to attain a high throughput, some methods are proposed. Stack decoding & List decoding established on SCD are proposed to enhance the property of correction of error of polar codes. Polar BPD has superiority of parallel processing. BP decoders are preferred in comparison with SCD due to latency. However, because of their iterative type, the energy dissipation and necessitate latency of BPD will change in proportion with the number of repetitions. B.Yuan and K.K Parhi in Ref. [4] describes an architecture optimization of BPD. They started from MS (minimum sum) algorithm then moved on to SMS (scaled minimum sum) algorithm with latest BPD. In order to bring down

CPD (critical path delay) in SMS (scaled minimum sum) algorithm, efficient critical path reduction method is proposed. Both MS and SMS algorithms are used in this optimized method. Without any change in hardware utilization, there is 0.5dB gain in decoding for this proposed (1024, 512) polar code. 30 % throughput is increased and 80% improvement in hardware efficiency.

Y.Zhang et.al developed BPD where each node is added by extra check node compared to basic BPD. From the new check nodes, propagated messages are changed by multiplying the bits. BP decoder got good performance compared to basic BPD [5]. Reference [6] describes an early stopping criterion for energy efficient low latency BPD for polar codes. Up to 42.5% at 3.5dB change in number of iterations by using two different stopping criteria for (1024, 512) polar code. For selecting stopping methods in different SNR areas, new channel condition estimated scheme was proposed. Chu Hsiang Huang et.al in [7] proposed two implementations of BP algorithms to censor BP and average BP which makes it immune to noise due to computation. Yuanrui Ren et.al proposed a low complexity. A low-complexity LLR-magnitude aided (LMA) early termination scheme was discussed in [8]. They reduced the iteration by 72.6%. They also proposed cyclic redundancy check (CRC) based faster ending method for better performance. Memory efficient BP decoder using stage combined algorithm has been presented by Jin Sha *et al* [9]. Junmei Yang *et al* have revealed the common factors between BP polar decoder and Fast Fourier transform (FFT) based processor and their proposed feed-forward and feed-back pipelined BP polar decoders with processing schedules [10]. Guiping Li *et.al* in [17] applied BP decoding to parity check matrix to improve the performance. Menghui Xu *et al*[12] proposed BPD for applications that need low complexity high fault tolerance and insensitive to processing speed based on stochastic principles. In the paper [13] by Menghui Xu *et al* , approximate BPD is proposed for applications which does not need very accurate results but need less complex hardware and hence less delay.

In our paper approximated BPD is further improved in implementation by optimizing the adder. It results in less delay compared to conventional one.

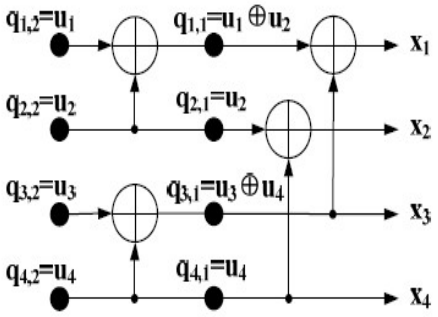

Fig. 1 Encoding of polar codes for n=4

Design and Analysis of Two-Stage Operational Amplifier for Biomedical Applications

Pabba Sowmya, Mamatha Samson, Mohd Javeed Mehdi, and Shaik Afifa Farman

Abstract The key purpose of this paper is to implement an amplifier that retains less power and large gain which is appropriate for precise biomedical applications. The circuit design of a two-stage opamp is executed with the help of LTspice tools employing 180 nm technology files. Numerous analog systems, for example, filters, integrators, data converters like ADCs, and summing circuits are carried out with operational amplifiers as it is the most necessary building block for the above-mentioned circuits. It is essential to design an effective amplifier that enhances the performance of analog circuits. Present work largely focused on executing a two-stage opamp with maximum gain. Further, utilizing this two-stage opamp, an instrumentation amplifier is realized. Several performance parameters, for example, voltage gain, AC gain, slew-rate, average power consumption, and bandwidth are calculated and observed.

Keywords Voltage gain · Bandwidth · Average Power · Slew-rate

1 Introduction

Most of the biomedical signals are with the amplitude ranging between 10 microvolts and 10 millivolts, the amplitude of Electrocardiogram (ECG) signals is nearly 1 millivolt, the amplitude of Electroencephalogram (EEG) signals is nearly 100 microvolts, the amplitude of Electromyogram (EMG) signals is nearly 5 millivolts, including a large amount of common-mode interference and noise signals [1]. Operational amplifiers being the most fundamental building block for most of the biomedical applications for signal acquisition, it is necessary to design an opamp that offers huge gain. Opamp is the short form used to refer to an operational amplifier [2].

P. Sowmya (✉) · M. Samson · M. J. Mehdi · S. A. Farman
GRIET, Hyderabad, India

M. J. Mehdi
e-mail: javeed954@grietcollege.com

S. Rawat et al. (eds.), *Proceedings of First International Conference on Computational Electronics for Wireless Communications*, Lecture Notes in Networks and Systems 329,
https://doi.org/10.1007/978-981-16-6246-1_10

Proceedings of the Third International Conference on Intelligent Communication Technologies and Virtual Mobile Networks (ICICV 2021).
DVD Part Number: CFP21ONG-DVD; 978-0-7381-1182-7

Design of Two Stage Operational Amplifier and Implementation of Flash ADC

Pahba Sowmya
M. Tech Scholar
Electronics & Communication Engg.
GRIET
Hyderabad, India
sowmyagoud217@gmail.com

Mamatha Samson
Professor
Electronics & Communication Engg.
GRIET
Hyderabad, India
mamata2001@gmail.com

Mohd Javeed Mehdi
Assistant Professor
Electronics & Communication Engg.
GRIET
Hyderabad, India
javeed954@grietcollege.com

***Abstract*—In this paper, Flash Analog to digital converter is implemented whose resolution is 3-bits. The designed Flash ADC consists of a resistive ladder network, comparators, the thermometer to a binary encoder and the entire design is carried out using LTspice tools employing 180nm technology. The reference voltage applied to the resistive ladder network is 1.8V. A two-stage operational amplifier is used as a comparator in the flash ADC. Binary code is obtained from the thermometer code by utilizing a priority encoder. The major problem that usually appears in flash ADC is as the number of resolution bits increases, the Area, as well as the power consumption of the circuit, also increases. In this paper, we principally concentrated to lessen the power consumption of the ADC by optimizing encoder circuitry. With the purpose of reducing power consumption, Encoder is implemented using 2:1 mux based on various logics such as switch logic, pass transistor logic as well as CMOS logic. In addition to this, the Wallace tree encoder was also implemented. Performance parameters of Flash ADC such as conversion time as well as average power are calculated and compared. It is verified average power obtained using Wallace tree encoder is 910pW and it is less compared to encoder implemented with other designs.**

Keywords—Average power, Conversion time, Thermometer to binary encoder, comparator.

I. Introduction

Digital signal processing has advanced intensely due to the rapid expansion of science and technology. In the majority of the digital domains, signal processing offers several advantages such as flexibility in design and programmability, reduced silicon area, high accuracy, as well as a smaller amount of power consumption. The design process is cost-effective and faster. Hence it is possible to design a system with a lesser area along with high speed. It is required to have an analog to digital converter that offers much higher speed in wireless communication, image processing, etc[1].

It is preferred to have digital systems that are portable and have prolonged battery life. This can be only possible by developing applications that consume less power. Since ADC's act as front-end components in the majority of mixed-signal systems, we focused to design ADC that consumes less power which in turn offers higher speed. We have various types of ADC architectures for instance successive approximation type ADC, Flash type, sigma-delta, etc. Among these Flash ADC is preferred since it offers high speed because of its parallel architecture, the conversion time is not limited by resolution hence these ADC's are utilized in those systems where bandwidth with a wide range and high speed is required[2].

Al-Ahsan Talukder and Shamim Sarker have implemented flash ADC with 3-bit employing threshold inverter quantization(TIQ). The main feature of this technique is the absence of separate reference voltage power supplies, unlike other Flash ADC implementations. It is possible to set the switching voltage of the inverter by choosing nmos as well as pmos transistors with suitable width to length ratios. This architecture comprises of TIQ comparator, the thermometer to the binary encoder in addition to gain booster. Because of the change in the dimensions of comparator Area changes[3].

Sonu Kumar and Anjali Sharma proposed a strategy employing CMOS technology that is demonstrated for implementing opamp. They preferred CMOS technology for designing an operational amplifier due to the fact that CMOS devices consume low static power and these devices are highly withstanding noise. The two-stage operational amplifier performance parameters are obtained whose gain is 44.98dB, the phase margin is 63 degrees, the gain-bandwidth product is 33.4MHz, power consumption 276μW[4].

Mirza Nemeth Ali Baig and Rakesh Ranjan have implemented high-speed flash ADC for wireless LAN applications. The designed 3-bit flash ADC is implemented using seven operational transconductance based comparators with the reference voltage of 250mV and a high-speed encoder is implemented using full adders. This design is a flash-based ADC converter with a finite output resolution of three bits and power consumption of about 223μW and resides in a chip area of 0.089287 mm2. The high-speed flash ADC is being designed and verified using the CADENCE Virtuoso tool with CMOS 180 nm technology. Since ADC is implemented by utilizing a full adder based encoder, The area is limited by the resolution[5].

Novel IOT Based Health Monitoring and Management System For Rural People

1st Tata Jagannadha Swamy
Electronics and Communication Engineering
Gokaraju Rangaraju Institute of Engineering and Technology
Hyderabad, India
tatajagan@gmail.com

2nd G. Pavan Krishna
Student-PGC-Software Engineering in Data Science
International Institute of Information Technology Hyderabad
Gachibowli, Hyderabad, India
iampavankrishna@gmail.com

3rd Hima Bindu Valiveti
Electronics and Communication Engineering
Gokaraju Rangaraju Institute of Engineering and Technology
Hyderabad, India
valiveti.bindu@gmail.com

4th Lakshmi Chaitanya D
Electronics and Communication Engineering
Pulla Reddy Engineering College
Kurnool, India
chaiturohini@gmail.com

***Abstract*—Internet of Things (IoT) is one of the emerging technologies. In recent years IoT technology spreads into all the areas which are, Agriculture sector, Industrial sector, Defense sector, Pharmacy sector, Science and Technology sector, and Irrigation sector etc. Due to its wide verity of applications, the human life becomes very much simpler than the previous. This IoT consists of many smart devices connected to each other with the help of the internet for communicate to each other for better results. With the help of IoT and other smart devices, online patient monitoring system and diagnosis are the innovative solutions for remote patients. Due to COVID-19 pandemic situations, online doctor, patient interactive system is very much essential. To further investigation of the disease or the health issues, initial test results measurements are safe. Consulting a doctor, diagnosing the disease, and Treatment a patient are very much possible through the proposed IOT Based Health Monitoring and Management System is very much useful for rural people. The proposed system is safe and the measured values are very much nearer to the physical patient test result.**

***Index Terms*—IOT, COVID-19, Patient, Doctor Interaction, Cloud Management, Hospital and Ambulance Services**

I. INTRODUCTION

Health care is the basic need to everyone. The problem associated with healthcare system is there are fewer amounts of medical facilities to monitor the patients condition to provide the treatment. So, it is necessary to optimize the healthcare system to make it more effective. Due to its huge rural population, requires more attention on their health conditions. Due to global and biological issues, they are far away from the minimum health facilities. Due to lack proper health and diagnosis facilities, and their living conditions, some novel systems are required to improve their health conditions as well as, to give proper diagnosis to them in-time[1].

With the help of advanced communication and information technologies, it has led to the Internet of Things (IoT) for various real world applications. Many physical devices capture transmit data, and provides data to various interoperability methods in IoT. The basic functionalities of IoT is for storage, display and communicate the information. Hence the Internet based Health monitoring system with IoT is beneficial for distant patient monitoring on a continual basis and aggregated, and analyzed the sensed data. It can bring about a massive positive transformation in the field of Internet-health system for the rural people.

In the pandemic situations like COVID-19, rural people are very much suffered due to lack of proper medical guidance and facilities. In COVID-19 like situations, tracing, testing, and treating are the three main processes for control the spread of any diseases, but due to less number of available facilities, testing and treating the diseases are much difficult. To give better health advises and treatments to COVID-19 patients, need to provide an IoT based human health monitoring and communicating and provide other facilities to them for better health conditions and it is working mainly based on Tele-Medicine concept for rural people. This type of technology very much useful for storing the data, communicating, and sending messages to nearby hospitals or ambulances through location identification as well as sending a request for treatment are the novel methods in the proposed research. It is very much useful to reduce the delay in diagnosis time as well it increases patient life span in emergency conditions [2].

There are many advantages and disadvantages in Internet of Things like, transferring data through a connected network which saves money and time, access information at anytime from anywhere through an internet. It improves quality of lives also reduces involvement of humans. Similarly it has some disadvantages. If any of the device which is connected to IOT having a malware or bug, then the whole systems gets corrupted, as number of users increases, security decreases and the data could be stolen. Some of the standards and frameworks in IoT as IPv6 over LOWPAN, Zig Bee, CoAP, LORAWAN, AWS, Azure etc.[7], [8], [9], [15]. In IoT technology, Wireless sensors are the key elements. With the help

978-1-6654-8035-2/22/ $31.00 © 2022 IEEE

Associative Memories Based on Spherical Seperability

1st Garimella Ramamurthy
School of Computer Science and Engineering
Mahindra University
Hyderabad, India
rama.murthy@mahindrauniversity.edu.in

2nd Tata Jagannadha Swamy
Electronics and Communication Engineering
Gokaraju Rangaraju Institute of Engineering and Technology
Hyderabad, India
jagan.tata@griet.ac.in

***Abstract*—The concept of spherical seperabilty was innovated by authors.In this research paper, based on the concept of spherical seperability, novel associative memories are proposed. The dynamics of the associative memories is shown to lead to a stable state or a cycle of length atmost 2, starting in an initial condition.**

***Index Terms*—Artificial Neural Networks, Spherical Seperability, Novel Associative memories, Hopfield Neural Networks, Hopfield Associative Memory**

I. INTRODUCTION

In an effort to understand the operation of biological neuron, McCulloch-Pitts proposed a model of biological neuron. This model of neuron was motivated by the concept of "linear separability" of patterns that need to be classified into two or more classes. Since McCulloch-Pitts neuron doesn't have the "training" ability, perceptron model was proposed. Using Perceptron learning law it was established that single "layer" perceptron can classify linearly seperable patterns. In an effort to classify non-linearly seperable patterns, Multi-Layer perceptron (MLP) was conceived and utilized successfully in many applications. Using McCulloch-Pitts neuron model, Hopfield proposed an Artificial Neural Network (ANN) which acts as an associative memory. The author, in his research efforts proposed the concept of "spherical separability of patterns and established that linear separability implies spherical separability but not the other way [1], [2]. Thus, a natural question that remained was whether it is possible to propose an ANN based on spherical separability that acts as an associative memory? This research paper is an effort to answer such a question.

In more clear terms, Artificial Neural Networks(ANNs), such as Single Layer Perceptron(SLP) were proposed based on the concept of linear seperability of patterns [3]. This model of neuron based on McCulloch-Pitts neuron was successfully utilized to arrive at Hopfield Associate Memory(HAM). The authors proposed the concept of "spherical seperabilityy" and reasoned that linear seperability implies spherical spereability (under mild conditions) but not the otherway. ANNs based on spherical seperability were proposed successfully [1],[2]. A natural question that remained was whether an associative memory can be arrived at using the concept of spherical seperability.

Vapnick, in an effort to increase the noise immunity of perceptron proposed the concept of Support Vector Machine (SVM). SVM in a well defined sense (maximization of "MARGIN") leads to the concept of "optimal linear seperability". Various researchers investigated SVM design in higher dimensions by suitably projecting the patterns (that are not linearly seperable) so that they become linearly seperable (using suitable kernel functions) in higher dimensional space. Various interesting theorems related to design of SVM's (such as Mercer's theorem) were proved.

Also, Radial Basis Function Neural Networks(RBFNN's) are proposed in which the activation function at each neuron computes the distance between an input vector and centering vector at the neuron. The centering vectors correspond to centers of clusters of patterns. Other than the pioneering effort by authors on spherical seperability, there is no related research literature. The closest related concept is "clustering".

This paper is organized as follows. In section II, various models of associative memory based on spherical separability are proposed.In section III, simulation results are presented. In section IV, recurrent laered neural networks are discussed. In setion V, we briefly discuss synthesis of associative memories based on spherical seperability. Conclusions are reported in section VI.

II. SPHERICAL SEPERABILITY ⋮ ASSOCIATIVE MEMORY ARCHITECTURES ⋮

We first summarize relevant details related to the concept of spherical seperability of patterns. It was first introduced in [1].

Definition: Patterns belonging to two classes are(in Euclidean space) said to be spherically seperable if and only if there exists a "hypersphere" which seperates the patterns belonging to the two classes.

Note:Patterns belonging to M-classes are "spherically seperable" if and only if any pair of classes are spherically seperable.

Note: The distance metric can be more general than a Euclidean distance (e.g.Hamming distance).

Note: It can easily be proved/reasoned that patterns(which are in a bounded region of Euclidean space) that are linearly

Materials Today: Proceedings xxx (xxxx) xxx

Contents lists available at ScienceDirect

Materials Today: Proceedings

journal homepage: www.elsevier.com/locate/matpr

Real time fruits quality detection with the help of artificial intelligence

Punna Sai Priya, Naga Jyoshna, Sireesha Amaraneni, Jagannadha Swamy

Dept of ECE, GRIET, Hyderabad, India

ARTICLE INFO

Article history:
Received 9 August 2020
Accepted 14 August 2020
Available online xxxx

Keywords:
Internet of things
Object management
Database management
Embedded system technology
Location identification

ABSTRACT

One of the major quality of grading fruits is its appearance. Appearance is effects the marketing and choice of consumer. Colour, texture, size, shape are used to find quality of fruit. But the sellers controlling the external quality of fruits to get high profit. In earlier observations, implemented products, computer vision systems for external controlling quality so grading and classification of fruits is based on observations. The proposed system depend on image processing to classify and grade quality of fruits by using mean of image, colour and HOG (Histogram of gradient) feature extractions are used to classify the fruit quality. All machine learning algorithms are used to find the better accuracy of data how it is predicting. In proposed method first data set is collected, then pre-processing is applied for better results. Machine learning algorithms (K-nearest neighbour (KNN), Support Vector Machine (SVM), and PCA is used for dimension reduction and to get good accuracy to implement the system. For big data pre-processing and to get better results Deep learning (CNN) is used to test the fruit in real time world with result and audio sounds. Audio is used to detect object by hearing also.

Selection and peer-review under responsibility of the scientific committee of the International Conference on Nanotechnology: Ideas, Innovation and Industries.

1. Introduction

India is associate degree agricultural country. International comparisons reveal the common yield in Republic of India is usually 30%-50% of the highest average yield within the world [1]. Agriculture and farming is one amongst the biggest economic sectors and it plays the most important role in economic development of Asian nation. Still in Asian nation, the standard examination of fruits is performed by human consultants. A lot of time is wasted within the fields for checking the standard of the crops. The foremost vital property is fruit size whereas colour resembles property. Hence, classification of fruit is important in evaluating agricultural turn out, meeting quality stands and increasing market price.

It's conjointly useful in designing, packaging, transportation and selling operations. If the classification and grading is completed through manual techniques, the method are going to be too slow and generally it shall be error prone. The labours classify fruits and vegetables supported colour, size, etc. If these quality measures square measures mapped into machine controlled system by victimization suitable programming language then the works are going to be quicker and error free.

In recent years, pc machine vision an image process techniques are found more and more helpful within the fruit The fruit business, particularly for applications in fruit quality examinations and shorting [7]. Analysing the vision may be a general characteristic of our brain. Our brain takes no effort to browse and perceive a symptom, or separate a lion and a felison a or acknowledge individuals by their face. All this can be too straightforward for humans. Wherever as for computers these square measure the particular difficulties to unravel. Thanks to advancement in vision based mostly computing capabilities and as algorithms will understand pictures and videos, systems will be ready currently which perceive what we tend to square meature gazing and what actions we tend toned to perform [2]. Several machine vision algorithms square measure available for agricultural applications too [3–5]. These algorithms area unit used often for speed, economic benefit and correct scrutiny, meature and analysis tasks. For exploit a spread of data from the farms, such as fruit and vegetable detection, estimation of fruit size and weight, fruit and vegetable identification, leaf space and yield estimation, plants, classification and grading. Among the on top of, fruit classification and fruit grading is one of the foremost vital and troublesome task as within the food market the cashiers ought to apprehend the various classes of a fruit element to see its value [6]. So as to scale back the manual work of classification and sorting to enhance the quality of the fruit grading, we are able to use the image process and machine learning algorithms. Form of the fruit, colour and size is

E-mail address: jagan.tata@griet.ac.in (J. Swamy)

https://doi.org/10.1016/j.matpr.2020.08.445
2214-7853/
Selection and peer-review under responsibility of the scientific committee of the International Conference on Nanotechnology: Ideas, Innovation and Industries.

Design of Power Efficient and High-Performance Architecture to Spectrum Sensing Applications Using Cyclostationary Feature Detection

Ms. Kadavergu Aishwarya * PG Scholar (MTECH VLSI)
Department of ECE GRIET, Hyderabad
Email: aishwaryaeng123@gmail.com

Dr. T. Jagannadha Swamy * Professor
Department of ECE GRIET, Hyderabad
Email: jagan.tata@griet.ac.in

Abstract— Cognitive Radio Spectrum Sensing is one of the novel techniques in wireless communications. In this process, wide variety of techniques are available for detecting the spectrum availability to send the secondary signal frequency signals in the absences of the other primary signal frequencies. In this Cognitive Radio spectrum sensing, speed of operation of the network is one of the important factors for efficiently data handling and transmission process. Cyclostationary feature detection is one of the efficient methods for Cognitive Radio spectrum sensing applications. The performance of the Cyclostationary feature detection-based spectrum sensing architecture in cognitive Radio networks can be improved by implementing the advanced multiplication techniques like Vedic multipliers for test statistic computing module deployed in the architecture. To detect the presence the signal over the provided spectrum band, continuous sensing of spectrum is required. This involves numerous multiplications. The proposed model with help of Vedic multipliers reduces the power consumption as well as increases the performance of the architecture and the simulation results are compared with BOOTH multiplier, when it is implemented in test statistic module shows better results. The complete design is implemented in Verilog and tested using Xilinx ISE and Xilinx Vivado tool.

Keywords: Cognitive Radio, Spectrum sensing, Cyclostatioary detection, Test statistic module, Booth Multiplication technique, Vedic multiplier.

I. INTRODUCTION

As the technology is increasing day to day, the need for the advancement in the communication system also increasing gradually. Cognitive Radio is one of the best used technology that enhances the system capacity by allocating the free licensed spectrum bands of primary users to the secondary by using the spectrum sensing technique [2]. Sensing techniques implemented with better performance will help in the speed of operation. There are several spectrum sensing techniques. These detection techniques have their own advantages and disadvantages. Matched filter detection technique involves precise information of the target user and it consumes huge power and has high complex architecture that leads to huge cost. On the other hand, Energy detection is well known for its simplicity and ease of hardware implementation. But it is not supportive to use under low SNR conditions [8].

Main focuses of this paper on the performance of test statistic module deployed in the Cyclostationary based spectrum sensing CR network. Cyclostationary feature detection is a technique for detecting primary user transmissions by exploiting the cyclostationary features of the received signal frequencies. It is best for low SNR calculation. In this sensing process, large number of multiplications are required to perform the test statistics. With the help of CORDIC, BOOTH technique, the filtering operation takes more time. So, it takes more power consumption to perform entire process. In this process, to reduce the power consumption we deployed Vedic multiplier in the design instead of the existing CORDIC and BOOTH. After the simulations and with the obtained results, the proposed Vedic multiplier shows good results and used to improves the speed of operation and also reduces the power handling efficiency and also improves the efficiency of the entire module for spectrum sensing applications.

The rest of the paper is presented as follows. In section II, discussed the system design and the importance of test statistic module in the design. In section III, the advantage of Vedic multiplier over Booth multiplier discussed. In section IV simulation results of Vedic multiplier and comparison results followed by conclusion and future scope in section V.

Proceedings of the Third International Conference on Inventive Research in Computing Applications (ICIRCA-2021)
IEEE Xplore Part Number: CFP21N67-ART; ISBN: 978-0-7381-4627-0

Implementation of Modified Dual-Coupled Linear Congruential Generator in Data Encryption Standard Algorithm

N. Akhila[1], Ch. Usha Kumari[2], K. Swathi[3], T. Padma[4], Padmavathi Kora[5]

[1] *M.Tech Scholar, Dept. of ECE, GRIET, Hyderabad, India*

[2,3,4,5] *Dept. of ECE, GRIET, Hyderabad, India*

akhilarao773@gmail.com, ushakumari.c@gmail.com

2021 Third International Conference on Inventive Research in Computing Applications (ICIRCA) | 978-1-6654-3877-3/21/$31.00 ©2021 IEEE | DOI: 10.1109/ICIRCA51532.2021.9544633

***Abstract*— Data transmission in cryptography is held by encipher and decipher processes. Data Encryption Standard is one of the symmetric key encryption algorithms. Data Encryption Standard (DES) is one of the simplest cryptography algorithms. Modified Dual Coupled LCG (MD-CLCG) is an essential element of Pseudorandom Bit Generator (PRBG) because it requires less area and it is more secured compared to previously executed different algorithmic techniques of linear congruential generator (LCG) family and other pseudorandom bit generators. In cryptographic schemes key generation makes an important role. This paper has implemented a modified dual-CLCG for the key generation with the utilization of shift register in Data Encryption Standard cryptographic technique. Usage of Modified Dual-CLCG in Data Encryption Standard algorithm is designed and coded by the Verilog-HDL language and prototyped on FPGA device Spartan3E XC3S500E.**

Keywords— Pseudo Random Bit Generator (PRBG), modified Dual coupled LCG (MD-CLCG), Data Encryption Standard (DES), symmetric key encryption.

I. INTRODUCTION

Securing data in various IOT applications is becoming more difficult by the day, and internet privacy is getting more sensitive. Transferring large amounts of data across the internet to a million or more components could result in privacy concerns [1] [2]. Pseudorandom bit generator (PRBG) is a critical aspect in IOT dependent systems for security.

The Pseudorandom bit generator is a aspect that manages user privacy in IOT devices because internet security in IOT apps and data privacy in IOT premised devices is both difficult to achieve presently. With limitations such as area, starting clock lag, randomness, and power, the huge bit size of PRBG VLSI design is challenging. The PRBG is said to be random if it passes the National Institute of Standards and Technology (NIST) fifteen benchmark statistical tests.

Pseudorandom bits can be generated using a number of different methods. Linear feedback shift register, linear congruential generator (LCG), Blum blum shub generator (BBS), Coupled linear congruential generator (CLCG) and dual-coupled linear congruential generator are different types of linear congruential generators.

Lenore blum, Manuel blum and Michael shub were created Blum blum shub generator (BBS) in 1986 year as pseudorandom generator. The hardware implementation is used to conduct modulo of the largest prime numbers and to calculate the size of a specific prime number [3]-[6]. The input to first output clock intermission is 2n+5 clock cycles, while the output latency is 2n+5 clocks [7] [8].

The simplest technique is to use a linear feedback shift register (LFSR). The LFSR is made up of simple flip flops and an XOR gate. The LFSR's architecture is straightforward. The LFSR takes up less space and has less hardware complexity. Because of its linearity structure, it fails to pass randomization tests. LFSRs are n-bit counters that produce pseudo-random bits. For n-bit, LFSR can only produce 2n-1 sequences [9].

LCG has a smaller footprint and less hardware complexity. It fails to pass randomization tests due to its linearity structure, as anyone may predict the following sequence after some time.

A coupled linear congruential generator is made up of two LCGs connected in parallel and a comparator [10] [11]. CLCG is safer than a single LCG [11]. CLCG fails the NIST five tests as well as the Discrete Fourier Transform test. The CLCG DFT test, which comprises two inequality comparisons, shows that sequences have a periodic shape [12].

Two connected LCG layouts with two comparators merge with one controller unit and memory to create a dual-coupled LCG (flip flops). Dual-CLCG generates pseudo random bits with clock latency of 2n+5 clocks at first, then only 2 clocks later to generate the data. For n-bit pattern formation, Dual-CLCG requires (2n-1) flip flops. Dual-CLCG fails to reach the NIST statistical randomness requirement and to achieve maximum length of sequence.

Cryptography is an essential component in used in the security of computers. Encipherment algorithms include substitution and transposition the main requirement is no data loss. When the transmitter and recipient share the same private pass code (key), the design is considered as a secret key, single key, or symmetric key/encryption. The mechanism is considered to be two key encryption or asymmetric encipher if the sender and receiver have distinct private keys. A symmetric encipher process is made up of five aspects: plain text, encryption algorithm, secret key, cypher text, and decryption of the data.

An invention of the DES algorithm was a valid interpretation in the early stages of surveillance systems. This

2021 International Conference on Intelligent Technologies (CONIT)
Karnataka, India. June 25-27, 2021

Performance Analysis of Pseudo Random Bit Generator Using Modified Dual-Coupled Linear Congruential Generator

N. Akhila
Dept. of ECE,
GRIET,
Hyderabad, India
akhilarao773@gmail.com

Ch Usha Kumari
Dept. of ECE,
GRIET,
Hyderabad, India
ushakumari.c@gmail.com

K. Swathi
Dept. of ECE,
GRIET,
Hyderabad, India

T. Padma
Dept. of ECE,
GRIET,
Hyderabad, India

N. Madhusudhana Rao
Dept. of ECE,
GRIET,
Hyderabad, India

2021 International Conference on Intelligent Technologies (CONIT) | 978-1-7281-8583-5/21/$31.00 ©2021 IEEE | DOI: 10.1109/CONIT51480.2021.9498354

***Abstract*— Pseudo Random Bit Generator (PRBG) is a key element to protect the data in various cryptography applications during transmission. To prove more secure among different previous pseudo random bit generator methods like Linear Feedback Shift Register (LFSR), Linear Congruential Generator (LCG), coupled LCG (CLCG), and Dual Coupled LCG (dual-CLCG) the modified Dual coupled LCG (MD-CLCG) is implemented. This method used is to generate a pseudo random bit with less area occupation and with single clock delay. In this paper three different ways of adder topologies ripple carry adder (RCA), carry skip adder (CSKA) and carry increment adder (CIA) are implemented in the place of modulo carry save adder to analyze the area, power and speed performance of the modified Dual Coupled LCG design using Verilog-HDL and prototyped on FPGA device Spartan3E XC3S500E.**

Keywords*— Pseudo Random Bit Generator (PRBG), Ripple carry adder (RCA), Carry increment adder (CIA), Carry skip adder (CSKA), modified Dual coupled LCG (MD-CLCG)*

I. INTRODUCTION

Day by day securing the data in various IOT applications is becoming complicate and privacy over the internet is more sensitive. Transferring big data in million number of components connected over internet may lead to privacy issues [1] [2]. Pseudo Random Bit Generator is a key element used in IOT based applications for the security purpose. The main aim of this project is enhance the performance of the PRBG with the Dual Coupled LCG method or for the efficient PRBG.

The Pseudorandom bit generator is a component used in IOT devices to manage user privacy. Because in today's, internet safety is complicated in IOT applications and protecting data in the IOT based devices. The large bit size of PRBG VLSI architecture is difficult with the limitations like area, initial clock latency, randomness and power. If the PRBG fulfils fifteen of the statistical benchmark tests of National Institute of Standard and Technology (NIST) then it is called random.

Pseudorandom bits can be generated using a number of different methods. Linear Feedback Shift Register, Linear Congruential Generator (LCG), Blum Blum Shub (BBS) Generator, Coupled Linear Congruential Generator (CLCG), and dual-coupled LCG are the different types of linear congruential generators.

Linear feedback shift register (LFSR) is easiest methodology. The area and hardware complexity of LFSR is less. It fails to satisfy randomness tests because of its linearity structure. LFSRs are n-bit counters exhibiting pseudo random bits. LFSR can produce only 2n-1 sequences for n-bit linear feedback shift register [3]. Blum Blum Shub (BBS) generator is a pseudo random generator developed in 1986 by Lenore Blum, Manuel Blum and Michael Shub. The hardware implementation is used to perform modulo of largest prime numbers and measures a particular prime number [4]-[7]. The initial clock intermission (input to first output) is 2n+5 clock cycles and output latency is 2n+5 clocks [8] [9]. Coupled linear congruential generator is designed using two LCGs in parallel and combined with a comparator [10] [11]. CLCG is more secure than single LCG [10]. CLCG fails the NIST five tests as well as the Discrete Fourier Transform test. The CLCG DFT test, which comprises two inequality comparisons [12], shows that sequences have a periodic shape. Dual- CLCG generates pseudo random bits with initial clock latency of 2n+5 clocks later on it requires 2 clocks to generate the data. Dual-CLCG requires (2n-1) flip flops for n-bit pattern generation. Dual-CLCG fails to achieve the NIST statistical randomness tests and to achieve maximum length of sequence [12].

In VLSI technology we have so many types of adder topologies. In that adder designs some basic adder topologies like ripple carry adder (RCA), carry skip adder (CSKA), carry increment adders (CIA) are going to be implemented instead of 3-operand modulo carry save adder.

II. EXISTING MODIFIED DUAL-CLCG

The PRBG method is designed to generate an efficient pseudo random bit patterns than the previous methods. The PRBG architecture is designed using dual- coupled LCGs, two n-bit comparators and XOR gate as represented in fig 1. So the block diagram of new PRBG method using LCG is simple compared to existing method [13].

International Conference on Communication, Computing and Electronics Systems pp 779–788

Collective Examinations of Documents on COVID-19 Peril Factors Through NLP

E. Laxmi Lydia, Jose Moses Gummadi, Chinmaya Ranjan Pattanaik, B. Prasad, CH. Usha Kumari & Ravuri Daniel

Conference paper | First Online: 26 March 2021

Part of the Lecture Notes in Electrical Engineering book series (LNEE,volume 733)

Abstract

The outbreak of the novel COVID-19 virus is identified across all experimental scientific tests that assist victims to fight against the pandemic situation. The problem seems to have a large number of scientific COVID-19 articles with different risk factors. The quick identification of documents allows the processing and interpretation of inevitable essential knowledge for investigators. This article provides a solution by creating an unsupervised framework for the

Space Debris Detection Unit for Spacecrafts

Publisher: IEEE

Shoaib Mohammed ; Maddela John Surya Teja ; Padmavathi Kora ; David Ephraim Vun… All Authors

Abstract: In the 21st century, tackling space debris has become one of the biggest challenges in space Technologies. Based on reports from European Space Agency, around 34,000 obje... **View more**

Metadata

Abstract:
In the 21st century, tackling space debris has become one of the biggest challenges in space Technologies. Based on reports from European Space Agency, around 34,000 objects are found bigger than 10cm poses serious threats to existing space infrastructure. The Estimated number of break-ups, explosions, collisions, or anomalous events resulting in fragmentation is more than 560(information updated on 8th Jan 2021). So, the proposed system can detect space debris from the lower earth orbit and transfer the data to the earth space stations so that the collision avoidance protocol can be activated. Alongside it also determines satellite health status which helps in identifying changes in spacecraft like atmospheric pressure and malfunction of sensors also providing relevant information about the outer space.

Published in: 2022 International Conference on Computer Communication and Informatics (ICCCI)

Date of Conference: 25-27 Jan. 2022 **DOI:** 10.1109/ICCCI54379.2022.9740771

Date Added to IEEE *Xplore*: 31 March 2022 **Publisher:** IEEE

ISBN Information:

Melanoma Detection Using Deep Learning

Dr. K. Padmavathi
Professor, Dept. of ECE
GRIET
Hyderabad, Telangana, India

Harish Neelam
Dept. of ECE
GRIET
Hyderabad, Telangana, India

Mora Prathap Kumar Reddy
Dept. of ECE
GRIET
Hyderabad, Telangana, India

Priyanka Yadlapalli
Assistant Professor, Dept. of ECE
GRIET
Hyderabad, Telangana, India

Koushik Sai Veerella
Dept. of ECE
GRIET
Hyderabad, Telangana, India

Karthik Pampari
Dept. of ECE
GRIET
Hyderabad, Telangana, India

2022 International Conference on Computer Communication and Informatics (ICCCI) | 978-1-6654-8035-2/22/$31.00 ©2022 IEEE | DOI: 10.1109/ICCCI54379.2022.9741010

Abstract—**Melanoma is one of the most deadly diseases in the world, and if not detected early enough, it can spread to other regions of the body. As a response, the medical industry has seen a significant advancement , with the introduction of automated diagnosis tools that may assist doctors and even laymen alike in determining the type of ailment they are dealing with. In this case, we're presenting a hybridized method for detecting melanoma skin cancer that could be applied to any worrisome lesion. An automated skin lesion classification approach is proposed in this study. A deep learning network that has been pre-trained and fine-tuned is used. The performance is then compared using various transfer learning methods. The performance is assessed using well-known quantitative criteria such as specificity, sensitivity, precision, and accuracy.**

Keywords-Convolution, Pooling, Deep Learning, Transfer Learning, Melanoma, Dermoscopy, Skin Cancer Classification.

I. INTRODUCTION

Melanoma is a cancer that affects melanocytes, which are the cells that produce the pigment melanin. Although most melanomas begin on the skin, they can also begin in any organ, including the eye, brain, and lymph nodes. If caught early enough, these melanomas can often be removed with minor surgery. Melanoma is more hazardous than other cancers because it has a greater predisposition for spreading to other regions of the body, resulting in significant illness and death. When the number of melanocytic nevi increases, the risk of melanoma rises.

Figure 1a. Data set Classification.

II. LITERATURE SURVEY

Skin cancers are a serious condition that affects people all over the world. Early diagnosis of cancer in dermoscopy pictures boosts the survival percentage substantially. However, precise melanoma detection is difficult due to issues such as low differentiation between lesions and normal skin, visible similarities among cancerous and non-cancerous lesions, and so on. As a result, efficient automatic identification of skin cancers is extremely beneficial to pathologists' accuracy and efficiency.

Yuexiang Li and **Linlin Shen** [2] split their study into three components: First, the abrasion segmentation, Second, abraision dermoscopic feature extraction, and finally, abrasion categorization. To provide the abrasion segmentation and rough classification results at same time, a deep learning network comprising (FCRN), a couple of fully convolutional residual networks is developed.

Sara Hosseinzadeh Kassani and **Peyman Hosseinzadeh Kassani** [3] employed ResNet50 with data augmentation procedures to prevent the detrimental effects of class imbalances, and it outperformed several other models in their investigation.

Region of interest dependant technique for the classifying the dermoscopic pictures of skin abrasions was described by

978-1-6654-8035-2/22/$31.00 ©2022 IEEE

Transfer Learning Using EfficientNet for Brain Tumor Classification from MRI Images

Dr. K. Padmavathi
Professor, Dept. of ECE
GRIET
Hyderabad, Telangana, India

Om Sri Rohith Raj Yadav Thalla
Dept. of ECE
GRIET
Hyderabad, Telangana, India

Sithagari Sujeeth Reddy
Dept. of ECE
GRIET
Hyderabad, Telangana, India

Priyanka Yadlapalli
Assistant Professor, Dept. of ECE
GRIET
Hyderabad, Telangana, India

Thakur Roshan
Dept. of ECE
GRIET
Hyderabad, Telangana, India

Thodupunoori Charan
Dept. of ECE
GRIET
Hyderabad, Telangana, India

2022 International Conference on Computer Communication and Informatics (ICCCI) | 978-1-6654-8035-2/22/$31.00 ©2022 IEEE | DOI: 10.1109/ICCCI54379.2022.9740923

Abstract— ***A benign or malignant brain tumour is a development of cells within the brain or skull that is abnormal. A primary tumour is one that grows directly from the brain's tissue, while a secondary tumour is one that spreads from another part of the body to the brain (metastasis). Depending on the tumor's kind, size, and location, there are a variety of treatment options.. Radiologist use MRI (magnetic resonance images) to classify them. Due to the complexity of brain tumours and their qualities, a manual examination might be error-prone. To aid physicians throughout the globe, we've proposed a solution that uses Deep Learning Algorithms like ConvolutionNeural Networks and TransferLearning (TL). In this paper we have classified MRI into four types (glioma, no tumor, meningioma, pituitary). We have trained our architecture using EfficientNet. From According to our findings, transfer learning works well when the dataset is limited. An accuracy of 99 percent is achieved by the suggested approach.***

Keywords-Convolution, Brain tumor · Transfer learning · EfficientNet · Convolution Neural Network · Magnetic resonance images · Deep Learning.

I. INTRODUCTION

A Brain Tumor is a mass of abnormal cells in the brain that have accumulated. A brain's skull is so hard that any development inside its confines might be problematic. Because of the increased intracranial pressure caused by these tumours, brain damage and even death may result. A new cell replaces the old one when the old one dies of old age or is injured. This procedure may go awry from time to time. When the body doesn't require them, new cells develop, and injured or old cells don't die as they should.. Tumors are masses of tissue that develop as a result of an abnormal accumulation of cells. There are a variety of symptoms associated with brain tumours, depending on where they develop in the brain. Some of the most frequent symptoms are headaches, seizures, eye problems, vomiting, and mental abnormalities.

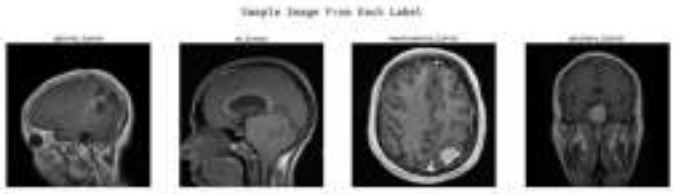

Figure 1. Data set Classification.

II. LITERATURE SURVEY

The brain is the most vital part of a person's body, hence it is critical to identify brain-related ailments at their earliest stages. Disease segmentation has been advocated by a wide range of experts using a variety of mechanical frameworks. Data from MRI brain scans as well as others have been used by several analyzers.

Amit Thakur and **Pawan Kumar Patnaik** [5] suggested employing multiple transfer learning algorithms to classify and identify brain tumours in MRI images. Transfer learning approaches were evaluated and assessed in this study, and VGG16 was shown to be the most accurate.

Transfer learning utilising CNN architecture for brain tumour classification and imaging has been suggested by **Ameur Ikhlef**, **Amina Hameulaine**, and **Sabir Jacquir** [6]. Pre-trained neural networks were used in this research to improve their classification accuracy and training time. A limited number of training samples results in excellent performance, which saves time.

Brain tumour segmentation and classification framework utilising deep learning techniques was developed by **Sunitha M Kulkarni** and **Dr G Sudharani** [7]. Gleoma and meningioma are again suggested as malignant tumours using this approach for detecting and classifying cancers MRI's.

978-1-6654-8035-2/22/$31.00 ©2022 IEEE

Proceedings of the Third International Conference on Inventive Research in Computing Applications (ICIRCA-2021)
IEEE Xplore Part Number: CFP21N67-ART; ISBN: 978-0-7381-4627-0

Automatic Segmentation of Polyps using U-Net from Colonoscopy images

Padmavathi Kora[1]
Professor, Department of ECE
GRIET
Hyderabad, Telangana, India

Boppana Haneesha[2]
B Tech Student, Department of ECE
GRIET
Hyderabad, Telangana, India

Damera Sahith[3]
B Tech Student, Department of ECE
GRIET
Hyderabad,Telangana, India

Sandra Prashanthi Grace[4]
B Tech Student, Department of ECE
GRIET
Hyderabad, Telangana

Benny Jasper K[5]
B Tech Student, Department of ECE,
GRIET
Hyderabad, Telangana

K Swaraja[6]
Professor, Department of ECE,
GRIET
Hyderabad, Telangana

K Meenakshi[7]
Professor, Department of ECE
GRIET
Hyderabad, Telangana

2021 Third International Conference on Inventive Research in Computing Applications (ICIRCA) | 978-1-6654-3877-3/21/$31.00 ©2021 IEEE | DOI: 10.1109/ICIRCA51532.2021.9544573

***Abstract*—Deep learning is a sort of neural network that has more processing layers than regular neural networks and can abstract and predict input at higher levels. It has swiftly established itself as a leading machine learning tool for image and computer vision applications. Deep convolutional neural networks are also quite good in automatically assessing photos, according to current research trends. Using a huge collection of colonoscopy and endoscopy images, this paper presents an effective U-Net architecture based on pretrained deep CNNs. We integrate U-Net architecture with data augmentation and patch extraction from colonoscopy images to detect polyps. The U-Net model is trained and validated to detect polyps in a set of colonoscopic and endoscopic images. The system can achieve overall high polyp detection precision and sensitivity using the suggested U-Net framework and our tuned hyperparameters. After the U-Net model is trained and validated, we evaluated mean Intersection Over Union (IoU) score as 0.9897 and dice loss as 0.0523. With the help of obtained evaluation metrics, the IoU score and dice loss curves are plotted. Furthermore, the proposed U-Net architecture is scalable and adaptable, allowing it to be readily upgraded in the future to include other forms of disease detection and to include more deep learning models to improve its generalising capabilities.**

***Index Terms*—Colorectal cancer,Polyps,CNN, U-Net.**

I. Introduction

Colorectal disease is one of the most common malignant cancer and the second most common reason for deaths due to cancer. [1]. Colorectal cancer screening is beneficial for both early diagnosis and prevention, and it greatly decreases colorectal cancer fatalities [2], [3]. Colorectal cancer usually starts as a polyp, which is essentially an overgrowth from the surface of the colon which undergoes a series of mutations and turns into a malignant condition. Thus, one of the primary goals of colonoscopy is the early detection of polyps, which considerably improves a patient's prognosis. Colonoscopy is a procedure that examines the colon or tailbone. Via the anal cavity, the tube will be inserted. A colonoscopy is an adaptive and visual assessment of the colon and rectum. It assists specialists with recognizing anomalies in the gut, including indications of

2021 2nd International Conference for Emerging Technology (INCET)
Belgaum, India. May 21-23, 2021

Quality Improvement of Retinal Optical Coherence Tomography

A Rajani
Dept. of ECE
JNTUH,
Hyderabad, India
rajani.akula@jntuh.ac.in

Padmavathi Kora
Dept. of ECE
GRIET,
Hyderabad, India
Padma386@gmail.com

K Reddy Madhavi
Dept. of CSE
Sree Vidyanikethan Engineering College,
AP, India
kreddymadhavi@gmail.com

J Avanija
Dept. of CSE
Sree Vidyanikethan Engineering College,
AP, India.
avans75@yahoo.co.in

2021 2nd International Conference for Emerging Technology (INCET) | 978-1-7281-7029-9/20/$31.00 ©2021 IEEE | DOI: 10.1109/INCET51464.2021.9456151

***Abstract*— This paper suggests a new approach for improving the accuracy of retinal OCT frames. This is referred to as the QIROCT (Quality Enhancement of Retinal Optical Coherence Tomography) procedure. Retinal optical coherence tomography *(OCT)* image is a layered structure. A mixture model, combination of multiple distributions, is used to represent retinal OCT image. A Gaussian-Mixture-Model (GMM), mixture of Gaussians, is proposed to represent the retinal OCT image as retina is a layered structure. Expectation maximization (EM) is an algorithm that fits the Gaussian mixture model (GMM). Gaussian components are obtained using the Expectation Maximization (EM) algorithm to match the Gaussian Mixture Model (GMM) to the retinal OCT results. Adaptive Gamma Correction with Weighting Distribution (AGCWD) is used to improve Gaussian components of the retinal OCT image. To understand the superiority of QIROCT method for OCT image processing, 30 healthy retinal OCT images are tested. The QIROCT approach is opposed to the contrast limited adaptive histogram equalization (CLAHE) method, and the difference between the two methods is visually and numerically illustrated. And segmentation is done for retinal OCT image using the QIROCT method and results are shown.**

Keywords*— *Optical Coherence Tomography, Gaussian Mixture Model, Expectation Maximization.

I. INTRODUCTION

Today, advances in data capturing technologies and the availability of datasets of unbelievable scale in research fields have altered our interpretation of certain standard practices in the real world [1]. Information securing is just a part of the procedure and the primary task remains the detachment of valuable data from the wealth of caught information. Mathematical portrayal is into strategy for this circumstance. For instance, demonstrating the results of numerous imaging frameworks can be utilized as an essential centre of numerous image handling undertakings [9], [10].

In this paper, another strategy for Optical Coherence Tomography (OCT) [2], [3] images is presented. Many past studies concentrate on contrast improvement in OCT images since they are frequently uproarious and of low visual contrast level. Contrast improvement considered as an essential part to change visual quality for computer processing.

A Gaussian mixture model (GMM) [7] is a linear mixture of several Gaussian distributions with various parameters such as mean, standard deviation, and weight coefficient that can be used to model any data distribution. The GMM is used to model an OCT image's probability density function [4]. After modelling with GMM, then the mixture components are enhanced with AGCWD.

II. PRODEDURE

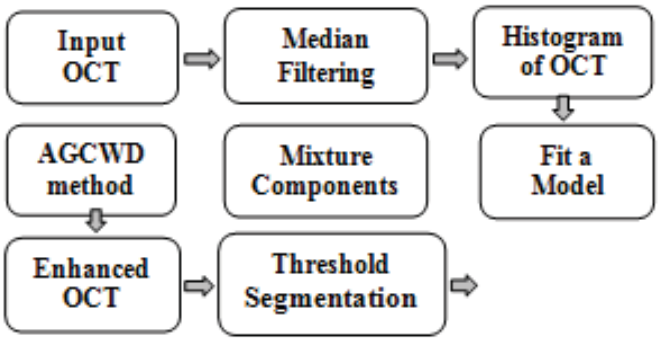

Fig. 1. Block diagram of proposed method

Naturally, QIROCT method comprise of two main parts. The median filter is used to minimize any of the speckle noise seen in OCT objects. First part fits a mixture model to OCT image by updating statistical parameters with Expectation Maximization (EM) algorithm. Second part gets the Gaussian components using statistical parameters and enhances each Gaussian component using AGCWD method. Fig.1 shows the block diagram for the proposed work.

A. Gaussian-Mixture-Model

The aim is to suit a simple model for the OCT intensities x likelihood density function g(x). The retina is thought to be a layered network of many layers of neurons linked by neurotransmitters from retinal existence systems. As a result, the whole retinal OCT study may be equipped with a mixture

Robust and Imperceptible Region Based Watermarking on Medical Images

K. Swaraja, K. Meenakshi, Padmavathi Kora, and G. Karuna

Abstract Telemedicine is the remote delivery of health care services to evaluate, diagnose and treat patients using common technology, such as video conferencing and smart phones, without the need for an in-person visit. There is likelihood in altering the medical images purposely or unintentionally while transmitting over covert channel. The Physician confirms the diagnosis region obtained from the medical image as region of interest (ROI), prior to interpreting any report on evaluation. Watermarking scheme for medical images exploring DCT domain is conferred in this proposal. Fuzzy c algorithm is utilized in segmenting the assessment region (ROI) and non-interest region (RONI), further the watermark is inserted through modulation scheme termed as M-ary. The scheme efficacy is determined for MRI medical images through simulation by computation of quality metrics such as PSNR and NCC.

Keywords Medical image watermarking · Region of interest · Fuzzy c-means · M-ary modulation

1 Introduction

Internet is the most innovative improvement in the existing technology. In our existence, health care is the most significant application of internet to health concern providers as Electronic Patient Record (EPR) is transferred to dissimilar organizations. The watermarking schemes in the telemedicine area [1–3] entail extreme caution while inserting extra data inside the medical images as the added data need not distress the quality of the image. Therefore, to overcome the difficulty of memory exploitation as well as to defend the medical details against illicit handling, watermarking for medical images is employed. Thus in this work, a watermarking system exploiting the M-ary modulation scheme is proposed. The image with medical details

K. Swaraja (✉) · K. Meenakshi · P. Kora
Electronics and Communications Engineering, GRIET, Hyderabad, India

G. Karuna
Computer Science and Engineering, GRIET, Hyderabad, India

A. Kumar et al. (eds.), *ICDSMLA 2020*, Lecture Notes in Electrical Engineering 783,
https://doi.org/10.1007/978-981-16-3690-5_78

A Robust Watermarking Using RDWT and Slant Transform Using Hybrid Firefly and Differential Evolution Optimization Algorithm

K. Meenakshi, K. Swaraja, Padmavathi Kora, and G. Karuna

Abstract In this work, an optimized watermarking framework is proposed with the hybrid combination of two metaheuristic algorithms-firefly optimization and differential evolution, namely HFADE. The cover image is partitioned into 4×4 sub-blocks, and the watermark is concealed in the slant domain using Quantized Index Modulation (QIM). The optimized thresholds obtained with HFADE used in quantization to improve imperceptibility and robustness. Peak Signal to noise ratio(PSNR) and Normalized Cross Correlation (NCC) are used for evaluation of the proposed watermarking scheme. The fitness function for HFADE is taken as the reciprocal of mean square error between the watermarked and cover image. Simulation outcomes convey that the proposed scheme maintains improved imperceptibility, and the watermark extracted from a seriously distorted image.

Keywords Differential evolution · Firefly · Slant transform · Quantization index modulation

1 Introduction

The improvement of Internet and computer input-output devices has made the broadcast and alteration of digital content without difficulty. With the advanced editing technologies, an edited copy appears similar to the original. So, the security of ownership of digital content has become the utmost concern. Digital watermarking [1–16] is evolved to protect the interests of owners from the copyright infringement. The three trade-off parameters of watermarking scheme are transparency, robustness and capacity. Further, it must not suffer from the false positive problems. Optimization algorithms such as Fuzzy logic [17, 18], Genetic Algorithm [19], Differential Evolution (DE) [1] are used to optimize the mutually conflicting parameters of transparency and robustness.

K. Meenakshi (✉) · K. Swaraja · P. Kora · G. Karuna
Department of ECE, GRIET, Hyderabad, India
e-mail: mkollati@gmail.com

A. Kumar et al. (eds.), *ICDSMLA 2020*, Lecture Notes in Electrical Engineering 783,
https://doi.org/10.1007/978-981-16-3690-5_79

2021 2nd Global Conference for Advancement in Technology (GCAT)
Bangalore, India. Oct 1-3, 2021

A Robust blind watermarking with integer wavelets and Hadamard transform using Gray Wolf Optimization algorithm*

*Note: Sub-titles are not captured in Xplore and should not be used

1st K.Meenakshi
(dept. of ECE.)
GRIET
Hyderabad, India
0000-0003-3145-3224

2nd Padmavathi Kora
(dept. of ECE).
GRIET
Hyderabad, India
0000-0002-1145-8442

3rd D.Kishore
(dept. of ECE.)
Aditya College of Engineering and Technology
Surampalem, India
0000-0001-9258-0847

4th K.Swaraja
(dept. of ECE.)
GRIET
Hyderabad, India
0000-0003-2638-2492

2021 2nd Global Conference for Advancement in Technology (GCAT) | 978-1-6654-1836-2/21/$31.00 ©2021 IEEE | DOI: 10.1109/GCAT52182.2021.9587641

***Abstract*—In this work, Gray-Wolf optimization (GWO) is applied to decrease the trade-off between robustness and imperceptibility. Initially, the cover image is applied with integer wavelet transform (IWT) and later the whole image partitioned into 4×4 blocks. After this, the Hadamard transform (HT) is applied for obtaining transform coefficients. The first three pixel intensities in the first rows of each 4×4 block HT coefficients are quantized with the watermark coefficients. These three-pixel intensities are randomized with a vector, and the threshold parameters are obtained from GWO. When these optimized parameters applied, and the GWO algorithm improves the transparency. The results show the proposed algorithm has high imperceptibility and robust to attacks than existing works in literature.**

***Index Terms*—Integer wavelet transforms Hadamard Transform, GWO, SSIM, NCC**

I. Introduction

Digital watermarking technology [1][2] is proposed as a remedy to prevent illegal and malicious copying and distribution of digital media. In the last decade, many multimedia watermarking algorithms have been proposed to protect the copyright of multimedia objects such as digital images, audio, and video clips. However, as the amount of digital multimedia production increases exponentially, the need for better and more advanced techniques for watermarking multimedia digital objects increases as well.

The twin prime requirements of any watermarking scheme are imperceptibility, and robustness[3].The watermarking technique conceals data into a cover image by incorporating invisible changes to the human eye but recoverable by a computer program. Robustness in watermarking scheme determines the amount of amendments to the stego medium can withstand before an adversary can destroy confidential information.

Watermarking can be carried in two domains, such as spatial and transform domain. Spatial domain watermarking [4],[5],[6] incorporate the watermark in the pixel coefficients of the image such as Least significant bits, 3d meshes or histograms. Transform based watermarking scheme incorporate the watermark in coefficients of transform such as Slant [7], DWT [8],[9], RDWT [10],[11],[12], Walsh-Hadamard transform [13],[14],[15], curvelet transform[16] and matrix factorization techniques [17]. If we improve the imperceptibility in the watermarking scheme, the robustness against attacks decreases. Contrary to it, if the robustness against attacks in watermarking improves, the imperceptibility suffer. To bring equilibrium between the imperceptibility and robustness optimization algorithms are used such as genetic algorithm [15], particle swarm optimisation (PSO) [18], Firefly algorithm [4], [19] and fuzzy logic [18],[20], [21],[22]. Ref.[23] developed a watermarking scheme based on DWT and SVD. The authors prevented the false positive problem by inserting watermarking in principle components of SVD. The algorithm is made robust to the geometrical attacks by employing SURF features.The scaling factors are optimized by Artificial Bee colony optimization. Existing literature prove that optimization algorithms can enhance the efficiency of the image watermarking method.

The contribution of the paper is

- The perfectly reconstructable IWT algorithm combines the Hadamard algorithm to obtain highly imperceptible and robust watermarking colour images.
- The optimized parameters for each block is obtained by the GWO algorithm and not taken manually.
- The algorithm is blind and does not require the cover image.

Recently, a novel bio-inspired algorithm inspired by Gray-

2021 Asian Conference on Innovation in Technology (ASIANCON)
Pune, India. Aug 28-29, 2021

A Robust watermarking using RDWT and Schur with Firefly optimization*

*Note: Sub-titles are not captured in Xplore and should not be used

1st K.Meenakshi
(dept. of ECE.)
GRIET
Hyderabad, India
0000-0003-3145-3224

2nd D.Kishore
(dept. of ECE.)
Aditya College of Engineering and Technology
Surampalem, India
0000-0001-9258-0847

3rd Padmavathi Kora
(dept. of ECE).
GRIET
Hyderabad, India
0000-0002-1145-8442

4th K.Swaraja
(dept. of ECE.)
GRIET
Hyderabad, India
0000-0003-2638-2492

5th Hima Bindu Valiveti
(dept. of ECE.)
GRIET
Hyderabad, India
himabindu@griet.in

6th Chaitanya D.L.
(dept. of ECE.)
GRIET
Hyderabad, India
chaitanya@griet.ac.in

2021 Asian Conference on Innovation in Technology (ASIANCON) | 978-1-7281-8402-9/21/$31.00 ©2021 IEEE | DOI: 10.1109/ASIANCON51346.2021.9544852

***Abstract*—In this paper, firefly optimization is applied to balance robustness and imperceptibility in image watermarking. First of all, the original image is partitioned into 4×4 blocks, and later Redundant Discrete Wavelet Transform (RDWT) and Schur applied for obtaining transform coefficients. The highly correlated pixels in the first column are collected from each 4×4 block and are amended by blindly concealing the watermark using quantization index modulation. These quantized values are amended with the randomized matrix and quantization factor randomly selected from the firefly algorithm to obtain the best performance in terms of robustness without compromising the quality of the image. Experimental results show that the proposed scheme maintains improved imperceptibility, and the watermark can still extract from a seriously distorted image.**

***Index Terms*—RDWT, Schur, PSNR, Firefly algorithm, NC**

I. Introduction

The improvement of the Internet, digitization of consumer electronics, and sophisticated image editors has resulted in the broadcast and editing of multimedia contents much more sophisticated than earlier. With this technology, it is possible to reproduce a replica of the original violating copyrights of owners [1], [2]. Therefore, the security of ownership of digital content has become the utmost concern. Digital watermarking proven to be a viable solution to protect the interests of original recipients of multimedia documents. The four essential concerns in watermarking are imperceptibility, robustness, security, and capacity. Robustness refers to the ability to watermark to withstand all possible distortion when watermarked multimedia passed through the insecure channel. Imperceptibility of watermarking scheme requires the watermarked image should be perceptibly similar to the original image. A watermarking scheme is meaningful only when it devoid of a false-positive problem. A satisfactory watermarking scheme should provide rightful ownership. Based on the domain in which the watermark concealed, watermarking techniques are classified into two types: pixel domain and transform domain. The pixel domain techniques are based on the Least significant bit technique [3], difference expansion [4] and histogram shifting [4]. Watermarking in frequency domain transforms the image from pixel to transform domain before concealing the watermark. Transforms such as Discrete Fourier Transform (DFT) [5], [6], Discrete Cosine Transform (DCT) [7]–[9], conjugate symmetric sequence Hadamard transform [10], Walsh Hadamard transform [11]–[13], Wavelet transform [14]–[16], Redundant discrete wavelet transform [17]–[19] and contourlet transform [20]. Applications of soft computing tools such as Fuzzy logic [21]–[23] and optimization algorithms [24] further improve robustness. The robustness is further enhanced by using multiple watermark strength factors rather than a single watermark strength factor [25]. The extraction of the optimal set of watermark strength factors is an NP-complete problem. Snehalatha and Maloo [26] proposed a Digital watermarking employing two transforms, DWT and SVD. Later, the authors utilized the modified whale optimization algorithm (MWOA) to derive multiple strength factors. The authors exploited the good characteristics of MWOA, such as a few parameters and low computational cost [26]. The drawback of the algorithm of the watermarking scheme is suffered from the false positive problem. Prabha and Sam [11] proposed watermarking employing Walsh Hadamard

2022 14th International Conference on COMmunication Systems & NETworkS (COMSNETS) | 978-1-6654-2104-1/22/$31.00 ©2022 IEEE | DOI: 10.1109/COMSNETS53615.2022.9668351

Wavelet based Non-Reconstructive Compressed Spectrum Sensing against Non-Gaussian Noise

Bandaru Bhavana and Samrat L. Sabat
CASEST University of Hyderabad
Hyderabad, India
18phpe03,slssp@uohyd.ac.in

Swetha Namburu
Dept. of ECE
GRIET
Hyderabad, India
swethakarima@gmail.com

Trilochan Panigrahi
Dept. of ECE
National Institute of Technology Goa
India
tpanigrahi@nitgoa.ac.in

***Abstract*—In cognitive radio, spectrum sensing in non Gaussian channel is a challenging task. In addition to non Gaussian noise channel, wideband sensing demands computational complex signal processing algorithm for spectrum sensing. Compressive sensing (CS) has emerged as one of the promising signal processing techniques for spectrum sensing. In CS-based sensing, the sensing is performed on the reconstructed signal that adds extra computational overhead. To mitigate the computational overhead, we present a non-reconstruction-based spectrum sensing technique that uses the energy of the discrete wavelet transform (DWT) coefficients of the compressed measurements in non Gaussian channel, as test statistics. We compare the performance of the proposed algorithm with the conventional energy detection against both non-Gaussian and Gaussian noise. Numerical simulation is carried out using a 5G Universal-Filtered Multi-Carrier (UFMC) signal. The simulation results demonstrate that the DWT-based sensing achieves nearly -8 dB and -8.5 dB SNR-wall against non-Gaussian and Gaussian noise, respectively. In contrast, the compressed DWT achieves -4.5 dB SNR-wall at a much lower computational complexity than conventional techniques.**

***Index Terms*—Compressed sensing (CS), Discrete Wavelet Transform (DWT), Energy detection (ED), Non-Gaussian noise.**

I. Introduction

Cognitive radio (CR) technology offers a promising solution to mitigate the spectrum scarcity problem exploiting the principle of opportunistic spectrum access [1]. In CR, spectrum sensing is an important stage that identifies the spectrum holes/vacant spectrum bands for cognitive radio /secondary users (SU) communication. The primary objective of spectrum sensing is to detect the low signal-to-noise ratio (SNR) signal without interfering with primary users (PU) [2]. Most of the literature analyses the sensing method assuming that the received signal at each SU is corrupted with Gaussian noise. However, the channel may also have non-Gaussian noise in real-time due to the different environmental effects. Hence, the development of a sensing algorithm that can mitigate both Gaussian and non Gaussian noise is of growing interest. The second critical aspect of CR is that each SU is equipped with battery-operated embedded processors that demands a simple and robust spectrum sensing technique.

Wide-band spectrum sensing using conventional Nyquist rate sampling requires computational complex algorithms for sensing. Recently, compressive sensing has been used for spectrum sensing by acquiring the received signal using sub-Nyquist rate [3]. It involves (i) acquisition of compressed samples, (ii) reconstruction of the original signal from compressed measurements, and (iii) spectrum sensing using the reconstructed signal [4]. The faithful reconstruction of the signal depends on the efficiency of the reconstruction algorithm. Thus, most of the literature focuses on the impact of the different reconstruction algorithms on sensing. However, it is not necessary to reconstruct the complete PU signal for spectrum sensing [5] [6]. Therefore, we present a computationally simple spectrum sensing algorithm using a non-reconstruction-based CS technique.

In literature, different spectrum sensing techniques like energy, matched filter, cyclo-stationary are used to decide the presence of a PU signal in the channel [7]. Energy detection (ED) technique is widely used in real-time test-bed [8]. Although it is a computationally simple algorithm, its accuracy i.e., threshold depends on the accuracy of estimated noise power. Any error in the estimation of noise power degrades the sensing performance. Moreover, it works better for Gaussian noise environment. However, the use of Discrete Wavelet Transform can mitigate the effect of impulsive non Gaussian noise to enhance the detection probability. In the proposed work, we evaluate the DWT of the compressed measurements corrupted with non Gaussian and Gaussian noise. Further, we find the energy of the approximate coefficients as the test statistics for spectrum sensing.

The contributions of the current work are

An Efficient Interconnection System for Neural NOC Using Fault Tolerant Routing Method

An Efficient Interconnection System for Neural NOC Using Fault Tolerant Routing Method

Dr.A.Pradeep kumar[1], Y. Devendar Reddy[2], Dr.T.Srinivas Reddy[3], K. Jamal[4]
[1]Professor, Mallareddy Engineering College (A), Hyderabad, Telangana, India
[2]Associate Professor, Nalla Narasimha Reddy Education Society's Group of Institutions, Hyderabad, Telangana, India
[3]Professor, Mallareddy Engineering College (A), Hyderabad, Telangana, India
[4]Assistant Professor, GRIET(A), Hyderabad, Telangana, India
Email: pradeepkumar@mrec.ac.in

Abstract. Large scale Neural Network (NN) accelerators typically have multiple processing nodes that can be implemented as a multi-core chip, and can be organized on a network of chips (noise) corresponding to neurons with heavy traffic. Portions of several NoC-based NN chip-to-chip interconnect networks are linked to further enhance overall nerve amplification capacity. Large volumes of multicast on-chip or cross-chip can further complicate the construction of a cross-link network and create a NN barrier of device capacity and resources. In this paper, this refer to inter-chip and inter-chip communication strategies known as neuron connection for NN accelerators. Interconnect for powerful fault-tolerant routing system neural NoC is implemented in this paper. This recommends crossbar arbitration placement, virtual interrupts, and path-based parallelization strategies in terms of intra-chip communications for the virtual channel routing resulting in higher NoC output at lower hardware costs. A lightweight NoC compatible chip-to-chip interconnection scheme is proposed regarding to inter-chip communication for multicast-based data traffic to enable efficient interconnection for NoC-based NN chips. Moreover, the proposed methods will be tested with four Field Programmable Gate Arrays (FPGAs) on four hard-wired deep neural network (DNN) chips. From the experimental results it can be illustrate that a high throguput can obtained effectively by the proposed interconnection network in handling thedata traffic and low DNN through advanced links.
Keywords: Network-On-chip (NoC), Deep Neural Network (DNN), Interconnection Architecture, Chip-to-chip interconnection, Hardware Accelerator,

1. Introduction

Technology can combine more and more logic circuits into a single chip. Therefore, the chips characters became more powerful. Processing units are integrated within a sigle chip which work with different clock frequencies [1] [2]. Traditionally, processing units have to interconnect the various sections of the SoC using bus structures.However, bus system on chip (SoC)s are key connectivity schemes because their scalability is too low [1]. Network on a chip has been suggested as a possible candidate for reduced scalability and poor connectivity efficiency issues presented in the previous SoC. Network connectivity is used by the NoC as a subtitut of bus systems to provide Globally Asynchronous and Locally Synchronous data transfer (GALS); that ensures that NoCs have increased the reliability of network connectivity and power usage by on-chip logic and device complexity [2].

The continuous increase in the size and complexity of the NoC interconnect infrastructure presents major challenges to the time-tested initiative of the architecture [3]. Chips up to 100 cores today rely on a wide range of NoC connectivity. In addition, active interconnecting architectures are being implemented to provide better efficiency and power utilization. This increasing maturity is obvious when one explores the growing concerts of features integrated into the router architecture, including complex arbitration processes, speculation as well as adaptive routing [4].

Proceedings of the Second International Conference on Electronics and Sustainable Communication Systems (ICESC-2021)
IEEE Xplore Part Number: CFP21V66-ART; ISBN: 978-1-6654-2867-5

Implementation of Cyclic Redundancy Check in Data Recovery

Nandivada Sridevi
ECE
GRIET
Hyderabad, India
nsridevi2222@gmail.com

K. Jamal
ECE
GRIET
Hyderabad, India
Kjamal24@gmail.com

Kiran Mannem
ECE
GRIET
Hyderabad, India
Kiranmannem14@gmail.com

2021 Second International Conference on Electronics and Sustainable Communication Systems (ICESC) | 978-1-6654-2867-5/21/$31.00 ©2021 IEEE | DOI: 10.1109/ICESC51422.2021.9532802

Abstract—**Cyclic Redundancy Check (CRC) technique can be widely used in data communication and storage devices in order to detect the sudden errors present in the data. The main motivation of this research was to detect the sudden, random or burst errors present in the transmission channels. This technique was very simple and easy to implement. It can be useful for the burst error detection and also to find the sequences of incorrect data present in the message signals. This technique was also good at detection of errors which were caused by the noise present in the transmission channels. The Conventional CRC Encoder and Decoder for 3 bits (101) and 4 bits (1100) was presented here.The proposed CRC Encoder and CRC Decoder were performed by using the binary division process and xor gate. Here, the generator or CRC polynomial or divisor was taken as $x^8 + x^2 + x^1 + 1$. It can be written as 100000111 which can be referred to 9 bits of polynomial. This polynomial was kept as constant in the whole binary division process for all random data bits. The novelty of this proposed work was the implementation of both CRC Encoder and CRC Decoder for input random bits such as 5 bits (10101), 8 bits (11000011) and 10 bits (1100110011). The CRC Encoder, Decoder and Test Bench for all these random data bits were simulated, compared and verified by using Verilog coding in Xilinx ISE 14.7 tool. This proposed CRC technique was implemented in Data Recovery application. This technique can be extended to various increased data bit sizes and different generator polynomial expressions as a future scope of this research. In this work, the simulation results were limited up to 5,8 and 10 random data bits.**

Keywords— **Cyclic Redundancy Check (CRC) , CRC Encoder, CRC Decoder, Burst or random errors, Xilinx ISE, Verilog coding, Data Recovery, CRC or generator polynomial, binary division, xor gate, RTL Schematic.**

I. INTRODUCTION

As there is a very high demand for increased functionality, low power, transistor width, length values and supply voltages, CMOS technology is scaling down. So, this led to a huge scope for memory applications. The demand for the functionality of a chip has caused an increase in the memory applications.

The main motivation of this research is to detect sudden, random or burst errors present in the transmission channels and also this technique is very simple, easy to implement.

The main objective of this research work is the implementation of Cyclic Redundancy Check (CRC) technique for random bits that is 5 bits (10101), 8 bits (11000011) and 10 bits (1100110011) and its application in Data Recovery by using Verilog coding in Xilinx ISE 14.7 tool.

The novelty of this work is the implementation of CRC technique that is CRC Encoder and CRC Decoder for random input data bits that is 5 bits (10101), 8 bits (11000011) and 10 bits (1100110011). The proposed CRC Encoder, Decoder and Test Bench for all these random data bits are simulated, compared and verified using Verilog coding in Xilinx ISE 14.7 tool. This is also implemented in the Data Recovery Application.

II. LITERATURE REVIEW

The CRC technique based on shift registers was proposed in [1] for parallel operation which can be used for high-speed applications. The parallel pipelining technique was used in [2] for the implementation of proposed CRC Encoder and Decoder systems in order to achieve higher throughput with less area. In [3] a unique architecture for CRC computation was proposed which can be used in high speed data communication. The CRC 32 method based on look up tables and slicing algorithm was explained in [4] which had lesser power and area. An efficient CRC-Eight Encoder and Decoder circuits were proposed and implemented in [5]. In [6] the state space transformation technique was proposed in order to reduce the circuit complexity. The errors present in the code word were detected in [7] by using CRC technique. By using simulation framework, several case studies were simulated in [8] in order to find the false positives present in the communication networks. In [9] the signal processing algorithms like pipelining and unfolding were used for the controller unit in both CRC encoder and decoder sections so that high-speed parallel circuitry can be obtained. The proposed scheme in [10] has improved area and decreased XOR stage when compared with the existing one. In [11] a novel algorithm was suggested in order to combine three CRC circuits into single unit so that the total area will be minimised in the system. In [12] CRC technique was used in data communication and storage devices for the detection of sudden changes present in the raw data. The CRC encoding and decoding processes was proposed in [13]. The application of CRC in radio frequency identification protocol was analysed in [14]. Few transforms in CRC such as multiplication, shift and complement were studied in [15].

M. M. Arifin, M. T. Hasan, M. T. Islam, M. A. Hasan and H. S. Mondal presented a technique called CRC which was used for the detection of errors present in the digital data. The CRC technique was simple to execute and it was fully performance oriented in identifying the deviations present in the channel. The implementation of CRC depends

Approximate Multiplier Architectures for Error Resilient Applications

Uppugunduru Anil Kumar[1]
EEE Department
BITS Pilani Hyderabad Campus
Hyderabad, India
p20170014@hyderabad.bits-pilani.ac.in

Ratna Kumari Chintakunta[2]
EEE Department
BITS Pilani Hyderabad Campus
Hyderabad, India

Sandeep Kumar[3]
EEE Department
BITS Pilani Hyderabad Campus
Hyderabad, India

K Jamal[4]
Department of ECE
GRIET
Hyderabad, India

Syed Ershad Ahmed[5]
EEE Department
BITS Pilani Hyderabad Campus
Hyderabad, India

2021 IEEE International Symposium on Smart Electronic Systems (iSES) | 978-1-7281-8753-2/21/$31.00 ©2021 IEEE | DOI: 10.1109/iSES52644.2021.00031

***Abstract*—Approximate computing is an emerging paradigm to achieve substantial improvement in the area, speed, and power in image processing applications where exact computation is not required. This paper proposes new approximate unsigned multiplier architectures which aim to reduce the power consumption and area with better accuracy. For the 8-bit multiplier scheme, experimental results show an improvement of 41.4% and 34.02% in power and area respectively, when the proposed design is compared against the exact design, and 22.88% and 26.72% respectively when compared against other approximate designs, without compromising on the accuracy.**

***Index Terms*—Approximate computing, approximate multiplier, partial product reduction, compressor.**

I. Introduction

Image and video processing applications requires huge power and has high latency to process the input image and video sequences [1]. Approximate computing is one of the emerging areas which is gaining a huge popularity because of its ability to reduce the area and power in digital systems [2]. The motivation behind approximate computing is that most of the image processing applications can tolerate error up to a specific limit.

Multiplication is the major power hungry module in the most of the image and video processing applications[3]-[6]. Multiplier is generally implemented in three steps (i) partial product generation (PPG), (ii) partial product reduction (PPR), and (iii) final accumulation. Since image and video processing applications are inherently error resilient, various approximate multipliers are proposed [9]- [14] to get the hardware savings.

In this paper, a new unsigned approximate multiplier is proposed to reduce the circuit complexity. The highlights of this work can be summarized as follows:

- A new PPR structure with an intent to reduce the computational complexity in approximate multiplier.
- Exhaustive hardware and error analysis has been carried out on the proposed and existing designs.
- The proposed and existing designs are implemented on image processing applications to validate the quality-effort trade-off.

II. Related Work

Generally, in multipliers approximation carried in partial product generation or partial products reduction stage. Various design have been proposed in the literature. Saeed et al. [7] implemented the higher order multipliers using two 4*4 sub multipliers. These sub multipliers are implemented using AND-OR encoding of partial products and used probability-based approximate 4-2 compressors for accumulation. Haroon et al. [8] proposed a recursive multiplier using 4*4 building blocks. High-performance approximate half and full adder cells are proposed for use in a 4×4 multiplier, which in turn are used for designing larger multipliers.

Partial product reduction is generally accomplished using a tree of compressors and approximating them result in hardware saving without significant loss in accuracy. Authors in [9] presented two approximate 4:2 compressors to reduce area consumption and power dissipation; but, they suffer from accuracy. Work in [10] implemented three approximate compressors for designing three different multiplier architectures; however, they have higher power dissipation. Minho [11] improved one of the Yang's compressor and incorporated an error correction circuit in the partial product reduction structure to improve accuracy without a significant increase in hardware. However, the improvement achieved by Minho is not substantial. Two different types of multiplier designs using approximate arithmetic modules were proposed by Venkatachalam [12], with an intend to improve speed and power consumption, but these designs suffer from low accuracy. Another variant of compressor-based multiplier of high accuracy was proposed by Xilin [13]. To improve hardware metrics such as area and power. Haoran et al. in [14] presented four different multiplier designs using three approximate compressors along with an error-correcting module but they suffer from delay.

III. Proposed Work

In this work, we proposed two new approximate multiplier using a novel approach that aimed to minimize error rate,

978-1-7281-8753-2/21/$31.00 ©2021 IEEE
DOI 10.1109/iSES52644.2021.00031

An Automated Rescue and Service System with Route Deviation using IoT and Blockchain Technologies

Sudhakar Yadav N
Department of Information Technology
VNR Vignana Jyothi Institute of Engineeing and Technology
Hyderabad, India
sudhakaryadav.mtech@gmail.com

Ravikanth Motupalli
Department of Computer Science and Engineering
VNR Vignana Jyothi Institute of Engineeing and Technology
Hyderabad, India.
ravikanth_m@vnrvjiet.in

K Jamal
ECE Department
GRIET
Hyderabad, India.
kjamal24@gmail.com

Chalumuru Suresh
Department of Computer Science and Engineering
VNR Vignana Jyothi Institute of Engineeing and Technology
Hyderabad, India.
suresh_ch@vnrvjiet.in

2021 IEEE Mysore Sub Section International Conference (MysuruCon) | 978-1-6654-3888-9/21/$31.00 ©2021 IEEE | DOI: 10.1109/MYSURUCON52639.2021.9641574

***Abstract*— The increasing population across the world globally increases the number of vehicles at an enormous rate. Detecting mechanical failures are one of the major issues to be resolved in the smart transportation. In addition to this, assisting the travel direction to save fuel and congestion is more important in improving the smart transportation to the next level. As the advanced technologies are shaping the modern world in an efficient and effective way. IoT and Block chain plays a vital role in offering the solution for smart transportation and automobile sector. The goal of this paper is to propose a smart automated automotive rescue and service giving system for highways using IoT and Block chain. This system also comprises of intelligent vehicle deviation module to assist in reducing traffic delays and thereby saving time and fuel consumption. As an extension of this paper, it intends to extend the work and demonstrate suitable results with an appropriate case study.**

Keywords—Automated rescue, IoT, Block chain, smart transportation, vehicle deviation, traffic delays, re-routing, data analytics.

I. INTRODUCTION

Internet of Things (IoT) has paved its path in connecting and communicating people with sensors and devices. This not only connects devices, moreover IoT assists in connecting smart buildings, smart infrastructure, smart cars, smart cities, etc. IoT has the capability to interconnect devices with any of the smart systems, which can also collect and organize the data with the hand of big data analytics. IoT and data analytics can integrated to develop an energy efficient framework for the smart transportation and automobile industry. On the other hand, block chain is growing tremendously at an extensible rate. It's a kind of distributed database which has the capability of holding the digital files with encrypted transactions in the forms of blocks, those are scattered across a peer network of machines. Block chain has shown its remarkable feature in holding the transactions in a transparent and organized manner, where decentralization or no third party shall be involved. Block chain was first created as a distributed ledger for the Bitcoin system in order to overcome the cryptocurrency's double-spending challenge [2,13 and 20]. The integration of IoT and Block chain results in a secured and trusted connection, this is most important in automobile and smart transportation [3]. The building blocks of IoT are shown in Fig.1.

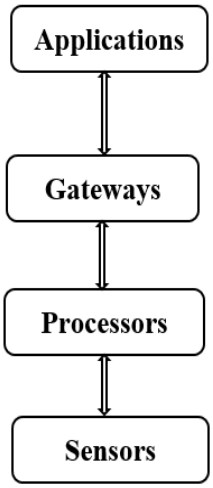

Fig. 1. Building Blocks of IoT

II. RELATED WORK

The current period is extremely fast-paced, necessitating the use of quick equipment and machinery to keep up. Automobile is one the main machine for travelling, luggage transfer and constructions. These heavy fuel based machines are now one of the most seen things on the earth. People are using them every day for saving the time and money but unfortunately these machine can do the opposite work for which they are made. If there are any problem with the vehicle it can stuck you in anywhere middle of the road/highway and that will be more time consuming as well as more expensive too for getting the help. As the working areas are expending day by day the use of automobiles are

978-0-7381-4662-1/21/$31.00 ©2021 IEEE

Proceedings of the Second International Conference on Smart Electronics and Communication (ICOSEC).
IEEE Xplore Part Number: CFP21V90-ART; ISBN: 978-1-6654-3368-6

A Low Power Binary CAM using 7T SRAM cell with increased substrate bias

Surekha G
ECE Department
Gokaraju Rangaraju Institute of Engineering and Technology
Hyderabad, India
yandamurisurekha@gmail.com

Dr. Balaji N
ECE Department
Jawaharlal Nehru Technological University, Kakinada
Kakinada, India
prof.balaji.ece.@gmail.com

Dr. Padma Sai Y
ECE Department
VNR Vignan Jyothi Institute of Engineering and Technology
Hyderabad, India
ypadmasai@gmail.com

2021 2nd International Conference on Smart Electronics and Communication (ICOSEC) | 978-1-6654-3368-6/21/$31.00 ©2021 IEEE | DOI: 10.1109/ICOSEC51865.2021.9591858

Abstract— **Leakage power reduction is an important metric to consider as technology progresses. A Binary CAM is introduced in this paper, which reduces leakage power caused by an increase in substrate bias in a transistor. This proposed design was tested in the virtuoso simulator using 45nm, 90nm, and 180nm tools. Investigation of the results show that the Binary CAM is reducing the dynamic power by 29.11%, 38.64%, 56.9% for matched condition and 34.78%, 41.51%, 75.48% for mis-matched condition in 45nm, 90nm and 180nm tools respectively. All these outcomes are compared with conventional Binary CAM and Binary CAM [25].**

Keywords— **Substrate Bias Voltage, SRAM, CAM, Dynamic Power, Leakage power.**

INTRODUCTION

A Memory is used in all electronic systems to store data. Memories types are Read Only Memory (ROM), Random Access Memory (RAM) and Content Addressable memory (CAM). Each word stored in the memory is compared with searched input data using Content Addressable memory (CAM), and it returns the address location of matching data. CAM gives a quick data search in only one clock cycle by comparing the search data with all of the stored data. CAM is a very elegant solution for more applications requiring fast searching functions, like network routers, look-up tables, and compression of data [1]. CAMs can execute a parallel search operation across several data systems. This parallel multiple data search makes CAM as a necessary component for high-associability caches, translation look-aside buffers [2], and register-renaming [3]. Lookup tables are also the main part of IP router tables and therefore CAMs are the key component of many router chips [4] [5]. Conventional CAM architecture is shown in Fig.1, consists memory cells, register for search, match circuit for checking the data, and an encoder for address. The CAM is designed using NAND and NOR CAMs. Types of CAM's are Binary CAM and Ternary CAM. The BCAM stores "0" or "1" ,and multiple searches are done by TCAM cell because it stores only "0," "1," or "X" [6].

Search data is stored in Match line and this data is compared with the stored data in CAM. A large amount of the power dissipated in CAM is produced by the Search Lines and Match Lines. In order to decrease the power spending of the CAMs, a variety of circuit techniques have been proposed. Less power dissipates in MLs for NAND CAM but it is less speedy [7]. More power dissipates in MLs for NOR CAM but it is fast, since all MLs are discharged through parallel transistors [8]. Power consumption is reduced by the NOR CAMs [9]– [20] and the searching speed improved by NAND CAMs [21]– [24]. Several techniques are proposed to reduce power consumption in the Matched Lines [8]– [24]. Mainly of them are based on the high-speed NOR CAMs [9]–[20]. A few techniques decreased the ML power by giving less power to mismatched MLs [10]– [13] or by reducing the voltage swing of the MLs using a sharing charge ML scheme [14] [15]. Further circuit designs reduced the activated MLs by employing a pre-computation method [16] or a pipelined hierarchical search scheme [17]. Though, they require added circuits for the pipeline registers. Without using extra registers the activated Matched Lines are reduced in pulsed NAND type –NOR type match-line scheme [18]. A few designs are based on low-power NAND CAM [21]– [24] and a fast searching speed is improved by the tree AND-type ML design [24].

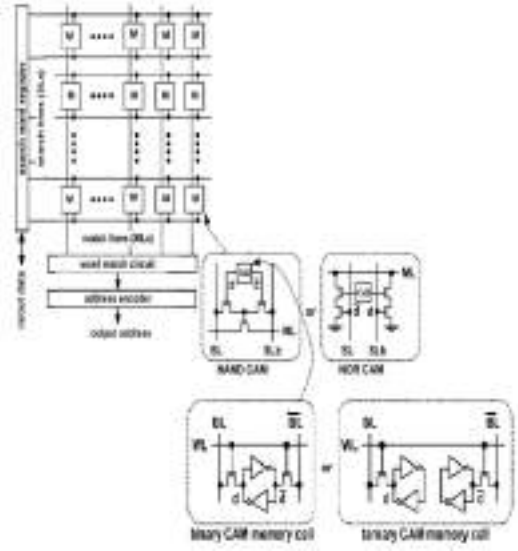

Fig.1. Architecture of Conventional CAM

To decrease the power consumption of Search Line (SL) numerous techniques have been proposed [17]–[19], [22]–[24]. Less number of sub-SLs is selected in the pipelined hierarchical search scheme [17]. This method increases area and latency because of stages connected in pipeline. Reducing the SL length and organizing the stored data value with "X" is achieved in segmented SL method [19] [22] [23]. One disadvantage of this method is complexity for the stored data while updating. By recycling the charge on the SLs reduced the SL power [18] [24]. A low-power BCAM is implemented [25] and it can be used for lower technologies to decrease the power consumption.

In this paper, a less leakage power Binary Content Addressable Memory using 7T SRAM cell as a memory

Proceedings of the Third International Conference on Intelligent Sustainable Systems [ICISS 2020]
IEEE Xplore Part Number: CFP20M19-ART; ISBN: 978-1-7281-7089-3

2020 3rd International Conference on Intelligent Sustainable Systems (ICISS) | 978-1-7281-7089-3/20/$31.00 ©2020 IEEE | DOI: 10.1109/ICISS49785.2020.9315883

The Ideal Block Ciphers - Correlation of AES and PRESENT in Cryptography

G.Sravya, Manchalla.O.V.P.Kumar, Y.Sudarsana Reddy, K. Jamal, Kiran Mannem

#1.Mtech student, ECE, GRIT, Hyderabad
#2, Asst. Prof, ECE, GRIT, Hyderabad
#3 #4, #5. Assocts Prof, GRIT

Abstract: In this digital era, the usage of technology has increased rapidly and led to the deployment of more innovative technologies for storing and transferring the generated data. The most important aspect of the emerging communication technologies is to ensure the safety and security of the generated huge amount of data. Hence, cryptography is considered as a pathway that can securely transfer and save the data. Cryptography comprises of ciphers that act like an algorithm, where the data is encrypted at the source and decrypted at the destination. This paper comprises of two ciphers namely PRESENT and AES ciphers. In the real-time applications, AES is no more relevant especially for segmenting the organizations that leverage RFID, Sensors and IoT devices. In order to overcome the strategic issues faced by these organization, PRESENT ciphers work appropriately with its super lightweight block figure, which has the equivalent significance to both security and equipment arrangements. This paper compares the AES (Advance encryption standard) symmetric block cipher with PRESENT symmetric block cipher to leverage in the industries mentioned earlier, where the huge consumption of resources becomes a significant factor. For the comparison of different ciphers, the results of area, timing analysis and the waveforms are taken into consideration.

KEYWORDS: PRESENT block cipher, AES cipher, Ultra-light weight, Area, Timing, Cryptography, IoT.

I. INTRODUCTION

Due to the existing plethora of devices and technologies to communicate with each other. The smart technologies like Interne of Things [IoT] at a rapid pace [1]. With respect to the data generated during communication, several security issues leading to data that result in wrong hands are analyzed. With the increase in use of IoT today it has become even more imperative to make sure that this technology addresses the emerging security concerns. Other factors like trust, privacy along security are influencing the outlook of IoT and further it will result in higher adoption of IoT across industries. One of the major concerns to be considered here is, it should handle data from ultra-data sensitive segments like finance, military and healthcare, etc. and it requires large amount of computational work in the vast number of computing devices and finally it becomes more prone to the physical attacks. Hence, in building solutions for the IoT space it is required to take these restrictions into consideration for proposing a better design. Accordingly, a portion of the gadgets in IoT is furnished with small sized Boards and oscillators with moderate movement, low end miniature regulators. For example, Sensor nodes in an organization of wireless sensors and also few of the software friendly light weight primitives can also be selected. Adding to this, all the IoT devices leverage power sources in limited levels, due to which it can determine dependencies on energy harvesting, [6] novel transmission, [2] and optimization techniques [7]. Cryptography secures and protects data in the likes of messages, documents, verbal and nonverbal communications, etc. It becomes very challenging to provide constrained environments for generating cryptographic solutions. As stated below, in [8] the power utilization, speed, cost and, area should be adjusted to multiple factors. Hence for IoT, the hardware based security is the right way to proceed further [1]. A quality breakthrough in the design along with optimization techniques remain more important in the future proposed security models and architectures. It further strengthens the premise that a Hardware based cryptography will be more secured and trustworthy over the Software based models. Many researchers have come up with

Materials Today: Proceedings xxx (xxxx) xxx

Contents lists available at ScienceDirect

Materials Today: Proceedings

journal homepage: www.elsevier.com/locate/matpr

Facial emotion recognition based music system using convolutional neural networks

S.k. Sana [a], G. Sruthi [a], D. Suresh [a,*], G. Rajesh [a], G.V. Subba Reddy [b]

[a] Department of Electronics and Communication Engineering, Gokaraju Rangaraju Institute of Engineering and Technology, Hyderabad, India
[b] Associate Professor, Department of Electronics and Communication Engineering, Gokaraju Rangaraju Institute of Engineering and Technology, Hyderabad, India

ARTICLE INFO

Article history:
Available online xxxx

Keywords:
Face Detection
Emotion Detection
CNN algorithm
Music Recommendation

ABSTRACT

Our face is amongst the most significant body organs. It is critical in determining a person's emotions and feelings. With the use of certain traits discernible on the face, the emotion of an individual can be approximated to a certain degree of precision. With new technology advances, recognizable features of the face can be retrieved as inputs utilizing a webcam. The gathered data helps in determining the mood and songs are played from a customized playlist. This eliminates that time-consuming procedure of physically selecting music or modifying playlists and allowed for the creation of an appropriate playlist dependent on the person's emotional level or mood. We will look at a variety of algorithms to come up with an automatic playlist generating methodology that uses emotion recognition to suggest songs. The facial expression-driven music player is set up in a way that allows you to listen to music based on your facial expression. In this work FER-2013, dataset and CNN algorithm are used for emotion recognition.

Selection and peer-review under responsibility of the scientific committee of the International Conference on Innovative Technology for Sustainable Development.

1. Introduction

Human emotions can be mainly categorized as happiness, anger, surprise, fear, disgust, sad and neutral. The other emotions including contempt (which is a variation of disgust) and cheerfulness (which is a variation of happiness) can be categorized under this umbrella of emotions. Facial muscle contortions are minimum, and determining these variations can be difficult as even a small variation results in different expressions. Also, expressions of different or even the same people might change for the same emotion, as emotions are hugely situation-dependent. Face expression identification is a technique for identifying essential human emotions. The facial expressions transmit important emotional information. Programs and systems that focus on the interplay of images may play a key part in the next generation of computer systems. Robotics, medicine, driving assist systems, and lie detector defense can all benefit from face expression recognition. The goal of the study is to recognize humans' emotions through facial expressions. Through the web camera (which captures the person's image) connection available in computing systems, a music player is meant to capture a human feeling. The software recognizes the user's image and then extracts characteristics from the face of the target human being using image segmentation and image processing techniques to determine the emotions that the person is attempting to express. The project's goal is to brighten the user's mood by playing songs from a specifically developed music player that fulfills the user's criteria by identifying the user's image.(See Figs. 1-5)

2. Literature survey

A paper was published by Renuka R Londhe et al. The mechanism for efficient facial expression analysis and classification is presented in this research. These tactical metrics entropy skewness and ptosis are used to do expression analysis. Different photos are used to extract features. The two-layer feedforward neural network is used to classify these features. The scaled conjugate gradient backpropagation algorithm is used to train this neural network. With 92.2% classification accuracy, Anger, disgust, fear, happiness, sadness, and surprise are six basic expressions that are recognized [1].

* Corresponding author.
E-mail addresses: sksunny8224@gmail.com (S.k. Sana), g.sruthi2018@gmail.com (G. Sruthi), snaik4698@gmail.com (D. Suresh), gandla.rajeshraja@gmail.com (G. Rajesh), gvsreddy2005@gmail.com (G.V. Subba Reddy).

https://doi.org/10.1016/j.matpr.2022.03.131
2214-7853/
Selection and peer-review under responsibility of the scientific committee of the International Conference on Innovative Technology for Sustainable Development.

Proceedings of the Fifth International Conference on Trends in Electronics and Informatics (ICOEI).
IEEE Xplore Part Number:CFP21J32-ART; ISBN:978-1-6654-1571-2

A Comprehensive Study on Automatic Speaker Recognition by using Deep Learning Techniques

[1]Venkata Subba Reddy Gade, Research Scholar, Dept. of ECE, Sathyabama Institute of Science and Technology, Chennai, India. E-mail: gvsreddy2005@gmail.com

[2]M.Sumathi, Dept. of ECE, Sathyabama Institute of Science and Technology, Chennai, India.
E-mail: sumagopi206@gmail.com

2021 5th International Conference on Trends in Electronics and Informatics (ICOEI) | 978-1-6654-1571-2/21/$31.00 ©2021 IEEE | DOI: 10.1109/ICOEI51242.2021.9452885

Abstract:

In Speaker, identifying or recognizing human voices is a challenging task. Recently, the automatic speaker recognition technique has been developed by using deep learning techniques. However, there is a lot of wide-ranging reviews on the implementation of deep learning techniques. The authors of this work examine numerous main subtasks of automatic speaker recognition, such as speaker verification and identification, focusing on deep learning-based solutions. This article offers the groundwork for establishing effective voice recognition, automatic speaker recognition planning, and accurate quantitative voice recognition evaluation using deep learning classifiers. Finally, the authors have analyzed robust speaker recognition with two primary techniques like domain mismatch and noise difficulties, for speech improvement and domain adaption.

Keywords: Convolution Neural Network, Deep Neural Network, Noise, Information**,** Speaker Recognition, Speech, Classifiers.

Introduction

The mode of communication for humans is speech and the identity of person can be identified from speech without seeing the face. The speech recognition is the method used for automatically identifying the person by using distinctive biological characteristics [1]. In speaker recognition, the main aim is to condense the details into the representation level of single utterance. Obtaining the representation level of good utterance has become necessary for speech and that is considered from unconstrained and noisy conditions, where the unwanted information present in speech signals need to be filtered [2]. The speaker recognition is divided into two sub fields such as speaker identification and speaker verification [3]. In speaker identification, the speaker tries to identify the voice of unknown person's among the voice of the group of persons. In speaker verification, the verified voice of the speaker and the claimed person's voice are compared through threshold which concludes the system with decision of accept or reject [4]. The speakers are identified in two different approaches such as text dependent and text independent. In the system of text dependent identification, the spoken text during the phase of testing should be similar to spoken text during training the system. In the system of text independent identification, the process will not be dependent on the text spoken by the speaker [5].

However, due to the impacts of extended fading ranges, complex sounds in the surroundings, and room reverberation, speaker detection in the distant field and complicated environments is difficult [6].Speech signal transmission over a longer distance is hampered by absorption, fading, and reflection of diverse objects, which alters the pressure level at various frequencies and lowers signal quality [7]. The existing frameworks for speaker recognition such as i-vector-based strategy which showed success in recognizing the speech[8]. The vector-based strategy assumes the enrollment and testing data includes similar distributions. But, the assumption failed in many real world scenarios and because there were frequent mismatch in the channel for enrolment and testing data. The mismatch in the channel significantly affected the performance of speaker recognition [9]. Many existing methods were developed for the recognition of speaker such Convolution Neural Network (CNN), Deep Neural Network (DNN), etc. However, in single speaker it was challenging to collect the training data from the different channels. So, the existing methods were difficult to represent the information of speaker among various channels [10].

The examination on speaker recognition can be traced all the way back to in any event 1960s [22]. In the accompanying forty years, many trend setting innovations advanced the improvement of speaker acknowledgment. For instance, various acoustic highlights (for example dynamic time warping and linear predictive cepstral coefficients) and later on, [21] favored representing the Gaussian combination model based general

2021 IEEE International Symposium on Smart Electronic Systems (iSES) | 978-1-7281-8753-2/21/$31.00 ©2021 IEEE | DOI: 10.1109/iSES52644.2021.00056

Energy Efficient Approximate Multiplier Design for Image/Video Processing Applications

L Hemanth Krishna and J Bhaskara Rao
Dept. ECE.,
GVP College of Engineering
Vishakapatnam, India
hemanth.krishna412@gmail.com

Ayesha Sk
School of CSE
VIT Chennai
Chennai, India
ayesha.sk@vit.ac.in

Sreehari Veeramachaneni
Dept. ECE.,
GRIET, Hyderabad
Hyderabad, India
srihariy2k4@gmail.com

Noor Mahammad Sk
Dept. CSE.,
IIITDM Kancheepuram
Chennai, India
noor@iiitdm.ac.in

***Abstract*—An energy-efficient approximate multiplier is designed by using an approximate compressor for image and video processing applications. This paper proposes an approximate 4:2 compressor design with an 18.75% error rate that consumes on an average 15% less energy compared with the existing designs from the literature. This paper proposes two variants of the multiplier, one with only approximate compressors and another one with approximate and accurate compressors.**

***Index Terms*—Energy Efficient Multiplier, Approximate Computing, Approximate 4:2 Compressor, Image/Video Processing applications.**

I. Introduction

APROXIMATE hardware-based computing is an emerging area for energy-efficient hardware design. Many real-life applications can be implemented using these approximate hardware. The applications that can tolerate errors in their output are the best suited for this kind of implementation. Signal processing, Image processing, and Video processing applications are best suited for approximate computing, and thereby one can reduce significant energy, delay, power, and area. The majority of the hardware will commonly use data path elements like adders and multipliers, etc.,. An efficient approximate multiplier will significantly reduce the energy of the system [1] [2].

In general approximate multiplier is designed by introducing approximate compressors in the partial product reduction stage as the partial product reduction stage consumes more area, power, and delay. Introducing approximation in this stage will significantly reduce the energy. There is a significant contribution has done by many researchers in designing a new compressor with different error rates at the output level [1] [2] [3].

The compressors produce two output bits from the n-input bits. Hence, it is popularly used in the partial product reduction stage of the multiplier [4]. The primary function of the compressor is to give the number of 1's present in the given input and produces the binary output. For example, let us consider the input to the compressor as 1111; the compressor produces the output as 100. The number of ones present in this input is 4; this can be read in the output as the most significant two bits 10 are Cout and Carry will have the same weight as 2^1 and the least significant bit is Sum and its weight is 2^0 as shown in equation (1).

$$A + B + C + D = (Cout + Carry).2^1 + Sum.2^0 \quad (1)$$

The accurate 4:2 compressor without Cin is designed using one full adder and one-half adder. Its corresponding circuit diagram is shown in Fig. 1, and Table I is the truth table of the circuit.

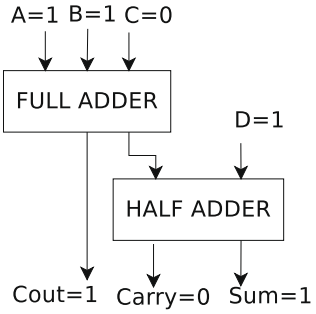

Fig. 1: Conventional Accurate 4:2 Compressor without Cin

TABLE I: Truth Table for Conventional 4:2 Compressor without Cin

A	B	C	D	Cout	Carry	Sum
0	0	0	0	0	0	0
0	0	0	1	0	0	1
0	0	1	0	0	0	1
0	0	1	1	0	1	0
0	1	0	0	0	0	1
0	1	0	1	0	1	0
0	1	1	0	1	0	0
0	1	1	1	1	0	1
1	0	0	0	0	0	1
1	0	0	1	0	1	0
1	0	1	0	1	0	0
1	0	1	1	1	0	1
1	1	0	0	0	1	0
1	1	0	1	1	0	1
1	1	1	0	1	0	1
1	1	1	1	1	1	0

The objective of the approximate compressor is to reduce the power and delay. Hence, the simple circuit can be designed only using primitive gates with slight variation from

978-1-7281-8753-2/21/$31.00 ©2021 IEEE
DOI 10.1109/iSES52644.2021.00056

the original output (which leads to error in the output for certain combinations); in such case, the use of XOR gates can be eliminated; as a result, power consumption reduces. The presence of error in the output will not change the visual information in image/video processing applications.

This paper proposes an approximate 4:2 compressor design, which uses primarily primitive gates. The proposed approximate 4:2 compressor design is used in the design of the multiplier to reduce the partial products. The proposed multiplier is delivering superior performance than the existing approximate multipliers.

The rest of the paper is organized as follows. Section II presents a detailed literature review about approximate multiplier. Section III proposes novel approximate 4:2 compressor design and approximate multiplier designs. Section IV detailed the results and discussion and followed by Section V Conclusion.

II. Literature Review

Approximate computing can be implemented at various levels, such as algorithmic level, module-level design, gate-level design, and transistor-level design. Many of the approximate computing works that are available in the literature are at gate-level implementations. In this paper, we are implementing approximate computing for the arithmetic circuit. This paper targets to design an approximate multiplier by designing approximate compressors for the Dadda multiplier.

The generic block diagram of the approximate 4:2 compressor is shown in Fig. 2, and the truth table is shown in Table II. Its equation is shown in 2.

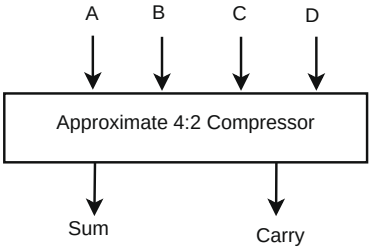

Fig. 2: Generalized Approximate 4:2 Compressor

$$A + B + C + D = Carry.2^1 + Sum.2^0 \quad (2)$$

[3] has proposed hardware-level approximate compressor at gate-level design. [3] has proposed two designs in his work, design2 uses 2 XNOR gates, 3 NOR gates, and one OR gate in his design with an error rate of 25%. He proved that his proposed design would have a lesser delay than the convention accurate 4:2 compressor.

[5] has proposed a approximate 4:2 compressor design as shown in Fig. 3 and Fig. 4 with 12.5% and 25% error rate respectively. In order to reduce the error rate, the author has used XOR, OR, AND, AOI, and OAI standard cells from the design library. The area, power, and delay of [5] are higher than the [3].

TABLE II: Truth Table for Approximate 4:2 Compressor

A	B	C	D	Carry	Sum
0	0	0	0	0	0
0	0	0	1	0	1
0	0	1	0	0	1
0	0	1	1	1	0
0	1	0	0	0	1
0	1	0	1	1	0
0	1	1	0	1	0
0	1	1	1	1	1
1	0	0	0	0	1
1	0	0	1	1	0
1	0	1	0	1	0
1	0	1	1	1	1
1	1	0	0	1	0
1	1	0	1	1	1
1	1	1	0	1	1
1	1	1	1	1	1

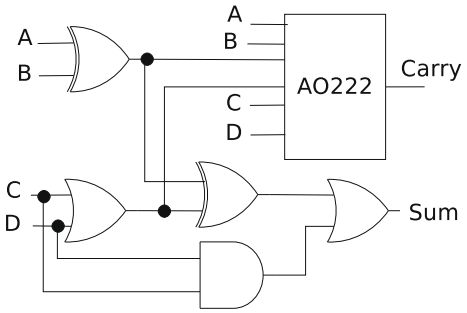

Fig. 3: Approximate 4:2 Compressor Design2 [5]

[6] has proposed three designs, where the hardware circuit for all the three designs remains the same as shown in Fig. 5, except the ordering of the given inputs. The input reorder is achieved using a 2:1 multiplexer, XOR, two OR gates, and one AND gate. All the design has same error rate, i.e., 25% with various delay characteristics. The author has mainly focused on reducing the delay and error rate. The approximate compressor with a different error rate is also present in [7] [8] [9].

A. Contribution of this paper

The objective of this paper is to reduce the power delay product with an acceptable output visual quality of the image.

- This paper uses an input reordering mechanism to reduce the number of inputs to a small number, thereby reducing the complexity of the circuit.
- Proposes a novel approximate 4:2 compressor with an 18.75% error rate.
- The proposed compressor design uses only primitive gates.
- To demonstrate the proposed compressor's effectiveness, this paper uses two multiplier designs.
- Estimated area, power, delay, and Energy (Power delay product) for existing and proposed compressor design and multiplier designs.
- Image processing application is chosen to prove the multiplier's effectiveness, and its metrics are presented.

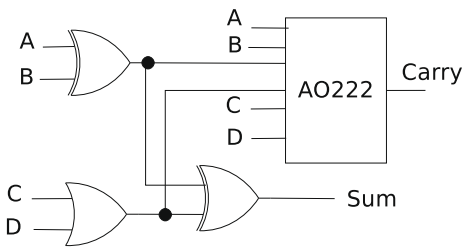

Fig. 4: Approximate 4:2 Compressor Design3 [5]

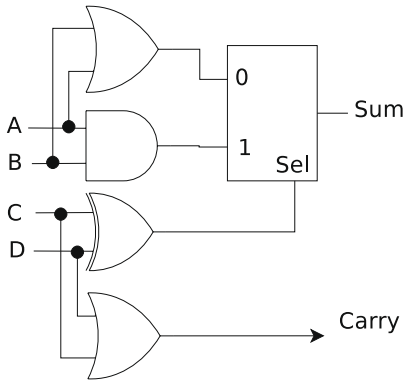

Fig. 5: Approximate 4:2 Compressor Design [6]

III. Proposed Energy-Efficient Approximate Multiplier

This section proposes a novel approximate 4:2 compressor, which is used for reducing the partial products efficiently. This section is organized into two parts. The first part will explain the proposed approximate 4:2 compressors and followed by the second part is an approximate multiplier.

A. A Novel Proposed Approximate 4:2 Compressor

The objective of this section is to design an approximate 4:2 compressor with reduced power, circuit area, delay, and energy. This section proposes a novel approximate 4:2 compressors. The compressor design is designed using only primitive gates, and as a result, delay and power are significantly reduced than the existing approximate 4:2 compressors from the literature.

The truth table of the conventional accurate 4:2 compressor without Cin is shown in Table I, and its circuit diagram is shown in Fig. 1. Based on the truth table I of the accurate 4:2 compressor without Cin, the approximation in the circuit is made by eliminating Cout in the output of the accurate 4:2 compressor design to make it as approximate 4:2 compressor as shown in Fig. 2 and the truth Table II. As accurate 4:2 compressor without Cin has four inputs and three outputs named Cout, Carry, and Sum. As it has four inputs, only one possible combination, i.e., $ABCD = 1111$, will give counted number of 1's like four and rest of the case it is only maximum three and this maximum number of 1's, three can be represented using two output bits, i.e., Carry and Sum.

TABLE III: Truth Table of Input Pairing Alignment Circuit

A	B	C	D	1's Count	Y0	Y1	Y2	Y3
0	0	0	0	0	0	0	0	0
0	0	0	1	1	0	0	1	0
0	0	1	0	1	0	0	1	0
0	0	1	1	2	0	0	1	1
0	1	0	0	1	1	0	0	0
0	1	0	1	2	1	0	1	0
0	1	1	0	2	1	0	1	0
0	1	1	1	3	1	0	1	1
1	0	0	0	1	1	0	0	0
1	0	0	1	2	1	0	1	0
1	0	1	0	2	1	0	1	0
1	0	1	1	3	1	0	1	1
1	1	0	0	2	1	1	0	0
1	1	0	1	3	1	1	1	0
1	1	1	0	3	1	1	1	0
1	1	1	1	4	1	1	1	1

The maximum count value counted for all the four input 1's is Sum=1 and Carry=1 with an error. The compressor count value depends on the number of 1's present in the input combination rather than the decimal value. Hence, this paper aligns all the 1's presents in the input towards to most significant bit (MSB) side using the input pairing alignment circuit as shown in Fig. 6. In Fig. 6 the inputs A and B are one pair and C and D are another pair. These two pairs align the 1's presents in the inputs towards the MSB side as shown in truth Table III. As a result number of 16 input combinations is reduced to 9 output combinations, as shown in Table III. As a result, compressor design with this logic will have lesser complexity, and circuit switching activity reduces than the existing design. The proposed approximate 4:2 compressor is designed using a truth table of the reduced number of combinations as shown in Table III.

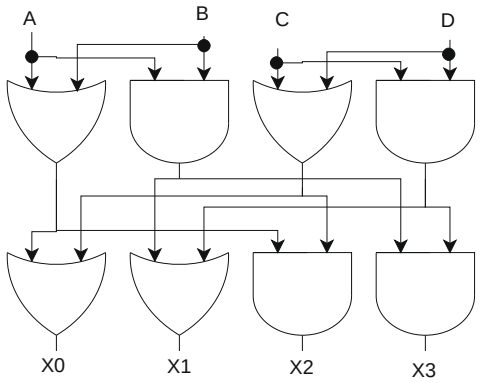

Fig. 6: Input Reordering Circuit

The proposed compressor will have three output combinations that have deviated from the accurate 4:2 compressor with an error rate of 18.75% as shown in Truth Table IV, and its equivalent circuit diagram is shown in Figure 7. The proposed compressor is designed with only primitive gates and one multiplexer.

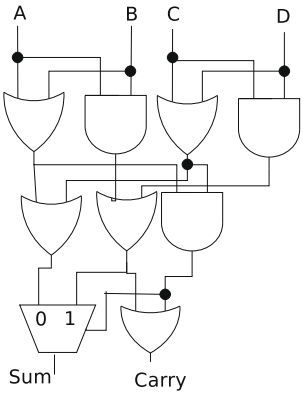

Fig. 7: Proposed Approximate 4:2 Compressor Design.

TABLE IV: Truth Table for Proposed Approximate 4:2 Compressor Design

A	B	C	D	Carry	Sum	Difference
0	0	0	0	0	1	0
0	0	0	1	0	1	0
0	0	1	0	0	1	0
0	0	1	1	1	1	+1
0	1	0	0	0	1	0
0	1	0	1	1	0	0
0	1	1	0	1	0	0
0	1	1	1	1	1	0
1	0	0	0	0	1	0
1	0	0	1	1	0	0
1	0	1	0	1	0	0
1	0	1	1	1	1	0
1	1	0	0	1	1	+1
1	1	0	1	1	1	0
1	1	1	0	1	1	0
1	1	1	1	1	1	-1

B. Approximate Multiplier Design

This section proposes two 8×8 multiplier designs [3] [5], where approximate multiplier design1 as shown in Figure 8 uses the only proposed approximate 4:2 compressors in the partial product reduction stage and adders. The approximate multiplier design2 is shown in Figure 9 uses lower half significant bits is added using the proposed approximate 4:2 compressors, and higher half significant bits of the multiplier is designed using accurate 4:2 compressor in order to reduce the overall error distance.

IV. Results and Discussions

All the existing and proposed designs are modeled using Verilog HDL and implemented in 45nm technology library using Cadence 6.1 EDA tools. The area, power, delay, and power delay product (PDP) of all the designs are estimated. The comparison results of area, power, delay, and power delay product (PDP) of all the existing and proposed approximate compressors are shown in Table V. From Table V, one can summarize that the proposed designs save significant energy (PDP) compared to the existing designs. The percentage of reduction in energy or power delay product is shown in Table VI.

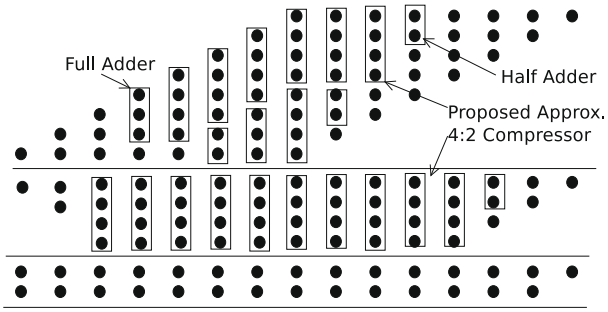

Fig. 8: Proposed Approximate 4:2 Compressors Mapping on Multiplier Design1

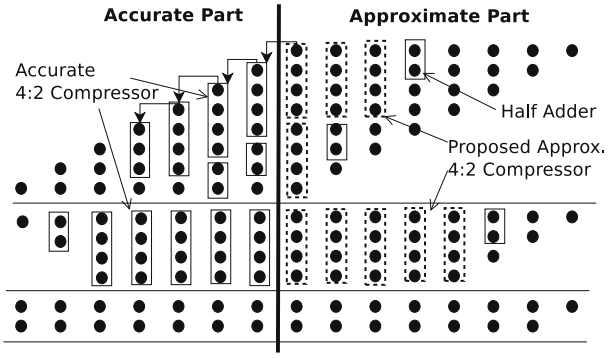

Fig. 9: Proposed Approximate and Accurate 4:2 Compressors Mapping on Multiplier Design2

TABLE V: Results Comparison for Existing and Proposed Approximate 4:2 Compressor Designs

Approximate 4:2 Compressor	**Area** um^2	**Power** nW	**Delay** ps	**PDP** aJ	**% of Error**
Existing Design2 [5]	7	613	70	42.97	12.50
Existing Design3 [5]	7	550	69	37.95	25
Existing Design [6]	7	634	53	33.60	25
Proposed Design	7	556	57	31.69	18.75

TABLE VI: % improvement of PDP of proposed Compressor designs compare with all the existing 4:2 compressors

Approximate 4:2 Compressor From Literature	**Proposed Design**
Existing Design2 [5]	26.24%
Existing Design3 [5]	16.49%
Existing Design [6]	5.68%

The proposed approximate 4:2 compressors are used in the design of the approximate multiplier. The area, power, delay, and power delay product (PDP) of the approximate multiplier design1 implemented using the existing and proposed compressors results are shown in Table VII. Implementation results of the multiplier design2 are shown in Table VIII. The percentage of improvement in multiplier design1 and design2 designed using 25% error based compressors comparison with the proposed compressor is shown in Table VII and Table VIII respectively. The proposed compressor-based multiplier de-

sign2 is compared with all the existing designs from the literature, and its percentage of improvement in power delay product is shown in Table IX.

TABLE VII: Results Comparison for Existing and Proposed Approximate 8-bit Multiplier Design1

Approximate 4:2 Compressor	**Area** um^2	**Power** nW	**Delay** ps	**PDP** fJ
Existing Design2 [5]	276	29835	477	14.23
Existing Design3 [5]	261	28489	558	15.89
Existing Design [6]	264	28430	642	18.25
Proposed Design	273	28016	579	16.22

TABLE VIII: Results Comparison for Existing and Proposed Approximate 8-bit Multiplier Design2

Approximate 4:2 Compressor	**Area** um^2	**Power** nW	**Delay** ps	**PDP** aJ
Existing Design2 [5]	286	34926	559	19.52
Existing Design3 [5]	278	34293	580	19.88
Existing Design [6]	279	34074	580	19.76
Proposed Design	296	34286	517	17.72

TABLE IX: % improvement of PDP of proposed multiplier design-2 compare with existence 4:2 compressor

Approximate 4:2 Compressor From Literature	**Proposed Design4**
Existing Design2 [5]	10%
Existing Design3 [5]	11%
Existing Design [6]	11%

TABLE X: Results Comparison for Existing and Proposed Approximate 8-bit Multiplier Design1

Approximate 4:2 Compressor Design Type	**PSNR dB**	**Mean Error Distance**	**Normalized Error Distance**
Existing Design2 [5]	35	83.28	0.32
Existing Design3 [5]	35.8	138.41	0.5
Existing Design [6]	28	$1.93x10^3$	7.59
Proposed Design	32.82	850	3.33

TABLE XI: Results Comparison for Existing and Proposed Approximate 8-bit Multiplier Design2

Approximate 4:2 Compressor Design Type	**PSNR dB**	**Mean Error Distance**	**Normalized Error Distance**
Existing Design2 [5]	63.31	11.22	0.04
Existing Design3 [5]	63.31	11.22	0.04
Existing Design [6]	61.45	18.46	0.07
Proposed Design	56.68	80.88	0.23

A. Application: Image Processing

The effectiveness of the approximate multiplication results can be proved by applying on the images and estimating the PSNR of the resultant images. The input for all the approximate multipliers is shown in Figure 10a and Figure 10b. The accurate multiplier resultant output image is shown in Figure 10c. The existing compressor-based approximate multiplier design1 resultant images are shown in Figure 11. The proposed approximate multiplier design1 resultant images are shown in Figure 13a.

The existing compressor-based approximate multiplier design2 resultant images are shown in Figure 12. The proposed approximate multiplier design2 resultant images are shown in Figure 13b.

The peak signal-noise ratio (PSNR), mean error distance (MED) [1], and normalized error distance (NED) [10] of the existing and proposed compressor-based multiplier design1 and design2 are compared in the Table X and Table XI. The proposed compressor-based multiplier is shown a significant improvement than the existing techniques from the literature. Multiplication is one of the basic operation in many image/video processing applications such as DCT (Discrete Cosine Transform) and DWT (Discrete Wavelet Transform) and etc.,.

(a) Input Image1 (b) Input Image2 (c) Output Image

Fig. 10: Input and Output Images of the Exact Multiplication

(a) Output [5] (b) Output [5] (c) Output [6]

Fig. 11: Output Images of the Approximate Multiplier Design1

(a) Output [5] (b) Output [5] (c) Output [6]

Fig. 12: Output Images of the Approximate Multiplier Design2

V. Conclusion

This paper proposed an approximate 4:2 compressor design with an 18.75% error rate. The proposed approximate compressor is compared with the existing designs in terms of area, power, and power delay product. The proposed approximate 4:2 compressors design delivers impressive energy savings

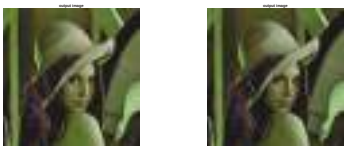

(a) Using Multiplier Design1 (b) Using Multiplier Design2

Fig. 13: Output Images of the Proposed Approximate Multiplier

with a low error rate, i.e., 18.75%. The proposed approximate compressors are used in the design of multiplier design1 and design2. The approximate multiplier design2 saves energy on an average of 10.8%, compared with all the existing designs. The PSNR values of the approximate multiplier design2 are better than the existing designs.

REFERENCES

[1] J. Liang, J. Han, and F. Lombardi, "New metrics for the reliability of approximate and probabilistic adders," *IEEE Transactions on Computers*, vol. 62, no. 9, pp. 1760–1771, Sep. 2013.

[2] H. Jiang, J. Han, and F. Lombardi, "A comparative review and evaluation of approximate adders," in *Proceedings of the 25th Edition on Great Lakes Symposium on VLSI*, ser. GLSVLSI '15, 2015, pp. 343–348.

[3] A. Momeni, J. Han, P. Montuschi, and F. Lombardi, "Design and analysis of approximate compressors for multiplication," *IEEE Transactions on Computers*, vol. 64, no. 4, pp. 984–994, April 2015.

[4] J. Gu and C.-H. Chang, "Ultra low voltage, low power 4-2 compressor for high speed multiplications," in *Proceedings of the 2003 International Symposium on Circuits and Systems, 2003. ISCAS '03.*, vol. 5, May 2003, pp. V–V.

[5] Z. Yang, J. Han, and F. Lombardi, "Approximate compressors for error-resilient multiplier design," in *2015 IEEE International Symposium on Defect and Fault Tolerance in VLSI and Nanotechnology Systems (DFTS)*, Oct 2015, pp. 183–186.

[6] F. Ranjbar, Y. Forghani, and D. Bahrepour, "High performance 8-bit approximate multiplier using novel 4:2 approximate compressors for fast image processing," *International Journal of Integrated Engineering*, vol. 10, no. 1, 2018.

[7] C. Lin and I. Lin, "High accuracy approximate multiplier with error correction," in *2013 IEEE 31st International Conference on Computer Design (ICCD)*, Oct 2013, pp. 33–38.

[8] J. Ma, K. Man, T. krilavičius, S. Guan, and T. Jeong, "Implementation of high performance multipliers based on approximate compressor design," in *6th International Conference on Electrical and Control Technologies, ECT 2011*, 01 2011, pp. 96–100.

[9] B. W. N. Braden J. Phillips, Daniel R. Kelly, "Estimating adders for a low density parity check decoder," in *Advanced Signal Processing Algorithms, Architectures, and Implementations XVI*, vol. 6313, 2006.

[10] N. Maheshwari, Z. Yang, J. Han, and F. Lombardi, "A design approach for compressor based approximate multipliers," in *2015 28th International Conference on VLSI Design*, Jan 2015, pp. 209–214.

Energy Efficient Approximate 4:2 Compressors for Error Tolerant Applications

L Hemanth Krishna and J Bhaskara Rao
Dept. ECE.,
GVP College of Engineering
Vishakapatnam, India
hemanth.krishna412@gmail.com

Ayesha Sk
School of CSE
VIT Chennai
Chennai, India
ayesha.sk@vit.ac.in

Sreehari Veeramachaneni
Dept. ECE.,
GRIET, Hyderabad
Hyderabad, India
srihariy2k4@gmail.com

Noor Mahammad Sk
Dept. CSE.,
IIITDM Kancheepuram
Chennai, India
noor@iiitdm.ac.in

2021 28th IEEE International Conference on Electronics, Circuits, and Systems (ICECS) | 978-1-7281-8281-0/21/$31.00 ©2021 IEEE | DOI: 10.1109/ICECS53924.2021.9665614

***Abstract*—In many real-life applications such as image/video processing, the error present in the output will not impact the output visual information. Approximation at the hardware level is one of the promising techniques to design energy-efficient circuits. This paper proposes an approximate 4:2 compressor design to reduce partial products in the multiplier design. The proposed approximate 4:2 compressor design consumes on an average 56% less energy compared with the existing designs from the literature, respectively. This paper proposes two variants of the approximate multiplier designs, where design1 uses only proposed approximate 4:2 compressors and multiplier design2's lower half of the multiplier is designed using proposed approximate 4:2 compressor and higher half of the multiplier is designed using existing accurate compressors to reduce the error rate and improve the output image visual quality.**

***Index Terms*—Energy Efficient Multiplier, Approximate Computing, Approximate 4:2 Compressor, Error tolerant applications.**

I. Introduction

AS the usage of portable handheld devices is continuously growing, and many real-life applications are also adapted on these devices. The battery life of portable devices doubles every ten years. Approximate computing is one technique to reduce the battery life for error-tolerant computing. Many researchers are started developing approximate hardware for error-tolerant applications. The majority of the real-life applications are error-tolerant, for example, signal, image, and video processing applications. Even the modern algorithms used for processing, such as machine learning, deep learning, etc., are error-tolerant. In processor multipliers, hardware will consume more energy, approximation in multiplier will make circuits energy efficient for image/video processing [1] [2].

Multiplier design has three stages in stage one, partial product generation. Stage two is partial product reduction; this stage consumes massive hardware to add the generated partial products, and stage three is the final adder. The approximation in the multiplier is introduced at the partial product reduction stage in multiple ways. The most commonly and popularly used technique is compressors and adders at the partial product reduction stage [1] [2] [3].

Compressors are hardware circuits that convert a n-number of input bits to 2-bit output, which is very much desirable in the case of the reduction stage of the partial products of the multiplier [4]. The primary function of the compressor is to give the number of 1's present in the given input and produces the binary output. For example, let us consider the input to the compressor as 1101, the compressor produces the output as 101. The number of ones present in this input is 3; this can be read in the output as the most significant two bits 10 are Cout and Carry will have the same weight as 2^1 and the least significant bit is Sum and its weight is 2^0 as shown in equation (1).

$$A + B + C + D = (Cout + Carry).2^1 + Sum.2^0 \quad (1)$$

This can be realized using an accurate 4:2 conventional compressor without Cin using one full adder and one-half adder, whose circuit diagram is shown in Figure 1, and its truth table is shown in Table I.

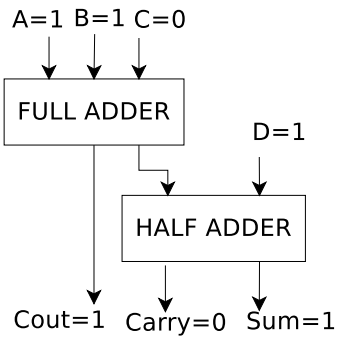

Fig. 1: Conventional Accurate 4:2 Compressor without Cin

The objective of the approximate compressor is to reduce the power and delay. Hence, the simple circuit can be designed only using primitive gates with slight variation from the original output (which leads to error in the output for certain combinations); in such case, the use of XOR gates can be eliminated; as a result, power consumption reduces. The presence of error in the output will not change the visual information in image/video processing applications.

This paper proposes an approximate 4:2 compressor design, which uses primarily primitive gates. The proposed approximate 4:2 compressor design is used in the design of multiplier to reduce the partial products. The proposed multiplier is

Design and Analysis of Obfuscated Full Adders

Sandeep Kolla
IIITDM Kancheepuram, India

Ayesha Sk
VIT Chennai, India

Sreehari Veeramachaneni
GRIET, Hyderabad, India

Noor Mahammad Sk
IIITDM Kancheepuram, India

2021 International Conference on Microelectronics (ICM) | 978-1-6654-0839-4/21/$31.00 ©2021 IEEE | DOI: 10.1109/ICM52667.2021.9664955

***Abstract*—In modern day semiconductor industry secure circuit/hardware is one of the major concern due to issues like IC piracy, Trojan insertion, IC over production and etc.,. Recently researchers has demonstrated various hardware based attacks and also expressed their concern towards the design of the obfuscated circuit. Securing the hardware circuit is one of the key concerns today. This work proposes design of the secure adders and its implementations. The objective of this work is to design minimal overhead based secure adders for secure system design. This can be achieved by encrypting the key into the hardware circuit at transistor level. The correct key ensures circuit's correct operation, else it produces an incorrect value. The correct and incorrect operation resultant output can not be distinguished by the malicious user.**

***Index Terms*—Secure Full adder, Obfuscation, Hardware Security, Key encryption, Logic Encryption**

I. Introduction

The construction and maintenance cost of semiconductor foundry or manufacturing plant for the fabrication of Integrated Circuits (ICs) is high. Semiconductor fabrication units has to continuously adapt to the newer technologies and its fabrication process as per the Moore's law. The entire IC design process can be broadly classified into two phases. Developing an GDS-II format from the idea is Phase-I, which can be done by modeling the design in HDLs (hardware description languages), synthesizing and physical design implementation. Phase-II is fabrication of IC using developed GDS-II format in the phase-I, which is done at the manufacturing plant. Majority of the semiconductor companies/organizations will end their in-house implementation with GDS-II format and they will outsource the fabrication to the third party fabrication unit. The loopholes in physical design are taken as an advantage by the malicious third-party fabrication units.

The fabricated chips are vulnerable for various hardware based attacks due to malicious third party fabrication unit. The malicious fabrication unit can leak the IP (Intellectual Property), reverse engineering, piracy and overproduction [1]. In order to protect from the above attacks the fabless organizations or companies has to go for hardware encryption, such that they can claim that their IP and take legal actions against the malicious fabrication unit. Typically, this hardware encryption is done at the layout level of the design by inserting a key using either EXOR gate or multiplexer or look-up-tables. The malicious foundry uses reverse engineering techniques using machine learning/AI algorithms to identify the security keys that are inserted at the layout and they will remove the keys and claims that the design is belongs to their own or its associative organization.

Adders are extensively used in the microprocessors and micro-controllers for program counter increment, branch target address generation, and arithmetic logic unit. Adders are the building blocks of the any hardware based encryption based ASIC (application Specific Integrated Circuit) chip. Secure arithmetic operations or control operations can be done by the design of the secure adders. Secure adders are adders with security key. Upon the supply of the correct key the correct addition result will come as output else it will produce the incorrect result [2][3][4]. This paper proposes a secure adder design.

The rest of the paper is organized as follows. Section II presents the detailed literature review. Section III elaborates the proposed secure adder design. Section IV presents results and discussions and followed by Section V conclusion.

II. Literature Review

Security key insertion in the circuit such that the circuit will produces the correct results for the correct key, else it produces the incorrect results. The process of insertion of security key in the original circuit is called logic encryption. This can be achieved by using XOR/ XNOR gate [5][6], where one input of the XOR/ XNOR gate is connected with key k and other input is connected with wire w of the intermediate circuit. Such that upon the correct key $k = 0$ output of the XOR/ XNOR is $w/\overline{w}$, else it is $0/1$.

Key insertion can also be done using the 2:1 multiplexer [7], where key k is connected to select line of the multiplexer and the first input of the multiplexer is connected to wire segment w of the circuit and the second input of the multiplexer is connected to any arbitrary wire in the circuit. Whenever the key $k = 0$ it produces the true value of the wire segment w, else it produces the arbitrary value.

LUT (Look-up-table) based logic encryption [8] uses one or more key(s), where a specific logic function or gate can be replaced with it. It uses a 4:1 multiplexer and whose inputs are connected to memory cells. The basic Boolean functions are realized in 4-bit memory cell. The logic function implemented on the memory cell is applied to the two select input lines of the multiplexer.

The above logical encryption schemes are applied on the Boolean circuits or gate level netlist and it will have overheads in terms of area, power and delay. Few of the works reported in the literature, where the encryption is also introduced at the transistor level. Kyle et. al., has proposed logic encryption at gate level by introducing the key using NMOS/PMOS switches. The security key(s) is/are introduced at PMOS and

Area Efficient Approximate 4-2 compressor for Multiplier Design

Chinthalgiri Jyothi , Kuruva Gayathri , Saranya Karunamurthi**, Sreehari Veeramachaneni, Noor Mahammad S *
Department of ECE, Gokaraju Rangaraju Institute of Engineering & Technology, Hyderabad.
*Indian Institute of Information Technology Design and Manufacturing (IIITDM) Kancheepuram,,Chennai.
**,Dr.MCET Pollachi,Coimbatore.

Abstract: In many applications like Digital Signal Processing (DSP), the multiplier is the basic building block, which uses the more complex circuitry. As the DSP applications are tolerable to outputs with some error, the replacement of exact multiplier with approximate multiplier gives the higher energy efficiency. In this paper a new approximate 4-2 compressor circuit is proposed for less complex multiplication process. The proposed compressor uses less hardware circuitry and less energy. The simulation results shows that the approximate multiplier by using the proposed approximate 4-2 compressor consumes less energy when compared with other multipliers with bit size of 8x8. The proposed multiplier gives 77.94% reduction in EDP when compared with the exact multiplier.

Key words: DSP, Compressor , Approximate multiplier, EDP

INTRODUCTION

With rising need and evolution in Internet of Things and portable devices, a great challenge on VLSI circuits to obtain energy efficiency. Many applications such as digital signal processing (DSP) and neural networks need approximate circuits to decrease delay and area with an acceptable accuracy.

Digital multiplier consists of three parts. Which are: generation of partial products, reduction of partial products, and proposed adder for result. However ,in multiplication the design has two approach for approximate multiplier. In the first approach, all partial products are reduced using full adders& half adders and at the last stage of calculation the proposed adder used. And in the second approach, all partial products are reduced by proposed 4-2 compressor and at the last stage proposed adder.

First approach is chosen to get low error rate, and second approach is chosen for better trade-off between error-delay. Here section II explains about Approximate 4-2 Compressor, Section III explains about Related works, Section IV explains the proposed work, section V tells about experimental setup, Section VI Results and conclusions, and in Section VII References are explained.

II. Approximate 4-2 Compressor

The compressors counts the number of 1's in the inputs. The mostly used efficient compressor is 4-2 compressor. The conventional 4-2 compressor has the 5 inputs and 3 outputs [1].The formula for the 4-2 compressor is as follows.

A+B+C+D+Cin =2(Cout+Carry)+Sum (1)

Where A,B,C,D,Cin are the inputs to the compressor and Cout,Carry Sum are the outputs of the compressor.

Figure 1 shows the 4-2 compressor which is implemented by using two full adders. The equations for the outputs of the compressor are given as follows,

$$Sum = A \oplus B \oplus C \oplus D \oplus Cin \qquad (2)$$

$$Cout = (A \oplus B) \bullet C + \overline{(A \oplus B)} \bullet A \qquad (3)$$

$$Carry = (A \oplus B \oplus C \oplus D) \bullet Cin + \overline{(A \oplus B \oplus C \oplus D)} \bullet D \qquad (4)$$

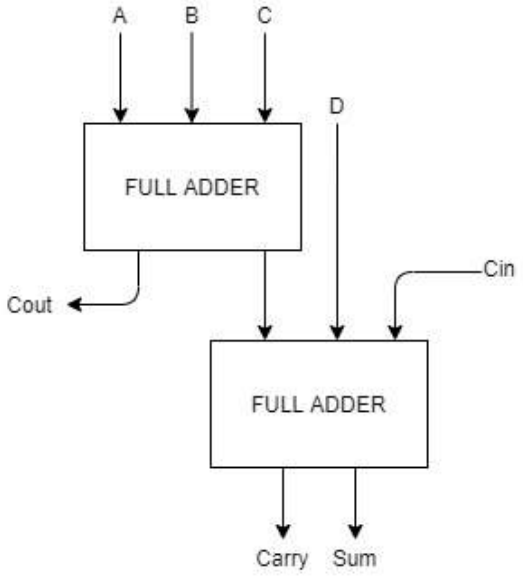

Figure 1: Conventional 4-2 Compressor

There are many approximate 4-2 compressors has proposed to reduce the area, power and delay of the system. The figure 2 shows the block diagram of approximate compressor which has 4 inputs(A,B,C,D) and 2 outputs(Sum, Carry) [2-4]. The approximate 4-2 compressor eliminates the Cin and Cout to reduce the complexity of the circuit.

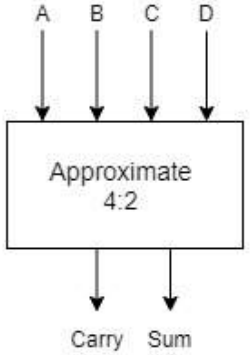

Figure 2: Approximate 4-2 Compressor

III. RELATED WORKS

There are two types of approximate compressors, one which counts the no of 1's in the value and other which gives the value [5,6]. But the final output will not effect by considering the

978-1-7281-8734-1/20/$31.00 ©2020 IEEE
DOI 10.1109/INDISCON50162.2020.00055

Area Efficient Nearly Accurate Approximate Adder Design

Chinthalgiri Jyothi , Kuruva Gayathri ,Sreehari Veeramachaneni, Noor Mahammad S *

Department of ECE, Gokaraju Rangaraju Institute of Engineering & Technology, Hyderabad.
*Indian Institute of Information Technology Design and Manufacturing (IIITDM) Kancheepuram,,Chennai.

Abstract : As CMOS technology is scaling down day by day to a few nanometre, there is a difficulty in improving circuit performance and energy scaling in a cost-effective manner. On the other hand, computational scaling from future workloads is increasing rapidly, because of this there is a gap between capabilities of CMOS technology scaling down and the requirement for future application workloads. In such scenario, either we have to accept computing systems that are good enough or look for alternative modifications to advance them without technological progress. There are several approaches, which can reduce this gap by improving system capabilities. Approximate computing is one of them. It is now becoming an interesting area for energy efficiency since computing-intensive applications such as visual processing, multimedia signal does not require accuracy to work correctly. In this paper, an approximate adder is proposed which is nearly equal to its accurate counterpart in terms of delay and accuracy. And have improvement in terms, power, and area over 50% when compared to conventional adder's implementation and 10% when compared to existing ones.

Key words: Approximate computing, approximate circuits, energy efficiency.

INTRODUCTION

A binary arithmetic operation such as addition, subtraction, multiplication, and division plays a vital role in digital computing systems. These operations use adders as the basic building blocks. The adders are used in multimedia applications as a prominent one. The area, power, delays are the main constraints of micro architecture system which depends on adder architecture. Among all traditional adders, Ripple Carry Adder (RCA) is the easiest one to construct and consumes less area, but the delay is more. Whereas the parallel prefix adder has less delay but the area is more. As the area is directly proportional to the power consumption, compare to RCA Parallel Prefix Adder consumes more power [1]. In contrast, any system prefers adders of less delay, low power consumption which any of these traditional adders does not meet the design metrics. By sacrificing the accuracy of system the delay, power design metrics can be improved. Many error resilient techniques are proposed in the previous work for the improvement of the delay and power [2]. The approximate computing technique attracted a lot of attention among the error- resilient techniques [3-9]. The main aim of the approximate computing is to implement the hardware and software systems by compromising the accuracy. The software approximate computing skips the algorithmic level computation. In hardware approximate computing the circuit level modifications can be done by truncation of the carry. In approximation computing technique the hardware level of approximation has been applied on arithmetic units. Among various arithmetic units adders are more significant. Here section II explains about Approximate Adders , Section III explains about Related works , Section IV explains the proposed work and section V experimental setup Section VI Results and conclusions and in Section VII References are explained.

II. APPROXIMATE ADDERS

Adders are extensively used in applications like digital signal processing. In multimedia, signal processing like many applications does not necessarily need the exact values; these applications can tolerate errors [2]. The main basic blocks can be replaced with an approximate one to reduce the delay and power metrics. Adders are the main basic building blocks of these applications. So modifying the adders will reduce the power, area, and delay [2-5]. The approximate adders can be implemented in the transistor level and gate level [2-5]. Here we are focusing on the gate level implementations. The approximate adder consists of two sub adder blocks, one is an accurate sub adder block and another one is the approximate sub adder block, shown in Figure 1 [5]. The accurate adder block contains higher order bits i.e., MSB bits, and the approximate sub adders block contains the lower order bits i.e. LSB bits. As MSB bits have higher weights the error percentage will be more compared to the lower order bits. So that the higher order bits cannot be approximated to reduce the error. The main aim of the approximate adder is to eliminate the carry chain. As because of the carry chain, the delay is more. By eliminating the carry chain the delay is reduced ,as because the carry circuit was reduced the power and area also reduces. The approximate adder will uses low power, area and reduces the delay by sacrificing the accuracy[5].

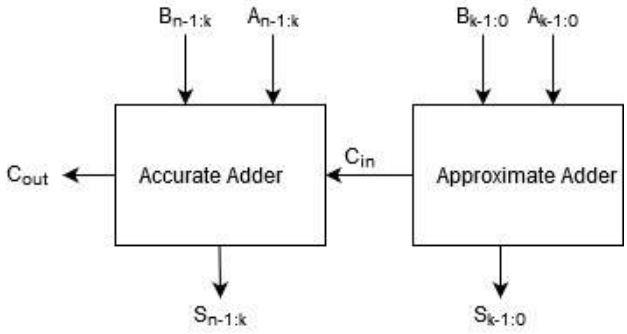

Figure 1: Approximate Adder Block Diagram

III. RELATED WORKS

Many approximate adders have been proposed previously [6]. The Approximate Full Adders (AFA) has been proposed by modifying the full adder architecture [6] . The carry circuit has been modified here. Full Adder equations can be expressed as

$$\text{Sum} = A \oplus B \oplus Cin \qquad (1)$$

$$\text{Cout} = (A \cdot B) + (B \cdot Cin) + (Cin \cdot A) \qquad (2)$$

Where A, B, C_{in} are the inputs to the adder and Sum, C_{out} are the sum and Carry out of the adder respectively [1]. The commonly used gate level implementation of the full adder is shown in

978-1-7281-8734-1/20/$31.00 ©2020 IEEE
DOI 10.1109/INDISCON50162.2020.00054

Implementation of Fault-tolerant techniques in Secure Non-volatile Main Memory Applications

SK. AFIFA FARMAN
M. Tech Scholar

Electronics & Communication Engg.
GRIET
Hyderabad, India
afifafarman642@gmail.com

CHAITANYA DUGGINENI
Professor

Electronics & Communication Engg.
GRIET
Hyderabad, India
chaiturohini@gmail.com

K. N. V KHASIM
Assistant Professor

Electronics & Communication Engg.
GRIET
Hyderabad, India
khasim.knv@griet.ac.in

2021 Second International Conference on Electronics and Sustainable Communication Systems (ICESC) | 978-1-6654-2867-5/21/$31.00 ©2021 IEEE | DOI: 10.1109/ICESC51422.2021.9532718

***Abstract*- Fault-tolerant techniques help detect and tolerate the faults in memories to improve the performance of the design. This article mainly considers the faults occurring in non-volatile main memories especially phase-change memory (PCM). Non-volatile memories have good performance advantages in recent market applications. Security of non-volatile memories is a key factor to focus on because data is present even after the shutdown of the power supply. Hence, to focus on security Advanced Encryption Standard algorithm utilized in this paper. Proposed Built-in self-test (BIST) fault-tolerant architecture shows better performance and reduction in area overhead compared to Randshift fault-tolerant architecture. These techniques are implemented in the Xilinx schematic software tool with the assistance of Verilog hardware description language. The simulation results show improvement in static timing analysis and reduction in area parameters. The motivation behind the proposed BIST architecture is to improve the performance of the design in consort with finding fault-free regions.**

Keywords- Stuck-at fault, Built-in self-test (BIST), Randshift technique, Linear feedback shift register (LFSR), Secure memories, Advanced Encryption Standard (AES), Circuit Under Test (CUT), Device Under Test (DUT).

I. INTRODUCTION

In this digital era, the popularity of computing systems has increased drastically. It has a huge impact on the storage of data. As technology grows day by day scaling down of the chip size causes significant challenges for volatile memories like DRAM and flash memory. It leads to a wider gap between processors and the memory capacity of cells [1]. This variation leads to cause a greater number of weak cells. These weak cells disadvantage in properties like data storage time which leads to cause a greater number of faults [2], [3].

Mainly memories are available as volatile and non-volatile. Because of cost and high-power consumption factors, volatile memories are not preferred. Fabrication is also complex hence designers preferring non-volatile memories over volatile memories.

Non-volatile memories for instance phase-change memory (PCM) in addition to resistive RAM (ReRAM) are providing high scalability and greater density which making them prefer over DRAM and flash memories [4],[5]. Even after the shutdown of the power supply, non-volatile memories contain data for up to a very long time when comes to volatile memories, they lose the data after the shutdown of the power supply. This is one of the main reasons to consider non-volatile memories over volatile memories. But these emerging memories like PCM and ReRAM facing endurance issues [6] which causes stuck-at faults in the memory cell.

In the present scenario phase-change memory (PCM) is considered as best and commercialized emerging non-volatile main memory. I am grabbing more attention from designers because of its excellent performance stated in articles [7],[8],[9]. Basic PCM cell consists of one transistor besides one resistor and is made up of chalcogenide material. To store ‘0’ and ‘1’ values the chalco-genide material present between two metals is heated. Recurrent heating of chalco-genide material causes stuck-at faults while storing ‘0’ or ‘1’ values in the memory cell. The storage array of a typical PCM cell as represented in fig (1) where BL represents bit line and WL represents word line and the selector can be a transistor, diode, or switches.

This paper compares two different fault-tolerant techniques, which supports to find the fault-free regions. This research work has proposed a BIST based fault-tolerant technique, whose test methodology helps in solving the issues like finding fault regions present in the design so that by removing or lowering the number of faults, the performance of the design can be improved. The area occupied by the BIST technique is very less as in recent years of integrated circuits. Hence BIST-based technique is preferred.

Proceedings of the International Conference on Electronics and Renewable Systems (ICEARS 2022)
IEEE Xplore Part Number: CFP22AV8-ART; ISBN: 978-1-6654-8425-1

2022 International Conference on Electronics and Renewable Systems (ICEARS) | 978-1-6654-8425-1/22/$31.00 ©2022 IEEE | DOI: 10.1109/ICEARS53579.2022.9752072

Ion Sensitive Field Effect Transistor as a Bio-compatible Device: A Review

1st Sankararao Majji
Research Scholar, Department of ECE
Centurion University of Technology and Management
Odisha, India
sankar3267@gmail.com

Chandra Sekhar Dash
Department of ECE
Centurion University of Technology and Management
Odisha, India
chandu0071@gmail.com

Asisa Kumar Panigrahy
Department of ECE
Gokaraju Rangaraju Institute of Engineering & Technology
Hyderabad, India
asisa.nist@gmail.com

***Abstract*—The ion-sensitive field-effect transistor (ISFET) is one of the most sensitive and adaptable sensors available, and it may be employed in modern complementary metal-oxide semiconductor (CMOS) techniques. As a result of its tiny size, low power consumption, and compatibility with industry-standard complementary metal oxide semiconductor (CMOS) technologies, potentiometric sensors like ISFETs are gaining appeal among sensor scientists and industrialists. These past decades have been broken down into three distinct time periods, which is described in detail in this paper to give an overview of what has been accomplished in the field over this. This work, briefly reviews about history, characteristic of the ISFET, and further discussion is performed about vivid applications of the ISFET.**

Keywords*— *ISFET, MOSFET, ISFET as biosensor, pH detection

I. INTRODUCTION

The ISFETs are comparable to MOSFETs with the former devoid of the gate material. The gate insulator which is the sensing layer of an ISFET is in direct contact with the electrolyte and requires a reference electrode to complete the gate to source circuit. The working of an ISFET may be explained effectively by the site binding theory and the electrical double layer theory. The ability of an ISFET device to be integrated with biologically active material helped it to explore into the field of biosensors [1]. It was noticed that ISFETs might be conveniently employed in conjunction with enzymes and other biological membranes generating an Enzyme Field Effect Transistor (ENFET). Since then, various different enzymes are being employed for different ENFETs. The enzymes are specific to a certain analyte. The enzyme Cytochrome P450 monooxygenase used in this work has the specificity of oxidizing n-hexadecane into n-hexadecanol. This enzyme has the potential of bio-monitoring as it oxidizes hydrocarbon which is an effective instrument in oil industry helping in monitoring environment deterioration by the oil spill [2].

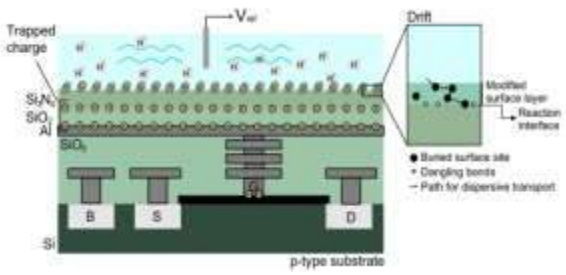

Fig. 1. Ion Concentration in ISFET [6].

Insulating membrane replaces the gate oxide in the ISFET, and the gate voltage is connected to an electrolyte reference electrode. It is possible to detect changes in the device's threshold voltage due to variations in ion concentration utilising specialized instruments [3-6]. When using traditional CMOS technology, the process metal is used as an electrode, as illustrated in Figure 1.

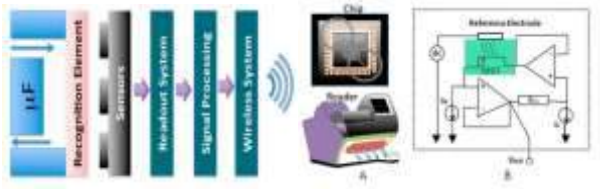

Fig. 2. Bio sensing Structure using ISFET [36].

A. I-V Characteristics of ISFET

I-V curves and transconductance plots of an ISFET biassed in the triode region are depicted in Figure 3 for illustration. V_{GS} vs I_D is virtually fully linear in biassing regions when gm approaches a rather flat peak [7-11]. As can be seen in the pH I_D graph, the projected pH to current conversion assuming a pH sensitivity that is close to ideal is easily discernible.

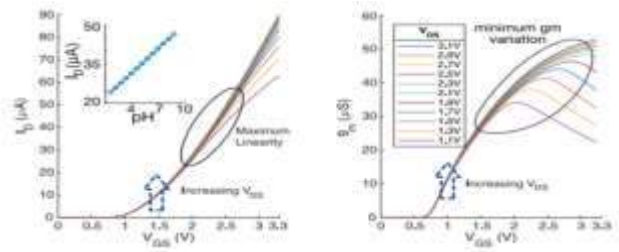

Fig. 3. I-V Curve of ISFET [4].

There was no need for an additional fabrication process to integrate ISFETs with ordinary silicon System-on-Chips, which resulted in essential advantages such as scalability and low cost. The device gains pH sensitivity thanks to this extended-gate approach, which utilizes the intrinsic top passivation material (Si3N4) as the insulating layer [12-14]. Figure 3 shows the reduced sensitivity that results from increased attenuation in the chemical input signal caused by capacitive division, which is one of the nonidealities. Capacitive effects regulated by the pH cause a corresponding shift in the device's floating gate voltage, which is simulated as the threshold voltage shift in this model. Dependency relationships look like this:

Proceedings of the Second International Conference on Electronics and Sustainable Communication Systems (ICESC-2021)
IEEE Xplore Part Number: CFP21V66-ART; ISBN: 978-1-6654-2867-5

2021 Second International Conference on Electronics and Sustainable Communication Systems (ICESC) | 978-1-6654-2867-5/21/$31.00 ©2021 IEEE | DOI: 10.1109/ICESC51422.2021.9532706

ARTIFICIAL INTELLIGENCE BASED MUSIC COMPOSITION SYSTEM-MULTI ALGORITHMIC MUSIC ARRANGER(MAGMA)

[1]Dr.R. Sabitha
Assistant Professor
Department of CSE
Karunya Institute of Technology and Sciences, Coimbatore
sabitha@Karunya.edu

[2]Sankararao Majji
Assistant Professor
Department of ECE
GRIET, Hyderabad, India
Sankar3267@gmail.com

Dr. M. Kathiravan,
Assistant Professor(SG), School of Computing Scineces, Hindustan Institute of Technology and science.
kathirrec1983@gmail.com

[4]S.Gopa Kumar
Assistant Professor
Department of ECE
Rohini College of Engineering and Technology, Tamil Nadu
sgopakumar1990@gmail.com

[5]K G Kharade
Assistant Professor
Department of Computer Science,
Shivaji University, Kolhapur
Maharashtra
kgk_csd@unishivaji.ac.in

[6]Santhoshachandra Rao Karanam
Assistant Professor
Department of IT,
Anurag University, Hyderabad
santoshit@anurag.edu.in

***Abstract*— A number of problems such as diagnosis, decision-making and optimisation were successfully solved through the methods of artificial intelligence (AI). However, any AI algorithm used for creative problems needs some replacement mechanism for human creative spark, as the computer has no creative potential. Randomness may not be the only mechanism to construct a creative structure, as created by a random number generator. This paper examines AI for music composition. In particular, the paper introduces MAGMA, which uses three different AI algorithms for music generation.**

Keywords- artificial intelligence, MAGMA, stochastic algorithm;

I. INTRODUCTION

Since the 1950s, computer-based music has been around [3]. The composition of the algorithm dates back centuries [4]. In the search of solutions to many problems, artificial intelligence (AI) techniques were applied, Includes emulation of human creativity in matters like composition of music. Through this review we will examine different AI applications and introduce in our edition three approaches to musical composition. We also analyse the findings and examine their strengths and limitations. The aim is to show AI approaches to automatic music composition. Composing and/or playing music is usually an artistic activity. It requires years of practice and study that people are skilled in composing or playing music. While music is an exciting and artistic form, there are several rules governing music composition, and the study of music theory is a wide-ranging endeavor. Computers and their running software are particularly suitable for the implementation of algorithms and rules. The effort to create music by computers and AI is therefore a way of recognizing and applying good music rules as software.

Music is composed in people in different ways. Some people "hear" and write music into their heads. Others prepare the music in a deliberative manner. Others spontaneously produce music by "jamming." Or, these techniques could be combined by musicians. These three methods may be viewed as applying music theory, applying the strategy, and using randomness in pruning music that "does not work," as calculated by some fitness assessment. Routine planning and genetic algorithms combined with a stochastic approach; we can use knowledge-based thinking in AI. The genetic algorithm is the primary method used in the current AI research (or some variation). Neural networks, fractal geometry and the chain of Markov are different methods.

There are several works with genetic algorithms, such as the Dash gene (4), which model each song as a different population., or the four-part harmonies and rhythms of Donnelly and Sheppard[5]. Contrary to the previous two systems, CONGA[6] uses people to analyse health of each piece of music and thus to determine how listenable a piece of music is using more than just music theory. In a harmonic sense, AMUSE is used in the development and evolution of improvised melodies[9] and BlueJam uses a mixture of genetic and heuristics[10].

II CONCEPT OF MAGMA

MAGMA is a currently under construction experimental AI system for composing music, in particular pop songs. To generate songs that are based on the chains of Markov, a routine plan algorithm and a genetic algorithm, a stochastic algorithm is used. The framework uses input user parameters and produces a song as a MIDI file.

MAGMA is designed to enable users to specify the song's preferences. The device produces a MIDI song file for one of the three algorithms based on these mood, repeat, variety, transition and range preferences. The database includes plain text files generated from musical sources, such as chord and melody progression songbooks and websites. Each database entry has its attributes marked so that MAGMA selects the entries that best fit the needs of the user to construct their transfer inventory arrays.

The routine planning algorithm uses a database of existing musical attributes to choose, similar to the stochastic process. In comparison to the stochastic approach using statistical information, a knowledge base for routine planning

Machine Learning Algorithms in 5g Cellular Network for Efficient Cognition

1st Chandra Sekhar Pasumarthi
Development Lead
Microsoft India Pvt Ltd
Hyderabad, India
pchandamama@gmail.com

2nd Akash Jain
Electronics & Telecommunication
SSIPMT Raipur
Chhattisgarh, India
jainakash007@gmail.com

3rd Narender Ravula
CSE Department
GITAM (Deemed to be University)
Hyderabad, India
narender7200@gmail.com

4th Shanthi Palaniappan
Sri Krishna College of Engineering and Technology
Coimbatore, India
shanthi@skcet.ac.in

5th Sankararao Majji
Department of ECE
GRIET
Hyderabad, India
sankar3267@gmail.com

6th S K Mydhili
Department of CSE
KGiSL institute of technology
Coimbatore, India
myura2u@gmail.com

2021 4th International Conference on Computing and Communications Technologies (ICCCT) | 978-1-6654-1447-0/21/$31.00 ©2021 IEEE | DOI: 10.1109/ICCCT53315.2021.9711802

***Abstract*— In today's communications and information technology business, cellular mobile networks are one of the technologies that has had the most significant impact on the industry. As part of the steps made to improve the overall quality of life, many aspects of everyday living, as well as technical breakthroughs, are becoming increasingly reliant on smart gadgets, which are becoming increasingly common. It is projected that, in the near future, every electric gadget will be a smart device that can be connected to the internet on a regular basis. A new network paradigm known as the vast cellular Internet of Things is created as a result, in which a large number of simple battery-powered heterogeneous devices work together for the improvement of humanity in all aspects. This system was developed in accordance with the standard simulation specifications for such systems, and the realistic data that will be extracted from it will aid in demonstrating the effectiveness of the proposed algorithms in order for them to be included in the 5G cellular communications technology.**

Keywords—5g Cellular, Internet of Thing, Network design.

I. INTRODUCTION

The scarcity of energy and bandwidth is a problem for wireless communication systems since it affects the quality of service and the capacity of the channels [1]. Most of the research in wireless networks focuses on new communication and networking paradigms that use these limited resources more intelligently and efficiently than previous paradigms. In order to make better use of limited network resources in a more effective and flexible manner, cognitive radio is a fundamental enabling technology that allows radios and other devices to adapt their operational settings to changes in the surrounding radio environment. The popularity of cognitive radio is rising. Cognitive radio is a critical enabling technology that helps radios and other devices make better use of scarce network resources by using them more efficiently and adaptably. Things like signal power, frequency, and modulation type fall under the category of transmission characteristics.

Different from ordinary radio devices, Cognitive Radio devices are equipped with cognitive capabilities and configurability, allowing them to adapt to the fluctuations in the surrounding radio environment [2]. In order for a device to have cognitive capabilities, it must be able to detect and receive important information about things like transmission power and frequency as well as modulation type. The cognitive user will be able to choose the best spectrum for his or her needs if they have this capability. When new information is detected, the cognitive user may quickly adjust the transmission settings to get the greatest possible performance out of the CR.

Machine Learning is a branch of Artificial Intelligence that has recently received a great deal of attention from researchers, owing to the advent of large amounts of data to analyse. Because there are numerous sources that generate the data, the data is available in a wide range of sizes and formats to suit the needs of the user [3]. It is also important to note that the data is generated at a rapid pace. As a result of their development, machine learning algorithms have proven to be extremely effective in a wide range of applications ranging from finance to telecommunications to healthcare to retail to education and other fields. Using historical examples, often known as training data, machine learning is used to improve performance indicators by identifying patterns. First, a model is constructed using the training data, and then learning is applied to the model in order to improve its performance metrics. The model can be predictive, in which case it is used to anticipate the outcome of test data [4]. descriptive, in which case it is used to characterise the data in order to gain information from the data; or both predictive and descriptive.

Figure 1: Components in Internet of Things (IoT)

Multihoming refers to a network that contains a large number of users who are dispersed around the physical Internet of Things environment [6]. We can improve the quality of life for everyone by utilising the Internet of Things to provide services such as real-time monitoring, information exchange, and other added-value features. In addition to providing smart environment and healthcare services, the Internet of Things (IoT) serves as a platform for smart transportation, smart agriculture, smart e-government, and other services connected to manufacturing products [7]. It is

5G Network Virtualization for the Remote Driving Enhancement

1st N Sendhil Kumar
Department of MCA
Sri Venkateswara College of Engineering and Technology
Tirupati, India
sandy.g05@gmail.com

2nd Upinder Kaur
Assistant Professor
Akal University
Talwandi Sabo, India
drupinder2016@gmail.com

3rd Dr. Anuradha T
Department of EEE
KCG College of Technology
Chennai, India
tanura1872@gmail.com

4th Sankararao Majji
Department of ECE
GRIET
Hyderabad, India
sankar3267@gmail.com

5th Santoshachandra Rao Karanam
Department of IT
Anurag University
Hyderabad, India
kschandra.rao@gmail.com

6th Radhika G Deshmukh
Department of physics
Shri Shivaji Science college
Amravati, India
radhikadeshmukh35@gmail.com

2021 4th International Conference on Computing and Communications Technologies (ICCCT) | 978-1-6654-1447-0/21/$31.00 ©2021 IEEE | DOI: 10.1109/ICCCT53315.2021.9711894

***Abstract* - For mobile machinery to be operated remotely, a dependable wireless communication system is required. With five generations of wireless networks, remote operations, real-time control, and data collection will be ultra-reliable and low latency. Using 5G radio, digital twins, hardware-in-the-loop development, and our own experiences with the system, we show how a remote mobile machinery control system works. According to our findings, future 5G networks will have a significant reduction in latency and jitter compared to existing LTE infrastructure when using a proper edge computing architecture.**

Index Terms – 5G networks, LTE, Digital twin, Jitters.

I. Introduction

There have been numerous life-changing technologies on the heels of the wireless data network's steady progress over the last 30 years. During the early 1980s, the launch of the first analogue cellular system marked the beginning of modern evolution. People could finally communicate while on the road, despite the fact that cell phones were still uncommon.

5G services have now been offered by more than 90 different providers in over 40 different countries, indicating that 5G commercialization is now becoming more commonplace. This launch's most notable feature is 5G's increased level of network complexity [1]. The bandwidth available for 5G can power a wide range of apps and services, as well as enabling new business applications like fixed wireless access. Due to the increased demand for private 5G networks and the integration of Sub-6 GHz and mmWave technologies, networks are adopting these new technologies to suit those needs.

Since there are so many potential use cases for 5G, it's evident that we'll need a more scalable and adaptable network architecture to support them all. Parallel to this, software virtualization in telecommunication networks is becoming more prevalent. It's becoming increasingly common for mobile operators and network equipment manufacturers to use virtualized radio access networks (vRAN) and open interfaces to connect their networks. Although increased data rates and processing loads associated with 5G Sub-6 GHz massive MIMO and millimeter-wave technologies necessitate optimised System-on-Chip (SoC) solutions, these solutions are still required.

People could exchange text messages using second-generation and 2.5G mobile systems by the early 1990s, but broadband internet access via 3G didn't become widely available until the turn of the new millennium [2]. Phones have progressed from being simple gadgets for placing and receiving phone calls to being multifunctional tools for communication, entertainment, and shopping.

As the most recent advancement, 4G is capable of sharing real-time information and location in real time. Due to this change, the sharing economy was made possible, and startups like Uber and Lyft were born. Though faster than a human reflex, it's still not fast enough to accommodate newer technologies. The answer to this problem will be provided by the advent of 5G.

A. Network Virtualisation

Our 5G Radio Access Network (RAN) Platform portfolio will include three new platforms by the second half of 2018: the Qualcomm Radio Unit (QRU) Platform, Qualcomm Distributed Unit (QDU), and the Qualcomm Distributed Radio Unit Platform. Qualcomm Technologies has a strong track record of delivering infrastructure solutions. A Qualcomm Radio Unit Platform-based SoC solution takes care of wireless front end and antenna issues [3]. The Qualcomm Distributed Unit includes integrated sub-6 GHz/mm Wave capabilities (QDU). Verizon Wireless (Cingular) (QDU). With the Qualcomm Distributed Radio Unit Platform, both units have been integrated into a single unit for compactness's sake

Consolidating hardware and software resources into a software-based virtual network is known as network virtualization. Mobile network operators (MNOs) are turning to network virtualization as a way to better manage their

Machine Learning Techniques for the Energy and Performance Improvement in Network-on-Chip (NoC)

1st Dr. J RamaDevi
CSE Department
PVP SIDDHARTHA Institute of Technology
Vijayawada, India
k.ramakarthik@gmail.com

2nd Dr. S Karunakaran
Department of ECE
Vardhaman College of Engineering
Hyderabad, India
s.karunakaran@vardhaman.org

3rd Sankararao Majji
Department of ECE
GRIET
Hyderabad, India
sankar3267@gmail.com

4th Dr. S Pathur Nisha
Department of CSE
Nehru Institute of Technology
Coimbatore, India
thanish05@gmail.com

5th Hemavathi S
Scientist, Battery Division
Central Electrochemical Research Institute
Chennai, India
hemavathi@cecri.res.in

6th Anandaraj Shunmugam
School of CS & IT
DMI-St. John the Baptist University
The Republic of Malawi, Central Africa
anandboyzz@gmail.com

2021 4th International Conference on Computing and Communications Technologies (ICCCT) | 978-1-6654-1447-0/21/$31.00 ©2021 IEEE | DOI: 10.1109/ICCCT53315.2021.9711872

***Abstract* - On resource-constrained embedded devices (e.g., Internet of Things nodes), deep neural network inference requires specialized architectural solutions to deliver the greatest possible performance, energy, and cost trade-offs. In this regard, a Network-on-Chip architecture with many parallel and specialized cores is one of the most promising (NoC). An architecture parameter that impacts deep neural networks' performance is the number and size of memory interfaces. Using these and other architectural criteria, we investigate the design space that can be created. We demonstrate how on-chip communication dominates delay while memory consumes the majority of energy. According to the findings, a new research area devoted to improving the performance and energy efficiency of on-chip communication fabrics and memory subsystems should be established.**

***Index Terms* - *Network-on-Chip*, neural network, Machine Learning.**

I. Introduction

Cores, last-level caches, and memory modules on a chip are now all connected via Network-on-Chips (NoCs). As of now, many-core devices have anywhere from a few dozens to several hundred cores, with thousands of cores expected in the future. The NoCs, on the other hand, use a significant part (between 10% and 36% of the chip's total power). The power issue will only get worse as transistor feature sizes continue to shrink and more power is used for communication than computation. In order to make future NoC designs more power-efficient, a number of studies have been proposed.

To save as much power as possible, it's critical to blend the advantages of numerous strategies. Static power can be reduced using the Power Gating (PG) approach. Reducing dynamic power is possible with the help of dynamic voltage and frequency scaling (DVFS). Static and dynamic power reduction can both be achieved with a combined PG/DVFS system. A poor outcome could be caused by the dynamic interactions between these methods and the network. Dynamic power is squandered when a DVFS decision is overstated. An overestimation of DVFS, on the other hand, could lead to network congestion, which reduces the amount of time $its are idle. This has an adverse effect on static power reduction because the PG decision is made during these idle cycles. For this reason, it is necessary to implement a preventative control policy. Exploring different application behaviour can also increase decision accuracy and power savings, but it complicates the control strategy in the process of doing so. The NoC, cache, and miss status holding registers' behaviour can be influenced in many ways by applications (MSHRs). Application-specific network utilization and message information are generated at the NoC level [1]. Examples of network communications that show the criticality of data include load/store and response/request. Processing power is connected with L1 instruction and data cache activity, whereas information regarding NoC traffic is gleaned from information in the L2 cache and in the MSHR. If this data can be gathered, decision accuracy and power savings may improve, but control policy is complicated and substantial engineering work is required. NoC design can be optimized using traditional control techniques or, more recently, supervised learning. When using a PID controller, the output variances are monitored and the logic is computed by taking the quotient of the proportional, integral, and derivative values. The empirically tuned parameters, on the other hand, may not be able to withstand changes in the applications or uncertainty in NoC behaviour due to their nature [2]. Similarly, in order to construct labelled training examples prior to the training phase, supervised learning necessitates human expertise and engineering.

A. NoC Architecture

Complex on-chip computing platforms necessitate an effective means of managing communication among the many on-chip components. The resources that communicate with one another do so via bus and crossbar architectures. The drawbacks of using a bus-based communication strategy include the need for a large amount of wire space, which can lead to a scalability issue as the number of resources increases due to serialization in the communication, as well as the possibility of significant latency and fan-out when arbitrating for a shared medium [3]. Although serialization is eliminated

Proceedings of the Fifth International Conference on Electronics, Communication and Aerospace Technology (ICECA 2021)
IEEE Xplore Part Number: CFP21J88-ART; ISBN: 978-1-6654-3524-6

Broadcasting of IoT-Connected Autonomous Vehicles in VANETs Using Artificial Intelligence

*1st Upinder Kaur
Department of Computer Science
Akal University
Talwandi Sabo, India
drupinder2016@gmail.com

2nd Dr. Anuradha T
Department of EEE
KCG College of Technology
Chennai, India
tanura1872@gmail.com

3rd Paparao Nalajala
Dept. Of ECE
Institute of Aeronautical Engineering
Hyderabad, India
nprece@gmail.com

4th Sankararao Majji
Department of ECE
GRIET
Hyderabad, India
sankar3267@gmail.com

5th Dr. Sushma Jaiswal
Department Of CSIT
Guru Ghasidas Vishwavidyalaya
Bilaspur, India
jaiswal1302@gmail.com

6th Dinesh Jamthe
Computer Science & Engineering
Priyadarshini Bhagwati College of Engineering
Nagpur, India
dineshvijayjamthe@gmail.com

2021 5th International Conference on Electronics, Communication and Aerospace Technology (ICECA) | 978-1-6654-3524-6/21/$31.00 ©2021 IEEE | DOI: 10.1109/ICECA52323.2021.9676127

Abstract* - *A future where computers take over driving could be paved by autonomous vehicles on Vehicular Ad-hoc Networks (VANET), a wireless network that spontaneously forms to exchange data about automobiles. In order to communicate properly amongst the cars, it helps transfer secure messages. Unauthorized access, such as sending bogus VANET messages, poses a serious risk. As a result, remedial action should be initiated early in the architectural process. To prevent a DoS attack, an equal balance between message authentication and DoS protection must be maintained while the VANET network is authenticating each message. A wide range of security-demanding circumstances and message transmission security solutions are discussed in this work.

***Index Terms –VANET, DoS,* Unauthorized access.**

I. Introduction

Ad hoc networks (VANETs) are mobile ad hoc networks in vehicles with infrastructure, such as cars and trucks (MANETs). In today's world, cars are necessities that are only getting better with time. To make judgments and assist the driver while driving, "smart" vehicles utilize a number of technologies including computers and sensors. They also use communications and artificial intelligence systems. As a result, new technologies are advantageous in a wide range of situations. Vast interest in VANET has been generated in academia and the automobile sector. For reasons of safety, convenience, and comfort, many automakers are incorporating communication devices inside their automobiles. Moreover, government groups have acknowledged the VANET's growing importance. The FCC has designated a specific portion of the radio spectrum for use by car networks. The National Highway Traffic Safety Administration (NHTSA) and the NHTSA have added intelligence layers to automobiles.

P2P, multiple hop, and vehicle-to-infrastructure (V2I) communication are just a few examples of VANET technology uses. There are a range of uses for the networked transportation systems known as Intelligent Transportation Systems (ITS). These communication mechanisms allow the car to react automatically to avoid collisions with other vehicles in its vicinity while still being completely transparent to the driver who is operating it. Vehicular-to-vehicle communication (V2V) involves vehicles communicating directly with one another on the road, while vehicle-to-infrastructure communication (V2I) involves vehicles communicating directly with existing road infrastructures like GSM, UMTS or WiMAX networks via fixed equipment. VANETs have a complex architecture that includes a wide range of hardware and software elements. There is an OBU (On-Board Unit) in VANET cars. When communicating with roadside infrastructure, RSUs (Road Side Units) is commonly referred to. Cameras are available as options on a few automobiles. To develop or alter routes based on computer vision, cameras capture images of scenarios in front of the vehicle and send them to sensors on board. Vehicles can be made to return to their proper lanes by using sensors that detect when they've drifted off course. Despite its success, this technology has drawbacks, especially in bad weather.

As a result of mobile communication technologies revolutionizing the automotive sector in the previous decade, gadgets can now communicate with one another no matter where they are or what they are doing. With such ease of connectivity, important data can be exchanged between devices while they're in use. The real-time flow of information has become a new paradigm in the industry because of how frictionless it is. As a result, developments in information and communication technology have made mobile device communication a no-brainer [5]. These advancements have led to new options for the use of safety applications, such as the VANET (Vehicular Ad-hoc Networks). Using a wireless channel, VANET connects various moving vehicles and connecting devices, exchanging important data. Vehicles and other equipment act as nodes in a tiny network that is being

Proceedings of the Fifth International Conference on Electronics, Communication and Aerospace Technology (ICECA 2021)
IEEE Xplore Part Number: CFP21J88-ART; ISBN: 978-1-6654-3524-6

Image Processing Approaches for Oral Cancer Detection in Color Images

1st Amarjeet Singh
Computer Science and Engineering
New Horizon College of Engineering
Bengaluru, Karnataka, India
dean.academics@newhorizonindia.edu

2nd T Ch Anil Kumar
Department of Mechanical Engineering
Vignan's Foundation for Science Technology and Research
Guntur, Andhra Pradesh, India
tcak_mech@vignan.ac.in

3rd Tiruvedula Mithun
Senior Software Engineer
Leanovate Info Solutions
Benguluru, Karnataka, India
tiruvedulamithun@gmail.com

4th Sankararao Majji
Department of ECE
GRIET
Hyderabad, India
sankar3267@gmail.com

5th Mooda Rajesh
Department of ECE
Mallareddy Institute of Technology and Science
Maisammaguda, Telangana, India
rajeshmrajum@gmail.com

6th Palagati Anusha
Computer Science and Engineering
KMM Institute of Technology and Science
Tirupati, Andhra Pradesh, India
palagatianushareddy@gmail.com

2021 5th International Conference on Electronics, Communication and Aerospace Technology (ICECA) | 978-1-6654-3524-6/21/$31.00 ©2021 IEEE | DOI: 10.1109/ICECA52323.2021.9675897

***Abstract*— Lips, two-thirds of the tongue and inner cheek lining are all common places for oral cancer to form. It can also arise in hard and soft palates, pharynx, and sinuses. Head and neck cancers are subtypes of this malignancy. Unless detected and treated early on, oral can be dangerous. Using microscopic biopsy images, the researchers were able to detect mouth cancer and non-cancerous lesions. Using cutting-edge techniques, it is possible to histologically diagnose oral lesions. For example, enhancing microscopic images involves transforming them from RGB to L*a*b color space, classifying the colors using k-means clustering, segmenting the nuclei, and obtaining and classifying their features.**

Keywords*— *Microscopic biopsy, RGB, Nuclei, k-means clustering

I. Introduction

Hippocrates created the term "cancer" (Latin for "crab") in the fifth century to designate a group of disorders. As the cells multiply and spread throughout the body, they suffocate the organism. Cancer is a disease produced by cells that have malfunctioned and lost control over their own proliferation, to put it simply [1]. Tumours and neoplasms, which are both medical terms for the same mass of cells, grow in size over time. It is possible for cancer cells to disseminate throughout the body, causing new tumours to grow in other parts of the body; this is known as metastasis. Several factors contribute to cancer, including faulty genetics and exposure to insults from the environment. Smoking and chewing tobacco are two practises that increase one's risk of developing mouth cancer, which is a life-threatening disease. A cancerous growth can appear anywhere in the body, and it is usual practise to label cancers depending on the organ or cell type from which they originate, resulting in more than 100 distinct forms of cancer. It is estimated that mouth cancer accounts for about 5% of all cancers in the head and neck region of people.

Oral cancer is the fifth most common cancer type and the eighth most common cause of cancer-related mortality worldwide, according to the World Health Organization. Globally, oral cancer is becoming increasingly burdensome despite advances in early detection and treatment technology. The incidence of oral cancer is on the rise across the globe. Oral cancer claims the lives of 30 percent of men and 12 percent of women over the world. There are numerous risk factors for oral cancer, but smoking and chewing tobacco are two of the most important. Tobacco smoking increases the risk of oral cancer in all forms. Smoking-free tobacco is a major risk factor for the onset of oral cancer (SLT).

Around 1,30,000 people die each year with this cancer because of tumours in the salivary glands, tonsils, neck, head, face, and oral cavity. For men, their mouth cancer risk is double that of women, and for men over the age of 40, their risk is even higher. Furthermore, over 25% of all oral cancers occur in non-smokers who also use alcohol on occasion [2]. 75 percent of oral cancer cases may be traced back to tobacco and alcohol use. Other risk factors include poor dental hygiene, malnutrition, and recurring infections. Cancer of the mouth and throat is known as oral cancer. Oral cancer is quite frequent, but if detected and treated early enough, it is highly curable. Mouth cancer, another name for oral cancer, is very common. This might occur in any of the oral tissues. Oral malignancies come in a variety of forms, but the most common is squamous cell carcinoma, which develops in the soft tissues of the mouth and lips. Oral cancer, often known as mouth cancer, most commonly affects the gums, lips, or palate roof in the mouth. Squamous cell carcinoma is the medical term for the majority of mouth malignancies. Initial signs and symptoms include things like tingling or numbness in the tongue or lips. If the tumour has spread, you may experience a burning feeling as well as swallowing difficulties and oral sores, among other things [3].

Modern methods allow for the histological diagnosis of oral lesions. Digital images of microscopic slides are an example of such a modality; they're an advancement in contemporary day diagnosis. The PC can handle several new highlights as a result of this digitization. It's possible to imagine new uses for image analysis, and those uses can be made more routine. The morphology of nuclei and cell shape are unaltered in a healthy tissue's cell-to-cell adhesion. No matter what the cause, alterations in the oral epithelium can lead to cancer in the mouth or throat. Squamous cell carcinoma of the mouth is the most common type of head and neck tumour (SCC).Cervical cancer has numerous dysplastic characteristics on a morphological and histological level. A new approach was used to distinguish between normal oral tissues and oral cancerous tissues in histology slides. There was more focus on building the programme for cancerous and non-cancerous tissues because this was a pilot project [4].

Proceedings of the Fifth International Conference on Electronics, Communication and Aerospace Technology (ICECA 2021)
IEEE Xplore Part Number: CFP21J88-ART; ISBN: 978-1-6654-3524-6

FPGA Implementation of Arbiter PUFs for ideal Cryptographic Key Generation

1st Komma Anitha
ECE Department
Prasad V Potluri Siddhartha Institute of Technology, Vijayawada, India
anithakomma108@gmail.com

2nd Kiran Kumar Gopathoti
Department of ECE
Institute of Aeronautical Engineering
Hyderabad, India
kirankumar.gopathoti@gmail.com

3rd J Rajeswari
Lecturer in ECE
Government Polytechnic for women
Kakinada, India
rajeswari.joga2@gmail.com

4th Sankararao Majji
Department of ECE
GRIET
Hyderabad, India
sankar3267@gmail.com

5th Tulasi Radhika Patnala
Developer
Shanax Technologies
Hyderabad, India
tulasichandra2010@gmail.com

6th Damaraju Sri Sai Satyanarayana
Scholar
Chalmers University of Technology
Goteborg, Sweden
errorbots01@gmail.com

2021 5th International Conference on Electronics, Communication and Aerospace Technology (ICECA) | 978-1-6654-3524-6/21/$31.00 ©2021 IEEE | DOI: 10.1109/ICECA52323.2021.9676119

***Abstract*— It is critical in today's security-conscious environments and communications to create unique identities, and this can be done with software or hardware. Hardware can create a reliable and unique identity with less complexity than software because software requires more complex algorithms to keep the secret hidden from the adversaries. PUF is the name of one such basic circuit. Even when made using a nominally identical process, no two physical objects are exactly the same. When presented with a binary input, a PUF circuit responds with a binary, device-unique output. A PUF circuit is designed to be sensitive to manufacturing process variations. PUF as a hardware primitive is used as an authentication device in the real-world practical application scheme. The proposed IoT node-to-node mutual authentication algorithm does not require a server or a trusted third party. FPGA boards are used to implement the algorithm's main modules, such as the Nonce generation logic and the unclonable response generation logic. In spite of identity theft, PUF-based authentication schemes have the assurance that malicious parties cannot replace the intended PUF-based node.**

Keywords—Arbiter PUF, FPGA, Ring Oscillator (RO);

I. INTRODUCTION

For security-conscious environments and communications, the creation of unique identities — whether software or hardware — is critical. Because software requires more complex algorithms to keep the secret hidden from the adversaries, hardware can create a reliable and unique identity with less complexity. One of these fundamental circuits goes by the name of PUF. No two physical objects are exactly the same, even if they were made with the same process. In response to a binary input, a PUF circuit generates a binary output that is specific to the given device. When designing a PUF circuit, the goal is to make it sensitive to changes in the manufacturing process. The real-world practical application scheme makes use of PUF as a hardware primitive as an authentication device. With this new IoT mutual authentication algorithm, there's no need for a server or third-party trust [1]. The main modules of the algorithm are implemented using FPGA boards, such as the Nonce generation logic and the unclonable response generation logic. Although PUF-based authentication schemes are vulnerable to identity theft, the assurance that malicious parties cannot replace the intended PUF-based node makes them a good choice in the face of these threats.

In cryptography, codes are used to protect data from unauthorised users by making them unintelligible. According to Wikipedia, the term "cryptography" comes from the Greek words "crypto" (meaning “secret”) and “graph” (meaning “writing”), respectively [2]. As a result, the term "cryptography" refers to the practise of writing confidentially. The context recently discussed the tools and systems defined to generate secure messages for member communication and defend against hacker's attacks. As a result, cryptography is critical for secure private communication over a public network. Cryptography Computing algorithms and mathematical theory are used in general in cryptography to work on secure transmission systems. As a result, encryption, decryption, watermarks, pseudo-random numbers, and so on all contribute to security.

Cryptography is based on four fundamental principles. Each of these terms refers to a different aspect of the security model. To ensure data privacy, it's important to follow the confidentiality principle. Consistency and accuracy of data are key components of the data integrity principle [3]. You recognise yourself to your communication partner through the process of authentication. Non-repudiation is the ability to verify the authenticity of a digital signature in order to ensure that the person who created a message is the real sender. There are two basic types of cryptography: symmetric and asymmetric. A symmetric system encrypts data using the same key on both systems. Symmetric cryptography can take many forms. The cypher algorithm uses a key, which is a generated value, to convert plain text into cypher text. In order to recover the plain text, the ciphertext must be decrypted using the same key as before. The execution time of symmetric cryptography algorithms is reduced. Symmetric cryptography algorithms include those that use mono alphabetic substitution [4]. This method uses a one-to-one correspondence between plain text and cypher text characters.

II. PUF MECHANISM

For a single Challenge C, the PUF mechanism implemented on similar ICs embodied with PUF generates a variety of Responses R1, R2, R3 and R4. This pictorial representation of the PUF mechanism shows this.

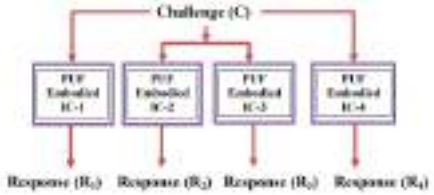

ISBN 978-1-6654-3986-2

Design, fabrication & control of modified SHRALA robot for campaigning in Indian Election

SHRALA – Social Humanoid Robot Based on Autonomous Learning Algorithm

Mounica Sakhinethi
PG Scholar, M.Tech Embedded Systems, Dept of ECE
Gokaraju Rangaraju Institute of Engineering & Technology
Hyderabad, India.
mounicasakhineti@gmail.com

Sudharsan Jayabalan
Associate Professor, Dept of ECE
Gokaraju Rangaraju Institute of Engineering & Technology
Hyderabad, India.
sudharsan.jayabalan@gmail.com

2021 International Conference on System, Computation, Automation and Networking (ICSCAN) | 978-1-6654-3986-2/21/$31.00 ©2021 IEEE | DOI: 10.1109/ICSCAN53069.2021.9526544

***Abstract*—During this covid-19 pandemic most of the countries have successfully conducted the parliamentary, state, and local elections. It was unfortunate that few candidates have been infected by the virus and lost their golden time in canvassing during their election campaign. One of the candidates (name and state kept anonymous) who was contesting elections in India was infected by the virus just 15 days before the election. The candidate isolated himself and was under medical treatment in hospital for few days. So, we intended to assist the candidate by modifying our SHRALA (Social Humanoid Robot based on Autonomous Learning Algorithm) as a campaign robot. Despite the challenging pandemic situation and limited availability of the resources the robot was designed, fabricated, tested, and deployed in less than 5 days. This paper discusses the approach and experience in the design, fabrication, testing and deployment of SHRALA robot in the election campaign. The robot performed beyond our expectation as it attracted more people towards it, most of them were curiously interacting with the robot and taking selfies. Based on our experience, future directions of the campaign robot are suggested as these robots can make huge impact in the election campaign strategy.**

Keywords— Social Robot, humanoid robot, election robot, campaign robot, SHRALA, Mobile Robot.

I. INTRODUCTION

Due to the widespread of the corona virus in 2020, the normal life has come to a halt in most of the countries. Countries have taken serious measures to curb and prevent the spread of the corona virus by implementing lockdown in several phases. Some of the countries have even faced third and fourth wave of corona viruses, which took so many people life and has put a huge dent in the economy of the middle- and lower-income group. The rate at which the corona virus spreads has increased drastically during the second wave and the third wave. Severe social distancing norms were followed in public places and in most of the places wearing of face masks and gloves has been made compulsory. It has been reported that in a wedding gathering almost 60% of the people who have been infected by coronavirus at the same time. almost similar amount of infection rate was reported in most of the large public gathering places like exhibition center, educational meeting, sports events, tourist places and places of worship etc. The worst part is that these viruses are so dormant for the first few days and slowly weaken your immune system and take over your body. A healthy individual with high immune system will not notice that he is an actual career of the corona virus for the first few days or until his immune system is weak. During these few days being an inactive career, the person spreads the virus to few other people around him in whatever the places he visits, and this cycle keep continues from one to view and waves of cases are being reported. There are only two ways to control this, the first way is through vaccine and the second way is through staying indoors the former seems to be a wise decision while the later one leaves the huge economic and career dent in that individual's life.

Despite knowing the severity of the situation some of the countries have successfully completed the lockdown while some other countries are in the process or yet to conduct them. The worst part is that during the election campaign and vote canvassing large number of public people will gather and which increases the possibility of infections to all these people. In some cases, some of the candidates who are contesting for the elections have also got corona virus. Most of these candidates have isolated themselves and were under proper medical treatment. Some of these candidates miss their golden time of vote canvasing, while few of them used digital media as their campaign platform. Even though so many robots like reception robot [1], social interaction robot [2-4] and food delivery [5-7] are available it was so hard to find these robots are similar robots being used as assistive mechanism during the election campaign for the candidates. This was mainly because as most of these robots are manufactured and imported from other countries. These robots are sold here with little modification to serve the necessary local application. During this pandemic because of ban in imports of the components and machinery it became difficult for the local people to develop the election campaign robot.

One of the candidates contesting in an election in India was infected by the corona virus and was isolated and was in a proper medical care. However, he was carrying out the election campaign using digital medium like others. So, considering this situation we have modified our existing SHRALA robot [8] and developed a new SHRALA –

Materials Today: Proceedings xxx (xxxx) xxx

Contents lists available at ScienceDirect

Materials Today: Proceedings

journal homepage: www.elsevier.com/locate/matpr

Recent developments in code compression techniques for embedded systems

Dumpa Prasad [a], P. Rahul Reddy [b], B. Sreelatha [c], Koya Jeevan Reddy [d], Sudharsan Jayabalan [e], Asisa Kumar Panigrahy [e,*]

[a] Department of Electronics and Communication Engineering, Sasi Institute of Technology and Engineering, Tadepalligudam, India
[b] Department of Electronics and Communication Engineering, Geethanjali Insititue of Science & Technology, Nellore, India
[c] Department of Electronics and Communication Engineering, Geethanjali College of Engineering & Technology, Keesara, Telangana 501 301, India
[d] Department of Electronics and Communication Engineering, Sreenidhi Institute of Science and Technology, Yamanapet, Ghatkesar, Telangana 501 301 India
[e] Department of Electronics and Communication Engineering, Gokaraju Rangaraju Institute of Engineering & Technology, Hyderabad 500090, Telangana, India

ARTICLE INFO

Article history:
Received 8 February 2021
Received in revised form 18 February 2021
Accepted 21 February 2021
Available online xxxx

Keywords:
Embedded systems
PDA
Code compression
LUT
Compressed instructions

ABSTRACT

Embedded applications software code is increasingly growing in size. Whereas the entire code of all control panels in a car provided for roughly a few 100 K code lines a decade ago, a single control panel such as the engine control can now have up to 1million code lines. With these help of good approach, common scenarios are developed for other, even for mobiles, embedded systems like PDA's, cell phones etc. However, increasing software size requires greater memory and can therefore raise the cost of an embedded system considerably. The starting of this pattern was already established in the early 1990 s. The compressed code is created by compressing the binary numbers using a code compression tool (at the time of design) is stored in the instruction memory of the embedded devices. The compressed instructions are decompressed and implemented by the processor at the time of startup. One of the serious challenges is that the tables will become wide in size and therefore decrease the benefits of compressing the code that could be accessed. Although the whole research in this area has mostly concentrated on improving greater code compression without specifically targeting the issue of wide look-up table sizes.

Selection and peer-review under responsibility of the scientific committee of the International Conference on Materials, Manufacturing and Mechanical Engineering for Sustainable Developments-2020.

1. Introduction

An extremely slower processor and limited memory sizes are commonly utilized by embedded devices to reduce costs. There is also an approximately 5 billion embedded microprocessors are being used now-a-days, as per the World Semiconductor Trade Statistics Blue Book. The major determinant for the rising prevalence of embedded device- driven portable devices like (Personal Digital Assistants) and web-platform mobile phones is the global expansion of their implementation, example the world demand for embedded devices will rise from about $1.6 billion in 2004 to $ 3.5 billion to 2009 a Average Annual Growth Rate(AAGR) of 16%. Because due to the requirements of the embedded industry, the memory chip of the embedded device must be tiny, various techniques are utilized to minimize the size of the embedded software by encoding it inactive and then decoding it active. In the field of individual instruction problem use generally a RISC processor, the concept of utilizing code compression as a method for chip size mitigation in microprocessors has most triggered concern. Furthermore many developments in IC integration techniques to explore another direction which surely impedes the speed of processing[1–7].

The method of compression of code can be utilized when the ISA (Instruction Set Architecture) may or may not be defined. When the ISA ids defined, to create the decoders hardware, the code compression algorithm uses the data in opcode or instruction format. In this situation, the compression ratio will be increased, as the amount and type of operands can be minimized as according o the operation specified by the opcode in the instruction format. If the ISA is not defined, the code compression method implements

* Corresponding author.
E-mail address: asisa@griet.ac.in (A. Kumar Panigrahy).

https://doi.org/10.1016/j.matpr.2021.02.643
2214-7853/
Selection and peer-review under responsibility of the scientific committee of the International Conference on Materials, Manufacturing and Mechanical Engineering for Sustainable Developments-2020.

IMPROVED IMPERIALIST COMPETITIVE ALGORITHM BASED ENERGY EFFICIENT PEAK TO AVERAGE POWER RATIO (PAPR) IN COOPERATIVE MIMO-AF SYSTEMS

S. Kanithan[1], Arun Ananthanarayanan[1], N Arun Vignesh[2*], Dr Thirunavukkarasu Kannapiran[3],
N. Srinivasarao[4], N. Kumareshan[5], S.Madhusudhanan[6]
[1]Department of ECE, MVJ College of Engineering, Bengaluru-560067
[2]Department of ECE, Gokaraju Rangaraju Institute of Engineering and Technology, Hyderabad-500090
[3]Professor & Head of Data Science, Unitedworld School of Computational Intelligence,
Karnavati University, Gandhinagar-382422
[4]Department of ECE, BVRIT Hyderabad College of Engineering for Women, Hyderabad-500090
[5]Department of ECE, Sri Shakthi Institute of Engineering and Technology, Coimbatore-641062
[6]Department of CSE, Koneru Lakshmaiah Education Foundation, Guntur-522502
*arunvignesh44@gmail.com

Abstract--**To enhance the performance of communication system, there are many cooperative techniques are available. The multi-input multi-output (MIMO) system has been analysed in this paper and its peak to average power is analysed with optimal available techniques. Such techniques are focused on various parameters and in this paper we have considered energy efficiency (EE). Practical implementations of realizing MIMO amplify and forward technique has some difficulties. In recent times, an algorithm such as Firefly fuzzy hybrid algorithm is being used. But in realizing the amplification and forward system, the performance may not be enhanced if the energy is not considered. The energy of the non linear system is associated with the average power and power efficiency. An improved imperialist competitive algorithm is proposed in this paper. The focus is mainly kept on energy efficiency. Algorithms such as EE HFFA (Energy efficient Hybrid Fuzzy Firefly Algorithm), amplify and forward system (AF) are analysed to bring out an algorithm called Improved Imperialist Competitive algorithm (IICA). It has been analysed in this paper that the simulation results of energy efficient IICA induces peak average power ratio (PAPR) which showed significant improvement in energy efficiency.**

Key Words— Energy Efficiency (EE), Multiple-Input-Multiple-Output (MIMO), Amplify-And-Forward (AF), Average power, Improved Imperialist Competitive Algorithm (IICA).

I. INTRODUCTION

Research in the field of Energy Efficiency is brings out sustainability for environment as well as economical in the sense of communication systems. Additionally, communication in cooperation is identified as one among the effective systems [1]. These types of systems would improve the performance. Recently many works have been made over in this research field.

In this research, methodology named EE-HFFA has been introduced to work for MIMO-AF. Many relaying techniques have been used for developing the MIMO-AF. One among those techniques is Amplify-and forward. Communication through MIMO-AF [4] would fascinate about many years.

EE-HFFA stands for Energy Efficiency with Hybrid Fuzzy Firefly Algorithm. It would obtain by merging the beneficial works of firefly and differential convolution shortly DE. This combination helps to improve the sharing of information between populations by parallel implementation. Even though large number of research has been going in this field, still difficulties are arising in MIMO-AF. One among those issues is its high PAPR.

PAPR [5] is the basically depends on relation between the powers. It is denoted in terms of db. The system like orthogonal frequency division multiplexing [7] would obtain high PAPR which is compare to system with single carrier.

Improved Imperialist Competitive Algorithm simply called IICA which aims to solve the nonlinear equations. In ICA [8], initial countries are defined using the initial population. In this population are getting select and bring out for evaluation to find the best countries. These

978-1-6654-8035-2/22/$31.00 ©2022 IEEE

An Ultrasonic Sensor-based blind stick analysis with instant accident alert for Blind People

Chandu Ramisetti [1], Talla Neeraj[1], Punna Surya[1], Mahesh Kumar G[1],
N Arun Vignesh[1*], Asisa Kumar Panigrahy[1], A M Viswa Bharathy[2], N. Kumareshan[3]

[1]Department of ECE, Gokaraju Rangaraju Institute of Engineering and Technology, Hyderabad-500090
[2]School of Computer Science and Engineering, GITAM University, Bengaluru
[3]Department of ECE, Sri Shakthi Institute of Engineering and Technology, Coimbatore-641062

*arunvignesh44@gmail.com

Abstract:

The project is about the blind people who can't move without a stick, so we thought of doing a smart stick for blind people which can sense the obstacles and make buzzer sounds so he can move forward with that, in addition to that, we add fire and water sensors it beeps with different intensities to get attention from it. we can use ultrasonic sensors for a variety of obstacles like a pit, wall, drainages, vehicles, people etc . whenever he forgot the stick through his mobile phone with an app on the home screen can speak to it and the stick responds through voice output like 'you forgot me here' with the help of Bluetooth connection. Apart from these things, there may be chances to meet with an accident then we connected vibrate sensor with certain intensity more than usual . If in case the vibrator sensor senses the accident level frequency we set before then it sends msg to relatives through GPS and GSM connected to the Arduino board.

Key words: Ultrasonic sensor, Blind, GPS, GSM.

I. INTRODUCTION

International Agency for the Prevention of Blindness (IAPB) and WHO researchers found that there were 285 million visually impaired people in the world, of which 39 million were completely blind. More than 90% of the data comes from sub-Saharan Africa and other developing countries. One million Egyptians are blind, with 14% of them being children. According to the WHO and IAPB, the number of people who are blind worldwide is expected to double by 2020.

Blind people have a hard time moving or living on their own. Consequently, they frequently employ a white cane to serve as a moving guide. Despite the possibility that it could be beneficial, there is no guarantee that it will protect blind people from harm. Using these traditional methods is only suitable for detecting low-level obstacles.

1.1. Assistive Technology

Disabled people rely on assistive technology to help them carry out everyday tasks, make their lives easier, and keep them safe while they are out and about. Personal care, navigation and orientation, and mobility assistance were all developed in the 1960s to assist people in their daily lives.

Electronic devices that use sensors to help the visually impaired locate and identify objects in their immediate surroundings have made this assistive technology available to the blind. The sensors can help with mobility tasks by determining the object's dimensions, range, and height. Vision replacement is more difficult to categorise because it involves both medical and technological aspects. An ocular nerve or direct display to the brain's visual cortex can be used to replace vision [9-12]. Vision enhancement differs from "vision substitution" in that the camera input is processed and the results are visually

978-1-6654-8035-2/22/$31.00 ©2022 IEEE

Two Stage Signal Processing of Channel Valuation and Recognition for millimeter MIMO Systems

K Murali[1], N Arun Vignesh[2*], S. Kanithan[3] N. Kumareshan[4], P Vidyullatha[5], Aruna Devi B[6], D Vijendra Babu[7]
[1]Department of ECE, Vijaya Institute of Technology for Women, Vijayawada, AP-521108
[2]Department of ECE, Gokaraju Rangaraju Institute of Engineering and Technology, Hyderabad-500090
[3]Department of ECE, MVJ College of Engineering, Bengaluru-560067
[4]Department of ECE, Sri Shakthi Institute of Engineering and Technology, Coimbatore-641062
[5]Department of CSE, Koneru Lakshmaiah Education Foundation, Guntur-522502
[6]Department of ECE, Dr.N.G.P. Institute of Technology, Coimbatore-641048
[7]Department of ECE, Aarupadai Veedu Institute of Technology, Tamilnadu- 603104
*arunvignesh44@gmail.com

Abstract-- In millimeter multi-input multi-output (MIMO) systems, signal processing is critical to support the detection and estimation of next generation millimeter wave communication channels. Due to the large number of antenna arrays used in transmitter and receiver, as well as mixed signal and radio frequency power limitations, new MIMO communication signal processing techniques are required. Two realistic millimeter waves can be seen as key targets.

- **The first is the massive MIMO channel matrix, which is necessary in millimeter wave systems because they require more displays at source and recipient to achieve adequate connection edge.**
- **Another point is that the sum of RF manacles that can be used in the set of transmitters and receivers is limited due to power and cost limitations.**

From mmWave MIMO, this research provides an accurate two-stage channel valuation system. First we use basic Bayesian learning to get a rough estimate of the channel. By maximizing the probability function in the second stage, the performance of mmMIMO is improved in the second stage. Compared with competitors, the performance of the proposed system is significantly better, and the computational complexity is moderate.

Key Words—**Level Shifter, Sub Threshold Voltage, Differential Cascode Voltage Switch , Less Power.**

I. INTRODUCTION

The millimeter wave (mmWave) frequency band is at the forefront of high capacity consumer wireless communication systems. Most wireless user systems use transmission frequencies below 6 GHz, while millimeter waves use the range of 30 GHz to 300 GHz. For the next generation of 5G cellular systems, millimeter wave communication is a technology essential. In any case, due to cost limitations, each set of millimeter waves can only use a limited number of RF links [1-6].At the same time, in millimeter wave practice, the number of radio frequency strings is less than the number of antenna units.

This encourages researchers to study the shape of the crossbar in the millimeter-wave MIMO structure. The channel data is needed to understand the signal processing required in mmWave MIMO. Although there have been many studies on station evaluation of classic narrow-range MIMO systems, such as [7-11], the methods used are not suitable for millimeter-wave. In combination of a huge scale millimeter wave MIMO channel network the strings of radio frequency creates an extraordinary test for channel evaluation. To solve these problems, a variety of channel estimation methods have been developed for millimeter wave MIMO systems. The channel estimate is injected into the compressed sensing structure. Orthogonal match search is used for channel estimation through precise multiple combination technology. Two techniques for channel estimation and detection for mm wave MIMO system is proposed in this paper.

978-1-6654-8035-2/22/$31.00 ©2022 IEEE

A Study On Wideband Spectrum Monitoring Using NI USRP

Laxmi Gouri Naga Sai Pratyusha [1], Kammela Keerthi[1], Kora Sathvika Reddy[1], Erukala Sai Sushma[1], N Arun Vignesh[1]*, V. Ayyem Pillai[1], N. Kumareshan[2]

[1]Department of ECE, Gokaraju Rangaraju Institute of Engineering and Technology, Hyderabad
[2]Department of ECE, Sri Shakthi Institute of Engineering and Technology, Coimbatore
*arunvignesh44@gmail.com

***Abstract*—Spectrum monitoring and signal analysis have various application areas, both civilian and defense. Spectrum monitoring is the bandwidth surveillance which is the study of a target signal group's frequency components which could be monitored in time as well as frequency varying fields. In this project we are implementing wide band spectrum monitoring using NI USRP Rio, LabVIEW. This programming language is often called 'G'. Thanks to the advent of SDRs, there has been a tremendous leap in wireless communication. All the components that were previously implemented in complex hardware can be implemented using software. They are flexible and go beyond the 'limited spectrum' assumptions of previous radio systems designs. Spectrum monitor is an device that allows the user to get an idea of signals that exist in that spectral area and also can notice if any other frequencies are present. Here we are limiting ourselves to observe the FFT (Fast Fourier Transform) power spectrum. In presence of a new frequency, the FFT power spectrum shows deviation from its original quite form.**

Keywords—Spectrum Monitoring, NI USRP Rio, LabVIEW, SDR, bandwidth, programming, software, FFT

I. INTRODUCTION

Nowadays, there has been tremendous growth in need for faster data rate applications, which in return brought about the need for new technologies that can deal with wideband signal data[6-9]. Wideband provides high throughput data, range resolution, low latency and more accuracy but is also associated with increase in noise, which in-turn is causes complexity in text and uncertainties [1-3]. Many a times, it becomes essential to analyse and understand the behaviour or nature of the spectrum, essentially on the receiver side of a communication system. One of the convenient and simplest methods to monitor spectrum is by using Fast Fourier Transform (FFT) power spectrum.

NATIONAL INSTRUMENT USRP RIO

USRP Rio from National Instruments is a low-cost software that can provide unrivalled performance for the construction of 5G wireless communication technology. Universal Software Radio Peripheral is the expansion of the acronym USRP which is the family of NI devices, that contain a Field Programmable Gate Array (FPGA), such as the USRP-294x and USRP-295x. The components include a cutting-edge 2x2 MIMO RF Transceiver, as well as a LabVIEW configurable DSP-oriented Kintex 7 FPGA.
The architecture of USRP Rio is shown in figure 1 [3].

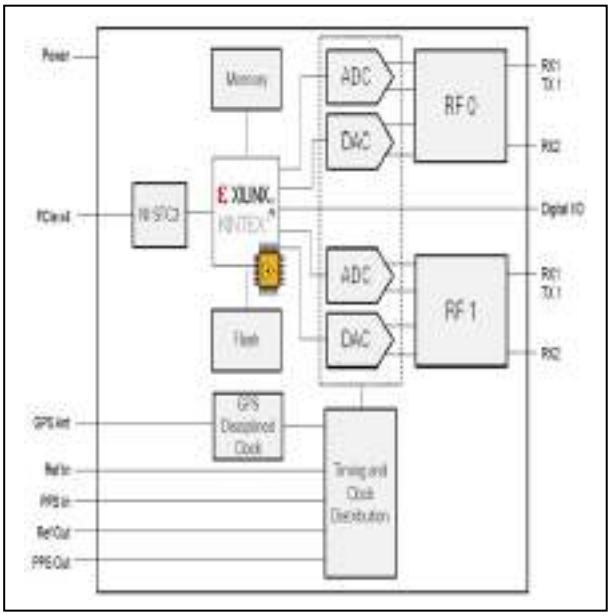

Figure 1: Architecture of NI USRP Rio Devices

In a half U column installed sleek design, it contains 2 full-duplex broadcast and receiving channel

978-1-6654-8035-2/22/$31.00 ©2022 IEEE

VIRTUAL IMAGE PROCESSING FOR ROBOT AUTOMATION

C. Gokul Prasad[1] , Shobana M[2], N Arun Vignesh[3], N. Kumareshan[4], E Konguvel[5], S.Madhusudhanan[6]

[1]Department of ECE, SNS College of Engineering, Coimbatore
[2]Department of ECE, SNS College of Technology, Coimbatore
[3]Department of ECE, Gokaraju Rangaraju Institute of Engineering and Technology, Hyderabad
[4]Department of ECE, Sri Shakthi Institute of Engineering and Technology, Coimbatore
[5]School of Electronics Engineering (SENSE), Vellore Institute of Technology, Vellore
[6]Department of CSE, Koneru Lakshmaiah Education Foundation, Guntur
[*]arunvignesh44@gmail.com

Abstract—A h**ypotheses underlying virtual environments have been focused on either a hard animal desire for freedom from the limits of the real world by accepting the digital world. Humans would be able to interact with all of this simulated space in a much more spontaneous manner right then and there, spawning new forms of human communication. Its goal would be to go above the conventional ways of collaboration in which most individuals do on a frequent basis, including the mouse and keyboard. All of that is viewed as an unreal method of operating because it requires individuals to respond to the needs of advanced technologies or is it the other manner only about. A online reality, but at the other hand, has the inverse result. This enables creating opportunities for more direct delve oneself together in visually stunning globe where they can discover using one's sensory perception. The above instinctual type of integration inside this reports indicate leads to innovative channels of information and comprehension.**

Index Terms - Augmented Reality, Virtual Reality, ZigBee,

I INTRODUCTION

A. *Embedded System*

A subsystem is indeed a mix of computer software and hardware that will either be static in capacity or customizable and therefore is specially built for a certain purpose. From among numerous conceivable servers for a microcontroller include manufacturing machinery, vehicles, hospital instruments, webcams, household products, aircraft, commercial systems, and entertainment [1]. Customizable operating device have ui components, and mechatronic coding is a specialist vocation [2]. Because the automated process is devoted to certain functions, system designers may optimise it to decrease device relative cost while increasing availability and security.

B. *Simulation*

These ideas underlying virtual technology were founded upon "a longstanding natural urge to transcend the limits of the current world" by adopting internet. There and then, people will be able to engage with this simulated space in an even more lifelike fashion, tailored to specific features of social communication. [3-6]. The Immersive Virtual device was created to address new kinds of brain connection. This advantage enables framework developers to easily, quickly, and perfectly incorporate a CPU with computer networks using UART.

C. *Features of Embedded System*

- An esp32 controller performs a single job and therefore can be configured to do other tasks [7-8].

- Digital logic possess relatively scarce resources, notably storage. They often lack auxiliary memory chips like as CDROMs and floppies [1-3].

- Microcontrollers will have to meet certain timeframes. Certain tasks must be accomplished over a certain timeframe. Dead lines are strictly enforced in certain integrated devices, referred to as real time systems. Overlooking hard zones can result in a disaster—loss of lives or

978-1-6654-8035-2/22/$31.00 ©2022 IEEE

Cross Coupled Power Effective Quick Level Shifter

N. Sai Kiran[1], N. Arun Vignesh[1*], S.Kanithan[2], E. Shobhana[3], N. Kumareshan[4], S.Madhusudhanan[5], Balambigai Subramanian[6], Prajith Prakash Nair[7*]

[1]Department of ECE, Gokaraju Rangaraju Institute of Engineering and Technology, Hyderabad
[2]Department of ECE, MVJ College of Engineering, Bengaluru
[3]Department of Physics, Kumaraguru College of Technology, Coimbatore
[4]Department of ECE, Sri Shakthi Institute of Engineering and Technology, Coimbatore
[5]Department of CSE, Koneru Lakshmaiah Education Foundation, Guntur
[6]Department of ECE, Kongu Engineering College, Perundurai
[7]Department of ECE, ACS College of Engineering, Bengaluru
[*]arunvignesh44@gmail.com

***Abstract*— A power effective and quick LS (Level Shifter) is proposed using cross couple structure. The designed LS will help to overcome the drawbacks of previous LS by utilizing cross coupled structure at the pull-up area, it will help circuit to increase its functional speed and power, energy needed for circuit is also decreased. Comparing to existing ones, the proposed LS need very low number of components to design and sizes of these components are minimized. This will help to lower the area required by LS. The advantage of proposed LS is it performs constructively when the input is lower than the V_{th} and offers very low delay. These simulations are performed by using LT spice tool which is of 180nm technology. The power utilization and overall delay of designed LS is 149.5nW and 23.6ns for 1 MHz and 0.4V/1.8V.**

Keywords*— Level shifter; sub-threshold; current mirror; leakage current.

I. INTRODUCTION

In the recent past by lowering the supply source voltage in electronic systems and electronic circuit will lower the SC (Short circuit) power. From the circuit's movement required dynamic power is achieved. Basically, the supply sources required are two, the first one is SC current and second is interchangeable capacitance. Above are the two major reasons for developing dynamic current and is produced by capacitor, when it is discharging and charging. While the two PMOS components and NMOS components are in dynamic state and leakage SC occurred in the circuit will results in loss of power. The power is calculated by the following expression

$$P_{switching} = \alpha . C_L . V_{dd}^2 . f_{clk} \quad (1)$$

Where α is factor of change. There are number of methodologies which can lower the dynamic current for instance lowering the size of component (here size of components are controlled by changing by value of width), reordering of components (here position of components are revised), swings in clock, by interchanging the pattern of components and by having various supply source voltages [1]. By lowering down supply source voltage will cause functioning of the circuit and its quickness is affected. To stop this cause from happening, various supply source methodologies can be used [2,3].

By giving the various supply source voltages, the minimum needed connections among different blocks are created by utilizing these LS. LS's must change less level of logics to higher levels of logic [3-5]. In between blocks LS is used as a bridge, so LS's may have chance to needed in very high quantity, hence it must be fast and make sure utilize low energy. By growth in technology one can lower the supply source voltage of components below its V_{th}, hence LS's must function for less supply source voltages.

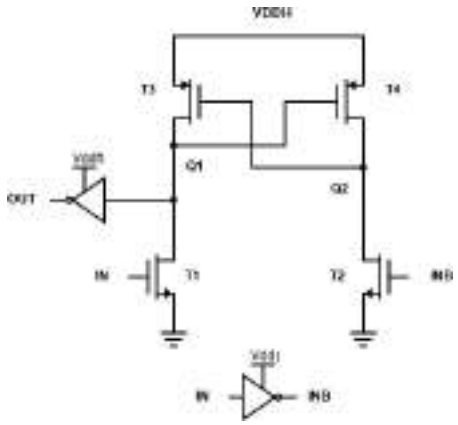

Fig 1: DVCS based conventional LS.

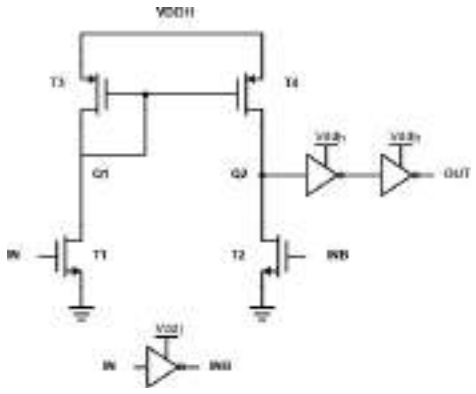

Fig 2: Current mirror based Conventional LS

Figure 1 displays, DVCS based conventional LS and Figure 2 displays current mirror based Conventional LS respectively. Major drawback of existing LS utilizing architecture of CM is, the interaction between components is not up to the level. The proposed design will overcome this advantage.

978-1-6654-8035-2/22/$31.00 ©2022 IEEE

Proceedings of the Fourth International Conference on Smart Systems and Inventive Technology (ICSSIT-2022)
IEEE Xplore Part Number: CFP22P17-ART; ISBN: 978-1-6654-0118-0

Deep Learning based Medical Image Classification

A.Sahaya Anselin Nisha
Associate Professor,Department of Electronics & Communication Engineering, Sathyabama Institute of Science and Technology,Chennai- 600 119.Tamil Nadu.India.anselinnisha.ece@sathyabama.ac.in

Vamsidhar Enireddy
Associate Professor,Department of Computer Science & Engineering,Koneru Lakshmaiah Education Foundation,Vaddeswaram, Guntur-522502. Andhra Pradesh.India. enireddy.vamsidhar@gmail.com

Bernatin.T
Assistant Professor,Department of Electronics & Communication Engineering, Sathyabama Institute of Science and Technology,Chennai- 600 119.Tamil Nadu.India.bernatin12@gmail.com

Karthikeyan.C
Professor, Department of Computer Science & Engineering Koneru Lakshmaiah Education Foundation,Vaddeswaram, Guntur-522502. Andhra Pradesh,India. ckarthik2k@gmail.com.

D.Vijendra Babu
Professor,Department of Electronics & Communication Engineering, Aarupadai Veedu Institute of Technology,Vinayaka Mission's Research Foundation,Paiyanoor-603104. Tamil Nadu.India. drdvijendrababu@gmail.com

N.Arun Vignesh
Associate Professor, Department of Electronics & Communication Engineering, Gokaraju Rangaraju Institute of Engineering and Technology, Hyderabad-500 090. Telangana.India.arunvignesh44@gmail.com

2022 4th International Conference on Smart Systems and Inventive Technology (ICSSIT) | 978-1-6654-0118-0/22/$31.00 ©2022 IEEE | DOI: 10.1109/ICSSIT53264.2022.9716383

Abstract*—With the advancement of the Computer Technology classification of Medical Images has become more viable. Use of the traditional features has made the system to lose the ability to represent the higher-level domain problem. Deep Learning models had paved a way for the development of a generalization ability even for the poor models. Medical Images have high resolution and availability of the dataset are also small, making these Deep Learning models deteriorate from various limitations and huge computational costs. In this paper a model is proposed a profound learning model that incorporates Convolutional Neural Network (CNN), Naïve Bayes, Support Vector Machine (SVM) and Multilayer Perceptron (MLP), which consolidates high level features that are separated from a CNN model and some chosen conventional features. The development of the proposed model incorporates the accompanying advances. To start with, a CNN is trained in a supervised manner and the outcome is that it can program the raw pels of Images into include vectors that address undeniable level ideas for characterization. In the next step, a bunch of chosen customary features dependent on foundation information on medical images are extricated. At last, a proficient model that depends on Neural Networks to intertwine the diverse element bunches acquired in the previous steps is proposed. The datasets used for the evaluation of the model are HIS2828 and ISIC2017. A general classification accuracy of 97%and 96%, separately, which are higher than the current techniques are accomplished.

Keywords*—Classification, Deep Learning, Feature extraction, Multilayer Perceptron, Naïve Bayes, Support Vector Machine

I. INTRODUCTION

In general, the Brain Tumor can be divided into two stages primary and secondary. Here primary stage is Benign where it is in the starting stage and the secondary stage is the Malignant stage. This stage is dangerous as in this stage the Cancer has spread to the other parts, and it is difficult to control the disease. Brain Tumor is defined as the uncommon growth of tissue due to the uncontrollable growth of cells [1]. The Tumor can be graded as Grade 1 to Grade IV as per the American Brain Tumor Association and WHO. Grade III and IV Tumor indicates a high-grade Tumor. Grade I and II are the low quality Tumor. If the inferior frontal cortex Tumor is left untreated, it is presumably going to shape into a high-grade mind Tumor that is an unsafe frontal cortex Tumor [2]. Patients with grade II Gliomas require consecutive checking and discernments by alluring Resonation Imaging (MRI) or enrolled Tomography (CT) channel every 6 to a year. Frontal cortex Tumor may affect any individual at whatever stage throughout everyday Life, and its impact on the body may not be a comparable thing for every individual.

The liberal Tumors of low quality I and II Glioma are seen as restorative under complete cautious excursion, while undermining frontal cortex tumors of assessment III and IV class can be treated by radiotherapy, chemotherapy, or a blend thereof. The term compromising Glioma consolidates both grade III and IV Gliomas, which is in like manner implied as Anaplastic Astrocytomas. An Anaplastic astrocytoma is a mid-grade Tumor that displays surprising or inconsistent turn of events and an extended advancement record diverged from other inferior Tumors. Besides, the most compromising sort of Astrocytoma, which is moreover the most raised assessment Glioma, is the Glioblastoma [3]. The uncommon fast advancement of veins and the presence of the defilement (dead cells) around the tumor are perceived Glioblastoma from the wide scope of different assessments of the Tumor class.

Assessment IV Tumor class that is Glioblastoma is for each situation rapidly improving and significantly perilous sort of Tumors when diverged from various assessments of the Tumors. Feature Extraction is a process in which the features are extracted from the Images and these features are used by the classification algorithms to classify the Images. Features are low level such as Edge, Color and Texture are useful in classifying the Images. Feature selection is a process in which the important features are identified so that the classification accuracy can be increased, and complexity can be decreased [14]. High level features extracted from

Proceedings of the Third International Conference on Inventive Research in Computing Applications (ICIRCA-2021)
IEEE Xplore Part Number: CFP21N67-ART; ISBN: 978-0-7381-4627-0

A Quick and Power Efficient Controlled Voltage Level-Shifter using Cross-Coupled Network

N. Sai Kiran[1] N. Arun Vignesh[1] K. Sravani[1] Ch. Usha Kumari[1] S. Kanithan[2] N. Kumareshan[3] C.Gokul Prasad[4]
[1]Department of ECE, Gokaraju Rangaraju Institute of Engineering and Technology, Hyderabad
[2]Department of ECE, MVJ College of Engineering, Bangalore
[3]Department of ECE, Sri Shakti Institute of Engineering and Technology, Coimbatore
[4]Department of ECE, PPG Institute of Technology, Coimbatore
[1 2 3 4]India
[*]nagaramsaikiran0@gmail.com

2021 Third International Conference on Inventive Research in Computing Applications (ICIRCA) | 978-1-6654-3877-3/21/$31.00 ©2021 IEEE | DOI: 10.1109/ICIRCA51532.2021.9544876

***Abstract*— This concise presents a quick and power efficient level-shifter (LS) using cross coupled network. This technique will eliminate the drawbacks of conventional LS using cross coupled network in the pull up region, this will make circuit to run fast and power required is also reduced. Compared to previous LS's the proposed level-shifter consists of less number of elements and their sizes are comprised to minimum, this will decrease the area of LS. The existing LS cannot convert voltages below V_{TH} and the voltage range offered is less and power utilization is more. In order overcome this with the use of crosscoupled network in the pull up region, the high switching speed achieved. By decreasing the transistor size, voltages are converted below V_{TH} and energy utilization is decreased. To design a high speed and low power LS by using RCC in pull up region. It is used in low power applications such as implantable medical components. Proposed level-shifter functions effectively with less delay for inputs below the sub threshold voltages. For simulations LT spice tool of 180nm technology is used. The total delay and power utilization of the proposed voltage LS for 0.4V/1.8V and 1 MHz are 21ns and 76.34nW.**

Keywords*— Level shifter; sub-threshold; current mirror; leakage current.

I. INTRODUCTION

Level shifter in electronics field is called logic LS or called as voltage level converter, this circuit used to convert signals from one logic stage to another logic stage, which is adaptable between ICs with various voltage specification, like CMOS and TTL. Present systems utilize level shifters to cross domains in between logics, sensors, processors and various circuits. At present years, the more common logics are 1.8V, 3.3V, and 5V, though the higher and lower levels such voltages are utilized.

Multiple voltage supply methods require LS depends on signals which change from one level to another voltage level. Signals which cross voltage stages cannot be sampled exactly without the level shifters. It is recommended that ideal methods are utilized in the flow design to recognize missing LS and finds out the missed one's which saves time while simulation and debugging. LS is added to make sure that blocks which are operating at various voltages would work properly when connected together in SoC. LS makes sure that particular drive power and timeframe such as switching signals from single stage to another voltage stage. Level shifters are installed at the beginning or start of the phase. Any signal that exceeds the MSV power source must have a standard shift attached. Although the transition from high to low power station is often optional, the conversion rate from low power to high power is compulsory. LS is placed near to the power based boundaries. It can be placed either at top or bottom or at the centre line of LS.

In recent days by decreasing the power supply voltage in digital systems and circuit will decrease the leakage power (short circuit, static and dynamic power). The requirement of dynamic power is developed from the movement of the circuit. Generally, the sources are two, one is short-out current and the other one is exchanged capacitance. These are main reason for dynamic power and it is occurred from discharging and charging of the capacitor. When both the PMOS transistor and NMOS transistor are in dynamic and the SC occurring between the ground and supply will cause the leakage power. The power is given as

$$P = I_{avg} . V_{dd}^2 \quad (1)$$

Here α is changing factor. There are many techniques that can decrease the dynamic power like transistor sizing (here transistors sizes are changed by controlling its width value), transistor reordering (here the revising of transistors is done), half clock swings, changing the structure of logic gates and by providing multiple power supply voltages [1]. But bringing down the power supply voltage will affect the quickness of circuit and its performance. In order to avoid this effect, we can use multiple power supply methods [2,3]. By providing the multiple power supplies, the required connections between the blocks are obtained using voltage LS. These LS's should convert low logic to up logic or voltages level. Hence, as LS's are using as intermediate blocks, these may be required in high in number so it should use less power and it must be fast. With increasing in technology for decreasing the low power

Implementation of Smart Energy Meter through Prepaid Transaction using IOT

P Rahul Reddy
Dept. of ECE, Geethanjali Institute of Science & Technology
Nellore, India
palvai.rahulreddy@gmail.com

Rajashekhar Kammanaboina
Dept. of ECE, Vidya Jyothi Institute of Technology,
Hyderabad, India
rajashekharkece@vjit.ac.in

Dumpa Prasad
Dept. of ECE, Sasi Institute of Technology and Engineering,
Tadepalligudam, India
prasadreddydumpa@yahoo.co.in

Prabhakara Rao Kapula
Dept. of ECE, B V Raju Institute of Technology,
Narsapur, India
prabhakar.kapula@gmail.com

Asisa Kumar Panigrahy
Dept. of ECE, Gokaraju Rangaraju Institute of Engineering & Technology,
Hyderabad,India
asisa@griet.ac.in

2021 International Conference on Recent Trends on Electronics, Information, Communication & Technology (RTEICT) | 978-1-6654-3559-8/21/$31.00 ©2021 IEEE | DOI: 10.1109/RTEICT52294.2021.9574015

***Abstract*— In India, energy meters are electro-mechanical and postpaid. The main drawback of this approach is that a person must walk from street to street, reading each house's energy meter and giving out the charges. According to that reading, the bill was paid. Even when bills are paid on time, issues like an over-billing amount or a provider warning are common. To overcome this problem, we proposed an IoT-based prepaid power recharge unit that will integrate with ordinary household energy meters and be capable of counting down energy use and switching off the main supply once the energy usage countdown hits zero, and a data collecting system using IoT. The recharge info and energy usage from the recharge station are saved in a Data Acquisition server connected to the energy meters to control the main power supply and monitor power consumption in real-time.**

Keywords— IOT; energy meter; prepaid; data acquisition.

I. INTRODUCTION

The As a result of post-paid connections, the consumer has a number of concerns. Prepaid power connections are often suggested as a viable solution to this issue Consumers will need to recharge the quantity of energy, they need to consume in this prepaid electricity meter circuit [1]. For this prepaid system to work, household electricity meters are to be equipped with a module that can identify the amount recharged by the consumer and tally down the amount recharged to zero depending on the electricity usage [2]. The main supply is automatically switched off when the meter count hits zero, and it may only be turned back on after the next recharge [3].

This concept was introduced using Arduino, a GSM board, and a node MCU [4]. We can refresh our energy balance by using an internet gateway [5]. The electricity supply link to the residence is automatically terminated if the balance is low or zero. Through the node MCU module, this device may also send energy consumption notifications from the meter to the substation at regular intervals, as well as alerting users about low balance, cutoff, and other difficulties [6]. The current system only gives customers feedback on how much power they have consumed in the form of a bill at the end of the month. The consumer has no way of tracking their energy usage in real time. Consumers are increasing at an exponential rate, and the load on electricity distribution divisions is also increasing. And in the current energy meter as shown in Fig. 1, chances of fraud and meter tampering also possible.

II. MOTIVATION

The concept of a prepaid entry system has been introduced in many countries. This notion is founded on the principle of "pay first, utilize later." From the perspective of the consumer, the concept is appealing because there is no fear of disconnection and reconnection for any reason.

The Electricity Board is unable to keep track of consumer usage of power under the current billing method (postpaid). Even if bills are paid on time, the consumer faces issues such as receiving late bills for payments that have already been paid [7] as well as inadequate electrical supply and quality [8]. Also, many researchers explored ways to reduce the interconnect length which in turn reduce the energy requirement of system [15]- [20].

III. EXISTIG SYSTEM

The local state electrical board is in charge of energy distribution and maintenance. A user's electricity usage is computed by multiplying the number of KWH consumed over the course of a month. On the metre, this reading is saved locally. This reading is taken manually by a worker from the power board who goes door to door. This information is then transmitted to the head electrical board for evaluation, after which an evaluation bill is prepared based on the monthly readings.

Fig. 1 Existing System.

The customers then pay their charges using their preferred

978-1-6654-3559-8/21/$31.00 ©2021 IEEE

2021 International Conference on Intelligent Technologies (CONIT)
Karnataka, India. June 25-27, 2021

Reduction of Electrical Signal Interference for future IC Integration-An Extensive Review

P Rahul Reddy
Dept. of ECE,
Geethanjali Institute of Science & Technology
Nellore, India
palvai.rahulreddy@gmail.com

A Kishore Reddy
Dept. of ECE,
Geethanjali Institute of Science & Technology
Nellore, India
krish.aduri2008@gmail.com

Dumpa Prasad
Dept. of ECE,
Sasi Institute of Technology and Engineering,
Tadepalligudam, India
prasadreddydumpa@yahoo.co.in

Koya Jeevan Reddy
Dept. of ECE,
SNIST
Hyderabad, India
jeevankoya@gmail.com

Asisa Kumar Panigrahy
Dept. of ECE, Gokaraju Rangaraju Institute of Engineering & Technology,
Hyderabad, India
asisa@griet.ac.in

2021 International Conference on Intelligent Technologies (CONIT) | 978-1-7281-8583-5/21/$31.00 ©2021 IEEE | DOI: 10.1109/CONIT51480.2021.9498394

***Abstract*— As per Moore's law, the dimensions of any system have been permanently scaling down to achieve the efficiency of Integrated Circuit (IC) since many decades. ICs have been waiting for a planar platform for a long time during their careful scaling. In the past few years, there have been two big requests. The primary demand is that the measurements of all devices have nearly reached a snag. Limiting the interconnect delay output of complete circuits or systems is the secondary and most significant demand. The most critical and real limitation is that there is none, but the interconnect delay is almost undistinguishable to that of the units. New interconnecting materials, as well as experimental architectures, must be designed to meet the demands of device efficiency. New integration methods called Three- Dimensional IC (3D IC) have been introduced to reduce interconnect delays. Noise coupling is a big issue in 3D IC. As a result, several researchers have applied and verified various materials through TSVs and substrates to minimize noise coupling issues. This paper presents an extensive survey on noise coupling reduction and future direction towards improvement of coupling issues in 3D IC.**

Keywords—3D IC; ETSV; Noise Coupling; Perylene-N; TTSV; Three-Dimensional.

I. INTRODUCTION

The successful transition from IT (Information Technology) to IoT (Internet of Things) has resulted in a rapid advancement in the ability to fit more functionality into a single Si chip. Since millions to billions of transistors are used, the issue of interconnections becomes more complicated. Till not many years prior expanding the quantity of interconnecting layers become a helpful arrangement however because of their parasitic capacitance, exceptionally elevated thickness interconnects in extending interconnect delay [1]. As a result, interconnect delay has become nearly equivalent to semiconductor deferral, and it has become a difficult in more scaling. To decrease the interconnect, defer the most ideal alternative is to search accelerative for a potential arrangement. Along these lines, for this the best arrangement is to utilize conspicuous innovation which relies upon their estimation and it is broadly known as 3D IC [2].

As a result, it has become a test for downsizing semiconductors by concentrating on signal postponement caused by interconnects rather than semiconductor execution. The interconnect delay enhancement was attained meritoriously by offering innovative engineering models, but their assistance became limited. The two major boundaries, gate delay and RC delay/signal defer, will specifically choose most active frequencies in this cutting-edge IC. The most common technique for reducing semiconductor delay is to calculate the system proportionally down. Lower interconnect delay would result in increased speed and bandwidth [3] – [5]. The main motivation for this 3D IC integration is that the electrical signaling between TSVs and Si substrate is very weak, resulting in noise coupling disruptions between aggressive and victim TVs, as well as between operational devices and substrate. A logical approach is used between TSVs and the Si substrate to solve the issue of noise coupling.

Noise coupling and heat are two issues that arise in modern IC integration approach called 3D IC. Presently a-days TSV's assumes a significant part in 3D IC reconciliation. TSV's are significantly arranged into two categories, ETSV (Electrical TSV) which transports electrical signal and TTSV (Thermal TSV) which transports heat form heat source to sink. 3D IC has major drawback of electrical signal interference between aggressive (current carrying TSV) and sufferer TSV's (grounded TSV). Due to the electrical signal interference system performance get degraded drastically.

This paper mainly focuses on the roadmap to decrease noise coupling between belligerent TSV and ground TSV. Many researchers have proposed various techniques to encounter the electrical interference between the aggressive TSV (ETSV) and sufferer TSV's by either shielding them or by choosing low constant dielectric material as liner, or by creating different TSV structures like Dielectric-metal-Dielectric structures. In the next section the brief report on the techniques adopted by researchers explored.

II. LITERATURE SURVEY

Metal, TSV, and RDL interconnects are the three types of interconnects used in 3D silicon interposer structures [6]. Individually and collectively, the study of these interconnects has been measured and checked. This examination additionally comprises of electrical qualities of coupling noise among all the interposers, this construction is

2021 International Conference on Intelligent Technologies (CONIT)
Karnataka, India. June 25-27, 2021

Hardware Based Voice Authenticated Security System

Nandan Goud Ambati
Dept. of ECE
Gokaraju Rangaraju Institute of Engineering and technology
Hyderabad, India
nandanambati@gmail.com

Jashwanth Chandhra Adama
Dept. of ECE
Gokaraju Rangaraju Institute of Engineering and technology
Hyderabad, India
jashwanthadama@gmail.com

Anudeep Chakiri
Dept. of ECE
Gokaraju Rangaraju Institute of Engineering and technology
Hyderabad, India
deepuchakiri99@gmail.com

Gohith Sai Vure
Dept. of ECE
Gokaraju Rangaraju Institute of Engineering and technology
Hyderabad, India
gohithsai123@gmail.com

Saikumar Dharavath
Dept. of ECE
Gokaraju Rangaraju Institute of Engineering and technology
Hyderabad, India
ksai88267@gmail.com

Durga Naga Snehit Kaliki
Dept. of ECE
Gokaraju Rangaraju Institute of Engineering and technology
Hyderabad, India
snehit.kaliki7@gmail.com

Naveen Eggadi
Dept. of ECE
Gokaraju Rangaraju Institute of Engineering and technology
Hyderabad, India
naveeneggadi@gmail.com

Nikhil Chandra Balne
Dept. of ECE
Gokaraju Rangaraju Institute of Engineering and technology
Hyderabad, India
balne.chandra@gmail.com

Asisa Kumar Panigrahy
Dept. of ECE
Gokaraju Rangaraju Institute of Engineering and technology
Hyderabad, India
asisa@griet.ac.in

2021 International Conference on Intelligent Technologies (CONIT) | 978-1-7281-8583-5/21/$31.00 ©2021 IEEE | DOI: 10.1109/CONIT51480.2021.9498365

***Abstract*—This paper explains a model that reflects technical development where computers and humans interact through voice UI. This model contains the code that uses comparisons between the common pitch of a recorded .wav file with that of test signal file. The vector differences between formant peaks within the Power Spectral Density of every file and most accurate one is detected. Feature extraction is obtained using MFCC. These features are trained using Vector Quantization for pattern matching [5]. Once signal matched then MATLAB code will send signal to the microcontroller unit via serial communication, so that microcontroller will control door open and close with time delay and send feedback message to user using Internet communication [1]. These entire operation users can monitor from remote location using BLYNK IOT application. So that this system will provide high security based locking systems for houses, banks etc.**

Keywords—IoT, voice user interface, power spectral density, mel frequency, Vector Quantization, Speech recognition.

I. INTRODUCTION

Voice recognition is one of the essential technologies to provide security and validate authenticity of a user [7]. Basically our home needs to be safeguarded and monitored whenever we are away from it. There are many locking technologies such as Biometric door locks or smart locks, which requires a person's biometric access, to antilock. But even stealing a person's finger prints is not a tough task these days, so in such cases this smart-lock system may fail. Hence in order to ensure the safety of our property, a simple and safe approach has to be followed. One as such is speech recognition, in which a lock opens by detecting the voice of an authorized user. Speech recognition is widely used in security applications, where you need to access your Pc by providing speech sample as password. This system stresses to identify the voice of the user irrespective of what he is saying. So it acts as a text-independent recognition system [10]. Hence we could able to develop a system, where machines can distinguish voice signals and respond accordingly.

II. PROPOSED ARCHITECTURE

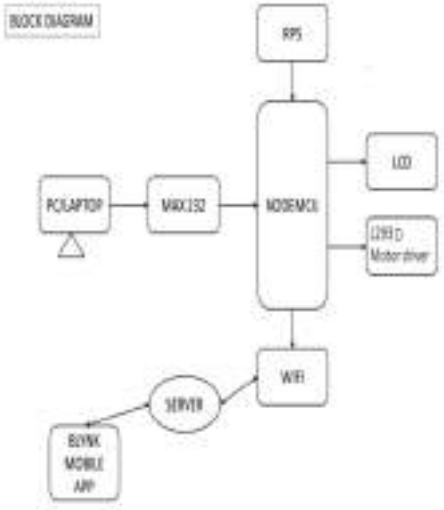

Fig. 1. Proposed Architecture.

The proposed architecture of speech recognition based door locking system is shown in **Fig 1**, whose components are described in the below section.

A. Components

The circuit consists of the following hardware components:

1. Node MCU
2. power supply unit

Materials Today: Proceedings xxx (xxxx) xxx

Contents lists available at ScienceDirect

Materials Today: Proceedings

journal homepage: www.elsevier.com/locate/matpr

Design of area-efficient high speed 4 × 4 Wallace tree multiplier using quantum-dot cellular automata

A. Arunkumar Gudivada [a], K. Jayaram Kumar [a], Srinivasa Rao Jajula [a], Durga Prasad Siddani [a], Praveen Kumar Poola [c], Varun Vourganti [d], Asisa Kumar Panigrahy [b,*]

[a] Department of Electronics and Communication Engineering, Aditya College of Engineering & Technology, Surampalem, East Godavari, Andhra Pradesh, India
[b] Department of Electronics and Communication Engineering, Gokaraju Rangaraju Institute of Engineering & Technology, Hyderabad 500090, Telangana, India
[c] Department of Electronics and Communication Engineering, Koneru Lakshmaiah Education Foundation, Hyderabad 500075, Telangana, India
[d] Department of Aeronautical Engineering, Institute of Aeronautical Engineering, Hyderabad 500043, India

ARTICLE INFO

Article history:
Received 16 July 2020
Received in revised form 28 July 2020
Accepted 29 July 2020
Available online xxxx

Keywords:
Nanotechnology
Full adder
QCA
Wallace tree multiplier
Quantum cell

ABSTRACT

Complementary metal oxide semiconductor (CMOS) devices are expected to face new challenges such as exponential current leakage, DIBL, hot carrier effects, and etc. at nano scale. Hence the CMOS technology is being supplanted by the nanotechnologies. Quantum-dot Cellular Automata (QCA) is key technology at nano scale which operates at tera hertz of speed. Comparing with the traditional CMOS technology, the QCA technology has low power consumption and high density. This technology also has a unique methodology such as "processing in wire" and "memory-in-motion". This work confers an area proficient, high speed full adder (FA) design with efficient clocking. The proposed full adder design comprises of 26 Quantum cells with delay of two clock phases, area occupancy of 0.03 μm^2. This paper utilizes the unique characteristics of QCA and the proposed Wallace tree multiplier is implemented with the mentioned FA and is designed by using QCA Designer 2.0.3 tool.

Selection and peer-review under responsibility of the scientific committee of the International Conference on Advances in Materials Research – 2019.

1. Introduction

Because of the advancements in the VLSI technology, we need to design transistors having dimensions less than 32 nm [1]. The CMOS technology is concerned with the problems such as sub-threshold leakage currents, heat, lithography etc. Various alterative techniques have been developed by researchers that can anticipate the problems occurred with CMOS devices. Even the ITRS road map had recognized some novel technologies like Resonant Tunnelling Diodes (RTD), Single Electron Transistor (SET), QCA, and Carbon Nano Tubes (CNT), which could replace the traditional CMOS technology. According to ITRS, QCA is regarded as the prominent technology. It was proposed in 1993 by Lent et al. [2]. The Quantum cell is the basic unit of design in QCA. The Quantum cell is a square like nanostructure comprising of four dots arranged at its corners. In these two are electrons which are diagonal to each other due to columbic interactions. This technology operates by a phenomenon called Columbic repulsion.

Arithmetic operations play a crucial responsibility in economics, mercantile and many domains. Multipliers are considered as one of the most important computational block in signal processing. The studies proved that one of the effective ways to reduce the multiplication complexity is by the use of Wallace algorithm. This work confers an area proficient, high speed multiplier based on Wallace algorithm which is used to reduce the complexity, delay and cell count by using an innovative full adder suggested in the previous works [3].

The manuscript is further organised as follows. Segment 2 presents the basic concepts of QCA cells. Segment 3 introduces the clocking process in QCA technology. Segment 4 describes the wire crossings in QCA. Section 5 explains the basic gates' design using QCA. Section 6 introduces the proposed QCA one bit FA layout. Wallace tree algorithm is explained in segment 7. Segment 8 describes the proposed layout of Wallace tree using QCA. Results and discussion is done in Section 7.3. Section 8 gives the conclusion. The scope of this paper is to develop the commonly used multiplier architecture in an optimized area using novel nanotechnology like QCA.

* Corresponding author.
E-mail address: asisa@griet.ac.in (A.K. Panigrahy).

https://doi.org/10.1016/j.matpr.2020.07.677
2214-7853/
Selection and peer-review under responsibility of the scientific committee of the International Conference on Advances in Materials Research – 2019.

Cluster Formation Algorithm in WSNs to Optimize the Energy Consumption Using Self-Organizing Map

Padmalaya Nayak, GK. Swetha, Priyanka Kaushal, and D. G. Padhan

Abstract Wireless Sensor Networks (WSNs) are considered as one of the most prevailing technologies in today's world due to the diversified applications. These applications are huge in the range such as environmental monitoring, health care, civil and military, disaster management to other surveillance systems. Minimization of energy is one of the most exciting tasks in WSNs as small sensor nodes are battery powered and deploy in remote environments. Clustering is one such imperative technique that can conserve energy more broadly, and evenly which makes the network operational for a longer period. This research paper aims at developing an energy-aware cluster-based routing protocol using Artificial Neural Network (ANN) which finds an optimal number of clusters and rotates the cluster head periodically to balance the energy consumption throughout the network. Typically, the proposed algorithm is developed based on Self-Organizing Map (SOM) to form the clusters, and the K-means algorithm is used to form different sizes of clusters. Finally, an optimal number of clusters is found that impacts the network load and balances the energy consumption. MATLAB is used as a simulation tool for experimental analysis. Simulation results prove that the proposed cluster-based routing protocol "LEACH-SOM" dominates the traditional LEACH routing protocol in terms of minimal energy consumption and makes the network active for long period.

Keywords WSN · SOM · K-means · LEACH

P. Nayak · GK. Swetha (✉) · D. G. Padhan
Gokaraju Rangaraju Institute of Engineering and Technology, Hyderabad, India

P. Nayak
e-mail: padmalaya@griet.ac.in

P. Kaushal
Chandigarh Engineering College, Landran, Mohali, India

P. Nayak et al. (eds.), *IoT and Analytics for Sensor Networks*, Lecture Notes in Networks and Systems 244, https://doi.org/10.1007/978-981-16-2919-8_2

Characterization of Bifacial Passivated Emitter and Rear Contact Solar Cell

[1]Dr. Suresh Kumar Tummala [*], [1]Dr. Phaneendra Babu Bobba, [2]Dr. Satyanarayana Kosaraju

[1]Electrical Engineering Department, Gokaraju Rangaraju Institute of Engineering & Technology, Hyderabad, INDIA

[2]Mechanical Engineering Department, Gokaraju Rangaraju Institute of Engineering & Technology, Hyderabad, INDIA

sureshkumar255@gmail.com

*corresponding author

Abstract Passivated Emitter and Rear Contact Cell (PERC) defines a new architecture of solar cell which differs from standard cell architecture. PERC enables to enhance light capture at the rear surface and to optimize electron capture. This leads to increase (or) achieve better efficiency than when compared with standard cell which are reaching their physical limits. In this paper, characterization of bifacial p-type PERC solar cell with various proportions of tallness and width, back Silicon Nitrate layer with various thickness are streamlined and most elevated back productivity of bifacial solar cell (~22%) was obtained at AM1.5, 1000W/m^2, 26^{0}C standard test condition.

Keywords—PERC; Bifacial; Finger; Generation Profile; Reflection; Absorbtion.

NOMENCLATURE

PERC	Passivated Emitter Rear Contact
LCOE	Levelized Cost of Energy
c-Si	Crystalline Silicon
PV	Photovoltaic

Chapter 5

An improvised control methodology for voltage sag mitigation, harmonics reduction with a dynamic voltage restorer to improve power quality: Considering fast-operating DSP

[1]A. Vinay Kumar, [1]J. Praveen & [2]S. Tara Kalyani
[1]*Gokaraju Rangaraju Institute of Engineering & Technology, Hyderabad, TS, India.*
[2]*Jawaharlal Nehru Technological University, Hyderabad, TS, India*

Abstract—Voltage sags are regarded as one of the largest causes of disruption in power supply systems.The voltage sags cause the adverse effects on sensitive equipment such as computers, adjustable-speed drives, process-control equipment etc. During sag, the nominal voltage drops between 60% and 90% and lasts between 10ms and 100ms. Though, the FACTS devices provide the solution to most of the PQ issues, but it was observed by that the drawback of these devices, however, is that they are very costlier. The Dynamic Voltage Restorer (DVR) is used to compensate the line disturbances by inserting a voltage in series with the supply mains of the distribution system. During this compensation with the magnitude and phase of the voltage, the DVR should be independent from an external power source, which requires a large energy storage device such as a capacitor bank, a battery or a dc link. The limitations of such external storage usage have been addressed by many researchers and here an attempt has been made to propose an improvised control methodology with the grid connected rectifier-based DVR controlled by a fast-operating DSP (Digital Signal Processor) to reduce the harmonics and to mitigate voltage sag.

Keywords—dynamic voltage restorer, voltage sag, harmonic reduction, power quality, DSP.

1. INTRODUCTION

The overall financial losses due to Power Quality (PQ) disturbances, mainly voltage sags in power systems are increasing with the increase in use of microelectronic control devices in modern industry. The voltage sags cause the adverse effects on sensitive equipment such as computers, adjustable-speed drives, process-control equipment etc. During sag, the nominal voltage drops between 60% and 90% and lasts between 10ms and 100ms. (Meyer et al., 2008). FACTS devices such as DVR is a well-developed custom device which has been reasonably widely applied in power systems around the world to solve the PQ problems (Ho and Chung, 2008). Though, the FACTS devices provide the solution to most of the PQ issues, but it was observed by that the drawback of these devices, however, is that they are very costlier (Milanovic and Zhang, 2010).

The DVR is used to compensate the line disturbances by inserting a voltage in series with the supply mains of the distribution system. During this compensation with the magnitude and phase of the voltage, the DVR should be independent from an external power source, which requires a large energy storage device such as a capacitor bank, a battery or a dc link. So, the dc link voltage can be supported by separate energy storage or by grid-connected rectifier.

5 Real-Time Solar Energy Monitoring Using Internet of Things

V. Vijaya Rama Raju and J. Praveen
Department of EEE, GRIET, Hyderabad, India

CONTENTS

5.1 INTRODUCTION

Electricity has become indispensable in our daily life. In every walk of human life, electricity is being used for various applications such as transport, illumination, cooking, freezing, cooling, and several other applications. Most of the appliances in residential, commercial, and industry sectors are run on electricity. The usage of electricity usage keeps on increasing with a positive gradient every day. To meet the exponentially raising demand, a parallel amplification of energy generation needs to be done as demand will also inflate with the increase of population. This could be observed by looking at the predictions about the number of units required to meet the exponentially raising demand and growth rate of 8% and 7%, respectively, for the upcoming 5-year plans in India alone as shown in Figures 5.1 and 5.2.

The majority of electrical energy is produced using three physical phenomena, namely, electromechanical, chemical, or photovoltaic effects. Electromechanical effect was the most popular among the three, and nearly 70% of the electrical needs

THD Optimization with Low Switching Frequency Control for 15-Level Reduced Switch Asymmetric Multilevel Inverter

Gireesh Kumar Devineni, Aman Ganesh*, Neerudi Bhoopal & DSNMRAO

Abstract. The Switching modulation techniques of high switching frequencies are not recommended in medium voltage drive applications with a power of megawatts because of high power losses and low converter performance. Fundamental strategies like selective harmonic elimination (SHE) are a popular alternative. Since the transcendental equations formulated by, SHE is simply non-linear in nature, it has proven to be an important challenge for the scientists to achieve a viable solution on the desired modulation index. This article presents the comparison analysis of the GA and PSO approach with good initial guess and its hybrid optimization of PSO-GA is used for solution of the SHE equation set to various modulation index values. The %THD generated at various modulation index values is also consistent with the harmonic standards of IEEE 519-1992.

Keywords: GA, PSO, PSO-GA, Hybrid algorithms, THD, SHEPWM

1 Introduction

Multilevel inverter technology has grown in popularity in recent decades due to its advantages of producing increased levels of output voltages using less power switch requirements for medium voltage and high-power applications. Multi-level inverters are currently available in three topologies: DC MLI, CHB MLI, and FCMLI. H-bridge MLI is typically favored for various industrial uses among all these topologies[1]–[3]. Low frequency switching and high frequency switching controls are two types of modulation techniques used to control multilevel inverters [4]. The following effects can be caused by high frequency modulation in inverters, such as carrier-based pulse width modulation schemes.

- Reduced system efficiency due to increased thermal losses.
- Motor bearing failure and insulation damage in case of drive control due to high dv/dt.
- Effect of electromagnetic interference due to the power frequency of side bands in the order 10-30 KHZ.
- Ripples & Harmonics in voltage and current waveforms.

However, low frequency switching modulation methods such as SHE has key features, like the less thermal loss, control on harmonic o/p voltage and a better harmonic profile. To generate an optimal solution at a specific modulation index for

---

Gireesh Kumar Devineni & Aman Ganesh*
School of Electronics & Electrical Engineering, Lovely Professional University, Phagwara, Punjab, India. **Corresponding author email**: aman.23332@lpu.co.in

Neerudi Bhoopal & Gireesh Kumar Devineni
Department of Electrical & Electronics Engineering, B V Raju Institute of Technology, Narsapur, Telangana, India. email: gireesh218@gmail.com

DSNMRAO
Department of Electrical & Electronics Engineering, Gokaraju Rangaraju Institute of Engineering & Technology, Hyderabad, India. email: dsnm.rao@gmail.com

RECENT TRENDS IN RENEWABLE ENERGY WITH POWER ELECTRONICS

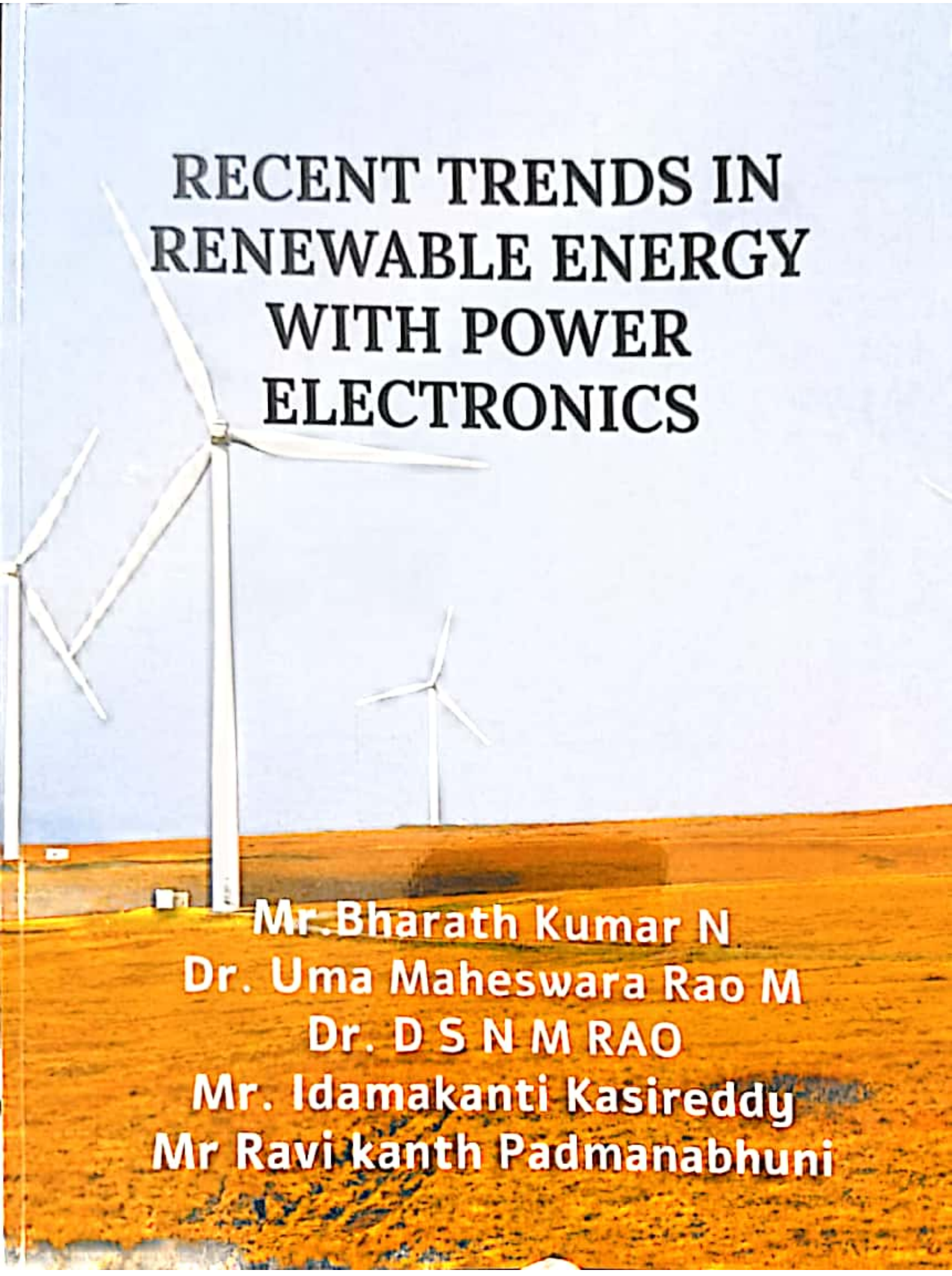

Mr. Bharath Kumar N
Dr. Uma Maheswara Rao M
Dr. D S N M RAO
Mr. Idamakanti Kasireddy
Mr Ravi kanth Padmanabhuni

Dr. M. Umamaheswara Rao

RECENT TRENDS IN RENEWABLE ENERGY WITH POWER ELECTRONICS

(For BE/B.TECH)

Text Book

Mr.Bharath Kumar N
Dept. of Electrical and Electronics Engineering,
Vignan's Foundation for Science Technology and Research,
Guntur, India.

Dr. Uma Maheswara Rao M
Dept. of Electrical and Electronics Engineering,
Vignan's Foundation for Science Technology and Research,
Guntur, India.

Dr. D S N M RAO,
Dept. of Electrical and Electronics Engineering,
Gokaraju Rangaraju Institute of Engineering and Technology,
Hyderabad, India.

Mr. Idamakanti Kasireddy
Dept. of Electrical and Electronics Engineering,
Vishnu Institute of Technology,
Bhimavaram, India

Mr Ravi kanth Padmanabhuni
Dept. of Electrical and Electronics Engineering,
Gokaraju Rangaraju Institute of Engineering and Technology,
Hyderabad, India

Xpress Publications
An imprint of Notion publications
India

MEASUREMENT AND INSTRUMENTATION: THEORY AND APPLICATION

Dr. D S N M RAO
T.Ch.Anil
Dr.P.M.Venkatesh
Dr. B. Mouli Chandra
Dr. B. Venkata Prasanth

MEASUREMENT AND INSTRUMENTATION: THEORY AND APPLICATION

(For BE/B.TECH)

Text Book

Dr. D S N M RAO
Department of Electrical Engineering
Gokaraju Rangaraju Institute of Engineering and Technology,
Hyderabad, India.

T.Ch.Anil Kumar
Department of Mechanical Engineering,
Vignan's Foundation for Science Technology and Research, Vadlamudi,
Guntur Dt., Andhra Pradesh, India - 522213.

Dr.P.M.Venkatesh,
Department of Electrical Engineering,
Vignan's Foundation for Science Technology and Research, Guntur,
India.

Dr. B. Mouli Chandra
Professor at QIS College of Engineering & Technology, Ongole,
Andhra Pradesh, India.

Dr. B. Venkata Prasanth
Electrical & Electronics Engineering, Department and Dean of
Administration & Monitoring, QIS College of Engineering and Technology,
Ongole, India.

Xpress Publications
An imprint of Notion publications
India

A study of Comparative analysis of fuzzy logic controller and neural network for dc–dc buck converter

Shaik Gousia begum[1], and *Syed* Sarfaraz Nawaz[2]

[1] EEE Department, GRIET, Hyderabad
[2] EEE Department, GRIET, Hyderabad.

Abstract. This paper presents the comparative analysis between fuzzy logic controller and neural network for DC-DC Buck converter. The major drawback in the conventional buck converter is when the input voltage or load change, the output voltage also changes which reduces the overall efficiency of the buck converter. So here we are using non linear controllers for buck converter which respond quickly for perturbations and maintains the fixed load voltage even when there are non-linearity's occurs compared to a linear controllers like P,PI,PID controllers which can't withstand when perturbations occur. Simplicity, low cost and adaptability to the complex systems without mathematical modeling are the best features of Fuzzy Logic controller and neural networks. The Two implementations are analyzed in detail and simulated in MATLAB/SIMULINK environment and results presented. Proposed approach is implemented on DC to DC step down converter for an input of 230V and performance characteristics like maximum overshoot, settling time and efficiency of the converter are studied.

1 Introduction

The design of dc-dc buck converter is to maintain a constant output voltage under the different load current and unregulated input voltage. The transient overshoot and recovery time of the output voltage should be minimized for stable operation in many electronic applications, which is ensured by the controller in the closed loop [1]. Classical controllers like PWM control, proportional (P) controller, proportional integral (PI) controller, proportional integral derivative(PID) [3] controllers only provides results which is either true or false. These controllers don't provide adequate results when there is nonlinearities in parameters or load. Recently, several methods have been proposed in the literature to alleviate the deficiency of the classical linear controllers for power converters. So non-linear controllers like fuzzy logic controllers and neural network etc are most widely used.

Now a days we are facing situations where we are unable to determine whether the state is true or false. Term "fuzzy" describes something that is non-linear or indefinite. Fuzzy logic is based on the observation that people make decisions based on imprecise or non numerical information. Neural networks are the set of algorithms inspired by the functioning of the human brain.So we are using non linear controllers for controlling the non-linearity's in the load because it responds faster to a transient condition, easy to design and implementation [4]. So here proposed controllers are used to stabilize buck converter's load voltage in transient state conditions [6].

2 Buck converter

The DC-DC buck converters are efficiently reduces the voltage levels as per our requirement. The basic circuit diagram of the Buck converter is shown in Fig.1. Here the MOSFET is controlled by duty cycles which are given by the non-linear controllers.

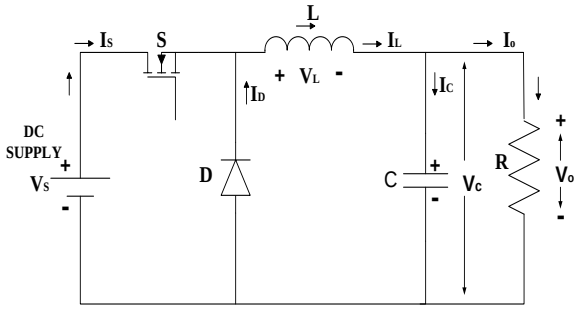

Fig 1. Circuit Diagram of DC-DC Buck Converter

Here, V_0 is the output voltage, V_L is the inductor current, I_C is the capacitor current, V_C is the voltage across the capacitor.

The modes of operation of buck converter are explained below.

Mode 1: When switch is closed, the current in the load and the charge of a capacitor is increase gradually because the energy also being stored in inductor. Throughout this

Frequency Analysis of Grid Connected EVS by using Artificial Neural Network (ANN)

Ranjith Kumar Reddy Banda[1], *Karunakumar* Davala[1], *Dola Gobinda* Padan[1], *Anil Kumar* Rajagiri[1]

[1]EEE Department, GRIET, Hyderabad

Abstract. The vehicle-to-grid (V2G) model is able to provide the power-systems that have been built to incorporate the hybrid electric vehicle model on a wide scale with distributed reserve. The authors suggested an amended V2G control model that would concurrently manage different renewable power sources, vehicle idle time and electricity generation on a vehicle consumer day basis. In respect of the desired status of battery and the detected plug-on terminal, vehicle-to-grid power is tested. This article presents an intelligent decision- making system based on an artificial neural network (ANN) that uses data logged by the M2MAMI for the planning and management of electricity charge. The ANN has been trained with household energy usage and EV energy requires the data and convention to determine when to charge the vehicle (G2V) or to discharge it (V2G). Charge Terminology, Electric Cars, Energy storage, Neural Network. Charge Scheduling. In this paper, MATLAB/Simulink implements the proposed control block. Different virtual images evaluate the performance of the control structure, interface, communications, device efficiency and time responses.

1.Introduction

Cars offered a comfortable lifestyle to society. Personal cars are preferred for freedom, protection and comfort over other modes, whereas travelling along greater distances is suitable for rail, aviation, etc. Without these carriages, animals would have drawn humans. Inventions, such as mechanical vehicles, balloon vehicles, steam-powered vehicles, push bikes, flights, helicoppers, aircraft etc. have reached up to one billion since 1350, in earliest known railway record. While these transport modes have generated many businesses, the environmental impacts they have had are devastating. And before they start moving, they use a lot of resources. The consumptive fuel and waste of the greenhouse, as well as other gases causing pollution such as carbon monoxide, nitrogen oxides and etc., are the main risks as the oxides of nitrogen and the hydrocarbons are reacting together trendy the eventof sunlight leading to the rise in the ground-level ozone. The transport sector primarily includes domestic combustion vehicles with an energy efficiency of up to 20%.

The other big effect of transportation is the mixture of petroleum in much of the world, such as environmental concern for fuel consumption, high petroleum prices and the potential for peak petroleum. In the mid-19th century, one solution was found to the threat posed by automobiles. This led to the demand for production of the cleaner alternative fuel or unconventional vehicle power systems. Although internal combustion engines remained the predominant motor vehicle power system for the next 100 years, electricity was used in different types of trains and smaller vehicles. Due to technological advances the electric vehicles (EVs) began to emerge as the burden of renewable energy was to change. When people came up with the concept, demand grew and engineers started sharing technical information to make electricity conversions[2-3]. Different kinds of EVs classified as their energy sources by the degree of electricity have appeared in industry. The major classes include: Electric Vehicle Batteries (BEV), Electric Hybrid Vehicles (HEVs) (PHEVs). Petrol and electricity are powered by HEVs. Regenerative braking produces the electric power to be used.This is a mechanism that helps to slow the vehicle down by the electric motor. It uses the energy transferred by the brakes to heat. You begin using the electric engine, followed by the gasoline engine as the cargo or the speed increases. The two engines are regulated by an internal computer that ensures the best driving performance. PHEVs are the same as HEVs, only distinction lying in another charge mode, namely, relation to the external power supply. The petrol engine expands the range of the car and when it gets low the battery also recharges. BEVs are completely EVs; i.e. they are only powered by electricity and have no fuel, oil only powered by electricity and have no fuel , oil or exhaust tube. They load either through

* Ranjith Kumar Reddy Banda: bandaranjithreddy93@gmail.com

Design of Fuzzy-PID controller using logarithmic approximations for IMC-LFC Model

Arunsai V[1], *Srividya Devi* P[2*], and *Vijaya Laxmi*.U[3]

[1]Research Scholar, EEE Dept., GRIET, Hyderabad, Telangana
[2] Associate Professor, EEE Dept., GRIET, Hyderabad, Telangana
[3] Assistant Professor, EEEDept., GRIET, Hyderabad, Telangana

Abstract. This paper provides a Artificial Intelligent controller layered to analyze the power system's logarithmic load frequency control problems. The control system ensures the preservation of steady frequency errors and of inadvertent bonding in a tolerance limit. The proposed control system was developed for a two-area hydrothermal heating system. The approach to control design is based on the two-degree internal model control (2DOF), which combines the fuzzy control technique for model order reduction to increase frequency excursions. Different techniques of the two-area reheating hydraulic energy system are integrated into the scheme and a correct combining of energy resources is seen in different operational conditions as a pragmatic solution. The IMC- FUZZY-PID architecture of the reduced order model, proposed with the original high order framework, delivers strong dynamic response and load sturdiness.

1 Introduction

Due to quick load disturbances, uncertainty of technical constants, operational differences, etc, performance can deteriorate in a broad power system. A ruggedness and reliability of a load frequency controller (LFC) for huge-scale systems are therefore extremely critical. However, due to its complexity, non-linearity and higher order, it is very tough to build the powerful controller in a wide-ranging, power system. a fundamental burden of a systems in a current power system scenario is maintaining equilibrium between electricity generation and a demand for electricity, in order to provide consumers with high-quality and reliable energy. Differences in energy demand can influence a power flow of a connecting line connecting control areas as well as a frequency of electrical services. As the result, a Large Frequency Controller (LFC) is configured to organize a system frequency, to change a generator units based principally on area control error, to zero under an infinite modulation of active electricity generation and therefore to balance a whole system with a load power well. This is because the better composition controller would have better control.

This can therefore be seen as a purpose enhancement or robust control problem [1–8] that counteracts unexpected disturbances, uncertain parameters, and can also operate effectively on a tie line under the defined overhead, set-up time, frequency and power variation [1]. Antipathy [8] proposed in 2009 to use multi-target evolutionary algorithms, with a Dead Band Governor and superconductive magnetic energy stores units (MESS), the decentralized LFC of interconnected energy systems(MOEA). For disrupted multifaceted power systems, the localized PID-LFC, where a power system's LFC performance depends on a locus on a stability border, was proposed by Sahaj et al. [9]. A design strategy, which was seen in the LFC literature to this day [9], causes parametric uncertainty. Uncertainty parameters in Swatietal were evaluated. [11] Considering the fractional order control principle ; a solid controller was designed to be similar to an internal model – proportional integrated derivatives [11] (IMC-PID).

In addition the method [12] for the application of load theory following an automatic power generation control has been seen in a reconstructed power system scenario. In light of contractual violations, a proposed hydrothermal energy system [12] is validated. The test device for various loads is an additional three-area unified electricity system [13]. There are several problems with goal optimization by improving the algorithm with a cluster-based set [14] with the proposal for the stabilization of the two-decker Multi-Driving Systems (SSSC), the magnetic energy storage (SMES), the thyristor control transfer, and more. Different technological optimizations have been suggested over the past decades [16–20] to maximize control gains in multi-area power systems to produce three degrees of 3DOF-PID and cascade controls [19,20]. A victorious 3DOF PID controller [16, 18] and a 3DOF ID controller [17] were respectively developed for different four/two-scale thermal and two-scale hydrothermal systems in the application of a highly optimized bio-geographic technique.

In addition, the data-based method [21] for repetition parameter adherence in the 3-DOF control structure was developed to improve a tracking efficiency. There are

* Corresponding author: srividyadevi.p@gmail.com

AVR SYSTEM ANALYSIS AND SIMULATION BY USING FOPID AND PARAMETERS VARIATION EFFECTS

Choppadandi Srikanth[1] , *Dola Gobinda* Padhan[1],*N. Kiran* Kumar[2].

[1]Department of Electrical and Electronics Engineering, GRIET, Hyderabad.
[2]Department of Electrical and Electronice Engineering, Vardhaman College of Engineering, Hyderabad

Abstract- The FOPID control units for an AVR system with a fractional filter are a unique fractional order. The main responsibility for controlling the reactive power and voltage level is an automated tensile regulator (AVR). PID controller, sensor, exciter, and stabiliser or amplifier are used for the module system. The system is designed according to state-space technology. The proposed controller must have seven independent parameters. A comparison of the published study with optimal adjusted AVR PID and FOPID controls also shows that the proposed controller is superior. The recommended controls derived from the bode analysis with their frequency response characteristics are shown. Finally, the resilience of the controller design is individually examined for both the parameter uncertainties of AVR system and outside storages introduced into AVR system. Given the overall results presented there are clear improvements to the performance of AVR system by a fractional filter in a proposed FOPID controller, and that the AVR system may successfully be applied to the suggested control.

1 Introduction

Reactive power is the foremost primary aspects for use and design in power systems. A constant tension output is the reactive force balance in the system. By shunting the reactive power injection, by transferring reactive power into the system via tap changes and lowering induction lane reagents through a succession of condensers, one may define the most common reactive power and voltage management systems. AVR systems are commonly used in exciter control systems. Major technique of the reactive power control is AVR generator excitation control. In typical operational conditions, AVR shall maintain the generator terminal voltage constant at varied load levels[1]. The Terminal Voltage Error is used to modify the voltage in AVR loop for an axle control system to administer the terminal-voltage[2]. Four important components – amplifier, sensor, exciter, and generator – are included in a controller exciter. Several articles discussed the AVR system control principles[2-5]. A Real energy losses in electricity generators are a general difficulty to solve. Researchers are studying automated voltage control units (AVR) to reduce these power losses in the power system. The major goal of this kind of AVR systems is to keep generator voltage at correct level highly precise. This precision enhances the life cycle of power system rated voltage equipment. The AVR system's stability and strength have a considerable impact on the power system's security[1]. Therefore, an efficiency of AVR system continues to be an important topic for the development of new control systems. In particular, many studies have been done to improve the AVR system's transitional reaction to the stability limitations. Researchers have devised several control ways to control the AVR generator voltage so far in an effort to get an enhanced system response. Some of the control techniques presented are the PID fractional order control (PRD) [2-4] [5,6]. Despite these enormous modifications, the scholars focus more on PID controller or its amalgamations because to its straightforward control structure and effectiveness.

PID controller parameters, like other controllers, must be adequately tailored to deliver a good system response. In addition, PID controller settings must be optimally modified in order to reach the best system answer. However, depending on industrial use, this perfectly adjusting method presents a serious problem.

ANN based LFC with Coordination strategies of DERs in Hybrid Isolated Micro-Grid Environment.

Srikanth Boyini [1], *Srividya Devi* Palakaluri[2,*], and *Rekha* Mudundi[3]

[1]Research Scholar, EE Department, GRIET, Hyderabad, Telangana
[2] Associate Professor, EE Department, GRIET, Hyderabad, Telangana
[3] Assistant Professor, EE Department, GRIET, Hyderabad, Telangana

Abstract. This paper provides a load frequency control (LFC) of a micro grid with renewable energy resources (RES). The operation of micro grid with a low inertia system leds to disturbances in power system. The disturbances in frequency is more in micro grid than conventional power system. So there should be a fast recovery of changes in frequency with existing system and interconnected system (RES). Active power injection is the main scheme to control frequency of a system. The matlab simulink tells us that different active power injection system contribute for the fast control of grid frequency with PID controller. The use of ANN technology to this system the load frequency control can be illustrated in faster rate of its recovery. An ANN controller is investigated which handles the inputs collectively in each sector of the power system. Back-transmission time is normally used in the study for neural network education. The performance of the power system is simulated independently with a typically integrated conventional controller and ANN controller. A complete spectrum of small signals is introduced for RESs in the isolated microgrid and a correct role in frequency control studies is taken into account.

1 Introduction

The prerequisite is to improve the confidence, economics and environment for conventional systems to introduce micro-grid (MG) into the energy system[1,2]. It seems obvious that the MG is a power storage device that includes everything. RES generators are commonly dispersed and employed in MGs[3,4] for load controlled and storage instruments (DGUs). RES is usually spaced out. The distributed generations typically included in the MG[5] studies are wind energy generators, photovoltaic (PV) panels, fuel (FCs), diesel (DEG) and battery storage equipment for flywheels (BESSs).The successful use of the DG units satisfies detrimental environmental constraints not only in order to achieve the spread of electricity consumption. Although the MG Framework for DGUs offers a lot of advantages, there are a number of issues associated with the monitoring, stabilisation, and efficiency of the MGs in terms of a greater variety of power sources with a wide range of dynamics[6]. The MG connection mode could in some way exacerbate the problems indicated. In two different ways the MGs work: (1) Isolated mode, and (2) Grid link mode[7], as prior study shows.

Unlike the RES structure in the island mode, a rendered-connecting mode involves intermittent change in RESs using smart, flexible AC MG management strategies to ensure robust performance and stability by remedying a connected power grid which reduces the disturbances in charge compared to the island mode. The SACP system in an island state has major obstacles and needs to be assessed for several reasons. The main generation of AC-MG fleets is mainly DER.This appears to result in a high frequency change in the separate microgrid from the synchronous generator (RoCoF).
The RoCoF is more than 0.2 Hz/s in the clearness of the Low Inertia Grid in conventional systems. Therefore, the necessity to provide suitable auxiliary services, such as inertia responses and primary frequency response, is unavoidable for all inverter-related technologies. Secondly, the provision of MG stable services does not provide the whole MG swiftly, which could lead to an aggravation of the issue. When the system fail and activates a safety system, the RoCoF in the MG reduces breakage rate to its contingency limit and is able to separate each electrical unit. Therefore, support for frequency in MG must be sufficiently swift in order to avoid the drop of frequency in low frequency conditions. Third, analysing the influence of the DERs on power storage systems. In this study, storages of non-existent DER units are employed to transform them into sendable units. However, other frequency support firms may have difficulty coordinating energy storage systems. Finally, In low- and medium-voltage distribution networks [8-10], the method for micro-grid management is a critical concern. In other words, there are inadequate distribution networks and unclear working conditions. DER's interaction with the production plan thereby minimises

* Corresponding author: srividyadevi.p@gmail.com

Speed control of robust position sensor less PMBLDC motor by Fuzzy controller

Shravani Sattu[1], *Vinay Kumar* Awaar[1*], *and Praveen* Jugge[1]

[1]Department of EEE, GRIET, Hyderabad, Telangana, India

Abstract. The aim of this work is to present a novel mechanical sensor-less control approach for permanent magnet brushless DC (PMBLDC) motors based on speed independent H functions. The starting of the motor and driving it from a low speed to the rated speed are two significant problems in sensor-less operation of PMBLDC motor drives. The commutation moment is determined using a speed-independent H function. Since the commutation instant is speed independent, it may be anticipated even at low speeds. The H function is entirely dependent on-line voltages, which simplifies and reduces the cost of the whole system. The suggested approach eliminates the need for analogue filtering and phase correction. Digital low pass filters and digital phase compensators are used to remove commutation ripple from line voltages. This results in a system that is small, simple to use, and cost effective. This economical option is ideal for low-cost equipment such as fans, air conditioners, refrigerators, and vacuum cleaners. The suggested method is implemented using a fuzzy controller to demonstrate the proposed sensor-less technique's efficacy for wide speed variations.

1 Introduction

In the last three decades the reduction of PMBLDCM functioning has always been an appealing study topic for academia (Permanent Magnet Brushless DC Motor). As the use of Hall-Effect electronic sensors is essential for rotor position assessments, due to the extra weather and circuitry a system is expensive and complex. A hall-effect sensor is also sensitive and successful with restricted temperature fluctuations. Therefore, the usage of a PMBLDC engine in both industrial and residential applications was restricted for those reasons. Many efforts have been made in a literature to overcome these deficiencies. The simple technique to estimate PMBLDCM's location is a strategy for EMF sensing [1-5]. A sensor in connection to a virtual soil of a zero-phase transmission is used to calculate the switching timings of this approach. However, a phase voltage zero-crossing instant is not a genuine moment. A null-crossing instant must be modified in phase to create the correct switching instant. A zero passing of line voltages is the extra approach in the category. A line voltage might be twice as – phase back veterinarian EMF. [6-7] has been demonstrated to offer the switch-up immediate to zero EMF return phase. The low-speed performance of these methods is a major disadvantage. The efficiencies of a technique above are not excellent because a low-speed EMF stage return is too low to be accurately sensed. A perceived back emf from a quiet phase is integrated into another technique [8] and [9] until a threshold is reached. Integration begins with a null crossing and returns a threshold value for the back phasing emf. It is established that a threshold value will nearly overlap with an exact time of switching. This method also shows inefficiency and low efficiency at lower speeds. A novel, technologically less sensor method has been outlined in the three-phase balanced star [4] and [10], which connects the three-star resistor with the neutral point, n. A voltage of three times the frequency of a trapezoidal rear emf between two neutral locations (Vnn'). This approach is hence termed as an EMF detection technique as a third harmonic back. A list of VNNs is added below and a decision is made at the time of switching. AVnnTes zero crossing was changed by 300 phases from an exact point of change, yet the integration corresponds precisely with a moment of switching. A neutral point of an engine is necessary for this operation. Another technique [11] for immediate switching measures the current of a quiet phase freewheeling diode. Because of inductive engine winding, freewheels through the diode are present in a quiet phase. A switching moment is picked by monitoring this current. There are six current measuring circuits that make this technology a complicated, costly, and large gadget. [1] for very

* Corresponding author: vinaykumaar.a@gmail.com

Analysis of Hybrid Energy Storage System for Hybrid Electric, Battery Electric and Plugin Hybrid Electric Vehicles using Bidirectional DC/DC converter

Vijaya Krishna Muragani[1], *and Anil Kumar* Rajagiri[1]

[1]EEE Department, GRIET, Hyderabad

Abstract. This paper deals with the Hybrid Energy Storage System (HESS) for Battery Electric, Hybrid and Plug-in Hybrid Electric Vehicles. Its performance is compared with conventional HESS design and also only Battery design, conventional design uses a bigger dc/dc converter between Battery and Ultracapacitor to satisfy the peak power demands in the real time, In this analysis a smaller dc/dc converter is used which maintains the voltage of ultracapacitor higher than the battery voltage by working as controlled energy pump. Battery will provide power directly only when voltage of the Ultracapacitor drops below the voltage of the Battery. Therefore, a constant and smooth load profile can be created for the battery. For the proposed HESS system Simulation results are presented to verify.

1 introduction

The world is developing by ensuring proper usage of advanced technologies for Electric Vehicles. The increase of vehicles has mainly caused major problems like traffic jams, CO_2 emissions, and therefore the extinction of fossil fuels. Decarbonization plays a crucial role in reducing the CO_2 emissions from transport vehicles. Electric vehicles are attracting attention within the vehicles market due to their low emissions of CO_2 and efficient reduction of CO_2 emission. The EV has higher engine efficiency and doesn't emit pollutants because it doesn't have any fuel. So, it's referred to as a zero-emission vehicle.

Energy storage systems (ESSs) have more importance in hybrid electric vehicles. Batteries, Fuel cells, Hybrid combinations are some of the commonly used among the energy storage systems. In Battery based Energy storage systems, the battery power density should be maintained higher enough to satisfy the peak power demand. Batteries with higher power densities also are available within the market, they're much costly than lower power density batteries. The solution to this problem is to increase the size of the battery [1]. However, this also increases the cost. In addition, balancing the cells in a battery system is an issue which concerns the battery life. Applications of instantaneous power input and output, find the batteries affected by the frequent charging and discharging operations. which affects the battery life. For this type of system it is necessary to keep an additional Energy Storage System which is more stronger to handle the surge current.

Hybrid energy storage systems have been analysed to reduce such problems. The general idea of a Hybrid Energy Storage System(HESS) is to combine ultracapacitors (UCs) and batteries to achieve better overall performance [1]. Ultracapacitors have a higher power density and lower energy density. This combination gives better performance when compared to the use of them alone.

One of the example is the hybrid energy storage system (HESS) using battery and Ultracapacitor, where the battery is used for compensation of low-frequency power fluctuations and the ultracapacitor is used for compensation of high-frequency power fluctuations [2]. Many researchers have demonstrated the efficiency of battery-ultracapacitor hybrid energy storage systems using theoretical models and experimental prototypes, however this is due to the drastically differing operational parameters of ultracapacitors and batteries. There are a variety of topologies that use both battery and UC hybrid energy storage systems, each with its own set of benefits and drawbacks, and researchers are still looking at them.

Table 1. Characteristics of Battery Cells.

Chemistry	Nominal Cell Voltage (Volt)	Energy Density (Wh/Kg)	Power Density (Kw/kg)	Life cycle (Times)
Lead Acid	2	30-40	0.18	Up to 800

* Vijay Krishna Muragani: vijaykrishnam6@gmail.com

ANN Based Current Controller for Hybrid Electric Vehicles

*Kavati.*Nagendar[1,*], *and V.Vijaya* Rama Raju[2]

[1]PG Student, Department of EEE, GRIET, Hyderabad, India.
[2]Associate Professor, Department of EEE, GRIET, Hyderabad, India.

Abstract. The use of Hybrid Electric Vehicles (HEVs) across the world is growing enormously every day. The single-phase bi-directional convertors are presented in this study for HEVs on-board charging(OBC). In HEVs, we use power electronics converters for the converting and inverting operations. Artificial Neural Network(ANN) is presented in this study for simple operation and high optimization approaches. ANN control technique regulates the system's THD and enhances charging system optimization, enables two-way power delivery that is from the grid to vehicle and the vehicle to grid. An ANN based current controller model that achieves fast-dynamic reaction and that improves grid current harmonic characteristics is proposed in this study. The system's THD is reduced by the ANN controller being suggested. The results prove the validity and feasibility of design and control technique of the proposed integrated charging system.

Keywords: DC-DC bi-directional converters (BDCs), Artificial Neural Network algorithms, Electric Vehicles.

1. Introduction

Hybrid Electric Vehicles (EVs) and Electric Vehicles (EVs) are generally the vehicles that must meet the standards for urban transportation emissions during the next 10 years. HEVs are a hybrid between traditional combustion engine vehicles and electric vehicles (EVs)[1], a compromised alternative that addresses issues such as air pollution, petroleum combustion, and limited driving range[2]. HEV [3] is made up of various components such as machines, gearbox, battery, charger, traction engine, and its driving inverter. A second power generator and its drive inverter are also included in system. The starter-generator system's goal is to start engine from a standstill and transform vehicle's kinetic energy into electric energy [4-5]. In this study, starter mechanism is modified to act as battery charger, rather of OBC, which is found in most HEVs (OBC). As result, upgraded start-generator system employs two distinct modes. The first is a motor drive that acts as a typical starter-generator. The charging battery is the other. Because this integrated charging method substitutes traditional OBC, it is possible toeliminate traditional OBC from HEVs. As a result, the redesigned circuit reduces the volume and weight of HEVs while also increasing power density. A feedback-based current control technology, such as proportional-integral controller, has emphasised the power converter's performance in recent decades[5-6]. The PI current controller achieves fine control results by translating time variable on synchronous frame into time-variable. Some of the flaws in this control strategy, however, are due to the controller's system parameter design. Furthermore, designing a controller for a sophisticated system is difficult. Model Predictive Current Control (MPCC) is introduced in this study as method for controlling 1-phase full-bridge inverter when integrated circuit is operating in battery charging mode. For high total harmonic distortion (THD) in output current, the typical MPCC produces eight separate voltage vectors because single phase two-level inverter only makes three distinct output voltages. THD in output current can be reduced by increasing sampling duration and reducing calculation time. Harmonic features of output current are limited and increased using an advanced MPCC method. Compared to typical feedback-based control method, the MPCC methodology has a faster dynamic response time. Output current has superior harmonic characteristics when compared to MPCC's normal method. Simulation results confirm the accuracy of proposed integrated charging design and control strategy of the system. There are several industries that look to bidirectional DC-DC converters (BDCs) as energy sources to improve the transmission and distribution of energy. As a result of system losses, efficiency is reduced and circuit elements' lifespan is shortened. Deshalb sollten in order to avoid power loss, better control systems be implemented whenever possible. A bidirectional power flow's efficiency is crucial to obtaining high-quality electrical energy. To improve the efficiency of the converter, a variety of control mechanisms are currently being explored. One of these control approaches is the artificial neural network (ANN), which is based on a variety of algorithms. Vector support (SVM) and autonomous map (SOM) approaches are used in ANN to feed forward information (FF). They are divided into two

Compensation of active and reactive power in PV- WIND battery system by using ANN technique

A. Ashwini [1,*], *V.* Usha Rani[2], *J.* Sridevi[3]

[1]PG student, EEE Department, GRIET, Hyderabad, Telangana
[2] Assistant Professor , EEE Department, GRIET, Hyderabad,Telangana
[3] Professor, EEE Department, GRIET, Hyderabad, Telangana

Abstract. This paper proposes the improvement of PV-WE system's energy usage and the battery energy storage system (BESS). PV, BESS. Surveillance, tension management, frequency control, energy distribution, power quality and artificial intelligence techniques (AI). The aim is to increase the power quality of the grid-connected PV-BESS system. In order to increase energy quality, technology is continually explored and evaluated. The PV-BESS system is built for the microgrid, which offers benefits including continuous supply, efficient load content and effective electricity utilisation. The flow of energy from source to source is controlled by ANN. The development of the MPPT algorithm for validation of the proposed approach is using an artificial neural network (ANN) technique. An extensive research and data finding demonstrates that output is accuracy with the ANN-based MPPT output. This study therefore proposes a new way for assessing the performance at a specific site of the microgrid. The power translation systems are therefore handled in an active and reactive manner taking into consideration their circumstances and limitations.

1. Introduction

The power balancing and load sharing are hierarchical control systems for voltage/frequency control, such as primary monitoring, secondary control and tertiary control[1], that are employed as a microgrid control. The decentralised drop-based control system also gives without communication an essential alternate control[2]. However, the following shortcomings are shown in various control systems:

1.1 System Coordinates

Generally, models were developed in the d-q synchronous frame of reference. However, this strategy presents some inconveniences. First of all, this technique takes the form of properly balanced three phase systems for loads, grids and models. However, a load normally involves several single-phase loads spanning three phases, and so a perfect load balancing, especially in a microgrid, cannot be achieved. A load does not necessarily represent a linear load and can be distorted or harmonic very easily. Models are therefore employed in this research in abc co-ordinates.

1.2 PLL (Phase locked loop)

In practise it needs to be monitored, and PLLs have been employed for this. This is a realistic technique. PLLs have their reactivity and characteristics, and both simulation models and control techniques have these characteristics. For the monitoring of the several models, the angles d-q to a-b-c and a-b-c to d-q are needed (e.g. the 3-phase inverter model). This work aims at the improving the dynamic performance of the available photovoltaic system.

1.3 Controller

A control approach that selectively limits the output of the control, taking into account also model line impedances, to achieve the control target.

In tandem with the RESs, the converters are utilised for transforming power into the grid. In the reference study[12], RES is connected to a bidirectional transformer and a hybrid configuration layout that includes PV and WE. Different characteristics like average wind speed, radiation, and temperature need to be taken into account when calculating PV and WE systems as weather-sensitive RESs. In several nations like India, China, Iceland, Sweden and the USA, there are a wide range of RES scenarios[2]. To be added in WE, on-shore and offshore output capacity is different[13]. Accordingly, flexible mathematical modelling and optimization methodologies must be designed to design seasonable WE and PV systems according to the many aspects affecting PV and WE systems. It is difficult to design the non-linear features of pv. Various optimization methods like as the optimisation of particulate swarm are therefore employed for estimating PV system parameters and improving the power production of PV and WE [14]. Ultimately, these strategies will aid configure the modelling of RESs. However, due to voltage drops on the line[4], the distributed generation (GD) units observed incorrect reactive power sharing. In order to overcome these restrictions[1],[3],[5]-[11] A secondary central control that requires dual-way communication

Reliability Analysis with Renewable DGs for Loss Reduction in Radial Distributed Generation

R. Kavyasree[1*], *J.* Sridevi[2] *and V.* Usha Rani[3].

[1] Student, EEE Department, Gokaraju Rangaraju Institute of Engineering and Technology, Hyderabad, India
[2] Professor, EEE Department, Gokaraju Rangaraju Institute of Engineering and Technology, Hyderabad, India
[3]Asst.Prof. EEE Department, Gokaraju Rangaraju Institute of Engineering and Technology, Hyderabad, India

Abstract. Nowadays, in the Evolving Power System, reliability testing plays an important role in the design and implementation of distribution systems that operate in a cost-effective manner with minimal customer load disruption. The distributed generation (DG) will play a major role in emerging Power systems as they use a variety of resources and technologies to harness energy in Power systems by reducing Power losses while maintaining the Voltage profile in the system within the limits set. In this paper, two case studies with one DG and two DGs were analysed. The results obtained showed that the DG Number with the plan will increase the reliability of the joint system. The proven system is verified before the IEEE 6-Bus Radial Distributed System to reflect exposure and impact on ETAP software.

1 Introduction

The DG (Distributed Generation) has been growing rapidly in reduced power systems resulting in their potential solutions to meet local needs at the distribution level and to reduce limited transmission power from central power stations[1-2]. The entry of the DG into the existing distribution system has many imputations for the system. However, incorrect size as well as arrangement of the units of weight units in a power system can jeopardize a reliable system performance[3] As a result, a good location and DG size should be established for the network distribution infrastructure In power systems, reliability analysis is defined as system flexibility analysis to satisfy load requirements [4-5]. The calculation of the reliability of a complete system depends on the reliability of all components included in that system. Each section has 2 locations, working conditions and unsuccessful conditions[6]. By specifying whether a component is active or not we will select the order of the program. reliability analysis and square measure assessment are key factors in the continuous performance of the system The main objective is to measure the effect of DG on the reliability of the system[7-8]. The IEEE 6-Bus distribution network was used in the study. [9] The precision and size of the DG have been changed, the insect particle development and the ETAP software packages have been used for model analysis and reliability [10-11].

There has been developing interest in renewable energy from renewable resources due to the need for extra electricity, global warming and therefore a strong elimination of fossil fuels. The onset or arrival of an expected energy source from a renewable source[12-13]. sources is likely to be a more reliable answer to the question than one perceived. Therefore, analysis before the merging of DGs into a distribution network is very famous [14-15]. Indeed, the position of the DG is the best place to live or work and the appropriate size bequeath in one can make different edges on the whole power such as living force lost or lost object and line deceleration, smooth reduction and sensitivity of the power profile [16].

Wind energy is a common high-performance renewable DG because it occurs as a rapidly growing energy source from renewable energy sources as it is a low energy cleaner and also requires minimum time to establish. Air production is happening very fast as part of a full-fledged news feed [17]. The ideal power supply for system winds on the earth's surface is 1.6x107MW approximately, which is equivalent to the energy produced by the earth's crust. Wind power exists as a result of expected delivery, because the size and location of the living or the production of wind farms constitutes a suitable disposal relationship[18-19].

Solar energy can be a superior source of energy and carry a large amount of energy in the form of an infinite energy source[20]. Its capacity is 178 billion MW, which is 20,000 times more than the demand for land. Solar energy can be used as photovoltaics[21]. PV systems can be used to provide a wide range of energy sources: fashionable homes, public spaces, limited businesses, crop production, health care, and available water. Another part of the PV action grid action, is usually as distribution units are distributed[22]. Due to the critical nature of the loads, the current system value exceeds its production capacity which makes connectivity resources unavailable and therefore a robust system structure cannot be exceeded. In a systematic way, in order to

* Corresponding author: kavyasree.rudroju@gmail.com

Battery, Ultra-capacitor based Hybrid Energy Storage System (HESS) for EV applications with PI and Fuzzy logic controllers

Jonnalagadda Santhosh[1], *Anil Kumar* Rajagiri [1], *Prashanth* Morri [1]

[1] Department of EEE, GRIET, Hyderabad

Abstract. The extensive use of vehicles based on IC engines has contributed to serious effects on the environment and accelerated depletion of fossil fuel reserves which has led to a rapid increment in fuel cost over the past few decades. By consideration of these undesirable effects, the automotive industry will move towards the electrified drivetrains for obtaining zero-emission and higher efficiency. In electrified vehicles, the drive is coupled entirely partially by e-motors powered by energy storage sources. The choice of the simple structured HESS topology is to make a better understanding of power flow and controlling circuits based on limits of existing energy storage sources and contribute to the electrification of the drive. The main intention of this paper, the excessive current which is required by the motor is to draw from the ultra-capacitor without burdening of battery. This will improve the efficiency of the storage sources and also smooth running of the drive. This document examines the feasibility and capacity of a HESS which integrates the battery and ultra-capacitor units and controlling through PI and Fuzzy controllers.

1 Introduction

The electrification of vehicular drives will make results in demanding of better performance and efficiency of Energy Storage System (ESS) for Electric Vehicle (EV) and Hybrid-Electric Vehicle (HEV) drives. Right now, no existence of only one type of energy storage source, which can provide all the requirements of vehicles while moving on roads. Li-ion batteries are a promising new scientific advance for the applications of vehicles because of their large specific-energy and comparatively larger specific-power than batteries of lead-acid and Ni-MH. If the Li-ion battery is subjected to quickly fluctuating charging/discharging currents due to coping with rapid fluctuations in torque and load power, the battery's life can be severely reduced. Ultra-Capacitor (UC) has superior in specific power and lower range of specific energy. By consideration of these properties, we can say Lithium-ion batteries are complement to Ultra-Capacitors, it is worth combining these energies to give appropriate results to run a drive [1]-[4].

2 HESS configuration

The literature on HESS topology has been discussed in [5], [6]. In all the simplest combinations of batteries and supercapacitors, the direct connection of the two units is achieved through a DC bus. Using DC-DC converters and controllers, this topology can be implemented very easily and at a low cost, but UC can't be used to its full potentials in this configuration since voltage of UC unit is restricted by the voltage of battery unit (BU).

The HESS topology is provided with a partially-decoupled technology with a single DC-dc converter that connects BU and UC. When especially in comparison towards the scenario of BU as well as UC are connected to the DC link via individual DC-dc converters, this arrangement will result in reduced weight. In this topology the DC link is coupled to either BU or UC. By considering the topology which the direct connection of BU with DC link and UC and DC bus are interfacing with DC-dc converter, here the unit of UC will be functioning of broader limits of voltage due to the converter and BU will affects from the rapid change of discharging/charging currents which are required or obtained from the electrified drive during acceleration or regenerative braking conditions respectively. To avoid this affects here we recommend partially-decoupled HESS design where fig.1 shows.

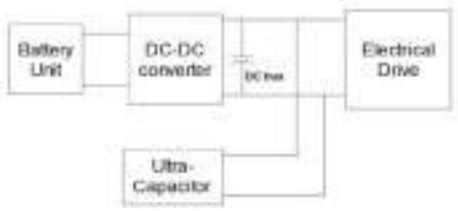

Fig.1. Proposed HESS configuration with Batter Unit, DC-DC Converter, Ultra-Capacitor directly interfaced to DC link.

As a result of this study, BU is protected in this configuration by providing the proper control technique to the DC-dc converter. In the contrast to the case where

* Jonnalagadda Santhosh: jsanthosh00@gmail.com

An Extensive Study on Machine Learning based Battery Health Estimation

Sai Vasudeva Bhagavatula[1], *Venkata Rupesh* Bharadwaj Yellamraju[1], *Karthik Chandra* Eltem[1], *Phaneendra* Babu Bobba[1] *and Naveen Kumar* Marati[2]

[1]Dept. of Electrical & Electronics Engineering, GRIET, Hyderabad, Telangana., India.
[2]Architect, Wipro Limited, Bangalore, India.

Abstract. This manuscript is a comparative study on various machine learning Regression methods like Decision Tree and Random Forest and SVM and other improvised methods along with unsupervised methods like Reinforcement learning, ANN methods like DNN are also discussed along with advanced methods like GRU, CNN, LSTM for estimating the battery health in order to estimate its life which is used in the modern-day technology of Battery Management System. The evolution of the present day BMS bought a great opportunity to study more about adaptive learning systems as it provides greater efficiency and tunes itself basing on environmental changes for battery health estimation studying on various methods on the subsets of artificial intelligence can be helpful to build more accurate correlation between the input and output. Adaptive learning even having a self-adjusting feature the computational limitations and the data being used is also important in producing correct result with a promising accuracy, so multiple algorithms, architectures and models are studied for better understanding in order to come to conclusions for selecting the apt model for satisfying results. Compared to other conventional methods Artificial Intelligence and their subsets learn from the error and adopt which outperforms other models in accuracy.

1 Introduction

A battery management system this helps to improve the robustness and performance of the battery. The BMS acquires information about the electrical and ambient parameters of the battery and not only protects it from electrical damages but also helps to enhances its functioning and battery life. The behavior of the battery can be understood by the State of Charge and State of Health or the Performance Characteristics are very useful is modern day technologies earlier many conventional methods were used for estimating these responses but later after the improvisation in the computational power of machines like computers old technologies like

Adaptive learning methods - machine learning and ANN (Artificial Neural Nets) started evolving that offer far better performance than the conventional approaches of estimating SoC and SoH. A representation of various ML techniques and their classification are mentioned below.

Fig 1. Representation of Machine Learning Methods

In the recent years the research in this particular field has grown enormous due its flexibility and accessibility.

From the vast research being conducted on these self- adjusting systems for the Battery health estimation some of basic attributes like voltage current and ambient temperature of the battery pack is being used for the estimation of SoC and for the estimation of health of the battery pack additional parameter like SoC, charge cycles, voltage, current, temperature and along with additional parameters are taken into consideration when dealing with these methodologies. A basic workflow any machine

https://doi.org/10.1051/e3sconf/202130901100

Power quality enhancement using Artificial Neural Network (ANN) based Dynamic Voltage Restorer (DVR)

Chaitanya Kasala[1], *Vinay Kumar* Awaar[1*], *Praveen* Jugge[1]

[1]Department of EEE, GRIET, Hyderabad, Telangana, India.

Abstract. The power quality, which can affect consumers and their utility, is a key concern of modern power system. The sensitive equipment is damaged by voltage harmonics, sag and swell. Therefore, as usage of sensitive equipment has been increasing, power quality is essential for reliable and secure operation of the power system in modern times. The potential distribution flexible AC transmission system (D-FACTS) device, a dynamic voltage restorer (DVR), is widely used to address problems with non-standard voltage in the distribution system. It induces voltages to preserve the voltage profile and ensures continuous load voltage. In this paper, the voltage sag and swell is compensated by DVR with an artificial neural network (ANN) controller. For the generation of reference voltage for voltage source converter (VSC) switching, and for the voltage conversion from rotating vectors to stationary frame, synchronous reference frame (SRF) theory is applied. The DVR Control Strategy and its performance is simulated using MATLAB software. It is also shown a detailed comparison of the ANN controller with the conventional Proportional Integral controller (PI), which showed ANN controller's superior performance with less Total Harmonic Distortion (THD).

1 Introduction

Electrical energy is a universal commodity available throughout the world and regarded as a daily consumer need [1]. The sources of renewable energies like solar, wind, etc are used to support the primary demand of energy. The intermittency of the renewable sources, reactive power issues and harmonics stop the performance of the power system by causing problems of power system stability [2], [3]. Flexible AC Transmission Systems (FACTS) devices are commonly incorporated to compensate reactive power, regulate voltage stability and improve power quality [4], [5]. FACT devices, however, also change different system parameters [6], so as to study the quality of power and determine the causes and solutions to these issues of power quality. In power systems, power quality has a major role during supply of variable power to the load. Consequently, the customers of domestic and industrial with sensitive loads will get affected by poor power quality. When any disturbance occurs in load voltage, results in voltage transient, sag, swell, harmonics causing high distortions and faults causing Total Harmonic Distortion (THD). The DVR can control the voltage from these problems and protect against tripping and resulting losses. Various problems and solutions related to DVR were reported, such as balanced voltage in a three-phase system and energy-optimized DVR control [7]. References [8], [9] give analysis of various control strategies for different voltage sag types. In [10] a comparison is presented for DVR between various topologies and control techniques. Paper [11] discusses the design of a DVR supported by a capacitor that protects distortions, sags, swells, or imbalances in supply voltages. The DVR's performance is discussed in [12] with a transformer of high frequency-link. This paper presents DVR's control and its performance with voltage source converter (VSC). In this paper synchronous reference frame (SRF) theory with artificial neural network (ANN) controller is used for DVR control.

The DVR is designed for balancing load side voltage with minimal injection of active power, even in the event of unbalanced disturbances compensation [9], through a cascaded H-bridge multilevel inverter. The use of DVR is a cost-effective way of mitigating sensitive load voltage sags and swells. The disadvantages of the existing method are solved through the application of the Artificial Neural Network (ANN) controller. The ANN controller is used for design and simulation of DVR to improve power quality and minimize harmonic distortions in sensitive loads [9]. DVR is utilized to increase the real power of the inverter in any disturbance. The DVR can be used as a voltage sag restorer and the voltage distortion compensator with

* Corresponding author: vinaykumaar.a@gmail.com

Grid-Connected Rectifier Based Dynamic Voltage Restorer To Improve Power Quality By Compensating Voltage Sag And Swell

Someshwara Thota[1], *Vinay Kumar* Awaar[1*], *Praveen* Jugge[1], and *Tara Kalyani* S[2]

[1] Department of EEE, GRIET, Hyderabad, India
[2] Professor, JNTUH, Department of EEE, JNTUH, Hyderabad, India

Abstract. Voltage sag and voltage swell are frequently occurred power quality problems in present power distribution system, which are cause more problems to avoid these problems and maintain constant voltage at sensitive load during sag and swell Dynamic voltage restorer gives solution .we propose self-supported DVR, to minimize the cost by preventing external dc source in DVR, it is controlled by SRF PI control along with an inner current loop to stabilize the system and outer voltage loop to increase the system robustness. The proposed model provides fast voltage restoration for a short and long duration of voltage sags and swells manage wide load current variation for short and long voltage disturbances. In this paper, we present the effectiveness of the proposed method by using MATLAB/simulation results**.** A laboratory prototype DVR is modelled and we are using CCS studio to interface DSPTMS320F28027F

1.Introduction

Power quality problems are classified based on quantity into voltage power quality and current power quality problems. Voltage power quality problems are classified as voltage sag, swell, interruption and voltage notch depending on magnitude variation of quantity [1-3]. The load connected to the power system is dynamic; when the load connected to the system is increased, it causes voltage sag and the load connected to the system decreases it causes voltage swell. During voltage sag and swell, the voltage across the load is not constant or rated due to these more problems that occur; the uneven operation of end-user equipment, cause production losses of process industries, and maloperation of relays and circuit breaker. The custom power devices STATCOM (static compensator), DVR (dynamic-voltage restorer) and UPQC (unified power quality controller) provide rated voltage across the load even voltage sag and swell occur. Still, the complexity of design and installation cost industries prefer DVR more than STATCOM and UPQC [3-7]. Dynamic voltage restorer is a series compensating device. It injects the voltage in series with the line; DVR injects voltage in phase and out of phase with supply voltage during voltage sag and voltage swell. To inject the voltage, DVR needs a certain amount of real and reactive power [8-13]; it is provided by using an energy source in DVR. Depending on the energy source, DVR is classified as capacitor-supported DVR, battery-supported DVR and Rectifier-supported DVR. The large magnitude and long duration sag condition require a large amount of energy storage capacity, increasing device cost. For avoiding high price for designing of DVR, we propose a self or grid-connected rectifier-supported DVR to compensate voltage sag and voltage swell [14-16], which is controlled by using SRF PI controller along with inner current loop it stabilizes the system and outer voltage loop it increases the robustness of the system. The proposed model provides fast restoration and reduces voltage disturbances. The proposed method can manage wide load current variations and avoids current distortions during short, fast and long

Corresponding author: vinaykumaar.a@gmail.com

Comparative Analysis of Coil Structures and Orientations of Single Transmitter and Multi Receivers Wireless Power Transfer System

CH Jagadeesh[1*] and *Phaneendra* Babu Bobba [1]

[1] Department of EEE, GRIET, Hyderabad, India

Abstract. Single transmitter and multi receiver (STMR) based WPT system is used to power multiple loads at a time. It consists of some limitations like long distance power transfer, mutual inductance between receiver coils and misalignment of receiver coils. this paper is going to give a detailed information about different designs of STMR, which are going to overcome the limitations of STMR. Different designs proposed by different authors are wireless power repeater system with single coil in each repeater, wireless power repeater system with two coils in each repeater, spherical strongly coupled magnetic resonant, square shape coils, maglev train IPT system and cube shaped unidirectional flux transmitter type. The above-mentioned designs are analysed and concluded a best design from it, depending up on applications and discussed about the control systems used in STMR.

1 INTRODUCTION

Wireless power transfer system (WPT) is a technology used to transfer power from one circuit to another circuit through an air. There are many types of models of transferring power from one circuit to other like single transmitter to multi receivers (STMR), A non-resonance inductive coupled system, a resonant inductively coupled system, an strongly coupled magnetic resonance (SCMR), etc., transferring power from a single transmitter to multi receiver (STMR) is a technology developing to increase the utilisation of wireless power transfer instead of wire transfer technology. STMR has many applications like charging of electronics devices, charging of electric vehicles, Etc. important parameter to control in STMR is size of the coils, due to utilizing of compensation technology in WPT, size of it is increasing. To make it compact, combining the compensation and main circuits is a possible method to decrease the size requirement and efficiency increment [3].

Fig1: Basic schematic diagram of STMR [26].

STMR is a system in which, there will be only one transmitter but "N" number of receivers as shown in fig (1), as application of drone battery charging. The main advantage of it is it can charge no of load at a time. limitations of STMR are Efficiency cannot be maintained high for long distance for many receivers by single transmitter, Coupling coefficient effect in receiver coils, Misalignment between transmitter and receiver coils. same frequency should be maintained between all the receiver coils to achieve high efficiency in the system.

This paper consists of different designs of STMR to overcome its limitations. Different designs of STMR are listed and analysed in section II, a comparison between different designs of STMR are given in section III, control systems used in STMR are explained in section IV and given detailed conclusion up on STMR's in section V.

2 Different Designs of STMR System

The following are the different evolutions in coil design to improve the efficiency in the STMR system

2.1 wireless power repeater system with single and two coil in each repeater

Control Techniques for the Cascaded and Cross-switched Multilevel Inverter - A Comparison

Sameera Shaik[1*], *Suresh Kumar* Tummala[2], *D Srinivasa* Rao[3]

[1,2,3]Department of Electrical and Electronics Engineering. Gokaraju Rangaraju Institute of Engineering & Technology, Hyderabad, India

Abstract Nowadays, the multilevel inverter has gained huge attention and has become more popularized in high voltage and high-power applications with low harmonics. As the number of output voltage increases, the harmonic content of the output voltage waveform decreases. In this paper, a comparison of cascaded H-bridge and cross-switched multilevel inverters for 7, 9, 15, 21 levels will be carried out. The different control techniques that will be used for carrying out comparisons are space vector pulse width modulation (SPVPWM), sinusoidal pulse width modulation (SPWM), and third harmonic injection pulse width modulation (THI-PWM) respectively. Here, the seven-level inverter is discussed mainly and can be extended to any number of levels.

Keywords—Multilevel Inverter, Total Harmonic Distortion, Sinusoidal Pulse Width Modulation, Third Harmonic Injection Pulse Width Modulation, Cross-Connected, Total Standing Voltage

Nomenclature

Abbreviation	Explanation
V_{ref2}	Reference voltage vector of a two-level hexagon
V_{ref4}	Reference voltage vector of four-level hexagon
V_{ndc}	Number of DC voltage sources
V(t)	The output voltage of the multilevel inverter (MLI)
A	Real axis
N_d	Number of switches in the current path respectively.
B	Imaginary axis
a_0, a_n, b_n	These are the coefficients of the Fourier transform
Θ	Angle made by V_{ref} vector
Θ_2	Angle made by V_{ref2} vector
Θ_4	Angle made by V_{re4}f vector
V_{ma}	The modulation signal
f_m	Modulating wave's peak frequency
F	Fundamental output frequency of the inverter
f_{cr}	Carrier wave's peak frequency,
V_m	Reference signal peak amplitude
V_{cr}	Carrier signal peak amplitude respectively, ma is the amplitude modulation index
V_{ref}	Reference voltage vector

* Corresponding author: sameera.250@gmail.com

1 Introduction

Multilevel inverters have become more focused and popularized in the past few decades. Multilevel Inverter is a power electronic device that can be used for high/medium voltage and power conditions with advantages of low harmonics, lower dv/dt stress on power electronic devices, lower device ratings, and reduced switching frequencies. In addition to the given advantages, some other advantages are low Total Harmonic Distortion (THD), efficiency, reliability, etc. Because of these advantages they are considered as proven technology and hence entered industry successfully. A three-level multilevel inverter was the first multilevel inverter that was introduced in 1975.

The different conventional topologies [1-7] of multilevel inverters are Neutral Point Clamped (NPC), Flying Capacitor (FC), and cascaded H-Bridge inverters (CHB). These regular geographies enjoy their benefits and weaknesses, however the fundamental downside of these three geographies is the requirement for high-power electronic parts, with an increment in the quantity of levels. This importantly builds the expense and intricacy of staggered inverters. In view of these disadvantages analysts have thought of new geographies of staggered inverters with less exchanging parts. Alongside presenting novel staggered inverter geographies, various strategies for control procedures for staggered inverters have likewise been presented. These control strategies can likewise be called adjustment methods which are characterized into two sorts. They are high recurrence and low-recurrence adjustment. Low-frequency modulation techniques cannot be applied for high power applications even though having better harmonic profiles. These are classified as space vector and selective harmonic elimination. High-frequency modulation can be

Remote Monitoring and Control for an Isolate Prototype Substation Model

Sandhya Rani G[1,*], *Vijaya Laxmi* U[1], *Srividya Devi* P[2], *Naga Sandhya Rani* M[1]

[1]Assitant Professor, EEE Department, GRIET, Hyderabad
[2]Associate Professor, EEE Department, GRIET, Hyderabad

Abstract. The objective of this paper is to monitor the electrical parameters like voltage, current, etc., remotely and display all the obtained real time values for a substation isolate. This paper is furnished to assure the load and electrical system equipment by the activation of relay, whenever the acquired parameters exceed the predefined values. Generally, this Proposed system design makes use of microcontroller, but the prototype of this circuit modelled in Proteus and can be executed by using ATmega 168 microcontroller. When supply is given to the designed hardware, all the sensors start sensing their respective parameters i.e., voltage, current, temperature etc., and modernize all the values on the display. Comparison between the problem-solving time values and the preordained values is continuously carried out by the microcontroller, if any of these values go beyond the pre-defined values, it sends fault alert to the relay, updates it on the screen and sends the same as an SMS through GSM for the rectification.

1 Introduction

Electricity is an exceedingly important and effective mode of energy. It plays a crucial act in contemporary world. Power systems are of highly complex and non-linear networks. Electric energy transmission and distribution structures are more required to function correctly and reliably to guarantee each continuity and high-satisfactory of supply [1]. Electrical power system is one of the key elements which play a vital role in both domestic and international framework and any damage to this system may lead to both fundamental direct and oblique impact at the countrywide financial system and security. As the functioning of power systems is hugely time-critical, low-latency communication should be considered for most control and monitoring applications [2]. Many advanced technologies are being developed today, even though electricity still suffers from power abnormalities and blackouts. Hence it has become necessary for a utility company to shift to automated analysis of the complex distribution network. The increasing complexity of huge electric power systems has resulted in a more prominent requirement for maintenance in order to keep a reliable supply of power [3].

The security and control systems comprise all segments and frameworks used to screen, control, ensure, and robotize the substation [4]. Home automation makes home more customized, comfortable, efficient, and riskless. Numerous applications of machine learning techniques to control power system security have been accounted [5]. These days research acquaints machine learning techniques to distinguish the flaw type, area identification and prediction [6]. Machine learning is appreciable for Problems for which the present solution depends up on a lot of fine adjustment or long details of rules: one Machine Learning design can often clarify code and perform better than the traditional approach. The applications of Machine Learning are 1) Analyzing images of products 2) Detecting tumors in brain scans 3) Automatically classify news articles. The harmony among supply and demand is the foundation of power system operations [7]. The purpose of this is to protect the load and substation equipment from damage due to any kind of faults like overload, short circuit, high temperature etc., Meanwhile, during fault an alert is sent by an SMS through GSM module and the same is displayed on the LCD display. Hence, by this it becomes very easy to notice the fault occurrence in the substation also the type of fault.

*Corresponding author:sandhyaranister@gmail.com

Artificial Intelligent Technique based Double-Frequency Analysis on a Single-Phase Grid-connected Inverter

Maheeth P V S[1,*], *Srividya Devi* P[2], *Sirisha* P[3]

[1]P G Scholar, EEE Department, GRIET, Hyderabad
[2]Associate Professor, EEE Department, GRIET, Hyderabad
[3]Assistant Professor, EEE Department, GRIET, Hyderabad

Abstract. Now a days more power losses can be seen in grid connected inverter. In order to reduce that double frequency in single phase grid inverter with Artificial Intelligent based fuzzy control is implemented. The inverter has two operating units High Frequency Unit (HFU) and Low Frequency Unit (LFU), low frequency reduce switching losses and high frequency suppress the symphonious currents. The fuzzy logic method expected towards deliver high yield, low total symphonious distortion, rapid response. Finally Total Symphonious Distortion (THD) contrasted among fuzzy including Integral controls (PI). The results are validated by using MATLAB/Simulink.

1 Introduction

The DC/AC Converter is always an important part of grid connected system [1]. Many switching symphonious are there in grid side current, to reduce that we will use passive filters like L or LCL filters to the grid [2-4]. The L filter has less complex structure, more reliability also have more inductance value and it has high voltage drop so it will reduce the system performance, instead of using L filter, LCL filter can be tried it has good capacity to reduce higher order symphonious[5], but it has the disadvantage of resonance. There are many new developments in semiconductor devices, that are widely used in many applications. These help to reduce the switching symphonious in a good way. Using these semiconductor devices in low and HFUs may add up some cost but the quality of the current will be good. The purpose of using controllers is when a system cannot fulfil the needs, then some variables will be used to achieve the wanted results.

The PLL (Phase Locked Loop) [6-8] is a closed loop system will generate an output frequency in relation with Phase and Magnitude of an input frequency it consists of variable oscillator and phase detector and feedback loop, these three are common parts of it. Through this process it will protect the grid from symphonious currents.

For controlling the inverters mostly PI controllers are used but to solve the mathematical model or transfer function will be complex to obtain that problem Fuzzy can be used. We can observe the importance of Fuzzy logic not only in computer science domain but also developing in industrial side [9-11], rocket engineering, and many domains. Fuzzy logic is a rule based controller, if any system uses fuzzy logic then it is called fuzzy model. We can observe some important applications of fuzzy in railway system, factories, air conditioner, camera control technique, in hospitals also while checking diagnostic procedure and diagnoses radiology and prostate cancer the machinery is installed with some of these fuzzy logics, washing machine controlling, vacuum cleaner, subway design for trains, it can tell the altitude of plane, range of it as this fuzzy is implemented in aerospace technology, traffic signal [12-14]. It has a good problem solving technique in the way its demand is increasing. Its decision making happens on three steps fuzzification, interfacing, and defuzzification. We can use this fuzzy in power electronics applications like controlling the speed of the motor, in electrical vehicles testing, this adds up a benefit to the systems. when compared to PI controllers this will be more beneficial because it thinks like human interface, it is faster and there is no mathematical approach to the fuzzy logic, it will show the results in the [0,1] format either the result produced will be false or true, it does not a give a situation in between them, and a membership graph will be seen with error and change in error it will relate those two graphs with rules that fuzzy had included in it. Fuzzy will simplify the data for itself to provide a valid reason to achieve the desirable output. A double frequency inverter proposed [15-19] will have two inverters used in different frequencies and achieves

* Corresponding author: maheeth333@gmail.com

Metadata of the chapter that will be visualized in SpringerLink

Book Title	Advanced Informatics for Computing Research	
Series Title		
Chapter Title	An Efficient Novel Approach for Detection of Handwritten Numericals Using Machine Learning Paradigms	
Copyright Year	2022	
Copyright HolderName	Springer Nature Switzerland AG	
Corresponding Author	Family Name	**Avvari**
	Particle	
	Given Name	**Pavithra**
	Prefix	
	Suffix	
	Role	
	Division	Department of IT
	Organization	Gokaraju Rangaraju Institute of Engineering and Technology, JNTU(H)
	Address	Hyderabad, India
	Email	pavithra.griet@gmail.com
Author	Family Name	**Ratakonda**
	Particle	
	Given Name	**Bhavani**
	Prefix	
	Suffix	
	Role	
	Division	Department of IT
	Organization	Gokaraju Rangaraju Institute of Engineering and Technology, JNTU(H)
	Address	Hyderabad, India
	Email	bhavani1592@grietcollege.com
Author	Family Name	**Sandeep**
	Particle	
	Given Name	**K.**
	Prefix	
	Suffix	
	Role	
	Division	Department of IT
	Organization	Gokaraju Rangaraju Institute of Engineering and Technology, JNTU(H)
	Address	Hyderabad, India
	Email	sandeepreddy283@gmail.com
Author	Family Name	**Kumar**
	Particle	
	Given Name	**Y. Jeevan Nagendra**
	Prefix	
	Suffix	

	Role	
	Division	Department of IT
	Organization	Gokaraju Rangaraju Institute of Engineering and Technology, JNTU(H)
	Address	Hyderabad, India
	Email	jeevannagendra@gmail.com
Author	Family Name	**Madhuri**
	Particle	
	Given Name	**T. N. P.**
	Prefix	
	Suffix	
	Role	
	Division	Department of IT
	Organization	Gokaraju Rangaraju Institute of Engineering and Technology, JNTU(H)
	Address	Hyderabad, India
	Email	madhuritelidevara@gmail.com

Abstract	The goal of recognizing handwritten numbers on paper is to extract the characteristics of the entered handwritten number. The human visual system is one of the wonders of the world. People can easily find and recognize the numbers as they are used for recognition and identification. Most people easily recognize numbers without effort. Humans are amazing at deciphering what our eyes show. All work is done subconsciously, and no additional training is required to recognize numbers. Generally, we do not need to assess the difficulty of a problem that our visual system solves. However, recognizing numbers for mechanical devices such as computers is not that easy. If we try to develop a computer program to detect numbers, the difficulty of visually recognizing patterns is significant. When it comes to coding, what seems simple when we see it will be quite complicated. Simple intuitions, for example, are for a system that recognizes strokes, circles, curves, straight lines, curves, and more. Example of recognizing a number like 9, you should recognize the loop at the top and a straight vertical bar at the bottom right. This is not easy to express algorithmically. That is why we came up with a prototype for number recognition. Although identification, classification and recognition are simple tasks with the help of machine learning, we are trying to develop a system that recognizes numbers as accurately as possible. The main goal of focusing on handwriting recognition is to learn about neural networks. Images are divided into pixels and recognized in pixel order.

Keywords (separated by '-')	K nearest neighbours - Stochastic gradient descent - Support vector machines - Neural networks - Deciphering - Metrics - Dataset hyperplanes - Regression

An Efficient Novel Approach for Detection of Handwritten Numericals Using Machine Learning Paradigms

Pavithra Avvari(✉), Bhavani Ratakonda, K. Sandeep, Y. Jeevan Nagendra Kumar, and T. N. P. Madhuri

Department of IT, Gokaraju Rangaraju Institute of Engineering and Technology, JNTU(H), Hyderabad, India
pavithra.griet@gmail.com, bhavani1592@grietcollege.com

Abstract. The goal of recognizing handwritten numbers on paper is to extract the characteristics of the entered handwritten number. The human visual system is one of the wonders of the world. People can easily find and recognize the numbers as they are used for recognition and identification. Most people easily recognize numbers without effort. Humans are amazing at deciphering what our eyes show. All work is done subconsciously, and no additional training is required to recognize numbers. Generally, we do not need to assess the difficulty of a problem that our visual system solves. However, recognizing numbers for mechanical devices such as computers is not that easy. If we try to develop a computer program to detect numbers, the difficulty of visually recognizing patterns is significant. When it comes to coding, what seems simple when we see it will be quite complicated. Simple intuitions, for example, are for a system that recognizes strokes, circles, curves, straight lines, curves, and more. Example of recognizing a number like 9, you should recognize the loop at the top and a straight vertical bar at the bottom right. This is not easy to express algorithmically. That is why we came up with a prototype for number recognition. Although identification, classification and recognition are simple tasks with the help of machine learning, we are trying to develop a system that recognizes numbers as accurately as possible. The main goal of focusing on handwriting recognition is to learn about neural networks. Images are divided into pixels and recognized in pixel order.

AQ1

Keywords: K nearest neighbours · Stochastic gradient descent · Support vector machines · Neural networks · Deciphering · Metrics · Dataset hyperplanes · Regression

A. K. Luhach et al. (Eds.): ICAICR 2021, CCIS 1575, pp. 1–11, 2022.
https://doi.org/10.1007/978-3-031-09469-9_8

1 Introduction

Our project aims at an automatic recognition of digits written by hand. The tendency of writing the digits in different forms is much higher as each person writes them differently. In such cases also, the system developed must be able to recognize the digits correctly and give out the accurate results. There exist many classification and pattern recognition algorithms in machine learning such as KNN, SVM, Neural Networks (CNN, ANN, and RNN) [1, 2]. We try to study how each algorithm works while training and testing the dataset. The project focuses on developing an easy methodology of recognizing the images for a plethora of things. The goal of this system is to provide information about the research project "An Efficient Novel approach for detection of handwritten numerical using Machine Learning paradigms" [12]. It includes what we did for the completion of project, requirements, description of modelling of the project, the technologies we have used for the project, implementation of the project and future enhancements [1, 2].

This project explains in detail about how a machine can identify human written digits. For this process, we are considering MNIST ("Modified National Institute of Standards and Technology") dataset which consist of 60000 images of 28*28 sizes in grey scale[15]. However, considering images as a dataset will not make our work easy. These images need to be pre-processed [2, 4]. As well as many other step need to be performed before entering into training the dataset. We are considering few classification and recognition algorithms like KNN, SVM and CNN [3]. We come up with a conclusion that no algorithm can beat up Neural Network in digit recognizer. We try to achieve the highest accuracy and prediction rates by applying best training methodologies [3, 4].

2 Related Works

The application identification of handwritten numericals using machine learning provides the following uses to the user: this application provides a chance for the user to allow their machine to recognize the digits from 0 to 9 written in any format with ease [2, 3]. It is useful for various kinds of future works like usage of this module in number plate recognition, number detection projects, etc. This also helps in performing multiple further operations like calculating attendance percentage, focusing on absentees, sending text messages to parents, etc. [14]. This document furnishes different diagrams for the "An Efficient Novel approach for detection of handwritten numerical using Machine Learning paradigms" using uml that clearly explains the model of building this particular application [3, 4]. The literary survey provides insights into the project in terms of the user experience and functionality of the project [9].

2.1 Feasibility Study

In the software development process, the feasibility study is critical. It provides the developer an opportunity to assess the operational flexibility of the product that is being developed[13]. The operational flexibility, technical support, the output of the project, and many others are treated as various criteria and parameters to analyse the feasibility of the project. Operational Feasibility, Technical Feasibility, as well as Economic Feasibility are the three basic types of feasibility studies.

2.1.1 Operational Feasibility

The application developed must be in such a way that it is feasible for the users to use with ease. How much the user is willing to use the application determines the operational feasibility of the system. Before checking the operational feasibility, the user must be adequately trained with regard to the application [11]. The user must not feel any difficulty in using the system. However, the percentage of the willingness of the user to use the application entirely depends on the way that the system is built with a user-friendly interface and the method that is taken to popularize the user about the system handling and usage. Our project employs a simple yet intuitive interface for the user to navigate through the application and operate it feasibly.

2.1.2 Technical Feasibility

This study is done to find the technical feasibility. This study determines to find out the technical requirements needed to develop the system.. Our project is developed with utmost care such that it is technically feasible [12]. Changes can be easily made and adopted according to the user's requirements. The trending programming language "Python" and its inbuilt libraries made the application development simple and easy.

2.1.3 Economic Feasibility

This study is done to find the economic feasibility of the developing system. The expenditures must be justified. The existing systems have the economy as one main backdrop because they require other specially developed devices [3, 15]. Thus, our project is designed well with a limited budget, and the hidden reason for this would be freely available technologies. The one and only customized product that has been used as an external device is a webcam which is always an economic-friendly device.

3 System Architecture

AQ2 See Fig. 1.

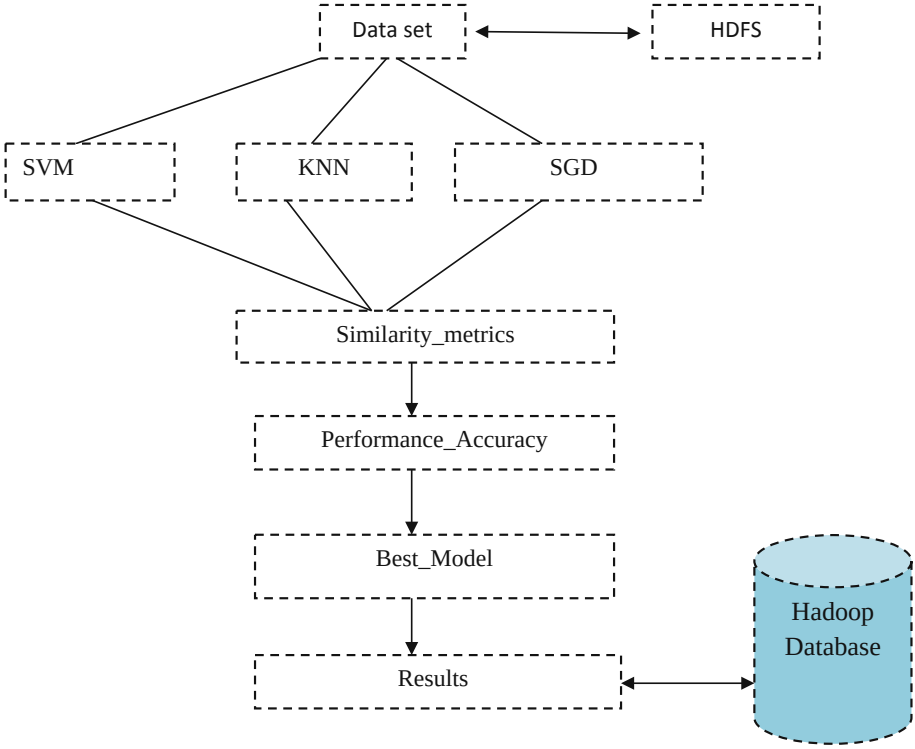

Fig. 1. Model framework

4 Methodology

4.1 Data

Handwritten digits were provided for a total of 70,000 photos from the MNIST (Modified National Institute of Standards and Technology) data set, with 60,000 examples in the training set and 10,000 examples in the test set, both with labeled images of 10 digits (0 to 9). This is a small part of the NIST broad set that was normalized to fit a 20 * 20 pixel frame without changing the aspect ratio [17]. The handwritten digits are images in the form of 28 * 28 grayscale intensities of images that represent an image, with the first column of each image being a label (0 to 9). The same has been decided in the case of the test set, which consists of 10,000 photos with labels ranging from 0 to 9 (Figs. 2, 3 and 4).

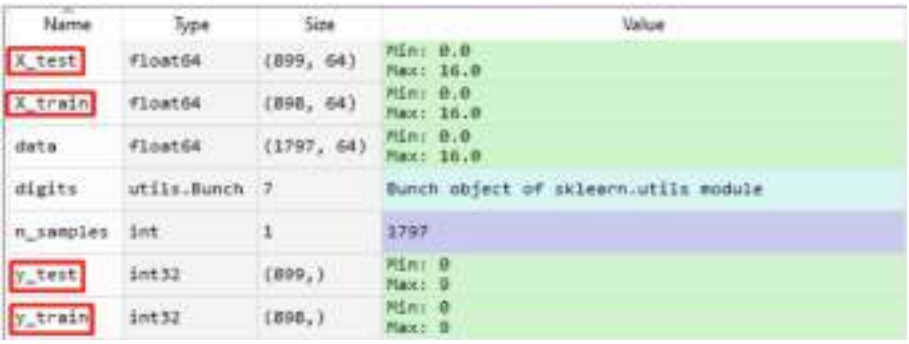

Name	Type	Size	Value
X_test	float64	(899, 64)	Min: 0.0 Max: 16.0
X_train	float64	(898, 64)	Min: 0.0 Max: 16.0
data	float64	(1797, 64)	Min: 0.0 Max: 16.0
digits	utils.Bunch	7	Bunch object of sklearn.utils module
n_samples	int	1	1797
y_test	int32	(899,)	Min: 0 Max: 9
y_train	int32	(898,)	Min: 0 Max: 9

Fig. 2. Data

Node	Transferring Address	last contact	configured capacity (GB)	used (GB)	non DFS used (GB)	Remaining (GB)	Used (%)	Remaining (%)	blocks	Block pool used(GB)
DN-1	172.16.9.31:50010	3	9112.91	14.80	71.01	8157.09	0.53	83.99	78.00	5.71
DN-2	172.16.9.32:50010	2	1154.19	14.68	77.66	1421.85	1.03	92.77	76.00	5.98
DN-3	172.16.9.33:50010	1	1450.26	14.84	87.56	1417.88	1.08	89.63	79.00	5.36
DN-4	172.16.9.34:50010	4	1450.26	14.84	87.56	1417.88	1.08	89.63	79.00	5.36
DN-5	172.16.9.35:50010	3	1450.26	14.84	87.56	1417.88	1.08	89.63	79.00	5.36

Fig. 3. Table of memory allocation in hadoop ecosystem

Data set(DS)	Size of the_fill	Replication®	Block_ size(BS)	Modification_ Time(MT)	Permissions (P)	Ownr (O)
				12/11/2020 16:24	rwxr-xr-x	IT
1	15.86 MB	6	128 MB	12/11/2020 16:54	rw-r--r--	IT
2	15.86 MB	6	128 MB	12/11/2020 17:24	rw-r--r--	IT
3	146.53 MB	6	128 MB	12/11/2020 17:44	rw-r--r--	IT
4	146.53 MB	6	128 MB	12/11/2020 18:54	rw-r--r--	IT
5	146.53 MB	6	128 MB	12/11/2020 19:24	rw-r--r--	IT

Fig. 4. Table of memory segregation in hadoop environment for file distribution

4.2 Support Vector Machines (SVM)

The ability of a machine with a reference vector to generate the highest level of precision is greater. SVM can be used for classification, which involves drawing a line between two categories or classes to distinguish [6]. Hyperplanes are the lines that connect different classes [8]. However, this distinction is not so clear [11]. In this situation, the dimension of the hyperplane must be changed from 1D to the N-th dimension, which is called the nucleus. Linear nuclei, polynomial nuclei, and functional nuclei with a radial base are the three types of nuclei [8, 9]. In multidimensional space, the created hyperplane divides different classes [17]. SVM iteratively develops an ideal hyperplane that minimizes the error [7, 13]. However, because it takes a long time to train and performs worse with overlapping classes, this classifier is not suitable for large data sets. It is also sensitive to the type of core used [8, 16].

SVM falls into the category of controlled learning and with a bonus for classification and regression problems. In general, SVM draws an optimal hyperplane, which is classified into different categories [18]. In two-dimensional space, we first draw the data points of the independent variable corresponding to the dependent variables. Then begin the classification process by looking at the hyperplane or any linear or nonlinear plane that distinguishes the two classes at their best (Fig. 5).

Algorithm:	
1.	*Identify the correct hyperplane which segregates the two classes better.*
2.	*Look for the maximum distance between nearest data point (of either any class) or hyperplane, the distance is measured as margin. So, look for hyperplane with maximum margin both sides equally. Hyperplane with higher margin is more robust, whereas low margin has changed for misclassification.*
3.	*SVM selects the classifier accurately to maximized margin.*
4.	*SVM is robust to the classifier and have a feature to ignore outliers and try to look for a hyperplane with maximum margin*

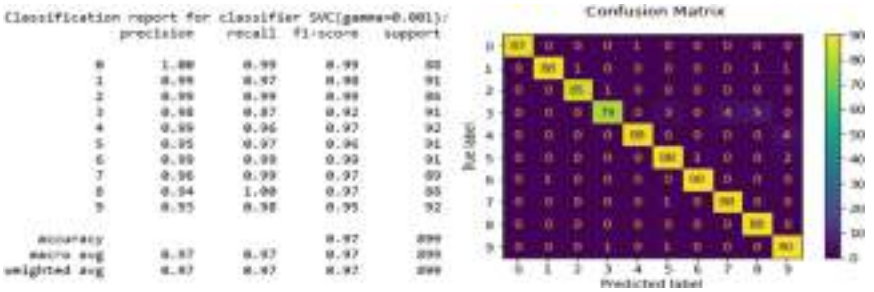

Fig. 5. Support Vector Machines (SVM)

4.3 K Nearest Neighbours (KNN)

This is the most basic classifier for categorizing images. This classifier is effectively explained with a simple expression in plain language: "Tell me your neighbors and I will tell you who you are." This approach is based solely on the distance between two illuminated vectors [7]. Finds the most common data among the closest K samples to distinguish the new data. Euclidean distance can be used as a distance metric [8].

This algorithm gave an accuracy of 92.8%. However, this algorithm has many significant drawbacks in terms of various aspects such as the choice of features [8], dimensionality reduction, etc. KNN is the nonparametric method or classifier used for both classification and regression problems [17]. This is the delayed or late learning classification algorithm, in which all the calculations are done until the last stage of the classification, and these are instance-based learning algorithms where the convergence is done locally. As it is the simplest and easiest to implement, there is no explicit training phase before and the algorithm does not perform training data aggregation (Fig. 6).

Algorithm:	
1.	*Compute the distance metric between the test data point and all labeled data points.*
2.	*Order the labeled data points in increasing order of distance metric.*
3.	*Select the top K labeled data points and look at class labels.*
4.	*Look for the class labels that majority of these K labeled data points have and assign it to test data points.*

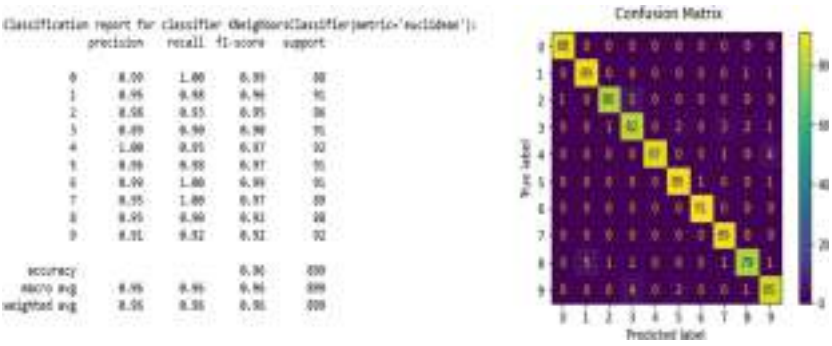

Fig. 6. K Nearest Neighbours (KNN)

4.4 Stochastic Gradient Descent

Stochastic gradient descent is a very popular and common algorithm that is used in various machine learning algorithms; the most important thing is that it forms the basis of neural networks. Gradient descent is an iterative algorithm that starts from an arbitrary point on a function and moves down its slope in steps until it reaches the lowest point of that function [18] (Figs. 7 and 8).

Algorithm:	
1.	*Find the slope of the objective function* ***with respect to each parameter/feature****. In other words, compute the gradient of the function.*
2.	*Pick a random initial value for the parameters. (To clarify, in the parabola example, differentiate "y" with respect to "x". If we had more features like x1, x2 etc., we take the partial derivative of "y" with respect to each of the features.)*
3.	*Update the gradient function by plugging in the parameter values.*
4.	*Calculate the step sizes for each feature as:* ***step size = gradient * learning rate.***
5.	*Calculate the new parameters as:* ***new params = old params -step size***
6.	*Repeat steps 3 to 5 until gradient is almost 0.*

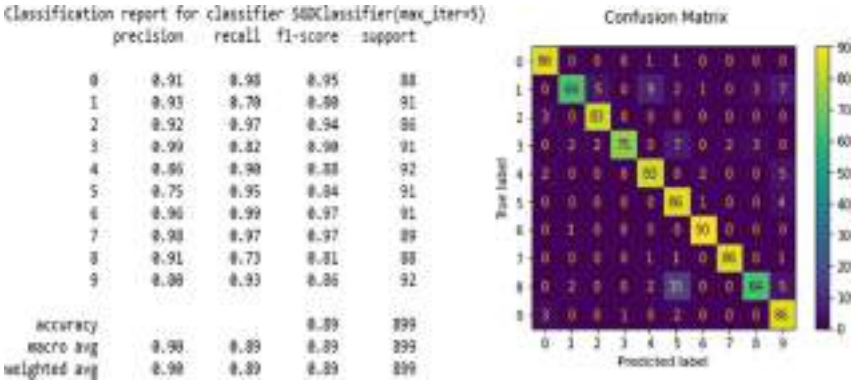

Fig. 7. Stochastic Gradient Descent (SGD).

Table: Comparison Analysis

Name of the Classifiers	*F1 Score*	*Accuracy Score*
SVM	0.92	0.96
KNN	0.90	0.95
SGD	0.81	0.89

In this section, the processed images are sent as input to various algorithms. The precision and F1 evaluation values are 0.96, 0.95, 0.89 and 0.92, 0,90, 0.81, respectively. Choosing the correct data set, pre-preparing the data with the right techniques, planning the model, and many other tasks combine to create better performance. The CNN model in our model efficiently organizes all the test photos with the names of the individual classes. This did not happen in any case. Each age group has its own data set [18]. Accuracy seems to increase with each generation. The pass set was tested after the

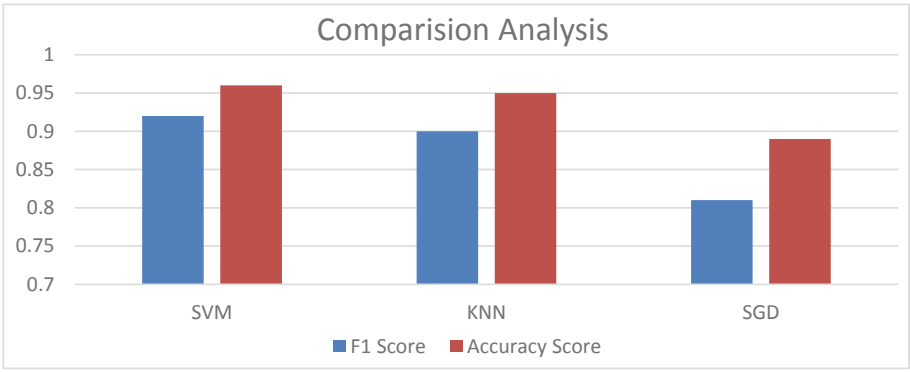

Fig. 8. Model accuracy

model was developed on the preparatory data set and showed a precision of 0.96. Then when the model was obtained with test data as input, the model showed an accuracy of 0.97%.

5 Conclusion

In this section we saw how the different algorithms work in handwriting recognition. There are many classification and recognition algorithms. K-Neighbor and Support Vector Machine are some of the most famous and widely used. All these algorithms consider various factors during training and testing. Also considered is the MNIST handwritten digit dataset used, consisting of approximately 60,000 images with sizes 28 * 28 grayscale images of handwritten digits 0 to 9. All images should be pre-processed using appropriate techniques. In the study, the main characteristics are extracted from each image for further processing for training. The processed images are sent as input to various algorithms. The precision and F1 evaluation values are 0.96, 0.95, 0.89 and 0.92, 0,90, 0.81, respectively. Choosing the correct data set, pre-preparing the data with the right techniques, planning the model, and many other tasks combine to create better performance. The CNN model in our model efficiently organizes all the test photos with the names of the individual classes. This did not happen in any case. Each age group has its own data set. Accuracy seems to increase with each generation. The pass set was tested after the model was developed on the preparatory data set and showed a precision of 0.96. Then when the model was obtained with test data as input, the model showed an accuracy of 0.97%. The excellent performance of the model is a direct result of the inclusion and structure of the authentic image of the model.

References

1. Abu Ghosh, M.M., Maghari, A.Y.: A comparative study on handwriting digit recognition using neural networks. In: 2017 International Conference on Promising Electronic Technologies (ICPET), 2017, pp. 77–81 (2017). https://doi.org/10.1109/ICPET.2017.20

2. Babu, U.R., Venkateswarlu, Y., Chintha, A.K.: Handwritten Digit Recognition Using K-Nearest Neighbour Classifier. World Congress on Computing and Communication Technologies **2014**, 60–65 (2014). https://doi.org/10.1109/WCCCT.2014.7
3. G. Vijendar Reddy, Sukanya Ledalla ,Avvari Pavithra: A quick recognition of duplicates utilizing progressive methods 'International Journal of Engineering and Advanced Technology (IJEAT)' at Volume-8 Issue-4, April 2019
4. Tuba, E., Bacanin, N.: An algorithm for handwritten digit recognition using projection histograms and SVM classifier. In: 2015 23rd Telecommunications Forum Telfor (TELFOR), 2015, pp. 464–467. https://doi.org/10.1109/TELFOR.2015.7377507
5. Gil, A.M., Costa Filho, C.F.F., Costa, M.G.F.: Handwritten digit recognition using SVM binary classifiers and unbalanced decision trees. In: Campilho, A., Kamel, M. (eds.) ICIAR 2014. LNCS, vol. 8814, pp. 246–255. Springer, Cham (2014). https://doi.org/10.1007/978-3-319-11758-4_27
6. Ahamed, Hafiz &Alam, Ishraq& Islam, Md. (2019): SVM Based Real Time Hand-Written Digit Recognition System
7. Al-Wzwazy, Haider. (2016): Handwritten Digit Recognition Using Convolutional Neural Networks. International Journal of Innovative Research in Computer and Communication Engineering
8. Ratakonda, B., Avvari, P., Rajarao, B., Sreevani, V., Ganapathi Raju, N.V.: Smart Parking for Smart Cities using IoT in 3rd International conference on Design and manufacturing aspects for sustainable energy(ICMED-2021) (2021). https://doi.org/10.1051/e3sconf/202130901128
9. Jeevan Nagendra Kumar, Y., Spandana, V., Vaishnavi, V.S., Neha, K., Devi, V.G.R.R.: Supervised machine learning approach for crop prediction in agriculture sector. In: IEEE - 5th International Conference on Communication and Electronics Systems (ICCES), pp. 736–741. ISBN: 978-1-7281-5370-4
10. Prasanna Lakshmi, K., et al.: Video genre classification using convolutional recurrent neural networks. Int. J. Adv. Comput. Sci. Appl. **11**, 170–176 (2020). ISSN: 2156-5570 (Online) ISSN: 2158-107X (Print))
11. Shailaja, V., Lohitha, R., Musunuru, S., Deepthi Reddy, K., Padma Priya, J.: Predictive analytics of performance bof india in the olympics using machine learning algorithms. Int. J. Emerging Trends Eng. Res. **8**(5), May 2020. ISSN 23473983
12. Zaguia, A., Raju, V., Jeevan Nagendra Kumar, Y., Rawat, U.: Secure Vertical Handover to NEMO using Hybrid Cryptosystem. Hindawi, Article ID 6751423, Hindawi
13. Jeevan Nagendra Kumar, Y., Rajini Kanth, T.V.: GIS-MAP based spatial analysis of rainfall data of Andhra Pradesh and telangana states using R. Int. J. Electr. Comput. Eng. (IJECE) **7**(1), February 2017, Scopus Indexed Journal, ISSN: 2088-8708
14. Ratakonda, B., Therala, A., Hanumanthu, C.K.: Driving license detection using QR code. In: International Conference on Design and Manufacturing Aspects for Sustainable Energy, 19 August 2020, ICMED (2020). https://doi.org/10.1051/e3sconf/202018401010
15. Prasanna Lakshmi, K., et al.: Efficient mining of data streams using associative classification approach. Int. J. Softw. Eng. Knowl. Eng. **25**(3), 605–631 (2015). ISSN (Online): 1793-6403. ISSN (Print) :0218-1940
16. Ledalla, S., Mahalakshmi, T.S.: Sentiment analysis using legion kernel convolutional neural network with LSTM. Int. J. Innov. Technol. Exploring Eng. **8**, 226–229 (2019)
17. Subbarayudu, Y., Sureshbabu, A.: Distributed multimodal aspective on topic model using sentiment analysis for recognition of public health surveillance. Expert Clouds and Applications, 16 July 2021, doi.https://doi.org/10.1007/978-981-16-2126-0_38 Springer, Singapore. Print ISBN978-981-16-2125-3 Online ISBN978-981-16-2126-0.

18. Rajiv, K., Rajasekhar, N., Prasanna Lakshmi, K., Srinivasa Rao, D., Sabitha Reddy, P.: Accuracy evaluation of plant leaf disease detection and classification using GLCM and multiclass SVM classifier. In: Sharma, H., Saraswat, M., Kumar, S., Bansal, J.C. (eds.) CIS 2020. LNDECT, vol. 61, pp. 41–54. Springer, Singapore (2021). https://doi.org/10.1007/978-981-33-4582-9_4

Author Queries

Chapter 8

Query Refs.	Details Required	Author's response
AQ1	This is to inform you that as the Institutional email address of the corresponding author is not available in the manuscript, we are displaying the private email address in the PDF and SpringerLink. Do you agree with the inclusion of your private e-mail address in the final publication?	
AQ2	Please check and confirm if the inserted citations of Figs. 1–8 are correct. If not, please suggest an alternate citations.	

Metadata of the chapter that will be visualized in SpringerLink

Book Title	Advanced Informatics for Computing Research	
Series Title		
Chapter Title	Analysing Sentiments of People Over Vaccines in Reddit Posts Using Natural Language Processing	
Copyright Year	2022	
Copyright HolderName	Springer Nature Switzerland AG	
Corresponding Author	Family Name	**Srinivas**
	Particle	
	Given Name	**J.**
	Prefix	
	Suffix	
	Role	
	Division	
	Organization	SR University
	Address	Warangal, India
	Email	jagirdar.srinivas@gmail.com
Author	Family Name	**Reddy**
	Particle	
	Given Name	**K. Venkata Subba**
	Prefix	
	Suffix	
	Role	
	Division	
	Organization	Kallam Haranadha Reddy Institute of Technology
	Address	Guntur, India
	Email	
Author	Family Name	**Rajasekhar**
	Particle	
	Given Name	**N.**
	Prefix	
	Suffix	
	Role	
	Division	
	Organization	Gokaraju Rangaraju Institute of Engineering and Technology
	Address	Hyderabad, India
	Email	
Author	Family Name	**Raju**
	Particle	
	Given Name	**N. V. Ganapathi**
	Prefix	
	Suffix	

	Role	
	Division	
	Organization	Gokaraju Rangaraju Institute of Engineering and Technology
	Address	Hyderabad, India
	Email	

Abstract	Misinformation on vaccines is deeply rooted in many major societies of the world which according to the World Health Organization is one of the main threats for public health globally in 2019. One of the main reasons for rapid spread of such misinformation on vaccines is social media posts. With proper analysis of social media posts, the main factors contributing for such misinformation can be identified. This paper performs sentiment analysis on Reddit posts related to vaccines using Natural Language Processing (NLP) techniques like stopwords, spacytextblob, wordcloud, subjectivity and polarity. The research found out that out of the total 1487 reddits 9.21% of them were positive reddits 83.86% of were neutral reddits 6.92% of them were negative reddits.

Keywords (separated by '-')	Vaccine hesitancy - Sentiment analysis - Natural Language Processing - Machine learning

Analysing Sentiments of People Over Vaccines in Reddit Posts Using Natural Language Processing

J. Srinivas[1(✉)], K. Venkata Subba Reddy[2], N. Rajasekhar[3], and N. V. Ganapathi Raju[3]

[1] SR University, Warangal, India
jagirdar.srinivas@gmail.com
[2] Kallam Haranadha Reddy Institute of Technology, Guntur, India
[3] Gokaraju Rangaraju Institute of Engineering and Technology, Hyderabad, India

Abstract. Misinformation on vaccines is deeply rooted in many major societies of the world which according to the World Health Organization is one of the main threats for public health globally in 2019. One of the main reasons for rapid spread of such misinformation on vaccines is social media posts. With proper analysis of social media posts, the main factors contributing for such misinformation can be identified. This paper performs sentiment analysis on Reddit posts related to vaccines using Natural Language Processing (NLP) techniques like stopwords, spacytextblob, wordcloud, subjectivity and polarity. The research found out that out of the total 1487 reddits 9.21% of them were positive reddits 83.86% of were neutral reddits 6.92% of them were negative reddits.

AQ2

Keywords: Vaccine hesitancy · Sentiment analysis · Natural Language Processing · Machine learning

1 Introduction

Over the years confusion over taking vaccines is largely prevalent in the society and therefore marked as one of the significant contributors of global sickness by World Health Organisation in 2019 [1]. According to the Strategic Advisory Group of Experts (SAGE) Working on Vaccine confusion defines confusion in vaccines as the "delay in acceptance or refusal of vaccination despite the availability of vaccination services. Vaccine hesitancy is complex and context-specific, varying across time, place, and vaccines. It is influenced by factors such as complacency, convenience, and confidence" [2]. Moreover the internet is a main factor for rapid dissemination of vaccine hesitancy as such myths and information can spread like wild fire [3]. Social media influences the decisions of the society to take, reject or postpone the vaccination. [4, 5] and could be a reason for the spread of avoidable diseases. One way to cope up with this hesitancy of accepting vaccines is to monitor social media posts related to vaccination. It is very significant to gauge the opinions and the social behaviour of people who have certain inclinations towards anti vaccinations. Opinion research or sentiment analysis of vaccination related

A. K. Luhach et al. (Eds.): ICAICR 2021, CCIS 1575, pp. 1–9, 2022.
https://doi.org/10.1007/978-3-031-09469-9_11

posts on social media can be performed to find out the reasons behind the vaccination hesitancy. In social media people are allowed to post their views on a certain topic freely. These posts if carefully analyzed may give some insights to the medical agencies to cope up with the existing problem of vaccine hesitancy. Social media can be effectively used to track people with vaccine hesitancy, communicable diseases and also for circulating health guidelines rapidly [6]. Text mining techniques can be used to detect vaccine hesitancy in social media posts [7]. Researchers also performed Sentiment Analysis (SA) [8] for finding out the stances of people on vaccines. The social posts can be analyzed and classified according to their polarity viz. positive, neutral and negative [9, 10]. In the literature there exists three methods of SA namely document-level SA, Sentencelevel SA and aspect-level SA [11]. Anti Vaccination campaigns also contribute to the hesitancy of public from taking vaccines. And mostly all the information is about such campaigns is circulated through social media. Investigating a persons' overt behavior towards vaccination on social media stages is a proved technique for finding the sources of such misinformation. On these platforms the main point of discussions will be vaccines. A study performed by some researchers showed that people are influenced over the internet against vaccination of children [12]. This research examines the individual's attitude towards vaccination on reddit posts. By using years of longitudinal data extracted from reddit posts, this research tries to identify individuals who are pro vaccine, individuals who are anti vaccine and finally neutral towards vaccination. This research hopes that this classification will later help health officials to encourage the neutral class of people to take vaccinations. Similarly the anti vaccination class of individuals can be convinced to take vaccines by properly counseling them. As the problem statement of this research clearly introduced now, in the coming sections of the paper related work, system architecture, experiments conducted and results obtained will be discussed. Finally, the paper will be concluded and insights into future work of this research will be discussed.

2 Related Work

A study in the past identified the confusions and apprehensions of individuals on multiple social media forums for solving the health issues of people globally [13]. One more set of investigators tried to understand the attitudes of twitter users on vaccinations by capturing four years of tweets. They applied NLP techniques for identifying the sentiments of individuals by analyzing user tweets [14]. A group of researchers tried to find the facts for refusing vaccinations by some individuals by analyzing their behavior on social media especially twitter [15]. They classified the tweets related to vaccination as positive and negative by using NLP techniques.

An alternate research explored the perspectives and experiences of advertisers of vaccination while they promote vaccines on the social media [16, 17]. They used qualitative methods to sample participants who were involved in promotion of vaccinations on social media. The work applied risk communication principles, framework analysis for analyzing the data generated by these participants. A survey performed by researchers found out that how people with infants were flooded with anti vaccination messages [18] over social media. One more study tried to investigate how social media influences the circulation of health related misinformation globally [19]. They investigate the vaccine

autism controversy. For this they collected data from Twitter, Reddit and also online news for around two years in the United States, the United Kingdom and Canada. One more study analyzed and later tried to address the health related misinformation on social media [20]. A group of analysts performed [21] investigations on twitter and concluded that sentiment analysis plays an important role in detecting the attitude of the public towards vaccination. In order to gauge the opinion of public towards COVID-19 vaccine a group of researchers performed sentiment analysis on twitter posts [22].Time series forecasting was performed on the current scenario of vaccination in USA. A group of investigators from Philippines [23] analyzed the sentiments of public over twitter using Naïve Bayes algorithm and attained an accuracy of 81.77%. A similar kind of research was performed by a group of researchers from Indonesia [24] on twitter data using Naïve Bayes algorithm. Their investigations revealed that in a total of 58,301 tweets 34 thousand were negative, 24 thousand were positive and three hundred and one tweets were neutral during a week. A group of researchers [25] analysed twitter data related to covid-19 tweets using three ML algorithms namely Multinomial Naïve Bayes (MNB), Support Vector Machine (SVM), and Logistic Regression (LR). LR gave an accuracy of 97.3% where as SVM gave an accuracy of 96.26% and finally MNB achieved an accuracy of 88%. The next section of this paper explains the system design that is followed for performing this research. NLP techniques were also used to identify the writers of text in social media by a group of researchers [26]. NLP techniques were applied on social media posts for determining whether they were fake or real [27]. Supervised text classification, an important aspect in NLP can be also performed using Artificial Neural Networks [28]. Before performing textual analysis some researchers created clusters of text streams in social media applications using tree based approaches and ternary features [29].

3 Work Flow and Results

The current section gives details of the various stages like data collection, pre-processing, word cloud representation and finally sentiment analysis. Figure 1 depicts the work flow model used by this research to perform sentiment analysis.

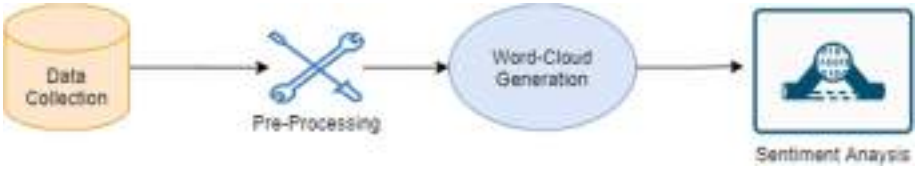

Fig. 1. Work flow of the system

3.1 Data Collection and Pre-processing

For this research the paper considered “reddit_vm.csv” dataset which is publicly available on Kaggle Dataset [30]. It has 1487 posts related to vaccination with eight columns.

Table 1 illustrates the column names and their type. Out of the eight column names, three belong to integer type and five belong to object type. Figure 2 represents the sample of the data set considered for this research. Out of the eight columns title, id, url, body and time stamp are categorical whereas scores, comms_num and created are non-categorical.

Table 1. Table captions should be placed above the tables

S. no	Column	Datatype
1.	title	object
2.	score	int64
3.	id	object
4.	url	object
5.	comms_num	int64
6.	created	int64
7.	body	object
8.	timestamp	object

Fig. 2. Sample records of the reddit dataset

The next step is to perform data pre-processing so that the NLP techniques applied for sentiment analysis become more effective. Data Pre-processing usually contains activities like checking for duplicates, checking for null values, remove punctuation, remove numbers and converting the text into lower case and Stop Word Removal. The dataset did not contain any duplicate rows. The 'url' column has approximately 1036 null values where as the 'body' column has nearly 366 null values. The rest of the columns do not contain any null values. Figure 3 represents a visualization of the number of posts published on reddit related to the topic 'vaccination'. This research used seaborn and matplotlib package of the python programming language for generating visualizations of the data. Figure 4 represents the heat map generated for 'score','coms_num' and 'created' columns that are non-categorical in nature. A heatmap is generated to see the correlation between non-categorical features. This research used Pearson Correlation. The next is to remove stop words from the data set. Frequently occurring words in the posts are identified and removed as they increase the processing overhead. Articles, pronouns found in the posts are identified and then removed. This research uses the

"stopwords" list already present in the nltk library of python programming language to remove the stopwords present in the dataset.

3.2 Word Cloud Generation and Statistical Analysis

The next step is to generate word clouds from the data present in the pre-processed dataset. The words that frequently appear in the posts will have bigger size in the cloud when compared to the words that have less frequency. In this paper, two word clouds are generated on the data present in the dataset. Figure 5 represents a word cloud where the column "title" was focussed and Fig. 6 represents a word cloud where "body" was the focussed column name. One can observe that words like "Vaccine", "Vaccination", "Vaccinate", "Vaccinated", "Anti", "Vaxxer", "covid", "measles", "children", "cause" e.t.c appear with large fonts in Fig. 5. Similar results are found in Fig. 6.

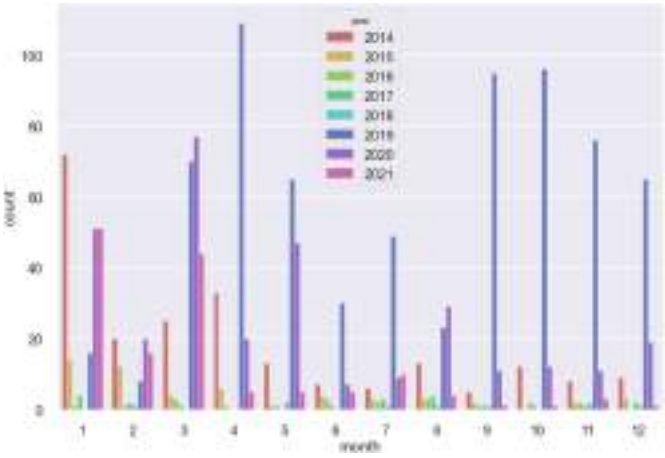

Fig. 3. Visualization of monthly published posts in a year related to topic vaccine

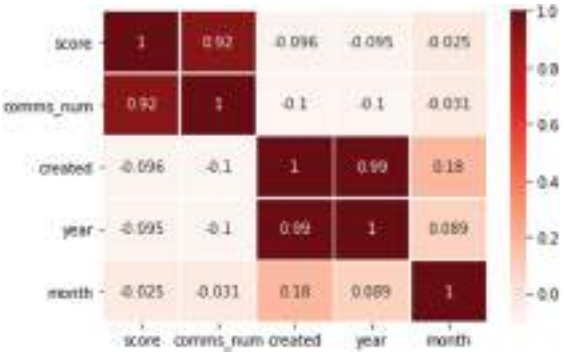

Fig. 4. Heat map of correlation between categorical values

Fig. 5. Word cloud on 'title' column

Fig. 6. Word cloud on 'body' column

3.3 Sentiment Analysis

The next step is to perform sentiment analysis of the text present in the dataset. Traditionally there exists three type of sentiments, viz. negative, positive and neutral. This research uses "TextBlob" package to perform sentiment analysis. Sentiment analysis is performed by finding out subjectivity and polarity of the text. Traditionally subjectivity refers to the metrics that are used to gauge personal opinions, emotions or judgments. It is a float value that ranges between [0, 1]. Polarity lies between $[-1, 1]$ where in -1 represents negative sentiment and 1 represents positive statement. 0 represents neutral. The following results are obtained from the sentiment analysis performed. Out of the total reddit posts 9.21% were positive posts on vaccinations, 6.92% of the posts carried

negative sentiment and 83.86% were neutral. Figure 7 graphically represents the sentiment analysis performed on the vaccine data set. The analysis found that a majority of posts were neutral. Government authorities can target the people who have posted these neutral posts and convince them towards vaccination. This will contribute to the betterment of the global health.

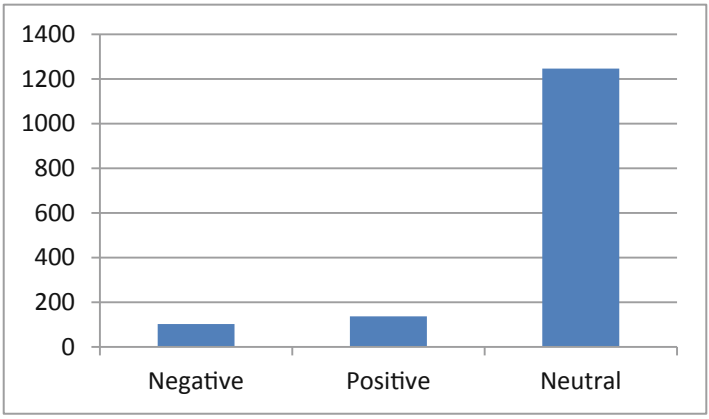

Fig. 7. Sentiment analysis on vaccine related reddit posts

4 Conclusions and Future Work

After performing this research the following conclusions related to vaccines are drawn out. It is observed that there is a lot of information and misinformation about vaccines on social networking sites like reddit, twitter, facebook and watsapp. This makes it absolutely necessary for authorities to monitor social media posts for effective implementation of vaccination strategies. An automatic system that effectively extracts and analyses the text related to vaccination on social media platforms is to be developed. Machine Learning based sentiment analysers are effective while dealing with current challenges. Due to induction of artificial intelligence, detection of sentiment polarity towards vaccination on social media posts has become easy and cost effective. This research analysed the sentiments of reddit users with respect to vaccines using NLP techniques and found out that a majority of users have a neutral attitude towards vaccination and they can be influenced by using concepts like target marketing. In a total of 1487, 83.86% were neutral reddits and 6.92% of them were negative reddits. As a future scope, the sentiment analyser can be equipped with tools to detect the origins of negative & neutral posts. Once location of such posts is detected health care professionals can plan vaccination drives more effectively in such areas. In future this research intends to analyse posts from twitter, facebook and watsapp.

References

1. World Health Organization: Ten Threats to Global Health in 2019 (2019). https://www.who.int/news-room/spotlight/ten-threats-to-global-health-in-2019. Accessed 27 May 2021
2. MacDonald, N.E.: Vaccine hesitancy: definition, scope and determinants. Vaccine **33**, 4161–4164 (2015)
3. European Centre for Disease Prevention and Control: Systematic Scoping Review on Social Media Monitoring Methods and Interventions Relating to Vaccine Hesitancy; ECDC: Stockholm, Sweden (2020)
4. Rosselli, R., Martini, M., Bragazzi, N.L.: The old and the new: Vaccine hesitancy in the era of the Web 2.0. Challenges and opportunities. J. Prev. Med. Hyg. **57**, E47–E50 (2016)
5. Broniatowski, D.A., et al.: Weaponized health communication: Twitter bots and Russian trolls amplify the vaccine debate. Am. J. Public Health **108**, 1378–1384 (2018)
6. Deiner, M.S., et al.: Facebook and Twitter vaccine sentiment in response to measles outbreaks. J. Health Inf. **25**, 1116–1132 (2019)
7. D'Andrea, E., Ducange, P., Bechini, A., Renda, A., Marcelloni, F.: Monitoring the public opinion about the vaccination topic from tweets analysis. Expert Syst. Appl. **116**, 209–226 (2019)
8. Yadollahi, A., Shahraki, A.G., Zaiane, O.R.: Current state of text sentiment analysis from opinion to emotion mining. ACM Comput. Surv. **50**, 1–33 (2017)
9. Mohd Azizi, F.S., Kew, Y., Moy, F.M.: Vaccine hesitancy among parents in a multi-ethnic country Malaysia. Vaccine **35**, 2955–2961 (2017)
10. Chou, W.S., Oh, A., Klein, W.M.P.: Addressing health-related misinformation on social media. JAMA **320**(23), 2417–2418 (2018)
11. Henriquez Miranda, C., Pla Santamaría, F., Hurtado Oliver, L.F., Guzmán, J.: Análisis de sentimientos a nivel de aspecto usando ontologías y aprendizaje automático. Proces. Leng. Nat. **59**, 49–56 (2017)
12. Salmon, D.A., Moulton, L.H., Omer, S.B., DeHart, M.P., Stokley, S., Halsey, N.A.: Factors associated with refusal of childhood vaccines among parents of school-aged children: a case-control study. Arch. Pediatr. Adolesc. Med. **159**(5), 470–476 (2005)
13. Suarez-Lledo, V., Alvarez-Galvez, J.: Prevalence of health misinformation on social media: systematic review. J. Med. Internet Res. **23**(1), e17187 (2021)
14. Mitra, T., Counts, S., Pennebaker, J.: Understanding anti-vaccination attitudes in social media. In: Proceedings of the International AAAI Conference on Web and Social Media, vol. 10, no. 1 (March 2016)
15. Dredze, M., Broniatowski, D.A., Smith, M.C., Hilyard, K.M.: Understanding vaccine refusal: why we need social media now. Am. J. Prev. Med. **50**(4), 550–552 (2016)
16. Steffens, M.S., Dunn, A.G., Wiley, K.E., Leask, J.: How organisations promoting vaccination respond to misinformation on social media: a qualitative investigation. BMC Public Health **19**(1), 1–12 (2019)
17. Royal Society for Public Health: Moving the needle: promoting vaccination uptake across the life course: Royal Society for Public Health (2018). https://www.rsph.org.uk/uploads/assets/uploaded/f8cf580a-57b5-41f4-8e21de333af20f32.pdf. Accessed 15 Jan 2019
18. Wolfe, R.M.: Vaccine safety activists on the Internet. Expert Rev. Vaccines **1**(3), 249 (2002)
19. Jang, S.M., Mckeever, B.W., Mckeever, R., Kim, J.K.: From social media to mainstream news: the information flow of the vaccine-autism controversy in the US, Canada, and the UK. Health Commun. **34**(1), 110–117 (2019)
20. Chou, W.Y.S., Oh, A., Klein, W.M.: Addressing health-related misinformation on social media. JAMA **320**(23), 2417–2418 (2018)

21. Yousefinaghani, S., Dara, R., Mubareka, S., Papadopoulos, A., Sharif, S.: An analysis of COVID-19 vaccine sentiments and opinions on Twitter. Int. J. Infect. Dis. **108**, 256–262 (2021)
22. Sattar, N.S., Shaikh, A.: COVID-19 vaccination awareness and aftermath: public sentiment analysis on Twitter data and vaccinated population prediction in the USA. Appl. Sci. **11**(13), 6128 (2021)
23. Villavicencio, C., Macrohon, J.J., Inbaraj, X.A., Jeng, J.H., Hsieh, J.G.: Twitter sentiment analysis towards COVID-19 vaccines in the Philippines using Naïve Bayes. Information **12**(5), 204 (2021)
24. Ritonga, M., Al Ihsan, M.A., Anjar, A., Rambe, F.H.: Sentiment analysis of COVID-19 vaccine in Indonesia using Naïve Bayes algorithm. In: IOP Conference Series: Materials Science and Engineering, vol. 1088, no. 1, p. 012045. IOP Publishing (2021)
25. Khakharia, A., Shah, V., Gupta, P.: Sentiment analysis of COVID-19 vaccine tweets using machine learning. SSRN 3869531 (2021)
26. Sheshikala, M., Kothandaraman, D., Roopa, G.: Natural language processing and machine learning classifier used for detecting the author of the sentence. Int. J. Recent Technol. Eng. **8**(3), 936–939 (2019)
27. Srinivas, J., Venkata Subba Reddy, K., Sunny Deol, G.J., VaraPrasada Rao, P.: Automatic fake news detector in social media using machine learning and natural language processing approaches. In: Satapathy, S.C., Bhateja, V., Favorskaya, M.N., Adilakshmi, T. (eds.) Smart Computing Techniques and Applications. SIST, vol. 224, pp. 295–305. Springer, Singapore (2021). https://doi.org/10.1007/978-981-16-1502-3_30
28. Kumar Ravi, R., Reddy, M.B., Praveen, P.: Text classification performance analysis on machine learning. Int. J. Adv. Sci. Technol. **28**, 691–697 (2020)
29. Raj, P., Srinivas, C., GuruRao, C.V.: Clustering text data streams – a tree based approach with ternary function and ternary feature vector. Procedia Comput. Sci. **31**, 976–984 (2014)
30. https://www.kaggle.com/khsamaha/reddit-vaccine-myths-eda-and-text-analysis. Accessed 10 July 2021

Author Queries

Chapter 11

Query Refs.	Details Required	Author's response
AQ1	Per Springer style, both city and country names must be present in the affiliations. Accordingly, we have inserted the country names in all the affiliations. Please check and confirm if the inserted country names are correct. If not, please provide us with the correct country names.	
AQ2	This is to inform you that as the Institutional email address of the corresponding author is not available in the manuscript, we are displaying the private email address in the PDF and SpringerLink. Do you agree with the inclusion of your private e-mail address in the final publication?	

Detection and Classification of Intracranial Brain Hemorrhage

K. V. Sharada, Vempaty Prashanthi, and Srinivas Kanakala

Abstract Computer

-aided diagnosis systems (CAD), as their name suggests, utilize computers to assist doctors to obtain a quick and correct diagnosis. They focused on several scholars as they are built upon the concept of processing and examining pictures of various parts of the individual body meant for a fast and correct outcome. CAD systems are generally area specific because they are augmented for some certain kinds of infections, various parts of the individual body, diagnosis methods, etc. They analyze dissimilar types of inputs given, for example, signs, test center, result, health pictures, etc. varying on their territory. One of the maximum common kind of diagnosis depends on medical pictures. Our approach is to develop a model to identify either a brain hemorrhage is present or not in Computed Topography (CT) scan of the brain and also identify the kind of hemorrhage. The process of detecting and identifying hemorrhage contains many steps like image pre-processing, segmentation of image, extracting the features, and classifying the images.

Keywords CT scan · Brain haemorrhage · Image processing · Image segmentation

1 Introduction

Brain hemorrhage implies blood loss within brain. In brief, one quite stroke which causes draining round the tissues by an artery within the cerebrum is observed as brain hemorrhage. Draining can happen in between the cerebrum and also the layers that cover it. The irritation that is caused by the blood from trauma leads to increase of pressure on brain tissues; this results in reduced percentage of oxygen from reaching the brain cells. This brain hemorrhage is observed as medical emergency which needs prompt treatment. There are several factors which might cause or result in

K. V. Sharada · V. Prashanthi (✉)
Gokaraju Rangaraju Institute of Engineering and Technology, Hyderabad, India

S. Kanakala
VNR Vignana Jyothi Institute of Engineering and Technology, Hyderabad, India

P. Nayak et al. (eds.), *IoT and Analytics for Sensor Networks*, Lecture Notes in Networks and Systems 244, https://doi.org/10.1007/978-981-16-2919-8_41

cerebral hemorrhage. These components include head injury, blood vessel anomalies, liver disease, brain tumour, extreme high blood pressure, bleeding disorders, and utilization of illegal medications. Anomalies within the blood vessels are the most explanation in the majority of the intracerebral hemorrhages that out of nowhere happen in youngsters, anyway there could be other potential causes which incorporate blood sicknesses, cerebrum tumors, septicemia, or the work of liquor or illegal medications. Many people who experience a hemorrhage have side effects as though they are having a stroke and can create weakness on one side of their body or a feeling of numbness. Sometimes brain hemorrhage can cause a scope of various indications like sudden, serious migraine, difficulty in gulping, vision problems, loss of coordination with the body, confusion or trouble in understanding, difficulty in talking or stammering discourse, seizures, torpidity or stupor.

Brain hemorrhage often leads to several complications. Because of the draining nerve cells one cannot speak with different pieces of the body and in this manner stops ordinary working. Additionally, there are scarcely any basic issues that emerge after a brain discharge which incorporates development, discourse, or memory issues. A few difficulties might be lasting relying upon the area of drain and the harm that happens. These intricacies may incorporate—loss of motion, vision misfortune, and decreased capacity to talk or get words, disarray, or memory misfortune. These complications made brain hemorrhage an emergency condition that requires immediate treatment. Diagnosing a brain drain could be troublesome as certain individuals do not give any physical indications. Specialists need to do take the assistance of a CT scan or MRI scan so as to locate the specific area of the seeping in the mind. CT pictures are known to claim numerous points of interest over MRI. Along these lines, the standard of CT pictures is sufficiently high to precisely analyse Intracranial Brain Hemorrhage. PC supported determination frameworks (CAD), as their name proposes, use PCs to assist specialists with arriving at a quick and exact conclusion. They have been the focal point of numerous scientists since they depend on preparing and examining pictures of various pieces of the human body for brisk and exact outcomes. Computer aided design frameworks are normally area explicit as they are advanced for certain particular sorts of infections, portions of the body, analysis techniques, and so on. They investigate various assortments of information, for example, manifestations, research facility test results, clinical pictures, and so on depending on their space. One of the most generally perceived sorts of determination is the one that depends on clinical pictures. Such frameworks are helpful on the grounds that they can be incorporated with the product of the clinical imaging machine so as to deliver a brisk and precise finding. Then again, they can be trying since they consolidate the components of man-made reasoning and advanced picture preparing (Fig. 1).

The rest of the paper is organized as follows: In Session 2 Literature survey is discussed, in Session 3 proposed system is described, Session 4 describes the implementation, Session 5 explains the experimentation and results and finally in Session 6 conclusion is given of our main proceedings series.

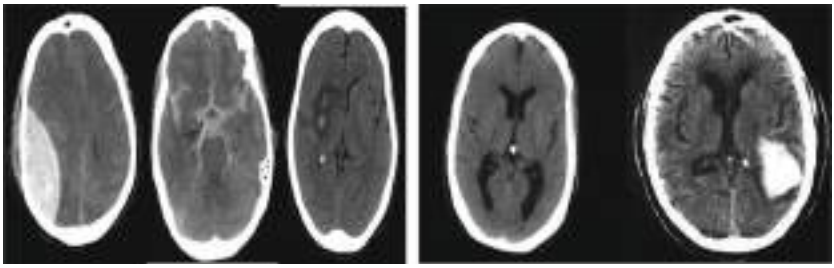

Fig. 1 CT scan images of five types of brain hemorrhages

2 Literature Survey

The paper [1] mainly discussed the pre-segmentation process. In this the techniques of dividing the input image into four quadrants using the method of splitting and merging are used. This is called as pre-segmentation of imaging. The pre-segmentation can be done with the following methods: (1) Thresholding: in thresholding the pixels of the input image is given certain threshold values and those pixels are mapped to related areas. (2) Region growing technique. (3) Supervised segmentation methods and unsupervised segmentation methods. Process of segmentation is as follows: as a first step the image is split into quadrants. Then histogram and pixel values are computed for each quadrant separately. The succeeding process for the above step is comparing each histogram value and pixel value with the predefined threshold criteria (or) histogram, pixel values. The final step is taking only the region of abnormality that is detected and feeding this as input to the segmentation process.

In [2] the method includes a combination of the machine with knowledge discovery techniques. During a CT scan the Intracranial pixel depth is noted. Based on the depth the pixel intensities are normalized using depth-dependent gray level normalization and the dense area of the intracranial region is segmented with the process of region growing and multi-resolution thresholding. The succeeding step is the construction of the decision tree by applying the algorithm. The first step in the method is pre-processing, and it involves the separation of pixels containing the extracranial part and the skull (intracranial pixels). This is used for recognition, measurement, and classification of a hematoma. In the next step the optimal threshold is chosen for hematoma segmentation by human experts and this differs from case to case which leads to instability. In the succeeding step the identification of the largest area containing Intracranial hematoma is done by considering the largest connected hyperdense region and excluding other smaller hyperdense regions. The final step is the construction of a decision tree using algorithm. Limitations: there is difficulty in recognizing subdural and epidural hematomas.

In [3] there is much focus on Cerebral Ischemia and had been said that if cerebral ischemia developed once there might not be a successful or complete cure for the abnormality. The method involved is based on the average thickness of the blood layer and based on thickness, and it is divided into grades such as good, recovery,

dead scaling them as 1, 2, and 3. Computed Tomography (CT) scanned images are given as input to the process. It is described in this process that a thick localized subarachnoid layer of blood or diffusion of blood might lead to delayed cerebral ischemia. This method only focuses on Cerebral Ischemia.

In [4] there is an automatic classification of images into two classes based on features. The two classes are abnormal and normal. This classification involves four phases. Pre-process includes the separation of pixels containing the extracranial part and intracranial part. In feature extraction the original dataset is restricted, and these extracted features serve as training data and saved into feature library. Next, they applied the SVM classifier and KNN classifier. While performing this method it was observed that the K-Nearest Neighbors classifier yielded better results in comparison with the SVM classifier. The postprocessing step is performed after image is classified as abnormal. In the post-processing step the image of the skull is removed and then the abnormal region is extracted. Generally, for removing skull we use brightest pixel cells as the brain matter appears in grey color. This approach categorizes only two classes (abnormal and normal) and gives generic results without any specific label.

In [5, 6] the cerebral microbleed is visualized by using susceptibility-weighted imaging (SWI). Here depending on susceptibility-weighted imaging they constructed rank based average pooling to identify cerebral microbleed. For detection of cerebral microbleed, Convolutional Neural Network is used which contains multiple layers. ReLU layer is used to map the convolution layer with SoftMax activation, tangent activation and Rectified linear unit activation. It is more effective than the convolution layer. So, it is more popular. The convolutional layer may have a greater number of elements in the feature set which will lead to dimension disaster termed as overfitting. In this situation pooling plays a major role that replaces the clusters of related elements in the feature set with statistic summary value. This is done using a pooling function. The last advance is rank-based normal pooling which incorporates a normal of non-zero negative actuations. Rank-based normal pooling can beat the issue of loss of helpful data which is brought about by normal pooling and most extreme pooling. This is a very complex method and has a computational burden.

In [7] the method proposed is a densely connected neural network which is called densenet. To detect cerebral microbleeds the algorithm used is densenet. A sliding window is utilized to cover the arrangement of unique pictures from left to right and through and through. The objective worth is chosen dependent on the focal pixel of the sub models. Later the cost matrix will be employed, based on the comparison between the entries in the cost matrix and target value final abnormality region is detected. Following are the steps included in this algorithm: (1) Traditional Convolutional Neural Network: the layer age of straight enactment, the capacity is done by means of convolutions [8]. The following layer, for example, ReLU layer, is utilized to outline convolution layer with SoftMax enactment, digression actuation, Rectified straight unit initiation, and so on. It is more effective than the convolution layer. So, it is more popular. (2) Densenet: It is used to establish connections between layers. These connections are used for feature maps. The layers that are between the blocks are called transition layers. Each layer receives information from its previous layer. (3) Transfer learning: it is based on fully convolutional multiscale residual

densenets. It considers the labeled samples to get high classification accuracy. It is meant to retrain the later layers of densenet. The usage of this transfer learning leads to an increase in accuracy rate.

In [9, 10] a complete CNN is trained with computed tomography (CT) scans. The algorithm resulted in high accuracy for the detection of acute Intracranial Hemorrhage. This algorithm has shown more accurate results than the measurements that are calculated by 2–4 radiologists.

The method used in [11, 12] is 3D quantitative analysis which performs 3D measurements of the parameters of the Intracerebral Brain Hemorrhage region based on computed tomography (CT) images. This resultant data is correlated with patient mortality. The image segmentation in this is done using a clustering algorithm whose strategy is based on fuzzy c-means which minimizes the objective function that represents the distance of feature vectors from the cluster centers. Based on the features of the clusters rule-based labelling is done whose components include fact-list, knowledgebase (or) rule-base, and inference engine. The labelling is done on the area, the color of the region. This is taken as input for the final step. This method not always perform correct segmentation.

In [13–15] the first step is pre-processing which includes division of the image into four quadrants called segmentation. Pre-processing is done using a tracking algorithm to separate skull images from the Gray dura matter in the CT scan image. Among these four regions the most vulnerable region which has the possibility of abnormality is considered and remaining regions are excluded. The next step is a grouping of all the identical homogenous regions to point out the abnormality. Following are the segmentation methods that are used: (1) Thresholding: it compares the pixel values with the threshold values. (2) Region growing techniques: it extracts useful or connected regions. (3) Supervised and unsupervised method: in this method there is the segmentation of the image in the training stage. Compared to supervised, unsupervised is efficient and less error sensitive. This method is not fully automatic. It requires a lot of human intervention.

3 Proposed Method

The proposed method includes CT scan images as the input datasets. Initially CT Scan images are converted into the format that a network/model can take as input. Images are converted into jpeg format. Later the images are processed so as to analyze the images accurately. Otsu's strategy is utilized with the end goal of segmentation. In general, it is a method to segment an advanced picture into numerous regions bolstered a few rules like arrangements of pixels, and so forth. Noise and unwanted pixels from the image are removed such as the skull part of the image which is of high intensity. The objective of the segment is to disentangle a picture to be increasingly significant and simpler to examine. Numerous methodologies for division exist, for example, thresholding and grouping. This stage sections the cerebrum picture into a few locales with the goal that we can segregate the ROI (the drain district). The result

of this stage is regularly used to distinguish the presence of hemorrhages with most extreme exactness. Later classification of images is done using the Weka tool. Otsu's method of segmentation also minimizes the within-class variance of the system by finding a threshold value automatically based upon the pixel values, probability values of a segment. Morphological operations and region growing techniques can be used to obtain further improvements on the segmented image and finally most filtered part of ROI is obtained and features like the area of ROI, the axis of ROI, the circumference of ROI, distance between skull and ROI are extracted, and they are fed into a neural network through a feature vector pattern. For the extraction of features accurately Region props tool of MATLAB is used. For the purpose of classification between various types of hemorrhages the shape of ROI plays a major role generally for Epidural and Intraparenchymal hemorrhages, there is a convex hull that is present in the region of Interest whereas for subdural hemorrhage it is concave in shape. The Region surrounding the ROI is called Bounding Box, which also plays an important role to extract features of region of interest (ROI). The extracted features from ROI will be stored as input to train the model. The kind of hemorrhage is then recognized based on the neural network which is trained. Once the set of input and output images are saved at that instance then there will be a saved network which is called a Network file. Later working of a network file is determined using a training percentage method.

3.1 Preprocessing

Preprocessing is the beginning step of the method that involves removal of high intensity pixel part of the image such as the skull part and removal of noise. Later the image is segmented into parts so that it becomes easy for the purpose of analyzing and it is done by the OTSU'S method which has 100% of accuracy and clustering of segments with similar properties is made so that identification abnormalities become easy.

3.2 Segmentation

Segmentation step is continued by the feature extraction step which is main step to group segments with similar properties together and then later feed into a neural network. The pixel intensity of the brightest part of the skull is about 250 pixels, and it must be removed in order to identify the part that has abnormality. It is done through MATLAB. Image based cad system is used for the purpose of image segmentation. Later based on the properties of segmented part the type of hemorrhage is detected using a classifier algorithm (Type detection algorithm).

Type Detection Algorithm (Segmentation)

1: BTD (Ss, p, q, Cc, W) ◁ Ss CT scan Data set. n count of feature. C classifier W is vector.
2: Dd ← BUILDDATASET1 (Ss, p, q)
3: for c ∈ Cc do
4: Acu ← TESTINCLASSIFIER (Dd, c, wc)
5: end for
6: return c Acu
7: end
8: BUILDDATASET1 (Ss, p, q) ◁ Ss Scan Dataset. n count of feature
9: Assign Dd to empty
10: for j ← 0,9 do
11: tt ← EXTRACINTFEATURE (j, n)
12: add tt to the end of Dd
13: end for
14: return Dd
15: end
16: EXTRACTINFEATURE (j, n) ◁ i brains CT scan
17: j is ≥ 251, j = 0; Apply steps 18 to 23
18: perform Otsu j
19: morphological j
20: regions growing j
21: region props
22: classifier
23: return vi
24: end
25: TESTINCLASSIFIER (Dd, c, wc)
26: partition Dd into 10 subset: Dd0..Dd9
27: for k ← 0,9 do
28: Ta ← Dk
29: Tb ← Sk = 0,…,9
30: calculate accuracy
31: return avg of Aj's for j = 0 to 9
32: end for
33: end procedure.

3.3 Morphological Techniques

The followings are the morphological techniques used Opening-by-remaking, shutting by-remaking, Supplement picture, Compute territorial maxima, Superimpose the picture, Process Background Markers, Watershed Transformation and the Segmentation, Imagine the Result, Evacuate Background Noise. Morphological operations basically remove the background and then dilates the inner segment region. An image

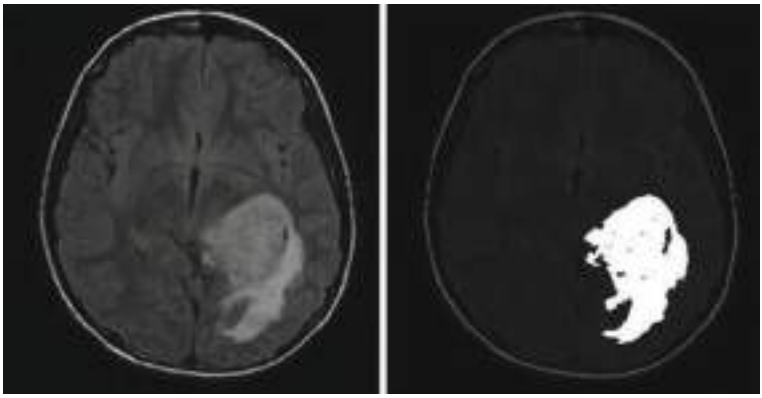

Fig. 2 Haemorrhagic region after applying segmentation and pre-processing techniques

containing potential regions with suspicious mass is the result of morphological operations.

3.4 Obtaining Region of Interest

Figure 2 highlighted images that indicate the hemorrhagic region after applying segmentation and pre-processing techniques. Region growing starts from a single point and then expand from that point by finding the region that is similar to that of the seed region. At the end of this step 'Region of Interest' is obtained which is utilized as contribution for 'Neural Network' and furthermore as training set. ROI is very crucial for the success of the proposed system. Resultant image after applying region growing techniques will be blank for normal brain image, whereas there will be some portion of image existing for brain image in abnormal condition after application of region growing technique.

4 Experimentation and Results

Experiments were done by changing the parameters given to the model: changing the way the data was split was tried by toggling the value of the shuffle argument—True or False as shown in Fig. 3. The change has not got any specific modifications to the output of the model. This has happened as little number of samples was utilized for performing segmentation. Next by changing the image size to 256X256 and the batch size to 64, the training process a lot more slower compared to when the values were set to 128 $\times$ 128 and 32 which trained the model approximately in 25 min. The training loss for the 256 $\times$ 256 images started learning later because the batch

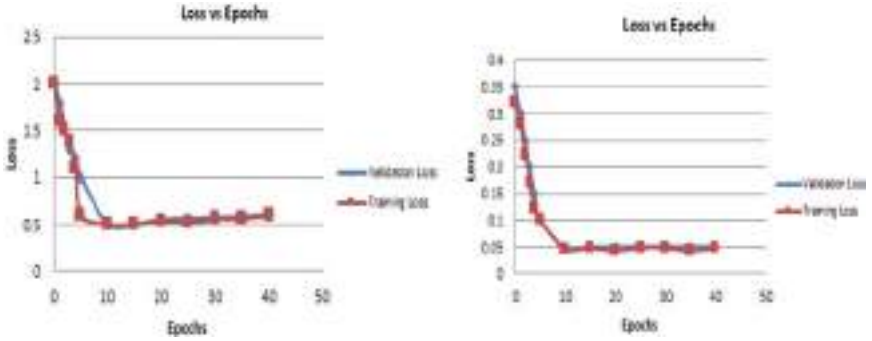

Fig. 3 (a) Loss vs Epoch: for 256X256 image size (b) Loss vs Epoch: for 128X128 image size

size was doubled and further we think it did not reach it. The model trained on 50 epochs but could have been appropriately trained for less number of epochs. This experiment mainly focused on segmentation of the data and localizing the affected area.

5 Conclusion

Automated frameworks for grouping medical images have increased a phenomenal degree of consideration recently. It has considerable impact in recognizing the existence of cerebral hemorrhage (the paired characterization issue) and in the event that it exists classification of hemorrhage is done and also problem of multiclass is also resolved. Although there are some algorithms which detect the hemorrhage efficiently and produce reasonable results, they are having few limitations like few algorithms find it difficult in recognizing subdural and epidural hematomas, few of them cannot detect subarachnoid hemorrhage, few consume more power and some are not suitable for large datasets, having longer computation time. Main cause for these limitations is existence of standardized procedures in less numbers. Since the diagnosis of Brain Hemorrhage is the very complicative and sensitive task, accuracy and reliability are given much priority. The investigations indicate that later prehandling CT Scans, the double arrangement issue untraveled with 100% exactness. Additionally, the actualized framework accomplished over 92% exactness for the order issue of deciding the discharge type utilizing convolutional neural systems as a classifier. The outcomes are truly promising and more elevated levels of exactness for the characterization issue will be accomplished by getting a vastly improved dataset with high-level goals pictures held legitimately from the CT scanner. Also, unique element extraction and highlight choice procedures could be utilized to improve the presentation of the framework.

References

1. Li, Y., Hu, Q., Wu, J., & Chen, Z. (2009). A hybrid approach to detection of brain hemorrhage candidates from clinical head ct scans. In *2009 Sixth International Conference on Fuzzy Systems and Knowledge Discovery*. vol. 1. IEEE.
2. Liao, CC., Xiao, F., Wong, J. M., & Chiang, I. J. (2008). A knowledge discovery approach to diagnosing intracranial hematomas on brain CT: recognition, measurement and classification. In *International conference on medical biometrics*. Berlin, Heidelberg, Springer.
3. Bhadauria, H. S., & Dewal, M. L. (2014). Intracranial hemorrhage detection using spatial fuzzy c-mean and region-based active contour on brain CT imaging. *Signal, Image and Video Processing*, *8*(2), 357–364.
4. Mohsen, F., Pomonis, S., & Illingworth, R. (1984). Prediction of delayed cerebral ischaemia after subarachnoid haemorrhage by computed tomography. *Journal of Neurology, Neurosurgery & Psychiatry, 47*(11), 1197–1202.
5. Kyaw, M. M. (2013). Pre-segmentation for the computer aided diagnosis system. *International Journal of Computer Science & Information Technology, 5*(1), 79.
6. Dou, Q., Chen, H., Yu, L., Zhao, L., Qin, J., Wang, D., & Heng, P. A. (2016). Automatic detection of cerebral microbleeds from MR images via 3D convolutional neural networks. *IEEE transactions on medical imaging*, *35*(5), 1182–1195.
7. Ramteke, R. J., & Monali, K. Y. (2012). Automatic medical image classification and abnormality detection k-nearest neighbour. *International Journal of Advanced Computer Research 2*(4), 190–196.
8. Wang, S., Jiang, Y., Hou, X., Cheng, H., & Du, S. (2017). Cerebral micro-bleed detection based on the convolution neural network with rank based average pooling. *IEEE Access*, *5*, 16576–16583.
9. Kuo, W., Häne, C., Mukherjee, P., Malik, J., & Yuh, E. L. (2019). Expert-level detection of acute intracranial hemorrhage on head computed tomography using deep learning. *Proceedings of the National Academy of Sciences*, *116*(45), 22737–22745
10. Loncaric, S., Dhawan, A. P., Cosic, D., Kovacevic, D., Broderick, J., & Brott, T. (1999). Quantitative intracerebral brain hemorrhage analysis. In *Medical Imaging 1999: Image Processing* (Vol. 3661). International Society for Optics and Photonics.
11. Kyaw, M. M. (2013). Computer-Aided Detection system for Hemorrhage contained region. *International Journal of Computational Science and Information Technology*, 11–16.
12. Magoulas, G. D., & Prentza, A. (1999). Machine learning in medical applications. In *Advanced course on artificial intelligence*. Berlin, Heidelberg, Springer.
13. Prashanthi, V., & Srinivas, K. (2020). Plant disease detection using convolutional neural networks. *International Journal of Advanced Trends in Computer Science and Engineering, 9*(3), 2632–2637.
14. Hayward, R. D. (1977). Subarachnoid haemorrhage of unknown aetiology: A clinical and radiological study of 51 cases. *Journal of Neurology, Neurosurgery & Psychiatry, 40*(9), 926–931.
15. Prashanthi, V., & Srinivas, K., Generating analytics from web log. *International Journal of Engineering and Advanced Technology, 9*(4), 161–165.

Obscuring of Data Leakage in Static Memory Cell and Optimization of WRITE Power

Cognitive Informatics and Soft Computing pp 429-443 | Cite as

- Gopala Krishna Pasumarty (1)
- N. V. Ganapathi Raju (1)
- Sankararao Majji (2)

1. Department of Information Technology, GRIET, , Hyderabad, India
2. Department of Electronics and Communication Engineering, GRIET, , Hyderabad, India

Conference paper
First Online: 02 July 2021

Part of the Advances in Intelligent Systems and Computing book series (AISC, volume 1317)

Abstract

With the limitations of CMOS technology scaling, rigorous research of alternate and competent technologies is emerged to impel the boundaries of digital computing. In this article, we proposed a simple, yet power and performance efficient methods of memory implementation. Present research attempts have been faithful to studying and performing these memory implementation techniques. In this article, we addressed the issues and described the current advanced methods of data storage. Conventionally, the WRITE operation in static memory consumes more power than the dynamic power associated with it because of the high-bit line voltage swing during the WRITE operation. This work presents the designing and characterization of ultra-scalable SRAM in terms of power and performance. The simulations are carried out using CMOS technology in cadence tool. The simulation results and functionality are distinguished with conventional memory units.

Keywords

CMOS technology Digital computing Static memory Voltage swing Data storage

Notes

Acknowledgements

We are very grateful to the reviewers for their valuable feedback and advice on further improving the manuscript. I thank the co-authors who have contributed immeasurably in making this manuscript possible, and I offer my sincere gratitude to each of them

References

1. Patnala, T.R., Majji, J.D,S., Valleti, M., Kothapalli, S., Karanam, S.R.: A modernistic way for KEY generation for highly secure data transfer in ASIC design flow. In: 2020 6th International Conference on Advanced Computing and Communication Systems (ICACCS), Coimbatore, India, pp. 892–897 (2020). https://doi.org/10.1109/ICACCS48705.2020.9074200 (https://doi.org/10.1109/ICACCS48705.2020.9074200)
2. Tulasi, R., Sankararao, P., Gopala Krishna, M.P.: Optimization of CSA for low power and high speed using MTCMOS and GDI techniques. Int. J. Eng. Adv. Technol. (IJEAT) **8**(5S3) (2019)
Google Scholar (https://scholar.google.com/scholar?q=Tulasi%2C%20R.%2C%20Sankararao%2C%20P.%2C%20Gopala%20Krishna%2C%20M.P.%3A%20Optimization%20of%20CSA%20for%20low%20power%20and%20high%20speed%20using%20MTCMOS%20and%20GDI%20techniques.%20Int.%20J.%20Eng.%20Adv.%20Technol.%20%28IJEAT%29%208%285S3%29%20%282019%29)
3. Makosiej, A., Thomas, O., Amara, A., Escu, A.V.: CMOS SRAM scaling limits under optimum stability constraints. In: International Symposium on Circuits and Systems , Beijing, China (2013)
Google Scholar (https://scholar.google.com/scholar?q=Makosiej%2C%20A.%2C%20Thomas%2C%20O.%2C%20Amara%2C%20A.%2C%20Escu%2C%20A.V.%3A%20CMOS%20SRAM%20scaling%20limits%20under%20optimum%20stability%20constraints.%20In%3A%20International%20Symposium%20on%20Circuits%20and%20Systems%20%2C%20Beijing%2C%20China%20%282013%29)
4. Bhoi, A.K., Sherpa, K.S., Kalam, A., Chae, G.-S. (Eds.): In: Advances in Greener Energy Technologies, Springer (2020)
Google Scholar (https://scholar.google.com/scholar?q=Bhoi%2C%20A.K.%2C%20Sherpa%2C%20K.S.%2C%20Kalam%2C%20A.%2C%20Chae%2C%20G.-S.%20%28Eds.%29%3A%20In%3A%20Advances%20in%20Greener%20Energy%20Technologies%2C%20Springer%20%282020%29)
5. Marques, G., Bhoi, A.K., Albuquerque, V.H.C. de, K.S., H. (Eds.): In: IoT in Healthcare and Ambient Assisted Living, Springer (2021)
Google Scholar (https://scholar.google.com/scholar?q=Marques%2C%20G.%2C%20Bhoi%2C%20A.K.%2C%20Albuquerque%2C%20V.H.C.%20de%2C%20K.S.%2C%20H.%20%28Eds.%29%3A%20In%3A%20IoT%20in%20Healthcare%20and%20Ambient%20Assisted%20Living%2C%20Springer%20%282021%29)
6. Kumar, P.S.A.M.S.M.A.: Real-time moving object detection algorithm on high-resolution videos using GPUs. J. Real-Time Image Proc. **11**(1), 93–109 (2016)
CrossRef (https://doi.org/10.1007/s11554-012-0309-y)

Google Scholar (http://scholar.google.com/scholar_lookup?title=Real-time%20moving%20object%20detection%20algorithm%20on%20high-resolution%20videos%20using%20GPUs&author=PSAMSMA.%20Kumar&journal=J.%20Real-Time%20Image%20Proc.&volume=11&issue=1&pages=93-109&publication_year=2016)

7. Ma, Y.: Nonvolatile multibit SRAM, bit level caching, and multi-context computing for IoT. In: Non-Volatile Memory Technology Symposium (NVMTS), Beijing, China (2015)
Google Scholar (https://scholar.google.com/scholar?q=Ma%2C%20Y.%3A%20Nonvolatile%20multibit%20SRAM%2C%20bit%20level%20caching%2C%20and%20multi-context%20computing%20for%20IoT.%20In%3A%20Non-Volatile%20Memory%20Technology%20Symposium%20%28NVMTS%29%2C%20Beijing%2C%20China%20%282015%29)

8. Prasanna Lakshmi, K.R.C.: A survey on different trends in data streams. In: ICNIT2010- 2010 International Conference on Networking and Information Technology, Manila, Philippines (2010)
Google Scholar (https://scholar.google.com/scholar?q=Prasanna%20Lakshmi%2C%20K.R.C.%3A%20A%20survey%20on%20different%20trends%20in%20data%20streams.%20In%3A%20ICNIT2010-%202010%20International%20Conference%20on%20Networking%20and%20Information%20Technology%2C%20Manila%2C%20Philippines%20%282010%29)

9. Mallikarjuna, R.K.A.: An efficient method for parameter estimation of software reliability growth model using artificial bee colony optimization. In: Lecture Notes in Computer Science (2015)
Google Scholar (https://scholar.google.com/scholar?q=Mallikarjuna%2C%20R.K.A.%3A%20An%20efficient%20method%20for%20parameter%20estimation%20of%20software%20reliability%20growth%20model%20using%20artificial%20bee%20colony%20optimization.%20In%3A%20Lecture%20Notes%20in%20Computer%20Science%20%282015%29)

10. Asaduzzaman, A., Gummadi, D., Yip, C.M.: A talented CPU-to-GPU memory mapping technique. In: IEEE SOUTHEASTCON, Lexington, KY, USA (2014)
Google Scholar (https://scholar.google.com/scholar?q=Asaduzzaman%2C%20A.%2C%20Gummadi%2C%20D.%2C%20Yip%2C%20C.M.%3A%20A%20talented%20CPU-to-GPU%20memory%20mapping%20technique.%20In%3A%20IEEE%20SOUTHEASTCON%2C%20Lexington%2C%20KY%2C%20USA%20%282014%29)

11. Wei, W., Namba, K., Lombardi, F.: Design and comparative evaluation of a hybrid Cache memory at architectural level. In: 2016 International Great Lakes Symposium on VLSI (GLSVLSI), Boston, MA, USA (2016)
Google Scholar (https://scholar.google.com/scholar?q=Wei%2C%20W.%2C%20Namba%2C%20K.%2C%20Lombardi%2C%20F.%3A%20Design%20and%20comparative%20evaluation%20of%20a%20hybrid%20Cache%20memory%20at%20architectural%20level.%20In%3A%202016%20International%20Great%20Lakes%20Symposium%20on%20VLSI%20%28GLSVLSI%29%2C%20Boston%2C%20MA%2C%20USA%20%282016%29)

12. Seevinck, E.: A current sense-amplifier for fast CMOS SRAMs. In: Digest of Technical Papers. 1990 Symposium on VLSI Circuits. Honolulu, Hawaii, USA (1990)

Google Scholar (https://scholar.google.com/scholar?q=Seevinck%2C%20E.%3A%20A%20current%20sense-amplifier%20for%20fast%20CMOS%20SRAMs.%20In%3A%20Digest%20of%20Technical%20Papers.%201990%20Symposium%20on%20VLSI%20Circuits.%20Honolulu%2C%20Hawaii%2C%20USA%20%281990%29)

13. Sim, J., Kwon, K., Choi, J., Lee, S., Kim, D., Hwang, H., Chun, K., Seo, Y.: A 1.0 V 256 Mb SDRAM with offset-compensated direct sensing and charge-recycled Precharge schemes. In: IEEE International Solid-State Circuits Conference, 2003. Digest of Technical Papers. ISSCC., San Francisco, CA, USA (2003)
Google Scholar (https://scholar.google.com/scholar?q=Sim%2C%20J.%2C%20Kwon%2C%20K.%2C%20Choi%2C%20J.%2C%20Lee%2C%20S.%2C%20Kim%2C%20D.%2C%20Hwang%2C%20H.%2C%20Chun%2C%20K.%2C%20Seo%2C%20Y.%3A%20A%201.0%20V%20256%20Mb%20SDRAM%20with%20offset-compensated%20direct%20sensing%20and%20charge-recycled%20Precharge%20schemes.%20In%3A%20IEEE%20International%20Solid-State%20Circuits%20Conference%2C%202003.%20Digest%20of%20Technical%20Papers.%20ISSCC.%2C%20San%20Francisco%2C%20CA%2C%20USA%20%282003%29)

14. Kim, Y., Tong, Q., Choi, K., Lee, Y.: Novel 8-T CNFET SRAM cell design for the future ultra-low power microelectronics. In: International SoC Design Conference (ISOCC), Jeju, South Korea (2016)
Google Scholar (https://scholar.google.com/scholar?q=Kim%2C%20Y.%2C%20Tong%2C%20Q.%2C%20Choi%2C%20K.%2C%20Lee%2C%20Y.%3A%20Novel%208-T%20CNFET%20SRAM%20cell%20design%20for%20the%20future%20ultra-low%20power%20microelectronics.%20In%3A%20International%20SoC%20Design%20Conference%20%28ISOCC%29%2C%20Jeju%2C%20South%20Korea%20%282016%29)

15. Raghav, N., Bansal, M.: Analysis of power efficient 6-T SRAM Cell with performance measurements. In: International Conference on Innovations in Control, Communication and Information Systems (ICICCI), Greater Noida, India (2017)
Google Scholar (https://scholar.google.com/scholar?q=Raghav%2C%20N.%2C%20Bansal%2C%20M.%3A%20Analysis%20of%20power%20efficient%206-T%20SRAM%20Cell%20with%20performance%20measurements.%20In%3A%20International%20Conference%20on%20Innovations%20in%20Control%2C%20Communication%20and%20Information%20Systems%20%28ICICCI%29%2C%20Greater%20Noida%2C%20India%20%282017%29)

16. Mishra, L., S.K.V., Mangesh, S.: Design and implementation of low power SRAM structure using nanometer scale. In: 2nd International Conference on Advances in Electrical Electronics Information Communication and Bio-Informatics (AEEICB), Chennai, India (2016)
Google Scholar (https://scholar.google.com/scholar?q=Mishra%2C%20L.%2C%20S.K.V.%2C%20Mangesh%2C%20S.%3A%20Design%20and%20implementation%20of%20low%20power%20SRAM%20structure%20using%20nanometer%20scale.%20In%3A%202nd%20International%20Conference%20on%20Advances%20in%20Electrical%20Electronics%20Information%20Communication%20and%20Bio-

Informatics%20%28AEEICB%29%2C%20Chennai%2C%20India%20%282016%29)

17. Kumar, A.S.V.S.V.P.D., Suman, B.S., Sarkar, C.A., Kushwaha, D.V.: Stability and performance analysis of low power 6T SRAM cell and memristor based SRAM cell using 45NM CMOS technology. In: International Conference on Recent Innovations in Electrical, Electronics and Communication Engineering (ICRIEECE), Bhubaneswar, India (2018)
Google Scholar (https://scholar.google.com/scholar?q=Kumar%2C%20A.S.V.S.V.P.D.%2C%20Suman%2C%20B.S.%2C%20Sarkar%2C%20C.A.%2C%20Kushwaha%2C%20D.V.%3A%20Stability%20and%20performance%20analysis%20of%20low%20power%206T%20SRAM%20cell%20and%20memristor%20based%20SRAM%20cell%20using%2045NM%20CMOS%20technology.%20In%3A%20International%20Conference%20on%20Recent%20Innovations%20in%20Electrical%2C%20Electronics%20and%20Communication%20Engineering%20%28ICRIEECE%29%2C%20Bhubaneswar%2C%20India%20%282018%29)

Copyright information

About this paper

Cite this paper as:

Pasumarty G.K., Raju N.V.G., Majji S. (2021) Obscuring of Data Leakage in Static Memory Cell and Optimization of WRITE Power. In: Mallick P.K., Bhoi A.K., Marques G., Hugo C. de Albuquerque V. (eds) Cognitive Informatics and Soft Computing. Advances in Intelligent Systems and Computing, vol 1317. Springer, Singapore. https://doi.org/10.1007/978-981-16-1056-1_34

- First Online 02 July 2021
- DOI https://doi.org/10.1007/978-981-16-1056-1_34
- Publisher Name Springer, Singapore
- Print ISBN 978-981-16-1055-4
- Online ISBN 978-981-16-1056-1
- eBook Packages Intelligent Technologies and Robotics Intelligent Technologies and Robotics (R0)

Personalised recommendations

Covid-19 Spread Analysis

Srinivas Kanakala and Vempaty Prashanthi

Abstract Based on the public datasets afforded by John Hopkins University and Canadian health authorities, we developed a forecasting model of Covid-19 after analyzing the spread. Data related to the cumulative amount of definite cases, per day, in each country and another dataset consisting of various life factors, scored by the people living in each country around the globe. We are going to merge these two datasets to see if there is any relationship between the spread of the virus in a country by preprocessing, merging and finding correlation between datasets we will calculate needed measures and prepare them for an analysis, then we will try to predict the spread of cases by using various methods. Time series data tracking the number of people affected by the coronavirus globally, including confirmed cases of the coronavirus, the number of people who have died due to the coronavirus and the number of people who have recovered from the deadly infection. Data science can give accurate pictures of coronavirus outcomes and also helps in tracking the spread. Secondly using Covid-19 data, we can make supply chain logistics decisions in spreadsheets supplies of personal protective equipment and ventilators to hospitals and clinics across the world. An analysis of the country, by state and region, identifying locations of highest need for supplies and ventilators according to the dataset collected. This is called a supply plan. Finally, create a set of visualizations and then add these visualizations to a presentation so that we can report on findings.

1 Introduction

The tale Covid that began in Wuhan, China, has spread to practically all nations and was announced as pandemic [1]. The degree of this flare-up is fast. It is difficult to precisely survey the lethality of this infection and it has all the earmarks of being

S. Kanakala (✉)
VNR Vignana Jyothi Institute of Engineering and Technology, Hyderabad, India

V. Prashanthi
Gokaraju Rangaraju Institute of Engineering and Technology, Hyderabad, India

S. C. Satapathy et al. (eds.), *Smart Computing Techniques and Applications*,
Smart Innovation, Systems and Technologies 224,
https://doi.org/10.1007/978-981-16-1502-3_5

unmistakably more deadly than the Covid that caused SARS and MERS. Researchers [2] have recognized two new strains of the Covid, demonstrating it is now been changed at any rate once. The greatest test is an obscure number of individuals have been contaminated by the infection without getting indicative. These individuals are transporters of the infection without themselves giving any indications. At first, individuals who gave no indications of disease were not isolated and this prompts the spread of the infection at a gigantic rate. The infection is additionally appeared to influence its hosts lopsidedly. Youngsters appear to be less inclined to be tainted while the moderately aged and more seasoned grown-ups are mysteriously contaminated. Men are bound to kick the bucket from the contamination contrasted with ladies, and furthermore individuals with a more fragile safe framework, Type 2 diabetes and hypertension. Be that as it may, as of late numerous alive and well youthful people have kicked the bucket from the contamination making it much harder to comprehend the impact of Covid-19 [3, 4].

2 Literature Survey

Coronavirus Fig. 1 is the overwhelming illness brought about by and was called Covid. This new virus was vague before and started in Wuhan, China, in December 2019. Coronavirus is a pandemic affecting many countries.

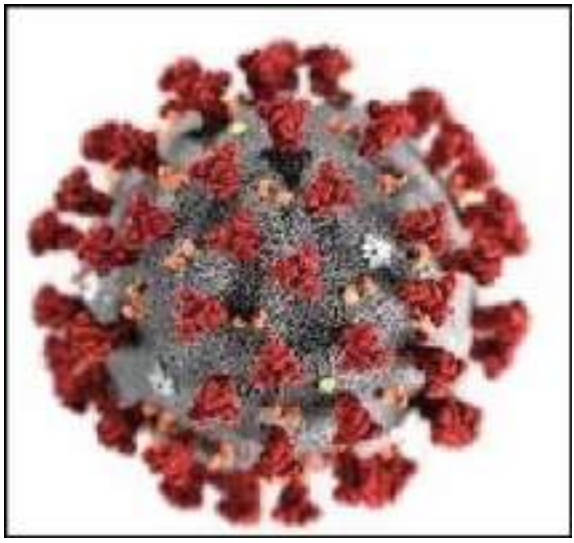

Fig. 1 Coronavirus

2.1 Symptoms

The indications of Covid-19 [5] are general influenza like and a few patients increase an great kind of pneumonia. Patients have fever, muscle pain and body throbs, hacks and sore throat about following six days of getting the contamination. The huge people feel truly desperate and frail and improve all alone, yet a minority of patients will deteriorate following 5–7 days of ailment and the patients have windedness and exacerbating hack. The hack is dry and not wet. It is even observed that patients have solid cerebral pains. Furthermore, the side effects are somewhat unique in relation to influenza. People tainted from the infection might not have a virus. However, a few people do not become ill while being contaminated and are spreading the infection to new has. These individuals ought not to be all over town spreading the illness. Individuals who got tainted and have been effectively restored have likewise got contaminated by the Covid-19 once more. Making it much harder to contain the episode. There is no anti-microbial to treat the Covid-19 and it may not be accessible until the spring of 2021. This makes it much more imperative to take preventive activities.

2.2 No Symptoms

Coronavirus is basically extended with respiratory beads detached by somebody who is hacking or has other effects, like fever or sluggishness [6]. Many people who have coronavirus experience just mellow indications. These are the symptoms in the beginning. Most as of late it has been indicated that elevated levels of the infection are available in respiratory discharges during the "presymptomatic period that can a days ago to over seven days" before the fever and hack normal for Covid-19. This capacity of the infection to be communicated by individuals without side effects is a significant purpose behind the pandemic. Some news show that persons who are not having any manifestations can communicate the virus.

2.3 Coronavirus Modes of Spread

The Covid spreads principally from one person to other [7]. This occurs among peoples who are close to each other. Beads which are created when a contaminated individual hacks or wheezes may land in the mouths or noses of individuals who are close by, or potentially be breathed in into their lungs. An individual contaminated with Covid—even one without any side effects may emanate vaporizers when they talk or relax. Mist concentrates are irresistible viral particles that can buoy or float

around noticeable all around for as long as three hours. One can be affected by Covid-19 when he touches an item which has virus and then touches their own mouth, nose, or conceivably eyes.

2.4 Importance of Social Distance and Self-isolation

Every person should maintain social distancing of about 6 ft or more from others. Schools, gatherings, occasions, malls, etc. do not maintain any social distancing. Therefore, these are closed during Covid. This will help the society from virus, as the spread will be controlled. Self-isolation is an important measure that should be taken by the people who is affected by coronavirus. He or she should be isolated in separate room, even from family members. These people should not go to crowdie places like schools, etc. Take clinical assistance. If you do not live in a region with intestinal sickness or dengue fever kindly do the accompanying.

3 Existing System

Aarogya Setu: It is an Indian Covid-19 APP. "Contact following, Syndromic planning and Self-evaluation" computerized administration, fundamentally a portable application, created by the National Informatics Center under the Ministry of Electronics and Information Technology (MeitY). The cause for this application is to make people familiar with Covid-19 for well-being of people. It is an app which needs the mobile phone's GPS and Bluetooth to follow the Covid contamination. The app can be accessed from Android and iOS versatile frameworks. With the help of Bluetooth, it indicates danger when one comes close (inside six feet of) to you who is with coronavirus, by viewing the database of cases around India. With the help of GPS, it can detect whether the region is a place with contaminated zone.

Drawbacks of Existing System:

- It is forced through leader request with no legitimization.
- Recently, Robert Baptiste has tweeted that safety weaknesses in Aarogya Setu permitted programmers to realize who is tainted or not well in their preferred region. He additionally gave subtleties of what number of individuals were unwell and contaminated at the PM's Office, the India Parliament and the Home Office.
- The application's Terms of Service (TOS) gives restricted obligation to the administration. In this way, there is no administration responsibility in the event of information burglary of clients.

4 Proposed System

We developed a new model of Covid-19 after analyzing the spread. Data related to the cumulative no of confirmed cases, per day, in each Country and another dataset consisting of various life factors, scored by the people living in each country around the globe. We are going to merge these two datasets to see if there is any relationship between the spread of the virus in a country by preprocessing [8, 9], merging and finding correlation between datasets we will calculate needed measures and prepare them for an Analysis, then we will try to predict the spread of cases by using various methods. Time series data tracking the number of people affected by the coronavirus globally, including confirmed cases of the coronavirus, the number of people who have died due to the coronavirus and the number of people who have recovered from the deadly infection. Data preprocessing [10, 11] is a data mining technique which is used to transform the raw data in a useful and efficient format.

Steps Involved in Data Preprocessing:

1. **Data Cleaning**: The information may have numerous insignificant and missed parts. To deal with such things, information cleaning is finished. This includes treatment of missed information, boisterous information and so on.
    (a) **Missing Data**: This condition comes when some information is not present. This can be obtained from different techniques such as:
        (i) **Ignore the Tuples**: This method is appropriate when the dataset is huge and different qualities are not present in a tuple.
        (ii) **Fill the Missing Qualities**: There are many methods to fill this. One can do this physically, by characteristic mean or the most likely worth.
    (b) **Uproarious Data**: Noisy information is a negligible information that cannot be deciphered by machines. It tends to be produced because of flawed information assortment, information section mistakes and so on. It very well may be dealt with in following manners.
        (i) **Binning Method**: This strategy chips away at arranged information so as to smooth it. The entire information is isolated into portions of equivalent size and afterward different strategies are performed to finish the errand. Each fragmented is dealt with independently. We can supplant information of section by the mean or limit esteems could be utilized to finish the errand.
        (ii) **Relapse**: Here information is turned smooth by fitting it into relapse function. The relapse utilized might be straight or various
        (iii) **Bunching**: This methodology bunches the comparative information in a group. The anomalies might be not detected or else it comes under outside the bunches.

2. **Data Transformation**: This progression is taken so as to change the information in fitting structures appropriate for mining measure. This includes Normalization, Attribute Selection, Discretization, Concept Hierarchy Generation.
3. **Data Reduction**: Since information mining is a method that is utilized to deal with colossal measure of information. While working with gigantic volume of information, examination got more diligently in such cases. So as to dispose of this, we utilize information decrease method. It means to expand the capacity effectiveness and decrease information stockpiling and investigation costs. The different strides to information decrease are Data Cube aggregation, Attribute Subset Selection, Numerosity Reduction, Dimensionality Reduction.

5 Proposed System

The supply logistics from the USA are considered. This set is cleaned by removing the unnecessary columns. It narrows down the data to information we need the most. This prevents distraction and enables a clear idea of what needs to be analyzed. Calculating the vent creating a pivot table in python. Since the values are extremely clumped, we can sort by a required filter such as region like MidWest. We use a legend to depict this. We have shown a pie chart representation to give a clear picture of the distribution in Fig. 2 since we have many states and matplotlib does a rudimentary view of the analysis. Calculating the ventilator requirements for each state in the US.

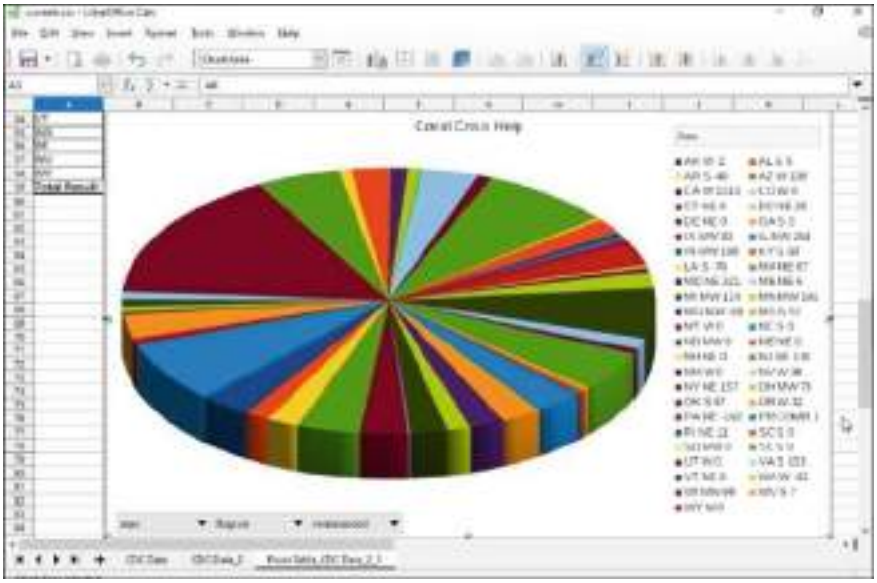

Fig. 2 Covid crisis pie chart

We take the number of patients hospitalized and the number of cumulative ventilators available to get the required number.

A specific case study to observe the number of cases in China, India and Japan show in Fig. 3. We can see that the rate of cases in the origin country of the virus has the maximum cases and since the other two countries are in close proximity, the cases have spread and also on a similar level in India and Japan.

The spread of the virus in India can be seen by the 21st day where the sudden spike is evident shown in Fig. 4. The government issued lockdown to flatten this spike of increase shown in Fig. 5.

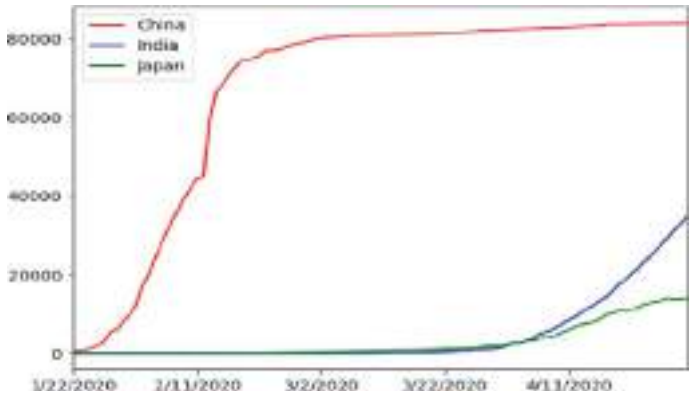

Fig. 3 Specific case study to observe the number of cases in China, India and Japan

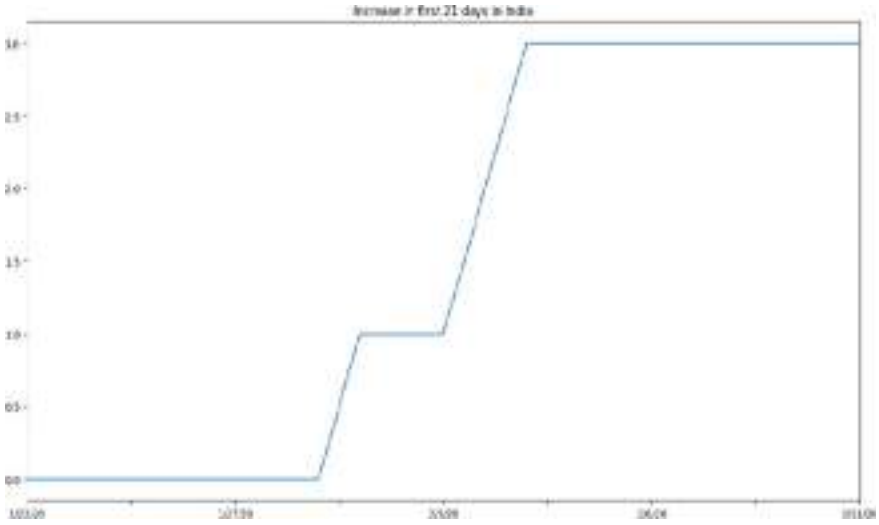

Fig. 4 Spread of the virus in India can be seen by the 21st day

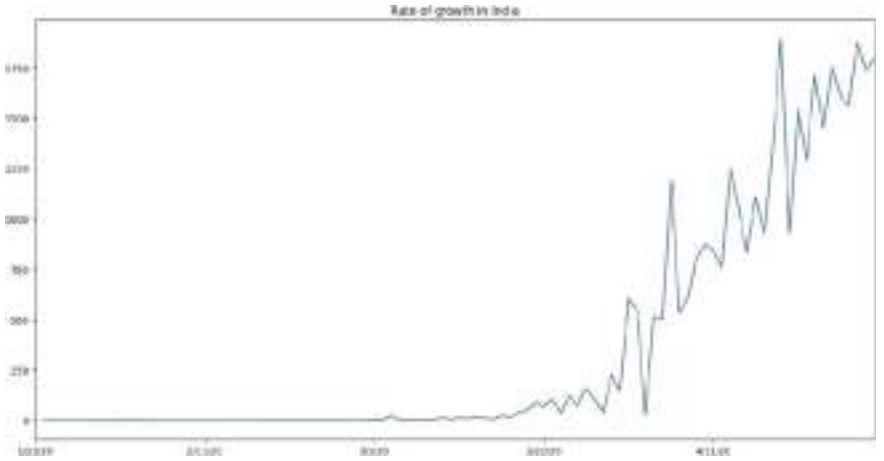

Fig. 5 For first 21 days coronavirus spread

Corona cases versus GDP: Does the wealth of a country mean less corona cases? It does not seem so. In fact, developing countries have a lesser risk than developed countries as per our studies shown in Fig. 7. We have tried to correlate the number of cases and the development of a country. This can be due to various reasons like climatic conditions, etc. However, this is not due to lack of testing kits on the contrary in developing countries (Fig. 6).

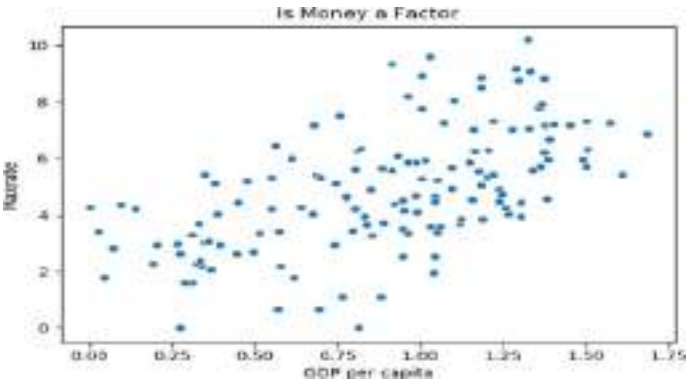

Fig. 6 Corona cases versus GDP

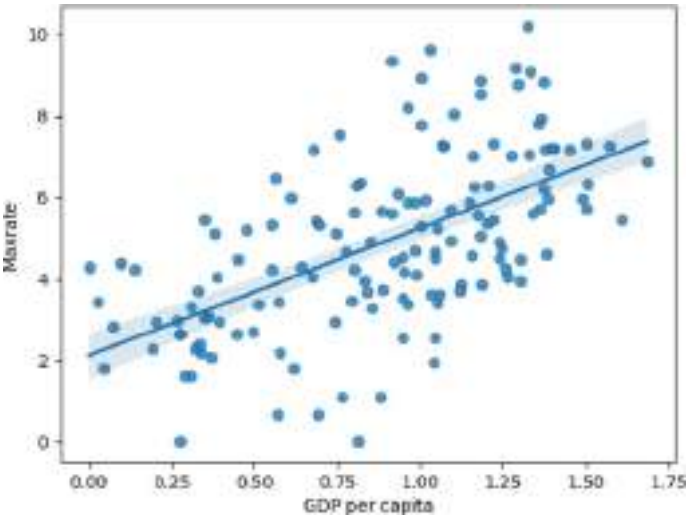

Fig. 7 Future spread based on cases and GDP per capita

6 Conclusion

In this digital world, new data and information on the coronavirus and the progress of the occurrence have become accessible at an exceptional pace. Even though, tough questions stay without answer and exact answers to predict the dynamics of the situation will not receive in such stage. Analyzing and predicting the spread of viruses with the existing data will help us to have a better understanding to prevent the spread and to take preventive measures. To fight with coronavirus, we have to take care of ourselves and follow all the safety measures and rules that have been given by the government. Everyone can play a part in helping scientists to fight the coronavirus.

References

1. Novel, Coronavirus Pneumonia Emergency Response Epidemiology: The epidemiological characteristics of an outbreak of 2019 novel coronavirus diseases (COVID-19) in China. Zhonghua liu xing bing xue za zhi= Zhonghua liuxingbingxue zazhi **41.2**, 145 (2020)
2. Perlman, S.: Another decade, another coronavirus, 760–762 (2020)
3. Abroug, F., et al.: Family cluster of Middle East respiratory syndrome coronavirus infections, Tunisia, 2013. Emerg. Infect. Dis. **20.9**, 1527 (2014)
4. Van Der Hoek, L., et al.: Identification of a new human coronavirus. Nat. Med. **10.4**, 368–373 (2004)
5. Guan, W.-j., et al.: Clinical characteristics of coronavirus disease 2019 in China. New England J. Med. **382.18**, 1708–1720 (2020)

6. Schoeman, D., Fielding, B.C.: Coronavirus envelope protein: current knowledge. Virol. J. **16**(1), 1–22 (2019)
7. Song, F., et al.: Emerging 2019 novel coronavirus (2019-nCoV) pneumonia. Radiology **295.1**, 210–217 (2020)
8. Kamiran, F., Calders, T.: Data preprocessing techniques for classification without discrimination. Knowl. Inf. Syst. **33**(1), 1–33 (2012)
9. Prashanthi, V., Kanakala, S.: Plant disease detection using Convolutional neural networks. Int. J. Adv. Trends Comput. Sci. Eng. **9**(3), 2632–2637
10. García, S., Luengo, J., Herrera, F.: Data preprocessing in data mining. Springer International Publishing, Cham, Switzerland (2015)
11. Prashanthi, V., Kanakala, S.: Generating analytics from web log. Int. J. Engi. Adv. Technol. **9**(4), 161–165

Exploring the Fog Computing Technology in Development of IoT Applications

Chaitanya Nukala, Varagiri Shailaja, A. V. Lakshmi Prasuna, and B. Swetha

Abstract In the 21st era, IoT is assuming a significant part in creating Smart urban communities. With the development of IoT, information is developing with increasing speed. As the information is developing the need to store information is likewise expanding. More the information, the dormancy will be high to store and recover information from the cloud. The idea of mist processing was started to reduce the inertness for getting to information to and from the cloud. Haze processing gives the capacity, figuring just as systems administration administrations toward the end purpose of the system. Haze hubs likewise have restricted computational abilities. Because of certain shortcomings, haze figuring and distributed computing can't continue alone, so both these advances are coordinated to fabricate keen IoT foundation for Smart city. Mist figuring have a significant job and preeminent duty being developed of a Smart city. This paper examines different utilization of mist registering and their usage in Smart urban areas. It additionally proposes a model for Waste administration framework in a city. Mist figuring can assist with overseeing the waste assortment of the city in a keen manner. Based on our survey, a few open concerns and difficulties of mist processing are examined, and the bearings for future analysts have additionally been talked about.

C. Nukala (✉)
Department of CSE, RGM College of Engineering and Technology (Autonomous), Nandyal, Andra Pradesh 518501, India

V. Shailaja
Department of IT, Gokaraju Rangaraju Institute of Engineering and Technology, Hyderabad, Telangana 500090, India

A. V. Lakshmi Prasuna · B. Swetha
Department of IT, Mahatma Gandhi Institute of Technology, Gandipet, Hyderabad, Telangana 500075, India

S. C. Satapathy et al. (eds.), *Smart Computing Techniques and Applications*,
Smart Innovation, Systems and Technologies 224,
https://doi.org/10.1007/978-981-16-1502-3_16

1 Introduction

A creating number of physical articles are being related with the IoT [1]. It is the interconnection of different physical elements that pass on and exchange data the sensors, shrewd meters, telephones and vehicles, radio-recurrence distinguishing proof (RFID) labels, and actuator [2]. The interconnection of these devices enables shrewd IoT applications like following on the web trucked merchandise, condition observing, medical services keen home and savvy framework, and so forth.

IoT devices make a great deal of data, which procure tremendous figuring office, stockpiling zone, and correspondence information move limit. Cisco said 50 billion gadgets could be associated by Internet in 2020 [3], and it will build 500 billion by 2025 [4].

The idea of mist figuring was presented by Cisco in the year 2012 [5]. The beginning objective of haze registering is to upgrade the profitability and to diminish volume of information which is moved to cloud for preparing. For ease, the board of all assets haze layer go about as a middle among gadgets and cloud server farms. Haze processing can offer types of assistance in different zones i.e. observation, transportation division, clever urban areas, medical services, and keen structures. Mist figuring can be utilized in various kinds of IoT administrations [5–7]. To start with, Smart E-Health Gateway can be utilized for patients to checking their wellbeing status [8]. Crisis caution can be enacted and send the alerts to the proprietor [9]. A haze based Electronic Data Interchange (EDI) is an exhaustive virtualized device outfitted with the capacity, transmission and registering limit [5].

Further segments of the article are clarified as follows: Sect. 2 contains Motivation of the investigation, Sect. 3 explains the Layered design of IoT and mist processing and how it can function for keen utilizations of IoT, Sect. 4 examines uses of IoT and haze registering, Sect. 5 clarifies load adjusting in mist figuring condition, Sect. 6 examine the proposed philosophy, Sect. 7 has been regarding open issues and supportive gestures lastly Sect. 8 finish up the paper and clarifies the opportunity of Future.

2 Motivation

This manuscript provides gives a short conversation of the application territories of IoT and FC. The fundamental ideas of IoT and FC are talked about that incorporates points of interest, hindrances, and engineering of FC.

Mist layer requires load adjusting to accomplish asset productivity, stay away from over-burden in the system, to improve framework execution, and furthermore to ensure the framework against disappointments. The inspiration of this paper is to investigating the keen waste administration framework which incorporates load adjusting on the haze layer. This paper likewise talks about different open issues and difficulties looked in mist conditions.

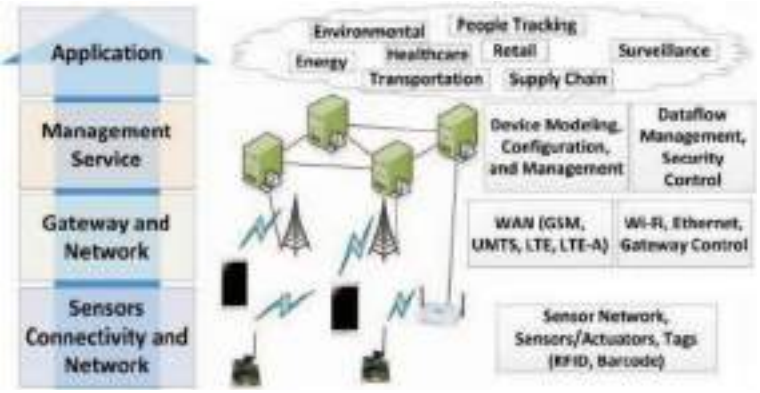

Fig. 1 Layers of IoT architecture [10]

3 Layered Framework of IOT and FC

3.1 Layered Framework of IOT

IoT has been arrangement of devices that send, share, and use data from the physical condition to offer types of assistance to individuals, endeavors, and society. The essential three-layer engineering is appeared in Fig. 1 [10].

(a) Layer of Sensors: This detect and collecting information from nature. Sensors, scanner tag marks, RFID labels, GPS, camera, and actuator are available in this layer

(b) Layer of Network: This utilized to assemble the information from sensor and sends to the web. Liable for organize layer is interfacing with other savvy things, arrange gadgets, and workers. Its features are moreover used for communicating and handling sensor data. Utilizing various advancements, different kinds of conventions and heterogeneous systems are accumulated.

(c) Layer of Middleware: This gets information from layer Network. Its inspiration is administration the board, information stream the executives, and security control. It moreover performs information taking care of and takes decisions normally taking into account results.

(d) Layer of Application: It gets information from the Middleware layer and gives overall administration of the application.

3.2 Layered Architecture of FC

The class of CC for example FC have three layer engineering. The lower layer contains IoT gadgets. Mist layer is the center layer. IoT gadgets are coupled to cloud

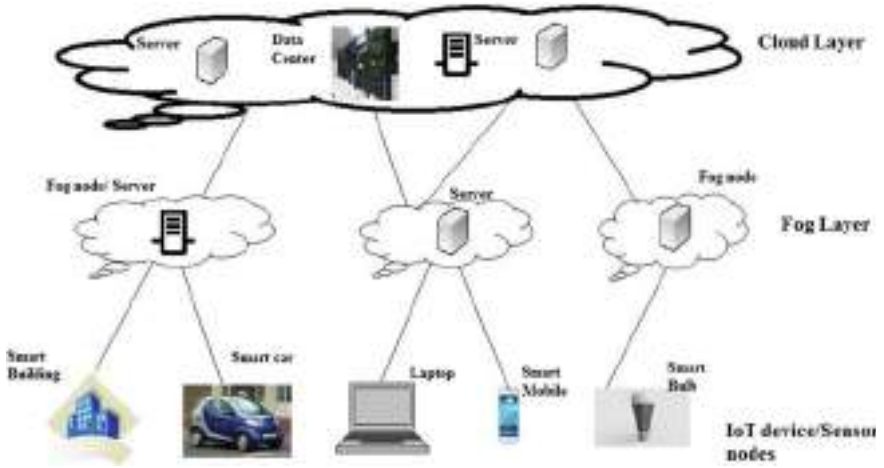

Fig. 2 Architecture of Fog computing

layer through mist layer. Entire gadgets store their information on the cloud. The haze layer channels information, and the information which isn't quickly needed is diverted to the cloud. The every now and again got to information is put away on the mist layer. Layered design of FC is clarified as beneath: Fig. 2 shows the engineering of FC.

- **Brilliant IoT gadgets**: The a great many sensors hubs and implanted frameworks having low transfer speed and low inertness are utilized at this layer. Savvy gadgets like brilliant structures, advanced cells, workstations, shrewd power bulbs, keen vehicles, and so forth can be considered as IoT gadgets which gather the information and send this information to the haze layer [14].
- **Haze Layer**: Network layer of haze is additionally partitioned into two sections: Fog system and Core organize.

Network of Fog: It incorporates 3G/4G/5G/LTE/Wi-Fi and so forth multi-edge benefits that are utilized to interface distinctive detecting gadgets with the haze hubs. Haze hubs are utilized to channel information assembled by method of IoT gadgets and not regularly utilized information is diverted to the upper layer for example cloud layer.

Network of Core: QoS, manifold protocol Label Switching (MPLS), manifoldcast, and security were deliberated at this phase [11].

- **Layer of Cloud**: It incorporates a great deal of server farms and cloud facilitating IoT investigation. The colossal information accumulated through various IoT gadgets are put away in the huge server farms situated at different areas on the planet.

4 Applications of FC and IOT

Haze works in dispersed condition. It offers types of assistance to the last client at the edge gadget. FC have different application regions where we can incorporate with IoT that can be examined as follows:

a. **Meticulous Healthcare**: In view of dirtied condition different sorts of microscopic organisms have been being spread noticeable all around which causes different ailments.
   Each individual has occupied today as a result of quick ways of life. Shrewd healthcare has the brilliant IoT which monitors exercises of individuals and measures different boundaries of their body and continues transferring the information on the haze hubs, which have been being seen by the specialists. The information put away on the haze hubs have been being utilized by specialists to treat the patients inside time. The individuals have been wearing insightful gadgets and these have been additionally connected to mist hubs which have been ceaselessly sending the estimations of body boundaries (temperature, pulse, and so on.) so as to the mist hubs. These wise wearable gadgets help to monitor individuals' wellbeing [7].
b. **Meticulous Parking**: Because of much increment in transportation in the urban communities, all the more parking spots have been required. Individuals need to meander to a great extent to locate the fitting parking spot for them. FC presented a novel thought of Meticulous stopping. With the utilization of FC the stopping spaces can be introduced with the sensors which continue following climate the parking have been a has vacant or full [12].
c. **Meticulous Agriculture**: Agribusiness has the wide territory to be given consideration since has zone has from where all the urban communities have been getting food. Brilliant agribusiness idea has been introduced in most recent couple of years. Shrewd detecting and figuring have been playing a critical obligation in keen agribusiness. A couple of savvy agribusiness approaches have been imagined around there. Brilliant water system frameworks have been given. Shrewd sensors have been being repaired in the fields [13]. FC gives a stage to working the sensors in the fields, which have been ceaselessly watching the yields. The sensors identify necessities of the harvests and persistently store information in the haze hubs which send the cautions to the ranchers about the prerequisites of the yields. The shrewd farming assumes an essential function for building a brilliant city.
d. **Meticulous Waste administration**: The earth has corrupting step by step, and to moderate the planet we require sharp consideration towards the normal assets. Presently days, day by day developing waste and water exhaustion from the earth looks for more consideration. Keen trash the board framework can be named the answers for improvement of condition in this time. Such keen frameworks will be created with the assistance of cloud just as FC to gather and deal with the waste all the more proficiently [8].

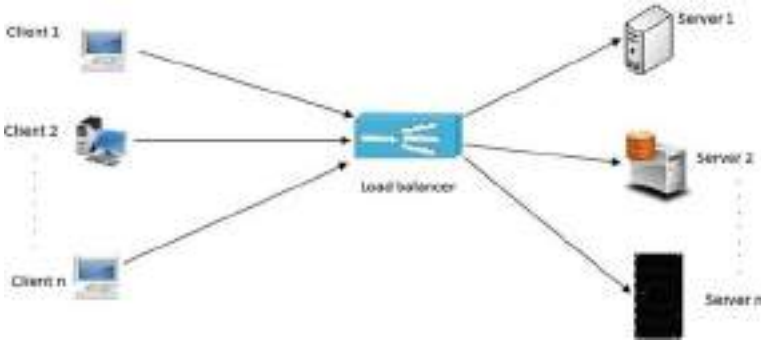

Fig. 3 Balancing of load in network

5 Load Balancing in FC Environment

In a system, scarcely any frameworks stay under-stacked sooner or later stretch, while the others convey the whole heap of the system. To keep up the heap in a reasonable plan, "Burden Balancing" gets vital. "Burden Balancing endeavors to disperse the heap in indistinguishable extents all through assets relying upon response capacity all together that each valuable asset isn't over-burden or underutilized in a cloud device" [14]. Burden adjusting additionally needed to be done to dodge halt and diminish the worker flood issue. Figure 3 shows the heap adjusting.

A portion of the objectives of mist based burden adjusting are talked about as underneath:

- In instance of failure of system, the balancing of load offers plans for backup.
- Consequently, performance could be enhanced.

6 Projected Methodology

The novel waste administration network has been projected in this manuscript by modifying the load at the layer of mist. Here, projected method comprises of three phases: mist, datacenters of cloud, gadgets related to sensor. It could be stated that comprise of sensors. Moreover, these canisters smart would tied up further over the layer of mist that data of channels have to be transferred towards cloud. The balancer of burden would adapt mist hubs heap. Moreover, it might distinct the similar heap on entire hubs.

These hubs of haze would readily create the messages for advising the transporters of trash for waster gathering. The sensors of security would established in canisters that lighten regarding receptacles. Further, in instance, anybody might try for canisters tempering, where these sensors would start signal clamoring that might spare by considering receptacles. Further, the containers smart would be linked by 3G or

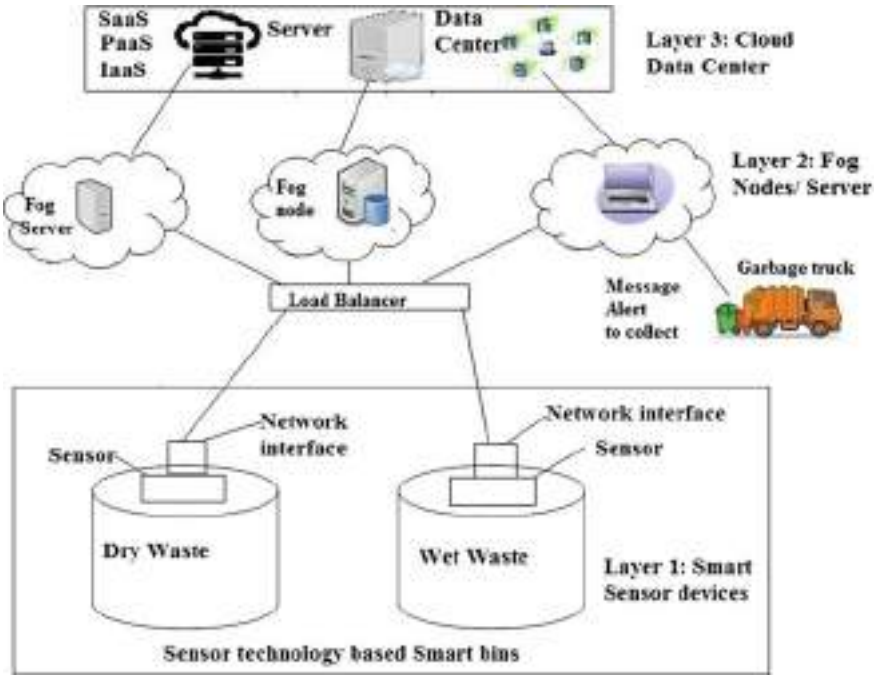

Fig. 4 Load balancing model

4G towards layer of mist. The application would be formed for contributing overall circumstance. The ensuing Fig. 4 shows the proposed model of burden adjusting framework.

7 Open Issues and Encouragements

There were divergent open issues, which could be worked in an addition. Here, accompanying could be examined further:

- Interaction among hubs: further, it might be examined in addition to explore the engineering by which hubs of haze might interact over one another.
- Recognition devices: the gadgets that are smart were exorbitant than another fundamental market components. Here, these could be deliberated deprived of any issue.
- It could be a significant issue in this contemporary world. FC pre-requisite more computations of security for real-time practice.
- It shall be in condition of mist. As it causes challenges when pair of workers have been loaded very much, while other workers would be stacked beneath.

- Effectiveness of energy: The effectiveness of energy could a prominent in FC test. The mist utilizing force has to be lessened.

8 Conclusion and Future Scope

The objective of this manuscript portrays joining of IoT and FC for assisting divergent implementations. What's more, load adjusting has been proposed. Next to, a couple of uses, including the brilliant farming, keen medical services, shrewd stopping, and savvy squander the executives showed. The basic purpose behind this survey is to give a significant perception and preferences of IoT and its fuse with mist/edge processing and how burden adjusting should be possible when FC incorporated with IoT. There are still more open regions for future analysts, for example, Haze organizing, asset provisioning, greater headway in transportation.

References

1. Al-Fuqaha, A., Guizani, M., Mohammadi, M., Aledhari, M., Ayyash, M.: Internet of things: a survey on enabling technologies, protocols, and applications. IEEE Commun. Surv. Tutor. **17**(4), 2347–2376 (2015)
2. Gubbia, J., Buyyab, R., Marusica, S., Palaniswamia, M.: Internet of things (IoT): a vision, architectural elements, and future directions. Futur. Gener. Comp. Syst. **29**(7), 1645–1660 (2013)
3. Evans, D.: The Internet of Things: How the Next Evolution of the Internet is Changing Everything. Cisco White Paper (2011)
4. Camhi, J.: Former Cisco CEO John Chambers Predicts 500 Billion Connected Devices by 2025. Business Insider (2015)
5. Luan, T.H., Gao, L., Xiang, Y., Li, Z., Sun, L.: Fog Computing: Focusing on Mobile Users at the Edge. arXiv preprint arXiv:1502.01815 (2015)
6. Emilia, R., Naranjo, P.G.V., Shojafar, M., Vaca-cardenas, L.: Big Data Over SmartGrid—A Fog Computing Perspective Big Data Over SmartGrid—A Fog Computing Perspective (2016)
7. Khan, S., Parkinson, S., Qin, Y.: Fog computing security: a review of current applications and security solutions. J. Cloud Comput. **6**(1) (2017)
8. Mahmud, R., Kotagiri, R., Buyya, R.: Fog Computing: A Taxonomy, Survey and Future Directions, pp. 1–28 (2016)
9. Desikan, K.E.S., Srinivasan, M., Murthy, C.S.R.: A novel distributed latency-aware data processing in fog computing—enabled IoT networks. In: Proceedings of the ACM Workshop on Distributed Information Processing in Wireless Networks—DIPWN'17, pp. 1–6 (2017)
10. Chi, Q., Yan, H., Zhang, C., Pang, Z., Xu, L.D.: A reconfigurable smart sensor interface for industrial WSN in IoT environment. IEEE Trans. Ind. Inform. **10**(2) (2014)
11. Chiang, M., Zhang, T.: Fog an IoT: an overview of research opportunities. IEEE Internet Things J. **3**(6), 854–864 (2016)
12. Perera, C., Qin, Y., Estrella, J.C., Reiff-Marganiec, S., Vasilakos, A.V.: Fog Computing for Sustainable Smart Cities: A Survey (2017)

13. Varshney, P., Simmhan, Y.: Demystifying Fog Computing: Characterizing Architectures, Applications and Abstractions. In: Proceedings—2017 IEEE 1st International Conference of Fog Edge Computing ICFEC, pp. 115–124 (2017)
14. Dastjerdi, A.V., Gupta, H., Calheiros, R.N., Ghosh, S.K.: Fog Computing: Principles, Architectures, and Applications, pp. 1–26 (2016)

Data-Driven Prediction Model for Crime Patterns

Smart Computing Techniques and Applications pp 47-58 | Cite as

- Y. Gayathri (1)
- Y. Sri Lalitha (1)
- M. V. Aditya Nag (2)
- Sk. Althaf Hussain Basha (3)

1. Gokaraju Rangaraju Institute of Engineering and Technology, , Hyderabad, India
2. Institute of Aeronautical Engineering, Dundigal, , Hyderabad, India
3. A1, Global Institute of Engineering and Technology, , Markapur, India

Conference paper
First Online: 08 July 2021

Part of the Smart Innovation, Systems and Technologies book series (SIST, volume 225)

Abstract

With the ever-increasing technology widgets and media, there is enough awareness of good and bad in the surroundings. Unemployment or abundant money is making people to indulge in crime. Throughout the world, crime prediction and prevention are the two major issues of all governments for the safety and security of their citizens. With machine learning and data mining techniques to predict unknown events, crime data analysis and prediction has attracted the attention of many researchers in recent times. There is still generalized, accurate and optimized requirement of crime data analysis and prediction models. This work proposes to address crime data analysis and prediction using visual analytics and machine learning algorithms on Kaggle crime dataset. The proposed models provide better insights on the crime zones and frequency of occurrences of certain crimes in a zone. We have compared Naïve Bayesian and Random Forest Machine Learning Models to predict the crime, and we have noticed that our models exhibited better accuracy.

References

1. Bogomolov, B., Lepri, J., Staiano, N., Oliver, F., Pianesi, Pentland, A.: Once upon a crime: towards crime prediction from demographics and mobile data. In: Proceedings of the 16th International Conference on Multimodal Interaction, pp. 427–434 (2014)

Google Scholar (https://scholar.google.com/scholar?q=Bogomolov%2C%20B.%2C%20Lepri%2C%20J.%2C%20Staiano%2C%20N.%2C%20Oliver%2C%20F.%2C%20Pianesi%2C%20Pentland%2C%20A.%3A%20Once%20upon%20a%20crime%3A%20towards%20crime%20prediction%20from%20demographics%20and%20mobile%20data.%20In%3A%20Proceedings%20of%20the%2016th%20International%20Conference%20on%20Multimodal%20Interaction%2C%20pp.%20427%E2%80%93434%20%282014%29)

2. Iqbal, R., Murad, M.A.A., Mustapha, A., Shariat Panahy, P.H., Khanahmadliravi, N.: An experimental study of classification algorithms for crime prediction. Indian J. Sci. Technol. **6**(3) 4219–4225 (2013)
Google Scholar (https://scholar.google.com/scholar?q=Iqbal%2C%20R.%2C%20Murad%2C%20M.A.A.%2C%20Mustapha%2C%20A.%2C%20Shariat%20Panahy%2C%20P.H.%2C%20Khanahmadliravi%2C%20N.%3A%20An%20experimental%20study%20of%20classification%20algorithms%20for%20crime%20prediction.%20Indian%20J.%20Sci.%20Technol.%206%283%29%204219%E2%80%934225%20%282013%29)

3. Chen, H., Chung, W., Xu, J.J., Wang, G., Qin, Y., Chau, M.: Crime data mining: a general framework and some examples. IEEE Comput. **37**(4), 50–56 (2004)
CrossRef (https://doi.org/10.1109/MC.2004.1297301)
Google Scholar (http://scholar.google.com/scholar_lookup?title=Crime%20data%20mining%3A%20a%20general%20framework%20and%20some%20examples&author=H.%20Chen&author=W.%20Chung&author=JJ.%20Xu&author=G.%20Wang&author=Y.%20Qin&author=M.%20Chau&journal=IEEE%20Comput.&volume=37&issue=4&pages=50-56&publication_year=2004)

4. Beshah, T., Hill, S.: Mining road traffic accident data to improve safety: role of road-related factors on accident severity in Ethiopia. In: Proceeding of Artificial Intelligence for Developments (AID 2010), pp. 14–19 (2010)
Google Scholar (https://scholar.google.com/scholar?q=Beshah%2C%20T.%2C%20Hill%2C%20S.%3A%20Mining%20road%20traffic%20accident%20data%20to%20improve%20safety%3A%20role%20of%20road-related%20factors%20on%20accident%20severity%20in%20Ethiopia.%20In%3A%20Proceeding%20of%20Artificial%20Intelligence%20for%20Developments%20%28AID%202010%29%2C%20pp.%2014%E2%80%9319%20%282010%29)

5. Zhang, Q., Yuan, P., Zhou, Q., Yang, Z.: Mixed spatial-temporal characteristics based crime hot spots prediction. In: IEEE 20th International Conference on Computer Supported Cooperative Work in Design (CSCWD), Nanchang, China (2016)
Google Scholar (https://scholar.google.com/scholar?q=Zhang%2C%20Q.%2C%20Yuan%2C%20P.%2C%20Zhou%2C%20Q.%2C%20Yang%2C%20Z.%3A%20Mixed%20spatial-temporal%20characteristics%20based%20crime%20hot%20spots%20prediction.%20In%3A%20IEEE%2020th%20International%20Conference%20on%20Computer%20Supported%20Cooperative%20Work%20in%20Design%20%28CSCWD%29%2C%20Nanchang%2C%20China%20%282016%29)

6. Sri Lalitha, Y., Govardhan, A.: Semantic framework for text clustering with neighbors. In: ICT and Critical Infrastructure: Proceedings of the 48th Annual Convention of CSI, Volume II, Advances in Intelligent Systems and Computing 249, pp. 261–271. © Springer International Publishing, Switzerland (2013). ISBN: 978-3-319-03095-1

Google Scholar (https://scholar.google.com/scholar?q=Sri%20Lalitha%2C%20Y.%2C%20Govardhan%2C%20A.%3A%20Semantic%20framework%20for%20text%20clustering%20with%20neighbors.%20In%3A%20ICT%20and%20Critical%20Infrastructure%3A%20Proceedings%20of%20the%2048th%20Annual%20Convention%20of%20CSI%2C%20Volume%20II%2C%20Advances%20in%20Intelligent%20Systems%20and%20Computing%20249%2C%20pp.%20261%E2%80%93271.%20%C2%A9%20Springer%20International%20Publishing%2C%20Switzerland%20%282013%29.%20ISBN%3A%20978-3-319-03095-1)

7. Mahmud, N., Ibn Zinnah, K., Ar Rahman, Y., Ahmed, N.: CRIMECAST: a crime prediction and strategy direction service. IEEE 19th International Conference on Computer and Information Technology. Dhaka, Bangladesh (2016)
Google Scholar (https://scholar.google.com/scholar?q=Mahmud%2C%20N.%2C%20Ibn%20Zinnah%2C%20K.%2C%20Ar%20Rahman%2C%20Y.%2C%20Ahmed%2C%20N.%3A%20CRIMECAST%3A%20a%20crime%20prediction%20and%20strategy%20direction%20service.%20IEEE%2019th%20International%20Conference%20on%20Computer%20and%20Information%20Technology.%20Dhaka%2C%20Bangladesh%20%282016%29)

8. Lin, Y.L., Yu, L.C., Chen, T.Y.: Using machine learning to assist crime prevention. In: IEEE 6th International Congress on Advanced Applied Informatics (IIAI-AAI). Hamamatsu, Japan (2017)
Google Scholar (https://scholar.google.com/scholar?q=Lin%2C%20Y.L.%2C%20Yu%2C%20L.C.%2C%20Chen%2C%20T.Y.%3A%20Using%20machine%20learning%20to%20assist%20crime%20prevention.%20In%3A%20IEEE%206th%20International%20Congress%20on%20Advanced%20Applied%20Informatics%20%28IIAI-AAI%29.%20Hamamatsu%2C%20Japan%20%282017%29)

9. Grover, V., Adderley, R., Bramer, M.: Review of current crime prediction techniques. In: International Conference on Innovative Techniques and Applications of Artificial Intelligence, pp. 233–237. Springer, London (2007)
Google Scholar (https://scholar.google.com/scholar?q=Grover%2C%20V.%2C%20Adderley%2C%20R.%2C%20Bramer%2C%20M.%3A%20Review%20of%20current%20crime%20prediction%20techniques.%20In%3A%20International%20Conference%20on%20Innovative%20Techniques%20and%20Applications%20of%20Artificial%20Intelligence%2C%20pp.%20233%E2%80%93237.%20Springer%2C%20London%20%282007%29)

10. McClendon, L., Meghanathan, N.: Using machine learning algorithms to analyze crime data. Mach. Learn. Appl. Intl. J. (MLAIJ) **2**(1) (2015)
Google Scholar (https://scholar.google.com/scholar?q=McClendon%2C%20L.%2C%20Meghanathan%2C%20N.%3A%20Using%20machine%20learning%20algorithms%20to%20analyze%20crime%20data.%20Mach.%20Learn.%20Appl.%20Intl.%20J.%20%28MLAIJ%29%202%281%29%20%282015%29)

11. Budur, E., Lee, S., Kong, V.S.: Structural analysis of criminal network and predicting hidden links using machine learning. arXiv:1507.05739 (http://arxiv.org/abs/1507.05739) (2015)

12. Chainey, S., Ratcliffe, J.: GIS and Crime Mapping. Wiley, USA (2015)
Google Scholar (http://scholar.google.com/scholar_lookup?title=GIS%20and%20Crime%20Mapping&author=S.%20Chainey&author=J.%20Ratcliffe&publication_year=2015)

13. Kim, S., Joshi, P., Kalsi, P.S., Taheri, P.: Crime analysis using machine learning. In: IEEE 9th Annual Information Technology, Electronics and Mobile Communication Conference (2018)
Google Scholar (https://scholar.google.com/scholar?q=Kim%2C%20S.%2C%20Joshi%2C%20P.%2C%20Kalsi%2C%20P.S.%2C%20Taheri%2C%20P.%3A%20Crime%20analysis%20using%20machine%20learning.%20In%3A%20IEEE%209th%20Annual%20Information%20Technology%2C%20Electronics%20and%20Mobile%20Communication%20Conference%20%282018%29)

Copyright information

About this paper

Cite this paper as:

Gayathri Y., Sri Lalitha Y., Aditya Nag M.V., Althaf Hussain Basha S. (2021) Data-Driven Prediction Model for Crime Patterns. In: Satapathy S.C., Bhateja V., Favorskaya M.N., Adilakshmi T. (eds) Smart Computing Techniques and Applications. Smart Innovation, Systems and Technologies, vol 225. Springer, Singapore. https://doi.org/10.1007/978-981-16-0878-0_6

- First Online 08 July 2021
- DOI https://doi.org/10.1007/978-981-16-0878-0_6
- Publisher Name Springer, Singapore
- Print ISBN 978-981-16-0877-3
- Online ISBN 978-981-16-0878-0
- eBook Packages Intelligent Technologies and Robotics Intelligent Technologies and Robotics (R0)

Personalised recommendations

International Conference on Advanced Informatics for Computing Research

ICAICR 2021: **Advanced Informatics for Computing Research** pp 65–77

Crop Identification and Disease Detection by Using Convolutional Neural Networks

K. Ravikiran, Ch. Naveen Kumar Reddy, P. Gopala Krishna, Mahendar Jinukala & K. Prasanna Lakshmi

Conference paper | First Online: 25 June 2022

Part of the Communications in Computer and Information Science book series (CCIS,volume 1575)

Abstract

The main Theme of this work is to implement a crop detector tool which is used to detect the type of crop and disease by taking crop images. The image of crop is given as input to the tool and it gives the name of the crop and disease if it effected with any disease. This work will help people to identify the crops which are not known to them. It is very difficult for the farmers to identify the crop disease with their naked eye to take what type of fertilizers to use on crops. For this work there is a require in depth knowledge to know the types of diseases. So to make it easier this tool also detects

if any leaf is infected with any disease. By using the machine learning algorithms such as convolutional neural network and training the dataset with various crop images, if the input matches with any of the trained data, the output is displayed that is the name of the crop and type of disease hence farmers can take immediate remedial to avoid the effect of disease.

Keywords

Crop **Crop diseases**

Convolutional neural network

Machine learning **Fertilizers**

References

1. Zhou, Y., et al.: Mapping paddy rice planting area in rice-wetland coexistent areas through analysis of Landsat 8 OLI and MODIS images. Int. J. Appl. Earth Observ. Geoinf. **46**, 1–12 (2016)

2. Khirade, S.D., Patil, A.B.: Plant disease detection using image processing. In: 2015 International Conference on Computing Communication Control and Automation, pp. 768–771 (2015). https://doi.org/10.1109/ICCUBEA.2015.153

3. Yeh, J.-F., Wang, S.-Y., Chen, Y.-P.: Crop disease detection by image processing using modified Alexnet. In: IEEE 3rd Eurasia Conference on Biomedical Engineering, Healthcare and Sustainability (ECBIOS-2021) (2021)

4. Heri Andrianto, S., Faizal, A., Armandika, F.: Smartphone application for deep learning-based rice plant disease detection. In: 2020 International Conference on Information Technology Systems and Innovation (ICITSI), pp. 387–392 (2020)

5. Wu, S., Bao, F., Xu, E., Wang, Y.-X., Chang, Y.-F., Xiang, Q.-L.: A leaf recognition algorithm for plant classification using probabilistic neural network. In: IEEE Symposium on Signal Processing and Information Technology 2007 (2007)

6. Li, L., Zhang, S., Wang, B.: Plant disease detection and classification by deep learning—a review. IEEE Access **9**, 56683–56698 (2021). https://doi.org/10.1109/ACCESS.2021.3069646

7. Yuan, Y., Xu, Z., Lu, G.: SPEDCCNN: spatial pyramid-oriented encoder-decoder cascade convolution neural network for crop disease leaf segmentation. IEEE Access **9**, 14849–14866 (2021). https://doi.org/10.1109/ACCESS.2021.3052769

8. Rajiv, K., Rajasekhar, N., Prasanna Lakshmi, K., Srinivasa Rao, D., SabithaReddy, P.: Accuracy evaluation of plant leaf disease detection and classification using GLCM and multiclass SVM classifier. In: Sharma, H., Saraswat, M., Kumar, S., Bansal, J.C. (eds.) CIS 2020. LNDECT, vol. 61, pp. 41–54. Springer, Singapore (2021). https://doi.org/10.1007/978-981-33-4582-9_4

9. To obtain data set. https://www.kaggle.com

10. Brahimi, M., Boukhalfa, K., Moussaoui, A.: Deep learning for tomato diseases: classification and symptoms visualization. Appl. Artif. Intell. **31**(4), 299–315 (2017)

11. Hemanth, D.J., Anitha, J., Naaji, A., Geman, O.,

Popescu, D.E.: Son, L.H.: A modified deep convolutional neural network for abnormal brain image classification. IEEE Access **7**, 4275–4283 (2019). https://doi.org/10.1109/ACCESS.2018.2885639

12. El-Kereamy, A., et al.: Deep learning for image-based cassava disease detection. Front. Plant Sci. **1852** (2017)

13. Huang, J., Wang, H., Dai, Q., Han, D.: Analysis of NDVI data for crop identification and yield estimation. J. Sel. Top. Appl. Earth Observ. Remote Sens. **7**(11), 4374–4384 (2014)

14. Fina, F., Birch, P., Young, R., Obu, J., Faithpraise, B., Chatwin, C.: Automatic plant pest detection and recognition using k-means clustering algorithm and correspondence filters. Int. J. Adv. Biotechnol. Res. **4**(2), 189–199 (2013)

15. Ravikiran, K., Sudhakar Dr., N.: Maximizing throughput in multi hope wireless network by considering intra and inter flow spatial reusability. J. Adv. Res. Dyn. Control Syst. JARDCS, 708–717 (2018). ISSN 1943-023X

16. Cao, J., Mao, D., Cai, Q., et al.: A review of object representation based on local features. J. Zhejiang Univ. Sci. C **14**, 495–504 (2013)

17. Ngugi, L.C., Abelwahab, M., AboZahhad, M.: Recent advances in image processing techniques for automated leaf pest and disease recognition—a review. Inf. Process. Agricult. **180**, 26–50 (2020)

18. Mohanty, S.P., Hughes, D.P., Salathé, M.: Using deep learning for image-based plant disease detection. Front. Plant Sci. **7**, 1419 (2016)

19. Garcia-Ruiz, F., Sankaran, S., Maja, J.M., Lee, W.S., Rasmussen, J., Ehsani, R.: Comparison of two aerial imaging platforms for identification of Huanglongbing-infected citrus trees. In: Computers and Electronics in Agriculture, vol. 91, pp. 106–115 (2013). ISSN 0168-1699

20. Krizhevsky, A., Sutskever, I., Hinton, G.E.: ImageNet classification with deep convolutional neural networks. In: Part of Advances in Neural Information Processing Systems (NIPS 2012) , vol. 25 (2012)

21. Kessentini, Y., Besbes, M.D., Ammar, S., Chabbouh, A.: A two stage deep neural network for multi-norm license plate detection and recognition. Expert Syst. Appl. **136**, 159–170 (2019)

Author information

Authors and Affiliations

Department of Information Technology, Gokaraju Rangaraju Institute of Engineering and Technology, Hyderabad, Telangana, India

K. Ravikiran, P. Gopala Krishna & K. Prasanna Lakshmi

Department of Information Technology, Vidya Jyothi Institute of Technology, Hyderabad, Telangana, India

Ch. Naveen Kumar Reddy

Department of Computer Science and Engineering, Malla Reddy College of Engineering and Technology, Hyderabad, Telangana, India

Mahendar Jinukala

Corresponding author

Correspondence to K. Ravikiran .

Editor information

Editors and Affiliations

Papua New Guinea University of Technology, Lae, Papua New Guinea

Ashish Kumar Luhach

Namibia University of Science and Technology, Windhoek, Namibia

Prof. Dharm Singh Jat

Universiti Malaysia Pahang, Pekan, Malaysia

Prof. Kamarul Bin Ghazali Hawari

University of Eastern Finland, Kuopio, Finland
Prof. Dr. Xiao-Zhi Gao

Saint Mary's University, Halifax, NS, Canada
Pawan Lingras

Rights and permissions

Copyright information

About this paper

Cite this paper

Ravikiran, K., Reddy, C.K., Krishna, P.G., Jinukala, M., Lakshmi, K.P. (2022). Crop Identification and Disease Detection by Using Convolutional Neural Networks. In: Luhach, A.K., Jat, D.S., Hawari, K.B.G., Gao, XZ., Lingras, P. (eds) Advanced Informatics for Computing Research. ICAICR 2021. Communications in Computer and Information Science, vol 1575. Springer, Cham. https://doi.org/10.1007/978-3-031-09469-9_6

.RIS .ENW .BIB

DOI
https://doi.org/10.1007/978-3-031-09469-9_6

Published	Publisher Name	Print ISBN
25 June 2022	Springer, Cham	978-3-031-09468-2

Online ISBN	eBook Packages
	Computer Science

978-3-031-09469-9 Computer Science (R0)

Design and Fabrication of a Solar Powered Autonomous Agricultural Robot

Bhukya Venkatesh Naik[1,a), R. Raman Goud[2,b)

[1]Design for Manufacturing, GokarajuRangaraju Institute of Engineering and Technology, Hyderabad, Telangana, India

[2]Department of Mechanical Engineering, GokarajuRangaraju Institute of Engineering and Technology, Hyderabad, Telangana, India

[a)]Corresponding author: Venkateshnaikbhukya@gmail.com

[b)]ramanrachala@gmail.com

Abstract: In the agricultural industry there's a necessity for a technology which is more easily understood and implemented by the farmers .machinerywhich require very less effort and less time with low cost are required for success in the field of agriculture. Traditional methods are still followed within the field of agriculture, which are outdated in the current world of technology. There is a huge demand for automation in various fields of agriculture. This project includesboth design and fabrication of an Autonomous Agricultural Robot which helps the farmer in different agricultural operations like pesticide spraying to inspection, control weeds, and material handling. This robot is equipped with four wheels which are independently connected to four L type geared dc motors. These motors are connected to a battery which is charged using a solar panel. This robot uses a Raspberry pi as a main controller which reacts as per the data received from the camera and ultrasonic sensors and whole system is operated using a mobile application. Thus, this robot completely automates the field monitoring by moving on the desired route map to follow which is given as a input to the controller using GPS technology.

Keywords: Automation, Crop Monitoring, Material Handling, GPS

1. INTRODUCTION

Automation basically refers to the technology by which processes or procedures are executed or performed without human assistance. Automation in the present trend has become very important in the modern manufacturing processessuch that, every company is implementing automation in its operations to sustain in the competitive market. In the field of automation, robots can be used in doing the repeated tasks. And in the agriculture, there's arequirement of a new technology which is much easyto implement by the farmers. machinery that requireminimum effort and time is much required to increase the yield to satisfy the growing demand for food. And hence the processes like crop maintenance, monitoring and material handling are to be automated.

In the present generation, most of the countries do not have sufficient number of skilled man power specifically in the field of agricultural sector which largely effects the growth and development of developing countries like India. To overcome this problem agricultural sector needs to be automated. In India directly or indirectly there are around more than 70% people dependent on different types of agricultural practices [1]. Even though the agricultural field operations are labour intensive, complex, diverse, and crop-directed, the amount of agricultural yield has been significantly growing over the past few years as a result of introducing new varieties of agricultural machinery to do the agricultural operations, and due to the introduction of automation in the field of agriculture [2,3]. Agriculture has been transformed tremendously from a labour intensive industry towards the one using lots of machinery and production system which is power intensive. Due to this transformation in agricultural industry there was a continuous labour outflow and around 40% of the work force has been decreased [4]. In the past 15 years the agricultural industry has grown digitally and new ways of farming has come into existence [5]. Lots of research has beendone on the implementation of intelligent automation systems and robots to do a huge variety of agricultural operations, and their technical usability has been vastly demonstrated [6]. The introduction of robotics into agricultural operationshelps in creating a new changeon the productivity ofthe labour. By imitating conventional skills or by expanding them, the robotshas the capability to overcome critical human constraints like the areas where a human can't reach, or the ability to work continuously without taking any rest etc. including an ability to work in difficult agricultural environments like outdoors, hazardous conditionsand have the potential to lower the impact of physically demanding jobs in agriculture. Clearly automation and robotics in agriculture helpsin mitigating the shortages which are seen in the labour markets. These technologies helps in providing high potential for increasedproductivity and shows good results [7,8].In spite of the hugenumber of robotic applications

2nd International Conference on Multidisciplinary Advanced Research and Engineering 2020
AIP Conf. Proc. 2358, 050005-1–050005-8; https://doi.org/10.1063/5.0057867
Published by AIP Publishing. 978-0-7354-4103-0/$30.00

Design, Analysis and Fabrication of a 3D Printed ABS Wheel Hub for an Autonomous Agricultural Robot

Bhukya Venkatesh Naik[1,a], R. Raman Goud[2,b]

[1]*Design for Manufacturing, Gokaraju Rangaraju Institute of Engineering and Technology, Hyderabad, Telangana, India*

[2]*Department of Mechanical Engineering, Gokaraju Rangaraju Institute of Engineering and Technology, Hyderabad, Telangana, India*

Corresponding author: [a]Venkateshnaikbhukya@gmail.com

[b]ramanreachme@gmail.com

Abstract: Wheel Assemblies in a Traditional Vehicle or a Robot Consists of a Knuckle, Hub, Bearings and Wheel usually assembled as a Single Part. The materials used to make these components are cast iron, Aluminium alloys, Ductile iron, mild steel etc. Usage of an alternative material like ABS (Acrylonitrile Butadiene Styrene) has been proposed in this work which is intended to reduce the overall weight of the wheel assembly. Due to the Lightweight of hub and wheel would reduce the Inertia, the work done to stop or move the vehicle will also be reduced. In this work 3D Printed ABS wheel hub has been proposed by conducting required analysis with suitable Trade-in-material design yielding reliable Factor of Safety with reduction in weight and hence making ABS a viable material for the wheel hubs. The characteristics of ABS (Acrylonitrile Butadiene Styrene) like good mechanical strength, mechanical damping ability with good fatigue resistance, Stiffness and ease of manufacturing gives the material an upper hand over other plastic polymers in reducing the mass without compromising on safety and strength

Keywords: ABS, Robot, 3D Printing

I. INTRODUCTION

The purpose of this project is to find out the credibility of an alternative material which helps to replace the conventionally used materials using Computer-Aided Design and Engineering Analysis. ABS is an opaque thermoplastic and it is a polymer which is comprised of three different monomers, one is acrylonitrile, second is butadiene and the third is styrene [1]. ABS is usually polymerised through the process called emulsification or by combining different components which don't combine into a single product. these three monomers are combined to form acrylonitrile whichhelps in developing a polar attraction with the other two components, resulting into a very highly durable and tough product [2].

Additive manufacturing which is also known as 3d printing is the process of creatingathree-dimensional solid object by rapidly converting a3D model generated in a computer into physical part. Additive manufacturing, which isalso referred as 3D printing, is a processing technology which has a range of potential in the manufacturing industry. The main principle of additive manufacturing is printing objects layer-by-layer using different materials like liquid, plastic,metal, polymer etc. by taking 3D computer aided designs as inputs [3] where thermoplastic filament is fed to a heated nozzle through filament extruder, melted, and parallelly deposited layer-by-layer onto a build plate or bed to create a desired three-dimensional geometry as per the design input given [4] The main difference between conventional manufacturing processes and 3D printing is that 3d printer involves additive approach and most of the conventional manufacturing processes involve subtractive approach which includes grinding, bending, forging, moulding, cutting, gluing, welding and assembling. Initially 3D printing was seen as a tool to shape and bring it to the artistictdesigns, but in the last few years this technology has been developing to a point where many crucial mechanical components with many crucial applications are been printed [5,6]. 3D printing causes very less harm to the environment and it can be environmentally sustainable than other conventional manufacturing processesas it uses less raw materials, generate less wasted by-products, and consumes less energy [7].

2nd International Conference on Manufacturing, Material Science and Engineering 2020
AIP Conf. Proc. 2358, 050004-1–050004-10; https://doi.org/10.1063/5.0053896
Published by AIP Publishing. 978-0-7354-4116-6/$30.00

ScienceDirect

Materials Today: Proceedings

Volume 49, Part 5, 2022, Pages 1885-1890

Near-dry wire-cut electrical discharge machining process using water–air-mist dielectric fluid: An experimental study

Sampath Boopathi [a], K.P. Arulkirubakaran [b], Ram Subbiah [c], G. Sivaraman [d]

[a] Department of Mechanical Engineering, Muthayammal Engineering College, Rasipuram, Namakkal 637 408, India
[b] Department of Aeronautical Engineering, Nasrul Islam Center for Higher Education, Thudaiyur, Kumarapuri, Tamil Nadu 629180, India
Department of Mechanical Engineering, Gokaraju Rangaraju Institute of Engineering and Technology, Hyderabad, Telangana 500090, India
[d] Department of Mechanical Engineering, Sona College of Technology, Salem, Tamil Nadu 636005, India

Received 26 May 2021, Revised 10 August 2021, Accepted 17 August 2021, Available online 25 August 2021, Version of Record 7 January 2022

Show less

Outline | Share | Cite

https://doi.org/10.1016/j.matpr.2021.08.077

Abstract

In this paper, Inconel 600 alloy has been cut by water mist wire-cut electrical discharge machining (WEDM) using a molybdenum wire tool. A little amount of tap water mixed with pressurized air (water-mist) was used to provide the dielectric insulation medium in the plasma zone. A new experimental arrangement has been made to conduct the near-dry WEDM using input parameters of the Current (K), Pulse-duration (PD), Pulse-pause time (PP), and flow rate (FR) of mixing tap water to predict the cutting speed (CS) and surface irregularity (SI). It was discovered that pulse-duration and current increase the CS and SI; conversely, the PT minimizes the CS and SI. The highest CS and SI are achieved by the highest flow rate of the tap water due to the quick flushing of debris. The percentage of contributions of K, PD, PP, and FR on CS is 20.04%, 22.22%, 42.86%, and 6.97% respectively and the percentage of contributions of K, PD, PP, and FR on SI is 17.06%, 39.1%, 26.50 %, and 27.34% respectively.

Previous Next

Keywords

Tap water-mist; Near Dry Wire EDM-Inconel 600 alloy; Taguchi analysis; Uncertainty analysis; Percentage of contribution

Sponsored articles Recommended articles

Cited by (7)

An experimental study on the hardness and wear rate of carbonitride coated stainless steel

2022, Materials Today: Proceedings

Show abstract

c 4

ScienceDirect

Materials Today: Proceedings

Volume 50, Part 5, 2022, Pages 1134-1137

Experimental investigation of lost foam casting process on aluminium

S. Ramesh [a], S. Mohan [b], N. S. S. Vakamulla [c], M. Boopathi [d], S. A. Sundar [e], M. Ponnuraj [f], S. Maruthi [g], Ravi Sekhar [h]

[a] Department of Chemical Engineering, Addis Ababa Science and Technology University, Ethiopia
[b] Department of Electrical and Electronics Engineering, Sri Sairam Engineering College, Chennai, Tamilnadu, India
[c] Department of Mechatronics Engineering, TISHK International University, Erbil, Iraq
[d] Department of Mechanical Engineering, Gokaraju Rangaraju Institute of Engineering and Technology, Hyderabad, India
[e] Department of Mechanical Engineering, Vinayaka Missions Kirupananda Variyar Engineering College, Salem, Tamilnadu, India
[f] Department of Mechanical Engineering, Bharath Institute of Higher Education and Research, Chennai, Tamilnadu, India
[g] Department of Mechanical Engineering, Sri Indu College of Engineering and Technology, Hyderabad, India

Received 6 July 2021, Revised 30 July 2021, Accepted 4 August 2021, Available online 17 August 2021, Version of Record 7 February 2022.

Show less

Outline | Share | Cite

https://doi.org/10.1016/j.matpr.2021.08.050

Highlights

- To achieve dimensional accuracy and surface finish on casting process is difficult task.
- Aluminium 6082 and silicon is fabricated through lost foam casting method.
- The different input constraints such as pouring temperature, slurry viscosity and cooling time were considered.
- The tensile strength was evaluated for the fabricated specimens
- Taguchi technique is applied to determine the optimal factor.

Abstract

The current scenario is to achieve dimensional accuracy and surface finish of the casting components which is identified to be a difficult task. It can be achieved through lost foam casting process. This casting process eliminate the difficulties in design considerations of casting products. Lost foam casting process has provided the quality of components through flexible manner. It's being used to create complex metal pieces with less production time. In this experimental investigation, aluminium 6082 and silicon is fabricated through lost foam casting method. During casting process, the different input constraints like pouring temperature, slurry viscosity and cooling time were considered. The tensile strength is evaluated for the fabricated specimens. Taguchi technique

ScienceDirect

Materials Today: Proceedings

Volume 50, Part 5, 2022, Pages 1341-1345

An overview on role of unconventional machining processes on different materials

Pradeep Jayappa [a], Santhosh Srinivasan [b], K. Vetrivel Murugan [c], C. Thangavel [d], M. Bala Theja [e], G. Phanindra Raju Varma [f], S. Manchary [g], Ram Subbiah [f]

- [a] Chemical Engineering, Bule Hora University, Ethiopia
- [b] Mechanical Engineering, Sri Krishna College of Technology, Coimbatore, Tamilnadu, India
- [c] Mechanical Engineering, Sri Sairam Engineering College, Chennai, Tamilnadu, India
- [d] Mechanical Engineering, Vinayaka Missions Kirupananda Variyar Engineering College, Salem, Tamilnadu, India
- [e] Mechanical Engineering, SVR Engineering College, Nandyal, Andhrapradesh, India
- [f] Mechanical Engineering, Gokaraju Rangaraju Institute of Engineering and Technology, Hyderabad, India
- [g] Mechanical Engineering, Sri Indu College of Engineering and Technology, Hyderabad, India

Received 7 July 2021, Revised 20 August 2021, Accepted 25 August 2021, Available online 6 September 2021, Version of Record [illegible] February 2022.

Show less ^

Outline | Share | Cite

https://doi.org/10.1016/j.matpr.2021.08.254

Highlights

- This article describes the unconventional machining processes on different materials.
- Hard materials are used for machining to get high dimensional accuracy.
- Machining of complex shapes, micro machining are possible using this process.
- The efficiency of production and machining precision are enhanced.
- The different metal removal mechanisms were discussed.
- The medium of energy are transferred through electrolyte, electron and high voltage particles.

Abstract

In present days, the development and applications of unconventional machining processes got rapidly increased in modern industries. The quality and performance of the product are improved through unconventional machining process. Hard materials are preferred to obtain high dimensional accuracy. The machining of complex shapes, super finishing, micro machining and surface is possible by unconventional machining process. The efficiency of production and machining precision were enhanced. The different types of machining methods were utilized to remove the materials. The different metal removal parameter such as erosion, Ionic dissolution, vaporization were analysed etc. The medium of energy were been transferred through electrolyte, electron and high voltage particles. This review article clearly describes the unconventional machining and hybrid machining processes on different materials.

< Previous | Next >

c. 6

ScienceDirect

Materials Today: Proceedings

Volume 50, Part 5, 2022, Pages 1502-1507

Investigating the effect of thermal cycling on thermal characteristics of the nano-silica based phase changing material (PCM)

R.T. Sathishkumar [a], M. S.R. Arunachalam [b], B. Bhuvan Manivannan [c], P. Manoj Kumar [d], Ram Subbiah [e], Vimal Kumar Eswarlal [f]

[a] Department of Automobile Engineering, Hindusthan Institute of Technology, Coimbatore 641032, Tamil Nadu, India
[b] Department of Mechatronics Engineering, Nehru Institute of Engineering and Technology, Coimbatore 641105, Tamil Nadu, India
[c] Department of Mechanical Engineering, Sri Ramakrishna Engineering College, Coimbatore 641022, Tamil Nadu, India
[d] Department of Mechanical Engineering, KPR Institute of Engineering and Technology, Coimbatore 641407, Tamil Nadu, India
[e] Department of Mechanical Engineering, Gokaraju Rangaraju Institute of Engineering and Technology, Hyderabad 500090, Telangana, India
[f] Mangla Smart Energy Solutions (P) Ltd., Erode 641604, Tamilnadu, India

Received 16 August 2021, Revised 1 September 2021, Accepted 7 September 2021, Available online 21 September 2021, Version of Record 7 February 2022.

Show less ^

Outline | Share Cite

https://doi.org/10.1016/j.matpr.2021.09.095

Abstract

Reliable thermal storage has become a critical factor for renewable energy-based thermal systems such as solar thermal collectors, because the incoming energy is inconsistent with time and, hence, an efficient energy management mechanism is required. Therefore, the collection of maximum possible energy during their availability and their uniform distribution during the lagging period has been the topic of research in recent times. The nano-enhanced phase changing materials (nano-PCMs) are recognized to be the eminent energy storage materials in terms of their thermal storage characteristics. However, their reliability over the period of thermal cycles is yet again in an interrogation. In this work, the nano-silica based paraffin was prepared through the dispersion of nano-silica in paraffin at three different lower volume fractions (0.5 vol%, 1.0 vol% and 2.0 vol%). Then, the thermal consistency and thermal properties of nano-silica/PCM such as latent heat, melting and solidifying temperatures were investigated using different instruments, namely thermogravimetric analyzer (TGA) and differential scanning calorimetry (DSC) after initial preparation and after 100 thermal cycles. The findings evidence that the nano-silica/PCMs are having good thermal consistency even after 100 thermal cycles up to a volume fraction of 1.0%. The deterioration of the properties has become prominent after 1.0% volume of nano-silica in paraffin.

< Previous Next >

Keywords

PCM; Nano-PCM; Nano-silica; Thermal cycling of PCM; Thermal properties of PCM

Special issue articles Recommended articles

ScienceDirect

Materials Today: Proceedings

Volume 50, Part 5, 2022, Pages 1015-1018

Effect of fly ash on metal matrix composites – An overview

[illegible] [a], N. [illegible] [b], R. Anton Savio Lewise [c], R. Anandan [d], S. Sathish [e], M. Dhanu Shatrughna [f], S. Manickam [g], Ram Subbiah [h]

- [a] Department of Chemical Engineering, Addis Ababa Science and Technology University, Ethiopia
- [b] Department of Mechanical Engineering, Sri Sairam Engineering College, Chennai, Tamilnadu, India
- [c] Department of Aeronautical Engineering, Noorul Islam Center for Higher Education, Tamilnadu, India
- [d] Department of Mechanical Engineering, Vinayaka Mission's Kirupananda Variyar Engineering College, Salem, Tamilnadu, India
- [e] Department of Mechanical Engineering, Sri Ramakrishna Engineering College, Coimbatore, Tamilnadu, India
- [f] Department of Mechanical Engineering, Guru Nanak Institutions Technical Campus, Hyderabad, India
- [g] Department of Mechanical Engineering, Sri Indu College of Engineering and Technology, Hyderabad, India
- [h] Department of Mechanical Engineering, Gokaraju Rangaraju Institute of Engineering and Technology, Hyderabad, India

Received 17 July 2021, Revised 20 August 2021, Accepted 24 August 2021, Available online 5 September 2021, Version of Record 7 February 2022

Show less

Outline | Share | Cite

https://doi.org/10.1016/j.matpr.2021.08.136

Highlights

- The substance property mainly depends on the nature of reinforcements.
- Fly ashes are added to the alloys to increase the properties.
- Fly ash improves the density of the materials.
- The tensile and impact strength are enhanced by adding fly ash particles.
- The mechanical properties of the alloys and its morphology were studied.

Abstract

The substance property mainly depends on the nature of reinforcements. Fly ash is one of the best reinforcement material added to the alloys in order to increase the properties. It is used to reduce the cost and improve the density of the material. The tensile and impact strength were enhanced through the addition of fly ash particles. The performance of castings and production of composites were developed by adding fly ash particles. The mechanical properties of the alloys and its morphology were improved through various volume fraction of fly ash. The properties, characterization of the fly ash and its effect on performance of the material were discussed.

Previous Next

Keywords

Fly ash; Reinforcement; Composite; Properties; Material

C 8

Materials Today: Proceedings

Volume 50, Part 5, 2022, Pages 2508-2519

An overview on characteristics and performance of ultrasonic welding process on different materials

N. Mary Jacintha [a], A. Arun Sasi Kumar [b], D. Rajasekaran [c], M. Murugan [d], B.S.V.S. Gowri [e], T.S. Amrutha Reddy [a], S. Hari Krishna [a], Bani Kalidindi [c] [f]

[a] Department of Mechanical Engineering, Timeria Engineering College, Narasaraopet, Andhrapradesh, India
[b] Department of Aeronautical Engineering, Nehru Institute of Engineering and Technology, Coimbatore, Tamilnadu, India
[c] Centre for Materials Engineering and Regenerative Medicine, Bharath Institute of Higher Education and Research, Chennai, Tamilnadu, India
[d] Department of Mechanical Engineering, Sri Sairam Engineering College, Chennai, Tamilnadu, India
[e] Department of Mechanical Engineering, Gokaraju Rangaraju Institute of Engineering and Technology, Hyderabad, India

Received 24 August 2021, Revised 2 September 2021, Accepted 7 September 2021, Available online 20 October 2021, Version of Record 7 February 2022.

Show less

Outline | Share | Cite

https://doi.org/10.1016/j.matpr.2021.09.095

Highlights

- An ultrasonic welding process plays an extraordinary role in all industrial applications.
- Metals and non metals were processed under USW with different melting points.
- Thin wires of foils are easily welded through this process.
- High quality of welded joints can be achieved through USW.

Abstract

In recent days, Ultrasonic welding processes are playing an extraordinary role in all industrial applications. Metals and non metals were processed under USW with different melting points. Thin wires of foils are easily welded through this process. High quality of welded joints can be achieved through USW without protective gas shield. The different process factors such as amplitude of vibrations, welding mode, down speed, pressure of trigger, weld time and clasp time were considered to determine the strength and quality of the joints. The varieties of joint designs were possible with definite features. The different ranges of frequencies have been applied in between the interface of the work piece. The plastic deformation of the metal occurred due to incorporation of vibrational energy and localized melting of the metal along the joint to be welded. The welded joints were quickly completed without any drying process which is suitable to soft and hard materials. The joint quality depends on the ultrasonic vibrations. The work pieces to be joined were detained together under pressure and applied to ultrasonic vibrations (range between 20 and 40 kHz). This review paper deals about the ultrasonic welding characteristics, interface of welding joints, performance and welding factors for different materials.

c 9

Materials Today: Proceedings

Volume 50, Part 5, 2022, Pages 2430-2439

Friction stir processing of boron carbide reinforced aluminium surface (Al-B4C) composite: Mechanical characteristics analysis

Somnath Bhopatrao [illegible]

a Department of Mechanical Engineering, Muthayammal College of Engineering, Rasipuram, Tamil Nadu 637408, India
b Department of Mechanical Engineering & Director Research and Development, Sreedevi College of Engineering and Technology, Peerancheru, Hyderabad 500066, India
c Department of Mechanical Engineering, Erode Sengunthar Engineering College, Perundurai, Erode 638057, India
d Department of Mechanical Engineering, Gokaraju Rangaraju Institute of Engineering and Technology, Hyderabad, Telangana 500090, India
e Department of Mechanical Engineering, Arulmurugan College of Engineering, Karur 639206, India

Received 3 September 2021, Revised 4 October 2021, Accepted 8 October 2021, Available online 10 November 2021, Version of Record 7 February 2022.

Show less

Outline | Share | Cite

https://doi.org/10.1016/j.matpr.2021.10.251

Abstract

In this article, the boron carbide reinforced Aluminium alloy surface composite material was fabricated through the friction-stir processing method. The Al6061 alloy and B4C particles were used as matrix and reinforced materials respectively. The influences of volume percentage of boron-carbide, traveling feed rate, and rotational speed on tensile strength and wear were investigated using the L9 Taguchi technique. The moderate rotating speed and traveling speed of the tool have been preferred to attain optimum responses. The highest tensile strength of 347 MPa and minimum wear of 35 μm were obtained from 12% of the volume of boron carbide particles, 1400 rpm of rotating speed, and 40 mm/min traveling speed of the tool. The optimum Al6061-B4C surface composites micro-structure has also been studied through scanning electron microscope images.

Previous Next

Keywords

Friction stir processing, Surface composite, Aluminium alloy, Percentage of B4C particles, Rotating speed, Traveling speed, Tensile strength, Wear

Spring issue articles Recommended articles

Cited by (7)

Materials Today: Proceedings

Volume [illegible], Part [illegible], 2022, Pages [illegible]

Analyzing an evacuated tube solar water heating system using twin-nano/paraffin as phase change material

Motilal [illegible] [a], S.D. [illegible] [b], P. Manoj Kumar [c], A.R. [illegible] [d], Rajasekaran [illegible] [e], Manoj Kumar Singh [f], R. [illegible] [g], S.G. Infant Tony [illegible], Vimal Kumar [illegible] [h]

- [a] Department of Mechanical Engineering, Government Engineering College, Jhalawar, Rajasthan 326023, India
- [b] Department of Civil Engineering, Sri Ramakrishna Engineering College, Coimbatore 641022, Tamil Nadu, India
- [c] Department of Mechanical Engineering, KPR Institute of Engineering and Technology, Coimbatore 641407, Tamil Nadu, India
- [d] Department of Mechanical Engineering, Gokaraju Rangaraju Institute of Engineering and Technology, Hyderabad 500090, Telangana, India
- [e] Department of Mechanical Engineering, College of Engineering, Jazan University, Saudi Arabia
- [f] Department of Mechanical Engineering, MJP Rohilkhand University, Bareilly 243006, U.P., India
- [g] Department of Automobile Engineering, Hindusthan Institute of Technology, Coimbatore 641032, Tamil Nadu, India
- [h] Mangala Smart Energy Solutions (P) Ltd., [illegible] 64[illegible], Tamilnadu, India

Received 30 August 2021, Revised 25 October 2021, Accepted 28 October 2021, Available online 22 November 2021, Version of Record 7 February 2022.

Show less ^

Outline | Share Cite

https://doi.org/10.1016/j.matpr.2021.10.[illegible]

Abstract

In this work, an effort has taken to improve the thermal storage capacity of the evacuated tube solar water heating (SWH) system by means of a new kind of twin-nano/paraffin as a thermal storage medium. Beforehand, the twin-nano/paraffin has been prepared by amalgamating 1% mass of twin-nanoparticles (comprising an equal quantity of SiO_2 and CuO nanoparticles) within the paraffin. The experiments were performed in three cases, viz., without paraffin, with paraffin, and with twin-nano/paraffin under the real-time solar conditions on the clear sunny days. The thermal storage characteristics had been measured in terms of the hotness of available hot water in the storage tank during the second day morning. The experiment for the each case was performed for twenty four hours continuously from the first day morning to next morning. During the experiment, the water was drawn-off after twelve hours, i.e., at 8 p.m. in the evening, so as to replicate the real-time hot water demand in households. The experiments proved that the integration of paraffin and further, twin-nano/paraffin enhanced the thermal storage capacity of the evacuated tube SWH, by improving the temperature of available hot water during the next morning. The results substantiated that the water temperature was augmented by 6.8 °C and 11.7 °C, respectively with paraffin and twin-nano/paraffin. The enhancement was noticed to be significantly higher for the case with twin-nano/paraffin.

< Previous Next >

Keywords

Thermal energy storage; Solar water heater PCM; Nano PCM; Hybrid nanoparticles

ASME International Mechanical Engineering Congress and Exposition

PROCEEDINGS PAPER

A Numerical Study on Springback of a Channel Through the Oscillation of Punch

Chetan P. Nikhare, Tanya Burdi, Nitin Kotkunde, Swadesh Kumar Singh

Paper No: IMECE2021-70171, V02AT02A050; 10 pages

https://doi.org/10.1115/IMECE2021-70171

Published Online: January 25, 2022

Abstract

To meet the demand of light weighting, environmental regulation, increase fuel economy, many innovations are underway. Options are light weighting the part to reduce the fuel consumption or decrease the gage in high strength dense material. In both cases during or after deforming the part these challenges occur like higher tonnage machine for deformation, sudden fracture, geometric defect, etc. One of the geometric defects which is very common in sheet metal forming is springback. Springback is the deviation of the part from the desired shape after the part is shaped and then load is released. It is the material tendency to relaxed back based on the accumulated strain and its elasticity. In lighter material or higher strength steels, the springback phenomena is very common due to lower elasticity or higher strength value. In this paper springback is analyzed by conceptualizing an innovative process. The innovative process is oscillation of the punch after the forming process is done. The 2D channel strip of the aluminum 2024 high strength alloy was used in the bending process. The process of bending with punch die and the blank was

Proceedings of the ASME 2021
International Mechanical Engineering Congress and Exposition
IMECE2021
November 1-4, 2021, Virtual, Online

IMECE2021-68756

OPTIMIZATION OF CNC MILLING OF GENERAL-PURPOSE POLY (METHYL METHACRYLATE)

J M Wambua[1] F M Mwema[1,2*] E T Akinlabi[3] Buddi Tanya[4]

[1] Department of Mechanical Engineering, Dedan Kimathi University of Technology, Private Bag, 10143, Nyeri, Kenya.
[2] Department of Mechanical Engineering Science, University of Johannesburg, South Africa
[3] Pan African University for Life and Earth Sciences Institute, Ibadan, Nigeria
[4] Mechanical Engineering Department, Gokaraju Rangaraju Institute of Engineering & Technology, Hyderabad, India

*Corresponding author fredrick.mwema@dkut.ac.ke

ABSTRACT

The purpose of this study was to investigate the impact of CNC milling parameters on the material removal rate (MRR) and surface roughness (Ra) of the general-purpose PMMA. The milling parameters considered were cutting speed, axial depth of cut and feed rate, each having four levels obtained through experimental trial and error. The levels were 300 rpm, 700 rpm, 1300 rpm, and 2000 rpm for the cutting speed, 0.3 mm, 0.8 mm, 1.5 mm, and 2 mm for the axial depth of cut; and 50 mm/min, 100 mm/min, 200 mm/min, and 350 mm/min for the feed rate. The Taguchi technique was used to design the experiments and carry out the analysis and optimization with an L16 orthogonal array. From the analysis, the optimal milling parameters for the maximum MRR were a cutting speed of 300 rpm, an axial depth of cut of 2 mm, and a 350 mm/min feed rate. The optimal CNC milling parameters for the least Ra were obtained at a cutting speed of 2000 rpm, an axial depth of cut of 0.3 mm, and a 50 mm/min feed rate. An ANOVA conducted depicted that all three factors were significant towards the MRR with the feed rate having the highest percentage contribution (46.8%), followed by the depth of cut (38.3%) and lastly, the cutting speed (9.8%). An ANOVA for Ra depicted that cutting speed and feed rate were the most significant factors. The axial depth of cut was insignificant towards the mean surface roughness. In terms of percentage contributions in the mean surface roughness, the cutting speed had the highest contribution (59.9%), followed by the feed rate (19.4%), and lastly, the axial depth of cut (13.9%).

Keywords: PMMA, Milling, ANOVA, Taguchi, Surface roughness, Material removal rate

1. INTRODUCTION

Poly (methyl methacrylate), otherwise known as PMMA, has been categorized as a hard-to-cut material owing to its mechanical and chemical properties, including the high brittle fracture at a temperature of above 80°C and also a low elongation-at-break of 5% [1]. These properties have limited the manufacturing of products from this material using conventional machining methods [2]. However, the material has attracted its applications in various fields due to its attractive properties such as moderately high flexural strength (110 MPa), high tensile strength (48 - 76 MPa), low density (1.19 gcm^{-3}), high glass transition temperature (105°C - 107°C), and high light transmission (92 – 93%) [3], just to mention a few.

The material has been widely applied in the medical field due to its chemical stability and biocompatibility [4]. However, the machining of the material using non-conventional methods is quite expensive. It is also associated with several defects on the finished products, such as the formation of bubbles in laser machining, which create a poor surface finish and affect the mechanical properties of the material [5-7].

Numerical Control (NC) milling has been identified as a potential method for machining polymeric materials with high efficiencies and surface quality. Studies conducted have revealed that the rate of production and surface quality during the machining of polymeric and other materials are affected by various machining factors, which include the spindle speed, the depth of cut, the rate of feed, the coolants employed, the cooling methods, machining temperatures, and among other factors [8-10].

Materials Today: Proceedings

Vol. 68, Part 3, 2022, Pages 1303-1309

Experimental investigations on properties of MoS_2 and TiB_2 reinforced aluminium composites

S. Rajkumar [a], T. Mahendra [b], K. Mageshkumar [c], M. Ravichandran [d], V. Mohanavel [e], P. Sathiyamurthy [f], Sunil S. Gouda [g]

[a] Department of Mechanical Engineering, Faculty of Manufacturing, Institute of Technology, Hawassa University, Shillapa

[b] Department of Mechanical Engineering, Saveetha School of Engineering, SIMATS, Chennai 602105, Tamil Nadu, India

[c] School of Mechanical Engineering, Vellore Institute of Technology, Vellore 632014, Tamil Nadu, India

[d] Department of Mechanical Engineering, K. Ramakrishnan College of Engineering, Samayapuram, Trichy 621112, India

[e] Centre for Materials Engineering and Regenerative Medicine, Bharath Institute of Higher Education and Research, Chennai, 600073, Tamil Nadu, India

[f] Department of Mechanical Engineering, Gokaraju Rangaraju Institute of Engineering and Technology, Hyderabad, Telangana 500090, India

Available online 28 December 2022. Version of Record 19 May 2022.

Show less ^

Outline | Share Cite

https://doi.org/10.1016/j.matpr.2022.11.521

Abstract

In this work, Aluminium Alloy (AA 6081) matrix composites reinforced with Molybdenum disulfide (MoS_2) and Titanium Diboride (TiB_2) have been developed through stir casting (SC) method. Influence of TiB_2 on the properties of the aluminium composite was studied. The incorporation of TiB_2 in the AA6081-2MoS_2 matrix improved hardness of the composite. The improved tensile strength (TS) and compressive strength (CS) was obtained for the AA6081-2MoS_2-12 wt% TiB_2 composite. The high impact strength (IS) is obtained for the AA6081-2MoS_2-8 wt% TiB_2 composite. The decreased elongation was observed for the increasing content of TiB_2. The high bending strength (BS) was obtained for the AA6081-2MoS_2-8 wt% TiB_2 composite.

Previous Next

Keywords

Composite; Stir casting; Molybdenum disulfide; Titanium diboride

Special issue articles Recommended articles

Cited by (4)

ScienceDirect

C. 14

Materials Today: Proceedings

Volume 64, Part 3, 2022, Pages 1319-1323

Performance study on phase change material integrated solar still coupled with solar collector

T. Vasudevan [a,*], C. Rajkumar [b], M. Arunkumar [c], V. Alphonsa [d], K. Arul [e], D. Mylsamy [f], Ravi Subbiah [g]

[a] Department of Mechanical Engineering, Saveetha School of Engineering, SIMATS, Chennai, India
[b] Department of Mechanical Engineering, Faculty of Manufacturing, Institute of Technology, Dilla University, Dilla, Ethiopia
[c] Department of Agricultural Engineering, Sri Shakthi Institute of Engineering and Technology, Coimbatore 641062, Tamil Nadu, India
[d] Centre for Materials Engineering and Regenerative Medicine, Bharath Institute of Higher Education and Research, Chennai, 600073, India
[e] Department of Mechanical Engineering, Agni College of Technology, Thalambur, Chennai, India
[f] Department of Mechanical Engineering, Academy of Maritime Education and Training (AMET) Deemed to be University, Tamil Nadu, India
[g] Department of Mechanical Engineering, Gokaraju Rangaraju Institute of Engineering and Technology, Hyderabad, Telangana 500090, India

Available online 9 December 2021. Version of Record 19 May 2022.

Show less

Outline | Share | Cite

https://doi.org/10.1016/j.matpr.2021.11.549

Get rights and content

Abstract

Drinking water is a global concern. Solar desalination minimizes the energy consumption. The present study combines solar stills with flat plate collector (FPC) with paraffin wax. The experiment is carried out for the different water depths at 10, 20 and 30 mm in the double slope basin. FPC imitates as preheater and phase change material (PCM) based heat storage provides heat energy during lean solar rays. Productivity of water at a smaller depth is observed higher. Still productivity increases to 23%, and the peak yield increases by 19%, with FPC and heat storage.

Previous

Next

Keywords

Solar energy; Solar stills; Heat storage.; Heat transfer fluid; Desalination

Special issue articles

Recommended articles

Cited by (4)

C 15

ScienceDirect

Materials Today: Proceedings

Volume 59, Part 2, 2022, Pages 1345-1349

Evaluation of mechanical properties on kenaf fiber reinforced granite nano filler particulates hybrid polymer composite

T. Raja [a], M. Mohamed [a], S. Suresh Kumar [a,b], S. Rajkumar [c], M. Ravichandran [d], Tamir Sabbir [e]

[a] Department of Mechanical Engineering, Vel Tech Rangarajan Dr. Sagunthala R&D Institute of Science and Technology, Chennai 600062, Tamil Nadu, India
[b] Centre for Materials Engineering and Regenerative Medicine, Bharath Institute of Higher Education and Research, Chennai 600073, Tamil Nadu, India
[c] Department of Mechanical Engineering, Panimalar Polytechnic College, Chennai 600025, Tamil Nadu, India
[d] Department of Mechanical Engineering, Faculty of Manufacturing, Institute of Technology, Hawassa University, Ethiopia
[e] Department of Mechanical Engineering, K. Ramakrishnan College of Engineering, Trichy 621 112, Tamil Nadu, India
[f] Department of Mechanical Engineering, Gokaraju Rangaraju Institute of Engineering and Technology, Hyderabad, Telangana 500090, India

Available online 18 December 2021, Version of Record 19 May 2022.

Show less

Outline | Share | Cite

https://doi.org/10.1016/j.matpr.2021.11.546

Abstract

Natural fibers are prime focus as a potential alternate material instead of synthetic fiber to making the composite material for automobile applications. In this work, kenaf fiber was selected as reinforcement material, granite powder act as a filler material and the epoxy polymer used as matrix material to fabricate the composite laminates by hand layup method with varying the fiber and filler weight ratio of three different samples. To analyses the mechanical properties of tensile, flexural strength, impact energy and hardness of hybrid composite. The results are revealed when the addition of kenaf fiber can improve the tensile and flexural strength are 50.16 MP and 39.54 MPa respectively. In the sudden force experiment was given maximum impact energy of 15 J for sample C, also the hardness number was varied in maximum of sample B is 54. The surface morphology of hybrid composite was conducted through microscopic analysis for all the fabricated samples before conducting the mechanical test.

Previous

Next

Keywords

Kenaf fiber; Granite powder; Microscopic analysis; Epoxy polymer; Mechanical strength; Hybrid composite

ScienceDirect

c 16

Materials Today: Proceedings

Vol. 66, Part 4, 2022, Pages 1765-1769

Performance of solar still powered water recovery system from moist air

A. Rajaseka Perumal [a], M. Jagannath [b], S. Sunil Babu [c], A.M. Shanmuga Sundaram [d], T. Vijay Muni [e], V. Venkatesh [f], Rani Subbiah [g, *]

[a] Department of Mechanical Engineering, Sri Sairam Engineering College, Chennai 600044, Tamilnadu, India
[b] Department of Mechanical Engineering, Bharath Institute of Higher Education and Research, Chennai 600073, Tamilnadu, India
[c] Department of Mechanical Engineering, Rajalakshmi Engineering College, Chennai 602105, Tamilnadu, India
[d] Department of Mechanical and Automation Engineering, MSN College of Engineering and Technology, Tirunelveli 627152, Tamilnadu, India
[e] Department of Electrical and Electronics Engineering, Koneru Lakshmaiah Education Foundation, Guntur 522502, Andhra Pradesh, India
[f] Department of Electrical and Electronics Engineering, Rajalakshmi Engineering College, Chennai 602105, Tamilnadu, India
[g] Department of Mechanical Engineering, Gokaraju Rangaraju Institute of Engineering and Technology, Hyderabad 500090, Telangana, India

Available online 31 December 2021, Version of Record 17 June 2022.

Show less ^

Outline | Share | Cite

https://doi.org/10.1016/j.matpr.2021.12.436

Abstract

In recent years, drinking water shortage has become an urgent concern. By contrast, our surrounding air contains a significant quantity of moisture content. Appropriate harvesting methods can alleviate the issue of water shortage up to a specific level. The purpose of this research is to examine a method for recovering drinkable water from the ambient air using a solar recovery system based on desiccant. The desiccants are capable material to adsorb the moisture from the surrounding medium and it can be recovered using a suitable method. In the present research, silica gel based adsorbent was employed as a desiccant, a substance that absorbed moisture from the ambient air throughout the nocturnal period. During the daylight, the taken moisture from the loaded desiccant was recovered utilizing a solar still type recovery device. Three comparable solar days were observed in March 2021 at Hyderabad, India, and the averaged findings are elaborated. Economically, the system was noticed to generate 0.94 L of drinkable water each day during the experimentation.

< Previous Next >

Keywords

Water production; Solar still; Desiccant; Silica gel; Water from atmosphere

Special issue articles Recommended articles

ScienceDirect

Materials Today: Proceedings

Volume 69, Part 2, 2022, Pages 1425-1428

Influence of heat storage materials in a concentrated solar absorber for space heating

T. Marcelo [a,b], D. Mahesh [c], S. Rajkumar [d], Anil Kumar Sahoo [e], M. Karthikeyan [f]

[a] Department of Mechanical Engineering, Saveetha School of Engineering, SIMATS, Chennai 602105, Tamil Nadu, India
[b] Department of Mechanical Engineering, Academy of Maritime Education and Training (AMET) Deemed to be University, Tamil Nadu, India
[c] Department of Mechanical Engineering, Faculty of Manufacturing, Institute of Technology, Hawassa University, Ethiopia
[d] Department of Mechanical Engineering, Agni college of Technology, Thalambur, Chennai 600130, India
[e] Department of Mechanical Engineering, Gokaraju Rangaraju Institute of Engineering and Technology, Hyderabad, Telangana 500090, India
[f] Department of Mechanical Engineering, K. Ramakrishnan College of Engineering, Trichy 621 112, Tamil Nadu, India

Available online 29 December 2021, Version of Record 19 May 2022.

Abstract

Industrial process-heating is usually counting on fossil fuels. It's preferred for using solar power due to its free availability and eco friendliness compared to fossil fuels. This experimental study of solar absorber crammed with metal chips is tested outdoor with a dish collector. The metal chips are aluminum, copper, and steel scraps, and therefore the selected mass is one kg. During the outdoor trials, the absorber with integrated materials undergoes sensible heating to store concentrated solar power. Using sensible and heat of transformation materials within the absorber improves heat storage capacity. While passing atmospheric air through solar absorber with a velocity of two 0.45 m/s and therefore the hot air is useful for process-heating. Absorber with aluminum fillings was observed effective in heat storage and warmth output of air. The general heat retention inside the absorber was maximum when integrating aluminum chips inside.

Previous Next

Keywords

Heat storage; Sensible heating; Process-heating; Solar collectors; Latent heat

Special issue articles Recommended articles

Cited by (0)

ScienceDirect

C. 18

Materials Today: Proceedings

Volume 59, Part 2, 2022, Pages 1434-1437

Comparison of Boron Nitride (BN) reinforced sintered and extruded AA2219 nano-hybrid composite particle size effects on mechanical and metallurgical characteristics

P. Arunagiri [a], S. Rajkumar [b], [illegible] [c], K. Mageshkumar [d], [illegible], Ram Subbiah [e], P. [illegible] [f]

- [a] Department of Mechanical Engineering, Rajalakshmi Engineering College, Chennai 602105, Tamil Nadu, India
- [b] Department of Mechanical Engineering, Faculty of Manufacturing, Institute of Technology, Hawassa University, Ethiopia
- [c] Department of Mechanical Engineering, Saveetha School of Engineering, SIMATS, Chennai 602105, Tamil Nadu, India
- [d] School of Mechanical Engineering, Vellore Institute of Technology, Vellore 632014, Tamil Nadu, India
- [e] Department of Mechanical Engineering, Gokaraju Rangaraju Institute of Engineering and Technology, Hyderabad, Telangana 500090, India
- [f] Department of Mechanical Engineering, Chennai Institute of Technology, Chennai 600 069, Tamil Nadu, India

Available online 31 December 2021, Version of Record 19 May 2022.

Show less

Outline | Share Cite

https://doi.org/10.1016/j.matpr.2021.12.190

Abstract

Aluminum metal matrix composites (AMMCs) exhibit extravagant characteristics that have sparked interest in developing new nanocomposite materials among the scientific world. In this paper analysis the effects of BN particle wt% micro and nano sized particles on the properties of the AA2219 hybrid nanocomposite produced via sintering and hot extrusion procedures. In comparison to sintered composite S3, the extruded composite S3 (340 MPa) has 1.234 times the compressive strength.

< Previous Next >

Keywords

AA2219; Compression strength; Sintering; Extrusion; Boron nitride

Special issue articles Recommended articles

Cited by (0)

C 19

ScienceDirect

Materials Today: Proceedings

Volume 62, Part 4, 2022, Pages 1722-1728

Lead time reduction and process enhancement for a low volume product

M. Balaji [a], S.N. Dinesh [b], ... S. Rajan, Ram Subbiah [d], ... Manoj Kumar [d]

- [a] Associate Professor, Department of Mechanical Engineering, Kumaraguru College of Technology, Coimbatore 641049, Tamil Nadu, India
- [b] Department of Mechanical Engineering, SNS Institute of Engineering and Technology, Coimbatore 641407, Tamil Nadu, India
- [c] Department of Mechanical Engineering, PSNA College of Engineering and Technology, Dindigul 624622, Tamil Nadu, India
- [d] Department of Mechanical Engineering, Gokaraju Rangaraju Institute of Engineering and Technology, Hyderabad 500090, Telangana, India

Available online 29 December 2021, Version of Record 17 June 2022.

Show less ^

Outline | Share Cite

https://doi.org/10.1016/j.matpr.2021.12.240

Abstract

Lead time management plays an important role in a company's success as reduction in lead time augments productivity and profitability. An efficient lead time reduction tool can reduce manufacturing costs, improves customer satisfaction in the longer run. However, ambiguity always lies in selecting a proper tool for lead time reduction based on the product volume and product mix. Amongst the major tools available for lead time reduction, process mapping, SMED, 5S, Kaizen, Value engineering, Seven-waste reduction are quite versatile and compatible. Nevertheless, for evaluating a product lead time and cycle time Value Stream Mapping proves to be an appropriate tool. VSM faces inabilities in measuring the product with low volume. In such cases, the paraphernalia such as MSOP, process mapping, spaghetti diagram and layout optimization is used to measure the lead time of the product and also account the value added and non value added process in the system, and thereby improve the quality of the product. This paper focuses on an Un-named company which produces low volume parts of caterpillar heavy truck assembly. The goal was to reduce lead time, enhance productivity and reduce the defects in the process by implementing lean tools. In turn, this improves the sales and market shares of the company, leading to better profitability and improve customer satisfaction.

< Previous Next >

Keywords

Lean tools; Low volume manufacturing; MSOP; Process mapping; Layout optimization; Spaghetti diagram

Special issue articles Recommended articles

Cited by (13)

ScienceDirect

C 2-0

Materials Today: Proceedings

Volume 56, Part 3, 2022, Pages 1411-1417

Taguchi optimization of metal inert gas (MIG) welding parameters to withstand high impact load for dissimilar weld joints

S.P. Arun kumar [a], C. Prabha [b], Rajasekaran Saminathan [c], Jamil A. Abdou [d], M. Vivekanandh [e], C. Ravi Anil Kumar [f], Ravi Subbiah P.S.R. [g], P. Manoj Kumar [h]

[a] Department of Mechatronics Engineering, Nehru Institute of Engineering and Technology, Coimbatore 641105, Tamil Nadu, India
[b] Department of Mechanical Engineering, Arjun College of Technology, Coimbatore 642120, Tamil Nadu, India
[c] Department of Mechanical Engineering, College of Engineering, Jazan University, Saudi Arabia
[d] Department of Mechanical Engineering, College of Engineering, Jazan University, Saudi Arabia
[e] Department of Mechanical Engineering, Hindusthan Institute of Technology, Coimbatore 641032, Tamil Nadu, India
[f] Heat Transfer Equipments (P) Limited, Coimbatore 641021, Tamil Nadu, India
[g] Department of Mechanical Engineering, Gokaraju Rangaraju Institute of Engineering and Technology, Hyderabad 500090, Telangana, India
[h] Department of Mechanical Engineering, KPR Institute of Engineering and Technology, Coimbatore 641407, Tamil Nadu, India

Available online 21 December 2021, Version of Record 11 Apr 2022

Abstract

The welding of two different kinds of metals has found greater applications and use in several fields of manufacturing in present days. A387 is a sort of grade steel used in the fabrication of pressure vessels that are widely used in applications requiring high thermal stability, such as heat exchangers, boilers, and pressure containers in the petroleum industry, among others. Additionally, in the majority of cases, it is necessary to attach A387 to stainless steel in the aforementioned applications. Metal Inert Gas (MIG) welding is a common method of connecting metals in industries. However, process factors such as welding voltage, current rating, as well as the weld bevel angle are critical for achieving a high-quality weld and appropriate mechanical qualities. The purpose of this work is to improve the critical variables of welding, viz., the welding voltage, current rating as well as, the weld bevel angle, in order to get higher impact strength when connecting dissimilar materials, such as A387 steel alloy and SS316 grade stainless steel, by means of Taguchi's well-known orthogonal array with L_9 Arrays. The optimal combination was found to be 140 A welding current, 20 V welding voltage, and 60° angle of bevel for achieving the highest impact strength. Additionally, ANOVA was employed to assess the most influential process variable that has a substantial effect on the weld joint's impact strength. The outcomes demonstrated that the most important variable affecting the welded joint's impact strength was welding current, trailed by welding voltage.

Previous

Next

Keywords

Taguchi optimization, MIG+ Welding dissimilar metals, Impact strength of weld joint

ScienceDirect

Materials Today: Proceedings

Volume [illegible], 2022, Pages [illegible]

Experimental analysis of the metal roofed industrial building using nano-silica disbanded crude wax (NDCW)

[illegible] [a], [illegible] [b], N. Vigneshkumar [c], Rakesh Sharma [d], Manoj Kumar Singh [e], Ram Subbiah [f], [illegible] Manoj Kumar [illegible]

a Department of Mechanical Engineering, Government Engineering College, Jhalawar, Rajasthan 326023, India
b Department of Mechanical Engineering, PSN College of Engineering and Technology, Tirunelveli 627152, Tamil Nadu, India
c Department of Mechanical Engineering, KPR Institute of Engineering and Technology, Coimbatore 641407, Tamil Nadu, India
d Department of Civil Engineering, Government Engineering College, Jhalawar, Rajasthan 326023, India
e Department of Mechanical Engineering, Faculty of Engineering and Technology, MJP Rohilkhand University, Bareilly 243006, U.P., India
f Department of Mechanical Engineering, Gokaraju Rangaraju Institute of Engineering and Technology, Hyderabad 500090, Telangana, India

Available online 29 December 2021, Version of Record 15 June 2022

Show less ^

Outline | Share Cite

https://doi.org/10.1016/j.matpr.2021.12.[illegible]

Abstract

The increased daytime temperature upsurges the energy need of the buildings for space cooling, particularly on days with strong sun exposure. The building's roof adds far more to this reason by allowing a big amount of heat to flow-in during the day. Additionally, single-storey structures with metal roofs allow for increased heat penetration, and so enhance the building's overall heat gain. They could do so by increasing the cooling load in order to achieve human comfort. The present work involved conducting an experiment to see whether a crude wax based Nano-silica (SiO_2) Disbanded Phase Changing Material (NDCW) might be used to lower the internal temperature of a metal roofed single-story industrial structure effectively. This approach attempted to minimize the building's total cooling load, hence reducing the amount of conventional energy required. The research was conducted using a scaled-down model of the planned building. The trials were done in three phases: normal roof (Normal Roof) without crude wax, with crude wax in the roof (CW Roof), and with NDCW inside the roof (NDCW Roof). The NDCW was prepared by disbanding 1.0% volume of nano-silica within the crude wax. The findings from the investigations shows that encapsulating crude wax and NDCW under the metal roofing of a single-storey structure significantly lowered the exterior roof's temperature, inner roof's temperature, and further enhanced the thermal comfort of the indoor building space. With the assistance of crude wax and NDCW, the daytime mean internal space temperature was decreased by 5 °C and 6 °C, respectively. Further, the corresponding daytime peak was diminished by 10.5 °C and 12.5 °C with crude wax and NDCW, respectively.

< Previous Next >

Keywords

Space cooling; Metal roofed building; Single storey building with PCM; Nano-silica; PCM; Roof with crude wax

Special issue articles Recommended articles

Materials Today: Proceedings

Volume 67, Part 1, 2022, Pages 1702-1707

Thermal analysis of a double-glazing window using a Nano-Disbanded Phase Changing Material (NDPCM)

Nitesh Kushik [a], P. Saravanakumar [b], S. Dhanasekaran [c], Rajasekaran Saminathan [c], Mohammad Rizwan Khan [d], Rajeesh Sreenivasan [e], Manoj Kumar [f], [g], [h]

[a] Department of Production and Industrial Engineering, Birla Institute of Technology, Mesra, Ranchi 835 215, Jharkand, India
[b] Department of Mechanical Engineering, Sri Ramakrishna Engineering College, Coimbatore 641 022, Tamil Nadu, India
[c] Department of Mechanical Engineering, Sri Ramakrishna Polytechnic College, Coimbatore 641022, Tamil Nadu, India
[d] Department of Mechanical Engineering, College of Engineering, Jazan University, Saudi Arabia
[e] Department of Mechanical Engineering, Government Engineering College, Jhalawar, Rajasthan 326 023, India
[f] Department of Mechanical Engineering, Gokaraju Rangaraju Institute of Engineering and Technology, Hyderabad, 500 090 Telangana, India
[g] Department of Civil Engineering, Government Engineering College, Jhalawar, Rajasthan 326 023, India
[h] Department of Mechanical Engineering, KPR Institute of Engineering and Technology, Coimbatore 641 407, Tamil Nadu, India

Available online 13 December 2021, Version of Record 17 June 2022.

Abstract

Building energy consumption is playing a key role in global energy demand. The previous researches demonstrated that the type and material of the windows influences the building energy consumption. The present study experimentally examines the heat transfer characteristics of a double-glazing window system which is united with a Nano-Disbanded Phase Changing Material (NDPCM) and the results are analyzed by comparing it with a window with the normal PCM and a standard double-glazing unit. The NDPCM had been synthesized beforehand through the dispersion of 1.0 vol fraction of nano-silica (SiO_2) within the technical grade paraffin. The interior thermal environment, inside temperature of the window glass, consumed energy via glazed windows, and glass transmittance with NDPCM were all critically evaluated. The results demonstrated that the transmittance of the window unit with NDPCM was sufficient enough throughout the day to permit adequate sun-light into the experimented space. Additionally, the NDPCM diminished the interior glass-panel temperature by 3.5 °C, abridged temperature variability of the investigated space by 5.5 °C, and enhanced energy conservation by 4.61%.

Previous Next

Keywords

Double-glazing window; Nano-PCM Window with nano-PCM; Energy conservation; Energy consumed by window

C 2.3

ScienceDirect

Materials Today: Proceedings

Volume 50, Parts 5, 2022, Pages 2547-2553

Influences of Friction stir tool parameters for joining two similar AZ61A alloy plates

V. Gokul Lal [a], A.R. Sampath Boopath [b], M. Mohammed Ashiq [c], Jovick Jino [d], Ravi Subbiah [e], K. Gokul Sasi Kumar [f]

[a] Department of Mechanical Engineering, Nandha Engineering Institute of Technology, Salem, Tamil Nadu 638052, India
[b] Department of Mechanical Engineering, Muthayammal College of Engineering, Rasipuram, Tamil Nadu 637408, India
[c] Department of Mechanical Engineering, Vignan's Lara Institute of Technology and Science, Guntur, Andhra Pradesh, 522213, India
[d] Department of Mechanical Engineering, Dhirajlal Gandhi College of Technology, Salem, Tamilnadu 64[illegible]04, India
[e] Department of Mechanical Engineering, Gokaraju Rangaraju Institute of Engineering and Technology, Hyderabad, Telangana 500090, India
[f] Department of Aeronautical Engineering, Noorul Islam Centre for Higher Education, Kumaracoil 629180, India

Received 30 August 2021, Revised 24 November 2021, Accepted 2 December 2021, Available online 18 December 2021, Version of Record 7 February 2022

Show less

Outline | Share | Cite

https://doi.org/10.1016/j.matpr.2021.12.074

Abstract

The welding of magnesium alloy plates is highly important to utilize lightweight applications such as aircraft, automotive, and space sectors. In this research, Friction stir welding (FSW) of two similar AZ61A Magnesium alloy plates has been performed to obtain the maximum micro-hardness and tensile strength. The tool parameters such as tool revolving speed, Tool traveling speed, tool force, tool pin, and shoulder diameters have been modified during the welding experiments. The percentage of contributions and significant various tool parameters on micro-hardness and tensile strength have been analysed using Taguchi's technique. The tool pin diameter and tool revolving speed are highly contributed factors to enhance the micro-hardness and tensile strength than tool revolving speed and shoulder diameter. The predicted best tool parameters values have been evaluated by confirmation experiments.

Previous

Next

Keywords

AZ61A Magnesium alloy; Friction stir welding; Taguchi technique; Tool parameters; Tensile strength; Micro-hardness

Special issue articles

Recommended articles

Cited by (7)

An experimental study on the hardness and wear rate of carbonitride coated stainless steel

2022, Materials Today: Proceedings

Show abstract

C. 2.4

ScienceDirect

Materials Today: Proceedings

Volume 56, Part 4, 2022, Pages 1923-1926

Investigating mechanical strength of a natural fibre polymer composite using SiO_2 nano-filler

Gopal Anandkumar Jadhav [a], Basanta Kumar Palai [b], Sumanta Bhattacharya [c], S Aravind [d], G. Sivakumar [e], Ram Subbiah [f], Madhusudhan Chandrakasan [g]

- [a] Department of Mechanical Engineering, D. Y. Patil College of Engineering and Technology, Kolhapur 416006, Maharashtra, India
- [b] Department of Mechanical Engineering, School of Engineering and Technology, GIET University, Gunupur 765022, Odisha, India
- [c] Research Scholar, Department of Textile Technology, Maulana Abul Kalam Azad University of Technology, Howrah, West Bengal, India, 711105
- [d] Department of Mechanical Engineering, Rajalakshmi Institute of Technology, Kuthambakkam, Chennai, 600124, Tamilnadu, India
- [e] Department of Mechanical Engineering, Panimalar Institute of Technology, Poonamallee, Chennai 600123, Tamilnadu, India
- [f] Department of Mechanical Engineering, Gokaraju Rangaraju Institute of Engineering and Technology, Hyderabad 500090, Telangana, India
- [g] Department of Civil Engineering, Road and Transportation Engineering, College of Engineering & Technology, Wollega University, Ethiopia

Available online 22 January 2022, Version of Record 11 April 2022.

Show less ^

Outline | Share | Cite

https://doi.org/10.1016/j.matpr.2022.01.176

Abstract

Introducing nano-fillers in natural fibre polymer composite materials have attained a greater attention in recent days due to their distinct behavior in improving the mechanical characteristics of the composites with less effort. In this study, the effect of introducing nano-SiO_2 filler in kenaf fibre polymer composite on their mechanical characteristics is analyzed. The nano-fillers with five different mass fractions namely 0%, 1%, 2%, 3%, and 4% were tested in this work. The tensile, compressive and impact strengths of the composites were investigated. The results evidenced that the increment in nano-filler content proportionally improved the strength of the composite until the addition of 2% of nanofiller and then, the improvement was not impressive. The maximum enhancement of 20.60% in tensile strength, 23.71% in compressive strength, and 22.89% in impact strength was attained with 2% fraction of nanofiller in composite.

< Previous

Next >

Keywords

Nano-filler; Kenaf fibre; Epoxy composite; Mechanical strength; Natural fibre

Special issue articles Recommended articles

Cited by (2)

Improving hydrophobicity and compatibility between kenaf fiber and polymer composite by surface treatment with inorganic nanoparticles

C 25

ScienceDirect

Materials Today: Proceedings

Volume 69, Part 1, 2022, Pages 1429-1433

Physical and mechanical properties of AA2219/BN composites

S. Rajkumar [a], K. Arul [b], K. Magesh kumar [c], T. Muralidharan [d], Ram Subbiah [e], V. Gokarajan [f], M. Ravichandran [g]

[a] Department of Mechanical Engineering, Faculty of Manufacturing, Institute of Technology, Hawassa University, Ethiopia
[b] Department of Mechanical Engineering, Agni College of Technology, Thalambur, Chennai, India
[c] School of Mechanical Engineering, Vellore Institute of Technology, Vellore 632014, Tamil Nadu, India
[d] Department of Mechanical Engineering, Saveetha School of Engineering, SIMATS, Chennai, 602105, Tamil Nadu, India
[e] Department of Mechanical Engineering, Gokaraju Rangaraju Institute of Engineering and Technology, Hyderabad, Telangana 500090, India
[f] Centre for Materials Engineering and Regenerative Medicine, Bharath Institute of Higher Education and Research, Chennai 600073, Tamil Nadu, India
[g] Department of Mechanical Engineering, K. Ramakrishnan College of Engineering, Trichy 621 112, Tamil Nadu, India

Available online 3 January 2022, Version of Record 19 May 2022

Abstract

The main purpose of this paper is to compare the impacts of multiple Boron Nitride particle weight percentages of micro-sized particles and nano-sized particles on the AA2219 hybrid nanocomposite produced via stirring and hot extrusion procedures. The finalized materials are structurally and metallurgically characterized. To conduct a comparative analysis the weight percentages of Boron Nitride-reinforced particles are varied. When compared to the other samples, the yield strength (270 MPa) and ultimate tensile strength (UTS) of the AA2219 hybrid composite sample-3 (S3) are greatly enhanced.

Previous

Next

Keywords

Composite materials; Porosity; Aluminium; AA2219; Physical properties

Special issue articles Recommended articles

C 26

ScienceDirect

Materials Today: Proceedings

Volume 55, Part 2, 2022, Pages 1457-1462

Parametric analysis and simulation of surface roughness and tool flank wear in machining of low carbon alloy steel

Rajaparthiban J, [illegible], A. Abinaya, S. Mahalingam, S. Suresh Kumar, M. Ravichandran, Ram Subbiah

- Department of Mechanical Engineering, Chennai Institute of Technology, Kundrathur, Chennai 600 069, Tamil Nadu, India
- Department of Mechanical Engineering, Kings College of Engineering, [illegible], Thanjavur, Tamil Nadu, India
- Department of Electronics and Communication Engineering, K. Ramakrishnan College of Engineering, Trichy 621 112, Tamil Nadu, India
- Centre for Materials Engineering and Regenerative Medicine, Bharath Institute of Higher Education and Research, Chennai 600073, Tamil Nadu, India
- Department of Mechanical Engineering, Panimalar Polytechnic College, Chennai 600029, Tamil Nadu, India
- Department of Mechanical Engineering, K. Ramakrishnan College of Engineering, Trichy 621 112, Tamil Nadu, India
- Department of Mechanical Engineering, Gokaraju Rangaraju Institute of Engineering and Technology, Hyderabad, Telangana 500090, India

Available online 24 January 2022, Version of Record 19 May 2022.

Show less ^

Outline | Share Cite

https://doi.org/10.1016/j.matpr.2022.01.086

Abstract

Austenitic SS influences in most frequently applied corrosion resistance or in higher surface loading were it is required. The present investigation represents the quality attributes namely surface roughness and tool wear rate in turning of AISI 316L steel using DoE. Taguchi method has been employed with L9 (3³) orthogonal array of the three significant factors, i.e., speed, feed and depth of cut, to achieve the minimum surface roughness and tool wear rate. The Analysis of variance was performed to identify the influencing factors which affect the responses. The outcomes from the research reveal that the minimum surface roughness was achieved at cutting speed 170 m/min, feed rate 0.10 mm/rev, depth of cut 0.15 mm and the minimum tool wear rate was attained at 170 m/min cutting speed, 0.07 mm/rev feed rate and 0.15 mm depth of cut was determined using the experimental study and compared with the prediction model from design of experiments. The results shows that both the values were good in agreement with experimental as well as prediction results.

< Previous Next >

Keywords

DOE; AISI 316L; Turning; ANOVA; Surface roughness; Tool flank wear

Special issue articles Recommended articles

Cited by (1)

c 2-7

ScienceDirect

Materials Today: Proceedings

Volume 62, Part 4, 2022, Pages 1854-1860

Numerical investigation of modified fin shapes for the improved heat transfer

Jagdish Lal Bishnoi [a], Prashant Chauhan [b], Rajnesh Sharma [c], Amarjeet Poonia [d], Hari Kumar Singh [e], Arun Kumar Sharma [f], Ram Sukhi [g, *]

[a] Department of Mechanical Engineering,Government Engineering College, Jhalawar 326023, Rajasthan, India
[b] Department of Physics and Materials Science and Engineering, Jaypee Institute of Information Technology, Noida 201309, Uttar Pradesh, India
[c] Department of Civil Engineering,Government Engineering College, Jhalawar 326023, Rajasthan, India
[d] Department of Information Technology, Government Women Engineering College Ajmer - 305002, Rajasthan, India
[e] Department of Electronics and Communication Engineering, M. J. P. Rohilkhand University, Bareilly 243006, Uttar Pradesh, India
[f] Department of Physics, D. A. V. (PG) College, Dehradun 248001, Uttarakhand, India
[g] Department of Mechanical Engineering, Gokaraju Rangaraju Institute of Engineering and Technology, Hyderabad 500090, Telangana, India

Available online 13 January 2022, Version of Record 17 June 2022

Abstract

An examination of fin surfaces with various shapes was performed in this work to determine the most efficient heat transfer rate. Models, investigations, and studies have been conducted on the geometry of fin surfaces, namely normal fins with rectangular cross section (R-Fin), fins with multiple steps (S-Fin), and multiple step fins with dimples (D-Fin). Fin surfaces with higher surface area have improved heat transmission, as determined by conceptual and numerical investigation. According to numerical data, dimpled fins improve the surface region and heat transmission of the fins. The dimples had been constructed with changing diameters to fit the fins, which are 5 mm, 4 mm, and 3 mm in diameter, and have been evaluated using a state computational approach. The purpose of this study is to demonstrate the construction, evaluation, and outcome of several fin shapes with constant input boundary conditions. The spherical grooves with various diameters were found to be more successful than the other fins, and creating notches increased heat transmission far more than augmenting the size of the stepped fin's depression.

Previous Next

Keywords

Fins; Dimples on fins; Heat transfer; Fin geometry; CFD; Sphere-shaped indentation

Special issue articles Recommended articles

Cited by (1)

Performance enhancement of phase change materials in triplex-tube latent heat energy storage system using novel fin configurations

Materials Today: Proceedings

Volume 56, Part 3, 2022, Pages 1561-1566

Study on influence of nano-filler content on the performance of natural fibre reinforced epoxy composites

M.G. Mohan G [a], K.S. Raghuram [b], J.N.S. Suryanarayana Raju [c], O. Ravi [d], M. Venkata Rao [e], Ram Subbaiah K [f], M. Mukendran Chandrasekar [g]

[a] Department of Mechanical Engineering, Panimalar Engineering College, Chennai 600123, Tamil Nadu, India
[b] Department of Mechanical Engineering, Vignan's Institute of Information Technology (A), Visakhapatnam, Andhra Pradesh 530049, India.
[c] Department of Civil Engineering, SRKR Engineering College, Bhimavaram 534204, Andhra Pradesh, India
[d] Department of Mechanical Engineering, Dhanalakshmi Srinivasan Institute of Higher Education and Research, Chennai 600073, Tamil Nadu, India
[e] Department of Mechanical Engineering, Gokaraju Rangaraju Institute of Engineering and Technology, Hyderabad 500090, Telangana, India
[f] Department of Civil Engineering, Road and Transportation Engineering, College of Engineering & Technology, Wolega University, Ethiopia

Available online 1 February 2022, Version of Record 11 April 2022.

Abstract

The purpose of this research is to determine the influence of nano-titania (nano-TiO2) on the impact strength and water absorbing capabilities of jute fibre reinforcement an epoxy polymer composite material. Compression moulding was used to fabricate the composite plates. By magnetic stirring and ultrasonication, epoxy was mixed with nano-titania at loading rates of 0, 0.5, 1.0, and 2.0 wt. fractions. Scanning electron microscopy (SEM) was used to characterise the microstructure. The results reveal that the inclusion of nano-titania significantly improves the impact strength of the jute fibre reinforced epoxy composite system. Particularly, 1.0% of nano-titania was determined to be the optimal fraction for obtaining maximum performance of the jute/epoxy composite. The impact strength was increased by 39.35%. The use of 1.0% of nano-titania nanoparticles lowered the water diffusion by 18.18%.

Previous Next

Keywords

Natural fibre composite; Jute fibre; Epoxy resin; Nano-titania; Water absorption; Impact strength

Special issue articles Recommended articles

Cited by (0)

ScienceDirect

C 29

Materials Today: Proceedings

Volume 68, Part 1, 2022, Pages 1478-1484

The influence of nickel on the mechanical and tribological properties of AA2219-CNT composites made by stir casting

J. Vijaya Kathir [a, b], P. Sivakumar [a, b], A. Senthil Kumar [c], G. D. Sivakumar [c], S. Siva Sundar [c], Ravi Sekhar [d]

[a] Centre for Materials Research Lab, Department of Mechanical Engineering, Sethu Institute of Technology, Tamil Nadu, India
[b] Mechanical and Industrial Engineering, University of Technology and Applied Sciences, Muscat, Oman
[c] Department of Mechanical Engineering, Sethu Institute of Technology, Tamil Nadu, India
[d] Department of Mechanical Engineering, Gokaraju Rangaraju Institute of Engineering and Technology, Hyderabad, Telangana 500090, India

Received 24 November 2021, Revised 3 January 2022, Accepted 5 January 2022, Available online 5 February 2022, Version of Record 19 May 2022.

Show less

Outline | Share | Cite

https://doi.org/10.1016/j.matpr.2022.01.306

Get rights and content

Abstract

AA2219 aluminium alloy matrix composite enhanced with CNTs(Carbon nanotubes) was investigated for its mechanical and tribological properties. Stir casting was used to add nickel to the aluminium matrix and the homogenization procedure was then used to homogenise the mixture. It was found that the interdimeric portions of the interdimeric CNT and aluminium compounds had a block-shaped structure. There was an increase in tiny needle-shaped Aluminum precipitates near interdimeric zones when nickel was added up to 1.5 wt%; additional nickel addition reduced their abundance in this location. It was found that the needle-shaped Carbon Interdimeric nanotube precipitates disappeared following normalisation treatment with nickel up to 4.5 wt%. Ni and CNT intermetallic were converted to CNT by adding nickel and homogenization. Furthermore, the aluminium matrix generated aluminium precipitates instead of al-Ni precipitates when nickel concentration increased from 3 to 4.5 wt%. Composite's coefficient of friction and wear rate were lowered by 13 percent and 12 percent compared to a control sample without nickel, while its strength was increased by roughly 42 percent.

Previous Next

Keywords

Nickel additives. Stir casting; Mechanical properties, AA2219, CNTs; Wear; Hardness

Special issue articles Recommended articles

Cited by (0)

C 30

ScienceDirect

Materials Today: Proceedings

Volume 64, Part 3, 2022, Pages 1532-1536

Studies on mechanical and morphological of TIG welded aluminum alloy

M. Magesh [a], K. Arul [b], M. S. [illegible] [c], R. Rangaraju [d], A. P., R. Aravind [e], S. Lakshmana Kumar [f], Ram Subbiah [g]

[a] Department of Aerospace Engineering, R.G. Abdul Rahman Crescent, Institute of Science and Technology, Vandalur, Chennai, India
[b] Department of Mechanical Engineering, Agni College of Technology, Thalambur, Chennai 600130, India
[c] Department of Mechanical Engineering, Shadan College of Engineering and Technology, Hyderabad, Telangana 500086, India
[d] Department of Mechanical Engineering, St. Joseph's College of Engineering, OMR, Chennai 600119, India
[e] Department of Mechanical Engineering, SSM Institute of Engineering and Technology, Dindigul 624002, India
[f] Department of Mechanical Engineering, Sona College of Technology, Salem, Tamilnadu, India
[g] Department of Mechanical Engineering, Gokaraju Rangaraju Institute of Engineering and Technology, Hyderabad, Telangana 500090, India

Available online 19 February 2022, Version of Record 19 May 2022.

Show less

Outline | Share | Cite

https://doi.org/10.1016/j.matpr.2022.02.001

Abstract

An automated TIG welding system was employed to increase the welding strength and weld quality of pure Aluminium (Al) plate in terms of bead width and depth of penetration. The control parameters during the welding process are the most critical factors, such as welding speed and arc length. TIG welding is a procedure that involves maintaining an electric arc between a non-consumable tungsten electrode and the weldable component. Due to its strong corrosion resistance, AA5059- aluminium alloy is the most often used in the ship industry across as a hull material.

Previous Next

Keywords

AA5059 Optimization. Mechanical properties. Microstructural studies

Special issue articles Recommended articles

ScienceDirect

Materials Today: Proceedings

Volume 59, Part 1, 2022, Pages 1544-1549

Effect of welding speed on the mechanical properties of AA6061 Al alloy joined by friction stir welding

S. Rajkumar [a], K. Nagesh kumar [a,*], K. Arul [b], S. Ravi [c], T. Mohanraj [d], Ravi Subhash [e]

[a] Department of Mechanical Engineering, Faculty of Manufacturing, Institute of Technology, Hawassa University, Ethiopia
[b] School of Mechanical Engineering, Vellore Institute of Technology, Vellore 632014, Tamil Nadu, India
[c] Department of Mechanical Engineering, Agni College of Technology, Thalambur, Chennai, India
[d] Department of Mechanical Engineering, Chennai Institute of Technology, Chennai 600069, India
[e] Department of Mechanical Engineering, Saveetha School of Engineering, SIMATS, Chennai 602105, Tamil Nadu, India
[f] Department of Mechanical Engineering, Gokaraju Rangaraju Institute of Engineering and Technology, Hyderabad 500090, Telangana, India

Available online 12 February 2022, Version of Record 19 May 2022.

Abstract

In this study, AA6061 alloys were connected via friction stir welding to a fixed rotation speed with different welding speeds (FSW). The hand tappers in the stirring tool in the welding process were made from a 15°-diameter shoulder and modified M6 × 1 HSS hand taps. The FSW was manufactured with the rotating velocity of 1500 to 30 r.p.m, 90 mm and 60 mm/min. To mechanical and metallographic tests and the mechanical and metallurgical properties of welding specimens, the effects of welding speed were examined in welded joints. The welding speed had a significant impact on the joint's macrostructure and mechanical characteristics. The findings showed that the soldering nugget has decreased on average at a higher welding speed. In addition, a high welding speed had negative consequences for the weld nugget's mechanical properties.

Previous

Next

Keywords

FSW; Aluminium alloy; Mechanical properties; Macro defects, Microstructure, Welding Speed; AA6061

ScienceDirect

C 32

Materials Today: Proceedings

Volume 59, Part 2, 2022, Pages 1537-1543

Mechanical properties of aluminium alloy AA7086 by equal channel angular press with parameters of die design

P. Rajkumar [a] [b], T. Mandavgane [b], Muthukannan Subiahiah [c], M. Saraj [d], K. MageshKumar [e], K. Anil [f], Ram Subbiah [f]

[a] Department of Mechanical Engineering, Faculty of Manufacturing, Institute of Technology, Hawassa University, Ethiopia
[b] Department of Mechanical Engineering, Saveetha School of Engineering, SIMATS, Chennai 602105, Tamil Nadu, India
[c] Department of Engineering, University of Technology and Applied Sciences, Higher College of Technology, Muscat, Oman
[d] School of Mechanical Engineering, Vellore Institute of Technology, Vellore 632014, Tamil Nadu, India
[e] Department of Mechanical Engineering, Agni College of Technology, Thalambur, Chennai, India
[f] Department of Mechanical Engineering, Gokaraju Rangaraju Institute of Engineering and Technology, Hyderabad, Telangana 500090, India

Available online 19 February 2022, Version of Record 19 May 2022.

Show less ^

Outline | Share Cite

https://doi.org/10.1016/j.matpr.2022.02.192

Abstract

ECAP is a highly successful method for generating ultra-fine grained bulk material because of its equal channel angular pressure distribution. Using a custom-made die, the material is fed via a channel and into the next step. Die design features such as corner angle and channel angle have an impact on fine grain development. Commercial aluminium AA7086 was used as a sample material to assess mechanical behavior/properties before and after the ECAP procedure. This material had 90° and 20° channel angles when it was conceived and made in the lab. A die designed with an ideal parameter for use with an ECAP die, the mechanical behaviour of economically pure aluminium is investigated and analyzed in the current study. Here, the keystrokes were performed anywhere from 0 to 3 times, following the BC path. ECAP runs reduced particle size to 320 nm, and the strength increased to 368.4 MPa after three runs, the researchers found.

Previous Next

Keywords

Aluminium; Mechanical behaviour; AA7086; ECAP; Design Parameters

Special issue articles Recommended articles

Cited by (5)

Influence of nano titanium oxide reinforced Al-7075 matrix composites by stir casting method

2022, Materials Today: Proceedings

Show abstract

Materials Today: Proceedings

Volume 59, Part 1, 2022, Pages 1094-1099

An experimental study on friction stir processing of aluminium alloy (AA-7024) and boron nitride (BN_p) surface composite

Santosh Boopathi [a] ✉, M. Jeyakumar [b], G. Robert Singh [c], Francis Gilbert A [d], M. Pandian [e], Ram Subbiah [f], V. Dhinakaran [g]

[a] Department of Mechanical Engineering, Muthayammal College of Engineering, Rasipuram, Tamil Nadu 637408, India
[b] Department of Mechanical Engineering, Christ the King Engineering College, Tamil Nadu 641104, India
[c] Department of Mechanical Engineering, Sasi Institute of Technology & Engineering, Tadepalligudem, Andhra Pradesh 534101, India
[d] Department of Mechanical Engineering, Sri Sairam Institute of Technology, Chennai, Tamil Nadu 600044, India
[e] Department of Mechanical Engineering, Gokaraju Rangaraju Institute of Engineering and Technology, Hyderabad, Telangana 500090, India
[f] Department of Mechanical Engineering, Kongu Engineering College, Perundurai, Erode 638057, India
[g] Department of Mechanical Engineering, Narasu's Sarathy Institute of Technology, Salem, Tamil Nadu 636305, India

Available online 1 March 2022, Version of Record 18 May 2022.

https://doi.org/10.1016/j.matpr.2022.02.435

Abstract

In this research the influences of percentages of boron nitride powder (BN_p) on the characteristics of friction stir Aluminium alloy (AA-2024) surface composite has been studied. Taguchi method has been used to design and investigate the effect of volume percentage of BN_p, welding speed, and tool rotational speed on tensile strength, and wear rate of surface composite. AA-2024 alloy has been used in aerospace and automotive industries due to its low weight-high strength. The optimum tensile strength and wear rate have been estimated and validated by confirmation experiments. The specimen made for confirmation experiments have been used to examine the fractures microstructure. The maximum tensile strength and minimum wear rate of the optimum specimen are 594 MPa and 1.37 mm^3/Nm respectively. The optimum process parameters settings, 15% of BN_p, 1200 rpm of tool rotation speed, and 50 mm/min. welding speed. It was also observed that the volume percentage of BN_p and tool rotational speed are significant FSP parameters on tensile strength and wear rate.

Previous

Next

Keywords

Friction stir processing, AA2024, Boron nitride (BN_p), Tensile strength, Wear rate, SEM analysis

Cited by (5)

An experimental study on the hardness and wear rate of carbonitride coated stainless steel

2022, Materials Today: Proceedings

c. 34

ScienceDirect

Materials Today: Proceedings

Volume 59, Part 2, 2022, Pages 1561-1565

Alloy 617 welding of similar and dissimilar materials: A review

K. Nagesh kumar [a], M. Balamurugan [b], S. Rajesh kumar [c], K. Arul [d], T. Muralikannan [e], Ram Subbian [f]

[a] Department of Mechanical Engineering, Sree Rishoa College of Engineering, Vellore - 632101, Tamilnadu, India
[b] Centre for Materials Engineering and Regenerative Medicine, Bharath Institute of Higher Education and Research, Chennai, India
[c] Department of Mechanical Engineering, Faculty of Manufacturing, Institute of Technology, Hawassa University, Ethiopia
[d] Department of Mechanical Engineering, Agni College of Technology, Thalambur 603103, Tamilnadu, India
[e] Department of Mechanical Engineering, Saveetha School of Engineering, SIMATS, Chennai 602105, Tamil Nadu, India
[f] Department of Mechanical Engineering, Sukaraju Rangaraju Institute of Engineering and Technology, Hyderabad 500090, Telangana, India

Available online 17 March 2022, Version of Record 19 May 2022.

Show less

Outline | Share | Cite

https://doi.org/10.1016/j.matpr.2022.03.105

Abstract

This review article shows the similar and dissimilar welding of UNS N06617 (Alloy 617). It is a nickel-based material that is highly chosen for hot environmental applications. This alloy is majorly composed of Cr, Co, and Mo elements which serve as solid solution strengtheners. To increase the life span and to prevent pollution to the environment, this alloy is highly preferred. Several welding techniques were taken part to fabricate this alloy using different filler metals. The presence of Molybdenum and chromium develops the cracking behavior in this particular alloy. Many researchers have reported this issue in all the similar and dissimilar weldments. that lowers the ductility of weldments. Due to the presence of secondary phases, most of the failures were detected in the fusion zone. This paper summarizes all the observations in the weldments of alloy 617 carried out by different welding techniques. So this could be very useful for industrial applications such as power plants, oil and refineries, and aerospace applications.

Previous Next

Keywords

Optical microscopy (OM); Scanning electron microscope (SEM); Energy dispersive spectroscopy (EDS); X-ray diffraction analysis (XRD); Fusion zone; Heat affected zone

Special issue articles Recommended articles

Cited by (0)

Materials Today: Proceedings

Volume 50, Part 7, 2022, Pages 1515-1519

Preparation and characterization of AZ63A/Boron Nitride composites using hybrid mechanical and ultrasonic assisted stir casting

J. Vasanthakumar [a] ✉, A. Senthil Kumar [b], G.D. Sivakumar [b], S.K. Rajeshwaran [c], Ram Subbiah [b]

[a] Centre for Materials Research Lab, Department of Mechanical Engineering, Sethu Institute of Technology, Tamil Nadu, India
[b] Department of Mechanical Engineering, Sethu Institute of Technology, Tamil Nadu, India
[c] Department of Mechanical Engineering, Gokaraju Rangaraju Institute of Engineering and Technology, Hyderabad, Telangana 500090, India

Available online 16 March 2022, Version of Record 19 May 2022.

Abstract

Magnesium (Mg) is become progressively used in the transportation business because of its low weight. The poorer mechanical properties of magnesium (Mg) compared to aluminium and steel limit its widespread use. Improved mechanical properties can be achieved through grain refinement in cast alloys. Particle substrates can be added to the liquid melt to serve as nucleation sites for the formation and development of grains, resulting in a finer grain size. Mechanical stirring (MS) with impeller is most common technique for dispersing inoculants into the molten metal. However, it is difficult to achieve uniform dispersion of inoculants using this method. Ultrasonic treatment (UST) has also been investigated as an alternative to MS treatment. Particle inoculants BN were studied to see how they would disperse inside the alloy AZ63A Mg in this study. To create the cast composites, either MS or UST were used. Thermal tensile tests and theoretical models were used to determine the mechanical properties of these materials. The UST-treated specimens outperformed the base alloy and the MS-produced samples in terms of mechanical properties. Inoculant dispersion in sonicated samples was shown to be improved due to the use of finer grains, a thermal development discrepancy between the refiner and matrix, and other factors. Using sonication and grain refinement, researchers were able to make a exclusive relationship between theoretic strengthening mechanism forecast models and the actual outcomes they attained. The mechanical properties of Mg alloy can be improved by utilising cutting-edge new technologies, such as UST, in the production of cast alloys.

Previous

Next

Keywords

Mechanical stirring (MS); Ultrasonic treatment (UST); Ultimate Tensile Strength (UTS); Sonication; Magnesium

c 36

ScienceDirect

Materials Today: Proceedings

Volume 62, Part 8, 2022, Pages 5228-5232

Study on wear properties of Aluminium alloy for different mass of SiC particles

Moti Lal Rinawa [a], Rajneesh Sharma [b], Prasad Ramchandra Baviskar [c], R. Santhoshkumar [d], Rashmi C. Deshmukh [e], M. Venkata Rao [f], Ram Subbiah [g]

[a] Department of Mechanical Engineering, Government Engineering College, Jhalawar, Rajasthan 326023, India
[b] Department of Civil Engineering, Government Engineering College, Jhalawar, Rajasthan 326023, India
[c] Department of Mechanical Engineering, Sandip Institute of Technology and Research Centre, Nashik, Maharashtra, 422213, India
[d] Department of Electrical and Electronics Engineering, KPR Institute of Engineering and Technology, Coimbatore, Tamilnadu, 641407, India
[e] Department of Physics, Shri Shivaji Science College, Amravati, Maharashtra 444603, India
[f] Department of Civil Engineering, SRKR Engineering College, Bhimavaram, Andhra Pradesh, 534204, India
[g] Department of Mechanical Engineering, Gokaraju Rangaraju Institute of Engineering and Technology, Hyderabad, Telangana, 500090, India

Available online 15 March 2022, Version of Record 23 June 2022.

Show less ^

Outline | Share Cite

https://doi.org/10.1016/j.matpr.2022.03.209

Abstract

Owing to its excellent dimensional consistency, low weight, mass strength ratio, cheap cost, and specific strength, aluminium 7075 has a wide range of applications in aircraft fittings, gears, worm wheels, shafts, missiles, and regulating valves. Considering the use aluminium alloy (Al 7075) in the aerospace and defence sectors, its wear qualities must be enhanced further to extend the life of the components used in these industries. Considering its wear resistance capabilities, silicon carbide (SiC) is commonly utilised in the production of wear-resistant blades, saws, surface coatings, and machine tools. The wear characteristics of Al 7075 alloy have been investigated in this study by fortifying it with varied weight percentages (1%, 2%, and 4%) of silicon carbide (SiC) and producing it using the stir casting technique. The experiment was carried out with a Taguchi L27 orthogonal array. A pin-on-disc wear measuring device is used to assess the dry sliding wear properties. SiC concentration, velocity, loading, and sliding length are the process parameters, and the outputs are the friction coefficient (CoF) and the rate of specific wear. The Signal-to-Noise (S/N) ratio was calculated with the help of Taguchi's analysis to discover the optimum effective combination for minimizing friction coefficient and rate of specific wear. According to the results, 4% SiC reinforcement results in a decreased friction coefficient and rate of specific wear under different dynamic conditions. A Scanning Electron Images (SEM) investigation was performed to detect the wear pattern, and it was discovered that the Al7075 strengthened with 4% SiC with a steady input variable shows the least wear. Investigation shows that increasing the weight percentage of SiC enhances the wear resistance of the Al 7075 alloy.

< Previous Next >

Keywords

Al 7075; SiC; Wear resistance; S/N ratio; Taguchi

Special issue articles Recommended articles

C 37

ScienceDirect

Materials Today: Proceedings

Volume 62, Part 8, 2022, Pages 5177-5181

Study on the impact of Nano-reinforcements on the fatigue strength of adhesive joints

M.D. Mohan Gift [a], V. Sharon [b], Saiteja Surakasi [c], B. Kameshwaran [d], M.S. Maurya [e], Manoj Kumar Singh [f], Ram Subbiah [g]

- [a] Department of Mechanical Engineering, Panimalar Engineering College, Chennai, 600123, Tamilnadu, India
- [b] Department of Mechanical Engineering, Panimalar Institute of Technology, Poonamallee, Chennai 600123, Tamil Nadu, India
- [c] Department of Mechanical Engineering, Lendi Institute of Engineering and Technology, Jonnada, Denkada Mandal, 535005, Andhra Pradesh, India
- [d] Department of Civil Engineering, B S Abdur Rahman Crescent Institute of Science and Technology, Vandalur, Chennai, 600048, Tamilnadu, India
- [e] Department of Chemical Engineering, MJP Rohilkhand University, Bareilly, Uttar Pradesh 243006, India
- [f] Department of Mechanical Engineering, MJP Rohilkhand University, Bareilly, Uttar Pradesh 243006, India
- [g] Department of Mechanical Engineering, Gokaraju Rangaraju Institute of Engineering and Technology, Hyderabad, 500090, Telangana, India

Available online 9 March 2022, Version of Record 23 June 2022

Show less ^

Outline | Share Cite

https://doi.org/10.1016/j.matpr.2022.02.593

Abstract

Single overlap joints had been created by combining two AISI 302 stainless steel sheets with the help of 3 M DP270 grade epoxy and their fatigue characteristics were examined under shear stress condition. Further, the effect of adding three distinct proportions of nano-titania with epoxy, on the mechanical characteristics of the joint was analyzed. The overlap lengths was selected as 20 mm and nano-titania proportions were elected as 1.0%, 3.0% and 4.0%, respectively during shear load condition. When the experimental findings were analyzed, it was shown that the mean damaging load associated with the usage of nano-dispersed adhesives rose significantly in general. As a consequence of the trials, it was discovered that the most effective nanoparticles proportion for boosting the fracture strength of adhesive joints is 4.0 percent, and the enhancement in rate of failure strength increase was noted as 85.52 percent. Additionally, it was shown that strain of nanoparticle had a noteworthy role in the shear characteristics of the adhesive junctions. Additionally, it has been shown that incorporating nanoparticles into the glue enhances junction extension. When the adhesive interfaces of the specimens were inspected, impairment was detected as adhesion dissociation, but nanoparticle replenishment had been detected as a combination of cohesive as well as adhesive characteristics.

Previous Next

Keywords

Nano-titania; Adhesive joints; Fatigue strength; Nano-reinforcement

Special issue articles Recommended articles

Cited by (0)

ScienceDirect

Materials Today: Proceedings

Volume 62, Part 8, 2022, Pages 5114-5118

Study on the impact of twisted tapes on the water temperature enhancement in solar water heater

G. Poonkodi [a], G. Prabhu [b], A. Vinodkumar [c], Ravuri Saisasi [d], B. Gowradasan [e], Shailendra Kumar Bohidar [f], Ram Subbiah [g]

[a] Department of Chemistry, Sri Sairam Engineering College, Chennai 600044 Tamilnadu, India
[b] Department of Mechanical Engineering, Panimalar Engineering College, Chennai 600123, Tamilnadu, India
[c] Department of Mechanical Engineering, Panimalar Institute of Technology, Poonamallee, Chennai 600123, Tamilnadu, India
[d] Department of Mechanical Engineering, Lendi Institute of Engineering and Technology, Jonnada, Denkada Mandal, 535005, Andhra Pradesh, India
[e] Department of Civil Engineering, B S Abdur Rahman Crescent Institute of Science and Technology, Vandalur, Chennai 600048, Tamilnadu, India
[f] Department of Mechanical Engineering, Kirodimal Institute of Technology, Raigarh 496001, Chhattisgarh, India
[g] Department of Mechanical Engineering, Gokaraju Rangaraju Institute of Engineering and Technology, Hyderabad 500090, Telangana, India

Available online 4 March 2022, Version of Record 13 June 2022

Show less

Outline | Share | Cite

https://doi.org/10.1016/j.matpr.2022.02.459

Abstract

This form of solar collector, known as an evacuated tube collector, is primarily utilized for water heating applications on both a domestic and commercial scale. When compared to other types of solar collectors, they discovered that theirs was greater in thermal efficiency. The evacuated tube is the most basic type of solar collector, and it has found its most widespread application as pump-less circulation solar water heating system for domestic and commercial applications, among other things. But they are plagued by an inherent problem that is caused by the inactive zone that has evolved at the base of each tube's interior walls. Twisted tubes constructed of aluminium are used in this study to overcome this issue, which is discussed in more detail below. The experimental findings demonstrated that the presence of twisting tape inserts expedited the transferring of heat inside the dormant zone; further, it assisted in maintaining a consistent temperature throughout the tube during the testing period. As a result of the use of twisting tape inserts, the water temperature at the dormant zone was raised to 71 °C, which was 39 °C higher than the temperature at the active region when the tapes were not utilized. The twisted tapes also increased the mean tube water temperature through the highest value of 11 °C.

Previous Next

Keywords

Solar water heating; Twisted tapes; Solar energy; Evacuated tube; Water temperature

Special issue articles Recommended articles

Cited by (0)

C 39

ScienceDirect

Materials Today: Proceedings

Volume 62, Part A, 2022, Pages 5314-5318

Investigation on wear characteristics of Al 2219/Si3N4/Coal bottom ash MMC

K. S. Vijayan [a] T. Arumugam [a] V. Mohanavel [b] S. Kalaiselvan [c] C. Ramasamudram [d] B. Boopathi Rajaram [e] Ravi Sahlajan [f] S. Suresh kumar [a] ✉

[a] Department of Mechanical Engineering, Vel Tech Rangarajan Dr.Sagunthala R&D Institute of Science and Technology, Chennai, Tamil Nadu, India
[b] Department of Mechanical Engineering, CMR Institute of Technology, Bengaluru, Karnataka, India
[c] Centre for Materials Engineering and Regenerative Medicine, Bharath Institute of Higher Education and Research, Tambaram, Selaiyur, Chennai 600073, Tamil Nadu, India
[d] Department of Mechanical Engineering, Sethu Institute of Technology, Virudunagar, Tamil Nadu, India
[e] Department of Mechanical Engineering, Gokaraju Rangaraju Institute of Engineering and Technology, Hyderabad, Telangana 500090, India
[f] Department of Mechanical Engineering, Panimalar Polytechnic College, Chennai 600027, Tamil Nadu, India

Available online 30 April 2022, Version of Record 23 June 2022.

Show less

Outline Share Cite

https://doi.org/10.1016/j.matpr.2022.04.425

Abstract

High-energy ball milling is used to create nanostructured materials from coal bottom ash (CBA) and silicon nitride (Si_3N_4). 36 h of ball milling coal bottom ash reduced it to 51.3 nm, while silicon nitride was reduced from 61.2 nm to 29 nm. Metal Matrix Composites (MMC) is fabricated through liquid stir method. The composites wear rate went up with nano coal bottom ash and nano silicon nitride reinforcements due to clustering, as well as a lack of interfacial connection between the base material and hybrid reinforcements employed. Increased frictional drive causes magnified debonding and easy exclusion of composite particles, accelerating the amount of wear. The friction coefficient reduces in all composite configurations as the average load increases.

Previous Next

Keywords

Al 2219 Coal bottom ash; Metal Matrix Composite; Nano powder; Reinforcement; Silicon Nitride; Wear rate; Wear load

Special issue articles Recommended articles

Cited by (2)

Tribological Behavior of AA7075 Reinforced with Ag and ZrO_2 Ceramic Particles Composites

2022, Advances in Materials Science and Engineering

ScienceDirect

c 40

Materials Today: Proceedings

Volume 66, Part 3, 2022, Pages 743-745

Investigation on corrosion and tensile Characteristics: Friction stir welding of AA7075 and AA2014

V.P.Lalitha [a], P.G.Venkatesan [b], Mohamed Ali Saleh [c], Mani Pandian [d], Gaur Subhash T.S. Boopathi [e] [f]

[a] Department of Mechanical Engineering, Nandha Engineering Institute of Technology, Salem, Tamil Nadu 638455, India
[b] Department of Mechanical Engineering, Hanamaya Institute of Technology, Hanamaya University, Ethiopia
[c] Department of Mechanical Engineering, Vignan's Lara Institute of Technology and Science, Guntur 522213 Andrapradesh, India
[d] Department of Mechanical Engineering, Erode Sengunthar Engineering College, Perundurai, Erode Tamil Nadu 638057, India
[e] Mechanical Engineering, Gokaraju Rangaraju Institute of Engineering and Technology, Hyderabad, Telangana 500090, India
[f] Department of Robotics and Automation, Muthayammal College of Engineering, Rasipuram, Namakkal, Tamil Nadu 637408, India

Available online 15 April 2022, Version of Record 8 September 2022

Show less

Outline | Share | Cite

https://doi.org/10.1016/j.matpr.2022.04.037

Abstract

In this article, the corrosion and tensile strength characteristics of Friction-stir-Welding(FSW) of AA7075 and AA2014 have been investigated. These Aluminium alloy materials have widely been used in making automotive, aerospace, and nautical industrial components. The nine specimens have been made by tool rotational speed and welding speed using full factorial design. The optimum tool rotational speed and welding speed were predicted using statistical analysis for both maximum tensile strength and minimum corrosion rate. The minimum corrosion rate (865.3 miles/year) was obtained from maximum speed of tool rotation (1400 rpm) and welding speed (60 mm/min); maximum tensile strength (194. 6 MPa) has been attained by moderate tool rotational speed (1200 rpm) and welding speed (45 mm/min). The specimens for the tensile and corrosion tests were prepared with optimum settings. The microstructure of corroded surface had been illustrated using scanning electron microscopy (SEM) images.

Previous Next

Keywords

Corrosion rate; Tensile stress; Microstructure; AA7075; AA2014

Cited by (2)

An experimental study on the hardness and wear rate of carbon/ride coated stainless steel

2022, Materials Today: Proceedings

Show abstract

C 41

ScienceDirect

Materials Today: Proceedings

Volume 66, Part 3, 2022, Pages 665-669

Experimental investigation of Machining of stellite alloy

N. Mary Jasmin [a], Y. Anil Reddy [b], A. Arul Sultan [c], Apparao Nakhil [d] & [illegible] Venkata Suresh [d], S. Sampath Reddy [d], Ram Subbiah [d]

- [a] Department of Mechanical Engineering, Tirumala Engineering College, Narasaraopet, Andhrapradesh, India
- [b] Department of Mechanical Engineering, Hyderabad Institute of Technology and Management, Hyderabad, India
- [c] Department of Aeronautical Engineering, Noorul Islam Centre for Higher Education, Kumaracoil, Tamilnadu, India
- [d] Department of Mechanical Engineering, Gokaraju Rangaraju Institute of Engineering & Technology, Hyderabad, Telangana, India

Available online 6 April 2022, Version of Record 8 September 2022

Show less

Outline | Share Cite

https://doi.org/10.1016/j.matpr.2022.03.659

Highlights

- In recent days, the applications of advanced alloys in manufacturing industries have been increased due its superior substance properties.
- Stellite alloy comes under the category of cobalt-chromium super alloys. In this paper the machinability performance of stellite using different unconventional machining process such as spark erosion (SE) and laser beam (LB) technique were discussed.
- The fine holes were produced on the surface of the stellite alloy. The comparisons of rate of material removal (RMR) were analyzed using different input constrains.
- The interaction and contribution of process factor on material removal rate were determined.

Abstract

In recent days, the applications of advanced alloys in manufacturing industries have been increased due its superior substance properties. Stellite alloy comes under the category of cobalt-chromium super alloys. In this paper the machinability performance of stellite using different unconventional machining process such as spark erosion (SE) and laser beam (LB) technique were discussed. The fine holes were produced on the surface of the stellite 1 alloy. The comparisons of rate of material removal (RMR) were analyzed using different input constrains. The interaction and contribution of process factor on material removal rate were determined. Finally, it was concluded that laser machining was provided high metal removal than spark erosion process. More than 25% of metal removal was achieved through laser machining process.

Previous Next

Keywords

C 42

ScienceDirect

Materials Today: Proceedings

Volume [illegible], Part [illegible], 2022, Pages [illegible]

Optimal parameters of microwave sintering process on nickel based composite

M. [illegible] [illegible] | Venkatesh [illegible] [illegible] [illegible] [illegible], S. Sampath Reddy [illegible], [illegible]

a Department of Automobile Engineering, Dr.Mahalingam College of Engineering and Technology, Pollachi, Tamil Nadu, India
b Department of Mechanical Engineering, PSNA College of Engineering and Technology, Dindigul, Tamil Nadu, India
c Department of Mechanical Engineering, [illegible] Engineering College, Narasaraopet, Andhrapradesh, India
d Department of Mechanical Engineering, Gokaraju Rangaraju Institute of Engineering & Technology, Hyderabad, Telangana, India
e Department of Mechanical Engineering, Kumaraguru College of Technology, Coimbatore, Tamil Nadu, India

Available online 9 April 2022, Version of Record 6 September 2022

Show less ^

Outline | Share Cite

https://doi.org/10.1016/j.matpr.2022.[illegible]

Highlights

- Microwave sintering process is the most economical and feasible technique to fabricate composite with superior quality of products.
- Nickel, aluminium and titanium alloy were reinforced with silicon carbide particles.
- The different microwave sintering constraints like sintering temperature, heating rate and hold time were considered to fabricate the composite.
- Taguchi approach was used to optimize the microwave sintering process factor.

Abstract

Microwave sintering process is the most economical and feasible technique to fabricate composite with superior quality of products. Nickel, aluminium and titanium alloy were reinforced with silicon carbide particles. The different microwave sintering constraints like sintering temperature, heating rate and hold time were considered to fabricate the composite. The fabricated specimens were processed under the evaluation of tensile strength and hardness properties. Taguchi approach was used to optimize the microwave sintering process factor. The parametric effect on tensile strength and hardness were analyzed through contour plot and variance analysis. Tensile strength of 360 MPa was attained at sintering temperature of 1400 °C, holding rate of 20 °C/min and holding time of 30 min. It was observed that sintering temperature has produced 87.04% of effect on tensile strength.

< Previous

Next >

Keywords

Microwave sintering; Nickel; Titanium; Tensile strength; Taguchi technique

Available online at ScienceDirect

Materials Today: Proceedings

journal homepage: www.elsevier.com/locate/matpr

The study of mechanical and microstructural properties of the AZ31 magnesium alloy using constrained groove pressing at elevated temperature: A review

Saikiran Sama*, Sashank Babbepalli, Akhil Budime, Tanya Buddi

Mechanical Engineering Department, CBIT, Hyderabad 500075, India

ARTICLE INFO

Article history:
Available online 29 April 2022

Keywords:
Mechanical properties
Constrained groove pressing
AZ31 magnesium
Severe plastic deformation

ABSTRACT

AZ31 magnesium alloy is used in different industries such as defense, aerospace, and biomedical applications, due to its high strength-to-weight ratio and it has a capability to expand its applications by improving its characteristics. Constrained groove Pressing (CGP) has a capability to produce ultrafine grained sheet (UFG) metals primarily based totally on severe plastic deformation, which can improve mechanical properties. Study on CGP of AZ31 magnesium alloy which has poor formability and low ductility at room temperature (RT), is still a challenge. The goal of this paper is to analysis the effects of constrained groove pressing (CGP) on the characteristics and applications of the AZ31 magnesium alloy at high temperatures. After the CGP process most of the specimens mechanical properties like strength and hardness had improved. Microstructural changes and mechanical properties are also varying with the number of passes.

Selection and peer-review under responsibility of the scientific committee of the International Conference on Materials, Processing & Characterization.

1. Introduction

Nowadays, in automobile and aerospace there is a necessity of utilizing of lightweight material for fuel consumption and reducing emission [1–3]. As magnesium is the commonly used lightest material, its alloys exhibit great potential in reducing weight since it has high specific strength and low density (1.74 g/cm³) that is almost three times less dense compared to titanium [4]. One of the major commercial applications of magnesium alloy is used in aircraft industry. It is used to manufacture the brackets. In automobile application, it is used to manufacture the steering wheel, seat frame, transmission case, intake manifold, and many more. In biomedical engineering, magnesium alloy can be used as metallic biomaterial [5]. And many more applications of magnesium alloys are restricted due to their low density at room temperature (RT) and poor formability because of the hexagonal close pack (HCP) structure [6]. Many experimentations were performed to improve and enhance the formability and ductility of magnesium alloy. It is well known that ultrafine grain (UFG) refinements can improve the ductility and strength of the material [11]. Ultrafine grain refinement can be achieved by severe plastic deformation (SPD) method [7]. Material produced by SPD improves tensile strength as well as other mechanical qualities such as super plasticity, fatigue resistance and fracture behaviour [8–10].

Severe plastic deformation process such as CGP have evolved into one-of-a-kind techniques for creating nano ultrafine grain structure for variety of metallic materials in recent years [11]. CGP can efficiently reduce grain size down to sub-micrometer level and even to nanometer level in some cases [12]. Grain refinement improves the material strength and strength to weight ratio, which are important characteristics [13]. Ultrafine grain material have more strength at RT and can be used in variety of applications and can be used in super forming operations at high temperatures. In the CGP process, a sample is repeatedly pressed beneath grooved and flat dies to produce orthogonal shear deformation [14]. Steps involved in the process is shown in below Fig. 1.

A pair of asymmetrically grooved dies are fixed to the punch rods. There are four steps in CGP process. Fig. 1a, b] shows the first step. A sheet is placed in between grooved dies and pressing is performed so that the gap between the dies is same as the thickness of the sample. When groove pressing operation is performed the sample takes the shape of the grooves. In the second step (Fig. 1c), the

* Corresponding author.
E-mail address: saikiranmech@cbit.ac.in (S. Sama), sashankbabbepalli@gmail.com (S. Babbepalli), akhilbudime@gmail.com (A. Budime), tanyabuddi@gmail.com (T. Buddi).

https://doi.org/10.1016/j.matpr.2022.04.429
2214-7853/
Selection and peer-review under responsibility of the scientific committee of the International Conference on Materials, Processing & Characterization

C44

Materials Today: Proceedings 5 (2018) 4481–4491

Contents lists available at ScienceDirect

Materials Today: Proceedings

journal homepage: www.elsevier.com/locate/matpr

Study on mechanical properties of AZ31-Mg alloy and effect of deformation using constrained groove pressing – A review paper

M. Akhil Sharma *, Ch. Shravan Kumar, M. Nathan Kunal Reddy, B. Tanya

Department of Mechanical Engineering, Vaagdevi Vaagdevi Institute of Engineering and Technology, Hyderabad, Telangana 502501, India

ARTICLE INFO

Article history
Available online 25 May 2018

Keywords
Mechanical properties
Constrained groove pressing
AZ31 mag alloy
Ultra fine grain structure

ABSTRACT

Constrained groove pressing (CGP), an intensive plastic straining process, is designed to fabricate plate-shaped ultra-fine grained metallic materials without modifying their basic dimensions. CGP works on the concept that a material is exposed to incremental shear deformation under plane strain deformation by using asymmetric alternate pressing. The constrained groove pressing (CGP) method is used on AZ31 Magnesium alloy sheets in this study as a severe plastic deformation (SPD). This approach can be a possibility to increase the mechanical properties of the material for wider scope of applications with improved mechanical properties. CGP is generally carried out at three different elevated temperatures.

Selection and peer-review under responsibility of the scientific committee of the International Conference on Materials, Processing & Characterization.

1. Introduction

Magnesium alloys are gaining a lot of demand for research in recent times because of its remarkable properties in contrast to its physical properties. They have very high stiffness and high specific strength, which is aided by its low density and great damping, these light weight alloys are can become the solution for many engineering problems we face today. Aluminium Steel and sometimes even cast iron is infused with magnesium to form alloys in various applications ranging from automobiles to high speed jets in aerospace sector, which makes the elements lighter and hence increasing their efficiency [1] (see Table 1).

However, due to multiple casting defects and poor mechanical characteristics of the casted material, typical casting magnesium alloys are unable to fulfil increasing industrial demands. Wrought magnesium alloys, which are made using plastic processing methods such as rolling, extrusion and forging, have gotten a lot of interest because of their superior mechanical properties. As a result, sheet forming processes involving wrought magnesium alloys can be viable alternatives, resulting in higher productivity and final strength [2]. Severe plastic deformation (SPD) procedures are carried out to lower the grain length of sheet and bulk metals and bring ultrafine grained metals. The SPD techniques include structured materials are Accumulative roll bonding, Asymmetric rolling, High pressure torsion, Equal channel angular protrusion Constrained groove pressing etc.

Constraint groove pressing is a severe plastic deformation technique, a material is subjected to repetitive shear deformation and straightened with a help of dies, without altering the initial dimensions, this comprises of two types of dies one is of grooved type and later with flat type. This is a new technique where a lot of research is going on with varied parameters and materials, performing at high temperatures which results in insertion of the microstructure which in turn has its implications on the grain size. With the arrangement of alternate pressing the material is subjected to shear deformation and plane strain conditions [4].

The primary concern about CGP process aroused in recent years, as this process has the capability to improve the grain structure and get very high ultrafine grain structure of the material. Parameters involved in the CGP are the groove angle, groove width, and groove height. The groove angle variation is observed a very little in constraint manner which affects the shear

2. Theory and procedure

The illustration of the CGP process is shown in Fig. 1. says that a complete pass of CGP has 4 stages. The upper and bottom dies were machined with a sequence of grooves whose depths are equal to the slope width, as shown in Fig. [3]. creating a 45° incline on the groove. Grooves on the top and lower halves of the assembly are asymmetric. During CGP, the thickness of the treated sheet

* Corresponding author.
E-mail address: akhil.sharma1729@gmail.com (M. Akhil Sharma).

https://doi.org/10.1016/j.matpr.2018.04.161
2214-7853/
Selection and peer-review under responsibility of the scientific committee of the International Conference on Materials, Processing & Characterization.

ScienceDirect

Materials Today: Proceedings

Volume 62, Part 6, 2022, Pages 3638-3641

Experimental studies and optimization of WEDM process in machining of Nitronic 60 using zinc coated copper wire

K. Satyanarayana [illegible], B. Sai Harshavardhan [illegible], Yaswanth Krishna [illegible]

Show more

Outline Share Cite

https://doi.org/10.1016/j.matpr.2022.04.[illegible]

Abstract

Nitronic 60 is an alloy steel that can be machined using an unconventional technique. Machining of Nitronic 60 is not an easy task as the surface roughness of the material should be very low and so is the Material Removal Rate. To Enhance the surface roughness and Material Removal Rate Wire EDM process is chosen as it reduces the time and complexity. For the present study Nitronic 60 of 25 mm diameter bar and zinc coated copper wire of 0.25 mm diameter was used for machining on Wire EDM. The experiment layout is based on Taguchi's L9 orthogonal array, and the experiments will be carried out by considering the Machining parameters like current, voltage, Pulse ON and Pulse OFF, and Material Removal Rate (MRR) and Surface roughness (SR) are considered for evaluation and optimised. It was observed from the study that Optimum condition for Material Removal Rate is current at level 3 (200 A), voltage at level 3 (20 V), pulse ON at level 3 (120 µs), and pulse OFF at level 1 (50 µs) and for Surface roughness current at level 3 (200 A), voltage at level 1 (10 V), pulse ON at level 1 (100 µs), and pulse OFF at level 2 (55 µs). additionally, from ANOVA analysis it was observed that for roughness interaction of Current*Pulse ON time with 25.53% for MRR current with 29.66% is most contributing factor.

Previous Next

Keywords

Wire EDM; Material Removal Rate; Surface Roughness; S/N Ratio; Taguchi

Special issue articles Recommended articles

Cited by (0)

ScienceDirect

C 46

Materials Today: Proceedings

Volume 66, Part 1, 2022, Pages 1255-1259

Investigating the performance of a NMPCM integrated heat sink for chipset cooling

J. Murali Krishna [a], A. Sree Sastha [b], R. Suresh [c], R. Gowrishan [b], S. Mohammed Nasrulla [c], Kaushik A. Josh [d], Ravi Subbiah [e] [f] [g]

[a] Department of Mechanical Engineering, Holy Mary Institute of Technology and Science, Hyderabad - 501301, Telangana, India
[b] Department of Mechanical Engineering, Saveetha Engineering College, Saveetha Nagar, Chennai - 602105, Tamil Nadu, India
[c] Department of Mechanical Engineering, Annamalai University, Annamalai Nagar, Chidambaram - 608002, Tamil Nadu, India
[d] Department of Mechatronics Engineering, Sri Krishna College of Engineering and Technology, Coimbatore - 641008, Tamil Nadu, India
[e] Department of Mechanical Engineering, PSNA College of Engineering and Technology, Dindigul - 624622, Tamil Nadu, India
[f] Department of Chemistry, GKV Arts and Science College, Jamnagar - 361008, Gujarat, India
[g] Department of Mechanical Engineering, Gokaraju Rangaraju Institute of Engineering and Technology, Hyderabad - 500090, Telangana, India

Available online 24 May 2022. Version of Record 8 September 2022.

Show less

Outline | Share | Cite

https://doi.org/10.1016/j.matpr.2022.05.121

Abstract

The demand for effective cooling solutions is critical for electronic chip sets, since it improves the operation and longevity of electronic equipment. The heat removal from a finned heat sink (HS) integrated computer processor with the aid of a nano-mixed PCM (NMPCM) is investigated in this work. The heat generation of the chipset is replicated with the aid of a plate heater and the plate-finned heat sink is studied under three conditions. The first configuration is the plate-finned heat sink containing no PCM (FHS), the second configuration is the HS containing the plain PCM (P-FHS), and the last configuration is the HS containing a nanoparticle mixed PCM (NP-FHS). The NMPCM was prepared through the careful mixing of 0.5% nano-titania within the paraffin. The results showed that the assimilation of PCM and NMPCM with the finned-HS (NP-FHS) was verified to be effective in reducing the heating rate of the chip sets, comparing to the FHS and P-FHS configurations. Explicitly, the NMPCM had assisted to postpone the baseline temperature of the HS by 32 min and 14 min, respectively at the heating rate of 3.5 kW/m^2 and 4.5 kW/m^2, respectively.

Previous Next

Keywords

Nano-PCM; Electronic cooling; Heat sink; Nano-titania; Paraffin

Special Issue articles Recommended articles

Cited by (0)

ScienceDirect

Materials Today: Proceedings

Volume 65, Part 8, 2022, Pages 3221-3227

Improving the productivity in carton manufacturing industry using value stream mapping (VSM)

V.N. Dinesh [a], B. M. Shafeeq [b], M. Vijay [c], R.C. Vijay Mohan [c], Rajesh Kumar Sambathkumar [a], Ram Subbiah [a]

[a] Department of Mechanical Engineering, KPR Institute of Engineering and Technology, Coimbatore 641407, Tamil Nadu, India
[b] Department of Mechanical Engineering, College of Engineering, Jazan University, Saudi Arabia
[c] Department of Mechanical Engineering, Gokaraju Rangaraju Institute of Engineering and Technology, Hyderabad 500090, Telangana, India

Available online 20 May 2022, Version of Record 8 September 2022.

Abstract

Almost every manufacturing business has been attempting to become 'lean' in recent years. Researchers and practitioners are under pressure to adopt new methods and strategies for dealing with diverse wastes as a result of a desperate hurry to be lean and responsive in order to deliver value to customers. One such process which helps the organization in achieving productivity is VSM. VSM is a tool to identify value and non-value-added activities in the process. The carton manufacturing industry employs VSM to create a lean manufacturing framework. VSM entails mapping the industry's current process and evaluating it for waste and bottlenecks by calculating value-added and non-value-added time. Based on the analysis of bottlenecks, solutions are suggested and a future state map is created. After then, metrics like cycle time and lead time are determined for the current and future state maps. The cycle time for each procedure is lowered as follows, based on the created maps. The productivity in corrugation, pasting, punching, and stitching increased by 5.83%, 11%, 11.05%, and 5.82%, respectively.

Previous Next

Keywords

Value stream mapping; Cycle time; Bottle necks; Value added activity; Non-value-added activity; Lean

ScienceDirect

Materials Today: Proceedings

volume 66, Part 1, 2022, Pages 1144-1147

Optimization and electro chemical grinding surface investigation on eglin steel

G.R. Kannan [a,*], R. Vijayakumar [b], T.T.S. Senthil [c], Prashant Sunagar [d], R. Karthik Kumar [e], Lokesh Parida [f], Ram Subbaiah [g]

[a] Department of Mechanical Engineering, PSNA College of Engineering and Technology, Dindigul, Tamilnadu, India
[b] Department of Chemistry, Panimalar Engineering College, Chennai, Tamilnadu, India
[c] Department of Mechanical Engineering, Panimalar Engineering College, Chennai, Tamilnadu, India
[d] Department of Civil Engineering, M S Ramaiah Institute of Technology, Bengaluru, Karnataka, India
[e] Department of Mechanical Engineering, St. Joseph's Institute of Technology, Chennai, Tamilnadu, India
[f] Department of Civil Engineering, Sharda Noida University, Greater Noida, Uttar Pradesh, India
[g] Department of Mechanical Engineering, Gokaraju Rangaraju Institute of Engineering and Technology, Hyderabad, Telangana, India

Available online 20 May 2022. Version of Record 6 September 2022.

https://doi.org/10.1016/j.matpr.2022.04.943

Highlights

- The present investigation is used to analyze the surface of ECG of eglin steel.
- The grinding wheel speed, voltage and flow rate are used to evaluate the rate of metal removal.
- The desirable rate of metal removal was found through taguchi technique.
- The parametric effect and their role were investigated through variance analysis.
- The grinding surface of the eglin steel was analyzed through atomic force microscopy.
- The surface texture was also studied through surface toughness plot.

Abstract

Surface technology is playing an essential role in metal industries to enhance the surface texture. The present investigation is used to analyze the surface of electro chemical grinding (ECG) of eglin steel. The methodology of the present work is to optimize the ECG process factors and analyze the machined surface. The grinding wheel speed, voltage and flow rate are used to evaluate the rate of metal removal. The desirable rate of metal removal (RMR) was found through taguchi technique. The parametric effect and their role were investigated through variance analysis. The grinding surface of the eglin steel was analyzed through atomic force microscopy. The surface texture was also studied through surface roughness plot. The optimal metal removal rate was performed at 15 V of voltage, 9 LPM of electrolyte flow rate and grinding wheel speed of 1400 rpm. The effect of voltage, flow rate and grinding wheel speed are 75.10%, 21.17% and 2.75% respectively. The average roughness of the electro chemical grinding surface is 24.15 nm. It was concluded that surface obtained from ECG was better than other process.

ScienceDirect

C 49

Materials Today: Proceedings

Volume 66, Part 1, 2022, Pages 1319-1323

Investigating the effect of nanoclay content on the mechanical characteristics of natural fiber epoxy composite

Ankit [a], Rajneesh Sharma [b], Ganesh Kumar Sharma [c], Rajeev Agarwal [c], Mul Lal Bishnoi [c], [d], Ram Subhash [e], Manoj Kumar [f]

[a] Department of Mechanical Engineering, Government Engineering College, Jhalawar 326023, Rajasthan, India
[b] Department of Civil Engineering, Government Engineering College, Jhalawar 326023, Rajasthan, India
Department of Mechanical Engineering, M.J.V. Textile & Engineering College, Bhilwara 311001, Rajasthan, India
[c] Department of Basic & Applied Sciences, M.J.V. Textile & Engineering College, Bhilwara 311001, Rajasthan, India
[d] Department of Mechanical Engineering, Gokaraju Rangaraju Institute of Engineering and Technology, Hyderabad 500090, Telangana, India
[e] Department of Mechanical Engineering, KPR Institute of Engineering and Technology, Coimbatore 641407, Tamil Nadu, India

Available online 20 May 2022, Version of Record 8 September 2022.

Show less

Outline | Share | Cite

https://doi.org/10.1016/j.matpr.2022.05.139

Abstract

The natural fibers have been recognized as the eco-friendly alternative for the synthetic fibers while preparing epoxy based polymer composite materials. Further, the nano-reinforcements have been acknowledged to be the better solution for enhancing the mechanical characteristics of the natural fiber based polymer composites. In this context, the present work investigates the influence of nanoclay reinforcement in luffa/epoxy (LE) polymer composite material at different loading fractions (0%, 1.0%, 2.0%, and 3.0%). The results revealed that the addition of nanoclay till 2.0% in LE composites had become more beneficial in terms of improvement in mechanical characteristics. However, the addition of nanoclay after 2.0% had ended-up in adverse effects due to the agglomeration of the nanoparticles. The highest percentage improvement in tensile, compression and flexural properties was observed as 20.0%, 18.69%, and 21.44%, respectively with the addition of 2.0% of nanoclay in LE composites. The percentage of enhancement in tensile, compression and flexural properties was suppressed by 6.44%, 8.5%, and 8.32%, respectively with the addition of 3.0% nanoclay comparing to the previous fraction.

Previous

Next

Keywords

Epoxy; Luffa fiber; Nanoclay; Mechanical characteristics; Composite

Special issue articles Recommended articles

C 5D

Materials Today: Proceedings

Volume 62, Part 6, 2022, Pages 4509-4514

Analysis of the effect of the process parameters on the mechanical strength of 3D printed and adhesively bonded PETG single lap joint

A. Vamshinath, A. N. Nitesh Kumar, P. Tarun Kumar, D.S. Nagaraju, M. Suresh, Ram Subbaiah

Gokaraju Rangaraju Institute of Engineering and Technology, Hyderabad, TS, India

Available online 25 May 2022. Version of Record 23 June 2022.

Abstract

The current study deals with the effect of 3D printing parameters on the strength of 3d printed and adhesively bonded PETG single lap joints. Polyethylene terephthalate glycol (PETG) is used to print standard specimens with different printing parameters (raster angle, raster width, and layer thickness) using fused deposition modelling (FDM) process. By conducting number of tensile tests on the single lap joint specimens, the effect of abovementioned 3D printing parameters on the mechanical behaviour of PETG joints is determined. Furthermore, a computational investigation was carried out to confirm the experimental results and gain a better understanding of the fracture behaviour of these types of joints. The effect of above mentioned 3D printing parameters in stress distribution and failure behaviour of the joints are examined and reported. Taking into consideration of a growing interest in FDM 3D printing technology in manufacturing and many other applications of adhesively bonded joints, obtained results are useful for future studies on new designs of 3D printed adhesively bonded products with a greater strength and improved structural performance.

Previous

Next

Keywords

Polyethylene terephthalate glycol; Raster angle; Raster width; Layer thickness; Adhesively bonded; 3D printing

Special Issue articles Recommended articles

Materials Today: Proceedings

Volume 62, Part 5, 2022, Pages 3069-3077

Achieving safety and weight reduction in automobiles with the application of composite material

N. Satyanarayana, K. Sai Kiran, S. Gopi Nookaraju, D. Siva Nagaraju

Show more

https://doi.org/10.1016/j.matpr.2022.03.516

Abstract

In the present scenario of cutthroat competition in automobile industry, the importance for sleek and efficient models of automobiles with aesthetics and passenger comfort is paramount. In addition to the comforts like air conditioning and spaciousness etc., the 'suspension' is also significant in the selection of an automobile. The main focus of this paper is on weight reduction by replacing conventional spring steels with composite materials. A successful attempt has been made at Gokaraju Rangaraju Institute of Engineering and Technology, Hyderabad laboratories to fabricate the composite leaf spring, which is having equivalent properties of Maruti800 car leaf spring. The transverse failures in steel leaf springs lead to rear axle dislocation. This problem could be successfully eliminated with composite leaf springs since the general failure in unidirectional reinforcement composites is in longitudinal direction. This paper suggests the design improvements in this direction.

Previous Next

Keywords

GFRP: Glass Fiber Reinforced plastic; Stiffness Resistance to deflection measured as load per deflection. Young's Modulus: Ratio of linear stress to linear strain with in elastic limit. Shear Modulus: Ratio of shear to shear strain. Poisson's Ratio: Ratio of lateral strain to linear strain

ScienceDirect

Materials Today: Proceedings

Volume [illegible], Part [illegible], [illegible], Pages [illegible]

Modelling and analysis of aircraft radome using different materials

M. Pavan Chandra, [illegible], P. Nikhilesh Goud, N. Sateesh

Show more

Outline | Share | Cite

[illegible]

Abstract

Radome is one of the most important part in aircraft. Radome protects the antenna which transmits and receives the signal in the form of radio waves. These radio waves are helpful in finding the location of aircraft. We can also say that radome is a structural protection cover for antenna as it protect antenna from environmental influences. Radome is constructed in such a way that it is transparent to the radio waves. The radome should be manufactured by a material which minimises the attenuation of signals transmitted or received by the antenna. For different aircrafts such as commercial planes, fighter jets etc. The shape and size of radome are different. In this project we have modelled different radomes in solid works software and analysis is done in the ansys software. The materials selected based on the strength and other good material properties. The different materials taken in this project are Kevlar composite, Fiberglass composite, Silicon nitride. Structural analysis and thermal analysis is performed to get the optimum suited material for the radome and to decide the best radome.

Previous   Next

Keywords

Aircraft radome; Ansys; Solid works

Cited by (0)

253

ScienceDirect

Materials Today: Proceedings

Volume 62, Part 8, 2022, Pages 4310-4315

Investigations on mechanical properties of jute fiber and epoxy resin composites with titanium oxide

M.S. Preethi, ... N. Saravan[illegible]

Show more

Outline | Share Cite

https://doi.org/10.1016/j.matpr.2022.05.[illegible]

Get rights and content

Abstract

The composite material is made up of a combination of materials with distinct chemical and physical properties. The utilization of jute fiber and epoxy resin composites is very extensive in the fields of aircraft and automobiles. These composites have a huge strength-to-weight ratio. Even so, modern applications require a significant increase in strength. The addition of Nano fillers had resulted in considerable changes in the mechanical properties of the composite. The present work aims at finding out the effects on mechanical properties of composites due to the addition of titanium oxide.

The specimens are prepared for tensile testing and hardness testing according to the ASTM standards by Hand Layup process with the combinations of jute fiber and epoxy resin. The composite is prepared by three variables with (0%,5%,10%)filler and three orientations(0°-90°,45°-45°, random). The specimens are tested on the Universal Testing Machine of model UTE-10 and shore hardness-A' the comparison process is laid down.

Previous Next

Keywords

Jute fiber composite; Strength to weight fraction; Titanium oxide; Hand layup process; Tensile test; Hardness test

Special issue articles Recommended articles

Cited by (1)

Tests of Physicochemical and Mechanical Strength Properties of Polymer Composites on an Epoxy Resin Matrix, Modified by a Constant Magnetic Field

2022, Materials

C56

ScienceDirect

Materials Today: Proceedings

Volume 62, Part 6, 2022, Pages 3963-3967

Effect of different reinforcements on aluminium composite properties – a review

K. Sunil Kumar Reddy [illegible], B.B. Chitra Lekha, Kota Uma Sakshi, Manoj Shreeya Chauhan, R. Karthikeyan, S. Aparna

Mechanical Engineering Department, GRIET, Hyderabad 500090, India

Available online 7 May 2022, Version of Record 23 June 2022.

Show less ^

Outline | Share Cite

https://doi.org/10.1016/j.matpr.2022.04.572

Abstract

In the automotive and aerospace industries, there has been a growth in demand for light-weight materials with high strength, good wear, and thermal qualities in recent years. Although traditional metals such as aluminium are preferred, aluminium alloys are unable to meet all requirements. To achieve the desirable qualities, composites are employed. To increase the material characteristics, the Aluminium Metal Matrix (AMM) is reinforced with other materials. To achieve the necessary qualities, more than one reinforcement might be added. Simple composites and hybrid composites can be employed in these applications according to their requirements. The impacts of different reinforcements added to an aluminium metal matrix, such as SiC, fly ash, Aloe Vera, rice husk, and so on, are discussed in this article. The reinforcements considered are low cost and readily available, and they have a significant impact on the metal characteristics of composites. The composites are made using simple manufacturing techniques.

< Previous

Next >

Keywords

AMM; Simple composites; Hybrid composites; Reinforcement; Hardness; Tensile strength; Impact strength

Special issue articles Recommended articles

Cited by (2)

Investigations on mechanical properties of aluminium alloy Al6061 hybrid metal matrix composite
2022, Materials Today: Proceedings
Show abstract ∨

INVESTIGATION ON CORROSION AND WEAR PROPERTIES OF Al-7075/TiC COMPOSITES FABRICATED BY STIR CASTING ROUTE
2022, Metallurgical and Materials Engineering

Materials Today: Proceedings

[illegible], 2022, Pages [illegible]

Experimental investigation on aluminium alloy AA6061 and AA8011 using friction stir welding

[illegible]

Show more

Outline | Share | Cite

[illegible]

Abstract

Friction Stir Welding (FSW) is a solid-state joining process that involves joining of metals without fusion or filler materials. The process is particularly applicable for aluminum alloys but can be extended to other products also like steels. The project was mainly founded by National Technological Agency of Finland. The friction stir welded joints of austenitic and ferrite stainless steels were implemented at different rotational speeds 500 – 1100 rpm. The results showed that increasing rotating speed enhanced heat input and material movement in the welded zone, and the nugget zone had a blocky, laminated, and vortex structure of austenite and ferrite. In this investigation, different combinations of tool rotation speeds and tool transverse speeds are used to connect different types of stainless steel. Following an overview of the macroscopic characteristics, the micro structure development and associated hardness tensile and impact results and distributions are discussed.

Previous

Next

Keywords

FSW, 6061 AND 8011 ALUMINIUM ALLOYS, HARDNESS, TENSIL, IMPACT, SEM FACTOGRAPHY

[illegible]

Cited by (0)

C 58

ScienceDirect

Materials Today: Proceedings

Volume 56, Part 3, 2022, Pages 1406-1410

Experimental investigation of the solar distiller using nano-black paint for different water depths

M.S. Chandra [a], J. Samson Isaac [b], Joeson Daniel [c], K. Kathiresan [d], C.L. Mathis [e], E. Fantin Irudaya Raj [f], Ilham Sobsion [g]

[a] Department of Electrical and Electronics Engineering, KPR Institute of Engineering and Technology, Arasur, Coimbatore, Tamilnadu, India
[b] Department of Biomedical Engineering, Karunya Institute of Technology and Sciences, Coimbatore, Tamilnadu, India
[c] Department of Electronics and Instrumentation Engineering, National Engineering College, Kovilpatti, Tamilnadu, India
[d] Department of Physics, PSNA College of Engineering and Technology, Dindigul, Tamilnadu, India
[e] Department of Mechanical Engineering, Rajalakshmi Engineering College, Chennai, Tamilnadu, India
[f] Department of Electrical and Electronics Engineering, Dr. Sivanthi Aditanar College of Engineering, Tiruchendur, Tamilnadu, India
[g] Department of Mechanical Engineering, Gokaraju Rangaraju Institute of Engineering and Technology, Hyderabad 500090, Telangana, India

Available online 9 December 2021, Version of Record 11 April 2022.

Show less ^

Outline | Share Cite

https://doi.org/10.1016/j.matpr.2021.11.449

Abstract

World nations are continuously thriving to find a prompt solution to the scarcity of potable water. In recent years, solar distiller has been suggested as a feasible technology for tapping drinkable water from saline water. In a solar distiller, the absorber surface has a significant impact on the solar distiller's performance. This work presents an attempt to increase the performance of a traditional solar distiller by improving the thermal conductivity of the absorber surface through spraying a nano-black paint over its surface. In this study, two distillers of identical size were used. One solar distiller was made by painting the absorbing plate with normal black paint and labelling it as a traditional solar distiller (TSD). Another distiller was prepared by painting the absorber of the traditional distiller with nano-black paint (TSD-Nano). The tests had been carried out over two days, with water levels of 0.1 cm and 0.2 cm in both solar distillers, respectively. For the fabrication of TSD-Nano, a nano-paint was prepared by thoroughly mixing 1.0 vol% of nano-CuO particles with black paint. The results showed that a coating of nano-black paint increased the thermal conductivity of the absorber and thereby increased the production of the solar distiller by 10.38% and 4.73% for 0.1 cm and 0.2 cm water depths, respectively, comparing to normal black paint.

< Previous Next >

Keywords

Traditional solar distiller; Nano-paint; CuO nanoparticles; Nano coated solar absorber; Solar distiller productivity